

structural analysis of historical constructions

possibilities of numerical
and experimental techniques

1

structural analysis
historical constructions

SAHIC

Edited by C. Modena,
P.B. Lourenço & P. Roca

Material com direitos autorais

Copyright © 2005 Taylor & Francis Group plc, London, UK

All rights reserved. No part of this publication or the information contained herein may be reproduced, stored in a retrieval system, or transmitted in any form or by any means, electronic, mechanical, by photocopying, recording or otherwise, without written prior permission from the publisher.

Although all care is taken to ensure the integrity and quality of this publication and the information herein, no responsibility is assumed by the publishers nor the author for any damage to property or persons as a result of operation or use of this publication and/or the information contained herein.

Published by: A.A. Balkema Publishers, Leiden, The Netherlands, a member of Taylor & Francis Group plc
www.balkema.nl and www.tandf.co.uk

ISBN 04 1536 379 9

Printed in Great Britain

Table of Contents

Preface	XV
Organizing committee	XVII
<i>Volume I</i>	
<i>Invited lectures</i>	
Seismic rehabilitation of heritage buildings in India – problems and prospects <i>S.K. Agrawal</i>	3
Research for seismic redesign of historic masonry buildings <i>M. Tomažević</i>	15
The importance of investigation for the diagnosis of historic buildings: application at different scales (centres and single buildings) <i>L. Binda</i>	29
Evaluation and analysis of the old timber structures <i>A. Ceccotti</i>	43
Remedial measures for the Cathedral of Porto: a post-modern conservation approach <i>P.B. Lourenço, Â. Melo & M. Carneiro</i>	51
Considerations on the significance of history for the structural analysis of ancient constructions <i>P. Roca</i>	63
Design approaches of interventions for the safety and conservation of historic buildings <i>C. Modena</i>	75
<i>Historical aspects and general methodology</i>	
Ancient binding materials, mortars and concrete technology: history and durability aspects <i>Ö. Kirca</i>	87
A system approach for examination and determination in historical buildings <i>D. Ekşi Akbulut & F. Aköz</i>	95
Analysis of steel-structure/masonry-wall interaction in historic buildings <i>D. Friedman</i>	103
Some considerations on the shape of the caps of vaults <i>D. Wendland</i>	111
An inquiry into an unbuilt monument: the mausoleum for the kings of the Italy of Alessandro Antonelli <i>G. Pistone & L. Re</i>	121
The industrial heritage of the Veneto between memory and project: what technology for conservation and reuse? <i>G. Riva</i>	131

<u>Technical state and renovation of buildings of Wrocław's 19th century city centre development</u>	137
<u><i>P. Berkowski, G. Dmochowski, M.Y. Minch & J. Szolomicki</i></u>	
<u>Constructive typologies investigation and approach proposals for the valuation of masonry arch state</u>	145
<u><i>C. Cennamo, S. D'Angelo & G. Voiello</i></u>	
<u>Structural damage prevention in the historical building site. Theory and praxis in the eighteenth century in Campania</u>	153
<u><i>G. de Martino & V. Russo</i></u>	
<u>Restoration of the bell tower on the Church of Vistabella del Maestrazgo, Castellón (Spain)</u>	159
<u><i>F. Vegas López-Manzanares & C. Mileto</i></u>	
<u>Palazzo Cittadini-Stampa: role of stratigraphy and cinematic analysis in the knowledge of a masonry building</u>	167
<u><i>S. Bortolotto, C. Colla, D. Mirandola & A. Sponchioni</i></u>	
<u>An architecture teaching program to rescue the historical town of Ouro Preto, Brazil</u>	177
<u><i>B.T. de Oliveira, E.C. de Araújo, J.N.S. Villaschi & L.C. Mancini</i></u>	
<u>Analysis of a Roman masonry flat-slab in Hadrian's Villa, Tivoli</u>	183
<u><i>D. Abruzzese, G.E. Cinque & G. Lo Gatto</i></u>	
<u>Emergence, development, and prevalence of brick nogging in American vernacular structures</u>	191
<u><i>D.F. Laefer</i></u>	
<u>Vernacular architecture and "historical seismography": an experience research</u>	203
<u><i>O. Niglio & D. Olivieri</i></u>	
<u>The traditional twig-knitted wooden construction techniques: a vernacular architecture, "the Huğ house"</u>	213
<u><i>Z.H. Tokay</i></u>	
 <i>Materials and laboratory testing</i>	
<u>An experimental study on the construction materials of the Ankara Citadel</u>	223
<u><i>Ö. Kirca & T.K. Erdem</i></u>	
<u>A material that has witnessed the past in Anatolia: adobe</u>	231
<u><i>T. Çobancaoğlu & U. Tuztaşı</i></u>	
<u>Investigation of the degradation of sandstones in Sydney's heritage buildings</u>	239
<u><i>K.H. Friolo, A.S. Ray, B.H. Stuart & P.S. Thomas</i></u>	
<u>Durability aspects of masonry stones used in the southern temple wall in Jerusalem</u>	245
<u><i>I. Wasserman</i></u>	
<u>Physical and chemical properties of pre-regulated American cements</u>	255
<u><i>A.S. Rush & D.F. Laefer</i></u>	
<u>Study of Place Stanislas coloured pavement for its historical restoration</u>	265
<u><i>J.M. Mechling & R. Elter</i></u>	
<u>Structural failure of historic buildings: masonry fatigue tests for an interpretation model</u>	273
<u><i>P. Ronca, A. Franchi & P. Crespi</i></u>	
<u>Experimental investigation on masonry elements subjected to eccentric axial loads</u>	281
<u><i>L. Cavaleri, A. Failla, L. La Mendola & M. Papia</i></u>	
<u>In-plane shear and tensile strength tests of small brickwork specimens</u>	291
<u><i>L. Malyszko</i></u>	
<u>Testing and modelling of multiple-leaf masonry walls under shear and compression</u>	299
<u><i>J. Pina-Henriques, P.B. Lourenço, L. Binda & A. Anzani</i></u>	

Non-destructive testing and inspection techniques

<u>On-site investigation techniques for the structural evaluation of historic masonry buildings – a European research project</u>	313
<i>C. Maierhofer, C. Köpp & A. Wendrich</i>	
<u>Combined in-situ tests for the assessment of historic masonry structures in seismic regions</u>	321
<i>V. Bosiljkov, M. Tomažević, L. Binda, C. Tedeschi, A. Saisi, L. Zanzi, F. da Porto, C. Modena & M.R. Valluzzi</i>	
<u>Structural evaluation of historic walls and columns in the Altes Museum in Berlin using non-destructive testing methods</u>	331
<i>C. Maierhofer, M. Hamann, C. Hennen, B. Knupfer, M. Marchisio, F. da Porto, L. Binda & L. Zanzi</i>	
<u>Geo-electrical techniques as a non-destructive appliance for restoration purposes</u>	343
<i>R. Keersmaekers, F. Van Rickstal & D. Van Gemert</i>	
<u>The use of radar techniques and endoscopy in investigating old masonry: the case of Dafni Monastery</u>	351
<i>E. Vintzileou, A. Miltiadou-Fézans, V. Palieraki & N. Delinikolas</i>	
<u>Identification of the mechanical properties of timber structures by combined non-destructive tests</u>	361
<i>M.R. Migliore & F. Ramundo</i>	
<u>Compressive behavior and NDT correlations for chestnut wood (<i>Castanea sativa</i> Mill.)</u>	369
<i>A.O. Feio, P.B. Lourenço & J.S. Machado</i>	
<u>Inspection & NDT to verify structural reliability of historic wooden roofs in the ex-Meroni spinning-mill</u>	377
<i>F. Augelli, C. Colla & R. Mastropirro</i>	
<u>The historic side-walls of the Navigli canals in Milano: in situ and laboratory tests for the structural conservative project</u>	387
<i>A. Migliacci, P. Ronca, P. Crespi, G. Franchi, F. Bianchi & S. Di Martino</i>	
<u>Application of ultrasonic Rayleigh wave to testing of masonry materials</u>	395
<i>M. Skłodowski</i>	
<u>Mosaic-grouting monitoring by ground-penetrating radar</u>	401
<i>P. Côte, X. Dérobert, A. Miltiadou-Fézans, N. Delinikolas & N. Minos</i>	
<u>Ultrasonic testing of properties of mortars</u>	407
<i>P. Cikrle, J. Adámek & M. Stehlik</i>	
 <u>Dynamic behaviour and structural monitoring</u>	
<u>The influence of bells' movement on the adjacent masonry vibrations</u>	415
<i>O. Fischer & S. Urushadze</i>	
<u>Validated structural analysis of Gothic vaulted systems</u>	421
<i>E. Erdogmus & T.E. Boothby</i>	
<u>A first approach to study an 18th century belltower</u>	429
<i>S. Ivorra, M.J. Palomo, G. Verdú & F. Pallarés</i>	
<u>Dynamic-based F.E. model updating to evaluate damage in masonry towers</u>	439
<i>C. Gentile & A. Saisi</i>	
<u>Seismic resistance of masonry towers</u>	451
<i>D. Abruzzese & A. Vari</i>	
<u>Techniques of structural identification for the monitoring of historical buildings: first experimental results for a masonry tower</u>	461
<i>P. Carusi, V. Sepe & A. Viskovic</i>	

The dynamic behaviour of the façade of the Basilica S.Maria di Collemaggio <i>E. Antonacci & G.C. Beolchini</i>	469
Earthquake performance of Suleymaniye Mosque <i>S.M. Kaya, O. Yuzugullu, M. Erdik & N. Aydinoglu</i>	477
Ambient vibration testing at N. Sra. do Carmo Church, preliminary results <i>M.A. Baptista, P. Mendes, A. Afilhado, L. Agostinho, S. Lagomarsino & L.M. Victor</i>	483
Experimental stress analysis of historical forged tie beams of archaeological museum of Spina in Ferrara, Italy <i>G. Bruschi, G. Nardoni, L. Lanza, F. Laudiero, N. Tullini, G. Mezzadri & S. Tralli</i>	489
Dynamic identification and model updating of historical buildings. State-of-the-art review <i>J.C. Araiza Garaygordóbil</i>	499
Structural monitoring in the Villa Reale of Monza (MI), Italy <i>A. Del Grosso, A. Torre, G. Corte, G. Brunetti & D. Inaudi</i>	505
Dynamic monitoring of an ancient masonry bridge on Carrara marble way <i>G. Chellini, P. Orsini & W. Salvatore</i>	513
Structural integrity assessment of medieval towers <i>A. Carpinteri & G. Lacidogna</i>	523
Experimental and numerical analysis of the structural behaviour of St Stefano's bell-tower in Venice <i>A. Lionello, I. Cavaggioni, C. Modena, F. Casarin, P.P. Rossi & C. Rossi</i>	533
 <i>Analytical and numerical approaches</i>	
Limit analysis of masonry structures <i>C. Anselmi, E. De Rosa & L. Fino</i>	545
A displacement-based approach for the safety assessment of masonry structures <i>J.A. Ochsendorf</i>	551
A simplified formula for the evaluation of horizontal capacity of masonry portal frames <i>A. De Luca, E. Mele, A. Romano & A. Giordano</i>	557
Staircases as cantilevers or arches? – a question for limit analysis <i>E.A.W. Maunder</i>	569
Systems of arches and columns strengthened with FRP at the extrados <i>U. Ianniruberto & Z. Rinaldi</i>	577
Ultimate behavior of masonry arches reinforced with FRP at the intrados: comparison between analytical and numerical models <i>U. Ianniruberto & Z. Rinaldi</i>	583
A probabilistic model for the assessment of historic buildings under permanent loading <i>E. Garavaglia, A. Anzani & L. Binda</i>	589
Out-of-plane behaviour of multiple-leaf stone masonry <i>G. Mirabella Roberti, L. Donati & A. Fontana</i>	597
Numerical modelling of a small mortar dome towards the restoration of a <i>cruzeiro</i> in Portugal <i>P.B. Cachim & A.L. Velosa</i>	603
The mechanical behaviour of mortars in triaxial compression <i>R. Hayen, K. Van Balen & D. Van Gemert</i>	611
The effect of the masonry pattern on the global behaviour of vaults <i>C. Calderini & S. Lagomarsino</i>	619

Non linear step by step analysis for masonry structures using changing shape finite elements – new developments and implementations <i>P. D'Asdia, A. Viskovic & C. Brusaporci</i>	629
Construction sequence in the finite element analysis of Romanesque churches <i>L.A. Van Gulick</i>	635
Structural scheme of the Cathedral of Burgos <i>D. Theodossopoulos</i>	643
Comparison of the masonry structures analysis using the co-rotational formulation and a simplified proposal <i>A. Agüero & F.J. Pallarés</i>	653
Analysis of masonry structures by discrete finite element method <i>I.H.P. Mamaghani</i>	659
Why does the Endless Column seem everlasting? <i>C.A. Safta</i>	667
Structural analysis of Küçük Ayasofya Mosque in İstanbul <i>M. Massanas, P. Roca, M. Cervera & G. Arun</i>	679
Prevision of settlement-induced cracking in historical building masonry façades <i>J.G. Rots & S. Invernizzi</i>	687
Cracking simulation in a plain structure using the finite element method <i>L. Pani, B. De Nicolo & Z. Odoni</i>	695
Author index	701

Volume II

Consolidation and strengthening techniques

Experimental investigation and analytical modeling of the effect of injection grouts on the structural behaviour of three-leaf masonry walls <i>E.E. Toumbakari, D. Van Gemert, T.P. Tassios & E. Vintzileou</i>	707
Application of mineral grouts. Case study and impact on structural behaviour: Church of St. Catharina at Duisburg (B) <i>S. Ignoul, F. Van Rickstal & D. Van Gemert</i>	719
Analysis of historic masonry shear walls strengthened by composite material <i>R. Capozucca</i>	727
Two techniques for repair and strengthening masonry constructions <i>R.A. Sofronie</i>	735
Structural restoration of vaults with extrados ties <i>A. Gubana & E. Giuriani</i>	745
The main cupola of the Dresden Frauenkirche <i>V. Stoll & W. Jaeger</i>	753
The medieval castle Spøttrup. Stabilization of the south wing <i>T. Jespersen</i>	763
Technologies for the prestressing rings of the Leaning Tower of Pisa <i>A. Lodigiani & G. Macchi</i>	771
A quick and low-cost method for strengthening high buildings: the case of St. Stefano's bell-tower in Venice <i>A. Lionello, I. Cavaggioni, P.P. Rossi & C. Rossi</i>	781

Intervention methodology on historical structures subject to distortions <i>A. Raffagli</i>	787
Strengthening of historical construction by using steel bracing inserted into brick walls <i>M.Y. Minch, J. Szolomicki, P. Berkowski & G. Dmochowski</i>	795
Confined masonry members: a method for predicting compressive behaviour up to failure <i>A. Mandara & G. Palumbo</i>	803
Castel Belasi's special underpinning and reinforcement project <i>P. Mazzalai, S. Torresani, L. Silvestri & L. Springhetti</i>	813
Non-invasive underpinning technologies in historic settings <i>E.E. Crocker</i>	821
Restoration and strengthening with fibre reinforced polymers: issues to consider <i>N.G. Shrive, M.M. Reda Taha & M.J. Masia</i>	829
Creep behavior of brick masonry panels strengthened by the bed joints reinforcement technique using CFRP thin strips <i>A. Saisi, L. Binda, M.R. Valluzzi & C. Modena</i>	837
In-plane shear strengthening of natural masonry walls with NSM CFRP strips and FRCM overlay <i>L. De Lorenzis, N. Galati & L. Ombres</i>	847
Numerical modeling of masonry structures reinforced by FRP plate/sheets <i>A. Failla, A. Cottone & G. Giambanco</i>	857
Stress transfer at the interface of bonded joints between FRP and calcarenite natural stone <i>M. Accardi & L. La Mendola</i>	867
Influence of environmental agents on bond between FRP reinforcement and calcarenite ashlar <i>M.A. Aiello & M.S. Sciolti</i>	875
Durability assessment of FRP wraps applied on high artistic "plaster and reeds" vaults <i>E. Quagliarini, M. D'Orazio & A. Stazi</i>	883
FRP strengthening systems for metallic structures: a state of the art <i>V. Zerbo, A. Di Tommaso & L. Ceriolo</i>	891
 <i>Historical timber and metal structures</i>	
Experimental analysis of ancient wooden beams for flexural and shear failure <i>F.M. Mazzolani, B. Calderoni, G. De Matteis & C. Giubileo</i>	903
A strengthening technique for timber floors using traditional materials <i>C. Modena, M.R. Valluzzi, E. Garbin & F. da Porto</i>	911
Experimental analysis of ancient chestnut beams by small specimens <i>F.M. Mazzolani, B. Calderoni, G. De Matteis & C. Giubileo</i>	923
Investigating causes of damages to historical timber structures by use of FEM <i>C. Thelin & K.G. Olsson</i>	935
Methodology for the analysis of complex historical wooden structures: a study case <i>F.M. Mazzolani, B. Faggiano & A. Marzo</i>	945
Strengthening and control methods for old timber trusses: the queen-post truss of the Trento theatre <i>M.P. Piazza, M.R. Riggio & G.B. Brentari</i>	957
Timber roof structures of the "Arsenale" of Venice <i>C. Menichelli, C. Modena, M.R. Valluzzi, E. Garbin & F. da Porto</i>	967
The furnace hall in Peitz – analyzing a 200-year old curved plank roof <i>L. Hahmann</i>	977

Viscoelastic analyses of a prestressed Howe Bridge <i>D.A. Gasparini, J. Bruckner & F. da Porto</i>	983
Ancient timber bridges: numerical modelling of connections behavior <i>C. Ceraldi & E. Russo Ermolli</i>	991
Long-term creep in wooden-iron bridges: a comparative study of different truss types <i>F. Lanza, A. Mattarucco & F. da Porto</i>	1001
Structural analysis and rehabilitation of a nailed railway bridge in Genoa <i>A. Brencich & L. Gambarotta</i>	1009
Historical railway bridges: tests and numerical analysis <i>M. Ferraioli, P. Malangone, M. Rauci & A. Zambrano</i>	1019
Restoration of the historical steel vault of the Goldoni Theatre in Livorno <i>M. Sassu</i>	1029
Numerical analysis of the steel roofing structure of the Umberto I Gallery in Naples <i>R. Landolfo, M. Manganiello & F. Portioli</i>	1039
 <i>Seismic analysis and vulnerability assessment</i>	
Vulnerability study in seismic areas: the role of on-site and archives investigation <i>A. Anzani, A. Baila, D. Penazzi & L. Binda</i>	1051
Guidelines for restoration and improvement of historical centers in seismic regions: the Umbria experience <i>L. Binda, G. Cardani, A. Saisi, C. Modena, M.R. Valluzzi & L. Marchetti</i>	1061
An analysis of the seismic vulnerability of the architectural heritage in Bhuj, Gujarat, India <i>D. D'Ayala & A. Kansal</i>	1069
Experimental testing in support of a mechanics-based procedure for the seismic risk evaluation of unreinforced masonry buildings <i>L.F. Restrepo-Vélez & G. Magenes</i>	1079
Mechanical models for the seismic vulnerability assessment of churches <i>S. Lagomarsino, S. Podestà, S. Resemini, E. Curti & S. Parodi</i>	1091
Seismic risk of monumental structures of Kathmandu Valley <i>P.N. Maskey & T.K. Datta</i>	1103
Assessing the seismic vulnerability of late Ottoman buildings in Istanbul <i>D. D'Ayala & D. Yeomans</i>	1111
On elastic models for evaluation of the seismic vulnerability of masonry churches <i>R. Meli & F. Peña</i>	1121
Probability of collapse of monumental buildings under seismic loads <i>G. Augusti, M. Ciampoli & E. Canalella</i>	1133
Out-of-plane fragility of historic masonry walls <i>G. de Felice</i>	1143
Failure mode in an industrial brickwork chimney using different criteria <i>F.J. Pallarés, A. Agüero, M. Martín & S. Ivorra</i>	1149
Seismic assessment of masonry structures by non-linear macro-element analysis <i>A. Penna, S. Cattari, A. Galasco & S. Lagomarsino</i>	1157
Correlation between tensile strength and the collapse mechanism of brick masonry constructions <i>F. Peña</i>	1165

Stochastic analysis of hysteretic degrading systems subject to earthquakes 1175
G.C. Marano & R. Greco

Seismic strengthening and innovative systems

Implementation of a methodology using “ties and injection” developed for repair and strengthening of historic monuments 1187

V. Sendova & P. Gavrilovic

Stabilization of the landmark Las Flores adobe: a case study of restrained seismic retrofit 1197

J.M. Barrow, E.L. Tolles & S.J. Farneth

Masonry strengthening by metal tie-bars, a case study 1207

G. Spina, F. Ramundo & A. Mandara

Modifying building response using energy absorbing diaphragm-to-wall connectors 1215

A. Lockrem, M. Schuller & R. Locke

Some considerations of structural restoration of S. Giacomo church's in Gavi (Alessandria) 1221

M. Corradi & V. Filemio

Seismic protection of monuments by shape memory alloy devices and shock transmitters 1229

M.G. Castellano & S. Infanti

Seismic protection of historical centers using innovative techniques, with focus on San Giuliano di Puglia after the 2002 Molise earthquake 1235

M. Indirli, P. Clemente, B. Spadoni, R. Cami, E. Speranza, M. Mucciarella & F. Pistola

Seismic upgrading of an old industrial masonry building by dissipative steel roofing 1247

F.M. Mazzolani & A. Mandara

Seismic isolation: a new approach to earthquake protection of historic monuments 1257

P. Gavrilovic, V. Sendova & S.J. Kelley

Case studies

Masonry structure in the Crusader's Castles – Syria 1267

W. Jaeger & E. Al-Khateeb

Library of Parliament of Canada – conservation, rehabilitation, upgrade case study presentation 1273

M. Petrescu-Comnene & S.R. Higgins

Pathology of the Dafni Monastery: survey, monitoring of cracks, interpretation and numerical verification 1285

A. Miltiadou-Fézans, E. Vintzileou, N. Delinikolas, E. Zaroyianni & E. Chorafa

The role of survey for a correct FE analysis: the case of the Monte Oliveto Maggiore church 1295

B. Belletti, E. Coisson, C. Ferrari & S. Pedroni

Researching the bearing system's capacity as an argument in solving a dilemma in the interpretation of the origin and development of architectural complex of the St. Donatus' church in Zadar 1305

E. Lokošek & H. Podnar

Analysis of Tapial structures for modern use and conservation 1315

P.A. Jaquin, C.E. Augarde & C.M. Gerrard

Preliminary investigation and monitoring for the design of a strengthening intervention on the Frari basilica, Venice 1323

A. Lionello, I. Cavaggioni, P.P. Rossi, C. Rossi, C. Modena, F. Casarin, G. Marchi,

G. Gottardi & A. Ragazzini

Fallingwater – structural intervention, in time <i>J.A. Matteo</i>	1335
The Nidaros Cathedral in Trondheim. The Norwegian National Symbol. Stabilization of the Choir <i>T. Jespersen</i>	1341
Structural restoration of a farm wing of the Park Abbey at Heverlee, Belgium <i>K. Brosens, S. Ignoul, D. Van Gemert, K. Van Balen, L. Schueremans & P. Stevens</i>	1349
Application of CFRP laminates as strengthening of cracked brick arches <i>R. Ciesielski, H. Ciurej & A. Kwiecień</i>	1357
Restoring the greenhouse at Lednice chateau <i>J. Hirs, M. Bajer, J. Kala & K. Ksandr</i>	1367
Saving minarets at risk in Afghanistan <i>G. Macchi</i>	1375
The vaulting structure of the Temple of Venus and Rome at the Roman Forum <i>C. González-Longo & D. Theodossopoulos</i>	1383
Structural analysis and project of reconsolidation of Italian Hospital, Montevideo, Uruguay <i>G. Valletta, R. Chaer, S. Nencioni, C. Pecora & L. Nisizaki</i>	1395
Theoretical and experimental studies for strengthening Bohemian brick vaults <i>I. Bucur-Horváth, M. Miklós & I. Popa</i>	1403
Structural studies developed on “The Miracles Roman Aqueduct” in Merida (Spain) <i>A.G. Palacio</i>	1409
Preservation and stability of industrial masonry chimneys <i>A.T. Vermeltfoort</i>	1413
A new load bearing structure for the conservation of the roofs of the Molino Stucky in Venice (Italy) <i>G. Boccanegra, S. Dobricic, A. Marchi & F. Amendolagine</i>	1421
Author index	1427

Preface

Structural Analysis of Historical Constructions IV continues the series of triennial international seminars started in Barcelona in 1995 and continued with increasing success in Barcelona 1998 and Guimaraes in 2001. This edition is organized at the University of Padova, at the beginning of its 783rd Academic Year, with a strong involvement of the country, Italy, where an exceptional concentration of historic construction and a long tradition of conservation actions exist: almost half of the about 160 accepted papers are in fact from Italy. Located near Venice, Padova is also a good lookout of what is happening for the conservation of one of the world's most famous historic centres. The occasion is in fact taken to have a close view of significant works being done in Venice, in the ambit of a special session organized inside its historic Arsenale. Venice is also the site of the UNESCO Regional Bureau for Science in Europe (ROSTE), so that the seminar is intended to offer a special chance for debating the very specific problems that have to be faced in countries of east Europe and middle and far east for the preservation of historic architectural heritage.

The number and quality of contributions, the number of countries, 27, from which the contributors came, is a clear indication of the importance have structural safety aspects for ensuring physical survival of the architectural heritage in all the world, and then the possibility to preserve its historic-artistic value with all the implied cultural-social and economical consequences.

The major challenges to specialized people – technicians, art historians, conservators – involved in the multi-disciplinary processes that are required to ensure the conservation of architectural heritage are all reflected in the written free and invited contributions, organized in ten topics: “Historical Aspects and General Methodology”, “Materials and Laboratory Testing”, “Non-Destructive Testing and Inspection Techniques”, “Dynamic Behaviour and Structural Monitoring”, “Analytical and Numerical Approaches”, “Consolidation and Strengthening Techniques”, “Historical Timber and Metal Structures”, “Seismic Analysis and Vulnerability Assessment”, “Seismic Strengthening and Innovative Systems”, “Case Studies”. In addition to the free presentations, height comprehensive plenary lectures have been provided by invited speakers.

As it is well known, it is not only a matter of dealing with a very difficult engineering problem, as it actually is. The very basic safety concepts are quite different, and much less established, in the case of existing structures with respect to the newly constructed ones. This is of course particularly true when the artistic/historic importance of existing structures is such to accept higher probabilities of “structural failures” than in the case of the new ones. Theoretical and experimental tools for analyzing the material and structural properties and performances are continuously evolving, in a very distinguishing way they are in the field of moderns constructions. Learning from practice is essential, even if the application are made always on “unique”, and for this only reason always important, objects.

But even more crucial is the fact that both in the phase of the evaluation of the exiting safety conditions and in the choice of the interventions an “appropriate balance” must by case by case found between “pure engineering” and “conservation” aspects.

It is of course the hope of the organizers that the seminar and the book will fruitfully help practitioner technicians and final users of their activity, and will stimulate scientists and researcher in further developing, stimulated by the presentations and discussions, new and more and more reliable tools and methodologies for ensuring “structural safety” while preserving historic/artistic values of the world's architectural heritage.

Padova, August 2004

Claudio Modena / Paulo B. Lourenço / Pere Roca

Organizing committee

Paulo B. Lourenço Universidade do Minho – Portugal
Claudio Modena Università di Padova – Italy
Pere Roca Universitat Politècnica de Catalunya – Spain

Scientific committee

Drazen Aninic University Josip Juraj Strossmayer – Croatia
Görün Arun Yildiz Technical University – Turkey
Luigia Binda Politecnico di Milano – Italy
Thomas Boothby The Pennsylvania State University – United States of America
Giovanni Carbonara Università di Roma “La Sapienza” – Italy
Ario Ceccotti Istituto per la Valorizzazione del Legno e delle Specie Arboree – CNR – Italy
Dina D’Ayala University of Bath – United Kingdom
Miloš Drdácý Institute of Theoretical and Applied Mechanics – Czech Republic
Gavrilovic Pedrag University St. Cyril and Methodius – Macedonia
Pietro Alessandro Vigato Progetto Finalizzato Beni Culturali – CNR – Italy
Maurizio Indirli Ente per le Nuove Tecnologie, l’Energia e l’Ambiente – Italy
Giorgio Macchi Università di Pavia – Italy
Christiane Maierhofer BAM, Federal Institute for Material Research and Testing – Germany
Roberto Meli Universidad Nacional Autónoma de México – Mexico
Ioanna Papayianni Aristotle University of Thessaloniki – Greece
Andrew Powter ICOMOS International Wood Committee – Canada
Michael Schuller Atkinson-Noland Associates – United States of America
Ramiro Sofronie University of Bucarest – Romania
Vito Renda European Laboratory for Structural Assessment – JRC – Italy
Miha Tomasevic Slovenian National Building and Civil Engineering Institute – ZAG – Slovenia
Koenraad van Balen Katholieke Universiteit Leuven – Belgium
Elizabeth Vintzileou National Technical University of Athens – Greece

The papers are published in the form submitted by the authors, after revision by the Scientific Committee. The Editors are relieved of any responsibility for possible errors or disagreements.

Organization



Università degli Studi di Padova



Dipartimento di Costruzioni e Trasporti

Sponsors



TNO DIANA



Fischer Italia S.p.A.



Industrie Cotto Possagno S.p.A



MOOG Italia S.p.A



Terreal Italia S.r.l



Tassullo S.p.A.

Supporting institutions



THE EUROPEAN COMMISSION'S
DELEGATION TO INDIA,
BHUTAN, MALDIVES AND
NEPAL
EU-India
Economic Cross Cultural Programme



CONSIGLIO NAZIONALE DELLE RICERCHE
Progetto Finalizzato – Beni Culturali

Patronage

Patrocinio
Regione del Veneto



Regione Veneto



United Nations Educational,
Scientific and Cultural Organization

Invited lectures

Seismic rehabilitation of heritage buildings in India – problems and prospects

S.K. Agrawal

Central Building Research Institute, Roorkee, India

ABSTRACT: History of earthquakes in India demonstrates vulnerability of our heritage buildings to seismic hazards. The recent past, devastating earthquakes in urban areas in India causing wide spread damages to these buildings, disruption of services and damage to environment have been of great concern; the experiences have prompted to carry out in-depth studies and come out with solutions and policies which will go a long way in minimizing the damages caused by seismic ground motions. In this context, seismic rehabilitation of heritage structures is a new discipline coming up in India and should be given a top priority. The paper discusses threadbare the problems associated with the heritage buildings, their modes of failures, rehabilitation actions and strategies. A recently accomplished restoration of a prestigious building damaged during 26th January 2001, Bhuj earthquake of India is discussed in the paper as a case study. Also, it is highlighted that there is urgent need of instrumentation, experimentation and monitoring of heritage structures to study the dynamic properties and safeguard them from future ground motion.

1 INTRODUCTION – HISTORY OF INDIAN HERITAGE BUILDINGS

Nearly 5000 years ago, on the lush green banks of river Indus, man started making sculptures from stones. In fact, he wanted to give shape to his own creativity. It was the copper age, iron had not appeared on the scene. He did not have fine chisel or sophisticated tools, but that did not deter him. He chose relatively softer rocks such as limestone and sandstone for making small statues. These creative people lived in twin cities of Mohenjodaro and Harappa, in the Indus valley, now in Pakistan, one of the oldest records of its kind in India. These were the earliest urbanized colonies of the Indian subcontinent. The great civilization left behind large monumental examples of carvings and construction skill. The artisans used either rocks and bricks or carved out temples and caves in rocks. These Heritage buildings are mute testimony in adobe, rubble, stone or brick of the ceaseless efforts of mankind to express his social and religious feelings. The progress of human civilization can be traced from the varied artifacts, motifs and artistic imagery carved in heritage buildings. These monuments not only reflect the rich cultural life of the ancient and medieval people but also show their technical skill in engineering construction and profound knowledge in the selection of sites, judgement of foundation conditions and choice of construction material.

India has been the seat of a great civilization for 5000 years or more. The ancient civilization has its manifestation in the sphere of religion, art, literature, music and sculpture – all these having been imprinted into the various monuments constructed through ages. The country is dotted with plethora of monuments, which include temples, Buddhist stupas, churches, mosques, rock-cut caves, minarets, palaces and forts. Many of these monuments are of considerable antiquity dating back to 1000 years or more.

The evolution of construction techniques is related to the gradual assimilation of knowledge of using construction materials of various types in a given environment. The earliest construction practice was confined mainly to the use of bricks and wood, and due to their low durability, the well-preserved heritage buildings of such kind prior to 3rd century BC are rarely found. However, the remains found in the Mohenjodaro site of Indus valley civilization (3000 BC) indicates use of shaped and dressed blocks of polished marble for building purposes.

The use of rocks by Emperor Ashoka (273–237 BC) as huge monolithic pillars and railings added a new dimension to the building history of India. Revolutionary thoughts and dynamic approach in utilizing *in situ* rock or the rock-mass gave birth to the rock-cut architecture in India, which now holds a glorious record of having nearly 12,000 rock-cut structures like shrines, chaityas and monasteries etc. constructed between 3rd

century BC and 9th century AD. In the construction of such rock-cut structures, knowledge of the right selection of the site including the character of the rocks, which are amenable to a sculptor's chisel and hammer, was vital. The world-famous rock-cut temples of Ajanta and Ellora, a treasure-trove of art, were chiseled out of the very resistant Deccan basalt at suitable sites.

Creative ideas for the utilization of local resources of building material like rock and clay brought in new concepts in architectural design and structural constructions. Where rock was available within a close proximity, it was used for durable construction material and lasting carvings. Thus we find, charnockite was used in the Mahabalipuram temple of Chennai, granite in the Meenakshi temple of Madurai, khondalite in the Konark temple of Orissa, Triassic limestone in the Avantipur temple of Kashmir, Vindhayan sandstone in the Ashoka Pillar and Dhameka stupa of Sarnath, and Siwalik sandstone in the Kangra fort of Himachal Pradesh. When beauty was the prime motive of construction, as in the Taj Mahal of Agra, the right selection of stone like the chaste-white Makrana marble of Rajasthan was the primary consideration irrespective of the distance of its availability. Hundreds of such splendid monuments of varied types of rocks have withstood the ravages of several centuries and are destined to stay for several centuries, if preserved meticulously and protected from natural disasters such as earthquake. The elegant terracotta sculptured brick temples of Bengal provide a classic example of the imaginative expression of artistry and construction talent in the use of local clay in the absence of rock.

Since the time immortal, these rich heritage buildings of India have been facing the wrath of man made cultural invasions, natural disasters and environmental degradation. However, they are the physical evidences of rich cultural values of our glorious past, which we inherit from our ancestors and are to be preserved in their authenticity i.e. aesthetic and historical values ensuring structural safety against external actions. The paper elaborates seismic rehabilitation of the heritage structures in India. The purpose of the paper is to highlight the problems and prospects connected with structural restoration and seismic protection in the areas of significant seismic hazard with special reference to the problems of the structures in India.

2 PERFORMANCE OF HERITAGE BUILDINGS DURING PAST EARTHQUAKES

Experiences of earthquakes in last decades in semi-urban & urban parts of India (Uttarkashi 1991, Latur 1993, Jabalpur 1997, Chamoli 1999, and Bhuj 2001) have caused deep concern with regards to seismic hazards and resulting risk. These devastating earthquakes in urban areas in India cause heavy economical losses



Figure 1. Monument at Bhuj damaged due to Gujarat Earthquake.

in terms of loss of life, property, disruption of services and damage to environment recurrently. The damages caused to the heritage structures during earthquakes are never given first priority and most of the times go unnoticed. However, thanks to the concerned organizations and people, who time and again bring upon these spectacular damages with the emphasis to restore them in their original glory. Among the many critical modes of failure experienced by heritage structures during earthquakes, the most relevant and recent with reference to India are discussed here.

2.1 Structural aspects

Most of the heritage buildings are made up of masonry of varied kinds, from adobe or rubble joined with mud/lime/surkhi mortars, to rock/stone conglomerates with cementitious materials of good quality. It is written in Indian literature that several kings used blood, pulses, and jaggery as binders and longevity. However, these heritage buildings seemed to perform badly during past earthquakes. The basic reasons has been the intrinsic weaknesses of masonry i.e. its great weight and low tensile strength, which is further aggravated by deterioration due to weathering. An important aspect of the masonry used in heritage structures is its heterogeneity and the significant variations in its quality among different structural members and even within the same member. Also, in masonry structures, it is difficult to give continuity to their structural members (among transverse walls and of the walls with the floors and roofs), as well as the difficulty to form stiff horizontal diaphragms capable of distributing inertia forces to the stiffest and strongest walls. Devastation caused to the heritage building in Bhuj during 26th January 2001, Gujarat earthquake is shown in Figure 1.

Another picture shown in Figure 2 is the old structure used as Road Transport office in Jabalpur, the meizoseismal area of 1997 Jabalpur earthquake, India. The structure undergone severe damage and is living perilously.



Figure 2. RTO building damaged during Jabalpur earthquake of 1997, India.



Figure 3. Wide spread damage was caused to temples all around the Gujarat during Bhuj earthquake causing complete failure.



Figure 4. Collapse of wall of a Bhuj fort.

Several temples of historical and cultural values went into rubbles and biting dust during past earthquakes of India as depicted in Figure 3.

2.2 Overturning of long walls

The most commonly encountered mode of failure during past earthquakes has been overturning of the walls due to out-of-plane inertia forces and normally precipitated by the outward thrust of the roof. Figure 4 shows



Figure 5. Chattris are very common in Gujarat area. Figure shows the view of Chattri before and after the Bhuj earthquake.



Figure 6. The Parag Mahal at Bhuj before and after the earthquake.

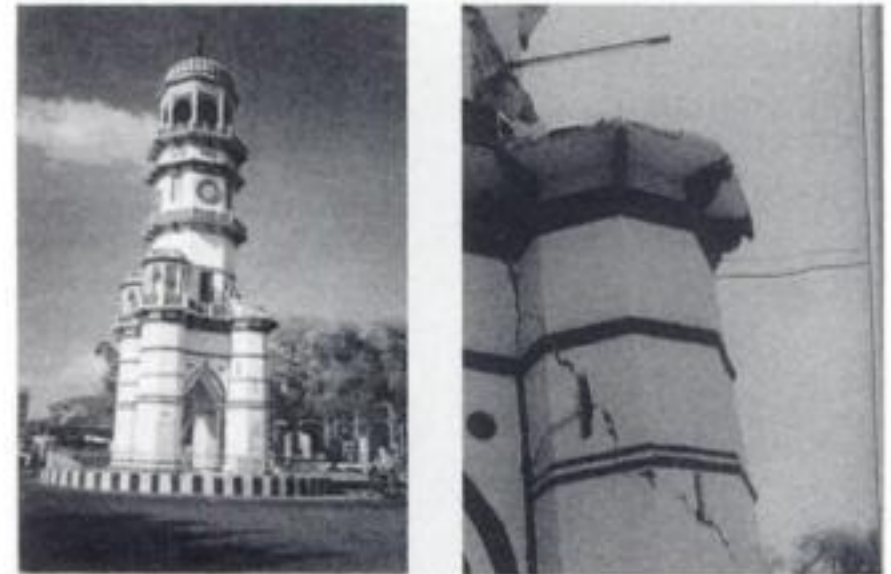


Figure 7. The Famous clock tower in the heart of Jabalpur city. One of the minaret fell down during Jabalpur earthquake, India.

the overturning of long wall of Bhuj fort leading to partial collapse.

Normally, the roofs of heritage buildings are jack-arched, vaulted or dome shaped. The failure starts with the separation of wall from its transverse supports, then by its vibration as cantilever of increasing length. Finally the walls overturn or open enough to produce the instability or loss of support of the roof, which collapses. Figure 5 shows the failures of Raolakha Chhatri and Figure 6 shows Prag Mahal at Bhuj, Gujarat.

2.3 Separation and overturning of facade

If the façades of the forts are not tied well to the rest of the monument, they tend to get separated, overturn and fell from the main structure. An example of Clock tower at Jabalpur whose one minaret fell since it was stiffer than the other minarets due to presence of stair is shown in Figure 7.



Figure 8. Mosque with collapsed minarets during Jabalpur earthquake.



Figure 10. Earthquake damaged clock tower at Morbi, Gujarat.



Figure 9. Partly broken and tilted minar of Idgah (the prayer place for muslims) during Jabalpur earthquake.

Also, the heavy and tall tower can become unstable owing to the inertia forces transverse to their plane. Roofs or intermediate floors do not provide proper restriction to the outward displacement of the façade. The failure of minarets during Jabalpur earthquake are shown in Figure 8 and Figure 9.

2.4 Diagonal cracking

The failure due to shear forces in walls through diagonal cracking is not very frequent in heritage structures, though, because the great thickness typical of the monuments gives the walls a significant capacity to resist shear forces, even if their unit shear strength is low. Nevertheless, the shear failure is commonly associated with walls with large openings such as in Figure 10.

Large openings can seriously undermine the in-plane shear strength of these walls. The shear capacity of masonry piers may not be enough to resist lateral loads imposed by earthquake forces. Poor in-plane

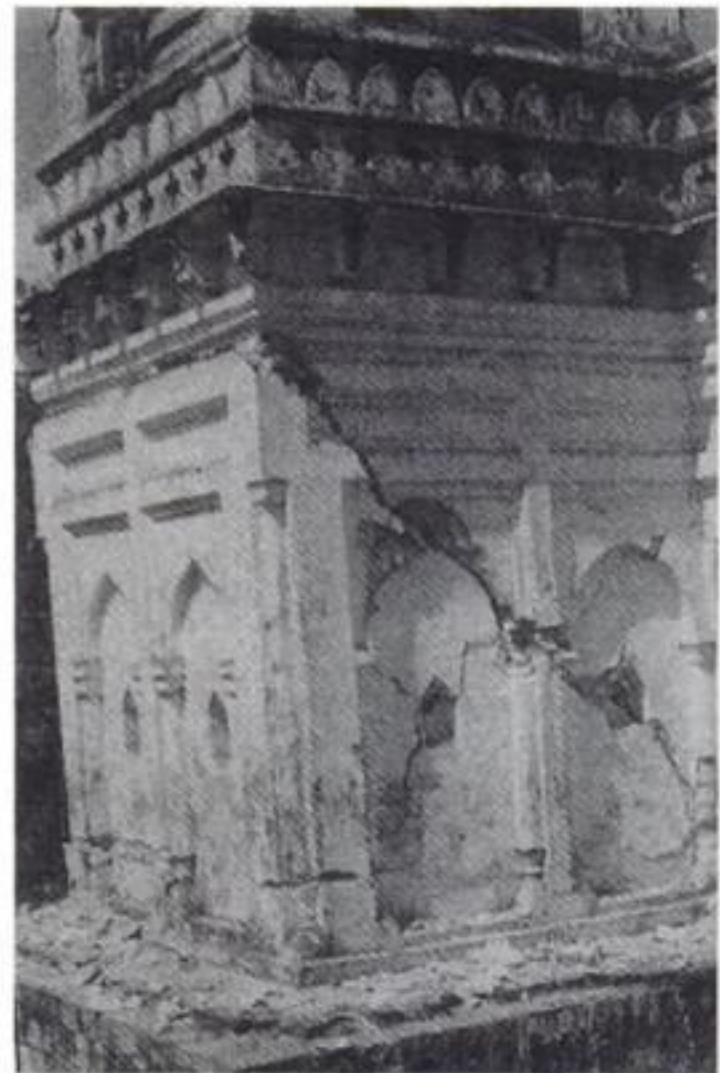


Figure 11. Development of shear cracks and partial collapse in Radha Krishna temple.

shear performance has been noted in heritage buildings in India. Diagonal shear cracking is common sight, due to reduced mortar shear capacity, however, in a few cases flexural (rocking) failures are also observed. The typical failure of a temple and church are shown in Figure 11 and Figure 12 during Jabalpur earthquake.

2.5 Tensile failure of structures

It has been found that artistic rooftops in most of the monumental buildings lack in proper floor and roof



Figure 12. 125 years old St. Paul Cathedral Church cracked with partial collapse of tower.



Figure 13. Collapse of Chattris made up of large block stone masonry during Bhuj earthquake.

diaphragms and the inertia forces thus generated in the large masses at roof levels get directly transferred to the walls supporting each portion of the roof, regardless of the relative lateral stiffness of the resisting members. Large concentrations of lateral forces can arise in some walls. Furthermore, it must be taken into account that during the vibration of the structure tensile stresses arise in roof that could generate large cracks, actually separating the structure in parts leading to partial to total collapse. Such a failure is shown in Figure 13 during 2001 Gujarat earthquake.

Also, the façade known as pagodas with its towers and buttresses can separate, due to longitudinal vibration, from the rest of the structure which must withstand the inertia forces generated on it, and whose buttresses do not contribute to the shear strength of the

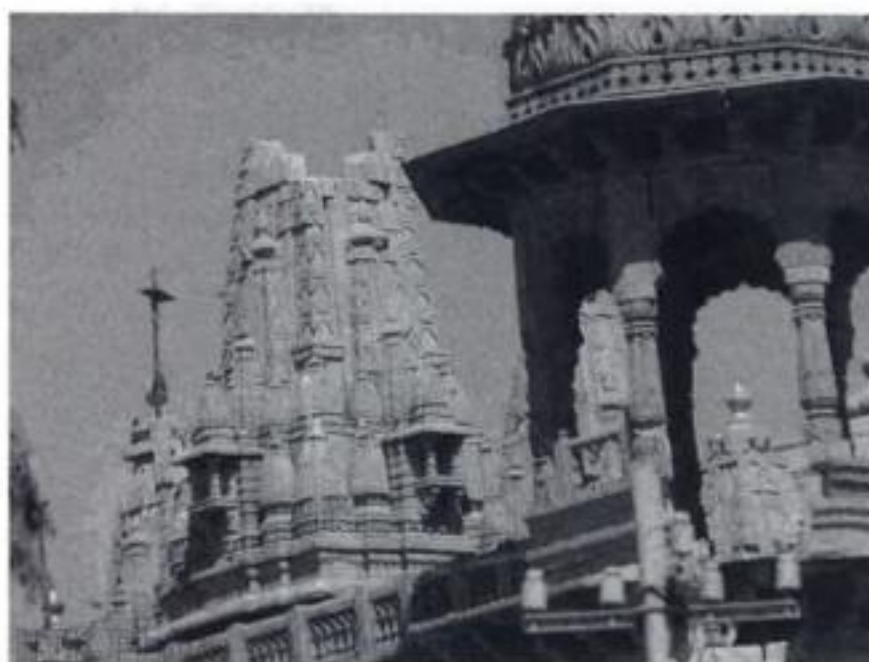


Figure 14. Partial toppling of temple top (pagoda) at the palace at Morbi, Gujarat.

rest of the structure. A failure of pagoda at the palace in Morbi is shown in the Figure 14.

3 SEISMIC REHABILITATION – AN OVERVIEW

Seismic rehabilitation is used as a comprehensive term to include all the concepts of *repair, restoring, upgrading, retrofitting* and *strengthening* that lead to reduce seismic vulnerability of any structure. A large number of existing structures in earthquake prone areas over the world need seismic rehabilitation due to various reasons and motivations, including codal modifications, deterioration of structures with age or change in use/modification of structure. Earthquake damaged structures may need strengthening along with repair of damaged portion for reuse (post-earthquake rehabilitation). Generally, they are rehabilitated so that their improved seismic performance is achieved from future ground motion. Seismically weak structures, the design of which do not comply with existing provisions, may also need rehabilitation (pre-earthquake rehabilitation). Seismic rehabilitation of existing structures by retrofitting is one of the most challenging tasks for structural engineers in the aftermath of earthquakes. This task more often poses challenge to structural engineers who find it difficult to retrofit a structure using conceptual retrofit schemes.

The failures of structures during the past earthquakes have clearly shown the vulnerability of our habitat. The problems in India are manifold. The construction practices are varied from region to region and moreover, it is the discretion of the owner, builder, or engineer whether or not to apply the seismic provisions in design and construction. Also, India has a very complex socio-cultural environment and its built environment encompasses the widest possible

range: from non-engineered dwellings built without any technical skills to the most modern buildings. Because all the earthquakes in recent years occurred in rural or semi-urban environments and because most of the deaths were caused by collapse of non engineered structures, the attention most of the time is diverted to repair/rehabilitation of these construction and thus trivializing entire rehabilitation process. The engineers and builders started strengthening buildings, as they deemed appropriate, even though most of them did not have a prior experience of seismic issues.

The seismic rehabilitation of existing structures is the most challenging task and one has to take advice of an expert instead of doing it oneself. Seismic rehabilitation in its strict sense calls for three kinds of improvement in the structure under consideration i.e. **Repair** only visual or cosmetic modifications are made, **Restore** structural repairs such as rebuilding of cracked walls, stitching of cracks, grouting, placement of reinforcement etc. are made such that the original performance of the structure are restored, and **Retrofit** structural modifications such as jacketing, external ties, buttresses, addition of shear/infill walls, bracing & anchorages are made such that a higher performance of the structure is achieved than that of original structure. However, the seismic rehabilitation has been used very loosely in the field. The cosmetic repairs are often confused with seismic rehabilitation. Seismic rehabilitation is to be carried out by structural engineer and requires proper planning and engineering judgment. Firstly, the structure is to be evaluated for its seismic resistance and then depending upon the requirements, it is to be rehabilitated. Seismic evaluation of existing buildings in itself is a tedious task and has been new in Indian scenario. There is no standardized document available for the said purpose. There has been meager data available on the structure retrofitted for their seismic resistance. The common methods in our country are to use traditional practices such as repair of cracks, stitching, guniting, jacketing etc. It has been experimentally verified that these techniques do not add to the strength and ductility and in turn render the structure precarious. We are actually carrying out repairs instead of strengthening. The newer techniques such as wrapping, addition of new frames, shear walls, bracing, introduction of energy dissipation devices, base isolation etc. are never tried despite of the fact that they perform well during earthquake and have been introduced all over the globe successfully. This is due to lack of awareness amongst engineers as regards seismic rehabilitation is concerned.

So far, the discussion was not specific to heritage structures. The problems get further complex when heritage structures are to be rehabilitated for their improved seismic resistance. Here the goal is manifold, the seismic rehabilitation means is to *preserve* and *reveal* the aesthetic and historical values of the

heritage structure and at the same time ensuring structural safety against external actions i.e. earthquakes. Heritage structures are defined as all those which merit special care on account of their individual historical or architectural importance, or their significance as surviving representatives of an earlier tradition. But the very definition is ignored and seismic rehabilitation is done with a syndrome known as cover-up of damage syndrome. This is put into practice after every deadly earthquake all around the world. The engineers try to cover-up the damages that appear in structural system and the associated paraphernalia. It is a quick and low-cost solution but precarious one. It is advocated that since the structure withstood the earthquake only with some cracks, there is no problem, which leads into ignoring the extent & pattern of damage as well as its influence on a possible future seismic loading, which could be fatal for the structurally degraded heritage structure. These antiseismic interventions also present a notable impact in the constructive reality of historical construction, and calls for precise awareness of the original structure and by structural choices, which are knowingly consistent.

Design and realization of the interventions for seismic rehabilitation should actually be characterized by concurring specialistic and multidisciplinary contributions, which ought to allow to take decisions so as to safeguard of historical, cultural and architectonic values is ensured in conjunction with the protection of both the construction itself and the human lives potentially involved from structural instability. Generally speaking the problem of seismic rehabilitation of heritage building differs radically from the problem of ordinary structures. Here the emphasis is on preservation of their aesthetic and historical values and then structural safety. As per Venice Charter (UNDP/UNIDO, 1984), the seismic rehabilitation of heritage structures must take into account the following:

- Respect for original material and authentic documents
- Respect to the valid contributions of all periods to the building
- Replacements of missing parts must integrate harmoniously with the whole, but at the same time must be distinguishable from the original
- Additions can not be allowed except in so far as they do not detract from the interesting parts of the building, its traditional setting and its relation with the surroundings
- The use of traditional techniques and materials are clearly preferable for seismic rehabilitation.

Modern techniques and materials are admissible where adequate capacity cannot be ensured by traditional techniques. In this case durability and compatibility of the interventions should be adequately

proven; otherwise, the modern techniques and materials should be used only in a manner that will permit easy corrective action at a later date if necessary.

4 SEISMIC REHABILITATION – METHODOLOGY

Any rehabilitation strategy is case specific and has to be dealt separately in a manner that it alleviates seismic deficiency from the structure under consideration. To adopt cost-effective and appropriate retrofitting scheme, quantitative seismic evaluation of building is prerequisite. Evaluation is a complex process, which has to take not only the design of building but also the deterioration of the material and damage caused to the building, if any. The difficulties faced in the seismic evaluation of a building are manifold. There is no reliable information/database available for existing building stock, construction practices, *in situ* strength of material and components of the building. The seismic evaluation mainly relies on set of general evaluation statements, since analytical methods to model the behavior of buildings during earthquake defining response spectra of structure are too complex to handle with the generally available tools and calls for rigorous engineering seismological exercise. The unavailability of a reliable estimate of earthquake parameters, to which the building is expected to be subjected during, its residual life poses another challenge. Probabilistic approach to evolve needful parameters, would call for elaborate studies. Hence, for preliminary appraisal, the ground motion parameters available in the respective codes may be at the macro level. As regards the effect of local soil conditions, which are known to greatly modify the earthquake ground motion, experiences of ground accentuation and data generated through collateral studies on site response should be considered. *Seismic evaluation* procedure is a comparison between some measures of the *demand* that earthquake place on a structure to a measure of the *capacity* of the building to resist. Evaluation is a complex process involving number of steps like visit to the site and data collection, selection of either the general set of evaluation statements; conduct of follow-up field work; structural analysis for seismic evaluation of building; characterizing seismic capacity, determine seismic demand and verify performance in light of global response limits, component acceptability and conceptual approval.

The Demand/capacity ratio (DCR), thus evaluated is measure of earthquake resistance of a building. The DCR less than unity indicate the building is safe for respective stresses under consideration. However, any DCR exceeding one indicates that the building is vulnerable to earthquake hazard as per respective codal provisions.

The following methodology is presented here for seismic rehabilitation, which is based on elastic method of analysis and is broken into three stages

Stage I – Develop knowledge of as built conditions:

- Step 1: Study of soil conditions at the site.
- Step 2: Measurement of actual geometry of building and its components.
- Step 3: In-situ non-destructive and destructive testing to estimate actual strength of building materials & components.
- Step 4: Tests to estimate material degradation, condition of the structure, extent of corrosion to carefully estimate their available diameters and verify the size, number and spacing of reinforcing bars etc.

Stage II – Analysis & Verification Stage:

- Step 5: Preparation of 3-dimensional model of structure, using measured geometry, and material properties.
- Step 6: Estimation of design lateral force on building using code specific design response spectra for 5% damping or site-specific response spectra, if available.
- Step 7: Application of design lateral force on 3-D model to determine stress-resultants (i.e. axial forces, shear forces, bending moments) in respective members & determination of displacements etc.
- Step 8: Determination of member capacities with actual cross section geometry & material properties as per respective codes (It is based on permissible stresses in flexure, compression, tension and shear) and Demand/Capacity ratios of members.
- Step 9: Identification of deficient members or deficiency in lateral stiffness of the structure if any and verification of the damages actually incurred in the structure.

Stage III – Retrofit Stage:

- Step 10: Identification of suitable retrofitting technique to rectify the deficiencies.
- Step 11: Estimation of the new member sizes, stiffness etc. for the proposed scheme, and/or the new members required.
- Step 12: Re-analysis of building to confirm the adequacy with the proposed retrofit techniques.
- Step 13: If strength and stiffness requirements are satisfied, then the proposed retrofit scheme may be adopted, else other more appropriate retrofit schemes may be identified and steps from 10 are to be repeated.

The above approach is based on elastic procedure and does not include failure patterns, ductility

and, therefore, can be used as a first cut method for retrofitting design. The non-linear analysis and pushover analysis approaches such as one outlined in ATC-40 can also be used for stage II and stage III.

5 SEISMIC REHABILITATION MEASURES – CONCEPTUAL DESIGN

There are umpteen methodologies available for seismic rehabilitation interventions so as to achieve the improved seismic performance and also to preserve historical and cultural values of the heritage structure. The complete list of techniques is beyond the scope of this paper and can be found easily in literature. The bottom line is that the selection of the specific type of element and material should be compatible with the structure under consideration and should be in harmony with the existing structural system. It is thus also an arduous task to develop guidelines for such selection. Conceptual design techniques, on the other hand, can be systematically categorized and design strategies formulated. The solution chosen for rehabilitation is to be always dictated by aesthetic and cultural values rather than merely satisfying technical demands. In heritage buildings, consideration of preservation of historic fabric usually controls the design. In many cases, even the performance objectives are controlled by limitations imposed by preservation. There are some basic issues that are of concern:

1. Aesthetics, including consideration of historic preservation
2. Improved seismic performance
3. Long term effect on building space planning and usage
4. Cost of construction (cost-benefit analysis).

All of these characteristics are always considered, but an importance will eventually be put on each of them, either consciously or subconsciously, and a combination of weighing factors will determine the scheme chosen.

6 REHABILITATION STRATEGIES

The primary focus of determining a viable retrofit scheme is on vertically oriented systems because of their significance in providing either lateral stability or gravity load resistance. Deficiencies in vertical elements are caused by excessive interstory deformations that either creates unacceptable force or deformation demands. The retrofit actions can be classified as:

6.1 *Connectivity*

It is defined as an arrangement consisting of assuring that individual elements do not become detached and

fall and assuring a complete load path. The connectivity deficiencies are within load path: wall out-of-plane connection to diaphragms; connection of diaphragm to vertical elements; connection of vertical elements to foundations; connection of foundation to soil.

6.2 *Modification of global behaviour*

This action normally focuses on decreasing deformations. Overall seismic deformation demand can be reduced by adding stiffness in the form of shear walls or braced frames. A significant time period shift is normally required to protect deformation sensitive elements in this way. New elements may be added, or created from a composite of new and old components. Examples of such composites include filling in openings and using existing columns for chord members for new shear walls or braced frames.

6.3 *Modification of local behaviour*

Rather than providing retrofit actions that affect the entire structure, deficiencies also can be eliminated at the local, component level. This can be done by enhancing the existing shear or moment strength of an element, or simply by altering the element in a way that allows additional deformation without compromising vertical load carrying capacity.

The yielding sequences such as beams yielding before columns, bracing members yielding before connections, bending yielding before shear failure in columns and walls can always be attained by local retrofit in variety of ways. The connections can be strengthened and the shear capacity of the columns and walls can be enhanced to be stronger than the shear demanded by earthquake.

Concrete columns can be wrapped with steel, concrete, or other materials to provide confinement and shear strength. Concrete and masonry walls can be layered with reinforced concrete, plate steel, and other materials. Composites of glass or carbon fibres and epoxy are becoming popular to enhance shear strength and confinement in columns and to provide shear-only strengthening to walls. Similarly, bending strength of unreinforced masonry walls can be increased by insertion of reinforcing or post-tensioning steel in field drilled cores. Deformation capacity can also be increased locally by uncoupling brittle elements from the deforming structure.

The above-discussed actions balance one another in that employing more of one will mean less of another is needed. It is obvious that added global stiffness will require less local deformation capacity, but it is often less obvious that careful placement of new lateral elements may minimize a connectivity issue such as a diaphragm deficiency, very common in Indian heritage buildings. Conceptual design of retrofit is seldom a

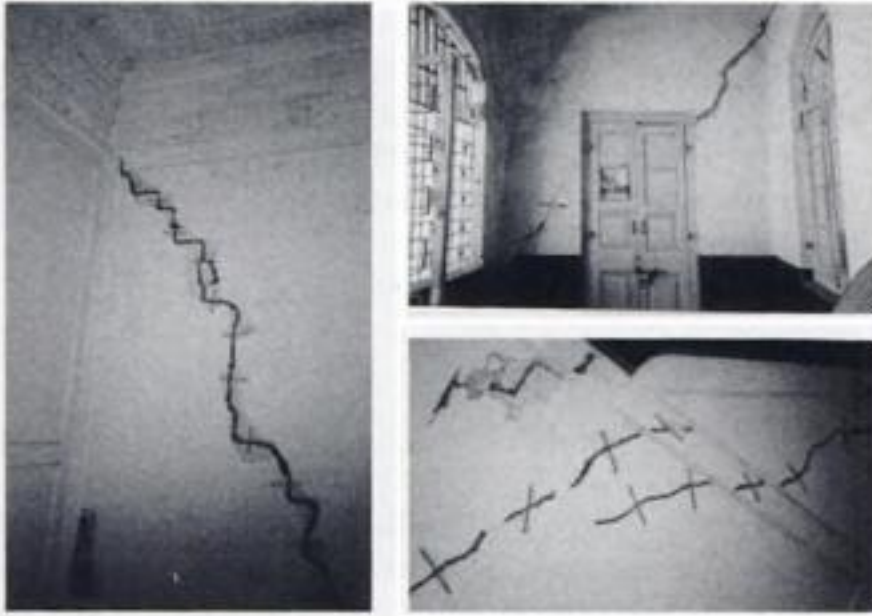


Figure 15. Internally stitched walls of circuit house immediately after the earthquake.



Figure 16. Jack arch floor of the circuit house which underwent severe cracking.

one step process, several trials are required to define satisfactory design, both to balance the retrofit actions discussed above and to determine the exact extent of each intervention (number and length of walls, size of braces etc.).

Case study – Seismic rehabilitation of circuit house (Lal bungalow) at Jamnagar, Gujarat.

January 26, 2001 Bhuj earthquake was one of the most disastrous earthquakes in India predominantly affecting the urban setting. This particular part of India had a very large number of small kingdoms and hence, the affected area is rich in cultural and heritage structures. Numerous such structures sustained heavy damages during the earthquake. A major challenge is to resolve the conflict between being conservative in demolishing many such damaged buildings considering them unsafe and salvaging maximum possible heritage. There have been number of retrofitting schemes and strategies suggested by experts from all over the world, a few of which have been successfully implemented. One such case study is circuit house at Jamnagar, which is a prestigious landmark structure with Roman architecture. The external and internal walls were damaged and then immediately stitched as shown in Figure 15 to aggravate the further damage.

The structure had jack arch flooring as shown in Figure 16, which got extensively damaged and later in the retrofit scheme were replaced with RC slab to reduce dead weight.

The suggested retrofit measures is implemented which comprises of the following:

- Making available most appropriate and effective load paths to the structure (It is done by providing steel framing system as an alternate loading frame system in addition to the exiting load bearing walls)
- Controlling the dead weight of the structures by replacing jack arch floors with RC slabs



Figure 17. Seismically rehabilitated circuit house with its past glory.

- Improving geometry of the structure by introducing framing for walls, openings and making them compatible with appropriate stiffness and integral connections
- Several arches over doors and windows were strengthened by providing steel arches below the existing ones
- Grouting and stitching of cracks
- Jacketing of walls with welded wire mesh, MS flats and chicken mesh from both sides
- Corner stiffening of walls with MS flats, lintel bands over openings.

The Figure 17 above shows the completely rehabilitated structure. Collapsed towers of the circuit house got improved with matching brickwork profile with crushed stones and polymer mortar. Artists who excel in the particular artwork used during the historical time were called to specially prepare the towers. The entire structure was plastered with suitable matching finish.

7 PROSPECTS: EXPERIMENTATION, INSTRUMENTATION AND MONITORING

The seismic rehabilitation of buildings is mainly based on assumptions and on mechanical properties, which are derived from an extensive experimentation performed mainly in laboratories. However, for heritage structures this is not the case, these structures do not lend themselves to laboratory experimentation except the behaviour of simplest forms such as arches, columns and walls. Most experimentation must be carried out directly on actual buildings.

Nowadays, several techniques have been developed for *in situ* measurements of structural properties. These techniques are reliable and non-destructive, or only slightly destructive, like sonic tomography, thermography, endoscopy, rebound tests, core sampling etc. The flat jack technique is also coming up as a powerful tool for determining Young modulus and the state of stresses on the structure.

Additionally, sophisticated techniques for monitoring the behaviour of heritage buildings in terms of displacements, settlements, out-of-plumb and crack openings are to be implemented in the structures at risk. In some of the countries, they are complimented by automatic data acquisition systems, which can be set to give alert signals when the response level exceeds a selected threshold. Instrumentation and monitoring of heritage buildings for the determination of seismic response is the future prospect and would be extremely useful for reducing associated risks.

One technique that is increasingly being used in high-rise buildings and that can give significant information also for heritage structures is the ambient vibration test. High-sensitivity accelerographs/seismographs are placed in different setups on critical points of the structure, to measure the vibration caused by traffic, wind or micro tremors. Averages of a large number of measurements over a period of time are used to obtain general trends, while eliminating noise and effects of specific inputs. By spectral analysis of the signals, natural frequencies of vibration and mode shapes can be determined, along with correlations between vibrations of different parts of the structure.

When these measurements are repeated after several years or after a significant earthquake occurred, changes in dynamic properties can be detected, which can be consequences of damage or of degradation of the structure. Ambient vibration measurements must be interpreted with great care when used to assess the structural response to actual earthquakes. The amplitudes of motions and the levels of stresses imposed by ambient vibration are so small that the structural behaviour remains essentially linear elastic and the effect of yielding and discontinuities in the structure is not completely reflected.

Much more representative of the earthquake response are the records obtained by permanent networks of accelerographs placed in the structure to measure its response to actual earthquakes. For this, first of all, one has to instrument the heritage structures in sufficient numbers so as to derive general conclusions about the earthquake response of typical heritage structures.

India is the ideal place to carry out seismic instrumentation of heritage buildings since more than 55% area could be subjected to damaging earthquake intensities. Also a variety of cultural heritage buildings made up of stone masonry, terracotta, bricks and rocks of different periods are available. The average return period of earthquake of magnitude more than 5 is less than two months in whole of India. The existence of a large network of ground motion instruments provides useful reference for the interpretation of the results.

Strong motion accelerographs are being installed in Indian cities nowadays and we have one such array in Delhi, the capital city of India. These are normally installed in the free-field or at the basement of modern buildings. There is need to put a few of them in heritage structures so that the difference in the motion recorded at the base of the structure and the free-field can be obtained. These results are important for the estimation of the maximum acceleration that can be induced by severe earthquakes.

8 CONCLUSIONS

Earthquakes have been the predominant cause of devastation of our rich heritage. For centuries, these structures have periodically suffered strong seismic actions and have undergone a kind of natural selection, so that only those that were well designed and constructed have survived. The paper reviews the critical modes of failures commonly encountered during past earthquakes.

As regards, the seismic rehabilitation, the concept of *preserve* and *reveal* the aesthetic and historical values of the structures shall have to be kept in mind in addition to the safety. Original structural system should in principle be kept unchanged. At most, only local improvement of the original structural system should be accepted. The original materials and authentic documents are to be respected. This imposes on the specialists responsible for rehabilitation, a duty, to consider what limitations these considerations place on the choice of techniques and materials of repair and strengthening. The thorough knowledge of the properties of the original materials used is prerequisite so that the compatibility of the new materials used for rehabilitation with the original ones can be ensured along with long term durability.

There are number of non-linear analytical design tools are available for seismic evaluation and retrofitting of existing structures, even then many structures are evaluated using relatively simple force-based methods that have little or no explicit consideration of realistic displacement demands from ground motion, displacement compatibility among dissimilar elements, non-linear response, failure modes etc. There is need to bench mark these procedures so that results obtained are reliable, consistent.

Code specified values of seismic coefficients and response spectra cannot be simply extended to heritage buildings while deciding the seismic action on these structures. The characteristics of the ground motion expected at the site must be taken into account and site-specific response spectra are to be generated. Particular attention is required for the heritage buildings founded on very soft or liquefiable soils.

Despite of advances in the field of modeling, experimentation and understanding the subject of seismic rehabilitation, published guideline and standards, engineer must continue to temper their decisions with experience and judgement, primarily based on past experiences of failures of real structures under earthquake loading.

Seismic rehabilitation of heritage structures is a highly specialized operation and requires close cooperation of experts of archaeology, architecture, surveying, structural engineering, geo-technical engineering and chemical engineering and should be supported by computation methods and well-equipped laboratories.

ACKNOWLEDGEMENTS

The author is grateful to Shri V.K. Mathur, Director, CBRI for granting permission to write the paper. I am indeed indebted to Dr. Paulo B. Lurenco, Portugal, Dr. Claudio Modena, Italy and Dr. Pere Roca, Spain for giving me such an opportunity and sharing the expert knowledge on the subject. The information gathered from web sites such as www.nicee.org, www.eeri.org, www.asi.nic.in, www.intach.org, www.gsdma.org is gratefully acknowledged.

REFERENCES

1986. Guidelines for earthquake resistant non-engineered construction, *The International Association for Earthquake Engineering*, Japan.
 1992. *Indian monument through ages*, Oxford & IBH Publishing Co. Pvt. Ltd., New Delhi, India.
 1999. Vulnerability Atlas of India, *Building Materials & Technology Promotion Council*, New Delhi, India.

2000. Jabalpur Earthquake 22 May, 1997, A geoscientific study, *GSI Spl. Pub. No. 51, Geological Survey of India, July, 2000*, India.
 2001. Bhuj, India Earthquake Reconnaissance Report, 2002 *Earthquake Spectra, July, 2002*, Supplement A to Volume 18.
 2002. Investigation of Earthquake Resistance of Multi-storeyed Buildings and Recommending Seismic Retrofitting Measures, *CBRI Report, Roorkee*, India.
 Abrams, D.P. & Costley, A.C. 1996. Seismic evaluation on unreinforced masonry buildings, *Eleventh World Conference on Earthquake Engineering, Acapulco, Mexico, June 23–28*, paper no 976.
 Agrawal, S.K. 2000. Strong motion array as response of layered elastic medium, *Ph.D. thesis, Department of Earthquake Engineering, Indian Institute of Technology, Roorkee*, India.
 Agrawal, S.K. 2000. Force Centre: A New Concept in SMA Data Analysis, *ASC 2000, Symposium on Seismology, Earthquake Hazard Assessment and Earth Interior Related Topics, October 10–12, 2000*, Tehran.
 Agrawal, S.K., Chourasia, Ajay & Parashar Jalaj 2001. System Identification of Eight Storied Steel Framed Structure, *Advances in Structural Dynamics and Design (ASDD), January 9–11, 2001, SERC, Madras*, India.
 Agrawal, S.K., Chourasia, Ajay, Parashar Jalaj, & Dutta, Jayanta 2001. Experimental Investigations on Earthquake Resistance and Retrofitting Measures of Masonry Houses – A Review, *International Conference on Civil Engineering (ICCE – 2001), 23–25 July, 2001, Indian Institute of Science, Bangalore*, India
 Agrawal, S.K. & Vipul Prakash 2001. An Engineering Approach for Earthquake Source Modelling, *International Conference on Seismic Hazard with particular reference to Bhuj Earthquake of January 26, 2001, 3–5 October, 2001, New Delhi, Govt. of India, Deptt. Of Science & Technology, India Meteorological Deptt, India*.
 Agrawal, S.K. & Chourasia, Ajay, 2002. Seismic safety aspects for historical monuments, *Strategy & methodology for conservation of heritage buildings & monuments in India, CBRI, Roorkee, April 4–5*, India.
 Agrawal, S.K., Chourasia, Ajay & Parashar, J. 2002. Seismic Evaluation & Retrofitting of Existing Building – A Case Study, *Proc. of 12th Symposium on Earthquake Engineering, Indian Institute of Technology, Roorkee*, India.
 Agrawal, S.K., Chourasia, Ajay, Parashar, J & Dutta, J. 2002. Experimental Investigation on Earthquake Resistance and Retrofitting Measures of Masonry Houses, *Advances in Concrete & Construction Technology, Publication –3, Interline Publishing, Bangalore*, India
 Agrawal, S.K., Chourasia, Ajay 2003. A pragmatic approach for Seismic Risk reduction of Megacities in India, *Indian Habitat & Infrastructure – need for innovative approach, 24–26 September, CBRI, Roorkee*, India.
 Agrawal, S.K. & Chourasia, Ajay 2003. Rehabilitation of RCC Structures – How Far From Reality, *Int. Conf. on 'Innovative World of Concrete 2003, Indian Concrete Institute, Pune, September, 2003*, India.
 Agrawal, S.K., Chourasia, Ajay & Parashar, J. 2003. Seismic Vulnerability of Jabalpur Urban Area, *Department of Science & Technology Report, Govt. of India*, India.

- Agrawal, S.K., Chourasia, Ajay 2004. Estimation of Seismic Vulnerability of Buildings in Delhi, *World Congress on Natural Disaster Mitigation, Institution of Engineers (India), New Delhi, India*, Vol. 2, 159–171.
- ATC-21 1988. Rapid Visual Screening of Buildings for Potential Seismic Hazards: A Handbook, *Applied Technology Council, Redwood city, CA, USA*.
- ATC-28 1991. Development of Recommended Guidelines for Seismic Strengthening of Buildings Phase: Issue Identification and Resolution, *Applied Technology Council, Redwood city, CA, USA*.
- ATC-40 1996. Seismic Evaluation and Retrofit of Concrete Buildings – Vol. I & II, *Applied Technology Council, California Seismic Safety Commission, Redwood city, California*.
- FEMA-172 1992. NEHRP Handbook for the Seismic Rehabilitation of Existing Buildings, *Federal Emergency Management Agency, Building Seismic Safety Council, Washington, D.C.*
- FEMA-178 1992. NEHRP Handbook for the Seismic Evaluation of Existing Buildings, *Federal Emergency Management Agency, Building Seismic Safety Council, Washington, D.C.*
- Gavarini, C. & Bruno S. 1996. Towards a complex approach to preservation and seismic protection of monuments, *Eleventh World Conference on Earthquake Engineering*, paper no. 2088.
- Giuffre, A. & Carocci, C. 1996. Vulnerability and mitigation in historical centers in seismic areas – criteria for the formulation of a practice code, *Eleventh World Conference on Earthquake Engineering*, paper no. 2086.
- Holmes, W.T. 2000. Risk Assessment & Retrofit of Existing Buildings, *Twelfth World Conference on Earthquake Engineering*, paper no. 2826.
- IS-456 2000. Plain and Reinforced Concrete – Code of Practice, *Bureau of Indian Standards, New Delhi, India*.
- IS-1893 2002. Criteria for Earthquake Resistant Design of Structures, Part-1: General Provisions and Buildings, *Bureau of Indian Standards, New Delhi, India*.
- IS-13920 1993. Ductility Detailing of Reinforced Concrete Structures Subjected to Seismic Forces – Code of Practice, *Bureau of Indian Standards, New Delhi, India*.
- IS-13935 1993. Repair and Strengthening of Buildings – Guidelines, *Bureau of Indian Standards, New Delhi, India*.
- Jain, S.K., Murty, C.V.R., Dayal, U., Arlekar, J.N. & Chaubey, S.K., 2001. A Field Report on Structural and Geotechnical Damages Sustained During the 26th January, 2001 M7.9 Bhuj Earthquake in Western India, *NICEE Report, Kanpur, India*.
- Mathur, V.K. & Agrawal, S.K. 2001. Safety and Security of Tall Buildings in India, *CTBUH London Conference, Council on Tall Buildings in Urban Habitat, December, 2001, London*.
- Mathur, V.K., Agrawal, S.K. & Chourasia, Ajay 2003. Demand-Capacity Approach for Seismic Rehabilitation of RC Residential Buildings, *9th International Conference on Civil & Structural Engineering Computing (CIVIL-COMP 2003), Heriot Watt University, Edinburgh, UK*.
- Mathur, V.K., Agrawal, S.K. & Chourasia, Ajay 2004. Microzonation Studies as impacted by recent earthquake in India, *World Congress on Natural Disaster Mitigation, Institution of Engineers (India), New Delhi*, Vol. 2, 81–91.
- Meli, R. & Ramirez, R.S. 1996. Considerations on the seismic safety of historical monuments, *Eleventh World Conference on Earthquake Engineering*, paper no. 2087.
- Murty, C.V.R. 2002. Quantitative Approach to Seismic Strengthening of RC Frame Buildings, *Proc. on Seismic Assessment and Retrofitting of Buildings, Indian Institute of Technology, Mumbai, India*.
- Penelis, G. Gr., 1996. Techniques & materials for structural restoration, *Eleventh World Conference on Earthquake Engineering*, paper no. 2089.
- SP-22, 1982. Explanatory Handbook on Codes for Earthquake Engineering, *Bureau of Indian Standards, New Delhi, India*.

Research for seismic redesign of historic masonry buildings

M. Tomažević

Slovenian National Building and Civil Engineering Institute, Ljubljana, Slovenia

ABSTRACT: Historic masonry buildings have been built on the basis of tradition and experience without taking into consideration specific rules for earthquake resistance. On the basis of the analysis of earthquake damage observations, the main causes of damage are determined and adequate measures to improve the seismic behavior developed. In order to assess the seismic resistance, mechanical properties of masonry materials should be determined by appropriate testing methods. Experimental research is needed to evaluate the observed mechanisms and propose numerical models for seismic resistance verification. Experimental research and testing is also needed to provide information regarding the efficiency of measures and technologies developed to improve the seismic resistance and obtain the data needed for seismic redesign. Experiences obtained at Slovenian National Building and Civil Engineering Institute in Ljubljana are discussed as an example.

1 INTRODUCTION

Historic masonry buildings have been built on the basis of tradition and experience. Only rarely some specific measures for earthquake resistance have been provided at the time of construction, such as the tying of the walls with iron ties and/or using connecting stones and cut stones in the corners and wall intersections to prevent separation and disintegration of walls in the case of stone-masonry buildings. Considering the response to earthquakes, the behavior of historic masonry buildings was generally not adequate. Therefore, in the cases of reconstruction of earthquake-damaged areas or seismic rehabilitation of historic urban and rural nuclei campaigns, seismic strengthening measures should be provided in most cases.

After several decades of experience, practice and research, rules and procedures have been developed which need to be considered in the redesign. They comprises seismic assessment of existing structures, deciding upon technical solutions to be used to improve the resistance, redesign to verify the efficiency of the selected measures, as well as execution of works. The decisions should be taken by considering many criteria, among them criteria for preservation and restoration of historical monuments which represent a specific case. General guidelines and recommendations are given in Eurocode 8-1-4: General rules – strengthening and repair of buildings (new draft of the document is under development).

Historic masonry buildings reflect the knowledge and construction technology of the time of their construction. Whereas in the case of the new buildings, material properties and structural characteristics are specified by the design, in the case of historic buildings the material properties and structural characteristics need to be determined on actual materials before redesign. Therefore, testing and experimental research is the only tool:

- To obtain reliable quantified data needed for structural assessment, such as the values of mechanical properties of materials, data about homogeneity and structural conditions, moisture, etc.;
- To understand the seismic behavior of buildings and develop numerical models needed for structural verification and redesign;
- To verify the efficiency of methods and technologies developed for strengthening and repair.

In this contribution, some experiences obtained at Slovenian National Building and Civil Engineering Institute (ZAG) in Ljubljana, Slovenia, regarding the testing and research in seismic behavior of historic masonry buildings, will be presented and discussed. Following the conclusions made on the basis of the analysis of earthquake damage observations, some basic test results and recommendations for their use in seismic redesign will be given. Some experiments to verify the most widely used strengthening techniques will be also presented.

2 MECHANICAL PROPERTIES, STRUCTURAL CONDITIONS AND RESISTANCE TO SEISMIC LOADS

In order to choose the appropriate technical interventions and ensure adequate seismic performance of historic buildings, the carrying out of a thorough structural diagnosis is unavoidable. The type of structural system and its elements should be identified and actual situation regarding the quality of structural materials should be verified. Information about the mechanical characteristics of structural materials should be obtained and quantitatively evaluated. In this regard, investigations and tests are unavoidable. Although sometimes costly and time consuming, they represent the only means to obtain reliable data for structural evaluation and subsequent redesign.

Many testing methods are available to obtain the relevant information, ranging from non-destructive, semi-destructive to destructive methods. However, by non-destructive testing, such as impact echo and radar tests, micro seismic wave propagation measurements etc., only qualitative data regarding the general structure of masonry walls (such as composition of layers and amount of voids) and possible existing damage can be obtained. Non-destructive tests are helpful in order to identify the general, qualitative situation of the building under consideration.

Semi-destructive tests such as flat-jack tests provide information regarding the stress state in the walls as well as strength of the masonry. However, systematic calibration tests still need to be carried out in order to quantify the obtained information in terms of mechanical properties of masonry needed in structural verification.

Unfortunately only by means of laboratory and/or in-situ destructive testing, some basic parameters, which determine the seismic behavior of historic masonry walls and structures, can be obtained. Within the framework of the research project named ONSITEFORMASONRY, a joint effort of 16 European universities, research institutions and companies has been recently made to study the possibilities of these methods and propose respective guidelines and recommendations.

2.1 Testing

Stone, mixed stone-and-brick and sometimes brick-masonry are the most common materials used for the construction of historic buildings, with lime mortar as the bonding material. Stone-masonry walls are usually built of two outer layers of uncoursed stone, with an inside infill consisting of a mix of smaller stones with lime mortar. Because of the method of construction of stone-masonry, many voids exist in the walls, uniformly distributed over the entire volume.

Since masonry is non-elastic, non-homogeneous and unisotropic structural material, the values of sectional forces and material properties are determined based on the gross-sectional geometrical characteristics and assuming the elastic, homogeneous and isotropic global properties, hence simplifying the analysis and redesign. The following mechanical quantities determine the load-bearing capacity and deformability of masonry walls:

- the compressive strength of masonry, f_c ,
- the tensile strength of masonry, f_t ,
- the modulus of elasticity, E ,
- the shear modulus, G .

Whereas compressive strength and modulus of elasticity define the load-bearing capacity of masonry walls at gravity loads, the tensile strength and shear modulus define the load-bearing capacity at seismic loads. In the latter case, however, information regarding the ductility and energy dissipation capacity, as well as strength and stiffness degradation and deterioration is also of relevant importance.

Because of specific characteristics of historic masonry it is not possible to determine the mechanical properties of masonry on the basis of tests of their constituent materials, such as bricks, stone and mortar, in the laboratory. In order to obtain reliable information from such tests, a correlation between data, obtained on constituents and data obtained on masonry wall specimens should be previously known. It is also difficult to reproduce existing masonry walls in the laboratory, even though thorough chemical and mechanical tests of the mortar and other constituent materials may have been carried out. The testing of specimens, cut out from the existing walls and tested in the laboratory (Fig. 1) and in-situ testing of the existing walls in the building (Fig. 2) is therefore preferred to testing of the laboratory constructed specimens (Fig. 3).

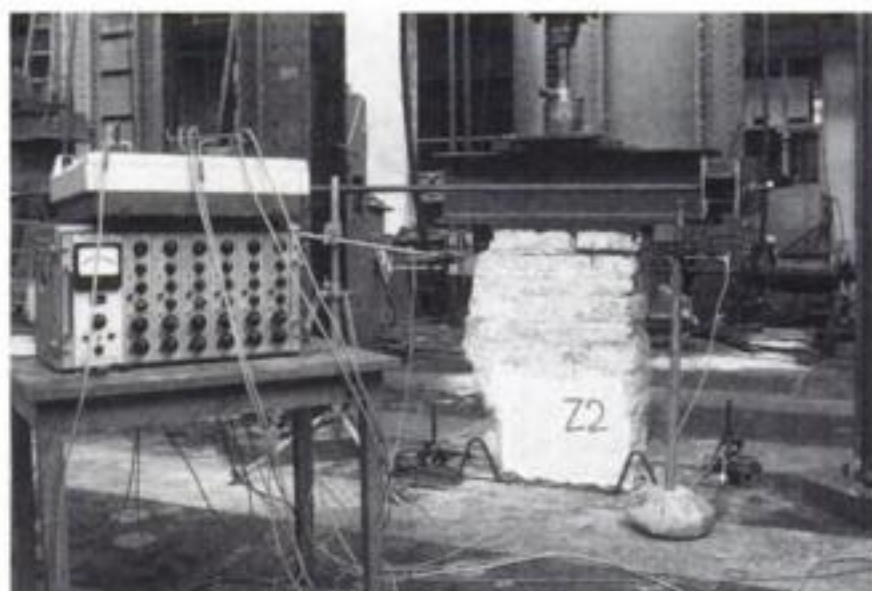


Figure 1. Lateral resistance test of a brick-masonry specimen, cut from the building, in the laboratory.

Standardized testing procedures are used in the case of vertical compression tests. In the case of lateral resistance tests, however, the seismic situation of loading is simulated by subjecting the specimens to constant vertical load, whereas the horizontal loads are applied cyclically, acting either in both or in one direction only.

In the laboratory conditions, vertical and horizontal loads are applied by means of hydraulic actuators. The

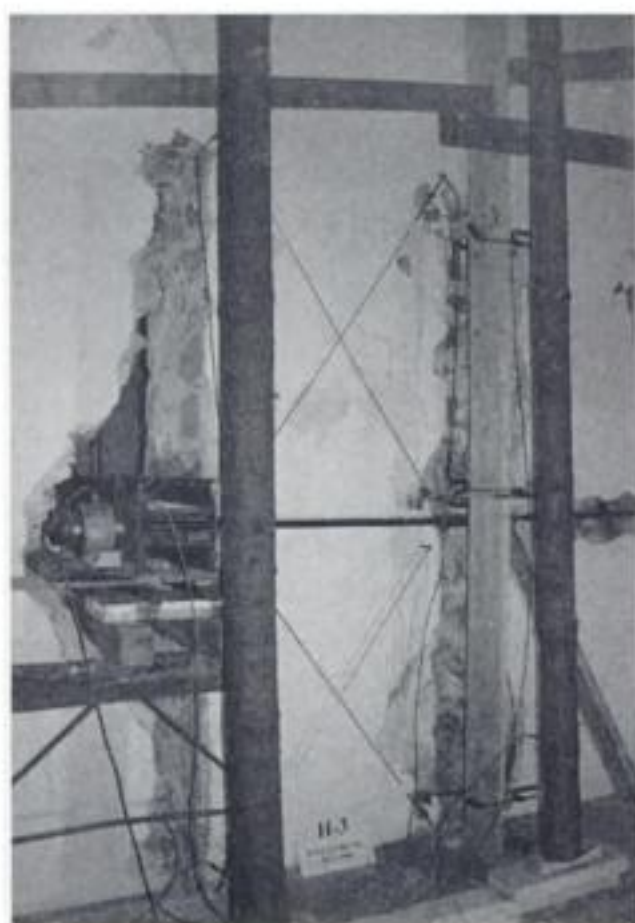


Figure 2. In-situ lateral resistance test of a stone-masonry wall.



Figure 3. Laboratory lateral resistance test of a laboratory constructed stone-masonry wall.

vertical load to simulate the working stress state in the wall is kept constant, whereas the horizontal load in the form of induced displacements is applied according to an appropriate pattern which simulates the cyclic character of seismic loading. Since the removing of specimens of adequate size from the building and their transport to the laboratory is usually a time consuming and costly procedure, the tests on the existing masonry are carried out on the site. At an appropriate location in the building, the specimen to be tested is separated from the surrounding masonry by vertical cuts on both sides. In order to prevent accidental collapse of the floor in the case of collapse of the specimen, the floor structure is supported with posts. A system of steel connectors and hydraulic jacks is provided to induce lateral loads.

2.2 Mechanical properties of masonry

In accordance with the principles of Eurocodes, characteristic values of strength of materials, reduced by partial safety factor for masonry materials γ_M , are used in seismic resistance verification. In accordance with standard EN 1052-1, which determines the testing of compressive strength of masonry, three specimens are tested and the mean value of compressive strength f evaluated. The characteristic compressive strength of masonry f_k is determined as the smaller value of either $f/1.2$, or the minimum obtained value f_{min} :

$$f_k = \min (f/1.2; f_{min}). \quad (1)$$

Although the testing procedures are not standardized, it is proposed that the same principle is also used for the evaluation of characteristic values of either compressive or tensile strength obtained from the laboratory or in-situ tests carried out on existing masonry walls. Since such tests are expensive, rarely more than two specimens of the same masonry type are tested. It is therefore also proposed, that either the average value of two test results or a single result, reduced by 1.2, be considered as the characteristic value.

Typical characteristic values of material properties for different types of existing stone-masonry walls, tested by Slovenian National Building and Civil Engineering Institute, are given in Tables 1 and 2 (Turnšek et al. 1978, Sheppard & Tomažević 1986, Tomažević et al. 2000).

According to Eurocodes, the values of partial safety factors for masonry γ_M are determined in dependence on the category of execution and manufacturing control. The values for the new construction in non-seismic situation vary from $\gamma_M = 1.5$ to $\gamma_M = 3.0$. In seismic situation, however, it is recommended that 2/3 of the usual values, but not less than $\gamma_M = 1.5$ are taken into account. Nevertheless, since in the case of the existing structures material properties are determined

by in-situ testing of actual materials, the γ_M values, as required for the new construction, can be further reduced. This is also suggested by Eurocode 8-1-4: Strengthening and repair of buildings.

Considering the correlation between the results of earthquake resistance analyses and earthquake damage observations, carried out after the past earthquakes, and following the guidelines given in Eurocode 8-1-4, the following recommendations regarding the values of partial safety factor γ_M to be taken into account in the redesign of historic masonry buildings, can be proposed:

- In the case where in the given region and for a given type of masonry the mechanical properties are determined either by in-situ tests or in the laboratory by testing specimens, taken from the existing masonry, the value of partial safety factor $\gamma_M = 1.0$ can be considered in seismic resistance verification;
- In the case where the characteristic values are obtained in the literature, as for example the values given in Tables 1 and 2, and identification of a given type of masonry is carried out by removing

Table 1. Characteristic values of tensile strength f_{tk} and design values of shear modulus G of stone-masonry.

Type of masonry	f_{tk} (MPa)	G (MPa)
Two leaf, uncoursed lime stone, poor lime mortar, rural	0.02	60
Two leaf, mix of uncoursed quartz sandstone, slate and lime-stone, lime mortar, urban	0.08	100
Two leaf, mix of uncoursed quartz sandstone, slate, lime-stone and brick; lime mortar, homogeneous, urban	0.12	40
Two leaf, uncoursed lime stone, poor lime mortar, rural dwellings	0.05	80
Two leaf, uncoursed lime stone, lime mortar, public buildings	0.07	170

Table 2. Characteristic values of compressive strength f_k and design values of modulus of elasticity E of stone-masonry.

Type of masonry	f_k (MPa)	E (MPa)
Two leaf, uncoursed lime stone, poor lime mortar, rural	0.40	1950
Two leaf, mix of uncoursed quartz sandstone, slate and lime-stone, lime mortar, urban	0.28	390
Two leaf, uncoursed lime stone, poor lime mortar, rural dwellings	0.82	2600

plaster and opening the walls, the value of partial safety factor $\gamma_M = 1.2$ can be considered;

- In the case where the characteristic values are obtained in the literature, but no identification tests have been carried out, the value of partial safety factor $\gamma_M = 1.7$ should be taken into account in the seismic resistance evaluation.

Mean values of in-situ test results are taken into account as characteristic values of shear modulus G and modulus of elasticity E .

As has been found, the mechanical properties of stone-masonry strongly depend on the structure of the wall and the way of construction. It has been also found that the values vary from region to region, so that individual values are not generally applicable.

Whereas a number of data exist about the values of the tensile strength and shear modulus, not many data are available about the compressive strength and modulus of elasticity. In particular, the results of in-situ tests are missing, difficult to carry out because of relatively large forces needed to test sufficiently large specimens. As the test results indicate, the compressive strength of stone-masonry is relatively low. Since even in the existing state the walls of stone-masonry houses do not possess a normal reserve in vertical load-bearing capacity, any removal of parts of the walls in the case of enlarging the existing, or making new door and window openings, or any adding of new stories to the existing building, may cause severe problems.

2.3 Resistance to seismic loads

As the analysis of earthquake damage and subsequent experiments indicate, three types of failure modes of walls, shown in Figure 4, can be observed, depending on the geometry of the wall (height/width ratio), quality of materials as well as boundary restraints and loads acting on the wall.

Shear failure is a typical failure mode in the case of historic brick and stone masonry buildings. It takes place where the principal tensile stresses, developed in the wall under a combination of vertical and horizontal loads, exceed the tensile strength of masonry materials. Characteristic diagonal cracks develop in the wall just before the attainment of maximum resistance.

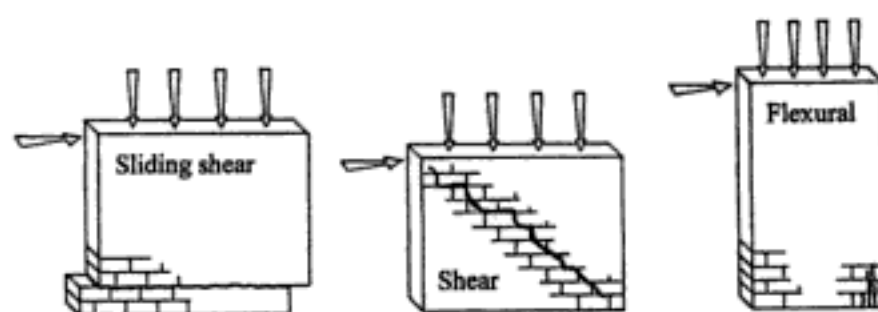


Figure 4. Typical failure modes of masonry walls, subjected to seismic loads.

For the case of the shear failure, the resistance of the walls is calculated by (Turnšek & Čačovič 1971):

$$H_{s,w} = A_w \frac{f_t}{b} \sqrt{\frac{\sigma_o}{f_t} + 1}, \quad (2)$$

where:

- $H_{s,w}$ = shear resistance of the wall,
- A_w = area of the horizontal cross section of the wall,
- σ_o = compressive stress in the wall,
- b = coefficient of distribution of shear stresses.

During the lateral resistance tests, the relationships between the cyclically acting lateral seismic load and displacements (rotation) of the wall are obtained in the form of hysteresis loops (Fig. 5). To use the information obtained by testing in the calculations, the envelope of the experimentally obtained hysteresis loops is idealized as a bilinear envelope (Fig. 6).

Three limit states are defined in the envelope:

- Crack limit, determined by displacement d_{cr} and resistance H_{cr} at the formation of the first significant cracks in the wall, which change the slope of the envelope.

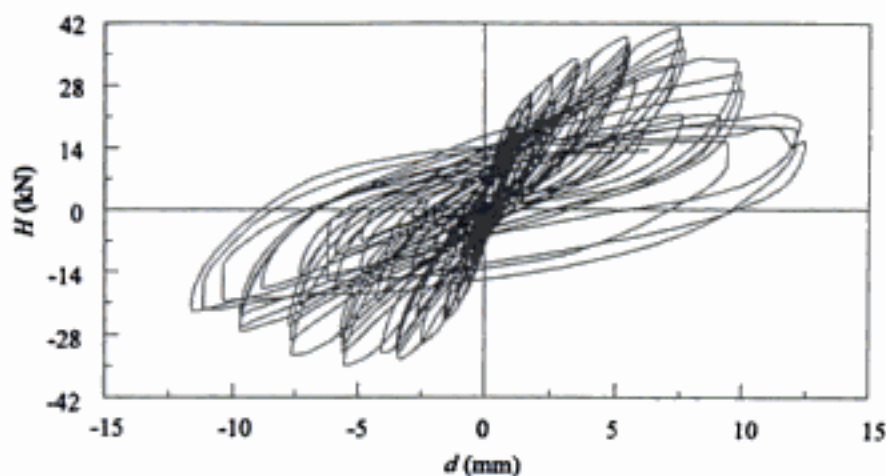


Figure 5. Typical lateral load–displacement hysteresis loops, obtained during laboratory test.

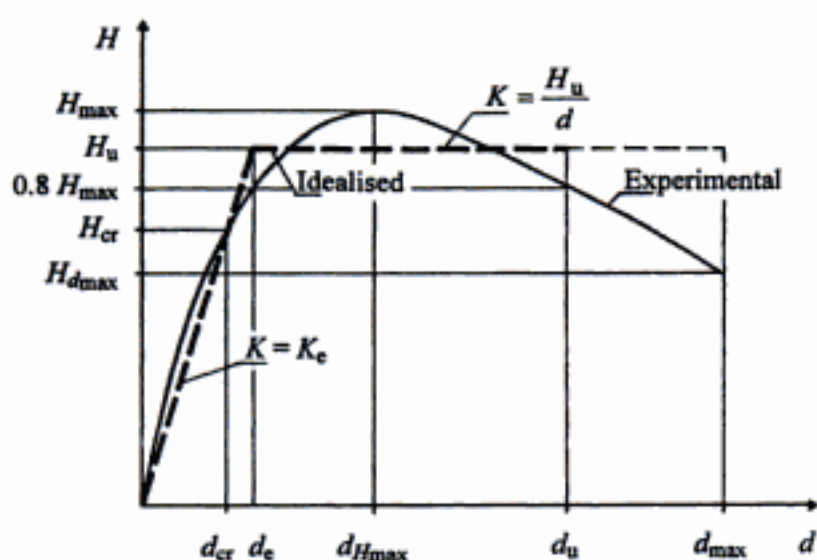


Figure 6. Idealization of experimental resistance envelope with bilinear relationship.

- Maximum resistance, determined by maximum resistance H_{max} , attained during test, and corresponding displacement $d_{H_{max}}$.
- Ultimate state, determined by maximum displacement attained during test d_{max} and corresponding resistance $H_{d_{max}}$.

Obviously, the initial slope of the idealized envelope is best defined with a secant stiffness at the formation of cracks, which is called effective stiffness of the wall $K_e = H_{cr}/d_{cr}$. Ultimate ductility factor μ_u , which defines the displacement (rotation) at which the wall does not resist any more to lateral seismic load, is defined as a ratio $\mu_u = d_u/d_e$. Usually, the displacement at which the resistance degrades to 80% of the maximum, is considered as ultimate, d_u .

3 SEISMIC BEHAVIOR AND REDUCTION OF DESIGN SEISMIC LOADS

3.1 Observations and numerical models

The analysis of damage caused by earthquakes to historic stone- and/or brick-masonry buildings in urban and rural nuclei, indicated that cracks at the corners and at wall intersections, which occur as a result of insufficient connections and lack of connection between the walls and floors, represent a characteristic damage pattern. Sometimes, separation of walls and even out-of-plane collapse occurred. Also, many times, despite the favorable structural layout of those buildings in plan and good connection of walls, the quality of masonry materials was not good enough to spare the walls from diagonal cracking, disintegration, and ultimate collapse.

Although the structural typology of masonry buildings varies in different regions, their damage resulting from earthquakes can be classified in an uniform way. The following typical types of damage can be identified by the analysis of the observed earthquake damage patterns:

- Cracks between walls and floors;
- Cracks at the corners and at wall intersections;
- Out-of-plane collapse of perimetral walls;
- Cracks in spandrel beams and/or parapets;
- Diagonal cracks in structural walls;
- Partial disintegration or collapse of structural walls;
- Partial or complete collapse of the building.

The analysis of damage patterns can clearly identify the weak and good points of different structural systems. On the basis of damage analysis, the failure mechanisms of individual structural walls and the entire structural system can be defined. On the basis of the observed mechanism, forces that develop in the structural system during earthquakes can be determined. On the basis of such analysis, causes of



Figure 7. Typical shear cracks in the walls of a historic stone-masonry house.

inadequate behavior can also be identified and subsequent measures for the improved seismic resistance proposed. The following typical causes of damage to masonry buildings may be identified:

- Inadequate structural integrity;
- Inadequate structural resistance;
- Inadequate structural layout, and
- Inadequate foundation system.

As a result of structural configuration and quality of masonry materials, typical observed damage patterns indicate that shear mechanism prevails in the case where historic buildings are subjected to seismic actions (Fig. 7).

Shear mechanism, which has been also observed by testing the models of historic masonry buildings on the shaking table (Fig. 8), is schematically presented in Figure 9.

Typically, unreinforced masonry walls, which fail in shear, are weaker than spandrels. Since the flexural capacity of the walls' bottom and upper sections is too low to allow the transfer of the bending moments to horizontal elements, i.e. lintels and spandrels, the individual walls can be considered as symmetrically fixed at both ends, what simplifies the calculations to a great degree. However, the assumption of rigid floor diaphragm action should be fulfilled in order to obtain reliable results as regards the distribution of loads and seismic resistance.

Different numerical models are used to calculate the seismic resistance of historic masonry buildings. The behavior of complex structures is modeled by means of kinematic and finite element models. However, in the case of regular historic buildings where the shear mechanism determines the behavior and resistance, good estimate of seismic resistance can be made by a relatively simple calculations (Tomažević et al. 1978, Tomažević 1997).

In the latter case, the resistance envelope of the critical story is obtained as a superposition of



Figure 8. Stone-masonry house model at collapse during laboratory shaking table test.

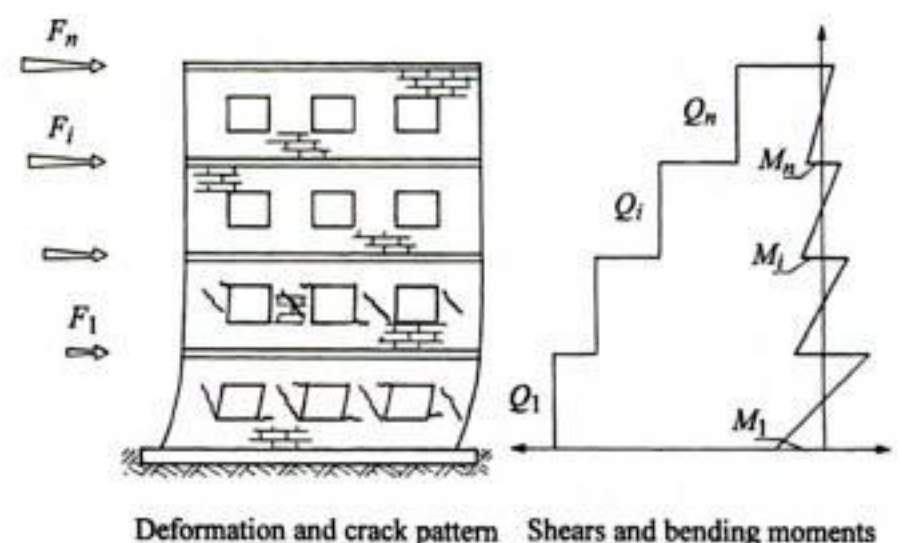


Figure 9. Shear mechanism: coupled shear wall with weak piers.

resistance envelopes of individual walls which compose that story. A push-over type method has been developed for the calculation of story resistance envelope. It is assumed that individual walls resist the imposed displacement up to the attainment of their ductility capacity. Ultimately, it is also assumed that they carry the vertical loads although they fail for lateral loads. The procedure is schematically presented in Figure 10 and validated with experimental results in Figure 11.

3.2 Reduction of design seismic loads

Seismic resistance of a historic building is the basic criterion for the decision whether the building should be strengthened or not. In the case where the seismic resistance verification indicates that the building

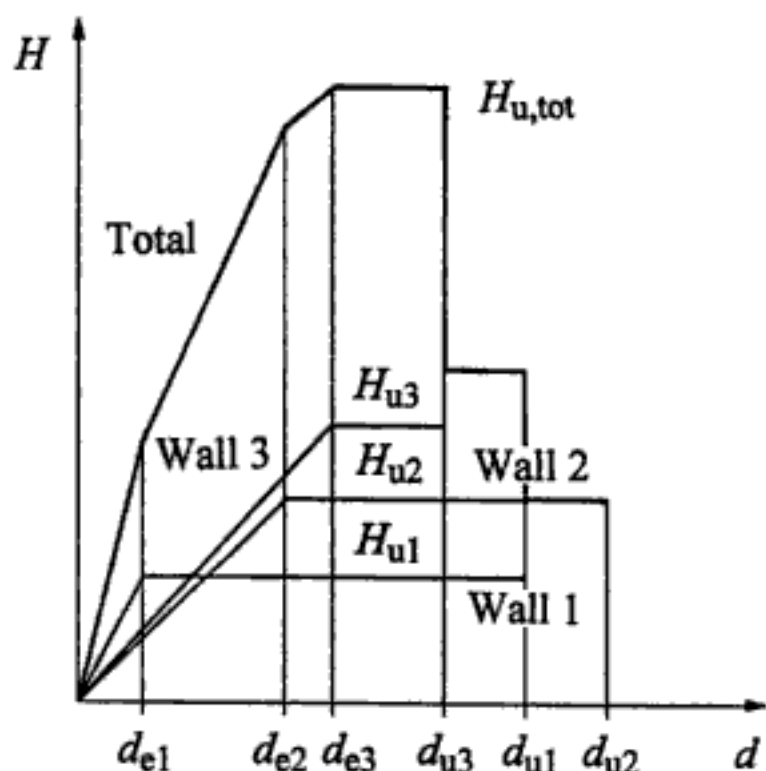


Figure 10. Construction of story resistance envelope on the basis of bilinear resistance envelopes of walls.

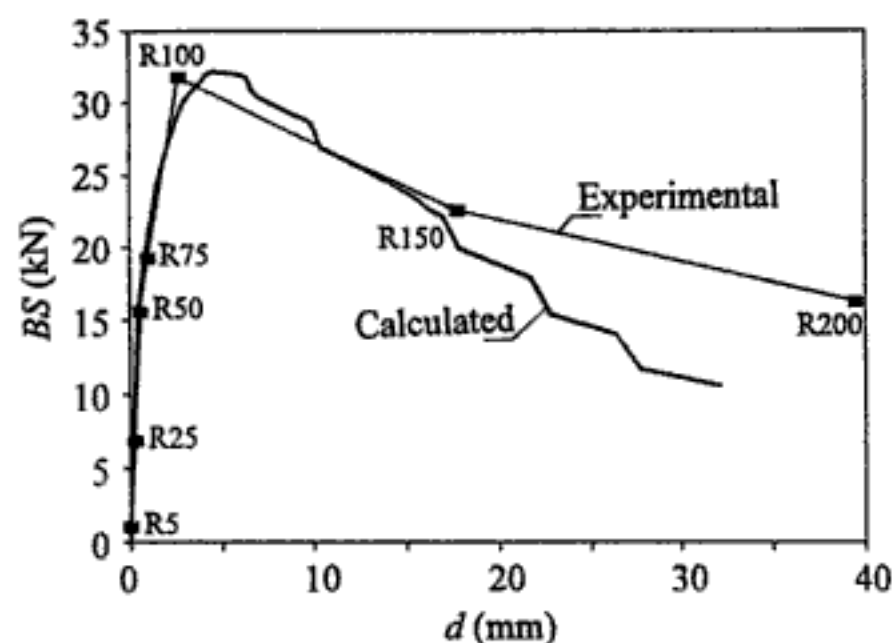


Figure 11. Correlation between experimental and calculated story resistance envelopes.

under consideration will not resist the expected seismic loads with an acceptable degree of damage, the building needs structural strengthening. By using adequate mathematical models, the weak elements of the structure where the strengthening is needed, can be identified.

Normally, the same level of design seismic loads should be considered in the redesign of historic buildings as in the case of the new construction. According to Eurocode 8, the design seismic load in terms of the ultimate design base shear coefficient $BSC_{d,u}$, i.e. the ratio between the design seismic load and weight of the building, is determined by:

$$BSC_{d,u} = \frac{a_g S \eta 2.5}{q}, \quad (3)$$

Table 3. Code ($BSC_{d,u}$) and proposed reduced values of ultimate design base shear coefficient ($BSC_{d,ur}$).

EMS intensity	VI	VII	VIII	IX
a_g	0.05	0.10	0.20	0.30
$BSC_{d,u}$	0.08	0.17	0.33	0.50
γ_n	1.00	1.00	0.84	0.67
$BSC_{d,ur}$	0.08	0.17	0.25	0.33

where:

a_g = seismicity depending design ground acceleration,
 S = soil factor,
 η = damping correction factor,
 q = structural behavior factor.

The resulting values of $BSC_{d,u}$ for different expected intensities of earthquakes (seismic zones) and firm soil are given in Table 3.

As the analyses and observations after earthquakes indicate, structural strengthening of historic masonry buildings is needed in most cases. Whereas the tying of the walls should be provided in every case, the experiences show that the strengthening of stone-masonry walls by cement-grouting is unavoidable in the zones of moderate and high seismicity, whereas in the zones of low seismicity, the decision whether the stone-and/or brick-masonry walls need to be strengthened or not, depends on the quality of existing masonry.

As the experience indicated, by applying the usual technical measures to historic masonry buildings, the values of the coefficient of seismic resistance CSR_u , i.e. the ratio between the ultimate resistance H_u and the weight of the building W , greater than 0.3 are difficult to attain, particularly in the case of buildings higher than 3 stories. It would be practically impossible to attain the resistance required for the new construction without adding new structural elements. On the other hand, however, there were many cases observed where even stone-masonry buildings resisted the earthquakes, although the calculated values of $CSR_{d,u}$ were lower than required for the given seismic zone.

According to Eurocode 8-1-4, the design ground acceleration may be reduced in the case where the anticipated total costs of strengthening the entire building inventory of particular urban areas would sharply increase if a_g values would be raised towards the code required level, as well as where code required a_g values for redesign of a monument would lead to completely unacceptable architectural alterations.

Taking into account the recommendations given in Eurocode 8-1-4, it is proposed that, for practical redesign of existing stone-masonry buildings in urban areas, maximum allowable reduction, i.e. reduction factor $\gamma_n = 0.67$ is used in the zone IX. Since there is no reduction proposed for the zones VII and lower,

Table 4. Seismic resistance of typical existing ($f_t = 0.06$ MPa) and strengthened ($f_t = 0.11$ MPa) 2-story stone-masonry houses in terms of coefficient of seismic resistance ($CSR_u = H_u/W$) in x- and y-directions.

Bldg. no.	Wall/floor area (%)		Existing building		Strengthened building	
	x-dir	y-dir	x-dir	y-dir	x-dir	y-dir
1*	12.0	9.1	0.21	0.19	0.25	0.25
2*	10.9	6.4	0.20	0.15	0.27	0.22
3	6.9	8.6	0.22	0.25	0.25	0.33
4	12.1	11.1	0.33	0.31	0.42	0.38
5	4.7	14.6	0.17	0.33	0.19	0.47
6	7.2	14.3	0.16	0.31	0.21	0.47
7	15.1	13.7	0.29	0.25	0.40	0.33
8	10.5	9.5	0.31	0.25	0.39	0.29
9	10.5	9.9	0.23	0.26	0.31	0.34
10	10.3	10.2	0.22	0.26	0.28	0.35
11	11.9	10.3	0.28	0.29	0.29	0.34
12	9.8	10.9	0.23	0.26	0.32	0.34
13	8.8	8.33	0.23	0.27	0.31	0.33
14	10.6	12.0	0.28	0.28	0.35	0.36
15	9.7	12.0	0.27	0.34	0.34	0.47
16	7.9	4.2	0.26	0.19	0.35	0.21

* $f_t = 0.08$ MPa for existing and 0.14 MPa for strengthened houses.

i.e. $\gamma_n = 1.00$, the value of reduction factor to be used in zone of EMS intensity VIII, $\gamma_n = 0.84$, is a linear interpolation between the values of reduction factors proposed for the zones IX and VII. The resulting reduced values of ultimate design base shear coefficient to be considered in the redesign $BSC_{d,ur}$ are also given in Table 3.

Typical results of a recent study of seismic resistance of buildings located in the zone, where intensity VIII earthquakes by EMS scale actually occurred in the time interval of 22 years, are given in Table 4 (Tomažević et al. 2000). Most of the buildings, analyzed in Table 4, have already been strengthened after the earthquake, which damaged the area in 1976. As the observations and analysis after the subsequent earthquake which occurred in 1998 indicated, the seismic behavior of strengthened buildings was adequate.

The results of this analysis confirm the possibility of reducing design seismic loads in the zones of high and moderate seismicity as proposed in Table 3, without risking inadequate seismic behavior. The behavior of historic buildings, strengthened to such level, is expected to be adequate. The buildings will not collapse, but the amount of damage will be larger than in the case of the new construction. However, the damage will still be repairable.

It should be emphasized that seismic resistance verification of historic buildings for seismic loads, given in Table 3, is only reasonable in the cases where

the integrity of structural system during earthquakes is ensured by means of the tying of the walls at floor levels. This only makes possible to utilize the available energy dissipation capacity of the structure, assumed by structural behavior factor q .

4 EXPERIMENTAL EVALUATION OF METHODS FOR STRENGTHENING AND REPAIR

As the studies of earthquake damage to historic masonry buildings indicated, the following basic requirements need to be fulfilled in order to achieve adequate seismic behavior:

- Structural integrity should be ensured, i.e. structural walls should be adequately tied and connected, and floors should be rigid enough and well anchored to the walls in order to provide uniform distribution of seismic loads onto the walls and prevent excessive out-of-plane bending;
- Structural walls should be uniformly distributed in both orthogonal directions as well as along the height of the building in order to prevent torsional and/or other phenomena;
- Structural walls should be resistant enough to resist the expected seismic loads;
- Foundation system should be capable of transferring the ultimate forces developed in the upper structure into the foundation soil.

Many methods have been developed for improving the resistance of historic buildings to meet these requirements. Not all have been experimentally verified. Different testing techniques are used for the verification of strengthening methods. In most cases, the efficiency of the proposed strengthening method can be evaluated by testing the masonry walls either in the laboratory or in-situ, using the same testing techniques as in the case of the walls in the original state.

However, to investigate the seismic behavior and mechanism of the entire buildings, models of buildings are tested on the shaking tables. The testing of models on simple seismic simulators has several advantages:

- Model tests are cheaper and simpler than prototype tests;
- Relatively simple testing facilities can be used;
- Global behavior and failure mechanisms can be reliably simulated;
- Modeling techniques can be adjusted to possibilities.

However, this testing techniques also has disadvantages, such as:

- Modeling scale is limited because of technological restrains;
- Structural details cannot be studied.

In the case of model tests, the general correlation between the prototype (P) and model (M) quantities is given by:

$$q_P = q_M S_q, \quad (4)$$

where:

q = physical quantity,
 S = scale factor.

Different modeling techniques are available (Tomažević & Velechovsky 1992). Depending on the basic correlations between the model and prototype materials, complete or simple models can be tested. If the dynamic behavior and failure mechanisms are studied, the following general requirements need to be fulfilled in the first place:

- Similitude of dynamic behavior which requires similar distribution of masses and stiffnesses along the height of prototype and model, and
- Similitude of failure mechanism which requires similar working stress/strength of material ratio in structural walls of the prototype and model.

At ZAG, the complete modeling approach is usually followed, and model materials have been developed, which conform with the requirements of this approach.

4.1 Tying of walls and interventions in floors

In order to evaluate the efficiency of steel ties and other measures, which are most commonly used to improve the integrity of historic masonry buildings, a series of shaking table tests of models of simple stone- and brick-masonry historic houses has been carried out (Tomažević et al. 1991, 1993, 1996).

To ensure the integrity of masonry structures during earthquakes, hence utilizing the available resistance of the walls, the walls are tied at floor levels with steel ties, placed on both sides of the walls and anchored at the ends on steel plates. In order to study the mechanism of action of steel ties, two series of models of typical simple historic stone- and-brick masonry houses with wooden floors have been tested on the shaking table. In each series of tests, referential models without any ties and models with tied walls have been tested. The models have been built as complete models at 1:4 scale by using either natural stone with mortar of reduced strength (Fig. 12) or model bricks, made of model mortar with composition of mix designed to meet the requirements of complete model similitude, respectively. Steel ties have been made of fully annealed wire and monitored with strain-gauges to measure the strains developed in the ties during shaking.

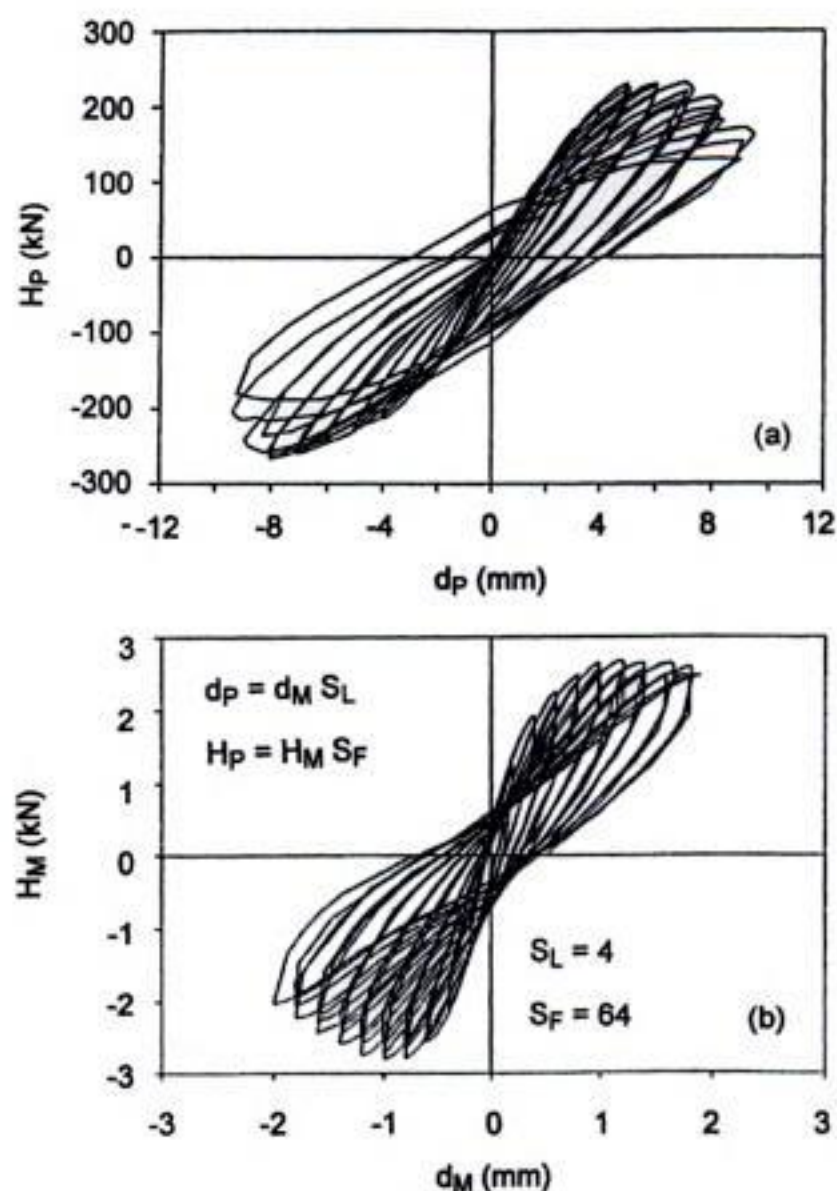


Figure 12. Hysteresis loops obtained by testing prototype (a) and model stone-masonry wall (b).



Figure 13. Brick-masonry house model without steel ties at collapse during laboratory shaking table test.

Whereas wooden floors of models without ties did not prevent the separation of the walls, excessive out-of-plane vibration and disintegration of the upper story (Fig. 13), the models with identical



Figure 14. Brick-masonry house model with steel ties at collapse during laboratory shaking table test.

structure, where the walls had been tied with steel ties, retained integrity up until the final collapse of the lower story (Fig. 14). As a result of retained integrity, the lateral load-resistance and deformability, as well as energy dissipation capacity was significantly improved.

Ties design recommendations resulted from this study. The ties of the walls, orthogonal to seismic motion and vibrating out of the plane, behaved similarly as reinforcing steel of a r.c. bond-beam made along the wall at floor level. Taking this into consideration, wall ties should be basically designed for bending moments developed in the equivalent bond-beam, formed by a strip of the wall between the ties, due to out-of-plane vibration of the wall.

On the other hand, steel ties should also be verified for forces which might develop in the critical segment of the structure in the direction of seismic motion (Fig. 15). As the shaking table tests have shown, a kind of truss mechanism develops in the structural walls in the direction of seismic loads, where the shear induced in the walls is carried over from story to story by means of tension developed in longitudinal ties. As indicated by the measurements, forces developed in the ties in the direction of seismic motion at ultimate state were of the same order of magnitude as seismic shear induced in the models.

The following formula has been proposed to calculate the minimum diameter of a steel tie:

$$D_{min} = \sqrt{\frac{H_{u,seg}}{n} \frac{4}{\pi} \frac{1}{f_y}} \quad (5)$$

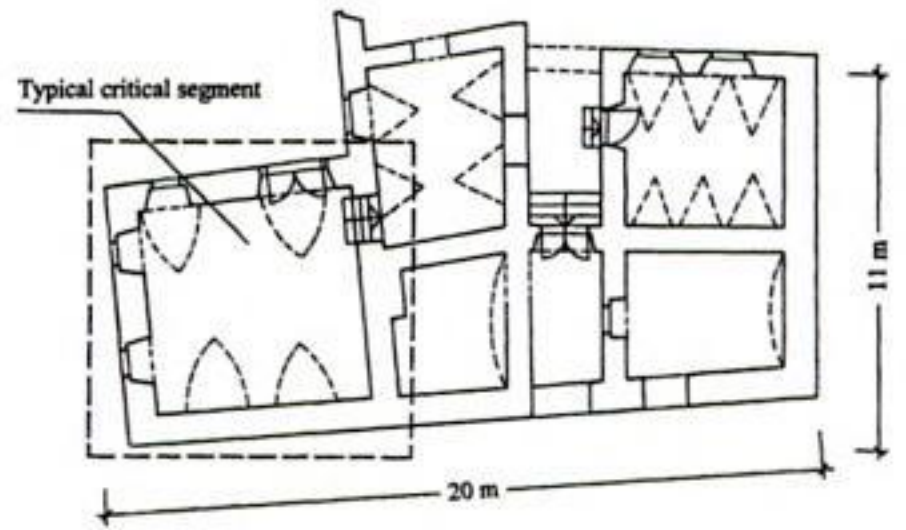


Figure 15. Critical segment of building used for the design of steel ties.

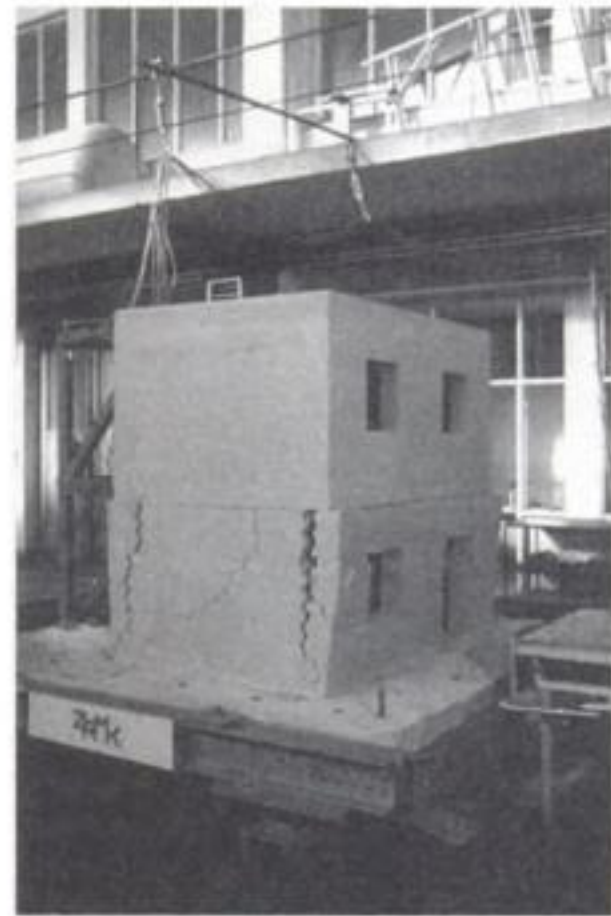


Figure 16. Sliding of the slab and pushing out of walls during brick-masonry house models with r.c. slabs shaking table test.

where:

D_{min} = minimum bar diameter,

n = number of bars,

f_y = yield strength of steel,

$H_{u,seg}$ = resistance capacity of a critical segment.

Within the same series of shaking table tests, the models where wooden floors have been replaced with rigid r.c. slabs, have been also tested. The experiments indicated, that the replacement of wooden floors with rigid slabs does not always provide the best solution. In case that the slabs are not properly anchored into the walls, they may slide on the bearing surface and cause separation and pushing out of parts of the walls (Fig. 16).

Similar phenomena have been observed in the case of stone-masonry buildings after earthquakes (Fig. 17).



Figure 17. Damage due to new r.c. slab, which pushed out parts of masonry wall.

This indicates that the slabs, which in the case of stone-masonry buildings are usually supported by the inner wythe of stone-masonry walls and are not properly anchored and/or connected with the outer wythe, may cause more damage to structural walls than what would have resulted from flexible wooden floors.

Both experimental research and on-site damage observations have indicated, that the replacement of wooden floors with r.c. slabs does not always provide the best solution.

4.2 Strengthening and repair of masonry walls

Different technical measures have been developed for strengthening and repair of masonry walls. Some of them are based on engineering judgment only and have never been actually verified. Others, however, have been verified by testing either in the laboratory or in-situ. Sometimes, the retrofitted or rehabilitated buildings have been even subjected to real earthquakes, so that the validity of some methods has been verified in the real situation. Different methodologies are available for strengthening of different types of masonry walls. Namely, the choice of the most suitable technical solution depends mainly on the type and quality of masonry, but also on the required degree of improvement.

While efficient interventions in stone-masonry are more or less limited to injecting the cementitious grout into the void parts of the walls, various possibilities are available for the repair and strengthening of brick-masonry walls.

Table 5. Characteristic values of tensile strength f_{tk} and design values of shear modulus G of cement-grouted stone-masonry walls.

Type of masonry	f_{tk} (MPa)	G (MPa)
Two leaf, uncoursed lime stone, poor lime mortar, rural	0.06	100
Two leaf, mix of uncoursed quartz sandstone, slate and lime-stone, lime mortar, urban	0.12	100
Two leaf, mix of uncoursed quartz sandstone, slate, lime-stone and brick; lime mortar, homogeneous, urban	0.16	450
Two leaf, uncoursed lime stone, poor lime mortar, rural dwellings	0.09	170
Two leaf, uncoursed lime stone, lime mortar, public buildings	0.17	400

The procedures of strengthening and repair can be classified into the following main groups:

- Repair of cracks;
- Repointing the joints with cement mortar;
- Coating (reinforced cement, ferrocement, PRFC) on one or both sides of the walls;
- Injections of cement-, lime- or epoxy-based grout;
- Prestressing the walls in vertical or horizontal direction;
- Reconstruction of the most damaged parts of the walls.

The efficiency of various strengthening methods has been verified by both laboratory and in-situ tests. Usually, the walls are first tested in the existing state. In this phase of testing, the data about the original strength and deformability properties of masonry are obtained, and the testing, even in the laboratory conditions, is terminated before the final collapse of the specimens occurs. Then, the damaged specimens are repaired and/or strengthened, and retested. In the case of laboratory tests (Fig. 3), the testing of walls in the strengthened state is carried out up until the final collapse of the specimens. In-situ, however (Fig. 2), the collapse is avoided so that the testing is terminated before serious damage occurs to the walls. However, the testing is carried out well after the attainment of maximum resistance.

4.2.1 Stone-masonry walls

Typical values of tensile strength f_t and shear modulus G , obtained by in-situ testing the cement-grouted stone-masonry walls, are given in Table 5. As the comparison of values of tensile strength and shear modulus of existing and strengthened masonry indicates (Tables 2 and 5), by means of grouting the wall with cementitious grout the lateral resistance

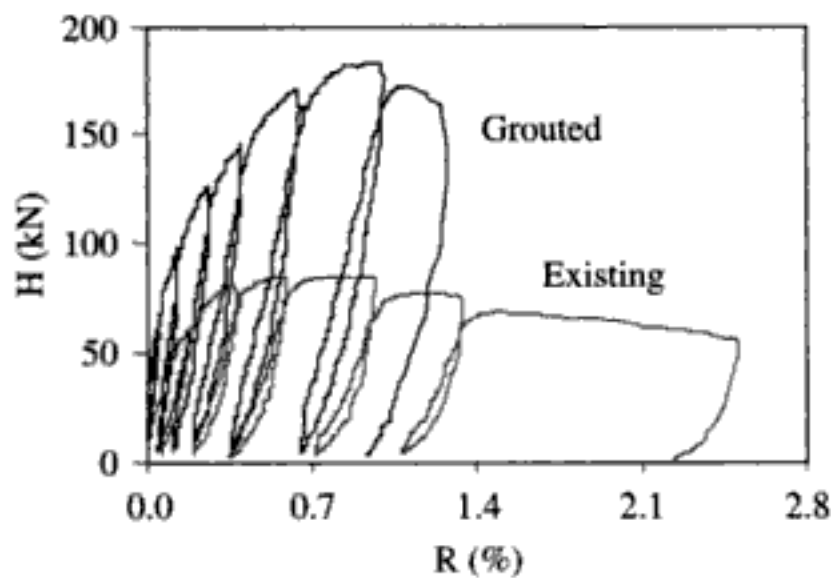


Figure 18. Lateral load-rotation relationships obtained by the in-situ testing of original and cement-grouted stone masonry wall.

Table 6. Characteristic values of compressive strength f_k and design values of modulus of elasticity E of cement-grouted stone-masonry walls.

Type of masonry	f_k (MPa)	E (MPa)
Two leaf, uncoursed lime stone, poor lime mortar, rural	0.80	8200
Two leaf, mix of uncoursed quartz sandstone, slate and lime-stone, lime mortar, urban	1.67	2600
Two leaf, uncoursed lime stone, poor lime mortar, rural dwellings	no data	no data

is improved. However, the degree of improvement depends on the quality of the existing masonry.

Typical relationships between the lateral load and displacements, obtained by in-situ testing of existing and cement-grouted stone-masonry walls, are shown in Figure 18. It can be clearly seen that not only the lateral resistance capacity, but also the rigidity of the tested walls significantly increased (Tomažević et al. 2000).

As was already mentioned, not many data are available as regards the compressive strength f and modulus of elasticity E . Some indicative results are given in Table 6. As can be seen by comparing the values given in Tables 3 and 6, the degree of improvement in load-carrying capacity to vertical loads, obtained by cement-grouting of the masonry, is significant.

In order to investigate the influence of grout strength on the resistance of stone-masonry walls, a series of walls has been built and tested in the laboratory (Tomažević & Apih 1993). Namely, to prevent the negative effects of pure cement grout, water repellent additives are added and/or part of cement is replaced with inert aggregates in the form of fine sands. The additives and reduction of the content of cement reduce the strength of the grout. However, as the experiments

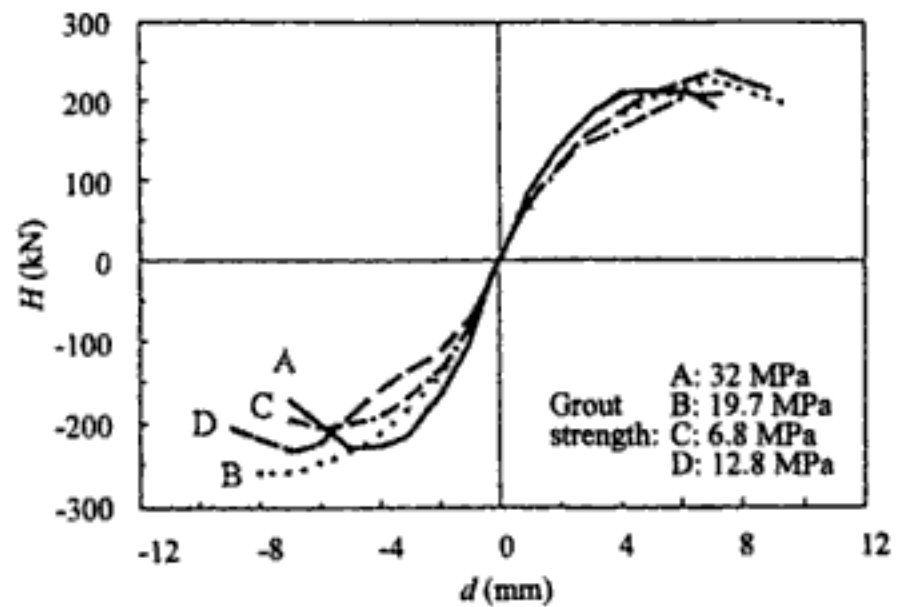


Figure 19. Comparison of hysteresis envelopes obtained during lateral resistance tests of stone-masonry walls, grouted with different grout mixes.

have shown, although the compressive strength of different grout mixes varied from 7 to 32 MPa, this had no influence on the lateral resistance of the grouted walls (Fig. 19).

It is believed that one of the possible reasons why strength of the grout did not influence the lateral resistance of the walls can be explained as follows. The potential resistance is determined by the strength of the original mortar and stone. Since the injection grout does not penetrate into the original mortar, the potential resistance does not change. However, by bonding the loose parts of the wall together into a solid structure and preventing the delamination and bulging when subjected to lateral loads, hence providing the integrity of the wall, the injected grout simply activates the potential load-bearing capacity.

On the basis of the results of this study, it can be concluded that an appropriate composition of the grout mix can be designed for each particular type of stone-masonry and for each particular problem to be solved in a historic stone-masonry building. Locally available materials compatible with the original texture of historic walls can be used to reduce the amount of cement in the grout and to reduce the expected side effects to an acceptable level.

4.2.2 Brick masonry walls

As regards the brick masonry walls, the efficiency of reinforced cement plaster coating has been tested by laboratory and in-situ testing. It has been observed that, depending on the geometry and quality of the existing wall as well as the way of application of the coating, the failure mechanism can be changed from shear to bending (Fig. 20).

As indicated by experiments, the improvement in the lateral resistance is inversely proportional to the quality of the original wall. It is significant in the case of poor-quality masonry, but not so in the case of good-quality walls. Typical example is shown in Figure 21.



Figure 20. Tensile rupture of reinforcing bar, observed during in-situ lateral resistance test of a brick masonry wall, strengthened by application of reinforced cement coating.

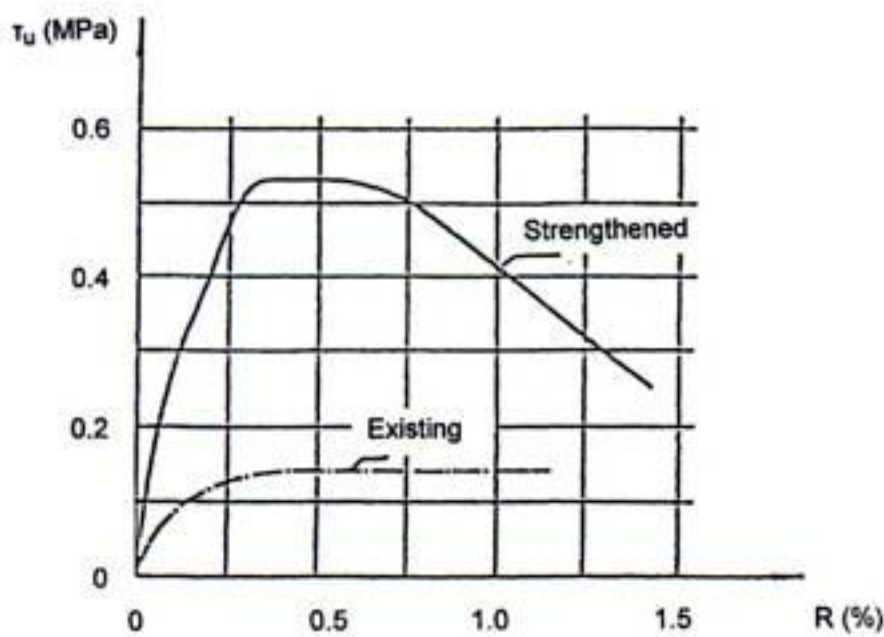


Figure 21. Average shear stress-rotation relationships obtained by the in-situ-testing of original and reinforced cement-coated brick-masonry wall.

5 STRUCTURAL EVALUATION

In the case where information is needed about dynamic characteristics of the building under consideration, such as natural periods of vibration and damping, special tests are carried out. Different methods and techniques are available. By means of dynamic exciters, fixed on the floors, vibrations of the building are induced. In this case, the frequency of rotating eccentric masses is electronically controlled and the response of the structure at different points along the height of the building at each frequency of excitation is measured. By evaluating the resonance curves

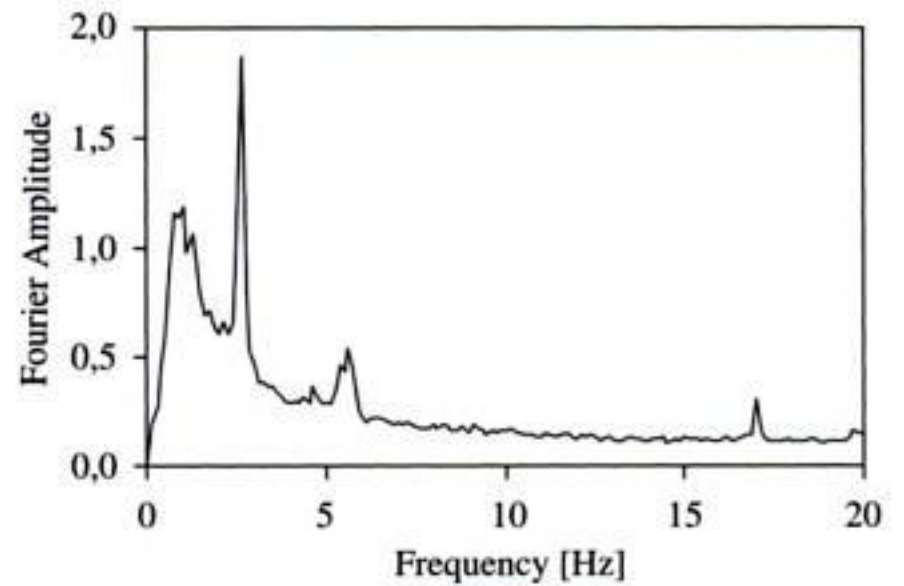


Figure 22. Frequency response spectrum, obtained by ambient vibration measurements of a stone-masonry tower.

measured during excitation, the coefficient of equivalent viscous damping can be also determined.

Ambient vibration tests are more simple to carry out. In this case, vibrations of the building caused by seismic microtremors, traffic, wind and other environmental influences are measured with sensitive transducers, placed on the structure at different locations along the height of the structure. The vibrations are measured for sufficiently long time and analyzed. On the basis of the calculated Fourier response spectra, information is obtained about the structure's natural vibration periods and damping (Fig. 22).

Both methods can be also used to determine dynamic characteristics of structural elements, if necessary. However, it is to emphasize that in both cases data about the dynamic characteristics are obtained in the range of very small amplitudes of vibration, especially in the case of ambient vibration tests. The data obtained by these methods are therefore only valid in the elastic range of vibrations and may be used for the verification of mathematical models developed for seismic behaviour of structures in the elastic range. On the basis of these data, no final conclusion can be drawn regarding the ultimate behaviour of the tested buildings, such as energy dissipation capacity, ductility and ultimate resistance.

In the case where the causes of damage, observed during visual inspection of the building, are not evident, long-term observations of building's behaviour are many times needed to definitely determine the reason for damage. Namely, not all observed damage can be attributed to previous earthquakes, but can also be a result of foundation settlements, temperature changes, vibrations induced by traffic, or other reasons. In order to successfully remedy the situation, the causes of damage should be removed before the intervention in the damaged structural element is carried out.

For this purpose, the structure is instrumented with displacement, strain and vibration transducers and other suitable instruments, and the readings are made either in regular time intervals at different

environmental conditions (summer, winter, wet, dry) or continuously. For example, settlements and tilting of the structure are measured with geodetic methods, the propagation and/or opening and closing of cracks with deformeters, whereas velocity transducers are in most cases used for monitoring the dynamic effects.

Sometimes, the structure is also monitored in order to verify the efficiency of structural interventions. Particularly, typical structures are monitored with strong-motion accelerographs to record their response during expected strong seismic events in the future.

6 CONCLUSIONS

The evaluation and redesign of historic masonry structures to remedy and/or improve the seismic resistance cannot be made unless reliable structural diagnosis had been previously carried out. In order to obtain the data needed for redesign, besides information regarding the type, geometry and conditions of the building and structural elements, quantitative data regarding the mechanical properties of structural materials should be determined. In order to make a reliable structural diagnosis, in-situ or laboratory destructive and non-destructive tests should be carried out. Different testing techniques and methods are available for this purpose. However, if non-destructive methods are used, a previous calibration is necessary.

Dynamic characteristics of the building's structural system may be defined by forced vibration or ambient vibration techniques. Sometimes, the structure is monitored so that short and long-term observations and measurements are performed to collect the relevant information for structural evaluation.

On the basis of the analysis of observations made after earthquakes and subsequent experimental research to simulate the seismic behaviour of historic buildings on earthquake simulators, mechanisms of seismic behaviour are defined and numerical models for seismic resistance verification are developed.

On the basis of structural evaluation, decision can be made as regards the necessary structural interventions. A large variety of different methods for seismic strengthening and repair of historic masonry buildings have been developed. Before practical application to buildings, however, the efficiency of these methods should be experimentally verified. Reliable data about the efficiency of such methods and numerical models to simulate their mechanisms of action during earthquakes, should be obtained and/or developed on the basis of experimental research.

ACKNOWLEDGEMENTS

The paper has been prepared on the basis of results of research, which the author and his colleagues have

carried out and published in the last decade. The reader may find more detailed information in the referenced publications.

REFERENCES

- Eurocode 8. prEN 1998-3. *Design of structures for earthquake resistance. Part 3: Strengthening and repair of buildings*. CEN, Brussels (under development).
- Eurocode 8. ENV 1998-1-4. 1996. *Design provisions for earthquake resistance of structures – Part 1-4: General rules – Strengthening and repair of buildings*. CEN, Brussels, 1996.
- Sheppard, P. & Tomažević, M. 1986. In-situ tests of load-bearing capacity of walls of old masonry buildings. *Proc. 4th Nat. Congress on Earthquake Engineering, Vol.2*, Cavtat: 85–92.
- Tomažević, M. 2000. Seismic redesign of existing masonry buildings. *European Earthquake Engineering*, 14 (3): 59–66.
- Tomažević, M., Klemenc, I. & Lutman, M. 2000. Strengthening of existing stone-masonry houses: Lessons from the earthquake of Bovec of April 12, 1998, *European Earthquake Engineering*, 14 (1): 13–22.
- Tomažević, M. 1999. *Earthquake-resistant design of masonry buildings*. London: Imperial College Press.
- Tomažević, M. 1997. Seismic resistance verification of masonry buildings: following the new trends. In Peter Fajfar & Helmut Krawinkler (eds.), *Seismic Design Methodologies for the Next Generation of Codes*: 323–334. Rotterdam: Balkema.
- Tomažević, M., Lutman, M. & Weiss, P. 1996. Seismic upgrading of old brick-masonry urban houses: tying of walls with steel ties. *Earthquake Spectra*, 12 (3): 599–622.
- Tomažević, M. & Apih, V. 1993. The strengthening of stone-masonry walls by injecting the masonry friendly grouts. *European Earthquake Engineering*, 7 (2): 10–20.
- Tomažević, M., Lutman, M. & Velechovsky, T. 1993. Aseismic strengthening of old stone-masonry buildings: is the replacement of wooden floors always necessary? *European Earthquake Engineering*, 7 (2): 34–46.
- Tomažević, M. & Velechovsky, T. 1992. Some aspects of testing small scale masonry building models on simple earthquake simulators. *Earthquake Engineering & Structural Dynamics*, 21 (11): 945–963.
- Tomažević, M., Weiss, P. & Velechovsky, T. 1991. The influence of rigidity of floors on the seismic behaviour of old stone-masonry buildings. *European Earthquake Engineering*, 5 (3): 28–41.
- Tomažević, M., Turnšek, V. & Terčelj, S. 1978. Computation of the shear resistance of masonry buildings. Report ZRMK-IK. Ljubljana (in Slovene).
- Turnšek, V., Terčelj, S., Sheppard, P. & Tomažević, M. 1978. The seismic resistance of stone-masonry walls and buildings. *Proc. 6th European Conference on Earthquake Engineering, Vol.3*, Dubrovnik: 275–282.
- Turnšek, V. & Čačovič, F. 1971. Some experimental results on the strength of brick masonry walls. *Proc. 2nd Int. Brick-masonry Conference*, Stoke-on-Trent: 149–156.

The importance of investigation for the diagnosis of historic buildings: application at different scales (centres and single buildings)

L. Binda

Politecnico di Milano, Italy

ABSTRACT: Investigation on historic buildings is needed for different reasons. Material properties, wall construction technique, hidden voids, inclusions, masonry and timber decay, structural damages, etc., are information used for the structure safety control and for the choice of appropriate materials and techniques for repair. Non destructive (NDT) or minor destructive (MDT) techniques are required, in order to avoid invasive tests. These techniques need a calibration both for the testing procedure and for the elaboration software of the collected data.

At the general level of historic centres, MDT and NDT can only be applied by sampling positions representative of a whole wall or group of constructions. In these cases the budget can be very low, but even few information can be meaningful for the diagnosis; this can be the case of historic centres in seismic areas. The paper introduces different strategies and different level of investigation also through some case histories.

1 INTRODUCTION

Restoration was in the past reserved to monumental buildings. Restorers were few experienced professionals who took care for years and sometime for their professional life of the same monument or group of monuments.

After the second world war, in Italy as in other mediterranean countries, houses and palace of the historic centres were frequently abandoned by the inhabitants for more attractive new modern buildings out of the centres, with heating and all the facilities not available in the old houses.

So the historic centres were left to the poorests and to the immigrants lowering the level of maintenance of historic building.

In many cases the entire historic centre was abandoned by the old owners searching for a job in the industrial cities.

On the other hand in high schools and the universities, teaching of old traditional materials as masonry and wood was substituted by concrete, steel and new high-tech materials.

So the knowledge about historic construction techniques and materials became lower and lower.

When some collapses occur or exceptional events cause heavy damage, then the structural engineers are called to produce projects for reconstruction or repair.

As frequently happened in the recent past, due to lack of knowledge and of appropriate analytical models, masonry was simply treated as a one type material, as homogeneous as concrete, steel, wood and what is

worse, as a “concrete”. The assumption for masonry structures in seismic areas were that, they should behave like a “box” with stiff floors and stiff connections between the walls, no matter which was their geometry or material composition.

As a consequence all the masonry buildings were treated as if they belonged to the same structural typology.

In seismic areas the strengthening project implied the use of the same intervention techniques: substitution of timber-floors and roofs with concrete ones, wall injection by grouts, use of concrete tie beams inserted in the existing walls.

This despite the typology of the structure and also despite the wall construction technology (one, two, three leaf, stone/brick). This type of intervention unaware of the construction typologies usually fails in seismic area (Figs. 1, 2) (Binda et al., 2003).



Figure 1. Collapse of a repaired walls.



Figure 2. Separation of leaves in repaired stone masonry.

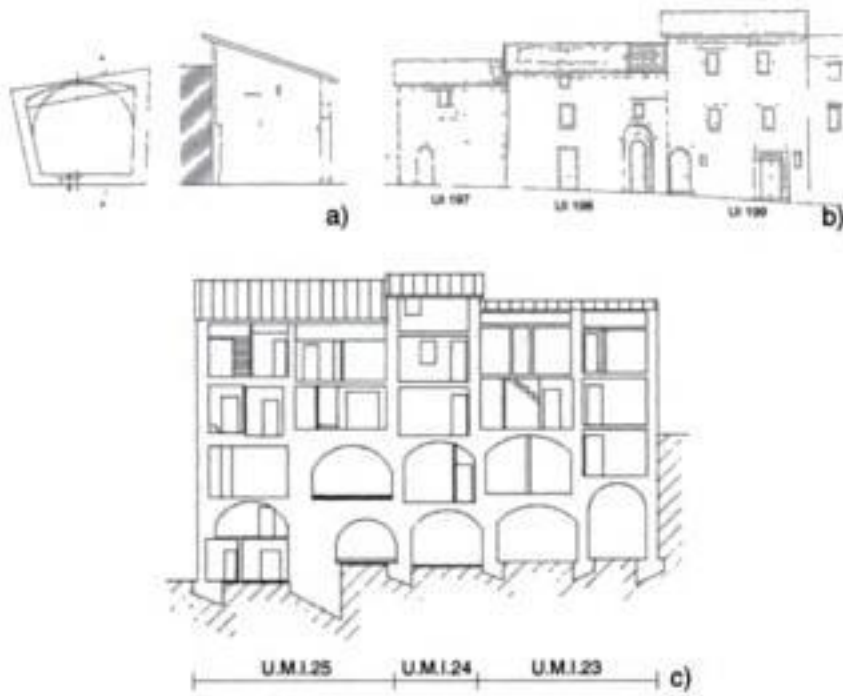


Figure 3. Example of: (a) simple isolated building; (b) row building; (c) complex building.

A remedy to the failure can only be an appropriate design for intervention based on a deep knowledge of the building typology and of the materials and structure behaviour, reached through an appropriate investigation.

2 WHY INVESTIGATION IS NECESSARY

After the above premises it is necessary to give an answer remembering that:

- the knowledge of the old building construction technique and materials was lost during the last century, therefore it has to be rebuilt;
- buildings belong to construction typologies (Fig. 3) which are different according to the building use and to the local materials;
- masonry is a composite with different section morphology: one-two-three leaves, regular irregular, made with brick and/or stones (Fig. 4);
- masonry should not be considered similar to the concrete; they are extremely different;
- analytical models should be calibrated by experimental investigation and applied appropriately to check the structural safety.

3 WHICH LEVEL OF INVESTIGATION

Investigation on site and in laboratory has an economic impact on the budget available for the preservation intervention.

If the level and type of investigation procedures is not clear and appropriate to the necessity of the building knowledge the available funds can be misused (Binda et al., 1999).

Furthermore if the questions to be answered by the investigation are not clear to the designer, the use of

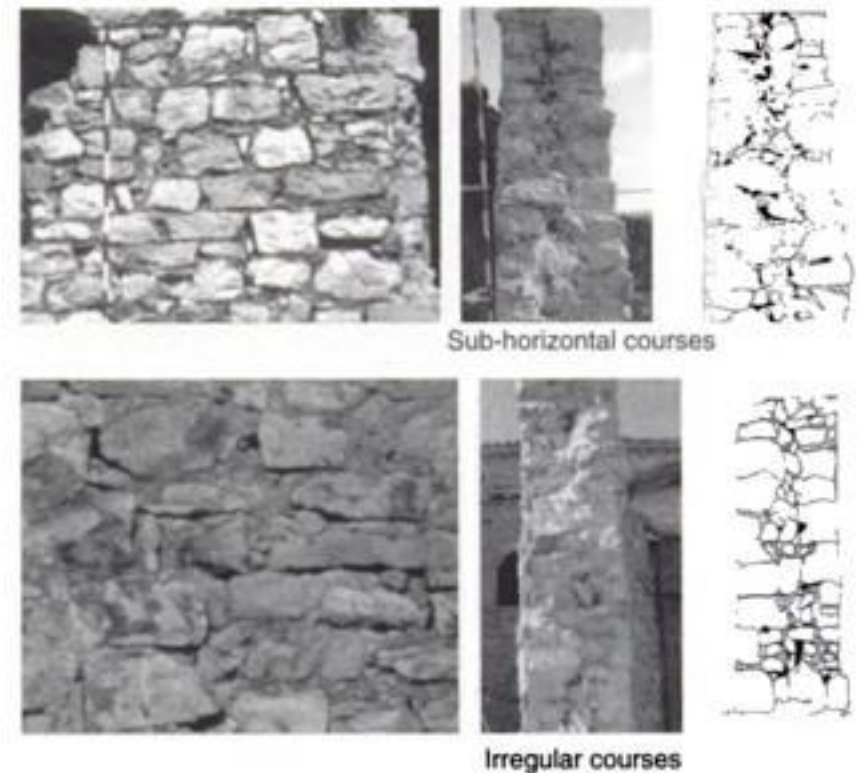


Figure 4. Prospect and section morphologies.

the results obtained can be unclear and even misleading (Binda et al., 1992) e.g. the stress values given by a flat jack test can appear unreliable if the designer chooses the test points without any hypothesis in mind or does not realise that the value obtained is a local one.

A design for complex and detailed investigation can be proposed if it concerns a complex building with many unsolved problems concerning: geometry, hidden features, high variability in materials and types of damage, a complex evolution of volumes and structural damages along the time (Binda et al., 2000b).

In some cases the investigation can be limited to geometrical and damage survey and to few laboratory and in situ tests.

Different level of investigation have then to be defined and guidelines can be given for each level.

3.1 Historic centres or urban aggregates

The necessity of investigation at urban level becomes very clear when dealing with urban areas under risk of exceptional events as earthquake, floods, eruptions, fires, or longterm events as slides, subsidence, etc.

In very old or antique centres where the buildings can be abandoned, misused or without maintenance for long-time, the knowledge on the behaviour of even largely distributed building typologies in the same area are lost or forgotten. In the case of earthquake or subsidence this knowledge at the level of similar typologies in the centre can be recovered by learning from the past events which are the most diffused types of damage (e.g. collapse mechanisms, crack pattern etc.) (Binda et al., 2004).

In those cases only the collection of geometry, material properties and type of damage characteristic for each building typology together with simplified mathematical models can be the base to study

and propose repair and preventive measure for the future, respectful of the existing buildings.

From basic investigation can also emerge clearly very difficult problems to be solved by more complex investigation procedures.

For very simple buildings as rural or two to three floor houses, the simple type of investigation can be appropriate if applied to every building and not only at urban scale even to study the choice of preservation techniques.

3.2 Preservation of complex and monumental buildings

If the aim is the preservation of buildings which have complexity of volumes due to their evolution in different subsequent times or monuments as palaces, churches, towers, arenas, etc., then the inspection and investigation have to be punctual and produce a deep knowledge of all the details of the structural and non structural parts.

A methodology of investigation has nevertheless to be applied to the knowledge of the building, from the basic operations to the more complex.

These operations can involve: geognostic investigation, geometrical, topographic, photogrammetric surveys, laboratory tests on materials sampled to be representative of the material used in the building, non destructive testing on the presence of humidity, voids, multiple leaf in masonries, slightly destructive testing.

Tests on timber structures, coring and visual inspections in depth, on site diffused mechanical test, etc. archive historical documentation and on site precise observation of the building evolution, should also be carried out (Binda et al., 2000b).

4 BASIC INVESTIGATION PROCEDURE

In order to give an appropriate methodology which can be applied with effectiveness taking into account the previous section 3, it is possible to state some priorities in the applications of investigation procedures.

Some operations must be always conducted due to their extreme importance.

Visual inspections, photographic campaign and collection of data on the site and on the single building from historic archives have to come first in order to understand the environment and the building features.

Then the geometrical survey, a map of the materials used, a decay map, the individuation of the structural elements, the crack pattern survey and the foundation and soil survey.

4.1 Geometrical and crack pattern survey

A design for intervention cannot be prepared if the geometry of the structural and non structural elements

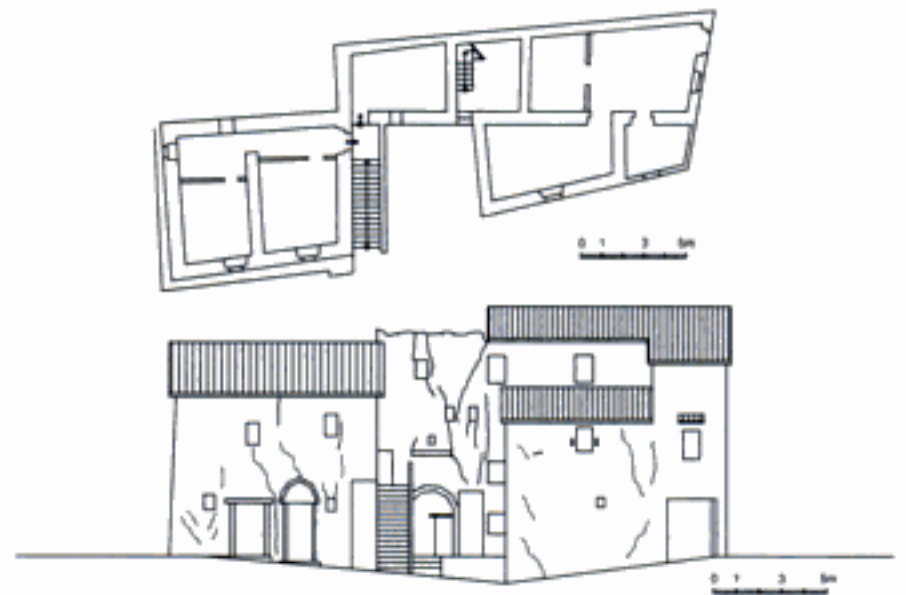


Figure 5. Crack pattern survey of a Montesanto building damaged by the earthquake.

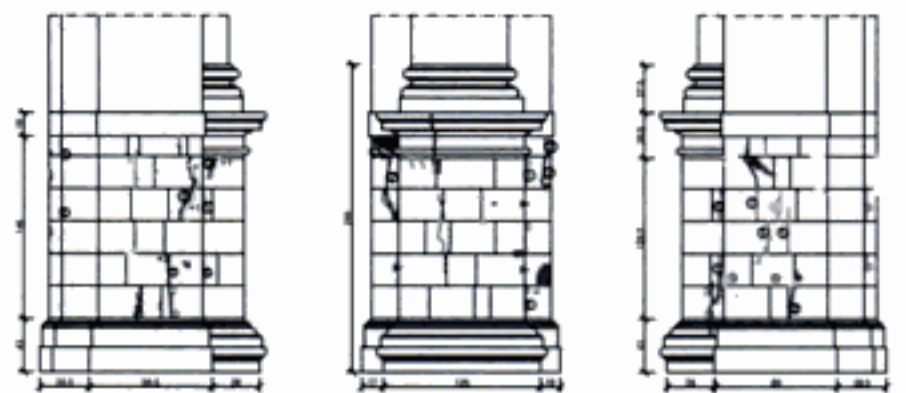


Figure 6. Typical crack pattern of a pillar under heavy compressive stresses.

is not available. The knowledge of the geometry is not only used from the architectural point of view, but also to understand the distribution of damage and decay, and is necessary for the structural analysis.

If the building is complex (row building, agglomerate), then the evolution of its volume should be detected by careful visual inspection to see the signs (lack of wall connection in the prospects at contact between two parts of the building built in different times, etc.). This is an important operation particularly in seismic areas when studying the vulnerability of the sites (Binda et al., 2004).

Essential for the safety of the building is certainly the crack pattern survey reported on plan and prospects. Cracks, out of plumb, loss of material, etc. when reported on the geometrical survey can give a clear indication of the phenomena interesting the structural movements (Figs. 5, 6).

The crack pattern can be in seismic areas also compared to a damage abacus (Fig. 7).

4.2 Survey of masonry texture and of the morphology of the wall section

This survey is very important for two reasons: (i) to understand the mechanical behaviour of the wall in order to avoid unexpected damages under earthquake

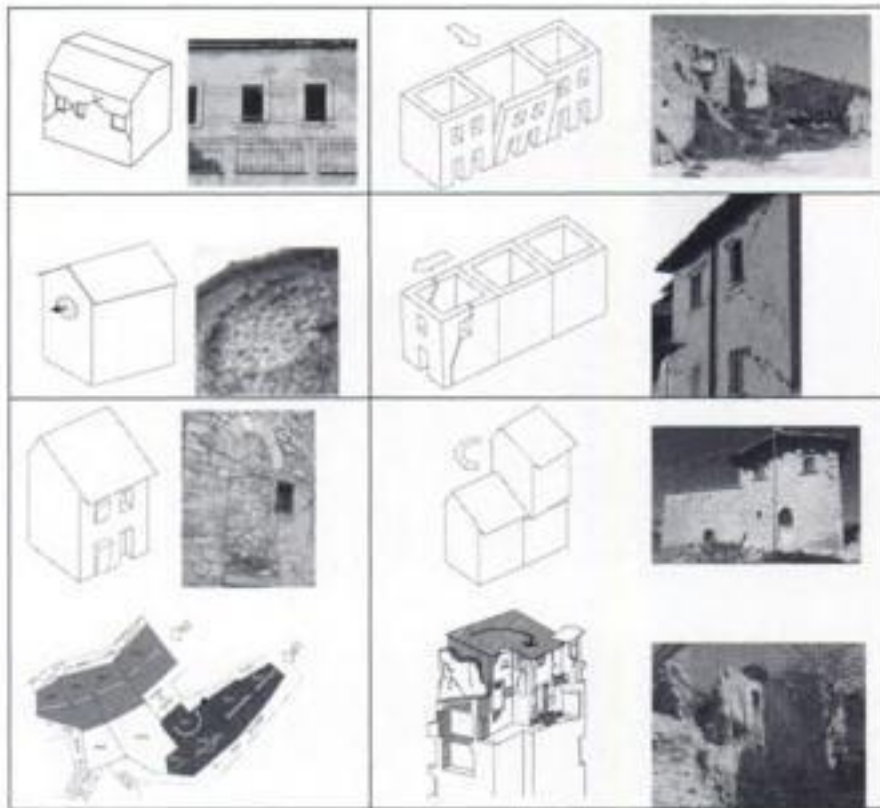
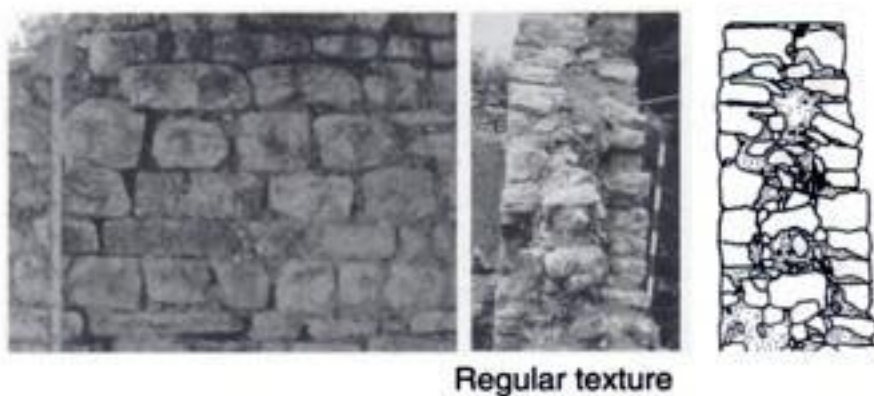


Figure 7. Some examples from the collapse mechanisms abacus.



Figure 8. Damages after Umbria earthquake: collapse of the outer leaf of the wall.



Regular texture

Figure 9. The regularity is also apparent, the section is very poor.

(Fig. 8), (ii) to understand the injectability of the wall in case of repair.

It should be clarified that an apparent regular wall can hide a very irregular section (Fig. 9). If the section is not visible local inspection have to be made.

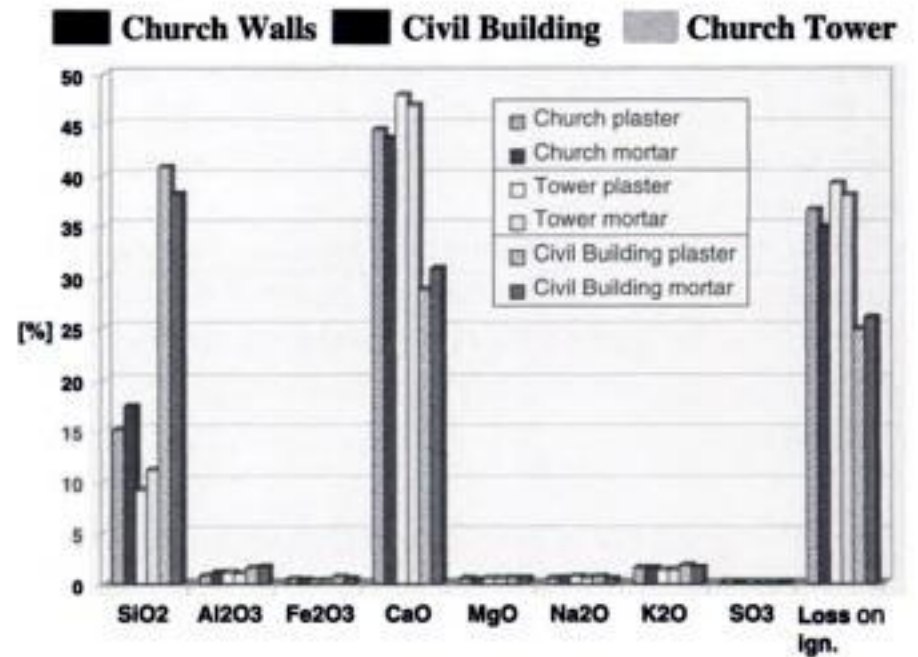


Figure 10. Results of chemical tests on mortars specimens sampled from an historic centre (Campi, Umbria).

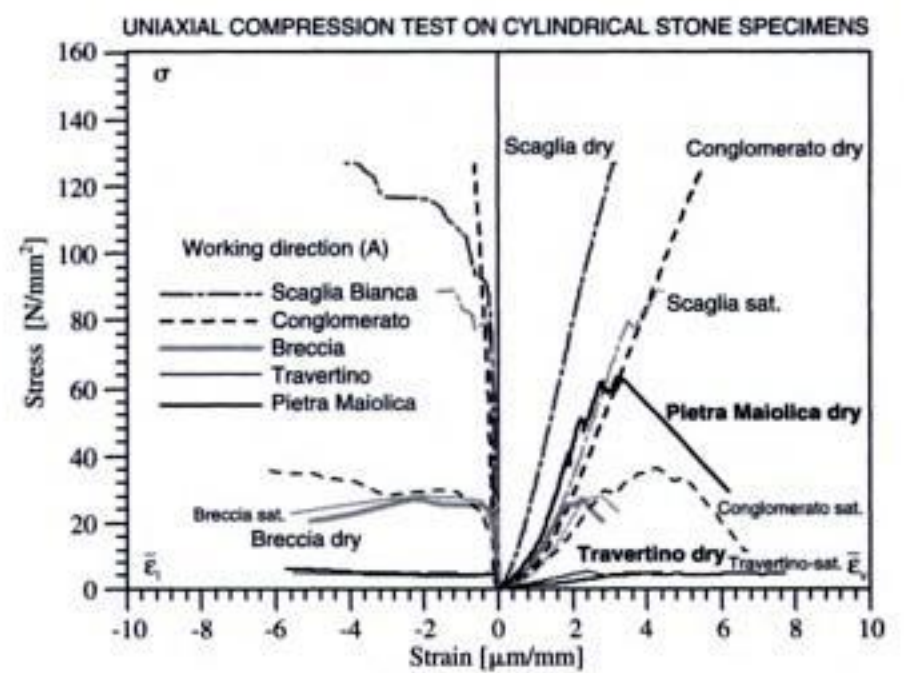


Figure 11. Some results on stones specimens sampled from an historic centre (Campi, Umbria).

4.3 Laboratory test

A minimum number of laboratory tests is necessary even for a basic investigation (Binda et al., 2004).

They have the aim of defining the chemical physical and mechanical characteristics of the component materials. In the case of masonry they characterise mortars, stone and bricks. For mortars mechanical tests are usually impossible, so chemical (Fig. 10) and petrographic tests can be made to identify the type of binder, of aggregates and the mortar composition.

For stone and bricks, petrographic analyses, physical and mechanical (Fig. 11) tests are important, particularly to detect states of damage and their causes and to choose new material for restoration compatible with the original ones.

4.4 Foundation and soil survey

Small exploratory shafts or core drilling have to be done for the geometrical survey of the foundations.

The material characteristics and the soil properties have also to be known.

In-situ and laboratory tests on the foundation soil are also needed in order to predict settlements or the state of stress and strain of the soil under new loading conditions after repair or to understand the causes of a collapse (Binda et al., 1992).

4.5 Minor destructive tests

To understand the morphology of a masonry wall it is important a direct inspection. Sometimes it could be performed by removing few bricks or stones and surveying photographically and drawing the section of the wall.

In some cases it is possible to core boreholes in the most representative points of the walls. Coring should be done with a rotary driller using a diamond cutting edge. This operation is rather simple but has limits. The drilled core is usually very decohesioned (Fig. 12) so it is almost impossible to detect the quality of the original materials. Inside the boreholes additional investigations can be made by the use of borescopy. A small camera may be inserted into the borehole allowing a detailed study of its surface and try a reconstruction of the wall section.

Nevertheless the interpretation of the results is a very difficult operation, sometimes hopeless; it should be remembered that boroscopy can only give a general stratigraphy of the section.

Other slightly destructive tests can be used to give more information on site about the masonry components as: (i) the Schmidt hammer rebound test; (ii) the penetration tests proposed in different ways, like probes, drillers, etc. correlate the depth of penetration to the material mechanical properties; (iii) the pull-out tests can only be used on bricks and stones. They can be considered as surface or small penetration techniques, which can be used for a preliminary investigation.

4.6 Flat jack test

The method was originally applied to determine the in-situ stress level of the masonry. The firsts applications of this technique on some historical monuments (Rossi, 1982), clearly showed its great potential. The test is carried out by introducing a thin flat-jack into the mortar layer, in masonry with regular and thin joints. The test is only slightly destructive (ASTM, 1991), (Binda & Tiraboschi, 1999).

The determination of the state of stress is based on the stress relaxation caused by a cut perpendicular to the wall surface; the stress release is determined by a partial closing of the cutting, i.e. the distance after the cutting is lower than before (ASTM, 1991). A thin

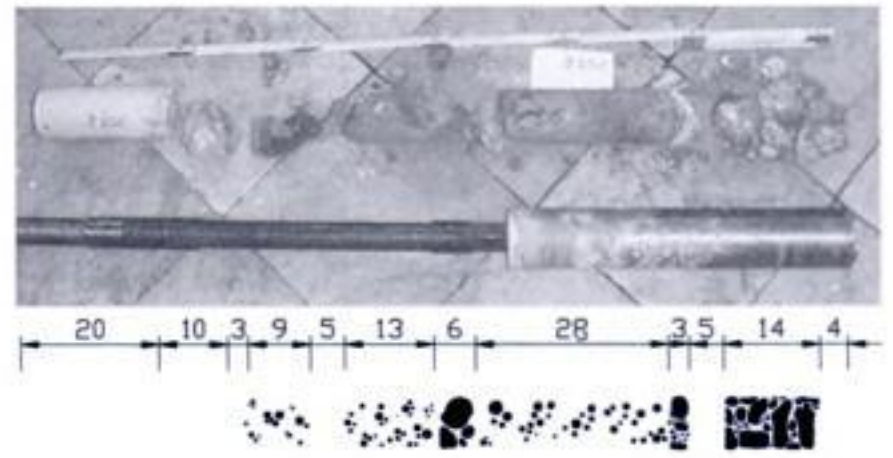


Figure 12. Drilled core and reconstruction.



Figure 13. Placing the flat jack.

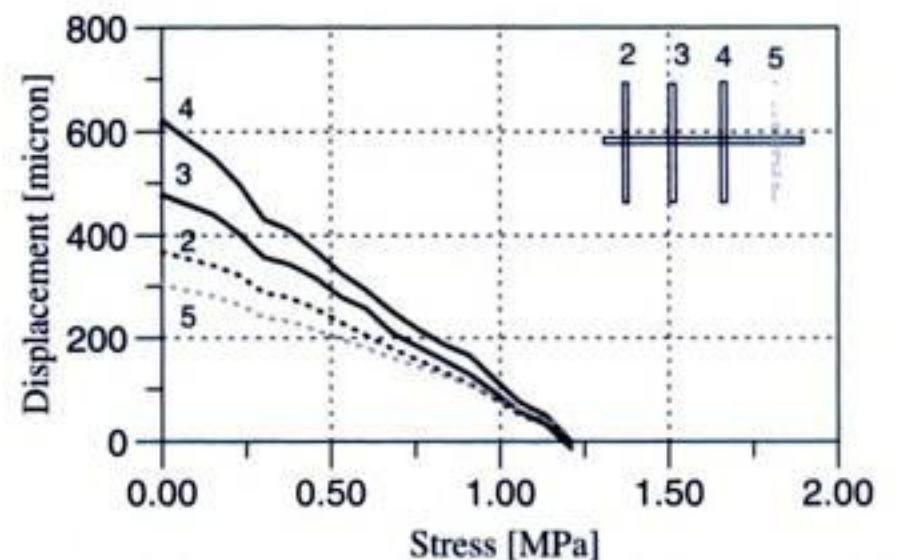


Figure 14. Single flat-jack tests carried out at the Monza Tower.

flat-jack is placed inside the cut (Fig. 13) and the pressure is gradually increased to obtain the distance measured before the cut (Figs. 13, 14).

The displacement caused by the slot and the ones subsequently induced by the flat-jack are measured by a removable extensometer before, after the slot and during the tests. P_f corresponds to the pressure of the hydraulic system when the displacement reach those read before the slot is executed, that is zero.

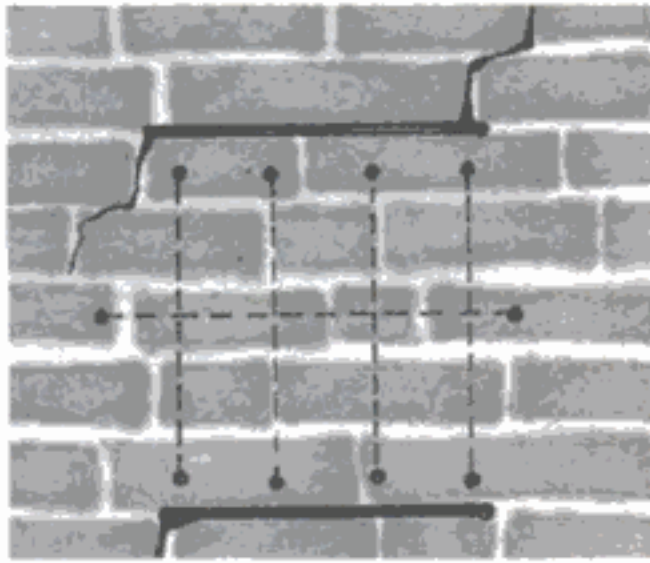


Figure 15. Double flat-jack test Tower of the Cathedral of Monza (Binda et al., 1998b).

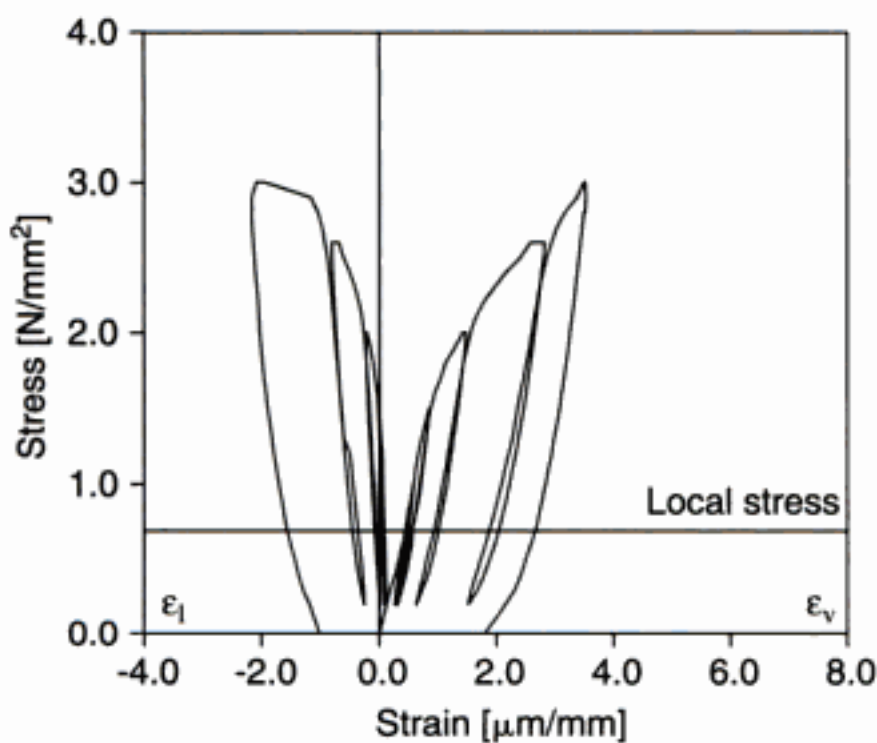


Figure 16. Double flat-jack test on West side of the Monza Tower (Binda et al., 1998b).

The equilibrium relationship is the fundamental requirement for all the applications where the flat-jack are currently used (ASTM, 1991):

$$S_f = K_j K_a P_f$$

S_f = calculated stress value

K_j = jack calibration constant (<1)

K_a = slot/jack area constant (<1)

P_f = flat-jack pressure

The use of flat-jacks for stonework made with irregular stones is not so easy, due to the difficulty of finding regular joints; therefore the cut for the insertion of the jack is done directly in the stone courses. It must be pointed out that the flat-jack test in the case of multiple-leaf walls gives results concerning only the outer leaves.

The test described can also be used to determine the deformability characteristics of a masonry. A second cut is made, parallel to the first one and a second jack is inserted, at a distance of about 40 to 50 cm from

the other (Fig. 15). The two jacks delimit a masonry sample of appreciable size to which a uni-axial compression stress can be applied. Measurement bases for removable strain-gauge or LVDTs on the sample face provide information on vertical and lateral displacements.

In this way a compression tests is carried out on an undisturbed sample of large area. Several loading could be performed at increasing stress levels in order to determine the deformability modulus of the masonry in its loading and unloading phases (Fig. 16).

It is interesting to compare these last results to the stress level measure in order to verify the present state of the masonry in relation with its last potentialities (Binda et al., 1998b).

5 NON DESTRUCTIVE PROCEDURES

The necessity of establishing the building integrity or the load carrying capacity of a masonry building arises for several reasons including: (i) assessment of the safety coefficient of the structure (before or after an earthquake, or following accidental events like hurricanes, fire, etc.), (ii) change of use or extension of the building, (iii) assessment of the effectiveness of repair techniques applied to structures or materials, and (iv) long-term monitoring of material and structural performance.

NDE can be helpful in finding hidden characteristics (internal voids and flaws and characteristics of the wall section) which cannot be known otherwise than through destructive tests (Binda et al., 2000b).

The types of tests available at present are mainly based on the detection of the physical properties of the wall.

In fact the only in-situ mechanical tests available are flat-jack, hardness, penetration and pull out tests. The flat-jack tests give local measurements and are slightly destructive: nevertheless they can give directly the values of mechanical parameters. In the case of ND tests, a correlation between the measured parameters and the mechanical ones is usually difficult, but they can give an overall qualitative response of the masonry. At present the most diffused ND techniques are represented by the sonic (or ultrasonic), radar and thermography tests.

Up to now most of the ND procedure can give only qualitative results; therefore the designer is asked to interpret the results and use them at least as comparative values between different parts of the same masonry structure or by using different ND techniques.

5.1 Thermovision

Thermovision is a NDT, which has been applied since several years to works of art and monumental

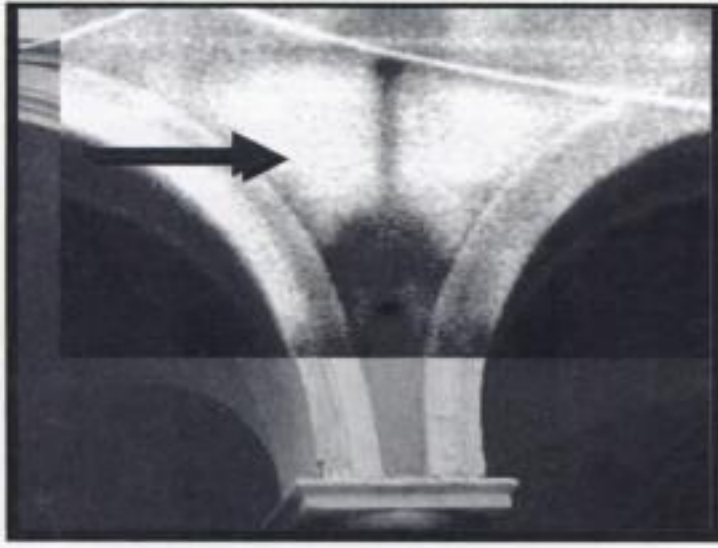


Figure 17. Investigation on hidden steel tie rods (Binda et al., 2003).

buildings. The thermographic analysis is based on the thermal conductivity of a material and may be *passive* or *active*. The *passive* application analyses the radiation of a surface during thermal cycles due to natural phenomena (insulation and subsequent cooling). If the survey is *active*, forced heating to the analysed surfaces are applied.

A camera sensitive to infrared radiation collects the thermal radiation. In fact each material emits energy (electromagnetic radiation) in this field of radiation; this radiation is characterised by a thermal conductivity, that is the capacity of the material itself of transmitting heat, and its own specific heat. The result is a thermographic image in a coloured or B/w scale. At each tone corresponds a temperature range. Usually the differences of temperatures are fraction of degree.

Thermovision can be very useful in diagnostic; in fact it is applied to identify areas under renderings and plasters that can hide construction anomalies. It is particularly interesting for studies on frescoed walls (Lenzi et al., 1997). Other applications can be: (i) survey of cavities (Fig. 17), (ii) detection of inclusions of different materials, (iii) detection of water and heating systems, (iv) moisture presence (Fig. 17). In the presence of moisture, the camera will find the coldest surface areas, where there is continuous evaporation (Fig. 17).

In the diagnosis of old masonries, thermovision allows the analysis of the most superficial leaves. It is necessary to point out that the penetration depth of this technique is limited, so it is unable to locate anomalies, which are hidden in the inner part of a thick masonry. The technique is often sensible to the boundary condition of the tests. Sometimes shapes are detected, caused by different local emissions and not by effective variations.

5.2 Sonic pulse velocity test

The testing methodology is based on the generation of sonic or ultrasonic impulses at a point of the structure.

An elastic wave is generated by a percussion or by an electro-dynamics or pneumatic device (transmitter) and collected through a receiver, usually an accelerometer, which can be placed in various positions.

The elaboration of the data consists in measuring the time the impulse takes to cover the frequency and amplitude of the walls of distance between the transmitter and the receiver. The use of sonic tests for the evaluation of masonry structures has the following aims:

- to qualify masonry through the morphology of the wall section, to detect the presence of voids and flaws and to find crack and damage patterns (Binda et al., 2001);
- to control the effectiveness of repair by injection technique in others which can change the physical characteristics of materials (Binda et al., 2001).

The first applications of ultrasonic tests to the evaluation of masonry materials and structures have been carried out on long time ago in the sixties (Aerojet, 1967). Several efforts have been put in the tentative of interpretation of the data from sonic and ultrasonic tests (Binda et al., 2001), (Abbanneo et al., 1996).

The limitation given by ultrasonic tests in the case of very inhomogeneous material made the sonic pulse velocity tests more appealing for masonry.

The fundamentals of wave propagation through solids allow to recognise the theoretical capabilities and limitations of the technique. The velocity of a stress wave passing through a solid material is proportional to the density ρ , dynamic modulus E , and Poisson's ratio ν of the material. Resolution in terms of the smallest recognisable features is related to the dominant wave-length (as determinate by the frequency) of the incident wave and also to the size of the tested element.

Wave-length, λ , is determinate by a simple relationship between velocity, v and frequency f : $\lambda = v/f$.

Hence for a given velocity as the frequency increases the wave length decreases, providing the possibility for greater resolution in the final velocity reconstruction. However there is also a relationship between frequency and attenuation of waveform energy. As frequency increases the rate of waveform attenuation also increases limiting the size of the wall section, which can be investigated. The optimal frequency is chosen considering attenuation and resolution requirements to obtain a reasonable combination of the two limiting parameters. In general it is preferable to use sonic pulse with an input of 3.5 kHz for inhomogeneous masonry.

Input frequency changes with the characteristics of the superficial material (e.g. presence of thick plaster or cracks). The sonic test in this case shows a very important limit. Due to the wall structure or to the presence of a thick plaster (with fresco) the high frequency components could be filtered.

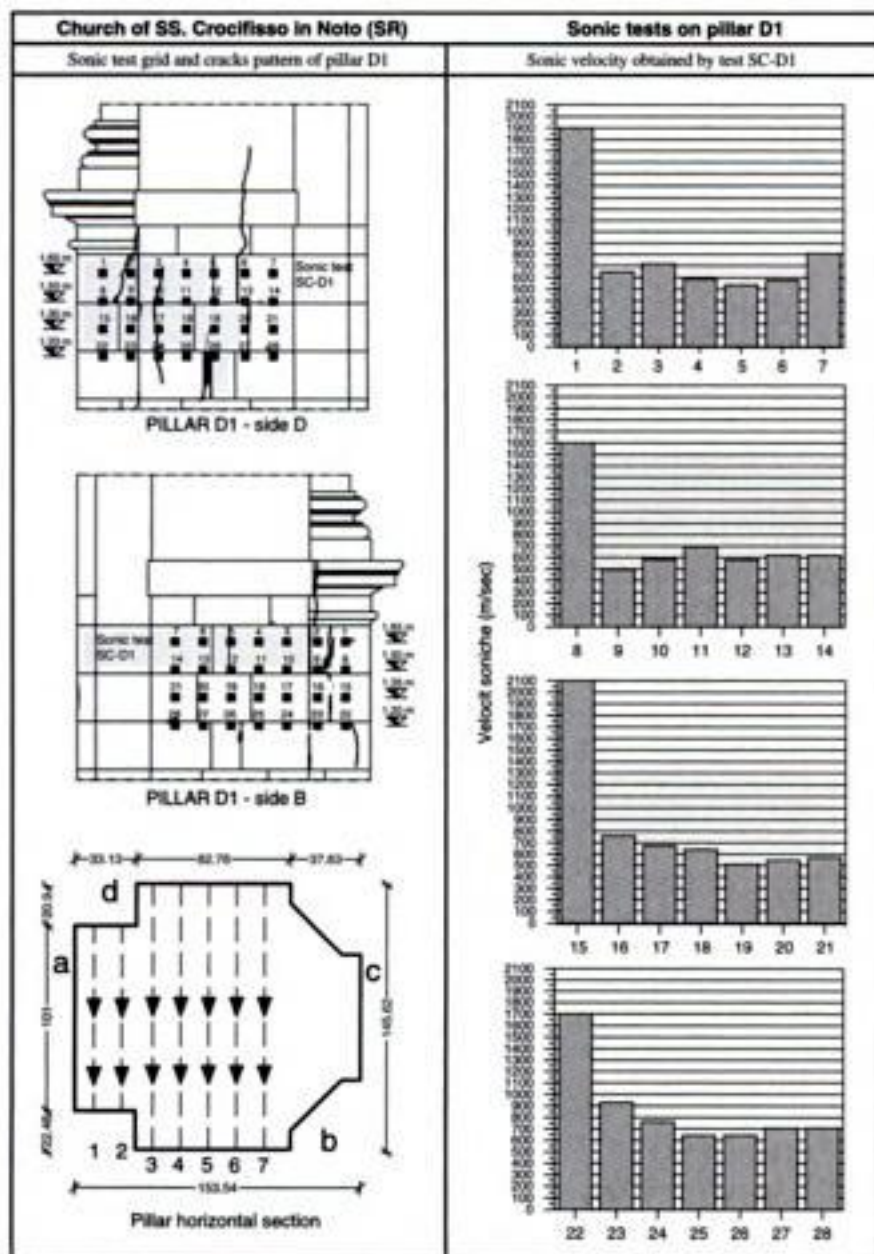


Figure 18. Crocifisso Church at Noto (Italy): results of sonic tests applied to a pillar.

It is important to stress that the pulse sonic velocity is characteristic of each masonry typology and it is impossible to generalise the values. The tests, then, have to be calibrated for the different types of masonry directly on site.

Figure 18 shows the crack pattern and the results of sonic tests applied to a pillar of the Crocifisso Church at Noto (Sicily – Italy).

5.3 Georadar

Among the techniques and procedures of investigation which have been proposed in these last years, georadar seems from one hand to be most promising, from the other to need a great deal more of study and research (Lenzi et al., 1997), (Binda et al., 1998), (Binda et al., 1999a). When applied to masonry, the applications of radar procedures can be the following: (i) to locate the position of large voids and inclusions of different materials, like steel, wood, etc. (Fig. 19); (ii) to qualify the state of conservation or damage of the walls; (iii) to define the presence and the level of moisture; (iv) to detect the morphology of the wall section in multiple leaf stone and brick masonry structures (Fig. 20).

Georadar seems to be a powerful tool to detect the presence of voids and structural irregularities, the

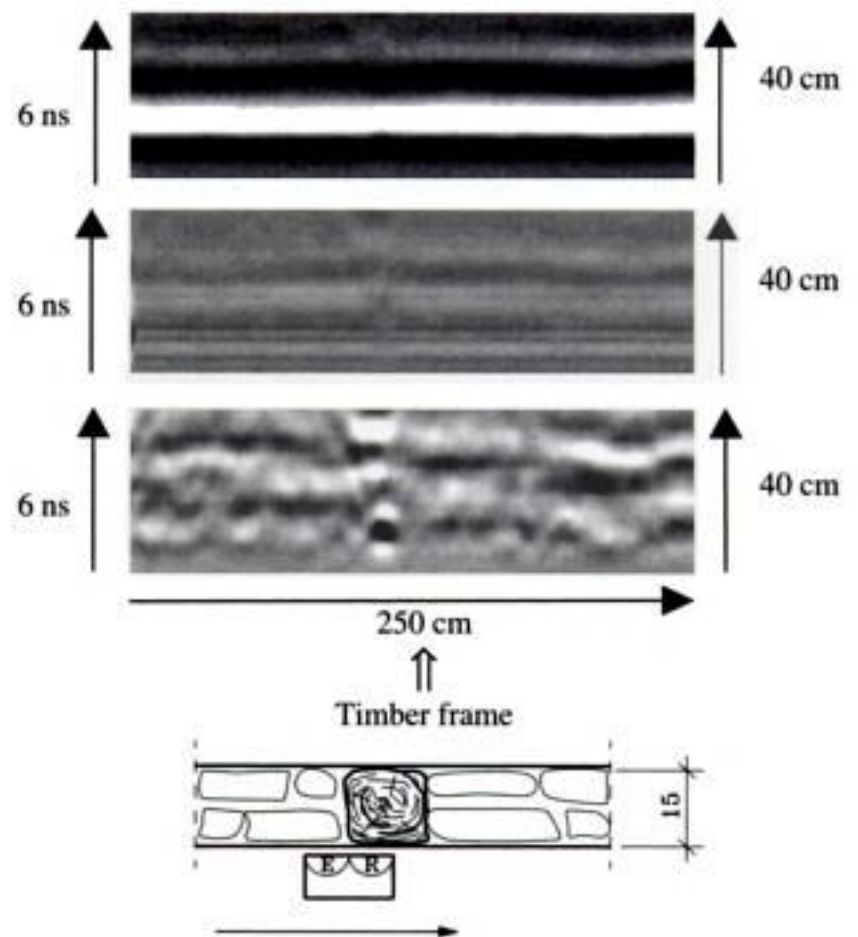


Figure 19. Localisation of a wooden element in a frescoed wall (Binda et al., 1998).

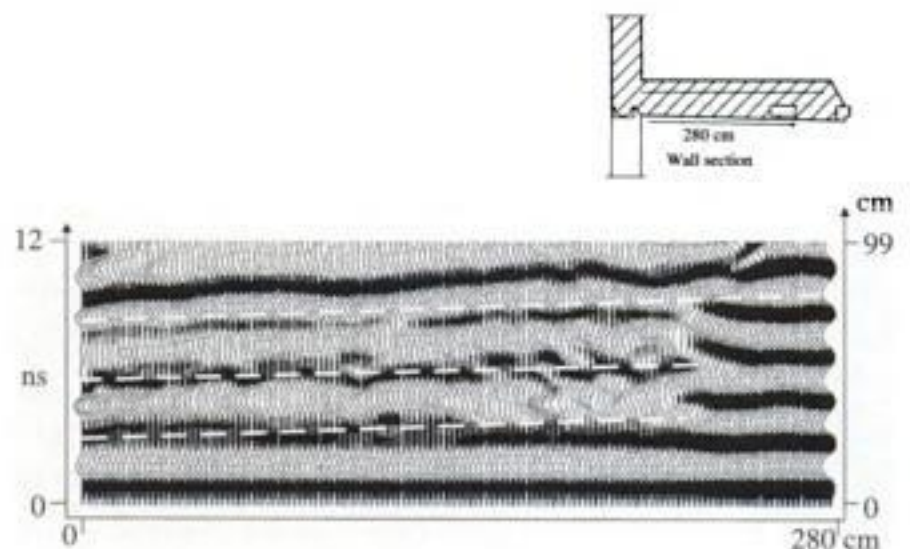


Figure 20. Radargram of the wall section at the Malpaga Castle. The leaves positions and the presence of a void on the right side are recognisable (Binda et al., 1999a).

presence of moisture and hopefully the presence of multiple-leaves in stone masonry.

The method is based on the propagation of short electromagnetic impulses, which are transmitted into the building material using a dipole antenna. The impulses are reflected at interfaces between materials with different dielectric properties, i.e. at the surface and backside of walls, at detachments, voids, etc. When the transmitting and receiving antennas, which are often contained in the same housing, are moved along the surface of the object under investigation, radargrams (colour or grey scale intensity charts giving the position of the antenna against the travel time) are produced. Measuring the time range between the emission of the wave and the echo, and knowing the velocity of propagation in the media it

would be possible to know the depth of the obstacle in the wall. In the real cases, the velocity is unknown because it changes from one material to the other or in the presence of voids. Furthermore the velocity is higher in dry walls, and lower in wet walls (Binda et al., 1999a).

The interpretation of the radar data involves the identification of significant anomalies. It should be a recognition process detecting features on the records that are characteristic of known signatures. Identifiable features on a radar record are continuous reflection from layers or reflection from discontinuities like voids and local inhomogeneities in the masonry.

The main problems in the data interpretation are caused by noises in the signals due to the following causes: (i) break-through effect. This effect is commonly visible on radar records and it hides partially the wall characteristics. It is caused by the fact that the antenna itself reacts to the electromagnetic wave. (ii) multiple echoes due to the presence of layers and joints. (iii) superposition of the lateral echoes that create images of parallel reflectors. This effect could be enhanced for a wall by the lack of mortar joints and the regularity of the stones.

Radar tests need always a preliminary calibration in order to verify if the emitted signal is enough powerful to detect the opposite side of the wall and the wave speed. This step allows to calibrate the relationship between the time and space scales. Some types of equipment give directly this transformation by setting up a value of the dielectric constant of the masonry. The value is an average of the characteristics of all the materials crossed by the wave.

The choice of the antenna frequency must be made on a site basis. During the test it is important to control the radar potentialities in relation to the frequency used (Padaratz & Forde, 1995).

One of the limits of the technique is the low readability of the results. In fact usually radar data are clearly readable only by experts. It is important to show results, as radargrams and graphics, which are significant to operators like architects and engineers.

5.4 Radar and sonic tomography

Among the ND applications the tomographic technique is quite attractive for the high resolution that can be obtained (Shuller et al., 1995), (Valle et al., 1997), (Valle et al., 1998). Tomography, developed in medicine and in several other fields, seems to be a valuable tool to give two or and three-dimensional representation of the physical characteristics of a solid. Tomography, from Greek "tomos" (slice), reproduces the internal structure of an object from measurements collected on its external surface (Fig. 21).

Tomographic imaging is a computational technique, which utilises an iterative method for processing a

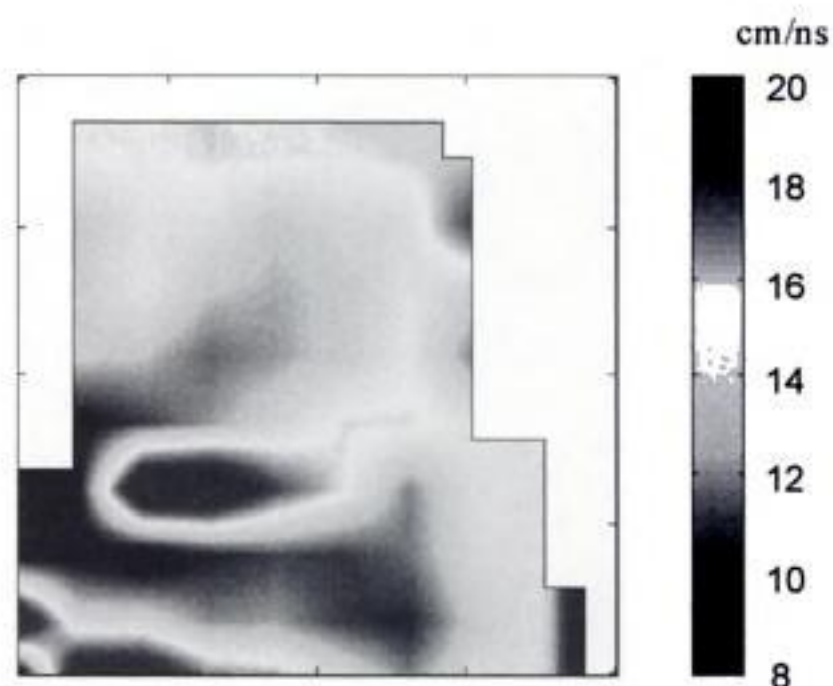


Figure 21. EM travel time tomography of a pier. The high EM velocities could detect a detachment of the structure (Valle et al., 1998).

large quantity of data. Standard pulse velocity data or radar data could be used to reconstruct a velocity distribution within a solid material, thus providing an "image" of the masonry interior. The testing technique gives a map of the velocity distribution on a plane section of the structure under investigation. The result of the tomographic inversion is a map of a property of the materials. In case of travel time tomography (TT) the measured quantity is the traveltime of the signal and the map is the distribution of the propagation velocity within the object. In case of amplitude tomography (AT) the measured quantity is the amplitude of the signal and the map is related to the distribution of the absorption coefficient.

6 STRUCTURE CONTROL BY STATIC AND DYNAMIC MONITORING

Where an important crack pattern is detected and its progressive growth is suspected due to soil settlements, temperature variations or to excessive loads, the measure of displacements in the structure as function of time has to be collected. Monitoring systems can be installed on the structure in order to follow this evolution.

This type of survey is frequently applied to important constructions, like bell towers or cathedrals (e.g. to the Pisa leaning Tower, to the Dome of the Florence Cathedral in Italy (Bartoli et al., 1992)) (Fig. 22) and the system may stay in place for years before a decision can be taken for repair or strengthening (Binda et al., 1995), (Binda et al., 2000a).

Very simple monitoring systems can be also applied to some of the most important cracks in masonry walls, where the opening of the cracks along the time can be measured by removable extensometers with high resolution (Fig. 23). This simple system can give very

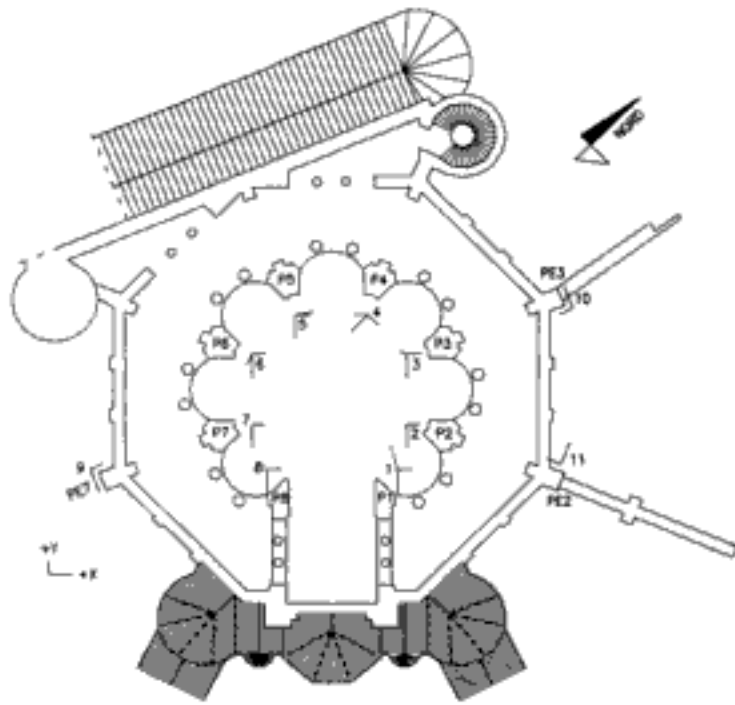


Figure 22. S. Vitale Church at Ravenna. Total variation of the out of plumb (November 1998–November 1999) (Binda et al., 2000a).

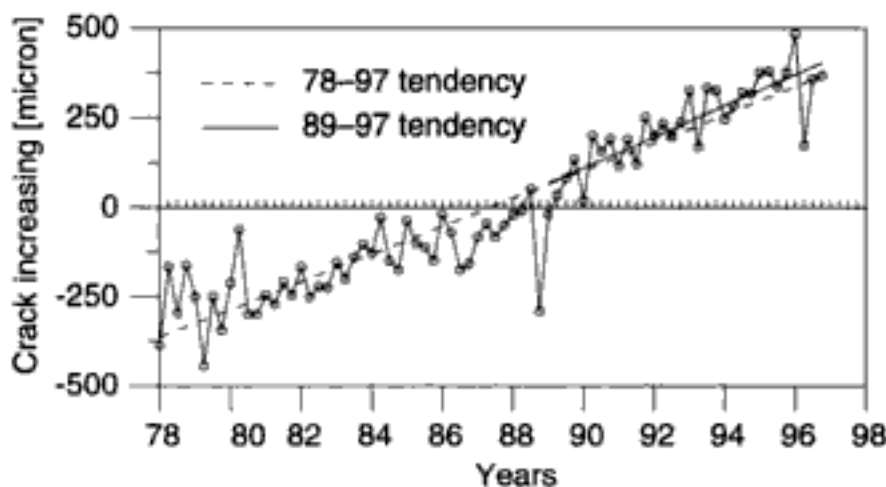
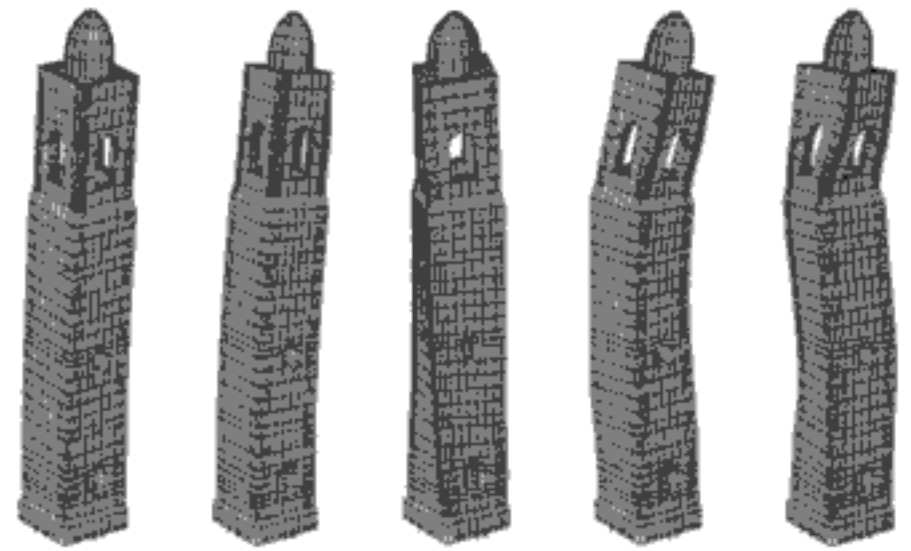


Figure 23. Crack monitoring made with a removable extensometer at the Monza Tower (28 Binda et al., 1998b).

important information to the designer on the evolution of the damage (Binda et al., 1998b).

In-situ testing using dynamic methods can be considered a reliable non-destructive procedure to verify the structural behaviour and integrity of a building. The principal objective of the dynamic tests is to control the behaviour of the structure to vibration. The first test carried out can be seen also as the starting one of a periodical survey using vibration monitoring inside a global preventive maintenance programme. Acceptance of vibration monitoring as an effective technique of diagnosis has been supported by different studies (Niederwanger, 1997), (Rossi, 1997).

These tests are very important to detect eventual anomalies in the diagnosis phase and to calibrate efficient analytic models (FEM) (Fig. 24) (Gentile et al., 2002). In this way it is possible to verify the effectiveness of the computational methods used in the analysis and control of the structure. The availability of an efficient numerical model allows for checking and predicting the structure behaviour to dynamic actions like, for example, strong winds effects and seismic actions.



$f_{FEM} = 0.585 \text{ Hz}$ $f_{FEM} = 0.709 \text{ Hz}$ $f_{FEM} = 2.455 \text{ Hz}$ $f_{FEM} = 2.726 \text{ Hz}$ $f_{FEM} = 5.698 \text{ Hz}$
 $f_{EMA} = 0.586 \text{ Hz}$ $f_{EMA} = 0.708 \text{ Hz}$ $f_{EMA} = 2.456 \text{ Hz}$ $f_{EMA} = 2.731 \text{ Hz}$ $f_{EMA} = 5.706 \text{ Hz}$

Figure 24. Vibration modes of the FEM model of the Monza Tower and comparison with the frequencies measured during the on site tests (Gentile et al., 2002).

The environmental excitation sources could be the wind, the traffic or the bell ringing in the particular case of towers (Binda et al., 1997), (Gentile et al., 2002), (Binda et al., 2000). The forced vibrations could be produced by local hammering systems or by the use of vibrodines. An accelerometer net is installed in chosen significant parts of the structure.

The dynamic tests allow to detect the frequencies, the modal shapes and the correspondent modal damping of a structure. These parameters are characteristics of the local and global behaviour of a structure.

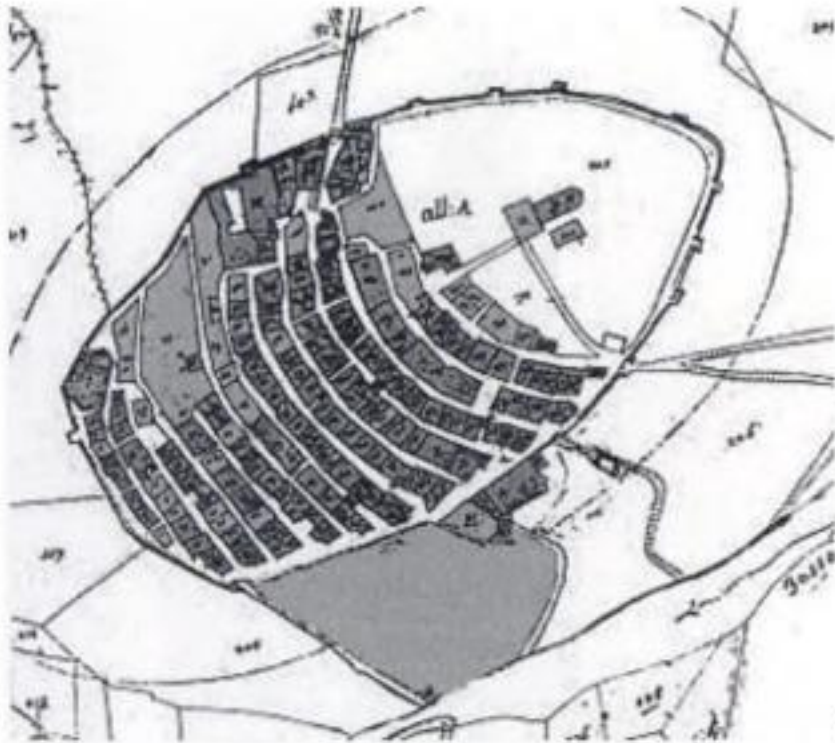
7 DIFFERENT LEVELS OF INVESTIGATION

As it was mentioned in the section 3, investigation procedures can be applied at different level following specific methodologies. Information on the building state of damage and on the material and structure characteristics are always needed, but if the processes are carried out at the level of the historic centre, only representative buildings of the most diffused typologies will be investigated and on site and laboratory tests will be carried out on samples of the most representative masonries, roofs and floors (Binda et al., 2004).

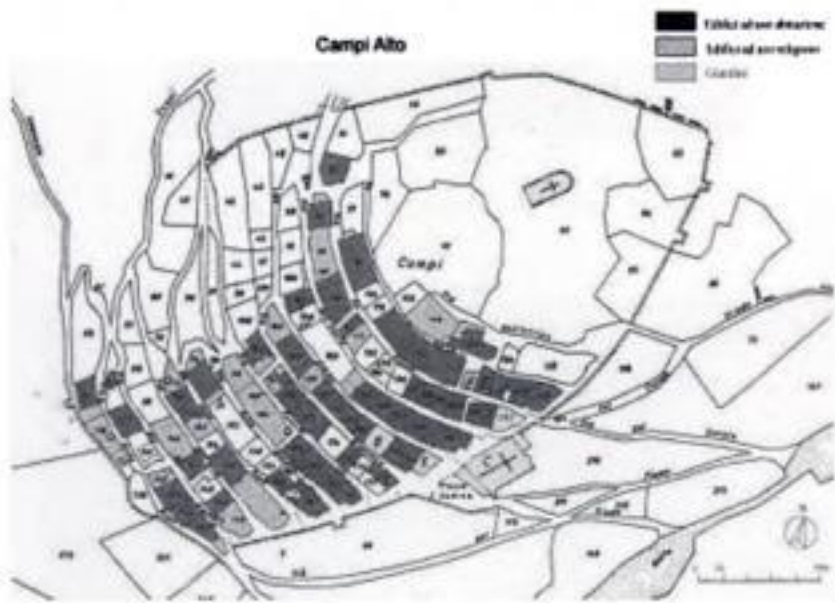
In case of important buildings and monuments when also a design for preservation is required, then the investigation must go into details intervention, the knowledge must be more detailed and also the investigation more sophisticated. In the following a description of the investigation procedures is given.

7.1 Investigation at urban level

As a first step the evolution of the centre during the different events or evolutions (e.g. earthquakes) is investigated (Fig. 25a,b).



(a)



(b)

Figure 25. Comparison between the state of Campi (Umbria) in 1835 (a), and in 1997 (b).

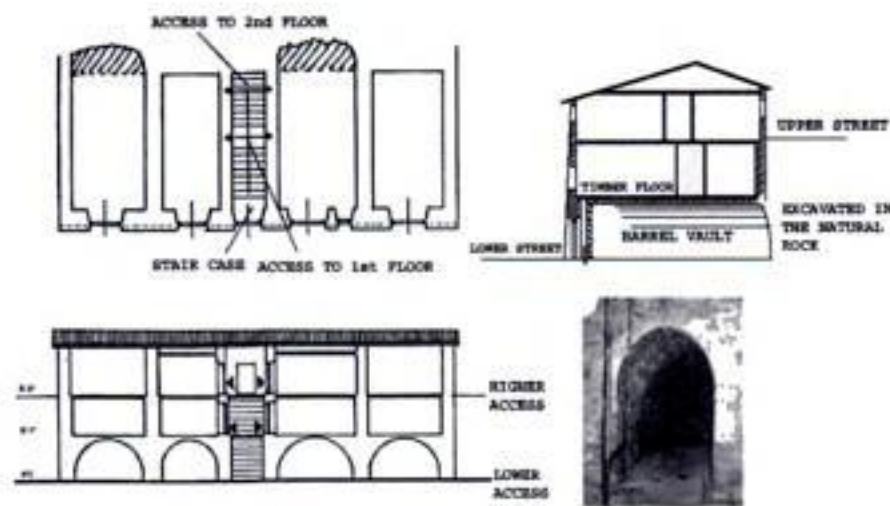


Figure 26. Row building typology.

Among the remaining buildings the most representative from the point of view of construction typology, structure and materials are chosen and on them the investigation procedure is applied. Geometrical, individuation of the building typology (isolated, in a row, complex) (Figs. 26, 27), crack pattern survey, comparison of the crack pattern to the abacus of the collapse mechanisms, laboratory tests (chemical, physical, mechanical tests are carried out on mortars

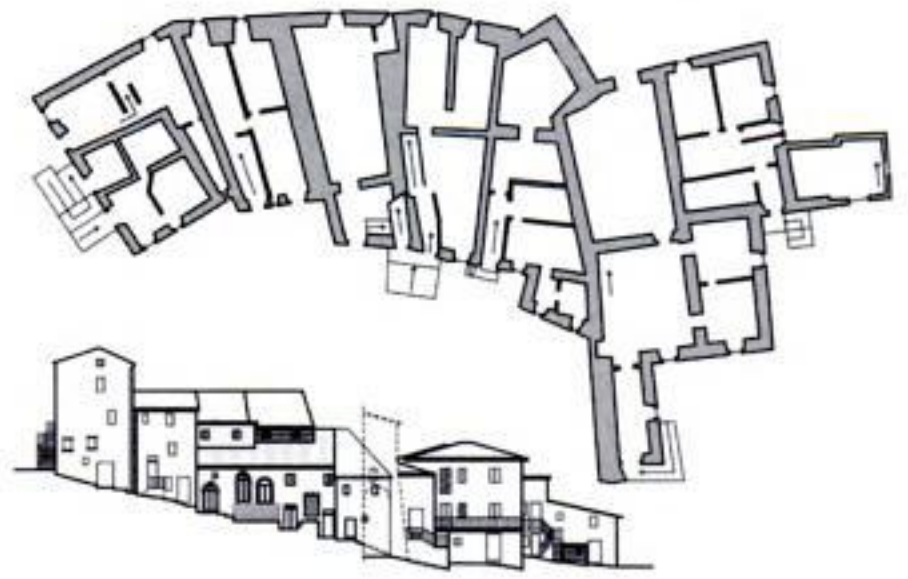


Figure 27. Complex building.

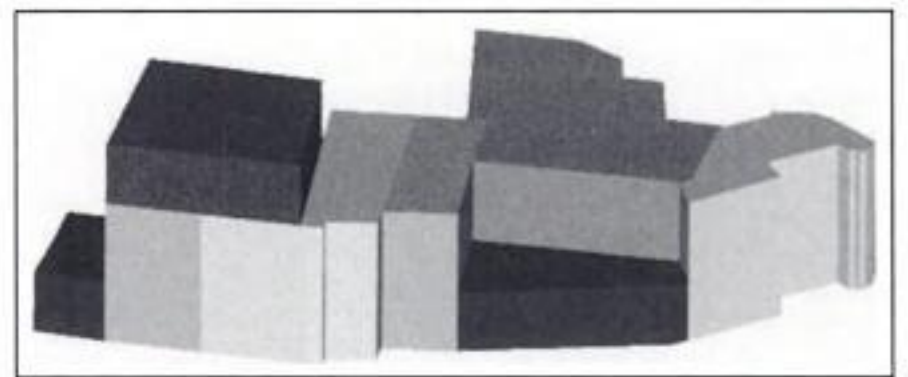


Figure 28. Example of constructive evolution phases of complex buildings.

and bricks and stones), simple on site tests (flat jack, sonic tests, drilling of cores, etc.).

In the case of complex buildings their evolution in time must be detected on site or through archive documents in order to study their vulnerability (Fig. 28).

Prevision of possible collapse mechanisms, analytical models for prevision of vulnerability of the centre and of the buildings.

Even if low cost and simple some on site NDT or minor DT can also be powerful at the level of urban investigation, in order e.g. to classify different masonry types and hence different building types (Fig. 29).

7.2 Investigation at building level

When the design for restoration or preservation of historic buildings has to be prepared, then a deep knowledge of the building is needed from its history and evolution in time to the geometry and typology of construction, to the structural elements (walls, columns, piers, floors, roof, etc.) to the possible decay and structural damages and their causes, to eventual monitoring systems to the effectiveness of the intervention. Then a design for investigation must be prepared by the future designer himself; he needs to at first inspect visually the building, understand the weakest points, formulate hypotheses on the damages and the causes,

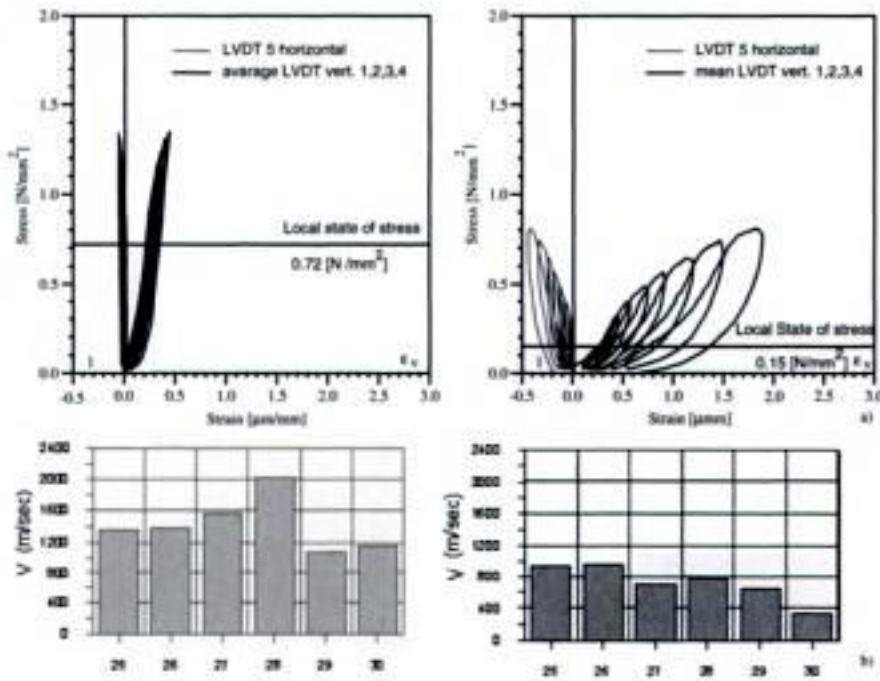


Figure 29. (a) Some results obtained with single and double flat-jack tests on the external wall of a church, of a bell tower and of a civil building; (b) representative results of the diagonal surface sonic measurements.



Figure 31. Tower and Cathedral of Cremona (Italy).

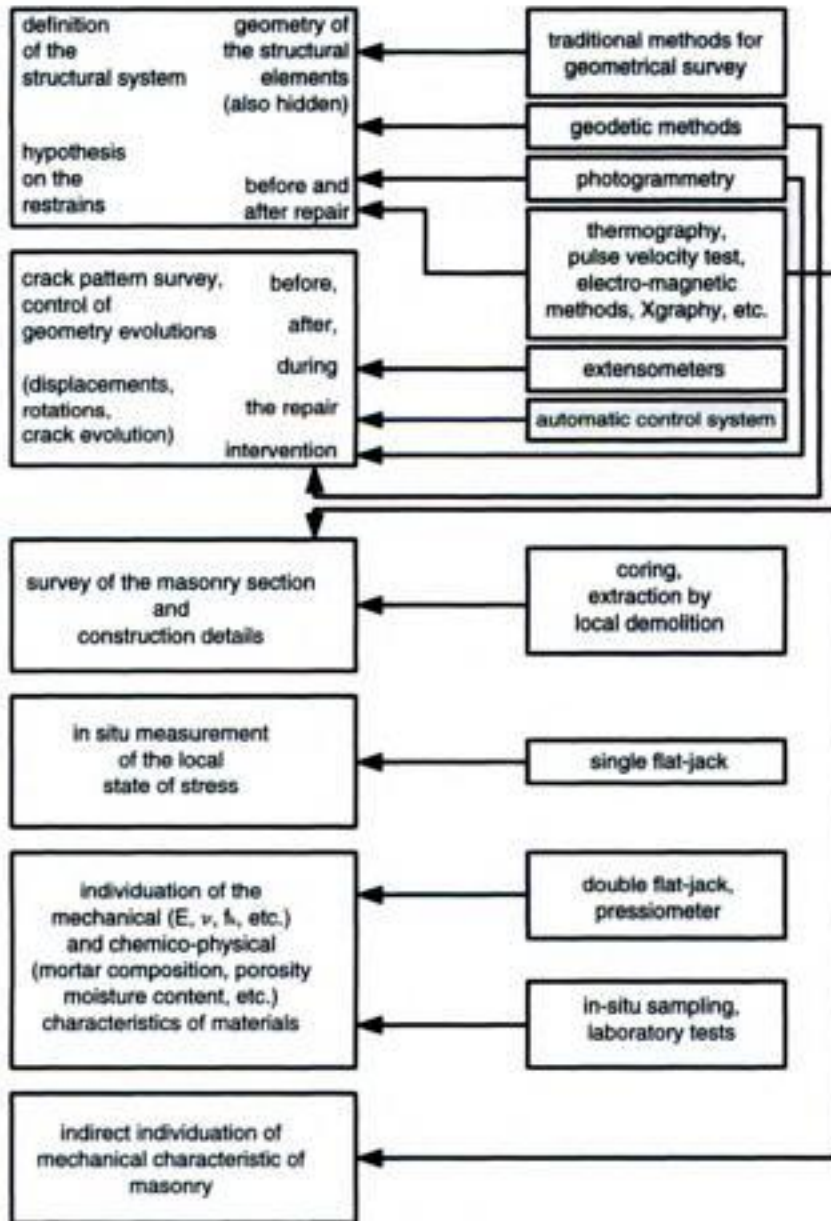


Figure 30. Information required and correspondent investigation techniques (Binda et al., 1994).

then to establish which investigation procedures better suit the building problems. This means that the architect or engineer who has to prepare the design for intervention, in order to choose appropriate techniques for repair, protection and strengthening must



Figure 32. S. Vitale Church at Ravenna (Italy).

choose appropriate investigation procedures and also apply them with an appropriate methodology.

The flow chart of Fig. 30 schematically presents a methodology to approach and solve the problem of structural investigation of an historic building, respectful of its integrity and applying the right investigation procedure to the different emerging problems.

On the left hand side the different unknowns are listed from the geometry of the structure to the crack pattern possible evolution, to the deep knowledge of material property and structural details.

This methodology was applied by the authors to various case histories with good success (Figs. 31, 32) (Binda et al., 2000; Binda et al., 2001).



Figure 33. Situation of a rural building in Milan in 1980 (a) and 1998 (b).

Obviously the designer has to remember that a single technique is frequently not enough to have the knowledge of defects, inclusion, voids in the structure but frequently techniques have to be used as complementary; this of course implies an appropriate budget reserved for investigation; therefore all the operations must be carefully chosen.

7.3 Investigation for maintenance

Lack of maintenance for a long time can be as destructive as exceptional events (earthquakes, floods) in a long range. Fig. 33 shows the effects of the environment on a historic building abandoned for twenty years. It has also to be remembered that most of the collapses occurring during earthquakes concern buildings which had no maintenance for a long time.

Therefore once the buildings has been repaired and starts functioning a project for maintenance must be prepared stating minimum investigation and monitoring operations in due times in order to fulfil the predicted service life.

The same investigation procedures mentioned in the previous sections can be applied. They should be NDT or MDT possibly easy, repeatable and at low cost.

8 CONCLUSIONS

An attempt has been made in the previous sections to point out the real necessity of a deep knowledge of the building before any intervention for its preservation is carried out. This knowledge in the case of historic buildings has been lost in the past century due to the use of new materials in the building industry. The only way architects and engineers have to follow in order to recover the lost information is to carry out an appropriate investigation, thanks also to the recent developments of sophisticated investigation procedures.

It must be clear that even if there is a need of consulting experts in the field, it is the designer, or a member of the design team, who must be responsible of the diagnosis and must: (i) set up the in-situ and laboratory survey project, (ii) constantly follow the survey, (iii) understand and verify the results, (iv) make technically acceptable use of the results including their use as input data for structural analyses, (v) choose appropriate models for the structural analysis, (vi) arrive at a diagnosis at the end of the study.

These operations can be accomplished with the help of experts in the field. Therefore information is needed for architects and engineers on the availability and reliability of the investigation techniques.

REFERENCES

- Abbaneo, S., Berra, M., Binda, L., 1996. "Pulse velocity test to qualify existing masonry walls: usefulness of waveform analyses", *3rd Conf. Non Destructive Evaluation of Civil Structures and Materials*, Boulder - CO, USA, 81-95.
- Aerojet General Corporation, 1967. *Investigation on sonic testing of masonry walls*, Final Report to the Dept. of General Services of Architecture and Construction, State of California.
- ASTM, 1991. *Standard test method for in situ compressive stress within solid unit masonry estimated using the flat-jack method*, ASTM C 1196-91, Philadelphia, ASTM.
- Bartoli, G., Blasi, C., Gusella, V., 1992. "Il sistema di monitoraggio della cupola del Brunelleschi: analisi dei dati rilevati (1988/1990)", *IV National Congress ASSI.R.C.CO.*, Prato, Italy, 445-455.
- Binda, L., Anzani, A., Mirabella Roberti, G., 1997. "The failure of ancient Towers: problems for their safety assessment", *Int. IABSE Conf. on "Composite Construction - Conventional and Innovative"*, Zurich, 699-704.
- Binda, L., Baronio, G., Gambarotta, L., Lagomarsino, S., Modena, C., 1999. "Masonry constructions in seismic areas of central Italy: a multi-level approach to conservation", *8NAMC 8th North American Masonry Conf.*, Austin, USA, 44-55.
- Binda, L., Cardani, G., Penazzi, D., Saisi, A., 2003. "Performance of some repair and strengthening techniques applied to historical stone masonries in seismic areas", *ICPCM a New Era of Building*, Cairo, Egypt, 18-20/2/2003, 2, 1195-1204.
- Binda, L., Cardani, G., Saisi, A., Modena, C., Valluzzi, M.R., 2004. "Multilevel Approach to the Analysis of the Historical Buildings: Application to Four Centers in Seismic Area Finalised to the Evaluation of the Repair and Strengthening Techniques", *13th International Brick/Block Masonry Conference*, RAI Amsterdam, July 4-7, CD-ROM.
- Binda, L., Falco, M., Poggi, C., Zasso, A., Mirabella Roberti, G., Corradi, R., Tongini Folli, R., 2000. "Static and Dynamic Studies on the Torrazzo in Cremona (Italy): the Highest Masonry Bell Tower in Europe", *Int. Symposium Bridging Large Spans: from Antiquity to the Present*, Istanbul, Turkey, 100-110.
- Binda, L., Gatti, G., Mangano, G., Poggi, C., Sacchi Landriani, G., 1992. "The collapse of the Civic Tower of

- Pavia: a survey of the materials and structure", *Masonry International*, 6(1), 11–20.
- Binda, L., Lenzi, G., Saisi, A., 1998. NDE of masonry structures: use of radar test for the characterisation of stone masonry, *Non Destructive Testing and Evaluation Int.*, 31(6), 411–419.
- Binda, L., Lenzi, G., Saisi, A., 1999a. "Radar Investigation for Diagnosis of Historic Buildings: Application to Stone Masonries", *8th Int. Conf. on Structural Faults and Repair*, London, CD-ROM.
- Binda, L., Lombardini, N., Guzzetti, F., 1995. "St. Vitale in Ravenna: a survey on materials and structures", *Int. Conf. on Historical Buildings and Ensembles*, invited lecture, Karlsruhe, Germany, 113–124.
- Binda, L., Lualdi, M., Saisi, A., Zanzi, L., Gianinetto, M., Roche, G., 2003. "NDT applied to the diagnosis of historic buildings: a case history", *3-Day Int. Conf. Structural Faults & Repair*, London, 1-3/7/2003, CD-ROM.
- Binda, L., Mirabella, G., Abbaneo, S., 1994. "The Diagnosis Research Project", *Earthquake Spectra*, 10(1), 51–170.
- Binda, L., Mirabella Roberti, G., Guzzetti, F., 2000a. "St. Vitale in Ravenna: A Survey on Materials and Structures", *Int. Symposium Bridging Large Spans: from Antiquity to the Present*, Istanbul, Turkey, 89–99.
- Binda, L., Saisi, A., Tiraboschi, C., 2001. "Application of Sonic Tests to the Diagnosis of Damage and Repaired Structures", *Non Destructive Testing and Evaluation Int.*, 34(2), 123–138.
- Binda, L., Saisi, A., Tiraboschi, C., 2000b. "Investigation procedures for the diagnosis of historic masonries", *Construction and Building Materials*, 14(4), 199–233.
- Binda, L., Tiraboschi, C., 1999. "Flat-Jack Test as a Slightly Destructive Technique for the Diagnosis of Brick and Stone Masonry Structures", *Int. Journal for Restoration of Buildings and Monuments, Int. Zeitschrift für Bauinstandsetzen und Baudenkmalpflege*, Zurich, 449–472.
- Binda, L., Tiraboschi, C., Tongini Folli, R., 1998b. "On site and laboratory investigation on materials and structure of a Bell-Tower in Monza", *2nd Int. RILEM Conf. on Rehabilitation of Structures*, Melbourne, Australia, 542–556.
- Gentile, C., Saisi, A., Binda, L., 2002. "Dynamic investigation of a historic masonry Bell Tower", *6th International Masonry Conference*, London, 4th–6th November, 192–199.
- Lenzi, G., Ludwig, N., Rosina, E., Saisi, A., Binda, L., 1997. "Analisi di tessiture murarie mediante termografia e georadar", *V Congresso Nazionale ASS.I.R.C.CO*, Orvieto – Italy, 142–146.
- Niederwanger, G., 1997. "Structural Repair of Damaged Old Bell Towers Based on Dynamic Measurements", *5th Int Conf. on Structural Studies, Repairs and Maintenance of Historical Buildings STREMAH97*, S. Sebastian, Spain, 447–456.
- Padaratz, I.J., Forde, M.C., 1995. "Influence of Antenna Frequency on Impulse Radar Surveys of Concrete Structures", *6th Int. Conf. on Structural Faults and Repair*, London, 2, 331–336.
- Penazzi, D., Valluzzi, M.R., Cardani, G., Binda, L., Baronio, G., Modena, C., 2000. "Behaviour of Historic Masonry Buildings in Seismic Areas: Lessons Learned from the Umbria-Marche Earthquake", *12th Int. Brick/Block Masonry Conf.*, Madrid, Spain, 217–235.
- Rossi, P.P., 1982. Analysis of mechanical characteristics of brick masonry tested by means of in situ tests, *6th IBMaC*, Rome, Italy.
- Rossi, P.P., 1997. "Possibilities of the Experimental Techniques for the Structural Analysis of Historical Constructions", *CIMNE*, Barcelona, Spain, 24–46.
- Schuller, M.P., Berra, M., Atkinson, R., Binda, L., 1995. "Acoustic Tomography for Evaluation of Unreinforced Masonry", *6th Int. Conf. on Structural Faults and Repair*, London, 3, 195–200.
- Valle, L., Zanzi, L., Binda, L., Saisi, A., Lenzi, G., 1998. "Tomography for NDT applied to masonry structures: sonic and/or EM methods", *2nd Int. Arch Bridge Conf.*, Venezia, 243–254.
- Valle, S., Zanzi, L., Lenzi, G., Bettolo, G., 1997. "Structure Inspection with Radar Tomography", *Int. Coll. on Inspection and Monitoring of the Cultural Heritage*, IABSE-ISMES, 223–230.

Evaluation and analysis of the old timber structures

A. Ceccotti

Trees and Timber Institute, IVALSA-CNR, Florence, Italy

ABSTRACT: A methodology for evaluating the actual load-bearing performance of an ancient timber construction is given in this paper based on a simple non-destructive approach. Materials and methods are illustrated and discussed. Examples are given emphasizing the key points of the decision making procedure. Final considerations with particular reference to the “minimum intervention” principle conclude the work.

1 INTRODUCTION

Before an ancient timber structure the structural designer is always asked for the fundamental question: what to do with this structure? That actually means: how sound are wood elements and joints? Is this structure capable of standing up for many years more, even under new service loads? Are any strengthening and repair needed?

Having in mind the conservation of the structure as main-guidance line, in order to take the most appropriate decision, the designer should follow a multi-disciplinary approach.

2 A METHODOLOGY FOR EVALUATION AND ANALYSIS

There are two basic and separate questions actually:

- is the wood still sound?
- is the wood enough resistant?

In fact resistance is a matter not only of wood soundness but also it is a matter of wood actual stress compared to wood actual strength. Evaluation of wood conditions and strength and analysis of forces and stresses are two moments of the same process. In Table 1 a synopsis of these points is given referring to a simple case of a single wooden rectangular cross section (b' original width, h' original depth) under a only bending moment M :

$$\frac{f_{m,k(5\%)}}{\gamma_M} k_{mod} = f_{m,d} \geq \sigma_{m,d} = \gamma_f \sigma_{m,k} = \gamma_f \frac{6M_k}{bh^2}$$

γ_M and γ_f safety coefficients (>1) cover further uncertainties about possible actual strength values and

Table 1. Evaluation and analysis process (schematic).

<i>Evaluation (Wood Technologist)</i>	
Decay detection – Residual cross section	$\rightarrow b, h$
Strength grading, in situ	\rightarrow timber grade
Anticipated strength	$\rightarrow f_{m,k(5\%)}$
Uncertainties	$\rightarrow \gamma_M$, material side safety coefficient
<i>Analysis (Structural Engineer)</i>	
Actions (loads, q_k)	
Structural scheme for calculations:	$q_k \rightarrow M_k$
Stresses on elements:	$M_k \rightarrow \sigma_{m,k}$
Uncertainties	$\rightarrow \gamma_f$, action side safety coefficient

acting load values (nominally intended for passing from 5th percentile to 0,5th percentile, lower tail for strength distribution and higher tail for load distribution, respectively). k_{mod} is a modification factor taking into account service conditions and duration of load effects (see Table 3).

2.1 Evaluation phase

Evaluation phase consists of:

- evaluation of possible biological decay across the member section and along the member itself. This allows to determine the residual cross-section dimensions along the entire length of the member to be used by the Engineer in his calculations (Bonamini, 1995).
- in-situ grading, i.e. evaluation of the strength of sound timber according to grading rules accepted for that kind of timber.

2.1.1 Important remarks

2.1.1.1 Grading

For a certain timber population (wood species, location of origin, grade) it will be possible to assign a set

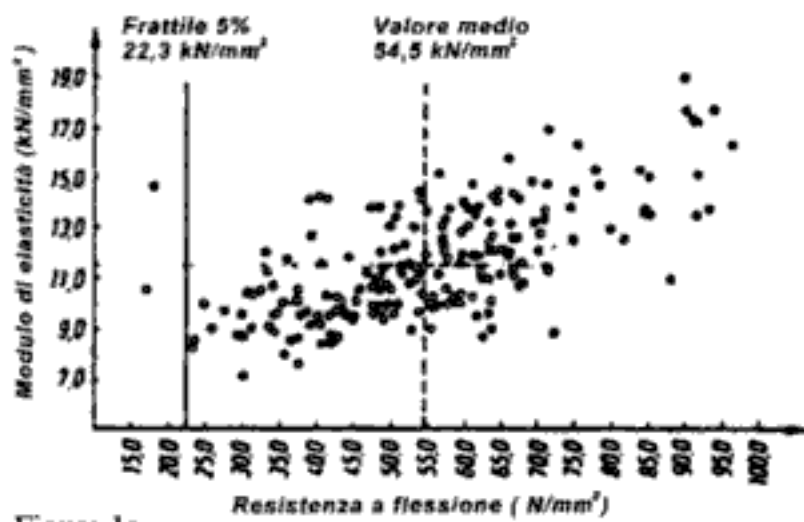


Figure 1a.



Figure 1b.

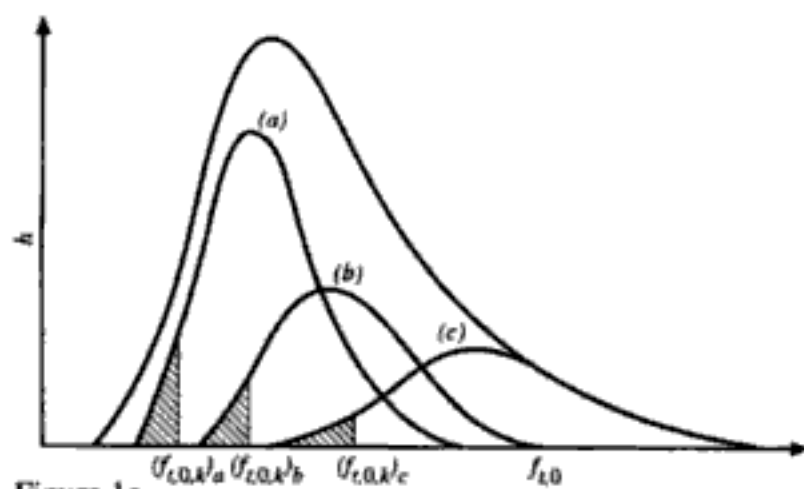


Figure 1c.

Figure 1a–c. Strength grading. Grading allows to separate better timbers from less resistant ones. With no grading, for the same timber population, strength could range from 15 to 95 Mpa (top, left) like in the case of Swiss pine beams. By grading pieces into strength-quality groups (a,b,c grades, for example) it is possible to classify timbers (top, right) according to their resistance. Grading rules are different over the world because locally calibrated on locally grown timbers. Grade determining defects are usually knots, slope of grain, annual rings thickness et cetera. For each grade, after an extensive testing campaign on that timber population, the relevant characteristic strength values (5th percentile) can be found (below). Grading rules are not 100% efficient because they do not allow to put all the best pieces in the upper class, for example, and the worst pieces in the lowest class neither (below), but they are nevertheless essential because they separate timbers according to their characteristic resistance anyway. Please note that in the same grade we have 95% of pieces more resistant than the 5% strength.

of strength values for different kinds of stress (strength profile). In fact everywhere in the world there are grading rules that allow to grade timbers according to their strength (Figure 1). Every country has its own rules calibrated upon home grown timbers peculiarities. Therefore there are tables available that attribute each timber population to a certain strength profile (strength class), see Table 2.

2.1.1.2 Strength

It is here necessary to remind the Reader that old timber characteristic strength values (e.g.: $f_{m,k(5\%)}$) are used as high as for “new” timber. It is actually acknowledged that timber is not losing its strength over time just because is becoming older (excluding of course any decay due to insects and fungi). In fact there is no real evidence that long lasting pre-loading of timber or timber structures to a limited load level has produced any damage (Kuipers, 1986), see Table 4.

2.2 Analysis phase

Analysis phase consists of:

- Internal forces analysis conducted by using the simplest structural scheme, at first. Then more and more accurate analysis which takes into account as much as possible of the actual restraints and of actual mechanical behaviour of materials. That include, for example, semi-rigid behaviour of joints (slip), and possible structural gross deformations and disorders. More and more sophisticated models (i.e. anisotropy of wood, II order analysis) should be adopted only when the complexity of the structure requires it. The more the scheme is reality-bound (e.g. considering hyperstatic behaviour, load sharing, et cetera) the more force peaks decrease so that verifications are facilitated, i.e. a better model, though more complex and time demanding, at the end of the entire process will be rewarding (see Figures 3–4).
- Stress analysis, it is possible to pass from internal forces to stresses using well consolidated calculation methods, as for example Eurocode 5, 1993 (usually the limit states design methods are more generous than allowable stresses methods). Then a safety check becomes possible referring to strength values given by standards, as said before.

3 DECISION MAKING

If the verification, by applying the previously illustrated method, is positive, this is sufficient to state that the structure is safe enough. However the opposite is not true. In fact it must be said that when using the above approach based on modern calculation codes and characteristic strength profiles and standard

Table 2a–2b. Strength classes and the “Magic” table, assignment of visual grades and species according to CEN/TC 124.215. Table gives coniferous timbers and source combinations matching strength class C24 profile.

	C14	C16	C18	C22	C24	C27	C30	C35	C40
in N/mm ²									
$f_{m,k}$	14	16	18	22	24	27	30	35	40
$f_{c,0,k}$	8	10	11	13	14	16	18	21	24
$f_{c,90,k}$	0,3	0,3	0,3	0,3	0,4	0,4	0,4	0,4	0,4
$f_{c,0,k}$	16	17	18	20	21	22	23	25	26
$f_{c,90,k}$	4,3	4,6	4,8	5,1	5,3	5,6	5,7	6,0	6,3
$f_{c,k}$	1,7	1,8	2,0	2,4	2,5	2,8	3,0	3,4	3,8
in kN/mm ²									
$E_{0,mean}$	7	8	9	10	11	12	12	13	14
$E_{0,05}$	4,7	5,4	6,0	6,7	7,4	8,0	8,0	8,7	9,4
$E_{90,mean}$	0,23	0,27	0,30	0,33	0,37	0,40	0,40	0,43	0,47
G_{mean}	0,44	0,50	0,56	0,63	0,69	0,75	0,75	0,81	0,88
in kg/m ³									
ρ_k	290	310	320	340	350	370	380	400	420

Strength classes and characteristic values according to EN 338. Coniferous species and poplar.

Table 2b.

Strength class	Grading rule publishing country (Grading standard)	Grade	Species commercial name	Source	
C24	Austria (ÖNORM B 4100-2)	G.BH	Spruce, Pine, Fir, Larch	CNE Europe	
	France (NFB 52001-4)	CF22	Whitewood, Douglas fir	France	
	Germany (DIN 4074-1)	S10	Spruce, Pine, Fir, Larch	CNE Europe	
	Nordic Countries (INSTA 142)	T2	Redwood, Whitewood	NNE Europe	
	The Netherlands (NEN 5466)	B	Spruce + fir	NC Europe	
	UK (BS 4978)		SS	Redwood, Whitewood	CNE Europe
			SS	Douglas fir, Larch, Hem-fir, S-P-F	USA + Canada
			SS	Southern pine	USA
			SS	Parana pine	Brazil
	USA + Canada (NGRDL + NLGA)		SS	Pitch pine	Caribbean
J + P Sel			Douglas fir, Larch, Hem-fir, S-P-F	USA + Canada	

CNE Europe: Central, North & Eastern Europe, NNE Europe: Northern & North eastern Europe, NC Europe: Northern and Central Europe.

grading rules, when the verification would fail at first approach, an appeal should be given to the structure.

We do not want to touch here the issue of possible reduced safety coefficients due to the fact that the structure is already existing (modern calculation codes are thought for not-yet existing structures). Therefore

uncertainties about the material still to be provided are much less because the material is already there and we can see it in place. Moreover, load standards are changed over the years increasing snow loads, for example, where our structure does exist from centuries with no interest in human discussions.

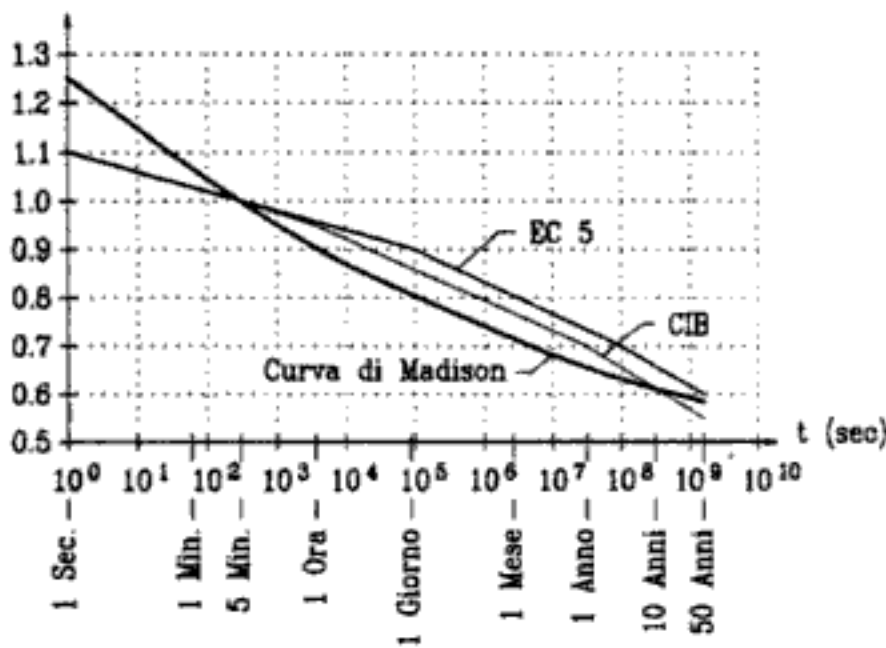


Figure 2a-c.

Table 3. Load-duration classes and k_{mod} for solid timber and glulam.

Load-duration class	Duration ^a	Examples of loading	k_{mod} for Service classes	
			1 & 2	3
Permanent	More than 10 years	Self weight	0,60	0,50
Long-term	6 months–10 years	Storage	0,70	0,55
Medium-term	1 week–6 months	Imposed load	0,80	0,65
Short-term	Less than one week	Snow ^b and wind	0,90	0,70
Instantaneous		Accidental load	1,10	0,90

^a The Load-duration classes are characterised by the effect of a constant load acting for a certain period of time. For variable action the appropriate class depends on the effect of the typical variation of the load in the life of the structure. The accumulated duration of the characteristic load is often very short compared with the total loading time.

^b In areas with a heavy snow load for a prolonged period of time, part of the load should be regarded as medium-term.

Figure 2 and Table 3. Duration of load effect. Duration of load effect is illustrated here according to EC5, CIB W18 code and Madison curve (Giordano, 1999) where time is in a logarithmic scale (x axis). Stress ratio as reported on y axis, is the ratio between the actual strength and the 5-minute-duration test strength. It is easy to see that under 50% of short term load resistance (so-called creep limit) the time-to-failure is almost infinite. That means that there is no damage at all inside the wood. Remember that when loaded under quasi-permanent load combinations the stress ratio is 15–20% of 5 minute strength. Possibility of internal damage due to long lasting action of loads that may overcome the creep limit for a certain duration of time is anyway considered by codes with the modification factor k_{mod} according to the time of accumulated duration of load at maximum level (characteristic, 5% fractile). Service conditions are: class 1, indoor; class 2, indoor or outdoor protected; class 3, outdoor not protected.

We want just to say that more sophisticated structural schemes, closer to reality, should be used in this case. In addition, grading of timber elements should be done ad hoc on the spot where the safety verification is actually performed (so called critical sections).

Actually a timber element is classified into strength grades according to some defects, basically. It is not possible to know a priori where in situ that element will be located, how it will be loaded, and where the most stressed section will stay (critical section). Therefore timber elements are classified by the timber supplier independently from the location of the grade determining defect along the timber element itself. Let's consider the case, for example, of an isolated big knot as the grade determining defect. Once the timber element has been put in place, if this knot is just near bearing supports or at the extra-dos of a bent beam, it will have much less importance than if it would be staying at the mid-span intra-dos of a bent beam. Old carpenters were actually used to put the best pieces in the most stressed parts of the structure! (see Figure 5).

In conclusion: if first safety check is not positive, before to make a life sentence (demolition or strengthening) a second chance should be given to the element, making an ad hoc re-classification of the timber element right around the critical section aiming for an up-grading of the element.

More: we have to say that even the ad hoc grading, refers to 5% lower fractile strength characteristic values, that means there is still a high chance that our element will be more resistant than that value.

Advanced research in wood mechanics field, for example using Non Destructive Testing methods coupled with analytical tools, could help to guess an actual strength value (see Table 4 and Figure 6).

4 CONCLUSIONS

Wooden cultural heritage's most dangerous enemy today is insensibility, and lack of maintenance, of course. However there is another risk equally frightening that appears just when conservation works have been launched.

This sneaking enemy is the "Do something, anyway" philosophy. "This wood is too old, it has lost its strength!" or "this element is going to fall down on us, it does not satisfy the last code on loads!" and so on, are typical examples, but many others could be given, that may lead to unnecessary reinforcement to the detriment of cultural authenticity.

Wood technologists and structural engineers have the privilege of mastering evaluation tools and analytical models that can help professionals in making the best decision in various circumstances, so that a new philosophy, with more respect and more knowledge will take over.



Figure 3a.

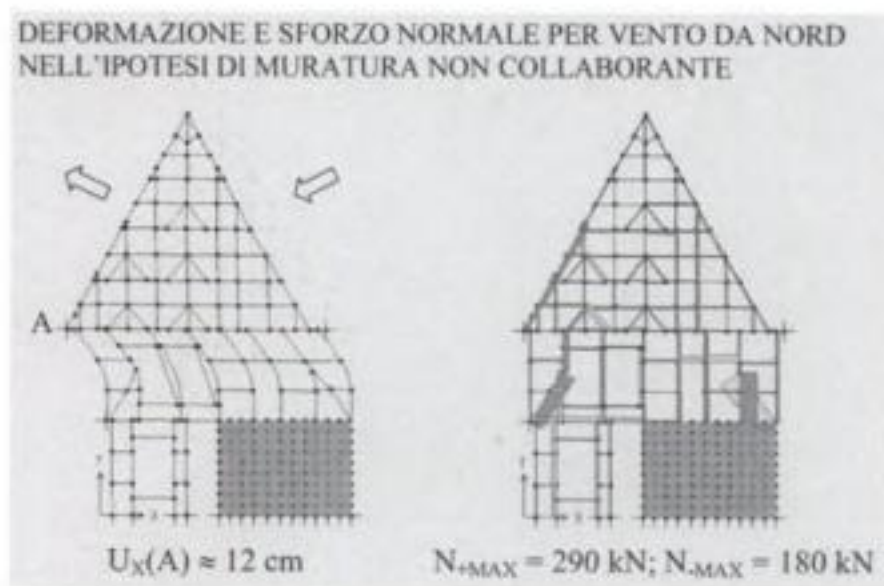


Figure 3d.

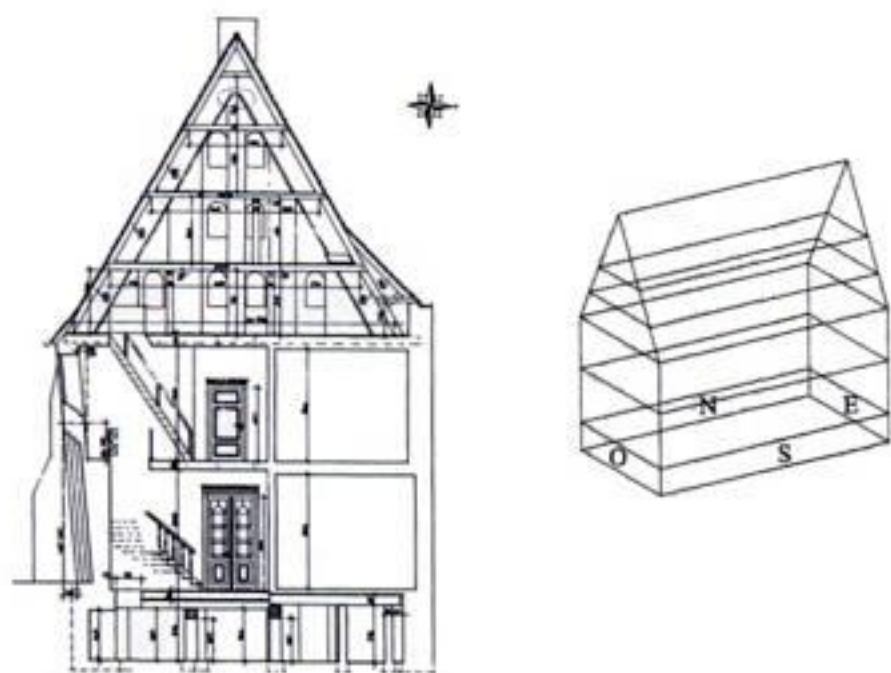


Figure 3b.

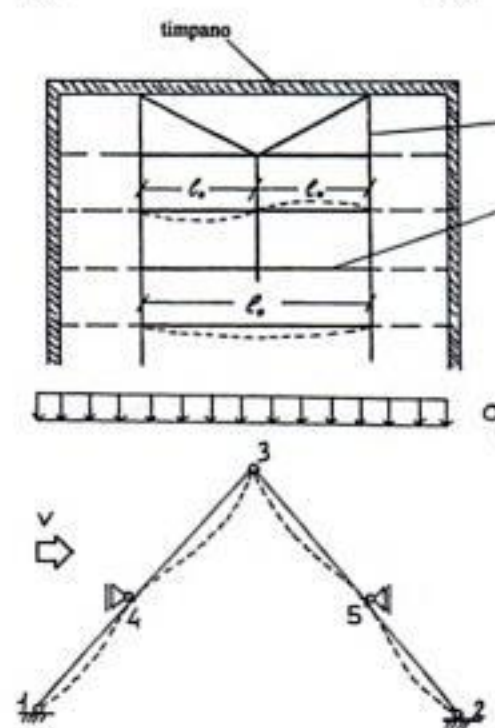
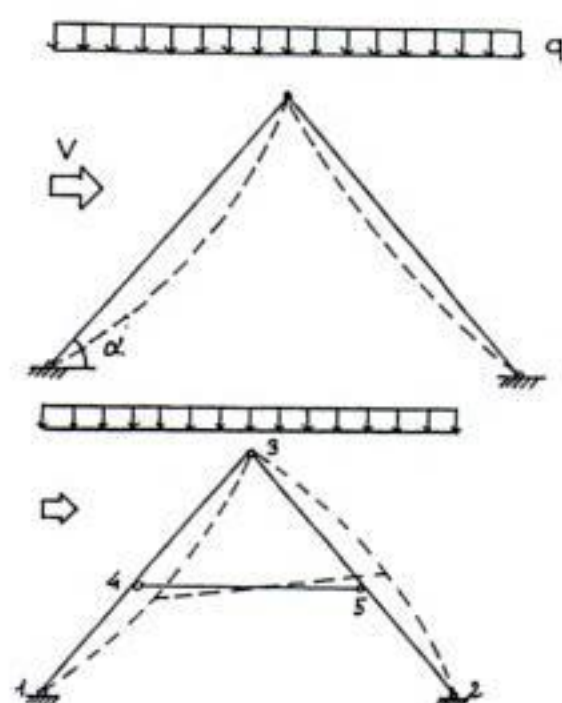


Figure 3e.

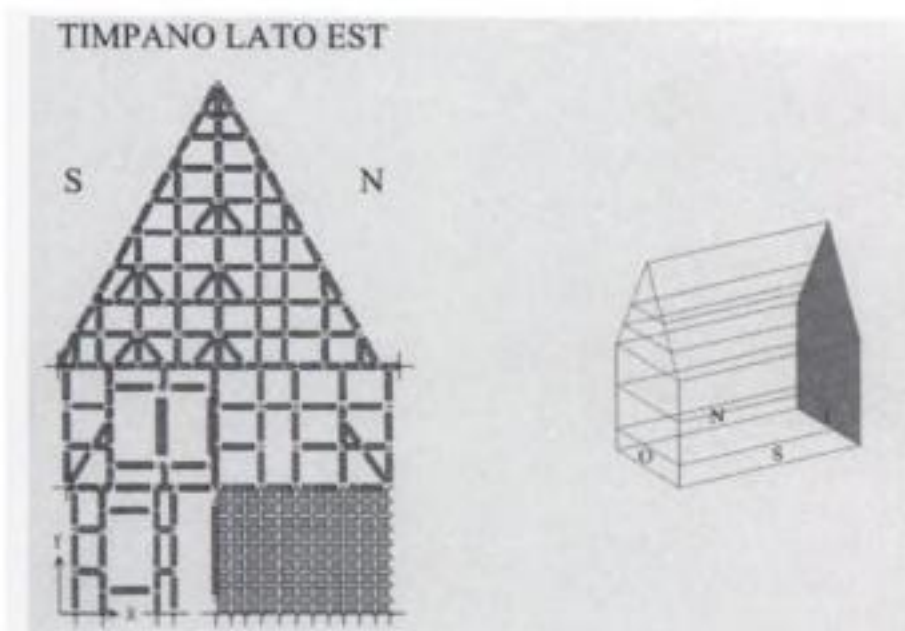


Figure 3c.

Figure 3a–3e. Simple models are very important in determining rapidly, even in a rough way the load distribution within the structure. This approach is usually conservative, because does not take into account possible re-distribution effects. More advanced models allow a finer evaluation of load distribution and give a better load-path with a reduction of peak forces.

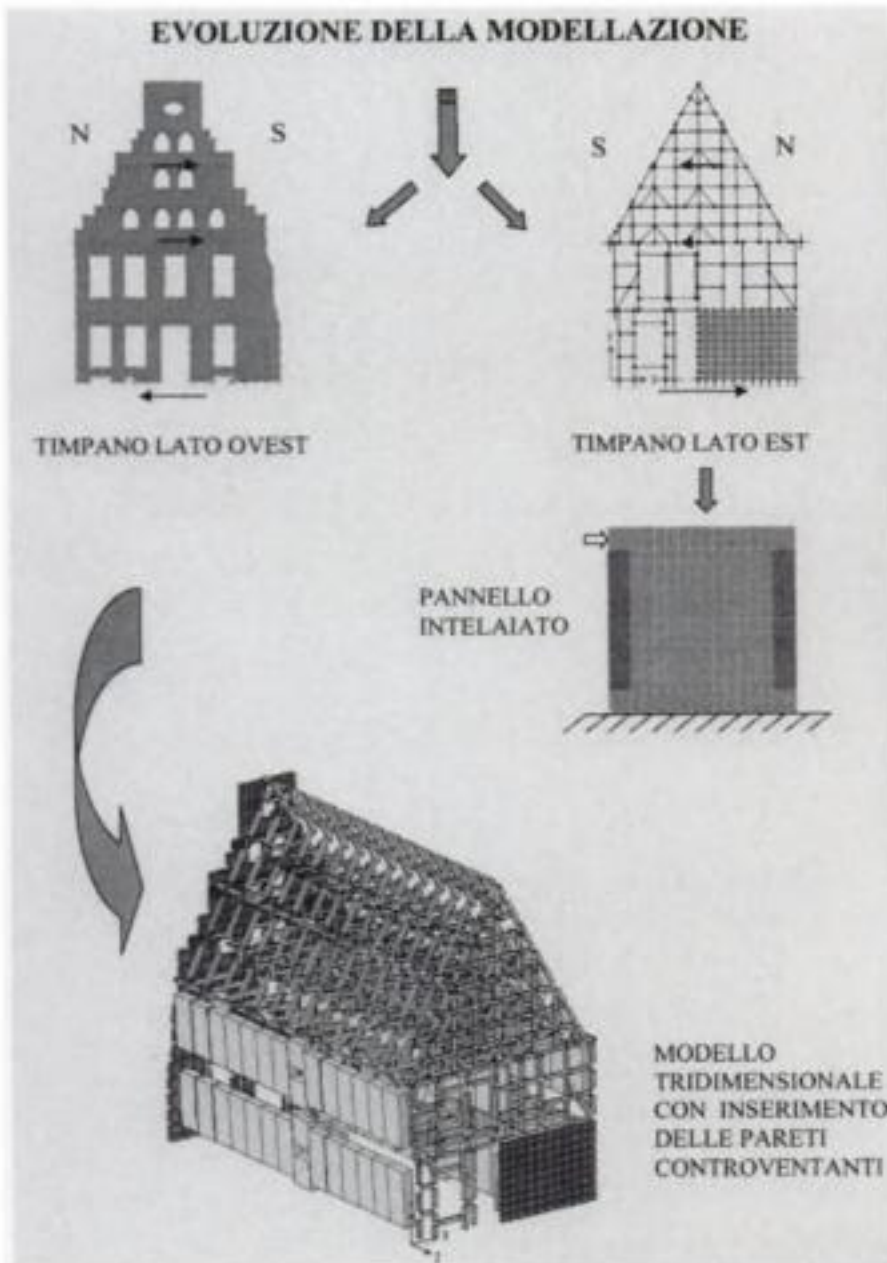


Figure 4a.

15 kN

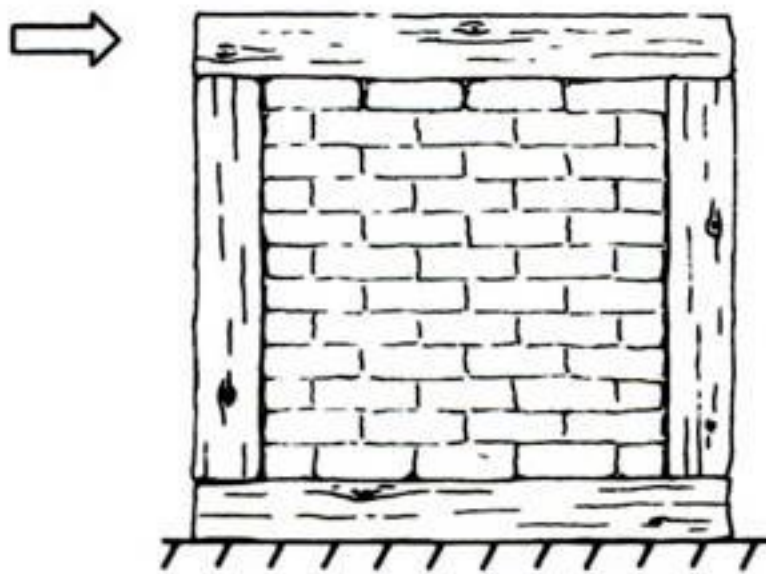


Figure 4b.

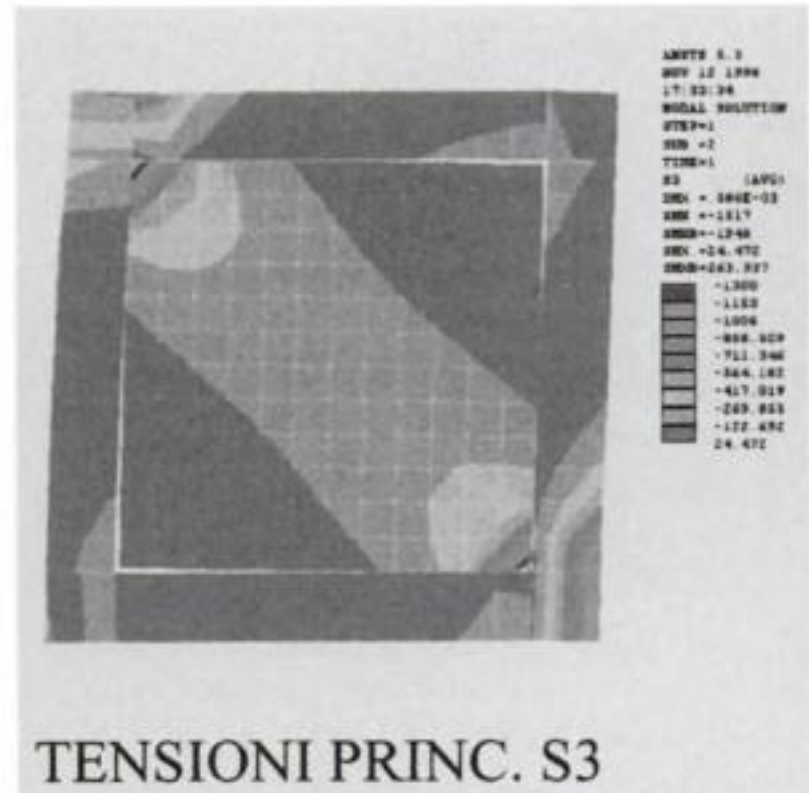


Figure 4c.

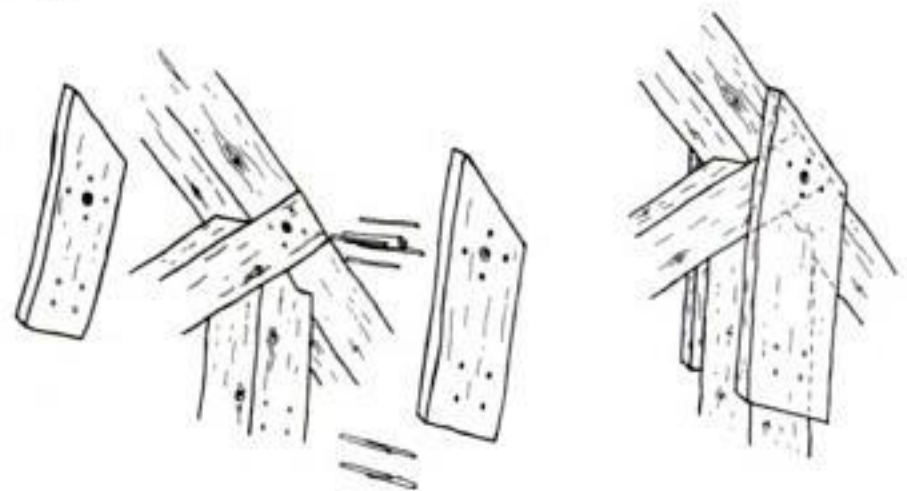


Figure 4d.

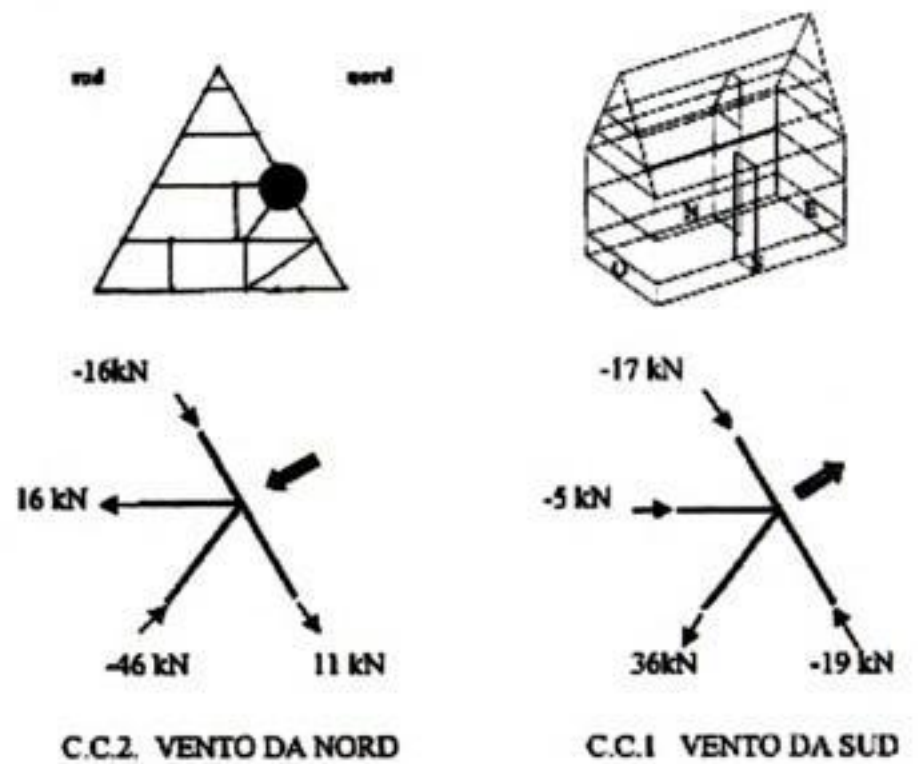


Figure 4e.

Figure 4a–4e. In some cases when the mechanical behaviour is very complicated to determine, tests should be performed, and/or highly sophisticated models used. This does facilitate verification and allows the adoption of very essential strengthening solutions. Tables 5a and 5b are a synopsis of the Master thesis of Ms **Angela Bevilacqua** on “Strengthening of 16th Century wood-masonry building in Wismar”, 1998, University of Florence, Italy.



Figure 5a.

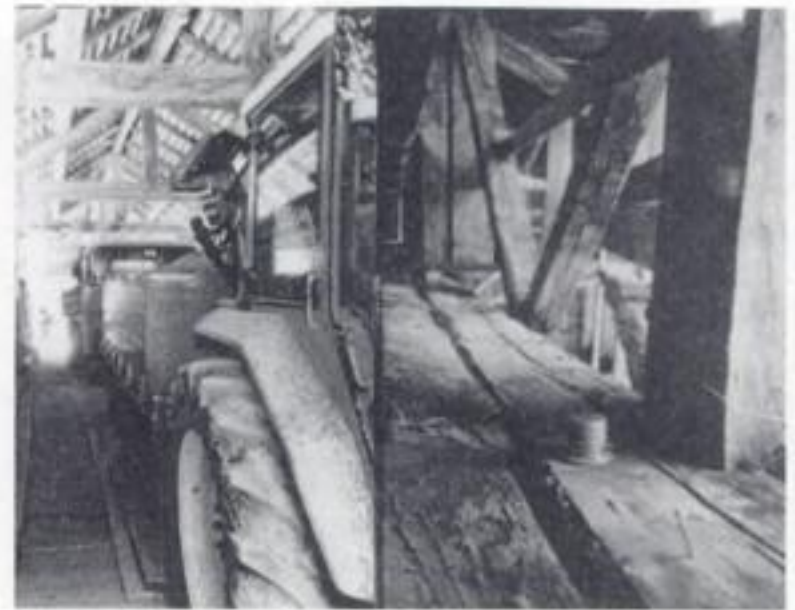


Figure 5b.

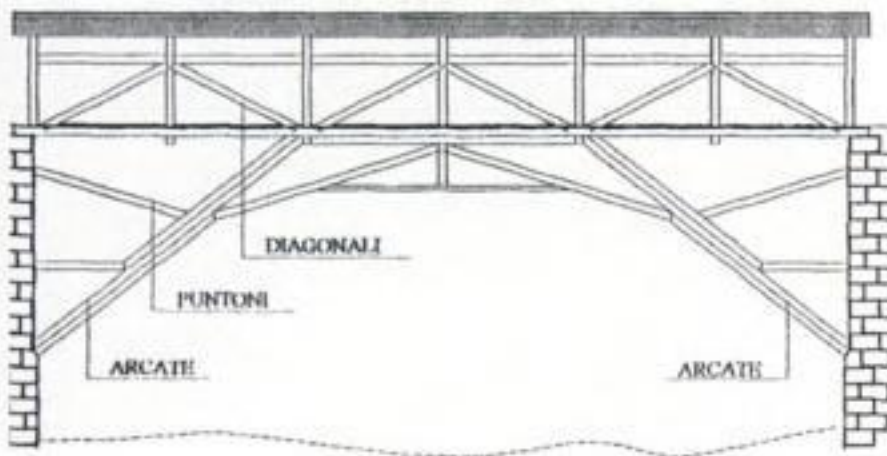


Figure 5c.

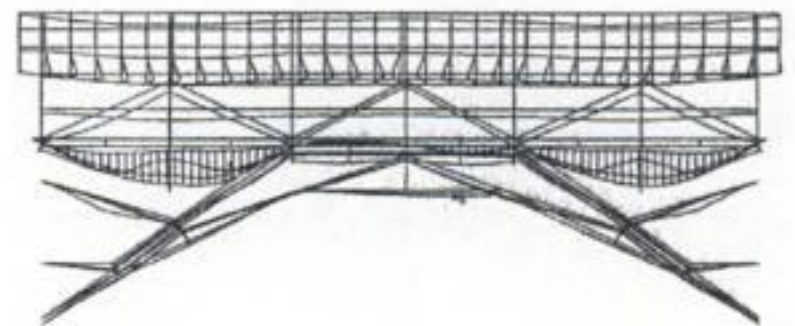


Figure 5d.

Figure 5a–d. Panchia (Trento, Italy) bridge. Accurate modelling coupled with in situ load tests allowed to identify the best way to preserve the cultural authenticity of the bridge without compromising users safety. To reduce car traffic induced bridge vibration the deck planks were simple inclined at 45° respect to traffic direction.

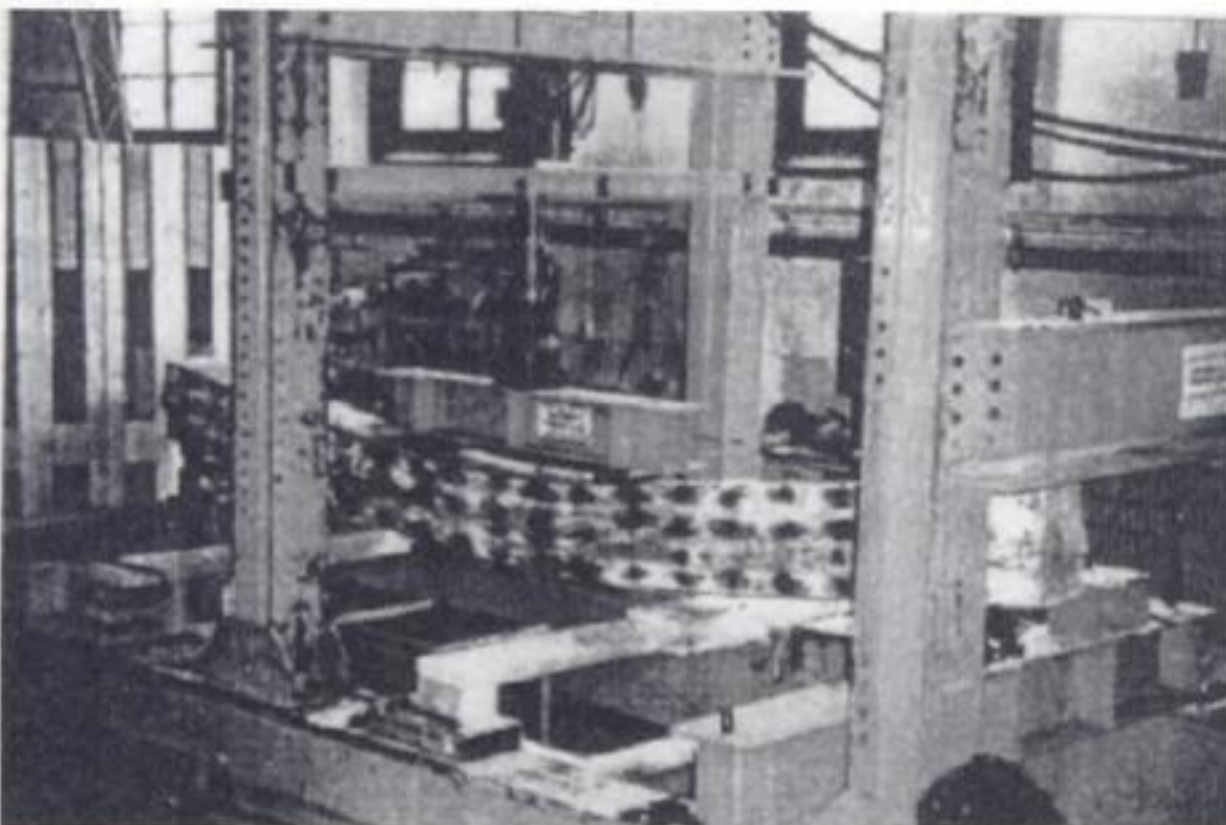


Figure 6a.



Figure 6b.

Table 4.

Beam	Density (kg/m ³)	E ₀ (N/mm ²)	F _m (N/mm ²)	Failure determining defect(s)
T1	480	8689	25.0	Ring shake, checks
T2	483	8273	28.0	Ring shake, checks
T3	516	18266	39.6	Checks
T4	464	13048	25.8	Ring shake, checks
T5	487	12906	44.8	Slope of grain, knot
T6	505	10355	33.9	Localised decay
T7	464	8102	30.9	Knots, diffuse decay
T8	513	14013	47.0	Checks
T9	498	11747	38.5	Knots
T10	478	12243	29.4	Checks
T11	469	7104	15.3	Diffuse decay
T12	449	11630	30.1	Checks

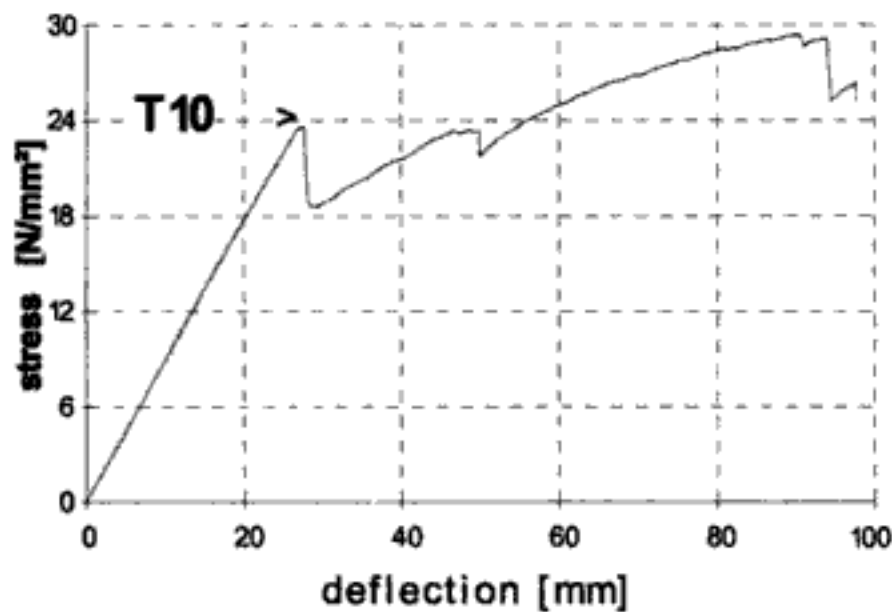


Table 4 and Figure 6a–6b. Large cross sections beams show an interesting semi-ductile behaviour because knots are collapsing one after the other allowing the beam to recover partially (if load sharing is permitted). In a series of results from Dr Marco Togni is shown that only 1 over 12 beams, discarded from the building site because considered not reliable, gave a strength low as 15 Mpa. **Marco Togni** (1995); “Elasticity and strength of large cross-section old timber beams: mechanical evaluation with NDT in situ”, Doctoral thesis, University of Florence, Italy (in Italian).

REFERENCES

- Kuipers, J. 1986. Effect of Age/or Load on Timber Strength. In *Proceedings of CIB W18 meeting, Paper 19-6-1*. Florence, Italy.
- Ceccotti, A & Uzielli, L. 1989. Reliability of Ancient Timber Structures. In G. Tampone (ed) *Proceedings of II National Italian Congress on Wood Restoration*. Firenze: Nardini (in Italian).
- Uzielli, L. 1995. Restoring timber structures – Repair and strengthening. *STEP 2 Timber Engineering, lecture D4*. Centrum Hout, The Netherlands.
- Bonamini, G. 1995. Restoring timber structures – Inspection and evaluation. *STEP 2 Timber Engineering, lecture D3*. Centrum Hout, The Netherlands.
- Giordano, G. & Ceccotti, A. & Uzielli, L. 1999. *Timber Engineering*. Milano: Hoepli (in Italian).

Remedial measures for the Cathedral of Porto: a post-modern conservation approach

P.B. Lourenço

University of Minho, Department of Civil Engineering, Guimarães, Portugal

Â. Melo & M. Carneiro

Portuguese Institute for the Architectural Heritage, Ministry of Culture, Porto, Portugal

ABSTRACT: The present paper presents the works recently carried out at the Cathedral of Porto as a case study of a difficult intervention that challenges current recommendations for the architectural heritage. The historical information is briefly reviewed and the general conservation approach for the different works is addressed. Afterwards, the aspects regarding the strengthening of the towers are treated with more detailed and the diagnostics of a chapel, incorporating the usage of limit analysis for safety evaluation, is presented.

1 INTRODUCTION

The cathedral is not a beautiful building, it does not surrender to love at first sight. In fact, stronger feelings and emotions can only result from a comprehension of the building's nature.

The works being carried out also fail to provide immediate adhesion. In the framework of a "restoration in continuity", the works resemble a "no-intervention" or a sort of zero level of architecture. Nevertheless, the authors believe that such a superficial impression is erroneous. The intervention is rooted in options clearly belonging to the disciplinary field of architecture, with an approach that evolved as a result of the knowledge of the building and not an *a priori* posture. The vanishing appearance of the intervention is not equal to a facing approach, because several levels of remedial measures co-exist, and some of them are profound.

2 THE INHERITED BUILDING – FROM THE EVOLUTIONAL TO THE RETURN TO ITS ORIGIN

The origin of the building is the middle of the 12th century. In this period it is possible to witness the construction of cathedrals in the main cities, across Europe, as a token of a renewed confidence within the urban communities.

The settlement is conceived as an answer to a program that can be referred to as the church where the

bishop celebrates, and where an elite of the clergies meet and advise their bishop in the administration of material and immaterial assets of the diocese.

For 800 years, the settlement was a repository of added parts. From this state of a continuous construction yard, the main fabrics are: romanesque and proto-gothic, gothic, renaissance, mannerist, baroque, neoclassic, contemporary works from the first half of the 20th century and, finally, the present intervention.

Although the works until the end of the 19th century can be identified by the style and the building techniques, all of them possess a severe common transforming attitude, that is, they add, superimpose, rebuilt, change or render. While the campaign of the 20th century, which lasted from 1918 to 1938 and was carried out after expropriation and classification of the settlement as a national monument, did not aim at transforming the building, but at restoring it, as a sort of time regression, performed with works aiming at bringing back the original style – the medieval.

During this period, the country kept itself at a distance from the industrial progress of the rest of Europe and, between modernity and tradition, Portugal chose the latter. The Medieval Age and Art, celebrated in the official culture as ethical and aesthetical patterns, participated in the construction of the imaginary associated to the valuation of a national identity, being particularly exalted in the public building, built from scratch or restored when historical.

This ideal identity incorporated values such as austerity, purity and trueness, which were then attributed

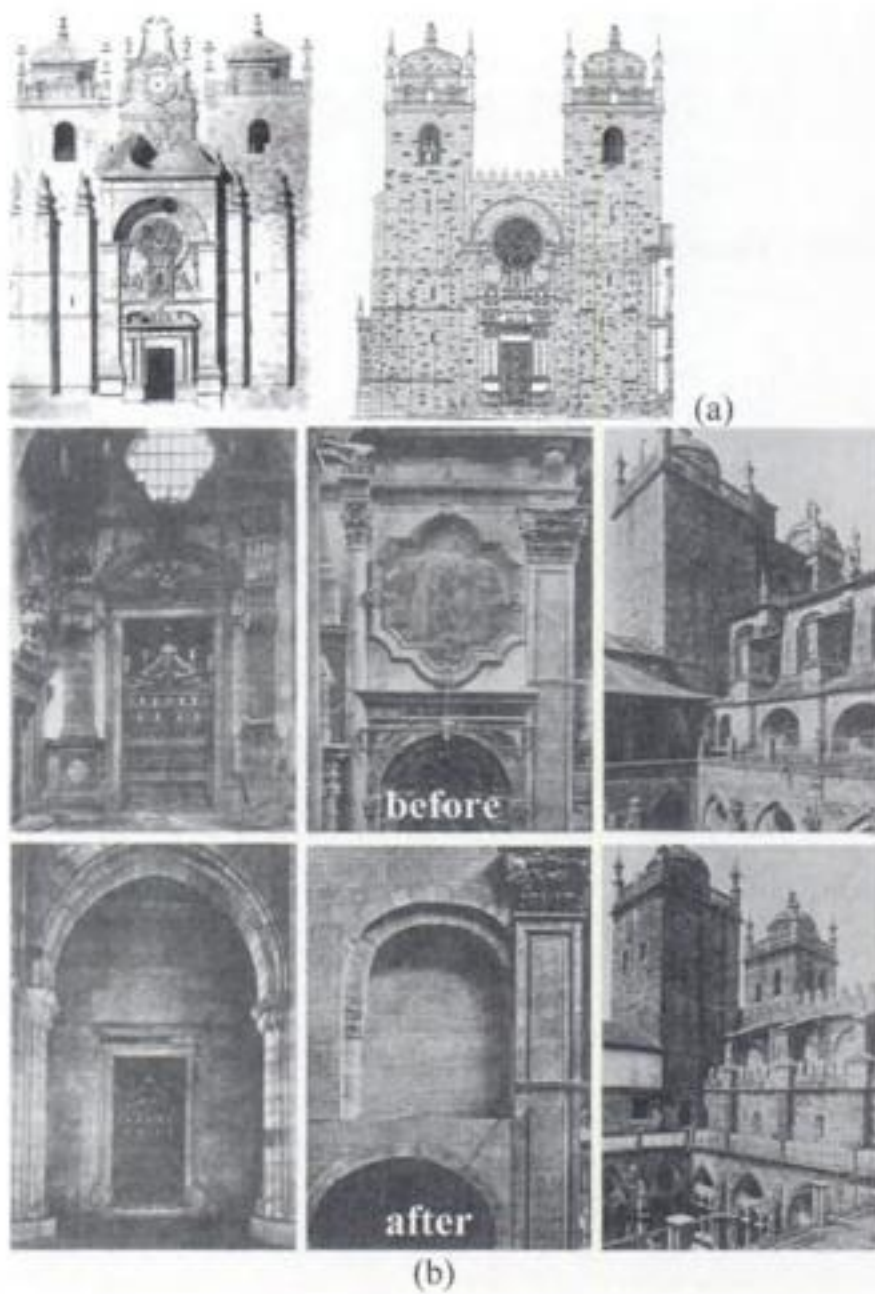


Figure 1. Aspects of the restoration work in the compound, carried out in the first half of the 20th century: (a) main façade and (b) details of the nave and view from the cloister.

to the “Portuguese race” and were present in the Medieval Art, especially the Romanesque.

In the process of declaring an identity and pursuing their values, styles and periods of the historical buildings were mutilated. In particular, the contributions of the baroque and neoclassic were aimed at, because their decorative heritage was not in agreement with the “austerity” of the architectural shapes and the “trueness” of the building materials.

Figure 1 illustrates some of the aspects of the Cathedral of Porto, before and after the restoration works of the first half of the 20th century.

2.1 The surroundings as a frame

After restoration of the building itself, also the surroundings were subjected to modifications. The narrow and labyrinth urban fabric that grew side-by-side with the cathedral was demolished, see Figure 2a. In its place a square was set up, see Figure 2b, and defined by straight alignments and monumental perspectives, see also Figure 2c, featuring a kind of frame aiming at isolating and stressing the importance of

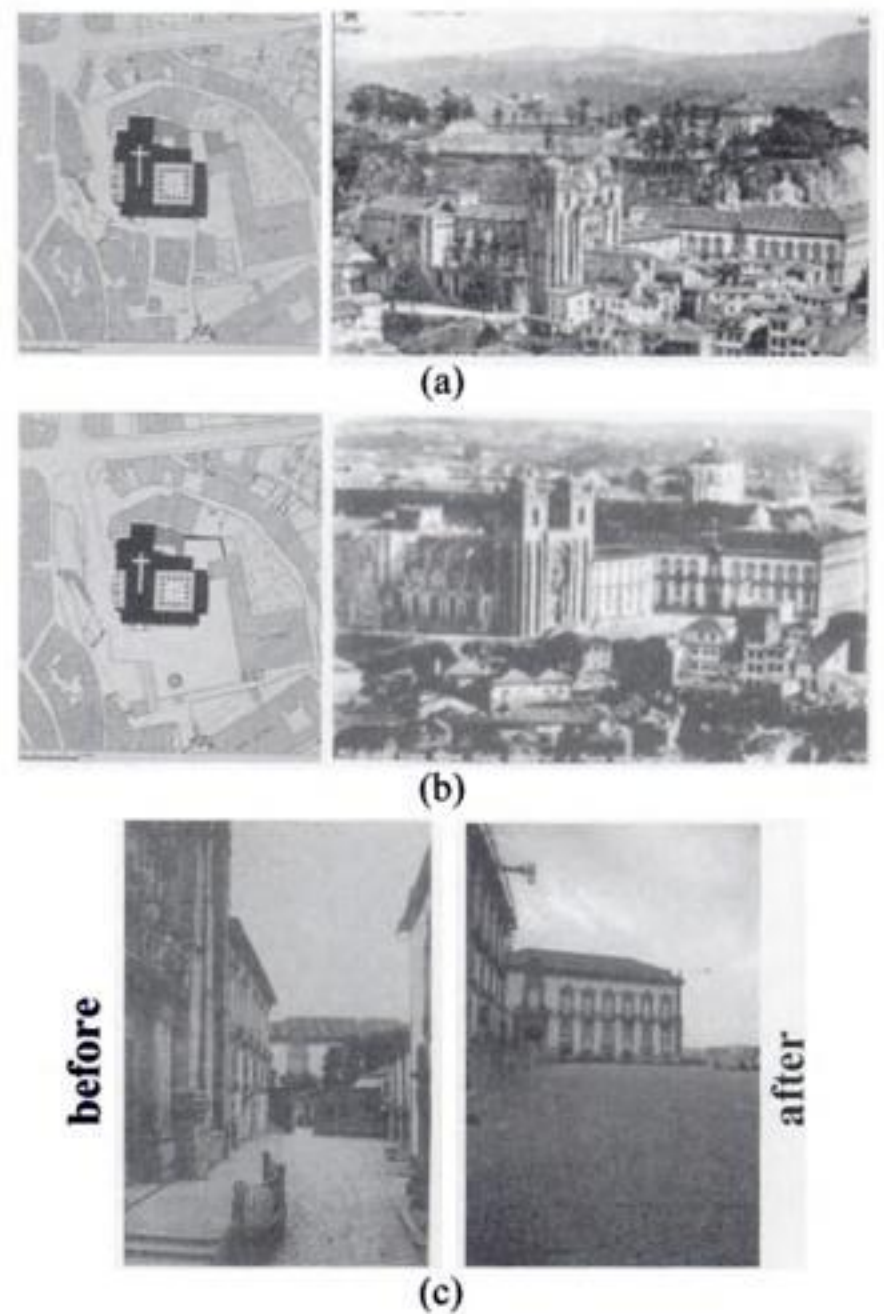


Figure 2. Aspects of the restoration work in the surroundings of the compound, carried out in the first half of the 20th century: general view and plan (a) before and (b) after the works, and (c) detail of the narrow street and square in front of the main façade.

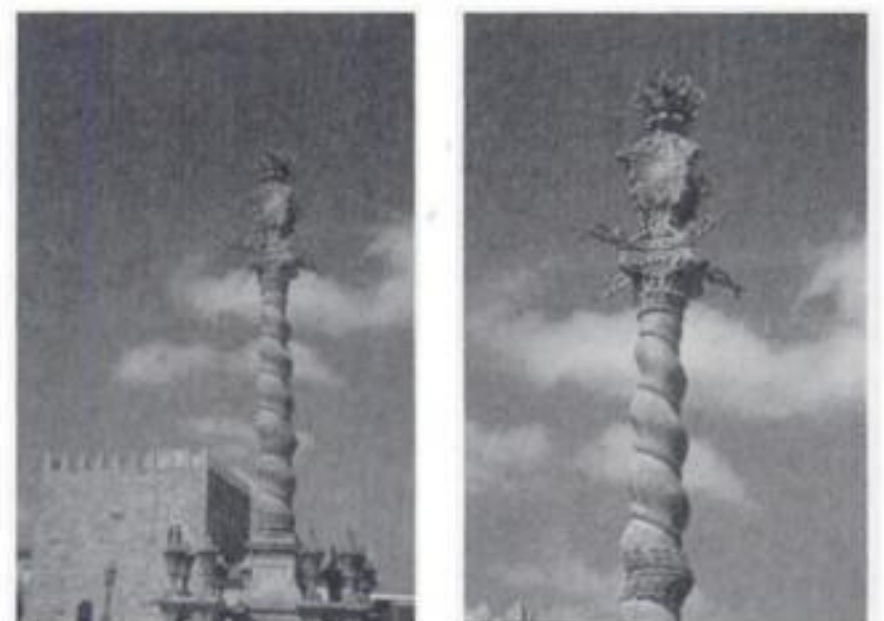


Figure 3. Details of the baroque pillory in the center of the square.

the monument, a syntax as inspiration to the way the cities were planned in the Illuminist period. The baroque was removed from the building but references to the baroque period were recreated in the surroundings, see the pillory in Figure 3. At the southwest limit

of the square, a tower-house with medieval appearance was built from scratch in 1940, with the purpose of hosting the Museum of the History of the City.

The scenic effect that resulted from the restoration produced a kind of representation of the past and the past in this way represented understated the representation. A kind of an alternative past or a commemorative allegory.

3 BASIS FOR CURRENT WORKS

3.1 *The rehabilitation of the restoration as a program*

The building, as it is found today, is hybrid and frozen in a perpetual past, where re-combinations or architectural redesign seem hardly acceptable in the near future. It is with the signs of anomalies and the absence of formal borders that the memory of the building is found and that the violation of authenticity, which is lacking, is understood. This process of learning is also a process of increasing identification and love between the authors and the building. Only then, it is possible to understand that the fake *self* of the cathedral, as a result of the previous restoration, is today the real *self* of the cathedral, transformed into a monument. This is a forged identity that cannot be considered a minor representation of the strength of a specific cultural period.

Therefore, the governing thread of the program of the current intervention is to rehabilitate the restoration. The aim is to reactivate, rehabilitate and upgrade the competence, where competence is understood as the performance capacity of the structures, the materials, the shapes and also the space, assumed as a support for functionality.

The intervention in the building was organized around five operations: removal of infestations, consolidation, water-tightness, ventilation and protection. And, finally, also monitoring.

From the functional point of view, the use was strengthened, which can be summarized by more "cathedral" and less "museum". In fact, several rooms had lost a meaning, either due to degradation or because they were changed into a kind of "museum" without a clear program, where loose artifacts of sacred art were exposed as an ornamentation of openings and empty spaces. Therefore, where possible, the aim was the rehabilitation of the function for which the spaces were created and the reintegration of the artifacts in their context. This program did not reduce but even increased the part of the compound open to the visitors.

3.2 *Dialogue as a methodology*

A constellation of professions has been mobilized and the dialogue has been applied as a methodology

to carry out the Works, which are only superficially from an author and much more from the collection of professionals.

Preliminary diagnosis was very brief and, therefore, the design project was not conceived in detail. On the contrary, the project was a directive kept open and continuously adapting to the unforeseen, which is often the case in historical buildings, where the anatomy is processed by successive approximations and under the lens of different disciplines. Of course, dissection as a knowledge tool cannot be a part of a modern intervention.

In this case, the lack of adequate preliminary diagnosis, which is in opposition with modern methodologies, was compensated with an intense multidisciplinary activity during the execution period (2002–2004), supported by research, consultancy and expertises in various fields. In the contingency of works that had started already, the reunion of efforts resulted in a process of effective cooperation, with the advantage of permanent in situ approaches and discussions.

4 SELECTED ASPECTS OF THE INTERVENTION

The restoration carried out in the first half of the 20th century used traditional construction techniques. Some of the structural deficiencies encountered were then solved with the dismantling and rebuilding of unstable parts, and with the replacement of deteriorated or damaged granite, with poor mechanical performance.

The sole concession to the industrial technology is the use of Portland cement, used as a common binder for repointing masonry joints, rendering walls and several reparations that during and after the restoration works, aimed at solving the following issues, without success: waterproofing of surfaces, glue and reconstitute volumes, stabilize cracks and stop movements.

It is precisely with respect to the above-cited issues that deeper interventions have currently been carried out, some without visible effects and other with the addition of parts, as in the strengthening of the towers. Therefore, the architects in charge of the works tend to joke about the fact that the only intervention being carried out is the strengthening of the towers.

Next, see Figure 4 to Figure 12, some of the aspects of the works being carried out are briefly reviewed. The works are mostly concentrated in the towers, and the roofs and façades in the west and south wings. Diagnosis and strengthening of the towers and the Saint Vincent Chapel are addressed in a separate section.

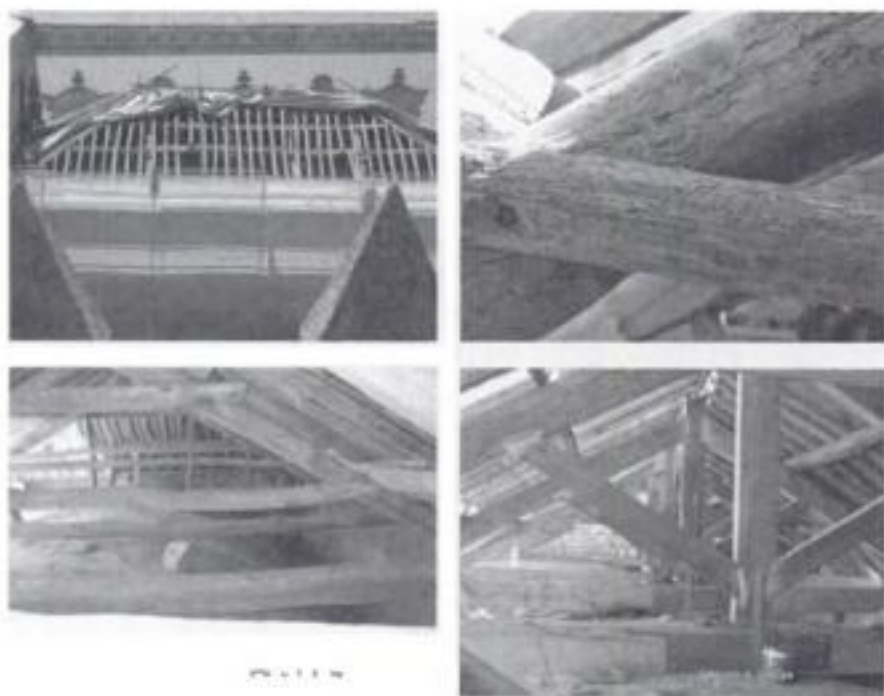


Figure 4. Remedial measures in the roof structures included cleaning, application of biocide, application of preservation products, consolidation, strengthening and local replacement. Experts were responsible for diagnosis and structural assessment.

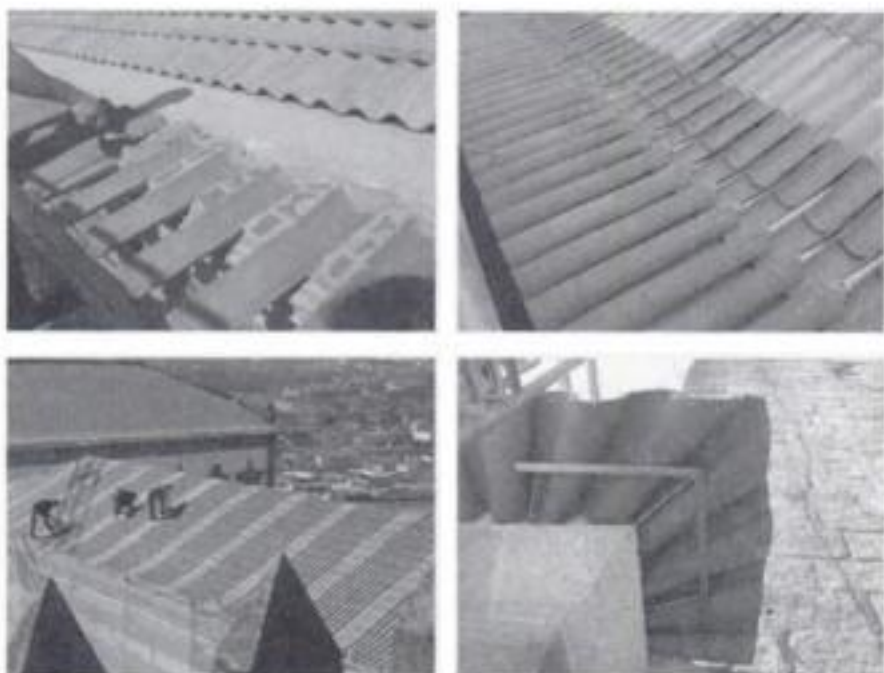


Figure 5. Replacement of the ceramic tiles including new anchors, traditional eaves, strengthening in the corners, introduction of under-roof sheeting and walkways.

5 INTERVENTION IN THE TOWERS

5.1 Introduction

A key aspect in the behaviour of ancient towers is that the collapse process usually excludes the possibility of ductile behaviour. In fact, there are hardly any possibilities of internal force redistributions between different critical sections, and failure of a single section is usually sufficient to provoke the entire collapse of the structure. This intrinsic feature leads to a high structural risk in tall masonry towers, because increasing height means large vertical loads and high compressive stresses at the base. Therefore, it seems easy to accept that masonry towers should possess a higher safety margin than the values normally found for other

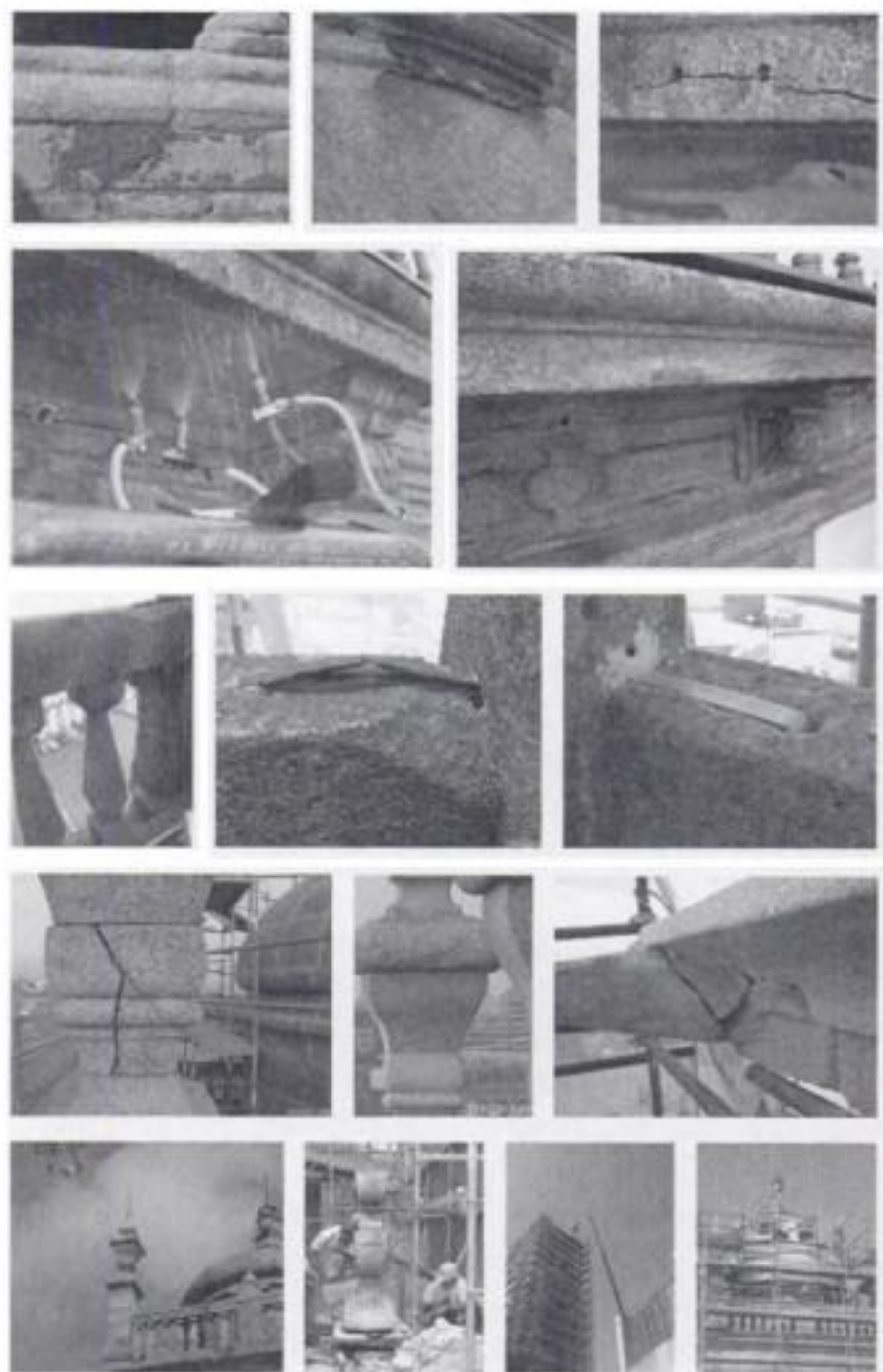


Figure 6. Remedial measures for stone, including removal of biological activity, dry and low pressure water cleaning, localised consolidation, application of water repellents, reconstitution of voids, crack closure and injection, replacement of iron ties, and, exceptionally, replacement of stone pieces. Experts were responsible for diagnosis and specific treatments.



Figure 7. Repair of grilles included control of anchors and new anchors, and measures for proper rainwater flow.

historical structures. But this is not often the case, see Binda & Anzani (1997).

A tower is usually a result of the need to create a symbol or the need to challenge structural stability (and nature itself). The interpretation of this desire to build higher, and simultaneously to reduce the safety of structures, was left to ancient builders in the context of almost no scientific basis. It is striking that the majority of the ancient high towers in Italy, e.g. in Pavia

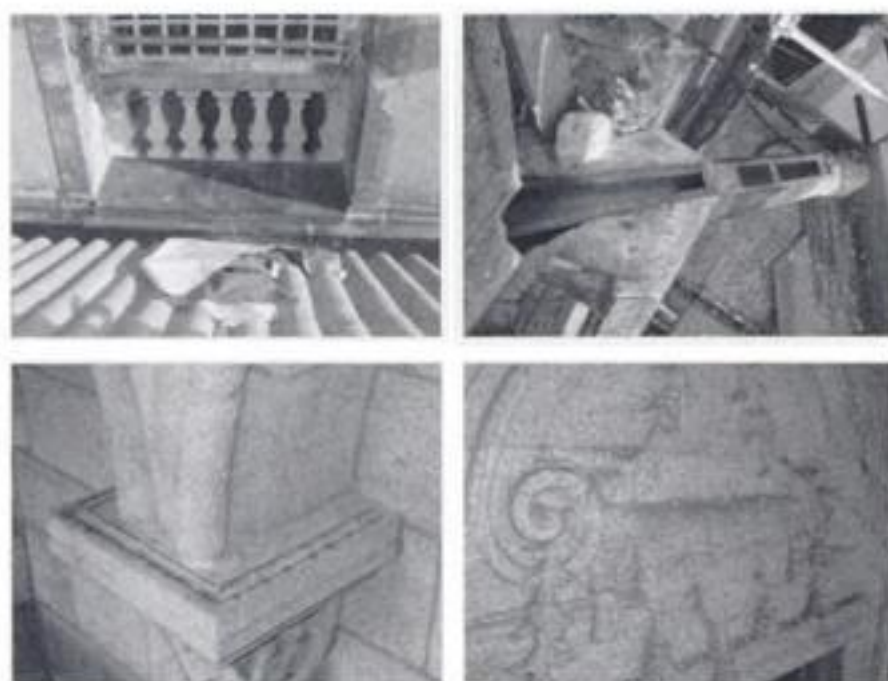


Figure 8. Physical protection of the granite stone include sheeting in the external horizontal planes and installation of a electrical anti-pigeon system.



Figure 9. Repair of finishings included repointing of masonry joints with lime mortar and repainting of wood with traditional oil paints.

and Bologna, are no longer present, Macchi (1998). The reality is that only a few of these structures survived until today, due to collapses, destruction due to lightning and even demolitions (often by precaution and concern of eminent collapse). In the recent history, there are well-known cases of collapse, namely the Campanile in Venice (1902), the Civic Tower in Pavia (1989) and the Santa Maria Magdalena Bell-Tower in Goch (1993). In the case of Venice, collapse was gradual, with signs of distress two days before collapse. Also, 20 minutes elapsed between the fall

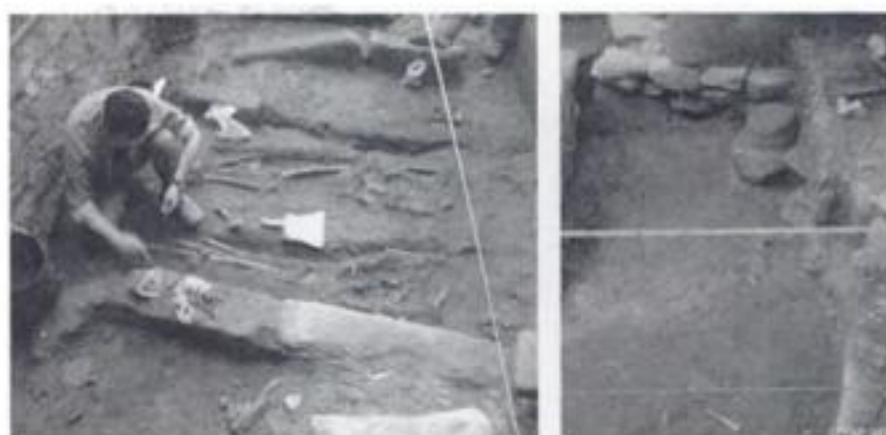


Figure 10. The historical survey aimed at study existing documents, drawing and bibliography to define the evolution of the cathedral. The archaeological survey included in situ excavation and stratigraphical records of the faces of the masonry walls.



Figure 11. For the time mechanisms, the works included diagnosis, conservation and reactivation of function.



Figure 12. Restoration and conservation of the heritage pieces included also diagnosis of stucco, full inventory, reintegration in the original location, pre-consolidation and cleaning of stucco.

of the first bricks and collapse. In the other cases, collapse occurred without previous warning. In Pavia, the collapse occurred in a few seconds and provoked four casualties (Macchi 1992).

Therefore, it seems unquestionable that the high structural risk of high masonry towers justifies detailed studies and carefully planned remedial measures in case of doubt about their behaviour. Several recent case studies have been reported, Modena et al. (2001), Valluzzi et al. (2003) and Lourenço (2004).

5.2 Description

The main façade was built between 1176–1200 (central part) and 1229–1325 (towers), see Figure 13. The towers evolved into a Bell-tower (North) and a



Figure 13. Main façade after the restoration works in the first half of the 20th century.

Clock-tower (South). In 1552, damage due to lightning is reported in the South tower. Between 1665–1669 the South tower was demolished up to mid-height and rebuilt. In 1717, it is recorded that the South tower was in the verge of collapse and, in 1727, buttresses were added, similarly to the ones that already existed in the North tower. Pinnacles were added in 1732. The construction of the Chapter House, contiguous to the South tower, also aimed at consolidating the tower. Also in this period, the two small windows in the main façade (South tower) were replaced by a single large window, similar to the one that existed in the North tower. Before 1841, a new lightning stroke the South tower.

The cross section of the towers is approximately square with a side of 10.0 m and exhibits a variable thickness, with a minimum of 1.7 m at the base. The height of the towers is approximately 35 m, which means that the average stress at the base is around 1.0 N/mm^2 . This value is rather low for regular granite masonry but it is rather high for rubble masonry (with or without mortar joints). In the main façade, two buttresses are apparent in each tower, see Figure 13. As addressed above, the structure suffered several major modifications through time, which resulted in a very complex internal structure with different load bearing internal elements at each level. The structure of the towers cannot be understood from structural reasons and several openings are closed, facing staircases or

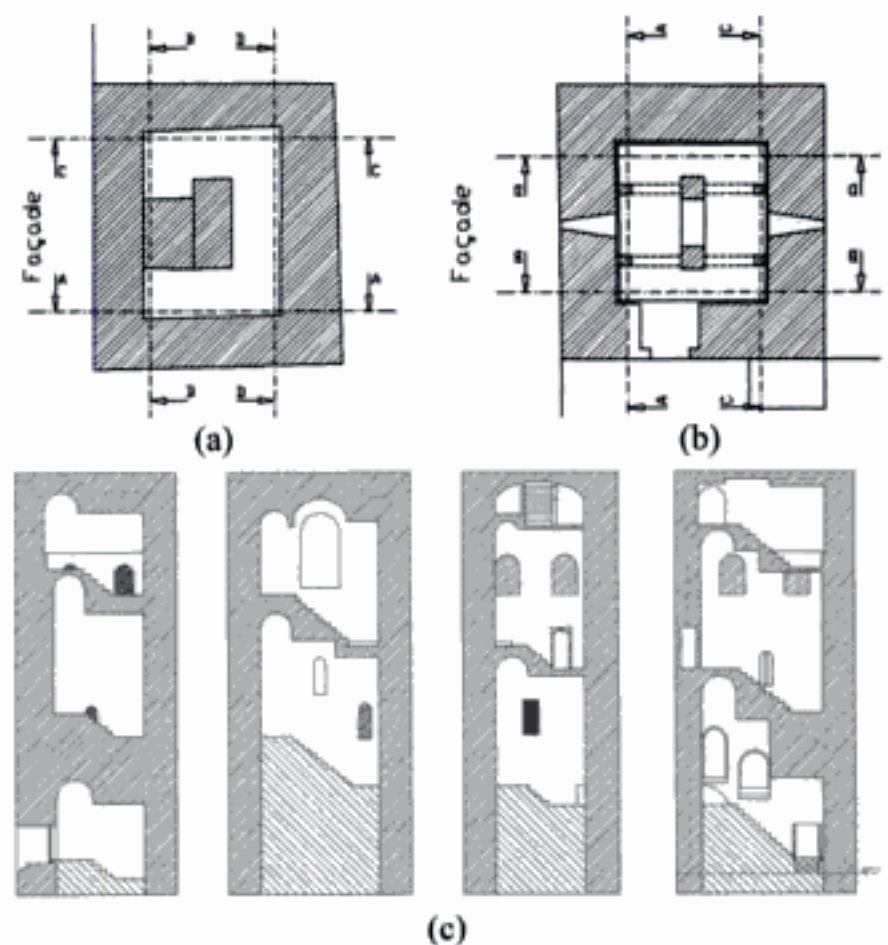


Figure 14. Partial sections of the towers: (a) horizontal section of the South tower, (b) horizontal section of the North tower and (c) sections A–D for the South tower.

vaults. The entrance for both towers is located at mid-height, with a connection between both towers from the top of the main vault. But the two towers have a rather different structure. The South tower possesses an internal core with a staircase shaped helicoidally, see Figure 14a,c. The North tower (presently with the bells and clock) features a horizontal mid-level with stone slabs and architraves apparently supported in columns and stone struts, see Figure 14b.

5.3 Constitution of masonry walls

The constitution of the masonry walls from the towers was characterized using visual inspection, both by removing smaller stones of the outer leaves and by using a boroscopic camera inserted in cracks or in holes drilled in joints, see Figure 15a. From the inspection, it was possible to conclude that the three-leaf walls have external leaves of granite ashlar with a thickness ranging from 0.30 to 0.70 m, while the middle leaf is made from loose smaller stones and/or silty soil, see Figure 15b and Figure 16. The combination of heavy rain in Porto, strong winds in the top of the hill where the Cathedral is located, and the open joints in the external masonry face, results in a wet infill even in the summer and the continuous washing out of the infill, see Figure 15c.

5.4 Existing damage

The towers exhibit distributed cracking and significant out-of-plane movements. The existing damage

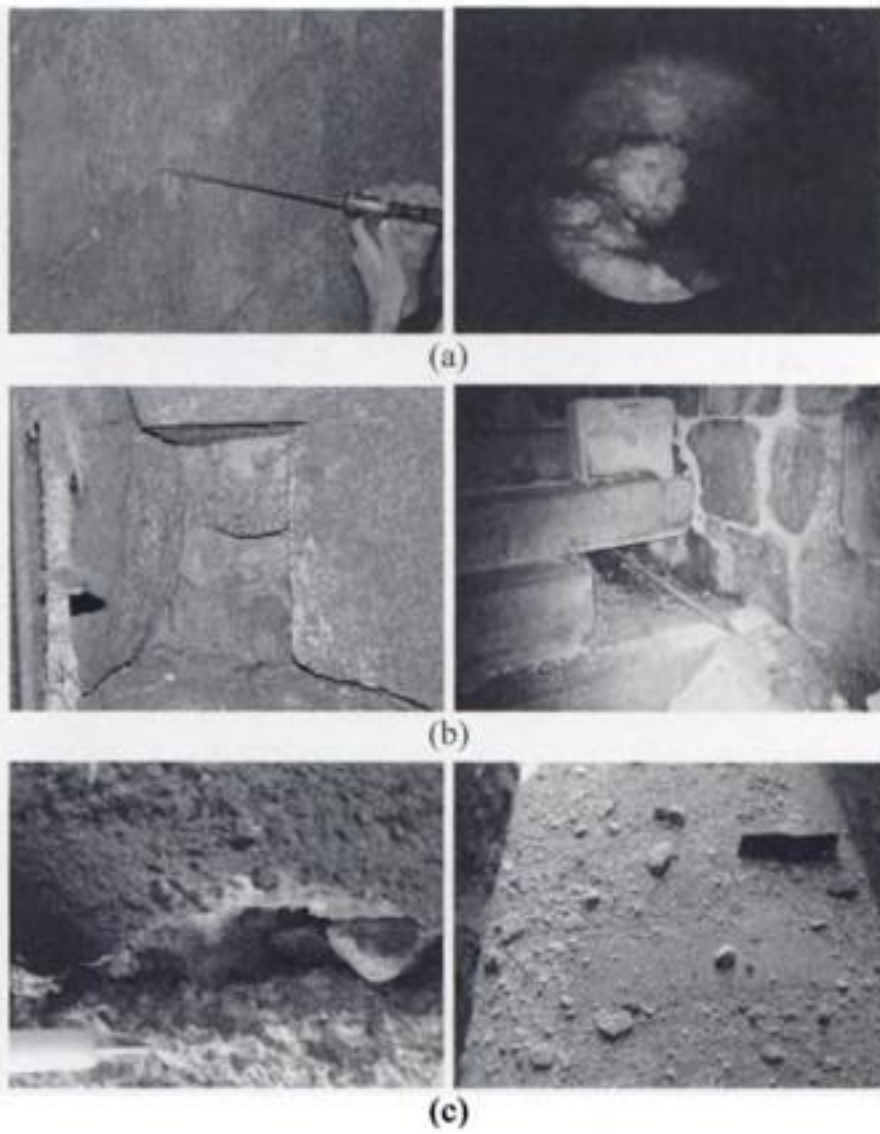


Figure 15. Visual inspection to define the constitution of masonry walls: (a) boroscopic camera, (b) opening up the structure (c) loss of material through central cracks in the openings.

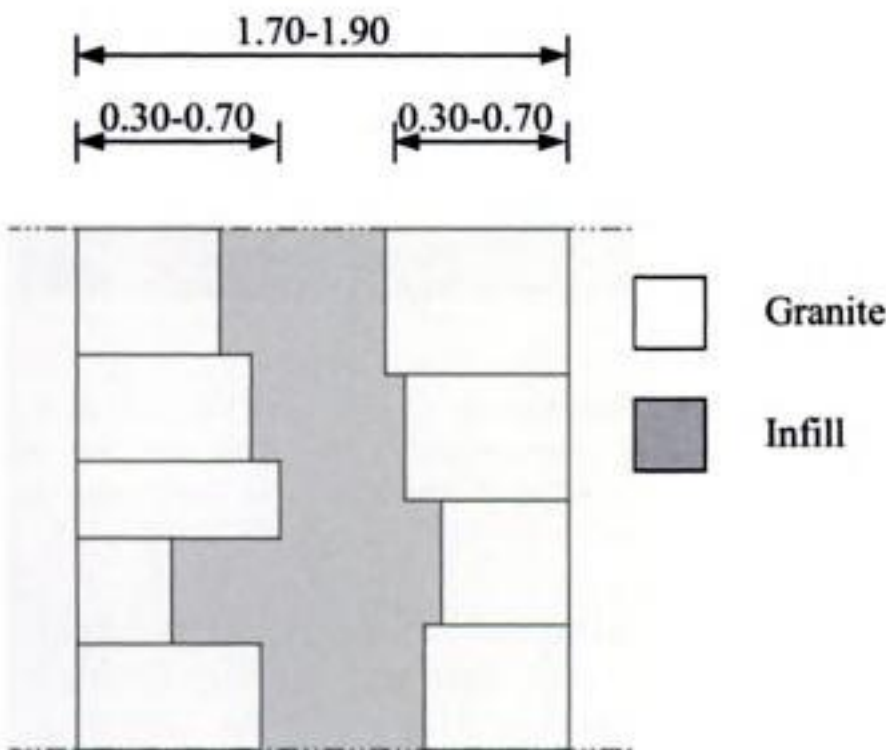


Figure 16. Typical cross section of the masonry walls.

resulted in the past addition of three iron ties (date unknown), see Figure 17a. Tie T_1 presents a severely deformed anchorage, see Figure 17b, and tie T_3 is corroded and broken, see Figure 17c. It is stressed that the separation between the East and West façades of the South tower continued after tie T_3 was broken. It is also noted that the masonry walls in the vicinity of



(a)



(b)



(c)

Figure 17. Ancient tower ties: (a) Deformed anchorage of tie T_1 and (b) details of broken tie T_3 .

the anchorages are also deformed, as expected due to the application of a large point load.

The South tower is more damaged than the North tower. Figure 18 exhibits the location of severe cracks and out-of-plumb walls in the South tower. Also the East façade of the South tower presents out-of-plane movements to the exterior. It is noted that the internal walls of this tower are straight, indicating crumbling or desegregation of the walls, with major cracks and voids in the interior, see Figure 19a. The separation between the internal and external leaves of the walls is further confirmed by the longitudinal cracking observed in most of the openings. Figure 19a illustrates such cracking, with a maximum width of some centimetres. Finally, it is noted that the North tower presents severe distributed vertical cracking at the base, see Figure 19c.

This cracking is only visible in the internal (medieval) face, while the external face seems undamaged. Moreover, the very large thickness of the walls

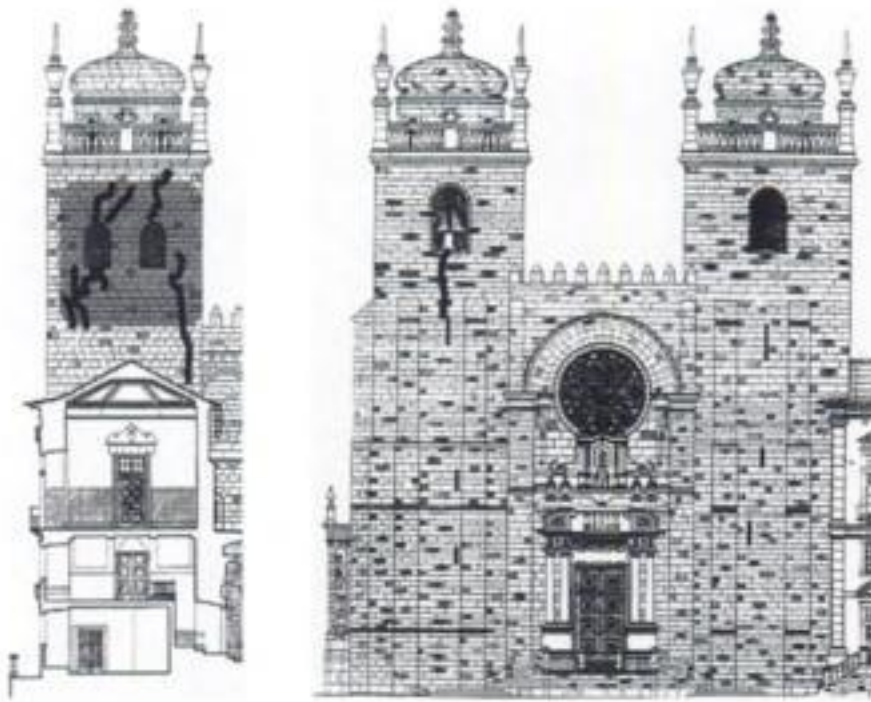


Figure 18. Location of most severe cracks and out-of-plumb walls, in the South view and main façade.

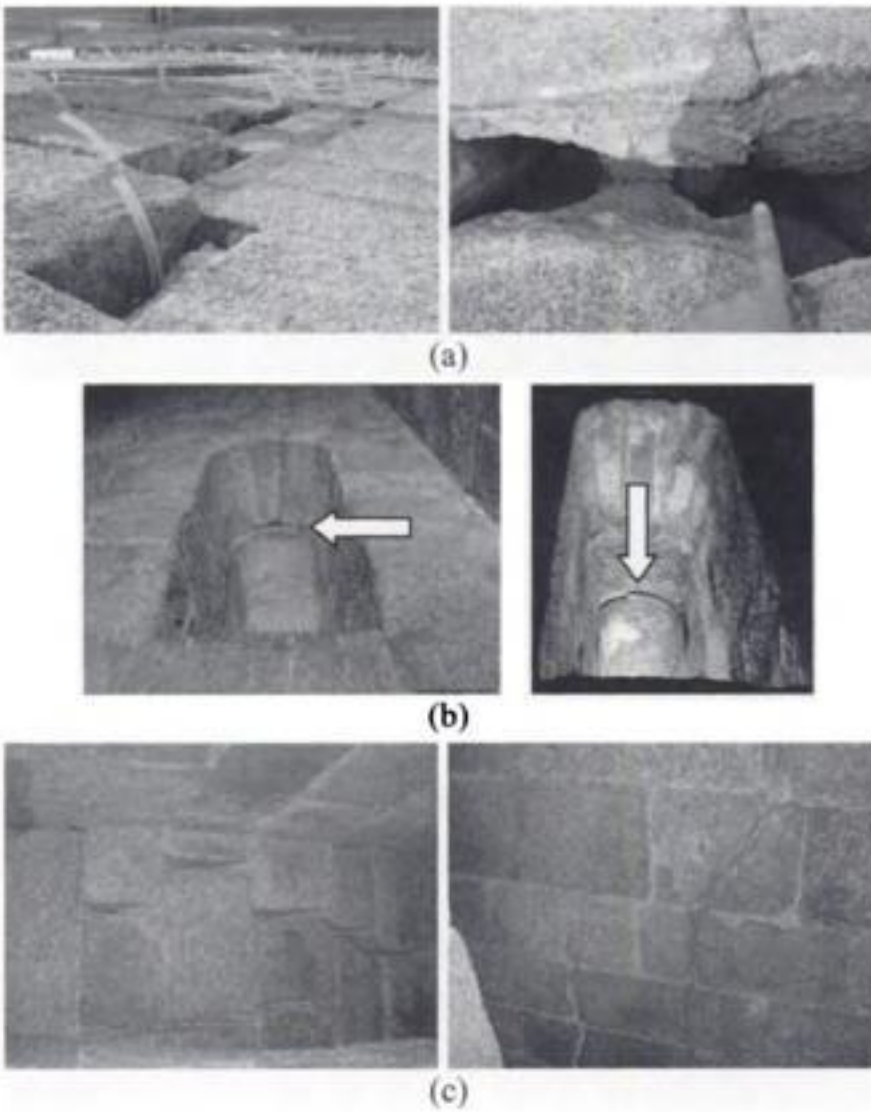


Figure 19. Details of the cracks in the towers: (a) cracks up to 0.20 m width in the South façade/South tower; (b) typical active cracks parallel to the walls at the openings; (c) vertical cracks at the base of the North tower.

are not replicated in the South tower, see Figure 20. For these reasons, it is believed that the damage is not recent and the helicoidal staircase belongs to the structure of an older tower.

Additionally, also the following damage is noted:

- Steel structure in the cupolas of the towers with advanced corrosion, see Figure 21a;

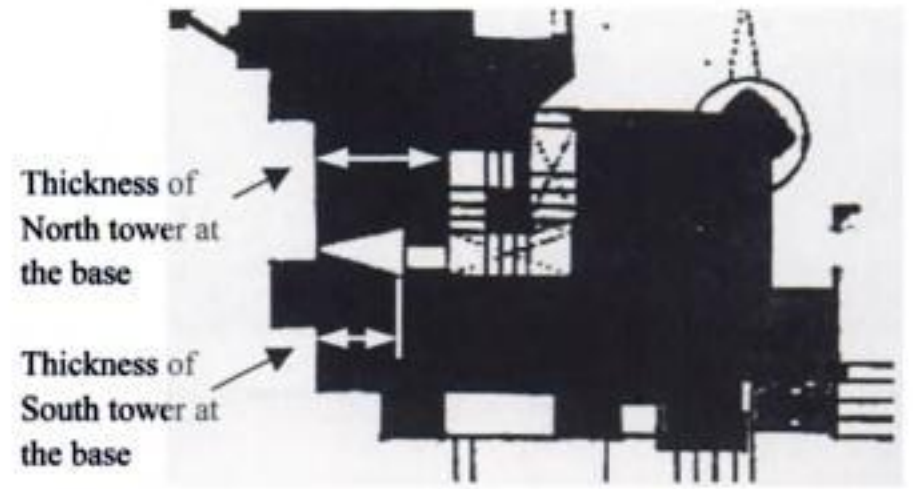


Figure 20. Plan of North tower at the base.

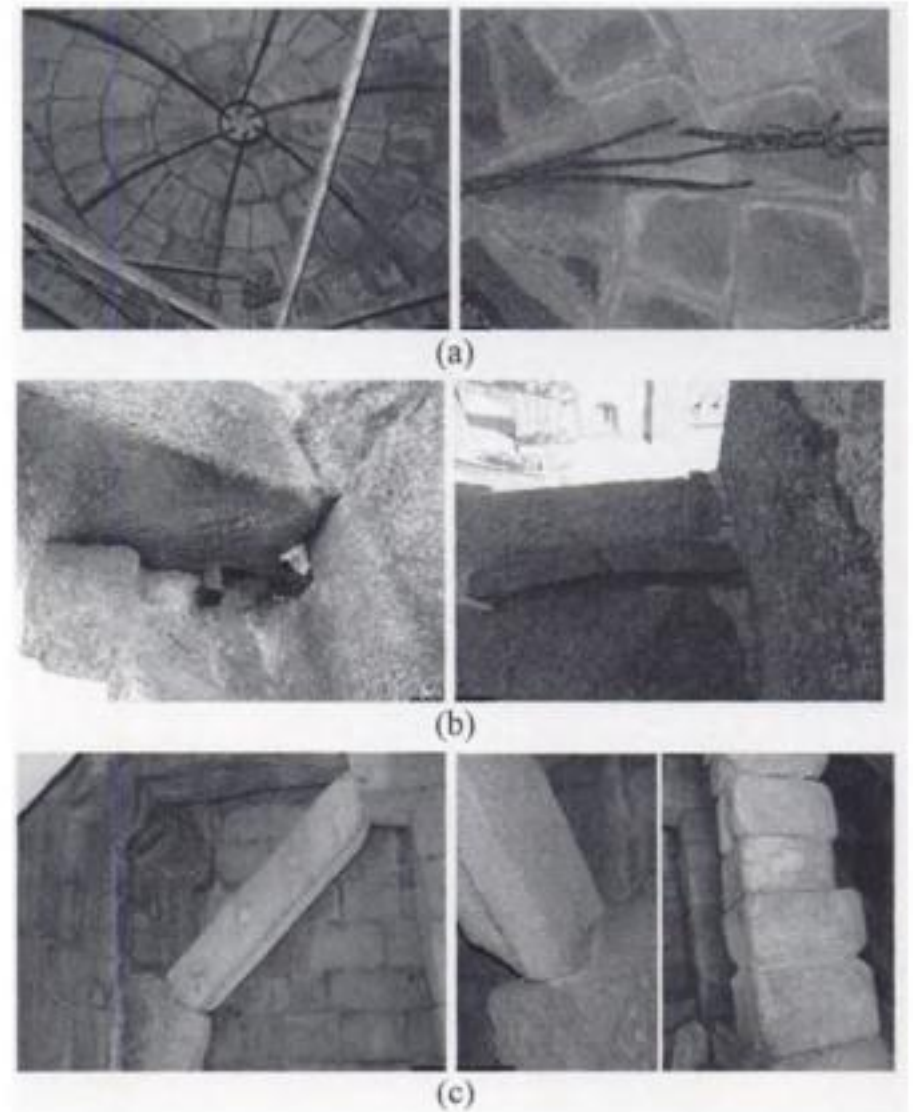


Figure 21. Other damage: (a) Corrosion of the steel structure of the cupolas; (b) corrosion of dowels and ties in balustrades and pinnacles; (c) deficient structural system to support the bell stone level floor.

- Balustrades and pinnacles under deficient stability conditions and with significant movements due to corrosion of dowels and ties, see Figure 21b;
- Misconception of the structure supporting the bells and clock in the North tower, see Figure 21c.

5.5 Remedial measures

As it arises from the history and survey, the towers seem to have been damaged in the past and rebuilt (particularly the South tower). The (re)construction seems to have been carried out under deficient execution conditions, no particular well defined structure and using improvised construction details. In addition,

different remedial techniques were already used in the past aiming at correcting and strengthening the towers.

The walls of the towers seem not to possess adequate connection between the external leaves and severe water infiltration in the walls contributed to the existing damage and to the loss of material in the rubble infill. Here it is again stressed that the Cathedral is located at the top of a hill, the masonry joints have lost all mortar and it was found that the rubble infill was wet by the end of the summer.

Besides other damage, the most relevant feature is that the North tower is divided in two similar U-shaped parts, from mid-height to the top, with full cracks along the West-East direction (in the other direction, the existing ties kept the tower together), and the South tower is bulging outwards both to South and to East (the existing West-East tie is broken).

The solution adopted for strengthening consists mostly of a steel ring in both towers, aiming at confining the structure along the two orthogonal directions, in the sole location possible, see Figure 22a,b. The rings are made with welded stainless steel plates (class AISI 316L), connected to the towers using long, inclined stainless steel anchorages inside of a cloth duct to prevent generalized injection, see Figure 22c–e. The length of the steel profiles is defined so that the elements can be transported to the location through the existing doors and can be easily assembled in situ, without any further welding.

In the North tower, the ring also aims at providing a support for the stone pavement for the bells. The reason being that the stone columns are very deteriorated and possess presently no structural function and the stone struts have very deficient conception, see Figure 22c. Here it is noted that it was decided not to recuperate the structural function of the columns (e.g. using injection) because the lower level seems to indicate insufficient strength of the inner core, see Figure 20c and Figure 21. The steel ring is made of U profiles (240×120 mm and 200×100 mm height).

In the South tower, a set of two ties was provided to the ring, because it was possible for aesthetic reasons and they are a witness of the ancient broken tie. The ring must cross the staircase at a selected location because the complex internal structure of the tower does not allow otherwise. Due to the lack of internal stiffening elements, a much more stiff steel frame is needed and the steel ring is made of I profiles (180×180 mm). Due to the bulging outwards of the East and South façades, and the severe cracks in the corners, several short ties have been added to the structure to stitch the East and South façades, and two long ties through the core of the South façade have been added to connect the West and East façades, see Figure 22f. Figure 22g presents details of the two types of anchorage plates adopted (circular plates and specially designed crosses).

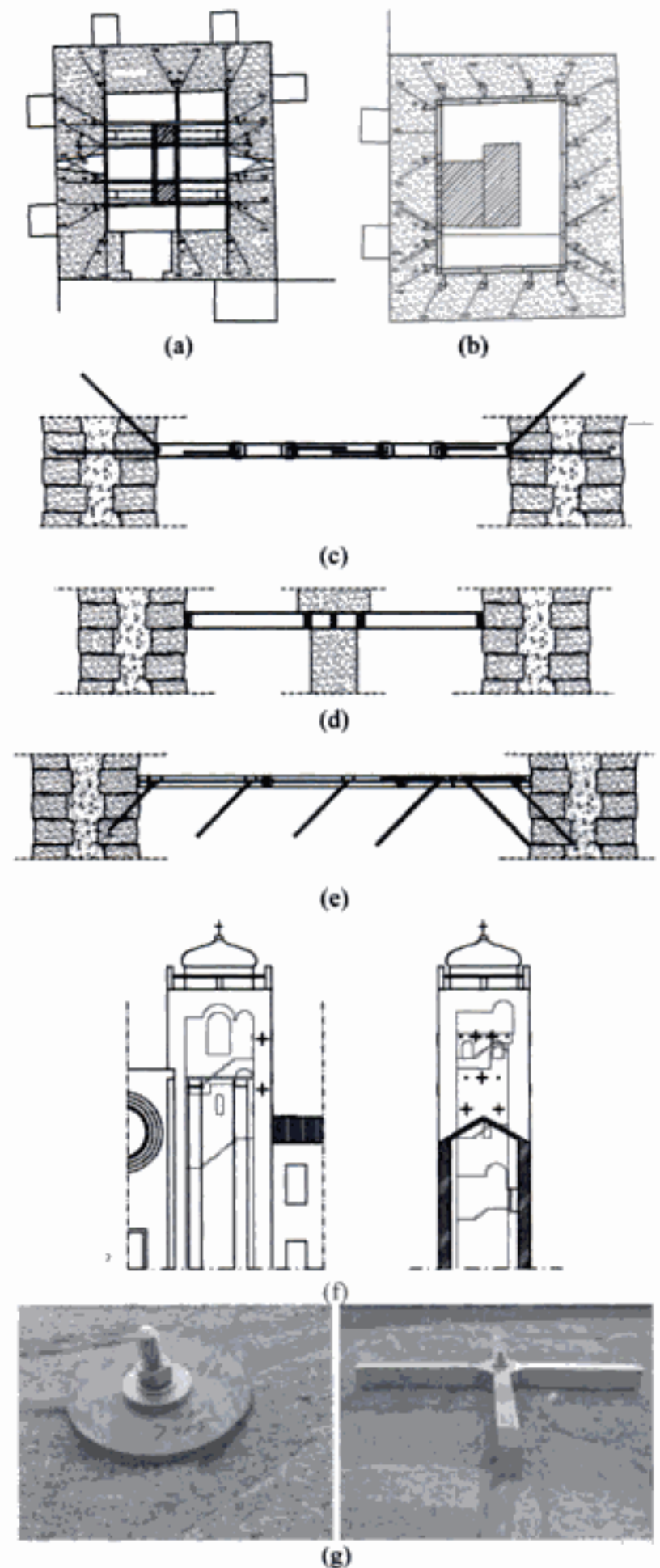


Figure 22. Aspect of the strengthening of the towers using stainless steel rings and long inclined anchorages: (a) plan of the ring for the North tower; (b) plan of the ring for the South tower; (c) North-South section for North tower; (d) West-East section for North tower; (e) typical section for South tower; (f) additional ties placed in the West and South façades of the South tower; (g) details of the anchorage plates.

Figure 23 illustrates the aspects related to repairing the pinnacles and balustrades, which consisted of replacement of iron dowels and ties by stainless steel. The large pinnacle in the top of the North tower cupola was totally loose at the time of the works and was jacketed with steel plates at the top and bottom necks.

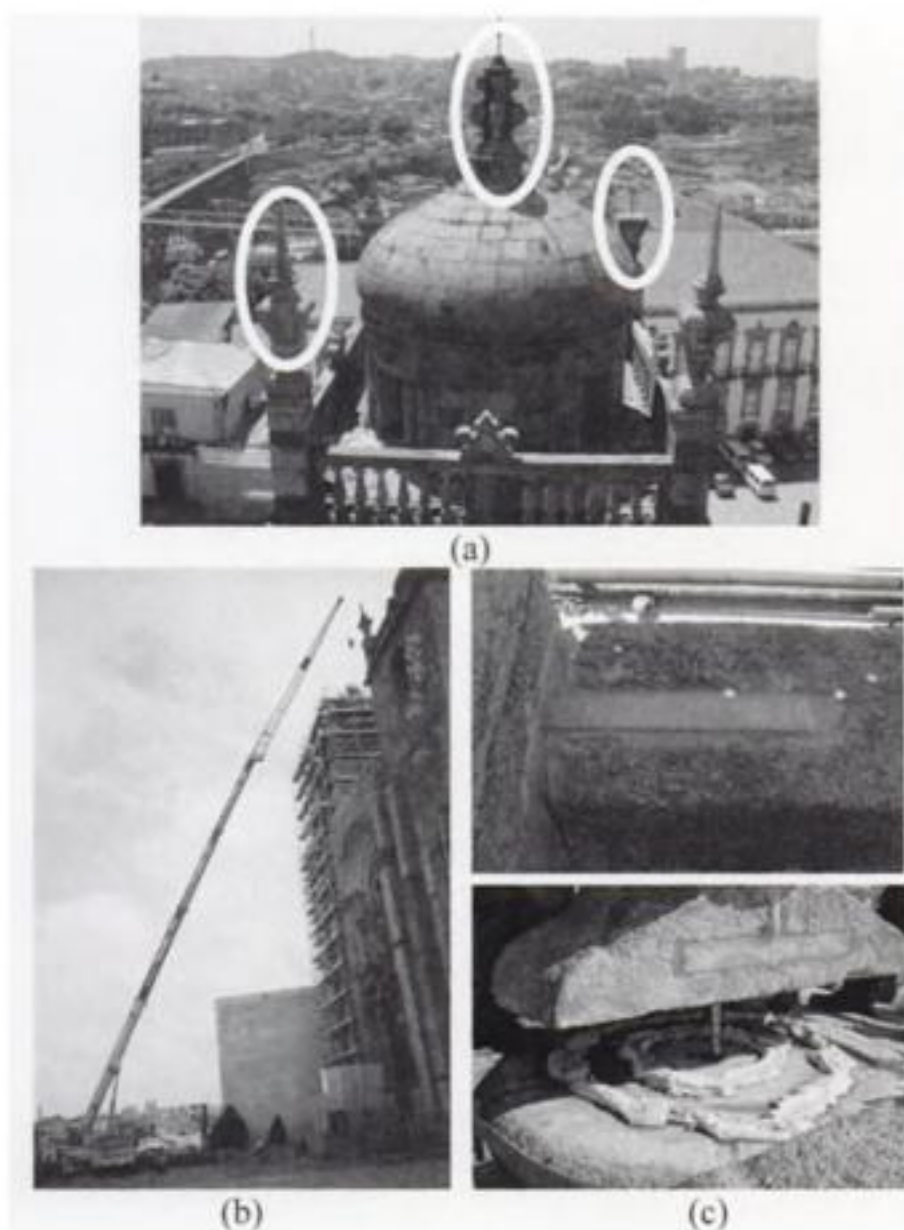


Figure 23. Pinnacles and balustrade removal and placement with stainless steel dowels and ties: (a) general view; (b) removal of the centre pinnacle; (c) aspect of stainless steel elements and placement.

The other works carried out include injection of the main cracks with lime based mortar grout, repointing all joints with two selected lime mortars (a traditional mortar for the filling and a more durable lime mortar for the finishing), protect against corrosion (the two ties in the North tower were kept in place) or replacing all existing iron.

5.6 Monitoring Plan

Given the cultural importance of the building and the significant damage in the South tower, a monitoring system was planned and installed.

The system includes four waterproof crackmeters in the largest cracks, two strain gages for the new ties, two biaxial clinometers to measure the tilting of the tower, as well as temperature, humidity and wind sensors. The system includes a GSM interface for remote monitoring.

6 SAINT VINCENT CHAPEL

The Saint Vincent Chapel is located next to the South wing of the Cathedral cloister. During the restoration works of the roof, it was found that the extrados of

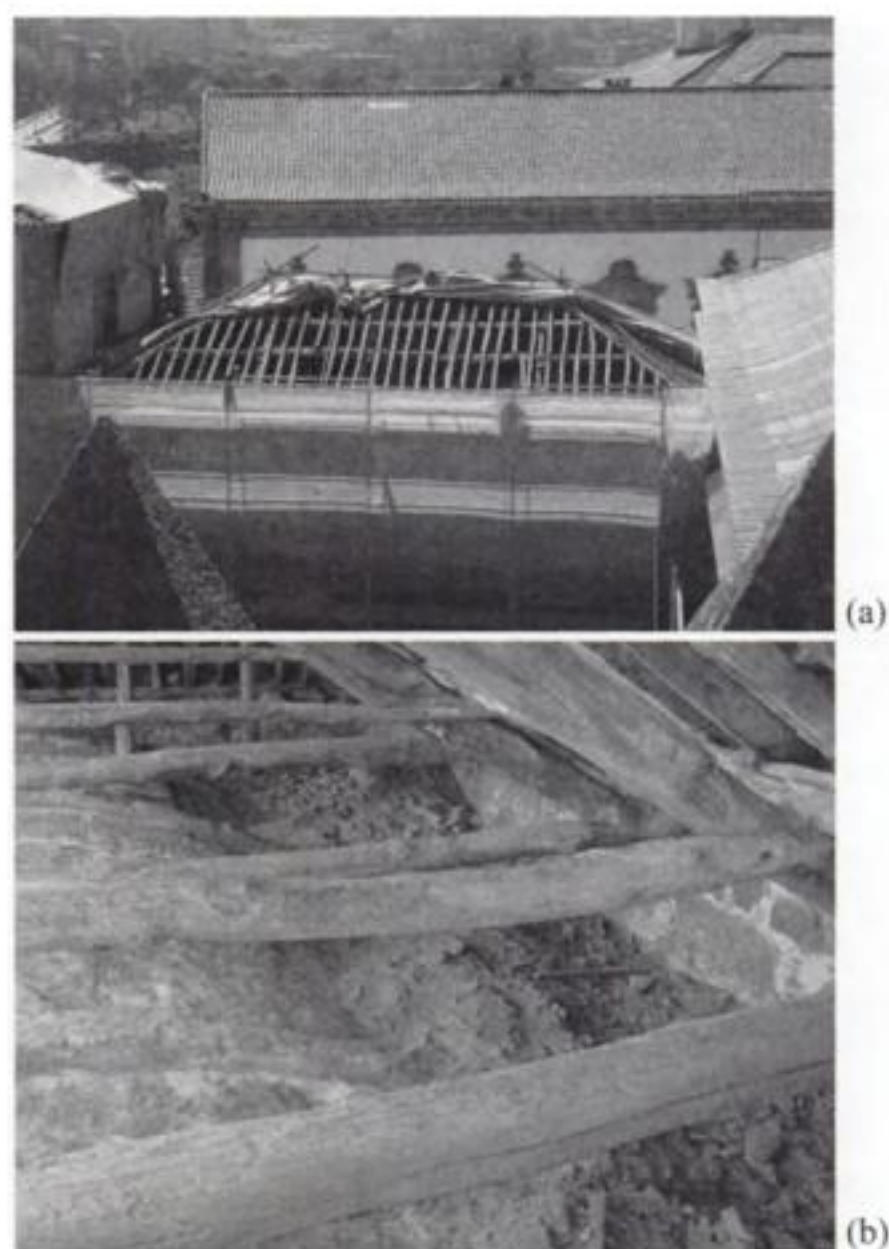


Figure 24. Roof of Saint Vincent Chapel: (a) aspect of restoration works; (b) aspect of vault infill with rubble.

the chapel vault was filled with rubble resulting from old demolitions see Figure 24. Also, and as usual in several historical constructions, the timber roof was partly supported by the vault, using later added struts.

The issue addressed here is the stability of the vault and the convenience of the removal of the infill.

6.1 Survey

The structure consists of a barrel vault with an approximate thickness of 0.25 m and a span of 6.8 m. On the North side, the cloister acts as a buttress but on the South side no buttresses are present. Even if the South wall (1.70 m) is thicker than the North wall (1.30 m), out-of-plumb movements outwards are clearly visible in the former, up to 1.5% (or 0.10 m at the springer of the vault), see Figure 25a.

Nevertheless, as the vault presents only minor cracking, see Figure 25b, it was believed that the vault has been built after the wall deformation. As it will be confirmed next, the vault replaces a previous timber roof at the same level.

6.2 Structural Analysis

A plane model was adopted for the structural analysis of the barrel vault. The analysis was carried out using

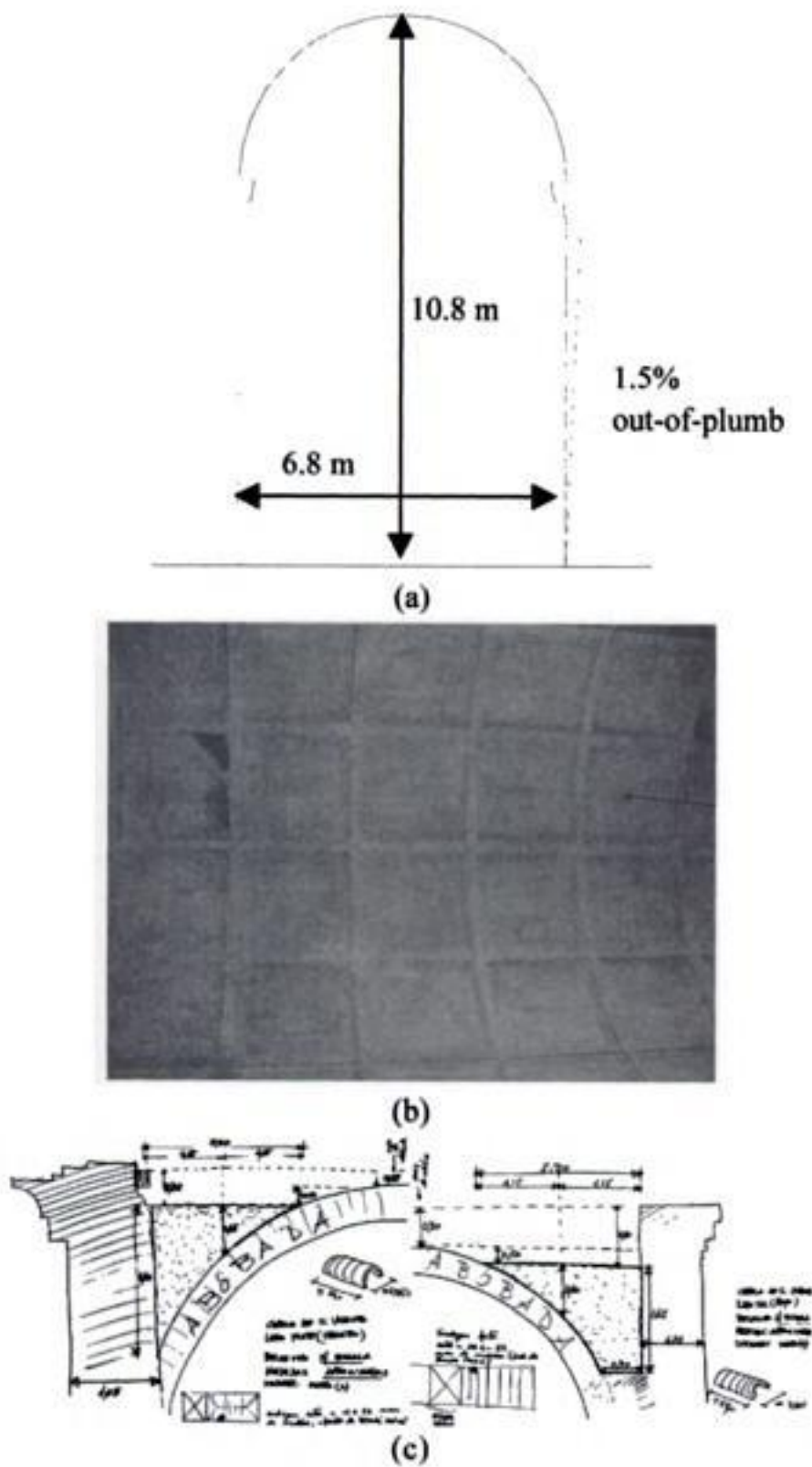


Figure 25. Saint Vincent Chapel: (a) cross-section; (b) aspect of vault intrados; (c) survey of inspection pits.

limit analysis, discretizing the walls and vault as a set of rigid blocks, see Orduña & Lourenço (2003). More complex approaches are available, Lourenço (1998, 2001), if necessary for more detailed studies. The assumed material properties include a tensile strength equal to zero, a tangent of the stiffness angle equal to 0.7, zero dilatancy and a compressive strength equal to 6 N/mm^2 . The actions included consist only of the self-weight of the structure.

As the objective of the analysis is to evaluate the influence of the infill, a sophisticated representation of the structure is not particularly relevant. Therefore, the influence of the cloister, openings of the walls and ribs of the vault were neglected in order to avoid the need of a three-dimensional model, Lourenço (2002).

The numerical results are given in Figure 26, in terms of thrust-lines and collapse mechanisms, both for the model with and without infill. The ultimate

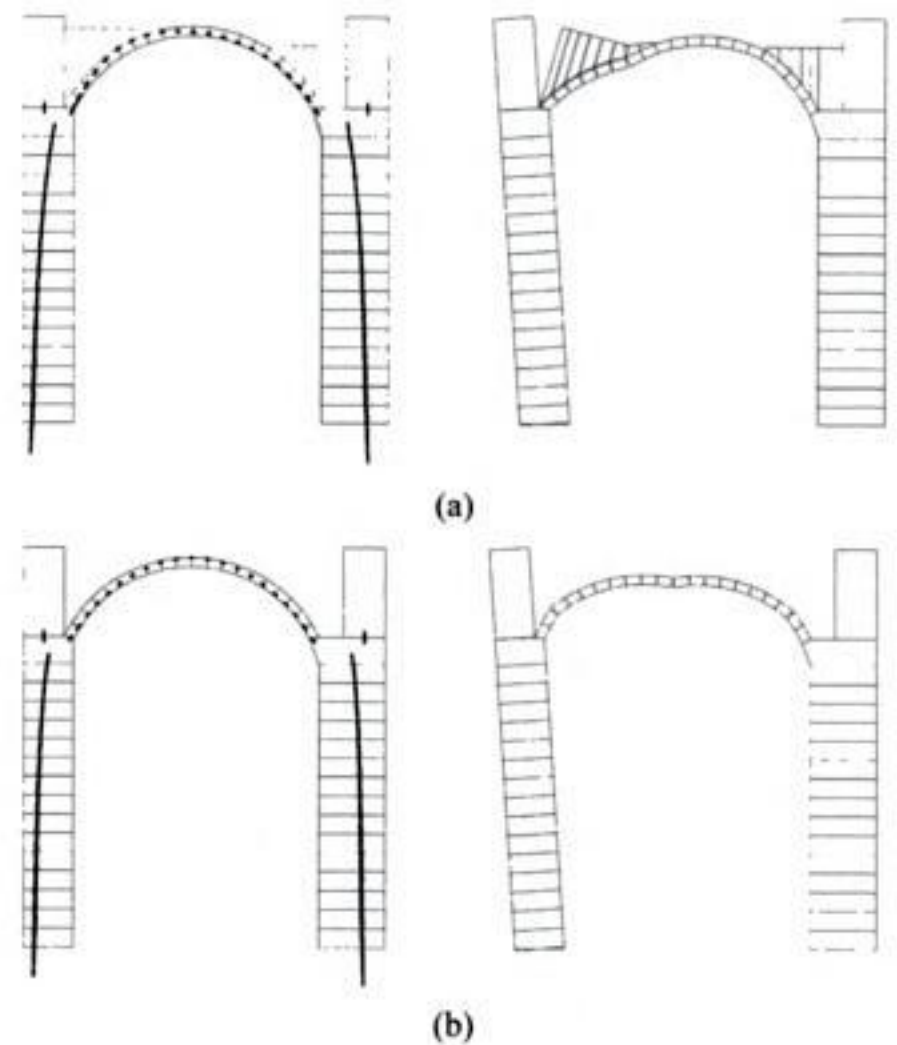


Figure 26. Results of the numerical analysis, in terms of thrust-lines and failure mechanisms: (a) with infill, for a ultimate load factor equal to 6.5; (b) without infill, for a ultimate load factor equal to 9.4.

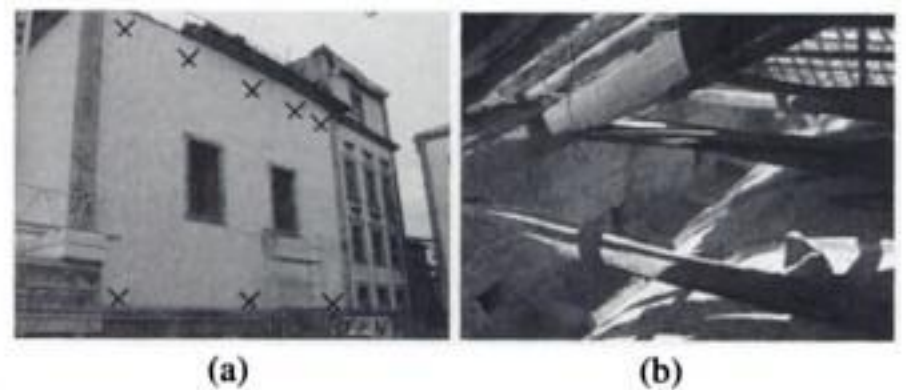


Figure 27. Infill removal: (a) location of topographic targets for monitoring; (b) aspect of the cleaned vault.

load factor increases 45% if the infill is removed, which seems also natural because it was not originally planned for this construction.

6.3 Remedial measures

The infill was removed but, for safety reasons, it was recommended to accompany this task with topographic measurements, see Figure 27a. The targets were read always at early morning to reduce temperature effects, daily during the process of infill removal (one week) and weekly during one month after load removal. Approximately 35 m^3 (7000 kg) of rubble were removed from the vault and no movements were recorded in the targets.

Figure 27b demonstrates that (a) the vault was never conceived to accommodate infill and (b) a timber roof

existed at the level of the vault, before the construction of the vault and the new roof at a higher level.

7 CONCLUSIONS

The present paper addresses the works recently carried out at the Cathedral of Porto as a case study. The methodology that governed the complete set of works is addressed and the conservation and repair works are briefly addressed. Two aspects are treated in detail, namely the towers and the Saint Vincent Chapel.

The towers exhibit severe global damage including cracking, crushing and separation between leaves and also local damage in the cupolas, pinnacles and balustrades. The global damage seems mostly due to water infiltration, deficient conception of the structure, ancient damage due to lightening and changes in the structures of the towers. For the purpose of increasing the structural performance, a rigid frame of stainless steel profiles and a set of long, inclined anchors have been designed to provide a confining ring. In addition, new ties and stitching of the external leaves were also included when necessary. The local damage is mostly due to corrosion of iron elements, which have been replaced by stainless steel elements or have been protected.

The chapel exhibits a significant overload due to a rubble infill resulting from previous demolitions and the external wall presents moderate out-of-plane displacements. From the diagnostics, it was possible to safety prescribe the removal of the infill (approximately seven tons). This operation allowed to confirm that the present vault is not contemporary to the walls and the external wall deformation is stabilized.

REFERENCES

- Binda, L., Anzani, A. 1997. The safety of ancient masonry towers: A survey on the effect of heavy dead loads. In G. Arun, N. Seçkin (ed), *Studies in ancient structures; Proc. intern. conf., Istanbul*. Istanbul: Yildiz Technical University.
- Lourenço, P.B. 1998. Experimental and numerical issues in the modelling of the mechanical behaviour of masonry. In: P. Roca et al. (ed) *Structural Analysis of Historical Constructions*, p. 57–91, Barcelona: CIMNE.
- Lourenço, P.B. 2001. Analysis of historical constructions: From thrust-lines to advanced simulations. In: P.B. Lourenço, P. Roca. (ed) *Historical constructions 2001*, p. 91–116, Guimarães: University of Minho.
- Lourenço, P.B. 2002. Computations of historical masonry constructions, *Progress in Structural Engineering and Materials* 4(3): 301–319.
- Lourenço, P.B. 2004. Strengthening design of the clock-tower in Mogadouro Castle, Portugal. Report 04-DEC/E-07, Guimarães: University of Minho.
- Macchi, G. et al. 1992. The collapse of the Civic Tower in Pavia: A survey of the materials and structure. *Masonry International* 1.
- Macchi, G. 1998. Seismic risk and dynamic identification in towers. In *Monument 98 – Seismic performance of monuments; Proc. intern. workshop, Lisbon, 12–14 November 1998*, p. K.3-K.17, Lisbon: DGEMN, LNEC and JRC.
- Modena, C., Valluzzi, M.R., Tongini Folli, R., Binda, L. 2001. Design choices and intervention techniques for repairing and strengthening of the Monza cathedral bell-tower. In *Structural faults & repair 2001; Proc. 9th intern. conf. and exhibition, London, 4–6 July 2001*. CD-ROM.
- Orduña, A., Lourenço, P.B. 2003. Non-linear cap model for limit analysis of masonry structures, *J. Struct. Engrg., ASCE* 129(10): 1287–1430.
- Valluzzi, M.R., da Porto, F., Modena, C. 2003. Structural investigations and strengthening of the civic tower in Vicenza. In: *Structural faults & repair 2003, Proc. 10th intern. conf. and exhibition, London, 1–3 July 2003*. CD-ROM.

Considerations on the significance of history for the structural analysis of ancient constructions

P. Roca

Universitat Politècnica de Catalunya, Barcelona, Spain

ABSTRACT: This paper presents some reflections on the role of structural modelling in the study of ancient structures and its relationship with other sources of knowledge, such as inspection, history, and monitoring. The relation between structural modelling and historical information is considered with special focus. A discussion is carried out on the capabilities which, ideally, numerical models and methods of analysis should include to obtain a fruitful connection with historical information. In particular, the need for procedures allowing the simulation of historical aspects such as the construction process, later structural alterations or long-term physical damaging phenomena is justified in the light of particular case-studies.

1 INTRODUCTION

The study of the structure of historical constructions poses a number of very significant challenges to the analyst. Difficulties stem not only from the need to model complex geometries, materials and actions, but also from the significance of history and the need for linking the structural analysis with the historical events. As can be observed apropos of the study of real cases, analysis disconnected from history may show sterile or may yield results in contraction with reality.

Certainly, part of the difficulties comes from the overall complexity of historical structures in terms of material, geometry and actions. Masonry, as a composite and brittle material, develops complex mechanical and resistant phenomena whose simulation is still challenging the capacity of advanced theories and computer methods.

Modelling the *materials* and the morphology faces also from the impossibility to reach a comprehensive characterization. This factual impossibility is due to the need for limiting the extent of destructive inspection and the preference for more indirect methods. Indeed, information on materials and internal composition remains very limited in many cases.

The organic *geometry* of many masonry constructions, resulting as a combination of linear, 2D or 3D, straight or curved structural components such as arches, buttresses, multi-layered walls, vaults and domes, must be described by means of capable versatile modelling techniques.

Historical structures are or may have been subjected to *actions* that are unfamiliar to our conventional

understanding of safety and our current techniques for the assessment of modern structures. Among these, major earthquakes of hurricane wind occurrences corresponding to long return periods, or the repeated effect of minor earthquakes or thermal cycles acting during long periods of time, can be recalled. Physical or mechanical phenomena developing through historical periods (such as those manifesting in the form of a slow decay) or more instantaneous but impacting events like destruction caused by wars, or important architectural alterations, are also to be taken into consideration. Besides the technical difficulties which may be found in the attempt of numerically simulating them, most of these actions may be insufficiently known not only historically but also from a phenomenological point of view.

Furthermore, all the cumulative effects of such actions contribute to cause a non-stopping, gradual transformation of the structure. Historical structures are not something inert or unchanging, but alive and always evolving towards, normally, a more sensitive and vulnerable stage, unless maintenance and restoration are carried out, meaning, in turn, more transformation. This gradual evolution is clear in what concerns geometry due to the constant increase of deformation produced by a variety of concurring actions (creep, soil settlements, thermal cycles ...). Anthropogenic alterations and repairs contribute to this changing nature as well (see also Roca, 2001).

Another difficulty coming from history is found in the understanding of the design concepts and construction methods originally used to produce the constructions. Ignoring the original aims, the design processes,

even the ideas inspiring the structures, will not help us in the understanding of them.

Because of all these considerations, conventional methods of calculation, as well as the conventional criteria for the assessment of structural safety, are hardly applicable to the study of ancient constructions. Official codes for structural design, normally oriented to modern constructions, are not either easily transferable to the case of historical buildings. (These facts are clearly addressed in the Recommendations of the Icarsah Committee, 2001.)

It is the footprint of history what makes the analysis of a historical building so challenging and what prevents from the applicability of conventional methods. However, history is also a possibility and a source of understanding, for history can also be interpreted as an experiment in the true scale of time and space. Knowledge on historical facts may provide precious empirical information.

Since conventional methods and concepts may not be usable, another more general approach is required which considers all the viable sources of evidence, including inspection, history, monitoring and structural analysis.

2 THE ELEMENTS OF THE ANALYSIS

2.1 Main activities

Studies on the structure of ancient constructions base on the combination of a set of activities which include (1) the *inspection* and characterization of the present state of the construction, based both on visual recognisance and deep observation by means of (preferably) non-destructive techniques, (2) the *historical research* carried out by expert historians from the available historical documentation, (3) the *monitoring* of the building by means of different types of sensors and (4) the *structural modelling and analysis* of the building. These are, in short, the main elements of the study from which the conclusions on the condition of the building and on the need for repair or strengthening are to be drawn (Fig. 1).

2.2 Historical research

As aforementioned, history can be understood as a natural experiment occurred at true space and time scales. This experiment accounts for the effect of real actions occurring in historical periods which can hardly (or just can't) be reproduced in laboratory or be monitored in the real building.

Because of that, historical research can provide important clues for the understanding of the present condition or to illustrate the response of the building when subject to major actions. Historical investigation provides extremely significant information and must

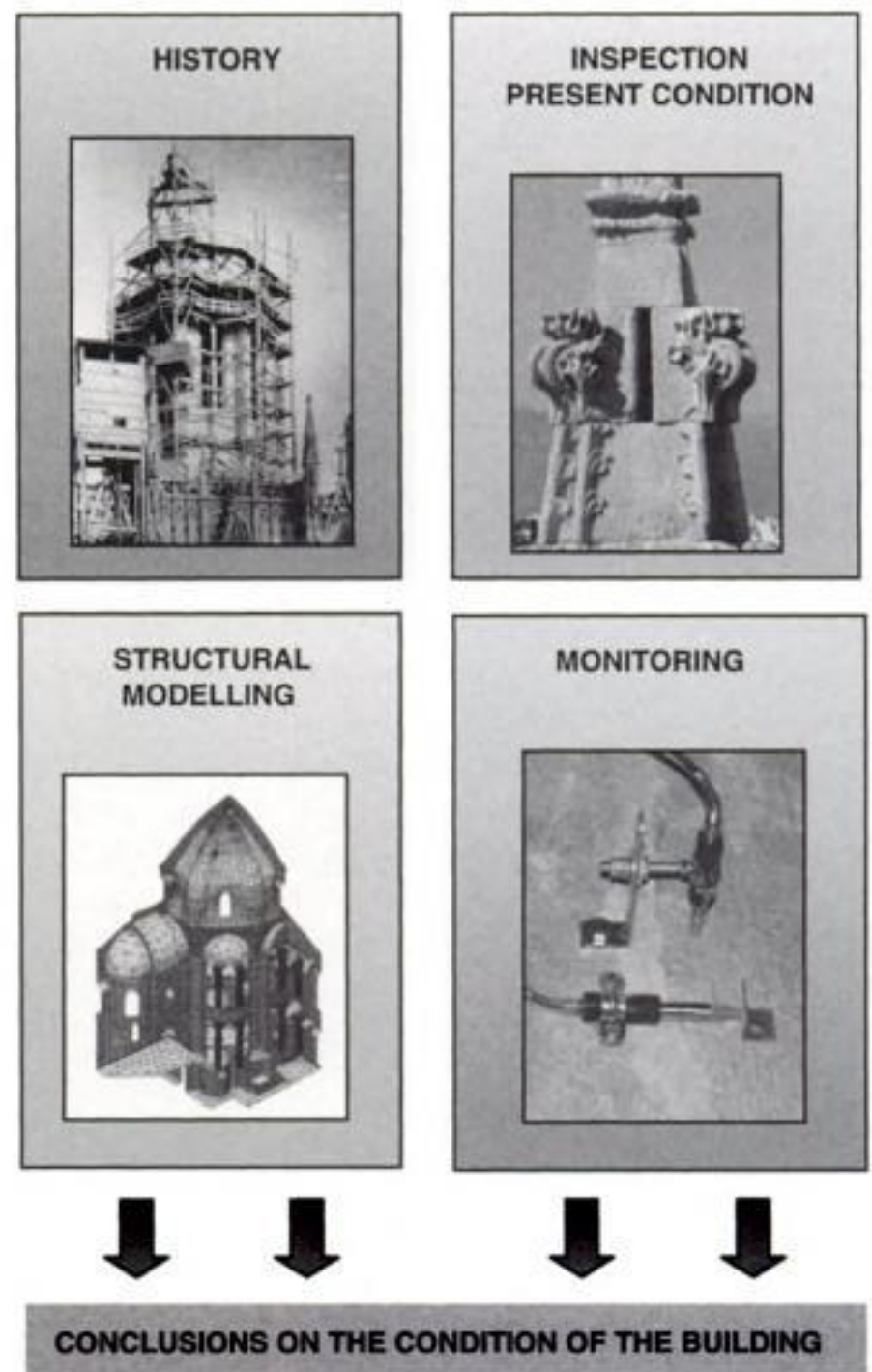


Figure 1. The elements of the analysis.

be considered as one of the most precious elements of the analysis. However, using historical information for the better understanding of an ancient structure is not always feasible or straightforward. The sources (such as the books available in the files of the chapters of Gothic cathedrals) must be investigated and interpreted by specialized historians, who later report to the structural analyst what they think is meaningful for the structure. Effective cooperation and communication between archaeologist or historians and structural analysts may face certain difficulties due to their very different specialization, vocabulary, and priorities. Nevertheless, a very enriching cooperation may take place between both specialists when communication is fluid and common objectives are shared and discussed. The tasks of the historian and the structural analyst are linked, in any case, by their wish to reveal and enhance all the value attributed to the building as part of the architectural heritage. They also share the common objective of contributing to preserve all what is historically genuine in the building.

This requires the development of an interest in history (at least, in history of construction) by the

structural analyst, while also demands a sensitivity or interest towards the structural and technological features of the constructions from the historian.

Unfortunately, a fruitful cooperation between historians and engineers or architects is not enough to ensure an accurate utilization of the information extracted from the historical files. Historical sources provide, most often, only partial and inaccurate information, while showing almost no technical insight. Interpreting the historical notices and linking them with real structural or morphological features (construction, failures, repairs, alteration, damage ...) may require much speculation, and thus give chance to possible subjectivity.

Having an accurate view of the properties of the structure in its original configuration, or systematically recorded details on its alteration may be extremely difficult in many cases. Documents (or historical evidence of any kind) describing the original construction or latter alterations are not always available and, when they exist, they may provide only ambiguous or partial information. Even in the case of important buildings with comprehensive information available, such information may experience significant lacks and thus leave unanswered crucial inquiries for the comprehension of the building. Mallorca Cathedral, as for instance, has been subject to comprehensive historical research; thanks to the effort in reviewing all the available documents, very interesting aspects have been clarified, such as the entire chronology of the construction (spanning for more than three centuries), the original quarries from which the different stones used were taken, or on the decisions leading to a set of important repairs (Domenge, 2004). In spite of it, no clear information has been found, for instance, about the reason for building the upper battery of flying arches. Such flying arches are not conveniently placed for an efficient contribution to overall equilibrium; they were not either built to counteract the effect of wind on a pitched roof which did not exist in origin (Fig. 2; Roca and González, 2001). No clear historical notice has been found on the reason for overloading the vaults and transverse arches with large pyramids of stone (in a way that cannot be seen in any similar building, Fig. 3); neither is any evidence either on the period in which the vaults were overloaded. On all those issues, historians and structural analysts have their own guesses, but no clear evidence coming from historical research. In Tarazona Cathedral, and also in spite of the historical research, the question whether the original cimborio collapsed because of structural problems, or whether it was just dismantled to build a new, larger one, remains unanswered (Aguerri and Rodríguez, 1998). In other buildings, information may be scarce or just inexistent. Notices on partial failures or structural problems are mentioned in historic files in a way which usually

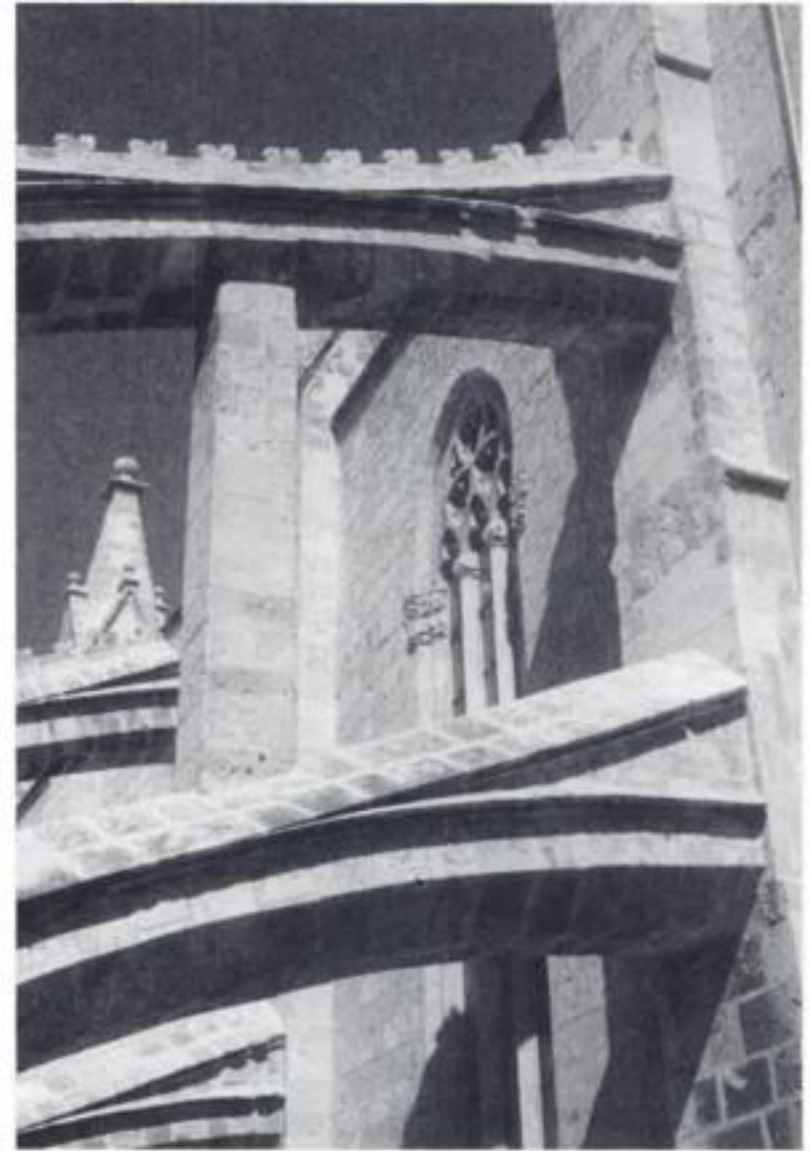


Figure 2. Double battery of flying arches of Mallorca cathedral, with the upper ones showing large deformation and occasional propping.



Figure 3. Dead weight on vaults and transverse arches of Mallorca Cathedral.

doesn't allow objective understanding of their actual material extent or structural significance.

It may be difficult to distinguish between mechanical alterations (cracks, deformations) arrived in the long-term, from those existing in the early configuration of the building. Masonry historical buildings deform, settle and crack during the construction process itself. In the case of the mentioned cathedrals, it is very difficult to guess which part of the settlements and deformations was experienced during the

construction process (when removing the centerings, for instance), and which part has been caused by later phenomena, such as earthquakes, long-term damage of the repeated thermal cycles.

Historical record is essential to understand the structure. Even if the historical information may be incomplete, we must try our best to gather as much historical evidence as possible. However, the available historical record may not be enough to really understand the structure; it is but one of the several sources which contribute to our knowledge.

2.3 Inspection

Activities related to both superficial or deep inspection provide qualitative information on the present condition of the building, encompassing geometry, morphology, construction details, material properties, alterations, historical repairs, and existing damage. Inspection provides the essential information needed to select the primary hypotheses on which the model is based. It also provides the amount of information needed to build a structural model in detail.

In some cases, realizations coming from inspection may permit a certain calibration of the model. This calibration may be achieved through the comparison of possible predictions of the model (in particular, those related to deformation or damage) with effects actually observable in the building. For instance, a first illustration of the validity (or inadequacy) of a model may be achieved by simulating the effect of gravity loading and then comparing the predicted distribution of cracking and deformation with their real manifestations in the building. However, this type of calibration may be hardly undertaken in practice because of the uncertainty on the actions having historically impacted on the building and the superimposition of effects involved in damage. Even if such aspects remain uncertain, results from inspection should be utilized to check the model and see that the predictions are not in frontal contradiction with reality. For instance, a model producing cracks, due to dead load, in parts which have remained intact from the construction of the building itself, should obviously be subjected to reconsideration. Inspection provides, at least, the possibility of a preliminary test for essential compliance with reality.

2.4 Monitoring

Monitoring provides quantitative information on the response of the structure across a short and contemporary period of time. Monitoring can be understood as a small window opened over the long term processes taking place in the otherwise inaccessible historical time (Fig. 4). In particular, monitoring may allow for the recognition of incremental processes in a term reasonable for engineering purposes and thus provide

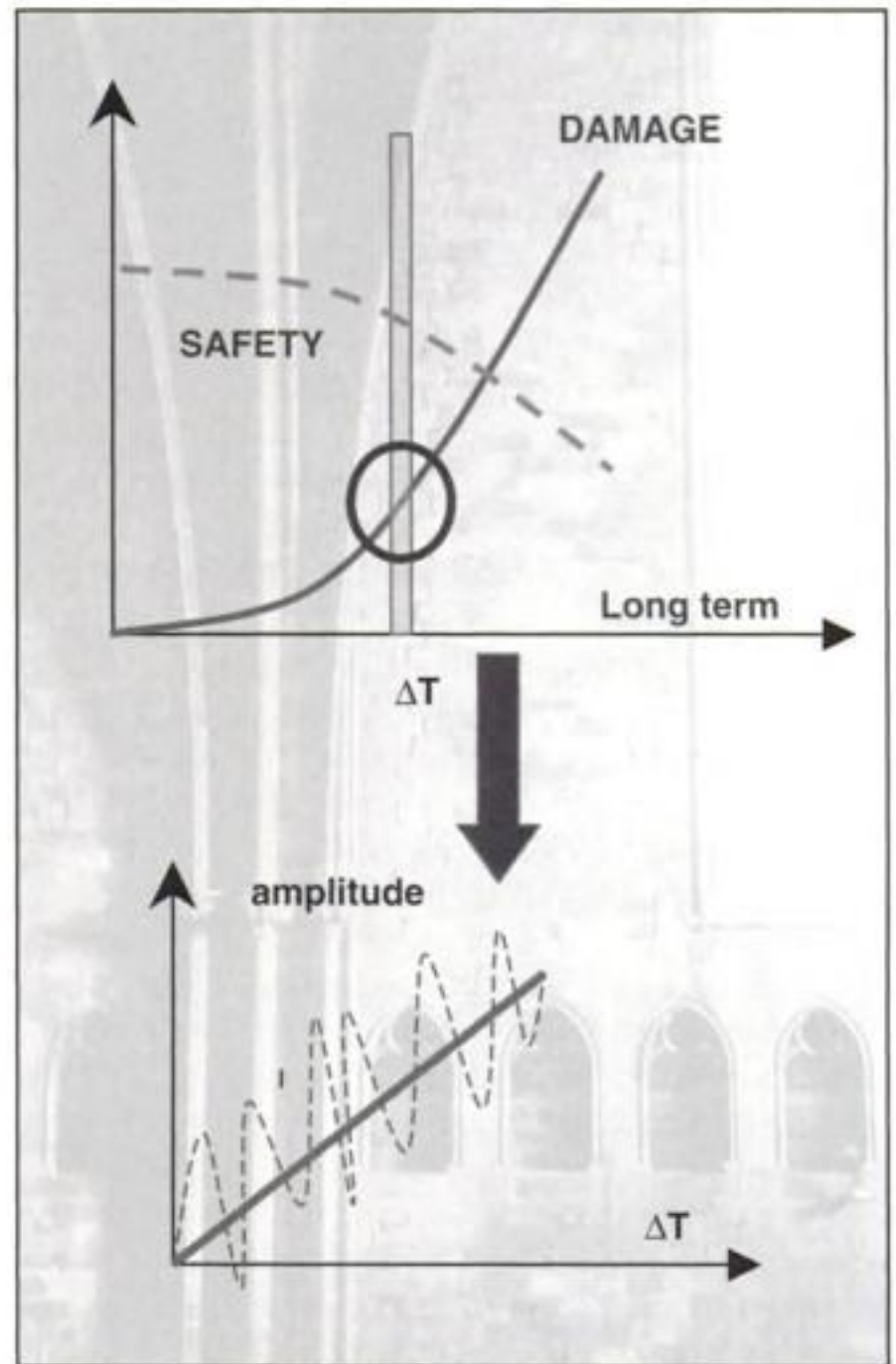


Figure 4. Monitoring as a window over historical time allowing possible insight on active processes long-term damaging processes.

information useful for the study and restoration of ancient constructions (see Roca et al., 2003, for a larger discussion on this issue).

However, characterizing long-term damage is a challenging task due to the slowness of the processes involved and the fact that they may be masked by more apparent, short-term variations caused by present actions. In order to characterise incremental, long-term processes, monitoring must be designed to allow a clear distinction between the reversible or cyclic components of the parameters measured, on the one hand, and the irreversible, cumulative components developing in the long term, on the other hand. In turn, the possibility of recognising both types of components demands the following requirements:

Monitoring must be extended to a period long enough to cover the entire duration of acting cyclic actions; since annual variations of temperature must be considered in any case, the minimum acceptable period is a complete year. Additional years will be of value to confirm the tendencies observed and appraise their possible evolution in the long term.

Monitoring must afford the characterisation of the environmental actions occurring during the studied period. This is particularly so in the case of the climate environmental actions; parameters such as the temperature and the humidity are to be measured at different stations in both the interior and the exterior of the building. Wind velocity and direction may be characterised by means of conventional measuring devices. Similarly, valuable information can be obtained if the effect of occurring low-intensity earthquakes or environmental vibrations is recorded by means of seismographs.

Structural analysis and monitoring do both handle quantities and thus permit a direct comparison. Results of monitoring can be used for calibrating a numerical model, provided that not only the parameters associated to the response (deformations, displacements, rotations, vibrations) are measured, but also those characterising the actions (environmental thermal effects, ground motion). In turn, simulation by a numerical model can help laying-out and adequate and truly informative monitoring by giving light on, for instance, the more significant variables to be measured, the expectable ranges of variation (which are meaningful to select the sensors) or the best location for the sensors.

2.5 Structural modelling

The role of the structural analysis within the frame of a general study and the requirements which should be taken into consideration to link it, in a profitable way, with the rest of the elements of the study (inspection, history, monitoring) are discussed in the following sections.

3 ROLE OF STRUCTURAL ANALYSIS

Drawing accurate conclusions from historical research, inspection, monitoring and structural modelling requires a clear statement on the real meaning of these activities and the way they are connected to each other.

Since conventional methods and theories may not be applicable to the study of ancient constructions, technicians working on them must base their investigation on the more universal and elementary approach given by the scientific method. In our understanding, all these activities are precisely the pieces needed to develop an investigation adequately based on the scientific method.

Applying the scientific method requires, first, the adoption of a set of hypotheses and, second, the use of available empirical evidence to prove them. To actually comply with the scientific method, the adopted hypotheses must allow demonstration or refutation based on the observation of reality. Proposed

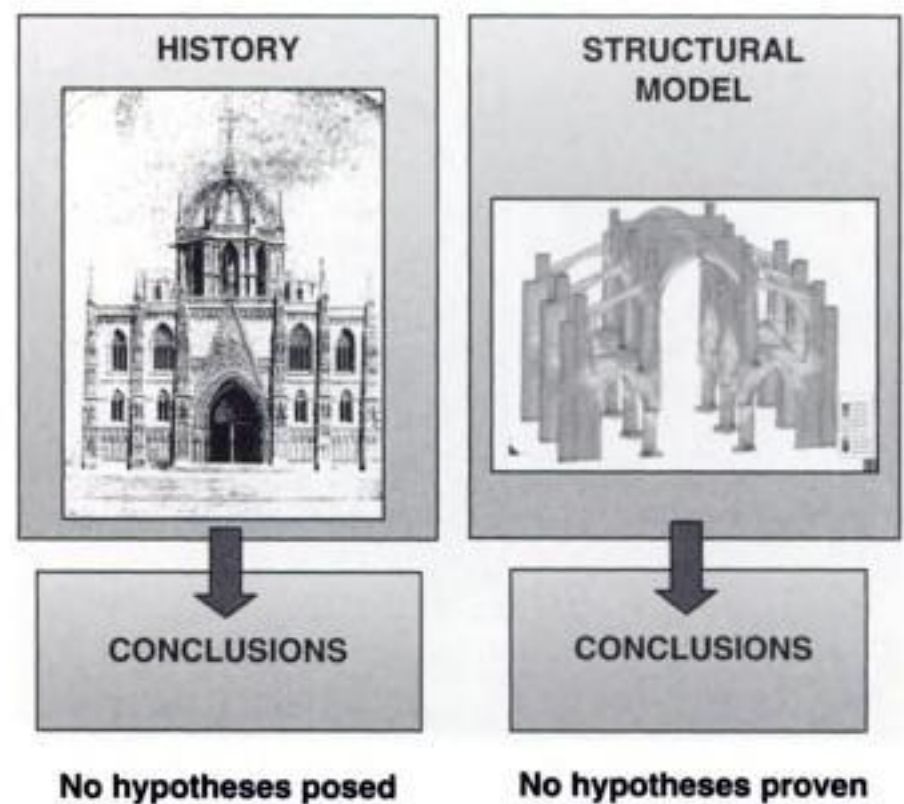


Figure 5. Debatable approaches not taking advantage of all possible sources of information.

hypotheses not allowing possible evaluation are in fact of null epistemological value; they will not add any valuable understanding and will be useless for a reliable prediction on the response and needs of the building analysed.

It is on the light of the above understanding that the different elements of the study are to be displayed and connected. Some of the mentioned activities (in fact, the structural modelling) are related to the first stage of the process, that is to say, to the adoption of the hypotheses. The model, whatever its nature (conceptual, analogical, numerical ...) is just the recipient of the hypotheses on the physical and mechanical nature of the construction. History, inspection and monitoring are activities oriented to the production of the empirical evidence needed to validate the hypotheses and, if needed, to disregard, correct or improve them to a satisfactory extent.

This understanding of the problem may seem obvious to any technician really committed with a scientific understanding of the study of ancient constructions. Unfortunately, some analysts did proceed, in the past, using incomplete reasoning schemes which, in some occasions, produced useless or incorrect conclusions (Fig. 5). As for instance, a blind satisfaction with an unproven conceptual or numerical model, from which results indicating the weakness of the structure were obtained, led, in some cases, to the implementation of an impacting strengthening causing a significant (and irreversible) transformation of the historical construction. Since the model had not been validated, no real demonstration for the need of such strengthening had been really provided. Furthermore, real examples exist (like in the case of the Segovia Aqueduct, Jurado, 1995) for which it has been possible to demonstrate that the already implemented strengthening was

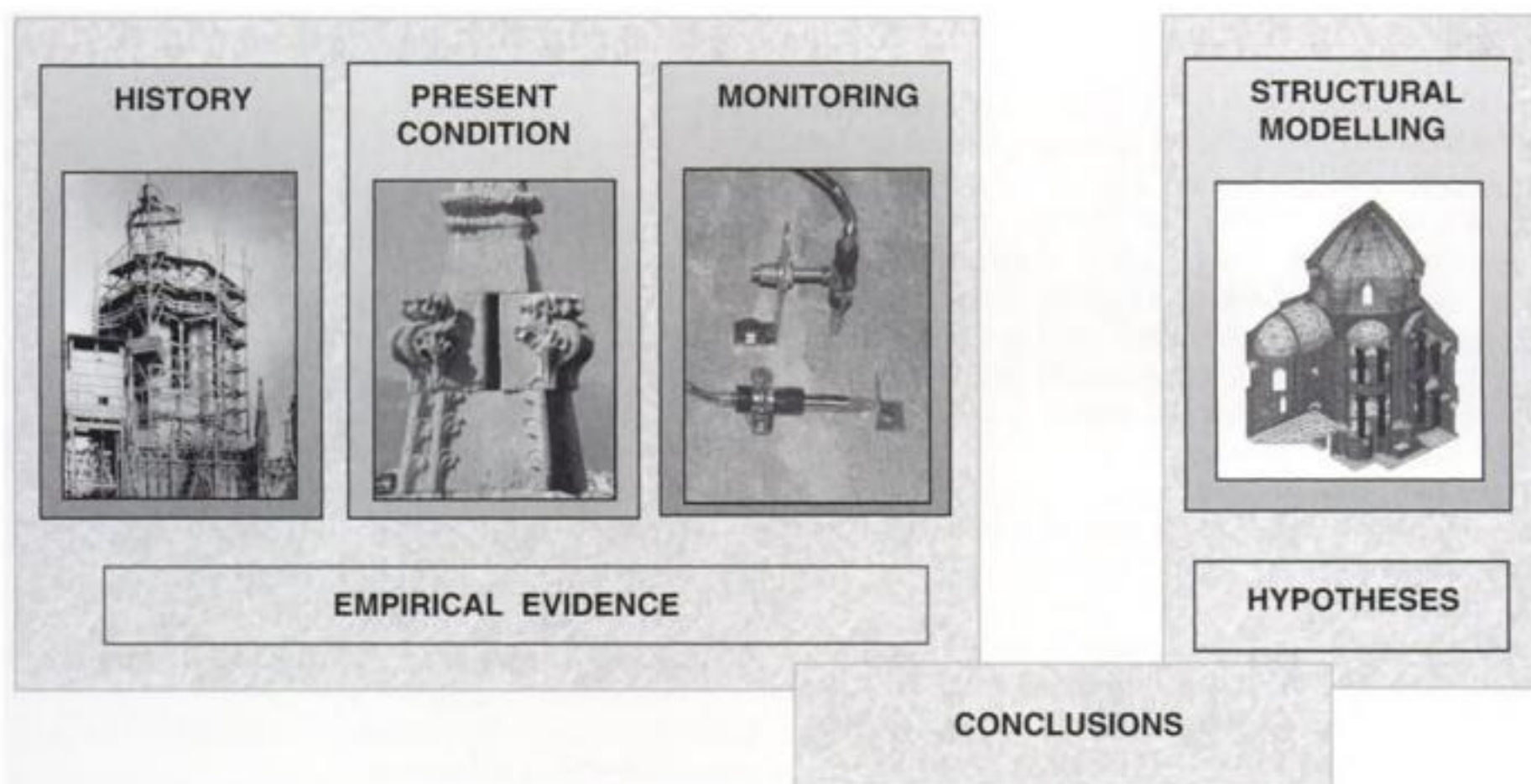


Figure 6. Role of the different activities in the study of an ancient construction. Conclusions on the condition of the building stem from the validation of hypotheses adopted to elaborate a model, once validated or calibrated in the light of available empirical or experimental evidence obtained from historical research, inspection and monitoring.

in fact not really needed and even unsuitable for the conservation of the structure.

Results from non-validated modelling may be simply in contraction with meaningful historical facts. For instance, the analysis may predict that an existing and well preserved dome can not resist a major earthquake having, in fact, occurred several times during the life-span of the building; if anything, this mere fact indicates that the model is not entirely correct and is still requiring further calibration. Although the hypotheses are (willingly or unwillingly) present, no previous effort has been devoted to gathering empirical evidence and using it to validate or calibrate the model before exploiting it for predictive purposes.

Another debatable approach consists of drawing the conclusions from the only knowledge of history. Certainly, the mere realization that a building is standing offers an empirical hint of its viable stability under the action of gravity. However, the actual meaning of this fact can only be completely interpreted in the light of a (conceptual, analogical, numerical) model of the structure. As shown by some real cases, ancient structures having been stable for centuries may collapse in a sudden manner without providing previous visible evidence of their precarious condition (as in the case of the Civil Tower of Pavia or Noto Cathedral, see Macchi, 1998, Croci, 1998, and Binda et al., 2003). Similarly, the fact that a building has been able to resist some historical earthquakes is not enough to conclude on its capacity to resist possible new earthquakes. The safety of the building in the case of a future earthquake is not guaranteed due to the structural decay (caused by the

progress of damage), possible architectural or structural modifications caused on the building, or because of the particular seismic features of the new earthquake (as in the case of the Basilica of St. Francis of Assisi, see Croci, 1998).

Even if history is regarded as the main and best source of evidence, complementary experimental and numeric analyses are needed to actually understand, in a rationale way, the condition and needs of the building. The problem of this second way or reasoning is in the lack of hypotheses actually being checked.

To our understanding, an adequate, scientifically based approach must consider both the structural modelling, as the recipient of the hypotheses to be checked, and the evidence coming from the inspection (providing qualitative evidence on the present condition of the building), historical research (as a source of qualitative evidence of the past performance of the construction the true scale of space and time) and monitoring (providing quantitative information of the current performance at a local time interval).

The need for a multidisciplinary approach stems not only from the variety of aspects involved by the study but also from the wish to apply the scientific method in a consistent and profitable way (Fig. 6).

4 REMAINING SPACE FOR UNCERTAINTY

It must be recognised that even if modelling (as recipient of the hypotheses) is used in combination with empirical evidence, and even if a model or a method

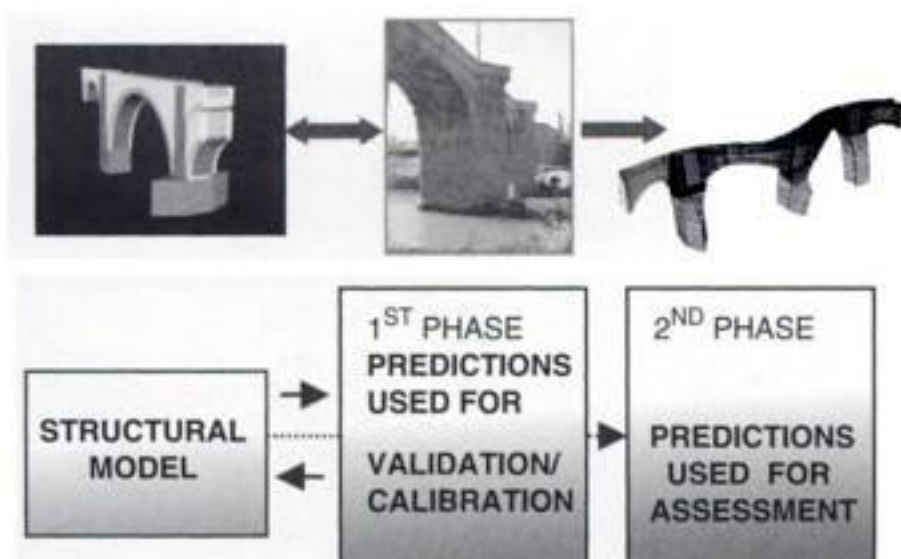


Figure 7. Two phases in the use of a structural model: validation and assessment.

of analysis is consistently validated and calibrated, a certain margin for subjectivity and uncertainty exists. The reason for remaining subjectivity is in the fact that the model or method will be validated for actions or general conditions with available information on the building, and thus different from those for which the model will be used for assessment (Fig. 7). For instance, an attempt may be undertaken to validate or calibrate a model using information from inspection which characterize the response of the building subject to dead load. Distribution of cracking predicted by the analysis for dead loading may be compared with cracks existing in reality. Or, deformation due to simulated thermal effects, vibration amplitudes or frequencies due to simulated traffic or wind may be compared with real measurements captured through a monitoring campaign. Once validated, the model will be used for the purpose of assessing the response of the building subjected to a variety of hypothetical actions (such as major earthquake). This operation requires, in fact, to extrapolate from the set of hypotheses or conditions for which the model has been consistently validated. However, this extrapolation – and the corresponding caused uncertainty – are an unavoidable effect inherent to the fact of predicting. The technician will have to base on his understanding and experience to determine whether the use of the model is reasonable or whether it is abusively trespassing the sphere of tolerable uncertainty.

In turn, and because of this remaining uncertainty, predictions and conclusions are always to be accepted as provisory. Further activity involving monitoring and periodical inspection of the already assessed or restored buildings are required to *a posteriori* validate the predictions – and the subjacent hypotheses – or review them.

5 THE STRUCTURAL MODEL

As aforementioned, the structural model constitutes the recipient of the hypotheses adopted during

the application of a scientifically-based analytical approach. The hypotheses contained in a model can be classified into two different categories.

On the one hand, a set of primary hypotheses, referring to physical or mechanical principles, is (consciously or unconsciously) adopted in order to select and adequate frame theory or formulation allowing the calculation. These include principles related to the technique used for the description of the geometry and the materials, such as the validity of continuum mechanics, or the adoption of particular constitutive equations. When it comes to brick or stone masonry, hypotheses on this respect are not yet conventionally or universally accepted; further research is still needed in spite of the significant effort carried during the last decades (see Lourenço 1998, 2001, for state-of-the art reports on this subject). Analysts must still undertake a certain contribution from his own in order to select and justify the optimal approach to be used in each particular case.

The failure of a model to represent real mechanical or strength phenomena observed in the building (at least, those that the analyst is trying to simulate) must lead to the conclusion of the need for another approach. In any case, the analyst must be aware of the limitations of the theory or formulation adopted; he must be able to interpret critically the results obtained and to reject those not being meaningful, or to recognize, if the case, the entire failure of the approach.

On the other hand, models are also based on a secondary set of more particular hypotheses on the geometry, morphology and material properties of the building. No matter the effort invested in the inspection and experimentation, the amount of information will never be enough to describe the full complexity of the structure, nor will any conceivable model be able to receive it comprehensively. The knowledge of the structure is always partial, which requires for additional hypotheses on its geometry, construction details and materials. Furthermore, viable models require an important level of idealisation – which is fact consistent with the very essence of modelling. Additional hypotheses are needed about the best way of simplifying or idealising the features of the particular building. Can a wall be described as a solid component, or should it (to the cost of larger computational effort and more accurate information available) be modelled as its real three-leaves counterpart? Can a column be described as a uniform, cylindrical body or should it be modelled as a geometrically and materially complex body composed of many different units having peculiar geometrical details? Do we need to include in model the mass of soil on which the building is founded?

Again, this second set of hypotheses must be critically checked and the possibility of having to improve them, even to large extent, must be accepted. These hypotheses may be improved through a calibration

process based on the comparison of the numerical predictions with the evidence available on the real response of the building.

In all this discussion, the requirement for the agreement between numerical results and experimental

or empirical evidence must be only extended to an engineering level. Aiming at a physically exact or extremely close agreement between model and reality may be sterile or prohibitively expensive for most purposes. Required cost and term must keep reasonable and consistent with the importance and complexity of the building and the resources available.

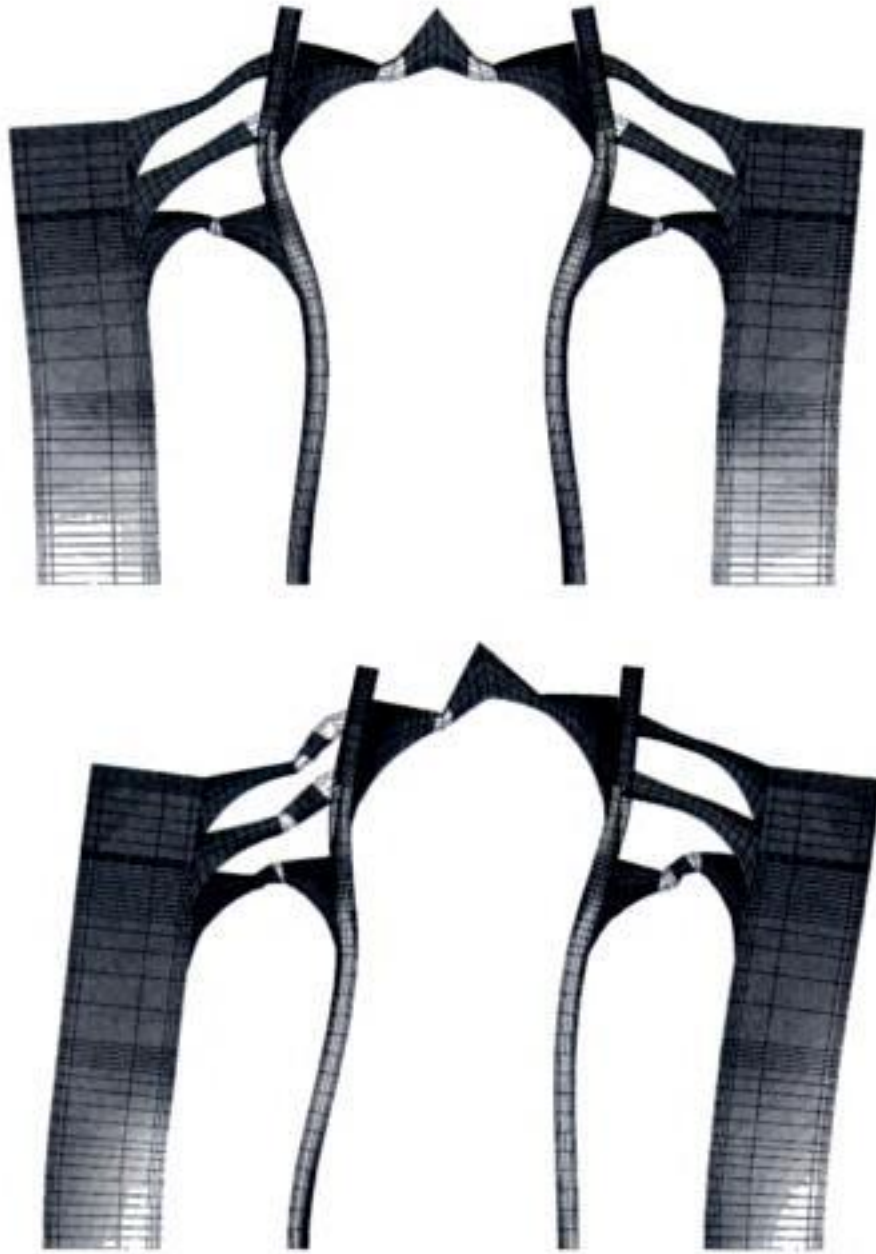


Figure 8. Analysis of the transverse section of Mallorca Cathedral. Above: deformation ($\times 2000$) and distribution of normal stresses ($10 \times \text{kN/m}^2$) in chromatic scale (white used for cracking) for dead load. Below: deformation ($\times 1000$) and distribution of stresses predicted for a major earthquake ($a_c/g = 0.12$).

6 CAPACITIES REQUIRED FOR THE ANALYSIS

Historical constructions may show a variety of structural alterations (such as large deformation, cracking or related damage in compression, and fragmentation due to cracking in tension or shear) caused by phenomena or actions developed during historical stages and long periods of time. In many buildings, such forms of damage do manifest in a very severe and apparent way. Conventional instantaneous analyses are not adequate for the study and the simulation of such effects.

In particular, it has been observed in a number of case-studies that instantaneous analysis may predict displacements orders of magnitude smaller than those shown by the real building; notwithstanding, the obtained deformed shapes are qualitatively similar to the real ones (Figs 8, 9).

More accurate studies intended to simulate aspects developing in the historical time may require specific capacities to simulate the following aspects:

- (1) the subsequent historical stages of the building (in particular, the construction process) through a sequential analysis,
- (2) the actions occurring in historical periods, such as major earthquakes or the repeated effect of minor earthquakes or thermal cycles, and
- (3) long term rheological or damage processes (such as those related to creep) developed through the life of the construction.

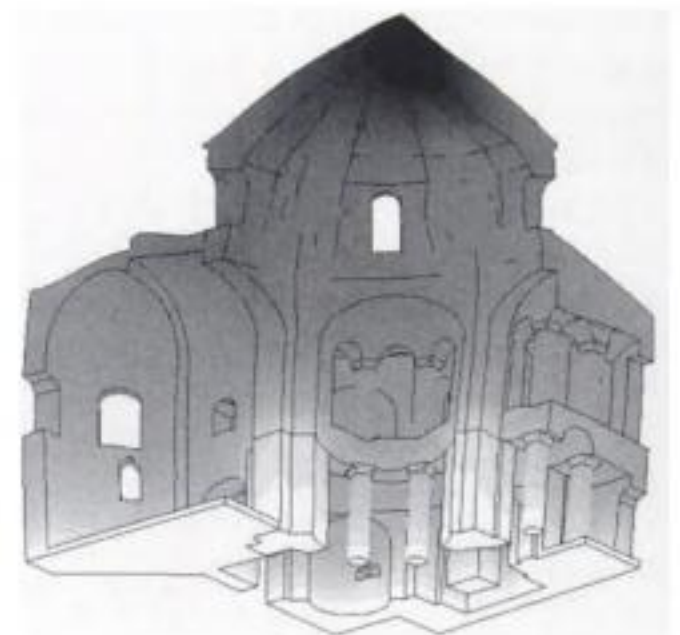


Figure 9. View of Küçük Ayasofya Mosque in İstanbul, compared with the deformation predicted by the analysis for gravity loading (amplified $\times 2300$).

It must be noted, however, that a realistic simulation of historical actions or long-term damage processes is still requiring additional experimental studies and numerical developments.

Faculties (1) to (3) may provide meaningful results in the frame of a non-linear method of analysis accounting for both the geometric and material contributions to a non-linear response. On the one hand, large displacements may affect the equilibrium of slender masonry constructions; this can be observed in slender arches or in more complex skeletal systems. On the other hand, masonry shows a highly non-linear response, even for moderate stresses, due to cracking in tension or other associated phenomena. Consequently, methods of analysis must be equipped with appropriate procedures for the description of the equilibrium of the deformed structure, and also with realistic constitutive equations for the simulation of the mechanics and strength of masonry. The capacity to account for these effects is of large importance since they act in a coupled way with the aforementioned historical effects (1) to (3). For instance, and from a theoretical point of view, additional flexibility due to cracking and progressive deformation due to creep might cause a very important increment of the eccentricity of the normal force at certain sections of a pier or an arch, leading, ultimately, to a differed collapse under the only action of gravity.

Simpler calculation methods, such as linear elastic analysis or limit analysis based on the plastic theorems may be very useful for the study of ancient constructions and may really contribute, when handled by an experienced analyst, to face complex problems. The above discussion is in no case oriented to discredit the use of these simpler tools in the study of ancient constructions. However, the possible simulation of complex actions and responses encompassing historical time calls certainly for more sophisticated approaches.

7 MECHANICAL DECAY IN THE LONG TERM

Long-term phenomena leading to progressive deterioration during historical periods must be accounted for in order to understand the existing damage. As observed apropos of the study of recent collapses (Papa and Taliercio, 2003, Binda, et al. 2001, 2003), the effect of creep under constant stress, at the long term, may induce significant, cumulative damage in rock-like materials. As mentioned by Binda et al. (2001), accumulation of damage (eventually leading to collapse) may occur for stress values significantly lower than the normal strength obtained by standard monotonic compression tests. The same authors found that such phenomena could start at 40%–50% of the normal strength value.

Effects due to historical actions may also contribute very significantly to the continuous increase of deformation. Extraordinary actions such as large earthquakes may produce important lesions and irreversible deformations (Fig. 8). Low-intensity earthquakes or repeated occurrences of hurricane-force wind may act cumulatively to cause ever increasing damage and deformation. Daily or annual thermal cycles individually have a minimal effect; however, a certain, irreversible increment of deformation may be produced after each cycle, thus contributing over very long periods of time to a meaningful increase in overall deformation. It must be noted that the effects of cyclic actions do not dissipate with time, but may increase in an accelerate way as the construction becomes more and more damaged.

The damage affecting the construction, which in normal conditions always increases due to the mentioned and other possible causes, will, in turn, enlarge the sensitivity of the construction towards a variety of actions. This situation contributes to constantly increasing (never-mitigating) deformation at the long-term or even accelerated long-term deformation which, in the worst case, can lead to the collapse of the construction. Since the more persistent action is gravity, it is not strange that such constant increase of deformation may manifest as a monotonic, non-asymptotic amplification of the initial deformed shape due to dead load.

Ideally, the numerical model used should be able to simulate most of the present or historical actions having affected the construction; it should also permit sequential analysis to simulate the construction process and the latter possible structural alterations or repairs. Having specific constitutive equations available for long-term creep of masonry or stone-like materials, such as the one proposed by Papa and Taliercio (2003), is of utmost importance for the purpose here referred.

8 THE LASTING INFLUENCE OF THE CONSTRUCTION PROCESS

Important effects related to deformation can be attributed to the construction process. The construction of historical structures lasted during large periods amounting to several decades or centuries. The construction included long intermediate stages during which the structure was stabilized by means of provisory supports or was forced to develop resisting mechanisms not entirely consistent with its structural arrangement and design. It is likely that the structures showed larger mobility during these intermediate phases due to the flexibility of the provisory supports and the more limited lateral confinement, so that significant initial deformations were produced. This phenomenon was amplified by the early settlement of

mortar in joints and the initial creep of compressed members.

Historical research on Mallorca Cathedral (built during 13th to 15th c.) has proven that the construction of each bay followed the same process, consisting on, first, the erection of the lateral chapels (with their vaulting) and buttresses, and, second, the construction of the collateral and then the central vaults

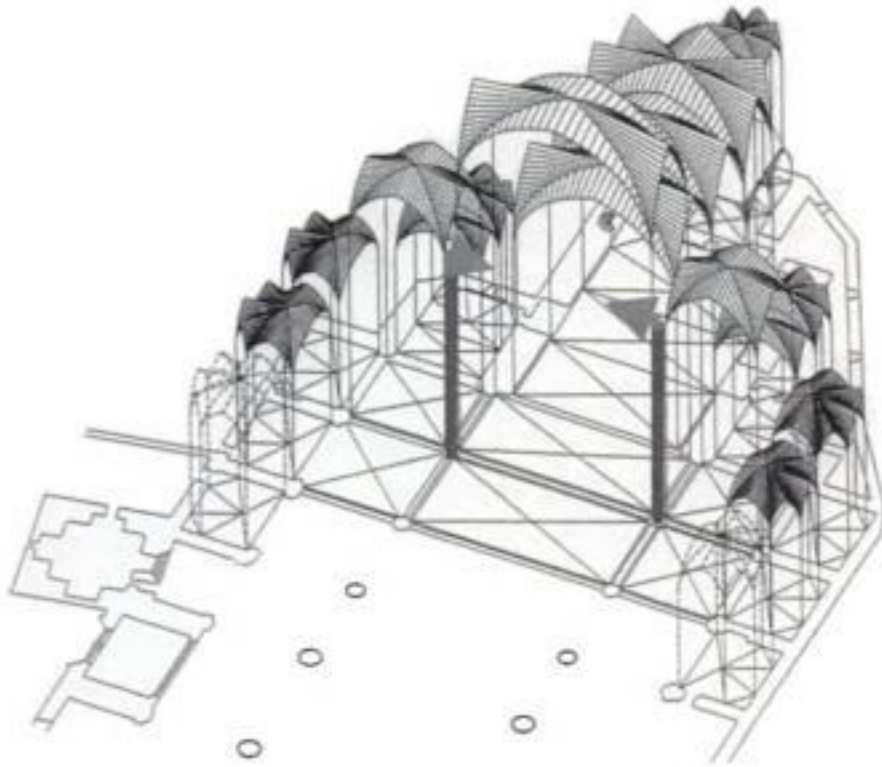


Figure 10. Construction process and temporary unbalanced forces in the transverse section of a Gothic cathedral.

(Fig. 10). Momentarily, the construction experienced an intermediate stage consisting of the partial structures shown in figure 11 (left). It is not clear, from the historical documents, whether the centering of the lateral vaults was removed prior to the construction of the central vault, or whether it was maintained during the entire operation. Removing the centering of the lateral naves would have caused a very significant inward thrust on the partial structure (Fig. 10) producing large lateral deformation. Given the characteristics of the wooden centering frames used at the time (with no foreseeable effective transverse ties to prevent from causing lateral forces against the capitals of the piers, it is likely that keeping them during the construction of the central nave would not have saved the piers from receiving a significant unbalanced lateral thrusts.

The numerical simulation of this stage, carried out by means of a FEM continuum damage model (see Cervera, 2003, for more information on the calculation technique used) has shown that equilibrium is possible for this particular condition at the cost of a very important deformation; however, no significant damage is experienced by the partial structures. The obtained lateral deformation is one order of magnitude larger than that predicted by an instantaneous analysis on the entire structure. Consistently, the subsequent completion of the central clerestory walls and vaults in the sequential analysis (Fig. 11, right) does not cause significant additional deformation.

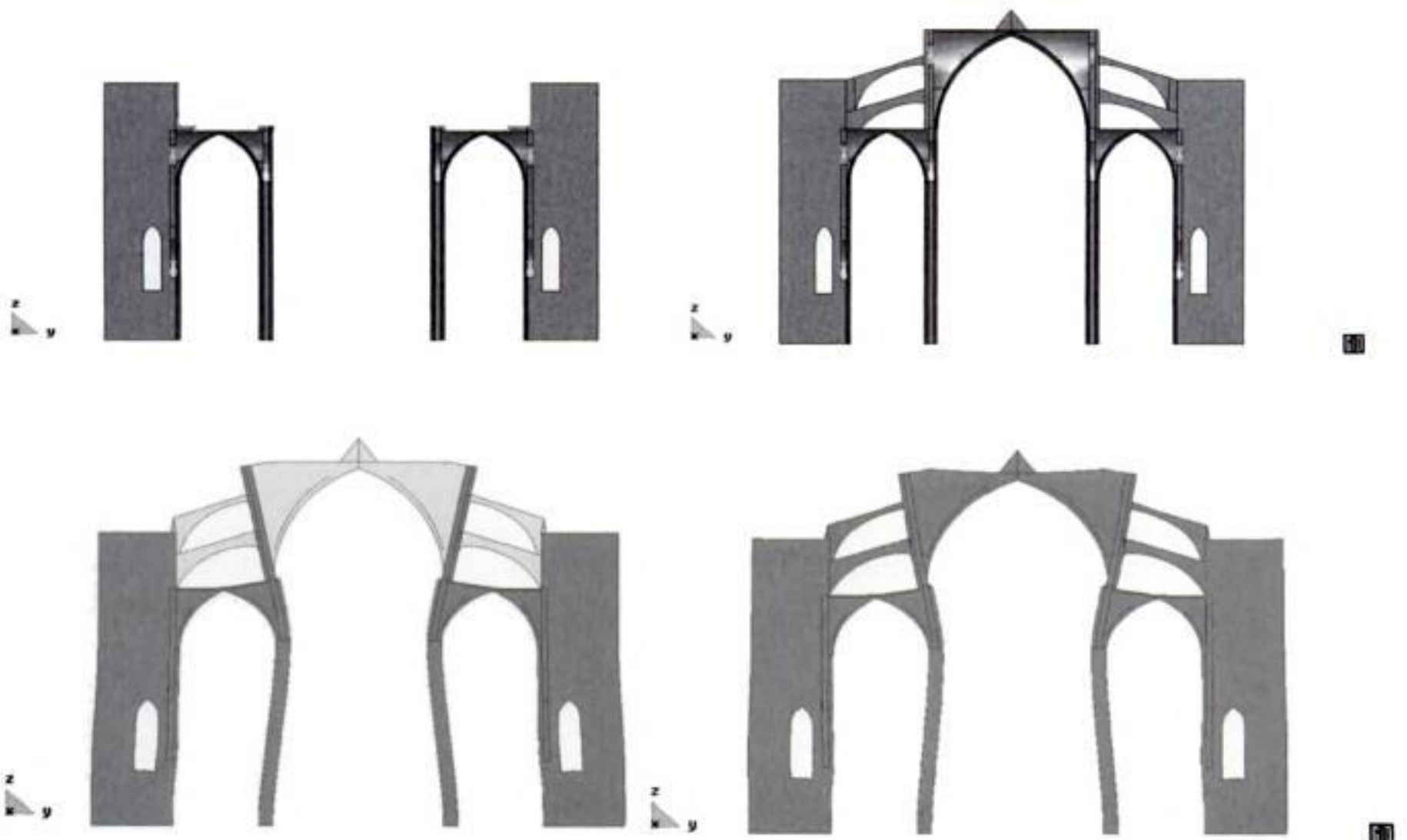


Figure 11. Simulation of the construction process. Intermediate (left) and final (right) configuration and accumulated deformation.

9 SIMULATION OF REPAIR AND STRENGTHENING ACTIONS

A model adequately validated and with demonstrated predictive capacity should not only be exploited for the assessment of the building in the past or in the present condition, but also to analyze its response during and after the restoration. The models should be chosen and selected in a way allowing the simulation of the possible repair or strengthening operations and the later response of the intervened construction. Using the model to assess the effect of a possible strengthening technique is not only a potentiality of the model, but also a requirement for a consistent method linking adequately investigation and restoration. Consistency also demands to assess the performance of the model representing the strengthened building by means of additional monitoring at the long-term.

A model allowing the simulation of possible strengthening techniques may also help to determine the more efficient one in improving the structural stability of the building, or may contribute to choose the minimal one yet providing the necessary strengthening effect.

10 CONCLUDING REMARKS

The role of modelling and structural analysis is found in predicting the response of the structure on the base of a set of adopted hypotheses. These hypotheses are related to (1) the physical principles governing the structural response and (2) the particular morphological and material features of the building. Inspection, historical research and monitoring may provide the empirical information needed to validate the hypotheses – and thus the model. Evidence on reality provided by the mentioned activities must be used, through a direct comparison with the predictions of the model, to validate or improve it until reaching a satisfactory agreement.

The purpose of using the model to assess complex structural phenomena occurring in historical periods calls for a set of demanding capabilities (see section 5), among which the simulation of the construction process (and its lasting effects), long-term damage processes, or the effect of persistent or extraordinary actions occurring in very long periods. These capabilities are still difficult to mobilize in practice due to the limitations of our understanding of complex physical and mechanical phenomena affecting ancient constructions (such as long-term damage). Limited or uncertain information on history and historical actions is an obstacle as well.

However, non-stopping research effort, covering both the experimental and the numerical fields, makes the possibility of having powerful and realistic tools of analysis in a near future foreseeable. Research on

history of construction, now experiencing much renewed interest, may also contribute with the necessary understanding of historical construction technologies.

REFERENCES

- Aguerri, F., Rodríguez, J. M., 1998, *Director plan for the restoration of the cathedral de Sta. Maria de la Huerta, Tarazona (in Spanish)*. Zaragoza: Diputación General de Aragón
- Binda, L., Saisi, A., Messina, S., Triangli, S., 2001, Mechanical damage due to long term behaviour of multiple leaf pillars in Sicilian Churches. *Historical Constructions*, Guimaraes: University of Minho
- Binda, L., Anzani, A., Saisi, A., 2003, Failures due to long-term behaviour of heavy structures: the Pavia Civil Tower and the Noto Cathedral. *Structural Studies, Repairs and Maintenance of Heritage Architecture VIII*, Southampton: WIT Press
- Cervera, M., 2003, *Viscoelasticity and Rate-dependent Continuum Damage Models*. Pub. M79, Barcelona: Center for Numerical Methods in Engineering (CIMNE)
- Croci, G., 1998, The collapses occurred in the Basilica of St. Francis of Assisi and in the Cathedral of Noto. *Structural Analysis of Historical Constructions II*, Barcelona: CIMNE
- Domenge, J., 2004, Chronology of the different construction phases of Mallorca Cathedral. *Study of the construction and structural response of Mallorca Cathedral* (in Spanish). Barcelona: Universitat Politècnica de Catalunya
- Iscarsah Committee, 2001, *Recommendations for the analysis, Conservation and Structural Restoration of Architectural Heritage*. ICOMOS International Committee for Analysis and Restoration of Structures of Architectural Heritage
- Jurado, F., 1995, The aqueduct of Segovia. *Structural Analysis of Historical Constructions I*, Barcelona: CIMNE
- Lourenço, P., 1998, Experimental and numerical issues in the modelling of the mechanical behaviour of masonry. *Structural Analysis of Historical Constructions II*, Barcelona: CIMNE
- Lourenço, P., 2001, Analysis of historical constructions: From thrust-lines to advanced simulations. *Structural Analysis of Historical Constructions III*. Guimaraes: Universidade do Minho
- Macchi, G., 1998, Problems related to the original conception. The case of Pavia Cathedral. *Structural Analysis of Historical Constructions II*, Barcelona: CIMNE
- Papa, P., Taliercio A., 2003, Creep modelling of masonry historic towers. *Structural Studies, Repairs and Maintenance of Heritage Architecture VIII*, Southampton: WIT Press
- Roca, P., 2001, Studies on the structure of Gothic cathedrals. *Structural Analysis of Historical Constructions III*. Guimaraes: Universidade do Minho
- Roca, P., González, J. L., 2001, "Morphology, Structure and History. The case study of the upper flying arches of Mallorca Cathedral". *International Millenium Congress. More than two thousand years in the history of architecture*, lb 22, Paris: ICOMOS
- Roca, P., González, J. L., Aguerri, F., Aguerri, J. I., 2003, Monitoring of long-term damage in Gothic cathedrals. *Structural Studies Repairs and Maintenance of Heritage Architecture VIII*: Southampton: WIT Press

Design approaches of interventions for the safety and conservation of historic buildings

C. Modena

Department of Structural and Transportation Engineering, University of Padua, Italy

ABSTRACT: Unconventional design approaches of repair/strengthening interventions on historic masonry buildings are more and more required and actually becoming popular among engineers and architects. This implies all the aspects of the design, and first of all theoretical/experimental ways and tools for evaluating the structural behaviour until failure of existing structures prior and after interventions are made. Primary scope of a conservative “attitude” in this field is in fact to avoid over-designing of interventions, which of course requires to limit as much as possible underestimations of the actual resisting capabilities of the existing structure. Important are, then, the proper use of materials and of their application techniques. What makes very critical this point is the fact that “new/innovative” materials are more and more proposed and actually used in structural restoration works. Appropriate preliminary investigations are in such cases necessary in order to avoid unexpected further problems.

1 INTRODUCTION

The conservation of architectural heritage is a very complex cultural operation, which was, and still is object of debates that greatly influenced – among many other aspects of the activity of the involved art historians, architects and engineers – the way how the crucial issue of “structural safety” is dealt with.

The problem is very well known. Modern structural safety concepts – based on the calculation of “accepted probabilities” that something considered “wrong”, first of all the failure, happens to the “load bearing components” – works very well for new constructions. The properties of the used materials and structural components can be precisely modeled in this case, thus allowing “precise” (even if substantially conventional) evaluations of the distance between a state of the structure that is considered “safe” and the state of the same structure can experience in any moment of its expected life. Materials and construction techniques are then selected with no substantial restrictions during the design process in order to make such distance complying with precise code prescriptions. In the case of existing historic structures, on the contrary, reliable and feasible structural models are difficultly available and in any case data on their mechanical properties are very scarce, generally insufficient to feed the models; on the other hand, substantial restrictions are imposed by conservation

criteria to the possibilities of intervening to “increase” the safety.

Absolutely relevant outcomes of the debates raised by this situation were new structural design concepts and tools which are more and more entering into the codes and then into the design practice (M.B.C.A. 1986 & 1996, M.L.L.P.P. 1996, ISCARSAH-ICOMOS 2001). It is enough to mention: the differentiation of the accepted safety level for different classes of existing structures; the use of qualitative evaluation of structural performances (observational approach); the evaluation of safety based on pure equilibrium considerations; the limitation of interventions at the minimum possible level, depending on the level of knowledge of the structure and then on the use of appropriate investigations/monitoring techniques; the compatibility of (traditional/modern/innovative) materials and construction techniques; the removability of the interventions. This situation is also stimulating the search for “new solutions”, i.e. new materials, new techniques, new investigation tools, etc. which can offer new possibility of better satisfying the new design concepts.

The design process is thus continuously evolving and becoming more and more complex and sophisticated. At this stage of the technical and scientific knowledge it must be necessarily based on a “case by case” approach. The continuous learning from practical applications is then essential in order to have

the above concepts more and more clear and “stabilized”, and then implemented into as much as possible generalized and controllable procedures.

With this aim some design experiences carried out in Italy are presented and commented.

2 LIMITING THE INTERVENTIONS BY USING INVESTIGATIONS AND MONITORING

An example where the strong influence on the design choices is very clear of having appropriate preliminary investigations and long term monitoring available is the timber roof of the “Palazzo della Ragione” in Padua (Figs. 1 and 2). The construction properties of the structure are really impressive: it covers a unique, skewed room, approximately 28 m wide and 80 m long, and is formed by slender ribs (the section is approximately $36 \times 40 \text{ cm}^2$, but obtained by joining curved boards 12 cm thick, whose length varies from less than

one meter to three meters), which 3 cm thick boards are simply nailed to. Preliminary design hypotheses assumed that only a complete dismantling could have permitted a “safe” repairing of heavily deteriorated zones of the ribs (Figs. 3 and 4) of such a “delicate audacious” structure, being conscious however that this solution could have caused unacceptable losses of the existing material and components and, in general, of its original character.



Figure 1. External view of the roof of the “Palazzo della Ragione” in Padua.

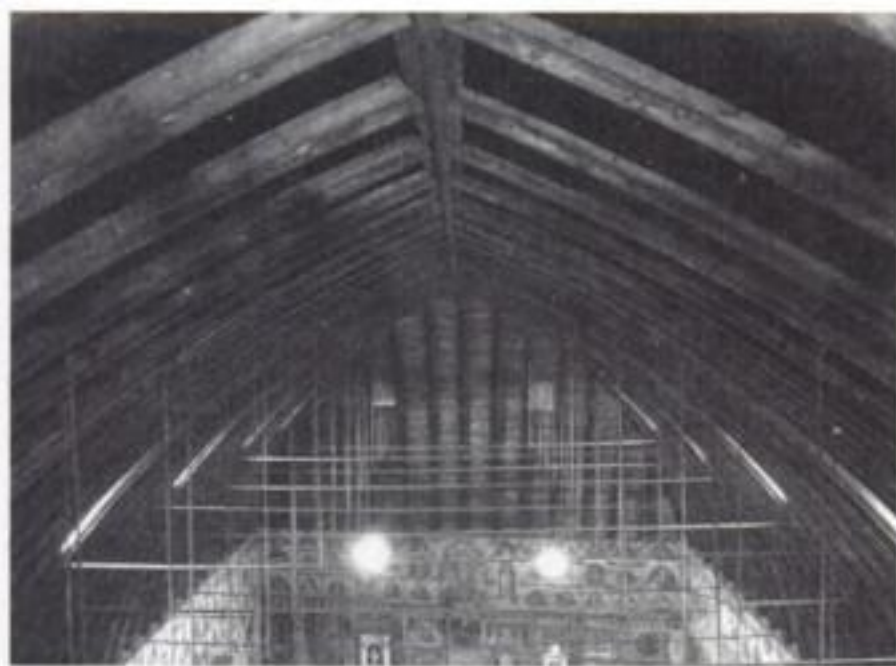


Figure 2. Internal view of the roof.



Figure 3. Detail of the deterioration of the ribs detected in the joints.



Figure 4. Deterioration of the internal part of the ribs.

A cautious and really conservative approach should have permitted to limit the repairing works to the pure substitution of the deteriorated parts of the timber ribs avoiding any previous dismantling but also extremely expensive and heavy (and dangerous for the remaining parts of the building) temporary supports.

This obviously implies the possibility of relying, during the works, on the capability of the structure to offer enough strength and stiffness, with minor "temporary aids", to resist with acceptable stresses and deformations, to the self weight and, even more crucial, to the most critical action which could cause severe damages to such a light structure, i.e. wind.

Major efforts were for such reasons primarily dedicated to a clear understanding of both static and dynamic effects of wind on the roof structure, taking into account its precise geometry and position inside the town (for static effects) and for its real wind/structure interaction (for dynamic effects).

Two different types of investigation were used for the analysis of static and dynamic effects of wind.

In situ measurements of wind pressure (Figs. 5 and 6) on selected points were in fact compared with wind tunnel tests (Fig. 7) on a reduced scale model of the building and of significant surrounding part of the historical center of the town, to determine static effects.

Dynamic characterization via in situ measurements of forced vibrations (obtained by a harmonic exciter applied to a rib) demonstrated that the fundamental period of vibration is far from giving dynamic interaction with wind (Figs. 8 and 9) (Modena et al. 1999).



Figure 5. Aerial view of the building and position of the wind pressure transducers on the external surface of the roof.

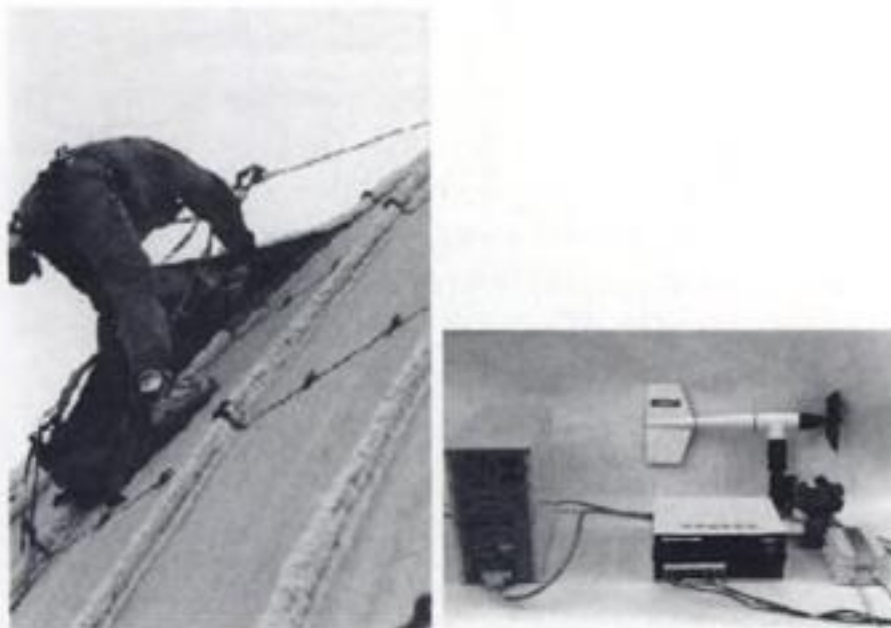


Figure 6. Phase of positioning of the transducers on the roof and view of the anemometer and of the acquisition system.

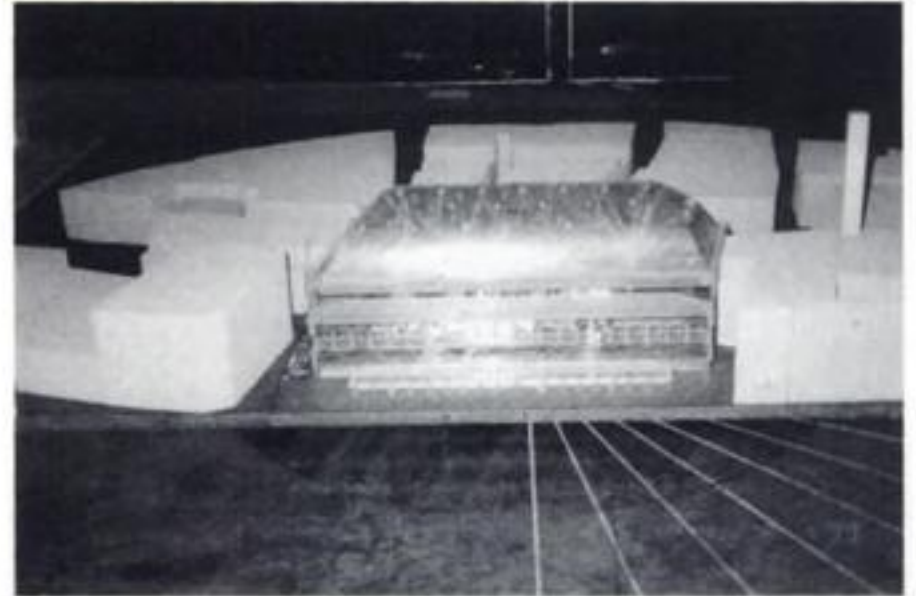


Figure 7. Aerodynamic measures in the wind tunnel of the reduced scale model.

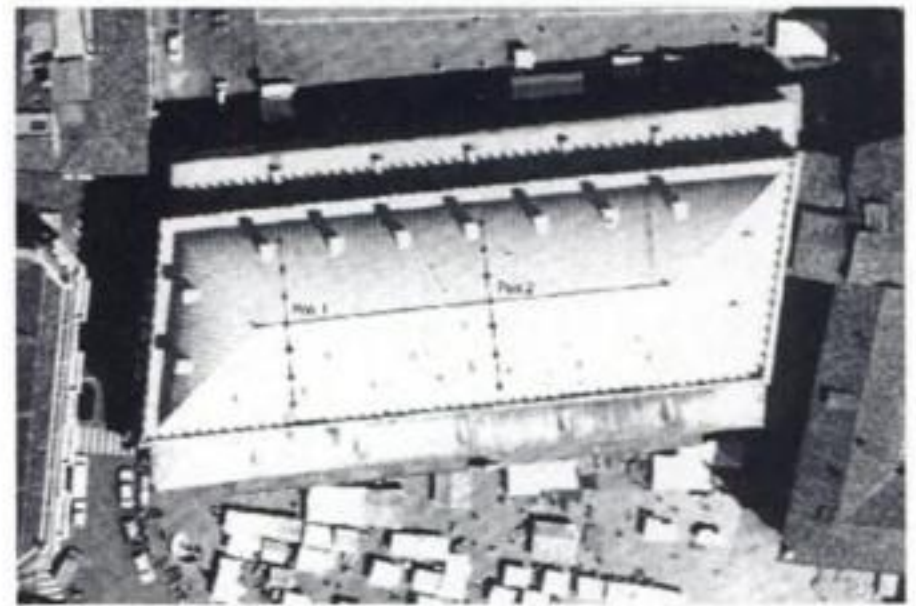


Figure 8. Position of the accelerometers on the external surface of the roof for dynamic acquisitions.

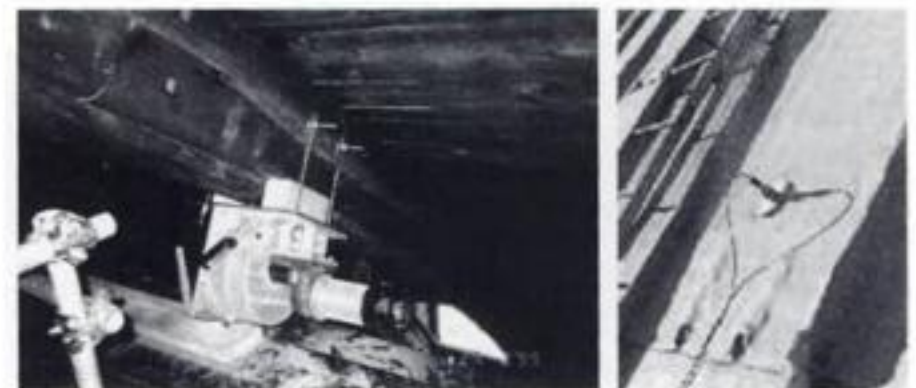


Figure 9. Positioning of the exciter on an internal rib of the roof and view of an accelerometer placed outside.

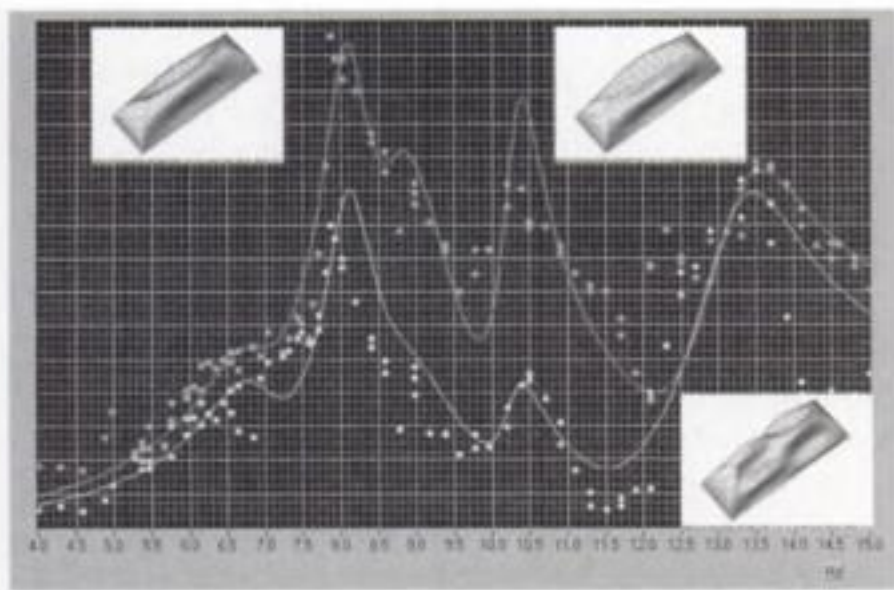


Figure 10. Results of the dynamic tests and comparison with the 3D FE modeling of the roof.

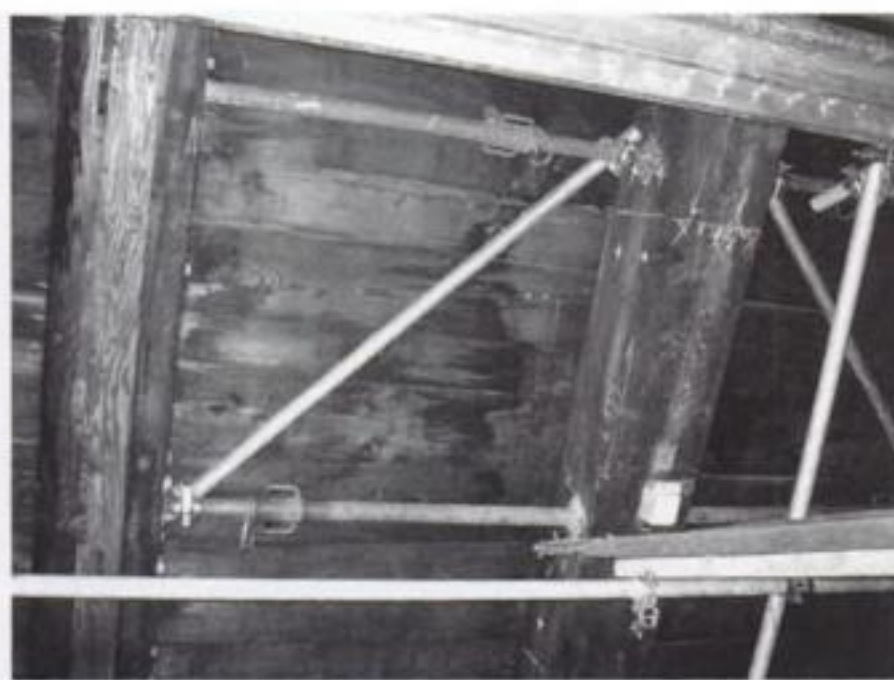


Figure 11. Lateral bracing of the ribs.

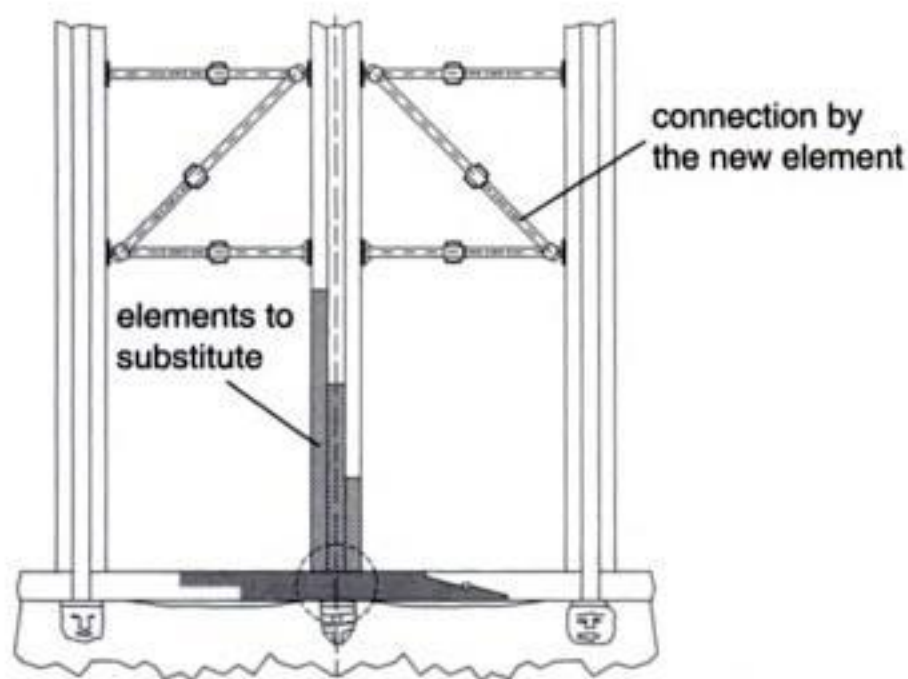


Figure 12. Detail of the intervention on the ends of the ribs.

In conclusion, the results of the investigations, combined with appropriate structural analyses (which were calibrated with the test results, as in Fig. 10), allowed to design the intervention being much more confident on the “robustness” of the structure, provided is full

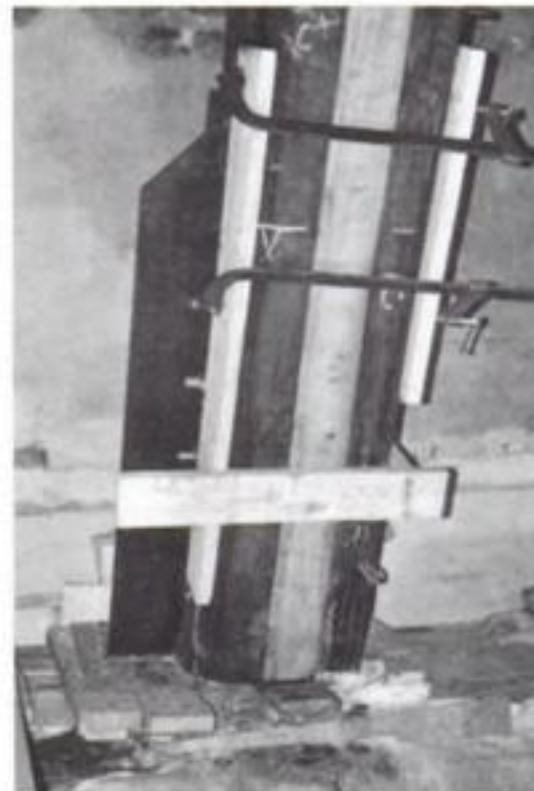


Figure 13. Substitution of the deteriorated central element of the ribs.

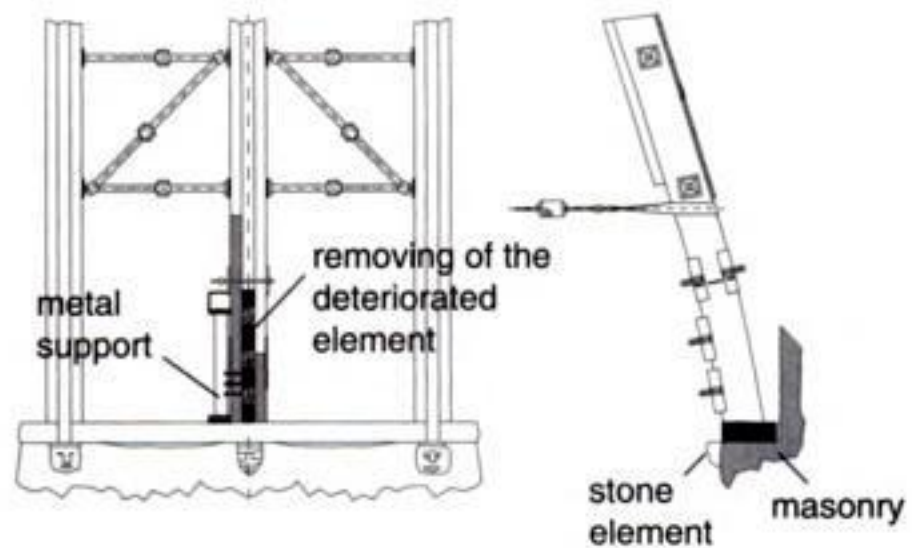


Figure 14. Detail of the phase of substitution of part of deteriorated ribs.

3D behaviour, and the essential contribution given to the stability by the “shell” formed by the nailed boards, would be in any phase maintained.

The design of the local repairing was made possible by taking simple temporary measures allowing for maintaining the stable 3D behaviour and inhibiting local buckling in any phase of the works. The first condition was assured by simply limiting the removal (when needed) of the boards forming the shell very locally, in order to permit local repairing, and the second through simple lateral support, as shown in (Figs. 11 to 14).

A supplementary measure was taken to avoid sliding at the supports during the works. To this scope a temporary tie was added as indicated in (Fig. 15). The force needed to ensure stability was theoretically calculated, and then monitored during the works (Fig. 15), together with relevant parameters of the overall behaviour of the timber and masonry structures (Fig. 16).

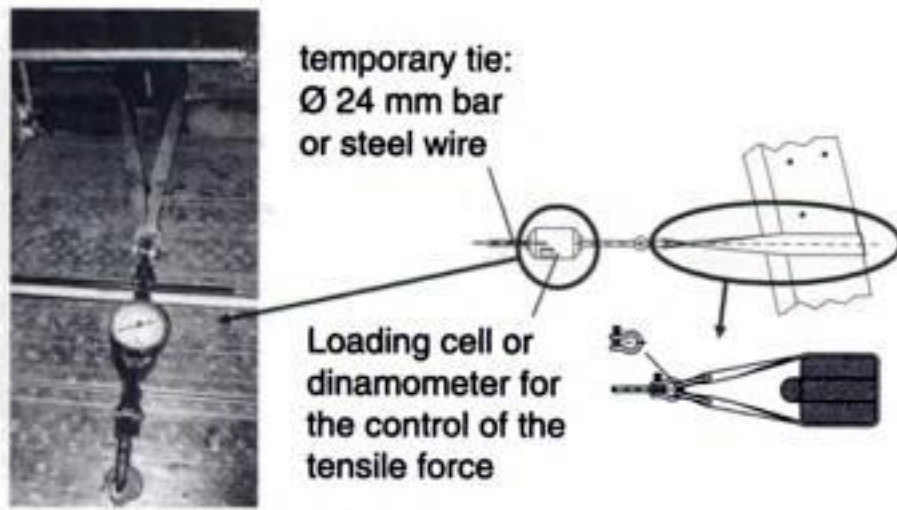


Figure 15. Scheme of insertion of a temporary tie and control of the tensile force.

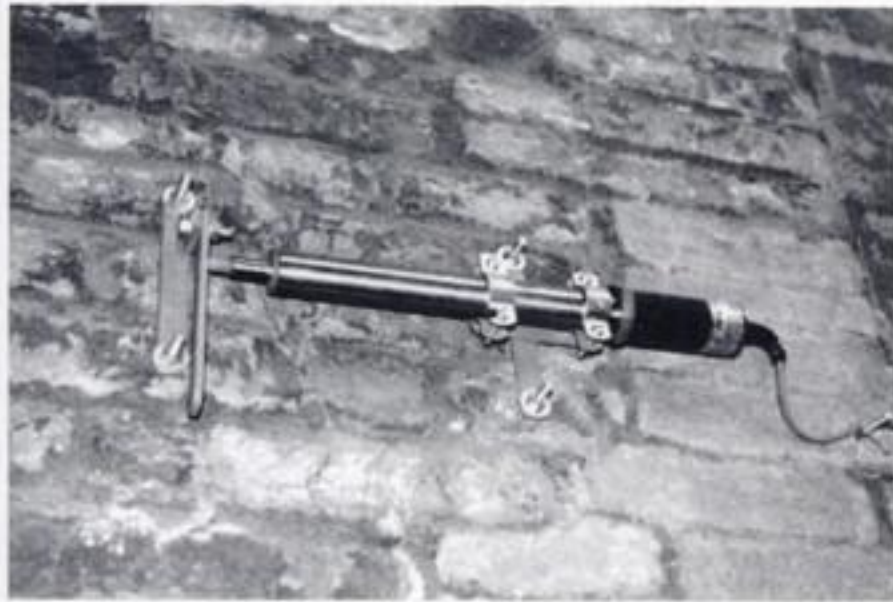


Figure 16. Monitoring of cracks: detail of a sensor.

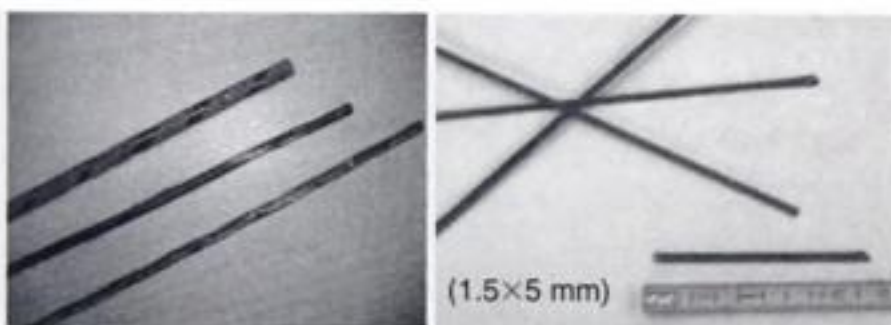


Figure 17. CFRP rods (left) and thin strips (right).

3 USING INNOVATIVE MATERIALS WHILE ENSURING COMPATIBILITY AND REMOVABILITY

Among innovative materials highly durable stainless steel and even more FRPs (*Fiber Reinforced Polymers*) have high potentiality for possible application on historic structures, due to several well-known advantages (for FRP especially corrosion immunity, low weight, etc.). In particular, the use of the more durable CFRP (*Carbon FRP*) bars combined with traditional mortars properly selected, can be proposed for the bed joint reinforcement of masonry structures (Modena & Valluzzi 2003) (Fig. 17).

In any case, what characterize the use of such sophisticated and high performance materials is the

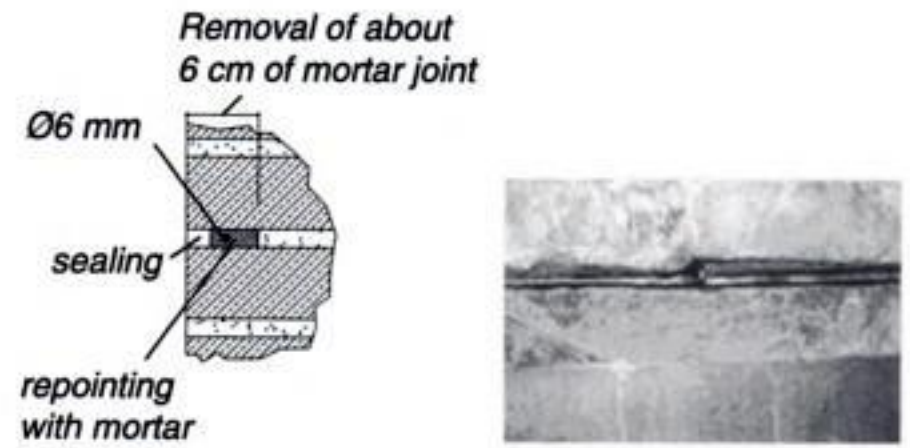


Figure 18. Bed joint reinforcement technique: scheme and detail of the reinforcement in a brick masonry wall by steel bars.



Figure 19. Application of CFRP strips in an experimental panel.

fact that the employ of traditional mortars, properly selected, to make them work together with the existing materials, is highly preferred. This is not only due to conservation considerations, but also to the search for reducing as much as possible high stress concentrations which could occur using high strength/high stiffness modern bonding materials like resins, high strength mortars etc., or, in other words, to ensure better “compatibility” from the mechanical point of view.

Specific applications of steel bars embedded superficially in the bed joints of massive structures (towers, curtain walls, large pillars), proved on experimental laboratory bases, demonstrated their high efficiency in counteracting typical masonry creep damage (Binda et al. 1999b & 2001) (Fig. 18).

More advantages can be achieved by the use of thin CFRP strips (1.5 × 5 mm in section size), assuring low obtrusiveness of the intervention and a better adaptability to the possible joints unevenness (Valluzzi et al. 2003b) (Figs. 17 and 19).

conditions are the Cathedral of Monza and the Civic Tower of Vicenza (Italy).

The bell tower of the Cathedral of Monza (XVI century) was suffering passing-through large vertical potentially dangerous cracks on some particularly weak portions of the West and East sides (Modena et al. 2001). They were slowly but continuously opening since 1927; moreover, wide cracks in the corners of the tower up top 30 m and a damaged zone at a height of 11 to 25 m with a multitude of very thin and diffused vertical cracks were detected (Fig. 20).

Design of intervention was mainly aimed in providing an overall confining action of masonry walls, limiting the dilation of the material. They consisted of: (i) metallic horizontal reinforcing rings applied on several sections along the height of the Tower, to improve the connection between the contiguous walls; (ii) the application of the reinforced repointing technique diffused on various portions of the walls, to counteract the creep damage, and concentrated on some pilaster strips to strengthen the corners; (iii) local interventions of injection, rebuilding, and pointing of the mortar joints, to restore the zones having high material deterioration (Fig. 21).

The intervention design was strictly based on the results of the investigations carried out on site and in laboratory both on materials and structure (also static and dynamic tests were useful to calibrate FE mathematical models). They allow to identify the bed reinforcement as a technique which, respecting as much as possible the original structure, provides an improvement capable to save the preservation concepts (Fig. 22).

The Civic Tower of Vicenza (XII century) is a slender structure with a base section of 6.2×6.5 m and a height of about 82 m. During centuries, it was subjected to several repairs and changes, due to several causes (earthquake, bombing, etc.). The Tower suffers a substantial out-of-plumb, and a damage characterized by localized deep cracks, diffused micro-cracks and material deterioration. Many of the main deep

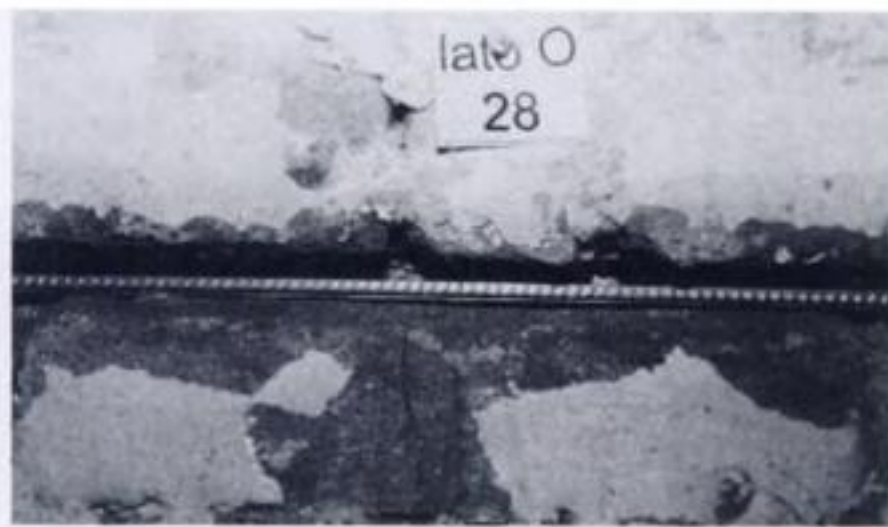


Figure 22. Insertion of a small diameter bar in an excavated joint of the West side of the Cathedral of Monza (Modena et al. 2001).

large cracks were located near the corners and complete or partial detachment of the external leaf and of local buckling of the masonry was found also in some areas of the façades (Valluzzi et al. 2003a) (Fig. 23).

The interventions (Fig. 23) consisted of: (i) grout injection at the base of the tower and on the belfry pillars, (ii) local rebuilding, (iii) pointing of mortar joints, to restore the areas characterized by high material deterioration; (iv) reinforced repointing applied on various portions of the walls and on the pillars, to counteract the creep damage and to strengthen the corners (Fig. 24); (v) metallic horizontal reinforcing rings and anchoring ties placed at different levels along the height of the tower to confine the masonry and improve the connection between contiguous walls.

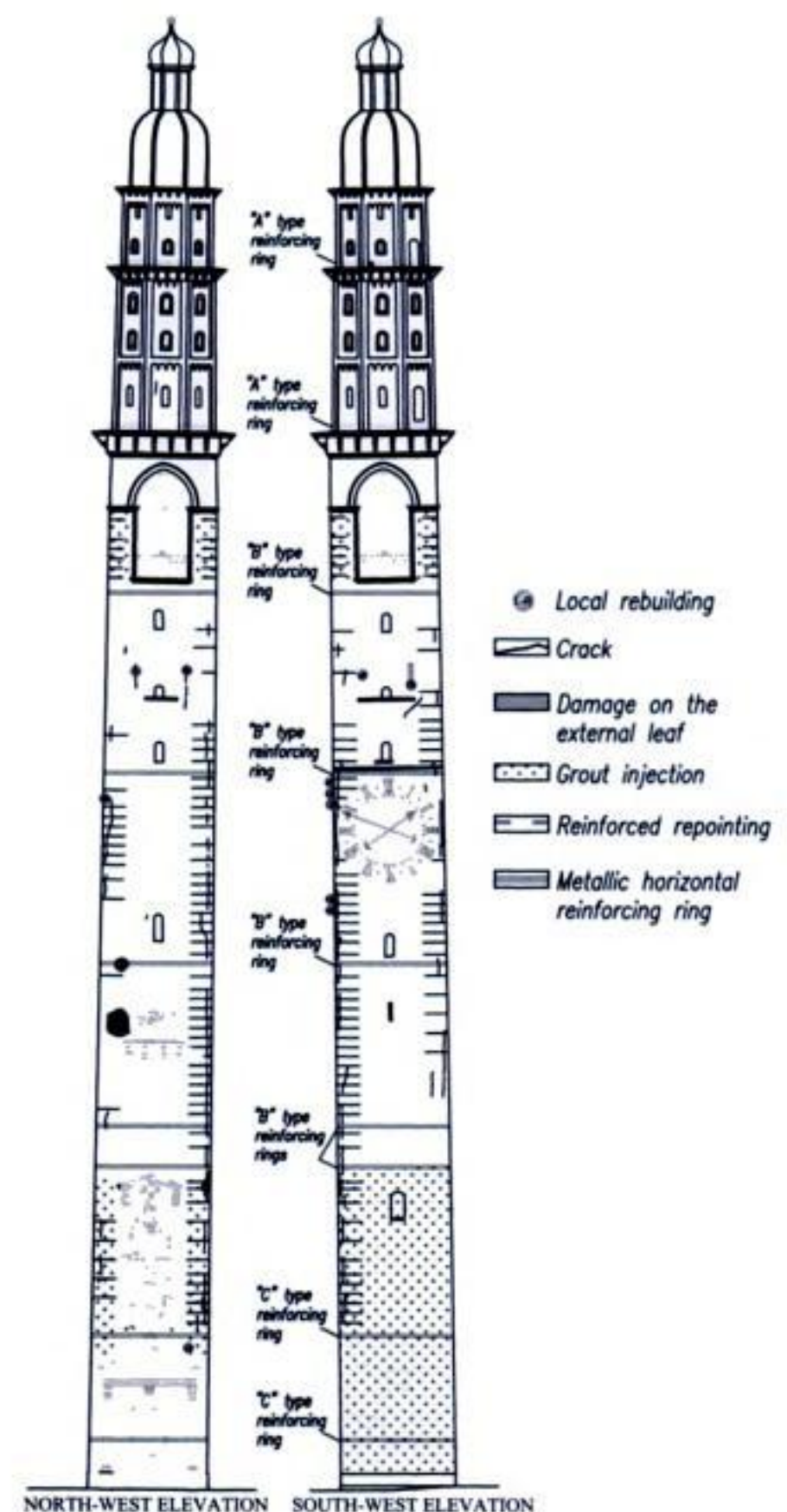


Figure 23. Civic Tower of Vicenza (Italy): scheme of the intervention measures on the damaged sides.

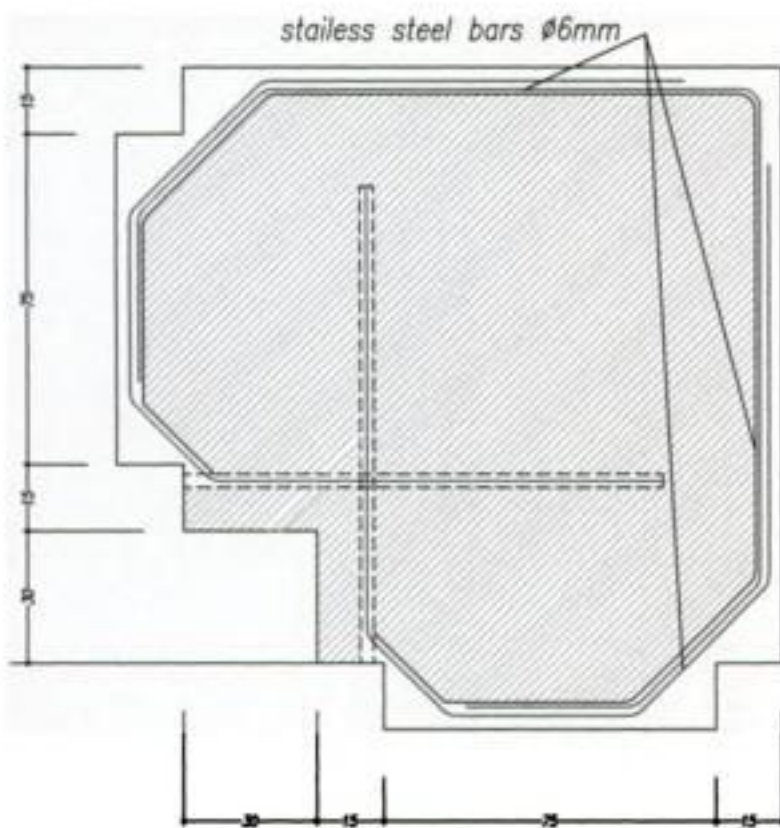


Figure 24. Reinforced repointing applied on the belfry pillars of the Civic Tower of Vicenza.

4 APPLYING EQUILIBRIUM ANALYSES FOR VULNERABILITY ASSESSMENTS AND STRUCTURAL IMPROVEMENT IN SEISMIC AREA

A complete limit analysis approach of existing masonry buildings, especially in seismic areas, is proving to be the most efficient way for making reliable safety evaluations without underestimating their actual resisting capabilities, thus avoiding over-designing repair/strengthening interventions.

Such method, based on single or combined kinematics models involving the equilibrium of structural macro-elements (Giuffrè 1993), is particularly addressed to existing masonry buildings in historic centres. They, in fact, often do not satisfy the general conditions which allow the application of common equivalent static procedures, based on the “box” behaviour of the structure (which requires the presence

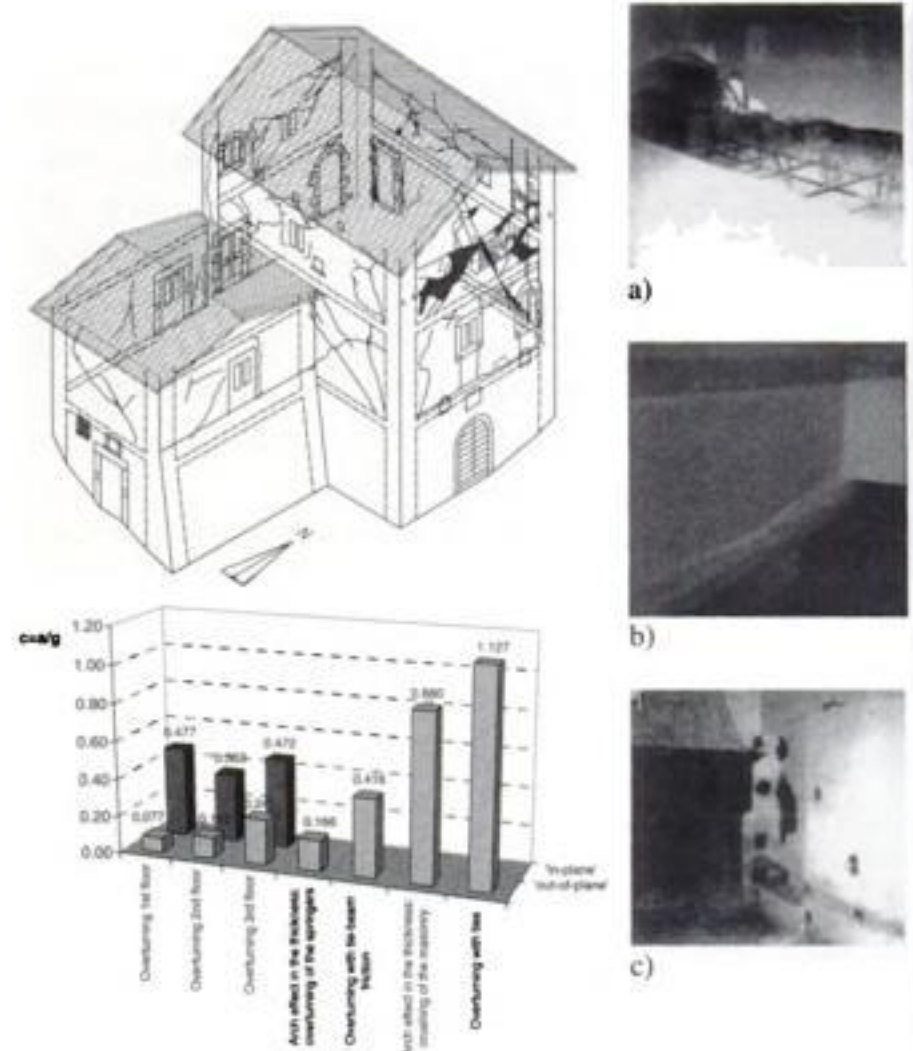


Figure 25. Damaged building after earthquake and intervention measures taken after a previous seismic event (a: ring beams at floor levels, b: superimposition of r.c. slab, c: rough injections). Analysis with equilibrium macromodelling showed that lowest seismic coefficients are related to the out-of-plane mechanisms involving the most damaged portions of the building.

of well-connected walls and floors and a proper horizontal stiffness of the floors) and on the elastic-plastic behaviour of the masonry. Common buildings in historic areas are often realized according to typologies (multi-material masonry, multi-leaf walls) and constructive details (poor connection between intersecting walls, between walls and floors and even among the layers in the thickness), which can evidence fundamental deficiencies for the stability and the safety under seismic actions.

The ultimate capacity of the building depends on the stability of its macro-elements, that is of portions of the structure bounded by the potential damage pattern (cracks, borders of poor connections, etc.) which can behave as a whole, following a kinematics mechanism. Macro-elements are defined by single or combined structural components (walls, floors and roof), considering their mutual bond and restraints (e.g. the presence of ties or ring beams), the constructive deficiencies and the characteristics of the constitutive materials. Once the critical structural configuration is defined, the subsequent step is the identification of the most probable collapse mechanism/s characterizing the macro-element.

Several studies based on the in-situ observations after seismic events allowed to systematize abacuses of

the typical damages occurring in constructive typologies (buildings, churches), which led to the consequent systematization of the mechanical models able to describe their specific behaviour by kinematics models, both for in-plane and out-of-plane mechanisms (Giuffrè & Carocci 1999, Binda et al. 1999a, Penazzi et al. 2001).

Those models, calibrated on the real damaged sites, are usefully applied for analyses of vulnerability for centres under seismic hazard, in order to examine the current condition and to prevent their future damage. Moreover, the simulation of possible interventions can be performed, both in damaged and undamaged conditions, evaluating their impact with the pre-existing situation (Avario et al. 2002, Valluzzi et al. 2004).

5 CONCLUSIONS

Some case studies have been presented and commented where efforts have been made to respond to “conservative” design criteria while intervening to ensure acceptable structural safety conditions of existing historic constructions.

As it is first of all expected in order to respect the existing features of the considered constructions, attention has been focused on avoiding unnecessary interventions and special care has been paid in order to limit in any case as much as possible variations not only of its external appearance, but also of its mechanical behavior.

This requires that special efforts are made to accurately analyze, theoretically and experimentally, the actual resisting properties of the considered constructions, prior and after interventions are made, in order to avoid over-designing approaches. Moreover, the actual contribution of any traditional/innovative material and technique, and of their possible combinations, can be adequately and scientifically exploited in order to ensure durability, compatibility and possibly removability of repair/strengthening interventions.

REFERENCES

- Avario A., Borri A., Corradi M. 2002. Ricerche per la ricostruzione. Iniziative di carattere tecnico e scientifico a supporto della ricostruzione, Regione dell'Umbria, DEI, Roma.
- Binda L., Modena C., Saisi A., Tongini Folli R. & Valluzzi M.R. 2001. Bed joints structural repointing of historic masonry structures, *9th Canadian Masonry Symposium 'Spanning the centuries', Fredericton, New Brunswick, Canada*, 12 pp., on CD-ROM.
- Binda L., Gambarotta L., Lagomarsino S. & Modena C. 1999a. A multilevel approach to the damage assessment and seismic improvement of masonry buildings in Italy. *On: Seismic Damage to Masonry Buildings*, Bernardini Ed., Balkema, Rotterdam.
- Binda L., Modena C., Valluzzi M.R. & Zago R. 1999b. Mechanical effects of bed joint steel reinforcement in historic brick masonry structures, *Structural Faults + Repair – 99, 8th International Conference and Exhibition, London, England*, 11 pp. on CD-ROM.
- Giuffrè A. 1993. Sicurezza e conservazione dei centri storici. Il caso Ortigia, Laterza, Bari.
- Giuffrè A. & Carocci C. 1999. Codice di pratica per la sicurezza e la conservazione del centro storico di Palermo, Laterza, Bari.
- ISCARSAH-ICOMOS 2001. Recommendations for the Analysis, Conservation and Structural Restoration of Architectural Heritage.
- M.B.C.A. 1986. Circ. 1032 18/7/1986: Raccomandazioni relative agli interventi sul patrimonio monumentale a tipologia specialistica in zona sismica.
- M.B.C.A. 1996. Istruzioni generali per la redazione dei progetti di restauro nei beni architettonici di valore storico artistico in zona sismica.
- M.LL.PP. 1996. D.M. 16/1/1996: Norme tecniche per le costruzioni in zone sismiche.
- Modena C. & Valluzzi M.R. 2003. Repair techniques for creep and long term damage of massive structures, *Proc. of the VIII STREMAH Conf., Structural Studies, Repairs and Maintenance of Heritage architecture, Haldikiki, Greece, 7–9 May 2003*, C.A. Brebbia Ed., WitPress, UK, pp. 141–150.
- Modena C., Valluzzi M.R., Tongini Folli R. & Binda L. 2001. Design choices and intervention techniques for repairing and strengthening of the Monza cathedral bell-tower, *9th Structural Faults & Repair, London, UK, 4–6 July 2001*, 12 pp., on CD-ROM.
- Modena C., Zonta D. & Riolfo A. 1999. Dynamic investigation on the Palazzo della Ragione roof in Padua, *Structural Faults + Repair – 99, 8th International Conference and Exhibition, London, England, July, 13–15, 1999*, 10 pp., on CD-ROM.
- Penazzi D., Valluzzi M.R., Saisi A., Binda L. & Modena C. 2001. Repair and strengthening of historic masonry building in seismic area, *International Millennium Congress 'More than two thousand years in the history of architecture safeguarding the structure of our architectural heritage', Bethlehem (Palestine)*, Vol. 2, Section V (7 pp.).
- Valluzzi M.R., da Porto F. & Modena C. 2003a. Structural investigations and strengthening of the civic tower in Vicenza, *Structural Faults & Repair – 2003, Commonwealth Institute, Kensington, London, UK, 1–3 July 2003*, 10 pp., on CD-ROM.
- Valluzzi M.R., Tinazzi D. & Modena C. 2003b. Strengthening of masonry structures under compressive loads by using FRP strips, *Proc. 6th International Symposium on Fibre-Reinforced Polymer (FRP) Reinforcement for Concrete Structures (FRPRCS-6), 8–10 July 2003, National University of Singapore, Singapore*, Vol. II, pp. 1249–1258.
- Valluzzi M.R., Cardani G., Binda L. & Modena C. 2004. Analysis of the seismic vulnerability of masonry buildings in historical centres and intervention proposals, *6th International Symposium on the Conservation of Monuments in the Mediterranean Basin, Lisbon, Portugal, 7–10 April 2004*, pp. 561–565 (on CD-ROM).

Historical aspects and general methodology

Ancient binding materials, mortars and concrete technology: history and durability aspects

Ö. Kırca

ÇimSA Cement Production and Trading Company, Mersin, Turkey

ABSTRACT: This paper deals with the history of technology related with binding materials. Lime, gypsum, and hydraulic binders, i.e. lime-pozzolan mixture have been the major types of binding materials survived in different regions of the world for 8000 years. Whatever type of binding materials the ancient civilizations used, it can be seen that those structures built by ancient binders, particularly lime-pozzolan mixture have survived for several hundred years. It can be claimed that even at that time architects were aware of the importance of the durability of binding materials. However, those structures belonging to modern civilizations and made by using modern binders, i.e. portland cement have experienced significant deterioration throughout their service life, generally lesser than 100 years.

In this research, the object of the study is to investigate the historical timeline of binding materials and to focus on their durability aspects by comparing the traditional technologies with modern ones.

1 INTRODUCTION

Binding material or cementing material in the general sense of the world can be described as a material with adhesive and cohesive properties, which make it capable of bonding mineral fragments into a compact whole. For constructional purposes, the meaning of the term “cement” is restricted to the bonding materials used with stones, sand, building blocks, etc (Neville 1989).

The use of cementing materials is very old. The first evidence of its existence dates back to 12 000 BC in Israel. Reactions between limestone and oil shale during spontaneous combustion occurred in Israel to form a natural deposit of cement compounds. Another example of ancient binder from the history of the human being is the use of naturally occurring bitumen by the Babylonians and Assyrians in their brick and gypsum plaster construction. The Egyptians improved the technology of lime and gypsum mortar and builded the pyramids by the use of such mortars. The Greeks made further improvements and finally the Romans developed a cement that produced structures of remarkable durability and that can set and harden even under water.

Lime was known to the Greeks and was widely used by the Romans. The Roman architect and engineer Vitruvius published the first specification for the use of lime in building in his celebrated work *De Architectura* (Vitruvius 1960). The Romans also knew how

to make hydraulic binder, i.e. lime-pozzolan cement by adding materials, such as volcanic ash or powdered bricks, tiles and pottery to lime.

The modern cement, i.e. portland cement was invented by Joseph Aspdin in England in 1824. After that time, modern Portland cement and concrete technology has proceeded till today by invention of new chemical and mineral admixtures and additions.

Although radical advances in cement and concrete technology have been observed for two centuries, there are still problems related with the endurance of cement and concrete. Many modern structures experienced significant deterioration within their service life, which is generally lesser than 100 years. Yet, many ancient Roman concrete buildings or structures are still in use after more than 2000 years. According to the Vitruvius’s book *De Architectura*, the magnificent quality of Roman concrete resulted from the extensive use of artificial pozzolanic mortars and concretes (Vitruvius 1960). In addition, placement, compaction, workability properties of ancient Roman concrete contributed to its magnificent survivability.

2 CHRONOLOGICAL SUMMARY OF BINDING MATERIALS AND MORTARS

The nature and usefulness of cement as a kind of artificial stone was probably first understood by the Romans; but it seems likely that they copied the

technology from Etruscans and Greeks and improved it drastically.

Concrete and/or cement itself is actually a phenomenon of nature, with the first evidence of its existence in Israel dating back to 12 000 BC, when natural deposits of cement compounds were said to have formed due to reactions between limestone and oil shale, employing spontaneous combustion. However, the earliest known concrete produced intentionally by human beings was discovered in the floor of a crude shelter built about 5600 BC on the banks of the river Donube in Yugoslavia. The floor was made from mixture of sand, gravel and red lime. That concrete was manufactured deliberately, rather than unintentionally by utilizing the red lime from a site 320 km away. For some reason, it appears that the technique for using lime-based cements was lost for at least 2500 years, until indications of use by the ancient Assyrians and Babylonian civilizations around 3000 BC. They used bitumen to bind stones and bricks. About the same time Egyptians used mud bricks mixed with straw to bind dried bricks and also this phenomenon furthered the discovery of lime and gypsum mortars as a binding agent for building the pyramids. Even at that time, the ancient Chinese people used cementitious materials to hold bamboo together in their boats and in the Great Wall, one of the Wonders of the world. By 500 BC the art of making concrete had spread to the Mediterranean island of Crete, and from there to the ancient Etruscans and Greeks.

Yet, it was the Romans who brought the manufacture and use of lime-based cement to an art form. 300 BC saw the Romans employing slaked lime and volcanic ash called pozzolan, named after the town of Pozzuoli, near Mt Vesuvius. This was a hydraulic cement that can set harden when mixed with water in air as well as under the water. Moreover, some natural additions such as animal fats, milk, and blood were also used throughout this era.

After the fall of the Roman Empire, knowledge of cement was lost till the 18th century.

The whole historical timeline of cement and concrete is summarised in Table 1, where the developments in modern era are also outlined.

3 TECHNOLOGY OF ANCIENT LIME AND LIME MORTARS

3.1 *Properties of lime*

There are two forms of lime: quicklime and hydrated lime.

Quicklime is produced by heating rock or stone containing calcium carbonate (limestone, marble, chalk, shells, etc.) to a temperature of around 900°C for several hours in a process known as ‘calcining’. It is an unstable and slightly hazardous product. Therefore,

in order to be used in construction it must be mixed with water to form a lime paste, which is defined as “hydration” or “slaking”.

To produce dry powdered hydrated lime just sufficient water is added for the quicklime lumps to break down to a fine powder. This material would have a “shelf life” of only a number of weeks, depending on storage conditions. “Old” hydrated lime would have partially carbonated and become a less effective binder. If too little or too much water is added, the properties of the slaked lime will be spoiled; the slaked lime will not harden and the paste will not be as plastic as it should be (Erdoğan 2002).

However, if quicklime is hydrated with a proper amount of water and well agitated, it forms a milky suspension known as milk of lime, which can be easily used in building applications.

Limestone containing a proportion of clay is often seen as an advantage in building as they produce hydraulic limes. In fact, limes do not possess hydraulicity, since it needs carbon dioxide for its hardening reaction (Erdoğan 2002). However, in the case of hydraulic limes, as the name implies, they can set and harden even under water and will produce stronger mortars.

In the construction industry, usually lime, in its hydrated or putty form, is mixed with aggregate and water to produce concrete or mortar for different purposes such as plastering sand-lime brick production etc. Plain lime-sand mortars are quite weak; any early adhesive strength results from drying out whereas longer-term hardening occurs as a result of carbonation of the lime.

Traditional lime plasters were often mixed with animal hair to improve cohesion and adhesion. Today addition of gypsum or portland cement and/or pozzolans to increase durability and give faster setting times is more common.

3.2 *Ancient lime technology*

Quarrying: The first step of lime production required finding a suitable raw material which was generally calcium carbonate based stones such as limestone and marble. Quarrying techniques had become well advanced during construction of the great Egyptian pyramids and further advanced during the Roman building era. The determination of raw material involved trial and error, as well as ages of experimental attempts. Once workable quarries and materials were located, workmen acquired skills for identifying and extracting suitable calcium carbonate raw materials. Then such materials had to be transported to sites where they were prepared for calcination. The major technological factors surrounding acquisition of the raw carbonate material, therefore, involved, identification of suitable stone, workable extraction,

Table 1. Historical timeline of binding materials.

12 000 BC	Reactions between limestone and oil shale during spontaneous combustion occurred in Israel to form a natural deposit of cement compounds.
5600 BC	Intentionally production of concrete from sand, gravel, and lime a natural concrete in Yugoslavia.
3000 BC	Bitumen to bind bricks and stones was used by Babylonians and Assyrians.
3000 BC	Egyptians used mud mixed with straw to bind dried bricks. They also used lime and gypsum mortars in the pyramids.
3000 BC	Chinese used cementitious material to hold bamboo together in their boats and in the Great Wall.
500 BC	The art of making concrete had spread to the Mediterranean island of Crete, and from there to the ancient Etruscans and Greeks.
300 BC–476 AD	Used pozzolan cement from Pozzuoli, Italy near Mt. Vesuvius to build several structures. They used lime as a cementitious material also Animal fat, milk, and blood were used as admixtures.
400–1779	The art of concrete was lost after the fall of the Roman Empire.
1779	Bry Higgins was issued a patent for hydraulic cement (stucco) for exterior plastering use.
1793	John Smeaton found that the calcination of limestone containing clay gave a lime, which hardened under water (hydraulic lime).
1796	James Parker from England patented a natural hydraulic cement by calcining limestone-containing clay, called Parker's cement or Roman cement.
1812–1813	Louis Vicat of France prepared artificial hydraulic lime by calcining synthetic mixtures of limestone and clay.
1818	Maurice St. Leger was issued patents for hydraulic cement. Natural cement was produced in the USA. Natural cement is limestone that naturally has the appropriate amounts of clay to make the same type of concrete as John Smeaton discovered.
1822	James Frost of England prepared artificial hydraulic lime likes Vicat's and called it British cement.
1824	Joseph Aspdin of England invented portland cement by burning finely ground chalk with finely divided clay in a lime kiln until carbon dioxide was driven off. The sintered product was then ground and he called it portland cement named after the high quality building stones quarries at Portland, England.
1828	I.K. Brunel is credited with the first engineering application of portland cement, which was used to fill a breach in the Thames Tunnel.
1843	J.M. Mauder, Son & Co. Were licensed to produce patented portland cement
1845	Isaac Johnson claims to have burned the raw materials of portland cement to clinkering temperatures
1849	Pettenkofer & Fuches performed the first accurate chemical analysis of portland cement.
1860	The beginning of the era of portland cements of modern composition.
1862	Blake stone breaker of England introduced the jawbreakers to crush clinker.
1867	Joseph Monier of France reinforced William Wand's (USA) flowerpots with wire ushering in the idea of iron reinforcing bars (re-bar).
1886	The first rotary kiln was introduced in England to replace the vertical shaft kilns.
1887	Henri Le Chatelier of France established oxide ratios to prepare the proper amount of lime to produce portland cement. He proposed that hardening is caused by the formation of crystalline products of the reaction between cement and water.
1889	The first concrete reinforced bridge is built.
1890	The addition of gypsum when grinding clinker to act as a retardant than the setting of concrete was introduced in the USA. Vertical shaft kilns were replaced with rotary kilns and ball mills were used for grinding cement.
1891	George Bartholomew placed the first concrete street in the USA in Bellefontaine, OH. It still exists today.
1893	William Michaelis claimed that hydrated metasilicates form a gelatinous mass (gel) that dehydrates over time to harden.
1900	Basic cement tests were standardized.
1903	The first concrete high rise was built in Cincinnati, OH.
1909	Thomas Edison was issued a patent for rotary kilns.

(continued)

Table 1. (continued)

1930	Air entraining agents were introduced to improve concrete's resistance to freeze-thaw damage.
1936	The first major concrete dams, Hoover Dam and Grand Coulee Dam were built. They still exist today.
1967	First concrete domed sport structure, the Assembly Hall, was constructed at the University of Illinois, at Urbana-Champaign.
1970's	Fibre reinforced in concrete was introduced.
1980's	Superplasticizers were introduced as admixtures.
1985	Silica fume was introduced as pozzolanic additive. The highest strength concrete was used in building the Union Plaza constructed in Seattle, Washington.

quarrying methods, and suitable means of transportation to a site for further treatment (Krumnacher 2001).

Calcination: In order to convert the calcium carbonate based raw material into quicklime, it was necessary to heat the mass of stone or shell up to required temperatures. By calcining the raw materials, the water and carbon dioxide was driven off from within the stone. Calcining of raw materials took place in either kilns or clamps customarily constructed of stone or brick with clamps sometimes representing an open heap of carbonate material and fuel (Krumnacher 2001).

"When the charge of calcium carbonate undergoes firing it transforms to a calcium oxide known as quicklime. This transformation involves the release of water and carbon dioxide, which are driven off after being heated through the calcining process. Through trial and error lime burners found that the raw limestone fired more completely if broken into pieces about the size of two closed fists. If the stones were too large there would remain unaltered clinkers, which would be found during the subsequent process. These clinkers would jeopardize the consistency and effectiveness of a resulting lime. Since quicklime was difficult to store and transport, clamps and kilns were set up near the site where lime was used and the raw material would be transported to the kiln site" (Krumnacher 2001).

"Constant attention and responsive orchestration of the firing were essential. Lime burners worked unusual hours and were highly skilled, although not always highly respected. In Roman times, inmates and criminals would often be sent to provide labour at the limekilns" (Krumnacher 2001).

Slaking: Quicklime intended for use in construction must first be mixed with water, to form a lime paste, by being slaked (Erdoğan 2002). All calcining process of calcium carbonate based stones had to be followed by slaking, which was necessary for construction purposes.

Throughout the Roman period, there were three different hydration methods for transformation of quicklime into the hydrated (or slaked) lime by the controlled addition of water. One of the three methods was followed: (1) sprinkling or 'drowning': ideally, water

equal in weight to 1/3 of the quicklime was sprinkled over it. Heat was given off, the material cracked open and became a powdered, and increased in volume. This method was considered the best. (2) Immersion: the quicklime, placed in a basket, was lowered into the water for the proper length of time, and drawn up to complete the slaking. The handling was tricky, at best, and demanded considerable skill. (3) Air-slaking: the quicklime was simply left exposed, to pick up moisture from air (Krumnacher 2001, McKee 1971).

The slaking procedure, like all other steps involving the preparation of mortar had a great influence upon the resultant properties and performance of finished mortar.

Mortar Mixing: In order to create a mortar for uniting brick or stone, workers introduced slaked lime to a sand aggregate. This practice involved proportioning the amount of lime, sand and water. According to McKee, in Roman period, three primary methods of mortar mixing predominated: (1) mixing dry slaked lime powder, sand, and water; (2) mixing wet slaked-lime paste and sand, adding water if needed; (3) mixing pulverized dry quicklime, sand and water, using the mortar while it was still hot (McKee 1971).

Fat lime or high calcium lime could be mixed with the aggregate and allowed to age, provided it was protected from exposure to the air. Exposure to the air would act to recarbonate or solidify the mass. Many ancient artisans practiced this custom of storing lime putty or lime mortar. Plasterers would keep their lime in sealed vats for considerable lengths of time. Nicholson describes the mixing and aging of mortar as follows (Nicholson 1850): "The mortar should be made underground, then covered up, and kept for a considerable length of time, the longer the better; and when it is to be used, it should be beat up afresh. This makes it set sooner, renders it less liable to crack and harder when dry... How very different was the practice of the Roman! The lime which they employed was perfectly burnt, the sand sharp, clean, and large grained; when these ingredients were mixed in due proportions, with a small quantity of water, the mass was put into a wooden mortar pan, and beaten with a heavy wooden or iron pestle, till the composition

adhered to the mortar: being thus far prepared, they kept it until it was at least three years old. The beating of mortar is of the outmost consequence to its durability, and it would appear that the effect produced by it, is owing to something more than a mere mechanical mixture" (Krumnacher 2001, Nicholson 1850).

3.3 Ancient lime applications

In order to understand the techniques associated with lime mortars it is necessary to review the lineage from which they arose. While the actual techniques involving preparation and application of lime remains less than fully understood, examples of finished materials still in existence testify on behalf of the early success acquired by those working with lime. According to Lazell, the picture of the early development of lime technology is as follows (Lazell 1915): "The art of using mortar in some form or other is as old as the art of building or as civilization itself. Evidences of the use of mortar are found not only in the older countries of Europe, Asia, and Africa, but also in the ruins of Mexico and Peru. The remains of the work of these artisans are evidence to us of the enduring qualities of lime mortar as well as the skill and knowledge possessed by the user" (Krumnacher 2001, Lazell 1915).

Lazell additionally describes ancient era as follows (Lazell 1915): "Plastering is one of the earliest instances of man's power of inductive reasoning, for when men built they plastered; at first like the birds and beavers, with mud; but they soon found out a more lasting and more comfortable method, and the earliest efforts of civilization were directed to plastering. The inquiry into it takes us back to the dawn of social life until its origin becomes mythic and prehistoric. In that dim, obscure period we cannot penetrate far enough to see clearly, but the most distant glimpses we can obtain into it shows us that man had very early attained almost to perfection in compounding material for plastering. In fact, so far as we yet know, some of the earliest plastering which remains to us excels, in its scientific composition, that which we use at the present day, telling of ages of experimental attempts. The pyramids of Egypt contained plaster work executed at least 4000 years ago, and this, where wilful violence has not disturbed it, still exist in perfection, out vying in durability the very rock it covers, where this is not protected by its shield of plaster".

"Development of masonry construction technology emerged and spread through empirical trial and error. Within the 1st century B.C. Romans borrowed and applied Greek and Etruscan techniques of lime preparation and applications for creating their mortar. Roman use of lime mortars reflected a keen insight into the material and its technological preparation and application toward their momentous building accomplishment. Although these accomplishments are

highly esteemed and respected, the techniques of preparation and application of lime and lime mortars have remained less than fully understood" (Krumnacher 2001).

Vitruvius, a 1st century B.C. Roman architect under Augustus, conveys the earliest comprehensive details regarding lime treatment and its use as a building material. Craft tradition was advanced by the Romans, who developed a strong infrastructure of labour, raw material, technological order and transportation. This craft tradition and supportive infrastructure facilitated a sophisticated building program (Krumnacher 2001).

4 TECHNOLOGY OF ANCIENT HYDRAULIC BINDER (LIME-POZZOLAN MIXTURE) AND ITS MORTAR

Throughout the history of human beings, for the first time, a hydraulic binder was used during the era of Roman Empire. This hydraulic binder has been called as Roman cement or concrete, as well. The techniques used by architects and artisans for the production of binding materials at the time of the Roman Empire were substantially based upon those described by Vitruvius in his splendid handbook *De Architectura* (Vitruvius 1960).

However, as Vitruvius says, the Roman art of building was the heritage of the Greek culture. On the other hand, the construction technique know-how, including building materials, came from the Egyptians and Persians through a slow transmission process of the original culture (particularly from East Iran) through the Mesopotamian and the Mediterranean civilization (Colleparidi 1997).

In the previous part, the primitive binder, lime, and its history of technology were examined. However, from now on, the technology of the Roman concrete, which is very similar to the modern concrete are going to be investigated. In fact, the fact that ancient Roman concrete has withstood the attack by elements for 2000 years, while the modern one undergoes premature deterioration within its service life lesser than 100 years, shows that the basic construction techniques of the Romans must be better than those of modern practice as judged by comparing the products (Moore 1993).

Mortar consisting of lime and sand has been used as an integral part of masonry structures for thousands of years. It also was applied to protect the earthen walls of ancient houses. When mixed with volcanic ash (pozzolan), it becomes a mortar that the Romans used to build rock walls. The Romans later discovered how to mix this mortar with small stones, bricks, and other materials to produce concrete called as 'Roman Concrete' (Moore 1993).

The constituents of Roman Concrete, aggregate and pozzolan, are going to be described in the following parts, except the lime, which was discussed previously.

4.1 *Aggregates*

Stone aggregate is a necessary part of the concrete because mortar by itself cannot sufficiently resist the crushing force of great weights. Aggregate gives concrete its necessary structural body by increasing the density of mass. It also reduces the amount of lime that must be burnt and slaked. The Romans used several kinds of stone for aggregates, ranging in weight from selce, a very heavy lava stone used in foundation walls, to lightweight tufa (a local granular stone) and pumice, both used in vaults. Other kinds of stone, as well as broken bricks and tiles were also used. All of these materials were found in and near Rome. Architectural sculptures and other stone members of demolished buildings were sometimes broken up and used as aggregate. In many structures different aggregates were used according to the loads to be carried. Certain vaults of the Flavian Amphitheatre contain pumice, and the five kinds of aggregate in the walls and dome of the Pantheon were separated into five horizontal zones, each containing a lighter aggregate than the one below. In foundations the aggregate often occupies two thirds of the total volume of the fabric (Singer et al. 1965).

Aggregate was added to the mortar during the actual construction of the wall or vault. Often the stones were spaced at random, having been dumped into the forms and left untouched, though sometimes they were raked out. In Trajanic and Hadrianic work they were frequently laid by hand in regular rows, spaced evenly in the mortar both horizontally and vertically in order to distribute evenly resistance to load. The stone in such cases is usually a yellowish tufa, roughly shaped into loaf forms about half-foot in length. Such aggregate takes up about half the volume of the concrete of walls and vaults. It is always completely surrounded by mortar, with the exception of the exposed irregular side of pieces laid against wooden shuttering or formwork (Singer et al. 1965).

5 POZZOLAN

Natural pozzolans are the naturally occurring siliceous or siliceous and aluminous materials which in themselves possess little or no cementitious value but will, in finely divided form and in the presence of moisture, chemically react with calcium hydroxide at ordinary temperatures to form compounds possessing cementitious properties. Volcanic glasses, volcanic tuffs, trusses, diatomaceous earths and some clays and

shales possess pozzolanic properties when they are in a finely divided form (Erdoğan 1997).

In fact, the name pozzolan comes from the town of Pozzuoli in the foothills of Mount Vesuvius, in Italy, where the ancient Romans had produced a hydraulic binder by mixing lime with volcanic soil more than 2000 years ago (Erdoğan 1997).

Likewise, Vitruvius describes pozzolan as a kind of powder, which from natural causes produces astonishing results. He says in his handbook *De Architectura* that this substance, when mixed with lime and rubble, not only gives strength to buildings of other kinds, but even when it is used in the sea, they can set and harden under water.

By the day the Romans had mastered the use of pozzolan, which they added to the dry mix in lieu of part of the sand. Pozzolan is a friable volcanic material, found in thick beds of chunks and gravel-sized pieces in Latium and Campania and easily reduced to usable form. It often has a distinct reddish or yellowish hue and has the property of forming hydraulic silicates in combination with lime, quartz sand, and water. The importance of pozzolan can be exaggerated, for some large Roman concrete buildings were built without it, but mortar made with it set readily under water, an advantage Roman engineers made good use of. The architects and builders of the high empire must have been convinced that pozzolan improved their concrete, for it was used in almost all buildings and rarely absent from high imperial construction in Rome and its environs (Singer et al. 1965).

6 DURABILITY OF ANCIENT MORTARS AND CONCRETE: COMPARISON WITH MODERN CONCRETE

Concrete experts talk today about how to make concrete durable. Many ancient concrete buildings are still in use after more than 2000 years. For these modern concrete experts, the Romans were fortunate builders in that they apparently simply used natural pozzolan deposits, which were found to be suitable for producing a hydraulic mortar. Contrary to this pronouncement, Vitruvius states in his book *De Architectura* that the magnificent quality of Roman concrete resulted from the extensive use of artificial pozzolanic mortars and concretes. Two artificial pozzolans were intensively used: (1) calcined kaolinitic clay, in Latin *testa*; (2) calcined volcanic stones, in Latin *carbunculus*. In addition to artificial reactive ingredients, the Romans used a natural reactive volcanic sand named *harena fossicia*. The ingredients *testa*, *carbunculus* and *harena fossicia* were intensively used in Roman buildings (Vitruvius 1960).

Dusty ancient history books taught us that Roman concrete consisted of just three parts: a pasty, hydrated

lime; artificial or natural pozzolan; and a few pieces of fist-sized rock. If these parts were mixed together in the manner of modern concrete and placed in a structure, the result certainly would not pass the test of the ages (Moore 1993). How did those Romans around the time of Christ build such elaborate, ageless structures in concrete is the question on which the durability of ancient concrete and its comparison with modern one will be discussed in the following part of this investigation.

“A most unusual Roman structure depicting their technical advancement is the Pantheon; a brick faced building that has withstood the ravages of weathering in near perfect condition. Solving the riddle of ancient concrete consisted of two studies: one was understanding the chemistry, and the other was determining the placement of ancient concrete. To understand its chemical composition, going back in time much before Moses is essential. People of the Middle East made walls for their fortifications and homes by pounding moist clay between forms, often called pise work. To protect the surfaces of the clay from erosion, the ancients discovered that a moist coating of thin, white, burnt limestone would chemically combine with the gases in the air to give a hard protecting shield. As a guess, the event of discovering pseudo concrete occurred some 200 years before Christ when a lime coating was applied to a wall made of volcanic, pozzolanic ash near the town of Pozzuoli in Italy” (Moore 1993).

A chemical reaction took place between the volcanic ash containing silica and small amounts of alumina and iron oxide and the lime (calcium hydroxide). Later Romans noticed that mixing finely ground volcanic ash with lime made a thicker coat, but it also produced a durable product that could be set and harden even under water. In order to understand the difference between lime and lime-pozzolan mixtures, the chemical reaction have to be examined separately. When only lime is used as a binding agent within lime-sand-water mixture, the strength development of the mix occurs as a result of carbonation, whereas in the case of lime-pozzolan mixture strength development is based upon the reaction between hydrated lime and finely ground amorphous silica. There is no need to carbon dioxide in the case of lime-pozzolan mixture, which means that it possess hydraulicity. It is also found that parts of the complex chemistry of the lime-pozzolan bonding gel matching the same chemical formula of modern concrete bonding gel, which is called as C-S-H or tobermorite gel in modern concrete world. And this is so; the pozzolan-wet lime gel gave the high performance to the ancient concrete. The placement technic used in ancient concrete was the other important point causing high performance (Moore 1993).

“Chemistry alone will not make good concrete; rather people will make good concrete. Although a new

concrete product called Roller Compacted Concrete (RCC) had been crudely developed, U.S. Bureau of Reclamation’s refinements made it an economical candidate for dam construction. In the construction of a dam in Utah, USA, a concrete consisting of a binding mixture of 40% Portland cement and 60% fly ash. By coincidence, the fly ash contained the same amorphous silica compounds as the ash from explosive volcanoes. And the hydrated portland cement released the calcium component recognized in the lime part of the ancient concrete formula. When Reclamation mixed these two parts for their dam, a bonding gel was formed to tie inert rock pieces of the hatch together. These rocks were used as a strong filler material much in the same manner as is used in standard concrete practices” (Moore 1993). So, a close relationship between the calcium hydroxide molecules from Portland cement and that of the ancient wet lime, and between the amorphous silica of the pozzolanic fly ash and the amorphous silica of the volcanic pozzolan can be constructed. As a result, such a reasonable relationship for the concrete components that make the gel for both modern and ancient concrete can be useful for comparison purposes (Moore 1993).

Although the similarity of the ingredients of modern and ancient concrete has been explained, there is more. Studies of the placement process are very important in making durable concrete. The Bureau of Reclamation mixed their components (cement, ash, and rock) with as little water as possible to give a stiff, ‘no slump’ concrete; spread it in layers on the dam; and pounded it into place by large vibrating rollers to make a new class of concrete. The ancients had mixed their components (wet lime and volcanic ash) in a mortar box with very little water to give a nearly dry composition; carried it to the jobsite in baskets placing it over pre-placed layer of rock pieces; and then proceeded to pound the mortar into the rock layer. Vitruvius mentioned this process in his history formulas for his concrete, plus the fact that special tamping tools were used to build a cistern wall. Close packing of the molecular structure by tamping reduced the need of excess water, which is a source of voids and weakness. But also packing produces more bonding gel than might be normally expected (Vitruvius 1960, Moore 1993).

Throughout the above paragraphs, the ancient concrete was compared with one type of modern concrete, RCC, which was invented few years ago and whose applications are restricted overall the world. The other modern concrete applications generally suffer from premature deterioration within their service or design life. Some of the reasons for that are as follows: (1) modern cement is too active, thus the rate of hydration reaction, which is exothermic, is too high; and thus modern concrete becomes more prone to thermal cracking and thus more permeable. (2) Expectation of high strength performance from concrete

induces use of higher dosage of cement or use of finer cement, which causes same result of (1). (3) Speed of construction induces use of high early strength cement and concrete or use of speeded curing methods (e.g. heat curing), and thus causes again the same result of (1).

7 CONCLUSION

The history of Portland cement, modern binding material invented in 1824 is too short, when the whole history of binding materials utilized by ancient people throughout several centuries is considered. Through the long history of human beings, several types of binding material have been invented sometimes intentionally, sometimes unintentionally. Mud, gypsum, lime, and lime-pozzolan mixture are some examples of ancient binding materials.

Whatever type of binding materials the ancient civilizations used, it can be seen that those structures built by ancient binders, particularly lime-pozzolan mixture have survived for several hundred years. It can be claimed that even at that time architects were aware of the importance of the durability of binding materials and their mortars. For instance, the Romans built many beautiful, massive structures such as the famous Pantheon lasting through several hundred years till today. However, those structures belonging to modern civilizations and made by using modern binders, i.e. portland cement have experienced significant deterioration throughout their service life, generally lesser than 100 years. As a result, it can be said that the whole process of modern binding materials, mortars and concrete should be re-examined beginning from raw materials, production processes of binding materials up to mixing, placing, compaction, finishing and curing processes of mortars and concrete. At that point, it is imperative to examine many good examples throughout the ancient centuries.

ACKNOWLEDGEMENT

Throughout this study some informations are quoted from several web sites i.e.

“www.auburn.edu/academic/architecture/bsc/classes/bsc314/timeline/timeline.htm”
“matse1.mse.uiuc.edu/~tw/concrete/hist.html”
“www.oneworld.org/itdg”

“www.portcement.org/cem/cementindustry_history.asp”
“realitytimes.com/rtnews/rtcpages/20000128_concrete.htm”
“www.romanconcrete.com”
“www.qcl.com.au”

This is sincerely appreciated by the author of this article.

REFERENCES

- Colleparidi, M. 1997. A Historical Review of Development of Chemical and Mineral Admixtures for Use in Stucco and Terrazzo Floor. *Proceedings of the Fifth CANMET/ACI International Conference on "Superplasticizers and Other Chemical Admixtures in Concrete"*, SP 173, pp. 673–694.
- Erdoğan, T.Y. 1997. *Admixtures for Concrete*. Ankara: METU Press.
- Erdoğan, T.Y. 2002. *Materials of Construction*. Ankara: METU Press.
- Krumnacher, P.J. 2001. *Lime and Cement Technology: Transition from Traditional to Standardized Treatment Methods*, MSc's Thesis in Virginia Polytechnic Institute and State University, USA.
- Lazell, E.W. 1915. *Hydrated Lime: History, Manufacture and Uses in Plaster-Mortar-Concrete*.
- McKee, H.J. 1971. *Early American Masonry Materials in Walls, Floors and Ceiling: Notes on Prototypes, Sources, Preparation and Manner of Use*. NY.
- Moore, D. 1993. The Riddle of Ancient Roman Concrete. "Spillway" a newsletter of the US Dept. of the Interior, Bureau of Reclamation. Upper Colorado Region.
- Neville, A.M. 1998. *Properties of Concrete*. New Jersey: Prentice Hall Inc. 4th Edition.
- Nicholson, P. 1850. *Encyclopaedia of Architecture: A Dictionary of the Science and Practice of Architecture, Building, Carpentry, etc. From the Earliest Ages to the Present Time*. Vol.2. NY: Johnson Fry Co.
- Singer, C., Holmyard, E.J., Hall, A.R., Williams, T.I. 1965. *History of Technology*. Vol. 1–5. Oxford: Clarendon Press.
- Vitruvius, P. 1960. *Vitruvius: Ten Book on Architectura*. New York: Dover Publications.

A system approach for examination and determination in historical buildings

D. Ekşi Akbulut

Architecture Department, Yildiz Technical University, Istanbul, Turkey

F. Aköz

Engineering Department, Yildiz Technical University, Istanbul, Turkey

ABSTRACT: In thousands of years in civilization history, these values, which were created by directly human beings or with nature, are named today as “Cultural and Natural Heritage”. Conservation of these values is a very important subject that has to be studied. These studies about conservation and restoration of historical buildings that are very important cultural heritage must be aimed at scientific principles, aesthetics, and conservation of their historic values.

Before the conservation, restoration and strengthening of a historical building, study stages have to be define in collecting and evaluating data towards observation and determination studies. In this paper, a system approach towards the criteria’s mentioned above that can be easily applied for each historical structure is proposed.

1 INTRODUCTION

Since early 20th century, some legal obligations such as Carta Del Restauero and Venice Charter are constituted for the studies about conservation and restoration of historical buildings which are very important cultural heritage.

In the past when the building has its own function its permanent maintenance has also provided its conservation. According to the famous Italian expert Piero Gazzolo; “If an architectural monument doesn’t serve to its own function, conservation becomes more than a practical necessity, turns into a cultural responsibility. The attention to this subject is depends on the next generations cultural knowledge and the sensitivity to the conservation of cultural heritage”.

Restoration and conservation methods continuously come into being discussions between the different disciplines. To cope with this problem, it has to determine the method and the conservation level in a point of historical and aesthetic appearance of historical buildings and it has to determine the procedures putting into practise relating the structural damages and their repairs. In these studies, specialists from different disciplines like architecture, archaeology, history of art and engineering have to collaborate.

2 STUDIES ON CONSERVATION

Even if the history of studies on conservation last out to past, the modern technique for conservation begins in 19th century. The congress in Athens in 1931 was the first congress about conservation of historical monuments. The congress expresses that each country constitute official records which shall contain all documents relating to its historical monuments and to deposit copies of its publications with the International Office. After the congress in Athens the principles are approved by Italy and called “Carta Del Restauero” becomes a legal obligation. And it recommends that the specialists from different disciplines have to collaborate and the experts have to agree that before any consolidation or restoration is undertaken. And also it is pointed that contributions of all periods of the building must not be destroyed, the additions which misleads the experts must not be built and the original materials that are come up with the analytic researches must be conserved.

In 1957 “I. International Conference of Architects and Technicians of Historic Monuments” is organized in Paris. In this conference it is explained that cultural heritage is common responsibility and some organizations like ICOMOS, ICCROM was proposed to establish.

“II. International Conference of Architects and Technicians of Historic Monuments” is organized in Venice in 1964. The Venice Charter which is constituted in the conference is examined the problems of architectural conservation in nearly hundred years of European history which become more complex and varied. This charter becomes a solution but not an ending, on the contrary it is affected the discussions in international perspective. Also in our days many associations and organizations are studying about this subject, many national and international conferences, symposiums are organized.

2.1 Venice Charter (1964)

The Venice Charter has an important role about theoretical progress of methods in conservation of historical buildings and monuments, and foundation of associations. It has 16 articles under the definition, aim, conservation, restoration, historic sites, excavations, publication headings. In this paper, as a system for conservation, restoration and strengthening of a historical building approach is proposed, the 9–13 articles are studied.

ARTICLE 9. The process of restoration is a highly specialized operation. Its aim is to preserve and reveal the aesthetic and historic value of the monument and is based on respect for original material and authentic documents. It must stop at the point where conjecture begins, and in this case moreover any extra work which is indispensable must be distinct from the architectural composition and must bear a contemporary stamp. The restoration in any case must be preceded and followed by an archaeological and historical study of the monument.

ARTICLE 10. Where traditional techniques prove inadequate, the consolidation of a monument can be achieved by the use of any modern technique for conservation and construction, the efficacy of which has been shown by scientific data and proved by experience.

ARTICLE 11. The valid contributions of all periods to the building of a monument must be respected, since unity of style is not the aim of a restoration. When a building includes the superimposed work of different periods, the revealing of the underlying state can only be justified in exceptional circumstances and when what is removed is of little interest and the material which is brought to light is of great historical, archaeological or aesthetic value, and its state of preservation good enough to justify the action. Evaluation of the importance of the elements involved and the decision as to what may be destroyed cannot rest solely on the individual in charge of the work.

ARTICLE 12. Replacements of missing parts must integrate harmoniously with the whole, but at the same time must be distinguishable from the original so that restoration does not falsify the artistic or historic evidence.

ARTICLE 13. Additions cannot be allowed except in so far as they do not detract from the interesting parts of the building, its traditional setting, the balance of its composition and its relation with its surroundings.

2.2 Code Ethique (1995)

ICOMOS International Training Committee agreed on responsibilities, documentations, examinations and applications in the meeting in Suomenlinna, Finland in 1995 which is named as “Code Ethique”. According to the articles about conservation, restoration and strengthening;

- a) As the conservation concept has a large extends and the attention of many different social groups need to be taken, conservation should be studied by trained and experienced person, carried out with the experts who have to collaborate with different disciplines with a scientific point of view and work with mass media associations.
- b) Before the conservation, restoration and strengthening applications are constructed; the general conditions, the physical properties, damage reasons and other problems of the historical monument should be examined.
- c) According to these examinations, a basic approach for each application must be improved and a conservation method which can be short term or long term must be programmed.
- d) There should always be a precise documentation of a technical report of the applications with drawings and photographs and should be copied for public institution archives. And also for the public use a summary report should be written.
- e) For the future existence of the monument there should be a limited applications with the examination of each effect through the monument and must be respected to its cultural heritage, environmental integrity, aesthetic, historical, physical originality.
- f) There shouldn't be any damage or changes to the original monument which are documentation of its history during the conservation, restoration and strengthening application.
- g) The modern techniques or new materials shouldn't be used without required experiments, scientific researches and discussions with an expert.
- h) The conservation, restoration and strengthening application shouldn't mislead the future studies, if it is necessary, the application can be removed, renewal as possible as can be and congenial with its surroundings (Binan, 1999).

2.3 Conservation studies in Turkey

In our country where there are many historic values and historical varieties, some associations and foundations related to conservation are also constituted. In recent years it is pointed that the symposiums organized by Cultural Ministry or the meetings Historical Cities Associations organized by municipalities are improved the point of view about the conservation of historical monuments and the public remaining interest to the subject. For healthy and permanent conservation not only the legal obligations but also active studies in micro and macro scale based on scientific data must be improved.

There is more maintenance of donations, economic sources for conservation and renovation of the historical buildings compare with the past because of commercial and touristical incomes. This kind of approach brings a danger of rebuilt of the monument or thoughtlessly change of functions. Whatever the aim is civilized usage of a historical monument is to keep the original by permanent attention. The basic and important aim is to keep the original not the damaged or copied one of the historical monument.

From the world heritage point of view our country is takes place on such a geographic place that many civilizations passed through and leave many work of arts which are now called cultural and historical heritage. Istanbul, in the end of southeast of Europe is the only city, which takes place both in two continents, Europe and Asia. Bosphorus flows between two continents, separate the city in two parts. Over 2600 years with a very interesting historical past, Istanbul is a unique city in the world. As a very special city of Turkey and World Istanbul, takes place in the list of historical heritage of UNESCO. So Istanbul is an uncovered laboratory with its historical monuments and buildings as all over our country. Although many of them could not resist to the natural disasters and wars and not exist today but many precious historical buildings have being lasted. Because of this reason these studies in Istanbul is very important by means of universal cultural heritage conservations.

2.4 Legal obligations of conservation in Turkey

The historical progress of the legal obligations of cultural heritage conservation in Turkey is mentioned below;

- In 1869 (*Asar-i Atika Nizamnamesi*) the Historical Monuments Obligations is constituted. This obligation is applied with some changes until the period of Turkish Republic.
- After 1930, Atatürk constituted "Committee for Conservation of Old Monuments and Preservation Delegation" for conservation the historical monuments.

- Property of Antiques and Superior Committee of Monuments is constituted in 1951 under the National Education Ministry related to control and observe the principles and applications of restorations, conservations, preservation of historical monuments and architectural buildings.
- Antiques Law is presented in 1973. The elements need to be conserved, including the residential buildings is attained a required level by this law. Between 1973–1982 years 100 urban sites, and 3442 monumental, 6815 residential architecture samples in 417 site area are officially registrated by Property of Antiques and Superior Committee of Monuments (Ahunbay, 1996).
- ICOMOS National Committee of Turkey is constituted in 1974 according to obligations of "International Council of Monumentals of Sites" in Turkey.
- In 1982 Republic of Turkey is approved to participate to UNESCO in accordance with "Conservation of World Cultural and Natural Heritage Charter". In 1983 Antiques Law is beared and Conservation of Cultural and Natural Heritage Law is constituted. By this law instead of antiques term cultural heritage term is consumed.

The cultural values which are under protection of government and named as Cultural and Natural Heritage are under the responsibility of Cultural Ministry. Conservation of Cultural and Natural Heritage Superior Committee under the Cultural Ministry carried out the cultural and natural heritage services according to the scientific basis.

These are the responsibilities and competences of Conservation of Cultural and Natural Heritage Superior Committee;

- a) To define the principles of the services about conservation and restoration of immovable cultural and natural heritage
- b) To provide the required coordination conservation committees
- c) To determinate the general problems caused by the applications and to assistant the ministry by consensus

There are many organizations like TAÇ, Turing, Chamber of Architects, Foundation of History, Çekül, Galata Society, Zeyrek Conservation Society, Cihangir Society except Government Institutions provides many contributions on determination studies, archives and library services.

The relations between responsibilities of committees about law and obligation regulations related to conservation of historical buildings is shown in Figure 1.

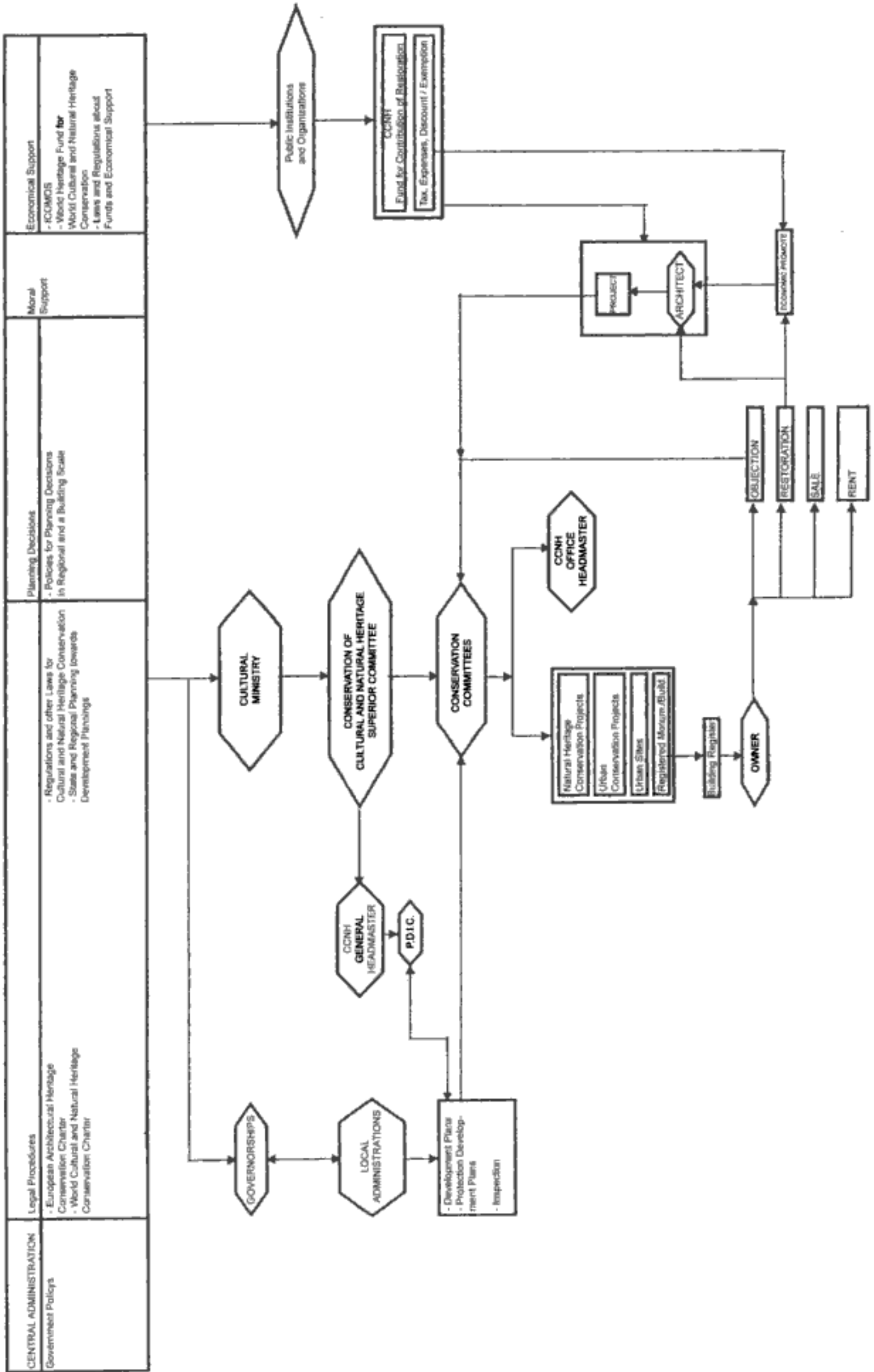


Figure 1. Organization scheme of conservation and restoration in Turkey (Akinci, 2000).

3 STUDIES ON MATERIALS

Every architectural shape is formed in a level of possibilities provided by technology and materials. In order to investigate the concept of aesthetics as much as perception of the building, material properties, applications and technological possibilities must be recognized. In historical buildings in comparison with comparison with today there are less materials and technical possibilities but variety of forms reaches to a high level.

Historical buildings construction typology is masonry. Materials used in masonry buildings, forming its structural system are also influenced its architectural features and its identity. The determination of material properties, which are used for masonry buildings, is very important subject as also for all types of structures. Architect, can design independently for a new structure but for the conservation and restoration of a historical building he has to work by respect to the history of building and its architectural features. In these studies to determine the present situation of building; researches about regional settlements and effects of these settlements, structural system of building and material properties, restorations that had been done before, strengthening and/or extension of building and their effects to the structural system and the examinations of the soil properties in micro and macro scale of building region have to be studied.

In the restoration studies, the properties of original materials must be investigate by experimental methods and the new materials, which will be used to have approximately same properties, must be taken into consideration. Otherwise fatal damages can be occurred and cannot be restored in the means of their aesthetics and historic values. For example; in the 1950's the materials like cement additive mortar and plaster which is very harmful for the historical buildings is applied by a volunteer firm who restored with a good intention in Konya. Because of this application there are significant physical damages on the structural materials like stone and bricks on the many Anatolian Seljuk Period buildings (Tunçoku, 2004).

The conservation, restoration and strengthening of a historical building is concerned measured drawing which is a documentation of architectural measurement and detailed drawings of building, restitution drawings which defines the original with the lost partitions or additions and restoration drawings for the determination of renewals must be prepared. However a healthy and permanent conservation must be carry out by experts with investigation of materials, scientific researches, laboratory analyses, preliminary studies, there is just a technical report which defines original material properties and defining the restoration materials.

There must be preliminary studies like determination of original construction techniques, damages occurred in time and the determination of physical, chemical, mechanical properties of original materials like stone, brick, mortar, plaster, adobe, wood, metal, glass which are used in historical buildings. For the experimental studies on materials the tests are generally performed on specimens taken from the structures. These specimens must be as small as possible for not damaging the building (Akman, 2001). Investigation of material properties of a historical building by using non-destructive methods usually includes rebound test, sonic test, radiographic tests, surface hardness test, permeability test and bonding test (Aköz, 2001).

In any case sampling a masonry specimen is not a simple operation also in the case of a regular and solid masonry. Being a highly destructive operation, only one or two specimens can be sampled and the test may be statistically unreliable in the case of a very poor masonry. Therefore, the only way to reach the goal seems to be an in-situ testing on the masonry as a composite (Binda, 1999).

The informations to determine the stages of building, construction dates, unexplained additions to the building can be obtained from a detailed material study of the historical building.

There are authentic construction methods, preparation methods of materials, authentic material properties of many historical buildings point out differences depend on the geographic aspects, construction periods in our country. So as to obtain detailed and straight historical documents and information, conservation and restoration of each building must be studied with material and technological perspective as well as its architectural and artistry perspectives. Otherwise conserving the historical buildings from the conservation studies or recovering the restored historical buildings must be taken into consideration.

4 A STUDY PROGRAM TO DETERMINE MATERIAL PROPERTIES FOR CONSERVATION, RESTORATION AND STRENGTHENING OF A HISTORICAL BUILDING

Before the conservation, restoration and strengthening of a historical building, study stages have to be define in collecting and evaluating data towards observation and determination studies. In Table 1, a study program which is proposed in this paper can be easily applied for each historical structure.

4.1 *Determination of the building identity*

The original name and current name of the building, its address, original function and current function should

Table 1. General study program for conservation and restoration of historical buildings.

Study Groups	Study Stages	Explanations	Check List		
			Yes	No	Explanations
I.GROUP	Determination Of The Building Identity Period : (day/month)	Name / Original Name			
		Address			
		Original Function / Current Function			
		Architect/ Constructor or Institution			
		Constrion Date / Period			
		Current Condition			
II.GROUP	Information About The Building Period: (day/month)	a) Literature and visional documentation			
		b) Plans, sections, elevations and photographs			
		c) Permissions from related intitutions for the investigations and determinations			
		d) Contacts with the responsible persons for studies			
		e) Drawing detailed and measured projects			
		f) Drawing restitution project			
III.GROUP	Examine Studies on Building Period : (day/month)	a) Coding of the elements on plans, sections, elevations with the informations from stage II			
		b) Confrontation of the documents with the current buildings in the site area			
		c) Determination of the elements, defining the damages by photography			
		d) Observation of the damage improvement by scaling and visual studies			
		e) Determination of the damage causes			
		f) Confrontation the current condition with the documents			
		g) Organization of study program by using the codings of elements for observation, measurements and tests			
		h) Determination of materials of each elements, measuremet of the elements, defining the craks and damages, detail photographs from required elements			
		i) Non-destructive tests and defining the test results on the program			
		j) Taking specimens from required and permitted elements			
IV.GROUP	Laboratory Studies Period : (day/month)	a) Preparing the samples and specimens for the laboratory tests			
		b) Physical, Mechanical, Chemical tests			
		c) Investigation of material properties			
		d) A statistical relation with the results from the laboratory tests and the non-destructive test for correlation			
		e) The determination of the material properties from the elements that no specimens are taken but non-destructive tests are studied by using the statistic correlation			
V.GROUP	Selection Of Materials Period : (day/month)	a) The selection of materials for conservation, restoration and strenghtening After the tests, determination of original material and defining the material properties,			
		b) Determination of some specimens in the application and investigate the quality, convenience to the original material.			
VI.GROUP	Conservation, Restoration And Strengthening of The Building Period : (day/month)	a) Project preparations , restoration project			
		b) Auctioning procedure			
		c) Conservation, restoration and strenghtening applications			
		d) A control system for quality and convenience to the original building and the projects			

be defined. Before all else architect of the building, the institution or the constructor who organized the construction and constructed date or period must be defined from the documents about the historical building than the information about past restorations, additions, renewals must be taken and current conditions of the building must be examined.

4.2 *Information of the building*

After determination of the building identity, literature study of the building, plan, section and elevation drawings of the building and the photographic of the building must be researched. So as to begin to investigate on the building area the permissions must be get from related institutions or organizations and contact with the responsible person. At the first stage, there must be visual determination by taking photographs and if there isn't any architectural drawing of the building, the measured, detailed drawing of the building must be studied on the building area.

4.3 *Examine studies on building*

Before the examine studies the groups must constitute a study program and define every single job as clear as possible.

4.3.1 *Coding*

The structural or any kind of element in the building must be coded on the projects and the photographs of the building. These elements must be check with the building so as to define current conditions and the damages of the building. This study must be done for also each decoration element on the building as well as the structural elements.

4.3.2 *Determination of damages*

The study stages and study schedule must be formed from the prepared, coded project. There should be determination of materials and measurement of dimensions from each element, detailed photography from required areas, and determination of damages and examination of the damage causes and investigation of damage improvements by using the visual and measurement methods.

4.4 *Non-destructive tests*

The non-destructive tests such as rebound test, sonic test, temperature test, humidity test and flat-jack test must be applied to determine the physical and mechanical properties of the materials in winter and summer conditions. Than so as to make studies in laboratory, the specimens must be taken from only required and permitted areas. The aim in taking specimens from a structural element is to investigate the quality of

materials as stone, brick, mortar to determine their strengths.

4.5 *Laboratory studies*

After preparing the specimens and samples taken from the building, physical and mechanical tests must be applied. A statistical relation with the results from the laboratory tests and the non-destructive test must be researched to find a correlation. The determination of the material properties from the elements that no specimens are taken but non-destructive tests are studied must be defined by using the statistic correlation.

4.6 *Selection of materials*

After the tests, determination of original material and defining the material properties, the selection of materials for conservation, restoration and strengthening studies must be improved. The required tests must be applied to the selected materials. In the application period again some specimens must be taken so as to make tests and investigate the quality, convenience to the original material.

4.7 *Conservation, restoration and strengthening of the building*

For the conservation, restoration and strengthening studies a restoration project must be prepared after the required tests and selection of materials. So as to define the application firm auctioning method can be used after all the studies, projects and documentations are obtained. There should be a control system for quality and convenience to the original building and the projects after the conservation, restoration and strengthening applications. An educated group of workers should for the proper, conscious and convenient to the original project study in the conservation, restoration and strengthening applications.

There should be expert groups, clarified job descriptions, detailed and defined study programs for each study stages in the study program defined in 6 stages which is mentioned above.

5 DISCUSSIONS

Although this study program seems detailed and long time work for the the conservation, restoration and strengthening studies that has many criterias it obtains determined system for application. The unconscious applications causes unreturn damages to the historical monuments. In this paper, the study program that has proper stages, defined experts and study descriptions and investigate the unconscious application is proposed. For example; Hırami Ahmet Paşa Masjid which

is restored between 1966–1968 the fresks are removed and exterior facade stone work restored without a respect to the original building with an unconscious study (Kuban, 2000).

The basic problems of restorations are not giving any importance to research studied before applications, lack of material investigations, to remain true to original materials and lack of scientific documentation. In this paper, the suggested study program obtains also detailed documentation, recorded knowledge about the buildings.

6 CONCLUSIONS

As it seen in the study program which is proposed in this paper;

- It may be improved by the experts from different disciplines according to their needs and study subjects
- These programs which improved by the experts may be gathered by director and transfer to the other experts and it may provide different disciplines collaborated study and may be viewed by the director of study program
- Such a study program like this, it may be scientific, aesthetic, conservative to the historical values and a scheduled study by the experts from different disciplines for conservation, restoration and strengthening as it is mentioned in Venice Charter and other documentations of ICOMOS

REFERENCES

- Ahunbay, Z., 1999, Tarihi Çevre Koruma ve Restorasyon, (Conservation and Restoration of Historical Environment) İstanbul, Yem Yayın
- Ahunbay, Z., 2002, ICOMOS ve Risk Altındaki Kültürel Mirasın Korunması, (ICOMOS and Conservation of Historical Heritage Under Risk) İstanbul Yapı Dergisi Sayı: 244, Sf: 27–29

- Akman, S., 2000, Yapi Hasarları ve Onarım İlkeleri, (Building Damages and The Principles of Restoration) İstanbul, TMMOB İnşaat Mühendisleri Odası, İstanbul Şubesi
- Akıncı, F.N., 2000, Geleneksel Sivil Mimarinin Sosyo-Kültürel Ve İşlevsellik Bağlamında Tarihsel Sürekliliği İçin Planlama/Finans Modeli, (A Financial Model for Historical Continuity in the Consistency of Social-Culture and Function of Traditional Residence Architecture) Doktora Tezi, Y.T.Ü. Fen Bilimleri Enstitüsü, İstanbul
- Aköz, F., 1995 Yüzer, N., "Investigation of Material Properties of Küçük Ayasofya Mosque – Sts Sergius and Bacchus – in Istanbul by Using Non Destructive Methods", STREMA 95, Structural Studies Repairs and Maintenance of Historical Buildings, Chania, Crete, Greece
- Aköz, F., 1996, Investigation of Material Properties of Küçük Ayasofya Mosque – STS Sergius and Bacchus by Using Non-Destructive Test Methods, EC Workshop on Non-Destructive Testing to Evaluate Damage Due to Environmental Effects on Historing Monuments, Trieste, Italy
- Aköz, F., 2001, Experimental Methods and Tests on Historical Structures, Workshop 3rd Meeting of IASS-WG17-Historical Structures, İstanbul, Türkiye
- Binda, L., Tiraboschi, C., 1999, Flat-Jack Test: A slightly destructive technique for the diagnosis of brick and stone masonry structures Aedification Publishers
- Binan, C., 1999, Mimari Koruma Alanında Venedik Tüzüğü'nden Günümüze Düşünsel Gelişimin Uluslararası Evrim Süreci, (International Conceptual Improvement of From Venice Charter to Today) YTÜ Basım Yayın Merkezi, İstanbul
- Erder, C., 1975, Tarihi Çevre Bilinci, (Historical Environment Conscious) ODTÜ Mimarlık Fakültesi Yayın no: 24, sf. 84–87, Ankara
- İpekoğlu, B., Böke, H., 2002, Türkiye'de Tarihi Yapılarda Malzeme Koruma Sorunları, (The Conservation Problems of Material in Historical Buildings) 1. Ulusal Malzeme Kongresi ve Sergisi, TMMOB Mimarlar Odası Büyükkent Şubesi, İstanbul
- Kuban, D., 2000, Tarihi Çevre Korumanın Mimarlık Boyutu, (Architectural Perspective of Conservation of Historical Environment) Yapı Endüstri Merkezi Yayınları, İstanbul
- Tunçoku, S., 2004, Günümüzde Koruma/Restorasyon Çıkmazı, (Contemporary Conservation/Restoration Problems) Mimarlık Dergisi, Sayı 315, Sayfa: 56, İstanbul
- Anon 3, T.C. Kültür Bakanlığı, Kültür ve Tabiat Varlıklarını Koruma Genel Müdürlüğü, yayın no: 1806, 2. Basım, Mart, 1996/Ankara

Analysis of steel-structure/masonry-wall interaction in historic buildings

D. Friedman

Consulting Engineer, New York, USA

ABSTRACT: Conservation of historic high-rise buildings requires analysis of the peculiarities of early modern construction. The beams, columns, and facades of large steel-frame, masonry-wall buildings experience complex undesigned interactions. Masonry curtain walls of these buildings are usually 300 mm thick, capable of resisting structural loads. American investigation of interactions between masonry curtain walls and steel frames began with facade inspection laws intended to find damaged masonry on high-rise buildings. Structural effects found include cracking, out-of-plane displacement, and spalls resulting from thermal stress, sidesway, and rust-jacking. This paper compares the effect on masonry curtain walls of various structural mechanisms, specifically for high-rise buildings as constructed in the United States between 1900 and 1930. For each mechanism, the stress and strain interaction of steel and masonry elements is considered, rather than analyzing them separately as in modern design practice.

1 INTRODUCTION

As the conservation movement has expanded to include modern buildings, and as the oldest steel-frame high-rise buildings have passed one hundred years since their construction, engineers have begun to study technical issues in maintaining and repairing historic high-rises. One of the most difficult issues is the interaction under load of heavy masonry curtain walls and steel frames, since this was neither anticipated in the original designs nor is common in the construction of current buildings. Much of the damage that is seen in these buildings – including cracking, out-of-plane displacement, and masonry spalling – is similar in appearance to that seen in traditional masonry construction but results from different causes. The causes can best be explained by analyzing these buildings as examples of a unique type.

New York City has been a center of study of historic high-rises, both formally within the conservation community and empirically by engineers and architects inspecting and designing repairs for facades. The historic reason for the study is the sheer concentration of such buildings in the city: in 1929, there were 2479 buildings in New York higher than ten stories out of 4829 in the United States. Chicago had the second greatest total, 449 (Regional Survey, 1931). The empirical reason for the study is the 1980 city law that requires periodic inspection and repair of all tall-building facades. Recognition of New York's unique tall-building history has not necessarily translated into

conservation and restoration techniques specific to the buildings. Simply put, architectural histories, technical descriptions of designated landmarks, and ad hoc conservation knowledge among designers and contractors focus more on the masonry envelopes of those buildings than their structural details. At one extreme, descriptions of tall buildings in architectural guides may omit critical details of a building, such as one description of the 320 m Chrysler Building that fails to mention that it has a brick-veneer exterior wall, let alone that it has a steel frame (White & Willensky, 2000). At the other extreme, technical literature specifically written for conservation typically emphasizes materials concerns over less-known structural ones. The New York Landmarks Conservancy, a non-profit advocacy and technical expertise organization, has created a useful guide to the repair of building facades that emphasizes work on high-rise buildings (Meadows, 1986). The guide correctly mentions steel deterioration and the effects of wind pressure and thermal changes as causes of damage, but is aimed at identifying and repairing materials damage. Unfortunately, there is no equivalent guide for identifying and repairing damage caused by interaction between steel and masonry elements, or, as they are often identified, structure and architecture. The lack of technical sources is exacerbated by the visual similarity between material deterioration and secondary damage from structural movement. For example, brick faces may spall because of incompatible pointing (a materials problem) or because of high compressive stress from

lack of expansion joints (a structural problem). Structural problems such as excessive sidesway are typically not visible in themselves, but become manifest in damage to non-structural elements.

2 HISTORICAL AND ARCHITECTURAL CONTEXT

The earliest steel-framed buildings in the United States, completed before building codes recognized the reality of curtain-wall construction, had very thick exterior walls, with 600 mm of masonry common in the 1890s. A trend towards 400 mm walls shortly before 1900 was finalized by the 1901 New York City Building Code, which required minimum 300 mm walls on all steel-frame buildings. Walls continued to be built thicker than minimum in order to carry architectural ornament. Various facing materials were used, most often brick and glazed terra cotta.

Steel-frame buildings constructed before the 1901 code vary greatly in structural type, and can be considered as partly experimental. Those constructed after 1901 and before the 1929 economic crash are much more structurally uniform, as described below.



Figure 1. 953 Fifth Avenue is the narrow building with a three window-wide street facade, directly above the truck.

This latter class of building is highly concentrated in New York and Chicago, as no other city had a large number of tall steel-frame buildings constructed in that era, and construction details from the post-World War II period are significantly different.

The character of large portions of Manhattan is marked by early twentieth century steel-frame buildings: the downtown and midtown business districts contain hundreds of office buildings of this type, while the north-south avenues of the uptown residential neighborhoods are lined with miles of mid- and high-rise apartment houses. Some of these buildings, such as the 240 m Woolworth Building of 1913, were planned as architectural monuments and have remained so since, but most of these buildings were meant as ordinary “background” architecture (Fig. 1). Individual buildings have been designated as protected landmarks by the New York City Landmarks Preservation Commission. There are also designated landmark districts containing many of these buildings, but the significant buildings within the districts (such as the Upper East Side district) are often low-rise, traditional-construction buildings such as churches and private residences. Despite the fact that so many steel-frame mid- and high-rise buildings in Manhattan are not considered architecturally distinguished, this type of building is of great interest because it quantitatively dominates use and repair.

3 BUILDING DESCRIPTION

The analysis in this paper concerns the structural effect of outside forces on all buildings of a given type – steel-frame high-rises built between 1900 and 1930 – using numerical examples from one such building. Generalizing from the analysis of one building to a class depends greatly on the assumption that the class has strongly marked properties that can be defined in advance. The author’s observations during restoration projects and the historical record both confirm this assumption – the existence of what architectural historian Carol Willis has called “vernaculars of capitalism,” where building codes, street layouts, and local economic conditions combined with the standard building technology of the day to produce “standardize[d] highrise design” (Willis, 1995). The description that follows is based largely on the author’s observations, but is similar to those in traditional architectural and technological histories such as Elliott (1992) and Condit and Landau (1996).

3.1 Characteristics of the general type

The defining characteristic of the type is the presence of a structural-steel skeleton frame designed to carry all gravity and lateral loads. Under the building codes in force during the period of interest (the first thirty

years of the twentieth century), the only lateral load explicitly used in the design of multi-story apartment, office, and industrial buildings was wind load; under current codes in the United States, wind load usually governs for steel-frame buildings except in the high-seismic areas (primarily the west coast) where relatively little high-rise construction took place until after 1945. Connections were typically riveted except for beam-to-girder double-angle connections, which were either riveted or bolted.

The most common lateral-load systems were moment frames with semi-rigid bracket connections, often top and bottom stiffened angles. Knee braces or more complex moment frames were used on slender or unusually tall buildings; full-bay bracing was used only in the tallest and most slender buildings. The reliance on moment frames is in part an artifact of design methods: the use of portal- and cantilever-frame analyses did not provide accurate lateral drift results that might have encouraged the use of stiffer frames. Matrix-based analysis was impractical without computers and moment-distribution was not yet available (Cross, 1930).

Several floor systems were in use simultaneously during the period of interest. In 1900, terra-cotta tile arches were the standard method of providing a floor between beams. By 1930, the most common system was the draped-mesh slab, often constructed using cinder-aggregate concrete. Ordinary bar-reinforced concrete slabs were sometimes used, although they were rare in New York during the 1920s and 30s. Patented reinforced-concrete slabs, such as the Kahn System, were most common in the 1910s, but appear throughout the period.

Building facades were solid masonry, consisting of a veneer of ashlar, terra cotta, or face brick over common-brick back-up. The 1901 New York Building

Code cleared the way for walls of constant 300 mm thickness by explicitly recognizing the frame structural support of the walls, in place of the codes based on masonry structure previously in use. The detail used for supporting the back-up masonry nearly always consisted of the masonry resting at each floor on either the spandrel beams or the slab above the spandrel beams. The veneer was commonly supported through mechanical interlock with the back-up (e.g., headers). Windows were simple rectangular openings with either loose lintels or, rarely, hung lintels. Masonry piers built integrally with the walls were typically used to provide fire-protection to the spandrel columns.

The most important structural aspect of these buildings is not obvious during cursory examination. Unlike modern construction, where great efforts are made to structurally isolate facades through the use of expansion joints and flexible ties, the exterior of these buildings is a system of masonry and metal elements in continuous contact. More specifically, there are no expansion joints of any kind in the curtain walls and the fire-proofing piers tie the columns to the walls. The presence of these piers and the close contact between masonry, spandrel beams, and floor-slab edges makes independent movement of the walls and frame impossible, and therefore negates a common design assumption.

3.2 Case study: 953 Fifth Avenue

The apartment house constructed in 1924 at 953 Fifth Avenue in Manhattan is typical structurally except for its bar-reinforced concrete slabs. At fourteen stories (46 m) above grade, it was not particularly tall when built, however it was built on a single 7.6-meter-wide lot and it therefore has a fairly high slenderness ratio of 6 (Fig. 2). In reality it receives no wind load in the

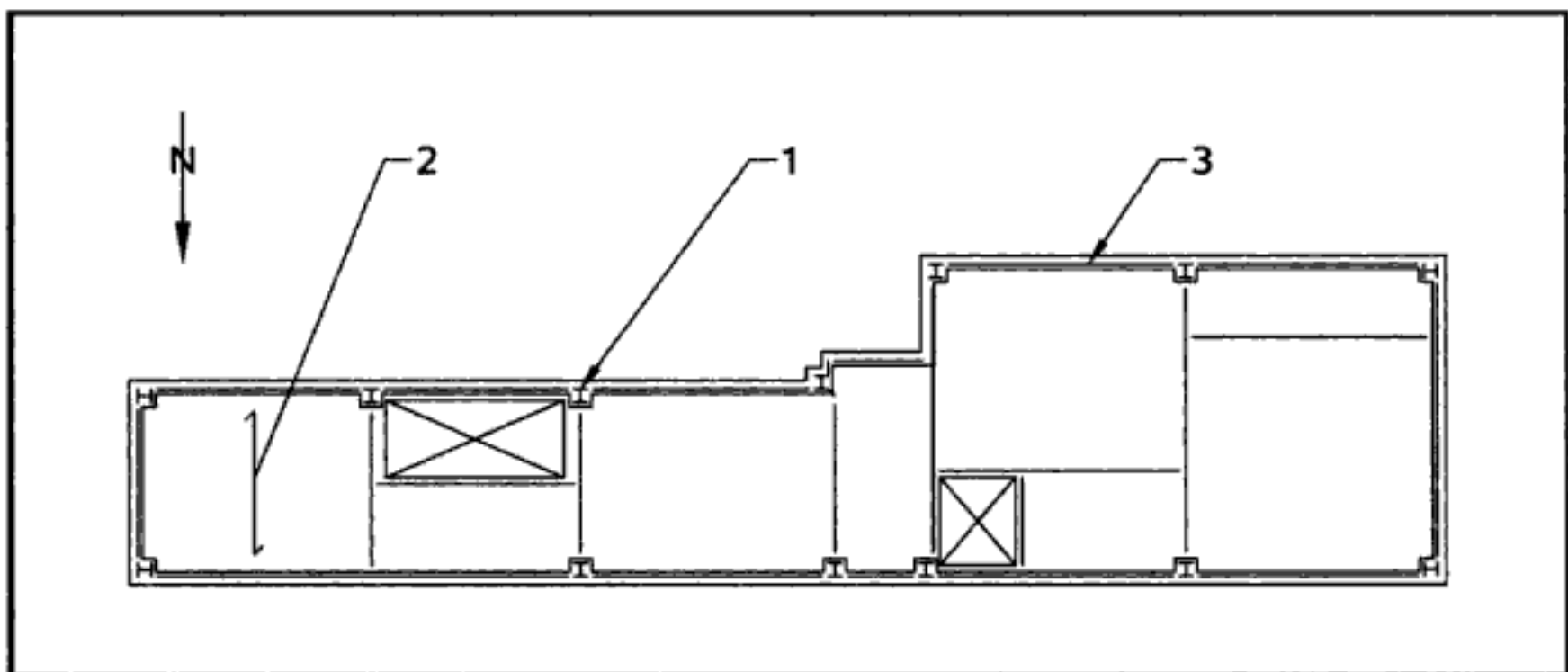


Figure 2. Typical floor framing plan, 953 Fifth Avenue. 1 is a spandrel column in a masonry pier, 2 is the typical floor slab, and 3 is a typical spandrel beam embedded in the wall.

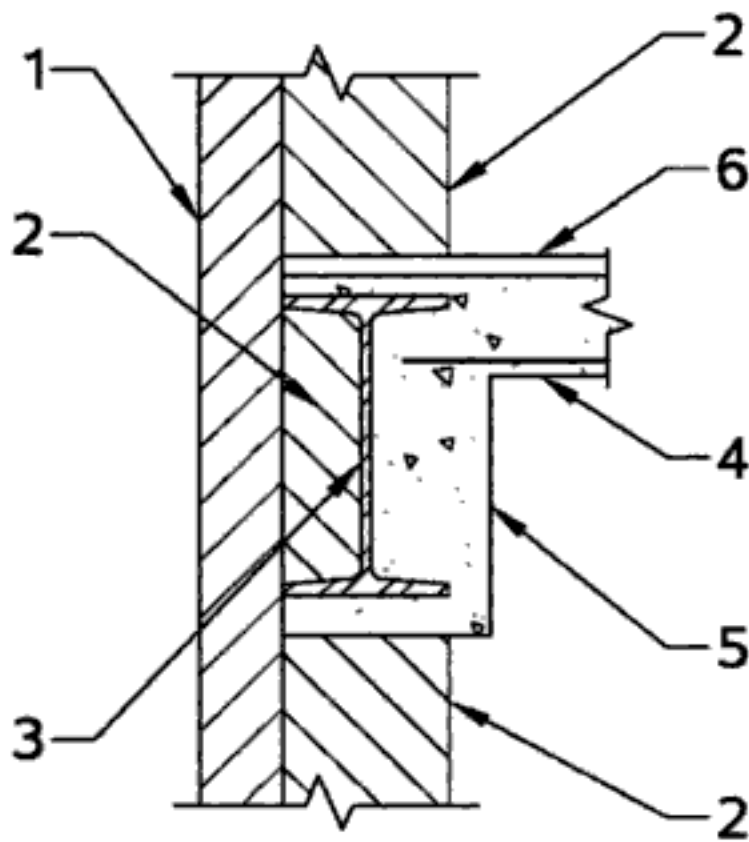


Figure 3. Typical spandrel section, 953 Fifth Avenue. 1 is the veneer masonry, 2 is back-up masonry, 3 is the spandrel beam, 4 is the floor slab, 5 is the concrete beam encasement and fire proofing, and 6 is cement floor topping.

short plan direction because it is sheltered on both the north and south sides by buildings of similar height and age, but it was, of course, designed as free-standing.

953 Fifth has always been a high-end apartment house. There is little difference in structure between luxury and ordinary buildings; the use of limestone veneer on the west (street) facade being the only noticeable departure from ordinary materials.

There is a light court at the south-east corner that is roughly half the east-west length of the building and one-third its north-south width. The basic frame consists of seven single-bay, knee-braced frames spanning north-south, connected to create three multiple-bay moment frames running east-west.

Two conditions were analyzed: the north facade, which is a wide and windowless lot-line wall, and the west facade, which is a narrow and slender windowed wall. Both walls are 300 mm of solid masonry, with all-brick construction on the north and limestone veneer over brick back-up on the west. The column centerlines are 356 mm back from the wall faces, with the spandrel beam locations varying to provide 100 mm of cover between the flange tips and the wall faces (Fig. 3). Commercial finite-element software (*Dr. Frame* version 2.0) was used to analyze the bare steel frame and the frame with masonry shear walls, and classical analysis was used for the walls as vertically-cantilevered beams.

3.3 Summary of analysis

Table 1 lists the movements associated with various forms of motion in the building. All loads are the maximum design loads (full dead and live load on

Table 1. Calculated movements under load.

Cause	Location	Structure	Movement (mm)
Sideway	North wall	Frame	5.6
Sideway	North wall	Frame & masonry	0.05
Sideway	North wall	Masonry	0.5
Thermal	North wall	Masonry	4.8*
Thermal	North wall	Masonry	7.4**
Compression	North wall	Column (live + dead)	15.8
Compression	North wall	Column (dead load)	11.4
Compression	North wall	Masonry (self-weight)	3.8
Compression	North wall	Masonry (live + dead)	9.7
Compression	North wall	Masonry (dead)	6.6
Sideway	West wall	Frame	15.7
Sideway	West wall	Frame & masonry	6.1
Sideway	West wall	Masonry	36.8
Sideway	West wall	Masonry (reduced wind)	6.1
Thermal	West wall	Masonry	1.3*

* Horizontal movement.

** Vertical movement.

interior floors, full wind load on exposed wall area, full thermal variation) unless otherwise noted. The details of each condition are described in the following text.

Several patterns are apparent in the calculated movements and described in detail below. First, load sharing between the frame and walls will occur under initial dead load and under some wind loads. Second, the slenderness of a given facade is a determining factor in load sharing from differential stiffness. Third, significant qualitative differences in results exist depending on whether full code loads are used or reduced loads that reflect more ordinary circumstances.

4 EFFECTS OF TEMPERATURE CHANGE

New York has large temperature swings every year, with winter average lows of -3°C to -1°C and a record low of -26°C and summer average highs of 27°C to 29°C and a record high of 41°C . The standard temperatures for HVAC design are -11°C for winter and 32°C for summer. Because of direct thermal gain from sunshine on masonry, it is common for masonry temperatures during summer days to exceed 38°C , therefore a maximum temperature swing of 32°C was used for examination of facade thermal effects. The masonry wall is assumed to have been built at the mean

temperature of 11°C, creating equally large thermal stresses at the minimum and maximum outside temperatures; for the sake of simplicity, the effects will be discussed for expansion only although equal effects exist for contraction.

The masonry of the facade is directly exposed to both the overall ambient temperature changes and (depending on orientation) direct heat gain from the sun. Buildings of this type have no dedicated insulation, but rather rely on the insulating properties of the masonry and the interior plaster. Since the columns are encased in masonry piers of equal exterior and interior thickness and the spandrel beams are encased on the exterior with masonry and on the interior with concrete fire-protection, the steel temperature is likely to be roughly half-way between that of the interior and exterior air. This tends to reduce the effects of extreme temperatures but this ameliorative effect is not considered here.

A wall plane exposed to a large temperature change will undergo both vertical and horizontal movement. The effect of vertical thermal expansion is limited by the geometry of the connection between wall and frame: since most of the wall is back-up masonry that is vertically bounded by spandrel beams, and the veneer is regularly tied to the wall by header bricks, any vertical expansion of the wall will be resisted by the spandrel beams and the forces transmitted to the columns. Vertical motion is ultimately not damaging because, pushing upwards from the foundation, it can simply lift the unrestrained upper portions of the facade and adjacent steel upwards. At worst, this creates differential movement between spandrel and interior columns, but this is resisted by the ductile-metal frame.

Horizontal thermal expansion is potentially more serious, because it is not resisted by gravity but it is restrained by structure. Unlike the foundations, which cannot be moved downward by thermal pressure, or the roof, which can be moved upwards relatively freely, the columns and walls that restrain horizontal movement have limited capacities for this undesigned load. There are various mechanisms that in theory restrain the horizontal thermal expansion: (1) shear at the intersecting wall at each plan corner, (2) friction between the wall and the floor structure along the wall length, and (3) resistance provided by the wall columns in bending from load transmitted through the fire-proofing piers. The second and third mechanisms depend on the geometry of construction, since the force transfer from masonry to steel can only take place where the materials are in direct contact. The practice of building the spandrel beams and columns into the wall provides such contact.

Resistance by the columns in bending cannot take place since the distributed load that is created along the columns (up to 200 kN/m) creates moments far larger

than the original wind-load design. The presence of intermediate masonry piers at each intermediate column is of no additional help, since those piers cannot resist the lateral load by themselves but will simply transfer it to the same columns. Resistance to the load through friction with the floor structure is resistance through horizontal shear in the walls; analysis of the long north wall shows a required friction/shear stress of 130 kPa on each of the two 200 mm by 30,500 mm contact surfaces per floor, which is realistic under the conditions described. However, on the short west wall, the required friction is 510 kPa, which is greater than the allowable shear strength for most clay masonry, and implies a large compressive force (which may not be present) in order to develop the friction.

Failure of all of the resistance mechanisms results in outward movement of the ends of a wall, cracking the corner masonry on the intersecting walls in line with the inside face of the wall in question. At an ordinary exterior corner, both walls are moving from roughly the same temperature change, and cracks develop on both faces.

5 EFFECTS OF DIFFERENTIAL STIFFNESS

Differences in stiffness between adjacent building elements is one of the most potentially damaging effects that can be found. Modern construction contains numerous provisions for movement to prevent accidental load transfer to relatively stiff elements, including slip joints in curtain-wall mullions, expansion joints in masonry curtain walls, and movement joints in interior partitions. Buildings of the studied type contain continuous masonry curtain walls in direct contact with the structural frames and interior terra-cotta- or gypsum-block partitions solidly built between floor slabs. The relative fragility of the partitions makes them less likely to carry structural load, so the focus here is on the exterior walls.

Similar to thermal effects, the effects of differential stiffness can be examined for vertical and horizontal movement. As thermal effects are limited to the wall plane because the amount of change in wall thickness from temperature variation is negligible, stiffness effects are effectively confined to the wall plane by the magnitude of the element stiffnesses. Masonry walls, subjected to out-of-plane forces are far more flexible than the structural frame to which they are attached and therefore act, properly, as non-structural elements. Walls subjected to in-plane loading have stiffnesses of the same order of magnitude as the frames – often greater than the frames – and therefore have a tendency to carry load. The simplest example is vertical movement under floor loading. As shown in Table 1, the shortening of the frame columns under dead load is greater than the shortening that the adjacent masonry

walls would undergo if they were carrying the load. This means that the load will be distributed between the wall and the frame in proportion to their vertical stiffness until and unless the wall suffers enough damage to release its load. A 300 mm wall would not be designed as the structural support for a 14-story building because the compressive stresses are too high; assuming that the curtain wall was built before all the dead load is in place implies that as the pressure within the wall increased, slip between wall and frame or local crushing of masonry relieved some of the load back to the frame. As live loads increased during and after construction, a similar effect would occur.

The more interesting effect of differential stiffness occurs with sideways from lateral load. The steel frame is strong enough to carry the loads, but is significantly more flexible than the combined frame-and-wall. Wind pressure can move a windward wall (bending in its weak direction) and the frame behind more than it moves the parallel walls. The long north wall is far stiffer by itself than the frame, while the short and fenestrated west wall is more flexible than the bare frame. The walls can only serve to fully stiffen the frames as long as they remain uncracked; each crack reduces the continuity of the walls and therefore their stiffness. This ad hoc composite structure has rarely been discussed. Stockbridge, in his paper on the Woolworth Building, lists a number of mechanisms but looks at all of them in terms of vertical compression within the wall (Stockbridge, 1981). He does not separately discuss the flexure and shear caused within the masonry by sideways.

Unlike thermal changes, wind loads are highly dependent on conditions immediate adjacent to the building in question. Tall neighbors can block winds, as is true for the north-south wind at 953 Fifth Avenue, and a grid layout such as exists in midtown and upper Manhattan and in the downtown area of Chicago prevents full wind load from being applied to buildings near or below the median height by preventing most winds perpendicular to facades. Exceptional conditions may allow for full wind load: the west face of 953 Fifth faces the 800-meter-wide open space of Central Park. The likelihood of sideways as the dominant mechanism for cracking can be judged by comparing cracking patterns to directions of possible wind loading.

As Table 1 shows, the absolute difference between frame and wall flexibility is greater for the slender west facade than the stocky north facade. More importantly, the maximum bending stress in the north wall is 97 kPa, acceptable for most masonry, while it is 455 kPa in the west wall under reduced load and 2760 kPa under full code load. In other words, while the masonry contributes greatly to the stiffness of both stocky and slender walls, it is not strong enough to carry the loads its stiffness attracts in the



Figure 4. Multiple-wing layout at Four Park Avenue.

slender walls. This difference applies in most buildings of this type since, in the era before air-conditioning and fluorescent lights, buildings with large overall plan dimensions had light courts that create multiple slender wings (Fig. 4).

6 EFFECTS OF RUST-JACKING

Unlike intermittent wind pressures and thermal expansion, pressures caused by rusting steel are continuous and (until repairs are made) ever-worsening. The pressure increases from zero as rust builds up behind the masonry, forcing it outward. The volume of rust compared to base metal varies with, for example, Gibbs providing values of seven to twelve times the original volume (Gibbs, 2000). These large values represent free expansion. When masonry is solidly built against a rusting piece of steel, the volume increase is restrained by the strength of the masonry. In technical terms, rust-jacking is the deflection of that masonry under load until failure (typically through cracking) and the forced movement of the masonry after failure, including bulging, spalling, and collapse.

In buildings of this type, the structural steel was protected with red-lead paint and, by virtue of being embedded within a masonry wall, has never been subjected to mechanical abrasion, impact, or exposure to attack by any non-water-soluble chemical agents. Experience has shown that the combination of paint and masonry skin performs well in flat and ordinary sections of wall. Where a greater than normal source of water entry into the masonry exists, such as parapets and the top surfaces of applied ornament including cornices and water-tables, damage is likely

to occur. Rust-jacking, in other words, is the structural equivalent of an opportunistic infection. While the masonry and paint that provide weathering protection to spandrel beams and columns fail over time, the most serious rusting occurs in those areas where the masonry fails first, from poor detailing that aids water entry, improper construction, or most often, cracks from thermal and lateral movements. This secondary effect is the most serious form of damage in high-rise buildings since it is the only one that is progressive and reduces structural capacity: if rusting of structural steel were not a concern, it might be possible to accept many of the cracks formed by movement as “naturally-occurring” expansion joints that posed no real danger to either people or property.

Because the effects of rust-jacking are non-linear – the restraint provided by masonry drops from full to zero after cracking – and are highly sensitive to voids in the column fire-proofing piers and in the veneer outboard of the spandrel beams, it is not possible to analyze this effect directly.

7 COMMON REPAIR TECHNIQUES

Since the passage of Local Law 10 in 1980, the New York City Department of Buildings has required inspection of all building facades higher than six stories every five years (Local Law 10, 1980). Conditions identified as dangerous must be repaired shortly after the inspection report is filed (Prior to the 1998 revision of the law, a category of “precautionary conditions” existed between “safe” and “dangerous;” conditions so noted had to be repaired before the next inspection.). A large industry has developed among architects, engineers, riggers, and masons in performing repairs. Given the physical similarity of buildings in the type under consideration, similar weathering exposure, a general lack of maintenance beyond ordinary joint pointing, and the small community of professionals and contractors involved in “Local Law 10 repairs,” standard methods of addressing problems developed quickly in the 1980s.

The most common repair performed is rebuilding masonry at external corners. Cracks on both wall faces are common, highly visible, and suggest a section of loose masonry. In the majority of buildings that have brick or terra-cotta veneer, the corner masonry units are typically removed, the steel painted, waterproofed, and repaired as required, and a new masonry corner constructed. Similar repairs are made at horizontal strips over spandrel beams where the beams have rusted (Figs 5, 6). Expansion joints may be created in conjunction with masonry replacement or by themselves. The removal of corner masonry provides an opportunity to create expansion joints at both faces of the corner with minimal effort and the removal of



Figure 5. Old beam and corner column masonry repairs at the rear façade 50 West 34th Street.



Figure 6. Corner column masonry removed and column cleaned and painted at Four Park Avenue.

masonry outboard of a spandrel beam provides a similar opportunity to create horizontal expansion joints below the level of wall support.

It may seem obvious to state that any steel exposed by the removal of masonry should be painted and waterproofed to prevent future deterioration, but this work is not always performed. It is not uncommon for workers to open up a ten-year-old repair to masonry and find unpainted, rusting steel. The use of self-adhering rubberized-asphalt sheet waterproofing has

made protecting complex steel shapes from water relatively simple as long as there is enough of a void between the steel and masonry at complex corners (such as the intersection of spandrel beams and corner columns) to allow for some movement of the sheets.

Steel repairs may be performed with masonry repairs, ranging from reinforcing plates welded to flanges and webs that have lost material to rust up to complete replacement of columns and beams. Repair is favored over replacement as it is far less disruptive to the occupied interiors and more safely performed from scaffolding over occupied sidewalks.

8 CONCLUSIONS

Regardless of the causes, damage to masonry curtain walls on high-rise buildings must be repaired to maintain public safety. However, different causes of damage may require different repair details. At this time, despite the large and growing body of experience in New York among designers and contractors with repairs, analysis is rarely performed to discover the causes of observed damage. The mechanism of rust-jacking is well understood, and the initial cracks are typically described as "thermal movement." Two aspects of thermal expansion are not obvious: first, that the force developed in restrained thermal expansion is independent of the length of the element; and second, that simple friction with the floor structure is, for long walls, more of a restraint on thermal expansion than that provided by intersecting walls and columns. The result for this type of construction, counter-intuitive for non-engineers, is that the longer a wall is, the less force it exerts from thermal change at corner intersections with other walls.

Lateral load is rarely considered in damage surveys of these buildings, since the steel frames are typically adequate for all lateral loads and current design practice does not typically treat steel and masonry as a composite structure. Analyzing this effect can give an upper bound on stresses in the masonry and, more importantly, can provide insight into patterns of facade damage, and therefore into repairs required. For example, if thermal expansion is believed to be an important

factor, vertical expansion joints may be cut into large flat wall planes as well as at corners, while if sideways is actually the dominant factor, the corner joints are all that is required.

The analysis and repairs techniques that have been developed in New York (and similar techniques in Chicago, since the 1996 enactment of a facade investigation law) are mostly empirical. The advantage to this approach is that only those techniques that produce acceptable results become commonly used. The disadvantage is that a lack of explicit understanding of a given problem leads to an iterative repair approach, which is wasteful of time and money. Analysis of facades as composite steel-and-masonry structures, as suggested here, is one method towards better focused repairs.

REFERENCES

- Condit, C. & Landau, S.B. 1996. *Rise of the New York Skyscraper, 1865-1913*. New Haven: Yale University Press.
- Cross, H. 1930. Analysis of rigid frames by the distribution of fixed end moments. *Proceedings of the American Society of Civil Engineers* 56: 919-928.
- Elliott, C. 1992. *Technics and Architecture*. Cambridge, Massachusetts: The M.I.T. Press.
- Gibbs, P. 2000. *Technical Advice Note 20: Corrosion in Masonry Clad Early 20th Century Steel Framed Buildings*. Edinburgh: Historic Scotland.
- 1980 Local law 10/80 in *The City Record* 108(32169).
- Meadows, R. et al. 1986. *Historic Building Facades: A Manual for Inspection and Rehabilitation*. New York: New York Landmarks Conservancy.
- 1931 Regional Survey of New York, vol. VI: *Buildings: Their Uses and the Spaces About Them*. reprinted 1974, New York: Arno Press.
- Stockbridge, J.G. 1981. The interaction between exterior walls and building frames in historic tall buildings. In Lynn Beedle (ed.), *Developments in Tall Buildings, 1983*. Stroudsburg, Pennsylvania: Hutchinson Ross Publishing Company.
- White, N. & Willensky, E. 2000. *AIA Guide to New York*, 4th edition. New York: Three Rivers Press.
- Willis, C. 1995. *Form Follows Finance*. New York: Princeton Architectural Press.

Some considerations on the shape of the caps of vaults

D. Wendland

Institute of History of Architecture, University of Stuttgart, Stuttgart, Germany

ABSTRACT: The ribs or groins of vaults are usually carefully designed in their geometry, and their geometrical layout is normally well analyzed. Less attention is usually given to the shape of the caps in between, as its understanding is not crucial for the interpretation of the architecture. The information available about the shape of the caps, either from historical building manuals as from secondary literature, in many cases appears not to be corresponding to the reality as it can be observed in historical vaults, or not describing it sufficiently.

This study is an attempt to describe their shape in regard to their construction process. A better understanding of the shape of these caps can be useful for their numerical modelling, as its shape has influence on the structural behaviour of a vault. Beyond that, such knowledge may be applied in the restoration, repairing or rebuilding of traditional or historical vaults.

1 INTRODUCTION

The basic elementary description of a cross vault is that of two intersecting cylinders. In such a first approach, the surfaces of its portions would be considered cylinders whose axes run parallel to the spring line of the vault. This idea can be also found extended to cross vaults with a pointed profile, conceiving the vault as composed of eight cylindrical portions (Fig. 1).

A comparison with the design procedures proposed in the historical technical literature and with the built

reality, however, reveals that this approach, if not in every case totally wrong, at least is far from being precise. Since scholars like Porter (1911) and Rave (1955) drew their attention on the shape of the caps of vaults, it is known that the problem is less trivial that it may seem at first glance, especially regarding those vaults that present a pronounced double curvature in their caps, so common in gothic architecture. Barthel (1991) elaborates a typological order and a systematic approach to the description of vault geometry which enables to model continuous surfaces on their webbing that correspond well to the reality as it can be observed in historical constructions.

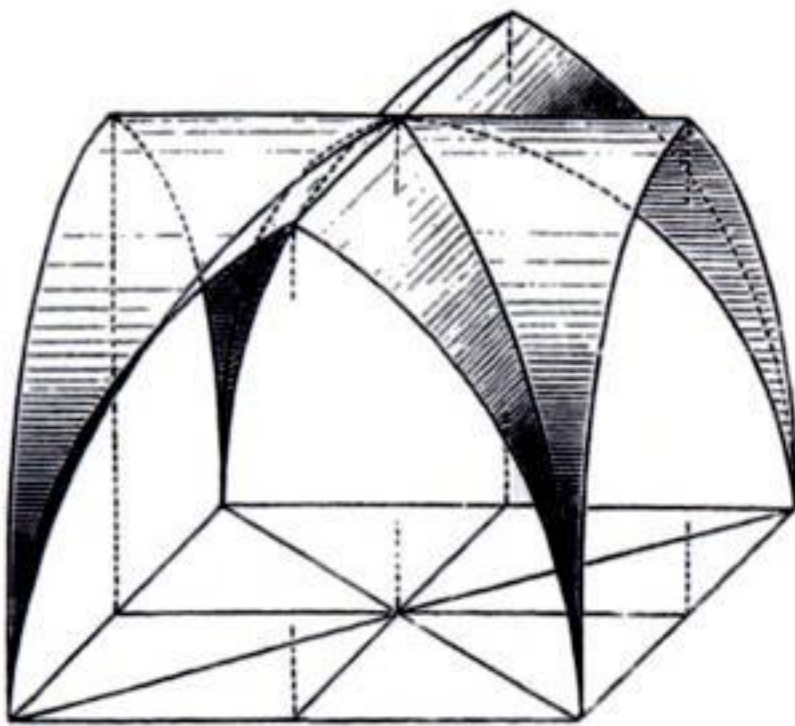


Figure 1. Elementary composition scheme of a pointed cross vault, conceived as being composed of cylindrical portions, after Breymann/Warth.



Figure 2. The extrados of a vault constructed without formwork. Note the difference of the shape respect to Fig. 1.

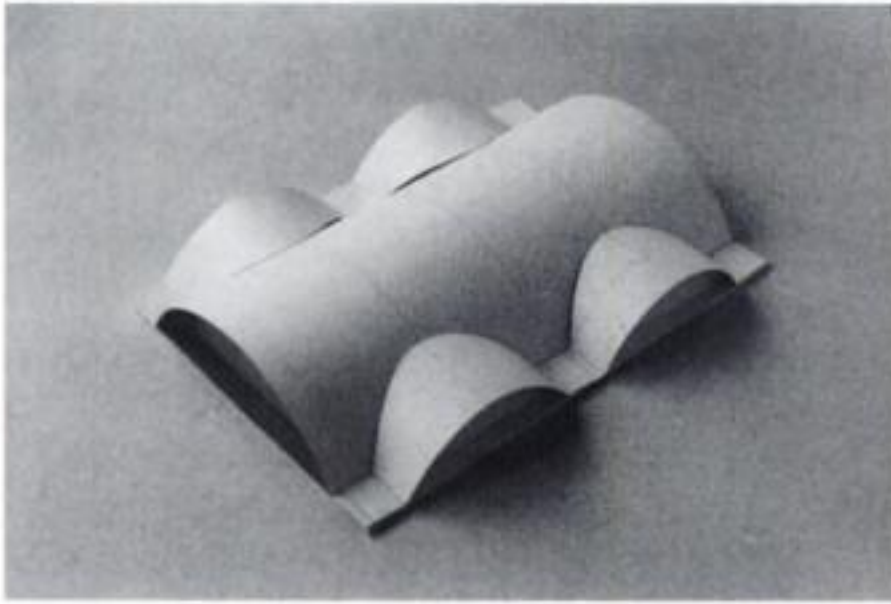


Figure 3. Model of intersecting cylinders, showing the spatial intersection curve.

2 THE CONSEQUENCES OF THE GEOMETRIC DESIGN OF THE RIBS AND GROINS FOR THE CAP GEOMETRY

The first reason for the geometrical complexity of the vaults' surfaces is the common practise to design preliminarily the "lines of discontinuity" of the vault, i.e. its formeret and transversal arches (those arches that confine the bay) and the groins, as these during construction are supported by centering frames which have to be drawn and pre-manufactured, and as these have the strongest impact in the visual appearance of the vaulted ceiling. These centering frames are usually designed according to elementary geometric patterns, sometimes as arches with more than one center but in most cases simply as circle segments; in every case with two-dimensional curvature and always arranged in vertical planes (leaving apart the groins of barrel vaults with lunettes built on a formwork, or the particular architectural features of the Guarinian tradition).

From this fact arises the difficulty to describe the vaults' surfaces as cylinders. This can be shown in vaults with elementary design. If, for instance, a barrel vault with large lunettes is conceived as consisting of intersecting cylinders with different radii, their curve of intersection must present a double curvature (Fig. 3). If, in the contrary, as usually practised, the groin is built with a single curvature (as circle segment or arch with more than one center) in a vertical plane, the surfaces of the vault in consequence cannot be cylinders (Figs 4, 5). The same is the case in cross vaults with semicircular profile but on rectangular plan where the groins would result double-curved, or even in "regular" cross-vaults on square plan, where usually the groin curves are circle segments.

In some cases the caps can be described by ruled surfaces between the arches which are generated with straight lines. This is the case where vaults have been built on a wooden formwork. An example can be found

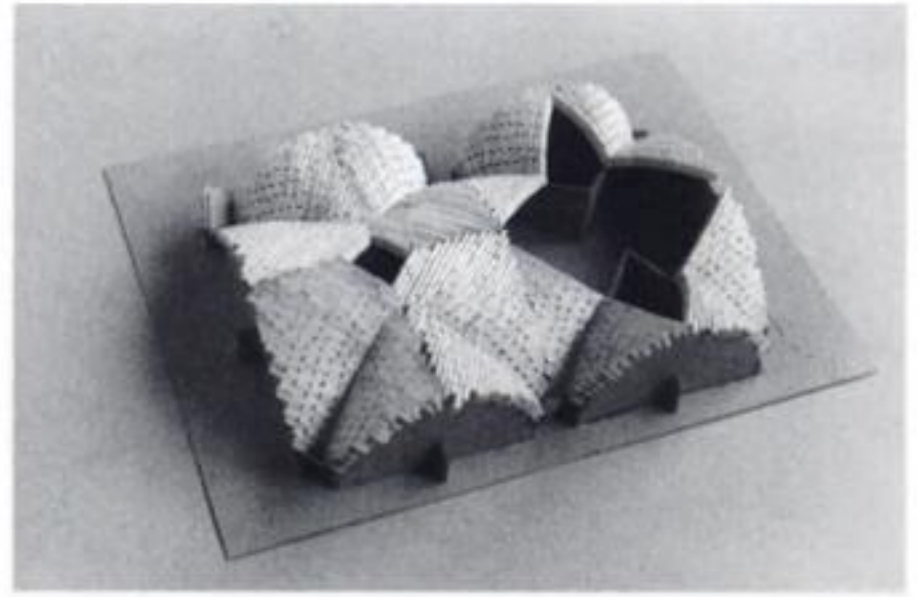


Figure 4. Model of a vault built on the same plan as the preceding one; as usual, the groins are not resulting from the intersection of cylinders, but describe curves on vertical planes.



Figure 5. Vault constructed with similar boundary conditions as Figure 4; the arches and groins are circular in vertical planes, the vault surface presents a slight double curvature.

in the Münster at Freiburg (Barthel 1991: 28). In some cases, traces of the wooden planks or laths of such formworks arranged on the stone ribs could be found in medieval buildings (Nussbaum & Lepsky 1999: 65).

3 THE SHAPE OF DOMED CAPS BUILT WITHOUT FORMWORK

In many cases cross vaults have been constructed without formwork. Where this is the case, no guidance is

available for the shape of the caps. Moreover, these vaults usually present a pronounced double curvature, as the shape was not restricted by the constraints of a wooden auxiliary structure, and as such a double curvature is extremely helpful during the construction process.

Some building manuals (e.g. Körner 1901) suggest that the shape of these domed caps could be spherical, thus describing them as spheres truncated by the circular groins and arches that confine the cap. In this case, the surface of the cap would have to be clearly discontinuous at its ridge, presenting a re-entrant groin along the ridge line. The profile of this ridge line, produced by the intersection of two similar spherical segments, would necessarily be circular.

Existing vaults with pronounced re-entrant groins in the ridge line, however, in contrast to statements that can be found in the historical technical literature since Ungewitter (1859), present in a vast number of cases a profile which is not a circle segment: in fact, the characteristic curve of such a ridge line usually has a curvature which is smooth but variable (see below, section 3.4). The surfaces of the caps that intersect in the ridge line therefore cannot be spherical. Moreover, besides those vaults that present such a re-entrant groin at the ridge, many cases can be observed where the ridge is smoothly curved, or where part of the ridge is smooth and part is a discontinuity of the caps' surface. Therefore we must consider the possibility of a variable curvature in the vaults' surface, and also different radii of curvature corresponding to the different directions at any given point of the surface. In reality, such a situation is far more frequent than a constant uniform double curvature as it would be the case in a spherical portion of a vault's surface.

Rave (1955), who systematically analyzed different vault typologies observing their level curves (looking at the intersection profiles of the vaults' surfaces with 5 horizontal planes – Fig. 6), compares the highest level curve of such “domed” caps with the shape of an almond or egg. The formula for a “simple idealization” introduced by Barthel (1991: 29–33) is that of a bundle of 2nd order parabolas which have their apex in the highest point of the cap (Fig. 7). This formula has the benefit of being simple while avoiding the constraints of Euclidean primitives; it is easy to adapt to a given geometry of groins and arches, defines a continuous surface and is still a good approximation to the reality of domed cross vaults.

3.1 The procedure of free-handed vault construction

Free-handed construction of vaults, as regards the current typology of half-stone vaults (i.e. those vaults where the units are placed in a running bond normal to the vault's surface, the resulting thickness of the shell

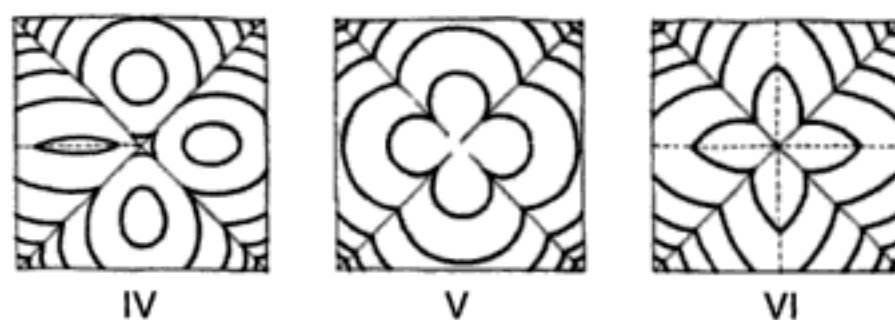


Figure 6. Level curves on double curved caps (Rave 1955).

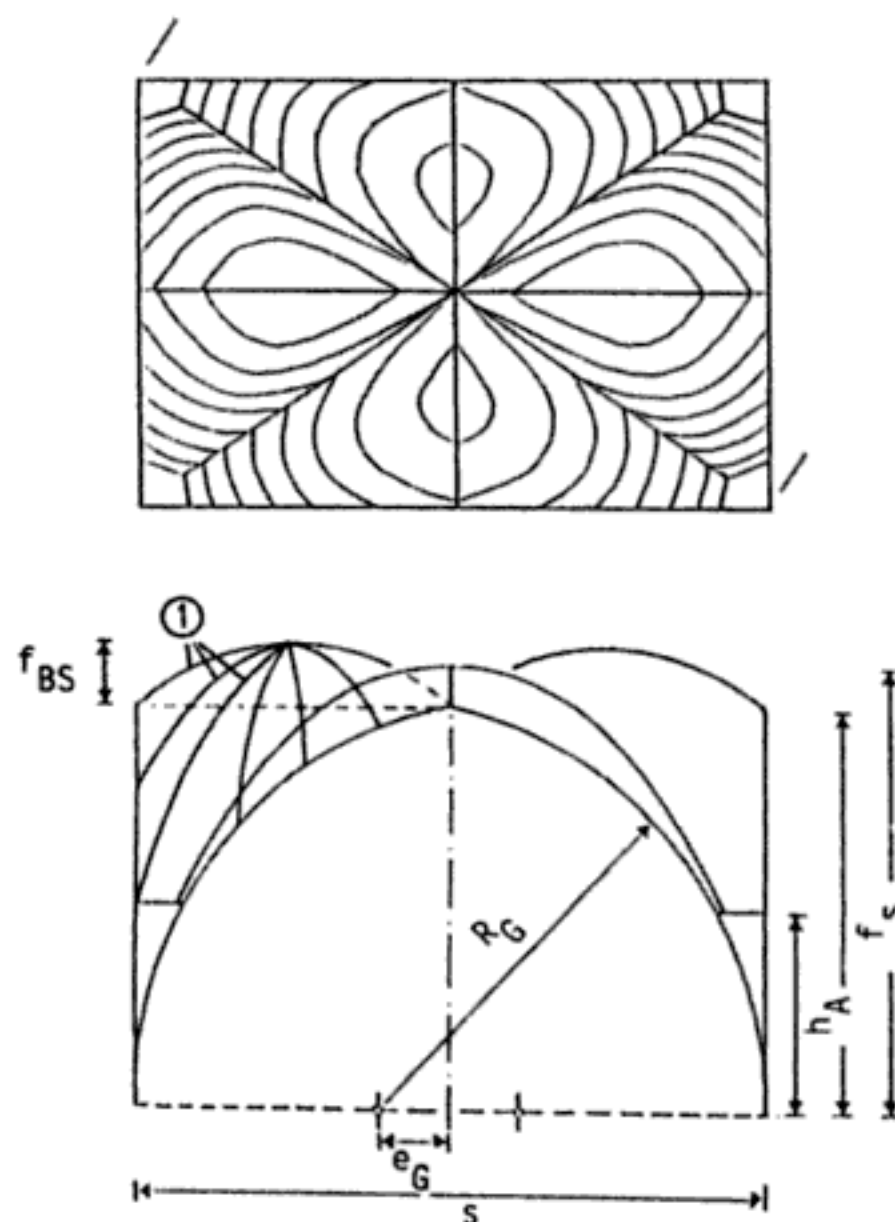


Figure 7. The surface of the caps as composed by a bundle of 2nd order parabolas according to Barthel (1991: 30).

equalling the width of the masonry unit), is mentioned in the technical literature since the end of the 18th century (e.g. Gilly 1805, first edition in 1795) – but it has certainly been practised since long before. Today it is still practised by few specialists. The basic principle has been formulated for the first time by the German architect J. C. von Lassaulx, whose essay (1829) had a considerable influence to the development of the topic in the technical literature (Wendland 2003). It consists in building the vault with self-supporting courses that are stable through their shape by forming arches. Every new course of the vault's masonry must be held in place by the adhesion of the mortar only until it is closed; once the course is complete, it is stable by having the form of an arch and it offers reliable stability for the units of the next course to be laid on top of it.



Figure 8. Domed caps of the vaults of St. Jan cathedral at s'Hertogenbosch. Note the double curvature.

In cross vaults, these arch-wise curved courses can be spanned conveniently between the centering frames of the arches and groins (or their respective ribs), which will offer sufficient abutment. The curvature of the courses necessary for their stability can be obtained by providing a double curvature to the caps ("domed" caps), by tilting the planes of the bed joints, or both in combination.

The caps can be built up independently without any continuity of the masonry fabric between them, connecting the single caps over the diagonal ribs with a mortar joint. In this way, in every single portion the best curvature is obtained by a modest doming and some tilting of the bed joint planes. Their spatial inclination can be corrected if necessary to optimize course curvature. The single caps should be built up more or less at the same time just not to cause asymmetric loads to the centering frames. This is the way Lassaulx, who has been mentioned above, built his neo-medieval vaults (Wendland 2003), and that has been commonly used in such cases where the groins were provided with stone ribs set on the centering before constructing the caps.

The most frequent masonry apparatus in cross vaults, however, is the dovetail pattern (Fig. 9). It consists in arranging the courses on diagonally tilted planes perpendicular to the groins. Hence, the masonry fabric is continuous through the neighbouring caps over the groin, avoiding the joint behind the groin rib. The diagonally tilted courses are seamed in the ridge of every cap. The continuity over the groins is beneficial

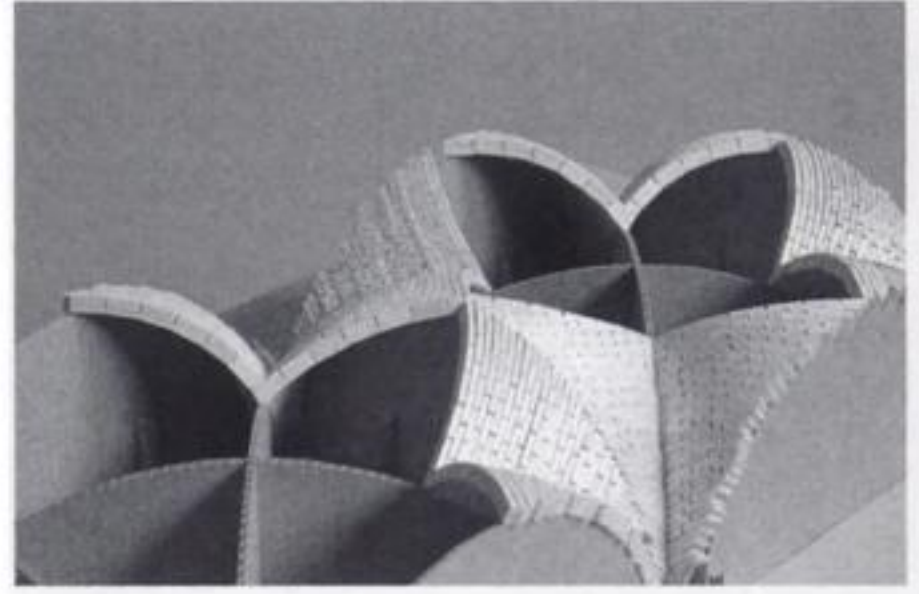


Figure 9. Model of a cross vault built with the dovetail pattern. Note the continuity of the masonry fabric over the groins.



Figure 10. Experimental construction of a cross vault without formwork, using the dovetail pattern. The design reproduces in scale 1:4 a late gothic church vault in northern Germany. Dimensions in plan: 2.50 × 2.30 m. Dresden University of Technology, 2003.

in those vaults which have no ribs or those where the groin ribs consist of small units within the masonry fabric of the caps.

3.2 *The masonry apparatus in the dovetail pattern: inclination of courses, course curvature and corrections*

In order to study the building process and its consequences on the shape in detail, a series of small-scale models simulating different typologies and vaulting patterns (e.g. Fig. 9) and a prototype in scale 1:4 (Fig. 10) were built.

From these trials it became obvious that the layout of a regular masonry apparatus, apart from its formal and structural benefits, is necessary in order to guarantee the stability of every new completed course during construction, and to facilitate an efficient geometric control to achieve a similar shape in all caps of the vault and to make sure that the portions rising from



Figure 11. Plane bed joint in the vault masonry (prototype).

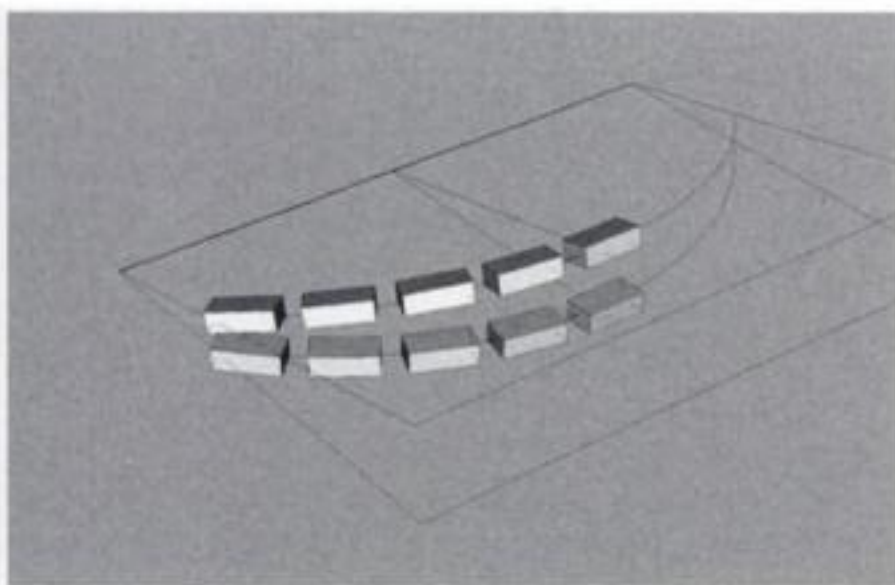


Figure 12. The variation in the thickness of the mortar joint in case of non-parallel bed joint planes.

the different spandrels come to meet correctly in the vertex.

In principle, the bed joint planes are lying normal to the curve of the groin. However, to follow strictly this rule would lead to a radial inclination of the bed joints and consequently to an angle of every bed joint plane respect to the preceding one. Such an arrangement is usually described in the building manuals since Ungewitter (1859: 104–114) (Fig. 13), although this author already admits that it could be debatable. Actually, in practise it is problematic to set the bed joint planes in an angle to each other, as this would lead to a variation in the thickness of the bed joints because the distance between the successive bed joint planes varies according to the local distance of the course to the turning axis of the planes (Fig. 12).

According to the observations on existing vaults and the trials on the prototype, such a turning of the bed joint planes is feasible only in those portions of the cap where the courses are very short and a manifest angular divergence can therefore be produced within the normal thickness of the mortar joint. This is the

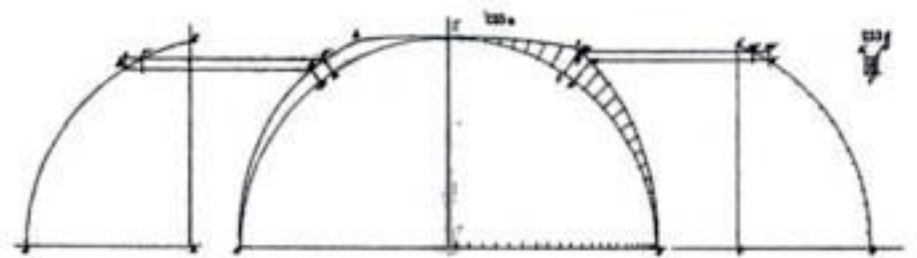


Figure 13. Radial inclination of the bed joint planes according to Ungewitter (1895), repeated in many other manuals.

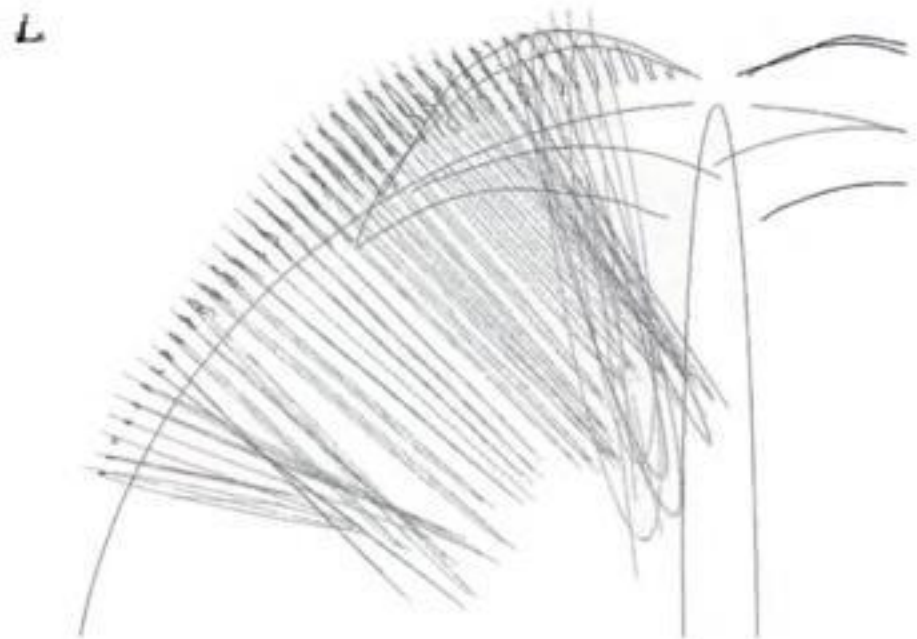


Figure 14. The bed joint planes as they appear from the measurement of the prototype at the TU Dresden: throughout the main part of the cap, the bed joint planes are parallel. In the drawing, the full circles of the course curvatures are also visualized.



Figure 15. Nearly parallel bed joint planes as measured in the vault built by J.C. von Lassaulx in the church of Treis (Germany), early 19th Century (Wendland 2003).



Figure 16. The shadow reveals the continuity between the course curve and the opposite cap surface (prototype).

case only in the lowest and highest portions of the cap. In the main part of the cap, in contrast to what has been stated before, the bed joints are always parallel, tilted in space with a constant angle.

For the curvature of the single courses, no precise indication can be found in the historical technical literature. Generally, a pronounced curvature serves to stabilize the courses during construction; Hörnig's manual (1836) says that less experienced masons will tend to give more curvature to the courses. Within a course, the curvature can be assumed as being constant, the resulting form of the courses therefore as circle segments. Over the entire cap, the curvatures need not be constant, but may vary from course to course or in different portions of the cap.

The area of the cap which is crucial for the choice of the course curvature is right above the summit of the transversal or formeret arch. Here, the courses have the greatest length and therefore most deserve to be stabilized through their curvature. The limit of possible curvature, i.e. the smallest possible radius, is defined in this area by the tangential continuity of the course with the surface of the opposite half of the cap (arising from the neighbouring groin), which causes a completely smooth vault surface at the ridge (Fig. 16). A greater radius, or minor curvature, in fact, leads to a re-entrant groin in the ridge, which is quite common and formally satisfactory, while a smaller radius, or greater curvature, would lead to an inverse discontinuity of the vault surface in the ridge that would appear as projecting to the inside, which would be a flaw. Hence, the limitations of the curvature are the stability of the longest courses and the disturbing of the surface continuity at the ridge of the cap.

It is rather difficult to carry out corrections in the curvature of the courses while proceeding towards the zone just mentioned. Such corrections are first of all limited by the obvious necessity of laying one course on top of the other. Also, they easily disturb the surface continuity, leading to an outward curvature of the



Figure 17. The cap masonry during construction; the shifting of the courses outwards is visible (prototype).

cap which must be avoided for formal and structural reasons.

Actually in many points of the cap masonry the courses are not exactly superposed upon each other (Fig. 17) – this happens because even if a radial inclination of the bed joint planes is achieved respect to the diagonal groin, these will not intersect the vault surfaces orthogonally in every point. As result, especially in the lower half the courses are shifting outwards in the part which is more distant from the groin. An attempt to exactly superpose them would be a mistake as it would successively reduce the curvature of the courses because the fleche would remain constant while the length is increasing – moreover, the starting point at the formeret or transversal arch itself is progressively shifting outwards. Such shifting of the courses must be restricted to a sufficient superposition of the courses, as basic principle of masonry construction.

3.3 *The continuity of the slope*

The rule for the building of the cap masonry, and therefore for the modelling of the cap's surface, is provided by the necessity of building curved courses on tilted bed joint planes between the diagonal groin and the formeret or transversal arch that confine the cap, i.e. between two continuous curves (usually circle segments), up to the longest course at the summit of the arch.

Above that point, one of the track curves is lacking, and the question is how to continue.

In a first hypothesis, it could be assumed that the surface continues as a translation surface, extending, as track curve, the curve of the formeret or transversal arch either with constant curvature or tangentially. However, such a surface generation is problematic because the length of the generating curves (coherent with the upper courses) continues to increase while rising upwards. If a constant curvature is assumed (Fig. 18), there is a high risk that the distance spanned by the course might exceed the diameter of the

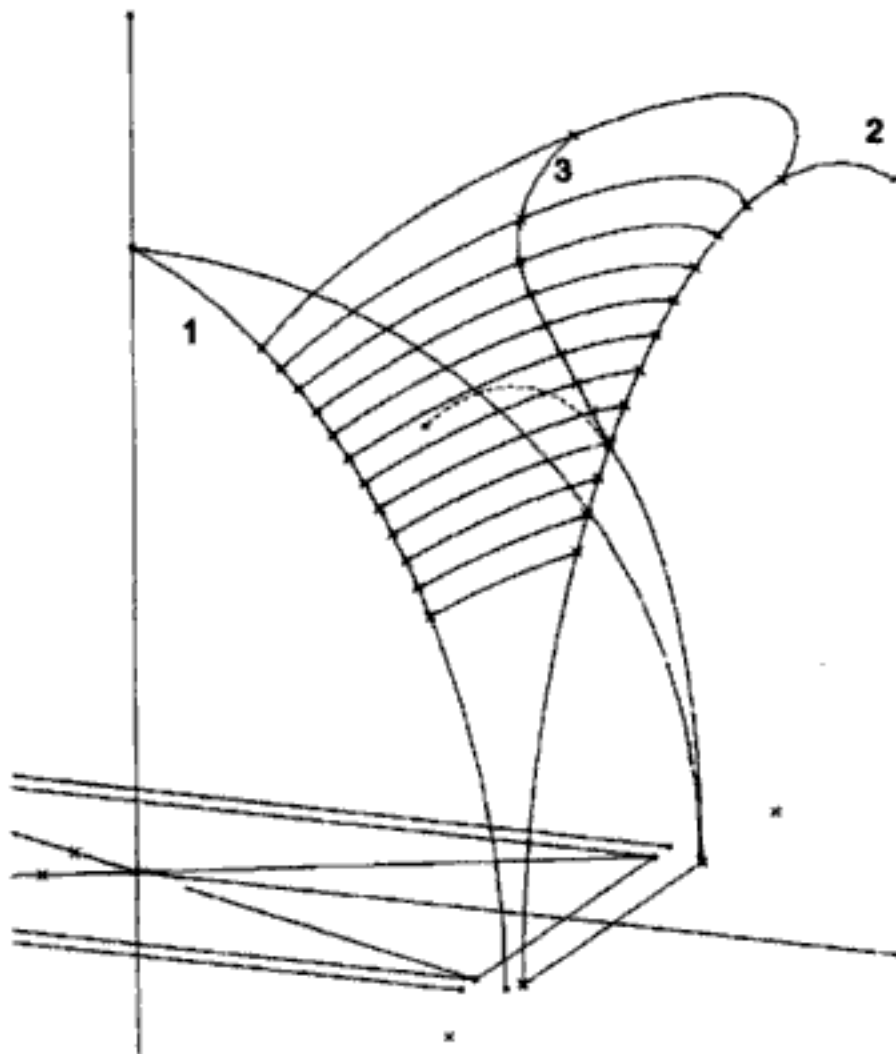


Figure 18. Hypothesis of a surface modelled on the diagonal groin (1) and the extended circular curve of the formeret arch (2) as track curves, and circle segments on parallel tilted planes with constant radius, coherent to the courses. Above a certain length of the generator curves, these are projecting outwards, and the ridge line (3) is bending to the outside. The next course could not be defined as it is lying beyond the track curve (2).

circles which the courses describe, which is impossible, and this modelling procedure therefore inconsistent. But even if the course length remains less than the diameter, the longest courses would project outwards, generating a surface which in normal direction to the courses is bending outwards, which is not acceptable in a masonry vault and not realistic.

In order to make this procedure consistent, a gradual reduction of curvature of the courses could be assumed. However, in reality such reduction does not happen. In the prototype, for instance, the measuring data show that the curvature of the courses within the region in question is nearly constant, with a radius of curvature considerably shorter than the length of the longest courses (Figs. 14, 19).

In the practical realization, building up the cap masonry, the way to continue beyond the summit of the arch is given by the demand of continuity in the slope of the cap. Any bending outwards is prohibitive, but also an abrupt change of the slope towards the inside would be problematic both under structural and formal aspects. Besides that, such a change in the slope would demand a drastic reduction of the course curvature and a strong shifting of the courses reducing their superposition; it would be feasible only by strongly

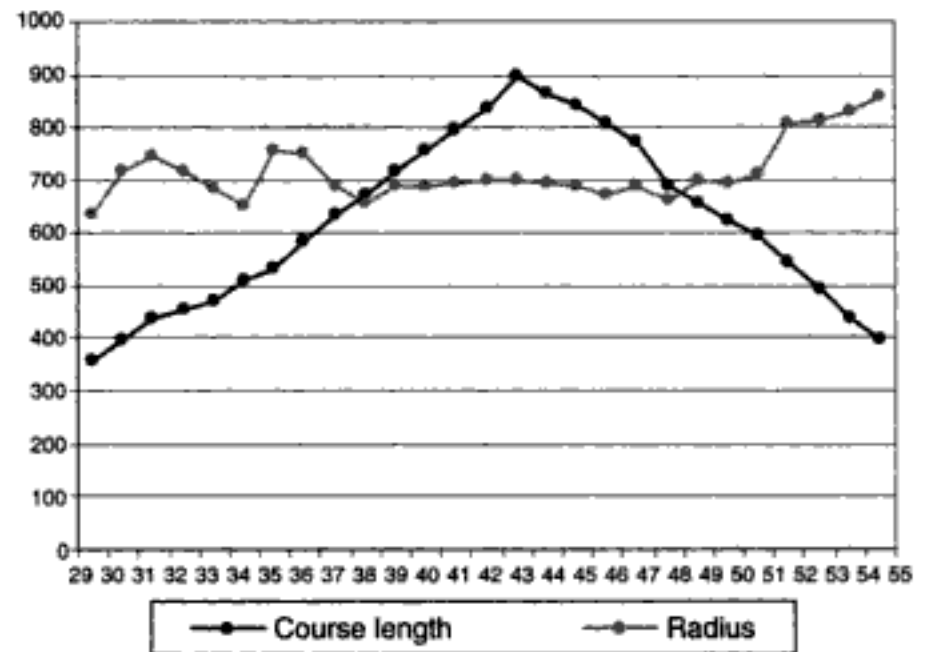


Figure 19. Real length of the courses and radii of curvature throughout one half cap, as measured in the prototype vault. The length of the courses is growing towards the summit of the formeret or transversal arch and then descending again. The radii are nearly constant especially in the area with the longest courses. For the visualization of the circles described by the courses, see Figure 14.

increasing the inclination of the bed joints planes, which due to the length of the courses in this area is impossible but by interrupting the masonry apparatus.

The demand that the longest courses should not project outwards due to their circularity can in some cases even oblige to reduce their curvature (increase the radius) respect to the preceding ones (which is not desirable if we remind the benefit of the curvature especially in the longest courses). In such a case, the slope of the cap would result straight in this portion – i.e. avoiding to curve inwards below the longest courses in order to reduce curvature the less possible, and in continuation aiming to regain the stronger curvature in the following courses. Otherwise, the slope normal to the bed joints will be very gently curved to the inside in the central part of the cap, while its curvature would increase in the lower part and near the keystone of the vault where the bed joint planes are radially turning as permitted by the short length of the courses in these areas.

Building the highest part of the cap is not very difficult, as the courses in this area are rather short. Therefore, the slope of the cap can easily be bent to the inside by shifting the courses, by inclining the bed joint plane and even by allowing some double curvature in the bed joint. Also the curvature of the courses can be easily reduced at one's convenience.

3.4 Surface models for the shape of the cap

The shape of the cap, described in these terms, is directly connected to the basic principles of masonry and their application in the building process of the vault. For the formulation of a geometric description, the profile of the slope, assumed to be straight or

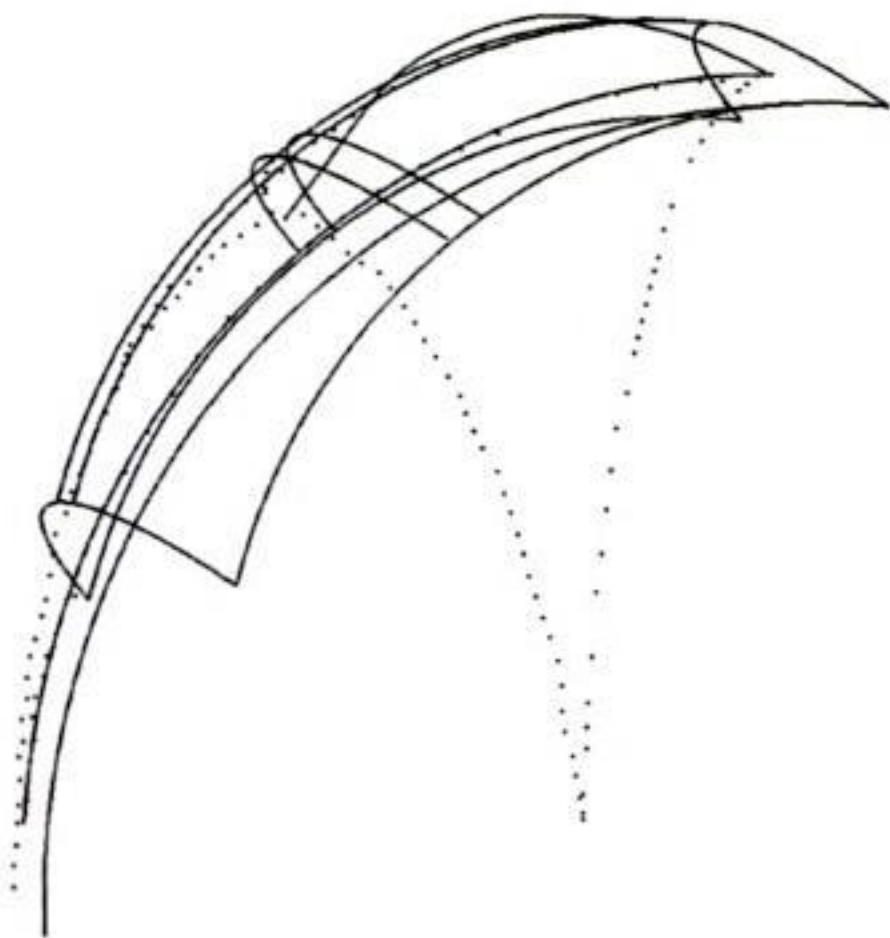


Figure 20. Approximation of the cap surface with a translation surface generated by parallel shifting of a circle segment.

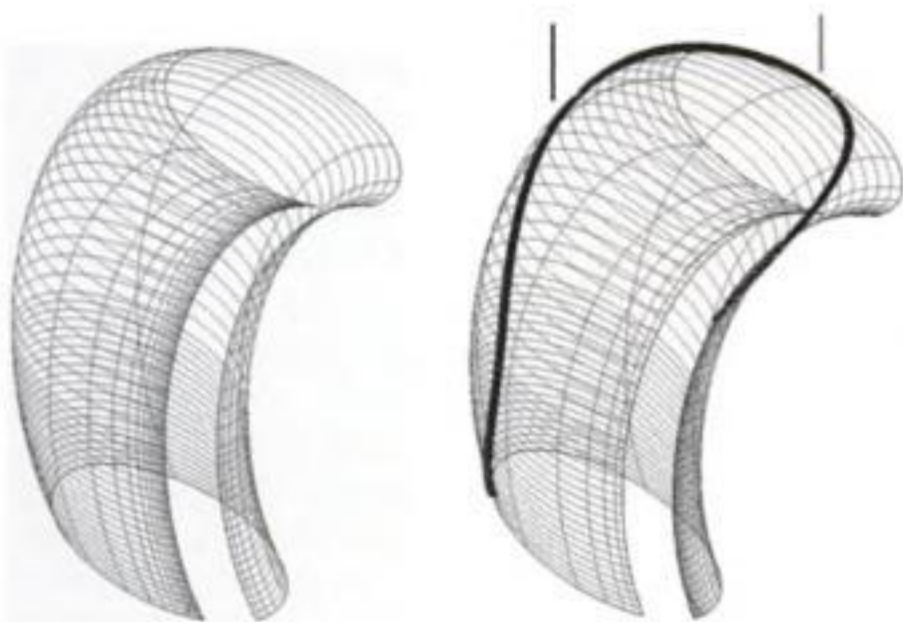


Figure 21. Surface generated by the parallel translation of a plane circular curve on an elliptical track. Right: intersection curve with a vertical plane; the portion that corresponds to the ridge line of a vault is indicated, limited by the position of the formeret (l.) and the center of the vault (r.).

gently curved in the main part of the cap, could be used for the procedure of surface modelling.

In some cases a torus may be considered a fair approximation for every half cap, although this would be accurate only in case that the bed joint planes were radial, which normally is not the case.

In the case of the prototype, a translation surface generated by the curves representing the courses sliding on the curve of the slope normal to the bed joints, proved to be rather accurate in the "critical" part of the cap surface (Fig. 20). In any case, the assumption of a translation surface is rather close to reality as it



Figure 22. Extrados of a vault. The ridge line shows a characteristic profile.



Figure 23. Ridge line profile on the extrados of the prototype.

takes in account both the fact that the bed joint planes are parallel and the fact that over the central part of the cap the radii of the curves described by the courses are more or less constant. Therefore, we may assume that the parallel translation of a constant curve sliding first on the curves of the groin and the formeret or transversal arch and then on a curve that running normal to the bed joints expresses the continuity of the slope, will lead to an accurate surface model, perhaps except for the highest portion of the cap. The generator curve can be assumed as being plane and circular, the inclination in space constantly normal to the central portion of the groin curve (this could be relevant in the cases of high pointed or surbased cross vaults) or simply by 45° .

The "theoretical" translation surface shown in Figure 21 could also explain the typical profile of the ridge line which, as mentioned, can be seen in many existing vaults (Fig. 22). In fact, the curve generated by the intersection of this surface with a vertical plane (analogous to an intersection with the symmetric counterpart of the opposite half cap) is quite similar in its shape to these ridge profiles: the curvature is stronger in the portion just above the summit of the formeret arch and decreases in the central part towards the keystone of the groins.

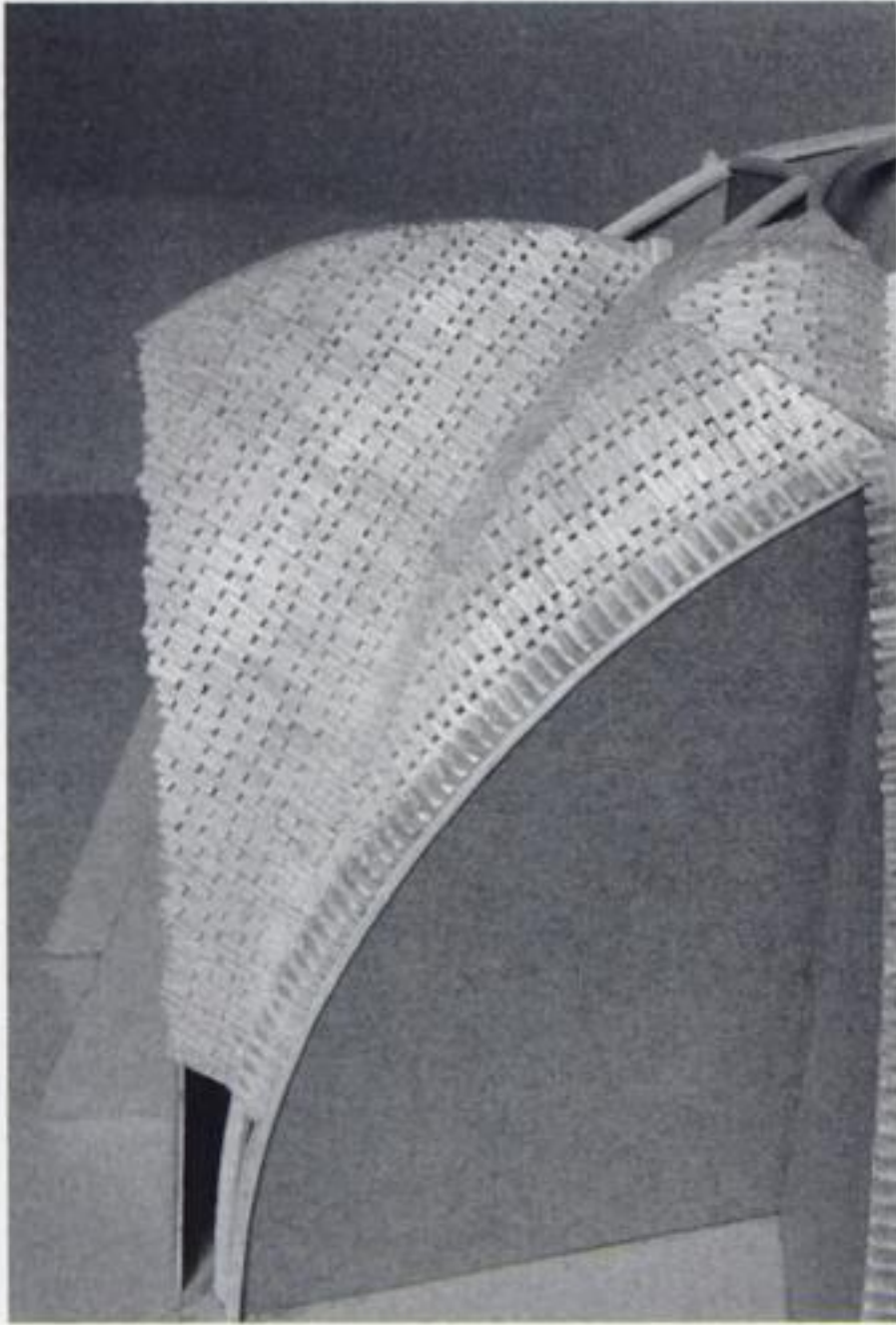


Figure 24. The vault shown in Figure 22 (a stellar vault with radial caps), reproduced in a model. In the head joints, the straight slope of the central part of the cap is visible.

4 CONCLUSION

In the considerations noted above, the terminology that has been employed is near to that of current CAD tools, as the problem discussed is essentially practical.

However, the formulation of an unequivocal answer of how to model the surfaces of a vault has been avoided. This is because, to the author's conviction, the solution to be adopted in a particular case cannot be generalized, first, as it depends on the tools to be used for modelling, the quality of the available information (the survey data) and the degree of accuracy needed (a high accuracy often implies a high complexity). Neither can the particular case be generalized beyond a certain point: Apart from the boundary conditions of a vault, like the layout and geometrical design of its arches and groins, which may present a great variety, the influence of the mason on the final shape of the cap is strong – it regards his choices, like that of the radii of curvature in the courses and the manner of closing the highest part of the cap, his strategy of correcting defective tendencies in the shape, and certainly his ability (including his manual dexterity



Figure 25. The extrados of the finished vault prototype.



Figure 26. The intrados of the finished vault prototype.

and his spatial imagination), and also the demand of perfection and pleasant appearance of the building in question.

Therefore, the way which the author has chosen to approach the problem is that based on a close view at the construction process, to formulate principles which must be adapted from case to case. The basic approach, starting from an elementary geometric design of the arches and ribs, is definitely according to the usual design process, which may be considered as a precondition for its accuracy. The modelling of the caps according to the basic principles of the construction process, as they have been pointed out, will lead to an accurate result.

NOTE

The present study is part of the author's doctor thesis in preparation, which is supervised by Prof. D. Kimpel, University of Stuttgart. Part of the research on traditional vault construction has been performed with the Fraunhofer-IPK Berlin within the EU project "iso-brick" (EU CRAFT Research Project G5ST-CT-2001-50095). The models have been built by María José Ventas Sierra and the author. The practical

experimentation has taken place at the Chair of Structural Design (Prof. W. Jäger), TU Dresden, under direction of the author. An acknowledgement is due to María José who gave strong support to the development of the contents and the text.

Photo credits: all photographs and CAD drawings are by M. J. Ventas Sierra and D. Wendland

REFERENCES

- Barthel, R. 1991. *Tragverhalten gemauerter Kreuzgewölbe*. Karlsruhe: TH Karlsruhe, Inst. f. Tragkonstruktionen.
- Breymann, G.A. & Warth, O. 1903. *Allgemeine Baukonstruktionslehre, mit besonderer Beziehung auf das Hochbauwesen. Vol. I: Die Konstruktionen in Stein*. 7th improved and enlarged edition by Otto Warth. Leipzig: Gebhart.
- Gilly, D. 1805. *Handbuch der Land-Bau-Kunst: vorzüglich in Rücksicht auf die Construction der Wohn- und Wirthschafts-Gebäude*. 3rd ed., Berlin (first edition in 1795).
- Lassaulx, J.C. 1829. Beschreibung des Verfahrens bei Anfertigung leichter Gewölbe über Kirchen und ähnlichen Räumen. *Journal für die Baukunst*, 1.4: 317–330.
- Lassaulx, J.C. 1846. Über Gewölbeformen: Vortrag des Bauinspectors von Lassaulx zu Coblenz in der Allgemeinen Architekten- und Ingenieur-Versammlung zu Gotha. *Zeitschrift für praktische Baukunst*, 6/1846, 423–427; also *Allgemeine Bauzeitung*, 376–380.
- Hörnig, G.S. 1836. *Theoretisch-praktisches Handbuch der verschiedenen Maurer-Arbeiten bei dem Land- und Wasserbau*. Dresden, Leipzig.
- Jäger, W. 1998. *Gutachten Dorfkirche Boitin* (unpublished).
- Körner, C. 1901. *Gewölbte Decken: Gewölbe*. 2nd edition. Stuttgart: Bergsträsser.
- Müller, W. 1990. Naturwerkstein in der Denkmalpflege: Die figurierten Rippengewölbe der deutschen Spätgotik. In *Geschichte des Konstruierens IV – Wölbkonstruktionen der Gotik I, proc. intern. colloquium Stuttgart 1989*. Stuttgart, Tübingen: SFB 230; 123–141.
- Nussbaum, N. & Lepsky, S. 1999. *Das gotische Gewölbe: Eine Geschichte seiner Form und Konstruktion*. Darmstadt: Wissenschaftliche Buchgesellschaft.
- Porter, A.K. 1911. *The construction of Lombard and Gothic vaults*. New Haven etc.: Yale Univ. Press etc.
- Rave, W. 1955. Das Domikalgewölbe. *Deutsche Kunst und Denkmalpflege*.
- Ungewitter, G.G. 1859–1864. *Lehrbuch der gothischen Constructionen*. Leipzig: Weigel.
- Wendland, D. 2002. Model-based formfinding processes: ‘Free forms’ in structural and architectural design. In: F. Levi, M. Chiorino, C. Bertolini (edd.) *Eduardo Torroja – From the philosophy of structure to the art and science of building* (proc. Seminar, Turin 2002), Milano: Franco Angeli 2003, S. 104–19.
- Wendland, D. 2003. A case of Recovery of a Medieval Vaulting Technique in the 19th Century: Lassaulx’s Vaults in the Church of Treis. In *First International Congress on Construction History, Madrid 2003*. 2107–17.
- Wendland, D. 2004. Zur traditionellen Technik des freihändigen Gewölbebaus. In: *Das Mauerwerk*, 4.2004.

An inquiry into an unbuilt monument: the mausoleum for the kings of the Italy of Alessandro Antonelli

G. Pistone

Dipartimento di Ingegneria Strutturale – Politecnico di Torino – Italy

L. Re

Dipartimento di Casa-Città – Politecnico di Torino – Italy

ABSTRACT: The study presented herein addresses an unusual theme: would it be possible to design a building of gigantic proportions, conceived by a great architect-engineer of the 19th century – Alessandro Antonelli – in keeping with the views and the specific techniques adopted by the author. The building in question is the temple-mausoleum for the Kings of Italy, imagined by Alessandro Antonelli, of which all we have is a few tables with sketches. In this paper, the significant signs taken into account for purposes of formal simplification are illustrated, and the hypothetical results are correlated to the respective stylistic references of Antonelli's life-size projects. Based on the foregoing, the concept of "consistency model" is formulated, to serve as a possible "validation" tool for architectural/historical virtual models. The first part is followed by a study of the structural check performed on the reconstruction hypothesis of the mausoleum for the King of Italy.

1 THE CULTURAL GENESIS OF THE PLAN

"It was in fact in these last years (after 1880, —) that he went ahead with his unyielding intelligence touching on and carrying out new and bold ideals; but there were two projects in particular that he dedicated his thoughts to, one was the façade of the Milan Cathedral and the other the mausoleum-temple dedicated to the Kings of Italy, which was to be erected in Rome either on Monte Mario or on Monte Cavi on the site of the ancient temple dedicated to Giove Laziale. But death, which he encountered while still standing in the breach, in spite of his being ninety years old, also interrupted the thread of thought of these two projects, even though of the latter and most grandiose there still remains the plans and the sketched altimetry which he had outlined and completed" (Crescentino Caselli, Alessandro Antonelli, Architect – born Ghemme 14 July 1798, died 18 October 1888, in "The Civil Engineer and Industrial Art", 1888, page 160 sgg.), (Caselli, C. 1884), (Caselli, C. 1889).

"There are basically two hypothesis that can be proposed for the six drawings that remain (one of which had already been put in fair copy): one in the form of a Greek cross with wings extended to various degrees, covered by a gigantic circular dome with a very ogival arch (...); the other is a circular plan with deep radial apsidal chapels. The first proposal, also developed in

height, could be the introduction to the second; but at the same time it cannot be excluded that it refers to another topic".

(Franco Rosso, Alessandro Antonelli 1798–1888, Milan 1989, page 121), (Rosso, F. 1989).

Even though the critical classification of these designs can go no further (as the chronological discordance between the national competition on the theme and the testimony of Caselli make the observation by Rosso legitimate – op cit., page 232-, this being supported by the date of 1887–1888 affixed by Costanzo Antonelli on the only table to be completed, which deals not of the monument dedicated to Vittorio Emanuele II, but "if anything, perhaps, of a project that wanted to be a piece of criticism"), these records of an "interrupted architecture", in which Antonelli proceeds in his faith in the rationalistic assumptions of art in unusual opposition to the trends of that time, seem to stimulate some hypotheses on those developments, that do not occur.

This was surely due to the advanced age of the architect, but perhaps also to the set of circumstances that we know nothing about, that led to the work being uncompleted. On the other hand, it is not possible to identify the topic of the mausoleum-temple dedicated to the Kings of Italy in the programme of the monument dedicated to Vittorio Emanuele II and the Unity of Italy, already achieved in 1885 at the

beginning of the works on the Vittoriano, on the project by Sacconi. The hypothesis of a specifically created mausoleum-temple was plausible, in consideration of the limits of capacity of the Pantheon where Vittorio Emanuele II had been buried, and which would have celebrated – apart from the foundation of the reign of Italy – the destiny of the dynasty (as had occurred for the Kings of Sardinia for almost two centuries with the Superga Basilica). However, it is also possible to object to the opportuneness of reaffirming the Piedmont supremacy, creating a symbolic building constituted of the extraordinary emphasised synthesis of the old and new buildings that symbolised Turin and Novara. The Antonelli approach to the theme was also in irreconcilable contrast with the eclectic tendencies of Italian culture at that time (those that produced the Palazzaccio and the Vittoriano, but also the concepts of D’Aronco and Basile); at least as far as his project for the Italian Houses of Parliament in Turin (1861) is concerned – an austere and rational project, functional and exemplarily economic in costs and in the use of spaces – another which was constructed was preferred with the stylistic imitations of Guarini buildings and the emphatic juxtaposition of a complex stylistic elaboration in memory of the French Renaissance and of constituent inventions. On the other hand, in an era of diffused eclectic typological-stylistic research, as those years were, the rigorous faith of Antonelli in Enlightenment rationalism, in the arrangement composition according to Durand’s trend, going beyond the courage and innovation of the construction and of the walled structures, programmatically leaving ornamentation to the refined and exclusive elaboration of the classical syntax (the only language of the “modern” architect, who does not give in to the allurements of historicism, of exoticism, of variously mixed vernacularism) was exactly the opposite of the linguistic orientations of that time. The weary incomprehension of the works of Antonelli by the critics of architecture, such as Camillo Boito, and also the majority of Italian historiographers, who, of all his works only mention the Mole and describe it as either gothic or metallic, was no different from that of the more competent experts, such as Tatti and Clericetti, who advised precautionary demolishing the pavilion of the Mole to substitute it with a light metallic neo-Moorish trellis; and analogous considerations can be made for the subsequent reinforced concrete consolidations for the Mole and for the Dome in Novara: “It is not the Dome that needs to be reinforced – but rather the spirit of those who are afraid of that courage”.

Among the six drawings for the presumed theme of the mausoleum-temple that are kept in the Antonelli Archives in The Gallery of Modern Art at the Turin Civic Museum (department S48, cupboard 6, shelf 2, file A, -5739-5739), two studies in pencil can be found, respectively for the horizontal sections and the

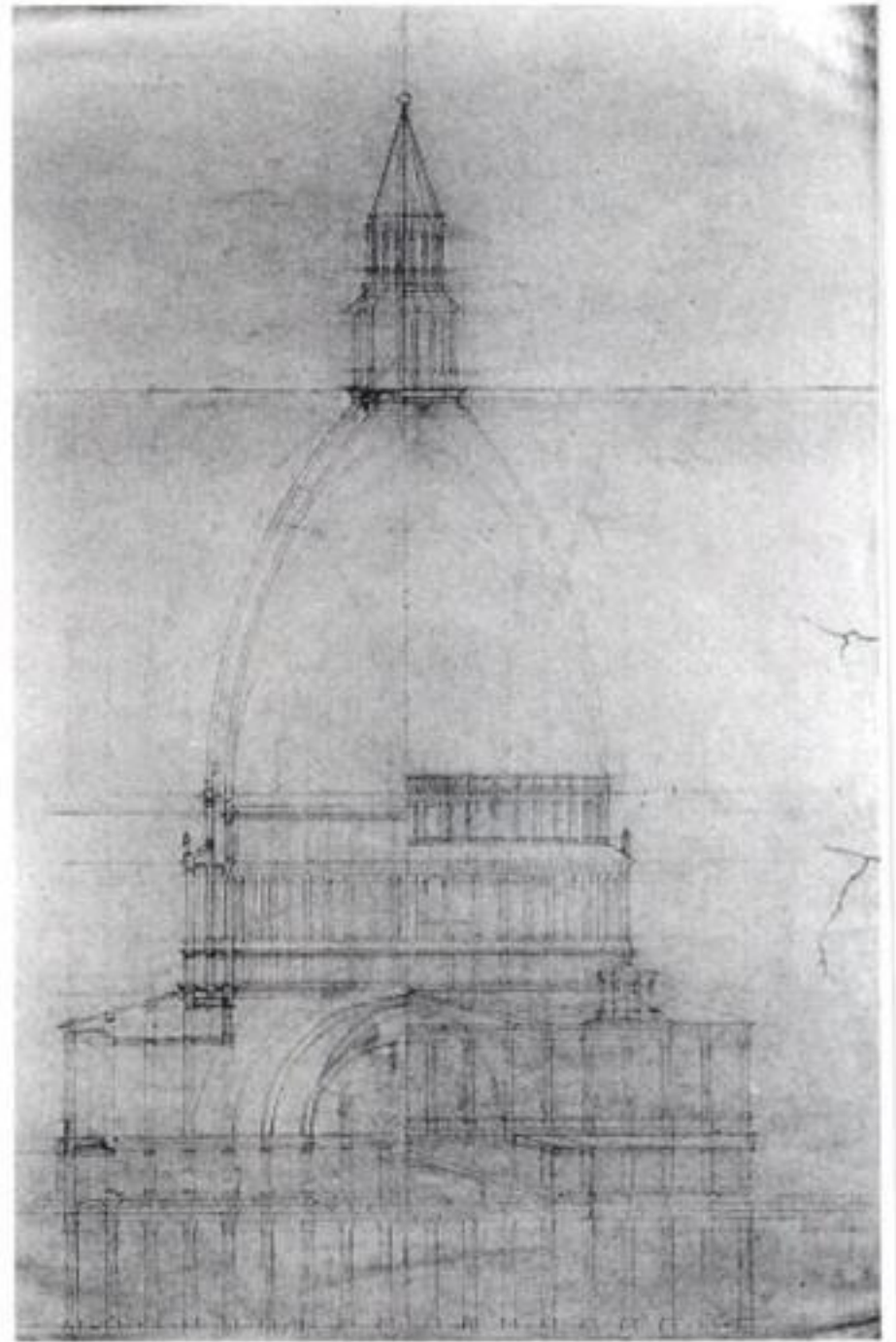


Figure 1. Section of the Mausoleum by Antonelli.

half raised and half in prospective sections, in a scale of 1:400 (Fig. 1), which outline a temple in the form of a Greek cross covered by an immense ogival dome with a double calotte closed by the lantern, of an overall height of about 225 metres (the lower level would have measured 23.60 metres, the internal beam of the ogive would have been 51.20 – eleven metres more than the Pantheon – and the double closing lantern would have developed from a level more or less in correspondence to the height of the Mole, which would therefore have been able to be completely contained within the internal space – Fig. 2). These drawings prevail to show, amongst others, in that they are connected to the exhaustive definition of the project idea (the other drawings are made up of a water-colour pen drawing of the considered plan and of a smaller version, of another plant articulated in Latin crosses – of a more specifically ecclesiastical type-, of a central plane on which a complex articulation of eight absidal chapel wings are imposed, of another different and even bigger plan where a wide exedra symmetrical to the temple and surrounded by other monumental buildings can be recognised.

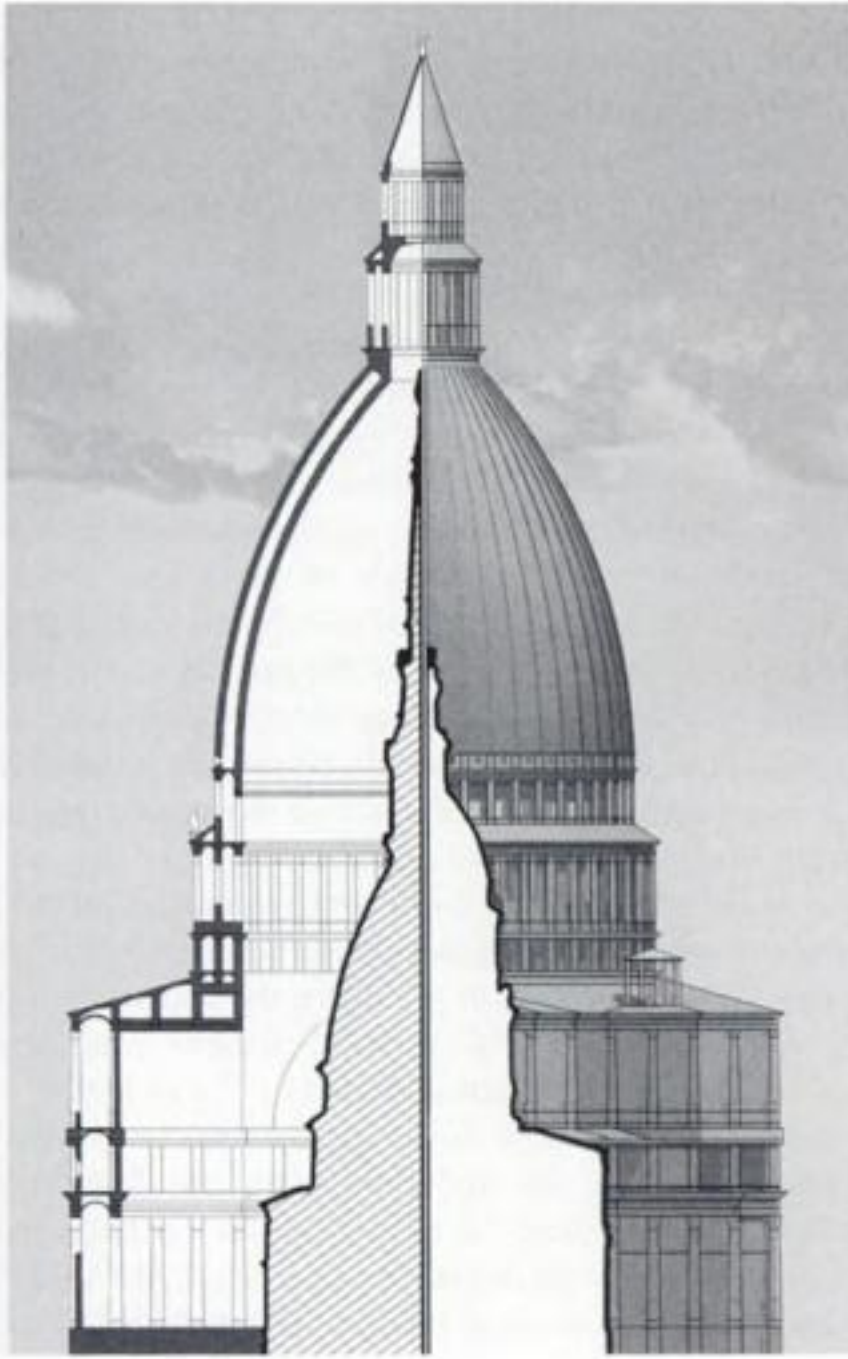


Figure 2. Comparison of the size of the Mausoleum, of the Mole (left) and S.Gaudenzio (right).

The scrawl of the two here considered drawings suggestively register the taking shape of the project in the assiduous autographical elaboration of the architectonic invention and stimulates two different considerations: on one hand the critical classification of this “interrupted architecture” in Antonelli’s production and in the context of history, and on the other, the curiosity of knowing or imagining more: what shape would it have had? Would its sublime dimensions allowed it to be made? These latter hypotheses have recently been developed from two standpoints, starting from the assumption of Antonelli’s designing as being a combination/elaboration of defined and constant constructive elements, intended prefiguring the building in a virtual manner (Fig. 3), from both the internal and external prospective points of view, building it with typical elements regularly used in Antonelli’s works, demonstrating the compositional coherence and architectonic relevance, among analogous constructions of his time and in the continuity of the historical series of large domes from the Renaissance onwards (in particular it can be seen how – apart from the dimensions – the structural conception of the double dome is simpler



Figure 3. Virtual representation of the Mausoleum.

and more experimented than that of the relationship between the ogive and conical towers of the Novara dome and of the square planned double pavilion of the Mole).

All these indications are in nuce and unequivocally present in the original drawing, the elaboration intended developing the graphic evidence without adding anything that was not present or which could reasonably be attributed for analogy reasons. In particular, the theme of the large dimensions (that recall the considerations of Galileo on the proportions of the colossal and the criticism of Boullée on the Vatican Basilica) is here resolved as in the Novara Dome and the Turin Mole not in the gigantism but rather in the multiplying and articulating of the members, with an unusual prevalence of thickly linked voids which give these large constructions a feeling of lightness and elasticity without comparison, conditions which are essential for their feasibility. On the judgement that one could make on this unprecedented conception, if it could have been put into concrete form, it is necessary to observe that its excellency would not only have consisted of its incredible dimensions and of the suggestion of a titanic site which would have been able to recall, in the progressing beauty of the in fieri building, the Tower of Babel by Brueghel, but also and even more so of its architectonic proposal which, like the other works by Antonelli, can be seen as a concept of ideal continuity, in the Enlightenment project rather than the heterogeneous tables that were prepared in his time, such as the Capitol in Washington. The sense of composition quality of the design is obvious and cannot be limited to the suggestion of incomparable dimensions.

Its compact syntactic articulation leaves no room for the redundancy or arbitrariness of the definition of its elements, of the most minute components; and it is based on the rigorous connection to the principles of classical composition and neoclassical rationalism: for example, in the indisputable Albertian identity between external order and internal order or in the classical predominance of axial moduli (an arrangement that Benedetto Alfieri had adopted on the Geneva Cathedral façade and which Crescentino Caselli had adopted for functional reasons in the Charity Hospice building in Turin). All the stylistic-syntactic questions would have found the principles to be developed with exemplary elaborations of the language of the orders, already experimented by Antonelli in many religious and civil buildings. The mausoleum-temple, contemporary of the Eiffel Tower, would have really sealed the season of Architecture of the Sublime and Reason, and would have reconnected – through the concepts of Boullée and the Enlightenment architects – with the Sainte-Genevieve by Soufflot and with the large domes that had progressively preceded them, as can be demonstrated by the continuing topicality of traditional construction in bricks and stones in the face of new technologies, in the intent of “attributing light to the progress in lateritious and stone construction for the large coverings”, in that “it is the most consensual for our Italian customs, the most convenient for our interests and duties, to preferably use the materials that nature has been lavish with” (as Antonelli himself wrote on other occasions).

The second legitimate curiosity was obviously to verify the feasibility of the project, from what could be deduced from the sketch. Obviously it is not possible to imagine which elaborations Antonelli would have made to the original idea (as he continued to do with open sites for the Dome and the Mole: it is possible to observe, but never in a restrictive manner) confiding almost exclusively in the intuition and experience of the architect (as it was for the Dome and the Mole) and which devices he would have gradually introduced to resolve the criticalities that have appeared from a verification method, which with respects to those of Antonelli’s time, has greatly reduced the difference between phenomena and hypotheses (and where it is difficult for those macroscopic differences in judgement that had caused diffidence on the part of scientists in the past to appear again). The invention, still at the draft stage, especially for the single development in sections, appears to be elaborate, above all for the definition of the volume and the internal spaces, rather than for the resolution and the joining of the members.

2 THE STRUCTURE

In view of clarifying the main problem, concerning the static equilibrium the second part of the study

addresses the problem of the stability of the building, and, in particular, it tries to determine whether static equilibrium could have been ensured with the knowledge and techniques available at the time. To this end, a series of FEM numerical models have been developed to reproduce the material and structures of the mausoleum identified during the first part of the investigation. The purpose of the models was to explore the numerous problems that would have had to be solved to create a structure so much bigger than any masonry building ever completed till then.

The computation code used applies to compression- and tension-resistant materials in the linear elastic field. This choice might appear unsophisticated, but in actual fact it was motivated by the consideration that the aim of a stability study is to identify the orders of magnitude of the parameters governing the behaviour of a construction and the efficacy of the spatial organisation of the resisting skeleton; accordingly, the purpose of the computation code is not to permit refined checks on the materials and the structure, but rather to serve as a quick tool to pin down the shortcomings and weaknesses and to identify the changes necessary to overcome the problems detected by the analysis.

In keeping with the results of earlier tests performed at our laboratory on materials from the Antonelli school, a Young’s modulus of 2,000 MPa was assumed for the masonry, with density of 18 KN/m³; the values assumed for granite were 55,000 MPa and 28 KN/m³ respectively, and for iron they were 210,000 MPa and 80 KN/m³, (Mattone, R., Pasero, G., Pavano, M., Pistone, G., Roccati, R., 1982), (Pistone, G., Roccati, R., 1988), (Pistone, G., Roccati, R., 1991).

2.1 *Modelling the structure*

For the sake of convenience, the model was subdivided into two parts, corresponding to a hypothetical subdivision of the building: the dome, including the drum and the lantern, and the base.

2.1.1 *The dome, the drum and the lantern*

The dome consists of two concentric ogive-shaped skins, 1.30 m thick and ca 70.0 m high. The 38.0 m high drum consists of three orders with binate columns, curtain walls with huge windows in them, and low columns arranged in three rows. The double lantern, measuring ca 54.0 m including the roof, also uses binate columns and repeats the visual motifs of the drum.

2.1.2 *The base*

The base, consisting of three orders, rises to a total height of ca 66.0 m. The entire plan is characterised by isolated columns spaced apart according to modules measuring 6.70 m, save for the central one, which measures 7.80 m. The model leaves out several elements

(the stairs, the pronaos, the small lanterns on the roof, which represent extensions of the stairs) whose absence does not affect the statics of the building. Initially, we assumed that the dome was supported by 4 big arches (Fig. 4) with pendentives, via a ring. The model was created on the basis of a highly simplified drawing, consisting of one-dimensional “beam” elements for the representation of columns and pillars, two-dimensional “plate” elements for the walls and the dome, and “brick” elements for the arches and the ring on top of them. These three elements are linked to one another at each common node in the frame. The two-dimensional and three-dimensional elements have been subdivided in their turn by means of a mesh running parallel to the reference axes, fine enough (ca 150–200 cm) to reveal clearly and in greater detail the behaviour of the structure under the load-effects; brick elements in particular make it possible to visualise the evolution of the state of stress inside them.

The horizontal elements – structural parts of which nothing is known – have been replaced with a hypothetical mesh consisting of “St. Andrew’s crosses”, conceived as infinitely rigid elements that can be used to simulate, by changing their dimensions, conditions as close as possible to the real situation (Arrigoni, R.,

Nascè, V., Pistone, G., Strona, P.P., 1989). These stiffening elements are also used between the outer and inner skins of the dome, where, in similar cases, Antonelli used to place stairs and pathways to simulate the action of the arches (including rampant and inverted arches – Fig. 5) and to make the two domes integral with one another.

The initial approach is based on a careful reading of Antonelli’s documents and the virtual model was defined on the basis of our knowledge of the techniques and construction principles available to the architect. This choice was dictated by the lack of sufficient evidence, in terms of surveys and records. Then, by identifying the structural function of each element, the most probable solution was identified account taken of the “language” of the building as a whole, and, above all, in accordance with the critical-scientific outlook of statics and the behaviour of materials.

The initial results were disappointing: through a careful scrutiny it became apparent that the reading was not so immediate and that the possible solutions could have been different.

Hence, it was decided to maintain this design approach as a starting point and then proceed through subsequent steps involving a continuous comparison



Figure 4. San Gaudenzio. A view of the two arches supporting the dome.

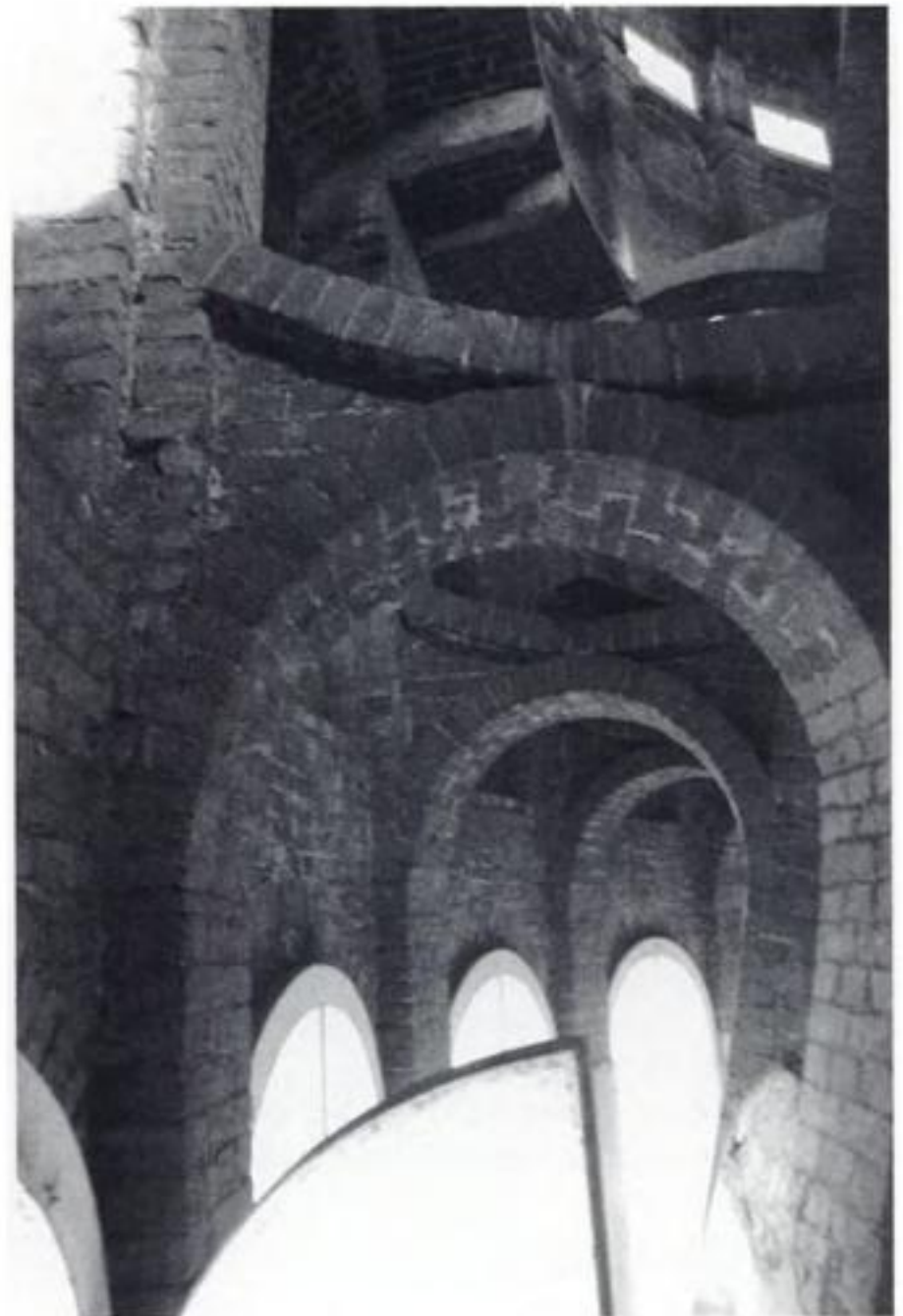


Figure 5. San Gaudenzio. Arch and inverted arch.

between the results and the most convincing hypothesis that gradually emerged. This method, strangely resembling Antonelli's ways of working by successive "adjustment", proved effective and, over time, yielded results of considerable significance, even though they differed from what we had anticipated.

For a better understanding of this approach, let us go over the different stages so as to provide a schematic overview of how the study evolved. It should be noted that the hypotheses described are the ones that proved most significant.

2.2 1st Hypothesis

The building is assumed to be made entirely of bricks.

The deformation configuration reveals an overall subsidence of the building $\Delta l = 136$ cm, with a symmetrical evolution in the transverse and longitudinal axes y and z . In addition to bulging conspicuously, the dome tends to sink vertically; in the drum this tendency meets with no obstacle, as the columns, vertical supports and windows yield under the enormous weight of the dome.

2.3 2nd Hypothesis

It is assumed that the structure as a whole has to be stiffened. The dome still tends to "sink" into the base, which, in its turn, is unable to support it. The "beam" elements, initially conceived as made of bricks, are replaced with stone: this is motivated by the need to enhance the stiffness of such a huge structure and to add a "precious" material befitting the aulic destination of the building. At all events, the materials are used according to functional criteria (placing the most precious materials in the most critical points). The only one-dimensional elements that are not replaced with stone are those making up the uprights of the windows, where bricks seem more fitting.

At the same time, granite ribs, conceived according to the same criteria adopted by Antonelli for Mole, are added to the dome and anchored to the masonry structure. Moreover, always with reference to the Mole, retaining chains are installed and connected with ties linking the two skins.

The deformation configuration shows an overall subsidence of the construction $\Delta l = 85$ cm. A slight improvement is observed, especially in the zone of the arches and the piers underneath. Maximum principal stresses are seen to decrease in the entire structure, especially in the dome.

The problem of how to carry the enormous thrust of the arches supporting the dome is still unsolved.

2.4 3rd Hypothesis

The great problem posed by the thrust of the dome and the arches that are unable to support it could not

be solved by fitting supporting elements, whether visible (something unconceivable in Antonelli's system) or hidden at the top of the arches, due to the lack of filling in the extrados of the pendentives. Nor would it have been possible to resort to retaining chains, even huge ones, and therefore the different attempts made did not yield any appreciable improvements. From an analysis of the plan, the presence of stairs at the four corners suggested the idea of linking adjacent columns in a double continuous wall, so as to obtain a system of symmetrical buttresses for the dome, forsaking the idea of having isolated fulcrums in these zones.

The deformation configuration reveals an overall subsidence of the construction $\Delta l = 74$ cm. Two considerations should be made at this stage: the first is that the situation has improved greatly, in terms both of the deformation configuration and of stresses. The deformation configuration clearly shows the favourable contribution of the partition walls, especially at the ring, though the latter is badly warped internally. The maximum values of the (tensile and compressive) principal stresses are also reduced, especially where brick elements are concerned. From the stresses in the vertical elements, it is possible to determine the evolution of the stresses inside the walls.

The other consideration is a persistent tendency of the dome to move away from the pendentives and assume a rhombus like shape (Fig. 6). This will be monitored during the subsequent stages.

2.5 4th Hypothesis

The next hypothesis entailed the use – as was often the case in Antonelli's system – of stone legati (linkage by stone) at the critical points of the structure. In this particular case, the critical points were the arches, having zones characterised by very high stresses, particularly at the keystone.

From the graphic viewpoint, the arches were already subdivided into 12 blocks, 6 in every half arch, but there was no "odd" block at the keystone; this was remedied by considering two blocks, one per side, plus two more blocks at the reins. The deformation configuration showed a reduction in the overall subsidence of the building of $\Delta l = 62$ cm, more significant than might have been logically expected.

The stresses in the vertical elements are smaller than under the previous hypotheses. From an analysis of the deformation configurations we find that the most important change has occurred in the brick elements (simulating the arches and the ring) which are directly affected by the legati. The ring displays a reduced tendency to warp internally, with a milder slant, and the arches appear less deformed. The values of maximum principal stresses and vertical stress are more acceptable, without substantial variations.

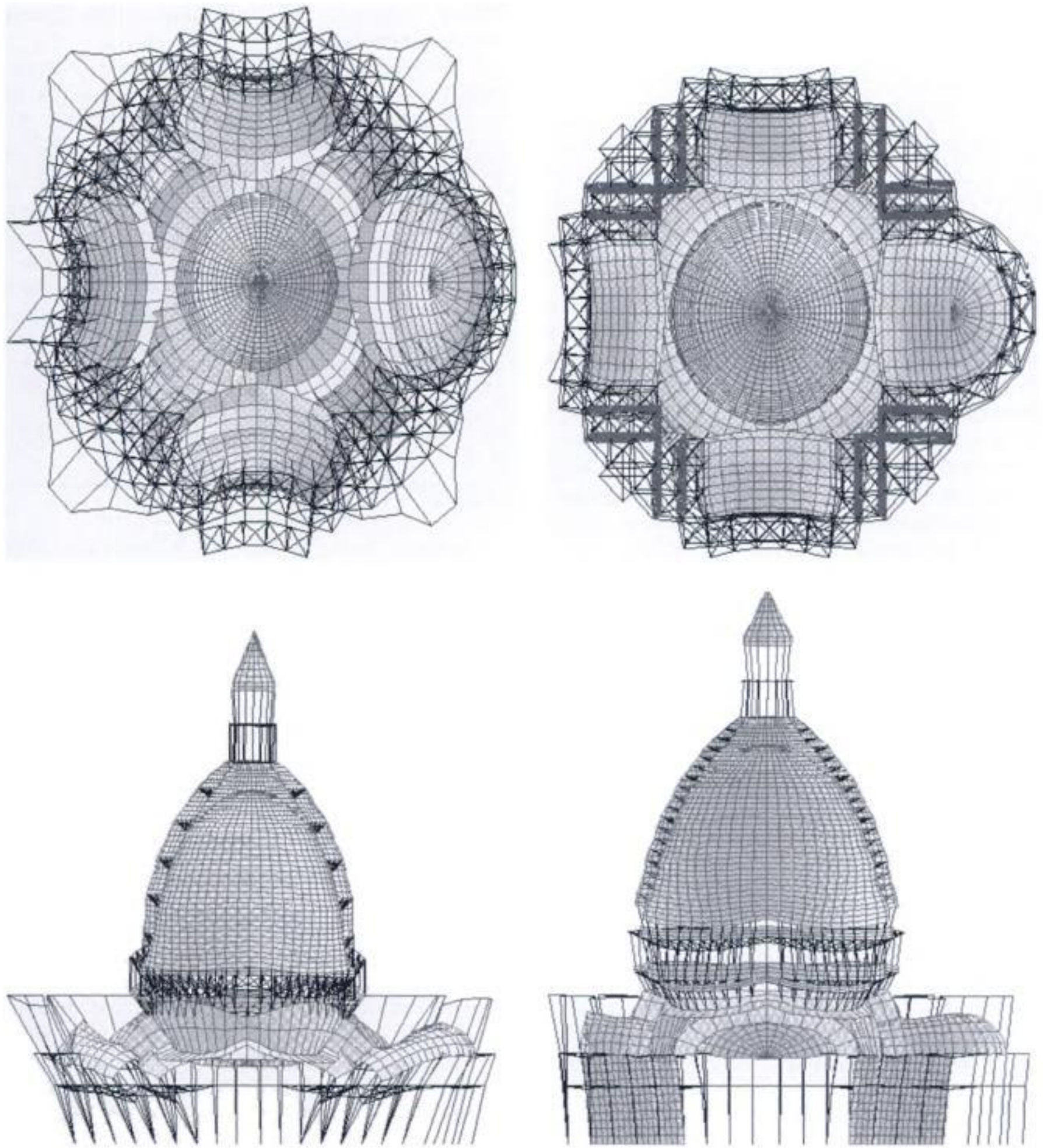


Figure 6. Deformed shape at first and final step.

2.6 5th Hypothesis

The arches supporting the dome are assumed to be rigidly restrained: this stage of the investigation was designed to explore the behaviour of the dome/arches system.

The deformation configuration indicates an overall subsidence of the building $\Delta l = 50$ cm. This stage proved fundamental to define a few essential points:

1. the arch displays a progressive lowering, which increases from the restraint to the keystone;

2. the deformation configuration reveals a settlement of the pendentives that increases with increasing the distance from the arches: a weakness already observed in the previous hypotheses, which is clearly reflected in the states of stress in the ring;
3. the windows, the only beam elements made of bricks, sag under the weight of the dome.

Based on these studies, it is felt that the only two solutions that can still be proposed are: the variant with from 4 to 8 arches, and the conversion of all columns to stone.

2.7 6th Hypothesis

The number of arches supporting the dome is raised to 8.

2.8 7th Hypothesis

All vertical elements are converted to stone.

2.9 8th Hypothesis

The arches supporting the dome are assumed to be rigidly restrained (as in the 5th hypothesis) to be able to assess the benefits arising from the changes introduced with hypotheses 6 and 7. The deformation configuration shows a total subsidence of the construction $\Delta l = 35$ cm. As for the other values, displacements are seen decrease further. A significant difference can be observed in the upper part of the drum, precisely at the three crucial points of the windows, where the values, as mentioned above, increased abruptly.

At these three points, in fact, the displacements are reduced to about half, from 43 to 28; from 46 to 28; and from 61 to 37. In view of the much greater incidence on the results of hypothesis 7 compared to hypothesis 6, it can be concluded that the choice of material plays a fundamental role in buildings of this type.

2.10 9th Hypothesis

As a final hypothesis, let us consider the possibility of moving the stairwell, ignoring the constraints imposed by the plan: this is done by moving back the partitions walls, so that they now oppose the 4 arches directly and perpendicularly, creating a sort of confining buttress. Both the stairs included the helicoidal one are moved by one module.

2.11 Results of the analysis

The analysis was performed by making successive changes to the original scheme, always using materials and structural elements that were available at the time of Alessandro Antonelli, in keeping with his structural conception.

The various steps achieved substantial improvements in terms of structural response, in addition to a general improvement in the distribution of the states of stress, and strains also gradually diminished. In this connection, see table 1, that shows how the lowering of the uppermost point gradually reduced to about one third of the original value (Fig. 6).

A number of basic problems remain unsolved.

a) The problem of the dome:

Its thrust cannot be carried with traditional methods. Metal chains cannot be used, because they would have to be gigantic, posing insurmountable

Table 1. Summary of the total displacements under the various hypothesis.

Hypothesis	Changes	Δl (cm)
1	Initial hypothesis	136
2	Stone columns (except at the windows), ties and ribs	83
3	Addition of wall partitions	73
4	Addition of legati	62
5	Restraint – study	50
6	The eight arches	59
7	Columns entirely made of stone	48
8	Second restraint – study	35
9a	The rearrangement of the stairwell – 4 arches	50
9b	The rearrangement of the stairwell – 8 arches	47

problems in the connections between the various segments, which could not be solved with the technologies available at the time.

b) The problem of the arches:

The arches cannot bear the exceptional load of the dome, both in terms of stresses, that exceed the failure strength of the material, and in terms of thrust, that cannot be effectively opposed. The impossibility of using visible supporting elements and hidden ties makes the problem insolvable. Though the use of partition walls might seem promising, it is not a viable solution for a building of this size.

c) The problem of the columns at the base:

The columns at the base are subject to extremely high stresses, that they cannot withstand, if they are made of brick masonry. But there is another aspect, of a practical nature, to be taken into account: if made of stone, the columns cannot be one-piece elements, but have to be conceived as a series of perforated blocks stacked on top of one another. This would entail stacking an extremely high number of blocks, given the height of the columns. A solution of this sort, might translate into a kinematic chain that would pose yet another challenge to the stability of the structure, regardless of the other problems already present in the mausoleum.

3 CONCLUSIONS

Seen through the eyes with which we had wished to examine it, the problem seems unsolvable.

But perhaps this is also the last project of Alessandro Antonelli, elaborated on a few tables that were not divulged to his contemporaries, but consigned to the memory of others who would come after him.

We therefore like to think that Antonelli wished to give shape and proportions to a dream that was

to be consigned to the new century, which was then close at hand, to the new materials that in those years were being tested for the first time and others which, little by little up to the present day, would have obtained increasingly better performances in the world of Construction Engineering and finally, for other designers, perhaps for constructors, who, looking again at his indications, would resolve the problems that appeared in our unsolved study, and bring his idea to a conclusion.

NOTE

This work has started from two degree theses, recently developed at Politecnico di Torino, under the supervision of G. Pistone and L. Re: Borra, D., 2003, *Architettura interrotte*, Architetture virtuali; Etzi, Antonella, 2003, *Ipotesi di stabilità di grandi strutture a volta: l'ideazione antonelliana per il mausoleo ai Re d'Italia*.

REFERENCES

Arrigoni, R., Nascè, V., Pistone, G., Strona, P.P., 1989, *Numerical Models for the Original Structure of the*

Mole Antonelliana", Structural Repairs and Maintenance of Historical Buildings, Berlin, Birkhauser Verlag Basel Boston.

Caselli, C. 1884. *Appunti e schizzi di Architettura Antica e Moderna*, raccolti all'Esposizione Nazionale di Torino del 1884. In *L'Ingegneria, le Arti e le Industrie*. Torino.

Caselli, C. 1889. Cenni sulla vita e sulle fabbriche dell'architetto Alessandro Antonelli. estratto da "L'Ingegneria civile e le Arti Industriali", Torino.

Mattone, R., Pasero, G., Pavano, M., Pistone, G., Roccati, R., 1982, "Prove sperimentali su campioni di varie dimensioni volte alla determinazione delle caratteristiche meccaniche delle vecchie murature", Atti del Sixth International Brick Masonry Conference, Roma.

Pistone, G., Roccati, R., 1988, "Testing of Large Undisturbed Samples of Old Masonry", Proceeding of the 8th International Brick/Block Masonry Conference, Dublin.

Pistone, G., Roccati, R., 1991, "Mechanical Characteristics of Masonry Rebuilt with Ancient Bricks and Fresh Mortars", 9th International Brick/Block Masonry Conference, Berlin.

Rosso, F., 1989, *Alessandro Antonelli 1798-1888*, Milano, Electa.

The industrial heritage of the Veneto between memory and project: what technology for conservation and reuse?

G. Riva

Department of Construction of Architecture, Iuav University, Venice, Italy

ABSTRACT: As regards the Veneto area, the panorama of the structures that can be classified in what is commonly defined as the Industrial Heritage is vast and compound and reflects the driving richness of the North–East. It is fully legible when investigating the historic roots of the industrial phenomenon, through the first signs – in town planning and building – of its appearance in the territory, and when seeking any traces that still survive. The language of technology is, in fact, more than ever an essential part of architectural language and, in these particular constructions, it is expressed in rigorous constructive forms, characterised by an honesty of expression that is associated with the clarity and solidity of the layout which features maximum simplification, even with solutions that may be demanding from the structural point of view. Sometimes they also possess innovative elements of great interest on the building scene of the time, regarding both the introduction of new materials and the way of using them, which was often unprecedented and pioneering.

1 FOREWORD

The panorama of the structures that can be classified in what is defined as the industrial heritage of the Veneto is very vast throughout the territory and constitutes a great wealth and a resource to be exploited, but also to be protected.

In our territories the birth and development of the factory were profoundly linked with the rhythms and times of agriculture, with which they have maintained a constant relationship. Early industrial structures were therefore influenced by rural building tradition and by the its characteristic materials (masonry and wood), which, in turn, directly conditioned both its shape and its constructive features. Only in works on a large scale and in those inspired by models from beyond the Alps, gradually introduced in the largest centres starting from the last years of the nineteenth century, are more free and original expressive forms encountered, produced by the introduction of the materials of the Industrial Revolution (cast iron, steel and, later, reinforced concrete).

The traditional constructive technologies (loadbearing masonry in brick and mixed brick and stone and roofs and floors of solid wood) would continue to survive indefinitely, till the mid twentieth century, for example in the realisation of the Hoffmann kilns for baking bricks and in the construction of industrial chimneys. But their use would also be prolonged in the factories located in the more peripheral industrial

districts or, on the contrary, in the most intensely man-made and representative environments, such as the old town centre of Venice, where the masonry shell would continue to be given a high-profile tectonic role (along the lines of the first examples of the Stucky Mill, the Tobacco Factory, the Maritime Station etc. . . .) and where the iron structure would be used alongside the traditional wood structure and even replace it until the arrival of reinforced concrete. Only much later, from the Thirties of the twentieth century, would traditional masonry techniques be widely used, first in a hybrid form with the introduction of reinforced concrete (in new buildings and in alterations carried out on previous structures for maintenance or reuse) which would finally replace it.

The use of reinforced concrete has given rise to original and at times unprecedented forms and pioneering construction experiences, which today deserve to be preserved and suitably valorised.

2 REINFORCED CONCRETE IN INDUSTRIAL BUILDINGS

2.1 *Its diffusion in the Veneto in the 20th century*

The diffusion of reinforced concrete in Italy came about much later than in other European countries, only as from the first years of the twentieth century, especially in the districts affected by the industrialisation processes in the North, such as a Piedmont,

Lombardy, Liguria and the Veneto. And in the Veneto the poles of industrial development at Schio-Valdagno-Thiene, Verona and Venice-Porto Marghera were the main driving centres for the success of the new material, able to assimilate the innovation brought by Hennebique's French patent and the great potential offered by its application.

The industrialisation of the territory was in fact the real driving force of the renewal of the building world, which was still stubbornly anchored to the tradition of masonry construction, because the introduction of the new material – reinforced concrete – made it possible to achieve rationalisation processes both in the sector of urban infrastructures (bridges, roads, subsidiary services, pipelines, etc. . . .), and in the sector of structures intended to bear high loads and characterised by large spans and high flexibility, such as the factories with their large machine rooms, large warehouses, silos, hangars, indoor markets, etc. . . . It also made it possible to ensure good resistance to fire and an expectation of long durability, which only later would be endangered when the problem of its behaviour over time was revealed, also in relation to the environmental conditions which with time had become more and more aggressive.

In the first period of its success, the new material was at an advantage on account of its particular characteristic of being able to be integrated in traditional masonry construction, at first only in horizontal structures (beams and floors), and then also for internal pillars (taking the place of cast iron and iron).

In the Veneto, the first constructions to use reinforced concrete date back to the very first years of the twentieth century, coinciding with the introduction in the territory of the French Hennebique method, of which they faithfully reproduce the type. They are slabs with a reduced thickness (with rectangular or square dimensions) resting on a crossed frame that is lower than the floor composed of secondary beams fixed into the main beams, which in turn are connected to the pillars by means of brackets with variable section.

Only later, from the Twenties of the twentieth century, do we gradually witness the evolution of an expressive language of the new material itself, able to interpret the union between the structural performance and the physical technical performance peculiar to the factory, and new types of construction become established. These are formed in such a way as to ensure structural reliability even for quite high loads, both fixed and moving (bridge cranes, stacks of deposited material, machinery with vibratory movement, etc. . . .), through solutions able to guarantee, at the same time, both large glazed surfaces of the shell (on sides and top) to illuminate the work areas, and openings for disposing of vapours and fumes and controlling the change of air.



Figure 1. View of the shed roofing structure of the machine room at the G.B. Conte Woollen Mill at Schio (VI) (Porcheddu Company, Turin, 1906) (*Il Cemento*, n. 1, 1909, year VI).

The result was load-bearing frames made entirely of reinforced concrete cast on the site with vertical point support structures, on square or rectangular mesh, which configure spaces with considerable flexibility and which “draw” the rhythm of the surfaces of the façades and mark the skyline of the spatial development of the volumes. These result in new, unprecedented expressions, full of strength, which show their constructive logic on the outside and are sometimes characterised by interesting architectural features.

From the typological point of view, the following four recurrent forms may be distinguished in industrial building (Nelva, Signorini, 1990):

- Structures having a frame complete with floors resting on beams and pillars, developed also on several storeys, with broad windows between the pillars on the perimeter walls, for non heavy work;
- Complexes based on the coupling of modular mesh of different heights to allow internal lighting with large windows;
- Sheds for heavy work (bridge cranes) with roofing of lattice girders and lighting obtained from windows between the floors located at different heights and from windows in the perimeter walls;
- Sheds with modular mesh with dimensions that are not too large, but generally very extensive horizontally, able to guarantee diffused lighting with shed solutions (machine room and weaving room in the G.B. Conte factory at Schio, 1906) (Fig. 1) or buildings with skylights obtained in various ways in flat roofs (spinning room in the G.B. Conte factory at Schio, 1906) (Fig. 2).

The photos no. 1–9 show some significant examples of the surviving industrial heritage in the territory of the Veneto, consisting of buildings of normal and pre-stressed reinforced concrete, chosen among the many still to be seen (sugar refineries, spinning mills,

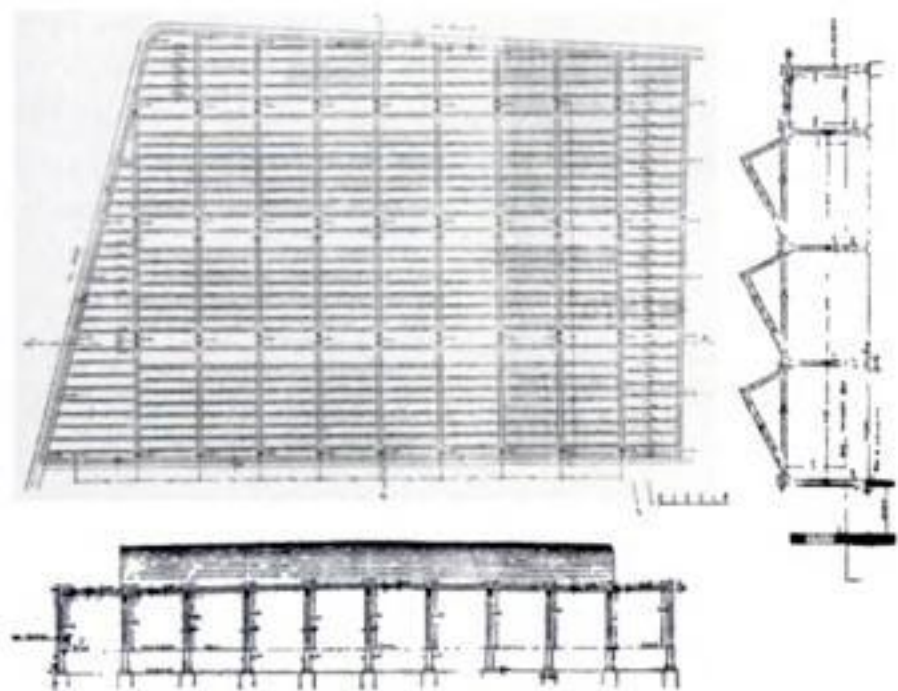


Figure 2.

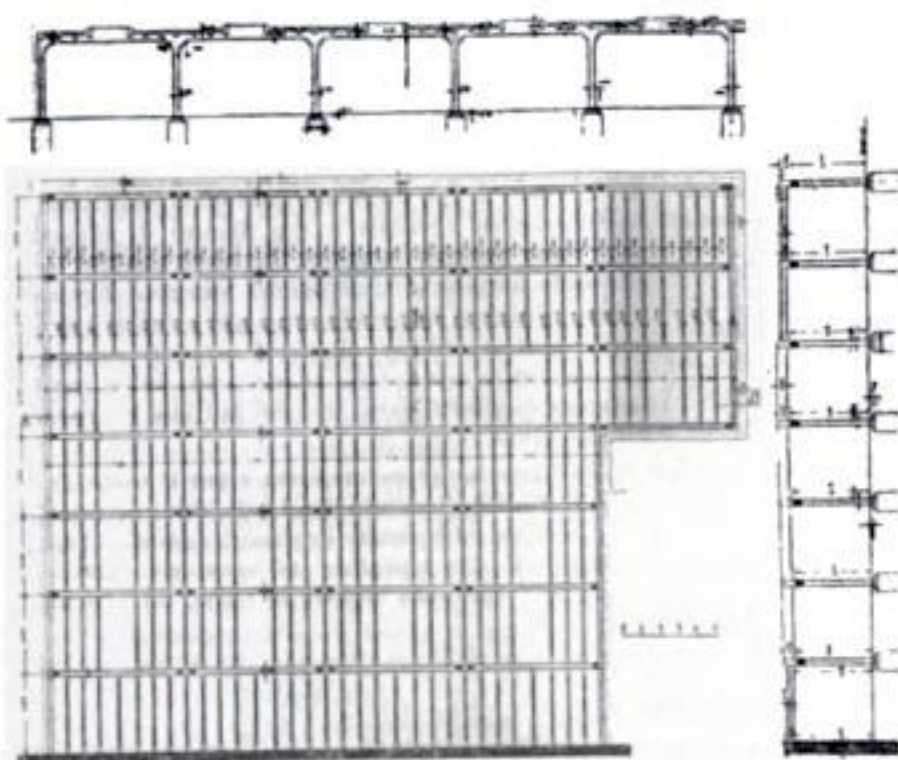


Figure 3.

Figures 2 and 3. Layout of the shed roofing structure of the machine room and of the flat roof of the spinning room at the G.B. Conte Woollen Mill at Schio (1906) (*Il Cemento*, n. 1, 1909, year VI).

kilns for making bricks, but also the milling industry, commercial activities, etc. . . .) made of reinforced concrete.

2.2 An innovative shed roof

Alongside the many examples made by better or lesser known designers, we wish to mention a structure built at Schio for Lanerossi s.p.a. on the site of the old "Francesco Rossi" factory along the Roggia Maestra at the end of the Fifties of the twentieth century. The building, on a large scale inspired by bridge-building techniques, is distinguished for the unprecedented typological solution of considerable structural and economic interest (Figs 4–7).

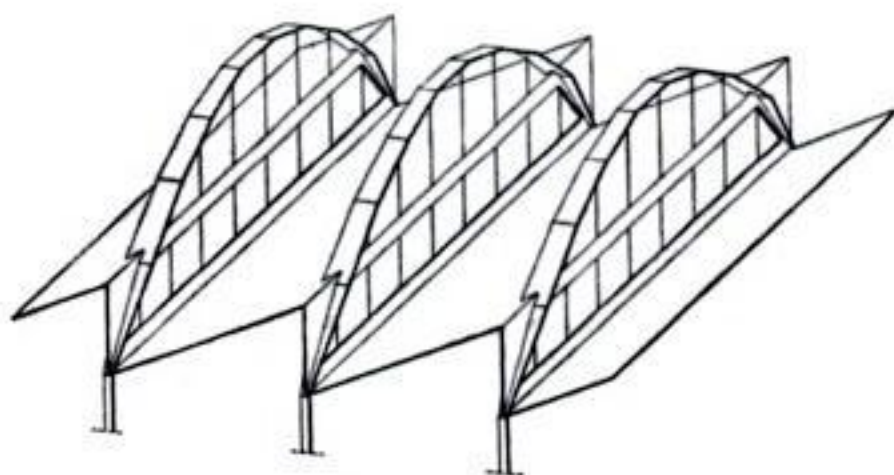


Figure 4. Axonometric view of the structural prototype of shed roofing based on the use of the stiffened flexible arch freely developed over the roof, erected on the sorting shed of the "Francesco Rossi" Woollen Mill at Schio.

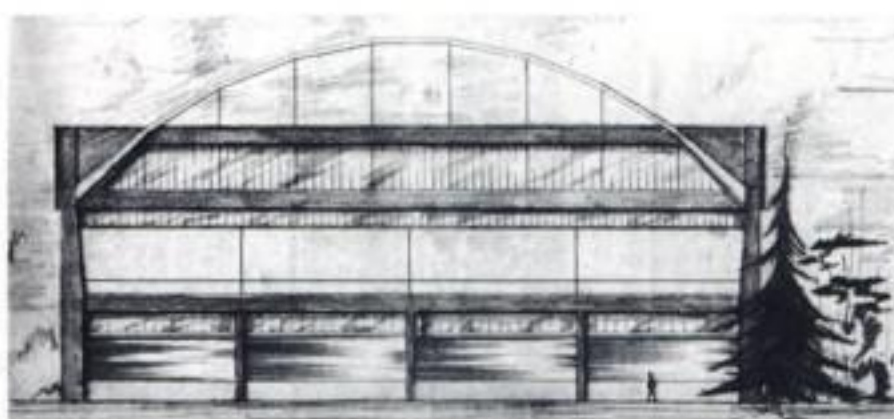


Figure 5. Front view.

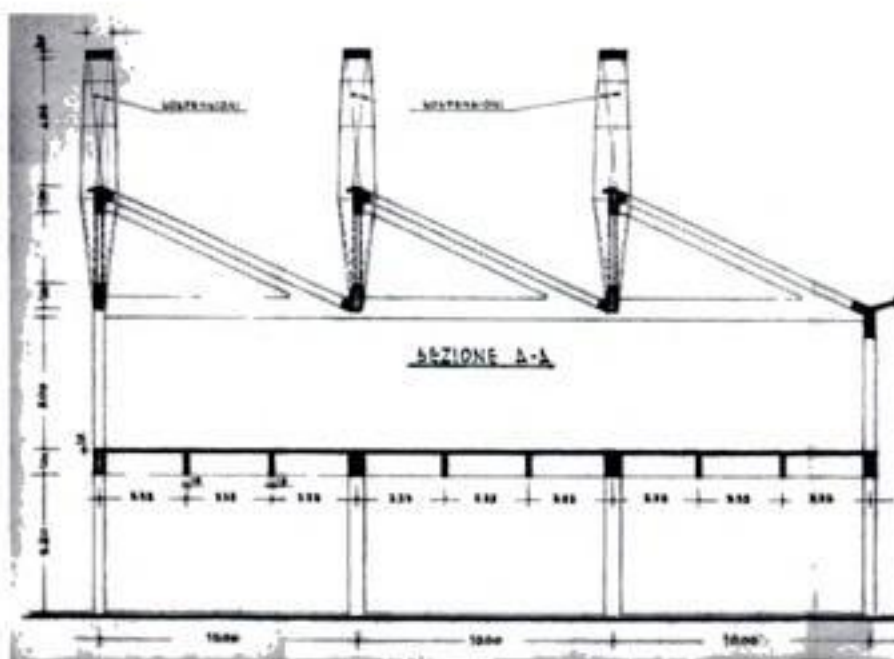


Figure 6. Section.

It is the sorting shed built in the years 1958–1961 by the Guaraldo firm to a structural design by the professor engineer Bruno Dall'Aglio. Particularly suitable for large-span roofs with only perimetral supports, the structural layout of the building combines the classic pitched shed roof, made with the usual floors of brick and reinforced concrete, with the use of stiffened flexible arches supporting the beams that define the borders of the windows, acting as chords, and makes it possible to obtain a surface free from structural impediments

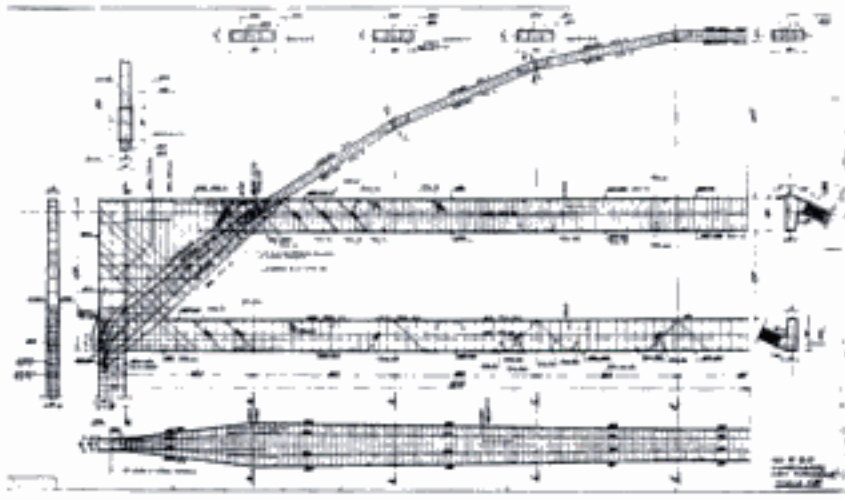


Figure 7. Original drawings, of the reinforcement of the arches, for the new sorting shed building in the Rossi industrial complex at Schio. Flexible arch with a span of 40.0 m using the same typology as the factory at Valdagno (Archive of the Guaraldo company).

with a span of 40.0 m. The designer commented, "Having considered a sequence of flat pitches with the same inclination forming the actual roofing and having realised the necessity of edging said pitches with beams defining the borders of the windows on vertical plains, I recognised the opportunity of exploiting the flexural rigidity of the beams as a 'compensating' rigidity to collaborate with flexible arches that would support them. Each pair of beams belonging to two consecutive pitches and lying on the same vertical plain are therefore horizontal elements that stiffen the arch developed on the same plain (. . .). With that in mind, it is useful to consider the particular adaptability of the constructive layout for large-span roofs with only perimetral supports, observing the quasi independence of the unitary dead load with respect to the span".

The stiffened flexible arch is freely developed above the roof with a rise of 9.0 m; its axis has been assumed as a funicular line of the permanent load uniformly distributed along the chord.

The edge beams, the pillars and the arches are of reinforced concrete, the tie beams of pre-stressed reinforced concrete and the shed floors of clay/cement mix with the joists laid according to the straight lines with the highest slope.

The prototype conceived and prepared in the sorting shed at Schio was taken as the basic model for working out the project of the Marzotto factory at Valdagno, optimising even more the quasi independence of the unitary dead load with respect to the span. The resulting space in the weaving room has layout dimensions of 57.80×156.50 m covered with twenty consecutive pitches supported by ten arches. In the new structure the theme of the collaboration between arches and beams is further developed, consisting the transmission of a pair of consecutive pitches to each arch. The stiffening system is thus composed of the four beams forming the edges of the a fore mentioned pairs of beams arranged on the vertical plain.

The Municipal Administration of Schio has promoted steps for buying both the shed buildings of the Conte Woollen Mill and the sorting shed at the Lanerossi Factory so that they can be suitably recovered and restored to the town's use with a new function.

3 A SUSTAINABLE RECOVERY FOR THE INDUSTRIAL HERITAGE?

In recent years in our country there has been a progressive awareness of the buildings in the industrial heritage, which has led to the refining of a culture of the recovery project aimed specifically at preserving them while respecting the original particular features of stratified memory in the man-made context and at valorising their residual potentials.

There are many reasons that make the interventions for the recovery of the industrial heritage competitive, on condition that they are assessed globally and refer also to parameters of quality as well as quantity, which include achieving a good level of *sustainability*. For this purpose the recovery of old buildings alone allows the saving of the resources necessary for a new building and makes it possible to keep down the consumption of vast surfaces of land. However, the essential condition for the survival of the old buildings is to ensure that they will have a function that will restore them to the production circuit, to all effects.

The evaluation of the *transformability* of these bodies concerns on the one hand their load-bearing frame and, on the other, the shell that encloses them, which in turn is closely connected to the frame.

With reference to the first aspect there is the widespread presence of relatively simple, repetitive and sturdy, types of loadbearing structures, characterised also by high internal *flexibility* (notable spans for distributions organised internally on point support structures), which generally allow good integration of the layout, favoured by the types of the structures themselves and by the presence of spaces intended for containing various types of equipment (*integrability*).

The original vertical bearing skeletons are in the majority of cases loadbearing brick masonry or reinforced concrete, or mixed structures, only rarely steel, while the floors and roofs are sometimes of wood, more rarely steel or reinforced concrete. This generally results in the possibility of adapting them to the current criteria of *structural reliability* without requiring too much work or upsetting the original systems, resorting to extraordinary maintenance work carried out over a period of time (generally to remove the effects of neglect, especially if the building has been unused for a long time); there is also ample possibility of adapting them for new uses, to be assessed case by case. This is above all due to the fact that the structures were originally intended to support high accidental overloads of



Figure 8. View of the Marzotto factory at Valdagno during construction 1961–1962 Span 60 m (from the P. Guaraldo catalogue). The structural layout is a development of the solution realised at Schio for the construction of the sorting shed at the “Francesco Rossi” Woollen Mill (figs 4–7).

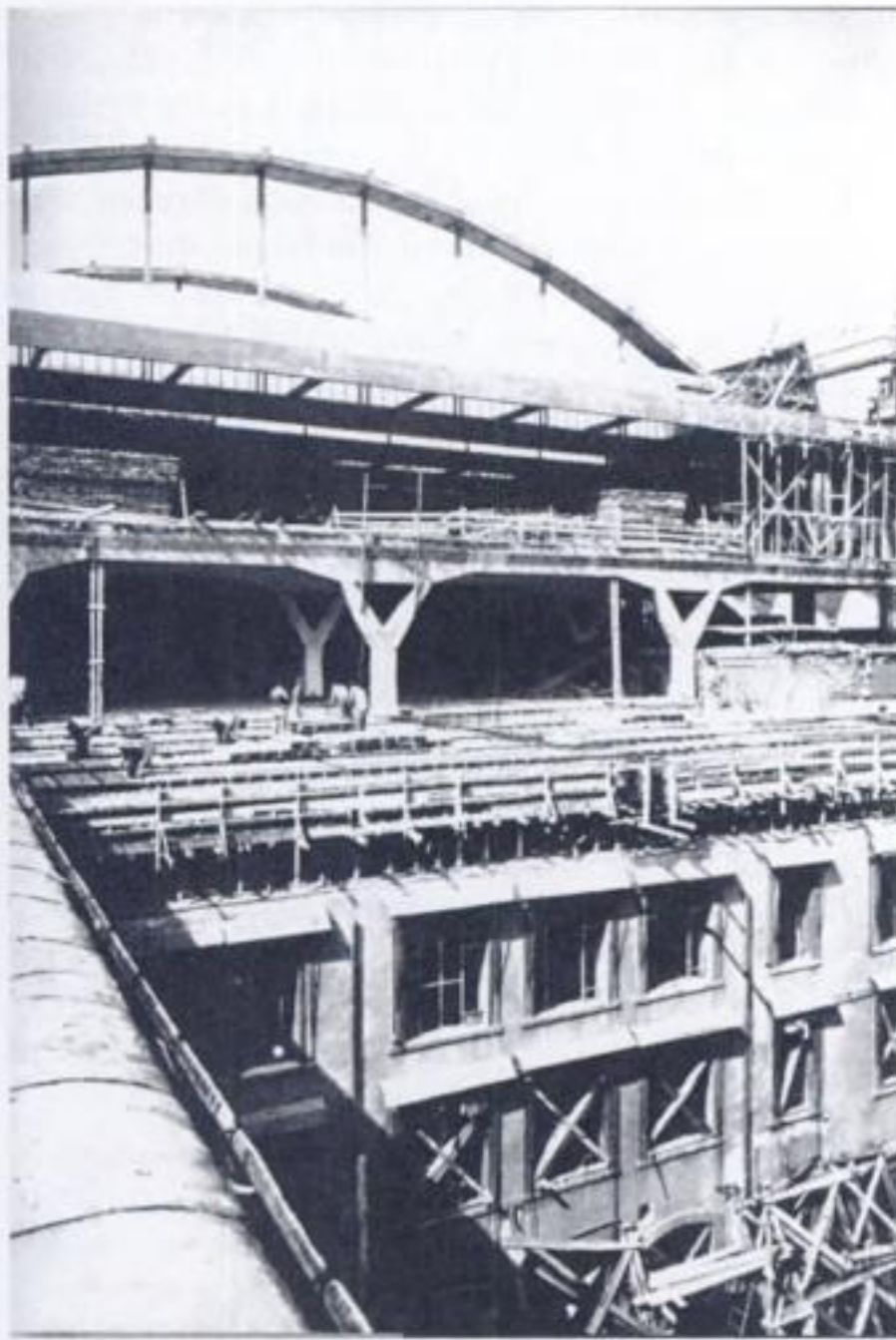


Figure 9. Another view of the building site of the Marzotto factory designed by professor engineer Bruno Dall’Aglia.

both a static and dynamic nature and the movement of people and goods, but they were also able to resist significant thermal stress, often accompanied by the aggressive action of chemical agents used for various purposes in industrial processes.

As regards the second aspect, that of the strategic decisions for the shell, these must consider the thermal-hygrometric and acoustic aspects and the levels of performance that generally ensure the *comfort*

of the internal environments with relation to the intended new uses.

When they are not made of a loadbearing structure of solid bricks, the shells are generally composed of curtain walls enclosed between the links of the loadbearing skeleton with beams and pillars, almost always visible on both the outside and the inside.

In these cases they are composite, discontinuous surfaces, with frequent openings, on which may still be seen traces of the transformations carried out on the factory over time. These surfaces are nearly always unsuited to perform the closing function and require specific intervention to correct their performance (introduction of ventilated cavities, etc.).

In most cases it is fairly easy to ensure good levels of natural lighting and ventilation of the premises, considering the particular features of the shells of the old factories, as has been demonstrated by many examples of recovery, while it seems to be more difficult to guarantee the thermal and hygrometric insulation of the closures (vertical, top and bottom) without altering the features of the old systems.

With reference to the possibility of reconciling examples of *sustainable development* with the need to transform the old industrial structures to adapt them to new functions, a series of aspects are summed up below which should be assessed in the design stage:

1. The structures are generally composed of well-designed, sturdy loadbearing skeletons, suited to resist high static and dynamic loads (structures with loadbearing masonry, spatial frames in reinforced concrete well wind-braced by cores and septums, mixed loadbearing masonry structures of brick and pillars, beams and floors in reinforced concrete) and are therefore adaptable to new functions, as long as they are compatible;
2. The loadbearing structures in reinforced concrete are very often used only on the inside, while the shells are made of massive loadbearing masonry, suited at the same time to ensure long-lasting behaviour of the structural skeleton they protect and good thermal inertia of the shell;
3. The interiors are generally well lit with large windows on the façades and/or with diffused overhead lighting obtained from windows created between roof slabs located at different heights or from various types of skylights in the flat roofs or from shed solutions;
4. The “out of scale” dimensions, typical of the built spaces of industrial factories, allow a good degree of transformability; they also allow the adoption of “double shell” solutions, aimed both at not loading the weights of the new overloads on the pre-existing structures, when the latter are unable to support them, and at solving the problem of ensuring the energy efficiency of the shells, without altering the visual impact of the original building;

5. In old industrial structures there are wide spaces, in which it is possible to install the equipment for the centralised management of the microclimate and for the backup of the natural circulation of air in the cavities (very often there are already many air ducts that can be easily used with the necessary technological integrations);
6. On careful analysis, many structures are themselves machines of systems that are suitable for being updated and exploited, using innovative solutions widely available today, but applying these together with traditional low-tech technologies of proven efficiency obtained by the recovery of the original systems.

On the other hand there are problematic aspects to be considered in the assessment of transformability for the recuperation of old buildings:

- Guarantee of acceptable levels of structural reliability and of fire resistance, without radically altering the structure and its image;
- Necessity of protecting the loadbearing skeleton from the direct exposure to the agents of decay, especially in the case of slender reinforced concrete structures, successfully reconciling it with the conservation of the particular characteristics of the work;
- Necessity of guaranteeing a good level of internal comfort without altering the value of the structure, taking skilful action on the shell.

4 CONCLUSIONS

What role should be assigned to technology on the horizon of the project, a decisive and strategic act, between the extremes of conservation and reuse, to be understood not as antagonists, but rather as poles between which to choose case by case, with relation to the particular architectural and technological-constructive features, while respecting the pre-existing elements and their recognisability over time?

The following general criteria may be listed:

- Reinforced concrete may be successfully subjected to restoration interventions of not only a cortical nature (that is, concerning only the concrete cover of the reinforcement), but also of a structural nature, that is concerning significant portions of concrete, but it must then be suitably protected against the aggression of the environment (both with local treatments and by excluding direct contact with the outside);

- The principle of the maximum respect of the original characteristics and of the original materials and technologies must be safeguarded, when the interventions concern the preservation of buildings of special architectural or historic-documentary interest;
- The suitability of the integrated use of traditional and innovative technologies must always be considered in interventions aimed at restoring old buildings for new functions, paying the maximum attention to the legibility and recognisability of the new interventions as distinct from the previous ones;
- Preference should always be given to the exploitation of the inherent potential of the old buildings to accept innovative energy solutions based on energy saving and aimed at sustainability, always trying to integrate the innovative approach with the existing traditional elements;
- The valorisation of local expressions of recent history must be stressed in order to favour the cultural identity of the territory and to establish hierarchies in the quality of the man-made fabric around the traces that best represent it, as historic, social, documentary and aggregating values.

REFERENCES

- Dall'Aglio, B. 1961. Su un nuovo tipo di copertura a shed per edifici industriali. Institute of Building Science of the University of Padua (15)
- Dall'Aglio, B. 1963a. La copertura del nuovo salone di tessitura del Lanificio Marzotto a Valdagno. Institute of Building Science of the University of Padua (19)
- Dall'Aglio, B. 1963b. Indagine sperimentale su un elemento di copertura a shed: struttura in foglio realizzata in laterizio e calcestruzzo armato. Institute of Building Science of the University of Padua (20)
- Franco, G. 2003. Riquilificare l'edilizia contemporanea, Milan: Franco Angeli
- Guaraldo s.p.a. 2000. 1945–2000. Cinquantacinque anni di attività. Paese (TV): Guaraldo
- Mancuso, F. 1990. Archeologia Industriale nel Veneto, Cinisello Balsamo (MI): Silvana
- Nelva, R. & Signorelli, B. 1990. Avvento ed evoluzione del calcestruzzo armato in Italia: il sistema Hennebique, Milano: AITEC, Associazione Tecnico Economica del Cemento
- Mazzotta, D. 1995. Archeologia Industriale, -La stagione del recupero, Venezia: Quaranta interventi negli ultimi vent'anni, IUAV – Dipartimento di Urbanistica Venezia
- Riva, G. 2004. Le radici di una comunità nello studio delle attività economico-industriali del primo Novecento a Spinea. Atti del Convegno promosso dall'Assessorato alla cultura della Città di Spinea. Spinea (VE): Helvetia
- Zorgno, A. 1985. La materia e il costruito, Milan: Alinea

Technical state and renovation of buildings of Wrocław's 19th century city centre development

P. Berkowski, G. Dmochowski, M.Y. Minch & J. Szolomicki
Wrocław University of Technology, Wrocław, Poland

ABSTRACT: Most of Wrocław's city centre development occurred towards the end of 19th and at the beginning of the 20th century. After the Second World War, major repairs were generally not conducted in the buildings that had survived destruction, it was assumed that they would be demolished and replaced by new buildings, once they became too dilapidated. This meant that it was barely 10 years ago when repair and renovation of these buildings began. These buildings have achieved expected mean time of service life, i.e. about 100 years, taking into account that they had not been repaired for so long. Now these buildings are in very poor technical condition. The review of about 80 buildings was carried out by the authors. This paper is an attempt to summarize the results of that assessment and to present ways of partially or fully revitalizing these structures.

1 INTRODUCTION

The authors performed several tens of technical assessments and did construction designs concerning fragmentary and major repairs of Wrocław's late 19th century city centre buildings. This article is an attempt to summarize the results of performed assessments, and to put forward ideas on ways of repairing these kind of buildings.

2 A GENERAL DESCRIPTION OF THE BUILDINGS UNDER REPAIR

Most of the city centre buildings in Wrocław were erected at the end of the 19th century or at the beginning of the 20th century, in a quarter settlement, with compact sequences of buildings along particular streets. These are generally four- or five-storey buildings with cellars and with what is called traditional construction. The walls and foundations are made of brick, and the ceilings above the cellars are solid, of the Klein type or in the form of segmental barrel vaults on steel beams. The floors between storeys are of wood with a sound boarding. The rafter framing is wooden, most commonly of bidding rafters and rafters, with a characteristic so-called false Wrocław roof, i.e. a slanted roof slope covered with roofing tile at the front and a flat part covered with roofing paper at the further back. The staircases are usually steel, of the stringer type, with wooden stair treads, based on solid staircase landings made of Klein board on steel beams. The

balcony structure is a solid bracket. Steel beams are the carrying items, and between them there is a Klein slab (a brick plate with steel reinforcement), brick placed on T-bars or prefabricated reinforced concrete slab.

3 A DESCRIPTION OF THE TYPICAL TYPES OF DAMAGE TO BUILDINGS AND THE REASONS FOR ITS OCCURRENCE

In Poland, the time of service life of the described buildings, by which we mean objects with brick walls and wooden floors, is estimated at about 80–120 years. After the war, it was assumed that as they achieved a high enough level of dilapidation, these buildings would be demolished and replaced with new ones. Thus no repair work was done, not even the most basic kind in many cases, which left the buildings in a significant state of disrepair, and some in almost disastrous condition. Not until only recently have overhauls of a few these buildings been done and repairs on other started. Since not enough funds are assigned for the latter purpose, these repairs are usually local, most often concerning elements in a failure or pre-failure condition.

3.1 Foundations

The foundations of the discussed buildings are made of common burnt brick on lime or cement-lime mortar. During their erection, the buildings did not have any horizontal insulation installed; there was usually a

circumferential pipe drainage made. During war activities, the draining system got damaged and was never repaired. This caused long-term saturation in the foundations and cellar walls and structural brick and mortar damage (slacking). At the moment, horizontal insulations are being done by resin injection, and the most damaged brick foundations are being strengthened by injections or by the placement of concrete.

3.2 *Load-bearing walls*

The walls of the buildings are made of common burnt brick on lime mortar. The thickness of the walls is between 62 and 72 cm in the cellars and on the ground floor, and up to 42 cm on higher floors. These walls are generally in a good technical condition. In general, it is only the decorative elements, external plaster and flashing work which have become got damaged. The wall brick became corroded on the surface, especially at ground level (Figs 1, 2) where it is most exposed to rainfall splashing. Here and there, on the walls inside the flats, there are traces of freezing and moistening. These walls do not fulfil requirements of currently obligatory thermal standard, but their insulating power is good enough, so the kinds of failure described above are local and are most often caused by a loss of cornices, plaster or flashing work on the elevation, or by leaks through the window woodwork. Due to the historic character of the buildings, there is no permission to additionally protect them from the effects of cold, but it appears that it will be enough to repair the described failures.

3.3 *Floors above cellars*

The floors placed above the cellars are of a solid construction. They are Klein slabs or segmental barrel vaults based on steel beams (Fig. 3). In most cases, the floors are humid, and the steel beams, brick vaults and their pointing are corroded on the surface. Increased humidity in the cellars caused by the lack of effectively operating drainage and horizontal and vertical insulation had an influence on the development of the corrosion. In extreme cases, complete corrosion of the intersection of the steel beams intersection may occur. Steel delaminating may also occur, because, due to its production process, the steel from this period of time is vulnerable to this kind of damage.

The repair procedures consist of exchanging the most damaged floor fragments, strengthening the existing beams, or cleaning and applying anticorrosion protection.

During the repairs, the cellars are dried, and the brick vaults are pointed. In the case of vault surface damage, strengthening work is done using appropriate substance, and the vaults are pointed.



Figure 1. An example of a deteriorated front façade.



Figure 2. An example of a deteriorated back façade.

3.4 *Floors between storeys*

The floors between the storeys are wooden, with sound boarding. In places, where the manner of their usage was not changed, they most often remained in good



Figure 3. A segmental barrel vault floor above cellar.



Figure 4. The deterioration of a wooden floor under a roof.



Figure 5. A toilet situated on a staircase landing.

technical condition. During the years after the war, in the majority of flats, the functional and spatial arrangement was changed. Before the war, in most cases, on every storey there were one or two flats and the toilets were usually situated on staircase landings (Fig. 5).

After the war, these flats were divided into a few separate flats, sometimes even five or six. This meant that new kitchen spaces, and later on bathrooms and toilet had to be created, on completely ill-adapted wooden floors (in the original layout, solid floors underlay the kitchens and bathrooms). While spaces were adapted for these goals, very often there were no moisture insulations made on the floors. This caused their saturation with moisture, and later, biological corrosion. Because of that, there have been a few serious ceiling failures, even involving injury as sections of inhabited flats collapsed into inhabited flats on lower floors. While the arrangement of the flats was being changed, some of the dividing walls were moved or removed. The original dividing walls had a timber construction with a brick filling. They were based on single wooden floor beams. The load capacity of these beams was too low to transfer live loads and the dividing wall weight, but these walls either had originally been placed up the whole height of the building, thus supporting one another, or had co-operated with floor beams, creating framework structure.

When new doorways were made in or removed from these walls, this structure was violated. Also, the floor beams loaded with the new walls were not adjusted to this purpose, and show deflections and damage. The beams exploited as per their original designation retained a suitable load capacity and are not excessively deflected. Most of them were not biologically corroded, because, although the wood was not protected against corrosion, the resin was not removed from the beams that were used; this was enough to prevent damage. At the moment, the damaged floor items are being exchanged with new ones, and in wet-use rooms (kitchens, bathrooms, etc.) solid floors are being installed. Renewed transformation of some flats to their original layouts is also occurring as smaller flats are purchased and joined back into one or two larger flats.

3.5 Roofs

The roof structure is wooden, mostly built of rafters and bidding rafters, distinguished by the fact that from the front of the building, the hipped roof end is slanted, covered with roofing-tile, while further back, it is flat, covered with roofing paper. The technical condition of the rafting framing depends on the tightness of the roofing and the condition of roof work, gutters and down-pipes. In the damaged parts of these elements, biological corrosion developed almost immediately, sometimes along the whole thickness of the intersection (Figs 6, 7).

The most endangered elements were the wall plates, which are almost completely damaged in most buildings. Within the correctly secured roof slopes, most of the elements are in a sufficiently good condition.



Figure 6. Deterioration of a wooden roof structure.



Figure 7. Details of wooden roof biological corrosion.

They are generally only superficially damaged by larvae of wood borer (woodworm larvae). Often, because of wide leaks on the hipped roof end, the wooden floor of the attic and even the floor of the storey below suffered biological corrosion.

The ends of the attic ceiling beams based on the external masonry are especially endangered by biological corrosion. This is caused by excessive moisture in a wall coping connected with leaks in the gutters and roof work.

The damaged elements of the roofing are being exchanged during the repair process.

3.6 Balconies

The bracket structure of the balconies is solid, based on steel beams. The filling is composed of Klein boards, prefabricated ferro-concrete slabs (Fig. 8) or bricks, based on T-bars (Figs 9, 10). The structural condition of all the c. 150 assessed balconies is bad. The fillings,



Figure 8. A prefabricated ferro-concrete balcony slab.



Figure 9. A balcony brick slab on T-bars.



Figure 10. A steel staircase.

composed of bricks or boards are corroded, there is loss of plaster and fillings, and there is also balustrade damage. In all the balconies, there is also a corrosion of carrying beams. In extreme cases, this damage caused the

possible risk in the evaluation of the building wear considers usually economical matters. Modern techniques used in building industry permit a quick reduction of errors in the evaluation and bring the building to the state that meets investor's demands (Marcinkowska & Berkowski 2001).

Depending on the degree of structural deterioration, the object is qualified for repair, major repair or demolition (Table 1), if other factors (social, maintenance or functional) do not decide about this. Then, depending on the gathered funds, a modernisation of the building is commenced. At the moment, because of a chronic lack of funds, this is often only a partial repair, securing the most damaged elements.

Below, in outlines, selected repair methods of basic structural elements of renovated buildings are described.

4.1 Foundations

In case of the necessity of foundations repair or strengthening, according to the type of damage or designed future functional assignment of repaired building, there are applied different techniques of repairing or strengthening (Zaleski 1987, Masłowski & Spizewska 2000):

1. widening of existing foundations by adding of one- or two-side concrete elements or underpinning with wider RC continuous footing
2. replacement of weak foundation's parts with ground strengthening
3. replacement of the whole old foundation with a new one, starting from its weakest part with introducing of walls strengthening rested on these foundation
4. underpinning using expansive concrete
5. leaning of foundations on grouting or drill piles in case of weak or wet soil.

It should be stated out that old foundations were generally designed with great safety factors, so these structures have rather significant strength reserves. In this cases, stresses in the soil ought to be verified before taking a decision of foundation strengthening.

4.2 Walls

In case of cracked walls the analysis of crack system is realised. Among other things, there are studied: lay-out and running of cracks, measurements of their width and depth, changes of their running during building life service. In many cases the lay-out of cracks helps to identify the cause of their formation. One can start to eliminate cracks after the elimination of the causes of their formation. According to the size of damage or the type of element to be repaired, the following techniques can be used (Zaleski 1987, Masłowski & Spizewska 2000):

1. mortar injections into small cracks that are running through joints between bricks
2. re-erection of cracked masonry with new bricks
3. in case of wide cracks, they can be additionally "quilt" using steel rods or strengthen with steel bars
4. column strengthening using steel or concrete reinforcement
5. repair of headers by introducing steel or concrete beams
6. in case of longitudinal and lateral walls, parting anchoring using steel strings or glued ties can be applied.

Wall repair is finished with plaster work, renovating of stuccowork and other decorative elements. If it is possible the walls are also protected from cold and wet.

Table 1. Technical condition classification of buildings.

Element condition classification	Building element deterioration percentage	Criteria of element assessment
Good	0–30	Elements of the building (or a sort of construction finish, fittings) – are well-kept and preserved, and correspond with standard specifications. Only current preservation is required.
Average	31–50	Elements of the building are kept appropriately. Local damage and losses are acceptable. Current preservation and repair work of single elements of the building are required.
Poor	51–70	Elements of the building have considerable damage or losses. Features and qualities of built-in materials have a reduced class and technical wear. Complex repair of the building is required.
Unsatisfactory	Above 70	Elements of the building show considerable damage and wear; they may endanger a security of tenants. The major repair or demolition is required.

4.3 Solid floors above cellars

In the repair of damaged solid floors above cellars there are used:

1. replacement of the whole floor structure, i.e. steel beams and masonry vaults with RC slabs on steel beams
2. in case of large-span vaults strengthening is made by applying RC shell.

4.4 Wooden floors and roofs

Repair of the damaged wooden inter-storey floors and rafting framing is conducted with classical technologies or using glued connections (Jasieńko 2003, Masłowski & Spizewska 2000). Conventional methods are as follows:

1. replacement of the wooden floor with the concrete monolithic or prefabricated slab floor on steel beams
2. strengthening of the floor structure by making an additional, independent steel bearing structure that can carry on all the loads except own floor weight
3. suspending of the existing floor structure to a new bearing construction; in this case all the loads are carried on by the new floor
4. strengthening by using new elements that collaborate with existing floor or roof elements: wooden or steel cover plates, replacement of damaged wooden beams parts, applying of concrete plate laid on the old wooden beams (Godycki-Ćwirko & Mielcarek 1997), strengthening with steel strings
5. replacement of the whole wooden roof structure with steel trusses.

Unconventional methods consist of applying the technology of steel rods or plates resin inserting or sticking reinforced carbon strips (Jasieńko 2003).

4.5 Balconies

The balconies are the most often repaired constructional elements of the old buildings. It is because of their great level of destruction and threat it means for their tenants. In the process of balconies repair there are used:

1. replacement of the whole structure, i.e. steel bearing beams and slabs, by using new RC slabs on steel girders
2. leaving the existing steel beams (in case of their good condition) and replacement of Klein or Wygasch plates with RC monolithic or prefabricated slabs.

In all these cases there are placed new modern insulations and all the decorations and railings are renewed.

5 CONCLUSION

After making overhauls in several tens of buildings from the turn of the 19th century, one may generally state, that their traditional structure with solid brick walls and wooden floors bore the passage of time passing.

In spite of great war damage, and later on, long-term lack of any repairs, the basic elements of these buildings were not damaged, and they preserved their service values (Figs 13, 14). Sometimes over 100 years from their being built, it is clearly visible that with suitable preservation, the term of their service life can be longer than theoretically assumed, i.e. 80–100 years.

At the same time, one can unambiguously feel that the basic factor which has an influence on the term of a building's existence is its current, careful preservation. Even a little negligence, such as a long lack of exchange of a damaged gutter, can lead to a malfunction of a whole fragment of a building.



Figure 13. An example of a well preserved building façade.



Figure 14. An example of a well preserved building façade.



Figure 15. An example of a renovated building façade.



Figure 16. An example of a revitalized building.

Even partial repair, removing the most damaged elements, leads to the housing community, which is generally the owner or co-owner of objects, more willingly decide to undertake further modernizing work, sometimes of a wide range (Figs 15, 16).

The second extremely important factor, determining the term of building service life is its use in accordance with its original functional and spatial arrangement. All functional changes should be reconsidered and adjusted to the character of the original building structure.

REFERENCES

- Godycki-Ćwirko, T. & Mielcarek Z. 1997. Renovation of old wooden roofs (in Polish). *Przegląd Budowlany* 2: 12–14.
- Jasiński, J. 2003. *Resin and structural compounds in repair, conservation and strengthening of historical wooden structures* (in Polish). Wrocław: DWE.
- Marcinkowska, E. & Berkowski, P. 2001. Evaluation of technical wear and modernisation of R/C structure from beginnings of the 20th century. In (ed.), *Developments in Building Technology; Proc. int. conf., Bratislava, 12–14 September 2001*. Bratislava: STU.
- Masłowski, E. & Spiżewska, D. 2000. *Strengthening of building structures* (in Polish). Warszawa: Arkady.
- Zaleski, St. (ed.) 1987. *Repairs and modernisation of houses* (in Polish). Warszawa: Arkady.

Constructive typologies investigation and approach proposals for the valuation of masonry arch state

C. Cennamo

Department of Cultura del Progetto, 2nd University of Naples, Aversa, Italy

S. D'Angelo

Interdepartmental Centre of Beni Culturali, University of Naples Federico II, Naples, Italy

G. Voiello

Department of Scienza delle Costruzioni, University of Naples Federico II, Naples, Italy

ABSTRACT: A great many among ancient bridges that are still used regularly for the urban mobility, have a lot of problems, caused often by the absence of appropriate maintenance interventions: in fact, an exact valuation of the general "state", for all the masonry structures and for the ancient masonry arch bridges in particular, is very onerous, also because the existent approach methods are not simply applicable; so, generally, work-assigned people prefer a "total restoration" of the examined structure, even if the real necessity could be lower: sometimes, just these interventions have created the biggest problems. For this reason, it is necessary to determine a no-intrusive approach technique that can be used to know, at every time, the situation of the arch bridges, beyond the entire monumental heritage.

1 INTRODUCTION

Masonry bridges – real structures of civil engineering – represent one of the most important examples of our Country historical-architectural heritage.

The most ancient ones – of Greek-Roman age – have the classic arch-shape allowing to stress the compression ashlar and keeping them together through reciprocal contrast.

Most of those structures have been lasting for centuries until now, thanks also to their great capability – given them mainly by their own weight – of strongly resisting to the stress of movable loads, in opposition to the lighter bridges made up of reinforced concrete and steel.

Many of them are still operating although without any routine maintenance in the course of time.

Other ones, on the contrary, collapsed because of unsuitable interventions both from structural and functional point of view and/or because of demolitions carried out in presence of their hydraulic incompatibility with the present design floods.

Assumed that, this research points out the crucial importance of the intervention criteria consistent with the building conception of those structures since, thanks to the new building materials and advanced

technologies of intervention, many of these works have been completely changed in their original structures causing some "gaps", which made them more vulnerable to external factors.

Indeed, all that shouldn't be done without a previous careful case-history of the historical period in which they were built and then of the building typologies and technique used.

2 THE ROMAN MASONRY BRIDGES: TYPOLOGIES AND BUILDING TECHNIQUES

Masonry bridges are an important evidence of a past civilisation and ancient building technique.

The bridge – whatever material its made up of: wood, iron, stone, concrete – is an architectural work that has been always deputed to link two places divided by a river, hill, ravine or something else, *leaving a space below for water flow or, sometimes, for the eventual traffic or structure discharge* (Galliazzo, 1995).

In this way, the bridge has played an important role, during the centuries, not only from the historical-building point of view, but above all for its capability

of connecting Regions, cities and villages making peoples of different civilisation meet together.

In particular, the most ancient ones, the Roman stone bridges, called *pons lapideus* or *pons lapidis*, in order to overcome difficult topographic situations, show a building typology – afterwards become a real reference model – characterised by several arches increasing according to the lights to be covered. They can be symmetric or asymmetric with lateral abutments perforated or not by arches or discharge windows.

Unfortunately, because of the important restorations and changes they have undergone during the ages, the existing Roman bridges often show a shape different from the original one and, contextually, their being different from each other makes a classification difficult to be done.

Generally, classifications are done starting from their usage destination, materials and building techniques used.

Indeed, the most common materials can be found in the several variety of tuff (the tuff of Grotta di Oseno, the Fidene tuff and so on), limestone (travertine) and sandstone, as well as iron and lead.

All those materials share a good resistance, easy workability and good adhesion to mortars.

By classifying the bridges with a particular similarity, both as regards materials and building techniques within the Campania Region, we pointed out a peculiar bridge typology, the “Campania type”:

“Its a particular technique entailing an already built bag core, while the faces consist in bricks (opus testaceum) and/or in opus mixtum ... even if there are tuff block curtains in opus vittatum or in opus vittatum mixtum, also, with a variegated displacement: in general, piers show sight faces or brick faces, or opus mixtum ones with bricks, or very seldom with square worked facing, while the arches are made up of opus testaceum, namely bricks, and often with header arches with double roll and overlapped bipedales” (Galliazzo, 1995).

Among that kind of bridges placed in Campania, we find: viaduct-bridge near the Agnano’s Thermae, viaduct-bridge in Monte Dolce near Pozzuoli, viaduct-bridge in Ronaco near Sessa Aurunca (Coletta, 1989) (Fig. 1).

A special interpretation of the Campania type is represented by the “Trajan type”, that is a typology based not mainly on materials, but on different levels of each pier overlapped layers and on the relation between the header arches of the arcade with the respective crowning frame (Galliazzo, 1995).

The typical example of that type is the Leproso Bridge (Fig. 2) that, dating back to the 1st century B. Ch., stands on Sabato river – left tributary of Calore Irpino river (Benevento), one of the most important river of South Italy hydrography.



Figure 1. Ronaco viaduct-bridge in Sessa Aurunca.



Figure 2. Ancient picture shown Leproso bridge in Benevento.



Figure 3. An old picture of Leproso bridge.

It has a typical Roman hog-backed structure, with quite short abutments despite its remarkably length (Fig. 3).

It consists of three – once five – arches (with discharge and flow windows), realised to repair the damages caused by the 1702 earthquake (Fig. 4).

Although it has been restructured many times, it still preserves some original elements such as: the



Figure 4. Comparison with a present picture shown Leproso bridge.

semicircular overhanging buttresses downhill with covers characterised by semi-pyramidal caps with a triangle base and a limestone slabs mat partly repaired.

3 ABOUT THE STATIC CONCEPTION OF ARCH MASONRY STRUCTURES

The problem of safety for arch masonry structures placed in the present historical/monumental building heritage, has become more and more crucial because of the progressive decay of environmental conditions and, sometimes, also arbitrary adaptation and consolidation interventions or, on the contrary, negligent maintenance. Besides, in those areas particularly affected by frequent seismic activity, there is need for preventing the damages produced by a violent and instantaneous earthquake stress, which suddenly transforms the static condition of those particular structures. In those cases, great importance is given to the mitigation of the so-called "seismic risk" and among the factors contributing to its assessment, the institutional competence of architects and engineers is the assessment of "vulnerability". The work of a structure expert consists in restoring the static functionality of arch bridges by integrally preserving the building logic and the original project, being conformed to the used technologies and materials, in order to obtain the whole structure restoration, without interfering with the layered architectural features of the environmental context.

The consolidation strategies should be chosen in order to ensure structural safety with regard to the staticmechanical (and historical) characteristics and should be conditioned by the destination of use, which binds many structural choices too.

In order to define a methodology on which basing a reliable checking criterion and a suitable intervention procedure, we should know the static behaviour

of the masonry building through working out mechanical models targeted to understand, in a satisfying – although not exactly – way, the structure response to external stress.

According to this view, it could be useful to investigate the former routes through a careful research on building methods, as well as the way of conceiving and proportionate the arch bridges used by past designers and builders. Besides, the careful investigation of ruins and collapses, individuation of their causes, comparison among the characteristics of ruined bridges and those well preserved, together with the codifications and rules contained in treatises and handbooks are the elements helping not only to perceive the behaviour but also to point out the structure capacity of bearing external perturbations and therefore its reliability and safety.

All that represents the "experience" heritage of the present-day structural expert undertaking a static restoration of an ancient structure. Indeed, it is the structure itself that gives instructions for its structural recovery to the person understanding its reading code, in the same way as few feeble traces give archaeologists important information about past civilizations.

Masonry resistance to compression and its non-resistance to traction have always conditioned the stone structures building, in particular the arch ones. The builders – more or less consciously – are engaged in conceiving structures bearing applied loads without provoking traction stresses in order to reach equilibrium by provoking only compression stresses – and of course that should be considered also in static restoring works.

What above said has been confirmed by Heyman's investigations on ancient monumental buildings and bridges. Indeed, by reviewing the eighteenth-century studies on vault static, he was the first to transfer the philosophy of Limit Analysis to stone structures (J. Heyman, 1966–1969).

Actually, when the hypotheses of elastic calculation fail, the logic to be followed is that of collapse analysis, used for metal structures, according to the hypotheses of non-deformability, no traction resistance and unlimited compression resistance.

In fact from studying old treatises on construction science and reading the ancient structural systems, it comes out how, already in the ancient times, they thought that planning masonry arch structures should be more based on a correct design of arch outline than to the compatibility of applied strengths with material resistance. Therefore the so-called "geometric methods" could be the premise for including masonry arch structures into the theory of Limit Analysis theory.

A formulation of the concept of arches cracking mechanism and the relative corollaries on the shape and location of ashlar rotation hinge as consequence of fractures can be already found in Leonardo's studies.

Although knowing either the basic theorems of Limit Analysis or static cardinal equations, he realized that arch resistance depended on the relations among the sizes of its components.

Only at the beginning of the eighteenth-century, we find the first methods based on assumptions connected with static equilibrium, even if Stevino (1608) and Roberval (1693) had already investigated equilibrium in terms of forces composition principles. It was in 1714, in France, that the first treatise dealing exclusively on bridges was printed, the *Traité des ponts*, edited several times until 1765. In that treatise, Hubert Gautier collects the principles of correct building, looking for the right relations among abutments, arches and piers but also those related to the easy connection with road network.

Among the hypotheses worked out in the eighteenth-century, the studies of De La Hire (1712), Bélidor (1729) and Couplet (1772) are really interesting. Following the principles of funicular polygon and static-graphic methods, they determine the arch outline, seen as a group of ashlar, subject to their own weight, all placed in equilibrium among the adjacent ashlar on which they exert thrusts and receive support and stability. At first, the joints without appeal to friction, afterwards the capacity of resistance to ashlar sliding is looked for in order to overcome equilibrium situations – paradoxical in that context – such as those of the section placed on the bearing base of a circular arch.

However, it was Columb (1773) the studier who, by introducing the concept of friction as basic element in masonry portal-arch equilibrium, finally solved the problem, changing deeply the eighteenth-century mechanic model.

In the nineteenth century, other investigation methods on arch structures stability were worked out and the most important contributions were given by Méry (1833) and Mosely (1840) who, by introducing the principle of “minimum thrust” to be associated to equilibrium, recognized the “hyperstatic” characteristic of the problem and worked out the most widespread method to verify and dimension arch structures until the end of the twentieth century.

In the meantime, with the development of the theory of elasticity and the contributions of Navier (1862), Winkler (1858), Clapeyron (1833), Menabrea (1858) and others, the foundations of the modern Theory of Structures were laid.

In those studies we get a clear view of the question concerning structures resistance both from the static and strain question, because they point out the need for checking that in all the building elements the stress state and strain one are included in the materials levels of admissibility.

That represents an important turning point: the attention of building experts is no more paid only to the “design” but also – and above all – to “verification”.

On summing up, in the eighteenth-century treatises, arch is seen as a system of rigid ashlar with a indefinitely compression resistance (rigid model). They pointed out the pressure lines, all meeting equilibrium requirements, but weren't able to univocally determine the “real” pressure line since, starting only from static, it was no possible to individuate the value of the keystone thrust as well as its exact application point.

All this static uncertainly comes from the fact that such attempts aimed at finding a solution to the hyperstatic problem with equilibrium as the only requisite, not recognizing the other basic aspect of the Structures Theory, i.e. the congruence of strains.

With the Theory of Elasticity development, arch was studied as an elastic beam with curvilinear axis fixed or hinged at the ends and so being hyperstatic and no more as non-deformable rigid solid.

At present the static of masonry arch structures can be investigated through the elastic analysis, or through the Limit Analysis. The elastic calculation can be used in the hypothesis of a structure perfect integrity and, therefore, dealing with masonry structures, only when there are compression stresses or a few traction. So it cannot be used in case of damage – the most frequent case in interventions of restoration and consolidation. By referring to a collapse situation, the Limit Analysis gives valid indications on structures safety levels, but it doesn't contribute to understand the intermediate states through which the examined structure has shown or is showing the first pathologic signs (Baratta, Voiello 1986).

Therefore, starting from those assumptions, we resorted again to more sophisticated calculation techniques, which take more into account the composition of masonry material being more suitable to the real behaviour of masonry structures and allow to investigate the fracture phase – being intermediate between elastic behaviour and collapse.

4 PRINCIPAL MASONRY BRIDGE PROBLEMS

The worst possible damage that a masonry bridge can undergo during its existence, is due to ground subsiding, caused by sudden alterations of the basement geology, or to the arising of horizontal loads caused principally by earthquakes; effects as dangerous can be provoked also by persistent and frequent vibrations, i.e. those provoked by trains crossing or by intense car traffic.

A masonry arch bridge, such as can be frequently found in Italy, often designed a lot of time before the seismic normative entry, and with resistance criteria valid only for vertical loads, resists the horizontal loads practically only thanks to the impressive mass that, through the inertial force action, tends to bring back

the structure into the initial configuration, contrasting the ground acceleration.

The expression of the inertial forces is, in fact

$$\begin{aligned} F_{IX_i}(\mathbf{x}, t) &= -\mu_i [\ddot{u}_i(\mathbf{x}, t) + \ddot{u}_{gx}(t)] \\ F_{IY_i}(\mathbf{x}, t) &= -\mu_i [\ddot{v}_i(\mathbf{x}, t) + \ddot{u}_{gy}(t)] \end{aligned} \quad (1)$$

where

$$\mu_i = \frac{\gamma_m \cdot A'_i}{g} \quad (2)$$

is the linear unity mass density;

$$\ddot{u}_{gx}(t) \text{ e } \ddot{u}_{gy}(t) \quad (3)$$

is the ground acceleration, respectively horizontal and vertical, γ_m is the material specific weight, A'_i is the transversal section area of a generic ashlar arch, and g is the acceleration gravity. So the inertial forces depend on the ground acceleration, on the structure mass and on the material specific weight that, in the masonry case, has a principal role for the resistance of the whole structure.

In the first years of the XVIII century, the bridges structural design were brought about by means of empiric formulations, i.e. as the Croizette-Desnoyers formula (Baratta, 1988) that reads

$$s = a + b\sqrt{2R} \quad (4)$$

where s is the arch key thickness, R is the radius of the circle concerning the imposts and a and b are two coefficients that change, respectively, the first in the case of an ordinary street or a railway one, and the second in accordance with the form.

The thickness s was multiplied by a coefficient depending on the overstructure thickness, on the overload value and on the stone break resistance; this one is the only parameter considering the material used for the bridge construction. The bridge arches are generally realized with stones, bricks or freestone; in a lot of cases, the parts considered of "secondary importance" were filled up with nogging. Also the "shoulders" were calculated with approximated formulas, i.e. the one used by the Genio Civile Italiano, that is valid for the circular arches

$$S = .05xh + .40xL + 2x(10 + L)xL/(100xf) \quad (5)$$

where h is the impost share, L is the arch span and f is the arrow.

In the case that the resultant thickness needs to be reduced, an artifice could be used consisting in the perforation of the lateral walls, so that the light can be subdivided in a lot of arches, characterizing, with this structural scheme, the whole bridge architectural aspect (Fig. 5). Generalizing under the term "masonry"

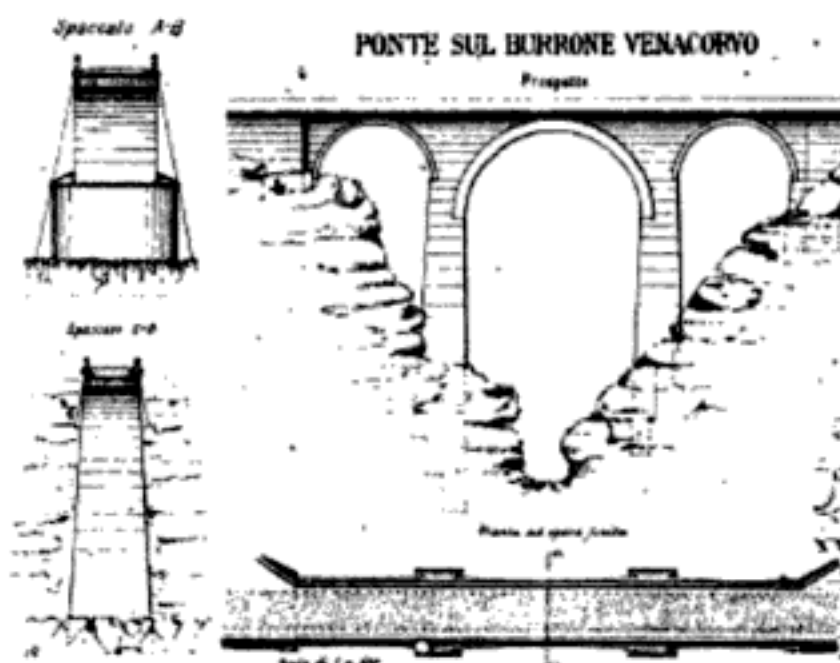


Figure 5. Plan, front and sections of the bridge built on Venacorvo ravine.

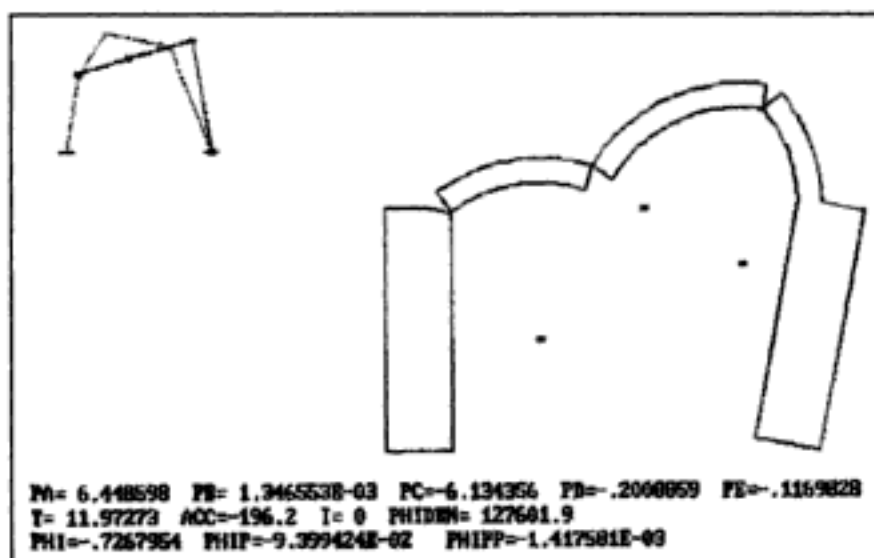


Figure 6. Collapse of a masonry arch subject to a monotonous forcing function.

all the materials that have an optimal traction resistance and a next to null pressure resistance, that have a "fragile" failure and can have either an isotropous behaviour (nogging) or an anisotropous one (squared block masonry), it is possible to say that, if a material with these parameters has certainly a good behaviour under vertical forces, it is not so good for structures subjected to horizontal forces, especially dynamics, that require the material to have a strong amount of ductility. In a special way, the ashlar masonry arch, whose resistance is given principally by the friction that the stones exercise between each other, collapses when a mechanism activated, i.e. by a seismic forcing, makes vain the "reciprocal contrast" action between the ashlar and makes impossible the return to the quiet configuration, which the inertial forces could instead favour in case the arch were kept solid (Fig. 6).

At present, in order to avoid these events, only two real ways exist: the "traditional" insertion of chains and tie rods that make the ashlar arch solid and maintain it anchored to the lateral walls and to the other structural elements, in the attempt to effect an improbable

aseismic equalization, or the whole “investigation” of the structure, grasping the history (the original project, the possible alterations, the breakages and strengthening intervention subjected in the last years, etc.) with the aim to “prepare” it for the event, to quote Giuffrè «se conosciamo il “cosa”, ne scaturisce il “come”», meaning as “come” the executed intervenes in an aimed way. In this background, the seismic vulnerability and the necessity of damage valuation must be considered, as well as the so-called “attempt damage”, whose knowledge could allow the limitation of negative effects on the structure.

4.1 The earthquakes question and the seismic vulnerability

Since it is difficult that these bridges, – built up, as can be seen, with structural concepts very far from the ones used at present – are equalized to the seismic laws, the only possibility to defend the historical bridges from the seismic effects (main and feared cause of monuments destruction in Italy), is to try to anticipate the impact in any way, whether it be “material” (on the structures) or “moral” (on people). In other words, the “attempt damage”, that is the problem to determine *a-posteriori* the risk level in order to prevent the damage. The seismic risk is treated in the probabilistic way through the old earthquakes catalogation that have occurred in a specific area, with the aim to define the place tendency to be an earthquake centre; some electronic programs, carried out by researches in the field, can localize, on the basis of probabilistic calculations given by the past earthquake catalogation, what is the probability that a seismic event will occur again in that specific site, what its intensity will be, and even when it will approximately occur. On the basis of these programs, that can be inserted in the “seismic risk” field, the structural damage can be defined; such a matter, concerns the field of civil engineering, together with the problem of structural vulnerability. As it was said, the structural vulnerability of any construction, in the specific case of a bridge built before the seismic law, refers to define the attempt damage in the earthquake shock case; so the vulnerability is linked to the seismic risk and to the earthquake foresight just in this sense. The probability matrix of damage, probabilistic expression of seismic vulnerability, is built defining a vector that contains the various levels of damage D_i included between 0 (unbroken system) and 1 (collapsing system); the seismic intensity vector is also defined, containing the different levels I_k , that are described through deterministic parameters (i.e. as the ground acceleration peak). So the vector I represents the seismic intensity medium value for a given event recorded within a specific area. In order to obtain the local value H_j it is necessary to introduce the probability $P(I_k)$ that in a given time space, a medium intensity

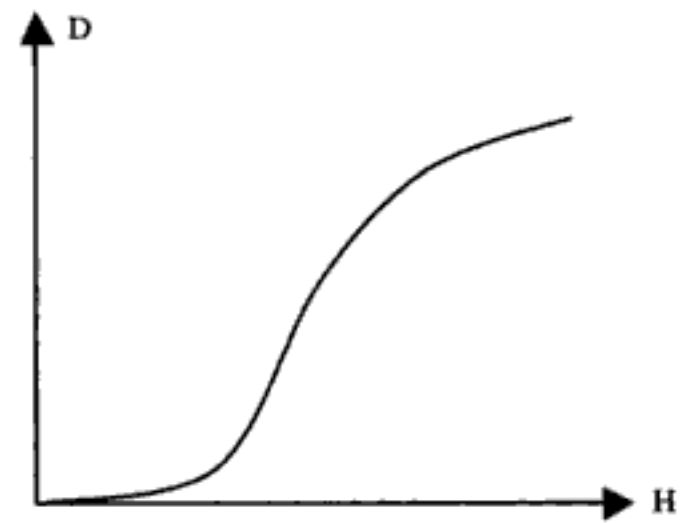


Figure 7. Scheme of vulnerability curve.

earthquake may occur. In this sense, the local value is expressed by the relation

$$P(H_j) = \sum_k P\left(\frac{H_j}{I_k}\right) P(I_k) \quad (6)$$

Finally, the probability that a damage level D_i is achieved, can be expressed by the relation

$$P(D_i) = \sum_j P\left(\frac{D_i}{H_j}\right) P(H_j) \quad (7)$$

The term $P(D_i/H_j)$ represents the elements of damage probability matrix, which expresses the seismic vulnerability in the probabilistic sense. In deterministic sense, diagramming the local seismic intensity and the damage level, the vulnerability curve is obtained (Fig. 7).

If a bridge shows an anti-symmetric plan and so some different structural characteristics and a behaviour variable with the action direction, the response of the structure or of the single resistant element can be influenced by the direction before than by the intensity of the forcing function. The response modality, as well as the element characteristics, lead to the individuation of a probable break mechanism, whose activation is subjected to the action explosion, to its intensity and to its duration.

The break mechanism involves the damage of a structural element, which occurs in the masonry arch when the material cracks itself and in that point a lateral hinge is activated; the relative rotation between the ashlar is so allowed. The hinges set, forms a so called “collapse mechanism”; in accordance with it, the arch can fall because of equilibrium loss (in particular, referring to Figure 5, the hinges are aligned) and its activation depends on motion intensity and duration.

The causes that contribute to the activation of the collapse mechanism are various: there is also the fact that the element is isolated – as in the case of bridges – the place conditions (ground subsiding etc.), the material degrade and its mechanical characteristics. At last,

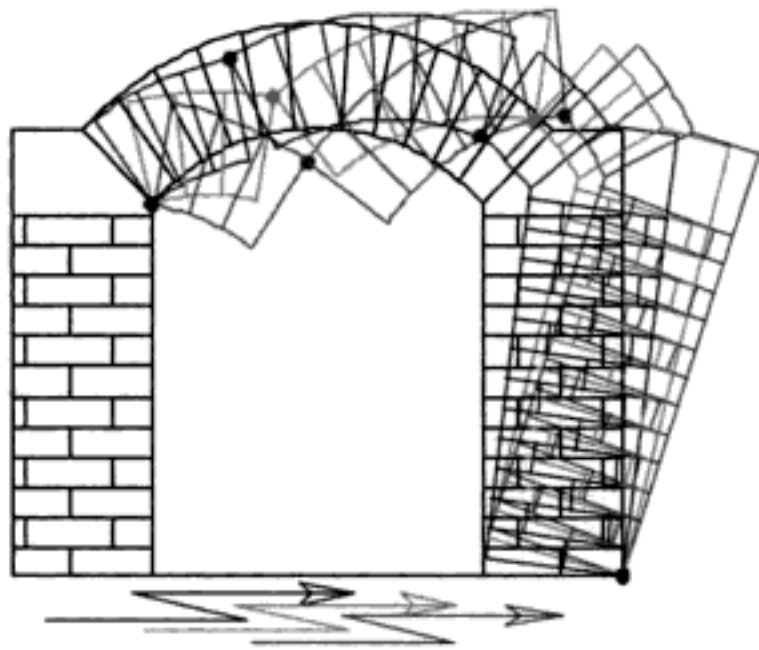


Figure 8. The arch model during the motion.

a mechanism activation doesn't necessarily imply the structural collapse, which, as already said, is very subjected to the motion duration.

From analytic view, the structural damage is related to the system plastic field excursion, and it is in connection to measures as deformations, displacements etc.; in the masonry case, the system can be schematized with a rigid-failure structural model; this model, as already said, arrives to the collapse for lost equilibrium (Fig. 8).

For this reason, for the attempt damage valuation, it is necessary to consider the action intensity and duration, both factors that determine the damage entity and the stress level in the material. So the vulnerability is estimated as the sum of two effects: the first doesn't depend on the ground acceleration characteristics, but i.e. by the material used for the construction or by the damage state and the second depends on the construction geometry or on its boundary conditions.

Other methods to determine the vulnerability curve are based on the constructions filing from experts, who fix belonging classes, according to the material used (i.e. masonry of lateral walls, of verticals etc.), with the structural state or with other parameters that are fixed on place and time by time judged suitable; on the basis of these comparisons and of one's own experience, they assign a vulnerability index that doesn't consider at all the above said boundary conditions.

The choice of the methodology to be used to define the vulnerability index and to give a given bridge a "supportability index" for a more or less serious event, and also to define the vulnerability curve and the damage probability matrix, depends on the construction age; this generally indicates whether the bridge is built up with aseismic criteria, or not: in fact it is necessary to consider that the post-law built up structures or those that have had aseismic equalizing works, can appear sufficient a qualitative investigation (vulnerability class belonging), while for the ante-law built up structures, it is necessary to use appropriate methods,

based on Mercalli and MSK scales. These scales, afterwards shortly illustrated as an example, must be equalized for the examined constructions, carrying out the single notices for the specific structures exploration, as the masonry bridges that are investigated in this work.

5 THE INTERVENTION POSSIBILITIES

5.1 The seismic intensity scales

The seismic intensity scale MSK (Medvedev, Sponhuer, Karnik, 1968), which subdivides the masonry construction according to the portant parts materials, is founded on three basic parts:

- (1) Three classes are considered, arranged in estimated way for growing seismic vulnerability (i.e. A, B, C).
- (2) Six damage levels are considered for every class, between "0" (no damage) and "5" (total collapse).
- (3) For every damage class a quantification is associated which, in the MSK formulation, refers to the construction percentage to which is possible to ascribe a given damage level.

The seismic intensity is ascribed on the basis of quantifications (3) found for each combination obtained crossing (1) and (2), for the intensity between V and X.

The tables obtained arranging the seismic degree in abscissas and the damage levels in ordinates for every typological class, can be used to estimate either the structure per cent that undergo a determined damage level for a determined seismic intensity or to value an earthquake intensity on the basis of the damage pointed out. The other valuation method used at present is based on the assumption of the Mercalli's scale; which is suitable to the same double aim, but which is also functional to direct observation (i.e. to value the bridge per cent that undergo a determined damage level for a determined seismic intensity, it is necessary to know this one and that is calculated with analytical methodologies; vice versa, to value the seismic intensity on the base of the pointed out damage, it is necessary to establish the damage amount). In the follow, two phases of Mercalli's scale.

- (1) Damage prevision (for seismic intensity between VIII-X and attempt damage description for every intensity).
- (2) Intervention strategy for every seismic intensity (i.e. <VIII \Rightarrow nothing intervention).

5.2 The techniques for masonry arches

The typological analysis allows to locate the constructive phases succession and these reveal the vulnerable belts. This way is obviously useful to the attempt damage preventive evaluation and to locate the restoration techniques that spring from the natural evolution

PONTE SUL FIUME PESCARA

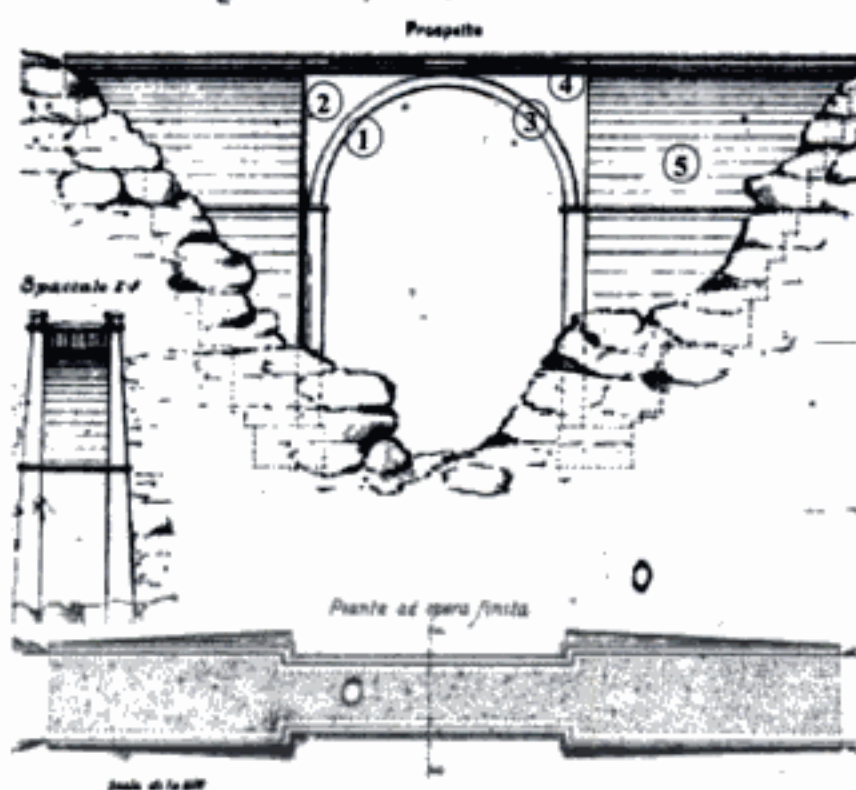


Figure 9. An example of simple arch bridge.

of the constructive formality that must be analyzed. In the latter, the Mercalli and MSK scales define a vulnerability empirical evaluation, analyzing time by time the structural elements. But these scales, formulated essentially for historical centres, must be reported to bridges problem and the single structural elements must be pointing out in precision way, thinking, over the other things, that structure isolated by the urban contest, if it is more vulnerable because it cannot rely on the aggregate capacity to be solid, on the other hand is more assimilated to a structural model, and it easily reports itself to a determined static scheme. Referring to the picture (Fig. 9), the most important structural parts of the arch bridge are pointed out: the arch 1 is the street support, the props 2 strengthen the lateral parts of the arch; the “shell” 3 attend to protect the arch masonry against water infiltrations; the headwalls 4 raise themselves from the arch extremities to the completion floor, interpose with a earth or gravel refilling, in order to reach the road level; the shoulders 5 sustain the arches and enter deeply into the ground with the foundations.

6 CONCLUSIONS

Well constructed masonry bridges – specially the realised with high quality materials and suitable building techniques ones – keep almost for ever.

Unfortunately, by reason of the important restorations and changes they have undergone during the ages, the existing Roman bridges often show a shape different from the original one and, contextually, a classification of the various typologies, became too complex and inaccurate to do.

In order to assure security and preservation, great restorations should be avoid; on the contrary, several routine and regular maintenance interventions in the course of time should be effected, to the aim to assure the old structure preservation, and at the same time, the “maximum duration” through the “minimum intervention”. A diligent classification of all bridges and viaducts in Italy, and a valuation of the attempt damage through the MSK and Mercalli scales – if it is possible – through probabilistic methods – in alternative – could suggest accurate interventions able to warrant the two most important requirement that the historical heritage needs: safety and functionality.

REFERENCES

- Baratta, A. Ponti a struttura muraria. *Istituto di Costruzioni Facoltà di Architettura Napoli*. Pubbl. n. 190. Napoli
- Baratta, A., Voiello, G. 1986. Modelli matematici per l'analisi delle strutture murarie. *Restauro* n. 87-88. Edizioni Scientifiche Italiane, pp. 81–251, Napoli.
- Baratta, A. 1988. La protezione antisismica dei beni architettonici: problematica e considerazioni di metodo. *Istituto di Costruzioni Facoltà di Architettura*, Napoli.
- Coletta, T. et al. 1989. La struttura antica del territorio di Sessa Aurunca. *Il ponte Ronaco e le vie per Suessa*. Ed. ESI.
- Baratta, A., Colletta, T., Zuccaro, G., 1996. Seismic risk of historic centre. *La città del sole*, Napoli.
- D'Agostino, S. 1994. Vulnerabilità del patrimonio costruito, prevenzione e conservazione. *Acta Neapolitana*, Ed. Guida, Napoli.
- D'Agostino, S. 1995. Manutenzione e protezione sismica delle aree archeologiche, *Atti 7° Convegno Nazionale "L'Ingegneria Sismica in Italia"* Vol. 2, 1063–1069 Siena.
- Galliazzo, V. 1995. I Ponti Romani, *Canova*, Treviso.
- Gautier, H. 1714–1765. *Traité des ponts*. Paris, chez la Veuve Duchesne.
- Giuffrè, A. 1993. Sicurezza e conservazione dei centri storici. *Editori Laterza*, Roma.
- Heyman, J. 1966. The stone skeleton. *Int. Jour. of Solids and Structures*, Vol. 2.
- Heyman, J. 1969. The safety of masonry arches. *Int. Jour. Mech. Sciences*.
- Jorini, A. F. 1927. Teoria e Pratica della Costruzione dei Ponti in legno, in ferro, in muratura. *Hoeppli*, Milano.
- Lemos, J. V. 1997. Discrete element modelling of historical structures, *New Technologies in Structural Engineering*, International Conference FIP, Lisbona.
- Resemini, S., Lagomarsino, S. 2004. Sulla vulnerabilità sismica dei ponti in muratura, *XI Congresso Nazionale L'Ingegneria Sismica in Italia*, Genova.
- Roca, P., Molins, C., Gonzalez, J. L., Casals, A. 1995. Analysis of two medieval stone masonry bridges, *Architectural Studies, Material & Analysis – Structural Studies of Historical Buildings*, IV, Vol I, STREMA, Creta.
- Torre, C. 2003. Ponti in muratura, *ALINEA*, Firenze.
- Zák, J., Novák, D. Modelling of Charles Bridge in Prague: numerical analysis and statistical simulation, *Architectural Studies, Material & Analysis – Structural Studies of Historical Buildings*, IV, Vol I, STREMA, Creta.

Structural damage prevention in the historical building site. Theory and praxis in the eighteenth century in Campania

G. de Martino

Università degli Studi di Napoli Federico II, Dip. di Pianificazione e Scienza del territorio

V. Russo

Università degli Studi di Napoli Federico II, Dip. di Storia dell'architettura e Restauro

ABSTRACT: The contribution focuses the attention on the methods which have been adopted in the past in order to prevent masonries damages, with particular reference to the context of Campania during the XVII and XVIII centuries. The examination of contemporary building sites, united to that of the scientific contemporary production, wants to put in light, particularly, the connections between instructions contained in scientific essays and the operating praxis. Historically, the period is really significant because of the birth of the “restoration”, as modernly intended. The conclusions of the essay want to point out that the deepening of the static history of the buildings of the past should be particularly attentive to less striking aspects and should make use of archival and bibliographical sources. This can provide an useful contribution to the present project of preservation.

1 NEAPOLITAN STRUCTURAL TREATISES

1.1 *Damage prevention: rules and regulations*

A very specific chapter in the history of “building art”, could be found in the set of devices pursued, in the last three centuries, in order to prevent structural damages, during building stages.

Beside the “reinforcement history”, but different from it, this topic seems to be not known so well because of the lacking in bibliographical and archival documents about historical technics of “pre-reinforcement”. Expedients used in the past – chains, buttresses, lightening methods, etc. – were part of the building know-how, handed on by oral tradition.

Luciano Patetta, in 1990, although the long lasting tradition about these techniques, underlined the difficulties to distinguish the pre-reinforcement devices, even after an accurate view, because of the frequent replacements or considerable weathering, as well as the similar ways used by the reinforcement techniques after structural decay. Furthermore, Patetta showed some cases of Italian buildings, starting from Middle Ages, where the chains became elements of architectural project, especially in “no tectonic” buildings where the shapes seem to overcome tectonic laws (Patetta 1990–1992).

Opposite to the habit usual to prevent structural damages since the beginning of architecture, several treatises hostile to this practice were written during

the Renaissance. For example, Leon Battista Alberti urged to avoid pre-reinforced arches and proposed the use of “whole arches which do not need chain, because they are able to remain intact” (“archi interi non abbisognano di corda, poiché essi sono in grado di mantenersi intatti da sé”, L. B. Alberti 1485, libro III, cap. XIII).

In the same way of L. B. Alberti, Vignola, Palladio and Scamozzi exhorted to “avoid misuse and errors of putting iron and chains in the structures” (“fuggire quegli abusi, e disconci di mettere ferramenta e catene”, Scamozzi 1615, p. II).

The wood as well as the iron is mentioned in the treatises as a material for preventive measures; wood scaffolding, put inside the city walls, is shown in the first volume of the Vitruvio’s treatise and repeated by Palladio in the illustrations of the “Commentarii of Caio Giulio Cesare” (1575).

A building model spreading in the practice and “scientifically” known since XVIII century is the “framed” (“intelaiata”) house, built with wood frames (Barucci 1990). A lot of space was given to this structural model in eighteenth century manuals, especially after the earthquake happened in Calabria in 1783. On that occasion, the most important scientific writings, conceived for something distant from the kingdom capital, were published in Napoli: Giovanni Vivenzio, *History of hearthquake of 1783 and what has been done until 1787* (“Istoria de tremuoti avvenuti nel 1783 e

di quanto fu fatto fino al 1787”) and Michele Sarconi, *Atlas of the earthquake which has taken place in Calabria and Valdemone in 1783* (“Atlante del fenomeno del tremuoto avvenuto nelle Calabrie e nel Valdemone nell’anno 1783”). The second one, in particular, was published by the Royal Academy of Sciences and Letters (“Reale Accademia delle Scienze e Belle Lettere”).

The neapolitan architects Pompeo Schiantarelli and Ignazio Stile were the illustrators for Michele Sarconi’s “Atlante...”. Both of them worked at the rebuilding in Calabria.

As for the above mentioned works, “Technical rules ...” (“Norme tecniche ...”), written by Francesco Pignatelli in 1784, represent the first “anti-seismic” rules manual, addressed to Bourbon Court and to intelligentsia around it.

Those rules concerned width of the roads and buildings height; the construction of domes and bell towers was prohibited, while the use of building “baraccato” was exhorted.

In the 1784 rules, a special attention was given to devices for containment of vaults and ceilings drifts, to get by “iron bends to fasten every building in its parts” (“fasce di ferro da stringere ogni edificio in tutte le sue parti”, De Ioanna & Piccarreta 2000).

All of these works, published after earthquake events, follow the studies of Vincenzo Lamberti and Nicola Carletti, of whom the most important works concerning structural topics were written in the seventies and eighties of 1700.

1.2 The contribution of Vincenzo Lamberti and Nicola Carletti

Vincenzo Lamberti, author, in 1773, of the *Right Vaultmetry* (“Voltimetria retta...”) and, in 1781, of the *Building Statics* (“Statica degli edifici...”), testify, as Nicola Carletti and Vincenzo Ruffo do, the state of art at his time in matter of construction theory in the capital city of Bourbon kingdom. In his writings, as in the *Institutions* (“Istituzioni...”) by Carletti, it is possible to find the most direct scientific references for his contemporaries involved in practice. The *Building Statics*, particularly, seems to be the local translation of theories matured beyond the Alps in the first half of the century, joining theoretic rules and useful examples of practical application, through a rational organization of the matter.

Rather than consolidation problems, Lamberti’s works deal with the matter of building methods in new parts of the fabric, explaining general rules for their calculations. The last part of the *Building Statics* is particularly interesting, as the author dwells upon the possible causes of static troubles in buildings. “Weakness of foundations” (“Mancanza del pedamento”), “shaking” (“scuotimento”), excess of load supported, bad construction, antiquity and the different exposition

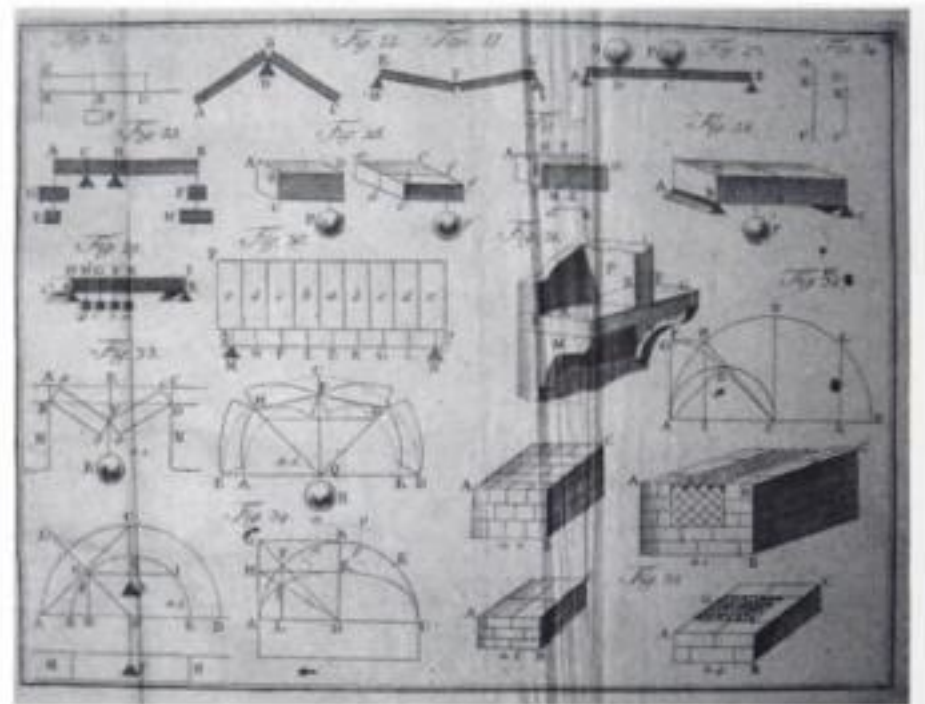


Figure 1. V. Lamberti. Building Statics. Tav. II.

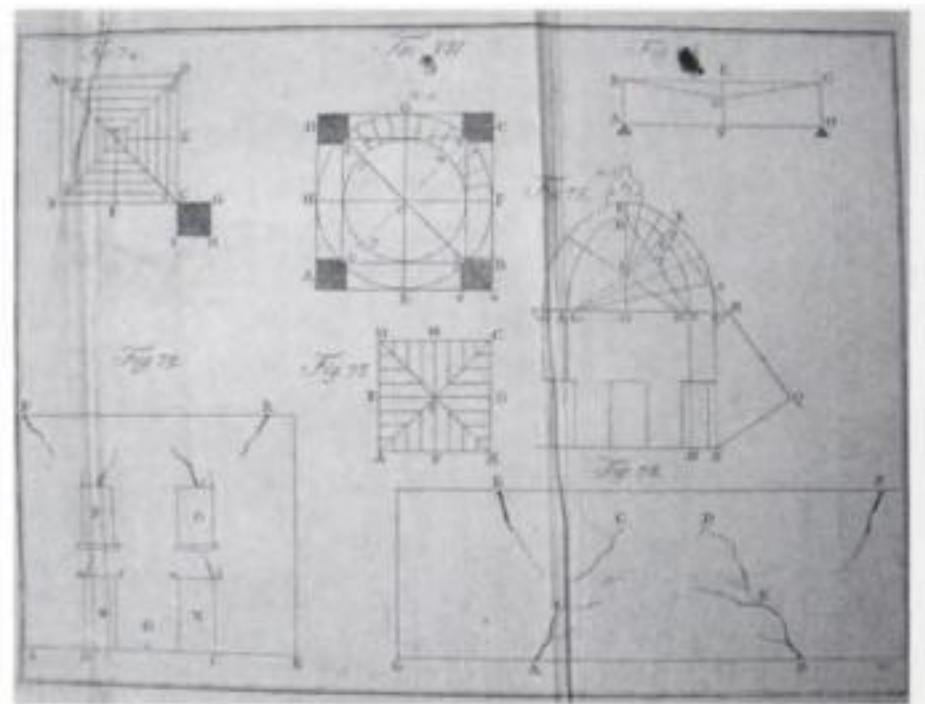


Figure 2. V. Lamberti. Building Statics. Tav. VII.

of the building parts to the sun are quoted as the principal causes of static troubles of a fabric. For each one of these, with a rational approach to the problem, Lamberti fixed a corresponding type of cracking.

Although he did not deal specifically with the vaulted structure troubles, he explained the case of cracking in arches bearing a dome. His instance is a typical explanatory model for contemporary architects for connecting the troubles of the arches with the ones of the impending vaulted structure. The work of Vincenzo Lamberti does not provide a solution to the question, but he writes in the conclusions of his writing: “For building repairs the Architect must reinforce it with wood structures, in the void parts of the building, because there is no loss possible for separate parts; and then damaged structures have to be rebuilt, according to places and circumstances; all this depending by abilities and knowledges of a professor” (“Per la riparazione dell’edificio dee prima l’Architetto assicurarlo con cataste, e puntelli in quei luoghi, ove le parti dell’edificio han descritto spazio nell’aere,

o sia nell'ultime parti dell'edificio prive di ostacolo, poiché non vi può esser mancanza sotto le parti distaccate, come dalle dimostrate teorie si è dedotto; ed indi si debbon rifar le parti patite secondo le teorie esposte nella presente opera, adattandole a' luoghi, alle circostanze, che concorrono, ed agl'usi; dipendendo ciò dalla prudenza, accortezza, perspicacia, ed avvedutezza di un esperto e dotto professore").

Carletti also afforded the study of domes ("volte a cupola"), dwelling several times with the risks of this kind of structures, "by nature light, imperfect, expensive and dangerous" ("di natura leggera, ed imperfette; spese, e pericolose"). The dome vaults are the results of a "joint of several pointed arches" ("concorso di più archi acuti"). Regarding their resistance to vertical stresses, the author made a difference between two types of structures: dome vaults and hemispherical vaults.

However, the question of intervening on existing buildings did not concern the 18th century architect, who simply meant to "rebuild the ruined parts" ("rifar le parti patite"), according to the good rules of *ars aedificatoria*.

2 VAULTS PRE-REINFORCEMENTS IN NAPLES

2.1 *Advances in neapolitan historical building site*

The direct knowledge of local structural theories and that of damage causes provided useful information to Campanian architects in order to avoid similar problems in designing new buildings.

Structures lightening, drifts control, masonries proportion were pursued in restoration and, in parallel, in new constructions.

It is possible to identify some examples of pre-reinforcement techniques both recurring to *in situ* exploration and, partially, from archival documentation. Especially regarding vaults, the recourse to hoop-iron bonds in neapolitan building sites spreads with evidence at the end of XVII century and in consequence of damages due to the earthquakes happened in 1688 and 1694.

Two significant cases can be considered the domes of the churches of St. Charles in Arena and St. George the Greater; in the first case, the architect Arcangelo Guglielmelli planned, in 1694, to encircle the dome and its lantern with an iron chain (Amirante 2000). The same architect planned, five years later, the enchainment, during the construction, of the lantern of St. George the Greater dome (Amirante 2000).

Significant advances of pre-reinforcement can be identified in two important historical structures in Naples: the domes of the Treasure of St. Gennaro's Chapel (Savarese 1986) and that of the church of Holy



Figure 3. Naples. Holy Mount of Mercy. The dome lantern.

Mount of Mercy. The first one, erected between 1608 and 1618, is composed of two calottes in order to reach the height of one hundred meters from ground floor. The dome, with its tuff masonry, is constituted of a windowed drum, regularly marked by piperno volutes. It is interesting focusing that, during the building process, the external calotte was connected to the internal one by eight buttresses and an internal lantern, replaced, because of its weight, by a lighter wooden pinnacle (ATSG, DA/9). The described structure was pre-reinforced, during the erection, with an iron chain at the top of the drum: Nicola dello Mastro, blacksmith, was paid in 1612 for going to Avellino in order to buy iron for the chain (ATSG, DA/8). Similarly, Francesco Antonio Picchiatti enchainned in 1660 the Holy Mount of Mercy dome with a double hoop-iron bond, made up of eight elements. The lantern was provided of a hoop-iron bond which connected masonry elements and pre-reinforced the top of the structure.

2.2 *Mario Gioffredo and the pre-reinforcement of the Holy Spirit dome*

The reconstruction of the dome of the Holy Spirit basilica, planned by the royal architect Mario Gioffredo, can be explanatory of the technical and



Figure 4. Naples. Treasure of St. Gennaro Chapel. The dome.

scientific knowledge reached in XVIII century in Naples.

The structure, started in 1768, presents a circular plan with an internal diameter of fifteen meters and an external one of eighteen meters. The drum upon the base is seven meters high and it is marked by columns among the windows. It is followed by the "attic", the vault and, finally, the lantern, surrounded by a balustrade and concluded by a groined little cupola.

Many archival documents, subscribed by Gioffredo, clear up the structural planning of the dome and illuminate on the technical aptitude of the royal architect (ASNa, Opere Pie-Spirito Santo, ff. 49–50). Gioffredo's competence results, particularly, from the methods adopted for lightening the dome vault (11 meters high); the architect used masonry in the vertical part and the first half of the curved one and had recourse to the very light pumice stone for the last five meters of the vault. Similarly, the groins were constructed with a "mixed" method related to materials' weight: the first part of them is made of bricks, the middle one of tuff and the last one, on the top, of pumice stone.

Mindful of the structural damages due to past earthquakes, Gioffredo supported masonries with a complex system of tie-beams. As archival documents

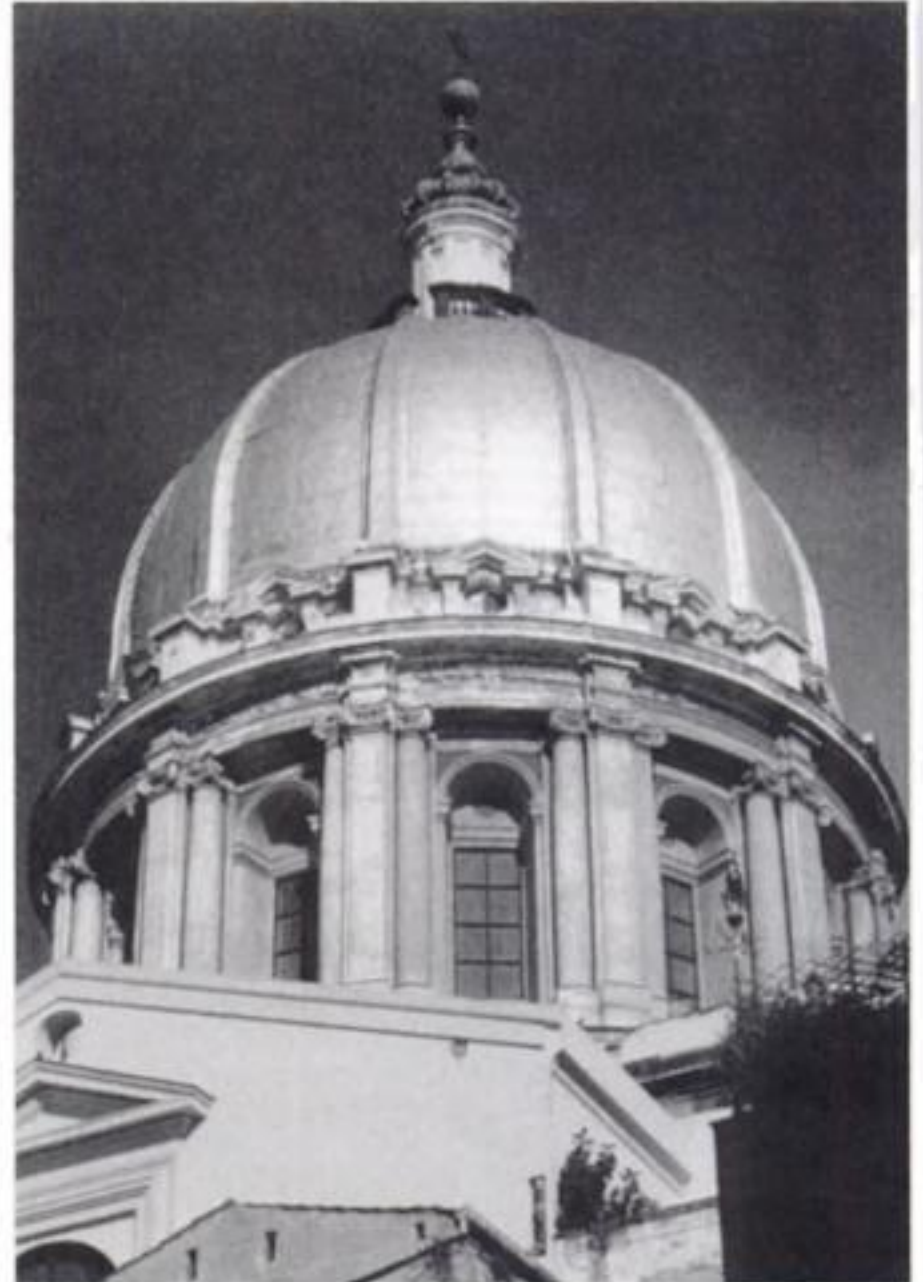


Figure 5. Naples. Holy Spirit Church. The dome.

show, iron was worked in order to realize two tie-beams for the choir's arch; moreover, they were placed on the windows of the drum, on the choir's vault, on the bell tower windows and even under piperno thresholds of the same windows. The dome was enchained at the middle of its height and the "attic" at the base was enchained, too. Tie-beams were put on the drum windows and into the staircase existing into the same drum. The four pendentives were braked with iron while the four dome's arches were pre-reinforced with tie-beams. The connection between the dome and the external walls of the transept was ensured by four couples of tie beams, placed in parallel with transept long walls (ASNa, Opere Pie-Spirito Santo, ff. 48–49–50).

Finally the structural dome's elegance was confirmed by the lantern's constructive modalities (ASNa, Opere Pie-Spirito Santo, f. 50). Aims as structure's lightening and drifts' reduction were reached by the recourse to wood for the top cupola and to iron tie beams. The first one was realized with the association of two buds made of oak and chestnut; the first convex bud was obtained by the connection of twelve radiate ribs in correspondence with the groins below. Above this bud, Mario Gioffredo planned another wooden element, constituted by 34 chestnut blocks, externally shaped.

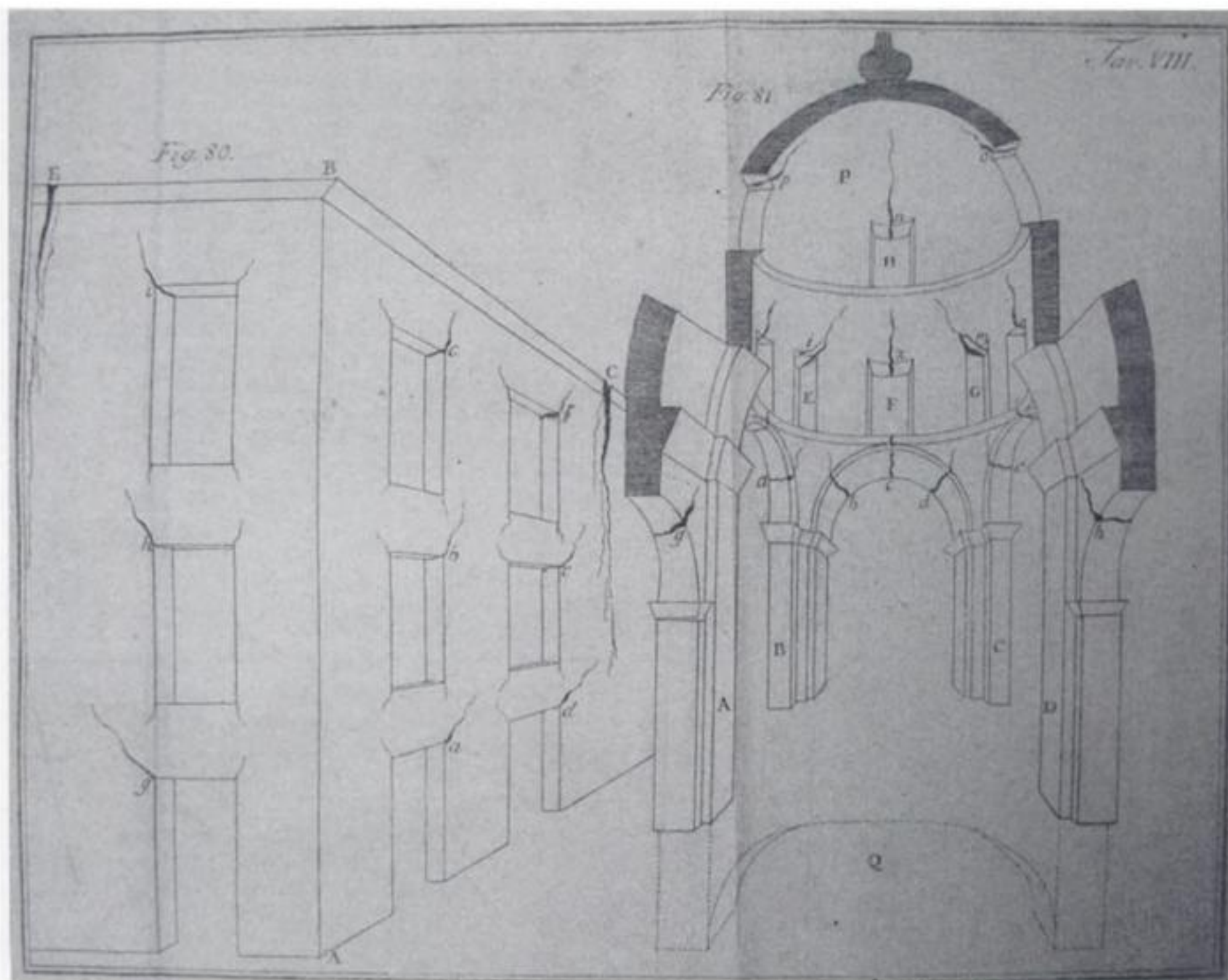


Figure 6. V. Lamberti. Building Statics. Tav. VIII.

As in dome below, the royal architect joined, in the lantern, an intelligent use of iron in order to absorb forces and connect the different parts. Two hoop-iron bonds were put at the base and at the upper part of lantern's drum; the structure was pre-reinforced by them and by transversal iron bars, necessary to maintain the cross at the top.

The plan of Gioffredo, well known rival of Luigi Vanvitelli in Royal Palace of Caserta, was especially praised by the neapolitan technical entourage, as many archival relations demonstrate. Among them, we can distinguish the agreement of the royal architects Giuseppe Astarita and Giovanni del Gaiso who, foreseeing the building future, praised Gioffredo for the adopted structural methods.

3 CONCLUSIONS

The mentioned cases provide a significant example of the importance of an in-depth historical study before any preservation programme. In fact, the only direct inspection does not enable to recognize complex

solutions adopted in the past in order to ensure the stability of structures; bibliographical and archival sources can provide useful information about materials provenance, details on working techniques and on specific pre-reinforcement or consolidation methods.

This kind of information make part of a "building art" oral tradition which does not emerge from "official" treatises. In any case, the knowledge of these latter is absolutely essential for the comprehension of the scientific progress in a particular geographical context and historical period.

Moreover, structural treatises can furnish useful information about the knowledges which architects of the past should have acquired in order to plan their structures.

The interrelation between in situ inspection and historical investigation helps to distinguish the specific solutions which have been adopted. Archival sources, often consisting of technical relations or advices, tenders, calculations, can form a solid base for a diagnostic programme, too. For instance, the forecast of invisible iron elements, just described in historical documents, can address magnetometric tests.

Similarly, the historical identification of “enlightened” or, on the contrary, reinforced parts helps to exactly localize “weak points” of the structure in the present.

Some more considerations can be done in relation to the conservation programme. An in-depth historical study must bring to the preservation of formal and aesthetic aspects of the building and, especially, to the preservation of historical and constructive values. It is possible to preserve a complex structural conception only recurring to the careful knowledge of the building techniques and to that of all the adjustments, “corrections”, transformations made in the past. These latter ones can be correctly distinguished by “pre-reinforcement” expedients only recurring to historical sources; moreover, their presence or absence in the analysed structure can prove pre-reinforcements’ineffectiveness or their efficacy, respectively.

A peculiarity of a preservation programme is its “complexity”; it can be obtained only as the result of an interdisciplinary elaboration in which history and technology talk to each other.

REFERENCES

- AA. VV. 2004. *Il Pio Monte della Misericordia nel quarto centenario*. Pisani Massamormile M. (ed.). Napoli: Electa Napoli.
- Alberti, L.B. 1485 (ed. 1966). *L'Architettura* [De re aedificatoria], Milano: Il Polifilo.
- Amirante, G. 2000. *Architettura napoletana tra Seicento e Settecento. L'opera di Arcangelo Guglielmelli*. Napoli: Edizioni Scientifiche Italiane.
- Barucci, C. 1990. *La casa antisismica. Prototipi e brevetti*. Roma: Gangemi Editore.
- Carletti, N. 1772. *Istituzioni di architettura civile*, Napoli: Stamperia Raimondiana.
- De Ioanna, A. & Piccarreta, F. 2000. Il consolidamento antisismico nell'edilizia del XVIII e XIX secolo: regola dell'arte e processo evolutivo della normativa antisismica. Le fonti storiche d'archivio a riscontro con l'osservazione “in situ”. *Palladio* 26: 93–124.
- Di Pasquale, S. 1996. *L'arte del costruire. Tra conoscenza e scienza*, Venezia: Marsilio.
- Di Stefano, R. 1980. *La cupola di San Pietro*. Napoli: Edizioni Scientifiche Italiane.
- Gravagnuolo, B. (ed.) 2002, *Mario Gioffredo*. Napoli: A. Guida.
- Lamberti, V. 1773. *Voltimetria retta, ovvero Misura delle volte*. Napoli: Donato Campo.
- Lamberti, V. 1781. *Statica degli edifici in cui si espongono i precetti teorici pratici, che si debbono osservare nella costruzione degli edifici per la durata di essi*. Napoli: Giuseppe Campo.
- Patetta, L. 1990–1992, Le ‘catene’ come scelta progettuale negli edifici tra il XIII e il XV secolo, in Corrado Bozzoni, Giovanni Carbonara, Gabriella Villetti (ed.), *Saggi in onore di Renato Bonelli*. Roma: Multigrafica.
- Pignatelli, F. 1784. *Norme tecniche ed edilizie per ricostruire le case distrutte*. Napoli.
- Savarese, S. 1986. *Francesco Grimaldi e l'architettura della Controriforma a Napoli*. Roma: Officina.
- Scamozzi, V. 1615. *L'idea dell'architettura universale*. Venezia.
- Strazzullo, F. 1953. *Il restauro settecentesco alla chiesa dello Spirito Santo a Napoli*. Milano: Casa editrice d'arte e liturgia Beato Angelico.
- Strazzullo, F. 1994. *La Cappella di San Gennaro nel Duomo di Napoli*. Napoli: Istituto Grafico Editoriale Italiano.

ASNa = Archivio di Stato di Napoli.

ATSG = Archivio Tesoro di San Gennaro.

APM = Archivio Pio Monte della Misericordia

Gianluigi de Martino has written par. 1.1 and 1.2 while Valentina Russo has written par. 2.1 and 2.2. Both of the authors have written par. 2.3 and 2.4.

Restoration of the bell tower on the Church of Vistabella del Maestrazgo, Castellón (Spain)

F. Vegas López-Manzanares & C. Mileto
Universidad Politécnica, Valencia, Spain

ABSTRACT: The bell tower of the church of Vistabella del Maestrazgo, Castellón (Spain) has recently been restored by the authors of this paper in its first phase under the pressure of an official emergency plan due to the bad state of the structure. The main pathologies were the general cracking of the four facades (some of them 20 cm wide and 1,20 m deep), the serious loss of mortar in the stone walls, the movement and distortion of the voussoirs of the arches, the risk of collapse of several of these voussoirs and deep abrasions on certain parts of the building. The urgent character of this commission required a quick intervention without time to study the pathologies of the stone wall properly beforehand. This paper describes this first intervention made to these major problems and the accurate surveys that were done to understand the causes of these pathologies.

1 INTRODUCTION

1.1 *Description of the church*

The village of Vistabella del Maestrazgo, Castellón (Spain) is located in a mountainous area, on top of a hill, in an isolated place with very cold winters. The Church of Nuestra Señora de la Asunción is built on the East side of the village, outside of the former medieval walls. This new bigger temple, in relation to the little church inside the city walls, was conceived with a view to enlarging the space for the pilgrims that passed by in their way to a famous sanctuary further up the mountains. The comparison of the dimension and the medieval fragmentation of the urban structure of the village with the shape of the new temple helps to evaluate the expectation that this new building aroused.

The church bell tower (fig. 1) was built at the foot of the nave on the right side, just at the end of the main street, where there was a historical gateway to the village. The location of the bell tower directly on the first vault of the right-hand nave, the foundation of the temple supposedly on the former ditch of the city wall where the soil usually comprises a pile of former rubbish, washed by water table pockets or underground streams, may have had an influence in the present conditions of vertical stability of the bell tower.

There is hardly any historical data concerning the construction of this church, and even less about its pathological history. It seems certain that the building of this church began at the end of the 16th century

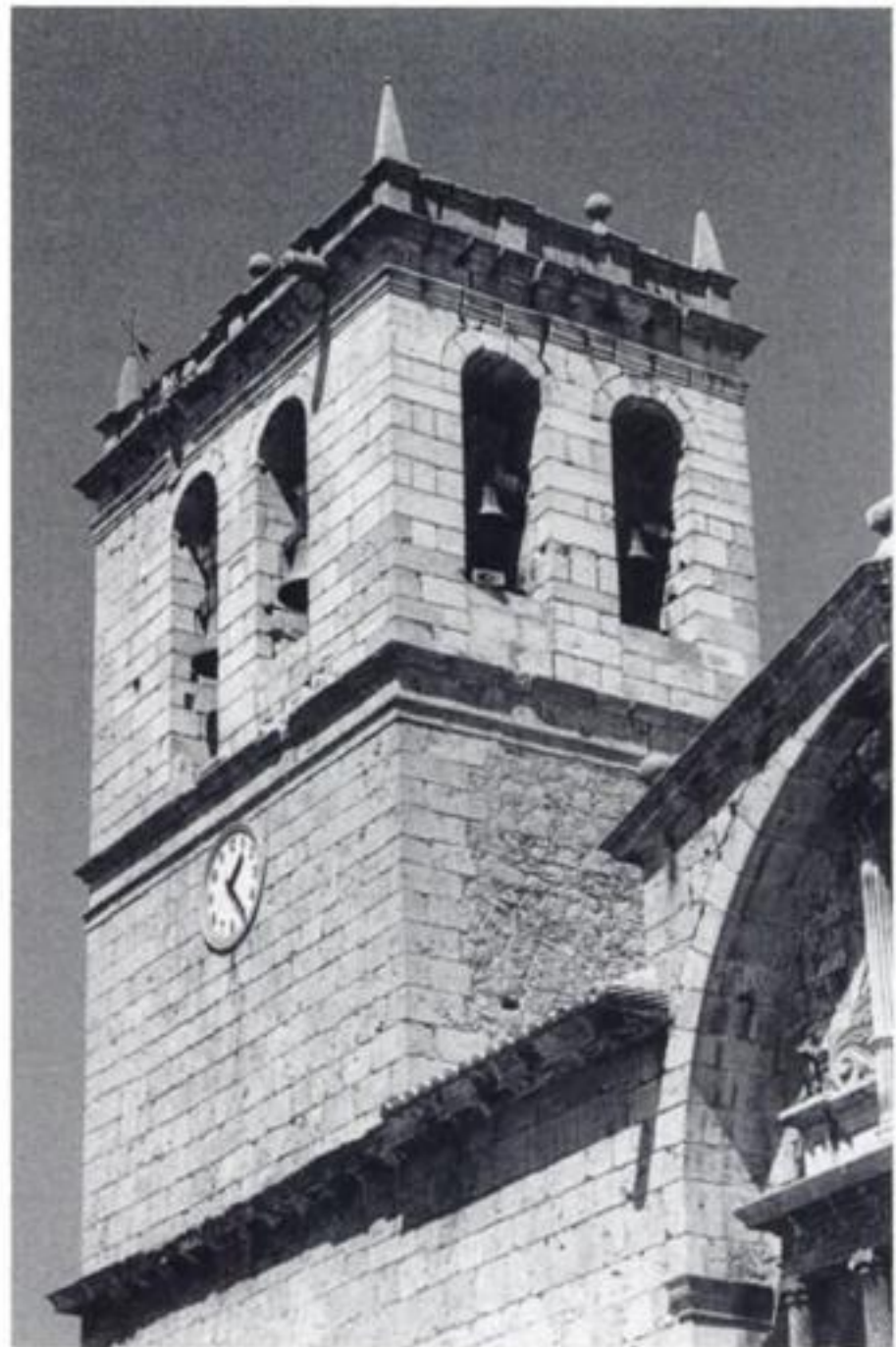


Figure 1. The church bell tower before restoration.

(Fernández 1995). The dates 1604 and 1624 are written on the main front, as the only historical reference that was available about the construction of this facade.

There is no other historical data about the birth of this church, its life, evolution and circumstances. The oldest live evidence about the bell tower was the last verger, who reached a very old age and said that the bell tower cracks had been degenerating due to the passage of time, rainwater and ice. That means that the present state of the bell tower does not correspond to a sudden change in its situation and evolution, but to a gradual and progressive worsening of its pathologies, starting four hundred years ago and continuing until today.

The church of Nuestra Señora de la Asunción is designed with three naves divided by two rows of big pilasters. The central nave is larger and higher than the lateral ones. All of them are covered by crossed vaults. The central nave is crowned by a big polygonal apse. The bell tower is located at the foot of the church, over the first vault of the right-hand nave, supported at the corner of the South and West walls of the church and the inside pilaster. Its thirty metres walls

are built with ashlar work in the most conspicuous areas of the facade, combined with masonry walls in the less visible areas of the tower.

It can be asserted that the master builder's decision to create a secondary large access under the bell tower does not help the stability of the whole in the least, because it reduces its supporting area at its foot to three simple big buttresses connected by arches and, as it will be possible to see, a masonry wall weakened by the presence of the round stairway that leads to the bells at the top precisely in the corner. Indeed, this stairway placed just on the Southwest corner of the bell tower (fig. 2) weakens the supporting wall and, on the other hand, makes the structural junction of the corner rigid, obstructing the transmission of the torsion movements of the bell tower.

In the second level of the bell tower, between the cornice of the temple and the base line of the bells body, there is a clock that was inserted in the ashlar wall at the end of the 19th century. This insertion was made by directly perforating the wall and installing the machinery inside on a wood slab, but no arch was added to support the weight of the upper wall.

Three crossed vaults of similar shape and construction cover these three internal spaces. The first is the same internal vault of the right-hand nave of the church. The second covers the wood slab that shelters the clock machinery and supports the base of the upper bell body of the tower. The third is the roofing vault. Both the second and the third, and particularly the third, show traces of multiple repairs and different plasters on their lower face.

2 METHODOLOGY USED IN THE SURVEY

The was made using traditional measure methods simultaneously with technological methods such as theodolite or laser measuring machines. Theodolite allowed a very precise measuring of spatial coordinates at long distances. The laser system allows a very accurate measuring of the deformations of the objects represented such as arches and vaults, whose exact shape can be drawn by taking as many measurements as there are joints between the voussoirs of these arches and the ribs or filling of crossed vaults.

The facades were surveyed with the help of calibrated and rectified photographs. Once the scaffold for the urgent intervention was built, this survey was enriched with the data that was obtained from direct contact with the stone wall. A topographical survey of the bell tower edges was also developed, and a precise laser survey of the three internal vaults of the bell tower in order to detect their respective deformations. Finally, from the scaffold a survey of the horizontal deformations of four entire sections of the bell tower was made.

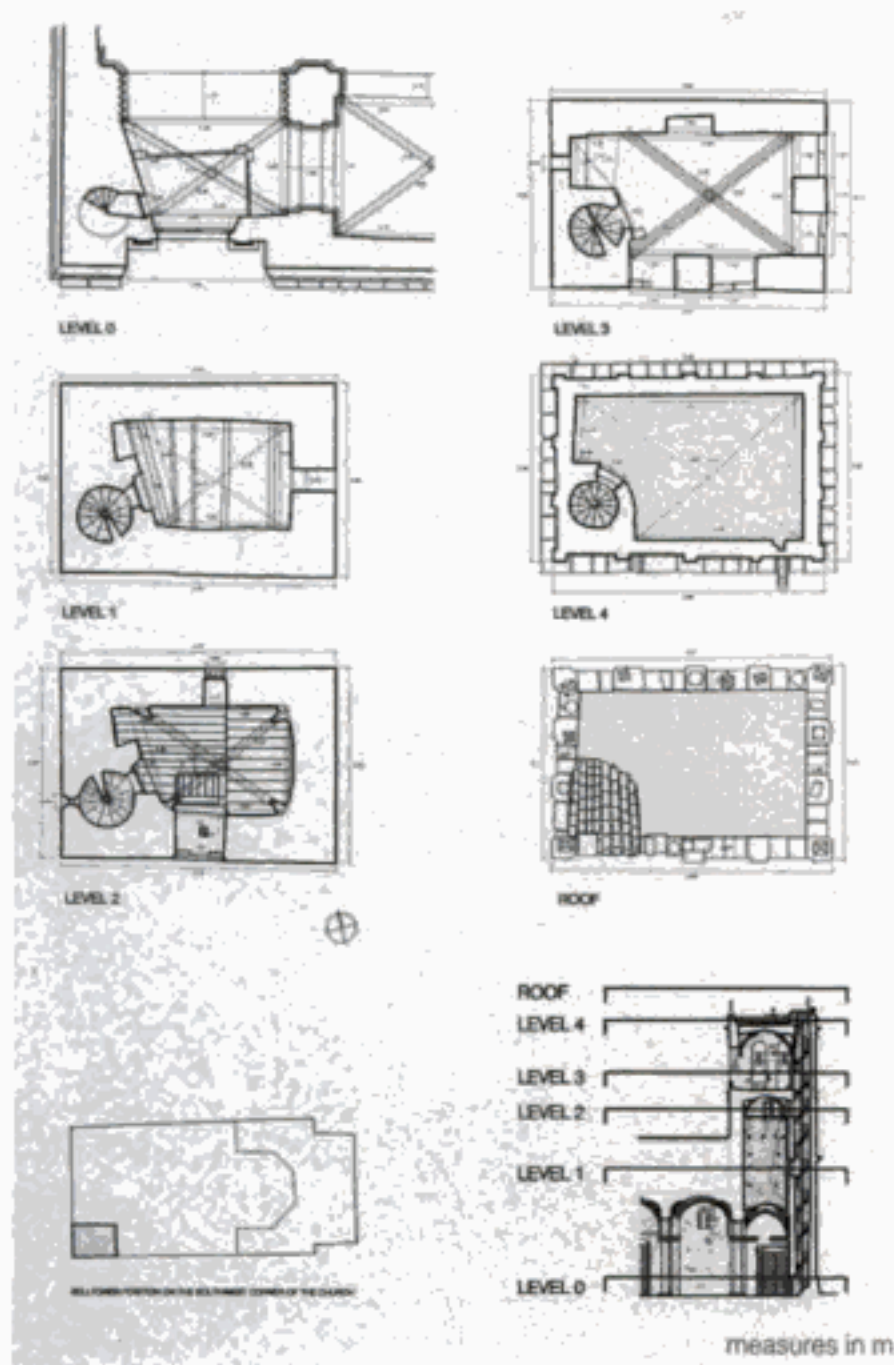


Figure 2. Layout of the bell tower at different levels.

2.1 Previous studies

All the previous studies that are explained in the following pages were developed parallel to the restoration works. Their aim was to assess the real influence and responsibility of every factor studied in the state of conservation of the bell tower.

2.2 Georadar subsoil studies

Several georadar explorations in the subsoil were made, in order to draw and identify building remains or other anomalies in the bell tower area that might have had an influence of these soil irregularities in the bell tower foundation problems and consequent overhanging, leaning or cracking (García 2002). The possible existence of these irregularities under the bell tower could be an explanation for its pathologies.

These explorations detected several anomalous areas at a depth of 1–1,5 m, and a uniform line at a depth of about 2 m that was identified as a possible water table pocket. This fact was corroborated by the presence of water at the same level in the underground crypt of the church, just near the bell tower.

2.3 Archaeological survey

These results obtained by the use of the georadar suggested us to dig two archaeological surveys at the bell tower base, which allowed us to identify remains of buildings related to the former Christian or even the Islamic wall (Rives 2002). Nevertheless these findings could not justify the bell tower pathologies. Perhaps the problem resided in a lower layer. These shallow archaeological surveys permitted us to make this type of identification but did not provide any information about deeper soil layers.

2.4 Geotechnical survey

This lack of information about the deeper soil layers suggested the idea of making a geotechnical survey around the bell tower to identify the irregularities in the layers underneath it that could have an influence on the state of the bell tower or, on the other hand, allow us to rule out the possibility of the soil as main cause of the bell tower pathologies. The final combination of the georadar diagrams with the archaeological surveys and the geotechnical survey allowed us to know the state and composition of the foundation soil very accurately.

The stratigraphic section of the geotechnical survey (compare with Igme 1981) detected three main levels: the first, from 0 to –1 m, is composed of concrete and filling; the second, from –1 m to –5 m, with grey clay and the inclusion of cracked sandstone; and the third, from –5 m to –10,60 m, with the presence of muddy sands with the inclusion of sandstone. In this stratigraphic section there is no mention of the water table pocket at a depth of –2 m, as the radargrams or the

partial flooding of the bottom of the crypt suggested, but only the location of the main water table at a depth of –7 m, approximately.

The results of the geotechnical survey analysed by competent professionals (A.T. Control 2002) made it possible to draw up a hypothesis of the behaviour of the foundation. Considering a foundation width similar or larger than the walls, with an approximate depth of 1 m to reach the grey clay layer, and considering that no soil irregularities had escaped the survey, this analysis concluded that there is a sufficient security coefficient against sinking, as the bell tower settling has occurred completely, saturating the clay of the subsoil. This hypothesis concludes as a result of the survey and the available data, that the subsoil is not the main cause of the bell tower pathologies.

2.5 Conclusion of the subsoil study

This hypothesis was assumed to be valid, although the unequal sinking in the Southwest corner of the bell tower had generated some of the vertical cracks in V shape that runs along its South and West facades. This unequal sinking may have been caused either by the presence of some irregularity under the Southwest corner (a bag of cracked sandstone inside the clay layer, which could have settled more than the adjacent areas), or by the influence of any of the building remains in the subsoil detected by the georadar, or by a phenomenon of flattening or plasticising of the ashlar of the corner, brought about by the reduction of the supporting section because of the void of the stairway in the corner.

2.6 Survey of the materials of the building

A parallel survey of the materials during the restoration works was made. The aim of this new survey was to determine the possible influence of the different materials in the pathologies that affected the bell tower. The main materials used in the bell tower are stone of two types (limestone and sandstone) and several forms of stonework (ashlars, rough ashlar, masonry) and lime mortar of different composition.

It was realized that the choice of a different type of stone had a direct relationship with the type of surface pathologies, even without taking into account the relative position or orientation in the bell tower. In any case, it could be demonstrated that this choice had no influence at all on the structural cracking of the bell tower.

As this possibility was ruled out, the idea that the mortar quality, really brittle in some places, could have had some influence on the disarticulation of the bell tower stone wall considered bell tower stone wall, since the following factor was taken into account. The mortar is the conglomerating material of the stone wall consisting of two faces of ashlar or masonry and an important amount of filling inside that adds or reduces

strength depending on its quality. Most of the mortar in the joints of the stone wall had been washed and lost, not to mention the cracks (some of them 20 cm wide and 1,20 m deep), which permitted rain and ice to seep inside the stone wall.

The stone wall was built with a similar aggregate, probably extracted from an area near the village. The proportion aggregate/lime is sometimes very diverse, although the most usual proportion to be found in the bell tower is 2/1 or 2,5/1 (Martin 2002).

The upper body of the bell tower has a very poor mortar, with proportions of 4/1 and even 4,5/1 (Martin 2002). This mortar is brittle and can be crumbled with the hand. The comparison of such different mortars with the irregular and chaotic distribution of limestone and sandstone ashlar suggest either a similar chaotic building site at this level of the bell tower or former undocumented restoration works on the upper body of the bell tower.

Maybe this historical restoration could be related to the collapse of the bell tower's upper vault, which happened at least twice in the past, but the absence of any trace on the main vault of the church (nowadays this vault is covered by a layer of concrete) does not allow this hypothesis to be confirmed.

2.7 *Monitoring of the cracks in the stone wall*

Nine movement monitors were installed on both sides of the significant cracks, and another one that exclusively measures the variation of temperature, all in order to obtain a two-year record of the possible movements of the bell tower cracks (Serna 2003).

At the moment of writing this paper, provisional measures that correspond to one year's monitoring have been already collected. These results are not definitive but permit us to make a structural hypothesis of the behaviour of the bell tower, to be confirmed at the end of these two years of monitoring. Special attention should be paid to the monitors on the main cracks in the South and West facades, which show an important opening of 1 and 1,5 mm, respectively in only one year.

3 STRUCTURAL PATHOLOGIES

3.1 *Roof vault*

The restoration works have helped to confirm that the vault had already been repaired, as could be seen from the patches of plaster. This vault collapsed, at least partially, at least twice, and was repaired afterwards. The causes of these collapses can be found in the opening of the crowning walls of the bell tower, owing to unequal foundation sinking, the opening of the side walls caused by the thrust of the vault, the important vibrations caused by the movement of the bells, or any combination of these three possibilities.

3.2 *Clock vault*

The crossed vault that shelters the clock machinery has some cracks in its lower part, particularly, at the joint of the ribs and the keystone. These cracks may respond to the same phenomenon of opening of the upper part of the bell tower stone wall, and a possible overload caused by an important amount of filling to constitute the base of the bell tower upper body.

3.3 *Deformation of the church arches under the bell tower*

The two interior arches of the church on the base of the bell tower that support the East and North facades walls show a deformation map that helped understand some of the movements of the bell tower. The arch under the East facade had settled in such a way that it had dragged the upper masonry wall down with it.

The arch under the North facade has also suffered deformation, settling and leaning towards the West wall at the foot of the church, accompanying the movement caused by the thrust of the last vault in the central nave on the closing wall at the foot of the church.

3.4 *Cracking in the stone walls*

The cracking picture of the stone walls is complex and due to multiple reasons (figs 3, 4). The general causes of cracking that can be found in the bell tower are fundamentally: settling of the stone wall, opening because of unequal sinking in the foundation, flattening and opening of the walls because of the settling and horizontal thrust of the arches and vaults, those inside the bell tower and those adjacent to the central nave of the church. All these cracks have been enlarged by everyday weather, particularly, rain and ice.

In the South facade, the map of the cracking corresponds to the unequal sinking of the bell tower foundations that, as it can be seen below, tilted as much as 15 cm westwards in the Southwest edge, compared with the 3 cm of the Southeast edge. The difference between these two degrees of tilting was absorbed by the V-shaped crack in the South facade.

In the West facade, the picture of the cracking is also due to an irregular foundation sinking that tilted 17 cm southwards on the Southwest edge, compared with the 2 cm of the Northwest edge. The difference between these two degrees of tilting was absorbed by the V-shaped crack in the West facade.

Besides, attention must be paid to the existence of a vertical crack in the joint of the temple wall and the bell tower wall, which took place because of the thrust of the last vault of the central nave in the West wall that is making it tilt it outwards, but does not affect the bell tower because of its greater rigidity and lateral position far away from this thrust phenomenon.

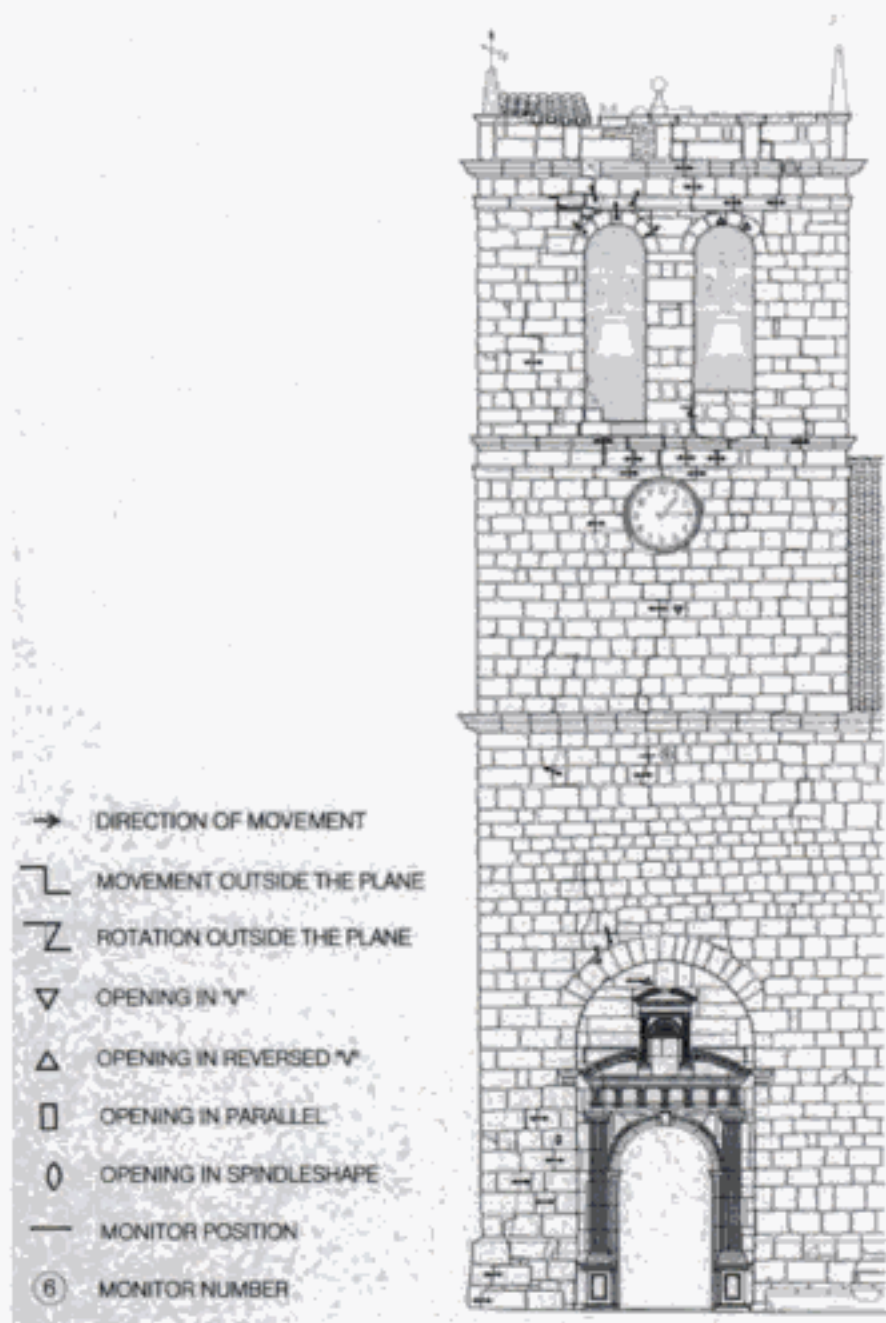


Figure 3. Map of the cracks in the South facade.

In the North facade, the map of the cracking again corresponds to an unequal sinking of the bell tower foundation that tilted 9 cm westwards at the Northwest edge, compared with almost no tilting registered at the Northeast edge. The difference between these two degrees of tilting was absorbed by the V-shaped crack in the North facade.

No doubt the opening of the walls caused by the horizontal thrust of the upper vault has enlarged cracking here, without forgetting the presence of ice during the winter, especially in this North facade with no sun at all.

In the East facade, the map of the cracking is partially due to the difference in tilting caused by the unequal sinking of the bell tower foundation, from the Southeast edge (4 cm) and Northeast edge (almost 0 cm), and partially to the settling of the interior church arch underneath this facade wall, which has dragged the upper stone wall down with it. In this case, the two arches of the bell tower crowning have suffered important voussoir settlements.

3.5 Dislocation of the upper bell arches

Indeed, one of the most alarming situations was the precarious state of balance that showed three of the

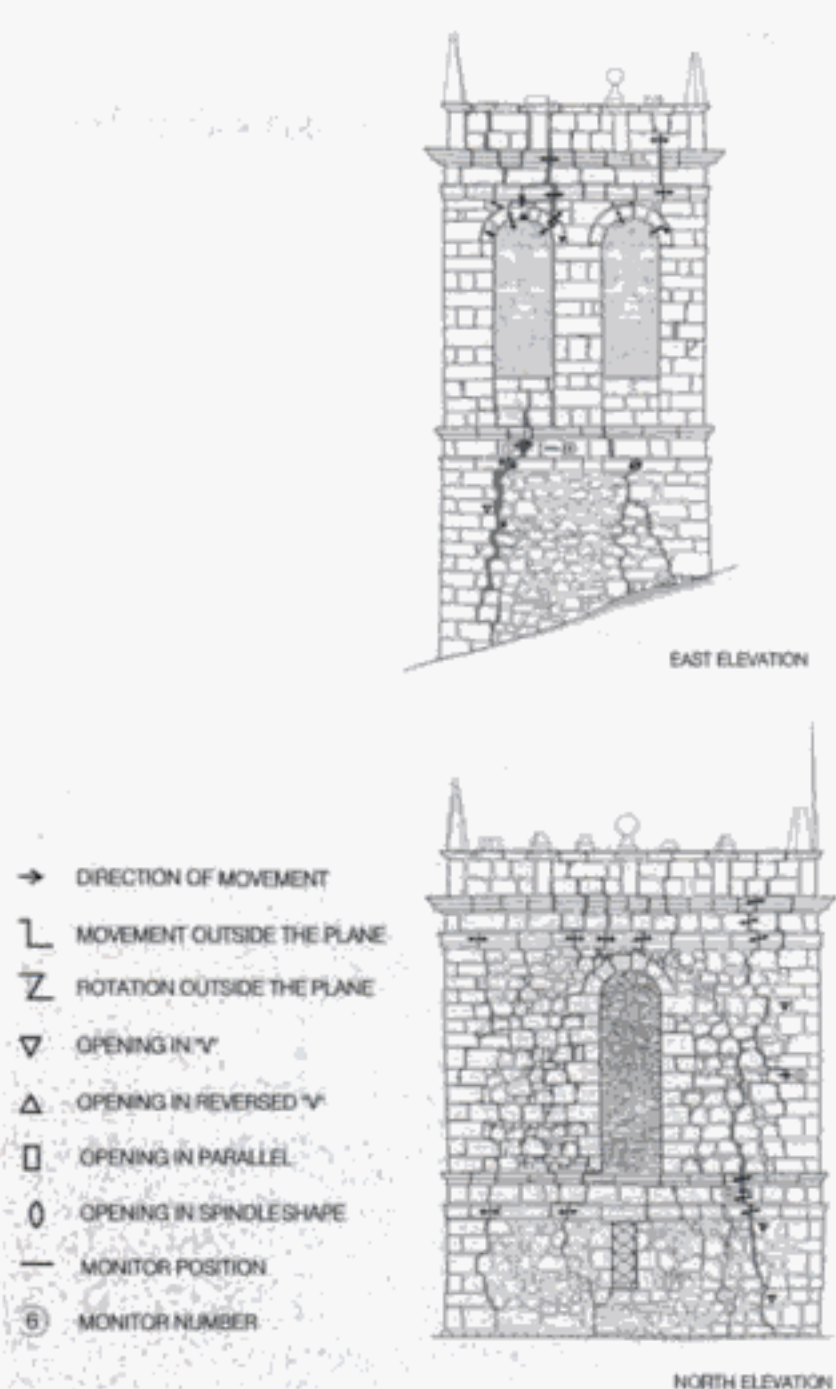


Figure 4. Map of the cracks in the East and North facades.

upper bell tower arches. The voussoirs and ashlar had lost support and unstable dislocation had taken place, especially in the arches of the East and West facades.

The reasons for this dislocation are the V-shaped opening from the very bottom of the bell tower, and the horizontal thrust of the roof upper vault.

3.6 Tilting and overhang

The bell tower shows a general leaning towards the Southwest, caused by unequal sinking of the bell tower in that direction (fig. 5). The overhangs are variable so that, as described in the cracking map of the whole, the difference between the tilting of Southwest edge compared with the tilting of the Northwest, Southeast and Northeast edges was absorbed by the appearance of cracks in the isostatic stone wall structure. The bigger overhang is more than 22 cm in the diagonal of the Southwest edge, compared with smaller ones in the Northwest, Southeast and Northeast edges.

3.7 Vertical deformation

These inclinations are not uniform in all the dimension of the edge because of some irregularities. Nevertheless, the vertical deformation is very clear in

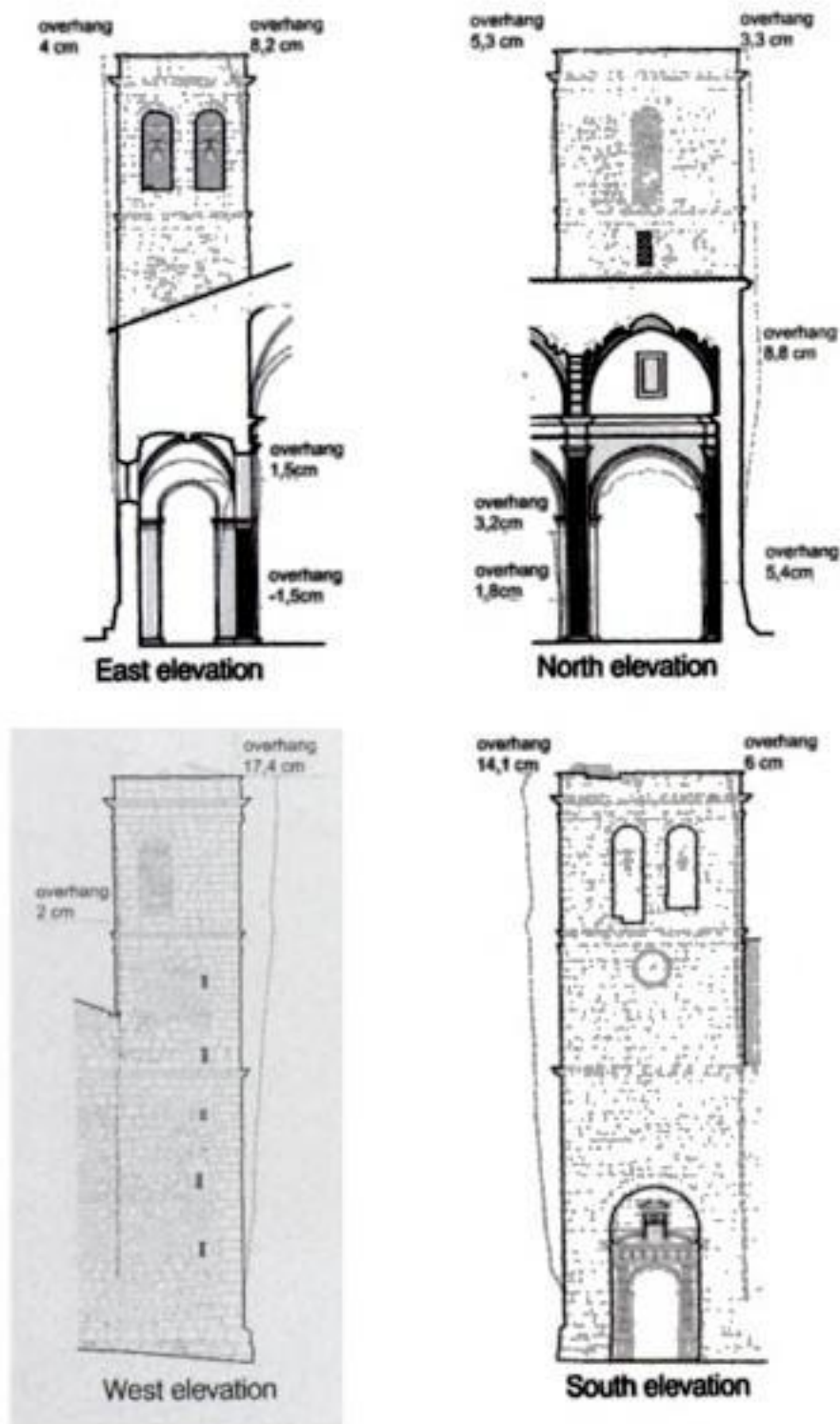


Figure 5. Vertical deformation of the bell tower.

the Northwest edge of the bell tower, where the influence of thrust of the last vault of the church caused particularly serious deformation in this point, combined with the edge overhang described above (fig. 6).

3.8 Horizontal deformation

The horizontal deformation of the bell tower's upper walls was measured in four complete sections. Convex and concave deformations were detected, in some cases reaching more than 4 cm (fig. 7). The convexities of the stone wall in the North, East and South facade sections may correspond to the actions described or dislocation and disintegration of the stone wall caused by the loss of the agglomerating mortar, together with the thrust of the upper vault, at the height of these sections.

3.9 Consequences of the insertion of the clock

As had been seen in the crack map of the South facade, the untimely insertion of the clock in the wall without creating an arch in the wall perforation, either on the

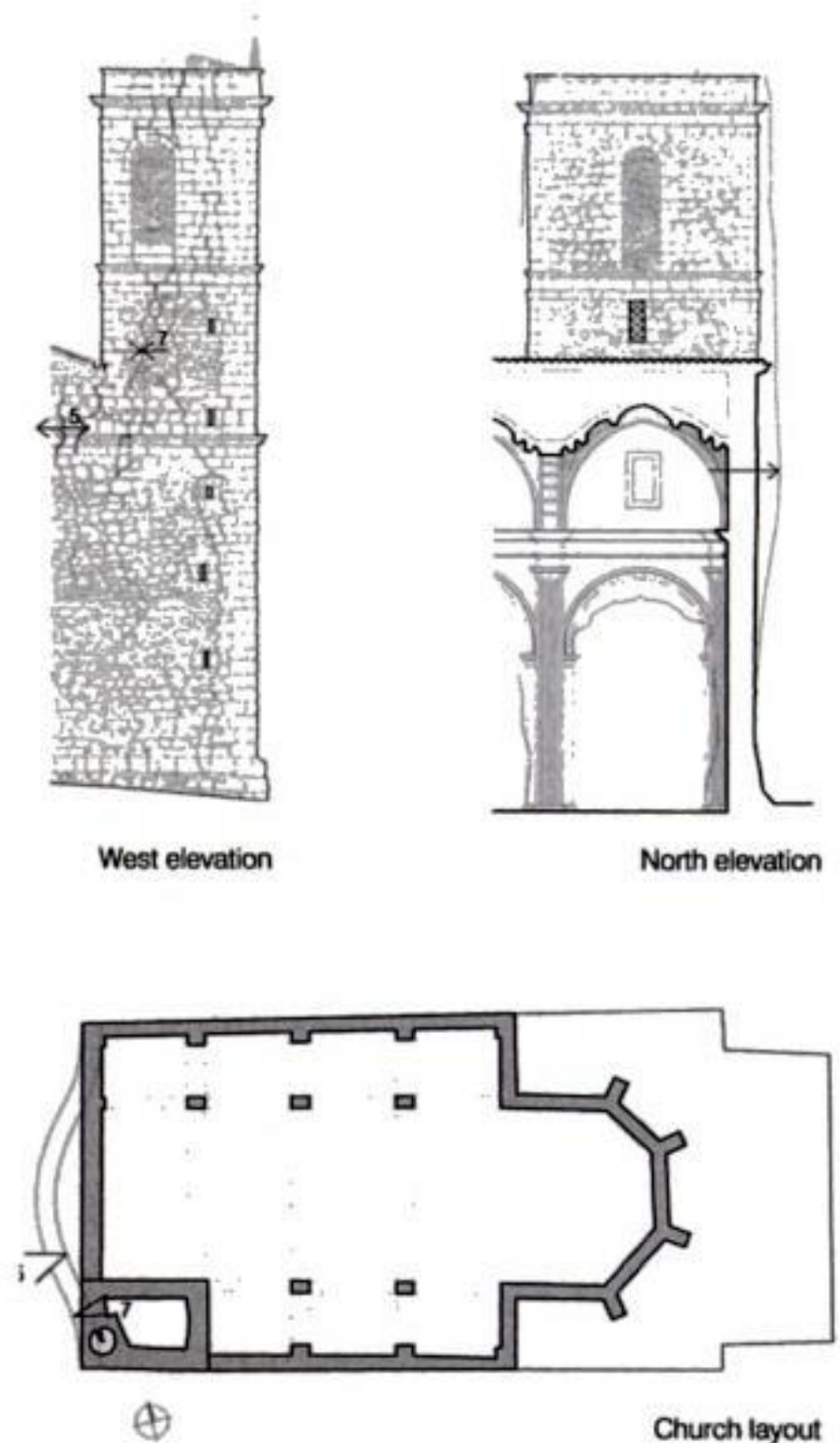


Figure 6. The thrust of the last vault in the church on the back wall.

outer or inner side of the facade or the filling, had caused the settlement of the ashlar over it, just where one of the upper buttresses of the facade is weighing on the fabric. The installation of a wood support inside to avoid more serious problems was successful, but the whole situation around the clock unnecessarily meant another weak point in the bell tower.

3.10 Stone flattening phenomena

A stone flattening phenomenon was detected at the base ashlar of the Southwest corner, with little vertical fissures. This problem is very serious and must be solved without delay to avoid the complete plasticisation of the stone and the ensuing collapse of the whole bell tower. The flattening phenomenon comes from the more than 22 cm tilt at this edge towards the Southwest and the weakening of the section in the Southwest corner because of the presence of the round stairway.

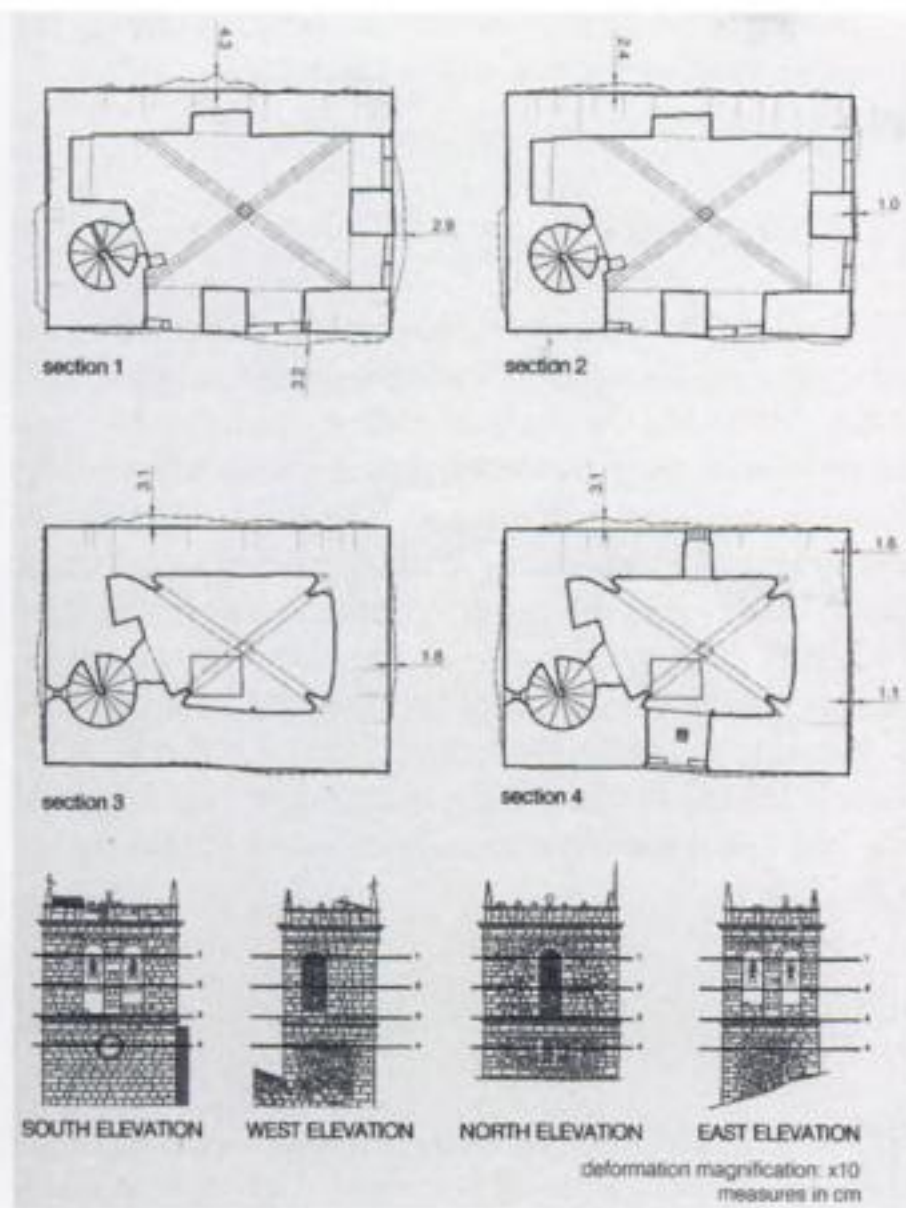


Figure 7. Horizontal deformations in the upper part of the bell tower.

4 RESTORATION PROJECT AND WORKS

4.1 *Reconstruction of the ashlar and voussoirs in the arches*

The reconstruction of the ashlars and voussoirs in the arches required the complete dismantling of two arches in the bell tower and the upper ashlars right up to its crowning (fig. 8). A third arch only required the relocation of one of its voussoirs by jacking up it to the former position. All these operations needed the implementation of several security measures to avoid the dismantling of one arch to affect the adjacent one.

For this reason, first of all, a restraint system for the bell tower's upper body was conceived consisting of four stainless steel cables that tied up the whole perimeter of the bell tower. Besides, it was necessary to shore up the arches in order to avoid the dismantling of one of them to cause the adjacent one to collapse. This shore system was created to serve simultaneously as support for the dislocated arches to be dismantled.

A very precise design was drawn of the arches to be dismantled to show which ashlars and voussoirs were to be dismantled and another design with their exact position in the restored fabric. Afterwards, they were dismantled with the help of a big crane, clamps

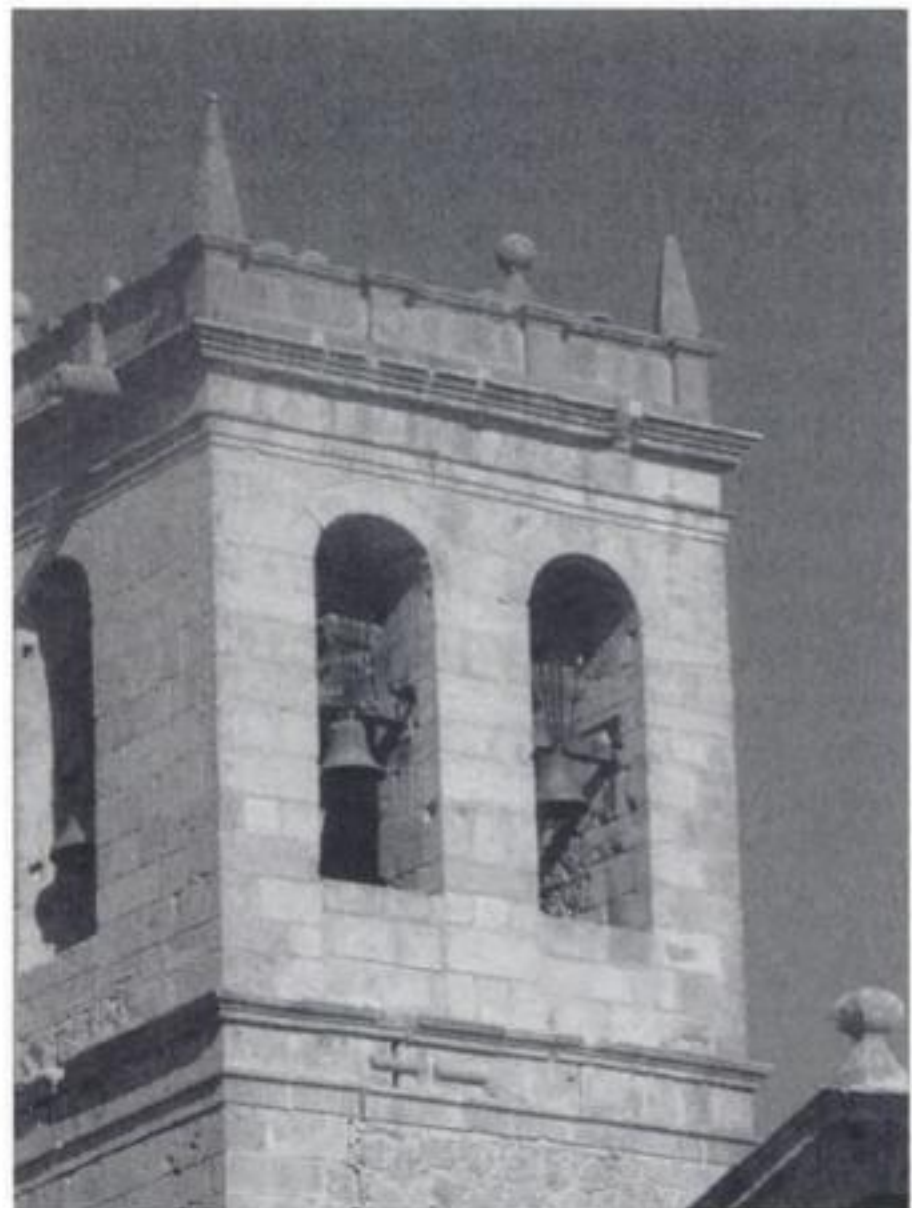


Figure 8. The church bell tower after the first phase of restoration.

especially designed for the occasion and double textile slings to extract the stones. The ashlars and voussoirs moved were numbered according as they were dismantled to ensure their relocation in the correct position.

After the dismantling came the rebuilding of the arches, using wooden wedges to distribute the new distances of the arches uniformly in all the stone wall joints.

4.2 *Reinforcement of the bell tower roof vault*

The bell tower roof was seen to have a very large amount of filling that was weighing heavily on it and causing a great horizontal thrust on the facades. The roof was then dismantled to unload the filling from the roof vault. The terrace had a modern ceramic pavement with cement mortar over a prefabricated concrete slab inserted in the nineteen seventies. That means that this terrace was no longer supported by the vault.

Once this slab was dismantled, the filling of the flat ceramic vault was unloaded (more than one metre at the corners). The precarious state of the vault needed urgent repairs and reinforcement, which consisted of applying a new layer of lime mortar and doubling it with a new ceramic vault to thicken the vault supporting section. The small budget forced us to relocate the prefabricated concrete slab on it provisionally.

4.3 Tightening of the bell tower roof vault and crowning

Once the weight of the filling in the vault had been unloaded, there was no more horizontal thrust on the walls, as the flat ceramic vault has almost no weight. But in any case it was necessary to tighten the bell tower crowning to avoid its continuous opening caused by the V-shaped cracks coming from the base.

It was decided to insert stainless steel braces in to restrain this opening. Six braces were installed in the bell tower crowning, three on each side, one central and one in every side, with inspection hatches that permit the tension to be regulated.

The installation of similar braces is foreseen all the way up the bell tower while the cracks are active and still opening, after the monitoring of these cracks has been completed.

4.4 Other works

The empty joints of the stone wall were injected and filled with to prevent rainwater from entering and the ensuing formation of ice and to restore lost strength to the stone wall. The parapets' ashlar work in the bell tower upper arches was dismantled and relocated and sewed with fibreglass to the existing buttresses to prevent them from collapsing as had happened shortly before the restoration. A structural metallic arch was designed and installed in the clock hole to permit the clock machinery to function normally. The cornices were consolidated, especially where they were threatening to come loose and collapse (Pita 2002).

4.5 Interventions still to be performed on the bell tower

Considering the urgent character of this first phase of intervention, the budget available was used for the more imperative repairs, but some equally urgent interventions still remain to be done, such as:

- Repair of the stone flattening in the Southwest corner
- Injection and filling of the joints of the rest of the bell tower

- Installation of new braces to restrain the living movement of the bell tower cracks.

5 CONCLUSION

The plight of the bell tower of Vistabella del Maestrazgo, Castellón (Spain) required a quick first intervention but the scaffold built to perform it helped to provide a very accurate survey to understand the reasons for these pathologies. The weak situation of the tower, supported only by buttresses and a hollow stone wall corner did not contribute to its present state of health. The precise survey together with the monitoring of the existing cracks in the bell tower made it possible to understand the origin of the problems, which can mostly be put down mainly to the design of the bell tower and the unequal sinking of the bell tower foundation.

REFERENCES

- AT Control 2002. *Informe del estudio geotécnico realizado para la rehabilitación de la torre de la iglesia de la localidad de Vistabella del Maestrazgo, Castellón*. Castellón, Inédito
- Fernández Núñez, J.M. 1995. *Vistabella. Centinela inmortal del Maestrazgo*. Barcelona. Avesta
- García García, F. 2002. *Estudio del subsuelo en la torre campanario de la iglesia de Vistabella del Maestrazgo (Castellón) con georrádar*. Valencia. Inédito
- Igme 1981. *Mapa geológico de España. Villahermosa del Río*. Madrid. Ministerio de Industria y Energía
- Martín Peinado, F. 2002. *Caracterización de morteros del campanario de la iglesia parroquial de Vistabella, Castellón*. Granada. Inédito
- Pita de Aguinaga, J. 2002. *Informe del biodeterioro de la torre campanario de la iglesia de Vistabella, Castellón*. Valencia. Inédito
- Rives Calbet, B. 2002. *Informe arqueológico de las catas de reconocimiento en la torre campanario de la iglesia parroquial de Nuestra Sra. de la Asunción en Vistabella del Maestrazgo, Castellón*. Valencia. Inédito
- Serna Ros, P. 2003. *Informe de las grietas del campanario de Vistabella, Castellón*. Valencia. Inédito

Palazzo Cittadini-Stampa: role of stratigraphy and cinematic analysis in the knowledge of a masonry building

S. Bortolotto, C. Colla, D. Mirandola & A. Sponchioni
Politecnico di Milano, Milan, Italy

ABSTRACT: The Cittadini-Stampa building is a 18th Century cultural heritage, whose abandon has caused its extreme decay. To approach correctly the building's heritage and material, the present work underlines the role of stratigraphy and cinematic analysis as preliminary knowledge phases. The survey of the superimpositions due to historic developments of this masonry building, and of the crack pattern which has developed, lead to evaluate the static equilibrium and to give indications for the strengthening intervention. A multidisciplinary analysis has defined the structural characteristics and precarious points of the construction. Careful inspections, survey and diagnostic investigations have served as essential tool to highlight the crack pattern, active and possible cinematic mechanisms and other specific vulnerability of this building, an aggregate of not-coeval structures. The knowledge gathered has supplied indications to formulate a targeted project of structural improvement.

1 INTRODUCTION

The Palazzo Cittadini-Stampa is located in Castelletto di Abiategrasso, within the western district-belt of Milan, along the Naviglio Grande, an artificial water channel of historical importance. It is a brick masonry, three-storey, rectangular-plan building, dating back

to the 18th Century (Figs 1–2). The northern front is plastered over and has a wrought-iron balcony and a wide, arched entrance. The windows have simple cornices and architectural framings which create a symmetrical central-axed rhythm throughout. The same architectural elements have also been used in the western and southern façades. The latter has



Figure 1. Palazzo Cittadini Stampa, main elevation on the Naviglio Grande, in a photo of the '80s.



Figure 2. The building settings in the present territorial context, at the meeting point of the artificial water channels of Naviglio Grande and Naviglio di Bereguardo (left); the relevant buildings in Castelletto with historical connections to the Cittadini-Stampa building (right).

a three-span portico and a wrought-iron balcony on the first floor. Interiors are partly frescoed and have coffered timber ceilings; the stone stairs have elaborate wrought-iron handrails.

Since 1915 the building has been included in the list of historical buildings (*ex lege* 364/1909) and was hence legally under State's protection, which was renewed 1950 (*ex lege* 1089/1939). In January 1980, local authorities through the commune's Technical Office started to take urgent measures for the preservation and maintenance of the building and financed works to replace the roofing and to consolidate the ceilings; the works were partially carried out in 1982. The building, a communal property, shows heavy signs of material and structural decay. Along the years it has been stripped of most of its most valuable decorative elements: fireplaces, stone cornices and terracotta floor tiles. In 2003, the "Laboratory of Diagnostic for the Preservation and Re-use of Buildings" operating within the Department of Architectural Planning at Milan's Polytechnic University made an agreement with the local authorities to set up an on-site workshop for students in the Cittadini-Stampa building. The workshop became part of a post-graduate training course for "Experts in survey and diagnostic techniques applied to historical buildings" which was held in January–June 2003 (see note 1).

The course was aimed at training professionals working on historical buildings and focused on the following aspects:

- study of historical records and cartography (Figs 3–4);
- analysis of construction techniques and materials;

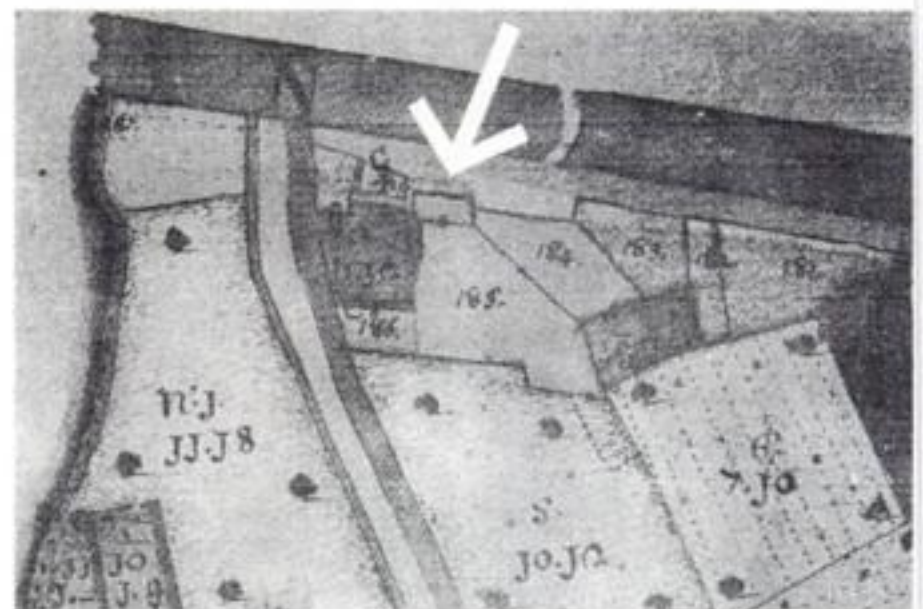


Figure 3. Portion of the Theresian Cadastre of 1751 showing the building on parcel number 185.



Figure 4. Detail of a fresco in the tower room at the first floor: ideal image of a XVII century palace.

- survey and elaboration of thematic maps (on paper and multimedia);
- diagnostic analysis (see note 2);
- preparation of analytical tables for preservation and re-use guidelines (see note 3).

Each course unit included practice within the on-site workshop, so as to gain direct experience of the complexity of analytical procedure and data analysis, preliminary steps to the drawing of any preservation project.

In July 2003, the Lombardy Region – together with Milan's Università degli Studi, Comune di Abbiategrasso, Milan's Province, Agenzia del Demanio (State property agency) and Aler (Lombardy Agency for Popular Housing) – signed an "agreement-plan" to locate some research laboratories, university and congress halls and one innovative museum in a number of historical buildings in Abbiategrasso. Accordingly, the Palazzo Cittadini-Stampa will house the "Water Museum".

The present study focuses on the evolution and structural analyses of this historic masonry building, and specifically on material "additions" and "subtractions", crack patterns and related "critical areas" (i.e. structural or potential weaknesses), which the preservation intervention will have to take care of.

2 STRATIGRAPHIC ANALYSIS

Intervention on historical architecture implies prior gathering of adequate information to describe the building in its geometric, morphological and material complexity.

Following this approach, the activities carried out on site started with geometric survey (see note 4) and then focused on various aspects: interpretation of the different construction phases of the building through stratigraphic analysis of the masonry walls, identification of the materials, analysis of present and past decay phenomena, crack patterns. The information gathered on site was integrated by stratigraphy survey in order to identify and understand the different construction phases. It has been ascertained that scientific methodologies borrowed from archaeological analysis can provide valuable results also in the field of architecture. This applied visual methodology favours direct observation of the source of interest, that is, reading off information from the walls themselves. It also contributes to in-depth study of specific aspects and suggests best practices to avoid irreversible loss of the genuine quality of the building and to preserve its multi-layered material history (Bortolotto 2004).

Stratigraphy analysis is a graphic methodology which allows to record layered construction phases which can be detected in a building. The archaeologist/architect's job is to reconstruct the chronological

sequence along with the material and structural decay process. The current debate on the relationship between archaeology, architectural archaeology and architectural restoration focuses precisely on codifying procedures to identify building processes and phases. To guarantee proper and efficient planning of preservation measures these must necessarily take into account all data deriving from the study of structural and material decay.

In the case of the Palazzo Cittadini-Stampa, only a limited amount of stratigraphy information could be obtained through visual observation (Mannoni 1984) due to the fact that the masonry patterns, the wall textures and toothing are largely not visible. In fact, the building is plastered on the outside and the rooms are plastered and largely covered by frescoes. Therefore, the procedure has been carried out where possible, non-invasively, and it granted detecting a sequence of building phases, as well as providing some structural indications of the construction. As a matter of fact, the static behaviour of the building has been affected by several additions which were made to the original core-structure.

Theoretical and methodological knowledge acquired during the study course has later permitted on site to acquire direct experience and to unveil several superimposing phases in the Palazzo Cittadini-Stampa. These stages have been ordered in a sequence which has disclosed the process of change and development that the building has undergone in the centuries. The study of the discontinuities in the masonry and of the many walled-up doors (revealed also through oblique-light observation), as well as the analysis of wall textures (with the help of active thermography), and above all the possibility to gain access to the garrets (where exterior elevations, plastered and painted, were discerned) permitted to detect the following main construction phases:

- a tower-house in the north-western portion of the present building. The "house" consisted solely of a ground-floor and reached as far as the present entry-hall, whilst the quadrangular "tower" had two storeys above the ground level. Two of its corners are still detectable in the North front and in the longitudinal spine bearing wall of the present building. On the top floor – which now corresponds to a garret – the tower had a projecting brick decoration, probably a windowsill for pigeons (Fig. 6);
- a "rectangular" body to the East of the tower-house, whose pristine South-front windows were walled up when the present Palazzo was built but are still visible in the garret, as well as parts of the corresponding plastered masonry wall;
- later additions to the above mentioned older structures, belonging to the present Palazzo Cittadini-Stampa. These are detectable through a number of elements: the absence of "toothings" or continuity

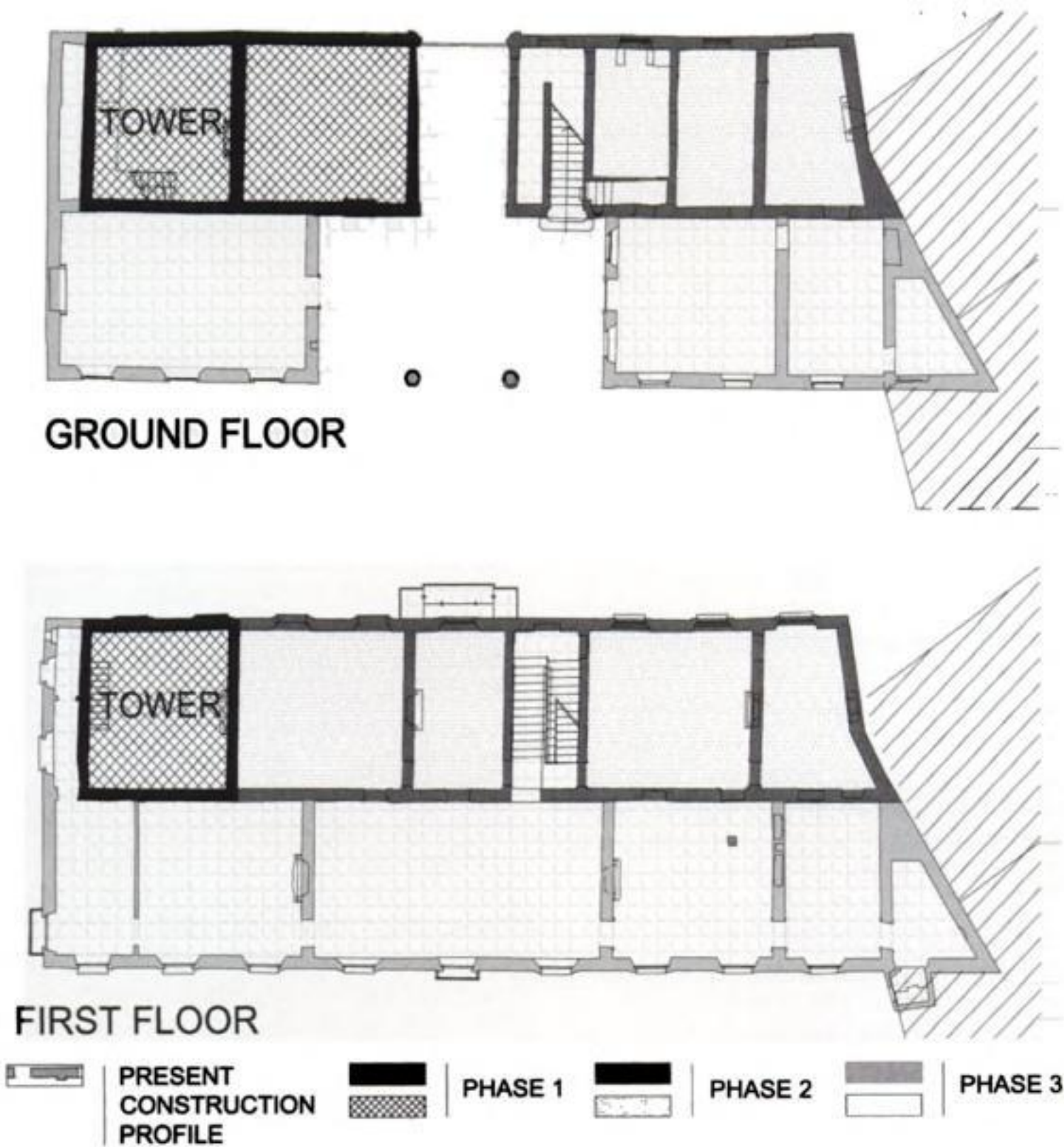


Figure 5. Building evolution as dated from its historic masonry.

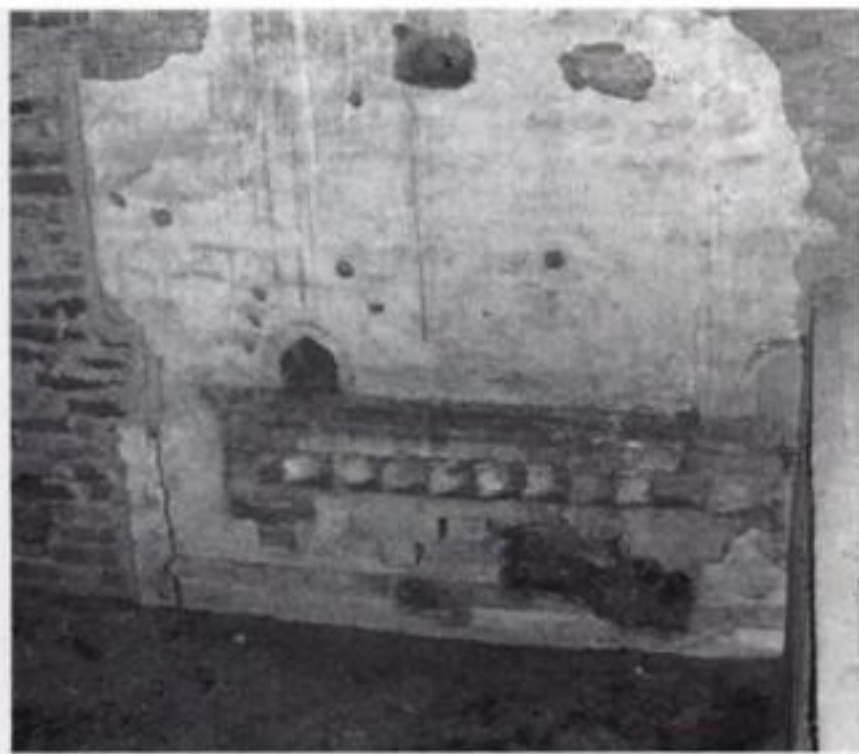


Figure 6. External projecting brick decoration of the ancient tower (visible in the garret of the present building).

between the newer and older masonry; alterations to the inner side of the tower's northern wall due to the opening of a window (on the first floor), which was meant to follow the new "rhythm" in the openings of the Palazzo itself; functional changes due to the construction of a new annex at north-west, housing secondary stairs, and a new grand staircase built on the previous flights but in a different way.

The main data have been summed up through simplified graphic schemes showing the different construction phases (Fig. 5).

3 STRUCTURAL DECAY ASSESSMENT

Through direct inspection of the site, a number of crack patterns have been described, which can be distinguished in passing-through cracks, non-passing cracks



Figure 7. Crack pattern of the main elevation (North) overlapped to that of the inner façade with projection of bracing walls.



Figure 8. Crack running vertically at the corner between bracing wall and longitudinal wall in the staircase.



Figure 9. Vista of the left portion of the North elevation with spalling of wall.

and some fissures which actually appear to be flaws in the plastering (i.e. several craquelure-like patterns in the coating). The most relevant fissure pattern involves the north-front external masonry. A visual survey of the crack pattern in this portion of the building

has been carried out along with a specular one on the inside of the same wall. The graphical output from both sides have been overlapped to obtain a more complete interpretation of discontinuities and structural damage (Fig. 7). Some axonometric projections are also

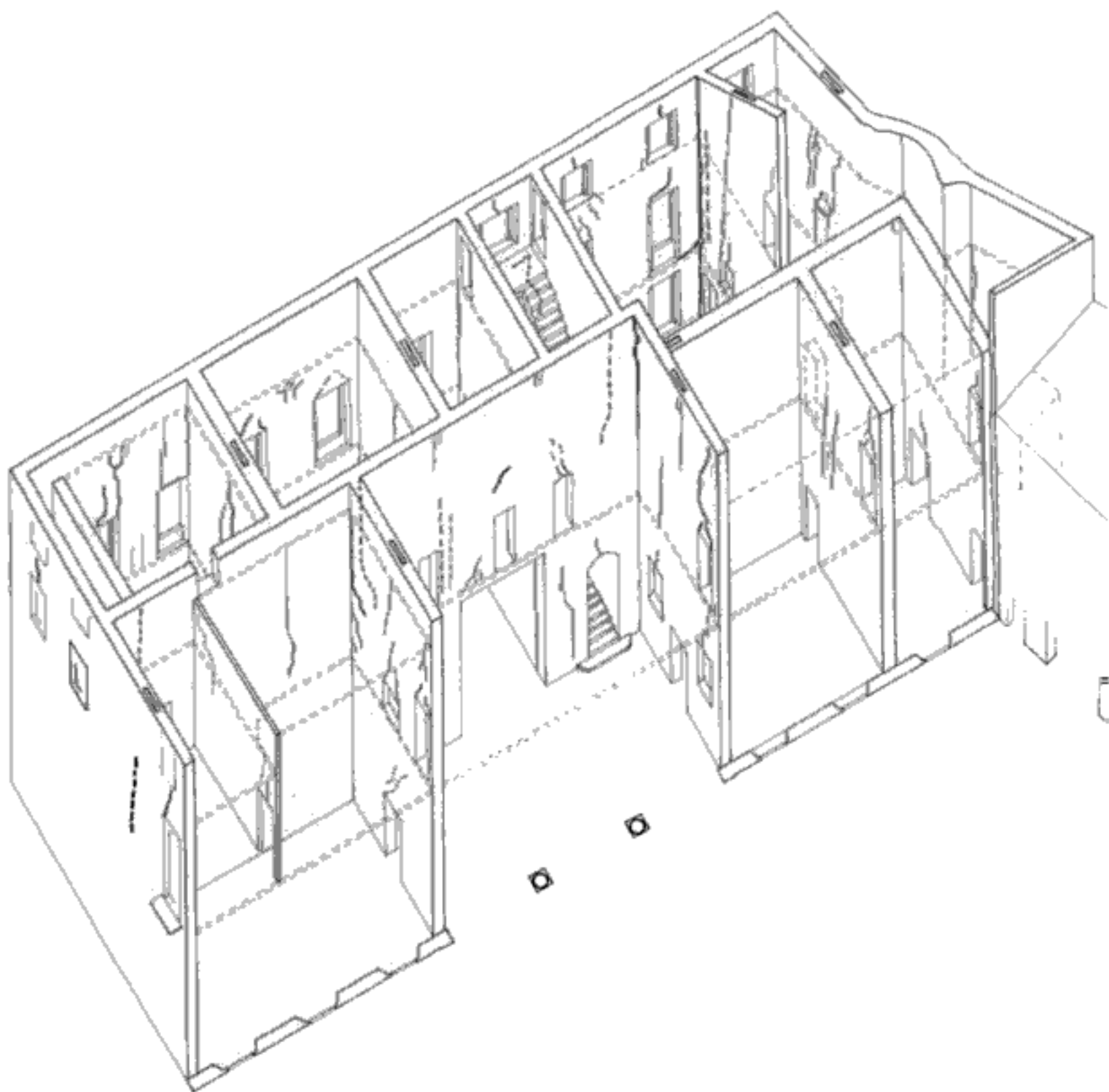


Figure 10. Axonometric projection of the crack pattern.

represented in Figures 10 and 11. As a result of this procedure and way of crack plotting, a three-dimensional reading of the decay phenomena in the building could be modelled and hence compared with the results of stratigraphy analysis in order to spot all “critical areas”. Indeed the results from both disciplines may be combined to enhance interpretation.

One essential step has been the identification of the original core-structure of the tower-house within the present building. This construction probably dates back to the 15th century and shows fair stability due to its “box-like” structural behaviour, and well-toothed coeval masonries.

The structure which was built to the East of the tower-house during the second construction phase, has undergone later major redesigning, especially when the Cittadini-Stampa family chose to enlarge and renovate the Palazzo. It is precisely in this portion of the building – which includes the new entry-hall to the

porch and the new grand staircase – that the heaviest structural problems have been discovered.

The third and last main construction phase involved both the “doubling” of the Palazzo through a “mirror” development to the South (its bracing walls abut against the longitudinal bearing wall) and the addition of a new portion to the west, leaning onto the first phase structure.

In order to attain consistency and unity with the pre-existing architecture and to increase functionality according to the owner’s new requirements, some partial or extensive demolitions were carried out in this last phase with the aim to improve inner communication through new stairs and new doors which were opened into the old bearing walls. To this phase also belongs the reorganization of the house main infrastructural services, in particular the heating system.

Discontinuities caused by the construction of new chimneys are easily detectable on the older walls.

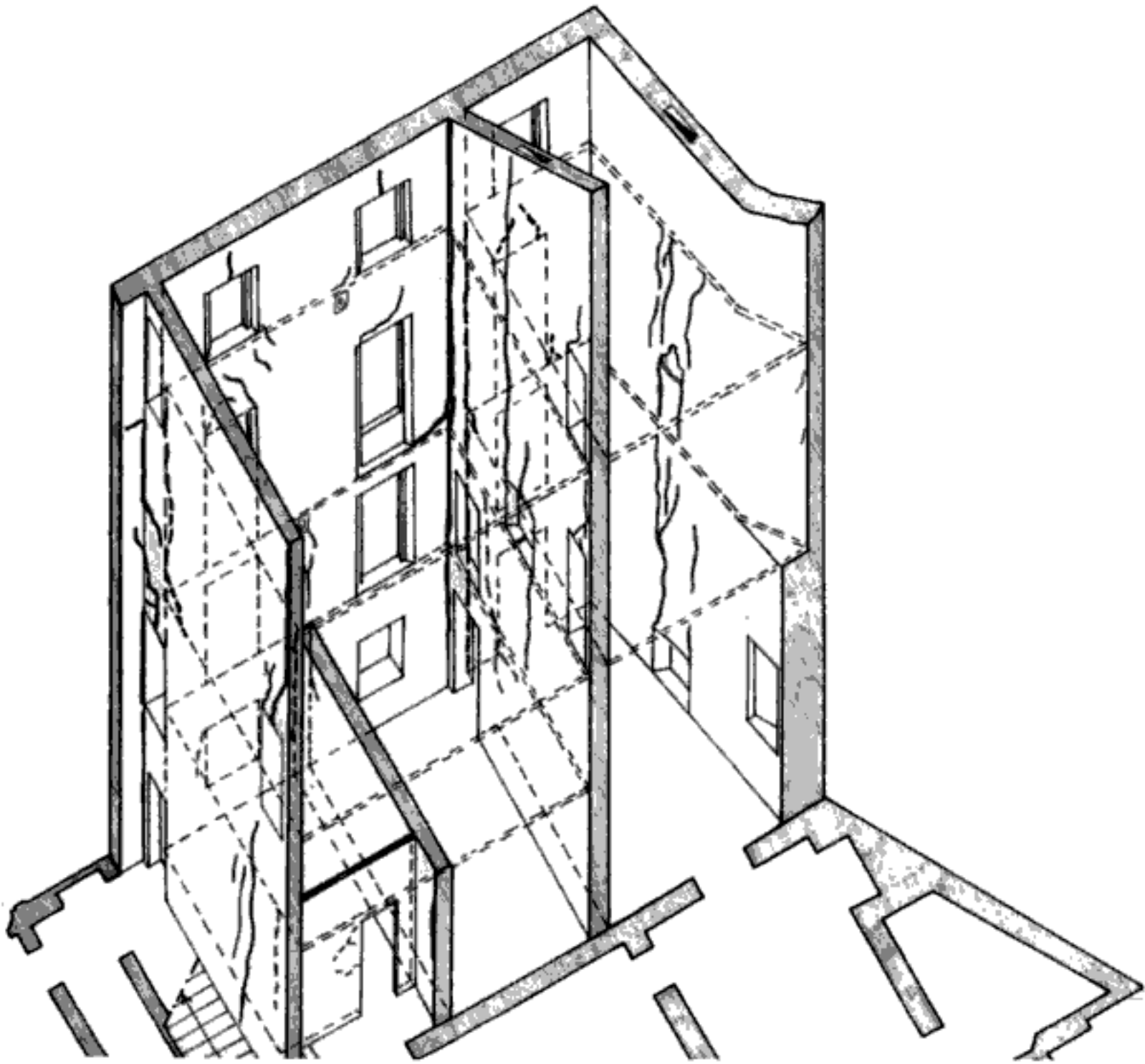


Figure 11. Detail of axonometric projection of the crack pattern with the crack running vertically the whole height between a transversal wall and the longitudinal North façade.

Openings and chimney wells are “weak points” as far as structural stability is concerned: extensive crack damage is easily detectable particularly where openings and chimneys are not coeval. Near the lintels are to be found “arched fissures” which occur when arches or lintels above the openings become weaker because of changes in the stress distribution in the wall.

Alterations made in the bearing walls, such as those mentioned above, have jeopardized the structural stability along the years. In the northeastern part of the building some large cracks have been spotted at the junction between North front wall and bracing walls, signalling a possible cinematic mechanism in the North wall. The most critical area is on the first floor where the wooden ceiling previously connecting the bearing masonry members is almost totally missing in one large room. Its collapse followed years of water leakage through the roof, caused by lack of maintenance and consequent material decay.

The cracks at the junction between transversal and longitudinal walls indicate the lack or loss of masonry “toothings”, which may produced a cinematic

mechanism. This construction defect is related to the multiple construction phases, as well as to the many doors, located in the orthogonal walls but too close to the north front wall (some of these doors were later walled up although with too thin masonry). In the third development phase, along with the walling up of some of these older doors, demolitions have taken place to open new doors in the same bracing walls, but this time too close to the longitudinal wall. These operations have further weakened the masonry.

Close examination of the crack patterns on the outer and inner faces of the north front revealed that a cinematic mechanism has taken place, limited to the portion to the east of the main entrance (Fig. 9).

A number of factors seem to have concurred to this situation, starting from the presence of the “void” created by the entrance-hall and the porch, continuing with the lack of connection between the walls built in second phase and the tower-house; as well as the new large windows added in the third phase; finally the thrust added by the orthogonal walls of the new structure built in third phase onto the northern walls.

The generated cracks run diagonally on the façade, along lines which, observed together, seem to draw an arch. This “arched” pattern clearly indicates a vertical translation in this portion of the façade (Mastrodicasa 2002).

To these cinematic mechanisms is to be added the outward rotation of that same wall, which can be attributed mainly to the above mentioned collapsing of the ceiling between the first floor and the garret – and consequent loss of a constraint – and further to the thrust of the rafters of the new roofing built in 1982. This thrust is unevenly distributed by the new concrete ring beam, which is not completely closed and, moreover, increases the load on the wall (Fig. 13). Therefore, this portion of the façade can be described as a “slender” wall, loaded on its extreme points, and outwards-bulging. To this wall remain two bonds: the corner wall to the East and the foundations which anchor it to the ground (Mastrodicasa 2002).

The following remarks regard the state of the foundations of the building and its urban and environmental context. The Palazzo Cittadini-Stampa was built very close to the meeting point between Naviglio Grande and Naviglio di Bereguardo. From these main water channels several ditches run southwards irrigating the land around the palazzo (mainly rice fields and water-meadows). To the East of the palazzo – right beyond the so-called “Osteria”, an ancient inn – there used to be an irrigation source (fontanile), which is still registered in the 1904 map of the Cesato Catasto (former register of the land property). Therefore, the “water” factor might have influenced the structural conditions of the Palazzo Cittadini-Stampa. Rising and sinking of the Naviglio’s water level, as well as twice-a-year draining in order to clean the river-bed may actually have varied the soil water content and therefore altered the state of the foundations.

4 A WORK IN PROGRESS

The detailed study and analysis of the Palazzo Cittadini-Stampa enables to draw few additional remarks on its present state of decay, although these do not mean to be conclusive and will require further in-depth research and monitoring.

The above description of the crack pattern present in the building has in fact been drawn without the help of an instrumental monitoring, prolong enough in time to detect possible cinematic mechanisms still active. It is suggested that further check and monitoring of damages be started as soon as possible, not because the present conditions of the Palazzo put at risk its structural stability but because data collection of this kind need to last over a year in order for the data to be significant. All data gathered until now can

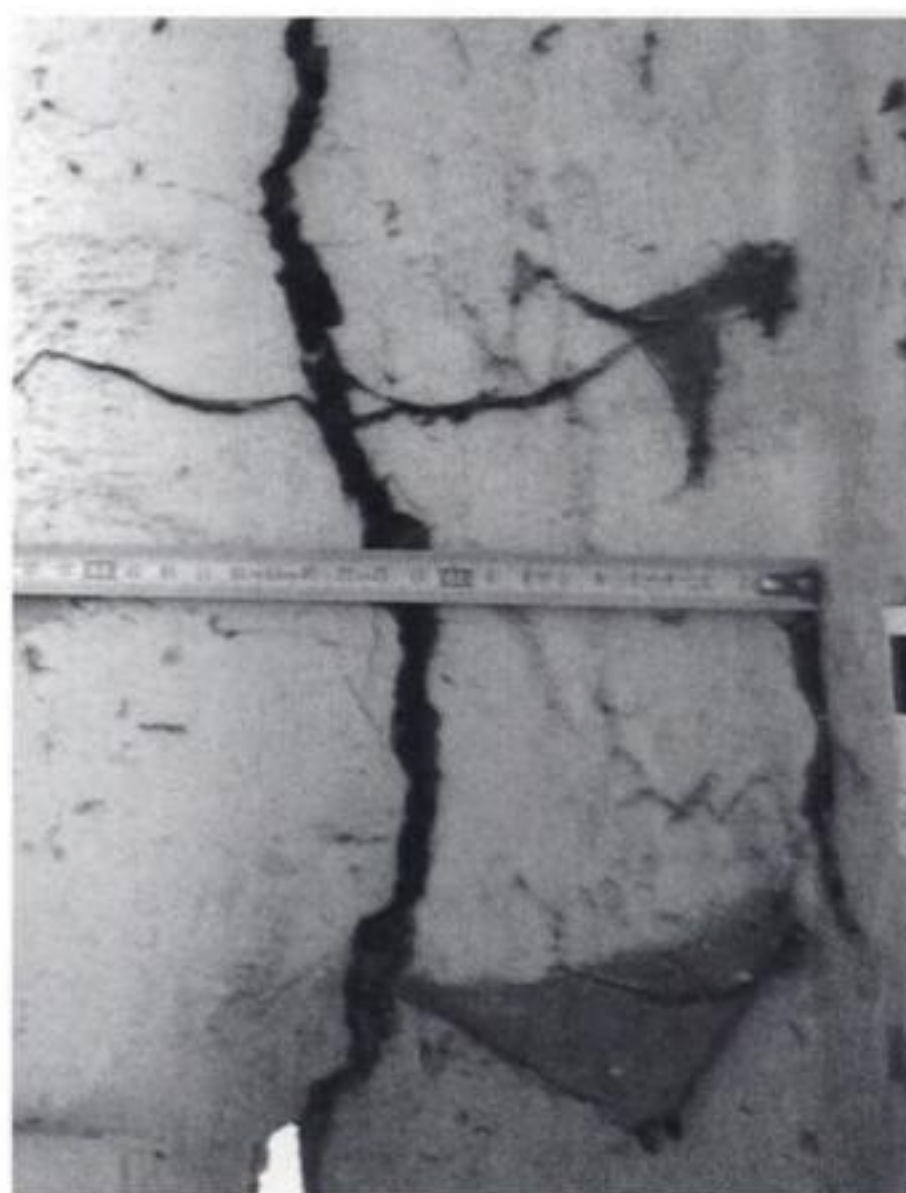


Figure 12. A detail of the crack of Figure 11.

nonetheless be of practical help in order to set up a plan for instrumental monitoring.

Therefore it is recommended to set up a monitoring systems over a significant period of time (18 months) in order to ascertain any changes in the crack patterns detected, as well as possible active cinematic mechanisms – translations, rotations, collapses – concerning structural macro-elements such as walls, openings, roofing, foundations etc. It would also be advisable to check the stress distribution and strength of the walls, for instance through diagnostic tests with flat-jacks both single and double (Binda 1979).

Only after the completion of a thorough diagnostic survey it will be possible to draw a suitable and well-focused consolidation project, which will presumably involve:

- closure of the reinforced concrete ring beam (Fig. 13),
- installation of metal ties both to contain the thrust of the roof and, at the ceilings, the walls’ relative movements,
- consolidation and partial substitution of the wooden ceilings to improve their bearing capacity,
- verify the existence of a basement with the possible aid of geo-radar technique or focused digging, in order to assess the actual depth of the foundations.

Further in-depth stratigraphic analysis will be possible on the basis of the outcome provided by historical



Figure 13. A detail of the ring concrete beam in the attic.

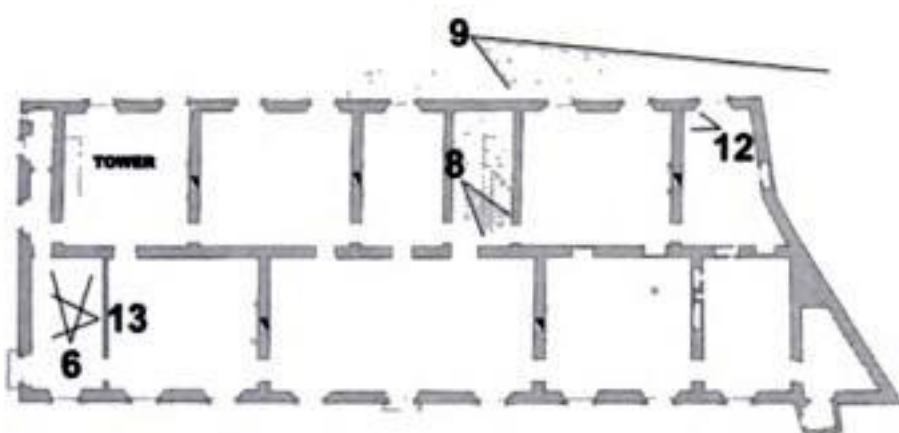


Figure 14. Photographic views location in the building.

and documental research and, if necessary, with the help of limited sample tests on the masonry.

It is here underlined the relevant role of non-destructive investigations in gaining specific as well as global knowledge related to the building and in assessing its environmental conditions. With this aim it is possible to integrate instrumental monitoring with psychometric and thermography tests (Binda 1997).

5 CONCLUSIONS

Thanks to a multidisciplinary analysis approach it has been possible to formulate considerations specific to the material and the structural decay of the building in object. and to highlight causes and effects, synchronicities and diachronicities.

The passing-through cracks, the weak points of the building, the active or possible future cinematic mechanisms, the rotation freedom of a portion of the North front are all parameters which indicate specific vulnerability of this building due largely to its configuration of aggregate of not-coeval structures.

The formulated observations have allowed to put forward some hypotheses related to the causes of the present structural decay. Although further deep analysis and monitoring will be needed, the collected information are already a valuable input to the intervention and strengthening project, contributing to direct and quantify it.

The analyses carried out and those still necessary to correctly define the building preservation project may well be specific and specialized studies, but with the ultimate purpose of punctually preserving the historical material which the building still houses. Therefore these will have to be coordinated and compared according to the multi-disciplinary approach which is necessarily involved in this kind of intervention.

The resulting analysis and interpretation outcome will provide clear guidelines for a careful and respectful re-use and strengthening intervention project.

NOTES

1. The post-grad course FSE n. 86947 (dir. S. Bortolotto) included the following units: Archeological, architectural and urban restoration: theory, history and practice; Historical and documental research methods; Direct and indirect sources for archaeological research on elevations; charting and plotting; diagnostics; multimedia techniques; business planning and legislation. Post-graduate students and researchers attended the on-site workshop: G. Capitanucci, C. Colla, M. Iezzi, C. Liverta, C. Miedico D. Mirandola, M.V. Piva, A. Sponchioni, M.P. Taliento; graduating students: C. Cipollini, M. Pozzi.
2. Diagnostic analysis included: thermography, moisture tests, microclimate charting, inspection of the wooden structures.
3. A CD-Rom was produced at the conclusion of the on-site workshop: "Il Palazzo Cittadini Stampa a Castelletto di Abbiategrasso" ed. by S. Bortolotto with M. Dell'Orto and R. Mastropirro.
4. Topographic survey with total laser station has also served to verify a series of the building's structural behaviour (out-of-plane, misalignments, spalling walls).
5. Special thanks to Professor Luigia Binda for her kind help and useful suggestions.

REFERENCES

- Binda, L. 1979. Sintomatologia del degrado statico, Course *Restauro edilizio nei Centri Storici*. Ord. Degli Ingg. Cremona: 36–65.
- Binda, L. 1997. *Sperimentazione ed indagini non distruttive*. Proc. V Nat. Congress ASS.I.R.C.CO, Orvieto, 119–126.
- Bortolotto, S. 2004. Il rilievo stratigrafico. In C. Campanella (ed), *Il rilievo degli edifici*. Milano: Il Sole 24 ore, 94–115.
- Mannoni, T. 1984. Metodi di datazione dell'edilizia storica. *Archeologia Medievale* n. XI. Firenze: all'Insegna del Giglio, 396–403.
- Mastrodicasa, S. 2002. *Dissesti statici delle strutture edilizie: diagnosi, consolidamento, istituzioni teoriche*. Milano: Hoepli.

An architecture teaching program to rescue the historical town of Ouro Preto, Brazil

B.T. de Oliveira

Architect D.Sc., IPHAN, Ouro Preto/MG, Brazil

E.C. de Araújo

Professor D.Sc., UFOP, Ouro Preto/MG, Brazil

J.N.S. Villaschi & L.C. Mancini

Architects, M.Sc., UFOP, Ouro Preto/MG, Brazil

ABSTRACT: Founded in 1698, Ouro Preto was, during two centuries, the capital of the State of Minas Gerais and stage of an intense nationalist feeling, that had influence on the independence of Brazil. As an alive testimony of secular traditions the city constitutes object of special cares in order to safeguard its integrity as the world largest baroque urban settle, and guarantee its historical, artistic and environmental heritage. In this sense, the Federal University of Ouro Preto proposes an Architecture and Urban Studies Course in order to face the social demand of the 21st century for professionals of the territorial planning as well as the preservation of its cultural values. The formation of critical mass on this professional performance area represents a most significant institutional relationship between the academic world and the daily community life, the urban space production and the destinies of Ouro Preto and its historical surrounding area.

1 HISTORICAL CONSIDERATIONS

1.1 *The Enlightenment in Ouro Preto*

Brazil, since its discovery in the 16th century, has never been isolated from the rest of the world. The process of its continental dimensions territory's occupation was held through successive economic cycles addressed to the satisfaction of the European market. Unlikely the first extractivist cycle of "Pau Brasil" (*Caesalpinia echinata*), which didn't favour any territory settlement, the mineral extractivism cycle generated deep transformations in the social and space structure and organisation, showing intense process of people displacement and the urbanisation of the country's interland.

During and after the two centuries of colonisation, the liberal ideas and philosophy, as well as other cultural influences were brought to Brazil, strongly inspiring revolutionary groups to promote the liberty and the necessary political changes.

The illuminist French thought "Libertè, Égalitè et Fraternitè" has greatly influenced the Minas Gerais people to become free from the colonial oppression and create our own national government. It also explains registers like the Minas Gerais flag "Libertas Quae Sera Tamem". Different from Bahia's disloyalty

in 1798, promoted by the people, the "Inconfidência Mineira" was led by the highly wealthy society that filtered and translated the illuminist purposes. They defended Brazilian liberation of the colonial power, even though in a partial and less democratic way, once they were owners of thousands of slaves and they wouldn't support the end of the slavery. According to Schmidt (1997), the Minas Gerais' disloyers had then planned the transference of the Minas Gerais capital to the town of São João del Rei, while Vila Rica, nowadays Ouro Preto, would become an excellent university centre.

Under pressure of the Portuguese Kingdom and alleging the collection of late taxes, the authorities arrested the military Silva Xavier, the only disloyer who did not belong to the powerful society group. Betrayed by his own conspiracy partners, he was hung in a public square, having his body divided in many pieces that were exposed in different points of the town of Ouro Preto, as a demonstration of the power of the king against the fight for independence.

1.2 *The gold cycle and the colonial times*

In the 18th century, Brazil had become the largest world producer of gold and diamonds. Discovered by



Figure 1. The Estrada Real (Royal Road).

the “Bandeiras”(expeditions in search of Indians and minerals), the main and more durable area of auriferous exploration was placed in Minas Gerais. The mining activities attracted immense number of people from all the world in search of immediate wealth, making the population in the colony to increase almost 10 times within just one century and the lack of infrastructure provoked hunger and conflicts in the area.

Portugal needed to create the “Minas’ Intendancy”, a fiscal organism directly linked to Lisbon and responsible for the administration and for the surveillance of the mining activities, but specially for the collection of tributes. The most important tax collected by the Kingdom was the “fifth”, which corresponded to 20% of all and any amount of gold found by any miner.

The official flowing of gold and diamonds to the closest port was concentrated on the “Estrada Real” (Royal Road), that covers more than 1400 km, constituted of two main roads converged in Ouro Preto: the Old Road that ties Ouro Preto to Parati and the New Road that links the city of Rio de Janeiro to Ouro Preto, later elongated until Diamantina. This road configuration turned Ouro Preto into the geographical and historical centre of the Estrada Real (Fig. 1).

In order to try to control the circulation and the transport of mineral wealth, some “Houses of Foundry” were created along the Estrada Real, where

the powdered and the nuggets gold, which circulation had been prohibited, were all melted and marked with the royal stamp.

1.3 The urban and architectural evolution of Ouro Preto

Ouro Preto has had an original space formation that disobeys all types of traditional radial or nuclear urban organisation in most of the other Brazilian Colonial cities. Its organic and lineal configuration advanced in more than two centuries the urban phenomenon nowadays known as “nucleation”, that is, the formation of a city starting from the connection of several close urban nuclei.

Several small settlements appeared in function of the discovery since 1698 of gold mines spread around the territory. Their connection (Fig. 2), was consolidated on the second quarter of the 18th century, by means of significant urban interventions promoted by the government of Mr. Gomes Freire of Andrade, called Earl of Bobadela (1735–63). In that period bridges and fountains were built, and the administrative centre was implanted, known at the present time as Tiradentes Square. It was delimited by the construction of the Palace of the Governors and later by the old House of Chamber and Prison. The new nucleus unified the two more important small villages, named Antônio Dias and Pilar. It highlighted Vila Rica as the main gold extraction centre of the 18th century, propitiating great innovations in the architecture, in the painting, and in the sculpture works. One of the most recognised is the artist Antônio Francisco Lisboa, known like Aleijadinho (the crippled).

In Minas Gerais, the buildings followed the models adopted in other Brazilian areas, developing simple architectural solutions standing out for the pleasant proportions and for the balanced rhythm of the whitewashed walls drained harmoniously by the empty spaces. The main constructive technique in the Brazilian popular architecture is still the “pau-a-pique”, which is constituted of wood barse covered of wet earth. Stone and whitewash walls were used only in the most important residences and in the monuments.

In the beginning of the 18th century, Vila Rica formed an architectural seatle of baroque style, constituted by white collar walls covered by ceramic tiles, harmoniously integrated with the topography and the surrounding nature.

In the religious architecture the Portuguese influences were assimilated, adapted and reformulated. In the beginning, the traditional conception of the first Brazilian Baroque style was adopted in Minas Gerais with rectangular plants and plane facades. Later, these facades were changed in curved formats and the heavy and robust proportions gave place to a larger lightness and harmony buildings. The curved plants

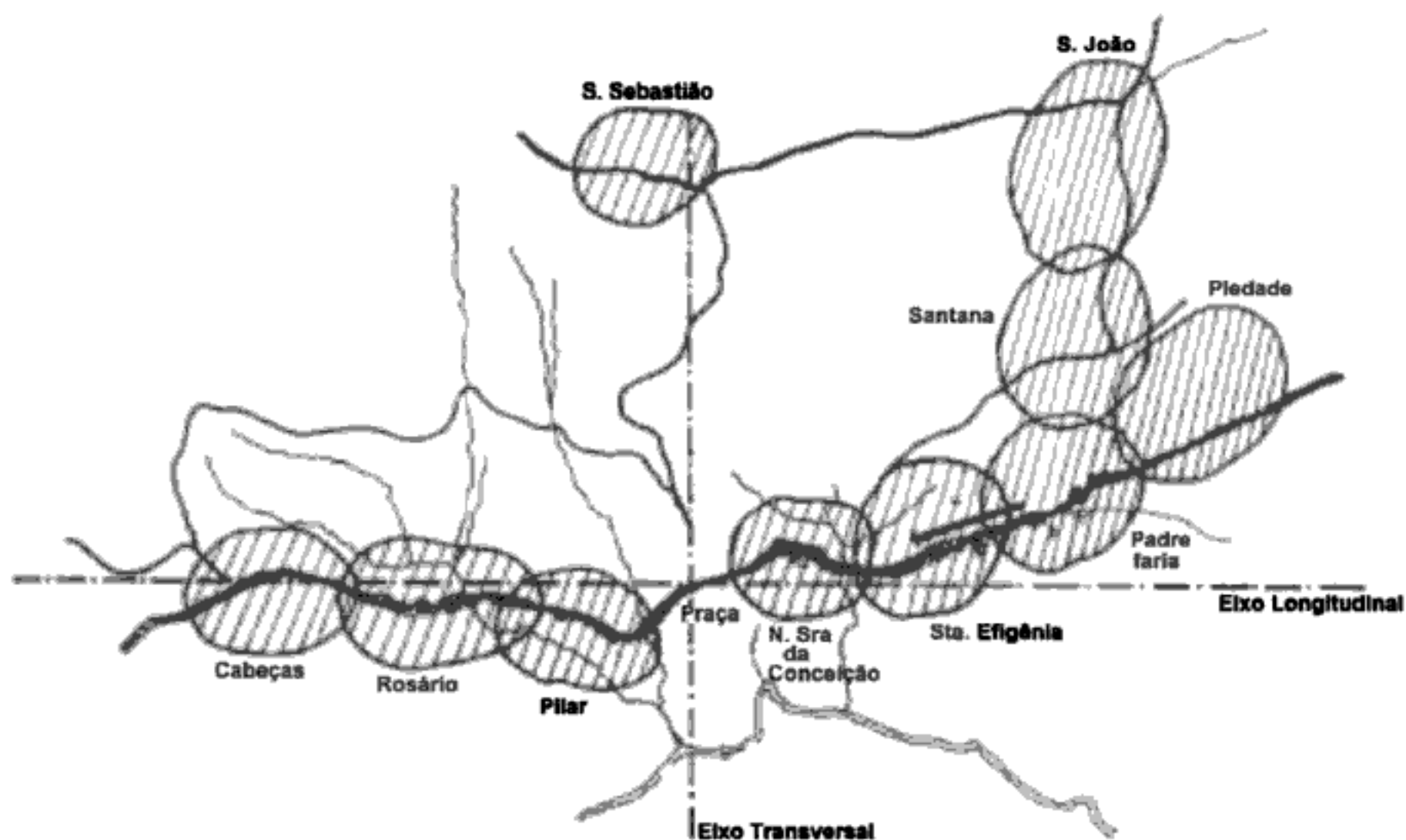


Figure 2. The urban evolution of Vila Rica.

and facades had strong influence of Borromini and German Baroque styles. The sumptuousness of the inside ornaments of the churches complete and accentuate the monumental aspect and the singular character of the religious architecture.

Another peculiar aspect of Minas Gerais history, comparing to other Brazilian areas, was the prohibition to install regular religious orders in its territory. This fact explains the lack of schools and convents in the urban landscape of the mining colonial cities.

The neoclassicist's premises in Vila Rica were first applied in the old House of Camera and Chain and later in the existent residence constructions and monuments, respecting its scales and old additions.

The first decline of the city happened at the end of the 18th century, with the exhaustion of the gold mines and the crisis of provisioning, resulting in a strong economic decadence and in the demography emptying from the old Vila Rica.

On March 20th, 1823, Vila Rica received the title of Imperial City of Ouro Preto, maintaining its function of capital of the province of Minas Gerais.

The following decades and in the 19th century, Ouro Preto was modernized with urban expansions in the Pilar Quarter in direction to Barra Quarter, besides the fixing of the railroad, of the telephony infrastructure, telegraph and illumination, as well as nets of water and sewer.

Several buildings of the colonial period were reformed and replaced for others, of neo-classic or

eclectic taste. The main church of the Pilar Quarter had its facade totally reformed between 1848 and 1852. The San Francisco de Paula's church was built in 1804 and was reformed in 1878, under neo-classical influence.

At that time, urban interventions were accomplished, fixing boulevards of classic taste and also appearing constructions of neo-classical facades with iron counters.

The inauguration of the rail station (1889) and the creation of the Pharmacy's School (1839), the Minas Gerais Lycée (1854), and the School of Mines were of great economic and social importance for the development of Ouro Preto in the 19th century.

With the proclamation of the Republic, in 1889, the image of the imperial city of Ouro Preto was revealed inadequate for the positivist purposes and for the scientific rationality of the republicans' ideals.

The change of the capital from Ouro Preto to Belo Horizonte, in 1897, produced an exodus of almost 50% of the population, provoking physical and economical damages to the city, characterizing its second decline process. As well as other historical cities, Ouro Preto preserved its physical and formal integrity because of the removal of the development that stimulates urban renewals.

In the beginning of the 20th century, the press had alerted about the abandonment of the cultural heritage of Minas Gerais and about the need of actions for its preservation. Starting from the twenties,

Ouro Preto begins to be visited by modern urbanists and architects as Lúcio Costa and Oscar Niemeyer, by poets as Cecília Meirelles and Carlos Drummond de Andrade, inspiring modernists like Mário de Andrade to classify the city as one of the most important bases of the national identity. Still in the twenties, several law projects were elaborated for the protection of the Brazilian historical and artistic heritage and, on July 12th, 1933, the Law-Decree 22.928 was promulgated leading Ouro Preto to National Monument. In 1937, at Gustavo Capanema's administration in the Education and Health Ministry, the National Historical and Artistic Heritage Service (SPHAN) was created, and in 1938 it promoted the integral recording of Ouro Preto.

In 1950, the installation of ALCAN enterprise (Aluminium of Brazil Limited), close to Ouro Preto, impelled the metallurgical and mining activities, provoking the growth of the population and the demand for new houses in the city. Such facts directed SPHAN to elaborate the first rules for approval of constructing projects, starting to recommend the traditional architectural elements of the colonial period, creating popularly architecture well known as "heritage style".

The decade of 60 presented important alterations for the life of Ouro Preto, like the creation of the Federal University of Ouro Preto (UFOP) and the asphaltting of the highway that links it to the capital of the State, Belo Horizonte. On that decade, fast urban transformations alerted the national public opinion and they stimulated public organisms to develop plans for the protection of the cultural heritage of Ouro Preto.

In the following years, successive attempts of cultural and environmental preservations and purposes of zoning were applied without solutions in the city and its surroundings. In September of 1980, Ouro Preto was declared as Cultural Heritage of the Humanity by UNESCO. Later, three state units of conservation in the surroundings were created: the State Park of Itacolomi, the Ecological Station of Tripuí and the Area of Environmental Protection (APA) of the Cachoeira das Andorinhas (Waterfall of the Swallows).

Successful, the settlement of the Addressing Plan proposed in 1996 constituted one of the county government's last initiatives in order to put together the urban development of the city with the protection of its cultural and environmental heritage.

The architectural and urban group of Ouro Preto has 45 monuments recorded separately and approximately a thousand constructions recorded together. The lines and the colours of its architecture are contrasting and they complement with the profiles, the textures and tonalities of the surrounding hills. According to Sylvio de Vasconcellos, in Ouro Preto the constructions marry the topography perfectly, accentuating its contours, the colours and the forms of the roofs, confusing itself

with the proper soils, its crests, looking like large nails or changing the natural foothills.

1.4 *The city at the present time*

Ouro Preto has a chaotic traffic, without an organized road system plan, with precarious traffic signals system and lack of areas for parking. There are few and an insufficient restrictions for traffic and the circulation of heavy vehicles is causing physical damages to the traditional structures of its stick-to-pricks, stone and adobe. A project for systemising the traffic was developed by the Monumenta/BID Program and it needs to be implanted with urgency.

The city also suffers a process of destruction of recurrent and temporary nature, with the realisation of megaevents at Tiradentes Square, without any planning or study of environmental impact.

Most of the protected properties are in reasonable conservation state and with compatible uses with their structures. The main problems are about compression, alterations of the internal spaces, replacing of materials and of the original constructive systems. There is a large demand of increments, additions and reforms, besides numberless irregular constructions. About a hundred processes against irregular behaviours are registered in the State and Federal public ministries. Another problem of difficult solution is said in despite of the fund subject, with the existence of ownerships and lands without owners, as well as many irregular division of urban portion.

Data of the IBGE, the official national statistic searching foundation, has already demonstrated that, if in 1970 the portion of the Brazilian population that occupied the cities in Brazil was about 50%, in the eighties, that value arose for almost 70% in 1990, and the urban population reached 77% of the total population of Brazil.

Attracted by non-existent, precarious or insufficient urban employments and services, large contingent of low income population, without means to survive in the country areas, has been more and more concentrated in the cities of medium and big loads. An approached scenery of the problems can be designed adding the rural exodus, the demographic explosion and the housing deficit, among other historical factors. It concerns the challenges related to the urban planning of any size of cities in Brazil at this so early century: the proliferation of slums and settlements on irregular urban portions, the lacking of basic infrastructure, the deterioration of urban environment, and the saturation of transport system, among others.

Through urban indexes, it has been verified the unequivocal perpetuation of a development model that concentrates opportunities, socialising the damages and the problems while it turns benefits private.

Ouro Preto has known, during the last decades, a fast process of total disordered growth, characterised by the occupation of its hills and lands located in life risk areas, the invasion of public spaces and green areas and even archaeological sites. The normative demands of projects, the latent fire loads, the surveillance and the existent systems of protection against the fire are precarious. The actual possibility of a reaction in chain, provoking fires of great proportion in the heritage architectural is a cruel reality. It has been contributing to deteriorate the life quality in the Ouro Preto, besides changing the face of the environmental surroundings and of the architectural group declared Cultural Heritage of the Humanity (Figs 3 and 4).

UNESCO organised a mission of technicians of the World Heritage Centre to come visit Ouro Preto in April 2003, in order to list the existent problems and to identify, in co-ordinated action with the several spheres of the public power, the necessary measures to stop the alarming deterioration of its environment and its built seatle, which is provoking substantial changes in the historical landscape of the city.



Figure 3. Ouro Preto in the beginning of the 20th century.



Figure 4. Ouro Preto at the present time.

A plan for the recovery of the cultural and environmental heritage of Ouro Preto means wide and diversified initiatives. It must contemplate actions in historical and archaeological research, for preventive maintenance of the cultural and environmental heritage. That task is immense and it can generate some hundreds of permanent jobs in the county, also contributing to the increase of the tourism and for the dynamical action of the regional economy. Only a collective action among the Municipal, State and Federal governments can remove Ouro Preto from its disordered and self-destructing expansion process, in order to replace the city on the way to the development over preservation patterns.

In that sense, some effective initiatives and purposes have been taken and, among them, it must be underlined the creation of an Architecture and Urban Studies course by the Federal University of Ouro Preto (UFOP), addressed to the preservation of cultural memories.

2 THE ARCHITECTURE TEACHING PROGRAM

The Brazilian Association of Architecture Teaching (ABEA) is working since 1989, on the settlement of a national politics for the establishment of profiles and patterns that assure the architecture professional's qualification in the depth of the social challenges related to the current process of globalisation.

The general curricular guidelines have for main goal the qualification of the students that will be graduated in courses recognised by the Ministry of Education for the professional exercise. It must provide to the future Architect the essential domain of the necessary matters to their performance, guaranteeing an unique qualification and strengthening their specialised knowledge, without losing the notion of group of problems of the architecture and urbanisation and their relationships with the society.

The purpose of structuring the Architecture Course in Ouro Preto is according to an old and wished institutional aspiration, within the growing social demand for professionals of the territorial planning. According to the intrinsically multidisciplinary of the academic formation and to the architectural professional practices, this course has been constructed with a vigorous potential of articulation of the several knowledge areas, gradually implanted in UFOP, especially in the last decade.

On the other hand, the formation of a critical mass in this professional area, that congregates slopes of the arts and of the applied sciences, represents significant depth of the institutional relationships between the academy and the society, the production of the city and the destinies of Ouro Preto. This double inside

and outside articulations punctuate clear perspectives of inserting UFOP and the city in the national and international subjects concerning the urban planning, the cultural heritage, the natural and built environment, the daily life quality, the renewed technological procedures in the civil construction, the aesthetic potential of our works, among others.

This course, proposed by the Escola de Minas (School of Mines) – UFOP, far away from representing just one more Architecture Course in Minas Gerais, have special characteristics in Brazil, as far as it proposes integral professional formation with two inside emphases in “Conservation and Restoration of Buildings” and in “Metallic Constructions”. It assists to peculiarities and historical potentials of the area, which are the important architectural sets of the mining colonial cities and other Brazilian historical nuclei, besides the traditional participation of Minas Gerais in the national metallurgy development.

The subject of the cities’ planning and administration should necessarily be a permanent subject of discussion inside public institutions and, particularly, in those dedicated to higher education. If the universities cannot be away from that mission, it is necessary to underline the important role that fits to UFOP in order to carry out this reflection and, above all, the formation of professional staffs, considering the most significant presence of this institution in the life of the community where it interferes. In this context there is a great need of performance of the very different professionals affected to the city planning, especially of the Architect and Urban Planning.

Base of the Brazilian colonial architecture, inspiring centre of the arts and strong pole of culture, science and technology, Ouro Preto has always been fertile source of professionals to the country. With all its tradition, UFOP has contributed, all along its history, with the formation of professionals in important areas, like mineral extraction, its transformation in steel plants, civil big works (highways, hydroelectric dams, airports) and, more recently, in the tourism. This concentrated know-how strengthens still more the credibility and the potential necessary for the creation of the Architecture Course, as well as the certainty of the success and of the benefits that will come from such academic enterprise.

3 CONCLUSIONS

Through a systemic research of the social, natural and architectural parameters it is easy to conclude that Ouro Preto suffer an accelerated process of complete decline. However, it’s necessary and it’s still time to save this historical monument from several types of

actions. The collective action among the national and international public powers can still avoid its entire destruction and place it on the way to the solemnity-sustainment. Besides, the settlement of an University Architecture and Urban Studies Course in the city will provide the teaching and the researching activities for the production of the city based on the preservation of the architectural, natural and cultural heritages, in order to promote a based critical context. This demand is about secular and the national and international organisms are about to unify their efforts in order to make possible the settlement of this Course in Ouro Preto. The supports can be financial or through institutional agreements.

A good example was given by UNESCO that highlighted: “*One good news is the next opening of the career of Architecture and urbanism, with emphasis on the protection of the cultural heritage, in the Federal University of Ouro Preto (UFOP). In addition, the university, in collaboration with the Historical and Artistic Institute of Patrimony (IPHAN), developed a Continued for Education Project for the sustainable preservation of the cultural heritage, available to the entire community of Ouro Preto*” (Paris, 2003).

REFERENCES

- BANDEIRA, Manoel. *Guia de Ouro Preto*. Rio de Janeiro MES, 1938.
- MEC/SESu/CEAU. 1994. Comissão De Especialistas De Ensino De Arquitetura E Urbanismo. *Ensino de Arquitetura e Urbanismo – Condições & Diretrizes*. p.187 Brasília.
- MEC/SESu/CEAU. 1997. *Perfis da Área & Padrões de Qualidade*. Dados do relatório, 65 p. Brasília.
- MELLO, S. de. 1985. *Barroco Mineiro*. São Paulo: Editora Brasiliense.
- MENICONI, Rodrigo O. de M. 1977. *A construção de uma cidade monumento: o caso de Ouro Preto*. Dissertação de mestrado. Escola de Arquitetura e Urbanismo, UFMG. Belo Horizonte.
- MOTTA, L. 1977. A Sphan em Ouro Preto; uma história de conceitos e critérios. *Revista do Patrimônio* n° 22, p.108 a 122. Rio de Janeiro.
- OLIVEIRA, Benedito. T. de. 2003. É urgente uma ação conjunta para reverter a deterioração de Ouro Preto, *Revista Projeto Design*, n° 279, p.24/26, São Paulo, SP.
- OLIVEIRA, B. T. de. 2003. Em defesa de Ouro, *Revista Arquitetura e Urbanismo*, n° 113, p. 63/66, São Paulo, SP.
- SCHMIDT, M. F. 1997. Nova história crítica do Brasil: 500 anos de história mal contada. *Câmara Brasileira do Livro (CIP)*, São Paulo, Brasil.
- VASCONCELLOS, Silvio de. 1977. *Vila Rica*. São Paulo: Editora Perspectiva.
- VICIOSO, E. P. 2003. State of conservation of the historic town of Ouro Preto, Brazil. Report on the ICOMOS Reactive Monitoring Mission to World Heritage Site. UNESCO, Paris.

Analysis of a Roman masonry flat-slab in Hadrian's Villa, Tivoli

D. Abruzzese, G.E. Cinque & G. Lo Gatto
University of Rome "Tor Vergata", Italy

ABSTRACT: The study concerns the research of the architectural and structural shape of an ancient building in villa Adriana in Tivoli, Italy. Particularly, the building has been investigated in order to answer questions about the status of its roof. The problem has been studied under geometrical assumptions based on data collected by the survey, but even under historical and architectural considerations reported in the literature about ancient roman building. The interesting result is that a large room of this Villa could be covered with a flat slab made with roman concrete and no reinforcement.

1 INTRODUCTION

1.1 Ancient Roman masonry

At the beginning of the II century A.D., when Hadrian was Emperor, Roman building techniques were improving.

The building technique for vertical walls was well known and widespread. Large areas could be covered by the use of the Roman concrete, because of its adaptability to the shape of the brick, used as casting mould.

Concrete vaults were the most common techniques for Romans to cover large rooms. Builders used simple and double curvature vaults: barrel vaults, groin vaults, dome vaults, and others with more complicated shapes. It is important to notice that the biggest concrete vault, covering the Pantheon was built under Emperor Hadrian. The diameter of the Pantheon's dome is 42 m.

1.2 Three Exedras building in Hadrian's Villa

Hadrian built his Villa during his own reign, between 118 and 138 A.D. near Tivoli, not very far from Rome (Fig. 1). The Villa is spread over approximately 120 hectares, but was probably larger. In ancient literature, Hadrian has always been considered an architect, and probably he himself was the architect designer of many buildings in the *Villa*.

In the Villa there was not only the emperor's residence, but even many other buildings, such as theatres, baths, *peristyles* and habitations for his large court, for the army and for servants. The *Villa* probably became the place where he and his architects tried to create new shapes and make new experiments, just like the dome of the Small Baths, whose shape reminds us of those of the later baroque period.

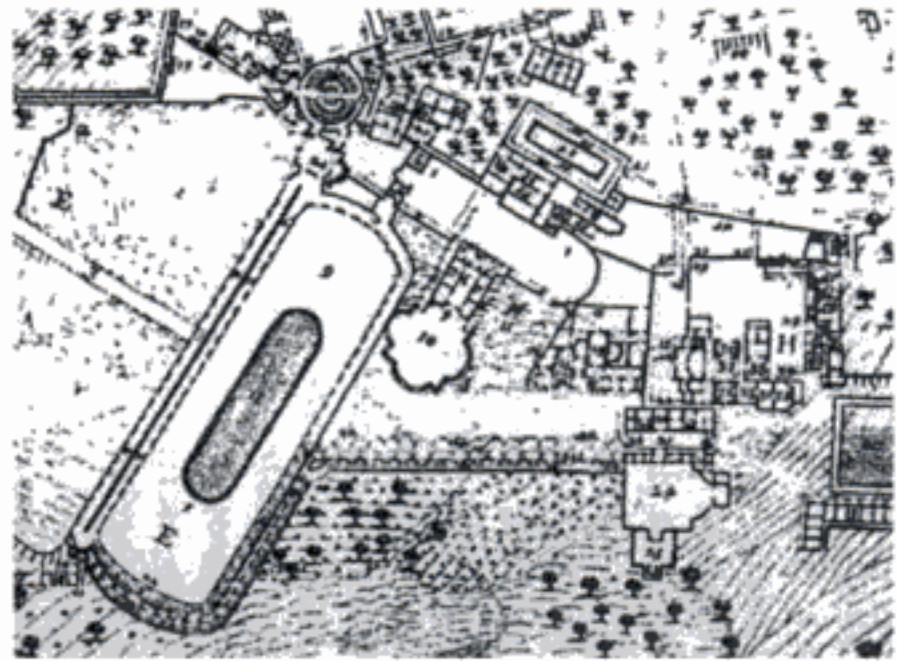


Figure 1. Plan of Hadrian's Villa (Contini, 1668).

The Three Exedras building is located in the Villa, in one of the areas first built.

The "building" case of this study lies near the so called *Poecile*, and in the literature is named "the east wing" of the *Three Exedras* building (Fig. 2). The building is unique because of its flat slab roof of very simple geometry. The building is symmetrical and its large central room is a rectangular area of 9 m × 16 m. The room was probably covered by a concrete flat slab, whose fragments now lie on the floor.

1.3 Methodology of study

The study of the roofing of the Three Exedras building was executed in three main steps:

1. The first step is the collection of geometrical and construction data of the building as we can see at present, and of the fragments of the masonry



Figure 2. Aerial view of Three Exedras palace (National photographic archive, Rome).

flat-slab on the floor. The collection of information has also been supported by a bibliographical research and by collecting paintings and pictures of old buildings belonging to the same period, or even much later (Renaissance) but referring to similar shapes.

2. In the second step, several hypothesis were formulated about the roofing and its structural behavior, and the hypothesis were then checked by structural analysis.
3. Finally, a virtual architectural model of the building was made according to the hypothesis checked analytically and with archaeological concepts. The model represents the building in its original state, in Hadrian's time.

2 COLLECTION OF INFORMATIONS

2.1 Structural characterization

This phase of study can be divided into 3 steps:

1. Geometrical survey of the building.
2. Survey of the flat-slab fragments and their characteristics.
3. Collection of bibliographical information.

2.2 Three Exedras building-description

The building's geometry is very simple and it is composed by a rectangular part and a semicircular one, whose diameter is 23.30 m (Fig. 3). This area is one of the Three Exedras of the building with that name, which is strictly connected with the east wing. The building is symmetrical and inside it has 7 rooms, two lateral rooms have an *apse*, while the large, rectangular central room, 16.2 m × 9 m wide, has another small room attachment at a slightly higher elevation (about 0.30 m). This part is like a balcony looking at

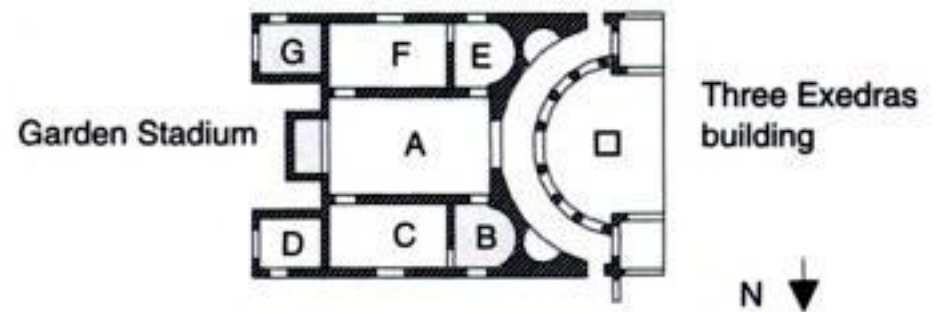


Figure 3. Plan of the east wing of the Three Exedras building.



Figure 4. One of the smallest fragments lying on the floor.

the near Garden Stadium. The function of the building is still unknown. The vertical walls have a regular thickness of 0.60 m (equivalent to two "Roman feet"), composed by three parts. In the external parts we have bricks arranged in the way of *opus reticulatum* used as casting mould into which the concrete was poured, thus becoming the core of the wall. The walls' height is 7–8 m, so they themselves bear witnesses of the skill of ancient Roman bricklayers.

The general condition of the masonry is still good, though many vandals during the building's life ruined it and stole marble and even deteriorated bricks. At any rate, the masonry's conditions have been improved by several interventions of restoration, the first of which was made in the early XX century.

The building's floor lies on *suspensurae*, which is an ancient roman heating system, composed by a square frame of small pillars made of bricks (0.30 m × 0.30 m). The information comes from a surveying program using geo-radar techniques. During the study, it was possible to use this investigative system directly because of a hole in the pavement of the room, originally hidden by soil, plants and stone fragments. The hole showed a *praefurnia* system, where the Romans lighted their fires to heat the building.

2.3 Fragments of the ancient flat-slab

Several fragments of an ancient concrete flat-slab lie on the building's floor.

The fragments, which are composed by several layers, had been surveyed and measured (Fig. 4).

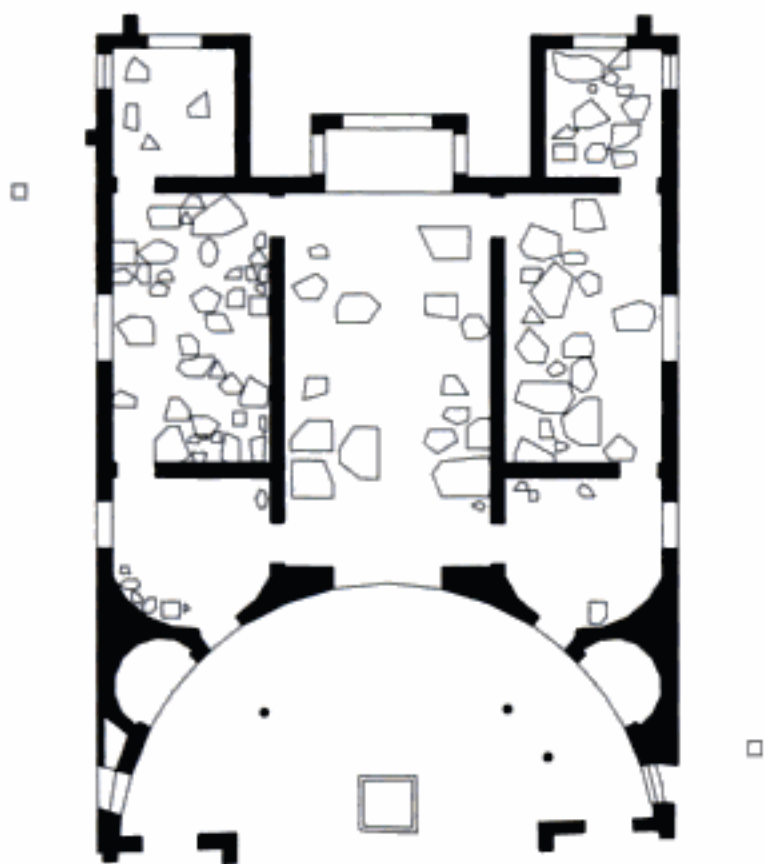


Figure 5. Plan of the flat slab's fragment on the floor.

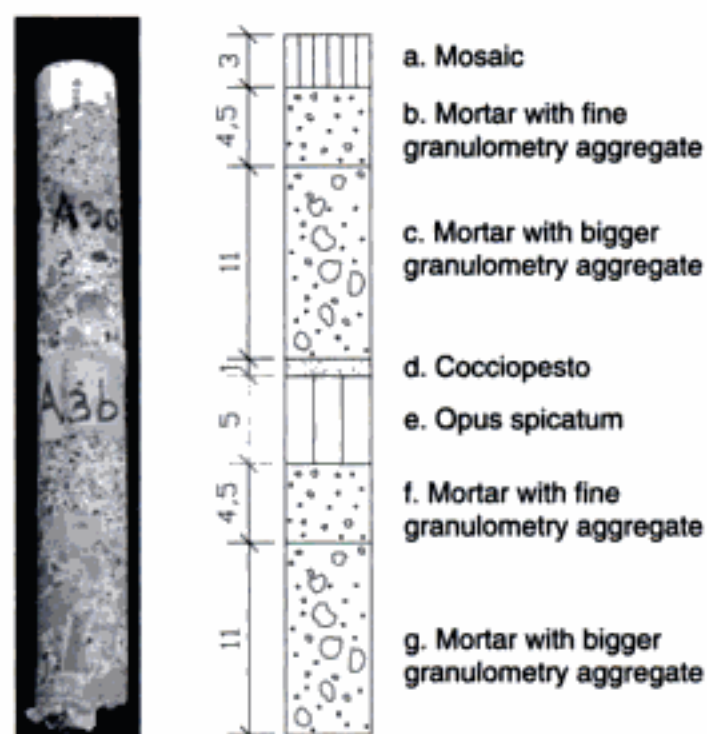


Figure 6. Layers in the flat slab's fragments.

Some of them still lie in the same position since the flat slab fell down (Fig. 5). It is evident because when they fell down they broke the floor which is supported by *suspensurae*.

The fragments' dimensions are very different: the largest has an area of about 2 m², and the smallest are about 0.20 m long. The lower and the upper surfaces are parallel and inside 7 different layers can be identified on variable thickness of 0.40÷0.50 m (Fig. 6).

The composition of the flat slab from the upper to the lower layer is showed in Table 1.

The same sequence of layers can also be found in the so called Winter Palace. Some lateral rooms are covered by a barrel vault, the extrados of which is plane and covered by mosaic, and has the same sequence of layers, although it is a vault.

Table 1. Composition of the flat slab.

- | | |
|----|---|
| a. | White stone mosaic, about 0.03 m thick. |
| b. | Lime mortar, about 0.045 m thick. The aggregate is fine grained. |
| c. | Lime mortar, about 0.11 m thick. The grain of this material is bigger than "b" material. |
| d. | Cocciopesto, with variable thickness, from some mm to 10 mm <i>Opus spicatum</i> : a layer composed by bricks 0.25 × 0.10 × 0.05 m in fishbone disposition. |
| e. | Lime mortar, about 0.045 m thick. The grain is fine but different from layer b because of the presence of pozzolana. |
| f. | Lime mortar, about 0.11 m thick. The grain is bigger than f, but different from c because there are more pieces of bricks. |

Even the ground floor is composed by two layers just like layer b and c, and of the same thickness, but above layer b there was an other one: the mortar to connect the flooring tiles.

The technique for the concrete flat-slab is described by many ancient writers, among whom is Vitruvius. However, no one wrote about *opus spicatum* inside a floor; usually used as a floor material.

The fragments lie on the floor of the whole building, but mostly in the lateral larger rooms. The total of the area covered by the fragments is 87 m², while the whole building's floor is 446 m² wide. The fragments' area represent 3% of the area of room E, and as much as 31% for room C. Totally they are 19%, but probably they covered the whole building's area at Emperor Hadrian's time, because the Villa had been plundered since it was abandoned by the Emperors and the court, until the early 1900. Besides, the fragments have never been measured and surveyed. So we don't know how many fragments there were before the great restorations in the early 1900. We just know that the fragments had been shifted during several restorations, except for those that were too large and heavy to be transported.

3 STRUCTURAL ANALYSIS

3.1 Structural model

Structural analysis of the covering needed to consider several models that could fulfil the requirements.

In particular, attention was paid on three problems:

1. Flat slab material characteristics: it was important to notice that there were different concrete layers and each one behaves in a different way if stressed by tensile stress or compressive stress.
2. Choice of restraints at the edge of the flat slab.
3. Structural behaviour according to the way it was poured.

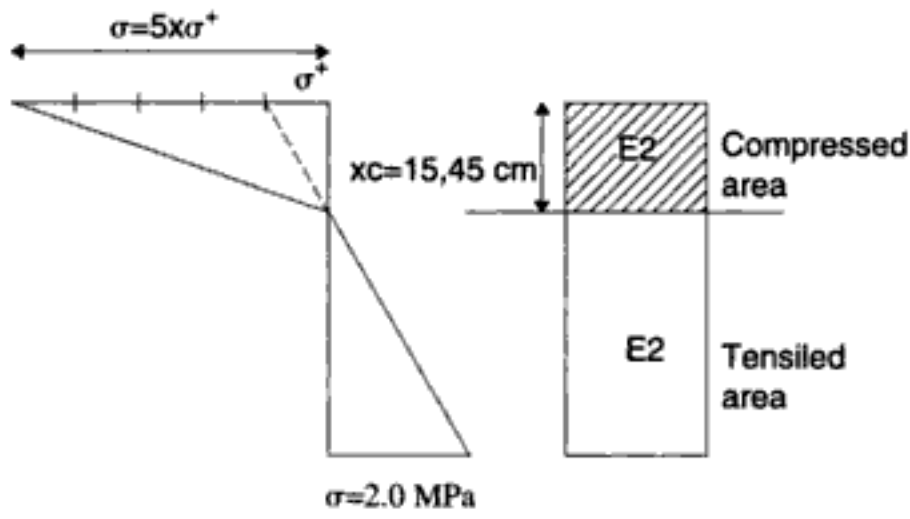


Figure 7. Stress distribution for bi-modulus material in a section under bending moment.

3.1.1 Material characteristics hypothesis

Nowadays, when we design a reinforced concrete structure, we do not consider that concrete could resist tensile stresses.

The most important problem of the hypothesis of this work is that the flat-slab necessarily should be stressed by high tensile stress.

In this kind of material, the critical stress is the cracking strength stress value. The real material composing the fragments is very good, so in this study we considered that the material of the model could resist to tensile stresses up to the value of 2.0 MPa.

It is noted that the material's behaviour is different if it is stressed by compressive or tensile stress: the concrete's modulus of elasticity decreases when passing from compressive to tensile stress; so neutral axis of a section under simple bending moment goes from the middle part of the section to the upper part.

Besides, the flat slab was composed of 7 layers, different in thickness and material, and each layer had its own modulus of elasticity. It would have been very difficult to make a model that considers both the characteristics (several layers and different behaviour).

The problem was first simplified to a concrete flat-slab composed of only one homogeneous and isotropic material. But other two examples were analyzed: 1. homogeneous material but anisotropic when stressed by compressive or tensile stress (Fig. 7); 2. isotropic material but the section is composed by 4 layers of the same thickness but each one with his own modulus of elasticity. The last example was just a theoretical case study, but quite close to reality if we knew all the characteristics of the material.

The mechanical characteristics of the model's material are those assumed by the architect Salza Prina Ricotti. The architect was the first one that tried to demonstrate that the building's covering was a concrete flat slab, and in this study the same material characteristics were used, in order to compare different results.

Table 2. Geometric and elastic characteristic of the concrete flat slab.

g	Density	2.000	kg/m ³
E	Modulus of elasticity	20.000	MPa
σ_{\max}^-	Tensile maximum stress	2.0	MPa
h	Height of the flat slab	0.50	m

3.1.2 Hypothesis on the flat slab's restraints

The flat slab is simply supported by the vertical walls, so the restraint in the model is that one of simple support. In fact it is impossible to think that the concrete of the flat slab and the walls could be merged and have structural continuity. Probably the flat slab was built when the construction of the vertical walls was finished, and it was simply posed on the walls. But the support's dimension depend on the model of the original building. We do not know the original architecture and the building process, that is why we had several different hypothesis, and some of the models we used are from Salza Prina Ricotti's work.

Since other details on the covering are not known, it is impossible to suppose the presence of vertical walls on the edge of the flat slab. These walls could improve the condition of tensile stresses in the concrete flat slab.

3.1.3 Hypothesis on the structural behaviour

The flat slab could have been built in two different ways: it could have been poured at one time in one big formwork or in more than one in many formworks. In this second case the formwork was 2.2 m long and the width of the same room dimension. This hypothesis is supported by the observation that a fragment lying in the central room 2.2 m long, has three sides orthogonal to each other.

A different structural behaviour would occur if the flat slab was poured all at one time or in several layers: in the first case it could be considered a plate, but in the second one it could behave as a series of beams.

Generally, considerations about masonry, assume inability to take tensile stress: this is the case when arching occurs within the thickness of the flat slab. But this could not be possible since the pressure arch had a low curvature and the thin and high walls could not resist to the high horizontal thrust.

In the next step analytical calculations were made for the various hypothesis on the restraints and the material characteristics (Table 2).

4 ANALYTICAL OUTPUTS

4.1 General characteristics

Different considerations have been made for the following models. The density of the chosen material

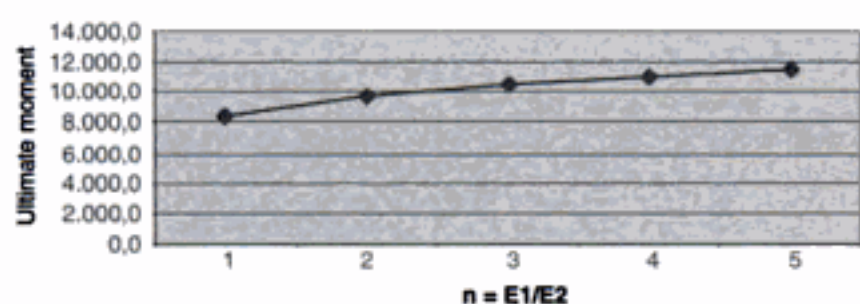


Figure 8. Graphic of the ultimate moment when ratio $E1/E2$ increases; tensile stress maximum at 2.0 MPa.

is $\gamma = 2000 \text{ kg/m}^3$, and the modulus of elasticity $E = 20.000 \text{ MPa}$ is constant in the whole thickness of the flat slab, however in some cases we considered a different modulus in order to make a careful study of the various examples.

The thickness of the flat slab has been fixed in 0.50 m, but we didn't consider the different layers, except for the case study with 4 layers of the same thickness but different values of the modulus of elasticity.

The calculation was developed for the covering of the large central room, but even for the lateral rooms. About the observation on restraints we considered always simple supports concentrated on one line in correspondence with the resultant of the distribution of the reactions at the supports.

These characteristics change if the width of the support changes or if the two parts – the support and the flat slab, or two flat slabs – have different stiffness.

Besides the crack value of concrete for tensile stress has been fixed at $\sigma = 2.0 \text{ MPa}$. This value is very high but we have to consider that the concrete of the fragments is still very good. The results of some test on sample of similar old roman concrete in the area of Hadrian's Villa gave values between 0.9 and 1.5 MPa, with indirect "brasilian" test (G.P. Giani, M.Candiago Zich, 1991), while compressive test gave value of the resistance between 10 and 30 MPa. We are still elaborating some new tensile test, but the high quality of the material leads to consider a higher value of tensile resistance, at least one tenth of compressive value. The crack value and the yielding stress are the same, so the material in the model doesn't have any plastic reserve. In order to study the ultimate resistance of a rectangular section some simulations have been done changing the isotropic properties of the material or the tensile crack stress maximum value. These studies showed that the ultimate moment of the section increases if modulus of elasticity ratio increases (compressive modulus/ tensile modulus) (Fig. 8).

This observation allowed a simulation of the stratification of different materials by creating a model composed by 4 layers of the same thickness. They had different modulus of elasticity but if the stiffer layer is on the upper part and the other are less and less stiff,

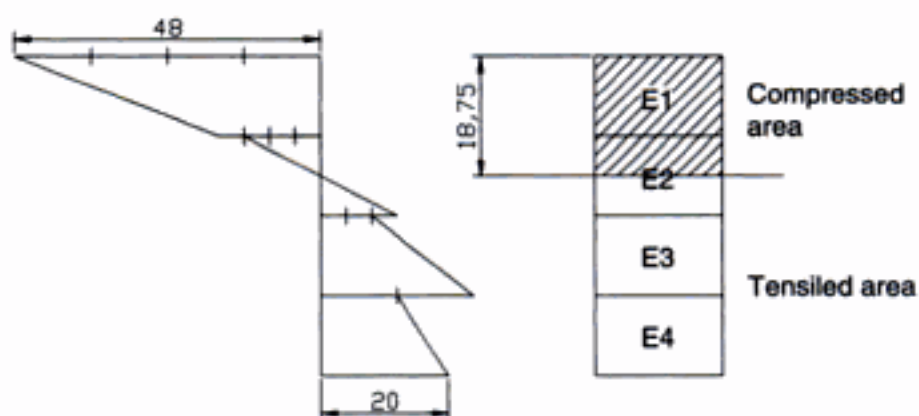


Figure 9. Stress distribution in a section with layers having different modulus E .

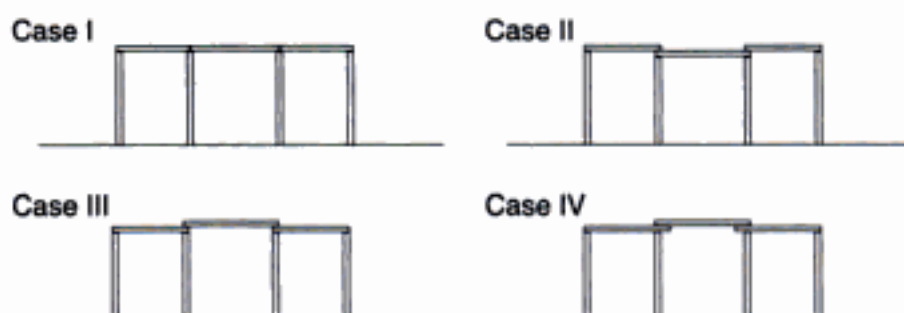


Figure 10. Scheme of the section of the building: position of the flat slab in the central room and in the lateral ones.

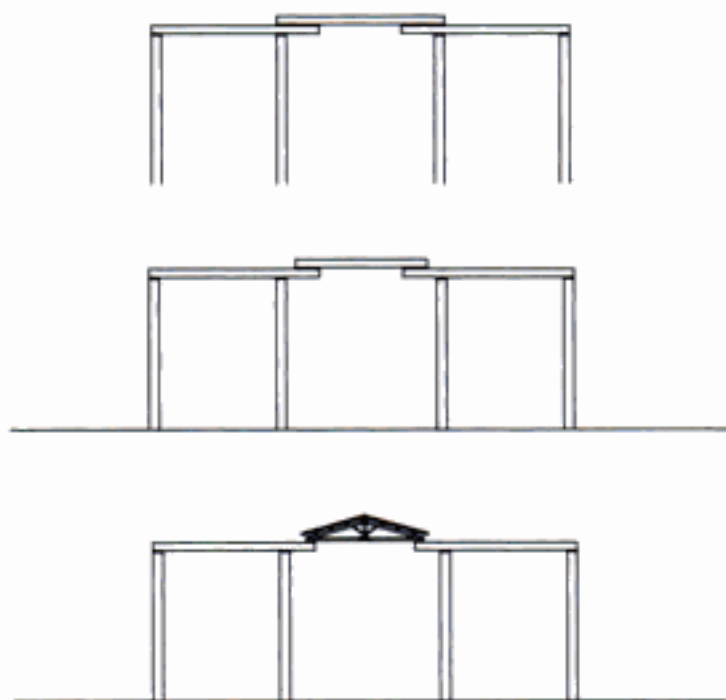


Figure 11. Cases deriving from IV case: the last one is the most likely model.

the section could have a higher ultimate moment. Thus, the use of material could be more efficient (Fig. 9).

The compressive crushing stress of the model's material is similar to the usual value of common masonry. Failure occurs because of the tensile crack value is achieved, while the material still has a compressive stress reserve.

4.2 Beam model

The beam model considered for the building's covering is similar to that one assumed by the architect Salza Prina Ricotti. The scheme has 4 main cases and 3 derived from the last one (Figs 10–11).

Tensile stresses were studied, where, in the moment diagram the values of the moment were maximum. The study was developed not only for the central room, but also for the lateral rooms. In some cases the tensile stress is too high in the lateral flat slabs, even if they are smaller than the central one.

The main schemes used were composed by simply supported beams but in some cases there were positive bending effects, because of observations on the point of the simple support and on other forces (Fig. 12).

In all the main 4 cases the crack tensile stress of 2.0 MPa was achieved. Other times, only little bit below the crack value was achieved, but this is highly unlikely in very real situations.

In the last 3 cases, derived from the 4th of the principal ones, the flat slab of the central rooms is stretched out, goes over the central wall and is the support for the central flat slab. The moment diagram reveals that the tensile stresses are too high in the lateral room flat slab, even if the dimension of the cantilever changes.

In the last of the 3 cases, derived from the principal one, the tensile stress value is acceptable. In this case the central room was covered by a wooden truss roof and it was supported by the two lateral concrete flat slab.

This solution is not in contrast with the information we have from the paintings or pictures that represent the building's front elevation. Particularly the drawings from Penna belonging to the 19th century before the great restoration of the early 1900, suggest that one of the three cases above could occur. In the drawing, a small cornice could underline the presence of the concrete flat slab. The cantilever part could span 1 m.

Besides, it is evident that some of the fragments in situ are in the same positions in which they were when the flat slab fell down: and their position is in keeping with this hypothesis. So the model has been accepted; but probably some of the previous models could provide interesting results if the material model was improved.

4.3 Plate model

This model would be useful if the flat slab was poured at one time in a large formwork large just like each

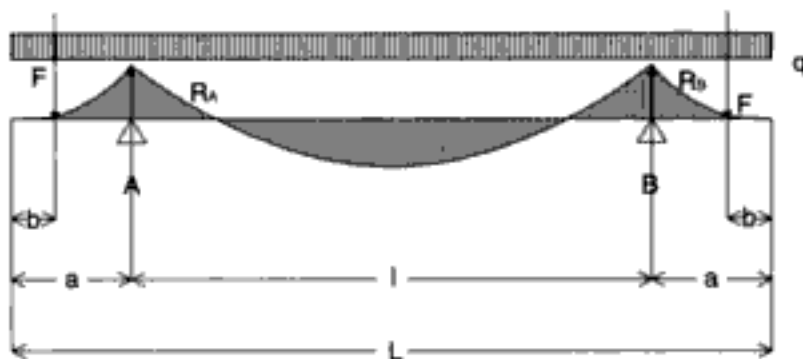


Figure 12. General scheme of the flat slab beam model: forces F and distances a , b , l , L change in the different cases.

room in the building. But in this case only the plate of the central room has been developed in this study because worst condition would occur in this room's covering.

The software used for the calculation of this model was Lusas Rel.13, a computer code for Finite Element Analysis. The main model for the roof is a plate of $9\text{ m} \times 16\text{ m}$, with 0.5 m of thickness, simply supported by the vertical walls on the lower edge (Fig. 13).

The software has been used to create a *mesh* that was useful to evaluate stress and displacement values in a more accurate way.

The first plate model that has been analyzed was made of an homogeneous and isotropic material whose characteristics are:

$$\begin{aligned} E \text{ (modulus of elasticity)} &= 20000 \text{ MPa} \\ \nu \text{ (Poisson's modulus)} &= 0.3 \\ \gamma \text{ (density)} &= 200 \text{ MPa} \end{aligned}$$

In the central part of this kind of plate, loaded with its own weight, there are the higher stresses in a symmetrical way:

$$\sigma_x = 0.993 \text{ MPa} \quad \sigma_y = 1.93 \text{ MPa}$$

In this model there is no difference between the material's behavior if it is stressed by tensile or compressive stress, so an other case study was developed: the material's characteristics are the same, but it is divided into two parts. In the upper part, above the neutral axis the modulus of elasticity is $E = 5000\text{ MPa}$ while in the lower part $E = 20.000\text{ MPa}$. The neutral axis line has been calculated for a rectangular section with pure bending moment.

In this simulation the maximum tensile stress is $\sigma_y = 1.31\text{ MPa}$. This value could be accepted but we should make a comparison between it and the beam model composed by a similar material.

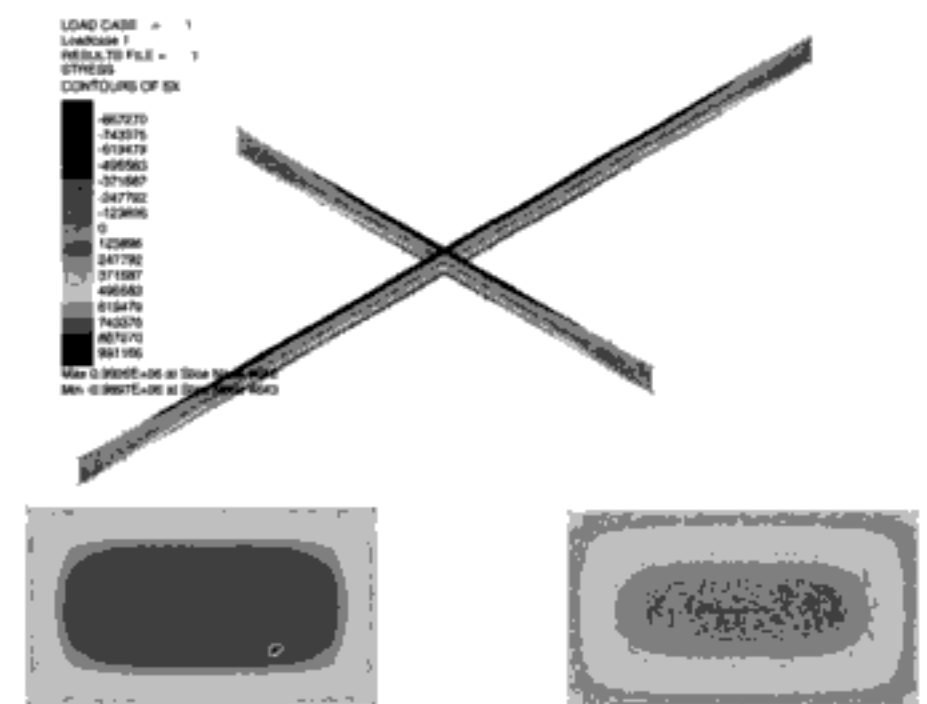


Figure 13. F.E.M. simulation of the central flat-slab ($9\text{ m} \times 16\text{ m}$) as a plate with Lusas.

Besides, as we don't know the real ratio between the modulus of elasticity, this example is just a simulation. At last another case study has been developed: if it was composed by different layers and the stiffer was in the upper part the tensile stresses would decrease.

5 GRAPHICAL HYPOTHESIS OF THE ORIGINAL STATE

The only believable analytical model, after the static analysis results, is the one in which the central room was covered by a wooden truss, but supported by the concrete flat slab stretching out of the lateral rooms.

So a graphical model was made using this hypothesis. The model shows the original state of the building at Emperor Hadrian's time (Fig. 14).

Not only static analysis results had been used in order to build the model, but even the information from ancient drawings and plants, bear witness to the building's conditions in past times. The drawings show the building before restorations, and give more information about it.

Besides the Regional Authority for Archeological Heritage ("Soprintendenza") for the Lazio Region, which is the tutor of the Villa, provided much information and suggestions about the virtual reconstruction model. Also some ancient roman example of similar architecture contributed to create the model.

It was impossible to ignore the presence of the other buildings surrounding the Three Exedras' East Wing in order to create the model, because all of them are strictly connected to each other from the architectural point of view.

In the model the height of the building and of the elements on it is strictly connected with the survey of the actual state; only when it was impossible to get information out of the survey some proportions have been chosen similar to building of the same age or of Renaissance times.

The three-dimensional model shown in Figure 13 presents the most likely shape of the building, according with the hypothesis assumed and the results of the structural investigation.

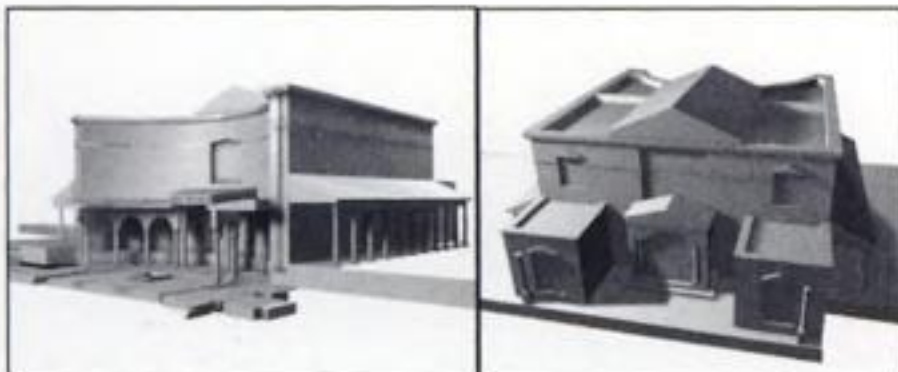


Figure 14. Final virtual graphic model of the building in the original state.

6 CONCLUSIONS

The study of ancient buildings can be developed in order to identify static problems not only to restore and reinforce them, but even to analyze various hypotheses and build a model of the original state.

The function of many of the buildings in Hadrian's Villa are still ignored, because the buildings in the Villa are not typical, such as basilicas or forum or residences.

We can imagine that the Villa was a particular place where the Emperor and his architects invented new forms and shapes, because of the 'architectural freedom' that the Villa allowed. These new architectural experiments also concerned structural and building novelties.

Sometimes buildings of the Roman age were not so solid and resistant and for the weaker ones, that probably ruined, there is no historical record. We have knowledge only of the stronger buildings that had characteristics of high resistance. It is noteworthy that the buildings and monuments, which remained in good conditions until today, were well designed in the framework of the architectural and building traditions, following the construction rules experienced over several centuries.

Most probably, new experimental buildings had low safety coefficient (the Romans couldn't evaluate the suitable safety coefficient until they experienced several new buildings). We can remember that several gothic cathedrals fell down during the middle ages.

The knowledge of the hypothetical original state of an ancient roman building contributes to give information to archaeologists, but it is also a sign of the technological progress that Romans had achieved in that period.

The simulation of the flat slab of the east wing of the Three Exedras building is living proof that, even with an extremely low safety coefficient, this kind of roof structure probably existed. This general hypothesis is also supported by some archaeologists, such as Salza Prina Ricotti, mostly from architectural considerations.

REFERENCES

- AA.VV. *Calcestruzzi antichi e moderni: Storia, Cultura e tecnologia*, Atti del convegno di studi, Bressanone, Luglio, 1993
- Abruzzese, D., Como, M. & Lanni, M., 1990, On the Horizontal Strength of the Masonry Cathedrals, *9th European Conference on Earthquake Engineering*, Moscow, U.S.S.R.
- Abruzzese, D., Como, M. & Lanni, M., On the lateral strength of multistory masonry walls with openings and horizontal reinforcing connections, 1992, *X World Conf. on Earthquake Eng.*, Madrid, 19-24 July

- Abruzzese, D., Como, M. & Lanni, 1999, Some Development on the lateral Strength of Historical Reinforced Vaulted Buildings, *6th Int. Conf. Struct. Studies, Repairs and Maintenance of Historical Buildings, STREMAH'99*, Dresden
- Adam, J.P., *L'arte di costruire presso i Romani*, 1988, Milano, ed. Longanesi C.
- Benedetti, D., 1982, Considerazioni teoriche e sperimentali sul comportamento sismico di edifici in muratura, in *Comportamento statico e sismico delle strutture murarie*, AA.VV., Milano, ed. Clup
- Calladine, C.R., 1983, *Theory of shell structures*, Cambridge University Press
- Cairolì Giuliani, F., 2000, La Villa Adriana, in AA.VV. *Adriano-architettura e progetto*, Milano, ed. Electa
- Cinque, G.E., 2002, *Rappresentazione antica del territorio*, Roma, ed. Officina
- Cinque, G.E., 1996, *I mezzi della conoscenza. Lettura storica della rappresentazione geometrica*, Trento, ed. Univerta
- Contini, F., 1668, *Pianta e spiegazione della Villa Adriana*, Roma
- Falsitta, M., 2000 *Villa Adriana-una questione di composizione architettonica*, Milano, ed. Skira
- Giani, G.P., & Candiago Zich M., 1991, Analisi di stabilità in condizioni dinamiche di speroni di contraffortatura del ninfeo di Villa Adriana, in *Analisi storica e comportamentale di sistemi di consolidamento tradizionali in muratura nelle aree archeologiche romane e laziali*, ed. S.Gizzi, Min. Beni Culturali, Soprint, Archeolog. del Lazio
- Lanciani, R., 1980, *Passeggiate nella campagna romana*, Roma, ed. Quasar
- Mac Donald, W. & Pinto, J.A., 1997, *Villa Adriana-La costruzione e il mito da Adriano a Louis Kahn*, Milano, Electa
- Manieri Elia, G., 2000, Stabilità delle strutture e conservazione, in AA.VV. *Adriano-architettura e progetto*, Milano, ed. Electa.
- Marta, R., 1985, *Architettura romana, tecniche costruttive e forme architettoniche del mondo romano*, Roma, ed. Kappa
- Penna, A., 1833, *Viaggio pittorico della Villa Adriana composto di vedute disegnate dal vero ed incise da Agostino Penna*, Roma, ed. Pietro Aureli
- Pacifici, V., 1984, I primi lavori a Villa Adriana dopo l'acquisizione allo Stato italiano (1872-73), *Atti e memorie della Società Tiburina di Storia e arte LVII*
- Roca, P., González, J.L., Mari, R. & Oñate, E., 1997, *Structural Analysis of Historical Constructions*, Barcelona, ed. Artes Graficas Torres
- Roca, P., González, J.L., Oñate, E. & Lourenço, P., 1998, Experimental and numerical issues in the modeling of the mechanical behaviour of masonry, in *Structural Analysis of Historical Constructions II*, Barcelona, ed. Artes Graficas Torres
- Salza Prina Ricotti, E., 2001, *Villa Adriana Il sogno di un imperatore*, Roma, ed. "L'Erma" di Bretschneider
- Salza Prina Ricotti, E., 1988, Villa Adriana, un singolare solaio piano in opus caementicium, *Palladio*
- Save, A. & Massonet, C. E., 1972, *Plastic Analysis and design of Plates, Shells and Disks*, Amsterdam-London, North-Holland Publishing Company
- Timoshenko, S.P. & Woinowsky-Krieger, S., 1959, *Theory of Plates and Shells*, Singapore, ed. Mc Graw-Hill
- Marco Vitruvio Pollione, 1990, *De architectura*, Pordenone, ed. Studio Tesi

Emergence, development, and prevalence of brick nogging in American vernacular structures

D.F. Laefer

University College Dublin, Dublin, Ireland

ABSTRACT: Despite being one of many seventeenth century American wall insulation systems, brick nogging, emerges as a prevalent construction type throughout all of the original colonies. Used in both framed and hewn-log structural systems, brick nogging is most typically found beneath clapboard siding. Because clapboard ultimately becomes a style in its own right, the presence of brick nogging beneath such clapboards becomes an unexpected complication for modern preservation and intervention efforts. The technique of placing fired and unfired bricks mortar, clayed, and dry laid, although poorly documented extends well into the nineteenth century increasing the anticipated weight of the structure by up to ten percent. Similarly, the presence of brick nogging substantially changes the structure's wall stiffness. Identification of clapboard covered, brick nogging structures is not straightforward, as their emergence was influenced by historical, fiscal and social factors, in addition to engineering considerations. This paper traces development and usage of this technique and presents information about the engineering properties of materials used.

1 INTRODUCTION

1.1 Background

A major challenge to the preservation of historic structures in the United States (US) is that the vast majority of resources and efforts have, to date, focused on the description and documentation of architectural elements. Such an approach may be a direct outgrowth of watershed architectural publications, such as Asher Benjamin's 1796 *Practice of Architecture – the Builder's Guide*, where the focus of this first American book related to building and architecture heavily concentrates on architectural details, ornamentation, and proportioning (Benjamin 1796). Conversely, the situation may reflect the history of preservation in the US as a discipline developed from chemistry. Regardless of the cause, the result is that critical information related to the affiliated underlying structural systems, the details of how these systems are assembled, and the dimensions and configurations of the foundations on which they sit are largely, if not entirely, absent in both the historical record and more recent publications. Without such knowledge, effective protection, preservation, and restoration is not truly viable, especially when structures are subjected to changing geotechnical conditions and structural deterioration. As population levels heighten and previously rural areas experience the tendrils of urbanization, an ever-increasing number of historic structures are subjected

to construction-induced ground movements. Tunneling, adjacent excavation, nearby blasting, pile driving, and dewatering may all imperil the architectural finishes of a building, if not its actual structural integrity, if a good understanding of its weight, stiffness, configuration, and load distribution is not available.

A key example of where this is problematic is with the presence of brick nogging, which significantly impacts all these factors, yet may be an entirely unknown phenomenon to the engineer charged with the protection or maintenance of the structure. This paper will serve as documentation of the emergence, development, and prevalence of brick nogging in American vernacular architecture.

2 BRICK NOGGING

In American architecture, brick nogging is a wall filling or insulation technique traceable to the English, fifteenth century wattle-and-daub construction found with half-timber construction (Fig. 1). Also known as pugging, brick nogging is often absent from architectural dictionaries. Poorly understood in the US, and even less appreciated is the evolution of this widespread technique and its persistence into the mid-nineteenth century. Its unexpected presence beneath what are thought to be clapboard structures poses significant challenges to the structural engineer due to



Figure 1. Brick nogging with protective plaster removed and viewing glass installed at a North Carolina plantation.



Figure 2. European half timber construction.

its additional weight, its composite nature of wood supports and filled centers, and its unknown stiffness characteristics.

2.1 Half-timber construction

There is evidence that the earliest colonial structures were replicas of contemporary English construction (Fig. 2), but even as early as the late nineteenth century none of these colonial examples of half-timber construction were in existence. Chandler (1916) attributes this degradation to the probable use of clay, instead of lime, as the binding and parging material, which would have easily been eroded with heavy rains.

There are, however, church structures from over 100 years later with exposed half-timber. Built by the Moravians from 1743 to 1745 in Oley Township, Pennsylvania and later in the towns of Savannah and

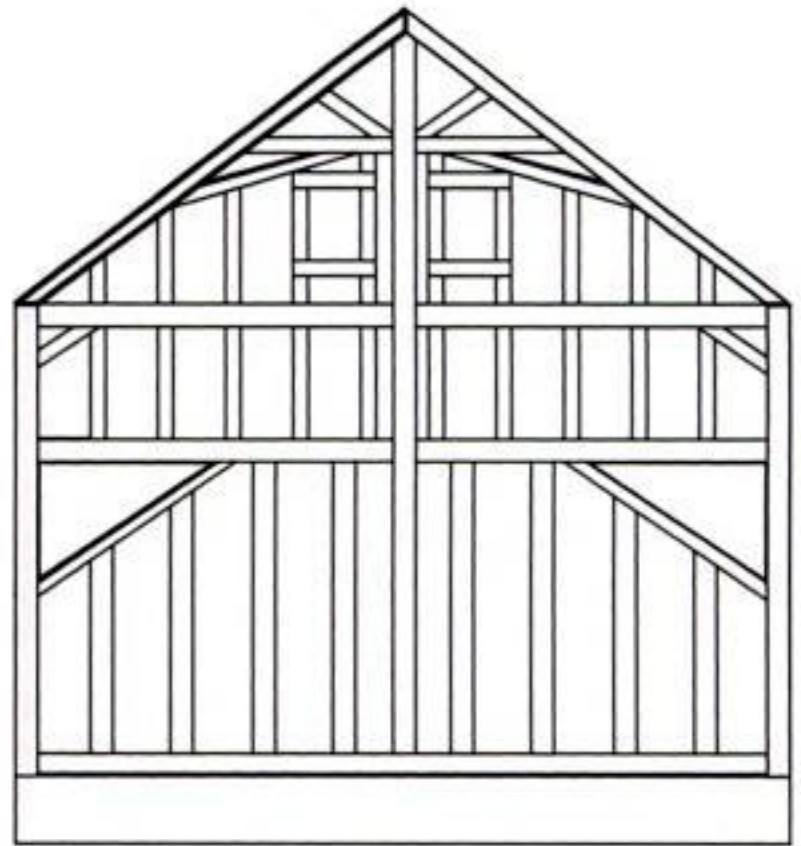


Figure 3. Section of framed construction of the Old Mud Meeting House in southeast Mercer County Kentucky, where the filling is placed in between the vertical boards (adapted from Lancaster 1991).

Augusta, Georgia and Winston Salem, North Carolina, these churches of half-timber are filled with clay and wood.

The framing of the exposed half-timber construction and the thousands of examples of cladded frame structures shared similar framing schemes. Typically, the studs of the frame were comprised of vertical timbers set on two-foot centers and framed into the sill below and the girt above (Chandler 1916).

2.2 Wall filling

Both in chimneys and building walls a wide variety of materials were employed for both basic construction and fill material. The spaces between the studs of the walls were filled with marsh grass, straw, clay, stone, and fired and unfired brick. Although traditionally considered as an exterior wall component, there are examples of its application to interior walls as well (Lane 1976). There is some evidence of a similar type of construction both with and without filling in Kent, England. According to Kimball (1927), "In England the most primitive form of filling, still common in many districts, was of wattle daubed on one side or both with clay, usually mixed with hay or straw, and finished with a thin coat of lime plaster for greater resistance to rain. In work of superior quality lathes were often used instead of wattle, still usually coated with clay, which was regarded in England as having its own advantage. Sometimes the clay was used alone as a filling. In 'cat and daub', the cats were pieces of 'straw and clay worked together into pretty large rolls and laid between the wooden posts.' Closely allied to this was

the use of sun-dried bricks, lumps of clay pressed in molds of a convenient size. The choice of materials was broad and influenced by local preferences even within a single English district” (Kimball 1927).

2.3 Configuration

The brick nogging could be laid in a variety of configurations. The bricks were often set on end sometimes or in neat lifts (Fig. 1). In other cases the placement was entirely random. What is not well documented is whether the nogging was typically laid in single or multi-wythes. Certainly multi-wythe brick walls were well established by the mid-seventeenth century (Marsh 1962).

2.4 Usage

Brick nogging was first found in New England vernacular structures in Portsmouth New Hampshire beneath clapboard homes (Howells 1937). There are a number of houses in Williamsburg with brick nogging, with no evidence that it was originally exposed. Kimball (1927) claims that no instance is definitively known of a framed building erected by the English colonists in which the filling of the frame was exposed on the exterior as “half timber,” as will be further discussed in section 4.0.

Brick nogging was used with both frame structures and those of hewn logs. There are also examples of mixed construction where some of a structure’s walls were filled and others of solid brick.

3 BRICK USAGE

Brick making and usage in the US is well documented even in the earliest years of most of the colonies. Skilled labor, kilns, and fired brick appear to have all been readily available from the initial years of the American colonies.

3.1 Brick availability

Bricklayers were among the first settlers at Jamestown in 1607 and brick making was begun no later than 1611. There are numerous reports throughout the colonies of clay and kilns being in abundance. At the Massachusetts Bay Colony a kiln was set in 1629, at Plymouth brick production occurred no later than 1643, and in New Amsterdam a kiln was operating as early 1628 (Kimball 1927 and Chandler 1916). Similar records are found for Hartford and New Haven Connecticut by 1653, and there were brick houses in Boston no later than 1654. In Virginia several brick homes were begun by 1651 or 1652 (Kimball 1927).

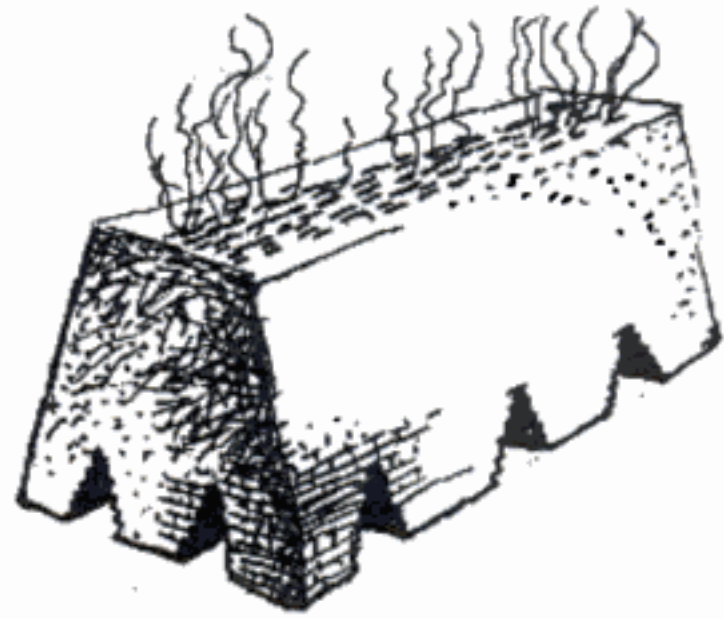


Figure 4. Scove kiln (Rhodes 1968).

3.2 Brick production

At the founding of the American colonies, the rudiments of brick making were fairly simple and easily accessible, even in the most rural locations thanks to the deployment of the scove kiln (Fig. 4). The scove kiln, also known as a field kiln, is a primitive but popular updraft kiln that was used extensively in the eighteenth century, with limited continued usage into the twentieth (Conner 1910 and Ritchie 1960). This temporary kiln was constructed out of raw bricks that were fired as part of the overall process. Thus, some of the bricks that were fired were stacked to form the outside structure of the kiln and became an inherent part of the firing apparatus (Rhodes 1968). The kiln incorporated several features including an enclosure in which to house the bricks, lower apertures to insert fuel, and a chimney mechanism up above. The bricks were placed in mounds creating the appearance of a long rectangle with slightly slanted sides and were strategically stacked to allow the flames and heat to access different sections of the mound via “passageways” (McKee 1973). The outer-bricks, prior to firing, were covered with a layer of clay and grass to allow venting of the vapors. In a single firing 40,000–50,000 bricks could be fired.

For scove kilns, initially brush, and then coal, was used as fuel (Rhodes 1968). The fires were fed and stoked for a week, and then the fire holes were covered with bricks and mortar to prevent the heat from escaping. During this period the fires burned out, but the greater portion of the heat remained. While the kiln remained closed the heat was allowed to dissipate for approximately one week.

Despite wide variability of the final product, the scove kiln was popular and commonly used, because it did not require the construction of a permanent facility (Rhodes 1968). The relative ease of constructability and mobility allowed the temporary placement of these kilns at the point of use, instead of miles away from the construction site, where transportation would have

posed economic and logistical impediments. Scove kilns are known to have been used in the construction of the College of William and Mary, and remains of seven of these temporary kilns have been found in Williamsburg, Virginia (McKee 1973). Despite extensive production, brick was not the predominant building material. Analyzing the means of production and the engineering properties of the resulting product provides a partial answer to why this was so.

3.3 Resulting products

During the firing, bricks were exposed to varying temperatures up to 982°C resulting in highly inconsistent strengths (Rhodes 1968). Bricks located close to the flames were over-fired and sometimes vitrified, while bricks far from the fire were softer and often more porous, causing them to be less desirable because of their lower strengths.

Replication of historic material has also shown highly variable performance. Quarter-scale, extruded clay units were fired in a permanent, updraft kiln (Laefer 2001). The bricks were dried for a minimum of 24 hours at 66°C. The units were fired in a stationary (porcelain) kiln with electrical heating elements on five sides (Fig. 5). The bricks were placed in 2 masses, each 464 mm by 597 mm by 127 mm high, containing approximately 1,400 brick per firing. Approximately 25,000 brick were fired in 12 firings at 496°C (verified by a #09 Orton cone) for at least 12 hours, with an additional day for cooling.

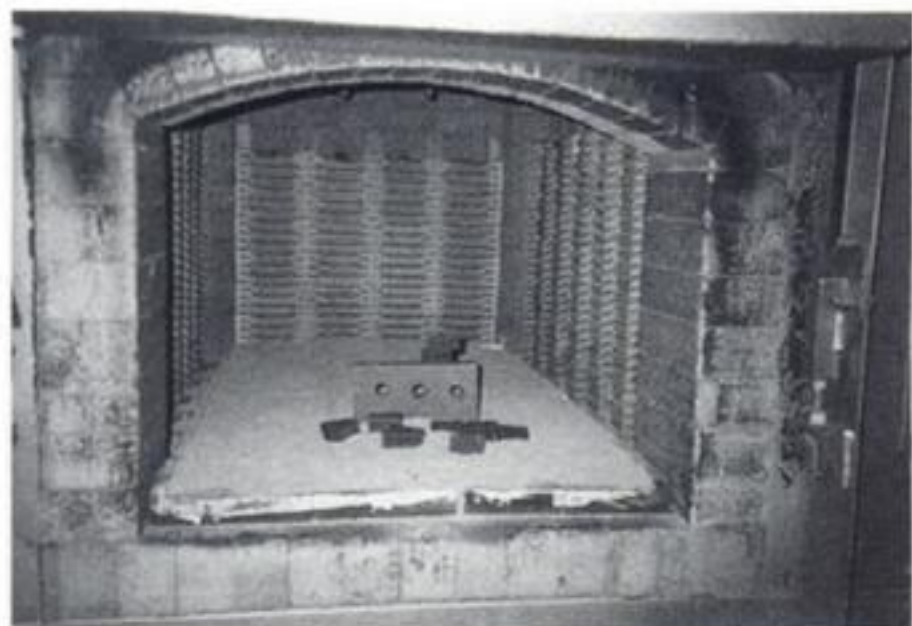


Figure 5. Electric kiln with miniature bricks.

Table 1. Brick absorption by coloration (Laefer 2001).

Brick designation	Absorption (%)	Average strength (kN/m ²)
1	16.4	3103
2-3	16.2	3916-5978
4-5	15.8	7350

The goal was to create high absorption, low strength brick, typical of low firing. Since the power source was electrical (as opposed to gas or coal), the oxidizing (as opposed to reducing) atmosphere facilitated a rough correlation between coloration and brick absorption and strength with the darker color being indicative of less absorptive and stronger brick; as the temperature increased the iron oxide within the clay reacts and exhibits color change (Tables 1 & 2). Using a Munsell Color Chart, the bricks were designated into categories and sorted according to color (Table 3). The classification numbers ranged from 1 to 5, 1 being lightly fired and 5 most fired.

The results of two firings demonstrated both the variability within a single firing and between firings that will occur, even under highly controlled procedures using Orton cones and timed firings (Fig. 6) (Laefer 2001). The variability from a single firing exhibited over a 100% strength difference between the strongest and the weakest brick. Although higher firing temperature or firings of longer periods of time would result in less variability, as well as a stronger product, the larger mass of bricks needs to be considered since such comparative data is not fully available. The data presented herein may be considered qualitatively, although not quantitatively, indicative. These model bricks were also compared to a similar miniature product produced in a modern tunnel kiln (designated by the number 20), which resulted in a profoundly different product achieving strengths nearly 5 times greater than any of the lightly fired products (Fig. 7).

Table 2. Compressive strength as an inverse of absorption capacity (Fried and Law 1995).

Clay brick type	Compressive strength (kN/m ²)*	Water absorption (%)
Low absorption, solid	79,299	5.7
Medium absorption, solid	45,004	12.0
High absorption, fog	31,800	21.8

*Tested as full single brick capped with mortar top and bottom.

Table 3. Color categorization.

Laboratory designation	Munsell hue page	Munsell classification
0	5 yellow grey	8/2
1	7.5 yellow red	7/4
2	5 yellow red	6/8
3	5 yellow red	6/8
4	2.5 yellow red	6/8
5	2.5 yellow red	5/10

Although there is some evidence, including the limited presence of mid-eighteenth century glazed bricks, that more sophisticated kiln arrangements (Upton 1998), as was perhaps the case in the city of Medford, Massachusetts, where shortly after the American Revolution, the city was known to have an annual brick production of about four million units. Despite this, the vast majority of bricks produced in the first

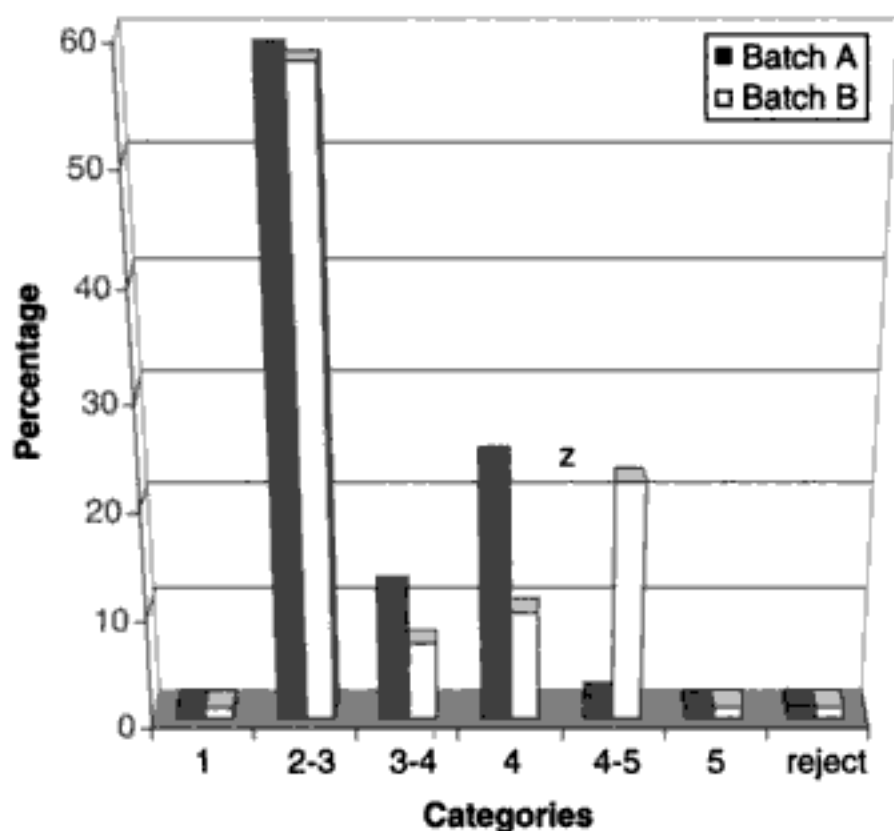


Figure 6. Compressive as a function of firing level.

200 years in North America, especially those outside highly urban centers were generally soft and weak by modern standards. Table 4 compares two sets of pre-Civil War brick (one from a plantation in rural, eastern North Carolina – Somerset Place and one from a railroad town in central Illinois – Jakes' House) to modern shale units. Even the more urban set shows tremendous variability in absorption and strength. Comparing mid-nineteenth century brick to the expectations of Benjamin (1796), a late eighteenth century architect is instructive. The values that Benjamin provides of a

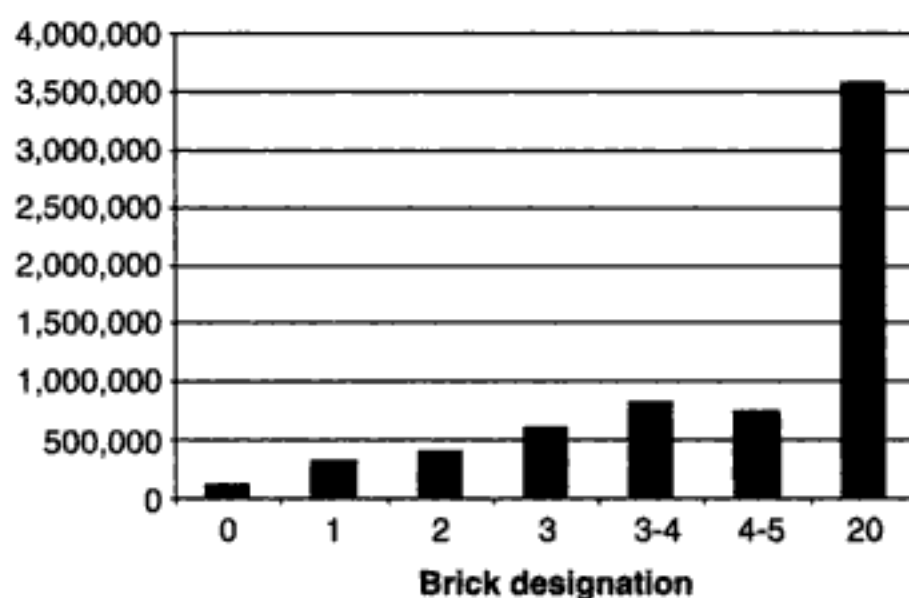


Figure 7. Compressive strength as an inverse of absorption.

Table 4. Physical masonry comparisons.

	Unit weight (kN/m ³)			Stress (kN/m ²) in end loading			Absorption (%)		
	New	Somerset House	Jakes House	New	Somerset House	Jakes House	New	Somerset House	Jakes House
	2191	1625	1777	60,545	2937	4371	2.00	12.07	25.00
	2136	1681	1638	34,344	413	3096	6.30	12.00	15.80
	2136	1750	1287	29,400	2627	6268	2.10	13.64	16.70
Av.	2154	1685	1567	41,430	1992	4578	3.47	12.57	19.17

	Unit weight (kN/m ³)			Stress (kN/m ²) in edge loading			Absorption (%)		
	New	Somerset House	Jakes House	New	Somerset House	Jakes House	New	Somerset House	Jakes House
	2191	1726	1416	27,745	4751	1338	2.00	10.77	19.50
	2191	1793	1393	35,075	5447	2420	4.10	11.36	22.50
	2136	1776	1394	42,556	3585	2930	4.20	10.20	22.90
Av.	2173	1765	1401	35,125	4594	2229	3.43	10.78	21.63

	Unit weight (kN/m ³)			Stress (kN/m ²) in flat loading			Absorption (%)		
	New	Somerset House	Jakes House	New	Somerset House	Jakes House	New	Somerset House	Jakes House
	2136	1775	1578	107,362	3220	11,715	4.20	13.73	22.90
	2191	1788	1518	112,540	3523	11,459	2.00	11.76	19.40
	2191	1714	1618	111,272	4792	37,709	2.00	11.90	17.10
Av.	2173	1759	1571	110,391	3845	20,294	2.73	12.46	19.80

Table 5. Eighteenth century material strengths and weights (adapted from Benjamin 1796).

Material	Crushing strength (kN/m ²)	Weight (kN/m ³)
Ash	2,494,096	762
Brick	395,955	1846
Granite	7,686,606	2632
Marble	1,275,934	2713
Oak	2,790,006	835
Pine	2,747,733	429

395,955 kN/m² crushing capacity (as opposed to the first crack testing in Table 4) with an unknown testing orientation and a 7 percent absorption are nearly equivalent to modern materials. The conclusion one must draw is that Benjamin was fortunate to live and work near modern brick making facilities or that familiarity with wood far outstripped his experience with masonry. Table 5 provides his material summary. Curiously, the unit weight of the proposed "typical" brick closely matches the historic material tested and not that of denser new brick (Table 4).

3.4 Brick importation

As an alternative to local production, there was also a lesser tradition of bricks being imported as ship ballast. Only in New Netherlands do brick seem to have been imported to any appreciable degree and there is limited documentation of this circumscribed but long-standing practice. In New England in 1628 there was a shipment of 10,000 brick. In 1773, the bricks, nails, and lumber for the Kincaid Plantation in Fairfield County, South Carolina were all brought from England (Marsh 1962). Even as late as the early 1800's bricks for ballast were carted from Charleston for Woodward Baptist Church (Marsh 1962). Imported brick may have been considered to be of higher quality, but American brick production was relatively inexpensive and widespread, with bricks from an early date being produced for export to Bermuda in exchange for limestone (Chandler 1916). The historical record is extremely strong that most of the brick found today was produced within a short distance of its final destination. The cost of transporting the material, particularly overland was simply prohibitive.

3.5 Transportation

For a small, two-storey house (100 m²) an entirely of brick would have required approximately 50,000 bricks in a double-wythe configuration and 75,000 in a triple-wythe one. The weight of the bricks at 1700 kN/m³ would have been over 120,000 kN for the thinner configuration. Given cart and horse

limitations, the shear weight would have made most brick transportation simply impracticable.

In port cities such as Charleston, South Carolina and Wilmington, North Carolina, brick structures were much more readily apparent than those that were beyond easy transport of such materials. These port city brick buildings may be a combination of transportation ease and brick as ballast.

3.6 Brick aesthetics

In terms of aesthetics, both the method of molding and the method of firing may have discouraged the use of locally made brick for building exteriors. Large variations in size, shape, and color were expected from a hand-molded, scove-fired brick. A random sampling of bricks from Somerset Place showed a color variation from light orange to medium red and a typical volumetric deviation of nearly 17 percent from the average sampled brick. Materials from the Jakes House generated highly similar results in the color range but with more of a brown cast (less iron oxide in the clay) and typical volumetric deviation also of nearly 17 percent from the average sampled brick.

Although in both structures the consistency of brick shape was hard discern after installation and more than 150 years of exposure, the bricks were clearly hand-molded. To compensate for shape irregularities a variety of mortaring techniques were commonly in practice by the time of the American revolution to generate the appearance of straight, even, rows of brick.

There are certainly a wide variety of stately and important structures built entirely of brick, even of hand molded brick, as was the case of the "Old Brick Church" dating from 1788 in rural Fairfield County, South Carolina, where the congregation built the structure (Marsh 1962). Depending upon the local there are early seventeenth century examples of highly unique and sophisticated brickwork, including glazed bricks and colors ranging from deep reds to bright yellows and orange (Chandler 1916). These structures tended to be some of the largest and most important in their respective communities and as such embody the exception of the materials produced.

The generally weak and highly absorptive nature of locally made bricks in rural and semi-rural areas would have strongly discouraged their use as exterior, structural members because of their high vulnerability to rapid weather-based deterioration resulting in pitting and scouring of the brick face. To prevent this, the brick would have needed to be covered with a coat of lime parging, a material was not readily available in most of the colonies.

3.7 Lime availability

A lack of lime has been cited by numerous authors as the reason for relatively few brick buildings in the early

colonies. Despite one early report of an abundance of lime, this was not the case, as extensively documented by Kimball (1927). Limestone was generally in scarce supply. Typically, lime had to be culled from oyster shells. Oyster shells were available from the Atlantic coast. Lime was eventually obtained from the limestone ridges of the Hudson (Chandler 1916) and parts of Pennsylvania, which was preferable as it produced a more durable mortar.

The need for lime was so extreme that alternative, inferior products were tried, which in Connecticut led to the explicit ban of mussel shells for use in lime production as late as 1724 (Felt 1845). When lime was not available, clay was used instead, leading to decreased durability and in the case of Governor Winthrop's house in Mistick MA, the complete loss of two walls during a violent rainstorm. Given the desperate shortage of lime, clay was used as parging, plastering, wall filler, and mortar, all functions traditionally served by lime. Surviving physical evidence of the employment of clay as an alternative to lime dates to 1675 in the Corwin house in Salem and persists in German houses of Pennsylvania well into the middle of the nineteenth century (Kimball 1927).

The argument that the lack of lime prevented full use of brick for structural building materials fails to account for a wide variety of competing factors as will be seen in the rise of clapboard structures. Additionally, even where lime from oyster shells was readily available, the local building practices often favored alternatives to load-bearing brick systems. A prime example of this is the rise of tabby (also known as tappy), a mix of lime and oyster shells which were squeezed, while moist, into square wooden boxes to produce building blocks. The technique was used throughout much of the southern colonies due to ease of handling, rapid construction, and low cost (Lane 1996). An early example is Frederica Georgia, which was planned as a military town as the southern outpost of the new colony and was described in 1743 as having a pretty strong Fort of tabby, barracks of tabby, and two, large, spacious buildings of brick and timber (Lane 1976).

3.8 Tradition of wood

The preference for wood seems to derive from a variety of economic, social, and historical factors.

3.8.1 Economic factors

Given that the new continent was densely forested, in most lots timber had to be felled before the ground could be tilled. Wood was plentiful and easy to shape. These factors combined with the early introduction of sawmills and their widespread use long before they became established in England (Kimball 1927) to provide low cost, highly available products for framing in the early years of the colonies.

Bricks were also time consuming as they were usually mixed and molded and then left to dry for an entire season. Chandler contends that because of the additional cost of kiln-fired bricks, sun-dried ones were often used instead (Chandler 1916), although time may have been an even more important factor during the earliest seasons in new each community.

Despite regulations dating as early as the seventeenth century requiring brick structures (Chandler 1916) and repetitive devastating fires that destroyed hundreds of houses in single incidents, wood construction persisted as the preferred vernacular construction material through the late nineteenth century until the Chicago fire, although in urban areas residences such as the cities of Boston, Philadelphia, and New York, the prevalence of brick was more substantial than in more rural locations. In Boston in 1722, after 3 major fires in 32 years, there were 12,000 people and approximately 3000 houses with roughly 1000 of them being of brick (Chandler 1916).

Availability of material should not be mistaken with economy. These materials required substantial labor and were considered dear. Even in the late eighteenth century, building materials were deemed as major capital as exemplified by in the 1774 property accounting on the death of architect William Buckland of Anne Arundel County, Maryland where 3500 bricks, 60 bushels of lime, and 30 bushels of hair were listed as major assets.

3.8.2 Social factors

Prejudice that houses of brick and stone were less healthy than those of wood was a wide standing belief and recorded by Thomas Jefferson in his Notes on Virginia in 1784. Stone or brick, unless laid in very thick walls or used in conjunction with other materials tended to be subject to damp penetration. Surviving examples include the Peter Tufts House at Medford, Massachusetts with 0.46 m thick brick walls (most likely four-wythes of brick thick) and Peter Sergeants house in Boston, built in the same period in 1667, with brick walls 0.61 m thick (most likely five-wythes thick). In contrast, by the beginning of the end of the nineteenth century, with the exception of high-rise office buildings, more than three-wythes of brick was unusual to find.

Damp was not the only climate-related concern. Frame houses were generally considered cooler than brick ones so that despite a series of successive fires in Charleston prior to 1740, frame houses predominated (Chandler 1916).

3.8.3 Historical factors

Historical precedent may have also been a controlling element. Kimball (1927) argues, "The use of wood by the colonists was ... not the adoption of an inferior material due to local conditions, but the perpetuation

of English custom where the need for abandoning it was lacking.” Certainly amongst the poor classes in England wood was the dominant house material.

4 CLAPBOARD USAGE

Clapboard structures have come to represent a highly American aesthetic but may be more rationally understood as an outgrowth of functional considerations.

4.1 Clapboard functionality

The traditional construction method of half-timber and wattle-and-daub was radically changed in the earliest colonies. Howells (1937) attributes the change in form and subsequent change in framing to the harsh nor-easter storms and general severe weather, which has also been ascribed to account for the changing roof styles from a double parallel to gambrel roofs. Certainly the climate played a large role. The wattle-and-daub was simply inadequate for the harsh winters. To retard the cold and damp the wattle-and-daub was covered.

The resulting configuration was most popularly seen as clapboard over a frame and filled walls. A prominent example of this is the 1705 House at 33-35 Deer Street in Portsmouth, New Hampshire. Howells (1937) contends that by 1701 a distinctive style had developed in the town of Portsmouth, New Hampshire and attributes the rapidity of which this style was adopted to the cultural homogeneity of the community of early settlers. Despite the town having been founded only a couple of decades before, an acutely uniform style had emerged.

Such uniformity was not typical throughout the colonies. Chandler (1916) documents many communities where a wide variety of construction materials and system were in evidence, including the early colony of Jamestown, Virginia where within a decade of its founding three permanent building types emerged including frame houses with hewn-timber frames covered by clapboards, brick houses and hewn-log construction. Kimball’s (1927) assessment is that material preference and amenities were a function of means and not opportunities or chronological sequence, which would support the physical record of brick construction dominating when funds prevailed or prestige required (mansions in the former case and churches in the latter).

Morrison (1952) notes that there was no physical evidence in extent structures that they were ever to have had wall fillings exposed, as the interior arrangements tended to appear completely haphazard. Conversely, there are written records that document the later addition of clapboards for both aesthetics and weatherproofing. A prime example is the John Roe House

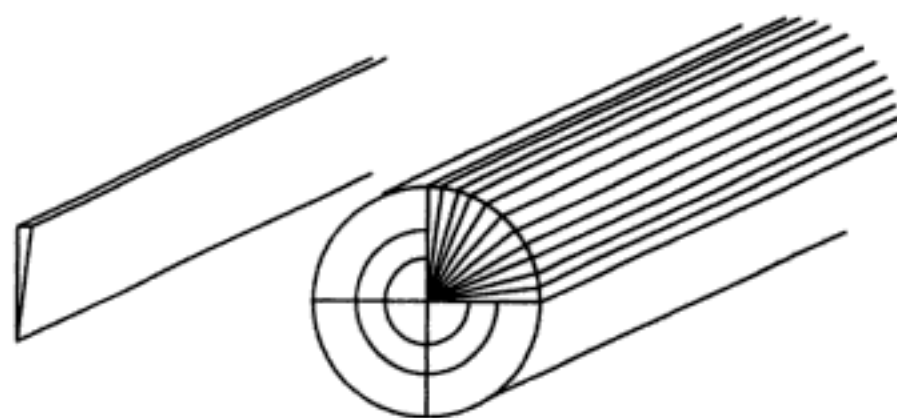


Figure 8. Original clapboard production.

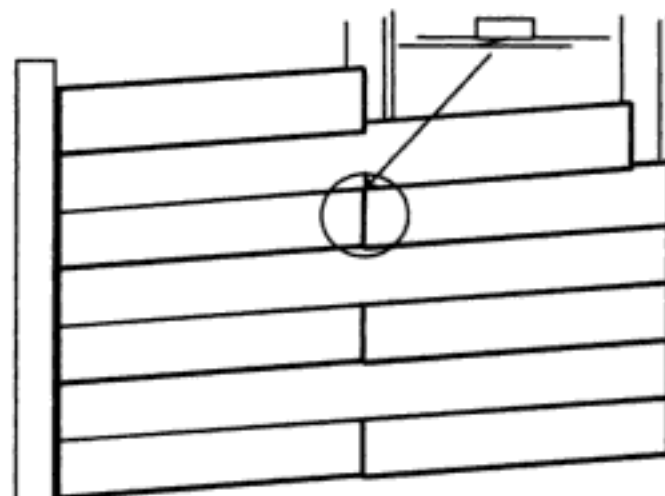


Figure 9. Clapboard elevation and detail of connection.

in Hancock County built between 1786 and 1803 with half-timber construction with clapboard added to the exterior walls after 1825 (Lane 1976). Whether done for warmth or prestige is unknown, although contemporary sources regarding Thomas Dudley’s house at Cambridge, Massachusetts claim warmth and not aesthetics for the requirement of clapboards nailed to the walls.

4.2 Clapboard manufacturing

Clapboards or weatherboards were first manufactured from pine by hand. Sawyers were recorded amongst the first settlers (Chandler 1916). Initially split from logs about four to six feet long, the log was first split into quarters through its length, then further split radially with froe and club into wedges (Fig. 8) (Lane 1996). The timbers were hewn square with a broad-axe, smoothed with an adze and notched joints cut with chisel, mallet, and auger. Clapboards appear to have been plentiful with some produced during the first winter at Jamestown for export.

The high cost of “pit-sawing” in terms of both time and labor encouraged the adoption of the water-powered sawmills. Although common in Europe from the middle of the fifteenth century, they were not used in England until 1663, by which time hundreds were used in New England alone. The first “sash” sawmills were modified pit-saws driven by a crank on the shaft of a water wheel. This method was later improved by incorporating several parallel saws (Chandler 1916).

The first mention of a sawmill in Virginia was in 1625 (Chandler 1916). The Dutch and Swedish settlers both built sawmill based on wind and water power. By 1760 there were 40 sawmills in Philadelphia County alone.

4.3 Clapboard alternatives

A contemporary alternative to the clapboarding was shingles. There are at least a few known examples of brick nogging beneath shingles in New Haven Connecticut, and they were especially popular in New Jersey and Long Island New York. In 1679 Jasper Dankers wrote "Houses in Boston are made of thin small cedar shingles, nailed against frames and then filled with brick and other stuff" (Chandler 1916). Sheathing may have first developed beneath shingled walls, where it was essential as a nailing base. The superior tightness of such a double layer led to the adoption of sheathing under clapboards beginning in 1700 and the gradual abandonment of clay or brick filling during the eighteenth century.

4.4 Clapboard usage

In New Amsterdam a 1642 contract specified 500 clapboards to be installed all around and overhead tight against the rain (Chandler 1916). In Massachusetts in 1638, the Symod's house was built with "very good oak-hart inch board ... (and) walls without to be all clapboarded beside the clay walls." (Kimball 1927). Similarly, the first record of an artisan house frame was in 1639, where "the rooffe and walles Clapboarded on the outsyde, ..." were to be used (Kimball 1927). Similarly, the church at Salem, Massachusetts in 1639 was "to be covered with ... board upon that to meet cloase...to be sufficientlie finished with daubings" (Kimball 1927).

Throughout the next century there is extensive remaining physical and recorded documentation of clapboarding structures. By 1736 in the newly formed settlement of Savannah, Georgia the structures were covered with split boards. The presence of the Moravians may have also been a contributing factor in this community and the Winston-Salem area in North Carolina. Locally available brick may also have been highly inappropriate for the highly damp climate as confirmed by the decay of a 1740 brick church that was parged with plaster but in demise soon after (Lane 1976).

Early examples are well documented as architectural historians are predominantly interested in the onset or introduction of a new element or style. The concept of the earliest date simply is revised backwards when new evidence emerges. What is more important to the practicing engineer is to establish how late certain practices persist and how widespread they remain. An extremely late eighteenth century example is the



Figure 10. Mid-nineteenth century plantation house with clapboard over brick nogging.



Figure 11. Mid-nineteenth century plantation's overseer's house and kitchen building.

Hinde house in Spring Hill Georgia (Lancaster 1991). Figures 10 and 11 show several mid-nineteenth century clapboard structures with brick nogging in rural North Carolina. Downing's 1850 book provides one of the most extensive description of the role and relationship of brick nogging to the wall insulation system instructing that a small gap be left on each side of the 4" brick nogging to create a cavity of dry air.

5 IMPORTANCE

Knowledge of the presence of brick nogging is critical to the proper assessment of an existing structure, primarily in terms of its weight and stiffness.

5.1 Weight

Critical to the presence of the brick is the weight of the material. Where wood is only a quarter of brick weight and the assumption of an older clapboard structure has an empty cavity within the framing the presence of even a single wythe of brick could substantially impact the total dead load. Based on a late twentieth century load take down of Somerset Plantation's large, main house, the total load was estimated at 803,770 kN (Fischetti 1980). Base on the floor plan and assuming

only noggin in exterior walls at a single thickness, the additional 1200 m² of material would increase the weight of the structure by 37,290 or nearly 5 percent. A double layer of the material would result in 10 percent increase. The critical point is in the understanding of the heightened load in specific piers, particularly if the house needs to be jacked or lifted.

5.2 Stiffness

Calculating stiffness is less straightforward. Tests of single-wythe low-strength brick showed elastic moduli around 3,000,000 kN/m² with a high amount of variability (Laefer 2001). What is unclear is how much of a composite section the walls behave. A conservative assessment approach would be to assume that the brick controls the building stiffness.

6 IDENTIFICATION

Identifying the existence of brick nogging is the most critical feature. The older and the more rural the



Figure 12. Gap between wall and floor exposes brick nogging.



Figure 13. Predecessor of the Somerset house by 30 years, approximately 45 km away.

structure is the more likely it is that brick nogging may be present. In frontier areas such as Kentucky architectural styles were influenced by the soldiers and settlers that entered the territory long after other parts of North America were well settled. The use of more traditional techniques decades, if not centuries, later than may have been expected from the architectural record in more urbanized areas should be considered as a direct outgrowth of the original factors that generated brick nogging beneath clapboards as a widespread construction style.

Determination of the presence of brick nogging may be achievable with only a minimal amount dismantling that may be done in a reversible and non-destructive manner. Figure 12 shows a gap between wall and floor, where the brick nogging was visible on a second story.

Another major clue may be the provenance of the original home builders. In the case of the Collins Mansion at Somerset Place, the family that built the structure had lived in a more urban area about 45 km away. The owner's previous home there and several other surviving structures from that period are nearly identical in many of their critical features with the Collins Mansion built 30 years later.

7 CONCLUSION

The wall filling technique of brick nogging is poorly known in part because the historical architectural books do not emphasize the details of the wall construction and configuration either because usage was so extensively employed that the knowledge was considered obvious or later considered *passé*. Subsequent documentation has also taken a highly superficial treatment of vernacular structures. The situation is further complicated by that fact that brick nogging was typically used beneath clapboards. The critical element to understand is that clapboard buildings may not be as they seem. The modern engineer working with even mid-nineteenth century clapboard structures should investigate the possible presence of such materials.

REFERENCES

- Benjamin, A. 1796. *Practice of architecture the builder's guide: two pattern books of American classical architecture (with new introduction by T.G. Smith 1994)*. New York: De Capo Press.
- Chandler, J.E. 1916. *The colonial house*. New York: Robert M. McBride & Co.
- Conner, E. 1910. The French brick trade. *Clay Record* (4)37 (August): 18–19.
- Downing, A.J. 1850. *The Architecture of country houses (with new introduction by J.S. Johnson 1969)*. New York: Dover Publications, Inc.
- Felt, J.B. 1845. *Annals of Salem Connecticut Houses* 2nd ed.

- Fischetti, D. 1980. *Subsurface exploration and analysis for the Collins Mansion, Somerset Place state historic site*. For State of North Carolina, Department of Cultural Resources.
- Fried, A.N., and Law, D.W. 1995. Factors influencing masonry flexural strength. *Proceedings of the British Masonry Society* (7)(October): 85–89.
- Howells, J.M. 1937. *The architectural heritage of the Piscataqua: houses and gardens of the Portsmouth district of Maine and New Hampshire*. New York: Architectural Book Publishing Co, Inc.
- [http:// www.shakespeares-globe.org/](http://www.shakespeares-globe.org/) last accessed May 12, 2004.
- Jefferson, T. 1784. Writings ed. P.L. Ford Vol. 3. 1894.
- Kimball, F. 1927. *Domestic architecture of the American Colonies and of the early Republic*. New York: Charles Scribner's Sons.
- Laefer, D. 2001. *Prediction and assessment of ground movement and building damage induced by adjacent excavation*. PhD Thesis. University of Illinois. pp. 903.
- Lancaster, C. 1991. *Antebellum architecture of Kentucky*. Kentucky: University Press of Kentucky.
- Lane, M. 1976. *The architecture of Georgia*. Savannah: The Beehive Press.
- Lane, M. 1993. *Architecture of the old south Kentucky & Tennessee*. Savannah: Beehive Press Book.
- Lane, M. 1996. *Architecture of the old south Georgia*. Savannah: Beehive Press Book.
- Marsh, B. 1962. *Plantation heritage in upcountry, South Carolina*. Asheville: Biltmore Press.
- McKee, H.J. 1973. *Introduction to early American masonry stone, brick, mortar and plaster*. Washington D.C.: Preservation Press.
- Morrison, H. 1952. *Early American architecture from the first colonial settlements to the national period*. New York: Oxford University Press.
- Rhodes, D. 1968. *Kilns: design, construction and operation*. Philadelphia: Chilton.
- Ritchie, T. 1960. Early brick masonry along the St. Lawrence in Ontario. *Technical Paper No. 93 of the Division of Building Research*. Canada: National Research Council, 115–122.
- Symonds, S. 1638. Personal correspondence to John Winthrop the younger. *Collection of the Massachusetts Historical Society*, 4th Ser., 7: 118–120, 1865.
- Upton, D. 1998. *Architecture in the United States: Oxford history of art*. New York: Oxford University Press.

Vernacular architecture and “historical seismography”: an experience research

O. Niglio & D. Olivieri

Faculty of Letters and Philosophy – University of Pisa – Pisa – Italy

ABSTRACT: The *history of earthquakes* can be defined as a very ancient discipline, which roots are on the tales and on records of the most calamitous events whose evidence is not easy to be found because not written but handed down orally. Our study based exclusively upon the analysis and the direct study of the architecture, aims to determinate the needs and the technical devices, peculiar to the art of building, but strictly connect to the local building culture of our territorial reference or research (the northern Tuscany). The rich store of informations has allowed us to study different constructive typology, often determined by needs connected not only to the building tradition but also to the *local seismic culture*. From this will of putting the basis for a systematic study of the “historical seismography” that promotes a technical normative of reference that is neither generic nor inducing interventions little respectful of a context that only asks to be left in alone.

1 INTRODUCTION

The knowledge of the urban environment and of its structures is the first step for the protection and the preservation of the rich architectural estate, both in terms of historical testimony and social safety.

The redaction of special plans for the recovery and safety, or even for the definition of infrastructures which are necessary when a structural collapse occurs, are not essential because the principal aim is to prevent well defined intervention through a careful study of the methodologies and the techniques which respect and which are compatible with the preexistence.

The principal aim of our research, mainly addressed on a sample area of the northern Tuscany given by the Garfagnana and Lunigiana, is to analyse the interventions and the seismic risk reduction techniques which have been carried out in the past, in order to evaluate their engineering validity.

The interventions used in the past, and even studied through some schedules of analysis, have shown an important coherence, both technical and structural, mainly related to the respect of the historical, architectural and typological estate.

2 THE VERNACULAR ARCHITECTURE

The architecture is a language whose main aim is to communicate, so it needs to have all the skills which belong to a language. Further, in architecture not only the experts are able to work out a message.

The activity of living belongs to all, until one has proof to the contrary, and “*nobody can be considered just public because everyone is involved in the continuous changing of the environment*” (Benevolo 1994).

In 1881 William Morris wrote: “*The architecture involves all the environment which surrounds the human life; we cannot escape it, until when we belong to the civilization, because the architecture is the whole of changes and alterations made on the earth’s surface in relation with the human needs, with the exception of the desert. We cannot limit our architectural interests to a small group of learned men, which are entrusted to search, to find out and to model the environment where we have to stay and that surprises us...; it is for us, for each of us, to watch and to take care of the right order of earth’s landscape, each with its spirit and with its hands, and in the proportion which is due*” (Benevolo 1994).

In 1936 Giuseppe Pagano highlighted, with deep regret, that “*the history of the architecture is interested, without exceptions, in the so called stylistic architecture, in other words, in that “small” part of the architecture which is considered worthy of attention for its aesthetic value*”.

In these words we can guess how is partial a judge which excludes the living culture and is limited to the cathedrals, to the palaces and to all emerging buildings. Since its origin, the living culture belonged to the individuals or to the communities which probably did not stamp the projects and, quite surely, did not draw their cities on the paper.

So the ability to work out a design activity or, in more general sense, to organize human settlements, does not necessarily belong to them that have studied manuals. There are communities that organize by themselves their residential system and they show to be able to write down their functional project.

This argument is rather complex and we risk to deal it with just a rural and artisan point of view which is quite reductive. In other words, we can leave out the urban universe, from the minor and anonymous building of the central areas to the noisy suburbs and the aggregates of unauthorized houses and huts.

For example, the historians have analysed Los Angeles and have studied works realized by famous architects using coded styles. Their interest excludes *"refreshment stands, hamburger stalls..., motorways, and other civil engineering works, which are essential for the human ecology and the environment of Los Angeles"* (Banham 1983).

This piece of architecture ignores their authors and hates *"the heroes, the first ladies, the too personal images which are added to the list of greats"*.

Rudofsky says that the proposed history is limited to a "who is?" of architects which celebrates the power and the richness. In fact, in these terms Rudofsky organized and showed in 1964 the exhibition *Architecture without Architects* at the MOMA of New York, which has been intended as *"a definitely desecrating action, a courageous act which gives attention to the anonymous and which is oriented toward new critic profiles and new research fields"* (Zevi 1997).

In the most parts of world the buildings built from their owners, from the communities and from local specialized builders do not represent the exception but the rule. These unknown builders, recently studied, have realised the most part of the areas built from men. It is not easy to define these architectonic and linguistic "koiné" and all trials which have been done to explain this obliged patrimony have been failed miserably.

We use and abuse of the adjective "popular", meaning a wide range of construction types and forms, but the use of this term is often inadequate in the context of the big variety of built environments.

We cannot even speak about "anonymous" architecture because this adjective reflects the prejudices which exist around these buildings.

On the contrary, the so called "spontaneous" gives the false belief that the communities organization is strictly related to the nature conditions. In this context Benevolo wrote about *"a strange figure, the Portulano, that each year was elected at the Pescocostanzo University (Abruzzo, Italy), and which had the power to regulate the restoration of the old buildings and the build on the new ones"*. No citizen was allowed to do any change to his home without the complete consent of the Portulano. The Portulano was elected each

year and so it was free from kickbacks, dispensations and permissions but he limits greatly the concept of spontaneity.

Paul Oliver used the term "cover" to define the main motivation of a building, but its application to all buildings was not appropriate.

As the interests and the research grow up, it was necessary to coin a word which, at least theoretically, can summarize the most part of these languages *"from the ancient farm house in Tuscany, to the fierce landscape of the huts placed at the end of a car-breaker field"* (Zevi 1997).

And so the "vernacular" term was thought.

In the language study, vernacular means native language, in other words sub-dialect of the common language, which derive from the Latin *vernaculus*. Extending this concept to the architecture, vernacular is the local or regional dialect that is the common language of the buildings.

It is not easy to find a single definition of the vernacular architecture. The vernacular builders usually belong to the communities, they use the buildings and they often are the owners, the builders and the occupants on them, and their knowledge is handed on the future generations.

The community decides collectively the project and the construction of its built-up area, without the presence of a designer. *"Each person gives its original contribution to a solidarity based on the real and objective needs of the community"* (Langé & Citi 1985).

It is clear that the different shapes of the constructions, the different uses, the meanings and the cultural complexities make the vernacular architecture various. So the attempts to reduce the richness and variety of these traditions to a simple description limits it to a process.

The *Encyclopaedia of Vernacular Architecture of the World*, edited by Paul Oliver, holds all the studies done in the last ten years about the vernacular architecture. It is a *vade mecum* for all researchers! (Oliver 1997)

This does not mean that the architecture without an author can be only vernacular but that a big part of architecture without authors is even vernacular.

It is interesting to ask, following Mannoni, if the concept of "monument", is only limited to context of the canonical architecture, if it *"is really related to cultural choices based on pure aesthetic values, or if it depends on the uniqueness of the constructions which are able to be studied and dated"* (Mannoni 1994).

In these interpretations, what is excluded from the historical and critical subject of investigation?

It is excluded everything has not left trace in the chronicle, in the archives, everything has not a signature or a name to remember, that is all the "architecture without the author".

Unfortunately the history of the architecture has been written by them which see a figure, and not a form, in a work of art, *“the person who sees the figure and not the process in a figurative work of art, don't see”* (Ragghianti 1974).

Unfortunately the history of the architecture, and all the history, is full of blinds.

The limit of this kind of historiography is that it is limited to the history of the dominant classes. Those classes which have always the economic and political power and which are allowed to intervene in the architectural action, delegating to specialists the build of cathedrals, palaces and new buildings; the same “monuments” which was of interest to the official historiography.

The preference of the category of some sources in place of others is not always fair and has heavy consequences for the historiography. In particular the traditional historiography is based on written sources usually controlled by the power groups; unexpectedly these same groups are able to build one hundred or five hundred monuments described in the manuals of the architecture's history.

These sources implies the use of historical material strictly related to well defined forms of culture and power which transfer their culture through traditional forms of communication (such as writing, painting, and architectural styles).

To investigate the “architecture without the author” means to stay in a new and original historical dimension where there are no cultural limits in listing and defining strict academic categories. In this context the architecture has a complex form which does not match the rigorous scheme, and this is the reason that does not allow all to understand it.

The architecture without the author is thought and realized by the mass which has not the opportunity to control the traditional historical sources. It is not common that an inhabitant of a shantytown is able to testify its presence in a treatise of architecture.

Usually the sources used in the official history are direct, authoritative, chronologically ordered and easy to interpret. This architecture is, for its own nature, very rich of contents and of information and all the investigations have to mainly pay attention to the use of materials intended as historical sources. The study of the history of that communities which are not testified in any document, imply a change in the research methodology because the study of the building projected and realized by a single architect is completely different than the analysis of the “product” wished, thought and used by the mass.

It is usual to have at home utensils realized by famous designers. They are so nice that we prefer don't use them daily and so they become just nice, but not usable, ornaments. In the same manner new buildings are built using expensive materials and economic

sources are invested so obtaining wonderful structures completely different from the “monotone” and common architecture of the others buildings. But these structures represent a too easy and evident subject in our discussions. They look like to stay in some place just to bring the observer to well defined conclusions. In fact they often declare what they want to be and what they want to represent. On the contrary the problem of the sources is more complex when they have to testify realities which are not so evident.

In fact this architecture is more complex and does not match a rigorous scheme and cannot be understood from all.

“The living is an activity even obvious, given its necessity, but for this reason it is very rich of contents and information” (Pierotti 1999).

The buildings are projected and built to give answer to all days needs; where the structures are created to meet extreme events, they are the result of an adaptation started after a failure. The igloo of Eskimos is a clear example. *“The project of the ice home cannot be referred to any architect or engineer. The shape and the structure have been designed by Eskimos. They have imitated the strong models and have refused those models that succumbed, so that this civility has formed the final project of its home”* (Pierotti 1999).

In terms of intervention on the soil, the experience has as much importance as the science.

Through this methodology of research *“we can rebuild all the living history and so to bring to light even on the history of the populations that usually did not leave written testimony but left traces related to the home problem on the territory”* (Pierotti & Ulivieri 2001).

“Even the built specks, provided that we are able to hear what the stones tell”.

This kind of historical analysis, applied to the study of local seismic culture, allows to develop a research able to recognize the so called protective “anomalies”, that are some characteristics of the historical buildings which cannot be explained if not interpreted as suitable measures which increase the resistance of the building in case of earthquakes.

2.1 *The “Ecostorico” method*

The recourse at the *Ecostoria*, that is the study of the human settlements mainly carried out using empirical data, represent an important help.

“The Ecostoria is the history of the oikos, that is the history of human settlements. To settle is as necessary as to live, all of us write our small pages of ecostoria starting when we leave the mark of our presence on the soil. The living belongs to all, and so the ecostoria will describe the history of all”. *“The ecistica is the discipline that organizes the human settlements on the soil (“ecista” was the founder of the Greek*

colonies starting from the VII century). This means that the sources ecistiche are handy for the ecostoria" (Pierotti 1999).

It is necessary to know what "local seismic culture" means, which is widespread and deeply rooted in a given area.

"Among the catastrophic events the earthquake perhaps leaves more traces than other events. It is common practice that after such earthquake more advanced building techniques are used and they are destined to make buildings more safe, at least in theory, and so this implies that even in the constructions science the earthquakes history represent a big help" (Pierotti 1997).

The seismic culture is in the character of the built. This "culture" is not intended in theoretical sense. In particular if we read the instructions contained in the manuals of the engineers of the XIX century which describe how to build a structures in a seismic area, we can see that they are all the same. On the contrary in this context we are not speaking about engineers, architects or geometries, we are discussing the abilities of the resident population to control the built.

In the regions with high seismic risk, the regularity in the arrive of earthquakes has induced the use of techniques and behaviours which have a clear protective function. In other words, if the earthquake is frequent, the population assumes a seismic culture which gives rise to not coded and not written rules but they are clearly observable in their constructions. Its knowledge is based on the experience which becomes science. An example is the traditional Japanese architecture where the risk awareness is included in the shape of their buildings.

It is not easy to recognize the traditional aseismic techniques. It is necessary to analyse the vernacular architecture of the well defined area to evaluate which elements have a aseismic validity. The study of the human settlements done through of empirical data is of great importance. The building is the source most objective and reliable. Each building is the testimony of its self and supplies a big quantity of information, with its damages, its reparations and the preventive interventions. We need to "read the earthquake on the stones", and to remember the Marangone and Ragghianti's words: "see before and read after". Even Mumford on the ways of its native city, New York, and visiting each of its areas, relied on its ability to see and he derived the history from the direct observation of the architectural objects.

The seismic culture does not grow only in inhospitable areas, such as the Japanese islands, but even in Italy where the earthquake is frequent and "a culture of building" is born.

The Lunigiana and the Garfagnana, for example, are two seismic areas of Italy. The last disaster has been held in 1920, even if many earthquakes are registered

every 4–5 years which have reached the seventh degree of the Mercalli's stair.

The population of Dalli di Sotto perceives one or two earthquake per year. They say that "the hens sing and they can heard, before the earthquake, a roar and even the dogs bark" (Pierotti & Ulivieri 2001).

One of the reasons which makes this area of interest, is that the most part of the ancient homes, mainly in the Lunigiana, have not the plaster and so it is possible to understand and to document, directly from the brickwork, the events that involved them. From the stones we can still see the prevention systems, the repairs, the reinforcements and the changes done by law (Pierotti et al. 2003).

In these areas, where the use of the bamboo canes is very improbable, the home built in brickwork is quite common (even if there are some elements in wood) and there are some components that try to reach the same aim of the bamboo. There are main walls with large sections, terraced homes or even streets with arcades which make the town as a single building block. Further there are arcs across the streets, architraves in chestnut, ceiling in wood and so on. The system to understand the earthquake on the stones of each building, integrate the opportunity to define micro-areas of observation which cannot be defined in other ways.

3 NECESSARY RESTORATION OR A NEED TO RESTORE?

It is a well known and widely recognized fact that, should a particularly catastrophic event occur, an earthquake for example, the damage to a piece of our "cultural heritage", taken in its broadest possible sense, is not only in its material and formal aspect, but also in its social value and cultural identity within the community of which it forms part.

Most certainly lost is that value defined by Cesare Brandi as "aesthetic" yet at the same time "historic" subjected first and foremost to immediate repair interventions on damage provoked by the sad event (Brandi 1995).

Consequential, on such occasions, is the planning of interventions principally on those cultural heritage structures that have suffered less damage, that have every potential to continue their life cycle and require works aimed at their structural and formal rebalancing without the implication of widescale transformation.

But interventions determined by events, often unexpected, such as an earthquake, flood or fire, fall within a category that certain experts have correctly defined as works "of necessity", by this term meaning a work (...) *imposed by an exceptional fact and not upon request – such as normal restoration – of an architectural or urban monument* (Boscarino & Prescia 1987).

It is likewise important to specify that the intervention subject falling within the above mentioned category concerns both individual buildings and areas of a city, but which are recognized as having a “documentary” value, a cultural, social and economic identity.

In fact, the intervention conditions have different meanings if the subject is classed as having a high historic and architectural value, or if it is more correct to describe the works as constructional recomposition or urban renovation.

Our attention in this case is addressed mainly to the first category, that of works which document a recognized collective value, testimonials to memory or ownership. In this framework we speak of restoration as that intervention aimed at guaranteeing the static safety of the construction and its subsequent return to order in full respect to its entire heritage role in the future.

In this respect it is important to quote a worthy description from the 1975 Amsterdam Treaty in which it declares the need to operate in terms of integrated preservation intended as *the result of the combined use of restoration technique and research of appropriate function* (Esposito 1996) in that the operational methodology requires the validation and reinstatement of the work in the framework of its existence and in its role in a social and environmental context.

But reality, when calamitous events have occurred, as reported often, has always been characterized by decisional and operational uncertainty caused mainly by the existence of obsolete and inadequate laws and regulations, as well as by organizations appointed to safeguard the heritage but who intervene with undue delay and lack of expertise.

We have witnessed a panorama of the most irregular, confused and inhomogeneous intervention solutions, the good fortune of which often derived exclusively from local contingencies rather than a solid and common cultural and operational methodology to confirm its interpretational differences on the subject of restoration.

3.1 *The Recommendations (1986)*

In 1986, the National Commission for cultural heritage risk prevention against seismic events produced the *Recommendations for specialist intervention on the monumental heritage in seismic areas* (Casiello 1990).

Said *Recommendations* systematically and accurately identify the analysis to be carried out prior to any intervention whatsoever, and lists in detail the project documents to be produced under the coordination of an architectural restoration specialist. In particular, the *Recommendations* aim to establish the correct intervention aims and confirm the main objective as that of prevention achievable by combining *improvement* works with the option of *general*

preservation. In a more detailed manner, the decree examines two kinds of intervention: adjustment and improvement. The first is intended as *the completion of a series of works proving necessary in order to render the building resistant to seismic activity*; the second is aimed at guaranteeing a higher degree of architectural stability *without substantially modifying its overall behaviour*. *Improvement intervention is mandatory for whoever intends to carry out local intervention aimed at renovating or replacing structural elements of the building*.

It is to this latter category that restoration interventions refer and which, first and foremost, require verification of the structural *status quo* and an in-depth knowledge of the building (the history of its constructional stages, materials and techniques used).

But a detailed analysis of the *Recommendations*, albeit with commendable attention also to preservation aspects, highlights a clear distinction between “subject” and “image”, that is between content and appearance, thus offering confirmation of the different methods and criteria used in *necessary restorations*.

The collective approach in these cases remains that of philological, sentimental, and “how it was ... where it was” restoration justifying many interventions, beginning with the reconstruction of the Campanile in Venice (1902) up to the current and contemporary debate over the reconstruction of the belltower of the Cathedral in Pavia (1989), but far from the true aims of reconstruction intervention determined by a clear desire to restore culture and national history (Pane 1959).

In this framework, experiments carried out over recent decades in the field of *necessary restoration* have involved many national territories: from Belice (1968), to Friuli Venezia Giulia (1976), Campania (1980), eastern Sicily (1990), Umbria (1998) and Molise (2002). All these cases demonstrate that impoverishment of the architectural and environmental heritage was not only caused by disasters, but also to the lack of timely and suitable renewal and recovery intervention.

With particular reference to the historic and architectural heritage, countless damage has been identified that more often than not has completely cancelled centuries-old historical evidence.

From analysis of the compromised construction, it has often emerged that the cause of the damage also resulted from previous interventions with little respect for the formal and structural characteristics of the building. In effect, for many years we have seen, and sadly still do, building restoration work using methodologies and technologies incompatible and often totally unsuitable to the real identified needs and in conflict with the original structure.

The problem in every case hinges on the real possibility of guaranteeing “seismic stability” with

respect for the preservation needs of the heritage, be it monumental or the so-called “lesser”.

In this respect it is fundamental to emphasise the content of the Law Decree of 24 January 1986 concerning technical regulations for constructions in seismic areas, quoted previously and later reconfirmed in the Law Decree of 16 January 1996.

Subsection 9.1 of the latter confirms two kinds of intervention: adjustment and improvement. With particular reference to improvement, in its clearest definition as illustrated previously, it contains the true principle of preservation, that of the function perceived by the original architect, as well as the awareness that history already partly proves the “testing” of the work itself.

Experience also, from particularly disastrous seismic events, has demonstrated the failure of a certain working method, aimed at the addition to the original structure of new elements in reinforced concrete, with mechanical characteristics that integrate inadequately with a brick wall structure (Mastrodicasa 1993).

There is no doubt that the true culture of *necessary restoration* finds its origins, differently, within the individual communities conditioned by the desire to reconfirm a lost cultural identity and to recover its function by adopting highly safe systems, as claimed by modern industrial technology, which then failed.

No less “invasive” are the indications imposed by organizations appointed to safeguard and protect, such as the state, regional, provincial and local (urban regulation) governments whose regulatory decisions on the subject are increasingly generic and do not integrate well with the reference subject. It is pointless recalling the lengthy delay recorded each day when analysing the conquests of scientific research against the difficulties they have met in acceptance by a public opinion geared increasingly towards consumerism.

Records increasingly show more cultural deviation between the world of research on the subject of cultural heritage preservation and interventions defined as *restoration* (but far from it) completed by engineers, architects, and more often than not also by surveyors, unspecialised and using operational methods and criteria closer related to economic and financial problems than to the real preservation of the architectural and urban heritage.

In this respect, we record a number of barely respectful interventions, and by no means preservational, contributing to an increased constructional vulnerability, illustrated and graphically represented in practices granted for and carried out upon architectural structures.

For example there is the replacement of ceilings (roofing and wooden floors) with heavy reinforced concrete slabs; curbing, again in reinforced concrete, inside a brick wall facing (both homogeneous and mixed); the application of reinforced beton for

consolidation of walls; extrados consolidation of vaulted structures capped in reinforced concrete; and so many other interventions adopted often.

On the contrary, as reconfirmed previously, the basis of a preservational intervention is an in-depth knowledge of the construction, and from here the important role of diagnostics, both archival (surveys, historical analysis) and instrumental (investigative techniques applied directly on the building), for which a study of specific and specialist literature on the subject is recommended.

From this it is deduced that the road to follow is that of systematic recovery of traditional intervention technique such as: buttresses, metal chains, stanchion hooping, light wind-bracing, etc... which, if correctly applied, are fully preservational in that they are coherent with the original structure, reversible and therefore not invasive.

In many cases the history of the building has demonstrated that interventions of this nature have fully respond to shock from seismic events without provoking further damage.

The wealth of resources of a highly technological content (both tools and composite materials) available on the market certainly constitutes a valid alternative to traditional technique only if applied with respect to the constructional principles of the building itself. Once again fundamental in this respect is a knowledge not only of the building but also of new materials and technologies that are often used in an uncivilized and compromising way. The problem, in fact, is to disseminate this knowledge at all professional levels concerned (both public and private) and make them part of standard operational practice.

In any event the eventual aim of preservation must certainly be that of not operating in the field of *necessity*, nor resort to unnecessary restoration in that, should this occur, it indicates that an adequate preservational methodology, with standard intervention to re-establish small-scale unbalance an accumulation of which leads to more costly and risky intervention, has not been adopted.

4 TWO TYPOLOGICAL EXAMPLES OF SEISMIC PREVENTION

4.1 *Habitable buttressing arches and arcades*

Habitable buttressing arches were devised and developed with the aim of providing a contrasting effect against the buckling tendency of walls perpendicular to the direction of seismic stress. The creation of these arches also resulted in an increase in volume and new space available in housing units.

These construction elements subsequently contributed to the appearance of a highly recognisable building type, known as *arcaded villages*, which are

characteristic of many villages and little hamlets in the region of this study.

In the majority of cases, habitable buttressing arches and arcades are composed of more or less extensive vaults built from local stone; only the arcades sometimes feature a small wooden floor instead of the vault. These elements are always built level with the wooden or vaulted ceilings of two opposite buildings, with the addition of new structures built between them, bridge fashion. This enables the arcade both to cover portions of the alleyways and to support new rooms, but above all to establish a form of collaboration between the connected structures.

4.1.1 *Methodological and preservation notes*

Habitable buttressing arches and arcades can be included in the class of the so-called “added” structures that we have called *arcaded villages*. These elements have a structural as well as a strictly defined functional purpose as they simultaneously solve both static shortcomings of the original system and satisfy new functional demands of the building with new paths, rooms, etc.

Conservative work is aimed at the critical analysis of the quality of this added element, the assessment of its actual structural consistency, and its material and formal qualities within the context that it occupies.



Figure 1. The habitable buttressing arch built with stones and bricks in the old town of Sillano.

The collocation of the building in a historical context often calls for work aimed at preserving and enhancing all of its constituent parts. These structural elements, especially in old town centres and medieval villages, are characteristic features of the local architecture and environment and as such should be protected without resorting to contrived solutions offered by the most innovative technologies.

4.1.2 *Structural behaviour*

In static conditions, the vaults composing the arcades and built-up buttressing arches exert limited thrusts on the outside walls of the two opposite buildings that are generally thus able to bear them without the onset of static problems and load-bearing deficiencies of the foundations.

However, a preliminary inspection of the consistency of the walls and the good quality of the materials of the sections that require buttressing is always necessary before commencing any kind of work.

In seismic conditions, this element enables the horizontal movements that are produced to be distributed more efficiently, but above all the structure added above the vault effectively counters the tendency of the two opposite walls to collapse, due to its continuity with the walls themselves, considerably reducing the collapse multiplier and thus the possibility of critical situations.

The horizontal thrust of these vaulted structures increased by the seismic thrust is often counterbalanced by that produced by the vaults that are very often featured inside the construction, or is absorbed by the walls on which it is built, due to their considerable thickness.

Finally, the increase of vertical loads caused by the building of these vaults results in a certain improvement in structural behaviour as it contributes to



Figure 2. The habitable buttressing in the old town of Albiano.

re-centering the ensuing forces, repositioning the centre of pressure within the core of inertia.

4.1.3 *Usage precautions*

The remark made earlier concerning buttressing arches, regarding the fact that care must be taken not to create any dangerous eccentricities due to the staggering of the ceilings, also holds true in this case. Indeed, the presence of differences in level of the floors produces bending stress in the vertical wall facings, and the slimmer the latter, the more dangerous the former will be. Indeed, the decompression of the section increases in direct proportion to its slimness.

In the case in which the opposite buildings have insufficiently thick walls and flat ceilings that do not produce counterthrusts able to centre the ensuing forces, the use of arcades and habitable buttressing arches may be counterproductive, and the possibility of eliminating these thrusts by means of metal chains should be carefully examined.

Finally, it must be remembered that also for this type of work, effective bonding between the old and new walls is of fundamental importance for their satisfactory structural behaviour, as is the preservation of the state of the walls, avoiding the introduction of any dangerous discontinuities.

4.2 *Buttressing arches*

Buttressing arches are premodern structural elements introduced in the attempt to halt collapse mechanisms, which are often triggered by defects in the connection of new buildings to pre-existing ones.

Indeed, the stretches of wall of the new houses that are perpendicular to the direction of the earthquake often display a tendency to collapse, even in the presence of slight seismic movements. In other cases, the original walls present problems related to their low resistance to horizontal seismic stress.

This reinforcing structural element consists of an arch that is often made from stone and less frequently from brick positioned level with the wooden or vaulted ceilings of two opposite buildings. These single or multiple arches were usually placed in correspondence with the façades of existing buildings. Consequently the arches and walls to reinforce belong to the same vertical plane as the buttressing arch, thus enabling the creation of a kind of collaboration between the horizontal and vertical structures.

4.2.1 *Methodological and preservation notes*

Following clearly visible static damage, provisional propping structures are commonly used to counterbalance the disequilibrium that has been accentuated in a construction system due to causes that must successively be verified and that have required the support of external structures.

This is not the place to discuss the problems associated with the application of provisional structures, but it is useful to point out that they must be positioned in such a way as to restore the equilibrium of the construction system and thus studied and calculated from a static point of view, as illustrated below.

In general, we are used to thinking of temporary supporting structures such as centering and buttressing and simple props, which may be made from wood or tubular metal. In many cases these temporary structures become permanent as the building awaits future restoration work.

However, sometimes it is possible to observe the use of one or more masonry arches built between the opposite façades of two houses, especially in the narrow streets of very stratified old town centres. These arches are commonly known as "buttressing arches" in technical language, and are used to contain the instability of one or both of the buildings in a certain point. Unlike masonry buttresses, this system is less visibly invasive and at the same time enables the problem to be solved without interfering with the underlying space (e.g. a pedestrian path, an entrance, a road, etc.). These counter arches are nothing more than protective safety structures positioned at the most appropriate points to counter stress that may be of a subsiding, crushing, combined compressive and bending or tensile nature originating in the imbalanced construction system. Their planning must bear in mind the characteristics of the building that they are designed to



Figure 3. The buttressing arch built with stones in the old town of Aiola.

protect, the type of wall and the kind and severity of damage. Consequently, it is very useful to perform a preliminary analysis of the consistency of the materials, especially in the area in which the provisional structure will be applied, where the flow of forces is most concentrated. In this respect, it is also very useful to study the type of joint and connection between the provisional structure and the wall that it is designed to protect.

In the sphere of restoration, it is useful to bear in mind the significance of these buttressing arches, which constitute real protective structures, whose value is not temporary but which have become part of the historical fabric of the buildings, characterising the place and environment in which they are featured. In many cases these arches have also assumed the function of small corridors, external walkways or covered arcades connecting the various buildings. Any restoration work must be aimed at preserving these structures, even if their protective function is no longer necessary due to the application of alternative solutions on a "case to case" basis.

4.2.2 *Structural behaviour*

In static conditions the presence of the arch does not have any noticeable influence on the structural behaviour of the two connected portions of buildings and the arch is not subject to any particular stress, as it only needs to bear its own weight.

Earthquakes produce horizontal movements at the level of the floors, which are redistributed amongst the vertical walls in proportion to their stiffness or to their area of influence according to the stiffness of the floors themselves.

The presence of buttressing arches enables these movements to be redistributed more efficiently due to their joining function of the various parts of wall, but above all provides an additional bond to the walls that would experience subsidence problems without them. Indeed, these structural elements became very widely used precisely because they enabled the consolidation of structures in which the collapse mechanism was already underway and halted its progress.

In static conditions the horizontal thrust of these arch structures on the adjacent walls is fairly low and consequently does not cause any particular problems, however during seismic events it can increase greatly, and in this case must be absorbed by the full section walls behind (i.e. those in which any openings are suitably spaced) or counterbalanced by that produced by another arch inside the building.

4.2.3 *Usage precautions*

Particular attention must be taken not to introduce any dangerous eccentricities that would subject the wall to excessive stress, creating hazardous tensile loads that are difficult for the wall facing materials to bear.

In the case in which the floors are at different levels, buttressing arches can still be used but must be "hump-backed", i.e. with the imposts positioned at different heights, in order to connect the different internal levels in some way.

If the main walls to be buttressed are not perfectly parallel, the arches must necessarily be slightly sloping, although this reduces their efficacy and in some cases makes their use inadvisable.

As we mentioned earlier, buttressing arches are often constructed after the houses themselves have been built in order to consolidate certain parts of them, and in this case the impost of the arch is created by demolishing part of the existing walls in the area in which it is to be positioned and then building it from the wall structure. However, in a few very rare cases, the impost of the arch is simply built up against the wall, without any connecting element, thus introducing an extremely weak element into the resistance mechanism. Finally, when these arches are built at the same time as the buildings that they are designed to sustain, the correct way of arranging the arch is to create its bearings by widening the vertical walls, thus avoiding the use of imposts that drastically interrupt the structural continuity of the load bearing walls.

5 CONCLUSIONS

The architecture of the old settlements cannot always be translated in project rules. So, when the safety of the old buildings is under analysis, we usually generalize the interventions for their preservation and we overestimate the seismic risk.

Given that, the present work intends to give the bases over which to define a new methodology for the risk "knowledge" and the intervention which can allow to write new local seismic laws. They need to take into account the different types of buildings and their complexity that cannot always be reduced to simple and limited schemes of structural calculus.

REFERENCES

- Banham, R. 1983. *Los Angeles. L'architettura di quattro ecologie*. Monza: Costa & Nolan.
- Benevolo, L. 1994. *Introduzione all'architettura*. Bari: Laterza.
- Boscarino, S. & Prescia, R. 1987. *Necessary restoration*. Milano: Franco Angeli.
- Brandi, C. 1995. *Restoration. Theory and practice*. Roma: Editori Riuniti.
- Casiello, S. 1990. *Restauro, criteri, metodi ed esperienze*. Napoli: Electa.
- Esposito, D. 1996. Papers, documents, laws, in Giovanni Carbonara (ed.), *Architectural Restoration Treaty*. Torino: Editori Utet.

- Langè, S. & Citi, D. 1985. *Comunità di villaggio e architettura*. Milano: Jaca Book.
- Mannoni, T. 1994. *Caratteri costruttivi dell'edilizia storica*. Genova: Escum.
- Mastrodicasa, S. 1993. *Dissesti statici delle strutture edilizie*. Milano: Ulrico Hoepli.
- Oliver, P. 1997. *Encyclopedia of Vernacular Architecture of the World*. Cambridge: University Press.
- Pane, R. 1959. *Attualità dell'ambiente antico*. Firenze: La Nuova Italia.
- Pierotti, P. 1997. *Paradigmi di architettura*. Pisa: SEU.
- Pierotti, P. 1999. *Imparare l'ecostoria*. Milano: Franco Angeli.
- Pierotti, P. & Olivieri, D. 2001. *Culture sismiche locali*. Pisa: Edizioni Plus.
- Pierotti, P., Olivieri, D., Niglio, O. & Palla, F. 2003. *Manual of Historical Seismography*. Pisa: Edizioni Plus.
- Raggianti, C. L. 1974. *Arte, fare e vedere*. Firenze: Vallecchi.
- Zevi, B. 1997. *Storia e controscoria dell'architettura in Italia*. Roma: Newton.

The traditional twig-knitted wooden construction techniques: a vernacular architecture, “the Huğ house”

Z. Hale Tokay

The Faculty of Architecture, Mimar Sinan Fine Arts University, Istanbul, Turkey

ABSTRACT: On the land of Anatolia where many civilizations have settled, each district has developed an individual housing architecture due to its climatic conditions, the characteristics of the settling area, local material facilities and social structure. “The Huğ House” that is an example of traditional housing architecture built by using timber, reed and mud-based organic materials is the oldest house type discovered in Çukurova District and East Mediterranean Basin, especially common around Adana, Mersin and Tarsus. This vernacular architecture and traditional building technique has continuously been used till the 20th century, but unfortunately only a few has managed to survive today as a result of many reasons. Therefore, the few examples of these buildings that have survived today should be taken under conservation.

1 INTRODUCTION

On the land of Anatolia where many civilizations have been born, different traditions and beliefs have articulated to each other in centuries, each district has developed an individual housing architecture due to its climatic conditions, the topographical features of the settling area, local material facilities and the social structure.

The traditional housing architecture that is the subject of this paper has a long-lasting past in Anatolia. This housing architecture built by using timber, reed and mud-based organic materials is still being used in Central and Eastern Blacksea Region, Trachea, The Balkan Peninsula and Çukurova. The concrete findings obtained from surface research and archeological excavations within these districts prove that this kind of architecture has been used since very ancient times.

At the excavations directed by Professor Önder Bilgi from İstanbul University in the İkiztepe Tumulus located 7 km away from Bafra in north-eastern direction in Central Blacksea Region, this kind of architectural layers from BC. 3000s during the first Bronze Age has been discovered. As no foundations made of stone or adobe have been found, it is understood that the buildings in İkiztepe were made of wood. Trunks of various dimensions that have not gone through any process have been used for the construction of these buildings and these have been covered with clay from inside and outside.

Under the scope of Thrace Archeological Project directed by Professor Mehmet Özdoğan also from

İstanbul University, remains of buildings with no foundation where load bearing poles cut off from trees knitted with binding tiny twigs make up a skeleton and is generally called as “twig-knitting”, have been revealed on each building layer between the years BC. 5500 and 4000. These kinds of buildings are still being used for different functions in this district today.

2 THE HUĞ HOUSE

2.1 History

The Huğ House is a traditional rural house type particular to that district and especially common around Adana, Mersin and Tarsus within the Çukurova Region and East Mediterranean Basin known as Cilicia during ancient times. It has been built with timber, reed and mud that are the natural building materials of this district.

The Huğ House is the oldest house type known within this district in Adana and Mersin in particular. Its history extends back to 9000 years from today. This data has been confirmed with the findings obtained during the archeological excavations in Mersin Yumuktepe Tumulus.

Mersin is generally known as a new city founded in the 19th century. However, in contrast to this belief, the history of the city extends back to 9000 years from today to BC. 7000s. Yumuktepe Tumulus that has been hidden among the suburbs located in the northern region of Mersin is the most important witness of this

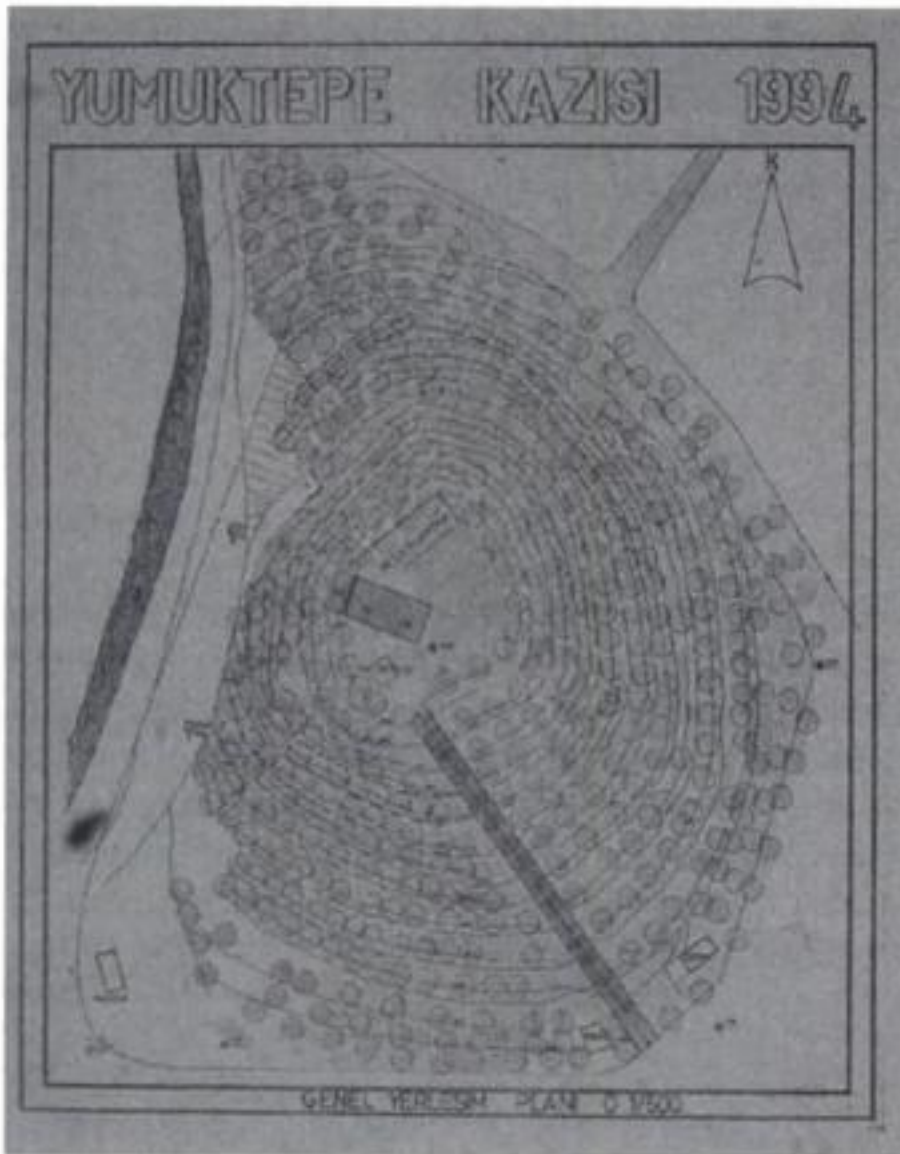


Figure 1. The general layout plan of the tumulus.



Figure 2. A general view of the tumulus, 1998.

history lasting for thousands of years. The Tumulus is restricted by Müftü Stream (Efrenk-Soğuksu) from west and Demirtaş neighbourhood from north and east. The height of the hill that covers an area, the diameter of which is approximately 300 meters, has decreased from 25 meters to 22 meters today. (Figures 1–2)

Yumuktepe holds a unique position in the world of Anatolia and Asia Minor because it is a hard-to-find establishment that had been settled for 7–8 thousands of years without having been abandoned at all. It means that this tumulus has been composed of the ruins of 30–40 establishment that were founded and collapsed one after another during thousands of years (from Neolithic to Islam). As it is clear, Yumuktepe Tumulus is a unique cultural asset and an outstanding place of

ruins that has witnessed the rooted past of Mersin. (Sevin, 1995)

The first excavations at the tumulus have been started by an English archeologist- John Garstang in 1936 and continued until the year 1947 with some intervals. In 1992, a team under the leadership of Professor Dr. Veli Sevin from İstanbul University has started the excavation again. (Köroğlu, 1993) The excavation is still being carried out by the cooperation of Rome La Sapienza University and Mimar Sinan Fine Arts University.

The findings belonging to the houses built with Huğ construction technique that has a very rooted past have been seen in Yumuktepe Tumulus since the earlier Neolithic period. We have found out from the findings revealed during the excavation works in the year 1998 that this housing technique has been used by Hittites during the second millennium BC. (Figure 3)

From the findings obtained during the excavation, we have understood that these houses were built in the form of cottages with a circular plan, no foundation and with load-bearing wooden poles – as we learn from the traces on the ground and carbonized little pieces of wood. It has also been understood that like the shelters of very ancient times, these houses with a circular plan and a flat base were made of fitted wooden poles cut off from trees, and tiny twigs and reeds knitted like basket were placed between these poles and covered with mud. (Acar, 1996) (Figures 4–5)

Evliya Çelebi who had passed by this region in the 17th century, has mentioned the existence of the Huğ Houses in Mersin in his “Book of Travels”. And in the Adana Almanac of 1860s, a description such as “a little village that consisted of a few Huğ’s among the greenness of myrtle trees inside” has been used.

2.2 Building technique and material

Huğ that can be pronounced as “Kuh” in Arabian accent means jerry-built shelter. The buildings were made of *quicksand bulrush, reed (kargı), twigs of myrtle tree (murt), zanzalak (zirinzak) tree* (Zanzalak is a local name. To which tree it refers has not been found out yet. The pith of this tree does not become worm-eaten as it tastes bitter, it becomes very hard and strong when dried.), *eucalyptus and katran tree* (Katran tree is also a local name.), and clayey soil mixed with *straw*. (Vural, ...)

The first houses of Mersin are these buildings called Huğ. These houses built of *reeds* obtained from the *canes* growing along Müftü Stream set an example for the rural buildings before urbanization with their primitive elevation.

Reeds that spontaneously grow in nature are cut off during winter and stored. These have been used either in the construction of houses and service buildings (sheep-fold, loft, depot, fence, wc ...) as constructive

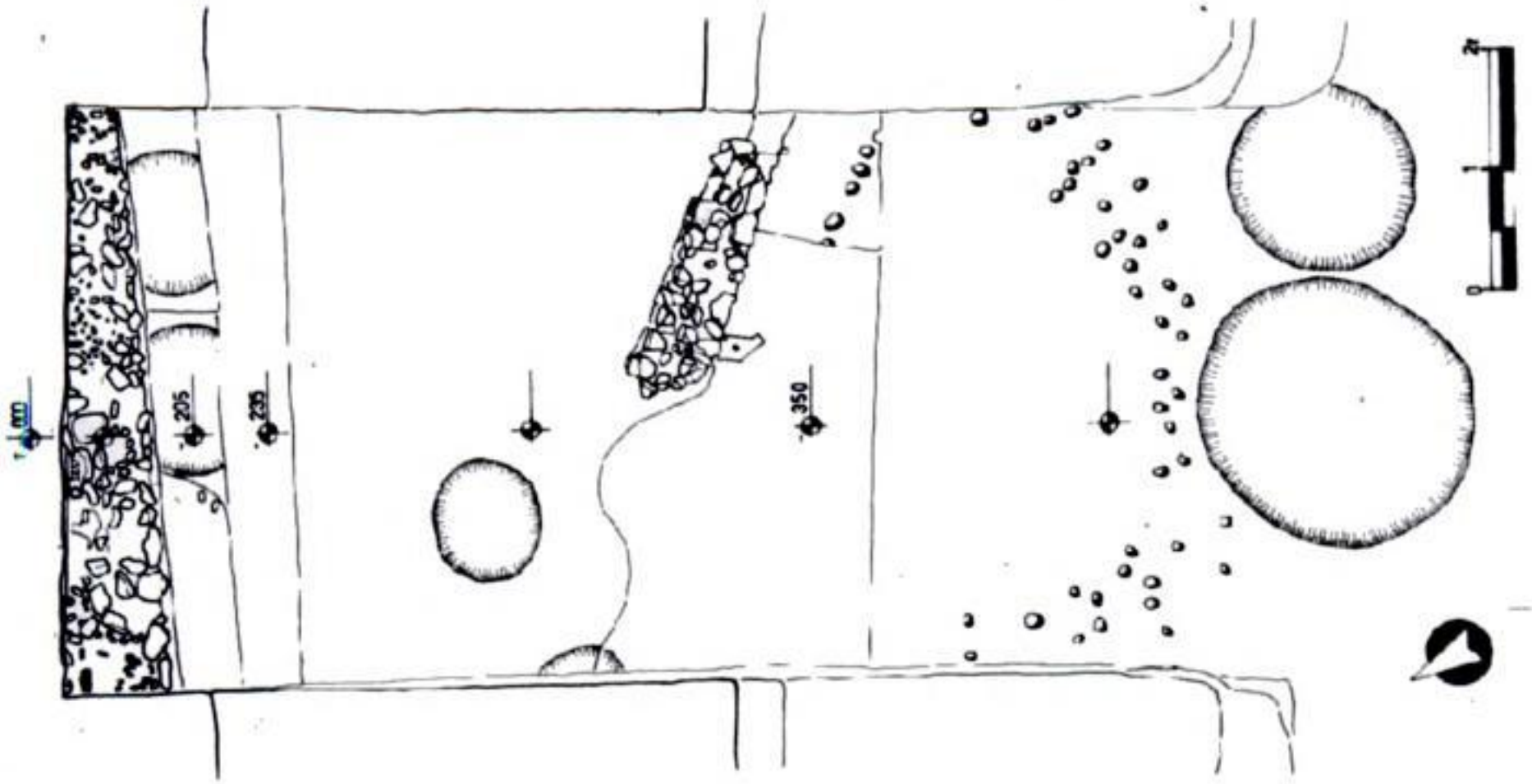


Figure 3. The findings that belong to the houses of Hittite Period and have been revealed during the studies in 1998.

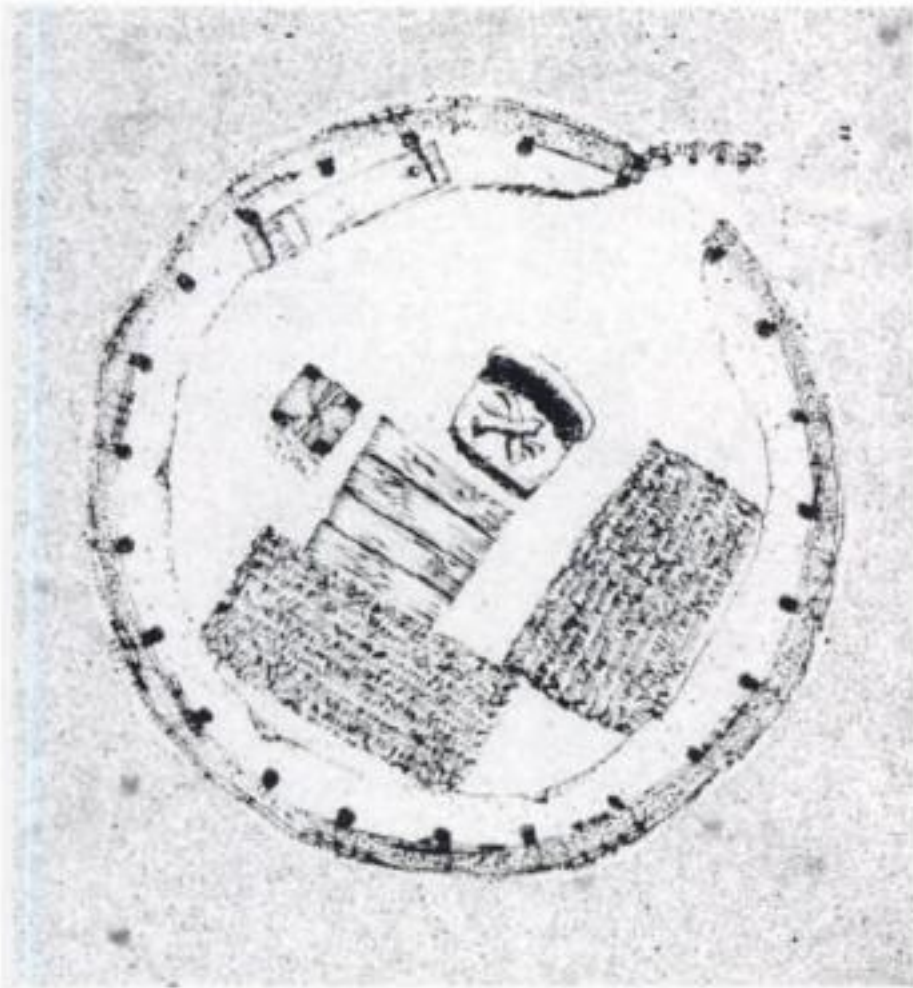


Figure 4. Circular shelter plan.

elements (Figures 6–7) or between garret beams (rafter) as covering or in place of lath in lath-and-plaster walls of traditional houses of the district and Mersin in particular that had been built in subsequent periods. Reeds are still being used today as one of the main building materials in the construction of shelters (houses) belonging to the people that have come as a result of immigration between cities and seasonal workmen. (Figure 8)

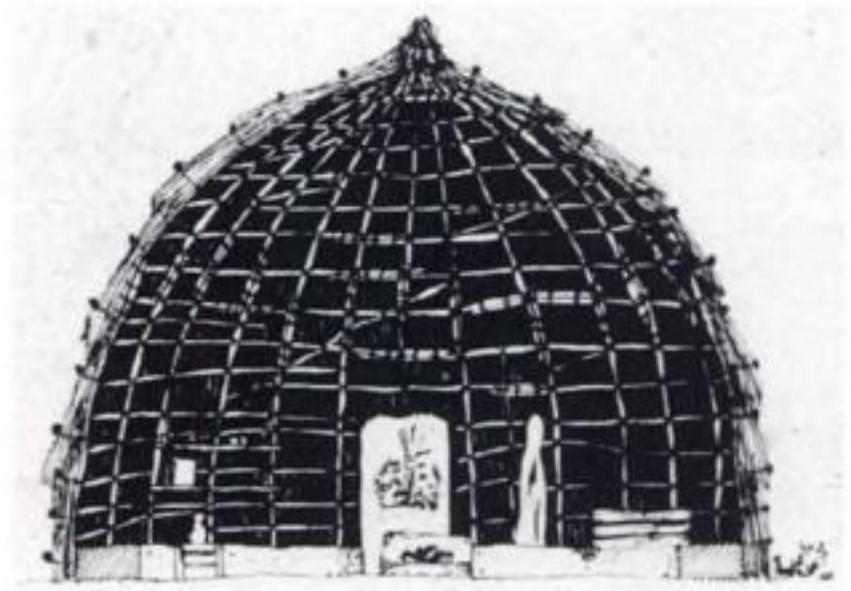


Figure 5. Circular shelter section.



Figure 6. Reeds that spontaneously grow in nature 1998.



Figure 7. The detail of masonry bond of traditional Huğ House, 1998.



Figure 8. The shelters of immigrants and seasonal workmen, 2000.

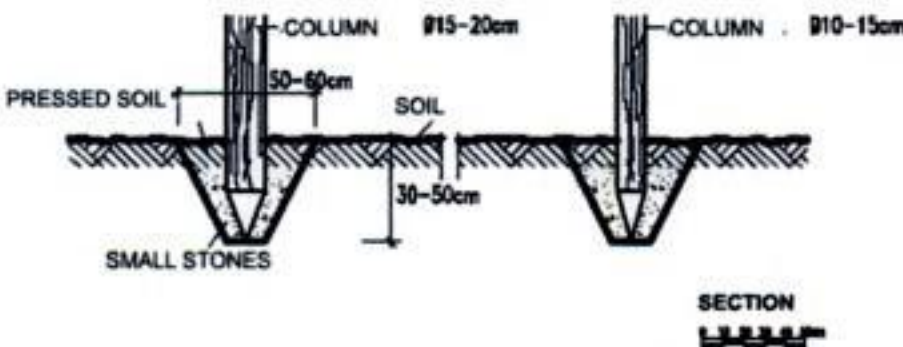


Figure 9. Foundation detail.

Foundations: As the buildings within this region have been built with lightweight materials such as timber and adobe mortar, they are not heavily loaded. For this reason, they do not need a continuous and deep foundation. In most of the examples examined, a continuous foundation pit has been dug for some walls and elsewhere a hole has been dug for each wooden pole that makes up the skeleton. So a continuous foundation has not been built. For load-bearing poles, holes with a diameter of 50–60 cm and a depth of 30–50 cm have been dug. As poles have been placed, they have been supported with small stones around. After having been wet with water, they are filled with soil and compressed (Figure 9).

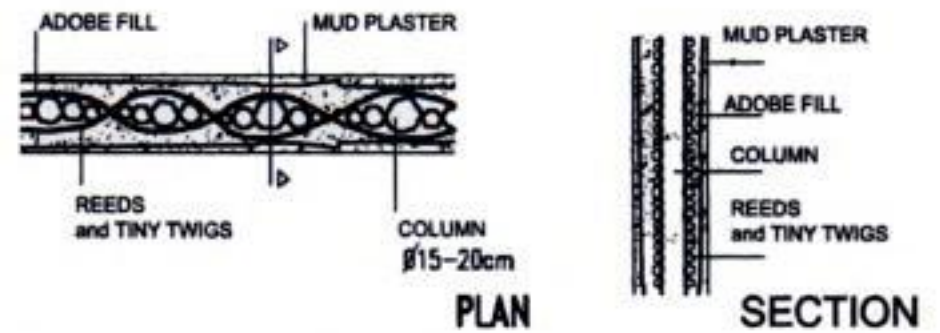


Figure 10. Wall detail.

Floors: A smooth floor is formed when a soil layer of 5–10 cm thickness is laid and compressed after the undulating areas on the ground have been cleaned and made smooth or when the surface of natural ground is covered with adobe mortar. As the floor is frequently renewed, the thickness of it gets higher in time. Then a mat is laid over the floor made of compressed soil or adobe mortar.

Walls: Trees of a large section ($\sim\varnothing 20$ cm), trees with a small section ($\sim\varnothing 10$ –15 cm) and reeds, bulrush and shrub are used besides tiny twigs ($\sim\varnothing 4$ –5 cm).

The main poles that make up the skeleton of the building have been chosen from *zanzalak*, *eucalyptus* or *katran trees* that are much resistant and common in this region. Then trees with smaller sections are placed and these poles are combined and consolidated with tree binding elements that act as a horizontal peripheral tie. Finally, the space between the main load-bearing elements and partitions is filled with *reed*, *supple myrtle*, *oleander* or *poplar-tree* knitted like mat and make up the wall skeleton. The empty space within the skeleton is filled with adobe mortar from inside and outside and both faces of the wall are covered with this mortar. The thickness of the wall varies between 20–25 cm. (Figure 10)

The traditional method of preparing adobe is difficult. The clayey soil that shall be used as adobe mortar is wet and left to rest. The humus layer that forms on the surface is taken away. Then, a ditch is opened and the clayey soil that has turned into sticky mud is laid inside this ditch. Small pieces of chopped *weed*, *straw*, *cotton* and other materials in the form of aggregate when necessary are added and mixed until it becomes a homogeneous mixture. The top of the ditch is covered for it not to be affected by natural conditions and the mixture is left to rest until the day it shall be used. On the day that it shall be used, the amount needed is taken, diluted again or mixed with straw until it reaches the required maturity. The walls are first filled with this adobe mortar until the wooden skeleton is completely covered, and then covered with a second layer of adobe mortar and a smooth surface is obtained. In wooden skeleton construction system, adobe is not used for load-bearing, it is a filling material. The adobe used for filling surrounds the wooden material and protects it from weather conditions. This causes the wood to last longer. Furthermore, as the adobe has become a

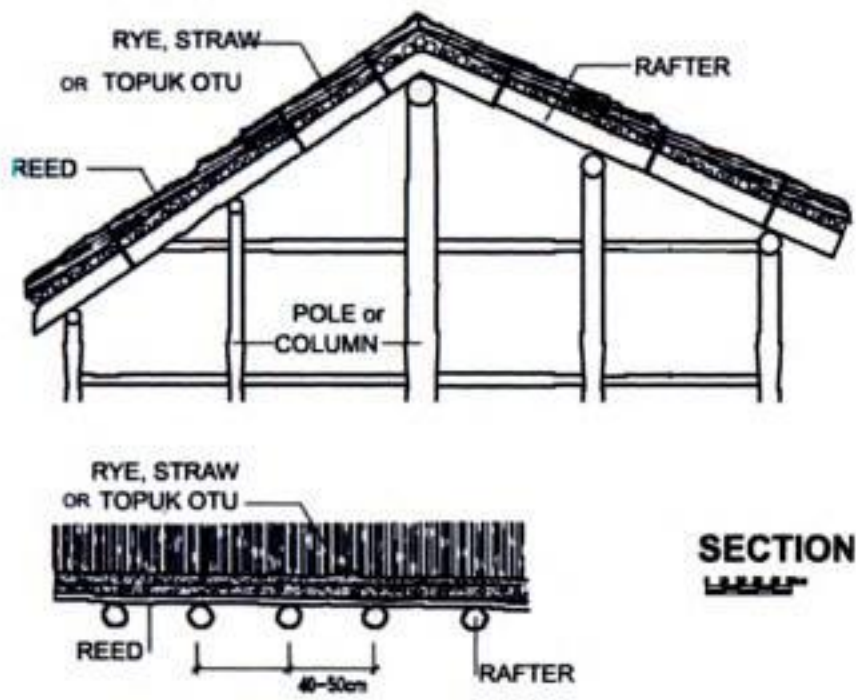


Figure 11. Roof detail.



Figure 12. One-storey Huğ House wall and roof covering, Adana, 2000.



Figure 13. Side elevation of the registered Huğ House next to Mersin Yumuktepe Tumulus, 1998.

light and hollow material as a result of vegetal additions, it is heat-insulating, hygroscopic and makes its environment a healthier place.

Roofs: The roofs within this region are built as either ridge or inclined towards one direction according to the formation of the building. The ridge roof can be built either with truss or without truss – with

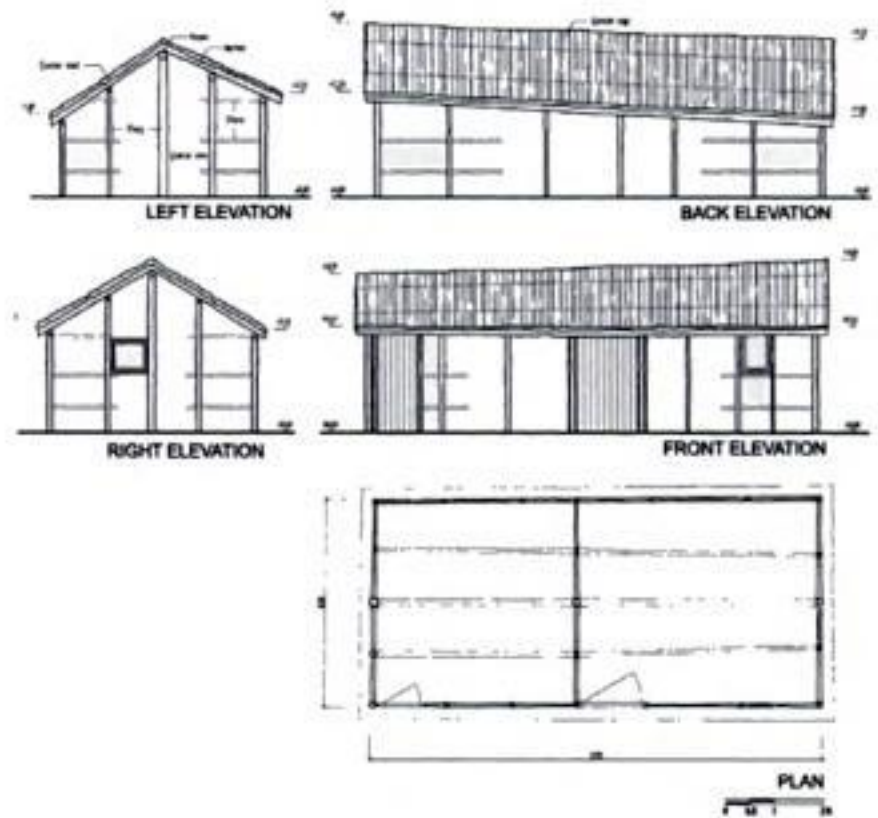


Figure 14. The Huğ House next to Mersin Yumuktepe Tumulus. This house is the only registered example. (plan, section, elevation).



Figure 15, 16. Ridge roof construction without truss, and reed covering material. Adana, 2000 and Huğ House's wall detail, Mersin, 1998 (demolished in 1999).

a central crown post. *Reed* or tiny twigs are knitted between the wooden skeleton of the roof and bunches of *rye, straw or a local herb called "topuk otu"* are laid above. This bunches arranged in a row with their stems up and ears down are tied up with a bond made of *bulrush or grass* and fixed. However, as a result of the unresistancy of the covering against the effects of time, the original roof covering of only a few buildings could have survived today, and tile, zinc and asbestos-cement have taken their place (Figure 11).

2.3 Examples

Although most of the buildings constructed with the Huğ technique usually have one-storey (Figures 12–14), there are also two-storey composite examples of these buildings that could have survived today (Figures 15–19).



Figure 17. Two-storey Huğ House, Kayışh Village, Adana, 1999.



Figure 18. Two-storey Huğ House, Adana, 1999.



Figure 19. Two-storey Huğ House, Sarıbahçe Village, Adana, 2001.

3 THE CONDITION TODAY – CONCLUSION

This vernacular architecture and traditional building technique has continuously been developed and used until the 20th century, but unfortunately these buildings have decreased very much in number because of the rapid urbanization today. Huğ houses and the

buildings constructed with this technique can only be seen in some suburbs of the city, gardens nearby the sea and in some villages, and they also face the threat of extinction day by day.

Mersin that has gone through a rapid development and change since 1830s has gained importance as a coastal city and harbour, become a cosmopolitan centre of commerce in time during the second half of the 19th century. Trade with foreign countries has caused an increase in the foreign population (Christians, Arabians, Maronites, people coming from Egypt and islands such as Cyprus, Crete, Rhodes, Europeans, Byzantine, Greeks, Jews ... etc.), consulates of foreign countries have been opened. A brand-new ethnic and cultural mosaic has been formed within the city. (... ,1978) This mosaic has naturally been reflected to urban structure and traditional Huğ houses and establishments made of this technique have slowly left their places to the buildings of a new style and a different urban texture in European style that includes houses, streets and monumental buildings has been formed.

These buildings in Mediterranean Levantine architectural style that came out in the 19th century in Mersin are far away from reflecting the traditional architecture of Mersin lasting for thousands of years. It is not possible to make a judgment of Mersin's development by just taking a look at these buildings of the 19th century and to understand the urban development within Mersin and Çukurova district by ignoring the traditional architecture.

The immigration from other cities towards Çukurova Region, new building period and the unhealthy development of cities have caused the traditional architecture of this district to enter a period of rapid extinction. For this reason, the very few examples of this architecture that could have survived today should be handled and evaluated in a systematic and detailed way.

In the direction of this aim, the very few examples of these Huğ buildings that are so fragile in the aspect of structure, unresistant to the effects of nature and people and can easily face extinction should be found, registered and taken under conservation. Only the one-storey building next to Mersin Yumuktepe Tumulus has been registered, unfortunately the other buildings within this district have not been registered yet.

There should be important lessons for us to learn from this architectural tradition that has the ability to adapt natural conditions of the past, and the knowledge and experience in using material. In my opinion, this tradition, knowledge and experience shall be the base in the formation of our comprehension of technique and art today.

As a result, this traditional architecture and building technique should be protected and it should not be forgotten that this architecture with its living, actual,

concrete assets could contribute to the creation of contemporary architecture.

ACKNOWLEDGEMENTS

This paper has been prepared by depending on the findings that came out as a result of regional surface and texture research besides the archeological and etnoarcheological (Etnoarcheology means, making it possible for us to make a healthy explanation about the remains that we come across in the form of base and trace at the excavation with the documentation of the existing examples of the architecture discovered) studies that İstanbul University, Rome La Sapienza University and Mimar Sinan Fine Arts University developed collectively in Mersin and Mersin Yumuktepe Tumulus. This study is still going on and is planned to be developed and carried on.

REFERENCES

- Acar, E., 1996. "Anadolu'da Tarihöncesi Çağlardan Tunç Çağı Sonuna Kadar Konut ve Yerleşme" *Tarihten Günümüze Anadolu'da Konut ve Yerleşme – Habitat II*, Beykan. M(ed.), Tarih Vakfı Yurt Yayınları, İstanbul
- Akman, A., 1995. "Kerpicingin Araştırılması ve Niteliklerinin Geliştirilmesi Üzerine" *Yapı Dergisi* 169: 104–105
- Eres, Z., 1999. *Tarihöncesi Kazı Yerlerinin Koruma, Restorasyon Sergileme Sorunu ve Çözümüne Yönelik Bir Uygulama Kırklareli – Aşağı Pınar Örneği*, İTÜ Mimarlık Fakültesi, Yayınlanmamış Y. Lisans Tezi
- Eriç, M., 1979. "Geleneksel Türk Mimarisinde Malzeme Seçimi ve Kullanımı", *Yapı Dergisi* 33: (42–45)
- Eriç, M., 1980. "Kerpiç Eski Eserlerin Onarımı ve Kullanılmasında Bir Araştırma" *III. Uluslararası Kerpiç Koruma symp*, Ankara, s. 79–86
- Eriç, M., 1982. "Geleneksel Türk Mimarisinde Malzeme Açısından Cephe Kuruluşu" *Yapı Dergisi* 45: (35–42)
- Gökçe, G., 1979. "Geleneksel Mimaride Strüktür", *Yapı Dergisi* 33: (19–28)
- Kazmaoğlu, M., Tanyeli, U., 1979. "Anadolu Konut Mimarisinde Bölgesel Farklılıklar", *Yapı Dergisi* 33: (29–42)
- Kouremenos, K.E., *the Sarakatsani*, Mellisa Publishing House, Athens
- Kurul, N., Eres, Z., Borotav, A., 1982. "Kırklareli'nde Deneysel Arkeoloji, Bir Neolitik Çağ Evinin Yeniden Yapılışı", *Arkeoloji ve Sanat* 82: (19–26)
- Kömürcüoğlu, E.A., 1962. *Yapı Malzemesi Olarak Kerpiç ve Kerpiç İnşaat Sistemleri*, İTÜ, Mimarlık Fakültesi Yayını, İstanbul
- Koroğlu, K., 1993. *5. Yılda Yumuktepe*, Eskiçağ Bilimleri Enst. Yayını, İstanbul
1978. *Mersin Evleri*, TC. Kültür Bakanlığı Yay. Tanıtma Dizisi: 63
- Özdoğan, A., 1984. *Tarih Öncesi Avrupa Dal Örgü Yapılarının Günümüz Örneklerine Göre Tümlene Önerileri*, İ.Ü, Ed. Fak. Yayınlanmamış Y. Lisans tezi
- Özdoğan, M., 1996. "Kulübeden Konuta: Mimarlıkta İlkler", *Tarihten Günümüze Anadolu'da Konut ve Yerleşme-Habitat II*, s.19–30, Beykan. M. (ed.), Tarih Vakfı Yurt Yayınları, İstanbul
- Sevin, V., 1995. "Yumuktepe", *İçel Sanat Klübü Bülteni*, 40: (28–29)
- Vural, S., "HUG En Eski Mersin Yapısı" Yayınlanmamış bilgi, Tarihsiz

FIGURE REFERENCES

- Figure 1; Sevin, V., 1995. "Yumuktepe", *İçel Sanat Klübü Bülteni*, 40
- Figure 2; Tokay, Z.H., 1998
- Figure 3; Measured drawing Tokay, Z.H., 1998
- Figure 4–5; Kouremenos, K.E., *the Sarakatsani*, Mellisa Publishing House, Athens
- Figure 6–7; Tokay, Z.H., 1998
- Figure 8; Tokay, Z.H., 2000
- Figure 9–11; Tokay, Z.H.
- Figure 12; Tokay, Z.H., 1998
- Figure 13; Measured drawing Tokay, Z.H., 1998
- Figure 14–15; Tokay, Z.H., 2000
- Figure 16; Tokay, Z.H., 1998
- Figure 17; Tokay, Z.H., 1999
- Figure 18; Tokay, Z.H., 1999
- Figure 19; Tokay, Z.H., 2001

Materials and laboratory testing

An experimental study on the construction materials of the Ankara Citadel

Ö. Kırca

ÇimSA Cement Production and Trade Company, Mersin, Turkey

T.K. Erdem

Middle East Technical University, Dept. of Civil Engineering, Ankara, Turkey

ABSTRACT: Ankara has been an important city throughout its history. Due to the geo-politic position of the city, Ankara was subject to many attacks by various civilizations. Therefore, the Citadel experienced many repairs by various people with different construction materials and techniques. Nevertheless, a great portion of the walls of today was reported to belong to Byzantine period. In this study, some mechanical and physical properties of the cut-stone taken from the inner and outer walls of the Citadel were determined. Compressive strength, point load, water absorption, density, and abrasion resistance tests were performed on stones. In addition, Schmidt Hammer and ultrasonic pulse velocity values were obtained. Compressive strength test values were correlated to the other data obtained to estimate the compressive strength in the further studies. Besides, the compositions of the two different types of mortar used in the fortification walls were also questioned through X-ray diffraction and X-ray fluorescence.

1 INTRODUCTION

Ankara was founded in the centre of Anatolia on the two main axes of transport running East-West and North-South. Thus, the city has been not only an important region for its geographic location throughout the history but also a transfer point for trade as well as military campaigns (Sağdıç 1994).

Ankara Citadel, which is the oldest portion of the city, had been utilised as a military garrison controlling the road passing through the plain in the rather old times. Unfortunately, it is not possible to give a certain date for the first construction of the Citadel (Sevgen 1959). Nevertheless, it can be said from the excavations that the Hittites founded a military garrison in İçkale (inner Citadel), the oldest portion of the city, in 4000–1200 B.C. This citadel had been constructed with mud brick on large rock blocks (Bakırer 2001, Bakırer 1987).

Due to the geo-politic position of the city discussed above, Ankara (and thus the Citadel) was subject to many attacks by various civilizations. Accordingly, the city was occupied by Hittites, Phrygians, Lydians, Persians, Galatians, Romans, Byzantines, Arabians, Seljuks, Ilhanids, and Ottomans. Therefore, the Citadel experienced many damages, repairs and restorations by various people with different construction materials and techniques. It is reported that the

fortifications of today belong to the Byzantine period (mainly in 7th and 9th centuries after Persian and Arabian attacks) (Bakırer 2001).

Andesite type of stone (Ankara stone) was used dominantly in the construction of the citadel fortifications. Marbles which belong to the ruins of the Roman structures, such as statues, entablatures, epigraphs, relief sculptures, marble blocks, column bases and capitals, etc. were also utilised very extensively. Rubble stone is used especially at the top of the walls with courses of bricks. The arches of the gates of the Citadel were also constructed with bricks.

Although there are many studies about Ankara Citadel, the authors of this report have not met any investigation about the mechanical properties of its construction materials. Actually, such a research is not easy because the structure have experienced many repairs by various people with several materials in different periods throughout its history. In this study, only a limited number of samples were tested but the samples were chosen carefully so that they characterise – to a certain extent – the materials used in the Castle.

The scope of this study is to determine the compressive strength, Schmidt Hammer values, ultrasonic pulse velocity values, abrasion resistance and water absorption capacity of the andesite, which is the dominant stone type used in the construction of the Castle. Besides, the X-ray diffractograms and chemical

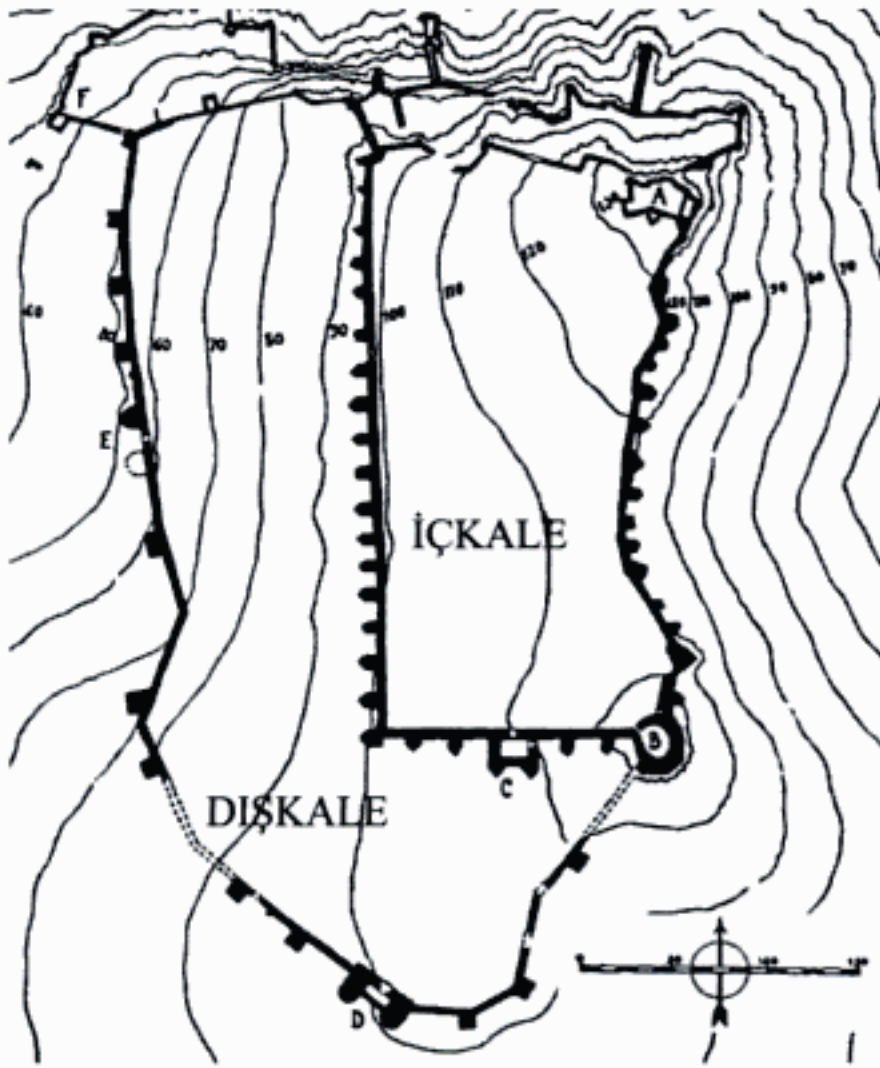


Figure 1. Plan view of the Citadel (Bakırer 2001).

analysis of the two different types of mortar used in the fortification walls are also questioned.

2 MATERIALS AND TECHNIQUES USED FOR THE CITADEL

It is reported that the Citadel was constructed mainly during the Roman and the Byzantine periods, and the walls of today belong to the Byzantine period (mainly in 7th and 9th centuries after Persian and Arabian attacks) (Bakırer 2001). The fortifications are the greatest work of Byzantine construction in Ankara (Foss 1989). Although there are various repairs and additions by the Seljuks, Ilhanids, Ahis, and Ottomans, the fundamental structure constructed during the Byzantine period has been conserved till now (Bakırer 2001).

The inner castle encloses a rectangular area of about 350 by 150 meters. The plan view of the Citadel is shown in Figure 1.

The main entrance to the Citadel is from the south. In the west, south and east walls, there are very closely spaced towers (only about 20 meters) (Fig. 1). Most of these towers have a pentagonal plan. Besides these, there are one square and two semi-circular towers. The inner walls were constructed over rubble stone by using cut-stones and huge blocks taken from ancient monuments up to a height of 8–10 meters. The upper portions are composed of courses of brick (Bakırer 2001). At the upper portions of the walls, generally,

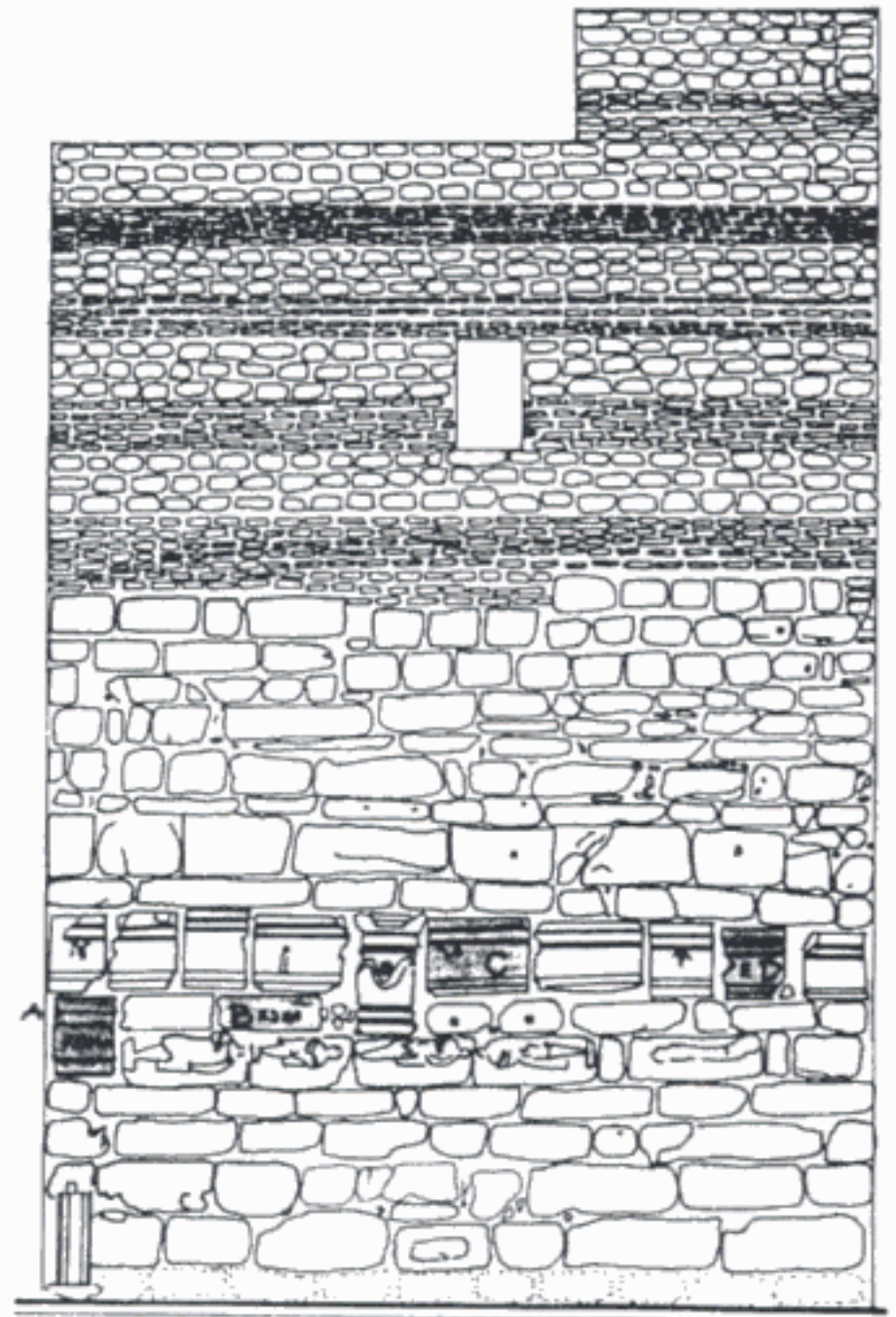


Figure 2. A wall from İçkale (Şimşek, et al., unpubl.).

brick and stone were used alternatively. (For example, in a wall at the south-side, stone/brick pattern is as follows: 5 brick / 3 stone / 5 brick / 3 stone / 4 brick / 3 stone / 5 brick / 3 stone.) The alternative use of brick and stone is shown in Figure 2. In some places, bricks were used randomly within the wall together with the cut-stones and rubble stones.

The materials used and the type of the construction of the outer walls are very similar to the inner ones, however, the workmanship is coarser in the former. The outer walls have a thickness of approximately 3.20 m and enclose the inner walls. There are 15 towers which are forty meters apart. 12 of them are square and the remaining 3 towers have semi-circular plans (Bakırer 2001).

Besides the use of brick in the fortifications, it is used in the arches of the gates of the Citadel. In Genç Kale Gate, the relieving arches are made of brick and lime mortar as the binding material. The vault coming just behind the arch is also made of brick. However, the arch of the Hisar Gate is built by using stones.

There are mainly three types of stones in the Ankara Citadel: andesite, white marble and limestone. Rubble stone and brick were also used in the fortification walls.



Figure 3. Two types of mortars.

The Citadel is dominated by andesite, however, marble is the most striking component of the walls.

Marbles used in the construction of the walls belong to the ruins of the Roman structures, such as statues, entablatures, epigraphs, relief sculptures, marble blocks, column bases and capitals, etc (Sağdıç 1994, Bakırer 2001, Bakırer 2001). This type of stones can be seen especially at the east and south walls of the Citadel (Fig. 2).

In addition, there are some stones with a hole at the middle, which had been used as water pipes in the Roman Period. After the failure of the water-supply system in the 4th century, the stone pipes of this system were utilised as a construction material in the Byzantine period (Bakırer 1987). These stone pipes are made of andesite and they exist especially at the east walls of the İçkale.

According to the observations at the lower parts of the fortifications, there are two types of binding material. The first one was nearly white in color, which was probably a lime mortar. The second type was used as flush jointing between the stones on top of the first binding material, which is thought to be Horasan mortar. Its color was pinky, and made of pebbles in different colors, tile chips and lime. These two types of mortar are shown in Figure 3.

3 EXPERIMENTAL PROGRAM AND TEST RESULTS

In this study, experimental program consists of two parts: a) Field work and b) Laboratory work.

In the field, the first step was the survey of the Castle. The types of the construction materials and their usage in the structure were determined. Then proper locations were detected to take samples which would characterise the materials used in the Castle. Andesite samples were taken from İçkale (inner Citadel) and

from Dışkale (outer Citadel). Two types of mortar samples were taken from the wall shown in Figure 3 for chemical and mineralogical analysis. Then, all of the samples were brought to the laboratory for testing.

Second part of the experimental program is the laboratory work, which is also composed of two parts: i) Tests on stone and ii) Tests on mortar.

3.1 Tests performed on cut-stone

Compressive strength, rebound Schmidt Hammer, ultrasonic pulse velocity, abrasion resistance and water absorption capacity tests were performed on andesite, which is the dominant stone type used in the construction of the Castle. Compressive strength, rebound Schmidt Hammer and ultrasonic pulse velocity can be used to estimate the mechanical properties of the materials such as compressive strength (Kırca et al. 2001).

Two andesite cut-stones were taken from İçkale. One cut-stone (andesite) was taken from Dışkale. In order to make tests on these stones, core specimens all having 50.3 mm diameter were taken from them.

After the water absorption and density tests, Schmidt hammer and ultrasonic pulse velocity tests were performed. Since it was not proper to apply hammer and ultrasonic tests on the core specimens with 5 cm height, these tests were performed only on the specimens with 10 cm height. Three rebound values were taken from each core specimen such that the distance between two data points is not less than 2 cm which is equal to two times the diameter of the impact plunger of the hammer. Then an average value was calculated for each location and this value was used in the related chart to obtain approximate compressive strength. Pulse time values taken from the ends of the core specimens were calculated from the formula:

$$V = (L / T) \times 10^6, \text{ m/s.} \quad (1)$$

where V = pulse velocity (m/s); L = length of the specimen (m); and T = calibrated average pulse time (μ s).

Then, the core specimens were subjected to compression until failure by using universal testing machine. Compressive strength values (σ) were determined by dividing the ultimate load (P) to the cross-sectional area of the specimens (A), that is

$$\sigma = P/A \quad (2)$$

The results for water absorption, density, rebound Schmidt hammer, pulse velocity, and compressive strength tests are given in Tables 1–4.

Moreover, point load strength tests were performed on the cut-stone taken from İçkale. The samples for this test were also taken from the same cut-stone whose test results are given in Tables 1 and 2.

The point load strength test is widely used to estimate the uniaxial compressive strength of the stones

Table 1. Test results for the first stone taken from İçkale.

Sample No	Length (mm)	Diameter (mm)	Weight (mm)	Density (g/cm ³)
1	100.4	50.3	463.3	2.32
2	101.0	50.3	455.5	2.27
3	100.5	50.3	456.0	2.28
4	100.1	50.3	461.9	2.32
5	100.9	50.3	453.5	2.26
6	100.8	50.3	464.6	2.32

Table 2. Test results for the first stone taken from İçkale.

Sample No	Pulse velocity (m/s)	Average Schmidt hammer value	Schmidt hammer comp. str. (MPa)	Comp. strength (MPa)
1	2960	45	50	42.8
2	3012	45	50	46.8
3	2872	43	46	38.3
4	2897	44	48	39.2
5	3087	47	53	52.2
6	3032	48	55	51.9

Table 3. Test results for the second stone taken from İçkale.

Sample No	Length (mm)	Dia-meter (mm)	Weight (g)	Density (g/cm ³)	Water abs. (%)	Comp. str. (MPa)
7	50.4	50.3	228.6	2.28	5.34	73.0
8	51.3	50.3	236.2	2.32	5.42	67.5
9	50.9	50.3	232.4	2.30	5.38	68.5
10	51.1	50.3	234.0	2.30	5.45	57.9
11	50.4	50.3	235.7	2.35	5.34	66.5
12	50.3	50.3	230.0	2.30	5.32	70.0

Table 4. Test results for the stone taken from Dışkale.

Sample No	Length (mm)	Dia-meter (mm)	Weight (g)	Density (g/cm ³)	Water abs. (%)	Comp. str. (MPa)
13	50.1	50.3	227.2	2.28	5.71	42.8
14	50.4	50.3	233.3	2.33	5.81	39.8
15	50.3	50.3	237.7	2.38	5.74	39.3
16	50.5	50.3	221.8	2.21	5.70	37.8
17	50.2	50.3	222.0	2.23	5.64	41.8

in fields and laboratories (Karpuz 1982). Point load test can be applied by 3 ways: diametrically, axially, and on irregular lumps. In this study, test direction was diametrical, that is, point load was applied in the direction perpendicular to its longitudinal axis. The

Table 5. Results for the point load test.

Sample No	Diameter, D (mm)	Failure load, P (kN)	Point load index, I _s (50) (MPa)
18	50.3	8.0	3.16
19	50.3	7.9	3.12
20	50.3	7.5	2.96
21	50.3	8.0	3.16
22	50.3	8.0	3.16

Table 6. Results Los Angeles abrasion test.

Initial weight, A (gr)	Amount retained on #12 sieve after		Abrasion ((A-C)/A)×100 (%)
	200 revolutions, B (gr)	1000 revolutions, C (gr)	
10000	9410	7410	25.9

Table 7. Chemical analyses of the mortars.

	Amount (%)	
	Inner mortar	Outer mortar
SiO ₂	60.21	44.41
Al ₂ O ₃	10.60	7.88
Fe ₂ O ₃	4.60	3.33
CaO	13.12	23.21
MgO	2.11	1.92
K ₂ O	1.49	0.86
Na ₂ O	1.07	1.01
SO ₃	0.13	1.44
LOI	12.61	20.33

results obtained according to the following formula are shown in Table 5:

$$I_s(50) = (P/D_e^2) \times F \quad (3)$$

where I_s(50) = point load index (MPa); P = failure load (N); D_e = equivalent diameter (mm), (D_e = diameter of the specimen for diametral test direction); F = correction factor = (D_e/50)^{0.45}, (F = 1 for this study).

Finally, as an additional work, Los Angeles abrasion test was performed on the cut stone taken from İçkale. This test is important from durability point of view. The results are given in Table 6.

3.2 Tests on mortars

As shown in Figure 3, two types of mortar were present in a wall of Dışkale. The first one was used in the inner

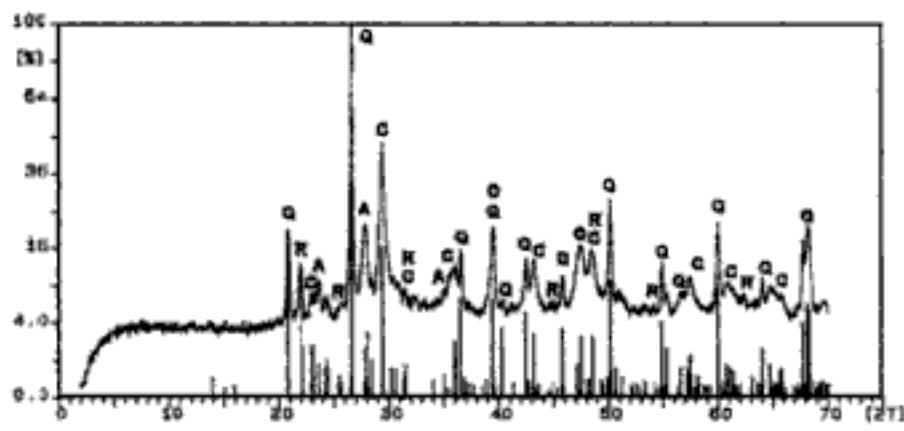


Figure 4. XRD pattern of inner mortar (Q: Quartz, C: Calcite, R: Cristobalite, A: Albite).

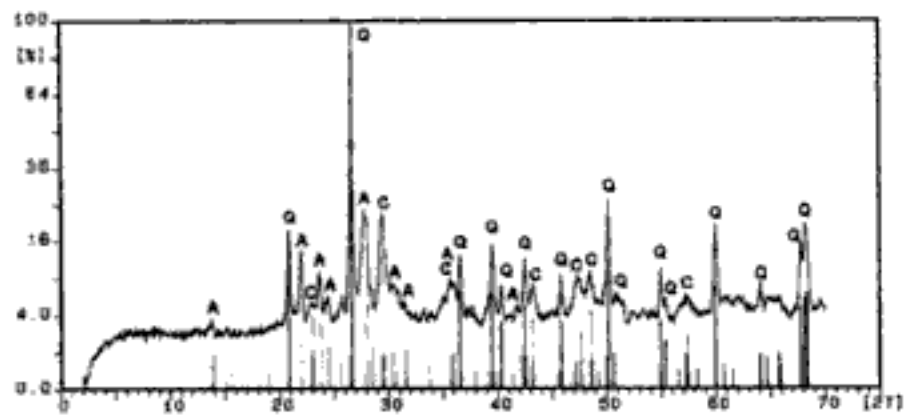


Figure 5. XRD pattern of outer mortar (Q: Quartz, C: Calcite, A: Albite).

portions of the wall and it was nearly white in colour, which was probably a lime mortar. The second type of mortar was pinky and used as flush jointing between the stones on top of the first binding material.

These mortars were powdered for X-ray diffraction (XRD) test to obtain mineralogical analysis. The chemical analyses of these mortars were obtained by X-ray fluorescence (XRF).

The chemical analyses of the inner and outer mortars are shown in Table 7.

X-ray diffractograms belonging to the mortars are given in Figures 4 and 5.

4 ESTIMATION OF UNIAXIAL COMPRESSIVE STRENGTH PROPERTY

4.1 Estimation of compressive strength from ultrasound pulse velocity test

A statistical study was performed to be able to find out an empirical formula that will give the relationship between compressive strength and pulse velocity values of the dimension stone core specimens. For this purpose, the experimental data of these core specimens tested in laboratory were used to form a data file in Microsoft Excel software. Trying to find the highest correlation factor, it was decided to make a non-linear regression analysis by using a Power function:

$$\sigma = A \times V^b \quad (4)$$

where σ = compressive strength value found in laboratory (MPa); V = ultrasonic pulse velocity value found in laboratory (m/s); A and B = constant numerical coefficients.

The formula, with a rather high correlation coefficient $R^2 = 0.95$ ($R = 0.97$), was originated as:

$$\sigma = 2 \times 10^{-15} \times V^{4.7354} \quad (5)$$

4.2 Estimation of compressive strength from Schmidt hammer rebound test

Similar to the procedure given for the estimation of uniaxial compressive strength from ultrasound pulse velocities, another statistical study was performed by using the rebound Schmidt hammer values (SHV). Highest correlation factor was obtained when the relation between the compressive strength and SHV was logarithmic, that is

$$\sigma = A \times \ln(\text{SHV}) + B \quad (6)$$

where σ = compressive strength value found in laboratory (MPa); SHV = Schmidt hammer values found in laboratory; and A and B = constant numerical coefficients.

The formula, with a rather high correlation coefficient $R^2 = 0.9038$ ($R = 0.95$), was originated as:

$$\sigma = 141.49 \times \ln(\text{SHV}) - 494.37 \quad (7)$$

4.3 Estimation of compressive strength from point load strength indexes

It is not possible to perform both compressive strength test and point load test on the same specimen since both of these tests depend on the failure of the specimen. Therefore, a one to one relation between the results of these tests can not be made for the same specimen.

In this study, compressive strength test and point load test were performed on the different core specimens of the same stone. Average value of the compressive strength values was found as 45.19 MPa and the average value for the point load strength index were calculated as 3.11 MPa. Then, a linear relationship was assumed and the following empirical formula was obtained:

$$\sigma = 15 \times I_s(50) \quad (8)$$

where σ = compressive strength (MPa); $I_s(50)$ = point load strength index (MPa).

5 DISCUSSION OF RESULTS

The results of the destructive and non-destructive tests performed on andesite cut-stone (dominant stone type

used in the Citadel) have been given in Tables between 1 and 6. These results lead to the following discussions:

The densities of the stone specimens were approximately 2.3 g/cm^3 . Abrasion of the stone was found to be 25.9% at the end of 1000 revolution. Since, the stones having an abrasion greater than 35% were said to be weak, the sample tested in the laboratory can be accepted as moderate from the abrasion resistance point of view.

The $5 \times 5 \times 5 \text{ cm}$ cube samples, taken from İckale, had water absorption values of approximately 5.4%. The uniaxial compressive strength values were found as between 58 MPa and 73 MPa. The water absorption capacity of the samples of Dişkale was approximately 5.8%, and their compressive strength values were between 38 MPa and 43 MPa. Therefore, as expected, it can be concluded that compressive strength decreases as their water absorption capacity, in other words porosity of the cut-stone, increases. So, the compressive strength property is inversely proportional to the absorption capacity was observed.

Non-destructive tests (Schmidt Hammer Rebound, and Ultrasound Pulse Velocity) and uniaxial compressive strength tests were performed on the core specimens having 5 cm diameter and 10 cm length. The compressive strength values of these samples were between 38 MPa and 52 MPa at the end of the tests. Ultrasound pulse velocity values lied between 2960 m/s and 3087 m/s. Schmidt hammer rebound values were between 43 and 48 at the end of the tests.

Point load strength test is widely used to estimate the compressive strength of stones in field and laboratories. In this study, this test was performed on the core specimens having 50.3 mm diameter. The average value of the point load strength index values, $I_s(50)$, was found as 3.11 MPa.

Table 8 gives a classification Ankara andesites. According to this classification, the results obtained from Schmidt hammer rebound values, ultrasound pulse velocity and point load tests suggest that the stones are slightly weathered.

A statistical study was performed to be able to obtain three empirical formulas giving the correlations between ultrasound pulse velocity, Schmidt hammer rebound, point load strength index $I_s(50)$ and uniaxial compressive strength property, respectively. These empirical formulas are given below as:

$$\sigma_v = 2 \times 10^{-15} \times V^{4.7354} \quad (9)$$

$$\sigma_{SHV} = 141.49 \times \ln(SHV) - 494.37 \quad (10)$$

$$\sigma_{I_s} = 15 \times I_s(50) \quad (11)$$

The results of the Schmidt hammer rebound tests were a little bit less reliable, when compared with the ultrasound pulse velocity test as expected, since, the

Table 8. The proposed sonic velocity, Schmidt hammer value (SHV) and point load strength (PLS) classification for Ankara andesites (Karpuz 1982).

Material description	Sonic velocity (m/s)	SHV	PLS (MPa)
Fresh	3900	54–61	3.16–6.63
Slightly weathered	3900–3050	39–54	2.24–3.16
Moderately weathered	3050–2250	28–39	1.22–2.24
Highly weathered	2250–1350	18–28	0.41–1.22
Completely weathered	<1350	<18	<0.41

rebound hammer value is affected by smoothness, surface hardness (carbonation effect), moisture content, size and age of the material.

The chemical analyses of the mortars have been given in Table 7. Although, it was not proved from the chemical analysis and X-ray diffractograms, a pozzolan is thought to be present in the mortars. Since, the relatively high amounts of Al_2O_3 and Fe_2O_3 , which were found at the end of the analyses, were the strong indicators of a pozzolanic material. Moreover, high background trends in the X-ray diffractograms showed the presence of an amorphous material, and this amorphous material is most probably due to binding material produced from the pozzolanic reactions with lime.

The results of the chemical analysis pointed out that, SiO_2 content of the mortar taken from the inner part was higher than that of from the outer part. This was partly due to higher amount of sand in the former (actually this was also observed by the visual inspection.). The case was reversed, when CaO contents were compared. The CaO content was higher in the outer part mortar. As a result of these comparisons, it can be said that, the binding material in the outer mortar was used relatively in higher amounts than that in the inner mortar. This result is quite logical and shows the indications of some advantages: The porosity (permeability) and the deleterious effects of weathering can be decreased by using mortars having high amounts of binding materials at the outer parts of the walls.

6 CONCLUSION

Any of these relations, determined experimentally and mentioned above, can be used to estimate the uniaxial compressive strength property of the andesite type cut-stones for the future rehabilitation and/or restoration works of the Citadel, when the corresponding tests are performed at site. However, it should not

be forgotten that, these rock formed cut-stones are not homogeneous materials. There may be some discontinuities due to the rock formation, and some defects throughout the surfaces because of external, weathering (abrasive) effects. Therefore, it should be noted that the estimated uniaxial compressive strength values by using the empirical formulas, all found out and given above, yield approximate results so they can differ a little from the exact strength values, determined at the end of destructive tests performed on core samples.

The binding material in the outer mortar was found to be used relatively in higher amounts than that in the inner mortar. This result is quite logical since the porosity (permeability) and the deleterious effects of weathering was tried to be decreased by using mortars having high amounts of binding materials at the outer part of the walls of the Citadel.

REFERENCES

- Bakırer, Ö. 1987. *Ankara Kalesi Koruma ve Geliştirme Projesi, I. Aşama Çalışmaları*. Ankara: ODTÜ Mimarlık Fakültesi, Restorasyon Ana Bilim Dalı.
- Bakırer, Ö. 2001. *Tarih İçinde Ankara II*. Ankara: ODTÜ Mimarlık Fakültesi.
- Foss, C. 1990. *History and Archaeology of Byzantine Asia Minor*. Hampshire: Variorum.
- Karpuz, C. 1982. *Rock Mechanics Characteristics of Ankara Andesites in relation to Their Degree of Weathering, Ph. D. Thesis*. Ankara: Middle East Technical University.
- Kırca, Ö., Erdem, T.K., Uslu, B., & Bakırer, Ö. 2001. Estimation of the In-Situ Mechanical Properties of the Construction Materials in a Medieval Anatolian Building, Sahip Ata Hanikah in Konya. *2nd International Congress on Studies in Ancient Structures, Proc. Intern. Cong. İstanbul Yıldız Teknik Üniversitesi*, July 9–13 2001. 691–701.
- Sağdıç, O. 1994. *Once Upon A Time Ankara*. Ankara: Santur.
- Sevgen, N. 1959. *Anadolu Kaleleri, Cilt 1*. Ankara: Doğu.
- Şimşek, G., Uslu, G., Bakacak, O., Karakul, Ö., & Akar, T. *Unpublished study in the Department of Restoration in Middle East Technical University, Turkey*.

A material that has witnessed the past in Anatolia: adobe

Tülay Çobancaoğlu & Uğur Tuztaşı

The Faculty of Architecture, Mimar Sinan Fine Arts University, Istanbul, Turkey

ABSTRACT: The traditional use of adobe in Turkey and especially Central Anatolia is known to have originated from the primary ages of settled civilization period. The building techniques that were used in Central Anatolia in BC 5000s and that can be seen in the examples that have survived today resemble one another. We can tell that this is an indication that the architecture defined as vernacular is not pure. The forms have affected each other and similar techniques have been used. Within the scope of this statement, vernacular examples of houses made of “adobe” that we have defined as a material that has witnessed the past in Anatolia have been examined and application methods that differ from region to region and their differences have been explained.

1 INTRODUCTION

Since the primary ages of settled civilization, the first building material that human being has produced and given shape has been adobe. The adobe becomes a brick after having been put into a stove. This property has given human beings the facility of an economical building material that is as hard as a stone and can be found anywhere. In every region where wood and stone are hard to obtain, the main building material of the house has been adobe and brick.

It is mentioned in the sources that the building material of rural houses located in the temperate zone of the world has been adobe and the most important historical data of building tradition based on adobe and brick has been produced in Mesopotamia, Iran and Central Asia (Kuban, 1990).

2 THE HISTORY OF ADOBE

It is observed in our country that the unrevealed parts of traditional houses during the digs in Anatolia have spread out a period of approximately ten thousand years. These have put forward the whole stages of development in the house concept and related building techniques that human beings have passed through. Natural materials have been used together since the earliest period that the archeological remains were found in. It is written in the documents that in the settlement area that was revealed within a digging area of nearly 8000 m² in Cayonu, a simple cottage built by twigs in a circular plan was changed into a building of rectangular plan with adobe brick walls standing above

a stone foundation, a flat roof, a door and a window (Ozdogan, 1996).

By depending on another example, we can also tell that there have been buildings made of adobe without a foundation or with a stone foundation or based on a stone wall in this settlement area of Anatolia during Trojan I period (Nauman, 1991). Although there are many stone walls found in Anatolia, a small number of solid adobe walls have been protected or seen.

In the applications of adobe in Anatolia, the adobe has been prepared within the site where enough amount of silt and water could be obtained. If the silt has been taken from the neighbourhood of the settlement area, the undesired mixture of broken pieces of cups, ashes and garbage, rubble usually comes out. Straw, animal food cut into small pieces, reed, sand and small pebbles have been added to silt on purpose, in order to loosen the mass of the brick and to provide a mechanical connection between the materials. It can be said that parts of plants have often been added into the adobe mortar in Anatolia. It is certified in the documents within sources that thousands of years ago this process was no different from the application today (Nauman, 1991) (Figures 1–2).

3 THE DESCRIPTION OF ADOBE

The mastery in adobe that was the traditional building material in Old Anatolia and Mesopotamia and has continued to be used for thousands of years requires a peculiar experience in the aspect of “building technique”. The selection of soil that shall be used in adobe production is important. According to the experienced

adobe craftsmen, the soil to be used should be taken from the surface of a field where an alluvial layer has been formed. This material should be cleaned out from other materials by filtration. The subsidiary element and binding material of loam is straw. The straw that shall be added to loam in a specific quantity is cut into very tiny pieces. The loam mixed with straw is left to rest for a long time and fermented. Then the loam is crushed by foot until it reaches its maturity. In the second phase, the loam is poured into wooden moulds of definite dimensions. This is called the cutting process of the adobe. Then it is left to dry and harden under the sun. The dried ones are stowed to be used later according to the rules (Tarhan, 1975).

The properties of adobe material can show some differences due to the type of the soil used, quantity of water, the methods and intervals of moulding and drying. The chemical composition of clayey adobe soil is an aluminium silicate. It is observed that soil with plant-based and organic materials have not been used in adobe production. Clay that has schist and

tiny pieces of sand shows a high plastic quality when kneaded by water. Pieces of stone bigger than 3 cm should not exist in adobe soil. The dimension of adobe and the preparation of the mortar used as the binding material differ according to the region where it is used (Eric, 1980).

4 THE APPLICATION OF ADOBE

The main building materials of traditional architecture in Turkey have been wood, stone and adobe. These materials have been used in the building systems according to the type that can easily be obtained within the district. Turkey can geographically be divided into seven regions: 1. Northern Anatolia, 2. Marmara Region and İstanbul, 3. Western Anatolia, 4. Southern Anatolia, 5. Central Anatolia, 6. Eastern Anatolia, 7. South-eastern Anatolia (Figure 3). Although there are not definite borders between the regions in the aspect of house building techniques, architectural building techniques are formed by vernacular effects. The adobe is mostly seen as the main building material of Central Anatolia Region and also can be observed in other regions in different techniques by the use of adobe with stone and wood. Within the scope of this statement, we are classifying the application of adobe by examining traditional adobe houses of nearly 150 years in three groups such as massive system, adobe filling between wooden skeleton system and the mixed system, and introducing these groups by original examples.

4.1 *Adobe houses in massive construction system*

The buildings that do not have load-bearing wooden elements between adobe materials and have walls made of adobe blocks are called massive adobe buildings. Massive adobe houses are usually common in the rurals of Anatolia. The most significant properties are a flat roof, one or two floors and a prismatic appearance (Figures 4–7). These houses are reinforced with 1–3 rows of horizontal peripheral ties due to the



Figure 1. Asikli Hoyuk settlement.



Figure 2. Asikli Hoyuk settlement.



Figure 3. The map of Turkey.

easiness of finding wood. Peripheral ties that have a circular section of 6–10 cm diameter and are placed in both sides of the wall are made of poplar or willow trees. These are placed inside the wall in every 1.50 or 2.00 meters and can be connected to each other at the corners. Lintels are pieces of wood of smaller sections. In some examples, vertical posts apart from the wall system have been used to support the span between massive walls (Kafescioglu, 1949).

The use of wooden peripheral ties causes a reduction in the dimension of the adobe. The dimensions of the adobe used in Asvan of the Keban district

where wood is used in the adobe walls ($30 \times 30 \times 10$), ($30 \times 15 \times 10$) are smaller than the adobe used in the district of Adiyaman and Urfa where wooden peripheral ties are not used (Erdim, 1979). Similarly, the adobe in Callı Village of Sivas ($32 \times 30 \times 10$), ($32 \times 15 \times 10$) is smaller than the adobe in Adiyaman and Urfa.

Massive adobe walls are classified into three groups according to the differences in the building technique of the wall: Building the wall with adobe blocks of same dimensions; using two kinds of adobe blocks – the big one, the dimensions of which are twice the other is called “mother”, the small one is called “lamb”; thick walls built with adobe on two sides and a filling material between them.

The most common technique is building up a wall with mother and lamb adobe blocks. The mother adobe block usually has a length of 40–30 cm, a width of 40–20 cm and a height of 15–8 cm. For example, ($30 \times 30 \times 10$), ($30 \times 15 \times 10$) etc. are used in the lower district of Ulupınar in Malatya and Balaban (Basakman, 1991). The thickness of the wall depends on the dimensions of the adobe. It can reach 70–80 or 50–60 cm. when muddy mortar mixed with straw is applied on both sides of the wall. In these houses the thickness of external walls is one and a half, and internal walls is one block of adobe. The use of adobe with larger dimensions makes the wall more durable.

If we make a brief explanation about the other horizontal building elements such as the roof covering, ceiling and floor covering; the flat roof made of soil that is an important characteristic of vernacular adobe architecture is composed of three layers: load-bearing beams, a floor made of reed and twigs supporting the soil and a layer of compact soil laying upon them (Kafescioglu, 1949).

First of all, wooden beams that are made of trees such as juniper, poplar, willow and are circular and decorticated, are arranged in parallel rows in definite intervals above the load-bearing walls of the building and make up the roof skeleton system (Barusta, 1990).



Figure 4. Kozluca village of Malatya.



Figure 5. Callı village of Sivas.

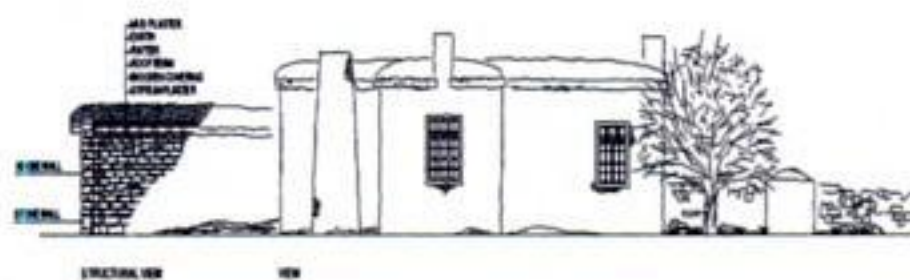


Figure 6. Callı village of Sivas.



Figure 7. Example for Hacibektas-Nevsehir.

The internal surface can either be covered with an ornamented ceiling covering or left bare with no paint or be painted. There are also independent posts used for taking away the load of roof skeleton from the walls. These posts are settled on a stone above the floor. Timber of smaller diameters or decorticated twigs of small dimensions (Ankara, Sivas, Mus, Van, etc.) are used to cover the wooden beams. So the wooden roof skeleton defined above is covered by a kind of fence consisting of reed or twigs. A mortar of soil and straw is applied on this fence and clayey soil is put on the muddy mortar. The soil of muddy mortar is sand with clay. This mortar is mixed better than adobe and wall mortar and left to dry. When it cannot be found, a soil that has absorbed water with saturated salt is used instead. This kind of roof or covering system is compressed by driving a cylinder made of stone and called as “stone roller” (Alioglu, 1991) on the soil layer. The material used in building the roof differ from one region to another. For example, reed has been used instead of twigs (Adiyaman, Konya, Isparta, Burdur, etc.) and small pieces of stone have been used instead of reed or twigs where stones with a large surface are common (Kayseri, Agirnas District). If the building consists of two floors, the end points of the twigs are not inserted into the walls. The barren flat roof has a low inclination within its borders and water is given out through waterspouts in definite points.

The flat-roof-houses located in the city centres of Anatolia were replaced by inclined roofs covered with tiles beginning from the XVIIIth century. Ridge roof with triangle pediment or hipped roof that were seen as a decorative element in the facade of privileged houses at first, have taken the place of flat roofs in time. The effects of this application were later seen in the countryside. The floor coverings of massive adobe houses are made of soil or stone due to the functions of the space.

4.2 Adobe houses with adobe filling material between wooden skeleton system

In the settlement areas of Anatolia where it is easy to find wood (for example, the inner districts of Northern Anatolia, Amasya (Figure 8), Safranbolu (Figure 9), Samsun-Havza (Figures 10–11), Kutahya in Central Anatolia (Figures 12–13), Sivas-Divrigi (Figures 14–15), we come across houses with adobe filling material between wooden skeleton system. In these houses, wooden skeleton is settled upon massive stone or adobe construction. The trees that make up the wooden skeleton are used as main and subsidiary vertical posts and horizontal beams and they are fitted together at some intervals. The main load-bearing material of this system is wood, and adobe is used as the filling material. The span between the wooden skeleton system is modified according to the dimensions of the

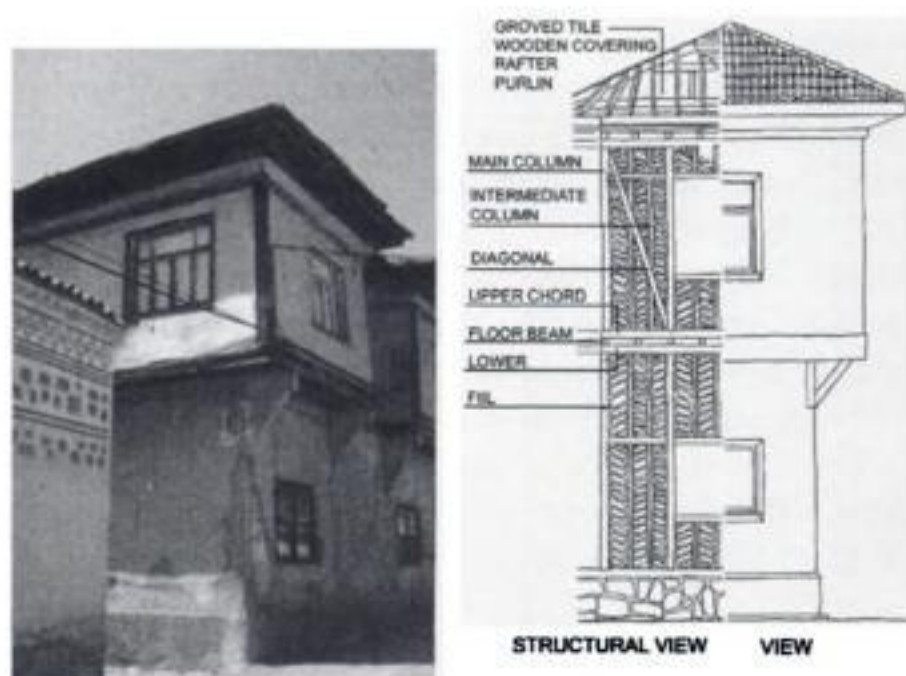


Figure 8. Example for Amasya.

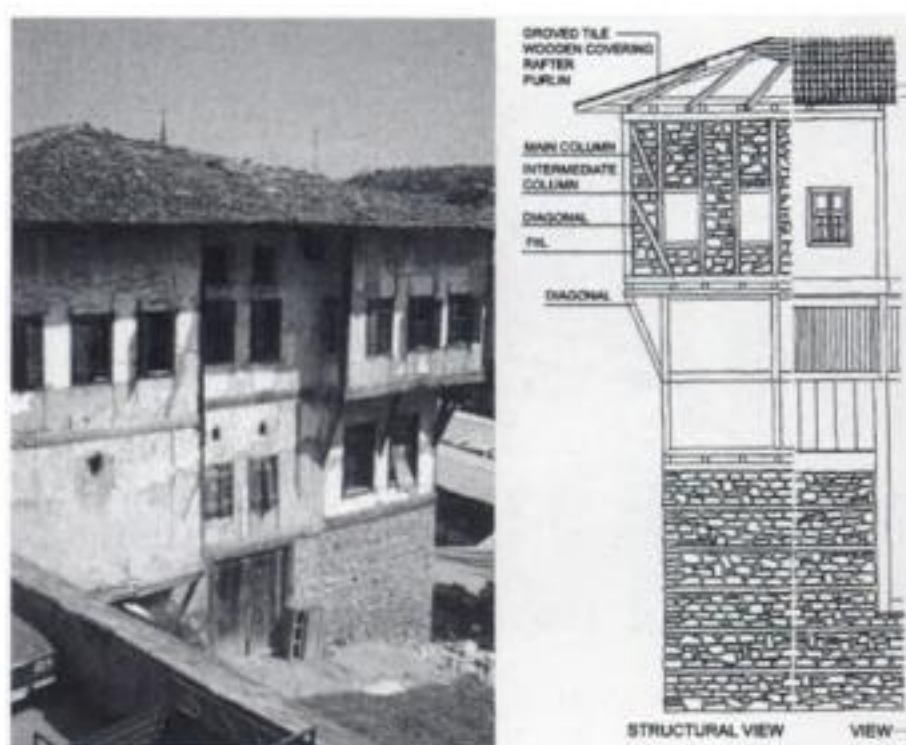


Figure 9. Example for Safranbolu.



Figure 10. Example for Havza.

adobe. In this building system that is generally called “HIMIS – post and pane”, the distance between vertical posts have become wider, for example 80 cm, by the advantages that adobe provide (Çobancaoğlu, 1998).

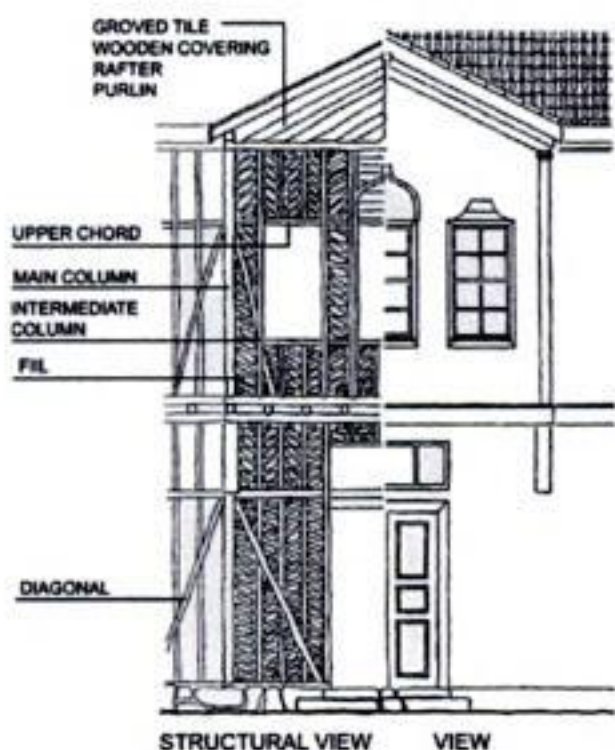


Figure 11. Example for Havza (Structural view).



Figure 12. Example for Kutahya.



Figure 13. Example for Kutahya (Structural view).



Figure 14. Example for Sivas – Divrigi.

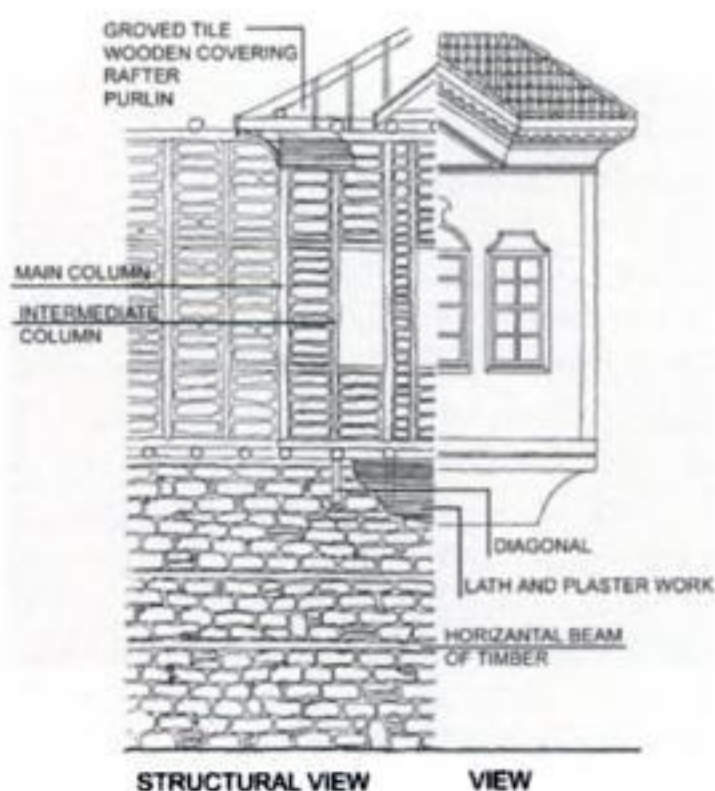


Figure 15. Example for Sivas – Divrigi (Structural view).

In most of the centres where wooden houses are located, walls are made of wooden skeleton and filled with adobe. Although the dimensions of adobe are similar, they show some vernacular differences. For example, $9 \times 12 \times 30 - 15 \times 30 \times 60$ in Kutahya (Eser, 1955), $15 \times 25 \times 30$, $15 \times 50 \times 50$ in Sivas–Divrigi (Sakaoglu, 1978), $27 \times 27 \times 10$, $27 \times 22 \times 10$, $27 \times 13 \times 10$ cm in Safranbolu (Ozeke, 2001). The most common dimensions are mother adobe of $40 \times 40 \times 12$ and lamb adobe of $40 \times 20 \times 12$ and $20 \times 10 \times 5$ cm. With the adobe blocks that are used as the filling material of this system, walls are built by using horizontal, diagonal or both bond techniques (Figures 16–17).

In some districts of Anatolia, the climate and the direction of the building has become an important factor; so adobe has been used as a material preferred for its heat insulation. In this skeleton system, plaster has been applied to the internal and external surfaces of the walls. The plaster can be applied on either adobe or little wooden lath that is called lath-and-plaster system.

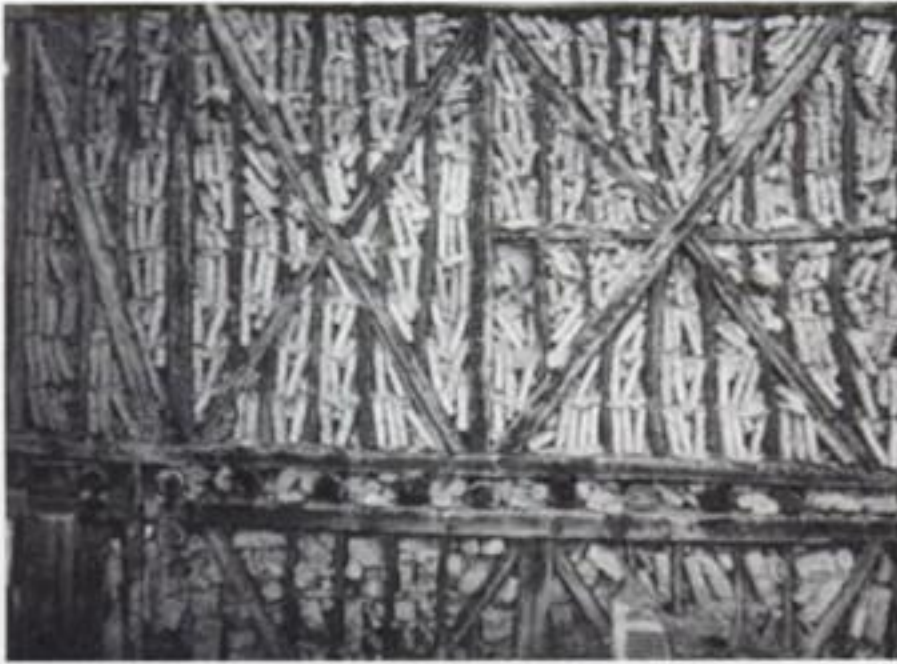


Figure 16. Example for Sivas.

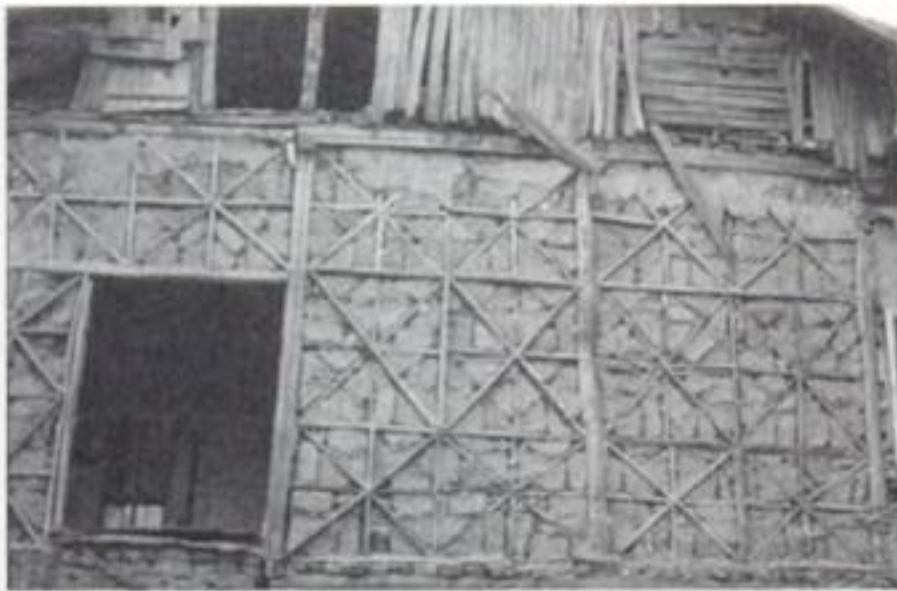


Figure 17. Example for Malatya.

The internal partitions of houses are different from each other due to the material used. Adobe and pieces of stone are used to fill between the wooden posts and then the wall is covered with plaster or the adobe blocks have been used in massive system, especially in the walls where the stove is located.

Wood has been used in the other elements of this building system, such as roof covering, beams supporting the roof and the floor, and also ceiling and floor coverings. In the courtyard or some service spaces, stone or compact soil has been used for floor covering. The roof is hipped and covered with mission tiles.

4.3 Mixed system adobe houses

The building system that we call the mixed system has generally been applied in the rurals of Anatolia and is an application where massive system and the filling between the wooden skeleton system can be seen together. In the external massive walls of these houses that are generally located in the city centres, vertical posts have sometimes been used due to the easiness of finding wood. And in some examples, the upper floor walls overlooking the landscape or the walls of the



Figure 18. Example for Van.



Figure 19. Example for Van (Structural view).



Figure 20. Example for Konya.

oriel have been built with adobe filling between the wooden skeleton; and the other external walls have been built in massive system. Internal walls have usually been built with adobe filling between the wooden skeleton. (For example Van (Figures 18–19), Konya (Figure 20), Mus, Malatya – Yediozonu (Figure 21), Malatya – Yesilyurt (Figure 22), etc.) The thickness of the external walls is one-and-a half or two blocks and internal walls are one or a half block with wooden skeleton inside. In two-storey houses, external walls on



Figure 21. Example for Malatya – Yediozonu.



Figure 22. Example for Malatya – Yesilyurt.



Figure 23. Example for SanlıUrfa – Suruc.

the ground floor are made of two, the external walls on the first floor are made of one and a half row of blocks. The internal walls on the ground floor are made of one and a half, and internal walls on the first floor are made of one row of blocks.

Adobe houses in mixed system are similar to the adobe houses in massive system in some aspects such as the massive wall system settled upon a stone foundation that is usually below the floor level and composed of round stones, adobe dimensions, covering the walls

with mud, building a flat roof (for example; Van, Adiyaman, Mus, etc.). They also have some similarities with the adobe filling between wooden skeleton system, such as walls made of adobe filling between skeleton and hipped roof application that has sometimes been used (Konya, Malatya, etc.). The similarity to both systems has made this system a mixed type.

The examples of one-storey mixed system adobe houses in rurals are bee-hive (stone, brick and adobe) houses of the Harran Plain and domed houses with curvilinear surface in the Suruc Plain (Figure 23). In the other districts of Anatolia where soil is used, these building forms have not been used.

5 CONCLUSION AND REVIEW

As a result, the adobe material has been a traditional building element that has always been chosen and preferred (because of the easiness of its production).

As a result, the adobe material that has sometimes served as the plaster on a block or as an adobe block with stone, and has always been chosen and preferred in massive construction system due to the easiness of its production, has been a traditional building element in the formation of our vernacular architecture since the primary ages of settlement in Anatolia. In this study, a structural classification has been made by searching the place of adobe architecture in Turkey and examining original examples. The structural differences caused by vernacular factors between the traditional adobe houses that are grouped as (1) In massive construction system, (2) In adobe filling between wooden skeleton system, (3) In mixed system, have been put forward.

Adobe buildings were accepted as cultural heritage with a judgement of ICOMOS after the 3rd International Adobe Conservation Symposium that took place in Turkey in 1980. As a result of migration from rurals to city centres, most of the unique adobe houses are not being lived in today or are facing many physical and structural problems by going through destruction as a result of losing their originality. The factors that cause the destruction of this system that requires maintenance at routine intervals can generally be classified in three groups, as heat, water and a variety of biological reasons. The most important defect of adobe is that it is not resistant to heat and humidity; so the structural problems depend on the relation between water and clay. The massive adobe buildings built in rurals are more influenced by water and humidity than the buildings in adobe filling between wooden skeleton system located in city centres as a result of their structural properties. Another important problem for adobe buildings is the earthquake. More than the half of the damage caused by earthquakes throughout world is linked to adobe buildings and there has not been



Figure 24. Example for Sivas.



Figure 25. Example for Sivas.



Figure 26. Callı village of Sivas.

any improvement in the structural systems of adobe buildings. This is another dimension of the structural problems of this system. For the renovation of the soil roofs in the flat-roof houses in Anatolia, a new layer of soil is added in place of the soil lost every year. The new soil layer causes the roof to become heavier and the static balance of the physically worn-out walls in wooden construction system to be lost.

This causes a negative influence against earthquake in the buildings. The culture of vernacular adobe buildings, the formation of which is the result of a long-lasting tradition especially in Anatolia, is beginning to get lost because of many factors (Figures 24–26). Furthermore, the differences between the systems of adobe building culture and wood and stone have not been fully examined during the research of vernacular architecture. For the adaptation of the adobe houses that have an important place in Turkey to contemporary conditions; they should be consolidated in the aspect of material and structural system and also be remodified according to the vernacular conditions of the district they are located in. The continuity of the adobe that has witnessed the past in Anatolia shall have been provided when these conditions have been fulfilled.

REFERENCES

- Barista, H. Orcun, (1991), *Duz Damli Konya Evlerinde Gorulen Kup Bacalar*, Turk Halk Mimarisi Sempozyumu Bildirileri, Konya, Turkiye, p. 35–45
- Basakman, M., (1991), *Asagi Ulupinar- Yukari Ulupinar, Balaban Yerlesmeleri Calismasi, Arastirma Projesi*, Firat Universitesi, Funah No: 33
- Çobancaoğlu, T., (1998), *Turkiye de Ahsap Evin Bolgelere Gore Incelemesi*, Basilmamis Doktora Tezi, MSU Fen Bilimleri Enstitusu, İstanbul
- Erdim, M. Murat, (1979), *Adiyaman 'dan Bir Kerpice Ev* ODTU Mimarlik Dergisi, Cilt 5, sayi 1, Ankara, Turkiye
- Eric, Murat, (1980), *Kerpice Eski Eserlerin Onarimi ve Korunmasinda Bir Arastirma*, Ucuncu Uluslararası Kerpice Koruma Sempozyumu, Ankara, ICOMOS-ICOM, p. 79–84
- Eser, L., (1955), *Kutahya Evleri*, İTÜ Mimarlik Fakultesi, İstanbul, p. 68
- Kafescioglu, R., (1949), *Orta Anadolu da Koy Evlerinin Yapisi*, İTÜ Matbaasi, İstanbul
- Kuban, Dogan, (1990), *Mimarlik Kavramlari*, YEM Yayınevi, İstanbul, p. 36–37
- Kuban, Dogan, (1996), *Ev Uzerine Felsefe Kirintilari*, HABITAT II, İstanbul, p. 4
- Naumann, R., (1991), *Eski Anadolu Uygarligi*, p. 47
- Ozdogan, Mehmet, (1996), *Kulubeden Konuta: Mimarlikta İlkler*, HABITAT II, İstanbul, p. 24
- Ozeke, A., (2001), *Safranbolu da Yorgun Ahsap Kulturu*, Anadolu nun Ahsap Evleri, T.C. Kultur Bakanligi Ozel Dizi, p. 62
- Sakaoglu, N., (1978), *Divrigi de Ev Mimarisi*, Kultur Bakanligi yayinlari, İstanbul, p. 23
- Tarhan, M.T., (1975), *Urartu Merkezlerinde Meydana Cikarilan Kerpice Mimarinin Korunmasi ve Onarimi Hakkinda Oneriler*, MTRE Bulteni, İstanbul, p. 46

FIGURE REFERENCES

- Figures 1–2; Acar, E., (1996), *Anadolu da Tarih Oncesi Caglardan Tunc Cagi Sonuna Kadar Konut ve Yerlesme*, Habitat II, İstanbul, p. 386 (Figures 1–2)
- Figure 4; Aran, K., (2000), *Barinaktan Ote Anadolu Kir Yapilari*, Tepe Grubu, Ankara, p. 88
- Figures 5, 16–17, 21–22, 24–26; Tuztasi, U., 2003
- Figure 7; Çobancaoğlu, T., 2003
- Figures 8–15, Çobancaoğlu, T., (1998), *Turkiye de Ahsap Evin Bolgelere Gore Incelemesi*, Basilmamis Doktora Tezi, MSU Fen Bilimleri Enstitusu, İstanbul
- Figures 18–19; Uysal, B. & Ozturk, S., (1997), *Tarihi Van Evlerinin Gunumuzdeki İzleri*, Mimarlik dekorasyon dergisi, sayi: 62, İstanbul, p. 54
- Figure 20; Karpuz, H., (2001), *Erzurum Konya Evlerinde Ahsap Malzeme Kullanimi*, Ahsap Kulturu Anadolu nun Ahsap Evleri, T.C. Kultur Bakanligi Ozel Dizi, p. 125
- Figure 23; Akin, G., Akin, N., Eres, Z., Ivedi, B., (2002), *Birecik- Suruc (SanliUrfa), Kirsal Mimarlik Envanteri Calismasi Raporu*, TUBA-TUKSEK, Turkiye Kultur Envanteri Pilot Bolge Calismalari, Ankara, Turkiye, p. 53

Investigation of the degradation of sandstones in Sydney's heritage buildings

K.H. Friolo, A.S. Ray, B.H. Stuart & P.S. Thomas
University of Technology, Sydney, New South Wales, Australia

ABSTRACT: Sydney, with many of its heritage buildings and monuments constructed as a result of the first European settlement in the 1800s, is a city built on a large block of sandstone. Although many of these buildings are still strong and sound, signs of deterioration have become evident in recent years. In order to prevent these precious buildings from further degradation, the weathering mechanisms of the stones must be thoroughly understood before suitable protection measures can be implemented. In this study, four techniques have been selected to detect chemical and physical differences between weathered and unweathered sandstones – Solid State Nuclear Magnetic Resonance (NMR) Spectroscopy, Thermogravimetric analysis (TGA), Differential Scanning Calorimetry (DSC) and X-ray Photoelectron Spectroscopy (XPS).

1 INTRODUCTION

The state of New South Wales has currently a stock of over 600 major stone structures built over the past 200 years and more than 60% of these have national heritage significance. Many of the ornate landmarks of Sydney, Australia's major city, are constructed from a rich golden yellow sandstone commonly known as "yellow block" sandstone. These sandstones generally contain 60–68% sand grains (quartz) and 16–25% cementing clay matrix (Franklin, 2000). It also contains up to 7% of siderite (FeCO_3 – an iron carbonate mineral) and small amounts of iron oxide, silica and gypsum. The newly quarried sandstones are usually grey in colour, but the oxidation of iron bearing minerals gives the stones a soft yellow-brown colour upon exposure to the atmosphere (Ray, 2000). The sand grains (quartz) not only provide the stone its hardness, durability and resistance to mechanical abrasion, but also produce the occasional sparkling character of the stone. Since quartz is a highly stable mineral, the investigation of the degradation process is largely focused on the weathering of the cementing material, clay, which is predominantly kaolinite. (Friolo et al., 2003).

The use of Sydney's sandstone in buildings reached its peak in the late 19th Century. One of Sydney's significant landmarks is the St. Mary's Cathedral built in the mid-1800s (Fig. 1). This magnificent Gothic style cathedral was constructed using entirely Pyrmont yellow block sandstones from different parts of the Darling Island quarry (Stuart, 1993).



Figure 1. Sydney's St. Mary's Cathedral.

St. Mary's Cathedral is located in Sydney's busy city centre. Apart from the high concentrations of pollutants produced from motor cars and nearby industries, the combination of various harmful elements

due to Sydney's climate and geographical location also accelerates the degradation process of sandstones in the area. These include long period of hot and dry weather, high UV radiation and frequent human contact from tourism. In addition, Sydney is also surrounded by coastal sea, regular sea spray introduce large amount of sea salt into the naturally porous sandstones. The rapid evaporation of water from the stones in hot and dry climate results in the recrystallisation of salts in the sandstone pores. This can have detrimental effects on the structure and integrity of the sandstones, as micro-cracks can form particularly at the boundaries between sand grains and their cementing materials.

Sydney's heritage buildings, like the St. Mary's Cathedral, not only display their architectural significance, but also represent their rich historical and cultural values. In recent years, rapid deteriorations of these buildings have been detected. An inter-disciplinary team of experts including scientists, architects, stone masons and engineers are working together to maintain these historic buildings.

The causes and deterioration mechanisms of Sydney's sandstone are not fully understood. The main aim of this investigation is to first determine the degradation processes of yellow block sandstones in Sydney's heritage buildings. Once these mechanisms are established, proper prevention measures, such as suitable stone consolidants, can be developed to slow down, or inhibit the degradation of these precious buildings.

In this investigation, solid state NMR was used to determine the porosity changes of sandstones upon weathering. TG, DSC and XPS were also employed to detect chemical changes in the sandstones.

2 MATERIALS AND METHODS

2.1 Sample preparation

This study deals with the investigation of extensively degraded sandstone blocks from the St. Mary's Cathedral. These samples were provided by the Gosford Quarries after being removed from higher of the cathedral. These sandstones were originally quarried at the Pymont area in Sydney, and are also known as Pymont sandstones. The weathered sandstones are generally still sound with the exception of the weathered surface (~1 cm). In this study, weathered surfaces were separated from the original stones and several sample treatments were carried out as follow:

1. Both weathered and unweathered sandstone samples were crushed separately and an ultrasonic probe was used to break the clay component from the sand grains. Fine clay particles were then obtained by using the gravity settling method (Carroll, 1970).

2. In order to observe the low concentration structural iron, $\text{Na}_2\text{S}_2\text{O}_4$ and NaHCO_3 were used to remove non-structural iron from a set of clay sub-samples to avoid interferences (Mehra et al., 1960).
3. Thin plates of weathered and unweathered sandstones were cut into pre-determined size ($5 \times 8 \times 13 \text{ mm}^3$). These sandstones plates were then saturated in water at room temperature overnight before NMR analysis.

2.2 Solid state (proton relaxation) NMR

A Resonance – Maran Ultra R1 (Version 2.1.4203) NMR spectrometer with a magnetic field strength of 0.046 Tesla was used to investigate the pore size distribution within the sandstone samples. The NMR spectra were obtained using the Resonance WinDXP software. It is based on the theory where the pore sizes are directly proportional to the NMR spin-spin relaxation time (T_2) of protons in water molecules in the pores (Dodge et al., 1995). Once these protons are NMR irradiated, the magnetization is transferred to the pore wall and the protons in water molecules relax back to a lower energy level (McCutcheon et al., 2002). Assuming all pores are spherical in shape, the relaxation time (T_2) for smaller pores will be shorter than that of the larger pores as shorter time is required for protons in smaller pores to transfer their energy to the pore walls. In this investigation, both weathered and unweathered sandstone plates were immersed in water overnight to ensure complete saturation before NMR analysis.

2.3 Thermogravimetric analysis (TGA) and differential scanning calorimetry (DSC)

A Setaram Setsys 16/18 TG-DSC 15 Thermal Gravimetric Analysis instrument was used for the thermal analysis of the clay samples. A Balzers Thermo Star 300 mass spectrometer with capillary interface was used together with a Chaneltron electron multiplier detector. Approximately 10–12 mg of unweathered and weathered clay samples were analysed from room temperature up to 1200°C at a heating rate of 1°C/minute.

2.4 X-ray photoelectron spectroscopy (XPS)

A Vacuum Generators XPS system with Al $K\alpha$ X-ray source was used to produce the XPS spectra of weathered and unweathered clay samples. The clay powder was secured onto the sample holder by double-sided tape (Nissen et al., 2001). The low-resolution scans were collected at 50 eV energy with step size of 1 eV every 0.5 seconds, and the high-resolution scans were collected at 50 eV energy with step size of 1 eV every 6 seconds.

3 RESULTS

3.1 Solid state (proton relaxation) NMR

The NMR spectra indicate that there are three populations of pores, small, medium and large pore sizes, in both the weathered and unweathered sandstone samples (Fig. 2). A significant increase in small pores and a moderate increase in large pores have been observed upon weathering. However, a moderate decrease in the medium pore population was also observed in the weathered sandstone samples.

3.2 Thermogravimetric analysis (TGA) and differential scanning calorimetry (DSC)

Figures 3a & 3b are curves of unweathered and weathered clay samples from the DSC and TGA analyses. These traces are of similar patterns to that of the Kaolin clay, where the typical three regions, dehydration, dehydroxylation and the formation of thermal product, are shown. The slight weight loss at $\sim 100^\circ\text{C}$ of the unweathered clay sample indicates the dehydration of the kaolin clay (K), where adsorbed water was lost. At 580°C , a typical peak denotes the dehydroxylation of kaolin clay was detected (Carroll, 1970). However, an addition peak at $\sim 680^\circ\text{C}$ was detected, which also arise from the dehydroxylation of a kaolin clay. At $\sim 1000^\circ\text{C}$, the formation of a thermal degradation product, mullite, was detected. The weathered clay sample showed relatively similar DSC patterns as the unweathered sample. However, a doublet was observed between $190\text{--}300^\circ\text{C}$ suggests the presence of iron compounds such as iron oxyhydroxide, $\text{FeO}(\text{OH})_x$, in the samples. In addition, it appears that the relative intensities of the peaks at 580°C and 1000°C in the weathered samples have decreased while that of the peak at 680°C has increased upon weathering.

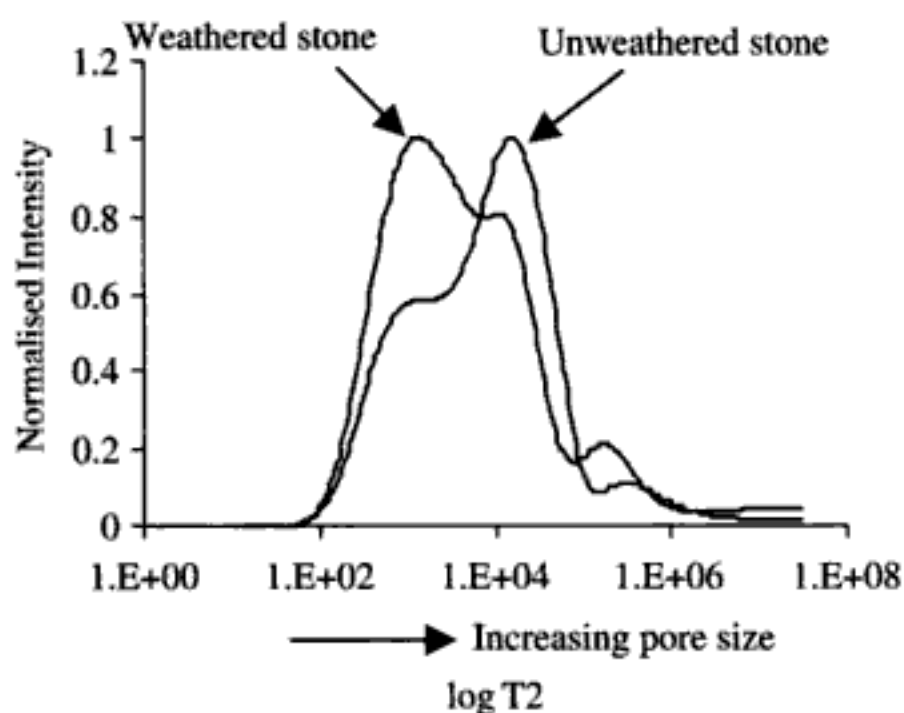


Figure 2. NMR spectra of weathered and unweathered sandstones from St. Mary's Cathedral.

3.3 X-ray photoelectron spectroscopy (XPS)

The low-resolution XPS scans show the presence of oxygen, aluminium, silicon and carbon in both weathered and unweathered clay samples (Fig. 4). In addition, small amount of iron was also detected in

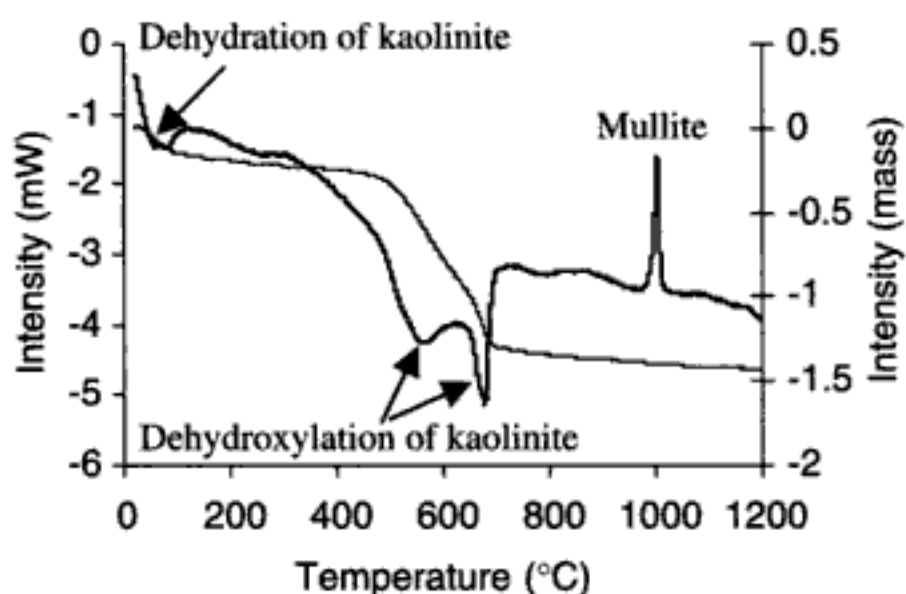


Figure 3a. DSC and TGA curves of unweathered clay sample.

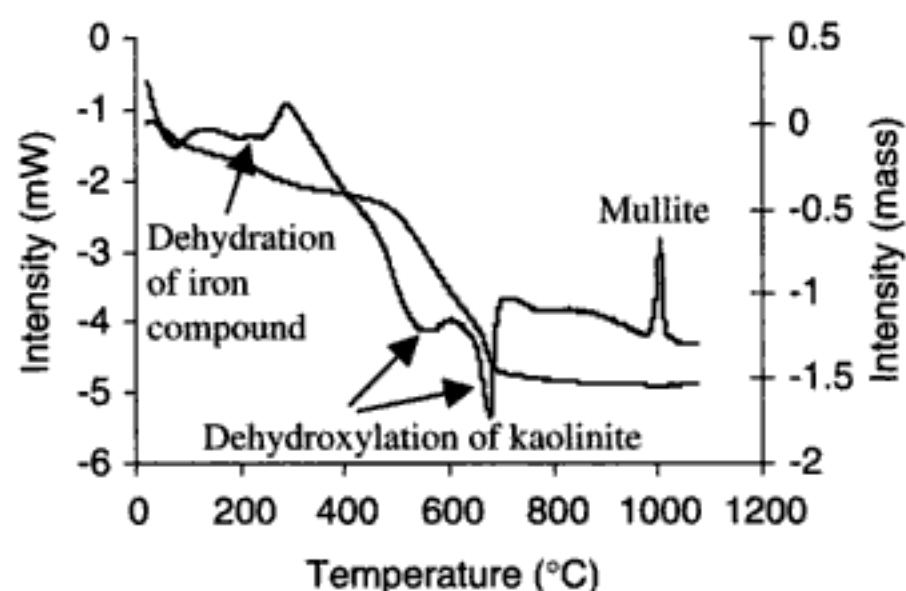


Figure 3b. DSC and TGA curves of weathered clay sample.

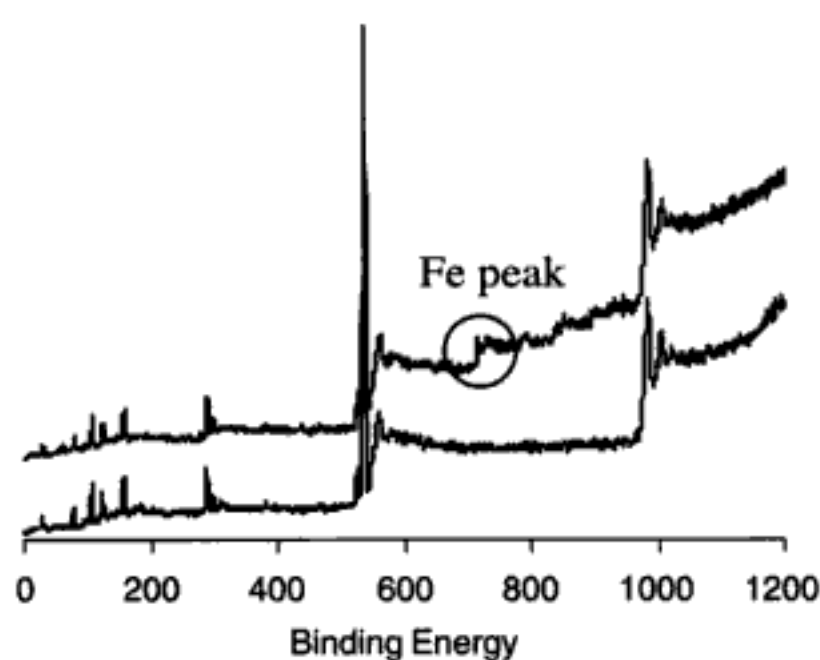


Figure 4. Low-resolution XPS spectra of weathered and unweathered clay samples.

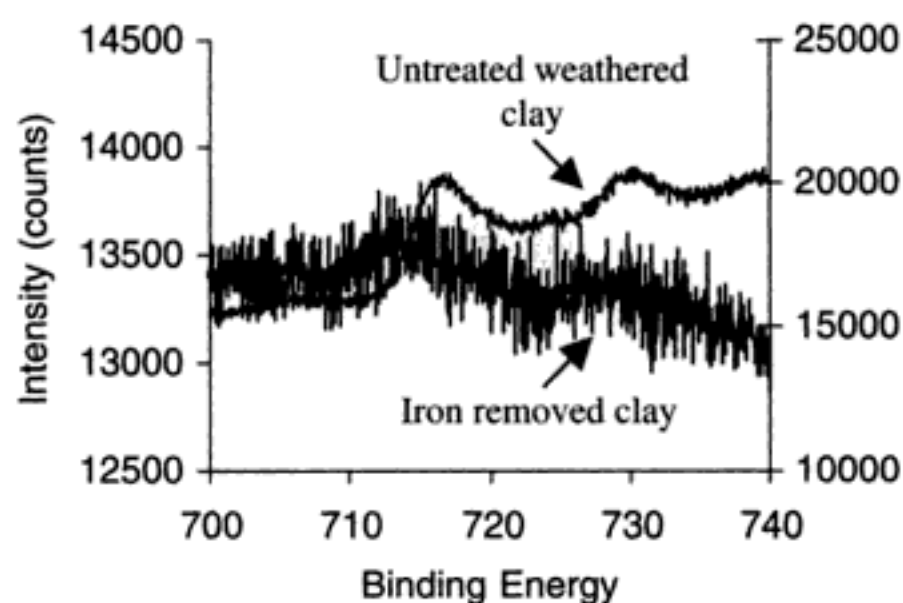


Figure 5. High-resolution XPS spectra of weathered clay samples before and after iron removal.

the weathered clay samples. Further investigation of the iron peaks from weathered clay sample after non-structural iron removal using high-resolution XPS was performed.

The high-resolution XPS spectrum of the weathered clay sample showed typical patterns of iron bonds in its two spin-orbits (Fig. 5). The clay samples were then treated by an iron removal process using $\text{Na}_2\text{S}_2\text{O}_4$ and NaHCO_3 (Mehra et al., 1960). The treated clay samples were analysed by high-resolution XPS under the same conditions. Although the spectrum of the treated clay is noisy due to the low iron concentration, it still illustrates the presence of iron in the clay samples (Fig. 5).

4 DISCUSSION

The results from the NMR analysis indicate a significant change in pore size distribution in the weathered sandstone samples. The increased intensities in both large and small pore sizes and the decreased intensity of the medium pore size compared to the unweathered samples suggest a major structural change within the sandstone upon weathering. The increase in large pore population may result from the disintegration of the cementing clay in the sandstone. For example, the break down of the clay structure and the collapse of the inner-boundaries between smaller pores upon weathering can result in the formation of larger voids and cavities in the remaining cementing medium. In addition, the destruction of the cementing clay also causes the dislodgement of sand grains due to the lack of binding medium. This can also lead to the formation of larger voids in the stone. On the other hand, small mineral particles or degradation products may redistribute into larger pores to produce greater number of smaller pores in weathered sandstones. The decrease in medium pore population may result from their breakdown to form larger pores.

The DSC and TGA patterns of both weathered and unweathered clay samples suggest that the cementing materials in Sydney's yellow block sandstones are largely belong to the Kaolin clay group. However, a significant difference was observed at the dehydroxylation region ($\sim 500\text{--}750^\circ\text{C}$). A typical dehydroxylation peak for kaolinite was detected at 580°C . On the other hand, a second peak at 680°C was also attributed to the dehydroxylation of kaolinite. This was confirmed by using the hot stage XRD technique where XRD patterns were obtained at a range of temperatures ($25\text{--}750^\circ\text{C}$). Both peaks were established to be kaolinite peaks. A plausible explanation is that a thermally more stable clay structure was generated upon weathering and iron has played a significant role by partially replacing Al^{3+} and/or Si^{4+} in the kaolin structure (Friolo et al., 2003). The Fe^{3+} substitution in this second generation clay has somewhat preserved the aluminosilicate structure. However, substitution of any kind into the crystal structure will contribute to the destabilisation of the structure. Upon physical examination of weathered sandstones, although the integrity and hardness of the overall stone are retained, all weathered sections of the stones were found to be relatively brittle and can be crumbled by the application of a small force. The dehydration of iron compounds were also observed in the weathered clay samples, where iron impurities were frequently detected in the weathered sandstones using other techniques. These non-structural irons were originated from the iron rich minerals, such as FeCO_3 and FeSO_4 , in the sandstone. The leaching and oxidation of these iron minerals provide the source of iron needed for Fe^{3+} substitution in the clay structure. In addition, the DSC trace of the weathered clay showed a decrease in intensity of the dehydroxylation peak of kaolinite, but increase in intensity of the dehydroxylation peak of the second generation clay in the cementing materials. A smaller mullite peak at $\sim 1000^\circ\text{C}$ compared to the unweathered clay was also detected. This finding suggests that only the original kaolinite in the cementing clay produces its thermal degradation product of mullite. The Fe^{3+} substituted clay may not generate the same thermal product upon heating.

The XPS results further confirm that iron exists as both structural and non-structural iron in the clay samples. The low resolution XPS indicates the presence of iron compounds in the weathered clay samples. Upon removal of the non-structural irons, further evidence in the high resolution XPS reveals the presence of iron in the aluminosilicate structure. Although iron was not detected in the unweathered clay samples using this method (detection limit: $\sim 6\text{ppm}$), it has been detected in low concentration using Inductively Coupled Plasma – Atomic Emission Spectroscopy (ICP – AES) analysis.

The above mentioned techniques, together with other analytical techniques used in the characterisation of sandstones in Sydney indicate the importance of prevention measures. The degradation process starts from the moment the sandstone is quarried. As the analytical results indicate, the kaolinic cementing clay is susceptible to Fe^{3+} substitution of Al^{3+} in its structure. Once this substitution occurs, the crystal structure of the cementing clay starts to destabilise until the point, where it cannot maintain its structure. As a result, the collapse of the clay structure leads to the loss of binding materials with a consequent change in porosity of the sandstone. If, at this stage, the sandstone is left untreated, it will be prone to attack by environmental elements, such as pollutants, sea salts, ground water and dirt due to its more porous nature.

The Centenary Stonework Program under the Ministry of the New South Wales Department of Commerce is actively involved in the maintenance of significant public buildings in the state of New South Wales. To date, their approach to preservation of significant sandstone buildings has been varied and radical at times, ranging from the stabilisation of existing structure to replacement of decayed stones. St. Mary's Cathedral, along with the Australian Museum in Sydney, are two examples where some of the extensively decayed yellow block sandstone were replaced in recent years as part of the restoration program. While the findings reported in this paper allow significant insight into the degradation of the kaolinite clay in decayed blocks which were removed and replaced, data from the current research suggest a new, less pragmatic approach may be appropriate in future restorations. For example, it is apparent from the data presented in this paper that a new generation of consolidants with a lower viscosity than a kaolinite clay binder has the potential to preserve partially decayed yellow block sandstones.

The newly developed consolidants must retain similar characteristics as the original binding materials in the sandstones. However, future research will also focus on other properties, such as desirable depth of penetration into the stone, permeability to moisture and UV and temperature stabilities. Research is currently underway in our laboratory to develop consolidants, which are based on different type of binders. Naturally occurring clay treated with polymeric materials in order to modify the clay layers in a way so that stronger bonding between layers can be achieved. The results of this investigation will be reported in future publications.

5 CONCLUSION

The study of weathered and unweathered sandstones using various analytical techniques ensures thorough

understanding of the degradation process of these dimension stones. In this investigation, the solid state (proton relaxation) NMR analysis indicated significant changes in porosity of sandstones upon weathering. These observations may be attributed to the leaching of minerals and the degradation of the cementing clay structure within the sandstones. Thermogravimetric analysis suggested the presence of iron compounds in the weathered sandstone samples. This may provide the Fe^{3+} to replace the Al^{3+} and/or Si^{4+} in the clay structure to produce a thermally more stable clay structure. Finally, the XPS analysis supports the hypothesis that structural iron is present in the weathered clay samples. Although many aspects of the degradation mechanisms of sandstones still remain unknown, the use of various analytical methods together with improved experimental techniques will ensure an in-depth understanding of these processes, so that suitable consolidants can be developed to prevent further deterioration of these historic buildings.

ACKNOWLEDGEMENT

An Australian Postgraduate Award (APA) to K.H. Friolo to carry out research for her PhD degree is acknowledged. The authors also acknowledge Gosford Quarries (NSW) Pty Ltd for providing yellow block sandstone samples from St. Mary's Cathedral.

REFERENCES

- Carroll D. 1970. *Preparation of Clays for X-Ray Examination – Clay Minerals: A guide to their X-ray identification*, The Geological Society of America, 57–61.
- Franklin B. 2000. Sydney Dimension Stone: the value of petrography in stone selection and assessing durability. Sandstone City, Sydney's Dimension Stone and Other Sandstone Geomaterials. McNally G. H. & Franklin B. J (ed.), *Environmental, Engineering and Hydrogeology Specialist Group (EEHSG)*. Geological Society of Australia.
- Ray H. 2000. The Sydney sandstone industry, past and present – Sandstone City, Sydney's Dimension Stone and Other Sandstone Geomaterials. McNally G. H. and Franklin B. J. (ed.), *Environmental, Engineering and Hydrogeology Specialist Group (EEHSG)*. Geological Society of Australia.
- Dodge W. M., Shafer J. & Angel G. G. 1995. Core and log NMR measurements of an iron-rich, glauconitic sandstone reservoir. *SPWLA 36th Annual Logging Symposium*, 1–6.
- Friolo K. H., Stuart B. & Ray A. 2003. Characterisation of weathering of Sydney sandstones in heritage buildings. *Journal of Cultural Heritage*, 4, 211–220.
- McCutcheon A., Wilson M. A., Hartung-Kagi B. & Ooi K. 2002. Relaxation of Protons in Pores in a Sandstone. *Journal of Physical Chemistry B*, 106, 2928–2932.

- Mehra O. P. & Jackson M. L. 1960. Iron oxide removal from soils and clays by a dithionite citrate system buffered with sodium bicarbonate. *Clays Clay Minerals*, 7, 317–327.
- Nissen K. E., Stevens M. G., Stuart B. H. & Baker A. T. 2001. Characterisation of PET Films Modified by Tetraethylene-pentamine (TTEPA). *Journal of Polymer Science: Part B: Polymer Physics*, 39, 623–633.
- Stuart G. 1993. *Secrets in Stone – Discover the History of Sydney*. Sydney: Brandname Properties.

Durability aspects of masonry stones used in the southern temple wall in Jerusalem

I. Wasserman

National Building Research Institute, Technion, Haifa, Israel

ABSTRACT: A swelling bulge that reached 0.71 m, approximately, has recently appeared in the Southern Wall of the Temple Mount Area in Jerusalem. In October 2002 the swelling rate was about 5 mm per annum. The properties of the masonry materials in the Southern Wall were unknown. Therefore, the current study has been essential and helpful for maintenance and the planned conservation measures of the Southern Wall. The current study established that the works done in the Southern Temple Wall in Jerusalem in the first half of XX century could be referred as *repair and not conservation measures*. Apparently, during their mandate, the British made repairs using inappropriate materials. The discrepancies in material performance between the “original” and “new” masonry seems to have led to the appearance of the bulge in the Southern Temple Wall.

1 INTRODUCTION

The current study was carried out in collaboration with the Israel Antiquities Authority (IAA) and aimed at clarifying the causes of a swelling bulge that has recently appeared in the Southern Wall of the Temple Mount Area in Jerusalem. In October 2002 the maximal bulge monitored by IAA, reached 0.71 m, approximately, whereas the swelling rate was about 5 mm per annum.

Archival documents that were published in 1860's and have been kept in the IAA, have shown an obvious deterioration and splitting of the masonry stones in the Southern Wall at that time (Warren & Conder 1881). Therefore, restoration measures have been implemented since then. However, the available archival documents have not included the detailed conservation plans. Therefore, this writer could not determine where the abovementioned reconstruction was carried out. Moreover, the properties of the stones and mortars in the Southern Wall were unknown. Therefore, the current study of the historic masonry materials has been essential and helpful for maintenance and the planned conservation measures of the Southern Wall.

2 HISTORIC BACKGROUND OF THE TEMPLE MOUNT COMPLEX

The Jewish Temples were particularly described in the Old Testament.

The Temple Mount Complex was destroyed along with the city by the Roman general Titus in A.D. 70.

Since this time Jewish people have not used the Complex as a place of their religious cult.

Since the Mediaeval period the Complex was used by Muslims as a Holy place of Islam. During that period, the level raising and the construction of the Dome of the Rock and the El Aksa Mosque were carried out.

3 ENGINEERING BACKGROUND OF THE TEMPLE MOUNT COMPLEX

Generally, the Southern Wall consists of two parts:

- (a) An internal part built during Herod's period (37–4 B.C.).
- (b) An external masonry part, about 1.2 m wide. This wall was constructed later than Herod's period. However, the exact term of its construction is still unknown.

The samples of historic materials investigated in the current research were bored only from the external masonry part.

According to calculations done in the Technion and the electromagnetic tests, the Southern Wall at its western corner is about 4.5 ± 0.5 m wide (Weisman 1968; Ben-Dov 1985; Mazar 1989; Peretz 1991).

4 OLD MASONRY PRACTICE IN ISRAEL

Since ancient times, a common building practice in Israel was masonry construction with sufficiently hard

and unblemished dimension stones. These dimension stones were set in courses fitted a desired designing height. Usually, a stone course in masonry walls was 0.5 to 1.5 m high (Peretz 1991; Sparai & Sason 2001). There was a common practice in ancient quarries located near Jerusalem, to hew the dimension stones about 35 to 55 cm long. The height and the width of such stones was about 20 to 30 cm (Sparai & Sason 2001).

In the Jerusalem area, soft chalks were also widely used in masonry construction. However, one should keep in mind that there was a widespread phenomenon of hard and dense calcrete formation occurring in the Israeli soft chalks (Buchbinder (1969)). Calcrete could be described as a natural concrete in which a micritic matrix consisting of calcium carbonate as cement, binds together pebbles, sand and desert debris (Judson & Richardson 1995).

Calcrete layers might be as deep as 1.5 to 2.5 m from the earth surface (Talesnik et al. 2001). The soundness of calcrete is much poorer than of unweathered soft limestone.

Wood and charcoal were universally used as fuel in the limestone kilns in the past. Therefore, wood ash and coal dust are common impurities observed in historic lime mortars and Roman concretes (Tsatskin 1999; Tsatskin et al 2000; Heritage Lottery Fund 2000; Siddall 2000; Krumnacher 2001).

5 GENERAL BACKGROUND OF THE LIMESTONE DURABILITY

Durability of limestone is strongly dependent on its chemical and mineralogical composition (Dana 1993) and the content of the secondary minerals. (Winkler 1982; Winkler 1997; Jarc et Mitric 2000). The smaller the content of the secondary minerals in limestone; the longer durability. Iron in the form of ferric iron, Fe^{3+} , is the most common and the strongest pigment in limestone (Winkler 1997). In limestone ferric iron, Fe^{3+} , is usually presented as hematite, Fe_2O_3 , goethite, $Fe^{3+}OOH$, and amorphous common rust, $Fe_2O_3 \cdot nH_2O$. Obviously, hematite is a much more stable mineral than goethite (Rezaie-Serej & Cook 1988; Oh et al. 1998; Cook et al. 1999). Stability of goethite is strongly dependent on acidity, pH. This mineral is stable only in a basic non-salty environment ($pH \geq 10$). According to (Park 1978), the rains in the Eastern Mediterranean have an average pH of 5.5. The contact of goethite with acid rain water in the presence of chlorine ions, Cl^- , promotes the formation of akagaenite, $Fe^{2+}O(OH)Cl$, instead of hematite, Fe_2O_3 (Rezaie-Serej & Cook 1988; Oh et al. 1998; Cook et al. 1999; Stahl et al. 1998). This process accelerates formation of the common amorphous rust in limestone, while a volume increase that occurs during conversion of

goethite to rust could be 20% to 70% (Winkler 1997). Thus, limestone that contains goethite and chlorine ions might deteriorate and even crumble.

Accelerated weathering and deterioration of limestone in polluted environments is an acute common problem of ancient and historic structures throughout the world (Winkler 1982; Torraca 1988; Moroni & Poli 1988; Johansson et al. 1988).

6 EXPERIMENTAL

6.1 Materials

Four stone fragments and two mortar pieces were drilled off from a central part of the swollen area in the external masonry part of the Southern Wall. The description of historic materials is given in Table 1.

6.2 Tests

The characterization methods used in the current investigation were:

- (A) *Chemical and mineralogical analysis of the historic stones*
- X-ray fluorescence (XRF);
 - X-ray diffraction (XRD);
 - petrographical investigation with polarizing microscope;
 - quantitative wet chemical analysis.
- All the abovementioned test procedures are described in details in Dana 1993.
- (B) *Physical properties of the historic stones*
- bulk density and total absorption (ASTM C97 1990);
 - capillary absorption (EN 1925 1999) and capillary absorption coefficients;
 - degree of saturation was calculated as a ratio of the capillary absorbed water and the totally absorbed water;

Table 1. Referring of the tested archaeological materials.

Name of the archaeological sample	Location in the southern temple wall	Length, m
Stone 1	Near external surface	0.1
Stone 2	From the edge of Stone 1 toward the internal part of the Wall	0.28
Stone 3	From the edge of Stone 2 toward the internal part of the Wall	0.22
Stone 4	From the edge of Stone 3 toward the internal part of the Wall	0.58
Mortar	Masonry joints	

- water evaporation rate (Wasserman & Bentur 2004). The measurements were carried out for the samples used in the capillary absorption test;
- Microerosion meter Digimatic Indicator IDF-150, Mitutoyo Corp., Japan was used in the stone swelling test (see Fig. 1). The microerosion meter is a simple micrometer tool that gauges surface height at a number of predetermined points, relative to initial datum points set into the stone (Price 1996). The test procedure used in the current research was as following:
 - oven-drying of the stone samples at temperature of $105 \pm 3^\circ\text{C}$ to constant weight;
 - cooling at temperature of $21 \pm 3^\circ\text{C}$;
 - water immersion of the stone samples for 24 hours. The changes in height of the samples were monitored. Mean swelling per unit height was calculated for each stone sample.

(C) *Mechanical properties*

- compressive strength (ASTM C170 1990). Samples used were $50 \times 50 \times 50$ mm or $40 \times 40 \times 40$ mm. Stone samples were oven-dried for 24 hours. Some samples were water saturated. Because of the limited amount of the investigated historic materials, the statistical processing of the strength data was not carried out. The results presented in this paper are given in the form of the minimal and maximal values of the strength. Compressive strength was measured in two directions:
 - (a) in parallel to the principal axis of the core drilled from the Southern Wall (subsequently referred to as A-A);
 - (b) transversely to the principal axis of the drilled core (subsequently referred to as B-B).
- wear resistance (220 rotation cycles) (Israeli Standard SI 6 1999).

(D) *Characterization of mortar*

Additional tests were carried out to characterize the chemical and mineralogical composition and the physical properties of two mortar pieces drilled off together with the Stones' samples.

7 RESULTS

7.1 Chemical and mineralogical analysis of the historic stones

7.1.1 Elementary analysis (XRF)

The main element identified in all investigated samples was calcium, Ca. In all investigated materials there were determined traces of silicon, Si, iron, Fe, and sulfur, S, which were presented in minor amounts. Potassium, K, and chlorine ion, Cl^- were detected in small amounts in the Stone 3, Stone 4 and in the mortars. The results of semi-quantitative estimation of secondary (impurity) elements in the Stones is presented in Fig. 2.

It could be suggested that the investigated stones might be classified into two groups: Stone 1 & 2 and Stone 3 & 4. Within each group, the occurrence of the secondary elements is similar; however, these two groups are quite dissimilar.

7.1.2 Mineralogical composition (XRD)

The main mineral in all investigated materials is calcite, CaCO_3 . In X-ray diffraction of all samples there were determined small peaks of goethite, $\text{Fe}^{3+}\text{O}(\text{OH})$. The results of X-Ray diffraction proved the classification of the Stones in two groups: Stone 1 & 2 and Stone 3 & 4. The former group contains a high rate of impurities, whereas, the latter group, on contrary, is characterized by slight traces of the secondary constituents.

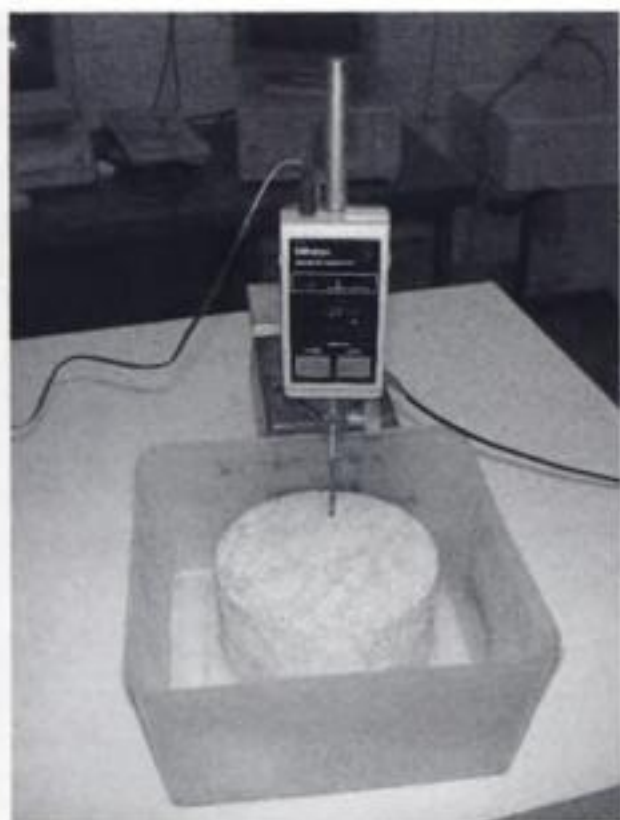


Figure 1. Image of swelling test with Digimatic Indicator IDF-150, Mitutoyo Corp., Japan.

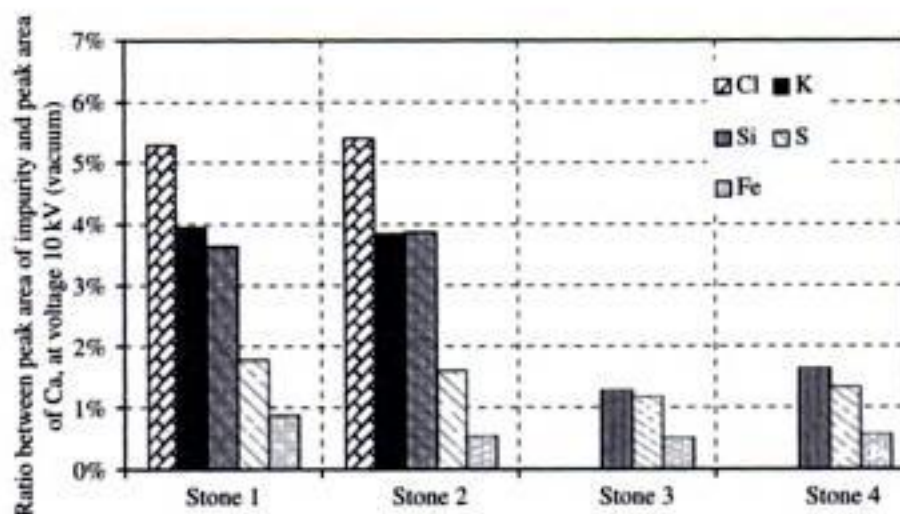


Figure 2. Presence of impurities in historic stones from the southern temple wall (XRF analysis).

7.1.3 Mineralogical composition (petrographical investigation with polarizing microscope)

The stones studied in the current investigation could be defined as weathered soft micritic calcite covered with an adjacent iron oxide impregnation, possibly of goethite, $\text{Fe}^{3+}\text{O}(\text{OH})$. It was found that Stone 1 is much harder than the other stone samples. All stones are partly transformed into calcrete. In contrast to the other samples, Stone 4 is far less weathered, and is transformed into calcrete to a smaller extent (see Fig. 2). There are minor amounts of adjacent iron oxide impregnation, probably goethite, in this stone.

7.1.4 Quantitative chemical composition of historic stones

Average chemical composition of Stone 1 & 2 and Stone 3 & 4 are reported in Table 2. As was previously emphasized, Stone 1 & 2 contains a high amount of impurities, while Stone 3 & 4 is more homogeneous.

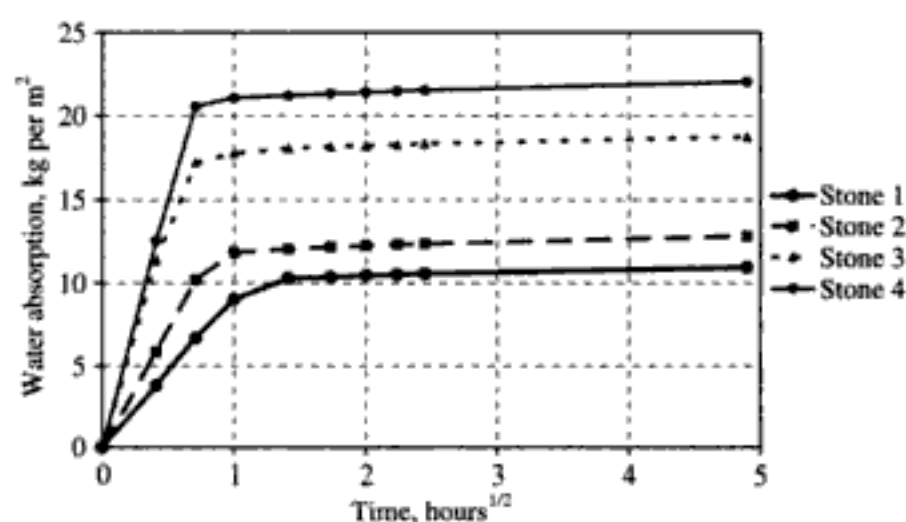


Figure 3. Capillary water absorption of historic stones.

Table 2. Chemical composition of the historic materials.

Component	Content, % (weight per cent)	
	Stone 1 & 2	Stone 3 & 4
CaO (total)	45.9	52.4
CaO (soluble in HCl)	45.7	52.4
Insoluble residue	8.5	2.8
SiO ₂	5.1	1.2
Al ₂ O ₃	0.9	0.9
Fe ₂ O ₃	0.45	0.3
MgO	0.9	0.5
Na ₂ O	1.0	0.04
K ₂ O total	0.49	0.12
K ₂ O soluble in HCl	0.44	0.12
CaO free	0.02	<0.01
LOI	40.6	42.3
Organic material	0.7	0.5
Cl ⁻ (estimated by content of soluble alkalis)	1.46	0.13

It could be concluded that the high content of secondary minerals and the advanced rates of natural aging of Stone 1 & 2, as well as their transformation to calcrete to a greater extent than Stone 3 & 4, indicates the potential differences in the durability of the two investigated groups of stones.

7.2 Bulk density, total water absorption and saturation coefficient

The results are given in Table 3.

Stone 1 and Stone 2 are similar in their physical properties. However, they are eminently different from Stone 3 and Stone 4. Moreover, Stone 1 and Stone 2 are much denser than Stone 3 and Stone 4, which have similar physical properties.

7.3 Capillary water absorption of historic stones

Fig. 3 presents the results of the capillary water absorption.

Capillary absorption coefficients of the investigated historic stones:

- Stone 1 – 9 kg per m² per hour^{1/2};
- Stone 2 – 12 kg per m² per hour^{1/2};
- Stone 3 – 18 kg per m² per hour^{1/2};
- Stone 4 – 21 kg per m² per hour^{1/2}.

All investigated stones are characterized by a very quick rate of water absorption. Capillary water uptake of Stones 3 & 4 is approximately as much as, that of Stones 1 & 2.

7.4 Evaporation rate of historic stones

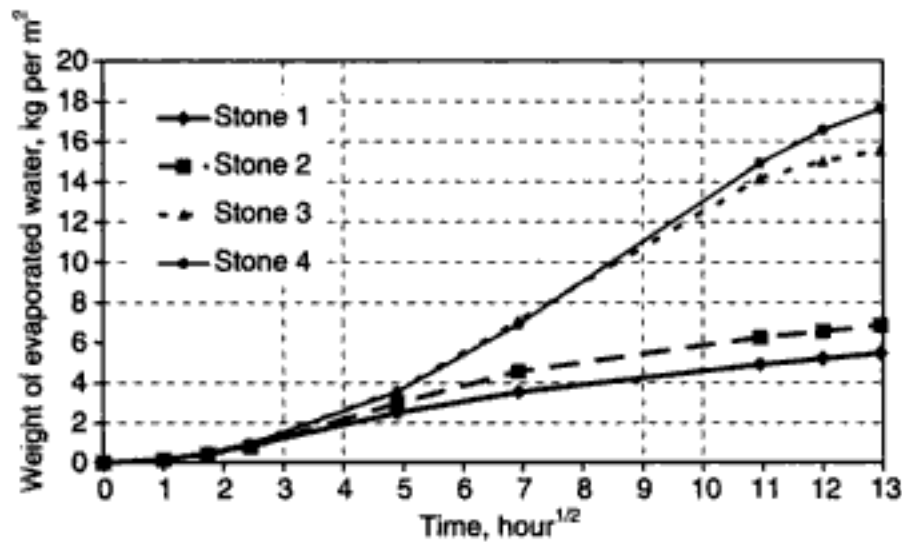
The results of the evaporation test carried out at 20°C/55% RH are presented in Fig. 4. Similarly to other properties, evaporation ability of Stone 1 & 2 strongly differs from Stone 3 & 4. Stone 3 & 4 have higher rates of water evaporation. High water evaporation capacity is very important for limestone durability, which is strongly affected by the moisture entrainment in stone.

Table 3. Bulk density and total water absorption of the historic stones.

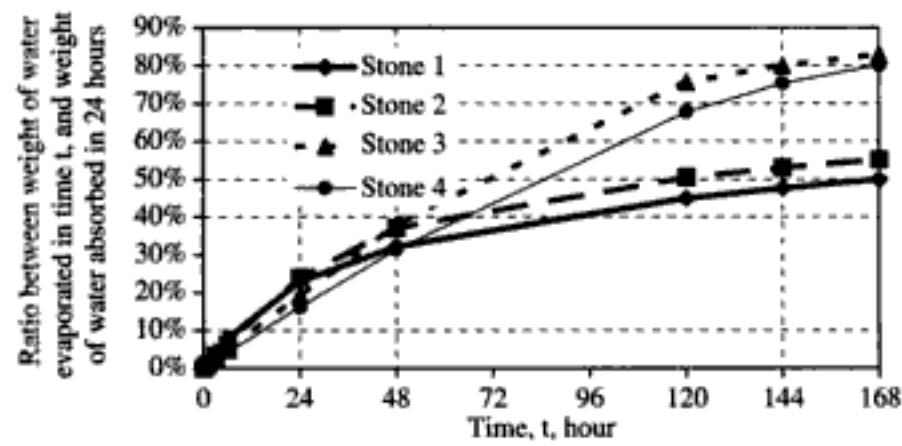
Material	Oven-dried bulk density, kg/m ³	Total water absorption, % (weight per cent)	Saturation coefficient
Stone 1	1,990	13	0.83
Stone 2	1,961	16	0.79
Stone 3	1,500	21	0.94
Stone 4	1,441	27	0.92

7.5 Swelling and swelling rate of the historic stones

Swelling due to moisture was measured only for samples Stone 2, Stone 3 & Stone 4. Swelling of Stone 1 was not checked because of the limited amount



(a)



(b)

Figure 4. Evaporation rate of historic stones. (a) evaporation rate of historic stones at 20°C/55%RH; (b) ratios between weight of water evaporated at different periods and weight of water absorbed during a 24 hour period.

Table 4. Swelling characteristics of the historic stones.

Stone 2			Stone 3			Stone 4		
Time, Δt , hour	Swelling, ΔSw_t , $\times 10^{-6}$, m per m	Swelling rate, $(SwR)_t$, $\times 10^{-6}$, m per m per hour	Time, Δt , hour	Swelling, ΔSw_t , $\times 10^{-6}$, m per m	Swelling rate, $(SwR)_t$, $\times 10^{-6}$, m per m per hour	Time, Δt , hour	Swelling, ΔSw_t , $\times 10^{-6}$, m per m	Swelling rate, $(SwR)_t$, $\times 10^{-6}$, m per m per hour
0.0	0	—	0	0	—	0	0	0
0.08	0.015	0.18	0.08	0.09	1.09	0.08	0.16	1.88
0.33	0.015	0.04	0.33	0.15	0.45	N/A	N/A	N/A
0.83	0.000	0.00	0.83	0.18	0.22	N/A	N/A	N/A
1.33	-0.103	0.08	1.33	0.21	0.16	1.25	0.24	0.19
1.83	-0.133	0.07	1.83	0.24	0.13	1.75	0.22	0.12
2.83	-0.163	0.06	2.83	0.30	0.11	2.25	0.20	0.09
3.33	-0.207	0.06	3.33	0.30	0.09	3.25	0.10	0.03
3.83	-0.237	0.06	3.83	0.30	0.08	N/A	N/A	N/A
20.83	-0.237	0.01	N/A	N/A	N/A	21.00	-0.51	0.02
24.00	-0.266	0.01	23.83	0.36	0.02	23.00	-0.55	0.02
Initial maximal swelling rate $\times 10^{-6}$, m per m per hour -0.2			Initial maximal swelling rate $\times 10^{-6}$, m per m per hour -1.1			Initial maximal swelling rate $\times 10^{-6}$, m per m per hour -1.9		

available. Swelling due to moisture was calculated as a ratio between changes in the height of moist sample at time t and its initial height ($\times 10^{-6}$ m per m per) after oven-drying and cooling. The results of measurements are shown in Table 4. Swelling rate was estimated as swelling at time unit ($\times 10^{-6}$ m per m hour), i.e.:

$$(SwR)_t = \frac{\Delta Sw_t}{\Delta t} \quad (1)$$

where $(SwR)_t$ = swelling rate at time t , $\times 10^{-6}$, m per m per hour; ΔSw_t = swelling at time t , $\times 10^{-6}$, m per m; Δt = time, hour.

Fig. 5 is presents the swelling kinetics.

As the test was carried out at constant temperature and humidity, the reduction in swelling during the test pinpointed the dissolution of some mineral compounds from the surface of the historic stones.

7.6 Compressive strength of historic stones

Compressive strength of the oven-dried historic stones is plotted in Fig. 6.

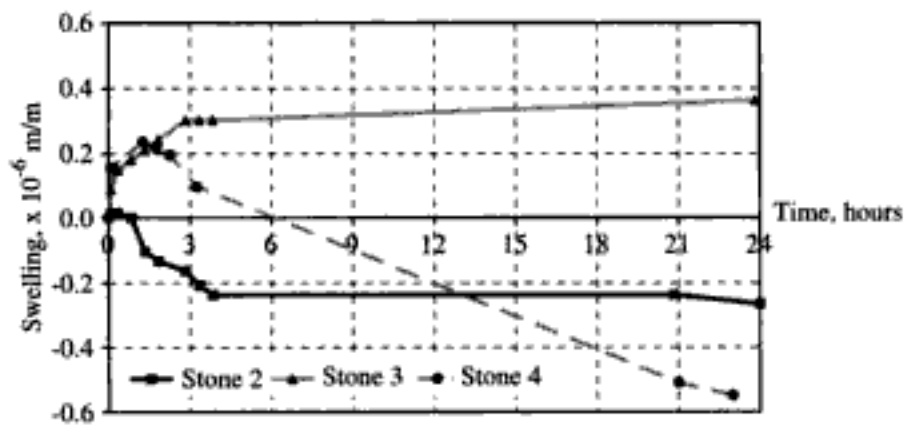
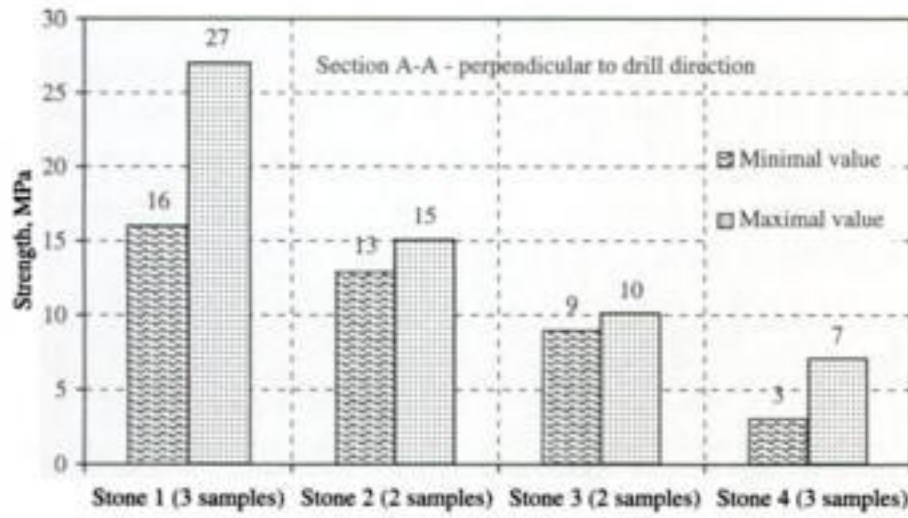
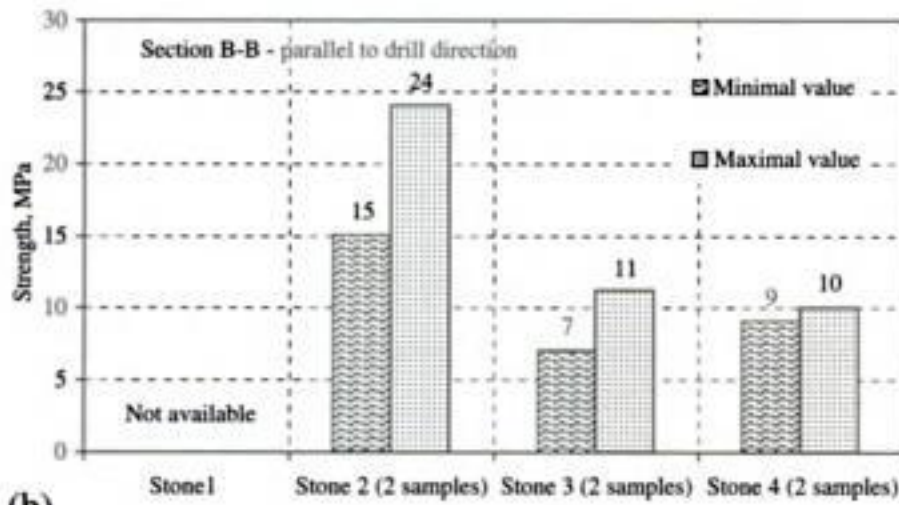


Figure 5. Swelling of historic stones caused by moisture.



(a)



(b)

Figure 6. Compressive strength of the oven-dried historic stones: (a) transverse to the principal axis of the drilled core; (b) parallel to the principal axis of the drilled core.

Compressive strength of water-saturated stones was measured only for samples Stone 2 and Stone 4, because of limit in the amount of Stone 1 and Stone 3. Compressive strength of water-saturated stones, as well as a wet-to-dry strength ratio are given in Table 5.

7.7 Wear resistance

The results of abrasion test are shown in Fig. 7. Wear properties of Stone 1 & 2 and Stone 3 & 4 are different. Stone 4 cracked during the test.

7.8 Mortar characterization

The results of the mortar investigation were discussed in Wasserman 2003. No residues of burnt wood or charcoal dust were observed in the investigated mortar. Therefore, quicklime used in the manufacturing of the mortar drilled off the Southern Wall has been calcined in an oil-based furnace.

8 DISCUSSION

All tests that were carried out showed the gap between the properties of Stone 1 & 2 and Stone 3 & 4. The differences in the mineralogical and chemical

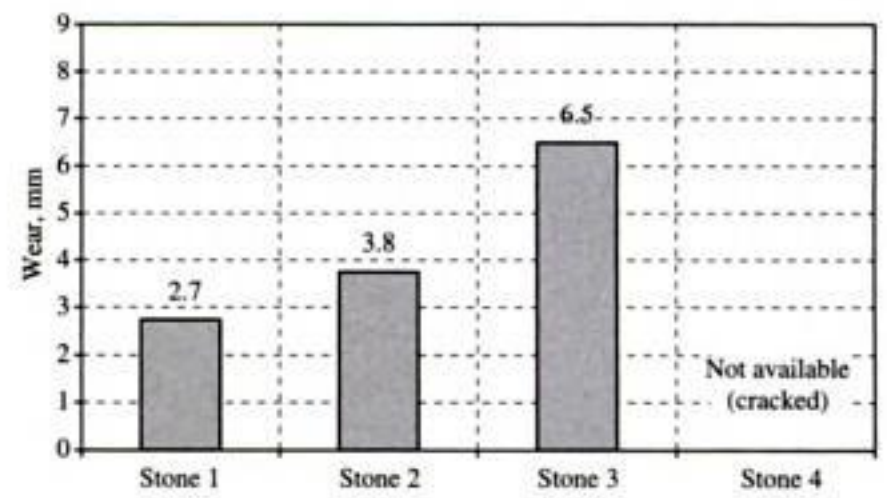


Figure 7. Wear resistance of historic stones.

compositions and in the character of water absorption and evaporation of these two groups of the stones caused their dissimilar physical and mechanical behavior.

The total absorption of Stone 3 & 4 is about 1.6 times more than that of Stone 1 & 2. The differences in the capillary absorption are also very sharp. However, the kinetics of the water absorption is very similar. This fact is well correlated with the similarity of the saturation coefficients. Therefore, the investigated stones have a similar ratio of capillary pores available for moisture uptake, whereas the total amount of absorbed water is less in Stone 1 & 2.

The character of evaporation kinetics of these two groups of stone allows us to assume that Stone 1 & 2 has less water evaporation capacity than Stone 3 & 4. Higher water retention of Stone 1 & 2

Swelling and wear characteristics are very valuable for clarifying the trends in stone decay. The results of swelling and wear tests carried out in the current research, correlated very well with the capillary absorption of the stones. A relationship between the capillary absorption coefficients, the initial maximal swelling rates and the wear resistance of the investigated historic stones are shown in Fig. 8 and Fig. 9, respectively. The relationships shown in Figs. 8–9 are of high significance, e.g.:

- (a) The correlation between the capillary absorption and swelling of Stone 2, 3 & 4 is described by the following equation:

$$\text{SwR}_{\text{initial}} = 6.3 \cdot 10^{-6} \cdot W^{1.2} \quad (2)$$

where $(\text{SwR})_{\text{initial}}$ – initial swelling rate, $\times 10^{-6}$ m per m per hour; W – capillary absorption coefficient, $\text{kg per m}^2 \text{ per hour}^{1/2}$.

Therefore, swelling rate of Stone 1 could be estimated as 0.06×10^{-6} m per m per hour, approximately.

- (b) the equation describing the correlation between the wear resistance of the stones and their capillary absorption is as follows:

$$\text{Wear}_{220} = 0.4 \cdot W - 1.3 \quad (3)$$

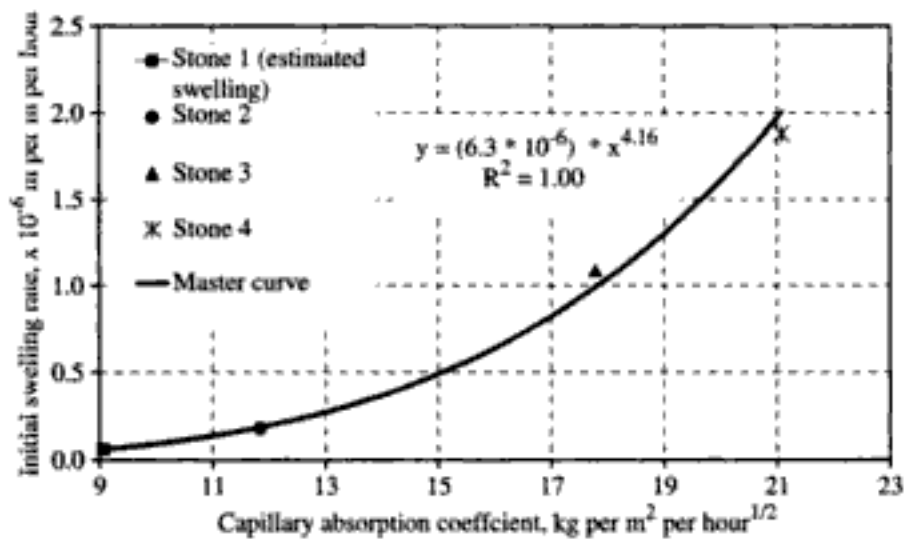


Figure 8. Relationship between capillary absorption and swelling due to moisture of the investigated historic stones.

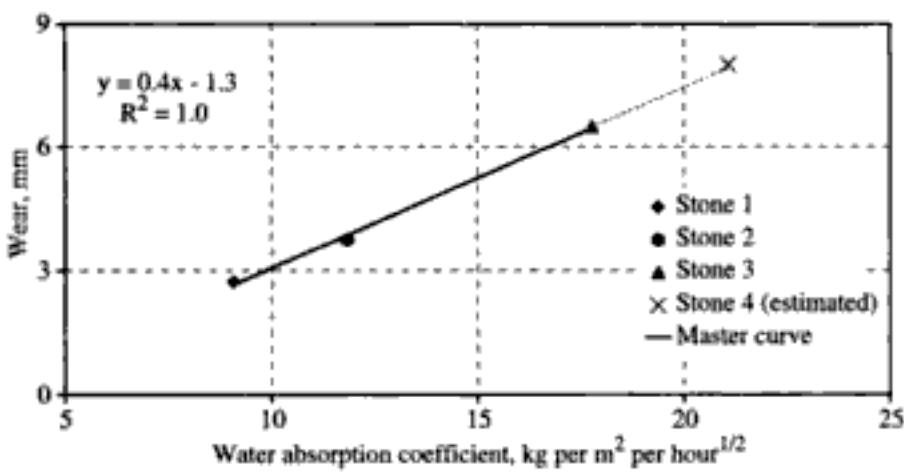


Figure 9. Relationship between capillary water absorption and wear resistance of historic stones.

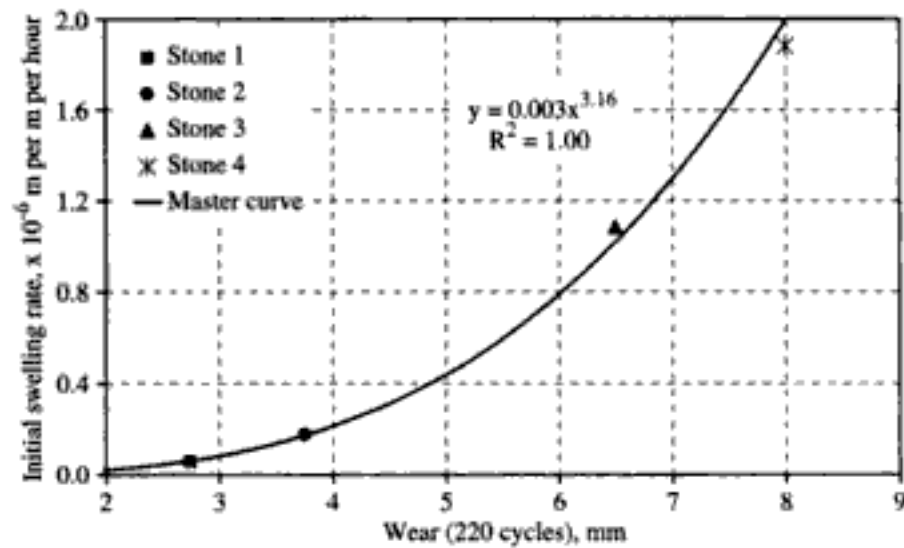


Figure 10. Relationship between the wear and the swelling of historic stones.

where $Wear_{220}$ – wear resistance (220 cycles), mm;
 W – capillary absorption coefficient, kg per m^2 per hour $^{1/2}$.

The reliability of measured and estimated results of swelling and wear characteristics could be proved by their high consistency, which is presented in Fig. 10.

The correlation between the results could be presented by the following equation:

$$SwR_{initial} = 0.003 \cdot (Wear_{220})^{3.16} \quad (4)$$

where $(SwR)_{initial}$ – initial swelling rate, $\times 10^{-6}$ m per m per hour; $Wear_{220}$ – wear resistance (220 cycles), mm.

The results shown in Figs. 8–9 and the equation (2)–(3) confirm a strong impact of moisture on the decay of chinks used for the erection of the South Temple Wall. However, the decay of Stone 3 & 4 caused by moisture might have been developed to a greater extent than Stone 1 & 2.

Consequently, the vast differences in the swelling characteristics of Stone 1 & 2 and Stone 3 & 4 might have effected in the differential behavior of the external and internal parts of the Temple Southern Wall and resulted in pushing off the stiff external layer by the bulging internal stratum.

Because of the dense structure, Stone 1 & 2 are characterized by much higher strength values than Stone 3 & 4. Consequently, Stone 1 and Stone 4 have the highest and the lowest strength values, respectively. Stone 2 and Stone 4 show the big difference between the strength observed in counter-cross directions, i.e.: the strength ratios in the counter-cross directions are about 1.4 and 1.9 for dry Stone 2 and 4, respectively. Therefore, anisotropy of Stone 2 and 4 could be suggested. Contrary, the strength ratio in the counter-cross directions of Stone 3 was 1.0. Therefore, the difference between Stone 3 and Stone 4 could be confirmed.

It should be emphasized that the total water absorption of Stones 3 is half as much as the total water absorption of Stone 4. Furthermore, the character of swelling is different in these two Stones, i.e. Stone 4 dissolved in a short period after water immersion; whereas, Stone 3 was swelling continuously during the experiment; see Fig. 5.

The cumulative length of Stones 1 & 2 is about 38 cm and of Stone 3 & 4 – 80 cm (see Table 1). The properties of Stone 1 and Stone 2 are very similar. In contrast, Stone 3 and Stone 4 have different total water absorption, various swelling behaviors and dissimilar mechanical behavior in counter-crossed directions. Therefore, Stone 1 & 2 seem to fit one dimensional stone block in the Southern Wall, and samples Stone 3 and 4 might have fitted the two next blocks behind the block of Stone 1 & 2.

Keeping in mind the similar mineralogical composition of Stone 3 & 4, we can conclude that Stone 3 & 4 might have been quarried at the same time from the same rock deposit and were used for the construction of the Temple Southern Wall at the same historical epoch. However, Stone 1 & 2 have properties, which are very unlike Stone 3 & 4. Therefore, it has to have had a different provenance. More comprehensive research has to be done to confirm this suggestion.

As was previously emphasized, quicklime used in the manufacturing of the mortar drilled off the Southern Wall has been calcined in an oil-based furnace. The use of this type of furnaces in the Israel lime industry

began in the 1920s during the British Mandate establishment (Sasson 2000). Thus, it could be suggested that the investigated mortar is about 80 years old. The writer received an information from the Israeli Antique Authority regarding the repair work carried out by the British Mandate in the Southern Temple Wall in the 1930s after a strong earthquake which occurred in the region in 1927 and which caused the destruction of many structures in Jerusalem (Amiran et al. 1994). Thus, it could be suggested that the Southern Temple Wall was repaired in the 1930s–1940s. Unfortunately, the properties of the stones, which were used for this repair (e.g. Stones 1 & 2), were strongly different from the historic masonry in the Southern Temple Wall (e.g. Stones 3 & 4). Therefore, the performance of the new and the historic masonry in the Southern Temple Wall was different during all the time after repair. Consequently, the bulk spot that appeared in the Wall might be a result of this dissimilar material performance.

9 CONCLUSION

The compatibility of materials used for conservation purposes is a well recognized prerequisite of the maintenance and rehabilitation of any historic building. However, the importance of the implementation of compatible material was recognized only after the adoption of the Venice Charta in 1964. The works done in the Southern Temple Wall in Jerusalem in the first half of XX century could be referred to as *repair and not conservation measures*. Apparently, during their mandate, the British did repairs using inappropriate materials. The discrepancies in material performance between the “original” and “new” masonry seem to have led to the appearance of the bulge in the Southern Temple Wall.

REFERENCES

- Amiran, D.H.K., Arieh, E., Turcotte, T. 1994. Earthquakes in Israel and Adjacent Areas: Macro seismic Observations since 100 B.C.E. *Israel Exploration Journal* 44: 290–305.
- ASTM C97 1990. Absorption and bulk specific gravity of natural building stone.
- ASTM C170 1990. Compressive strength of natural building stone.
- Ben-Dov, M. 1985. In the shadow of the Temple: the discovery of ancient Jerusalem (translated from the Hebrew by Ina Friedman), Keter Pub. House, Jerusalem.
- Buchbinder, B. 1969. Geological map of Hashephela region, Israel, with explanatory notes, Part 1–2, Jerusalem.
- Cook, D.C., Oh, S.J., Balasubramian, R., Yamashita, M. 1999. The role of goethite in the formation of the protective corrosion layer on steel. *Hyperfine Interactions*, 122 (1): 59–70.
- Dana, J.D. 1993. Manual of Mineralogy. 21st Edition, John Wiley & Sons, Inc., New York.
- EN 12525, 1999. Natural stone test methods – Determination of water absorption coefficient capillarity.
- Heritage Lottery Fund 2000. Limestone Heritage Project: Limekilns. Programme Report. Published by Arnside/Silverdale Area of Outstanding Natural Beauty, UK.
- Jarc, S. & Mirtic, B. 2000. The Study of Weathering Effects on the Slovenian Limestones by SEM. *Journal of Conference Abstracts*, 5(2): 553, Cambridge Publications.
- Johansson, L.-G., Lindqvist, O., Mangio, R.E. 1988. Corrosion of Calcereous Stones in Humid Air Containing SO₂ and NO₂. *Durability of Building Materials*, 5: 439–449.
- Josephus Flavius 1984. The Jewish Wars. Penguin Classics (translated by G.A. Williamson, revised by E.M. Smallwood).
- Judson, S. & Richardson, S.M. 1995. Earth: An Introduction to Geologic Change, Englewood Cliffs, NJ, Prentice Hall.
- Krumnacher, P.J. 2001. Lime and Cement Technology: Transition from Traditional to Standardized Treatment Methods. Thesis (M.Sc.). Virginia Polytechnic Institute and State University.
- Mazar, B. 1989. Excavations in the south of the Temple Mount, Institute of Archaeology, Hebrew University, Jerusalem.
- Moroni, B. & Poli, G. 1988. Corrosion of Limestone in Humid Air Containing Sulfur and Nitrogen dioxides: a Model Study. *Durability of Building Materials*, 5: 367–373.
- Municipality of Jerusalem 1996. Statistical yearbook of Jerusalem 1994/1995. Municipality of Jerusalem and the Jerusalem Institute for Israel studies.
- Oh, S.J., Cook, D.C., Townsend, H.E. 1998 Characterization of iron oxides commonly formed as corrosion products on steel. *Hyperfine Interactions*, 112 (1): 59–65.
- Peretz, A. 1991. The management and economic aspects of the erection of the Temple Mount. M.Sc. Thesis, Technion – Israel Institute of Technology, Haifa.
- Price, C.A. 1996. Stone conservation: an overview of current research, The J. Paul Getty Trust, Santa Monica, CA, USA.
- Rezaie-Serej, S. & Cook, D.C. 1988. Environmental Influence on the formation of α -FeOOH on the surface of weathering steel. *Hyperfine Interactions*, 41(1): 701–704.
- Sasson, A. 2000. The lime-burning plant at the Ali-Muntar Hill in Gaza. *Bulletin of the Anglo-Israel Archeological Society*, 18: 83–103.
- SI 6 1999. Terazzo floor tiles (Hebrew).
- Siddall, R. 2000. Conservation: Material Science. Plaster, Mortar, Cement & Concrete. Course notes, Department of Geological Science, University College of London, UK. Available from: <http://www.ucl.ac.uk/~ucfbrxs/limes/G123notes.htm> [Accessed 10 December 2002].
- Sparai, Z., Sason, A. 2001. Stone excavation and quarries in ancient Israel, Eretz Hefetz Institute “Israel Lights”, Education academic college.
- Talesnik, M.L., Hatzor, Y.H., Tsesarsky, M. 2001. The elastic deformability and strength of a high porosity, anisotropic chalk. *Int. J. of Rock Mechanics and Mining Sciences*, 38: 543–545.
- Torraca, G. 1988. Air Pollution and the Conservation of Building Materials. *Durability of Building Materials*, 5: 383–392.

- Tsatskin, A. 1999. The petrography of hydraulic and other building materials in Caesarea. *Caesarea Papers* 2, *Journal of Roman Archaeology*, Suppl. Ser. 35: 419-429. K.G. Holum, A. Raban, and J. Patrich (eds).
- Tsatskin, A., Rohrlich, V., Soroka, I., Raban, A., Berner, A. 2000. Analysis of ancient hydraulic concrete from Caesarea by petrographic and material science techniques. *Israel Geological Society, Annual Meeting*: 95.
- Vitruvius, 1931-34. *De architectura libri decem* (English translations by M.M. Morgan, Cambridge, Mass., 1914, and by F. Granger in the Loeb Classical Library), 2 vols.
- Warren, C., Condor, C.R. 1881. *The Survey of Western Palestine*. The Committee of the Palestine Exploration Fund, London.
- Wasserman, I. 2003 "Material Characterization of Masonry Stones and Mortar from the Southern Temple Wall in Jerusalem". *Proceedings of the 4th Symposium of the Hellenic Society for Archaeometry, Athens (Greece), May 28-June 3 (in press)*.
- Wasserman, I., Bentur, A. 2004 "Efficiency of Surface Treatment on Enhancement of Durability of Limestone Cladding in the Eastern Mediterranean Offshore Zone". Submitted for the publication in *Materials and Structures*, September 2003.
- Weisman, G. 1968. *Stability of the Southern Temple Wall*. Technical Report, Technion - Israel Institute of Technology, Haifa.
- Wingate, M. 1985. *Small-scale lime burning, a practical introduction*, Intermediate Technology Publications, London.
- Winkler, E.M. 1997. *Stone in Architecture: Properties, Durability*. 3rd Edition. Springer-Verlag, Berlin, Heidelberg.
- Winkler, E.M. 1982. *Problems in the deterioration of Stone. Conservation of Historic Stone Buildings and Monuments*. Commission on Engineering and Technical Systems, US National Academy on Science, Engineering and Medicine.

Physical and chemical properties of pre-regulated American cements

A.S. Rush

North Carolina State University, Raleigh, North Carolina, USA

D.F. Laefer

University College Dublin, Dublin, Ireland

ABSTRACT: The characteristics of pre-regulated American cements differ fundamentally from those manufactured afterwards, both in terms of physical and chemical properties and with regard to cement consistency. This paper presents an overview of cementitious products available in America from 1875 to 1909. Historical testing data is compared to that expected of modern materials. The data presented show that a lack of consistency and a less rigorous manufacturing processes resulted in an original product much inferior to modern expectations regarding the compressive capacity of concrete and that this was true for both natural and Portland cements.

1 INTRODUCTION

The advent of widespread usage of reinforced concrete and a myriad of related fatal accidents caused the regulation of the concrete industry. Fundamental to this was cement regulation. The resulting products in a post-regulated environment distinctly differ from those manufactured prior to regulation. For modern engineers to effectively evaluate the potential capacity and behavior of structures built prior to regulation, a more fundamental understanding is needed as to how cements manufactured before 1909 differ from those in use today. This paper provides an overview of major chemical and physical distinctions between pre-regulated and post-regulated cements, along with reasonable historical performance expectations.

1.1 *Regulatory agencies within the United States*

During the nineteenth century, cement and concrete in the United States (US) were unregulated materials with respect to manufacturing, testing, and usage. In 1904, the American Concrete Institute (ACI) was established and began to standardize the industry. Prior to 1904, the American Society for Testing Materials (ASTM), an agency originally founded in 1898 to improve railroad safety, began investigating cement properties. Along with other engineering organizations, these two agencies advocated for increased regulation of cement and concrete design and production. The first ASTM requirements for tensile strength of cements were published in 1909. Prior to that, concrete design was on a

comparative basis. Many different “authorities” published results from their testing of cements in the form of neat and sanded concrete, and a designer was forced to individually determine a confidence level to ascribe those tests.

Prior to the formation of these agencies, there was no data published that was produced in a consistent manner related to the physical and chemical properties of cement within the US. The manufacturing processes varied by cement producers, as did the chemical compositions of the materials. For modern engineers, the period of greatest concern ranges between 1875 and 1909. These dates demarcate the period between Monier’s experiments with iron reinforced concrete and some of the earliest official test guidelines for cement (Ransome 1912). ASTM created these initial guidelines to establish boundaries of allowable tensile strengths for concretes. The tests were based on neat and sanded mixes.

Although Americans were relatively slow to adopt reinforced concrete compared to European usage, substantial buildings were constructed in the US with these materials, including the Academy of Sciences in San Francisco, California, the Pacific Coast Borax Works in Bayonne, New Jersey, and the Loomis Building in Cleveland, Ohio (Ransome 1912). Unfortunately, a detailed list of buildings constructed with pre-regulated cement is not available. Consequently, buildings that may have been erected with cements that by modern standards would be considered sub-standard, either because of their variability or their strength capacity, are hard to identify without chemical

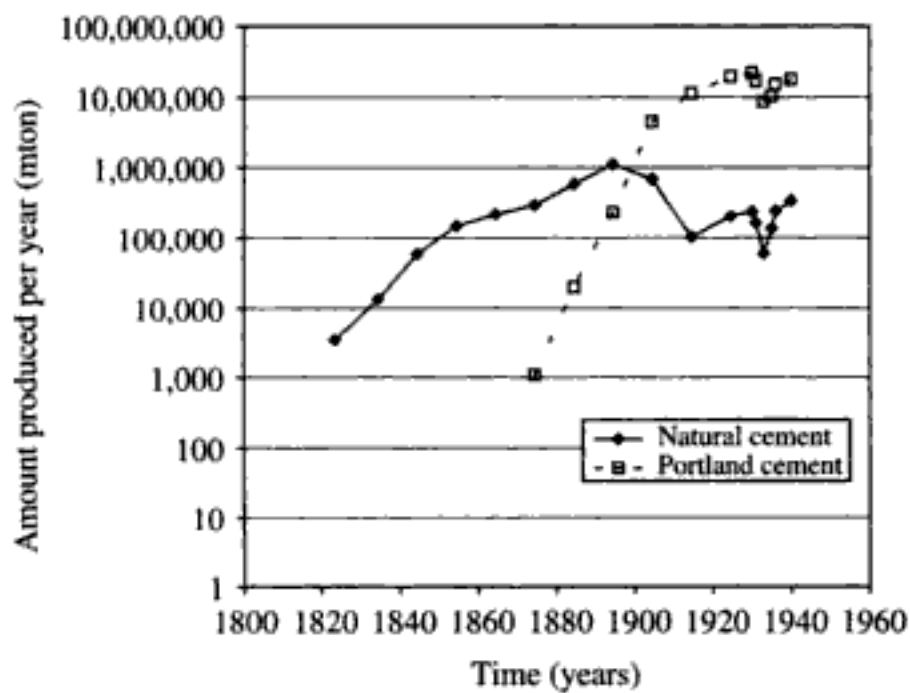


Figure 1. Natural and Portland cement production 1820–1940 (data adapted from Kemp 2002).

analysis from destructive testing, except potentially by construction their date. Production of these materials was substantial (Fig. 1) through the turn of the previous century.

2 NATURAL CEMENTS

2.1 Definition

Natural cements are hydraulic cements produced from burning limestone at low temperatures, around 1000 degrees Celsius (Richardson 1897f). Usage dates back to the Roman Empire, which explains why natural cements are often called Roman cements. In the US, natural cements were primarily used as mortar for masonry but were also used for highway construction and structural members in buildings. In the US, millions of tons of this material were produced and used throughout the late nineteenth and early twentieth centuries. As an example, in 1903, natural cement output was about 845,000 metric tons and begins to mark a decline from previous years (Eckel 1928).

2.2 Types of natural cements

At the end of the nineteenth century, the most typical natural hydraulic cements were created from limestone. The differences between cements varied because of chemical distinctions in the various limestone deposits.

Two common natural cements were regularly referred to as magnesian and lime (Table 1). Although similar to each in their production processes, they differed in setting time, heat of hydration, rate of strength gain, and chemical composition (Richardson 1897h). Differences between the two originate primarily from the chemical compositions of the limestone (Table 2). Magnesian cements were typically quarried in upstate

Table 1. Physical properties of natural cements (data adapted from Clifford 1897h).

Type of natural cement	Brand	Fineness (% retained)		
		200	100	50
Magnesian	Rosendale, best, NY	10	7	2
	Rosendale, average, NY	24	12	3
	Buffalo, NY	32	24	6
	Akron, "Star," NY	12	7	2
	Milwaukee, Wis.	18	10	2
	Utica, Ill.	25	15	4
Lime	Round Top, Md.		15	8
	Cumberland, Md.		19	
	Cumberland & Potomac, Md.	30	17	4
	Antietam, Md.		7	
	Sherpherdstown, Md.		14	
	Unspecified	Louisville, "Anchor," Ky.		24
Louisville, "Speed," Ky.		24	16	10
Sellersburg, Ind.			27	12
Fort Scott, Kans.		12	4	
Double Star, Kans.		9	3	1
Mankato, Minn.		31	9	1
Union, Penn.			7	
Improved Union, Penn.		30	15	3
Anchor, Penn.			10	2
Milroy, Penn.			20	
Utah		14	4	

New York, where the magnesia content in the limestone was generally 13 to 15 percent, while lime cements were typically quarried in the Potomac Valley, where the magnesia content was usually lower than 4 percent (Richardson 1897h). The importance of magnesia content is explained below.

2.3 Manufacturing process

The manufacturing process for natural cements begins with the quarrying of hydraulic limestone. The stone is then burned in a kiln until the carbonic acid burns off and some of the free lime bonds with the silica and clay, thereby forming compounds with hydraulic energy. This process is called calcination. Common lime is obtained by heating, i.e. calcining, pure or nearly pure limestone. Such heating produces quicklime, CaO, by driving off the carbon dioxide from CaCO₃ at a temperature of around 400 degrees Celsius. The addition of water to this substance then causes the quicklime to slake with the liberation of heat and a gain in volume. Natural cements are formed by calcining the limestone at a higher temperature around 1100 to 1200 degrees Celsius (Kemp 2002), which in the processing was often unsustainable in a consistent manner at the end of the nineteenth century. After a single burning, the burnt stone typically contained excess free lime.

Table 2. Chemical composition of natural cements by brands (data adapted from Richardson 1897g).

Percent composition											
Brand	Lime CaO	Magnesia MgO	Silica comb. SiO ₂	Alumina Al ₂ O ₃	Iron oxide Fe ₂ O ₂	Combined alumina and iron oxide	Combined soda and potash	Sulphuric acid SO ₃	Loss on ignition CO ₂ + H ₂ O	Silicates undec.	Total
Rosedale											
Hoffman, 1897	34.64	14.82	16.49	10.96	4.68	15.64	1.80	1.04	4.50	12.43	101.36
Hoffman, 1890	35.84	14.02	18.38		15.20	15.20		0.93	3.73	11.46	99.56
Newark & Rosedale	34.14	19.61	24.43		8.68	8.68	1.52		3.57	6.35	98.30
New York - Eastern											
Hudson River	36.67	14.35	18.17		11.30	11.30		1.32	4.27	13.11	99.19
New York & Bridge	33.18	19.61	11.28		9.40	9.40			4.40	14.64	92.51
Rock Lock	35.35	14.75	14.82		17.50	17.50		1.41	4.68	12.18	100.69
New York - Western											
Akron Obelisk	37.54	26.14	13.94		10.02	10.02	2.12		4.58	6.81	101.15
Star	41.60	22.24	16.20	4.40	2.80	7.20	1.62	2.06	6.90	4.00	101.82
Buffalo	39.20	26.52	13.24	4.40	2.00	6.40	1.85	1.39	6.80	3.24	98.64
Pennsylvania											
Slegfried	45.95	11.53	5.78		6.86	6.86		0.69	26.17	13.83	110.81
Milroy	41.90	29.73	13.56		5.00	5.00		0.74	6.40	4.68	102.01
Western											
Sellersburg, Ind. Anchor.	38.28	11.94	18.52	4.78	3.24	8.02		1.97	10.39	6.24	95.36
Milwaukee	33.40	22.60	13.80	4.00	2.80	6.80	2.51	2.59	9.50	11.20	102.40
Louisville	46.64	12.00	20.42	4.76	3.40	8.16		2.57	6.75	3.74	100.28
Utica, Ill.	29.99	19.79	9.58	2.76	2.16	4.92	1.77	1.35	15.96	17.42	100.78
Kansas											
Ft. Scott	49.80	12.16	17.60	4.00	5.00	9.00		2.04	4.50	4.20	99.30
Minnesota											
Mankato	45.51	15.02	16.30	3.34	3.80	7.14	2.03	1.94	10.00	5.06	103.00
Potomac											
Shepardstown	34.83	11.33	22.89		9.36	9.36	1.25	1.49	5.13	13.62	99.90
Antietam	29.38	13.37	14.54	10.44	3.25	13.69		1.15	7.15	18.96	98.24
Lime Cements											
Round Top	45.66	2.86	21.68	8.34	4.14	12.48		1.31	8.13	7.96	100.08
Cumberland & Potomac	39.54	3.80	20.42	8.38	5.38	13.76			10.20	9.80	97.52
Cumberland	41.96	3.19	20.25		14.76	14.76			7.97	9.41	97.54

Table 3. Statistics of chemical compositions for natural cements (data adapted from Richardson 1897g).

Parameters	Lime CaO	Magnesia MgO	Silica comb. SiO ₂	Combined alumina and iron oxide	Combined soda and potash	Sulfuric acid SO ₃	Loss on ignition CO ₂ + H ₂ O	Silicates undec.
Mean	38.68	15.52	16.47	10.06	1.83	1.53	7.80	9.56
Standard deviation	5.62	7.28	4.46	3.68	0.37	0.58	5.06	4.65
Lower extreme	29.38	2.86	5.78	4.92	1.25	0.69	3.57	3.24
Median	37.91	14.55	16.40	9.18	1.80	1.39	6.78	9.61
Upper extreme	49.80	29.73	24.43	17.50	2.51	2.59	26.17	18.96
Range	20.42	26.87	18.65	12.58	1.26	1.90	22.60	15.72

When mixed with water, this free lime caused a high temperature of hydration, which created overly rapid curing, thereby resulting in lower concrete strength (Richardson 1897g). After this primary burning, the limestone was mill ground or further processed to slow its setting time.

To combat excessively high hydration heat, three methods were employed. Air slaking the dry ground cement particles was one method, which allowed the free lime to naturally slake, through a chemical reaction with air. The large storage facilities and time required, however, discouraged use of this process. The burnt stone could also be sprinkled with water to produce the same effect. The amount of water varied for each type and size stone and, thus, had to be established through experience. The final option was to steam the burnt stone in baskets until the free lime was slaked (Richardson 1897g).

Following the removal of excess lime, the stones were then repetitively crushed and sieved to ensure the product's fineness. The sieving process consisted of separating the larger grained stones from the smaller ones by passing them through a series of wire meshes, which were designated by a sieve number that indicated the quantity of holes within a 2.54 cm square area of wire mesh.

2.4 Fineness

The percent retained on the #100 sieve and above acted as an indication of cement fineness. Typical magnesian cements ranged between 7 and 24 percent retained on or above the #100 sieve. The fineness of lime cements ranged between 3 and 20 percent retained on or above the #100 sieve. The lime cements had a much broader range of fineness across different brands (Table 1), but were generally finer than those of the magnesian cements (Richardson 1897h).

2.5 Chemical composition and specific gravity

The chemical composition of natural cements varied greatly between different brands (Tables 2 & 3). The range of magnesia content varied about 3 percent to

Table 4. Comparison of magnesian and lime cements (data from Richardson 1897d, g, & h).

	Magnesian	Lime
Typical brands	Rosendale	Round Top, Potomac Valley
Heat of hydration	Low	High
Strength gain	Slow	Rapid
Initial	Low	High
Long term	High	Low
Resistance to frost	None	Some
Basic chemical composition	Average percent composition	
Lime (CaO)	37	42
Magnesia (MgO)	18	3
Silica (SiO ₂)	15	21
Combined alumina & iron oxide (Al ₂ O ₃ & Fe ₂ O ₂)	11	14
Sulfuric acid (SO ₃)	1	1

30 percent. Despite all materials being manufactured from limestone, the differences between the stones resulted in significant chemical and physical properties. For instance, magnesian cements typically had a percentage of magnesia between 15 and 27 percent (Richardson 1897g). The high amounts of magnesia created slower setting cements better suited to use in mortar for brick construction. For projects where the structure had to withstand early loading, faster setting cement was desirable. For these projects the lime cements were preferred, where the magnesia content was kept below 3 to 4 percent (Richardson 1897g). As per the actual amounts of magnesia present in typical magnesian and lime cements after burning, Table 3 provides a basic chemical composition of these cements.

The highest specific gravity of magnesian cements was about 3.04, slightly less than Portland cement. A typical range given of natural cements was between 2.70 and 3.04 (Richardson 1897g). The lower the



Figure 2. Tensile testing arrangement (Skempton 2001).

specific gravity, the more water is needed to obtain the same strength as a mix of Portland cement with the larger specific gravity.

2.6 Physical properties

There is only limited performance data available on these historic materials, but critical physical properties that could be easily measured were tensile and compressive strengths.

2.6.1 Tensile Strength

Researchers at the end of the 19th century believed that the data gained from tensile tests were of greater value than that from compression tests, because the tensile test measured the weakest performance mode. Figure 2 is a schematic representation of a tensile testing apparatus. Briquettes of the material were cast in a form in the shape of a letter "I" and loaded along the y-axis. Typical tests included mixes of cement with only water (neat cement), and those with varying quantities of sand, cement, and water (referred to in the literature as part quartz concrete). The results in Table 5 were generated from a mix of 2 parts sand (quartz) and 1 part cement.

Generally, magnesian cements tended not only to gain strength at a much slower rate than lime cements but reached a lower final tensile strength a (Figure 3). Due to inherent inaccuracies with tensile testing, results varied greatly between technicians resulting in data sufficiently accurate for only general comparisons. Problems with this test included premature crack propagation at the corners of the briquettes and inconsistent testing briquettes both in concrete mixtures and shape (Cummings 1897d).

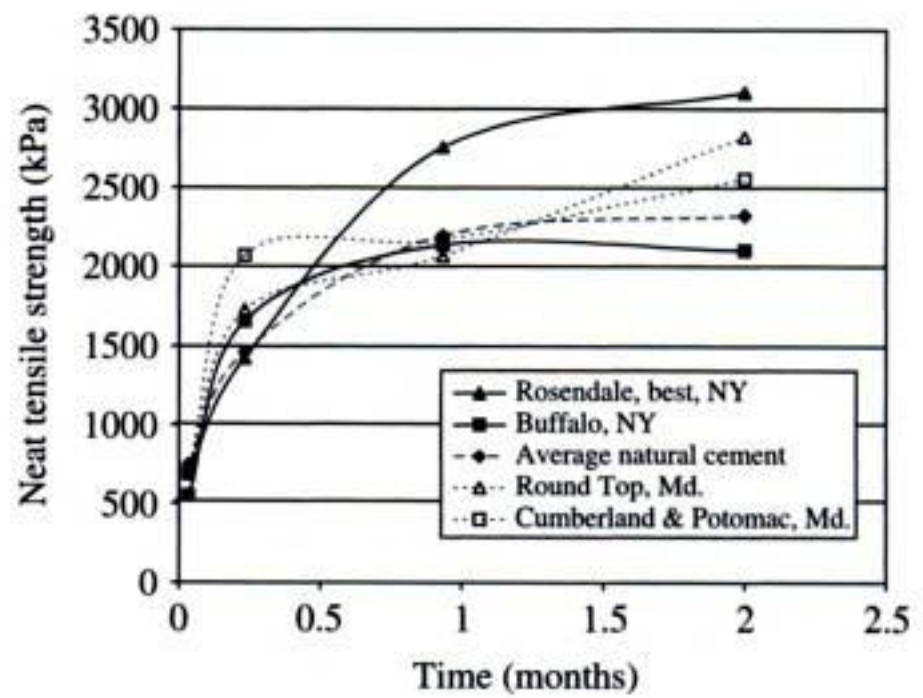


Figure 3. Neat cement tensile testing results from various natural cements (data from Richardson 1879h).

2.6.2 Compressive strength

In an attempt to further understand the properties of cements; compressive tests were conducted in a manner similar to the tensile tests. Several 7 day and 28 day results are provided in Table 5. As mentioned below, these tests are difficult to compare to compressive tests done today due to the different consideration of concrete mixes as being just sand, water, and cement. Although little testing information exists within the US, in Europe compressive tests were conducted on such historic materials (Skempton 2001).

2.7 Quality control

The quality control for natural cements consisted of visually spot checking the sprinkled burnt stone to ensure that most of it had slaked properly and that the ground cement in each barrel sold was properly blended (Richardson 1897g). These quality control measures for slaking and sieving were considered by many to be insufficient and eventually led to designers' distrust of natural cements for structural concrete. Many of the natural cements sold on the market at the end of the nineteenth century were considered too fast setting to be effectively used in structural concrete (Brooks 1911).

3 EARLY PORTLAND CEMENT

3.1 Brief history

Joseph Aspdin invented the first form of artificial cement in England in 1824. He ground and then burned limestone and clay in a kiln and found that the resulting mix acted as a hydraulic cement, which hardened with the addition of water (Skempton 2001). Eventually referred to as Portland cement, this material was first imported to the US in 1865, received a US patent

Table 5. Various physical properties of natural cements (data adapted from Richardson 1897h).

Type of natural cement	Brand	Neat tensile strength (kPa)						2 Part quartz tensile strength (kPa)***			Neat compressive strength (kPa)		2 Part quartz compressive strength (kPa)		Specific gravity		
		1 day	7 days	28 days	3 mos.	6 mos.	1 year	7 days	28 days	3 mos.	6 mos.	1 year	7 days	28 days		7 days	28 days
Magnesian	Rosendale, best, NY	689	1420	2758	3103	3151	3447	552	1034	1724	2551	3103					3.04**
	Rosendale, average, NY	517	1034	2068	2241	2586	3172	310	896	1448	1862	2344					3.04**
	Buffalo, NY	552	1655	2137	2103*	1999*	2386*	552	1048	793*	710*	669*			4826	6757	
	Akron, "Star," NY	772	2068	2206	2186*	2510*	2544*	745	1586	1048*	1027*	793*			4826	8963	
	Milwaukee, Wis.	827	1103	1613	2330	2255*	2565*	414	552	931*	1048*	1076*			3489	5667	
	Utica, Ill.	1310	1717	2317	1772*	1669*	1786*	814	965	1379	841*	924*			7412	9997	2.70**
Lime	Round Top, Md.	689	1724	2068	2827	3075	3627	841	1758	2358	2668	3551					2.84**
	Cumberland, Md.	689	2068	2586	2558	2710		1076	2048	2455	2413	3020					
	Cumberland & Potomac, Md.	689	2068	2172	2558	2710		1296	1551	2779	2737	3006					
	Antietam, Md.	448	1007	2068				483	855	1117	1558	1600					
Unspecified	Sherpherdstown, Md.	483	1103	2068				731	1448	1827	1937	2523					
	Louisville, "Anchor," Ky.	758	1531	2137	2255*	2537*	2868*	676	1048	758*	993*	1110*			3447	7343	
	Louisville, "Speed," Ky.	1241	1710	2717				496	1131								
	Sellersburg, Ind.	276	414	2206				207	896								
	Fort Scott, Kans.	359	689	1103				248	593								
	Double Star, Kans.	800	1448	2103	1903			786	1765	2744					2875	4688	2.79**
	Mankato, Minn.	1296	1641	2386	1786*	1931*	2199*	772	1103	827*	869*	1055			6812	10,135	
	Union, Penn.	1172	1586	2586				1034	1724						3964	5750	2.81**
	Improved Union, Penn.	965	1510	2165	2234	2737		1000	1593	2041	2475	2758					
	Anchor, Penn.	1034	2068					621									
	Milroy, Penn.	345	1172	2758				483	1379								
	Utah	552	1407	1931	2689			359	1586	336							

* Data included in original table but from separate testing source.

** (data adapted from Richardson 1897g).

*** Cement mixer is 1 part natural cement to 2 part sand.

Table 6. Chemical composition comparison of modern and pre-regulated Portland cement (data adapted from Kostmatka 2002 & Skempton 2001).

Modern Portland cement			Pre-regulated Portland cement		
Primary compounds	Chemical formula	Modern Portland cement (%)	Primary compounds	Chemical formula	Early Portland cement (%)
Tricalcium silicate	3CaO-SiO ₂	50-70	Silica	SiO ₂	22-25
Dicalcium silicate	2CaO-SiO ₂	15-30	Lime	CaO	54-60
Tricalcium aluminate	3CaO-Al ₂ O ₃	5-10	Alumina	Al ₂ O ₃	6-9
Tetracalcium aluminoferrite	4CaO-Al ₂ O ₃ -FeO ₃	5-15	Iron oxide	Fe ₂ O ₂	4-8
Anhydrous calcium sulfate	CaSO ₄		Magnesia	MgO	1-2
Gypsum	CaSO ₄ -2H ₂ O				
Calcium sulfate hemihydrate	CaSO ₄ -1/2H ₂ O				

in 1871, was manufactured in the US in 1872, and first produced in excess of one million barrels in 1896 (Concrete 1909).

3.2 Manufacturing process

Portland cements were ground into a powder, burned, and then reground into a finer powder, unlike natural cements, which were burned in a kiln prior to grinding. Portland cements were also burned around 1700 degrees Celsius, a substantially higher temperature than the natural cements. With the firing temperatures at this level, tricalcium silicates and aluminates were produced, which affected the setting time and hydraulic bonding reaction (Kemp 2002). This process yielded a finer, stronger, and more consistent product (Skempton 2001).

3.3 Chemical composition and specific gravity

The tricalcium silicates are the primary bonding agents within Portland cement today, yet many of the chemical compositions for pre-regulated Portland cement existed in the same chemical form as natural cement (Table 6). For the past 100 years there have been important changes in the production of Portland cement. Where early Portland cement was typically burned once, modern Portland cement undergoes several complex processes including burning of the stone through a rotating kiln, the addition of additives, like gypsum, within the actual cement clinker to increase the consistency of the final product, and finally through a similar, but slightly more complex grinding process which produces an extremely fine powder able to pass through sieves that would retain water (Kosmatka 2002).

Regardless of procedures for the production of Portland cement over the decades, the specific gravity has remained relatively unchanged at 3.15, a value substantially higher than natural cements (Richardson 1897g); the higher specific gravity requires less water to generate the same strengths as those created with natural cements.

3.4 Physical properties

3.4.1 Tensile strength

Early Portland cements generated at higher tensile strengths than natural cements during the course of the first year, and thus were thought to be superior (Fig. 3). Yet, early tests also indicated that as Portland cement continued to age over a period of years, tensile strengths began to decrease, while those made of natural cement continued to increase in tensile strength up to 100 percent (Cummings 1897b).

3.4.2 Compression strength

Compressive strength tests of early American Portland cements are difficult to locate; however, many tests conducted in Europe on similar cements resulting in 28 day compressive strengths for 1:3 part cement to sand mixes between 5520 kPa and 19,300 kPa (Skempton 2001). Although data is difficult to compare across continents due to the differences in the native stone, the same general conclusions were found in the US, namely that even pre-regulated Portland cement was consistently stronger than natural cement. In 1916, Portland cement was advertised as being to develop equivalent strengths to that of natural cements in "leaner" mixtures meaning those with less water (Kidder 1916). As with modern concrete this offered many benefits including higher ultimate strengths and less likelihood for freezing during setting because of the reduced free water.

3.5 Quality control

The other difficulty in the period of cement is that at the end of the 19th century, demand for Portland cement often outpaced the production capabilities to generate a consistently high quality product. According to contemporary sources, manufacturers would often sell inferior cements as Portland cements, in order to make a profit. These inferior cements consisted primarily of ground clinker and improperly burned cement rock. Natural cement producers also sold ground, over burnt

stones as Portland cement, even though, as explained above, the process of production was distinctly different (Richardson 1897g).

4 COMPARITIVE ANALYSIS

4.1 Natural and early Portland cements

Distinctions between natural cements and artificial cements were based on the production processes for each. From the specific processes, the cements gained their chemical and physical properties. Natural cements utilized the inherent hydraulic bonding properties of limestone, whereas artificial cements increased the stone's bonding properties by increasing the surface area by grinding the limestone prior to burning and by increasing the burning temperature, therefore, allowing more of the quicklime to bond to available silica and form tricalcium silicate. This process produced a more uniform and consistent final product. The result was a larger initial tensile and compressive strength for Portland cements over natural cements (Fig. 4).

Eventually builders concluded that natural cements were unfit for construction. By 1909, textbooks claimed, "Natural cement is not suitable for concrete." (Concrete 1909). Natural cement production decreased 78 percent between 1903 and 1913, dropping from around 845,000 metric tons per year to 90,000 metric tons per year (Eckel 1928). Even as early as 1896, Portland cement production was approximately twice that of natural cement production in the US (Fig. 1) (Kemp 2002).

4.2 Pre-regulated and modern cements

The chemical and physical properties of pre-regulated cements between 1875 and 1909, a period when

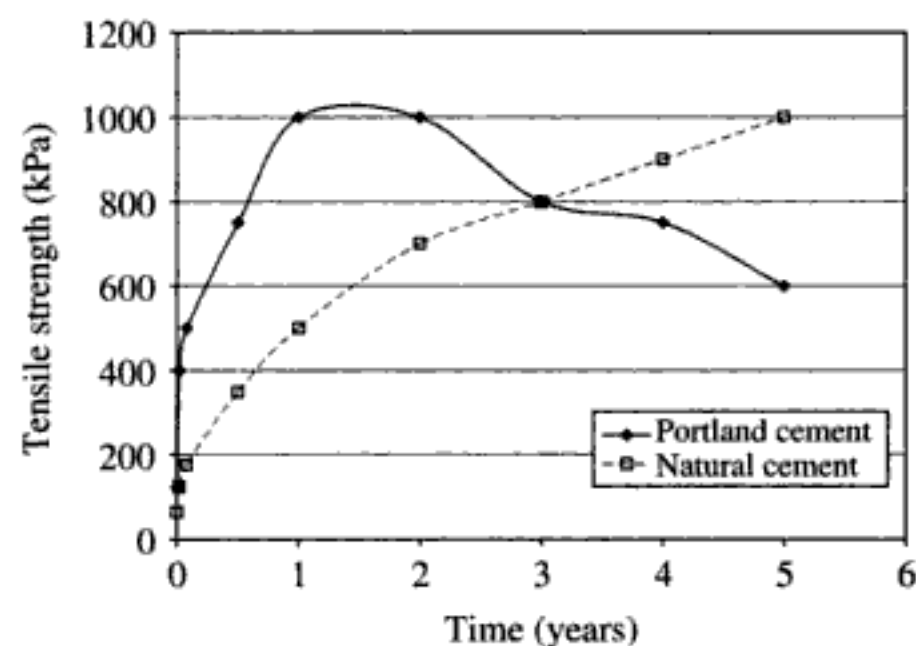


Figure 4. Tensile strength of Portland and natural cement over 5 years (Cummings 1897b).

reinforced concrete came into use, were inconsistent, varying in degree between the different types of cements and the different brands. Unlike modern cement, early cements rarely produced a concrete mixture with similar tensile and compressive strengths in testing briquettes and cubes. By the 1930s, the variability in setting time of natural cements eventually caused their demise. Portland cements of this period, although more consistent, still had flaws in the production procedure, namely with quality control. With the apparent variance in historic cements, modern engineers when confronted with such projects may consider coring multiple samples from various locations within a building that dates from this time frame to ensure an accurate prediction of the concrete capacity of the structure. Unlike today, where the production process for cements is heavily regulated by ACI, PCA, and ASTM, the late 19th century in the US can for all essential purposes be considered as unregulated.

5 CONCLUSIONS

Today's designers often mistakenly assume modern performance values for historic materials. Such a course of action may prove especially imprudent when evaluating buildings constructed with pre-regulated cements as the material did not consistently achieve 20,000 kPa. Adequate precautions should be taken when considering materials from this period.

REFERENCES

1909. *Concrete Construction About the Home and on the Farm*. New York: The Atlas Portland Cement Company.
- Brooks, J. P. 1911. *Reinforced Concrete – Mechanics and Elementary Design*. London: McGraw-Hill Book Company.
- Cummings, U. 1897a. American Cement – Chapter VII – Cement Testing. *The Brickbuilder*. 6(3): 55–57.
- Cummings, U. 1897b. American Cement – Chapter VII – Cement Testing. *The Brickbuilder*. 6(4): 76–78.
- Cummings, U. 1897c. American Cement – Chapter VII – Cement Testing. *The Brickbuilder*. 6(5): 100–101.
- Cummings, U. 1897d. American Cement – Chapter VII – Cement Testing. *The Brickbuilder*. 6(6): 124–127.
- Eckel, E. 1928. *Cements, Limes, and Plasters – Their Materials, Manufacture, and Properties*. New York: John Wiley & Sons, Inc.
- Kemp, E. L. 2002. Hydraulic Cement – The Magic Powder. In Bernard G. Dennis, Jr. et al (eds), *American Civil Engineering History – The Pioneering Years*: 273–319. Reston: American Society of Civil Engineers.
- Kidder, F. & Nolan, T. 1916. *The Architect's and Builder's Pocket-Book*. New York: John Wiley & Sons, Inc.
- Kosmatka, S. H. et al 2002. *Design and Control of Concrete Mixtures*. 14th Ed. Skokie, IL: Portland Cement Association.
- Ransome, E. L. & Saurbrey, A. 1912. *Reinforced Concrete Buildings*. London: McGraw-Hill Book Company.

- Richardson, C. 1897a. Characteristics of Various Brands of American Natural Cements. *The Brickbuilder*. 6(12): 280–281.
- Richardson, C. 1897b. Lime, Hydraulic Cement, Mortar, and Concrete II. *The Brickbuilder*. 6(4): 78–79.
- Richardson, C. 1897c. Lime, Hydraulic Cement, Mortar, and Concrete III. *The Brickbuilder*. 6(5): 101–103.
- Richardson, C. 1897d. Lime, Hydraulic Cement, Mortar, and Concrete IV. *The Brickbuilder*. 6(7): 151–152.
- Richardson, C. 1897e. Lime, Hydraulic Cement, Mortar, and Concrete V. *The Brickbuilder*. 6(8): 175–180.
- Richardson, C. 1897f. Lime, Hydraulic Cement, Mortar, and Concrete VI. *The Brickbuilder*. 6(9): 202–205.
- Richardson, C. 1897g. Lime, Hydraulic Cement, Mortar, and Concrete VII. *The Brickbuilder*. 6(10): 228–230.
- Richardson, C. 1897h. Lime, Hydraulic Cement, Mortar, and Concrete VIII. *The Brickbuilder*. 6(11): 253–255.
- Sabin, L. C. 1905. *Cement and Concrete*. New York: McGraw Publishing Company.
- Skempton, A. W. 2001. Portland Cements, 1843–1887. In Frank Newby (ed.), *Studies in the History of Civil Engineering: Early Reinforced Concrete*: 61–95. Burlington: Ashgate Publishing Limited.
- Turneure, F. E. & Maurer, E. R. 1914. *Principles of Reinforced Concrete Construction*. New York: John Wiley & Sons, Inc.

Study of Place Stanislas coloured pavement for its historical restoration

J.M. Mechling

Université Henri Poincaré – Nancy 1, Dpt Génie Civil – IUT de Nancy-Brabois, Villers-lès-Nancy, France

R. Elter

INRAP, Ludres, France

ABSTRACT: Listed as a World Patrimony by UNESCO, the Place Stanislas (Stanislas Square) in Nancy (France) was built in 1755. The ground of the Square will soon undergo a complete remodelling which aims at restoring it to its original glory. To prepare the project, a historical and geological study was carried. The research into the archives helped us to discover some unpublished documents. They present the initial state of the ground and appearance of the Square, previously unknown. They gave some valuable indications about the cobblestones (red and black limestones, layout, geometric design ... etc.) and information about the approximate cobblestone quarries. A geological study was necessary to define the nature and origin of the black cobblestones but doubt remains about the real coloured aspect of the red ones. Some chromatic analyses indicate that all the different red rocks likely to have been used relatively close to the same ochre brown colour.

1 INTRODUCTION

1.1 Stanislas Square origin

Listed as a World Patrimony by the UNESCO, Stanislas Square was built from 1752 to 1755 by Stanislas Leszczynski, former king of Poland (1677–1766). It is located south of the *Carrière Square* between the medieval town and the seventeenth century new town (Pfister 1974). The Square was named *Place Royale* until 1792 (French Revolution), to become *Place Stanislas* in 1831. The Square used to feature the statue of King Louis XV of France, Stanislas' step-son

but has since been replaced by a statue of the Polish King and last Duke of Lorraine.

1.2 Restoration goal

To celebrate the 250th anniversary of the Square's completion, the urban council of Nancy and its agglomeration are undertaking a complete remodelling of the Square which aims at restoring the original ground and the vicinity of the Square. The current weight constraints used for a public square have to be respected (pedestrian space with some occasional heavy weight



Figure 1. Actual aspect of the Stanislas Square (photography: Town of Nancy).

vehicles passages for special events that demand bleachers or stands, tents, etc.). The Chief Architect at Historical Monuments is supervising the project. A study of the archives has been conducted to prepare the ground restoring project.

The aim was to discover documents about the original pavement. Search has to be conducted by a geological study to detail the different aspects and colours of the pavement mentioned in the archives.

2 NEW HISTORICAL DATA

Until recently, the official known documents of the Stanislas Square didn't indicate the use of colour nor geometric design of the pavement. In May 2003, original documents were discovered in the Public Record Office of Nancy (Archives 1755). One of these documents, a quantity survey conducted by the architect to pay the pavers reveals the component and the exact geometric designs of the Square grounds at the time of its inauguration. Some contracts agreed with the pavers and the quarrymen gave information concerning the origin, the quality and the sizes of the cobblestones.

2.1 Geometric design of the square

The pavement was essentially red in colour, underlined with black cobblestones lines. The black cobblestones were located around the base of Louis XV's statue and along the square lateral gutters. They represented the four diagonals between the corners and the central statue (Fig. 2).

2.2 Quarries location

Other documents gave a wide range of information about the work order from the quarry to the grounds. The stones were all extracted from less than ten kilometres from the Square. They came from different local towns, *Art-sur-Meurthe* for the black cobblestones, *Dommartemont*, *Malzéville*, *Pixérécourt* and *Vandoeuvre* for the red ones. Today, these sites are too vast and contain different rocks than the past black and red cobblestones. Special geological investigations will be necessary (refer to below).

2.3 Cobblestones and characteristics of the builder's yard

The cobblestones were sized on the quarrying place. As shown in an agreement between the architect and the local paver *Jean Maizières* on July 15th 1754 and as found in the archives, the work had to be very precise. Indeed, the layout of the pavement prescribed a selection of cobblestones in the quarries;



Figure 2. A view of the Stanislas Square sourced from the painting of Pange. (Photography: Town of Nancy).

sizes had to be of approximately 0.25 to 0.29 m in length, 0.20 to 0.26 m in width and 0.26 to 0.29 m in high. They couldn't be sensitive to frost. Another document specifies the use of a good quality rock without imperfections particularly the clay beddings.

The cobblestones were carried to the builder's yard by the pavers (Archives 1755). Thereafter, the cobblestones were placed on a sand or gravel level with a disposition that allowed for crossed joints. The pavement was then covered with sand.

2.4 Remarks about this new documentation

Surprisingly, the documents found in the archives gave new information about the two colours of the pavement and their geometric designs totally ignored by the official iconography.

Only one painting, which can be seen in the castle of *Pange* (sixteen kilometres to the north of Nancy), shows how the cobblestones were installed (Fig. 2). Red and black cobblestones are visible as the black diagonals that leading to the corners to the statue of Louis XV. This pavement was preserved as far as the French Revolution. A new quantity survey from May 30th 1789 indicated that refection works were necessary (Archives 1789). They were eventually stopped by the Revolution. The monarchy marks as the statue disappeared in 1792. The first geometric pavement design to highlight the statue were changed and disappeared from the collective memory of the inhabitants.

3 FIRST GEOLOGICAL ARGUMENTATION

3.1 Nancy geological context

From a geological point of view, Nancy is located on the eastern fringe of the sedimentary basin of Paris. The town and its vicinity grow in a clayey dip, surmounted by a calcareous table-land and its residual hill, respectively to the west and north-east. A river *the Meurthe* runs inside the dip not far from Nancy's city centre. Local stratigraphy (dated from the Jurassic period) also shows two blocks. At the bottom the first layer (geological stages Hettangian-Sinemurian, Pliensbaschian, Toarcian) mainly contains clays with a few limestones and sandstones on 250 to 270 metres

high. The second layer (geological stages Aalenian and Bajocian) is a continual succession of several limestones lithofacies on 120 metres deep. The rocks susceptible to have been used for the pavement have to be found in some geological strong sedimentary beds in exclusion of too many clayey materials. These rocks must correspond to the initial colours criteria. Historical archives could help us to determine more precisely locations of ancient quarries.

3.2 Colours present in local lithostratigraphy

In this lithostratigraphy, we can effectively find again the different colours described in the historical written documents. The oldest sedimentary beds from Hettangian-Sinemurian, Pliensbaschian and Toarcian contain dark lithofacies of grey, blue-ish and black colours. With the exception of a particular limestone bank of a 1 or 2 metres thick, named *Calcaires ocreux*; initially black, it can progressively takes a rusty colour with the weather alteration.

Just above, Aalenian geological stage coincides with the regional iron ore well known as *Minette Lorraine* and extracted during the nineteenth and the first part of the twentieth centuries. Its petrographical aspects and colours do vary. In this geological sedimentary bed, shades encountered are caused by iron oxides variation and concentration. They can be grey, green, red, brown, with many sort of rust or orange shades (Bubenicek 1961).

Above, lower Bajocian allows calcareous rocks still containing a few iron oxides. The shades are therefore systematically ochre brown, rust or even red with a more or less grey colour adjunction. Local encrinitic limestone, *Calcaires à entroques*, is occasionally named red rock, *Roche rouge*, by quarrymen and geologists.

At the top of the local stratigraphic series, colours from the middle Bajocian are very different from the previous rocks. Shades are typically white-ish like the white oolite sedimentary bed, *Oolithe blanche*, or grey-ish like coral limestone, *Calcaires à polypiers*. These different specific colours are easily recognizable in the road slopes that climb the table-land over Nancy.

3.3 Preliminary results

The local towns of *Malzéville*, *Pixérécourt* and *Vandoeuvre* match the Aalenian and Bajocian geological stages, whereas *Art-sur-Meurthe* relates to the Hettangian-Sinemurian.

The comparison of these quarries coming from the different towns above named and as mentioned in the archives, with the first geological argumentation and the colour of their extracted rocks is consistent (Tab. 1) and allow us to make initial conclusions. Hettangian-Sinemurian limestones have been extracted for the

Table 1. Links between the Archives localities and the geological stages.

Stages	Petrography	Colours	Local towns
Mid. Bajocian	Limestone	White, grey	Malzéville Pixérécourt Vandoeuvre
Low. Bajocian	Limestone	Ochre brown	
Aalenian	Limestone	Grey Red, orange Brown Green, grey	
Toarcian	Marle	Dark grey Black Blue-ish	Art/Meurthe
Pliensbaschian	Marle/ Sandstones		
Hettangian – Sinemurian	Marlous- calcareous		

black cobblestones whereas Aalenian and/or lower Bajocian limestones have furnished red materials.

We have to complete these previous indications with some field observations to confirm the real aspects of the two sorts of cobblestones.

4 PETROGRAPHICAL ASPECTS OF THE COBBLESTONES

4.1 Black cobblestones

The case of the black cobblestones is simple because sedimentary bed *Calcaires à Gryphées* is the only one allowing black or dark grey limestone in the local stratigraphy. Furthermore, they could be no doubt about the black cobblestones origin as its presents in *Art-sur-Meurthe*, was mentioned in the archives.

Today, there isn't any quarry visible in this local area but archives also mentioned a special tenancy rental contract for the purpose of extracting those stones. The original cobblestones sources was about 30 cm cubic and covered approximately 7.5% of the Square (about 850 m² compared to 11300 m²) representing a total volume of 240 m³. A very small production of quarry was necessary for as the stripping and the waste rocks. At the end of the lease and the extraction being finished, farm cultivation replaced the quarry activity. Fifteen kilometres to the west, an important quarry is currently in use in this sedimentary bed by a cement company.

This *Calcaires à Gryphées* is an alternance of calcareous and marly banks of 10 cm to 60 cm high. Fossils (ammonites, ancient bivalvia like *Gryphea arcuata*) can be very abundant in particular places and the limestone characteristic aspect is generally constant. The stone texture sub-lithographic is very thin (Fig. 3) and therefore cobblestones are not very difficult to size. On the other hand, these limestones are generally a little clayey (about 5%) and also present some low resistances to the freeze and thaw action.



Figure 3. Aspect of the black limestone *Calcaires à Gryphées*, note the very thin texture (width of the field of view: 14 cm).

4.2 Red cobblestones

Find the original colour of the red cobblestones is more complex than for the black stones for two main reasons. At first, a red-ish colour could correspond to three geological calcareous sedimentary beds of geological stages Aalenian and lower Bajocian. Secondly the archives from the local towns previously mentioned report these three different red rocks sedimentary bed for systematic extraction. For each one, *Minette Lorraine*, *Calcaires sableux* and *Calcaires à entroques* we have to consider, petrography and colours of the limestones, aptitude for stone cutting and performances, and the eventual presence of historical quarries.

Minette lorraine (Aalenian):

In Nancy area, this formation is the only one that can have some really pronounced red colours among others like those previously named in Section 3.2. It's a set of carbonaceous (oolites, ossicles) or siliceous (quartz) detrital deposit, from 10 m thick. There is a high concentration of ferruginous minerals such as iron sulphurs (pyrite ...) and iron oxides (limonite ...). The rock cementation is made with carbonates (calcite ...) and ferruginous compounds.

Around Nancy, this sedimentary bed has been intensively and industrially used in underground mines and presents a characteristic microfacies of ferruginous oolitic limestone (Fig. 4). However these rocks are generally too clayey and have insufficient mechanical properties to cut cobblestones. Only a few blocks have been used in a wall of a mediaeval castle established at 40 km south of Nancy in the village of *Vaudémont* however nobody is aware of any quarry used for blocks extraction.

Calcaire sableux (lower Bajocian):

This geological level is defined by a thin ochre brown limestone layer that contains a variable quantity of

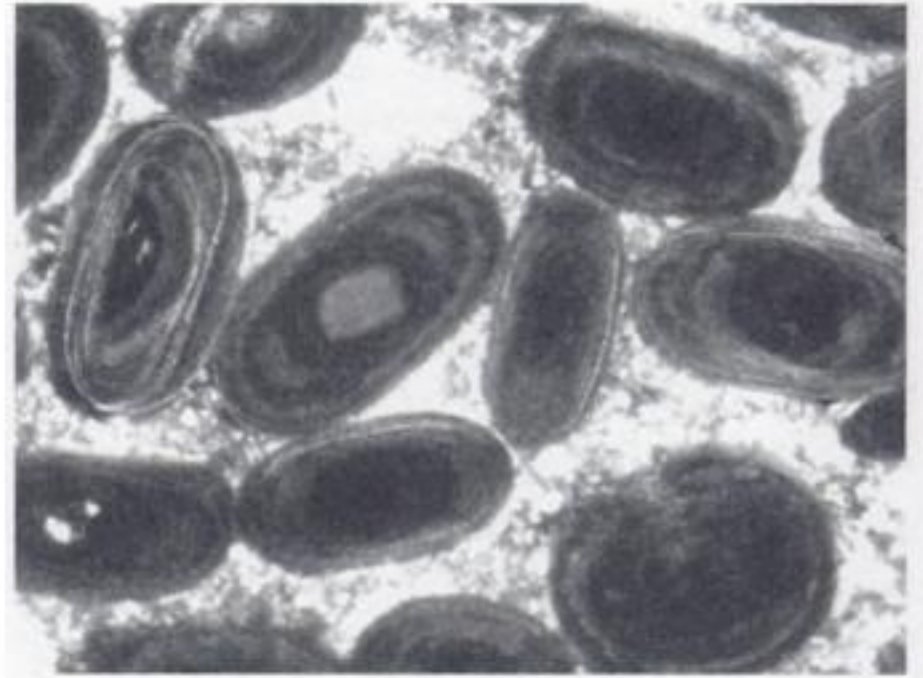


Figure 4. Microscopic view of the ferruginous oolites in *Minette Lorraine* (magnification: $\times 25$).



Figure 5. Homogeneous aspect of the *Calcaires sableux* (width of the field of view: 10 cm).

quartz grains (between 5 and 40%) and clayey minerals. Observed through a microscope, most of the others elements are bioclastic materials as fragments of echinoderme, serpula and small bivalvia wich are coloured in ochre brown. Their good wide spread among the rock combined to the iron oxides present in the carbonaceous cement, give a stable colour and aspect to the rock (Fig. 5).

In a lot of reefs, clays and quartz induce the formation of thin lamina (1 to 2 mm high), responsible of an important rock breakdown (Castaing 1972). In these conditions, a production of cobblestones is not easy and requires the selection of the most favourable banks of stone.

An ancient quarry is known in the local area of *Vandoeuvre* and is now used for modern urbanization.



Figure 6. Heterogeneous aspect of the *Calcaires à entroques*. Note the difference between the bottom part of the sample (grey limestone with many small blank ossicles) and the large red spot above (width of the field of view: 15 cm).



Figure 7. Relatively homogeneous appearance of the *Calcaires à entroques* presenting a thin spotty aspect (width of the field of view: 10 cm).

It may be possible that other ones existed and progressively disappeared for the same reason. We don't find any indication concerning their eventual location and period of activity.

Calcaires à entroques (lower Bajocian):

This sedimentary bed named, *Calcaires à entroques*, is immediately placed above the previous (*Calcaires sableux*). There is no real evident limit between those two calcareous layers and their aspects can sometimes be similar. Nevertheless, the frequently encountered rock is a massive encrinite as a result of an accumulation between marine animal fragments (ossicles) and cemented by calcium carbonates (calcite).

In the past, two ancient important quarries existed in this geological formation and are now localities, *Vandoeuvre*, and *Dommartemont*. The first one is located on a cadastral survey from 1805 (50 years after the ground edification) while the second was in use during the 14th century for the construction of a gate on *the Meurthe*. Our field observations especially

close to those two quarries have shown that encrinite usually have two coloured different aspects. The more common is a grey facies with red orange milimetrik or a couple of centimetres large spots (Fig. 6) caused by a high enrichment of iron oxides (limonite ...). But this limestone can regularly be more homogeneous with a very thin orange spotty aspect (Fig. 7). In this particular case, iron oxides are well scattered in carbonaceous cement and porosity from small size.

The sedimentary bed gives acceptably good mechanical properties but is not really suitable for a cutting. Actually many quarries uses this rock for crushed granulates generally used as seating of roads. From a normative aspect, impact strength (Los Angeles test, NF P 18-573) or attrition strength (Micro Deval test, NF P 18-572) present some moderate results (LA = 30 and MDE = 40) (Zennir, 1996). However those mechanical properties are better than those of the two previous formations (*Minette Lorraine* and *Calcaires sableux*) that are never used in the actual public works.

4.3 What does the red rock really look like?

It's very difficult indeed impossible to give the real aspect of the red rocks as simply named in the archives. In some cases, it can correspond to an unvarying rock aspect with a more or less pronounced ochre brown colour (*Calcaires sableux* and *Calcaires à entroques* in several banks). In some other cases, it corresponds to a spotty rock resulting from the combination of a greyish colour with red orange to rusty spots (*Calcaires à entroques*).

This first aspect is the same than the one represented on the painting kept in the castle of *Pange* (Section 2.4). Meanwhile, many ancient quarries would principally furnish the second aspect. The uncertainty persists.

In our historical remodelling, we can only define the prevailing colour of the different rocks and three corresponding facieses. During the initial ground edification, many quarries were used and most cobblestones had probably not the same aspect. We can estimate the total red cobblestones volume about 3200 cubic meters (92.5% from 11300 m², 30 cm thickness). This volume is too high for a constant production in those geological beds.

The lower Bajocian doesn't allow any good rock for quality building stones. As we can see in the next section, the mechanical properties of those limestones are not sufficient for actual technical applications.

5 SUBSTITUTION MATERIALS FOR THE RESTORATION

The use of the original black and red limestones raises a lot of issues for the remodelling of the Stanislas Square. We shall remember that the cobblestones were

carefully chosen before their use and despite those precautions, the original pavement was rapidly damaged (see Section 2.4).

In first instance difficulties appear into making the different cobblestones. It would be very difficult to dress cobblestones in the ochre brown limestone from the lower Bajocian, at reasonable cost. Furthermore, the existing quarries open in those limestones produce crushed granulates and consequently use a very different quarrying technique that the one used for the cutting stones. Furthermore, greater difficulties stand with regards to the durability of the cobblestones in relation to the weather or occasionally heavy weight vehicles circulation (special events, march past). Most of those limestones are easily cracked by the frost and show bad impact and attrition strength, except the encrinitic limestone, *Calcaires à entroques*, for acceptable characteristics. These limestones full of iron oxides would tend to change and generally become red with high temperature. At times, political demonstrations takes place on the Stanislas square and it is necessary to anticipate, an eventual fire started by the demonstrators and its consequences on the ground.

For those above reasons, the local authorities and the Chief Architect at Historical Monuments decide to choose stronger materials such as better quality limestones or siliceous rocks. These substitution materials will have to be in conformity with the norms and will have to match to the colour of the original pavement. The previous descriptions gave any qualitative colours descriptions that greatly depend on personal perception. To avoid this mistake, we carried some specific analyses: colour of representative samples had been measured with an accurate chromatic study.

6 COLORIMETRIC ANALYSES

6.1 Methodology

The colorimetric analyses were carried with two types of three dimensional colour spaces, *Lab* and *LCh*, defined by the CIE, *International Commission on Illumination* (CIE 1986).

CIE Lab system is the most commonly used colour space and is based on human perception of colour; the three colour receptors being red, green and blue in the eye. This result in three sets of signals are sent to the brain: light or dark, red or green, and yellow or blue. They are opposite meaning one receives a red signal or a green one but not both. This opponent type colour space is derived mathematically from the CIE values.

CIE LCh system is similar to the *CIE Lab* colour space, except that it describes the location of a colour in space by using polar coordinates, rather than rectangular coordinates.

L is a measure of lightness of an object, and ranges from 0 (black) to 100 (white). It indicates the reflecting properties of an object and also reveals its more or less dark surface.

a is a measure of redness (positive *a*) or greenness (negative *a*).

b is a measure of yellowness (positive *b*) or blueness (negative *b*).

C is a measure of chroma (saturation), and represents the distance from the neutral axis.

h is a measure of hue and is represented as an angle ranging from 0° to 360°. Angles that range from 0° to 90° are reds, oranges and yellows. 90° to 180° are yellows, yellow-greens and greens. 180° to 270° are greens, cyans (blue-greens) and blues. From 270° to 360° are blues, purples, magentas, and return again to reds.

6.2 The samples and results choice

Eight representative samples (noted A to B) were chosen in the different geological sedimentary beds having supplied the cobblestones. Most of those samples came from the reddish rocks (Aalenian and lower Bajocian) with reference to the problem of the red cobblestones. The black limestone has already the same aspect (colour and structure), so only one measure was necessary.

For each sample, a polished plane surface was made and several tests were carried on it. The above Tables 2a, b contains the obtained values.

6.3 Reading

At first, it is not surprising (but normal) to see a significant difference between the results of the black limestone (sample H) and those of the red ones. Parameters *a*, *b*, *C* and *h* respective values are -0.29, 0.45, 0.53 and 123.30, to 8.19, 17.90, 19.73 and 65.54 for the average values of the red rocks. On the other hand, it's difficult to clearly characterize the differences between the red rock sample values.

That is why we express ΔE_{ab} , the difference or the distance between two colours, in the *CIE Lab* system, with the above equation 1:

$$\Delta E_{ab} = \sqrt{(\Delta L)^2 + (\Delta a)^2 + (\Delta b)^2} \quad (1)$$

where ΔE_{ab} is the colours difference; ΔL the difference between the *L* values of the two different colours; idem for Δa and Δb , with *a* and *b* values.

From 0 to 1, the colours difference is tiny. If this value is above 3, the visual difference is not very flaggering. Beyond, the difference becomes more and more visible.

All the values between each pair of samples have been calculated and figured in the next table (Tab. 3).

Table 2a. Lab, Colorimetric results.

Sedimentary beds	Samples	Colorimetric analyses		
		L	a	b
<i>Calcaires à entroques</i>	A	52.43	7.49	17.69
	B	56.92	6.60	16.99
	C	51.53	6.22	14.52
<i>Calcaire sableux</i>	D	52.62	6.90	16.91
	E	53.59	8.52	20.28
<i>Minette</i>	F	45.72	10.04	21.85
	G	42.67	11.58	17.06
<i>Calcaires à Gryphées</i>	H	41.31	-0.29	0.45

Table 2b. LCh, Colorimetric results.

Sedimentary beds	Samples	Colorimetric analyses		
		L	C	h
<i>Calcaires à entroques</i>	A	52.43	19.21	67.06
	B	56.92	18.22	68.76
	C	51.53	15.79	66.82
<i>Calcaire sableux</i>	D	52.62	18.26	67.81
	E	53.59	21.99	67.21
<i>Minette</i>	F	45.72	24.05	65.32
	G	42.67	20.61	55.83
<i>Calcaires à Gryphées</i>	H	41.31	0.53	123.3

Table 3. Colour differences ΔE_{ab} between the different samples of red rock.

	A	B	C	D	E	F	G
A	0	4.63	3.63	1.00	3.02	8.30	10.60
B		0	5.94	4.30	5.05	12.70	15.09
C			0	2.71	6.54	10.10	10.66
D				0	3.86	9.04	10.99
E					0	8.16	11.78
F						0	5.88
G							0

At first, we can comment the results obtained between the samples taken in the same sedimentary bed. For the *Calcaires à entroques* (three samples), the values vary between 3.53 and 5.94. In the formations *Calcaires sableux* and *Minette Lorraine* (two samplings, each) the respective colour difference values are 3.86 and 5.88. The differences ΔE_{ab} are superior to 3 and some colour variations appear as it was described in the petrography (see Section 4.2). The smallest value, 3.86, corresponds to the *Calcaires sableux*, the most homogeneous sedimentary bed.

Regarding the values of the black limestones, *Calcaires à gryphées*, it is possible to take those results

Table 4. Average values for the two cobblestones colours.

Colour	Average colorimetric values				
	L	a	b	C	h
Red limestone*	53.42	7.15	17.28	18.69	67.53
Black limestone	41.31	-0.29	0.45	0.53	123.30

* limited to the *Calcaires sableux* and *Calcaires à entroques* sedimentary beds.

as a reference. Indeed we regard (see Section 4.1) this geological level as a homogeneous one.

Now we can compare the different colours differences ΔE_{ab} average values calculated between each formation. For the two sedimentary beds *Calcaires à entroques* and *Calcaires sableux*, the average difference is only 3.77. This value is approximately on the same scale of size that the ones previously obtained between the samples of an individual formation. We can then rely on the colours difference in and between those two sedimentary beds as equivalent. It is not the case with the *Minette Lorraine*, where the typical colours differences ΔE_{ab} vary between 8 and 15.

Summarize those colour analyses, we can note that the two sedimentary beds named *Calcaires à entroques* and *Calcaires sableux* are relatively similar. Their average parameters (Tab. 4) could be used as a colorimetric reference for the choice of alternative materials similar to the original colours of the Stanislas Square pavement. This colour represent a good arrangement as it takes in account most of the lithofacies that could be initially used on the eighteenth century. Whatever taken decision as whether to use a regular or a spotty ground aspect, the general new aspect will be relatively close to the historical colour.

7 CONCLUSION

Upon their accuracy the newly discovered archives completed with some geological investigations allow a real knowledge enrichment for the project and constitution specifications.

This study allows to find the historical red and black colours, the geometric design of the pavement as well as information about the growth and cobblestones hewing or installation. The original black limestones used for cobblestones are precisely defined while a small doubt remains between two adjacent sedimentary beds for the red cobblestones. The red colour that is in fact an ochre brown tone, could be from a homogeneous aspect or a fine spotty one. However, a careful observation of the colours linked with an accurate chromatic study (*CIE Lab* and *LCh* methods, reflexion spectrometry) indicate that all the different reddish rocks likely to have been used are relatively close in term of colour.

This research also gives a clear indication of the poor mechanical properties of the initial materials. Consequently, the shortly true historical restoration will have to use stones of greater quality that allow the elaboration of a pavement globally similar to the original one.

The conclusion of this study is useful and can be used as a basis for a new substitution materials choice.

REFERENCES

Archives 1755. *Série CC 630–691*. Public Record Office of Nancy.

Archives 1789. *Série AA n°15*. Public Record Office of Nancy.

Bubenicek L. 1961. Recherches sur la constitution et la repartition du minerai de fer dans l'Aalénien de Lorraine. *Annales de l'ENSG et du CRPG* tome 8: pp 5–204.

Castaing J. 1972. *Contribution à l'étude sédimentologique du Bajocien de la région de Nancy*. Ph-D Université Henri Poincaré, Nancy 1.

CIE 1986. *Colorimetry, Technical report 15.2*. Vienna: Bureau central de la CIE.

Pfister C. 1974. *Histoire de Nancy*. Paris: Berger-Levrault Ed.

Zennir A. 1995. *Bétons calcaires en Lorraine – Utilisation des granulats du Bajocien de Viterne pour la formulation de bétons courants*. Ph-D Université Henri Poincaré, Nancy 1.

Structural failure of historic buildings: masonry fatigue tests for an interpretation model

P. Ronca, A. Franchi & P. Crespi

Depart. of Structural Engineering, Politecnico di Milano, Milan, Italy

ABSTRACT: A better understanding of the mechanical behavior of masonry, considered as a material, under small variations of the remarkable sustained loads, needs, to clarify the real mechanism responsible of structural failures of historic buildings. Despite a number of analytical models, trying to describe the processes of damage accumulation in the long term, are available, however very few experimental tests have been done, probably because of the uncertainties and difficulties on choosing and controlling the leading parameters for the setting up the tests and for interpreting the related results. The present paper describes and comments the experimental tests and results on a number of small scale masonry specimens, with the intent to better understand the effect of repeated loads on the masonry strength. The damage accumulation due to repeated loads may lead to a better understanding of failure behavior of old massive masonry, like, for example, bell towers, high ditch walls, where the static capacity is stressed by average heavy load conditions.

1 INTRODUCTION

A better understanding of the influence of the so-called “long term actions” on old masonry structures is significant for the evaluation of static efficiency and safety of old historic buildings. The nowadays concerns on the conservation of historic heritage structures are motivated by some recent damages or collapses occurred to important monuments. We can mentioned either geometrical complex structures, like gothic or flat vaults, either geometrically more simplex structures, like bell towers; in both cases significant crack patterns, or even collapse, occurred, due to important shocks, like seismic action, or due to minor or even not manifest load perturbation. In the first case a number and relevant studies are available, concerning directly structures, structural elements or material samples generally tested following the LCF (Low Cyclic Fatigue) procedure (Carpinteri 1994, Calzona & Dolara 1996).

In the second case, the damage accumulation due to long term actions may be explained by different hypothesis, following, in any case, the mechanical behavior resulting from deformation and propagation of successive micro-cracks. As for a number of structural materials, even for masonry such a behavior is generally due to High Cycle Fatigue. The structural failure due to H.C.F. phenomenon may occur in the range of admissible loading conditions, therefore pretty insidious.

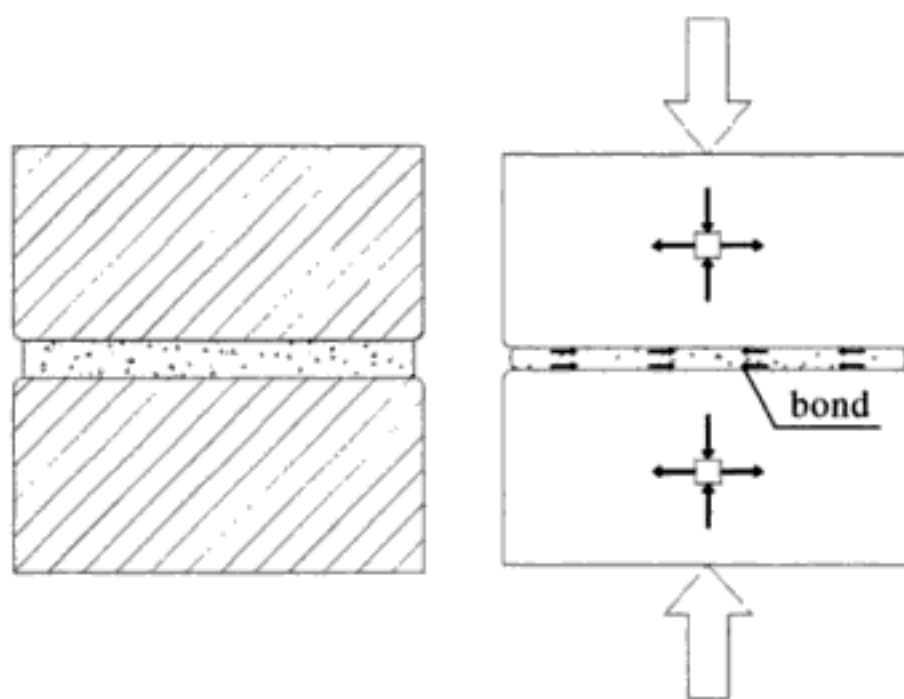


Figure 1a. Interaction mechanism between brick and mortar.

As a matter of fact, starting from the situation of internal micro faults of a fragile material (like in the case of old masonry), external actions inducing alternate loads, even of small intensity may produce a picture of micro-fractures, not stable in-time. It is known that, as shown in Figure 1a, the stress state in a brick depends not only by the loads, but also even by the interaction mechanism between brick and mortar, which may cause tensions of traction. The presence of even a micro-crack, due for example to imperfections

in the brick material, may be emphasized by this state of traction, as shown in Figure 1b.

The irreversible strains at the apex of fracture produce residual tensions, which are responsible,

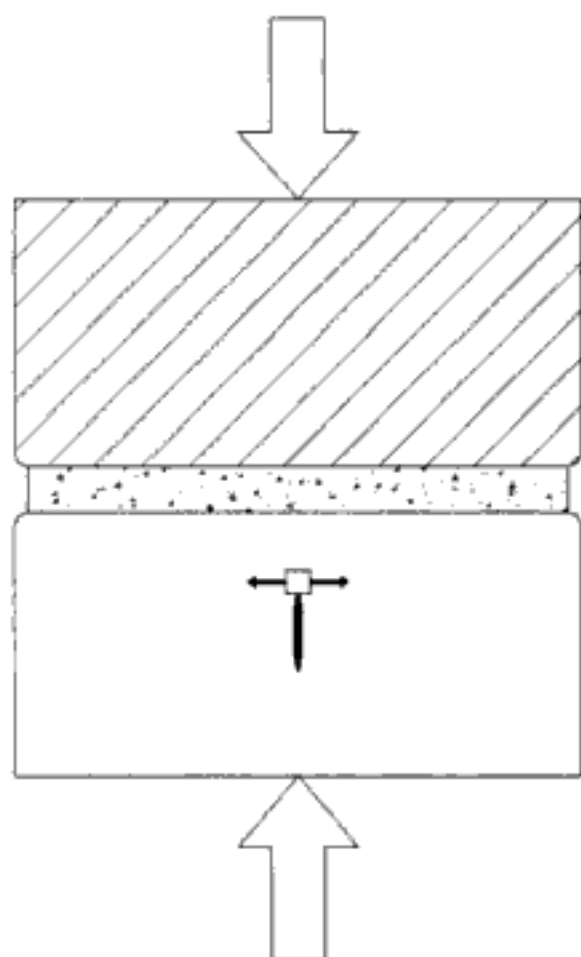


Figure 1b. Tensile tension due to micro-crack.

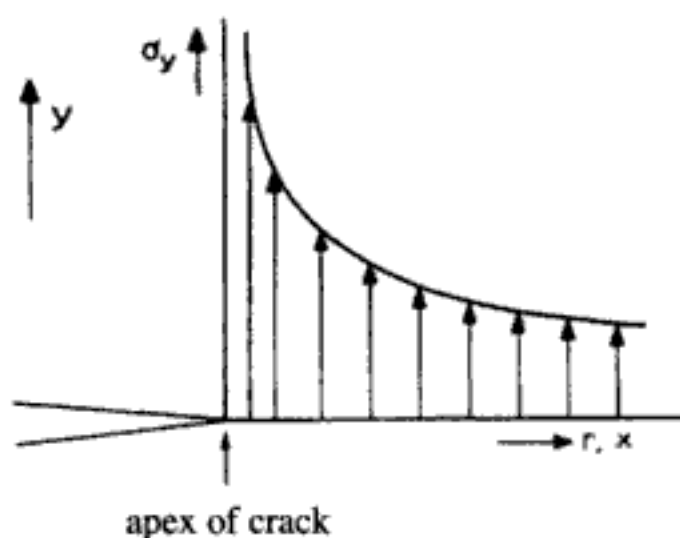


Figure 2a. Elastic stresses at the apex of crack.

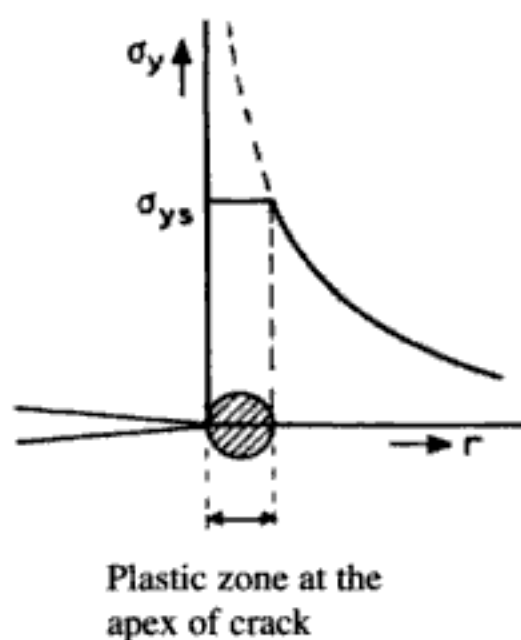


Figure 2b. Plastic zone.

during successive cycles, of the fracture propagation (Figs 2a, b). The propagation of the micro-fractures, in successive steps, may develop in a preferential direction, resulting in a real structural fracture and inducing a progressive failure mechanism.

The interpretation of structural failure of ancient masonry structures under loading conditions below limit loads has been recently studied with creep models and tested on samples under quasi-static sustained loads (Binda & Anzani 1993, Anzani et al. 1996, Edgell 1999).

2 PREVIOUS SIGNIFICANT STUDIES AND SCOPE OF THE PRESENT WORK

The scope of the present study is to better understand the behavior of the masonry materials under the two combinations of actions perpendicular to bed joints: sustained heavy load and high cycle alternating loads.

Significant researches on masonry fatigue tests are, among others, those published in (Naraine & Sinha 1988, Naraine & Sinha 1989, Abrams et al. 1985, McNary et al. 1984).

The papers Naraine & Sinha (1988, 1989) refer on tests performed on bidimensional samples. The definition of a model describing the stress-strain curve for a masonry under repeated load is explained, on the basis of experimental evidence. However, the research work is still on the range of low cycle compression loads, alternating from zero to the maximum established value. More significant for our purpose are the experimental studies described in Abrams et al. (1985), where a total of 120 stack-bond tests prisms with different mortar type were subjected to different combination of sustained alternating axial forces. On the basis of previous-studies (McNary et al. 1984), they assume that the behaviour of masonry under compressive stress is dependent primarily on the dilatants properties of the mortar.

However, the tests carried out in Abrams et al. (1985) on masonry samples are characterized by a very low frequency (0.1 Hz) and, consequently, a range of alternate loads pretty high (even up to the value of 40% of the ultimate stress). With this frequency/alternate loads combination the maximum number of 180 cycles have been stated. Significant elaboration of the test results are shown in Figure 3, where, for two different types of mortar, is obtained the "safe zone" for the combination "sustained load versus alternate load", i.e. the zone below the heavy line.

However, different parameters have to be stated during the project phase of a specific test programme on masonry samples subjected to high cycles fatigue loads.

Among these, it is important to state clearly either the material mechanical parameters and those parameters with particular significance for

clearly defining the validity of the test; in the case of high cycle compression loads, very significant parameters are: the frequency and the amplitude of the alternate applied loads.

Being the scope of our study to verify the behaviour of masonry with mechanical properties similar to old masonry, (i.e. mortar with low strength) under actions and conditions similar to that of old structure, we have chosen the following parameters for the elements: according to the Italian code for masonry structure (D.M. 20/11/1987) the class of used mortar is M4 (volumetric composition: concrete 1, hydraulic lime 2, sand 9) with a ratio water/concrete equal to 1.94; the average strength of used brick is 48.86 MPa; and the following parameters for our samples (more details can be found in Del Bono 2000): (1) average ultimate

strength of masonry of 10–13 MPa; (2) the magnitude of sustained load around 70–80% of the ultimate; (3) actions in the range of High Cycle Fatigue; (4) low value of compression cyclic loads (around 5–10% of the ultimate).

For this purpose 30 samples have been prepared, whose dimensions are shown in Figure 4. With the same material and procedure (Del Bono 2000), 5 samples have been prepared to check the monotonic resistance (see Table 1) and to obtain the average ultimate strength: $f_m = 12.84$ MPa.

3 DEFINITION OF HIGH CYCLE FATIGUE TEST PARAMETERS FOR MASONRY SAMPLES

The hydraulic dynamic press, available in the laboratory of Civil Engineering Department of the University of Brescia, has been used, as it is shown in the photograph of Figure 5 and in the scheme of Figure 6.

As mentioned before, we want to investigate the effects of a typical condition of historic masonry wall, generally subject to loading condition due to a permanent load not so far from the ultimate and an alternate load (due for example to traffic vibrations) variable in a small range. In these conditions, serious damages or even failure of the masonry can eventually occur with high number of cycles (much more than those performed in Abrams et al. 1985); the direct consequence of it is to assume higher frequencies for alternate loads. This aspect leads to problem of

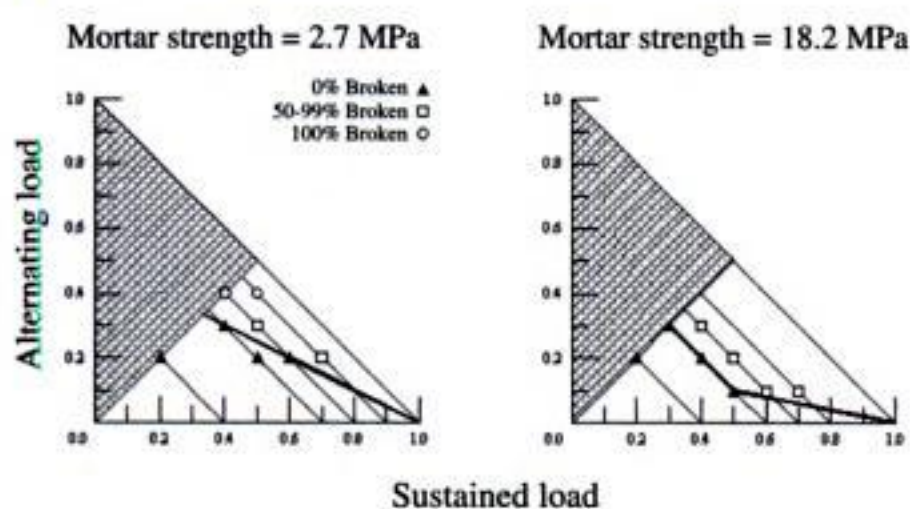


Figure 3. Summary of specimens results from Abrams et al. (1985).

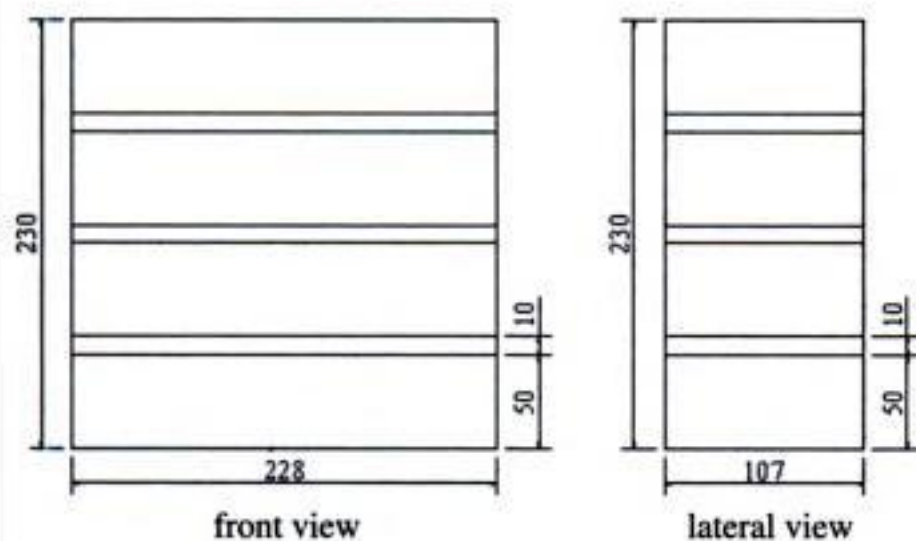


Figure 4. Dimensions of the specimens.

Table 1. Compression strength of the masonry samples.

Sample	Ultimate load (kN)	Strength (MPa)
1	245.3	10.05
2	339.4	13.91
3	310.5	12.73
4	274.7	11.26
5	331.2	13.58
Average	313.2	12.84



Figure 5. The hydraulic pulsar.

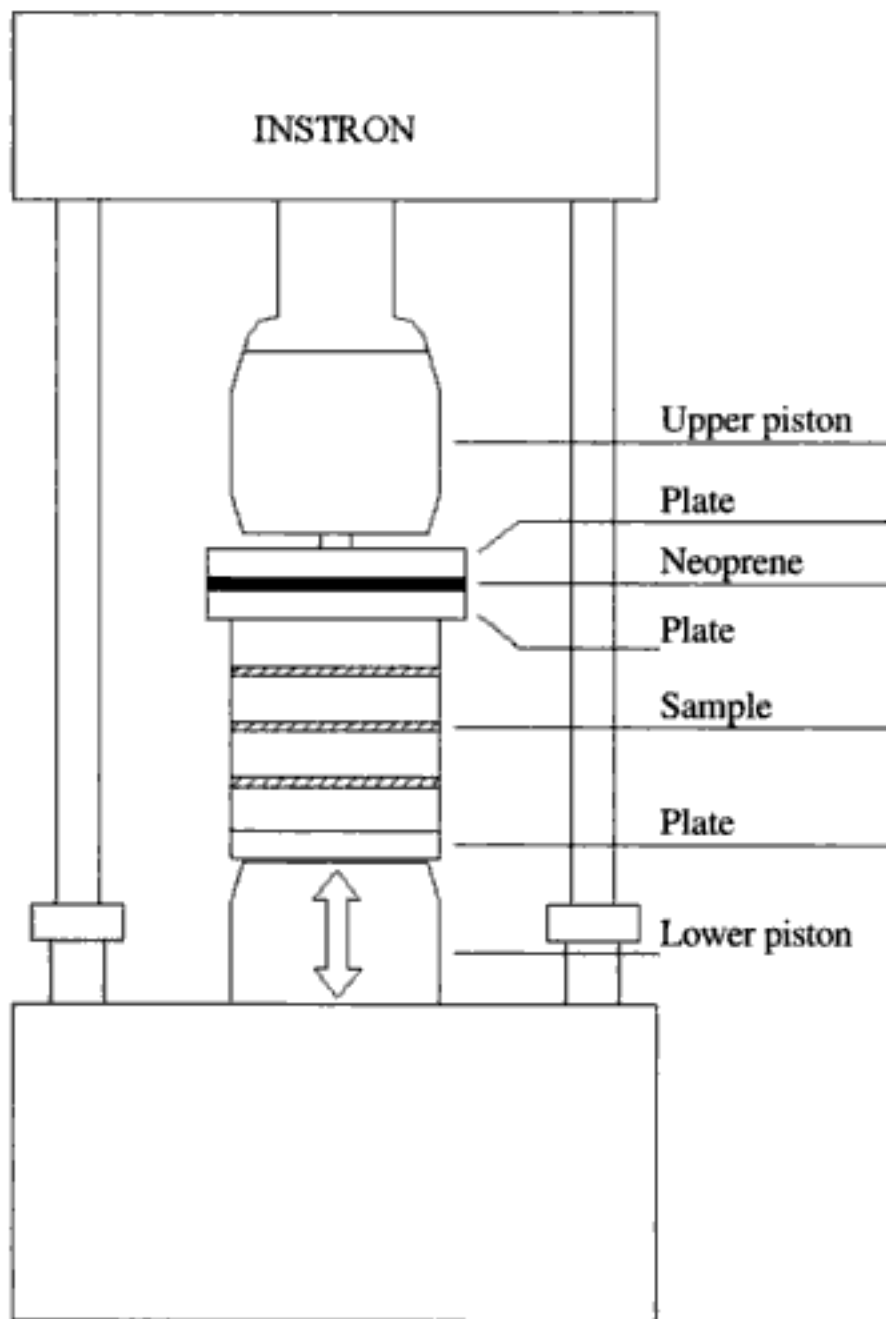


Figure 6. Sample and equipment for the test.

controlling the strain rate for fatigue tests on masonry sample. While for other materials (steel, concrete) curves relating the velocity of the alternating load and the deformation are available, in the case of masonry there are no specific studies and references. In this chapter the work done to establish a possible correlation frequency-deformation, at least for masonry samples of our dimensions will be briefly illustrate.

For this purpose tests on similar masonry samples have been performed, with the intensity of the permanent load corresponding to the 55% of the ultimate capacity of the example and the variation for the alternating loads of the 10% of the ultimate load. The variation of the alternating load have been imposed with three different frequency: 1, 5, 10 Hz. The tests have been stopped at 11600 cycles. The graph of Figure 7 shows the curves displacements-cycles for the 3 frequencies, and the Figure 8 shows the relative discretized curves. It is possible to note that the axial deformations grow up more in the case of 5 cycles/s.

More details on this preliminary checks are in Del Bono (2000). Having in mind to better understand the behaviour of old massive masonry (like for example in bell towers), we focused the attention on the behaviour of a group of examples loaded at 65% of the average ultimate load capacity and an alternating load of 10%

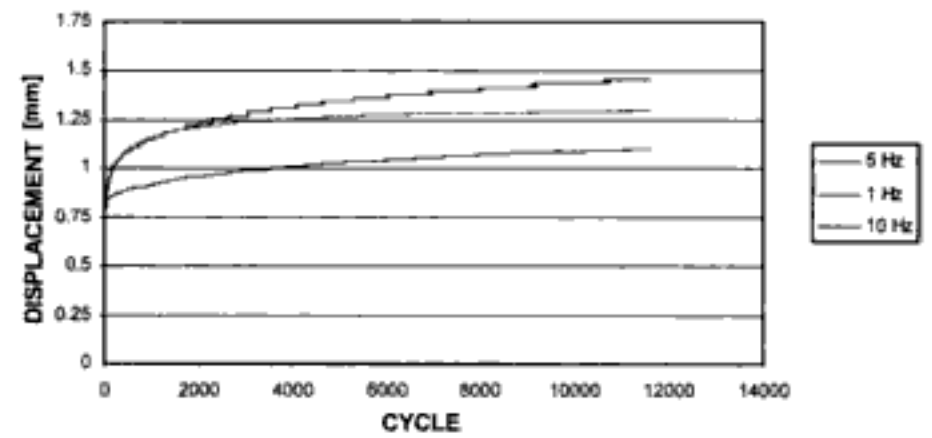


Figure 7. Cycles-displacements curves for the 3 samples (permanent load = 55% of ultimate; alternate load = 10% of ultimate load).

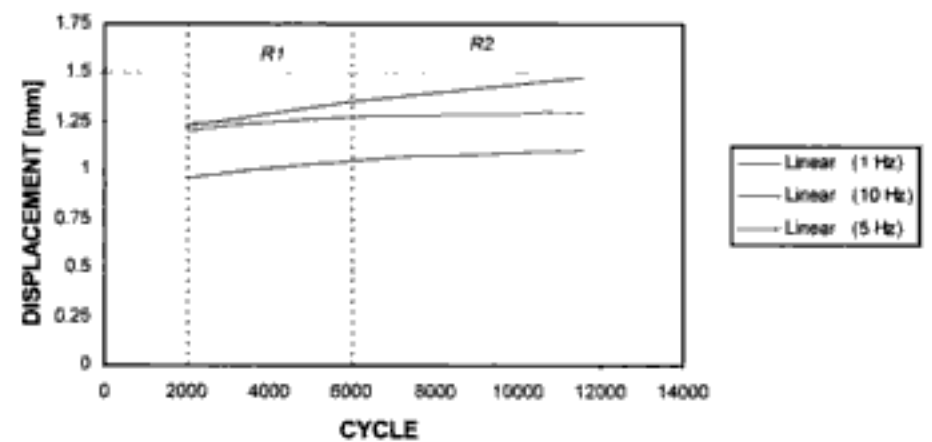


Figure 8. Linear representation for curves of Figure 7.

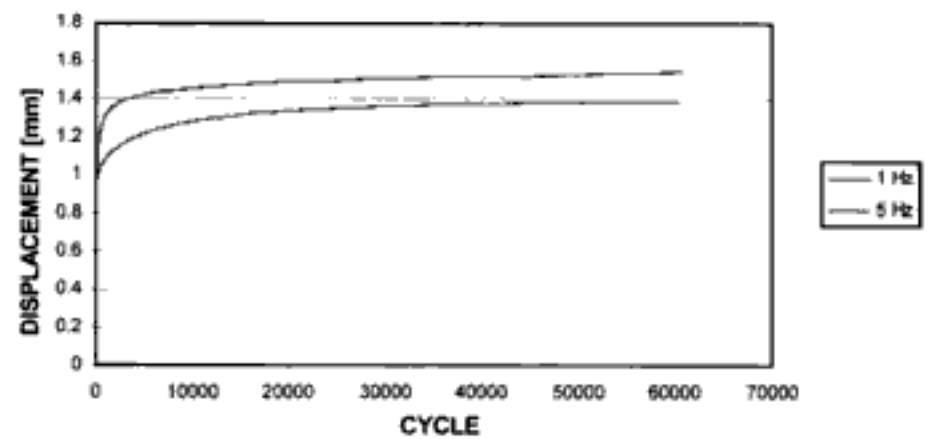


Figure 9. Cyclic test on two samples with permanent load of 65% of the ultimate capacity and the variable load equal to 10% of the ultimate.

(Fig. 9), with a rate of cycle of 1 and 5 Hz. In both cases, the strain-rate reach a stable behaviour after 30000 cycles, and the displacement seems to following linear growth.

After more checks, the overall behaviour of our samples seems to prove that, after a value of about 11000 cycles, the strain-rate (in the case of variable load, stated for our purpose, of 5–10% of the average ultimate load) is more sensitive to the different mechanical characteristics of the sample, than to the frequency of loading–unloading cycles.

4 COMMENTS OF THE RESULTS ON MASONRY SAMPLES

As already mentioned, the aim of the works is to clarify, by means of experimental tests, some question

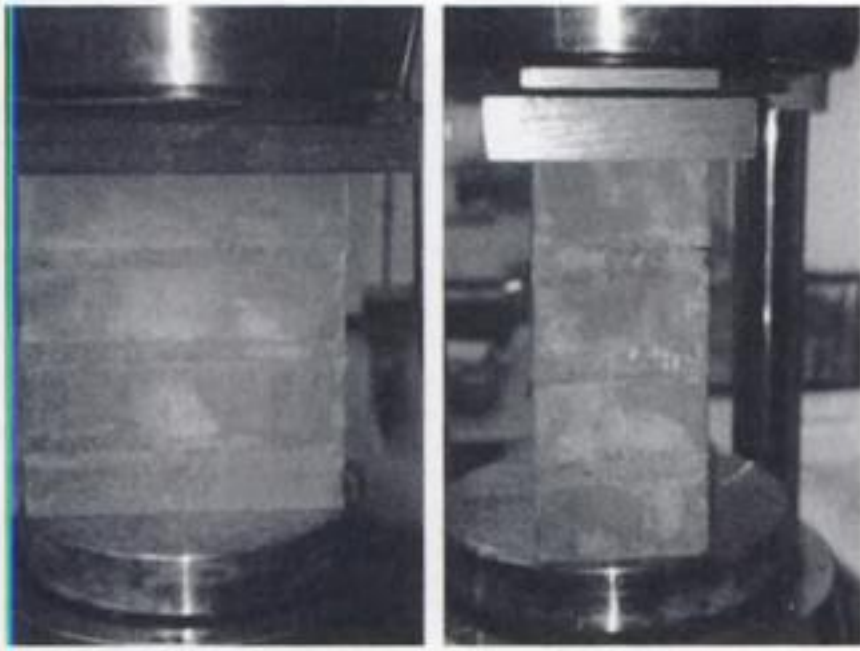


Figure 10. Frontal and lateral view of one of the samples.

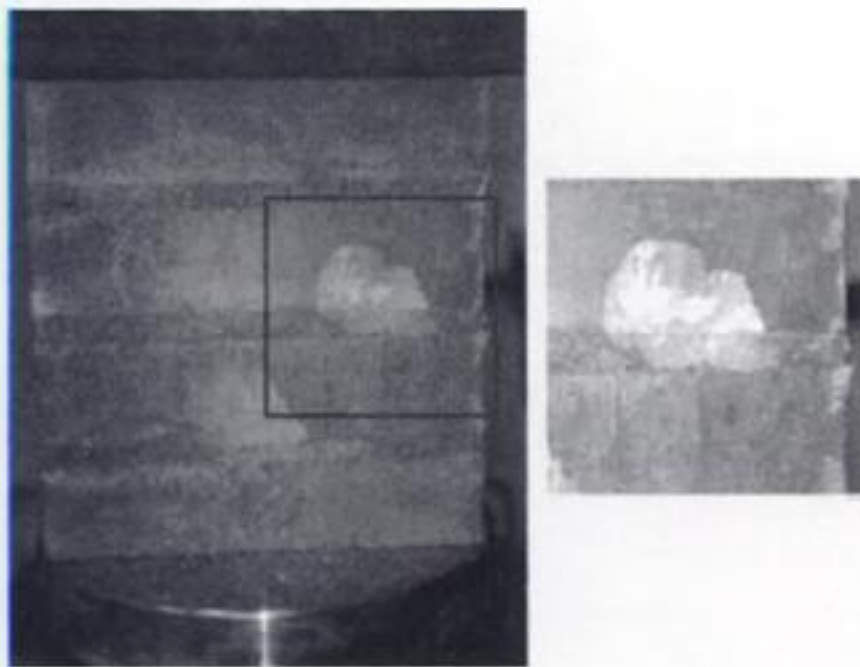


Figure 11. Frontal view of the sample after 24800 cycles.

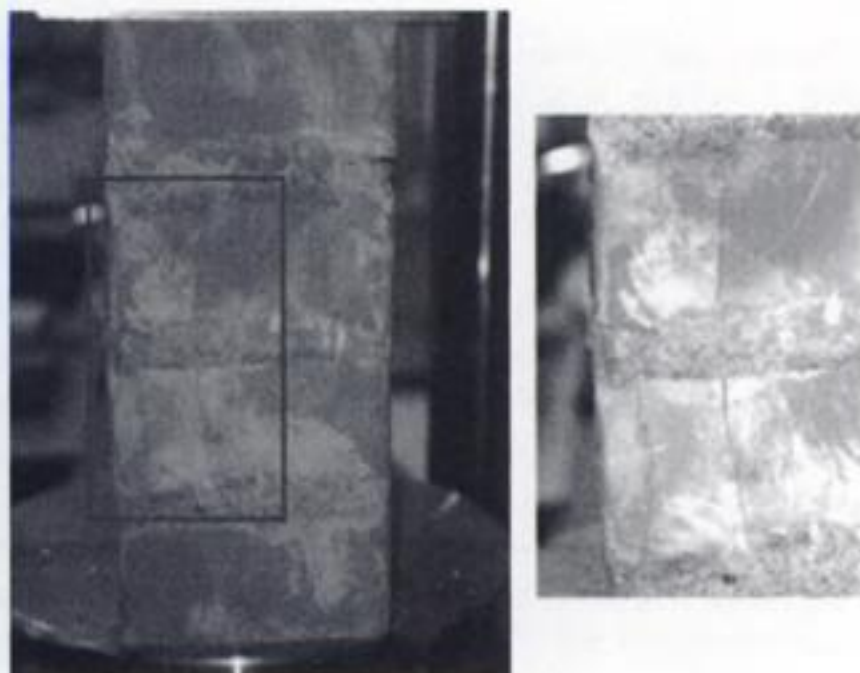


Figure 12. Lateral view and enlargement of the damaged zone after 24800 cycles.

typically regarding toll historical structures, like bell towers, on which the static actions are at quite high level and the alternating loads is a small variation of the ultimate average load capacity. An important question is if there are and which are the ranges of loads

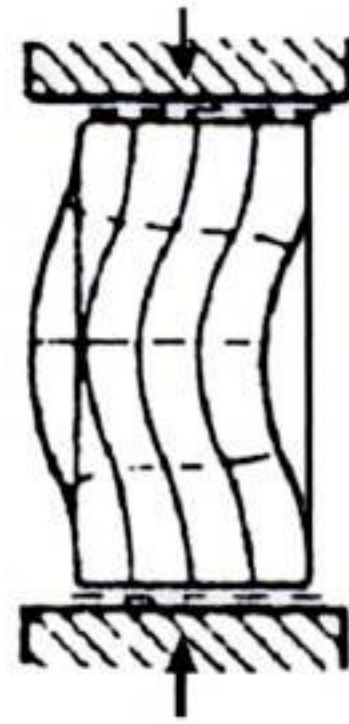


Figure 13. Hypotheses of collapse mechanism.

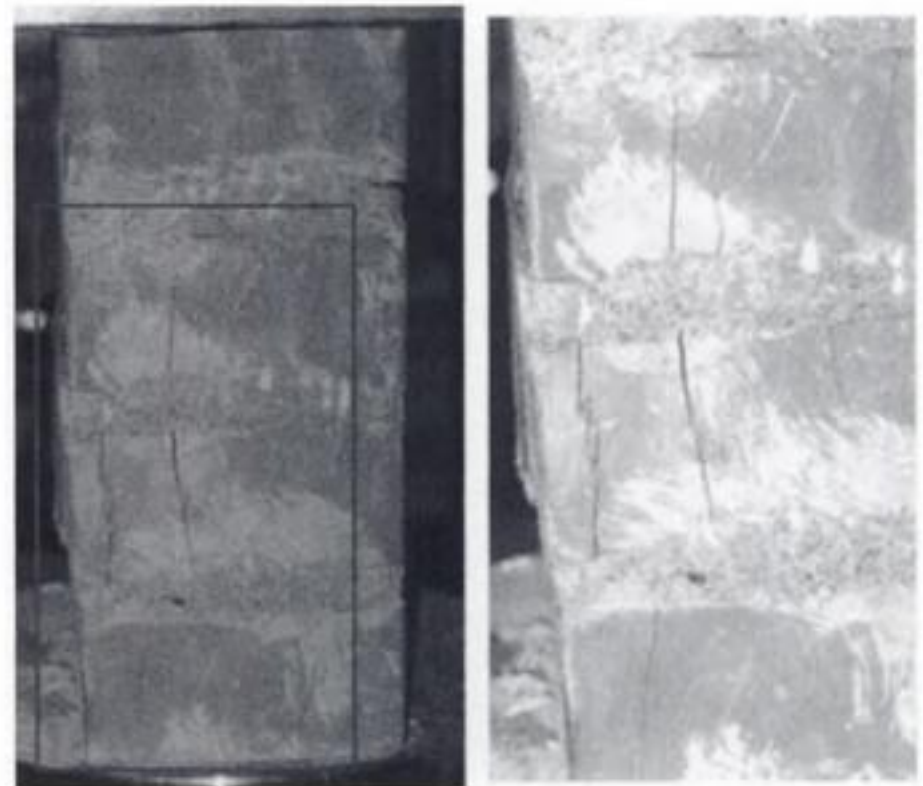


Figure 14. The sample after 105800 cycles (left side).

for which the masonry may be considered insensitive to a fatigue load history. For this purpose, after having defined the range of the strain rate for our samples, as mentioned in the previous chapter, we show here the results concerning samples loaded even at the 80% of the ultimate capacity with an alternate load of 5% of the ultimate load with the frequency of 1 Hz. The sequence of photographs of Figures 10–12 shows the progressive fatigue damages for a sample (in particular after 105800 cycles): it is possible, from the number and flow of the cracks to state an incipient failure mechanism as drawn in Figure 13. In Figures 14 and 15 the lateral displacement is also geometrically evident. After 135414 cycles a sudden failure of the samples occurred, with its explosion (Fig. 16). The duration of the test has been of 37 hours. Some other samples, in the same conditions did not reach the collapse after the same number of cycles.

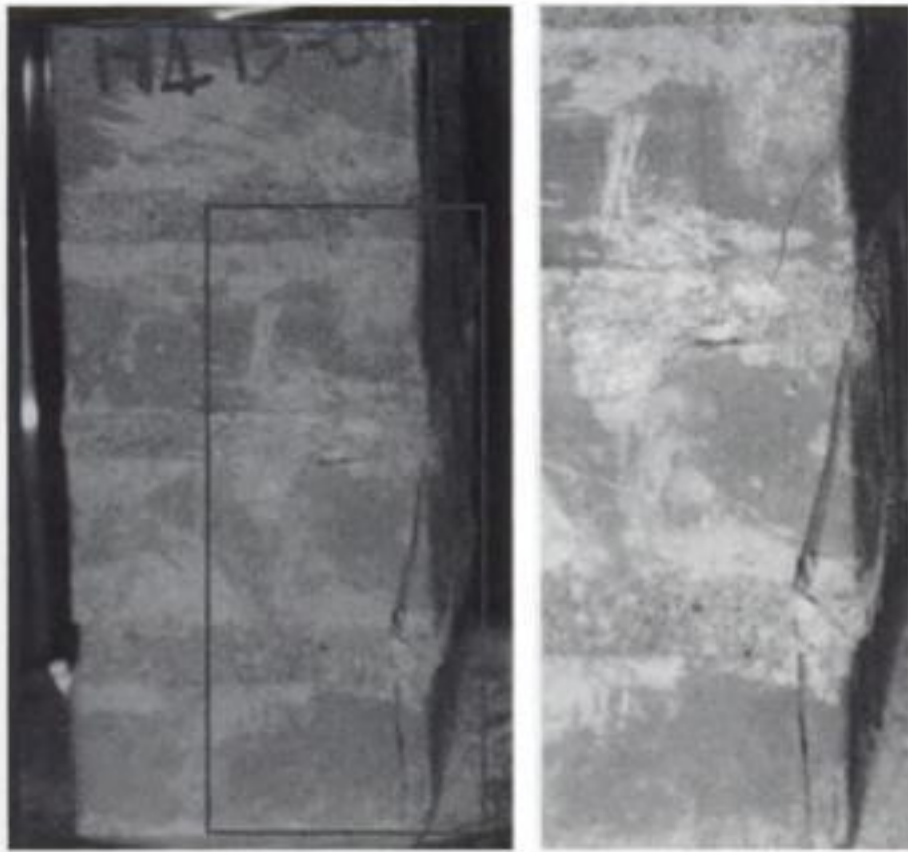


Figure 15. The sample after 105800 cycles (right side).

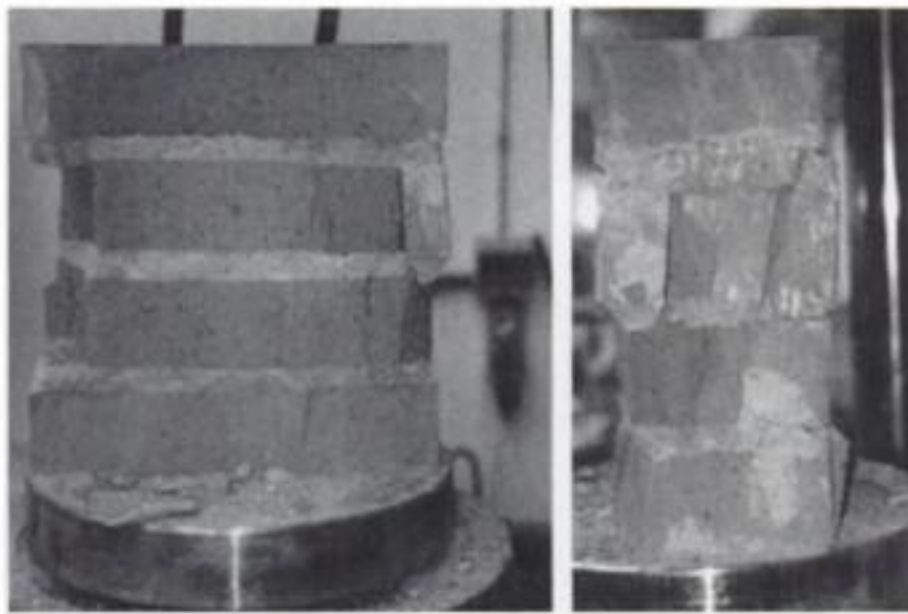


Figure 16. The sample after collapse (135414 cycles).

Table 2. Tests parameters.

N° of samples	S_m/F_c	$\pm S_a/F_c$	Frequency (Hz)
3	0.80	0.10	1
3	0.80	0.075	1
3	0.65	0.10	1
1	0.65	0.05	10

Successive tests have been conducted with different combinations: sustained load-alternating load-frequency.

Table 2 shows the parameters and load ratios chosen for the remaining groups of tests, being F_c the average collapse load, S_m the average sustained load, S_a the alternate load, f the frequency.

Table 3. Overall significant results.

S_m/F_c	$\pm S_a/F_c$	f (Hz)	Failure cycle (n°)	Maximum cycle (n°)
0.80	0.100	1	27	–
0.80	0.100	1	57	–
0.80	0.100	1	351	–
0.80	0.075	1	4838	–
0.80	0.075	1	221	–
0.80	0.075	1	39	–
0.80	0.050	1	135414	–
0.80	0.050	10	–	2500000
0.80	0.050	10	–	1000000
0.65	0.100	1	–	60600
0.65	0.100	5	–	65000
0.65	0.100	5	156007	–
0.65	0.050	10	–	220000

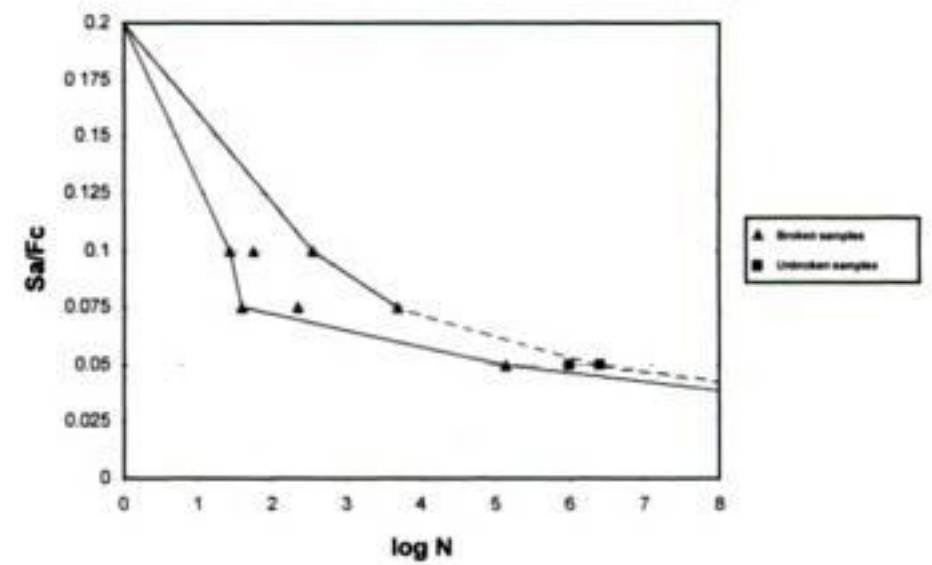


Figure 17. S-logN experimental diagram.

The overall significant results are summarized in Table 3, where it is possible to read the following indications:

- reducing the permanent load level to the 0.65 of the average ultimate load while maintaining the ratio S_a/F_c very low (0.10–0.075), the structural samples result in a more stable conditions respect to the samples with the ratio S_m/F_c of about 0.80. Under these conditions, the specimens seem insensitive to the fatigue action.
- Samples with a ratio S_m/F_c of about 0.80 reach the collapse with a very small alternate load, i.e. with a ratio S_a/F_c of ± 0.05 –0.075.

The number of the tests with the ratio $S_m/F_c = 0.8$, and related results, allow to trace and propose a curve S-N for the tested masonry samples, as shown in Figure 17.

Recalling the elaboration of the results of Abrams et al. (1985), and shown in the second chapter of this paper, we can complete the diagram adding our results, having used materials with similar mechanical characteristics (Fig. 18).

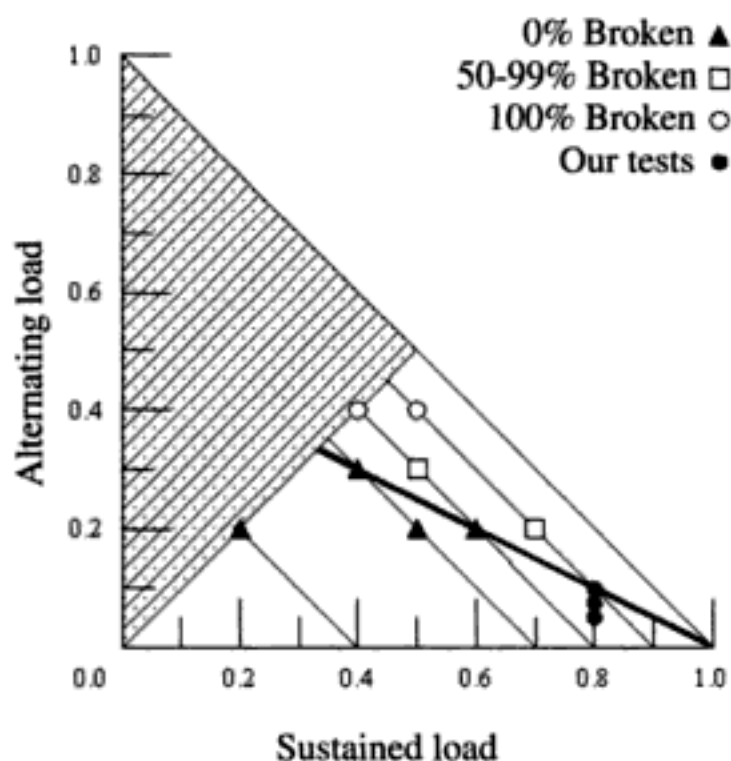


Figure 18. Abrams's diagram for masonry with M4 mortar.

5 CONCLUSIONS

The paper presents, describes and comments the experimental tests and results on a number of small scale masonry specimens, with the intent to better understand the effect of repeated loads on masonry structural strength.

A first group of specimens have been tested in order to assess the role of loading rate on the material response; a second group of specimens have been tested with the scope of deriving an S-N curve, having in mind in particular the situation of a masonry subjected to heavy sustained loads and small perturbations, mostly due to environmental conditions (traffic vibrations, differential thermal excursions, etc.). Failure mechanisms are pointed out and discussed; fracture mechanics principles helps to interpret the crack propagation in the brick element and possible arrest in the interface brick-mortar.

At this stage of the research, we are able to underline some overall physical behavior remarks:

- (1) Generally there are no splitting lesions on the frontal side of the examples.
- (2) On the minor side vertical cracks are better visible, which propagate with the cycles increasing.

These two points confirm the hypothesis of the formation of not stable micro rods between the cracks, especially on the weaker plane, i.e. the short side of the sample, with failure mechanisms similar to those shown in Figure 19.

The successive tests, done with similar conditions, but with $S_a/F_m = \pm 0.10$ (S_a = alternate load, F_m = average ultimate load capacity), have reached the

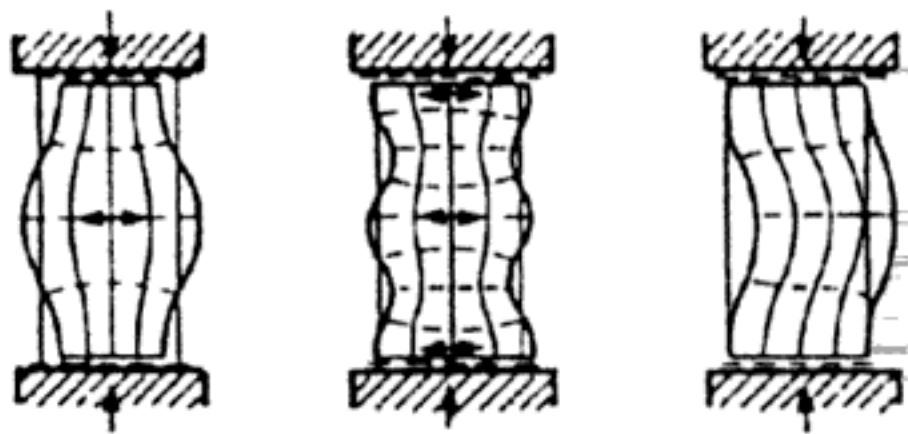


Figure 19. Hypotheses of failure modes (from Calzona & Dolara 1996).

collapse of all the samples with a very low number of cycles respect to the cycles necessary to reach evident damages (even if not collapse) in the previous groups of samples with $S_a/F_m = \pm 0.05$ (but all other conditions equal).

BIBLIOGRAPHY

- Abrams, D.P., Noland, J.L. & Atkinson, R.H. 1985. Response of Clay-Unit Masonry to Repeated Compressive Forces. *Proc. of 7th IB2MaC*. Melbourne.
- Anzani, A., Binda, L. & Melchiorri, G. 1996. Il Comportamento Dipendente dal Tempo di Antiche Strutture Murarie. *Atti del Convegno Nazionale "La Meccanica delle Murature tra Teoria e Progetto"*. Messina. Sett. 1996.
- Binda, L. & Anzani, A. 1993. The Time Dependent Behaviour of Masonry Prisms: an Interpretation. *J.T.M.S.*, 11.
- Calzona, R. & Dolara, E. 1996. *Fatica e Decadimento dei Materiali e delle Strutture Sottoposte ad Azioni Cicliche*. Università "La Sapienza", Facoltà di Ingegneria, Ed. Ferrocemento, Roma.
- Carpinteri, A. 1994. *Handbook of Fatigue Crack Propagation in Metallic Structures*. 1-2. Elsevier.
- Del Bono, I. 2000. *Comportamento della Muratura di Mattoni Sottoposti a Carichi Ciclici di Compressione*. Degree Thesis in Civil Engineering. Faculty of Engineering, University of Brescia. Italy.
- Edgell, G.J. 1999. Creep Eccentricity in Masonry: Review of Previous Creep Work up to 1995. *Masonry International*. 13.
- McNary, W.S., Atkinson, R.H., Abrams, D.P. & Noland, J.L. 1984. Basic Properties of Clay-Unit Masonry in Compression. *Proc. 8th World Conference on Earthquake Engineering*. S. Francisco. July 1984.
- Naraine, K. & Sinha, S. 1988. Test of Thick Masonry Models under Cyclic Compressive Loading. *Proceedings of the 8th IB2MaC*.
- Naraine, K. & Sinha, S. 1989. Loading and Unloading Stress-Strain Curves for Brick Masonry. *J. of Structural Engineering*. 115(10). ASCE.

Experimental investigation on masonry elements subjected to eccentric axial loads

L. Cavaleri, A. Failla, L. La Mendola & M. Papia

Dipartimento di Ingegneria Strutturale e Geotecnica, Università di Palermo, Italy

ABSTRACT: The flexural behaviour of masonry rectangular cross-sections is studied in order to characterize the mechanical behaviour of structural elements under axial eccentric loads by means of a proper law. First the experimental response of walls under vertical centred loads is observed and a stress–strain law depending on two parameters is given in order to fit the experimental results. Subsequently the behaviour of walls nominally equal to the walls mentioned before is investigated under eccentric vertical loads, and the response is observed in terms of moment–curvature relation. Then a comparison is made between the moment–curvature response obtained experimentally and the moment–curvature response obtained by means of the stress–strain law given, in the hypothesis of a plane strained section. Once the accuracy of the model is proved the limit domain of the cross-section is calculated in order to be used for practical applications.

1 INTRODUCTION AND STATEMENT OF THE PROBLEM

In masonry buildings vertical loads are often transmitted to the walls eccentrically and sometimes due to thrusting elements or seismic events horizontal loads are also applied. In some cases, due to the low level of the constraint with the transversal ones or because of the high ratio between the distance of the lateral constraints and the height of the wall (Fig. 1-a), these walls can be considered as one-dimensional elements (Fig. 1-b) whose response can be simply predicted if the limit conditions of the cross-section of the wall are known.

Referring to the problem of the identification of the cross-section behaviour under eccentric loading, few studies can be found in the literature. Further, experimental works are mainly addressed to the characterization of the stability of slender elements made of clay blocks (or bricks) and mortar, and not always devoted to the definition of analytical tools for the identification of the limit condition of the cross-section.

Yokel (1971) studied the stability condition of members made of material without tensile strength, giving the limit conditions for those members. In his work a linear behaviour is hypothesized for the material that can be proper for very slender elements in which failure can be reached before the material can exhibit a non-linear behaviour but may not be proper for not very slender elements. A similar study was carried

out by Schultz et al. (2001) considering the additional effect of laterally distributed loads.

Drysdale & Hamid (1983) analysed the behaviour of small walls constituted by different types of concrete blocks and mortar in order to observe the failure modes and specifically the effects of the eccentricity of the load on the failure modes with respect to the case of a centred axial load. A similar investigation was carried out by Hatzinikolas et al. (1980) basing on solid concrete blocks. In each of the two cases the problem was not analytically treated.

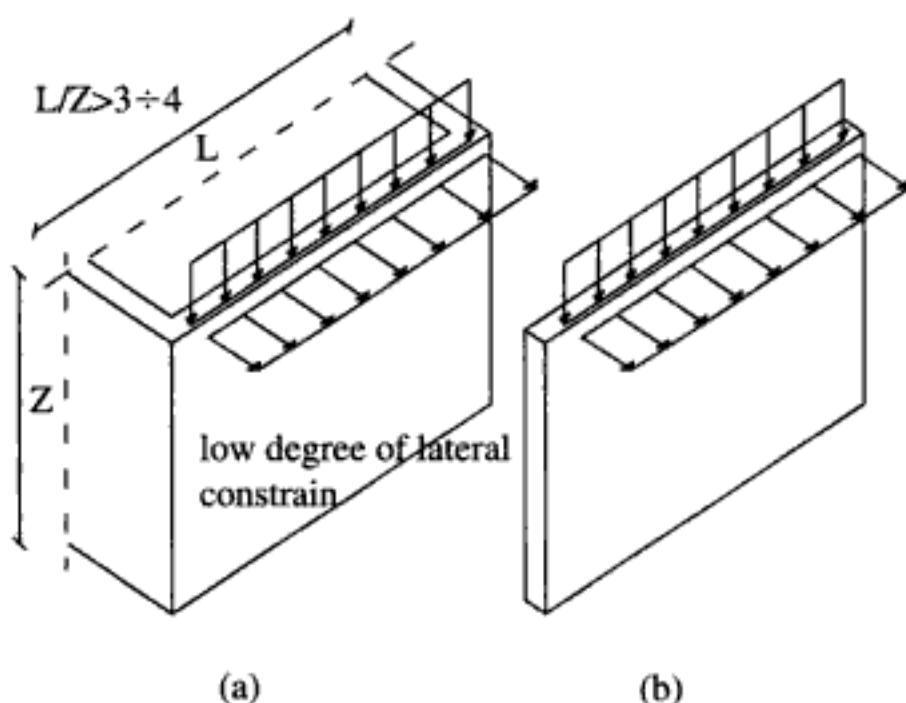


Figure 1. Examples of tridimensional (a) and plane (b) schemes for analysis of walls.

Cantù (1982), basing on an experimental investigation and an analytical one, tried to determine the moment–axial load limit domain for walls under eccentric loading. In this case the masonry was made of hollow clay blocks and mortar.

Crook (1982), basing on five types of solid and hollow concrete blocks, observed the failure mechanisms of walls under an eccentric axial load, identifying some key parameters.

Furthermore, analysis of the works mentioned and of some others not specifically commented on here (e.g. Macchi 1982, AlShebani & Sinha 2000), highlights the fact that concrete block and clay block masonry is considered in the greatest number of cases while calcarenite block masonry, which represents the most diffused masonry in the Mediterranean area, is not investigated so much.

In this context an experimental study was carried out and an analytical law was formulated for the behaviour of the cross-section of walls made of calcarenite masonry under bending moment and compressive forces basing on the non-linear behaviour of the material evidenced by the experimental tests.

Firstly, masonry specimens were tested in compression and the stress–strain law for the material was identified. The same law was subsequently used for obtaining the limit domain compressive axial force–bending moment for the cross-section basing on the hypothesis of a plane deformed cross-section. This hypothesis was verified comparing the experimental response obtained from specimens eccentrically loaded with the analytical response of a section, nominally equal to that of the specimens, under the same loads, obtained by using the non-linear law mentioned before, as will be better explained in the next sections.

2 EXPERIMENTAL INVESTIGATION

2.1 Test specimens

Three-layer walls were considered that were 520 mm high, 360 mm wide and 205 mm thick. The geometric characteristics are shown in Figure 2.

Calcarenite blocks from a Sicilian mine were used for the resistant elements while mortar was used for the vertical and horizontal joints. The mortar was obtained by combining the following volumes: 1/7 cement, 1/7 hydraulic lime and 5/7 calcareous sand; water was added to the mixture in such a way as to maintain the water-binding ratio equal to 0.5 (by volume). The vertical and the horizontal joints were 10 mm wide.

The mechanical characteristics of the mortar and of the calcarenite were measured by proper tests. For the mortar the compressive strength was obtained by using cubic specimens having 100 mm sides, while the compressive and the tensile strength of the calcarenite

were obtained by using cylindrical specimens having 100 mm diameter and 200 mm height. For the evaluation of the tensile strength the Brazilian test was performed. In Table 1 the mean values of the above mechanical characteristics evaluated on 10 specimens are summarized.

2.2 Test program

Two kinds of tests were carried out under compressive force. In the first case force was centred in the section while in the second case eccentric force was applied with different levels of eccentricity. Specifically three value of eccentricity were considered along the thickness of the specimen: 35 mm, 50 mm and 60 mm. The number of specimens tested in each case is summarized in Table 2.

2.3 Test setup

The tests were executed by two different types of devices. For the centred compression tests a hydraulic

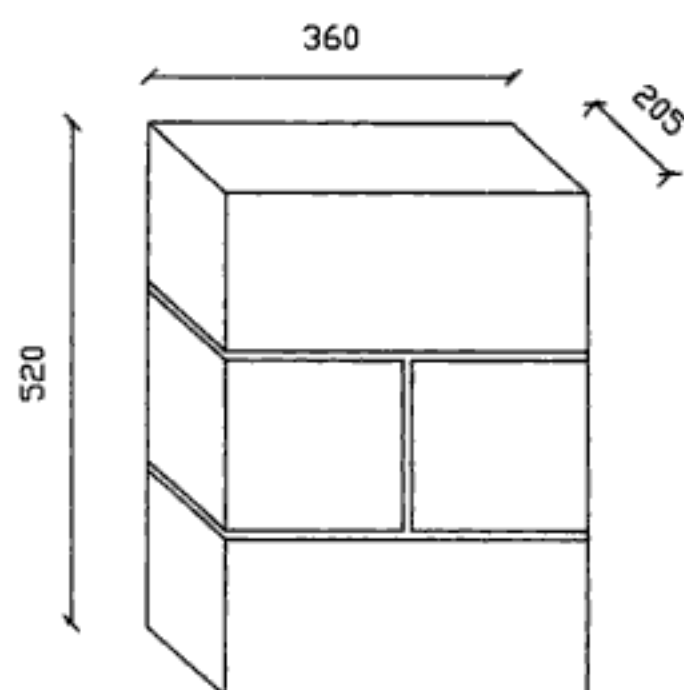


Figure 2. Test specimen.

Table 1. Mean mechanic characteristics of the masonry components.

	Compressive strength (MPa)	Tensile strength (MPa)
Mortar	5.9	–
Calcarenite	7.06	0.99

Table 2. Number of specimens and type of test.

Eccentricity (mm)	Number of specimens
0	6
35	4
50	4
60	4

press was used in displacement control having a 600 kN nominal capacity. On the top of the specimen a rigid beam was placed in order to ensure the spreading of the load. On each specimen four digital transducers were applied symmetrically (two for each of the longest sides) for measuring the shortening on a basis of 350 mm (see Fig. 3). The accuracy level of the transducers was 0.001 mm. The level of the force was measured by means of a loading cell located in the press. In Figure 4 the specimen in the loading machine is shown.

For the tests under eccentric loads the same press was first used in agreement with the scheme described by Cucchiara et al. (2003). Nevertheless, the test was repeated with the device described in the next paragraphs having a capacity to follow the rotations of the cross-section, near to the collapse condition, better than in the previous case. In this way a longer post-peak branch of the moment–curvature response was obtained for each specimen and reliable data about the ultimate curvature was obtained.

Hence, for the tests under eccentric loads a horizontal screw jack was used for the application of the load. In order to simulate a vertical eccentric load the specimen was rotated 90 degree with respect to its natural position.

The specimen was supported by a horizontal plate and properly contrasted along the horizontal direction. Between the plate above and the specimen a layer of sand was set in order to reduce the friction produced by the specimen's own weight.

The deformations of the specimen were monitored by means of the instrumentation shown in Figure 3. Between the screw jack and the specimen a load cell was placed for measuring the force. Furthermore, a plate connected to a T-shape steel element was inserted between the specimen and the load cell in such a way that the plate could transversely slide with respect to the T element for the application of the eccentric load.

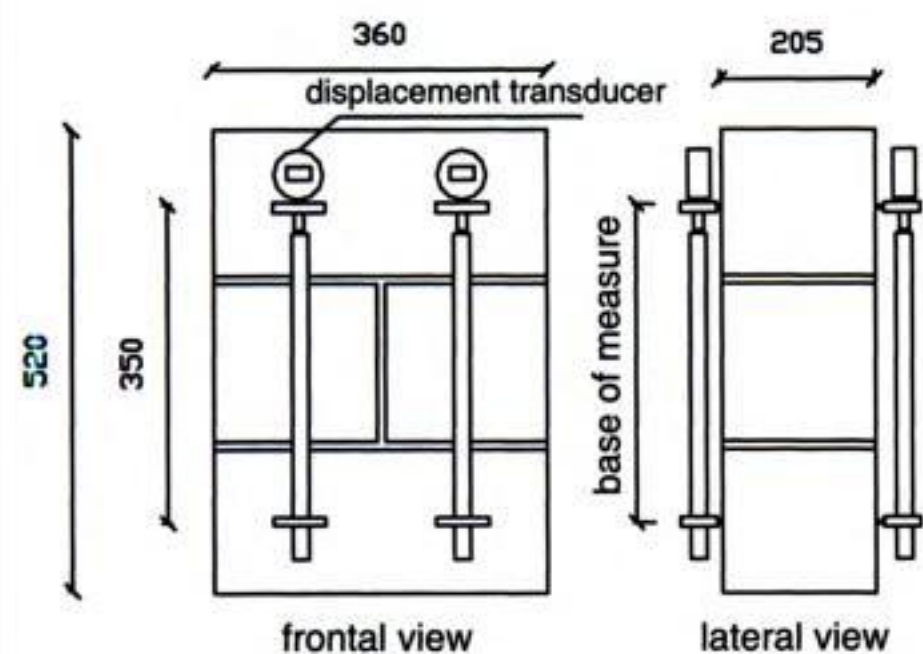


Figure 3. Location of displacement transducers on specimen.

The test was executed by controlling the displacement. In Figure 5 the scheme described before is shown, while in Figure 6 a picture of the test devices is shown.

Observe that the specimen's own weight, acting in a non-natural direction, did not condition the test because of the level of the horizontal forces applied, much greater than the weight itself.



Figure 4. Specimen under centred load.

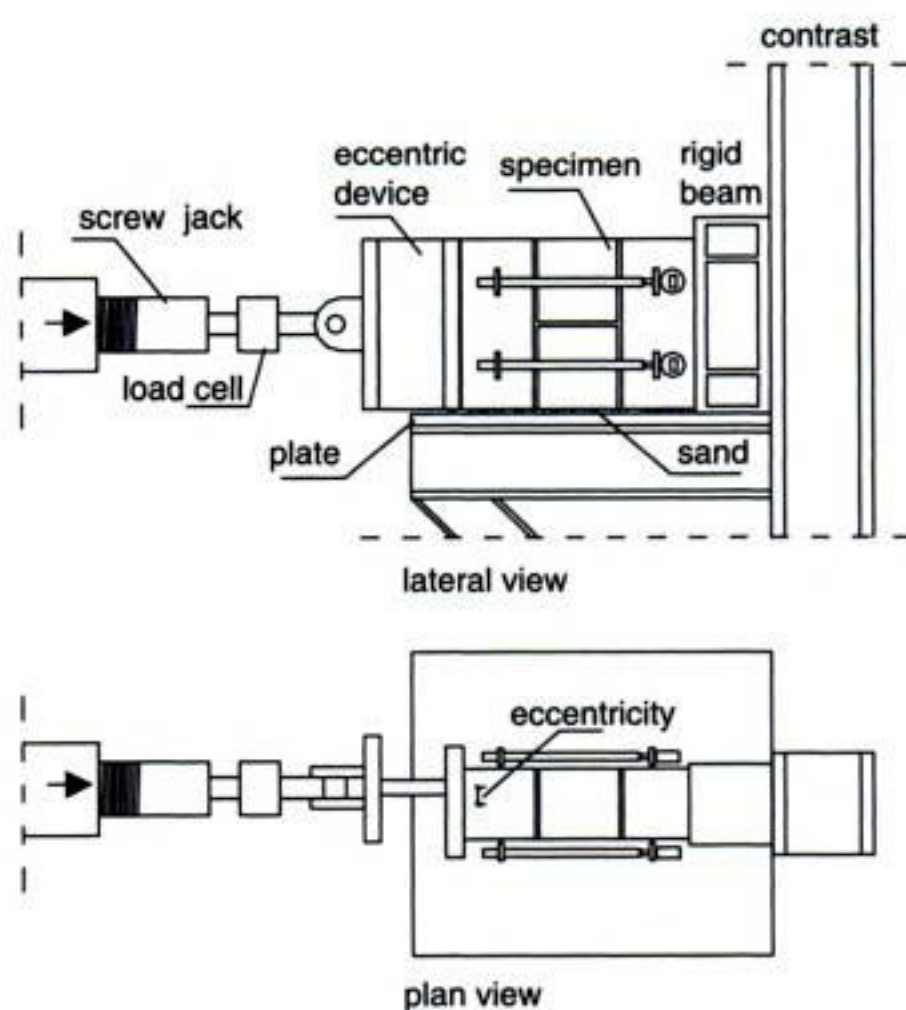


Figure 5. Test setup for specimens under eccentric load.

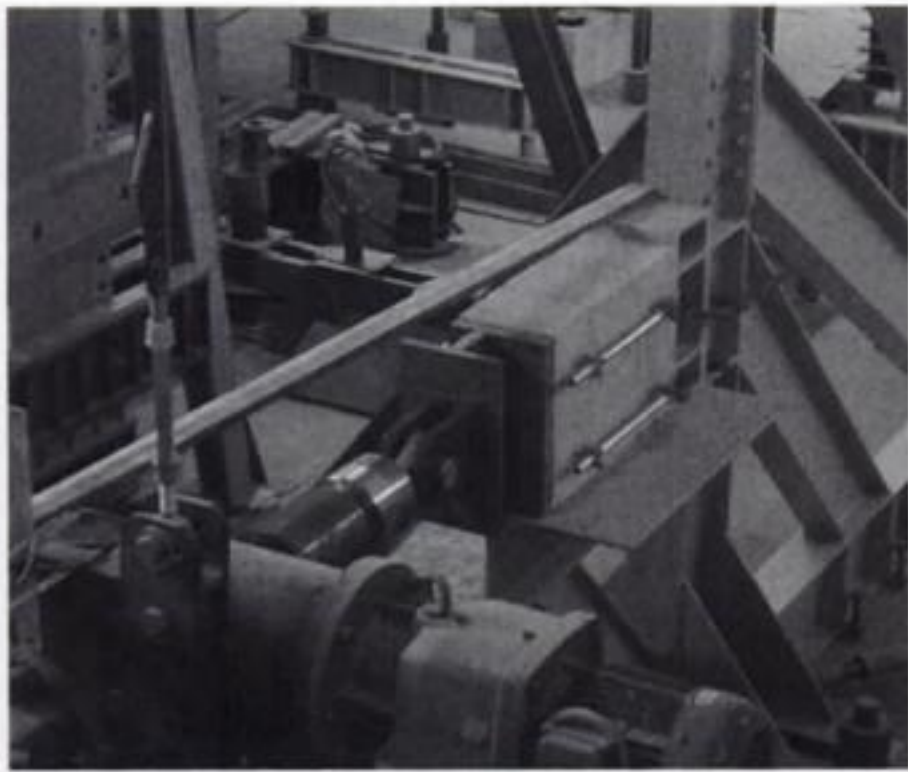


Figure 6. Specimen under eccentric load.

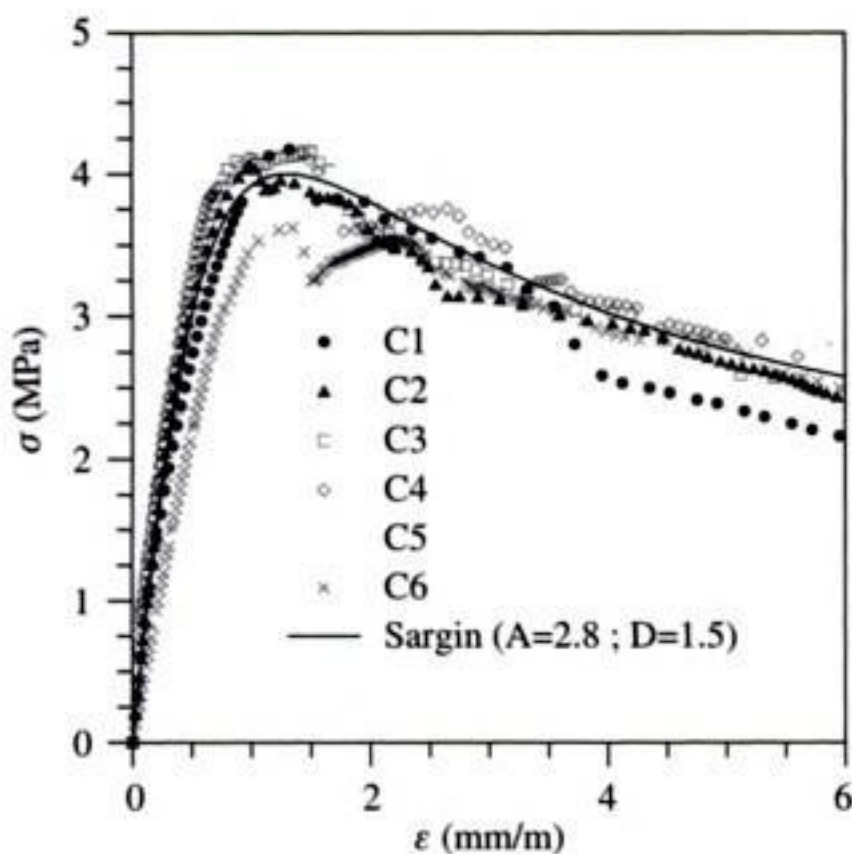


Figure 7. Stress–strain curves for specimens under centred load.

2.4 Test results

2.4.1 Specimens under centred load

The specimens exhibited a quasi linear behaviour for a low load level and reduced their stiffness when the load exceeded approximately fifty percent of the maximum load. When the maximum load was reached the specimens did not show a rapid decrease in resistance; on the contrary a good capacity of deformation beyond the peak of resistance was exhibited. In Figure 7 the stress–strain results obtained for each specimen (labelled with the symbol C) are inserted. Observe that the strain (ϵ) is obtained as the mean of the strains determined by the displacement measures at each of the four transducers located on the specimen, while the stress (σ) is obtained by dividing the force measured at the load

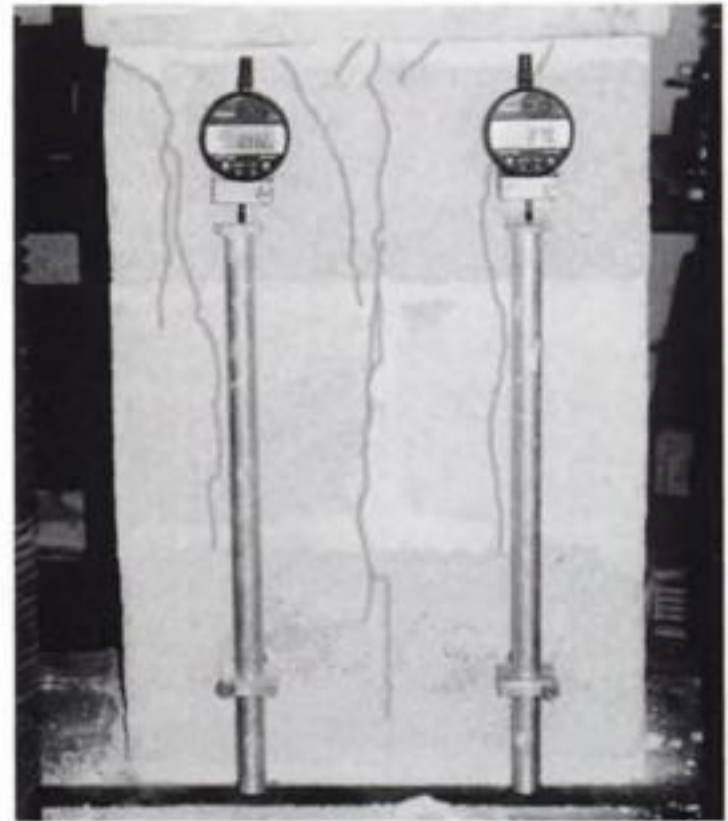


Figure 8. Specimen at the end of the centred compression test.

cell for the nominal area of the cross section of the specimen.

In Figure 7 the analytical model of the experimental results is also inserted but it will be discussed in the next section.

Figure 7 shows that the peak of resistance is comprised between 3.75 and 4.25 MPa, while the corresponding strain is about 1.25 mm/m. Further, it can be observed that at 6 mm/m strain a reduction in resistance of less than 50% occurs. Hence the material altogether exhibits a good ductility level. The results show a no high degree of dispersion.

In Figure 8 one of the specimens at the end of the test is shown. The picture highlights the vertical cracks produced by the state of compressive stresses. The same situation was observed on each of the other specimens.

2.4.2 Specimens under eccentric load

As mentioned before a load cell was used for measuring the force while four displacement transducers were used for measuring the deformations of each specimen. The data were electrically acquired and stored in a PC. Subsequently the data were processed for determining the response of the specimen in terms of moments and related curvatures. The moment was obtained by multiplying the level of the force by the fixed eccentricity while the curvature was obtained by dividing the mean strains at each side of the specimen by its thickness augmented twice the distance of the measurement point from the surface of the specimen (see Fig. 9).

In Figures 10, 11, 12 the moment–curvature diagrams for the different values of investigated eccentricity are presented. The good rotation capacity of the cross-section can be observed in addition to the moment peak in agreement with the deformation

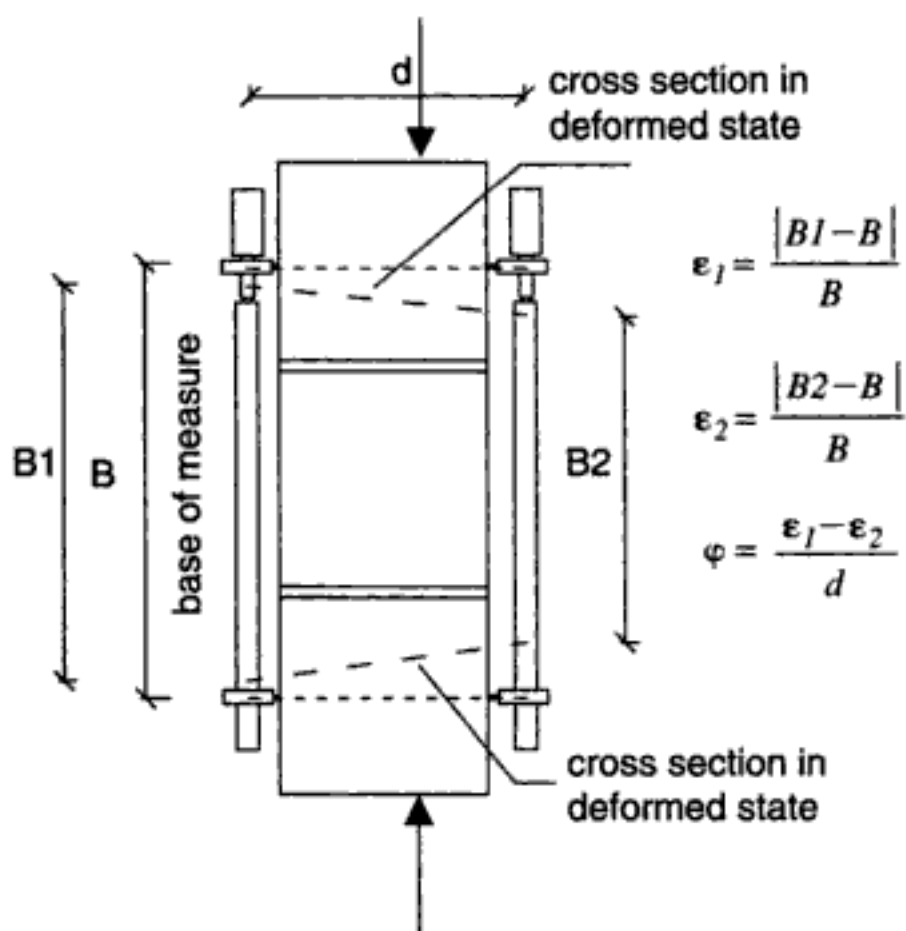


Figure 9. Scheme for the evaluation of the curvature.

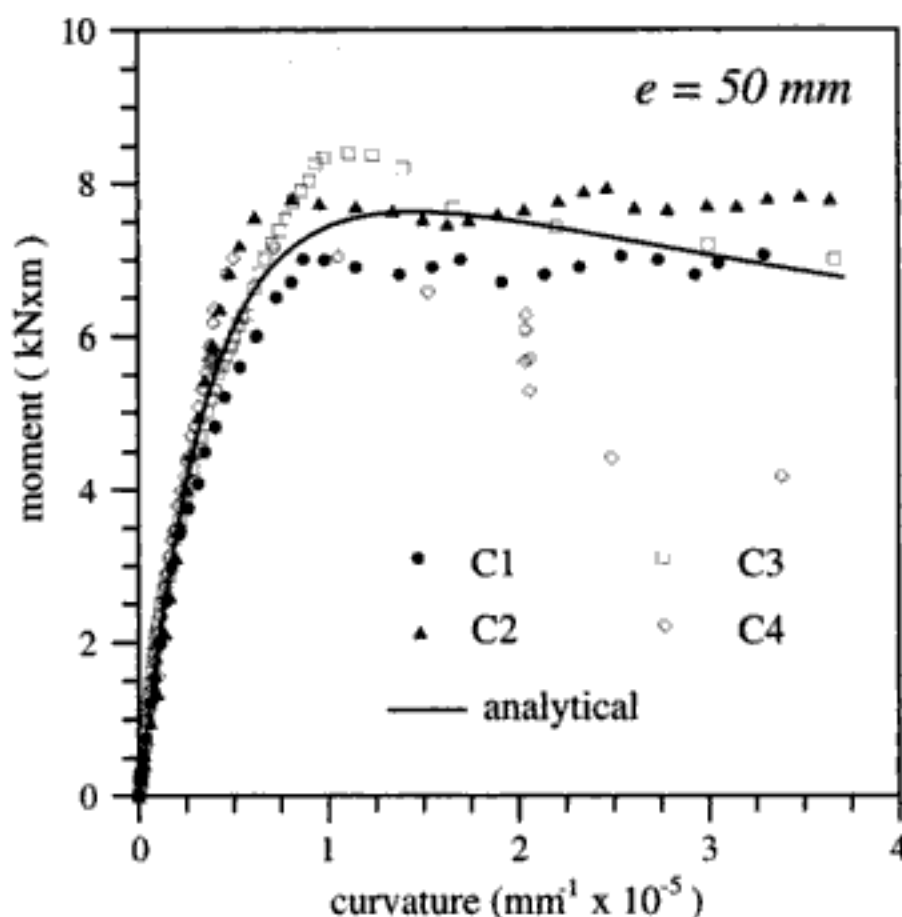


Figure 11. Moment-curvature curves: 50 mm eccentricity.

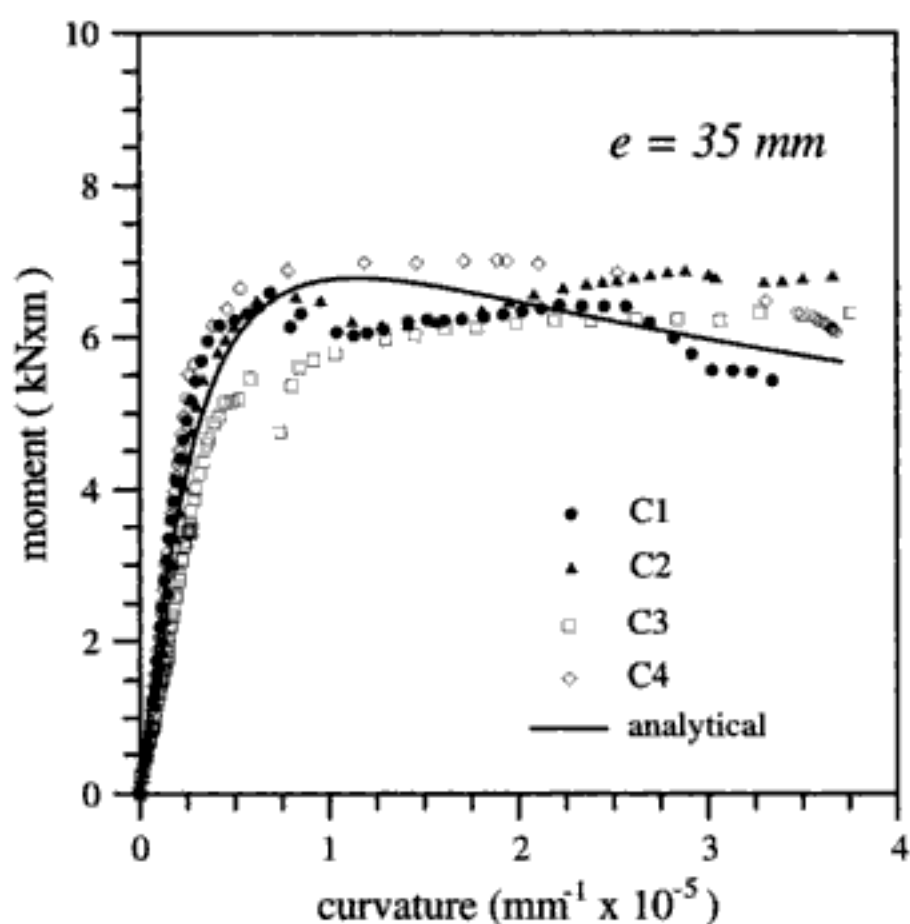


Figure 10. Moment-curvature curves: 35 mm eccentricity.

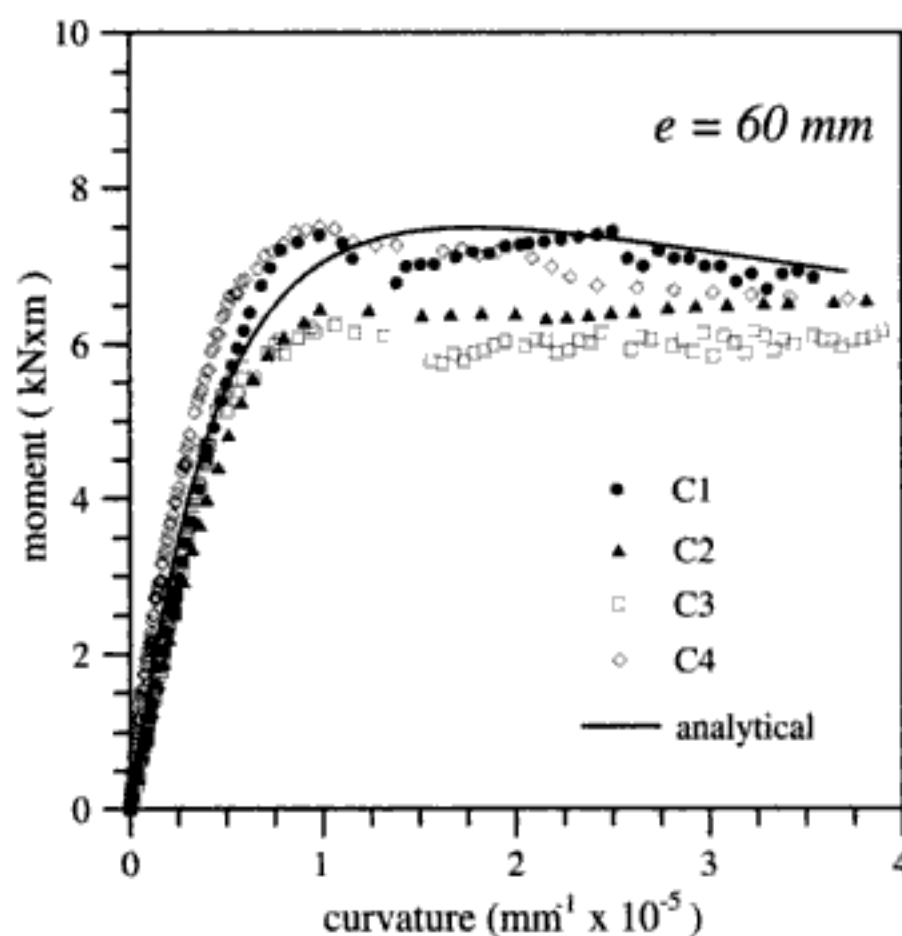


Figure 12. Moment-curvature curves: 60 mm eccentricity.

capacity of the material simply compressed. With big variation in the eccentricity not very big variation in the moment peak was observed.

A higher level of dispersion of the results was observed for the tests executed with 50 mm and 60 mm eccentricity in the post-peak branch, also due to the occurrence of premature local failure.

While in the case of 35 mm eccentricity the failure was mainly caused by a crisis in the material in compression, in the other two cases a progressive reduction

of the resistant cross-section was the main cause of failure.

In Figure 13 the state of a specimen subjected to a load with 60 mm eccentricity can be observed at the end of a test. In this case the partialization of the cross section occurs in the central blocks while in the other cases the partialization of the cross-section is activated in the mortar joint. The possibility of having these two different mechanisms is a further cause of the dispersion of the results.

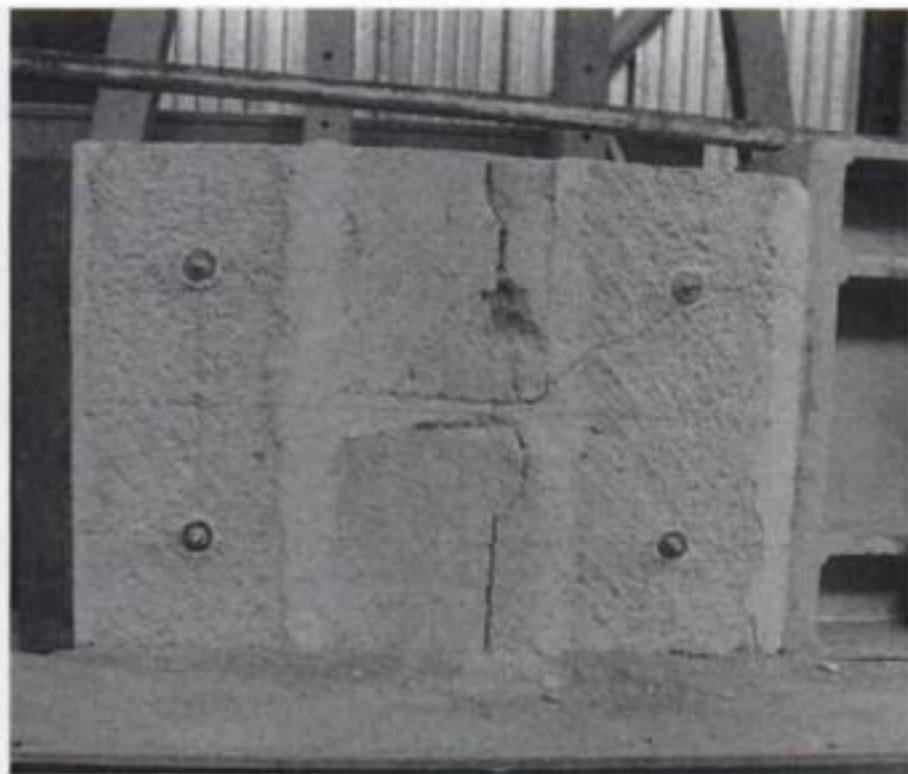


Figure 13. State of a specimen at the end of the test.

3 MODELLING OF EXPERIMENTAL RESULTS

The results of the tests with centred loads made it possible to define a stress–strain law for the masonry to be used for the analysis of the cross-section under bending moment and centred load. At this point the resolution of the problem of evaluating the distribution of the stress in the cross-section requires definition of the strain distribution. In the most simplified case the strain distribution can be considered linear, that is to say the cross-section remains plane. This hypothesis makes it sufficiently simple to evaluate the limit condition of the cross-section in the case of non-linear mechanical behaviour of the material. Nevertheless, it must be verified.

In this framework the tests under eccentric loads had the aim of proving the reliability of the hypothesis of plane cross-sections, as is explained in the next paragraphs.

3.1 Analytical law for masonry in compression

In order to model the behaviour of the masonry in compression the masonry itself was considered as a continuum homogeneous governed by a constitutive conventional law that gives the overall real response of the elements. This approach disagrees with techniques based on the definition of a constitutive law for each component and/or a constitutive law for the interface between them.

In this study the analytical law given by Sargin (1971) for concrete was used, that is

$$\tilde{\sigma} = \frac{A\tilde{\varepsilon} + (D-1)\tilde{\varepsilon}^2}{1 + (A-2)\tilde{\varepsilon} + D\tilde{\varepsilon}^2} \quad (1)$$

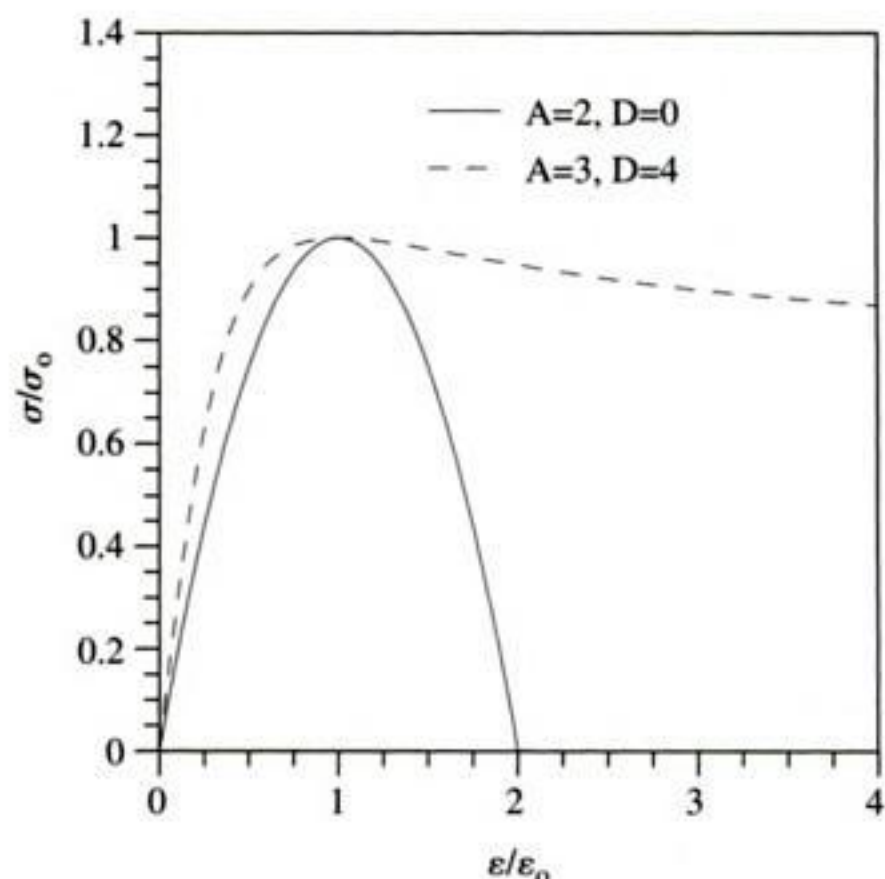


Figure 14. Plotting of Equation 1 for the limit values of the parameters A and D.

where A e D are parameters to be calibrated by experimental tests while

$$\tilde{\varepsilon} = \frac{\varepsilon}{\varepsilon_0}, \quad \tilde{\sigma} = \frac{\sigma}{\sigma_0} \quad (2)$$

In Equation 2 σ_0 is the maximum compression stress and ε_0 is the corresponding strain.

With variation in A and D many types of materials can be modelled. Generally, for masonry, A has to be chosen in the range $2 \div 3$ while D has to be chosen in the range $0 \div (1 - A)^2$. In the limit conditions ($A = 2$ and $D = 0$, $A = 3$ and $D = 4$) the curves inserted in Figure 14 can be obtained corresponding respectively to brittle and ductile behaviour.

For the case examined, 2.8 and 1.5 are the values chosen respectively for A and D, these values giving a good accordance between the experimental and the analytical data. In Figure 7 the good agreement can be observed with the mean of the stress peaks, with the increasing branch and the softening branch.

It must be said that, after the experimental study was concluded, these parameters seemed to be the most adequate to represent the constitutive law, while when the last two tests were to be done, the values 2.8 for A and 1.2 for D seemed more appropriate, as discussed by La Mendola & Papia (2002).

Observe that the parameter A conditions the increasing branch of the curve represented by Equation 1 since it defines the slope of the tangent to the curve at the origin of the axes. Further, it conditions the non-linearity of the increasing branch of the curve

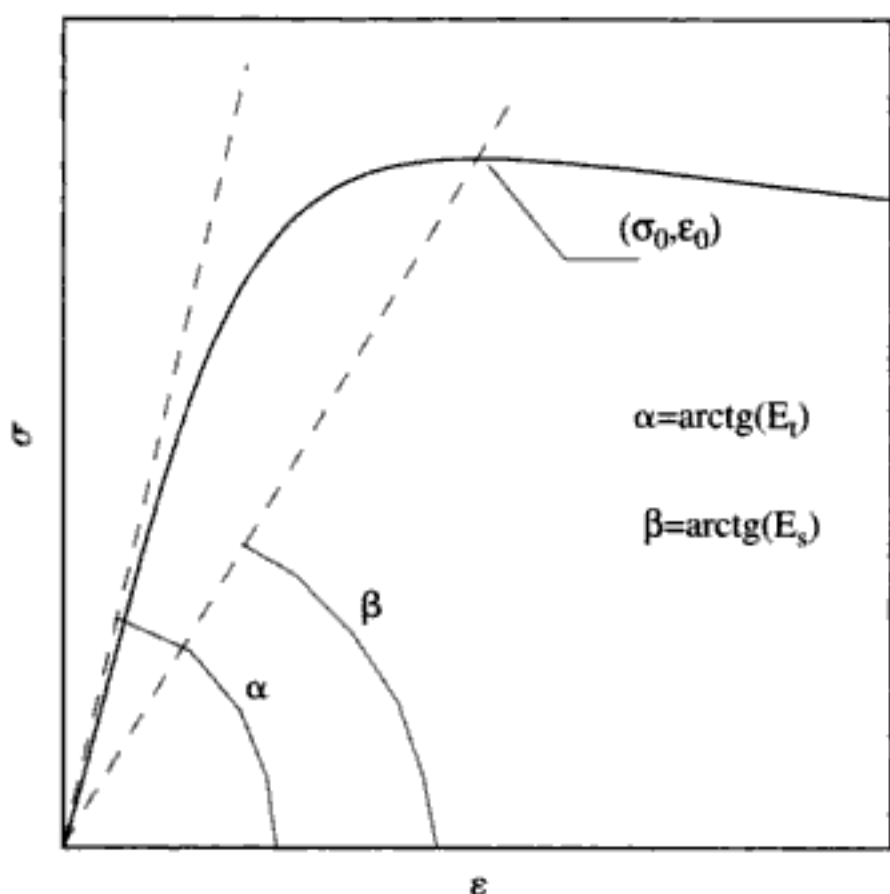


Figure 15. Some parameters defining the path of the $\sigma - \varepsilon$ law.

$\sigma - \varepsilon$ obtainable using Equation 1, since it is simply verifiable that

$$A = \frac{E_t}{E_s} \quad (3)$$

E_t being the tangent modulus at the origin and E_s the secant modulus at the peak of the curve (see Fig. 15).

Obviously if $A = 1$ the increasing branch becomes linear.

The parameters D conditions the post-peak branch, that is the increasing of D reduces the absolute slope of the post-peak branch augmenting the ductility.

The complete definition of the $\sigma - \varepsilon$ law for the material requests to fix appropriate values for the peak of resistance σ_0 and the corresponding strain ε_0 . These values were fixed by examining the experimental results in such a way the analytical curve was compatible with the experimental results themselves: 1.3 mm/m was chosen for ε_0 and 4 MPa for σ_0 .

3.2 Evaluation of the moment-curvature law and comparison with the analytical results

Once the stress-strain law for the masonry is known the behaviour of the cross section of an element in compression could be analysed under proper hypotheses.

First observe that if the deformed state of the cross section is fixed the state of stress can be determined by means of the stress-strain law before defined. Hence, the evaluation of the state of stress implies the assumption of a law of distribution of strains in the deformed state of the section: in the simplest case a linear distribution can be assumed, that is the maintaining of the

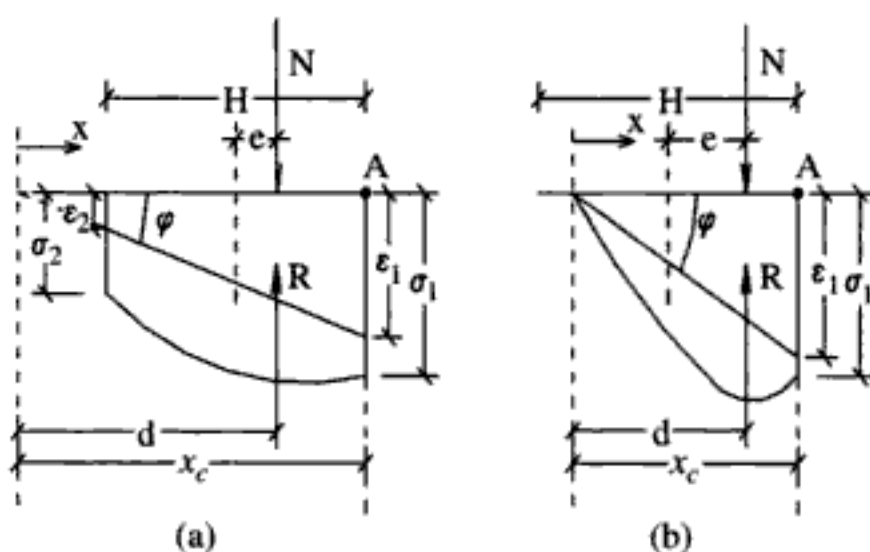


Figure 16. Distribution of stresses and strains in the cross-section: a) uncracked state; b) cracked state.

section plane in the deformed state. In order to validate this hypothesis a section like that of the tested specimens was supposed under an eccentric increasing load and, referring to the strain-stress law in the hypothesis of plane section, the moment-curvature response of the section was calculated and successively compared with the experimental results before described.

In order to evaluate the moment-curvature response of the cross section the no-tensile strength of the material was supposed. Once the eccentricity was fixed, the curve was obtained by increasing the level of the eccentric load and searching at each increase the curvature of the section which verified the equilibrium conditions.

It is worth to note that in the section, taking Equation 1 and Equation 2 in to account, the following equation hold

$$\sigma = \sigma_0 \tilde{\sigma}(\varepsilon) \quad (4)$$

in which, under the hypothesis of plane cross section, the strain ε at the distance x from the neutral axis can be written as

$$\varepsilon = \varphi x \quad (5)$$

Referring to the symbols inserted in Figure 16, the equilibrium conditions of the cross-section can be expressed by

$$N = \int_0^{x_c} \sigma(x) b dx \quad (6)$$

$$N \left(\frac{H}{2} - e \right) = \int_0^{x_c} \sigma(x) (x_c - x) b dx \quad (7)$$

b being the width of the specimen.

In the uncracked state, by operating a change of variables in the integrals quantities, Equation 6 and Equation 7 can also be written as

$$N = \int_0^{x_c} \sigma(x) b dx = \frac{H}{\varepsilon_1 - \varepsilon_2} b \int_{\varepsilon_2}^{\varepsilon_1} \sigma(\varepsilon) d\varepsilon \quad (8)$$

$$N\left(\frac{H}{2}-e\right)=\frac{H^2}{(\varepsilon_1-\varepsilon_2)^2}b\int_{\varepsilon_1}^{\varepsilon_2}\sigma(\varepsilon)(\varepsilon_1-\varepsilon)d\varepsilon \quad (9)$$

while in the cracked state, by operating in an analogous way, one obtains

$$N=\int_0^{x_c}\sigma(x)b dx=\frac{x_c}{\varepsilon_1}b\int_0^{\varepsilon_1}\sigma(\varepsilon)d\varepsilon \quad (10)$$

$$N\left(\frac{H}{2}-e\right)=\left(\frac{x_c}{\varepsilon_1}\right)^2b\int_0^{\varepsilon_1}\sigma(\varepsilon)(\varepsilon_1-\varepsilon)d\varepsilon \quad (11)$$

The integrals on the right side of Equations 8–11 are solvable in an exact form thanks to the particular form chosen for the function $\sigma(\varepsilon)$. This circumstance makes the procedure simple for solving Equations 8 and 9 in the case of an uncracked section or Equations 10 and 11 in the case of a cracked section to determine the curvature associated with an assigned axial load N for fixed eccentricity e . The same equilibrium equations can be found in nondimensional form in (Cucchiara et al., 2003) where the numeric procedure for their simple solution is also explained. The construction of the moment-curvature response of a calcarenite masonry section under an axial load of assigned eccentricity leads to the continuous curves plotted in Figures 10, 11, 12. Comparison with the experimental results shows that the response evaluated basing on an analytical non-linear law of the masonry considered as a homogeneous continuum, under the hypothesis of plane section, is in good agreement with the real response. However, it must be observed that for higher values of eccentricity (60 mm in this study) the results derived from the analytical approach given tend to overestimate the actual response.

Observe that the maximum of the moment for the section obtained analytically (denoted as \bar{M}) is associated with a value of \bar{N} .

$$\bar{N}=\bar{M}/e \quad (12)$$

All the couples of values $\bar{N}-\bar{M}$ obtained varying the eccentricity e in the range $0-H/2$ (the axial force obviously cannot exceed these limits) define a convex limit domain. In Figure 17 the corresponding dimensionless domain is plotted, which is obtained in terms of the following dimensionless axial load and dimensionless bending moment.

$$n=\frac{\bar{N}}{\sigma_0 b H}; \quad m=\frac{\bar{M}}{\sigma_0 b H^2} \quad (13)$$

This domain represents a tool to be used in practical applications for the determination of the safety level of a section. The limit domain obtained analytically is compared with the dimensionless experimental

results, showing that the optimal behaviour of the section with respect to the bending capacity occurs for 50 mm eccentricity ($e/H=0.243$).

In the limit domain plotted in Figure 17 the value of the eccentricity e associated with the limit value of the dimensionless axial load is not explicitly represented. Nevertheless, a different representation of the limit domain is possible, giving this information directly. From Equation 12 it is clear that, once \bar{N} is fixed, \bar{M} corresponds to the maximum value of the eccentricity associated with \bar{N} , and hence the information contained in the curve plotted in Figure 17 can be explicitly contained in a curve that relates \bar{N} to the maximum possible value of e . In Figure 18 this kind of representation of the limit condition of the section

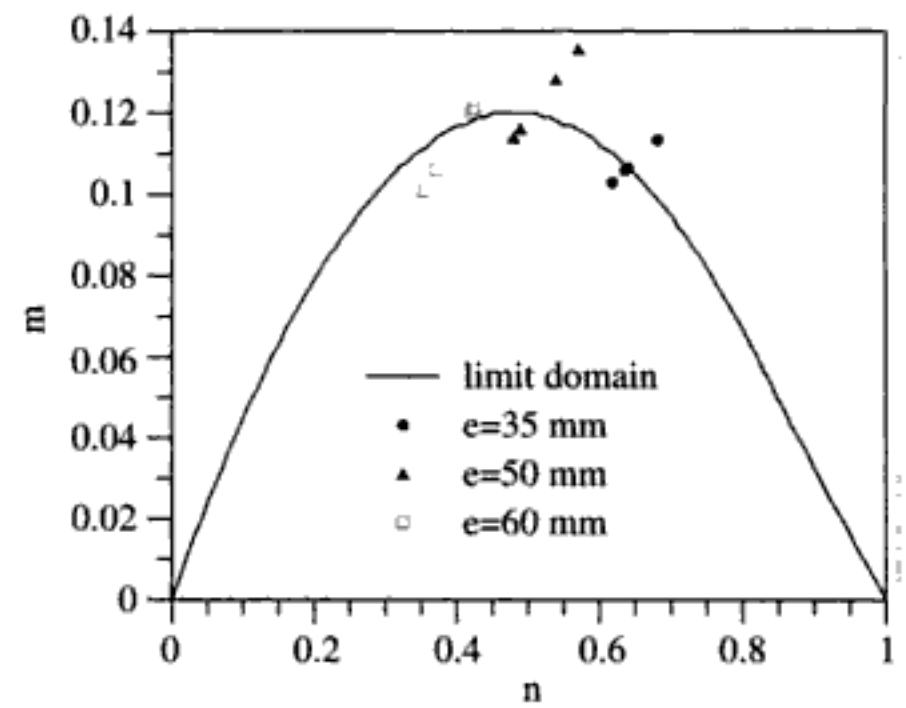


Figure 17. Dimensionless limit domain $m-n$ for masonry elements under eccentric loads.

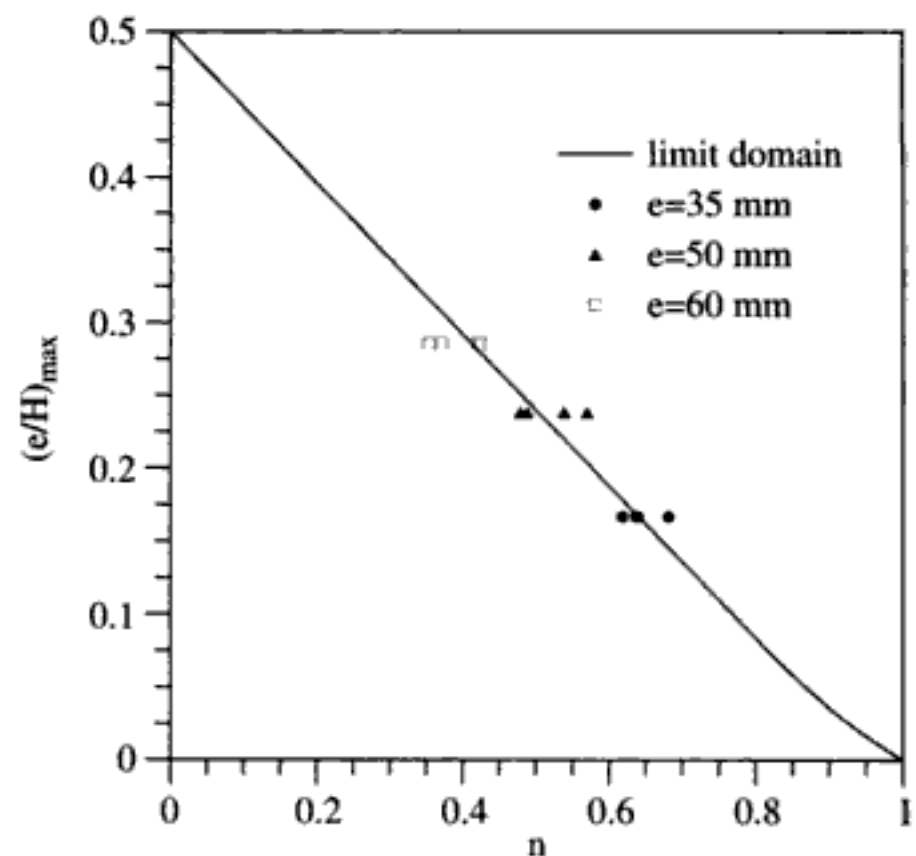


Figure 18. Maximum dimensionless eccentricity compatible with an assigned value of n .

is given, the dimensionless data obtained through the experimental tests also being given.

4 CONCLUSIONS

The research carried out for the characterization of the behaviour of calcarenite masonry sections under eccentric vertical loads showed that:

1. the material can be considered as homogeneous and characterized by a global $\sigma - \varepsilon$ law in compression;
2. when we are a long way from the instability state of eccentrically axial loaded elements, it is basic to define the $\sigma - \varepsilon$ characteristic law also including the non-linear branch up to collapse;
3. the response of not very slender elements under eccentric loads exhibits a very extended non-linear branch of the moment-curvature diagram;
4. the use of the $\sigma - \varepsilon$ law mentioned before, associated with the hypothesis of zero tensile strength of the material and plane behaviour of the section lead simply to the definition of a limit domain of the section itself represented in terms of axial force bending moment curve or in terms of axial force–maximum value of associated eccentricity;
5. the reliability of the limit domains was proved once the hypothesis of plane section was observed to be reliable by comparing the response obtainable analytically and the one obtainable experimentally from eccentrically loaded specimens.

REFERENCES

AlShebani, M.M. & Sinha, S.N. 2000. Cyclic compressive loading-unloading curves of brick masonry. *Structural Engineering and Mechanics* 9: 375–382.

- Cantù, E. 1982. Axially loaded reinforced masonry walls under cyclic bending. *Proceedings of Sixth International Brick Masonry Conference*, Rome: 1043–1055.
- Crook, R.N. 1982. The behaviour of concrete block masonry units under vertical loads. *Proceedings of Sixth International Brick Masonry Conference*, Rome: 627–638.
- Cucchiara, C., La Mendola, L. & Papia, M. 2003. Flexural bearing capacity and related ductility demand for masonry sections under nonlinear constitutive law. In C.A. Brebbia (ed.), *Structural Studies, Repair and Maintenance of Heritage Architecture (STREMAH); Proceedings of eighth international conference*, Boston WIT Press: 791–800.
- Drysdale, R.G. & Hamid, A.A. 1983. Capacity of concrete block masonry under eccentric compressive loading. *ACI Journal* 80: 102–108.
- Hatzinikolas, M., Longworth, J. & Warwaruk, J. 1980. Failure modes for eccentrically loaded concrete block masonry walls. *ACI Journal* 77: 258–263.
- La Mendola, L. & Papia, M. 2002. General stress–strain model for concrete or masonry response under uniaxial cyclic compression. *Structural Engineering and Mechanics Journal* 14(4): 435–454.
- Macchi, G. 1982. Behaviour of masonry under cyclic actions and seismic design. *Proceedings of Sixth International Brick Masonry Conference*, Rome: 51–74.
- Sargin, M. 1971. Stress–strain relationship for concrete and analysis of structural concrete sections. *Study N.4, Solid Mechanics Division*, University of Waterloo, M.Z. Cohn (ed.). Waterloo, Ontario.
- Schultz, A.E., Ojard, N.J. & Stolarski, H.K. 2001. Critical axial loads for transversely loaded masonry walls. *Proceedings of ninth Canadian Masonry Symposium*, New Brunswick, Canada.
- Yokel, F.Y. 1971. Stability and capacity of members with no tensile strength. *Journal of the Structural Division*, ASCE, 97: 1913–1926.

In-plane shear and tensile strength tests of small brickwork specimens

L. Malyszko

Faculty of Technical Sciences, University of Warmia and Mazury in Olsztyn, Poland

ABSTRACT: Under monotonic force control several strength tests were performed on coupon-size masonry panels (dimensions mostly $520 \times 520 \times 120$ mm) in order to get information on the in-plane response of brickwork walls. All specimens were made up of polish standard clay bricks ($250 \times 120 \times 65$ mm) and a 1:0.5:4.5 portland cement-lime mortar. The response to direct shear was investigated by means of both the standard triplet test and the test with the predetermined single plane of the shear failure. In the latter test there is not need to measure the strength at a number of the precompression levels in order to predict the initial shear strength. Tests with the single shear plane normal to the bed joints were also performed. The diagonal compression test has been chosen to simulate in-plane shear phenomenon related to the diagonal cracking. The test was carried out on ten masonry panels capturing the failure modes and the splitting strength. Additionally, the various strength characteristics of bricks and mortar were investigated. The strength criteria related are also discussed. For the experimental data the simplest form of the criteria are presented in the shear-precompression stress state. The three basic failure modes are distinguished: shear slip along the bed joints, diagonal tension cracking and shear compression failure. Some remarks on taking advantage of the strength parameters from triplet and diagonal compression tests are also given.

1 INTRODUCTION

A large number of buildings are constructed with masonry walls that significantly affect the distribution of lateral loads to various parts of the building if the tensile and shear strengths of masonry are sufficient. Unfortunately, the combination of relatively low tensile and shear strength and brittle behavior results in masonry being susceptible to cracking. In addition to the potential for developing horizontal cracks corresponding to the shear slip along the bed joints, various forms of diagonal cracking can occur. These important in-plane failure modes are the crucial effects in the infill panels and the shear wall design. In loadbearing masonry buildings, shear walls carry vertical loads and resist the lateral in-plane loads due to wind or earthquakes. This combined loading creates a biaxial tension-compression stress state in the wall leading to cracking when the tensile or shear strength of masonry is exceeded. Therefore, although unreinforced masonry is primarily designed to withstand compression, it is important that these types of failure can be properly predicted for a complete description of the material behavior.

In the present experimental work, which was performed on coupon-size masonry panels under monotonic force control, several tests have been carried out on the same masonry panels in order to get information

on the in-plane response of brickwork walls under lateral loads.

In order to predict properly the masonry shear capacity, it is necessary to first identify the most anticipated failure mechanism and next to formulate the strength criteria applicable to the specified mechanism. In the paper the simple forms of the failure criterion are proposed that are taking advantage of the strength parameters obtained. The strength criteria can be represented by three independent analytical expressions, each being the condition of limit equilibrium of masonry applicable to specified failure mechanism. The failure surfaces in the shear-precompression stress space are similar to those known from the appropriate literature.

The paper sums up experimental and theoretical research performed at the University in Olsztyn on solid clay brick masonry. The results have been partly published by Malyszko (2002, 2003).

2 MATERIALS CHARACTERIZATION

Masonry mechanical properties depend on the characteristics of the constituent elements (bricks and mortar), as well as on the workmanship and the interaction within the assemblage. Thus, an extensive program of tests, ranging from the units to the small assemblages

Table 1. Synthesis of the additional program.

Material	Type of test	Number of tests	Mean strength [N/mm ²]
Brick 250 × 120 × 65 mm ³	Standard compression	6	27.1
	Flexural tension (modulus of rupture)	6	3.86
	Splitting tension	6	2.84
	Direct tension	12	0.60
	One-plane shear	10	3.21
	Dual-plane shear	10	0.85
Mortar	Compression	6	8.50
	Flexural tension	6	2.21
Triplet	Sliding along mortar bed joints	3 × 4	0.53 0.54
	Masonry	Standard compression	5
	Horizontal compression	5	14.09

scale, was additionally performed. However, accurate prediction of assemblages behaviors using properties of the constituent materials is rather hard to do due to the interactions between the individual materials being too complex to be accurately modeled using a few basic material properties. Table 1 gives the scheme of the whole additional program with mean strengths obtained.

The main mechanical properties of the bricks have been determined by axial compressive and tensile tests. Knowledge of the tensile strength of bricks was expected to be important for the development of a proper understanding of failure mechanisms in the diagonal compression test. When the failure plane passes through the bricks, as can be expected for diagonal cracking and for tension parallel to the bed joints, the in-plane tensile strength should be affected by the tensile strength of the brick. Therefore, apart from the modulus of rupture test, direct tension and splitting tests were also performed to obtain a comparative measure of tensile strength. In the splitting test, the nearly constant tension developed over the central part of the brick height between the line loads is closer to a direct tension than to a flexural tension condition. However, the calculated average strengths tend to be much higher (almost five-times) than the direct tension results but with much less variability. The flexural tensile strength of bricks, also denoted as modulus of rupture, is 36% higher than the splitting tensile strength.

Although a certain amount of testing of shear in masonry units may be essential for verification of strength criteria and failure mechanism, there has been

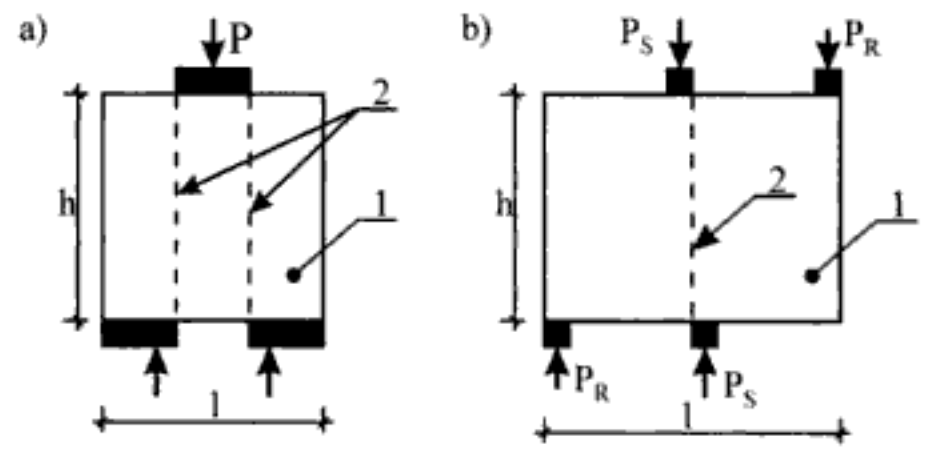


Figure 1. Set-up of shear tests on single brick specimens: a) two planes of shear failure, b) single plane of shear failure, 1 – brick, 2 – shear planes.

little attempt to standardize procedures. Results in Table 1 are given according to the experimental set-up from Figure 1. Mean values indicate much higher shear strengths in the single plane tests than those obtained in the dual-plane tests. This is because of different failure mechanisms. In the dual-plane shear test, the failure mechanism is strongly influenced by flexural tensile stresses.

3 STRENGTH OF PANELS IN DIRECT SHEAR

3.1 Triplet tests

Triplet tests are commonly used as a standard test to obtain experimental data relating to masonry joint shear strength. Here, triplet shear samples were used according to Polish standard, which is quite similar to Eurocode 6 (1996). In order to investigate the local interaction between mortar and bricks, three series of sliding tests were performed on four triplets (12 specimens in total). Interpolating the experimental points obtained at three levels of confining compressive stress – 0.2, 0.6 and 1.0 N/mm², it was possible to detect the parameters describing the strength for shear slip along mortar bed joints. According to Eurocode 6 and Polish standard the Coulomb equation representing the dry friction mechanism during joint sliding is:

$$f_v = f_{v0} + \mu \sigma_c = 0.53 + 0.54 \sigma_c \quad (1)$$

The tests were performed by keeping constant the confining compressive load normal to the bed joints and by increasing monotonically the in-plane loads parallel to the joints in order to evaluate the mortar-brick friction coefficient μ and the shear strength for null compression f_{v0} . Assuming that under pure shear the limiting strength is defined either by the diagonal tensile strength of the mortar (equals to 0.46 N/mm², that is 21% of the flexural tensile strength) or by the direct tensile strength of the brick (0.60 N/mm²), it can be seen that the cohesion value ($f_{v0} = 0.53$ N/mm²) is in good agreement with this assumption.

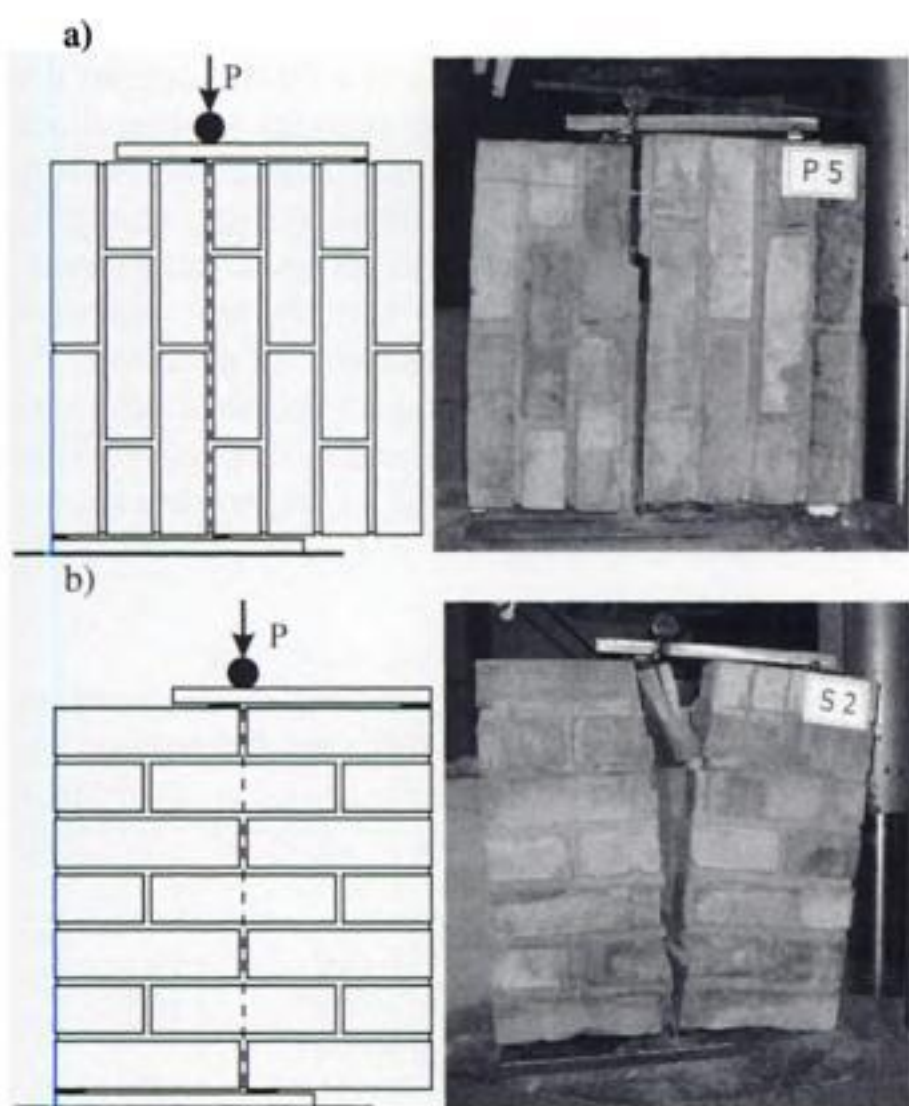


Figure 2. Shear strength test with the predetermined single plane of a failure: a) for loading tangential to the bed joints (C_z), b) for loading normal to the bed joints (C_x).

3.2 Tests with the predetermined single plane of shear failure

Apart from triplet test, the other test has been used to obtain the initial shear strength related the adhesion and shear-friction resistance between the mortar and the units. Although the triplet test is assumed to be performed without a flexural tension due to the precompression, the failure mechanism is yet influenced by flexural tensile stresses, especially at the low precompression level. Besides, in the triplet test there is need to measure the strength at a number of the precompression level in order to obtain the initial shear strength, i.e. the strength for null precompression. Alternatively, the response to direct shear may be investigated by means of the test with the predetermined single plane of the shear failure, similar to that from Figure 1b. In the test there is not need to measure the strength at a number of the precompression levels in order to predict the initial shear strength. However, that strength is the only value obtained. The test may be performed both for tangential and normal to the bed joints loading, Figures 2a and 2b, respectively. Shear strength may be calculated as a ratio P_S/A , where A is the average area of the cross section along the failure plane and P_S is a shear force caused by the applied load P . The specimens with the dimensions $520 \times 520 \times 120$ mm were used, although the test may be performed on a triplet if a suitable loading

Table 2. Tests with predetermined single plane of shear failure.

C_x (vertical) and C_z (horizontal) shear strengths				
No.	P_{MAX} [kN]	C_z [N/mm ²]	P_{MAX} [kN]	C_x [N/mm ²]
1	55	0.83	68.5	1.00
2	50	0.75	73.0	1.07
3	38	0.57	68.5	1.00
4	40	0.60	90.5	1.32
5	47	0.70	90.3	1.32
Mean value		0.69		1.14
Standard deviation		0.11		0.17
Coefficient of variation		0.15		0.14

rig is made. Ten specimens were used in total. The maximum values of applied load P and the calculated strengths are given in Table 2.

It is expected that both the shear strength for tangential and normal loading are related to the initial shear strength from the triplet test and to the shear strength of brick, respectively. However, the shear strength for tangential loading ($C_z = 0.69$ N/mm²) is higher than that obtained from the triplet test ($f_{v0} = 0.53$ N/mm²). On the other hand, assuming that under direct shear for loading normal to the bed joints the limiting strength is defined by the shear strength of bricks in three courses, i.e. is equal to 1.2 N/mm² = $3.21 \times 3 \times 65/520$, it can be seen that the obtained strength value ($C_x = 1.14$ N/mm²) is in good agreement with this assumption.

4 DIAGONAL COMPRESSION TEST

4.1 Test method

The RILEM standard LUMB6 (1991) describes test method to determine the capacity of masonry under conditions that can produce diagonal cracking. The diagonal compression test, shown in Figure 3 for the brickwork panels made of solid clay bricks, is based on subjecting a square section of wall to diagonal compression through steel or polymer concrete shoes (loading plates) on two diagonally opposite corners of the specimen. The loading shoes should be dimensioned such that the sides of the vee are one tenth of the height of the specimen (i.e. the length of the side). The specimen should contain sufficient units (a minimum of four units wide) to be reasonably representative of finished masonry. This test can be carried out with standard equipment. The strength parameter S_{pt} is calculated from the equation:

$$S_{pt} = 0.707P / A_n \quad (2)$$

where P = the load value at failure; A_n = the net area of the specimen = $(l + h)/2 t n$; t = the wall thickness and l and h the face dimension; n = the fraction of the gross area of the specimen that is solid.

This corresponds to the principal tensile stress in the centre of the panel assuming isotropic elastic properties.

Similarly, ASTM (1988) describes test method based on a 4 ft (1.2 m) square section of wall allowing axial load normal to the bed joints to be also applied. The shear capacity is significantly affected by the level of axial compression, which has the effect of delaying tensile cracking and enhancing the shear-friction component of the shear strength.

Due to some difficulty of relating the strengths and behaviors from diagonal tests to diagonal cracking in walls, there are other tests, like racking tests or splitting tension test of disks and square masonry assemblages. In the racking tests, larger specimens have been used consisting of panels several bricks in length by several courses in height. The results of these tests depend rather critically on the form of the specimen and method of loading. They are also relatively expensive to carry out and require a special loading rig. The splitting tension tests of disks or square masonry assemblages have been used to study the parameters affecting in-plane tensile strength.

4.2 Results

The diagonal compression tests were carried out on ten $520 \times 520 \times 120$ mm masonry specimens (labeled as P1-P10), made from polish standard clay bricks and a 1:0,5:4,5 portland cement-lime mortar. Tests were performed under monotonic force control. Both vertical and horizontal displacements were measured on the two main faces of specimens (Fig. 3). The results are given in Table 3. The average value of the failure load, calculated on the 8 samples according to the equation (2), is equal to 93,500 N and results in the average value of diagonal tensile strength equal to 1.01 N/mm^2 . The considerable higher values of the failure load were

obtained in two tests (P2 and P4). This is because of different failure mode relating to a formulation of the diagonal compression strut between the loading shoes on opposite ends of the diagonal. These values were rejected and not taken into consideration, since they are likely connected to the improper test arrangements. As one can see in Figure 4, where the representative force-strain diagrams are presented for specimen P6 (splitting failure) and P4 (compression strut), the vertical and horizontal strains (ϵ_1 and ϵ_2 respectively) are smaller at the same load level if a compression strut is likely to form (Fig. 4b).

Table 3. Results of diagonal compression test

Specimen	P [N]	S_{pt}
P 1	100,000	1.09
P 2	150,000*	1.63*
P 3	108,000	1.17
P 4	170,000*	1.85*
P 5	98,000	1.06
P 6	100,000	1.09
P 7	80,000	0.87
P 8	96,000	1.04
P 9	93,000	1.01
P 10	71,000	0.77
Mean value	93,500	1.01
Sample standard deviation	12	0.02
Coefficient of variation	13%	

* Formulation of the compression strut; values of both specimens were rejected.

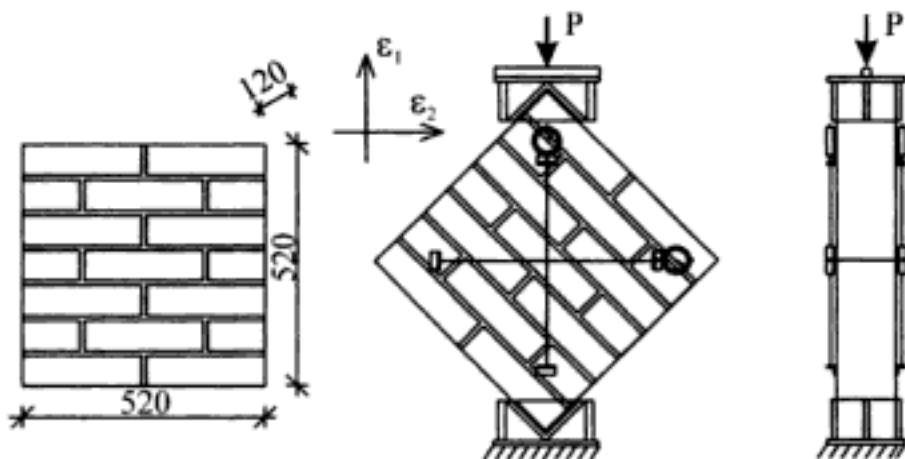


Figure 3. Experimental set-up for the diagonal compression test

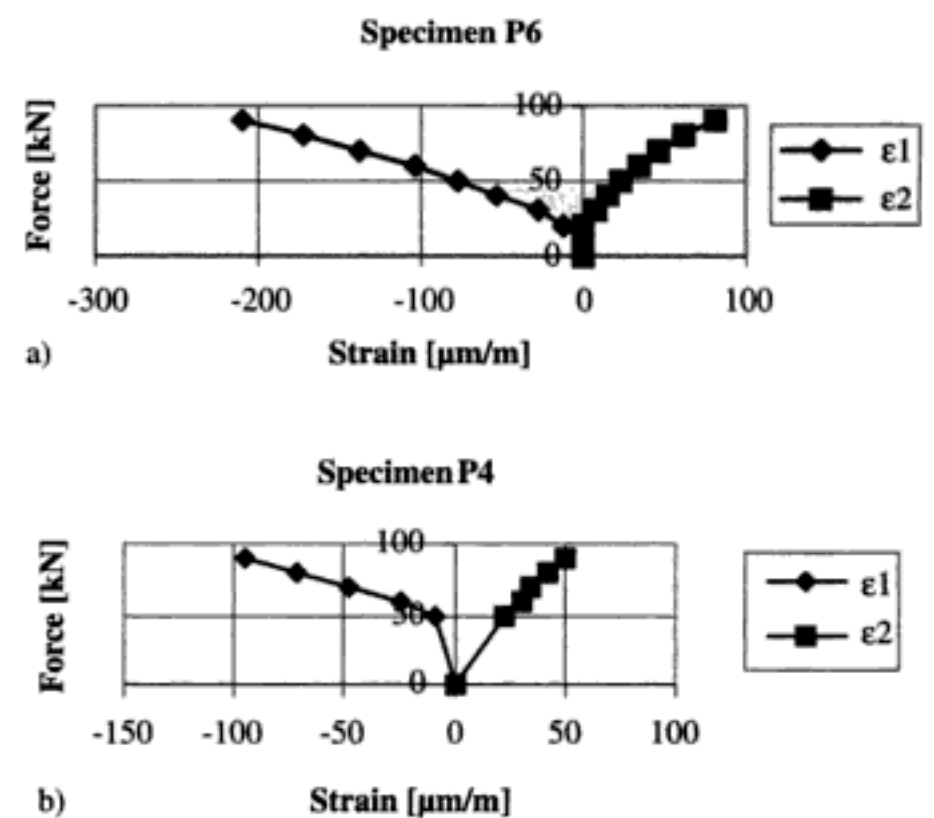


Figure 4. Force-strain diagrams: a) for the case of combination of shear slip along bed joints and diagonal tension failure, b) for the case of compression strut failure.

4.3 Failure modes

The diagonal compression tests tend to produce three basic failure modes (Fig. 5). In general, the stress field tends to force the cracks to follow the line of action of the compression load. The splitting tension stress results in diagonal tension at 90° to the line load. Typical failures are shown in Figure 5b and 6a. In this case, the tension crack may have a rougher surface as the weakest path along combinations of head and bed joints and through units is followed to some extent. However, depending on the path of least resistance, the combination of diagonal splitting and step-pattern sliding along the mortar joints may occur (Fig. 5c and 6b, c). For practical purpose this is the more important

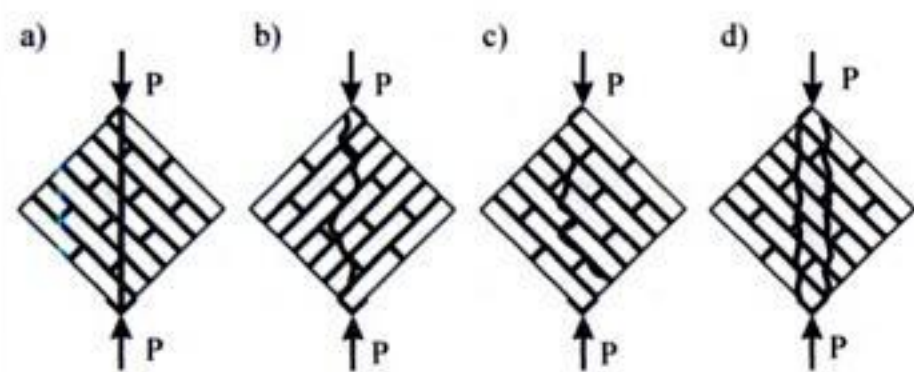


Figure 5. Typical crack pattern of masonry panels: a) theoretical splitting failure, b) diagonal tension, c) combination of shear slip along bed joints and diagonal tension, d) compression strut.

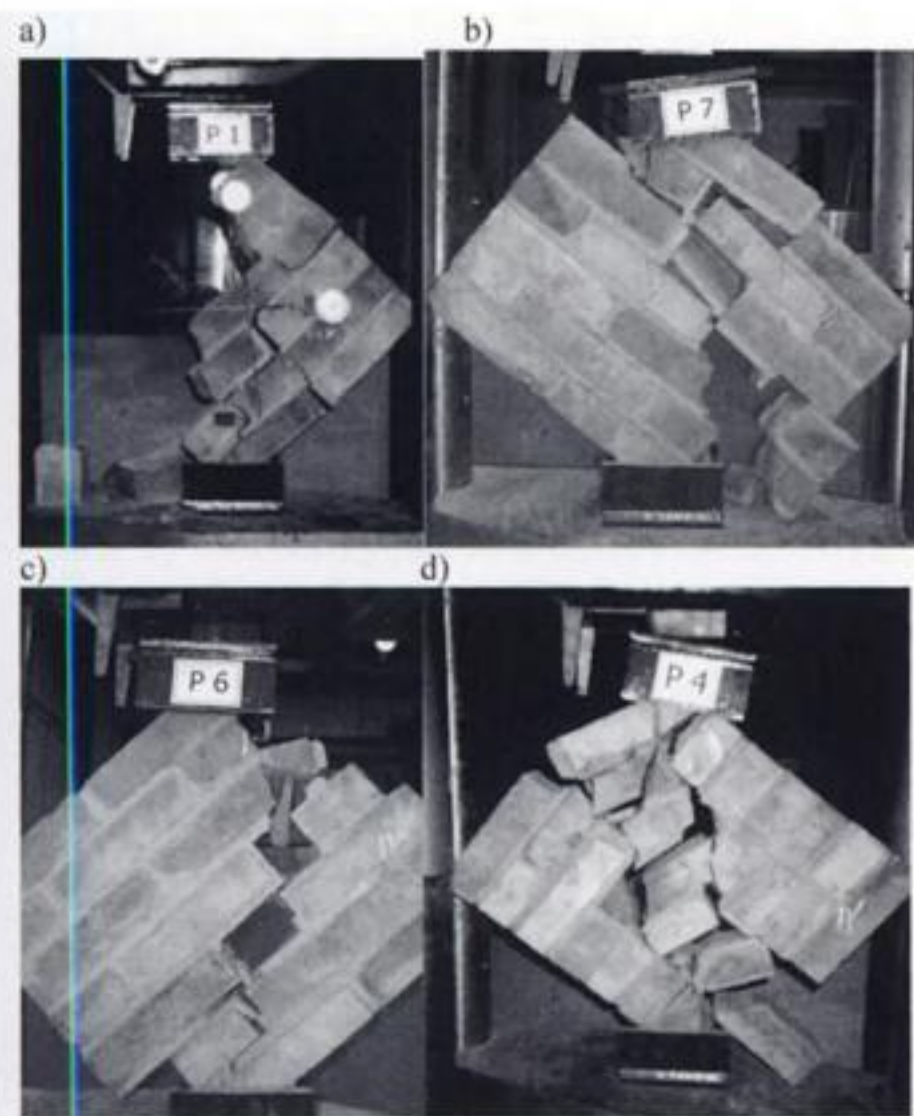


Figure 6. Experimental failure modes of masonry panels: a) diagonal tension, b) and c) combination of shear slip along bed joints and diagonal tension, d) compression strut.

case related to diagonal tension in the wall, because the shear mode of failure will be either shear slip along a bed joints or a stepped diagonal crack by breaking the bricks or the bond along a combination of head and bed joints. This type of failure may be captured in the diagonal compression test. In some cases, the loading shoes on opposite ends of diagonal can transfer compression load through a fairly large compression strut formed after the appearance of diagonal cracks (Fig. 5d and 6d). This compression strut can carry higher loads than those required to produce diagonal cracking, as it happened in the case of specimens P2 and P4.

The diagonal compression test belongs to the indirect test methods and is easy to perform and yields reliable results. Although not difficult to carry out in standard testing machine, it seems that the application of this form of test has not been fully explored.

5 DIRECT TENSILE STRENGTH OF PANELS

The tensile behavior of masonry can be also investigated by direct methods. They are characterized by applying directly the tensile force to the specimen. The main drawbacks of direct tests are their sensitivity with respect to eccentric application of tensile force and to shrinkage. For direct tensile loading perpendicular to the bed joints, the masonry strength is generally under influence of the relatively low tensile bond strength between the bed joint and the unit. In the paper the tests were performed for direct tensile loading parallel to the bed joints. The specimens (dimensions $520 \times 215 \times 120$ mm) were regained from the tests with predetermined single plane of shear failure (see section 3.2). In the case of direct tensile loading parallel to the bed joints, two different types of failure are possible, depending on the relative strength of joints and units (Fig. 7). In the first type of failure cracks zigzag through head and bed joints, in the second one cracks run almost vertically through the units and head joints. The failure load and the calculated strengths are given in Table 4. The tensile strength were calculated as a ratio of the failure load and the area A , where $A = 215 \times 120 \text{ mm}^2$.

Observations of the behavior of masonry in tension have been recorded in the literature (see Schubert 1997 for example). The simple formulae have been deduced



Figure 7. Failure modes for masonry under axial loads along the bed joints.

Table 4. Results of determination of direct tensile strength.

Direct tensile strength [N/mm ²] and failure load		
Specimen	Load [N]	Strength
1	43,000	1.67
2	34,500	1.34
3	52,500	2.03
4	38,000	1.47
5	37,500	1.45
6	46,500	1.80
Mean value	42,000	1.63
Standard deviation	6,700	
Coefficient of variation	15.9%	

to determine the masonry tensile strength as the lowest value of two possible forms of failure: failure of the unit due to tension and shear slip along the bed joints. However, in this case none of these formulae can be applied, since they are deduced by equilibrium, assuming that there is a uniform distribution of tensile stress and shear stress. The test without a vertical precompression is rather sensitive to applied load and stress peaks are likely to occur.

6 ANALYSIS OF RESULTS

Depending on the in-plane lateral and axial loads, as well on the form of wall construction, the shear failure mode may be characterized by three basic mechanisms: shear slip along the bed joints, diagonal tension cracking and shear compression failure. In unreinforced masonry, the first failure mode results from lateral shear forces exceeding the adhesion and shear-friction resistance between the mortar and the units or the floor. The diagonal tension cracking occurs either as a diagonal splitting or as step-pattern sliding along the mortar joints, depending on the characteristics of the constituent materials (mortars and bricks). Both of these two modes may be captured in diagonal compression tests. The third failure mode is attributed to predominance of the axial load leading to vertical cracking failure or to the more localized biaxial compression failure. Therefore, in order to predict properly the masonry shear capacity, it is necessary to first identify the most anticipated failure mechanism, based on the knowledge of the involved materials. To this end, the failure criteria are needed. For practical purposes however, it is necessary that the calculation of the shear strength of a wall should not be unduly complicated and that related test methods should be such that they can be carried out economically and without the need for highly specialized equipment. The failure criterion commonly adopted in codes of practice for combined compression and shear relates the strength

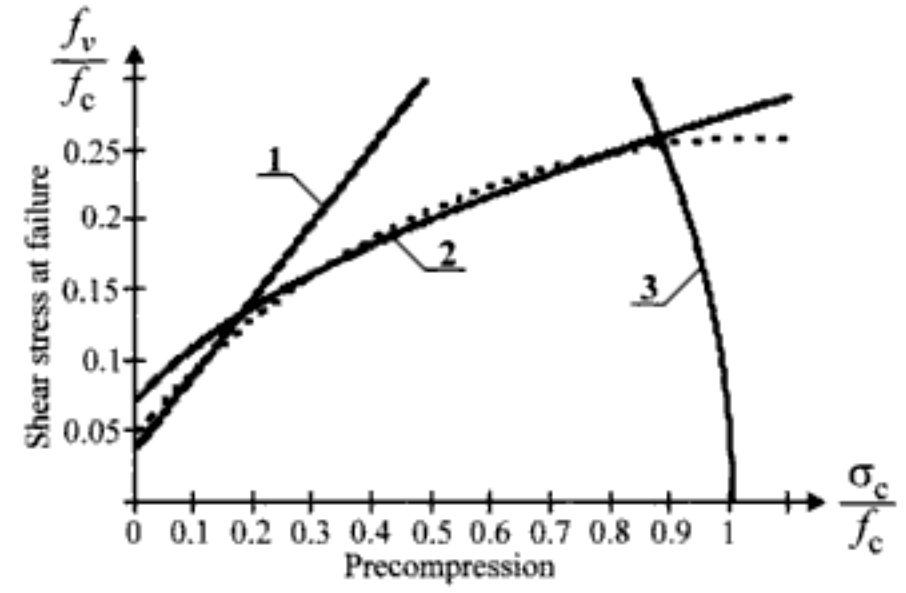


Figure 8. The comparison of the strength criteria for the experimental data: 1 – the Coulomb criterion, 2 – the principal tensile stress criterion, 3 – the compressive stress criterion.

to the compression by a Coulomb type equation (Equation 1). This relationship is in accordance with experimental results at least up to a certain value of the compressive stress. The Coulomb criterion is related to the shear slip along the bed joints failure mode. An alternative criterion may be based on the assumption that failure will be related to the attainment of a limiting value of the principal tensile stress (see Hendry 1997). Application of this criterion depends on being able to determine the principal tensile stress at failure. Assuming that the principal tensile stress at failure is constant and equal to the diagonal tensile strength, the criterion may be written in the simplest form as:

$$f_v = S_{pt} \sqrt{1 + \frac{\sigma_c}{S_{pt}}} \quad (3)$$

where f_v = shear strength of masonry (shear strength at failure), σ_c = precompression normal to the bed joints. By using the diagonal tensile strength S_{pt} , this criterion is related to the shear failure mode defined by diagonal cracking.

The third failure mode may be related to the principal compressive stress criterion for the case of biaxial compression state (see Malyszko 2002). This criterion may be written in the simplest form as:

$$f_v = n_c \cdot f_c \sqrt{1 - \frac{\sigma_c}{f_c}} \quad (4)$$

where f_c = the compressive strength of masonry for axial loading normal to the bed joints; n_c = ratio of the compressive strengths for parallel and normal loadings to the bed joints, respectively.

The comparison of the strength criteria for the experimental parameters obtained is shown in Figure 8. The plot is formatted in the dimensionless axes σ_c/f_c and f_v/f_c . The lines are drawn according to the following criteria: line 1 – Coulomb friction (Equation 1),

line 2 – the principal tensile stress (Equation 3) and line 3 – the principle compressive stress (Equation 4). The dash line denotes the shear failure criterion adopted from the paper Malyszko (2002). This criterion is not discussed here. The area between the lines and the horizontal axis describes the loading conditions for which the shear strength of the wall is not exceeded. The area is similar to that developed by Mann & Muller (1985) based on consideration of the equilibrium and strength of a unit within a wall. From the comparison of the principal tensile strength criterion (line 2) to the Coulomb criterion (line 1) for the experimental parameters i.e. for the cohesion value $f_{v0} = 0.53 \text{ N/mm}^2$ and the friction coefficient $\mu = 0.54$ and the diagonal tensile strength $S_{pt} = 1.01 \text{ N/mm}^2$ (Tables 1 and 3) it is seen the shear slip along the bed joints should be expected in the wall for the precompression stress below about 2.5 N/mm^2 . Above this value, which may be outside the range of the practical design, there is failure of the bricks as well of the bed joints, so, the diagonal cracking mechanism is likely to occur. This case is beyond the validity of Equation 1 and the assessment of the shear strength should be done based on Equation 3.

It is interesting to note that the ratio of f_{v0}/S_{pt} , i.e. the ratio of the initial shear strength from the triplet test to the diagonal tensile strength, may determine the shear failure mode. By comparing Equation 1 to 3 following inequality may be establish:

$$\frac{f_{v0}}{S_{pt}} \geq \frac{1+4\mu^2}{4\mu}, \quad (5)$$

for which the diagonal cracking mechanism should be expected. If this inequality does not hold the shear failure mode depends on the precompression level. Both the shear slip along the bed joints and the diagonal tension cracking are then likely to occur. The justification of these remarks, however, is not entirely clear since it would not appear possible to compare results from full scale tests on shear walls or panels for which small specimen strengths from triplets and diagonal compression tests are also available.

7 CONCLUSIONS

With the use of shear walls or infill walls built within a structural frame, in-plane shear and tensile strengths may be often of prime importance in loadbearing structures. Strength tests of masonry assemblages are used as the basis for assigning failure load and, in some cases, as a quality control measures or as a control of strengthening efficiency. Many test methods have been proposed for determining the shear strength of brickwork, including the effect of precompression. Most

of these are joint tests on small specimens, the simplest being the triplet type consisting of three bricks. In applying the Coulomb type equation, problems arise from difficulty in defining the limit of practical design compressive stress. Also, it could be said that control test is on a joint which is not representative of conditions in a wall. Beyond the validity of Coulomb criterion, it seems that the application of the diagonal compression test has not been fully explored. This test is not difficult to carry out in standard testing machine and uses larger masonry assemblages. The use of the diagonal compression test requires at present some further verification against shear wall test results.

Some problems may arise in devising a test which will reliably measure the initial shear strength – the parameter f_{v0} . New type of test is being currently investigated at the University in Olsztyn on the same masonry panels like in the diagonal compression test in order to predict this parameter (Fig. 2). In this test, it is not necessary to evaluate the strength with null compression by measuring the strength at a number of precompression levels. There is also not need to find then the value by extrapolating the best fit line to these results to null compression. However, the initial strength is the only value obtained. The test may be performed both for tangential and normal to the bed joints loading. As it is expected, the shear strength for tangential loading is related to the initial shear strength from the triplet test. However, for the experimental brickwork specimens its value is 25% higher than that obtained from the triplet test. For loading normal to the bed joints the limiting strength is defined by the strength of brick in direct shear.

The estimation of shear strength is clearly empirically based and approximate. Shear resistance is calculated on the mean shear strength in the wall, whereas the stresses are not uniform and the strength is to some extent dependent on the length of the wall. Nevertheless, both the strength criteria and tests related would appear to be sufficiently well validated for practical purposes.

ACKNOWLEDGEMENTS

The author wishes to express his gratitude for the support of the Scientific Committee of the University in Olsztyn, under university grant reference 0602-0214.

REFERENCES

- ASTM E 519-81. 1988. *Standard Test Method for Diagonal Tension (Shear) in Masonry Assemblages*. Philadelphia.
- EN 1996-1-1, EC 6: *Design of masonry structures*. Part 1-1: General Rules for reinforced and unreinforced masonry.

- Hendry, A.W. 1997. Shear Strength Criteria and Related Tests for Brick Masonry. *Advances in Structural Engineering Vol. 1 No. 2*: 135–141.
- Malyszko, L. 2002. Failure Criteria for Masonry as Anisotropic Material. In Proc. of the 4th Intern. Conf. "AMCM": 111–115. Cracow, Poland, 5–8 June.
- Malyszko, L. 2003. In-plane Tensile Strength of Masonry Panels Subjected to Diagonal Compression Tests. In Proc. of the Local Sem. of IASS PC: 63–66. Warsaw-Rzeszów Dec. 5: Micro-Publisher JBO WN. ISBN-83-908867-7-4.
- RILEM LUMB6. 1991. Diagonal tensile strength tests of small wall specimens.
- Mann, W. & Muller, H. 1985. Schubtragfähigkeit von gemauerten Wänden und Voraussetzungen für das Entfallen des Windnachweises. *Mauerwerk-Kalender*. Berlin: Ernst & Sohn Verlag.
- Schubert, P. 1997. Biegezugfestigkeit von Mauerwerk. Untersuchungsergebnisse an kleinen Wandprüfkörpern. *Mauerwerk-Kalender*: 611–628. Berlin: Ernst & Sohn Verlag.

Testing and modelling of multiple-leaf masonry walls under shear and compression

J. Pina-Henriques & P.B. Lourenço

University of Minho, Department of Civil Engineering, Guimarães, Portugal

L. Binda & A. Anzani

Politecnico di Milano, Department of Structural Engineering, Milano, Italy

ABSTRACT: Predicting the behaviour of multiple-leaf masonry walls is a challenging issue, given the influence of a wide range of factors as the mechanical properties of the leaves, their dimensions and the way they are connected to each other. In the present paper, experimental results in large specimens are carefully reviewed together with numerical interpretation of the shear and compressive behaviour of multiple-leaf walls. Simplified calculations for practical assessment of existing walls are also addressed.

1 INTRODUCTION

Multiple-leaf walls are frequently found in ancient buildings. They usually consist of two or three leaves made up of different materials such as stone, brick or rubble masonry. For an appropriate repairing/strengthening of masonry walls with minimum intervention, the bearing capacity of the structure has to be known prior to the intervention. However, this task is especially complex in the case of multiple-leaf walls, because the stress distribution is largely dependent on the mechanical properties of the leaves, on their dimensions and on the way they are connected to each other. In particular, the load transfer between leaves is a key issue when studying compressive damage of heavy pillars in monumental buildings, see Binda *et al.* (2003a).

References in literature can be found on this topic, see e.g. Binda *et al.* (1991), Egermann & Neuwald-Burg (1994), Binda *et al.* (1994) and Drei & Fontana (2001). Yet, further experimental and numerical insight on the shear and compressive behaviour of composite walls is needed. For this purpose, a set of twelve three-leaf stone wallets (regular-rubble-regular) with dimensions of $310 \times 510 \times 790 \text{ mm}^3$ were built and tested at the Politecnico di Milano, within the frame of a National Research Contract (responsible L. Binda), see Binda *et al.* (2003b). Two types of collar joints (with and without shear keys) and two types of stones (a limestone named Noto and a sandstone named Serena) have been considered. The wallets were tested according to three

different procedures:

- Shear tests. A monotonic load was applied to the inner-leaf while the outer-leaves were supported. This test is similar to the EN 1052-3 (CEN, 2002).
- Compression tests on single leaves. Outer and inner leaves were tested individually under uniaxial compression.
- Compression tests on full wallets. A monotonic load was applied to the complete transversal section of the wallets.

This paper addresses the results obtained in the experimental tests and their critical analysis, resorting to simplified calculations and, also, to sophisticated numerical tools.

2 EXPERIMENTAL TESTS

Tests were carried out on the wallets given in Table 1. The specimens dimensions are shown in Figure 1. The same type of stone was used both for the outer and inner leaves.

Table 1. Designation of the wallets according to the type of stone and connection.

	Straight collar joints	Keyed collar joints
Noto limestone	NS1, NS2, NS3	NO1, NO2, NO3
Serena sandstone	SS1, SS2, SS3	SO1, SO2, SO3

2.1 Characterization of masonry components

Physical and mechanical tests were carried out on cylindrical samples cored from the stone units used to build the wallets. The units were cored considering two different orientations: along the loading direction L and along the bedding direction B , so that the anisotropy of the material could be characterized.

The physical tests consisted on the determination of the bulk density and open porosity, according to EN 772-4 (CEN, 1998). Six cylindrical specimens with a diameter of 80 mm and a height of 145 mm were considered for each type of stone. The average results obtained in terms of the bulk density $\rho_{b,s}$ and the open porosity P_o are given in Table 2. In addition, the coefficient of variation CV is also given. The values found illustrate the significantly different physical properties of the two stones. The Noto limestone exhibits high open porosity and low weight while the Serena sandstone exhibits a 1.5 times larger weight and seven times less porosity.

Uniaxial compressive tests were carried out after the physical tests, on the same cylindrical samples, according to EN 772-1 (CEN, 2000). Three specimens for each combination type of stone/orientation were tested. The average values for the compressive strength f_c , the peak strain ε_p , the modulus of elasticity E and the coefficient of Poisson ν are given in Table 3. According to the results obtained, the Serena stone exhibits, in the loading direction, a strength about five times larger than the Noto stone and about the double of the stiffness.

The tensile strength was obtained resorting to the indirect tension test (splitting test), according to the

RILEM recommendation CPC6, RILEM (1994). The tests were carried out on six cylindrical specimens for each type of stone with a diameter and height of 80 mm. The specimens were cored along the bedding direction of the units. This direction is the most relevant with respect to the tensile strength as it is the direction where the principal tensile stresses occur when units are vertically loaded.

The average results obtained are given in Table 4. In the case of concrete, the splitting tensile strength $f_{t,s}$ is about 5 to 12% higher than the direct tensile strength f_t , see Neville (1997). Here, f_t has been considered equal to $0.9 f_{t,s}$. According to the results obtained, the Noto stone exhibits an average tensile strength three times smaller than the Serena stone. Relatively to the ratio between the compressive and tensile strengths, a value of ten times was found for the Noto stone and a value of seventeen times was found for the Serena stone.

A commercial premixed hydraulic lime mortar denominated *Albaria Allettamento*, Italy, was adopted to build the wallets. Flexural and compressive tests have been carried out according to EN 1015-11, (CEN, 1999). The tests were performed at four ages: 28 days, 75 days (corresponding to the beginning of the tests), 90 days and 172 days (corresponding to the end of the testing programme). For each curing stage a total of six prisms were tested.

Table 5 gives the average results obtained for the flexural strength f_f and for the compressive strength f_c . The results found yield average values for the flexural and compressive strengths during the testing period (75 to 172 days) of 2.2 N/mm^2 and 10.3 N/mm^2 . Generally, a factor of 1.5 can be assumed for the ratio between flexural and tensile strengths, see Van der Pluijm (1999) and Lourenço (1997).

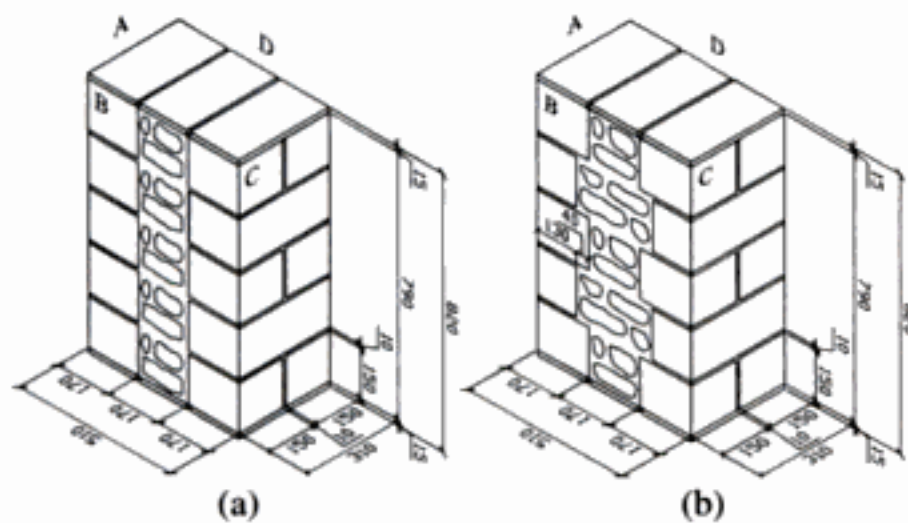


Figure 1. Wallets dimensions in mm: (a) straight collar joints and (b) keyed collar joints.

Table 2. Average results of the bulk density and open porosity of the stones.

Type of stone	$\rho_{b,s}$ (kg/m^3)	$CV\%$	$P_o\%$	$CV\%$
Noto	1760	1.5	15.4	4.5
Serena	2570	0.3	2.1	5.7

Table 3. Average results obtained from the compression tests on the stones (values in brackets give the CV).

Type of stone	Orientation	f_c (N/mm^2)	ε_p 10^{-3}	E (N/mm^2)	ν
Noto	L	20.6 (7%)	2.4	9475	0.10
Noto	B	17.6 (22%)	2.3	8525	0.09
Serena	L	104.2 (1%)	*	18218	0.19
Serena	B	89.0 (15%)	*	23293	0.21

*The Serena specimens had to be tested in a machine with a higher capacity, which did not allow recording the displacement values.

Table 4. Average results obtained from the tension tests on the stones (values in brackets give the CV).

Type of stone	Orientation	$f_{t,s}$ (N/mm^2)	f_t (N/mm^2)
Noto	B	2.05 (13%)	1.8
Serena	B	6.00 (12%)	5.4

Table 5. Average results obtained from the flexural and compression tests on the mortar (values in brackets give the CV).

Curing time (days)	f_f (N/mm ²)	f_c (N/mm ²)
28	1.5 (6%)	7.4 (3%)
75	1.9 (13%)	9.2 (6%)
90	2.3 (10%)	9.7 (7%)
172	2.2 (9%)	11.2 (5%)

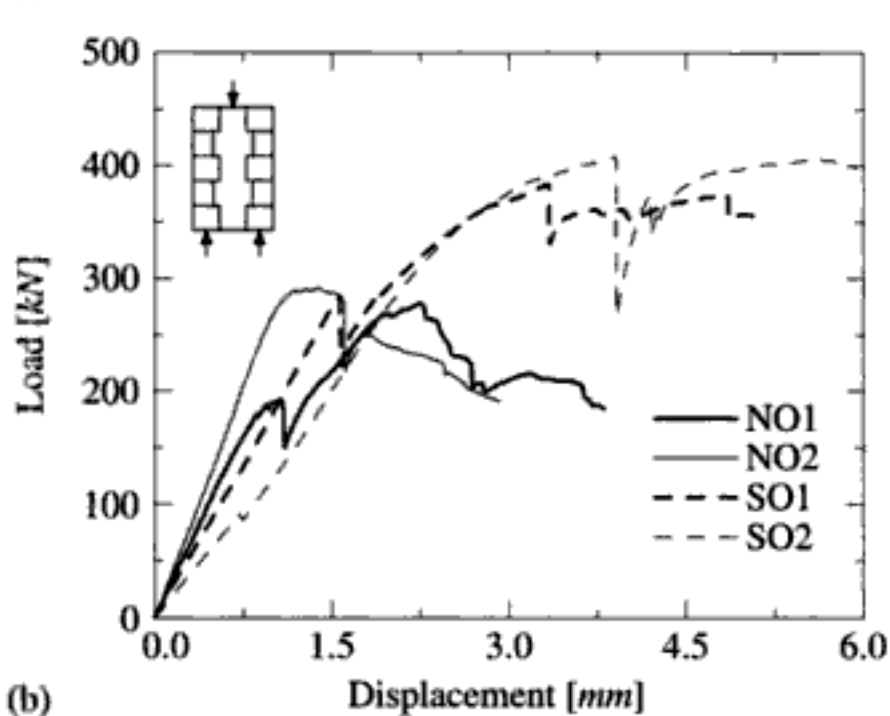
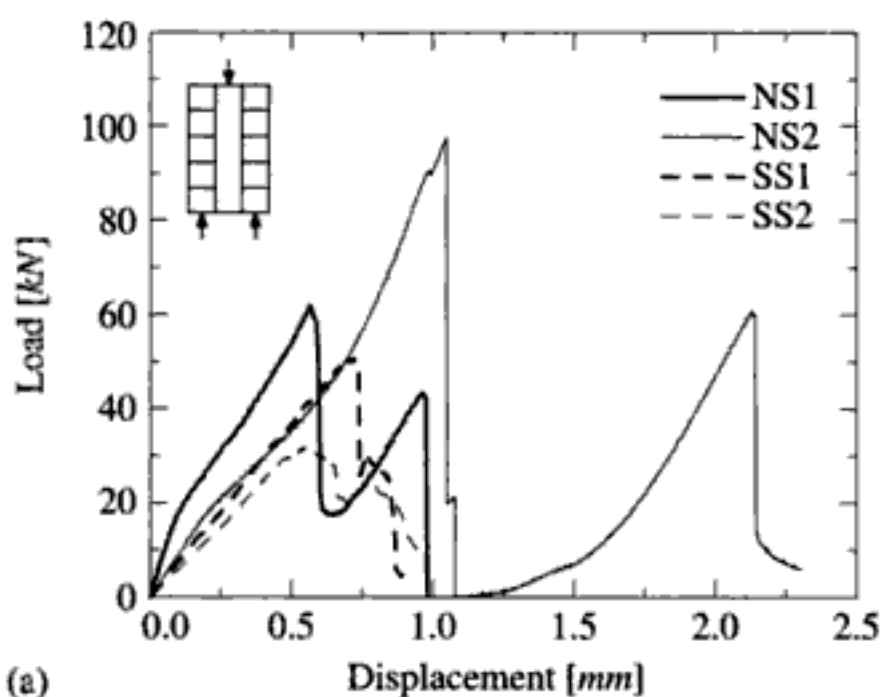


Figure 2. Load-displacement diagrams obtained for the shear tests: (a) straight collar joints and (b) keyed collar joints.

Table 6. Average results obtained from the shear tests.

Wallets	Type of stone	Type of connection	τ_r (N/mm ²)	δ (mm)	τ'_r (N/mm ²)	δ' (mm)
NS1,NS2	Noto	Straight	0.17	0.81	0.22	1.55
SS1,SS2	Serena	Straight	0.09	0.64	0.11	0.78
NO1,NO2	Noto	Keyed	0.58	1.82	–	–
SO1,SO2	Serena	Keyed	0.81	3.62	–	–

2.2 Results of shear tests

Two wallets for each combination type of stone – type of connection were tested in a total of eight specimens, see also Binda *et al.* (2003c) and Anzani *et al.* (2003).

The load-displacement diagrams obtained are illustrated in Figure 2. In the case of the wallets with straight collar joints, a non-symmetric response of the connections was found, with failure occurring non-simultaneously. Such behaviour had also been found by Lourenço *et al.* (2004) in triplet tests performed on three courses brick masonry panels and must be considered characteristic of the triplet test.

The first peak in the diagrams of Figure 2a corresponds to the failure of the weakest connection and provides the shear strength τ_r for a shear area of $2 \times 310 \times 790 \text{ mm}^2$. After failure of the first connection a minor rotation of the two leaves still connected was observed due to the eccentricity of the applied load. From that point on the test cannot be intended as a triplet test due to the change in the loading scheme and, therefore, the values related to the second connection to fail should be considered carefully. Namely, the second peak represents the combination of a higher shear strength for the second joint and some minor friction in the first joint due to bending. If the effect of bending is neglected the second peak provides the shear strength of the strongest joint τ'_r , for a shear area of $310 \times 790 \text{ mm}^2$. This holds true only because no confining pressure is present.

For the wallets with keyed collar joints, the shear strength was calculated assuming straight connections and, thus, the value represents an “equivalent” shear strength.

Table 6 gives, in the case of straight collar joints wallets, the average shear strengths (τ_r and τ'_r) and displacements (δ and δ') corresponding to the first and second load peaks. For keyed collar joints wallets, the average values of the shear strength and the corresponding displacements are given.

It is possible to verify that the shear strength of the straight collar joints wallets is mainly influenced by the physical properties of the stone (larger porosity yields better adhesion stone-mortar) while for the keyed collar joints wallets, the strength of the stone is an issue that must be considered.

In terms of ductility the specimens with straight collar joints show a similar behaviour for both types of

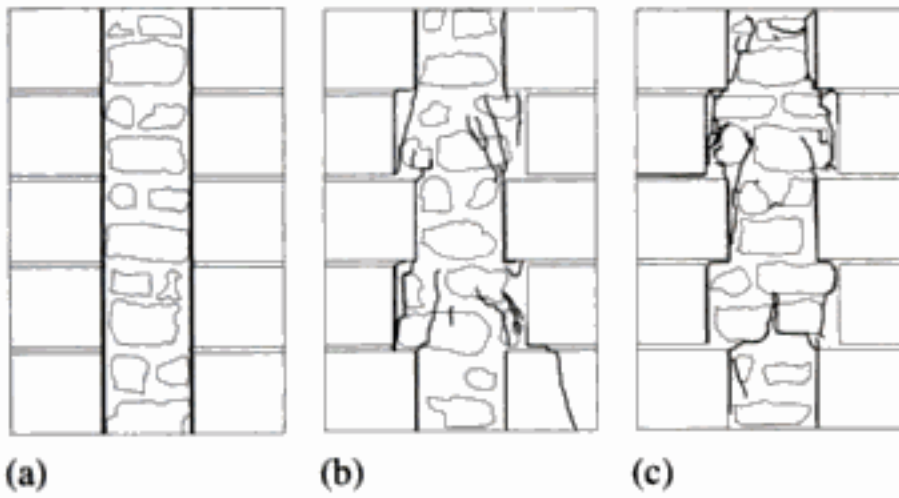


Figure 3. Typical ultimate crack patterns for (a) straight collar joints wallets (NS1) and keyed collar joints wallets: (b) Noto (NO1) and (c) Serena (SO2).

stones. The failure is quite brittle and without showing any residual strength, given that the test set-up allows the wallets to move freely outwards. Regarding the wallets with keyed collar joints, the Serena specimens exhibit a less brittle behaviour than the Noto specimens. This is probably due to the different behaviour found for the inner-leaves as it will be shown below.

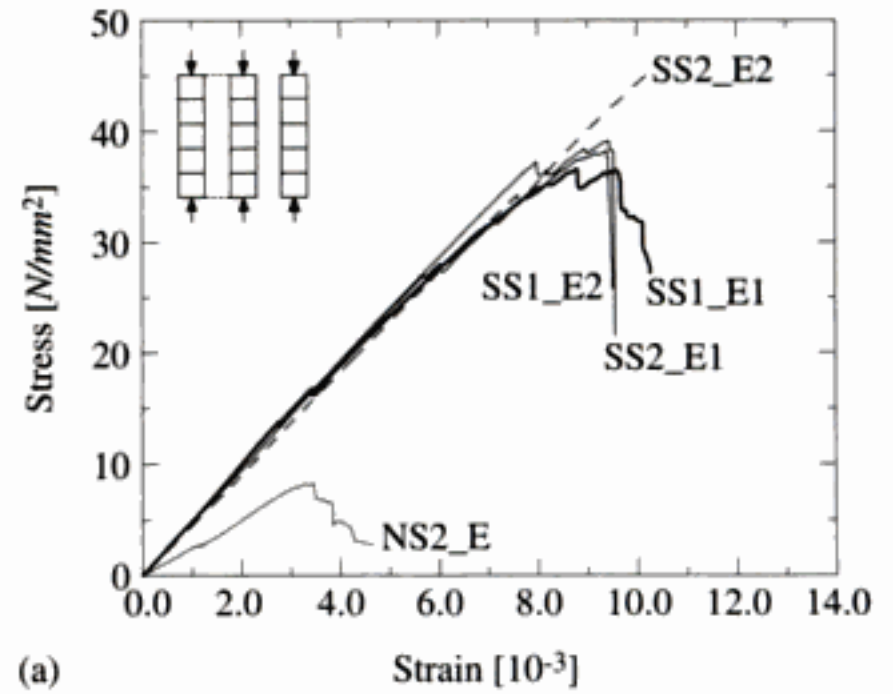
Typical ultimate crack patterns are illustrated in Figure 3. The wallets with straight collar joints failed due to the development of two vertical shear cracks along the connections. No other visible damage was observed at the end of the test.

In the case of the specimens with keyed collar joints, the cracking pattern was different according to the type of stone. For the Noto specimens, damage was observed in both outer and inner leaves. In the inner-leaves, more severely damaged, diagonal cracks were observed, developing from the shear keys and passing through the inner-leaf stones. Relatively to the outer-leaves, diagonal cracks near the base appeared. At ultimate stage, full separation in three irregular leaves could be observed.

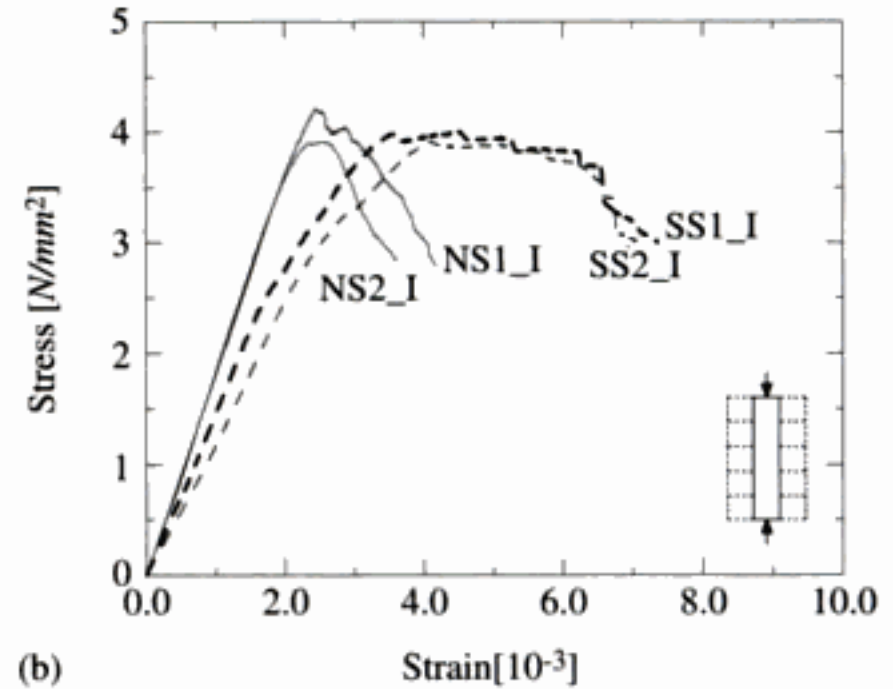
In the Serena specimens, the cracks developed only in the inner-leaf. However, in this case, cracks usually went around the stones instead of breaking them, due to the larger strength and smaller adhesion stone-mortar. At ultimate stage, it is clearer to observe that only the inner-leaf collapsed.

2.3 Results of compression tests on single leaves

The tests were performed on the leaves of the wallets with straight collar joints, previously tested in shear, see Section 2.2 and Binda *et al.* (2003c). In the case of the Noto specimens, both outer-leaves were tested simultaneously, trying to reproduce what may happen in real composite walls: shear failure of the connections followed by transfer of almost all the load to the external stiffer elements. This can explain the type of damage found in massive pillars, see Binda *et al.* (2003a) In the case of the Serena leaves, which were much more resistant, the same procedure could not



(a)



(b)

Figure 4. Stress–strain diagrams obtained: (a) outer-leaves and (b) inner-leaves. A problem in the acquisition system prevented fully capturing the NS1_E diagram and, thus, it is not shown. It is also noted that failure of specimen SS2_E2 could not be attained within the capacity of the testing machine.

be adopted due to the limited capacity of the testing machine and, thus, the leaves had to be tested separately.

A comparison between the stress–strain diagrams obtained for the outer and inner leaves is shown in Figure 4. The average results obtained, including the strength f_c , the peak strain ϵ_p , the elastic modulus E and the Poisson coefficient ν are given in Table 7.

From the given results it is possible to verify that the Noto outer-leaves exhibit a strength of about 45% the stone strength and the inner-leaf about 20%. In the case of the Serena leaves, the same ratios are about 40% for the outer-leaves and only 4% for the inner-leaf. It is further noted that Serena inner-leaves exhibit a less brittle behaviour than Noto specimens, due to the higher strength of the stones, forcing cracks to go around them instead of passing through.

Typical ultimate cracks patterns are illustrated in Figure 5 and Figure 6 for the outer and for the inner leaves, respectively. The shaded areas indicate spalling of the stone.

Table 7. Average results obtained.

Specimen	Stone type	Leaf	Peak load (kN)	f_c (N/mm ²)	ϵ_p (10 ⁻³)	E (N/mm ²)	ν
NS_E	Noto	Outer	912	8.7	3.3	3150	–
SS_E	Serena	Outer	2095	39.8	9.5	4870	–
NS_I	Noto	Inner	214	4.1	2.6	1830	0.15
SS_I	Serena	Inner	209	4.0	4.3	1405	0.18

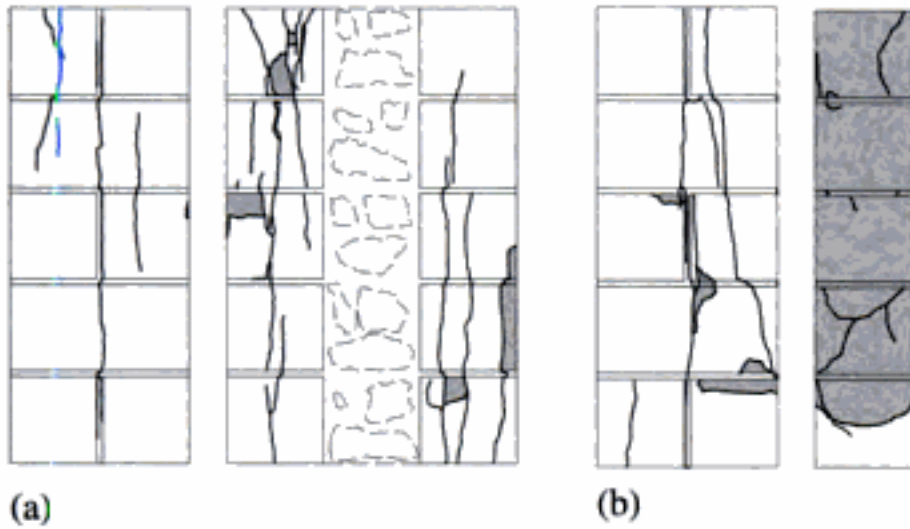


Figure 5. Typical ultimate failure patterns for the outer-leaves: (a) Noto stone and (b) Serena stone.

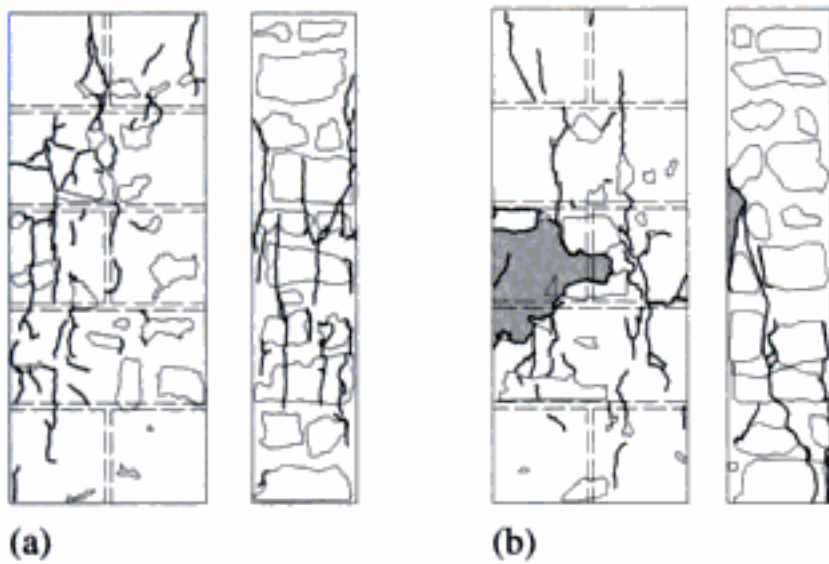


Figure 6. Typical ultimate failure patterns for the inner-leaves: (a) Noto stone and (b) Serena stone.

2.4 Results of compression tests on full wallets

One wallet of each type (stone/connection combination) was tested in compression, in a total of four specimens. Yet, the peak load for the Serena wallets was beyond the capacity of the testing machine and a maximum load of 2380 kN was applied. The stress-strain diagrams obtained are shown in Figure 7. Table 8 gives the results found.

The following observations can be made from the results, even if the limited number of tests precludes any conclusive statement:

- The strength of the Noto wallet with keyed joints seems to be about 10% higher than the wallet with straight collar joints.

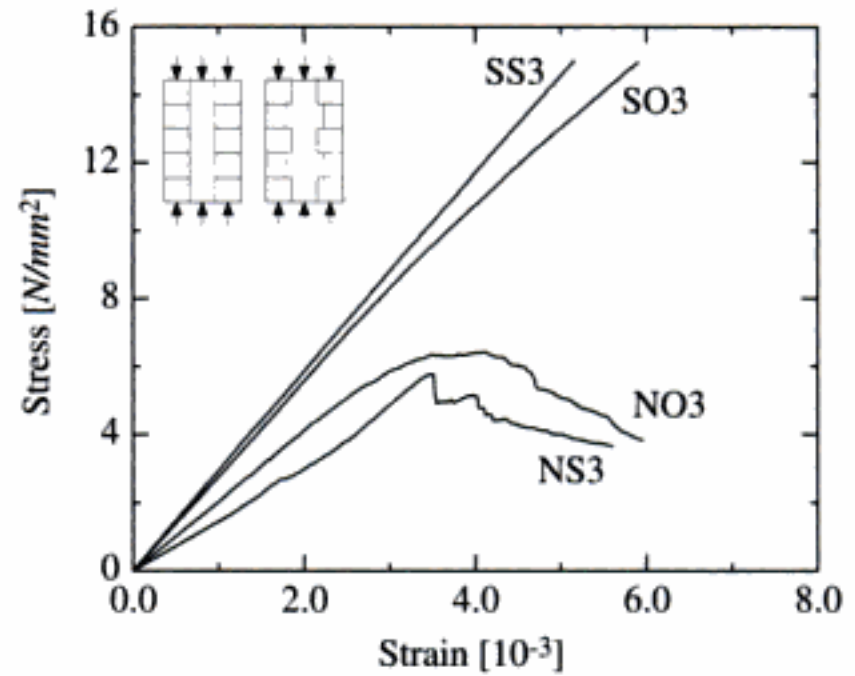


Figure 7. Stress-strain diagrams obtained.

- The Noto wallet with keyed collar joints seems to exhibit a less brittle behaviour than the wallet with straight collar joints.
- The peak load of any of the two Noto wallets tested is not much higher than the peak load of the single outer-leaves: 912.3 kN.

The ultimate failure patterns are illustrated in Figures 8 and 9. The shaded areas indicate spalling of the stone. The Noto wallet with straight connections failed due to the development of several vertical cracks in the outer-leaves while the inner-leaf was practically undamaged.

In the case of the Noto wallet with keyed connections the outer-leaves exhibited a more severe and diffuse cracking pattern with several vertical cracks developing in the inner-leaf near the peak load. Regarding the Serena wallet with keyed connections and despite the fact that the peak load was not attained, the development of some cracks in the inner-leaf could be observed.

3 PRELIMINARY SIMPLIFIED CALCULATIONS

This section contains a first analytical interpretation of the test results, with simple calculations being used to predict the compressive strength of the wallets

Table 8. Results obtained for the compression tests.

Wallet	Type of stone	Type of connection	Peak load (kN)	f_c (N/mm ²)	ε_p (10 ⁻³)	E (N/mm ²)
NS3	Noto	Straight	913	5.8	3.5	1770
SS3	Serena	Straight	>2380	>15.1	>5.2	2940
NO3	Noto	Keyed	1013	6.4	4.1	2085
SO3	Serena	Keyed	>2380	>15.1	>5.9	2725

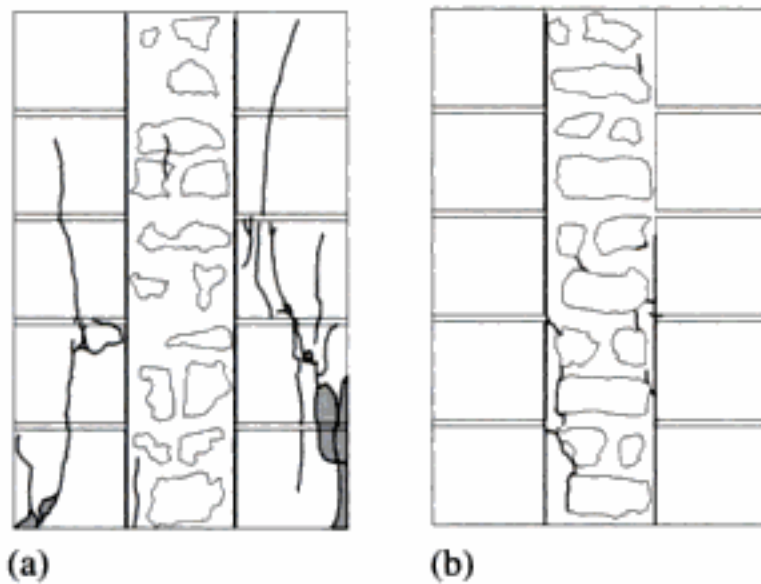


Figure 8. Ultimate failure patterns for the wallets with straight collar joints: (a) Noto (NS3) and (b) Serena (SS3).

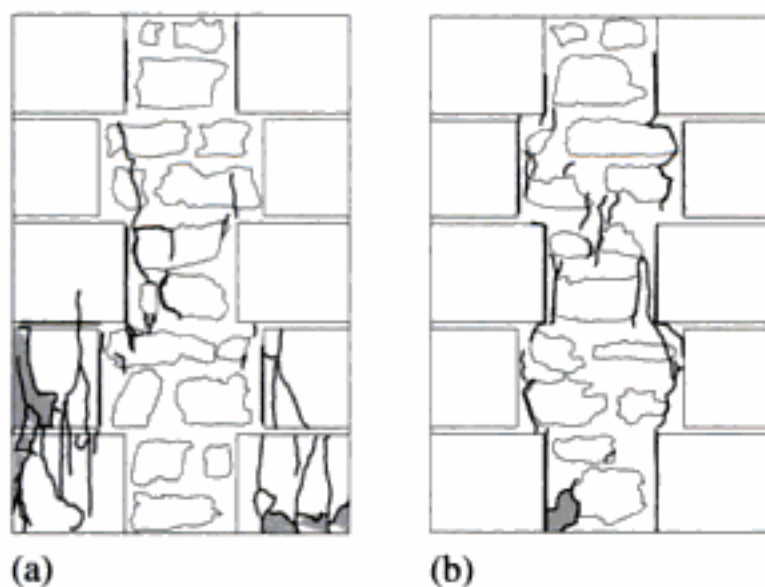


Figure 9. Ultimate failure patterns for the wallets with keyed collar joints: (a) Noto (NO3) and (b) Serena (SO3).

tested. It is noted that the experimental results found should be considered as indicative and conclusions should be taken carefully due to the small number of specimens.

The compressive strength of composite sections f_c can be estimated resorting to the following equations, each one assuming different hypotheses:

(a) the external load is completely supported by the stiffer elements, i.e., the outer-leaves

$$f_c = \frac{2t_e}{2t_e + t_i} \cdot f_e \quad (1)$$

(b) the external load is supported by each leaf according to its cross-sectional area ratio

$$f_c = \frac{2t_e}{2t_e + t_i} \cdot f_e + \frac{t_i}{2t_e + t_i} \cdot f_i \quad (2)$$

(c) the external load is supported by each leaf according to its area ratio and adjusted by a correction factor, see Egermann and Neuwald-Burg (1994)

$$f_c = \frac{2t_e}{2t_e + t_i} \cdot \theta_e \cdot f_e + \frac{t_i}{2t_e + t_i} \cdot \theta_i \cdot f_i \quad (3)$$

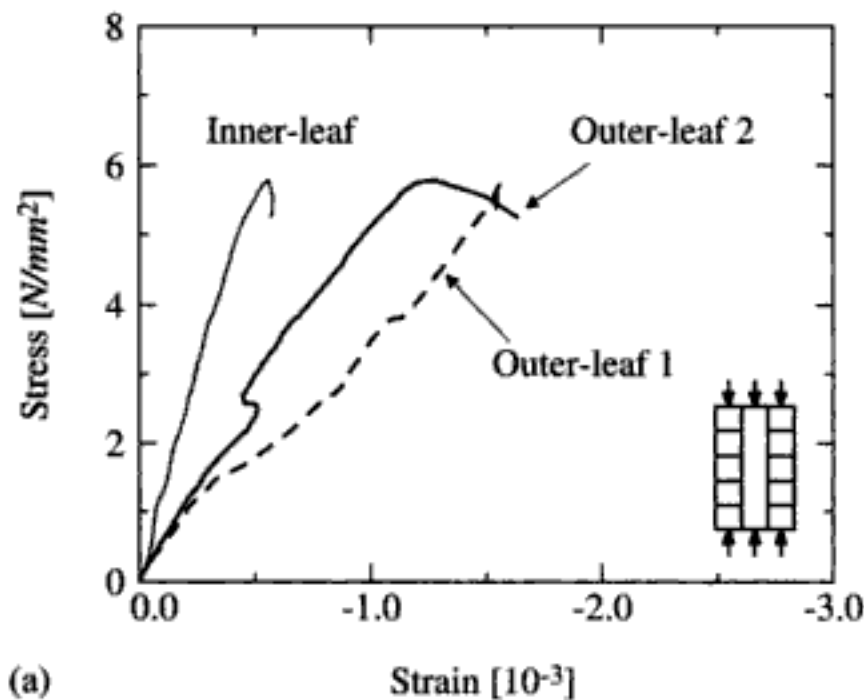
In the above, t_e and t_i are the thicknesses of the outer and inner leaves and f_e and f_i are the uniaxial compressive strengths of the outer and inner leaves. The parameters θ_e and θ_i are correction factors for the outer and inner leaves, assuming that the outer-leaves are under biaxial compressive stresses and bending moments and, thus, their uniaxial strength should be reduced and that the inner-leaf is under a biaxial compressive state of stress and, therefore, its uniaxial strength should be increased.

The results obtained for the wallets with and without shear keys are given in Table 9. In the case of the wallets with keyed collar joints, the thickness assumed for the inner-leaf includes the length of the shear keys. With respect to the application of Eq. (3), the values adopted for the correction parameters were $\theta_e = 0.7$ and $\theta_i = 1.3$, see Egermann and Neuwald-Burg (1994). It is further noted that Eq. (1) was not used to estimate the strength of the wallets with keyed joints because, in this case, it is clear that the inner-leaf is collaborating in the composite response.

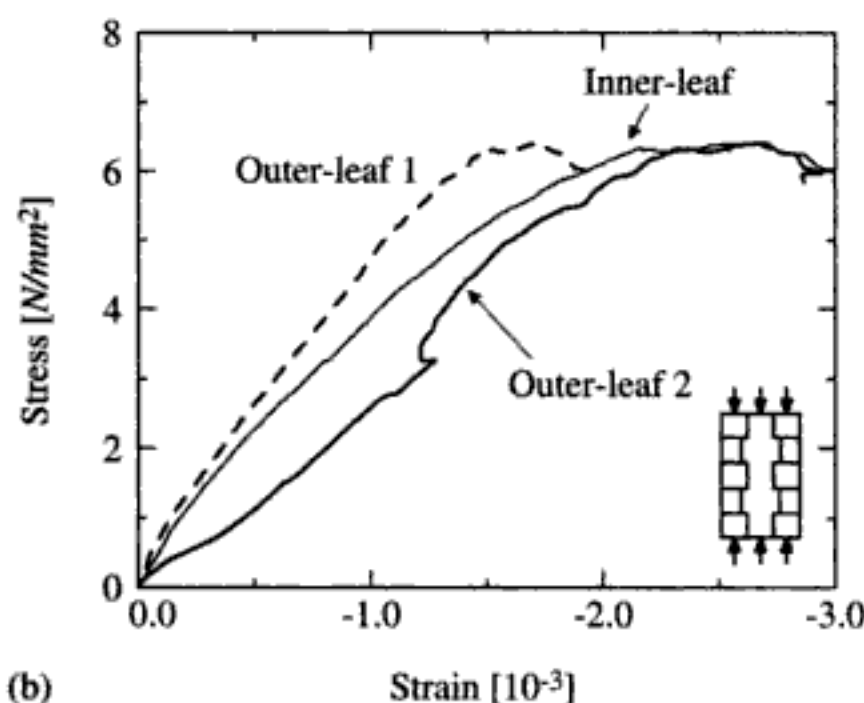
The value predicted for the compressive strength of the wallets with straight collar joints using Eq. (1) and Eq. (3) show an excellent agreement with the experimental results. Note that, however, the fact that the experimental and the predicted values are exactly the same should be considered just as a coincidence. The stress-strain diagrams illustrated in Figure 10a show that the inner-leaf vertical deformation do not accompany the vertical deformations of the outer-leaves and that, at failure, the inner-leaf strain is quite less than its peak strain, see also Figure 11a. As a consequence, the bearing capacity of the inner-leaf is

Table 9. Predicted compressive strength values for the tested wallets.

Wallet	Type of stone	Type of connection	Exp. f_c (N/mm^2)	Predicted f_c [N/mm^2]		
				Eq. (1)	Eq. (2)	Eq. (3)
NS3	Noto	Straight	5.8	5.8	7.2	5.8
SS3	Serena	Straight	>15.1	25.3	26.6	19.4
NO3	Noto	Keyed	6.4	–	6.4	5.7
SO3	Serena	Keyed	>15.1	–	21.3	16.1



(a)

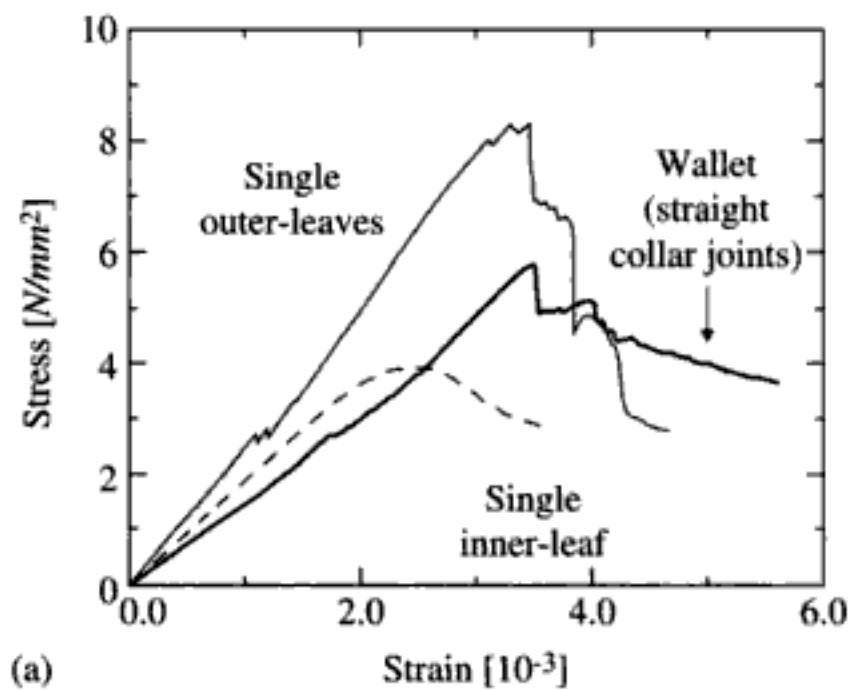


(b)

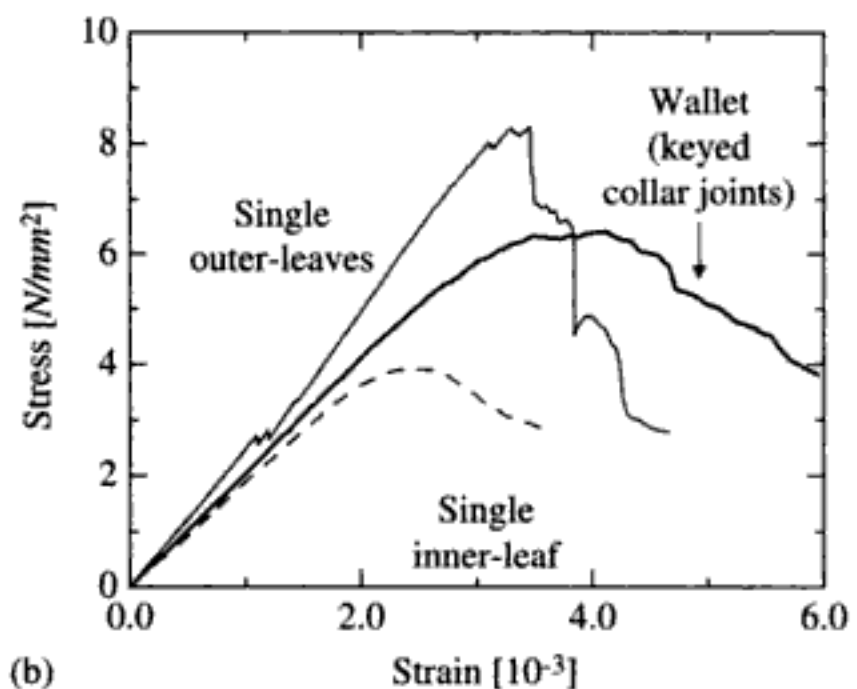
Figure 10. Compression stress–strain diagrams of the leaves inside the composite Noto wallets: (a) straight collar joints (NS3) and (b) keyed collar joints (NO3).

only partially mobilized and the hypothesis of Eq. (1) holds fairly true. The causes for the different deformations in the wallet leaves are not completely clear but a possible reason may be attributed to settling of the inner-leaf prior to testing.

In the case of the wallets with keyed collar joints, Eq. (2) yielded the best result while the strength predicted by Eq. (3) is less than the experimental value for the Noto wallets. This indicates that the inner-leaf is collaborating in the wallets response, as confirmed



(a)



(b)

Figure 11. Compression stress–strain diagrams of the single Noto inner and outer leaves and of the full wallets with: (a) straight collar joints (NS3) and (b) keyed collar joints (NO3).

by Figures 10b and 11b, but the assumptions of a strength reduction of the outer-leaves due to bending and a strength increase of the inner-leaf due to confinement do not apply. This can be explained by the test boundary conditions, which allow horizontal displacements at the top and bottom of the wallets. In such way, the effects of outer-leaves bending and inner-leaf confinement are diminished.

Finally, it should be noted that each equation considered independently predicts a larger strength for the wallets with straight collar joints than for the wallets

with keyed collar joints. This is due to the reduction of the cross-sectional area of the outer-leaves in the case of the specimens with shear keys. However, the opposite behaviour was found in experiments. The reason of such behaviour can be attributed to the fact, as already mentioned, that the inner-leaf was almost not collaborating in the experimental response, in the case of wallets with straight collar joints.

4 NUMERICAL SIMULATIONS

This chapter deals with the numerical simulation of the tests performed and represents a relevant contribution towards the interpretation of the results. The leaves of the wallets were represented using plane stress continuum elements (8-noded) with 2×2 Gauss integration while line interface elements (6-noded) with 3×3 Lobatto integration have been adopted for the collar joints. The analyses were carried out with indirect displacement control with line searches. It is further noted that the self-weight of the wallets was not considered.

For the material behaviour, a composite plasticity model with a Drucker-Prager yield criterion in compression and a Rankine yield criterion in tension was adopted. The inelastic behaviour exhibits a parabolic hardening/softening diagram in compression and an exponential-type diagram in tension. The material behaves elastically up to one-third of the compressive strength and up to the tensile strength. For the interface elements a combined cracking-shearing-crushing model developed by Lourenço (1996a) was adopted. The compressive mode was, however, not active and interface failure could only occur by shear or/and tensile yielding. Both shear and tensile modes exhibit exponential-type softening.

The elastic material properties adopted for the wallets leaves are given in Table 10 and the inelastic

Table 10. Elastic properties for the wallets leaves.

Material	E (N/mm^2)	ν
Outer-leaves	3150	0.10
Inner-leaf	2100	0.15

Table 11. Inelastic properties for the wallets leaves.

Material	c (N/mm^2)	f_t (N/mm^2)	$\sin \phi$	$\sin \psi$	Gf_c (N/mm)	Gf_t^* (N/mm)
Outer-leaves	3.7	1.8	0.17	0.09	5.0	0.070
Inner-leaf	1.7	0.3	0.17	0.09	5.0	0.035

* For the shear simulations of the keyed wallets, the values adopted for Gf_t were 0.150 (outer-leaves) and 0.070 N/mm (inner-leaf), so that numerical convergence could be found.

properties in Table 11. Here, E is the elastic modulus, ν is the Poisson coefficient, c is the cohesion, f_t is the tensile strength, ϕ is the friction angle, ψ is the dilatancy angle, Gf_c is the compressive fracture energy and Gf_t is the tensile fracture energy. The cohesion is obtained from Eq. (4), which derives from the Drucker-Prager yield function applied to uniaxial compression. Here, f_c is the compressive strength. The tensile strength of the outer-leaves was considered equal to the tensile strength of the stone, assuming, thus, vertical cracking. The tensile strength of the inner-leaf was obtained according to $f_t = f_c/15$, which is a relation often found for masonry specimens. The value adopted for the friction angle was 10° (a larger value in plain stress would implicate an overestimation of the biaxial strength) and, for the dilatancy angle, a value of 5° was assumed. For the tensile fracture energy, a value in agreement with the experimental results reported by Van der Pluijm (1999) for brick specimens was adopted. Values of the elastic modulus and of the compressive fracture energy were adopted so that the numerical response of the specimens resembled the experimental response, see Figure 12.

$$c = \frac{1 - \sin \phi}{2 \cos \phi} f_c \quad (4)$$

The elastic material properties assumed for the collar joints are given in Table 12 and the inelastic

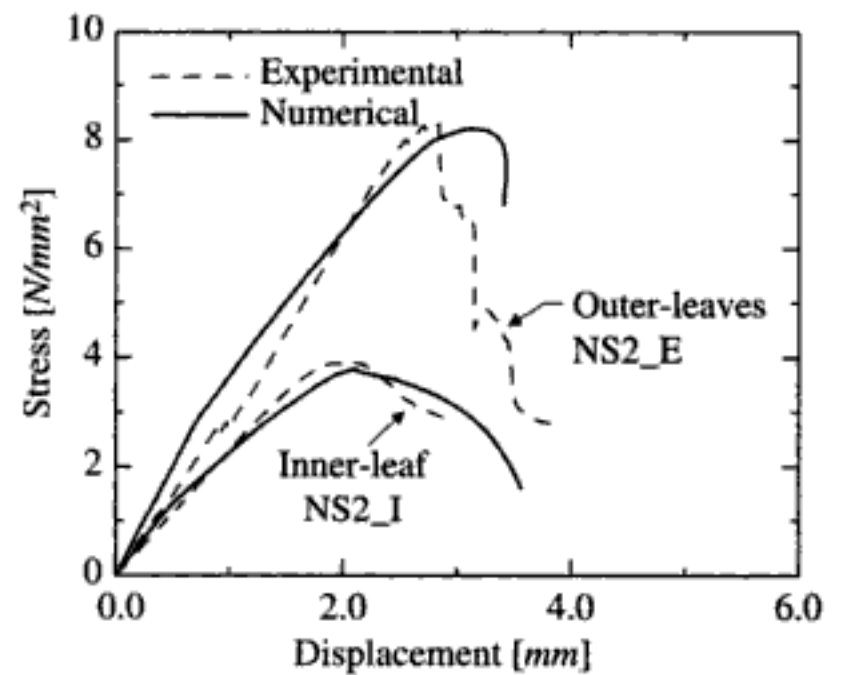


Figure 12. Stress-displacement diagrams for the leaves of the Noto wallets.

properties are given in Table 13. The parameters were obtained, whenever possible, from the shear test on wallet NS1 but most of the inelastic parameters are unknown and must be estimated. The interfaces shear stiffness k_s was adopted so that the numerical and experimental elastic responses showed a good agreement. Based on elastic assumptions, the normal stiffness k_n can be obtained according to $k_n = k_s \times 2(1 + \nu) = 1.0 N/mm^3$, where $\nu = 0.2$ is the coefficient of Poisson. However, higher values had to be adopted in order to avoid interpenetration of the two continua separated by the interfaces. The cohesion c for the first connection to fail was given experimentally but for the second connection a value was adopted so that the numerical response resembles the experimental response. The values of the remaining inelastic parameters (tensile strength f_t , friction coefficient $\tan \phi$, dilatancy coefficient $\tan \psi$, mode I fracture energy Gf_I and mode II fracture energy Gf_{II}) were adopted in agreement with the values experimentally found by Van der Pluijm (1999) and recommended by Lourenço (1996b) for unit-mortar interfaces.

4.1 Shear simulations

The shear tests for both types of wallets, either with or without shear keys, have been numerically reproduced. As it will become clear later in the text, the testing boundary conditions are a key issue for the correct interpretation of the results. The experimental test set-up was composed by two steel plates at the bottom, supporting the outer-leaves, and a third plate over the inner-leaf, through which a vertical load was applied. Additionally, sheets of Teflon were placed between the steel plates and the wallets. Therefore, the shear interaction between the plates and the wallets is not a clear issue and must be further investigated.

Table 12. Elastic properties for the collar joints.

Collar joint	k_n^* (N/mm^3)	k_s (N/mm^3)
1 (left)	150	0.4
2 (right)	150	0.4

* For the shear tests on straight collar joints wallets a lower value of $10 N/mm^3$ was adopted.

Table 13. Inelastic properties for the collar joints.

Collar joint	c (N/mm^2)	f_t (N/mm^2)	$\tan \phi$	$\tan \psi$	Gf_I (N/mm)	Gf_{II} (N/mm)
1 (left)	0.13	0.09	0.70	0.00	0.015	0.050
2 (right)	0.21	0.14	0.70	0.00	0.015	0.060

For the wallets with straight collar joints, this aspect has been assessed by considering four different shear stiffnesses k_s at the supports:

- $k_s = 0$, the specimen is free to slide over the steel plates.
- $k_s = \infty$, shear slip is precluded between the specimen and the plates.
- Intermediate $k_s = 0.01 N/mm^3$, a constant shear stiffness is applied and, thus, shear slip can occur but the horizontal reactions at the boundaries increase with increasing displacement.
- Non-linear k_s . At the level of the upper plate, shear slip is free to occur up to a certain relative displacement, beyond which, shear slip is completely restrained. A transition phase for k_s was also considered. At the level of the bottom supports, shear slip is precluded.

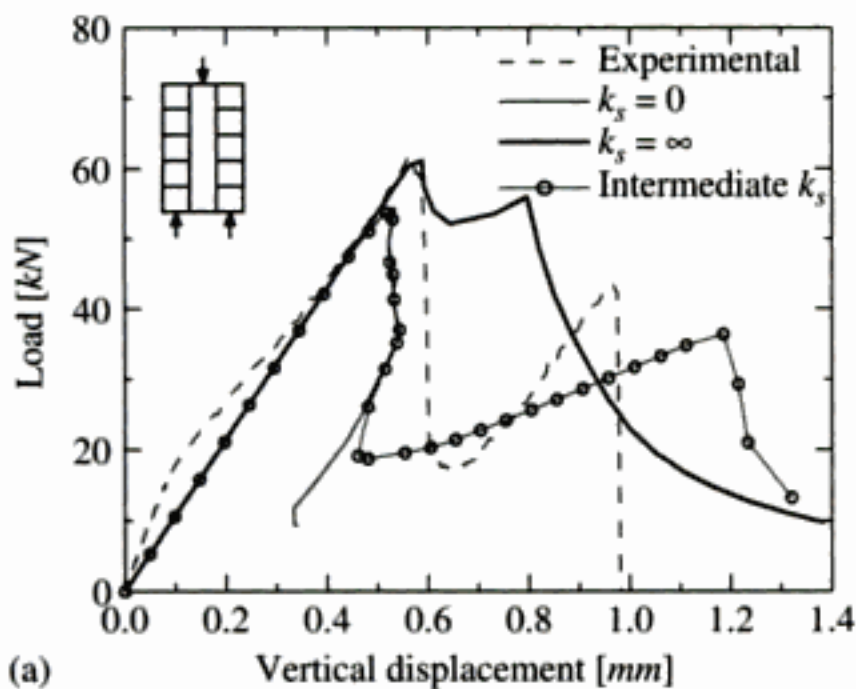
Regarding the normal stiffness k_n given to the boundaries, the same behaviour was adopted for all cases. Zero stiffness in tension and infinite stiffness in compression were considered.

Figure 13 illustrates the experimental load-displacement diagram obtained for the wallet NS1 and the numerical diagrams obtained according to the different boundary conditions. It is noted that the two experimental load peaks correspond to the failure of each connection, see Section 2.2.

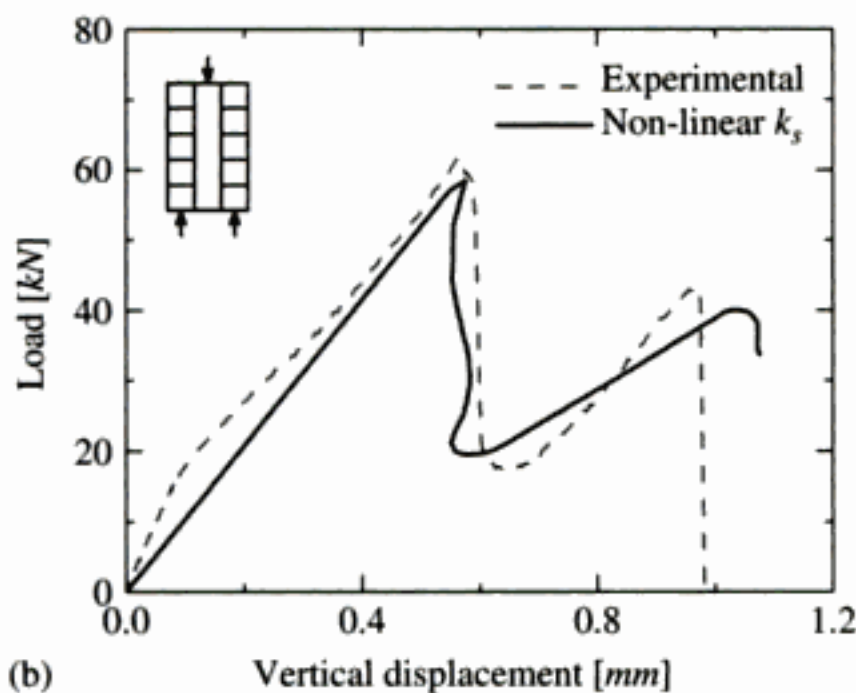
Regarding the numerical diagrams, some relevant remarks are now given. For boundaries with $k_s = 0$, after failure of the first connection the specimen starts sliding until complete degradation of strength is obtained and, thus, only one of the two connections fails. Another interesting point is that the collapse load is underestimated. Such difference is due to the absence of horizontal constraints at the bottom, which leads to a failure that is not exclusively governed by shear but is accompanied by flexural tensile stresses.

For supports with $k_s = \infty$, a smooth load drop due to material softening follows the failure of the first connection. Yet, it is not as sudden or as deep as the experimental load drop. In terms of collapse loads, the first load peak shows a good agreement with the experimental results but the second load peak, corresponding to the failure of the second connection, is largely overestimated. This is, again, due to the softening behaviour of the first connection to fail, which is still contributing to the specimen strength when the second connection fails.

For an intermediate shear stiffness $k_s = 0.01 N/mm^3$, the value of the first load peak equals the value for $k_s = 0$ and, thus, is also underestimated. After the failure of the first connection, the specimen starts sliding over the boundaries with the load suddenly dropping. However, in this case, after some amount of shear slip,



(a)



(b)

Figure 13. Numerical and experimental (NS1) load-displacement diagrams for straight collar joints wallets. Different shear stiffnesses were considered at boundaries: (a) constant, (b) non-linear.

the horizontal reactions at the supports become mobilized and a load increase is observed until failure of the second connection occurs. The comparison with the experimental response shows, nevertheless, that an understiff response was obtained for the second increasing branch.

These results demonstrate that to capture correctly the experimental behaviour found, the boundary conditions adopted must allow some amount of shear slip at the supports after the failure of the first connection and, afterwards, restrain it completely. Therefore, a non-linear k_s was adopted for the upper boundary together with complete shear slip restriction at the bottom boundaries. Good agreement with the experimental response was found, see Figure 13b. Even so, the slope of the second increasing branch is slightly underestimated. This shows that the hypothesis assumed of equal shear stiffness for the two connections is, probably, not true for this specimen, with the second connection showing a stiffer behaviour than the first

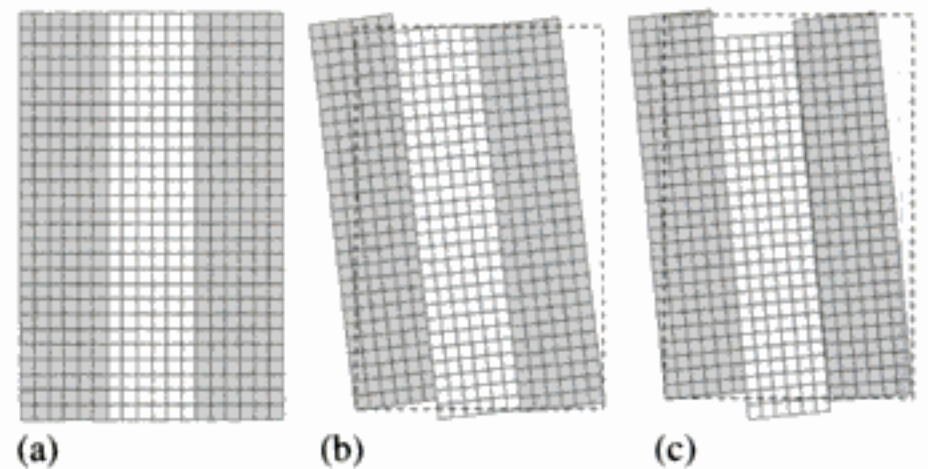


Figure 14. Progressive shear failure for non-linear k_s boundary conditions: (a) mesh adopted, (b) deformed (incremental) mesh after failure of the first connection and (c) deformed (total) mesh after failure of the second connection.

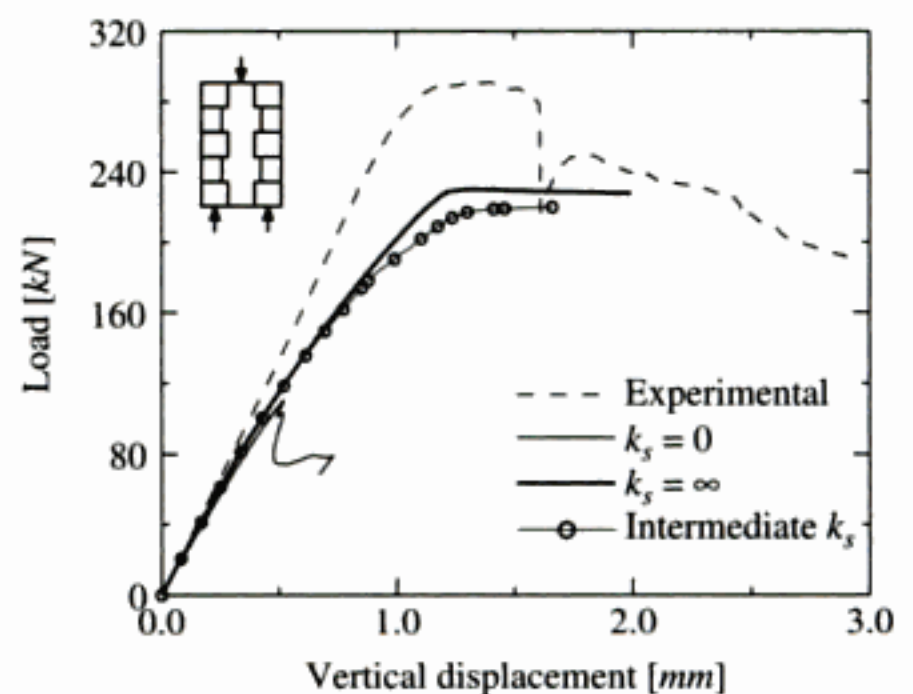


Figure 15. Numerical and experimental (NO2) load-displacement diagrams for keyed collar joints wallets. Different shear stiffnesses k_s were considered at the boundaries.

connection. Figure 14 depicts the progressive shear failure of the wallet.

In the case of keyed collar joints wallets, the influence of the boundary conditions in the response was assessed by a procedure similar to the one utilized for straight collar joints wallets. Here, three different shear stiffnesses at the boundaries were considered: (a) $k_s = 0$, (b) $k_s = \infty$ and (c) intermediate $k_s = 2.0 \text{ N/mm}^3$.

The comparison between numerical and experimental load-displacement diagrams is given in Figure 15. The deformed meshes at failure for each numerical diagram are depicted in Figure 16. The collapse load obtained for zero shear stiffness at the boundaries is significantly lower than the experimental collapse load. In this situation, the specimen fails due to a vertical crack that arises in the weaker connection (left), developing along the shear keys. For infinite shear stiffness at the boundaries, a much better agreement with the experimental collapse load is found. Here,

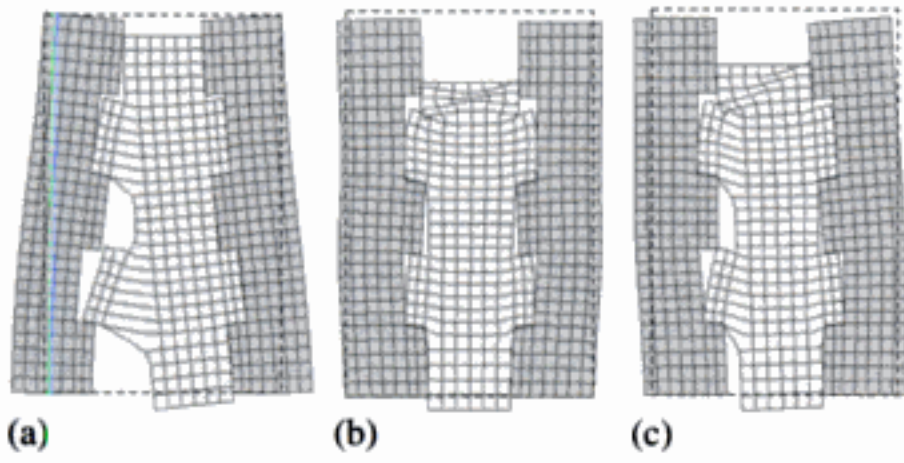
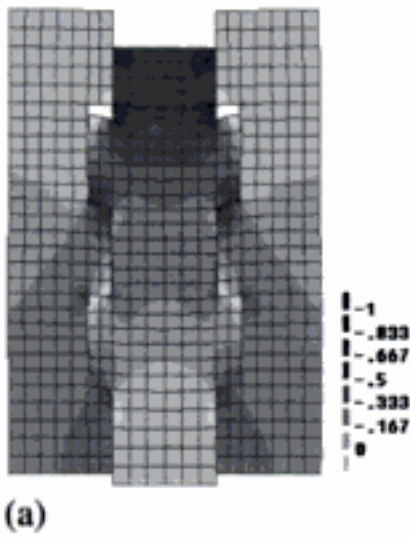


Figure 16. Deformed meshes at failure for different shear stiffnesses k_s at the supports: (a) $k_s = 0$, (b) $k_s = \infty$ and (c) int. k_s .



(a)

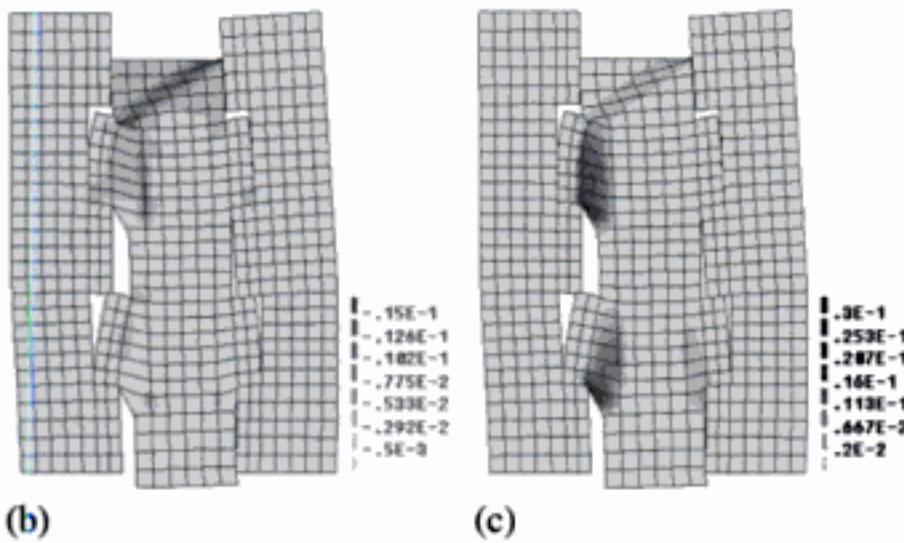


Figure 17. Results obtained for the shear simulations on keyed wallets, adopting the intermediate k_s : (a) principal minimum stresses for an applied load of 50 kN (elastic regime) and principal plastic strains at failure: (b) minimum and (c) maximum.

failure is governed by crushing of the inner-leaf near the top.

In experimental failure, both described modes seem to be present and, thus, an intermediate k_s was considered in order to reproduce more accurately the behaviour found. The collapse load obtained was almost the same as for $k_s = \infty$ and is about 80% of the experimental collapse load. In this case, failure occurs due to combined shearing-crushing of the inner-leaf near the top and due to the development of vertical cracks along the shear keys, see Figure 16c.

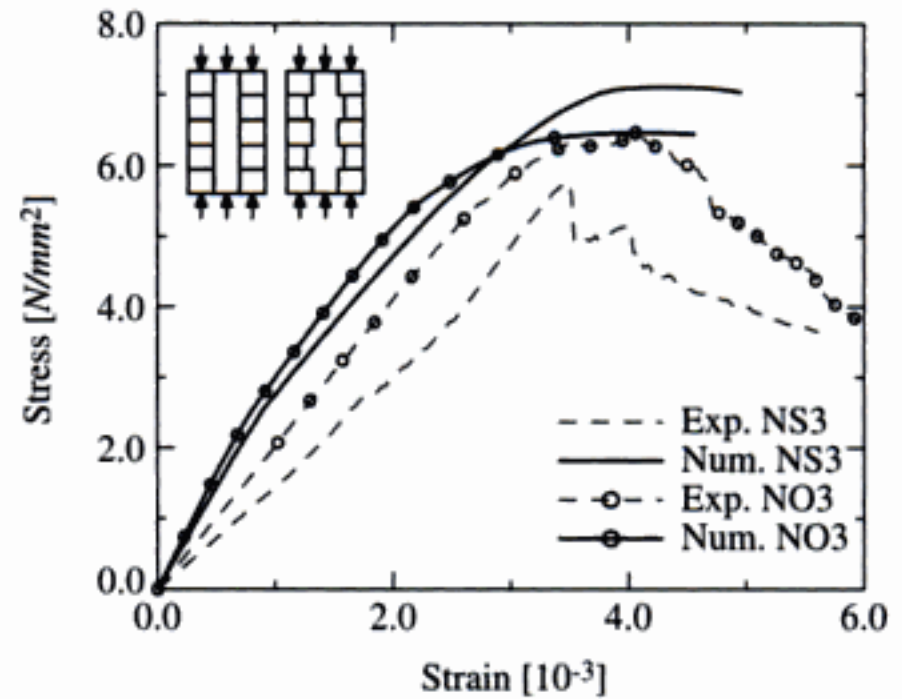


Figure 18. Stress–strain diagrams obtained for compression on wallets with straight collar joints (NS3) and keyed collar joints (NO3).

For the intermediate k_s at the supports, Figure 17 illustrates the contour of minimum principal stresses for the elastic regime and the principal plastic strains at failure. In Figure 17a, it is visible the transfer of compressive stresses from the inner-leaf to the outer-leaves, through the shear keys. In Figure 17b,c, the shearing-crushing of the inner-leaf near the top and the tensile damage in the inner-leaf, along the shear keys, is confirmed as failure mechanism.

4.2 Compression simulations on the full wallets

The compression tests on wallets with and without shear keys have also been analysed. Friction between wallets and boundaries has been precluded in the simulations. In the case of the wallet with straight connections, a row of mesh elements at middle height was made slightly imperfect and a 10% lower compressive strength was given. The objective is to trigger the strain localization.

A comparison between numerical and experimental stress–strain diagrams is given in Figure 18. Good agreement is found in the case of the wallet with keyed collar joints. In the case of the wallet with straight collar joints, the predicted strength is about 20% higher than the experimental strength. As discussed in Section 3, the inner-leaf is almost not collaborating in the experimental response, which can partially explain the difference found between the experimental and numerical strength values.

Another point is that the numerical strength of the wallet with keyed connections is lower than the strength of the wallet with straight connections, as predicted also by the simple expressions discussed in Section 3. Such behaviour is explained by the smaller cross-sectional area of the outer-leaves in the case of the wallets with keyed collar joints.

5 CONCLUSIONS

The present paper addresses the shear and compressive behaviour of composite masonry walls, which seems to be not a sufficiently debated issue in the literature. From the experimental tests, the following conclusions can be withdrawn:

- Shear strength values found for straight collar joints are between $0.09\text{--}0.17\text{ N/mm}^2$, whereas for keyed joints the values are in the $0.58\text{--}0.81\text{ N/mm}^2$ range.
- In wallets with straight collar joints, shear failure occurs due to vertical cracks that arise in the connections while in wallets with keyed collar joints, failure is mainly due to the development of diagonal cracks in the inner-leaf.
- Further compression testing on composite wallets is needed, considering also specimens with different ratios between inner and outer-leaves thicknesses.

Numerical assessment of experimental data was also addressed. Good agreement has been found by utilizing a plasticity based finite-element model, in which units and mortar were smeared out in a continuum.

Simplified calculations for predicting the compressive strength of composite walls have also shown good agreement with experimental results and with advanced numerical methods. Thus, simplified expressions may be used as a first estimate of the wallets strength.

ACKNOWLEDGEMENTS

The experimental research was supported by MURST – Cof. 2000, 2002. Authors wish to thank M. Antico for technical assistance and M. Brazzale for data elaboration. FCT is gratefully acknowledged for the fellowship awarded to J. Pina-Henriques.

REFERENCES

- Anzani, A., Binda, L., Fontana, A., Pina-Henriques, J. 2004. An experimental investigation on multiple-leaf stone masonry, in: *Proc. 13th IBMaC*, Amsterdam, the Netherlands.
- Binda, L., Fontana, A., Anti, L. 1991. Load transfer in multiple leaf masonry walls, in: *Proc. 9th IBMaC*, Berlin, Germany.
- Binda, L., Fontana, A., Mirabella G. 1994. Mechanical behaviour and stress distribution in multiple-leaf walls, in: *Proc. 10th IBMaC*, Calgary, Canada.
- Binda, L., Saisi, A., De Benedictis, R., Tringali, S. 2003a. Exp. Study on the Damaged Pillars of the Noto Cathedral, in: *Proc. 8th Int. Conf. STREMAH*, Halkidiki, Greece.
- Binda, L., Anzani, A., Pina-Henriques, J., Tongini Folli, R. 2003b. Sperimentazione su provini in muratura a tre paramenti, in: *Workshop: Danneggiamento, conserv. e manut. di strut. murarie e lignee*, DIS-Politecnico di Milano, Italy.
- Binda, L., Anzani, A., Fontana, A. 2003c. Mechanical behaviour of multiple-leaf stone masonry: experimental research, in: *Int. Conf. Structural Faults & Repair*, London, UK.
- CEN 1998. *Methods of test for masonry units: Det. of real and bulk density and of total and open porosity for natural stone masonry units*. EN 772-4, CEN, Brussels, Belgium.
- CEN 1999. *Methods of test for mortar for masonry: Determination of flexural and compressive strength of hardened mortar*. EN 1015-11, CEN, Brussels, Belgium.
- CEN 2000. *Methods of test for masonry units: Det. of compressive strength*. EN 772-1, CEN, Brussels, Belgium.
- CEN 2002. *Methods of test for masonry: Determination of initial shear strength*. EN 1052-3, CEN, Brussels, Belgium.
- Drei, A. and Fontana, A. 2001. Influence of geometrical and material properties on multiple-leaf walls behaviour, in: *Proc. 7th Int. Conf. STREMAH*, Bologna, Italy.
- Egermann, R., Newald-Burg, C. 1994. Assessment of the load bearing capacity of historic multiple leaf masonry walls, in: *Proc. 10th IBMaC*, Calgary, Canada.
- Lourenço, P. 1996a. *Computational strategies for masonry structures*. Dissertation, TU Delft, Delft, the Netherlands.
- Lourenço, P. 1996b. *A user/programmer guide for the micro-modelling of masonry structures*. Report 03.21.1.31.35, TU Delft, Delft, the Netherlands.
- Lourenço, P. 1997. *An anisotropic macro-model for masonry plates and shells: implementation and validation*. Report 03.21.1.31.07, TU Delft, Delft, the Netherlands.
- Lourenço, P.B., Barros, J.O., Oliveira, J.T. 2004. Shear testing of stack bonded masonry. *Const. and Building Mat.*, 18.
- Neville, A. 1997. *Prop. of concrete*. Wiley, New York, USA.
- RILEM 1994. *Tension by splitting of concrete specimens*. CPC6, RILEM tech. rec., E&FN Spon, London, UK.
- Van der Pluijm, R. 1999. *Out-of-plane bending of masonry, beh. and str.* Dissertation, TU Delft, Delft, the Netherlands.

*Non-destructive testing and
inspection techniques*

On-site investigation techniques for the structural evaluation of historic masonry buildings – a European research project

C. Maierhofer, C. Köpp & A. Wendrich

Federal Institute for Materials Research and Testing (BAM), Berlin, Germany

ABSTRACT: The main objective of the EC project ONSITEFORMASONRY is the development and improvement of methodologies for the evaluation of the structure and material properties of historic masonry Cultural Heritages. These methodologies are based on non-destructive (NDT) and minor destructive (MDT) testing methods like radar, sonics, microseismic, impact-echo, ultrasonics and active thermography which are adapted and optimised to assess selected damages and testing problems. In this paper, the so far achieved results of the projects are outlined.

1 INTRODUCTION

The highest percentage of the European Cultural Heritage consists of brick and stone masonry buildings. Due to the effects of an aggressive environment (earthquakes, settlements, traffic vibrations, air pollution, microclimate etc.) and to the fact that many old and ancient buildings and historic centers were no subject to continuous maintenance, now most of this patrimony is affected by structural problems which menace safety of buildings and people.

ONSITEFORMASONRY is a research project funded by the European Commission under the 5th Framework Program 1998–2002 in the Thematic Program *Environment and Sustainable Development* and the action *The City of Tomorrow and Cultural Heritage*.

ONSITEFORMASONRY will provide improved methodologies for the evaluation of the structure of historic masonry Cultural Heritages based on non-destructive (NDT) and minor-destructive (MDT) testing techniques. The main objective of the research project is the improvement of the cost/benefit ratio for investigation and diagnosis as follows:

- Optimisation of current techniques (radar, ultrasonics, impact-echo, sonics, microseismic etc) for better analysis, prediction and early prevention of environmental damages as well as for the diagnosis and control of the efficiency of intervention.
- Development of investigation methodologies to allow more frequent assessment with lower costs (combined methods, software for automation and data fusion).
- Evaluation and use of the results and data as input for structural analysis.

- Contribution to future standards of building assessment by developing guidelines.

The consortium is well balanced bringing together all the needed expertise and including partners with complementary roles: equipment manufacturers (Mala Geosience, Sweden), developers of NDT methodologies (BAM, Germany, Politecnico di Milano, Italy, University of Pisa, Italy), NDT and MDT users (BAM, Geotecnica Y Cimientos S. A., Spain, University of Padua, Italy, Slovenian National Building and Civil Engineering Institute, Slovenia, University of Castilla La-Mancha, Spain, Institute for Research in Materials and Applications, Slovenia, Institute of Theoretical and Applied Mechanics of the Academy of Sciences of the Czech Republic, Czech), experts for structural models (University of Castilla La-Mancha, University of Padova) and owners of Cultural Properties (Luther Memorial Foundation in Saxony-Anhalt, Germany, Regione Toscana, Italy, Regional Government of Castilla La-Mancha, Spain, Province of Verona, Italy) which play an important role as potential users of the methodology.

With the developed technologies, environmental influences on historic buildings can be assessed at an early stage. Small and medium enterprises (SMEs) will be able to develop new technologies and to offer services with faster, cheaper and more accurate measurement and analysis systems. Final users like the operators of historical buildings will benefit from more possibilities and enhanced efficiency of investigations, enabling reconstruction of more historic sites. This leads to increasing the safety of historic structures, allowing an opening of extended areas for public access which will have a clear influence on tourism

and thus on employment and economic growth in the region.

2 DAMAGE CATALOGUE

To achieve a wide base of knowledge for the investigations ONSITEFORMASONRY is aiming at, in a first essential step it had to be determined which types of damages typically affect historic masonry.

All project partners contributed to this state of the art by providing their case studies of former or ongoing investigations concerning historic masonry. These include the characterisation of the structural element, a description of the damage, the building materials, the probable origin of the damage and a significant picture from the *wanted poster* of the particular case study, completed by a proposition of applicable NDT-methods and relevant measurement parameters. When collecting the case studies, it appeared rather quickly that the term *Damage Catalogue* would have to be extended, since a lot of the investigations dealt with questions about the recognition of structures (one- or multiple-leaf walls, thickness of walls, presence of voids, etc.) which is a major aspect in restoration and preservation of monuments and historic buildings and which is as important as the survey of damages.

The collection of case studies is now called *Standard Damage Catalogue and List of Structural Typologies and Related Requirements* and comprises currently more than 100 examples, still being extended in the course of the project.

The document developed under supervision of the Spanish partner Geotecnica Y Cimientos S. A. represents thus far more than just a collection of damages. It is a comprehensive classification of problems, questions and damages related to historic masonry.

The crucial point of the overview is the definition of structural typologies and the classification of damages together with a compilation of measurement parameters needed for their characterisation. The structural typologies comprise among others a systematic structuring of:

- Construction typologies (buildings, bridges, etc.)
- Structural elements (arch, vault, wall, dome, etc.)
- Singularities of masonry structures (number of leafs, construction technology, history)
- Masonry cross sections (types of wall cross sections)

For an all-embracing assessment of the structures the chemical, physical and mechanical properties of the components have to be determined. The measurement parameters necessary for characterisation (e.g. mineralogical composition, mechanical properties, dynamical properties, dimension, morphology, etc.) have been compiled and described in detail.

The damages typical for historic masonry have been divided into two main groups:

1. Damages due to material deterioration including:
 - Moisture and related damages
 - Erosion and other damages due to wind and air pollution and
2. Damages due to mechanical effects on the structure including:
 - Static direct actions (increase and decrease of loads, traffic)
 - Static indirect actions (differential settlements, thermal deformation, etc.)
 - Combination of static direct and indirect actions
 - Dynamic and exceptional actions (earthquake, explosion, etc.)

For the determination of damages measurement parameters (e.g. salt and moisture content, shrinkage-swelling cycles, dynamic actions, presence of pollutants, etc.) have been compiled as well.

The *Standard Damage Catalogue and List of Structural Typologies and Related Requirements* offers the user the opportunity to make a first estimation of the extent, the cause and the kind of damages and indicates, which of the available investigation methods can be used for an evaluation. Relevant measurement parameters are described in detail. Additionally the Catalogue visualises representative types of damages and thus helps to identify problems occurring at historic masonry.

3 METHODOLOGIES AND TEST SPECIMENS

3.1 Methodologies

The combination of several NDT and MDT methods like ultrasonics, impact-echo, sonics, microseismic, radar and flat-jack can give more reliability for the interpretation of results and for the detection of irregularities like voids, cracks, presence of moisture and/or salt etc. If a void is detected by more than one method, the presence of this irregularity can be regarded with a higher level of reliability. Furthermore, it can help to clarify the morphology of the structure investigated, to give information about the presence of weakened areas and about the state of stress in masonry structures. In ONSITEFORMASONRY, methodologies containing various system combinations related to different testing problems are evaluated.

The impulse-echo methods to be applied can be used in reflection as well as in transmission configuration. Therefore, data recording and data processing was optimised to analyse indirect (reflected) and direct (transmitted) signals as well as signals collected for tomographic reconstruction (Lualdi et al, 2003).

Table 1. Methods developed, optimised and applied in ONSITEFORMASONRY.

Method	Field of application	Development and modification
Radar (impulse-echo and tomography) (Maierhofer et al, 2003) (Lualdi et al, 2003)	Geometry, internal structure (voids, delaminations), moisture content and distribution, salt distribution using different frequencies, location of inclusions (metal targets, wood)	Optimisation and application for tomographic measurements, tomographic data analysis Development of a new light high frequency radar antenna consisting of separable transmitting and receiving elements, enabling tomography with enhanced resolution Development of the positioning system for 3D acquisition
Microseismic (Marchisio et al, 2000)	Geometry, internal structure (voids, delaminations)	Improvements of transmitter and receivers to obtain a higher frequency band of the signal and a better signal/noise ratio Development of tools for positioning transmitter and receivers to speed up the measurements A specially modified seismograph should help to obtain quickly a very sharp time-picking
Impact-echo (reflection and transmission) (Sansalone et al, 1997)	Geometry, thickness of first leaf, internal structure (voids, delaminations)	Development of automated data acquisition at masonry in reflection and transmission Selection of optimum sensor and detector Development of software for tomographic data analysis
Sonics (direct and indirect) (Abbaneo et al, 1995) (da Porto et al, 2003)	Geometry, internal structure (voids, delaminations), density variations, estimate of elastic moduli, weak areas	Optimisation to reduce acquisition and elaboration times, especially for tomography New devices (low cost transducers and controlled wave sources) for multichannel sonic tomography Extension of the software for tomographic reconstruction by including the attenuation analysis with the frequency downshift method
Ultrasonics (impulse-echo and tomography) (Krause et al, 2003)	Geometry, thickness of first leaf, internal structure (voids, delaminations)	Selection of optimised pulse form and frequency range depending on material and masonry structure Application of array technique for tomography

The main field of application of each method and the developments and optimisations performed during the project are summarised in table 1.

3.2 Test specimens

The strategies for an evaluation of historic masonry, which were developed in the project, have to undergo comprehensive tests, before they can be incorporated in guidelines or recommendations. Previous experiences with measurements at real masonry have shown that very often unexpected difficulties occur because of the distinctive inhomogeneity of many brickwork structures.

A first step was therefore the construction of some masonry specimen, which, featuring a diversity of properties (material, thickness, presence of voids),

represent several aspects or characteristics of real historic masonry. These specimens are used to perform measurements under specific conditions. If for example the exact position of voids is known in the specimen, it is particularly qualified for proving the effectiveness and reliability of the respective investigation method.

Among others, a large historic masonry wall has been constructed at BAM in close cooperation with Luther Memorial Foundation in Saxony-Anhalt (Wittenberg, Germany), Institute for Diagnostic and Conservation at Monuments in Saxony und Saxony-Anhalt e. V. (Halle, Germany) and Institute for Applied Science in Civil Engineering (IaFB), (Berlin, Germany). This wall features a diversity of typical materials, structures and inhomogeneities (e.g. brick and stone, multiple leave structure, voids, wooden pile,



Figure 1. Top: Historic Masonry Specimen at BAM. Bottom: Simulation of voids.

metallic beam, metallic anchors) and thus represents several aspects of real historic masonry (see figure 1). This specimen with the dimensions $7\text{ m} \times 3\text{ m} \times 1.5\text{ m}$ has been planned and constructed in consideration of traditional manufacturing techniques, partly using historical materials from demolished buildings. It represents a large variety of problems and characteristics of real historic masonry (mixed masonry, multiple-leafed walls, hidden inclusions, cracks, voids, etc.). Each of the characteristics or properties of this *Historic Masonry Specimen*, which has been erected by a very experienced building company specialised in the restoration of cultural heritage buildings, is known in detail. This specimen is in a way the link between usual masonry specimen and real historic masonry buildings and will make the validation and calibration of the investigation techniques possible. It enables investigations under more or less defined conditions. The detailed documentation compiled during construction, permits a reliable interpretation of the recorded experimental data.

In figure 2, a radargram of a horizontal trace along the test specimen is displayed. Layers as well as some voids can be detected.

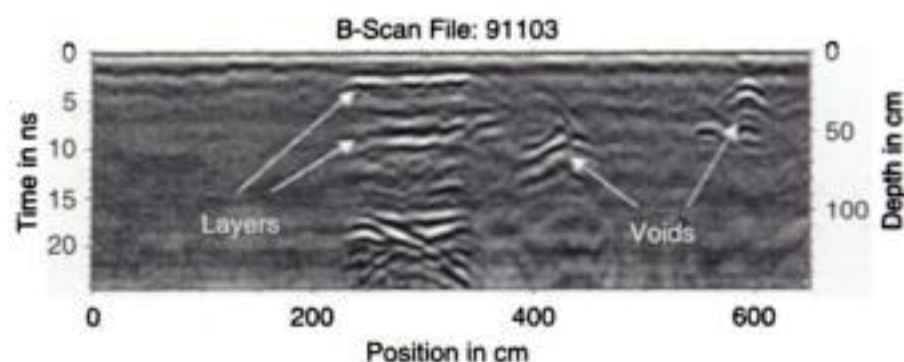


Figure 2. Radargram of a horizontal trace along the historic test specimen recorded with the 900 MHz antenna.

4 CASE STUDIES

For the performance of on-site calibrations and testing of methodologies, a preliminary selection of pilot sites has been made considering the following aspects:

- Material: regular brick and stone masonry, masonry made with irregular stone.
- Typology: single and multiple leaf walls and columns.
- Deterioration mechanism.
- Environmental conditions.

These sites should allow the evaluation of the reliability of the results through the comparison with a priori information and /or with coring or other destructive investigations. The assessment of the pilot sites includes also structural modeling based on the measured parameters. This is the way of integrating the NDT techniques considered within the project focusing on the final aim of every end-user: to determine the actual state and the load carrying capacity by considering data obtained from NDT and MDT methods. The applications will be carried out at the partners' countries to optimise integration and co-operation and to compare the obtained results.

Recently, the following sites for detailed case studies have been selected (the responsible partner is given in brackets):

- Pisece Castle in Slovenia (Slovenian National Building and Civil Engineering Institute and Institute for Research in Materials and Applications, Slovenia).
- Veltrusy Castle in Czech Republic (Institute of Theoretical and Applied Mechanics of the Academy of Sciences of the Czech Republic).
- Altes Museum in Berlin, Germany (see paper at this Conference).
- Wartburg in Eisenach, Germany (Luther Memorial Foundation in Saxony-Anhalt, Germany).
- St Alessandro Church in Lucca, Italy (University of Pisa, Italy).
- Palazzo Bottagisio in Verona, Italy (University of Padova, Italy).



Figure 3. Left: Pisece Castle in Slovenia built at the first half of the 13th century as defense fortification against the Hungarian threat by archbishop of Salzburg. Right: Crack at the main tower.

- Avio Castle in Italy (Politecnico di Milano, Italy).
- Convento de la Asunción in Almagro, Spain (Geotecnia Y Cimientos S. A., Spain).

Detailed reports of these case studies will be published as deliverables at the end of the project. In the following, some of these objects will be described in more detailed.

4.1 Pisece Castle in Slovenia

Pisece Castle in Slovenia (see figure 3) was built at the first half of the 13th century as defence fortification against the Hungarian danger by archbishop of Salzburg. Here, structural investigations related to cracks (see figure 3 right), multiple leaf, inhomogeneous masonry and localisations of metallic inclusions have been performed.

Apart from the real NDT methods, the complementary MDT methods (flat-jack, endoscopy, bore-hole extraction, etc.) as well as destructive testing methods (in-situ shear tests) have been applied here. This is often impossible at highly protected historic buildings.

Figure 4 shows the results from radar investigations at an outside wall showing the presence of a large void at a depth of about 20 to 25 cm. This void can be most probably related to the presence of a chimney.

4.2 Veltrusy Castle in Czech Republic

The baroque-classical Veltrusy Castle was constructed from 1720 to 1820. It is surrounded by a large English park with a system of channels and small pavilions. During summer 2002, the castle was affected by the flood disaster as shown in figure 5. Therefore, the main objectives of the investigations were the determination of remaining moisture content and moisture distribution and structural investigations for the analysis of

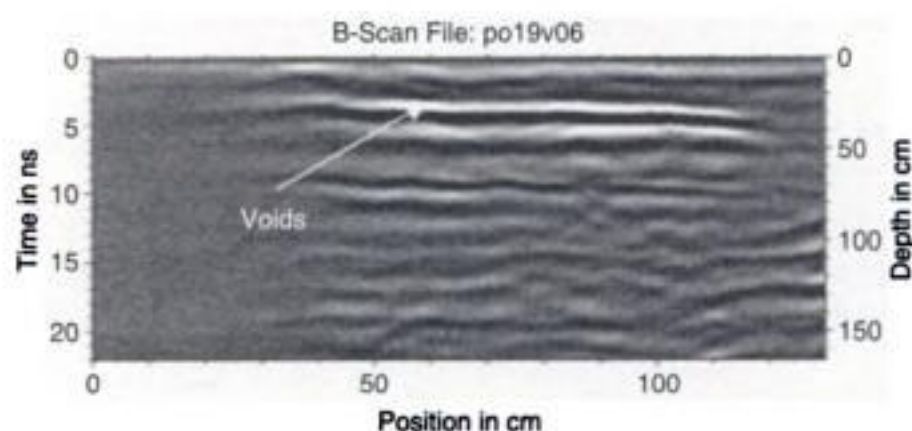


Figure 4. Top: Investigated wall containing a large void (chimney). Bottom: Radargram of a vertical trace at the wall showing the reflection from the void at a depth of about 20 to 25 cm.



Figure 5. Veltrusy Castle during the flood disaster in summer 2002.

damages related to structural movement and foundation settlements during and after the flood. Another aim was also the structural assessment of load bearing walls consisting of different materials.

Therefore, investigations have been performed with radar, microwave borehole method and powder drilling to evaluate the moisture situation. Structural characterisations have been carried out with radar, thermovision and microseismic. Mechanical extensometers



Figure 6. View of Wartburg in Eisenach, Germany.

and some automatic electrical sensors were used for structural monitoring.

First results from the moisture investigations show that in spring 2003, the walls have already been dried up.

4.3 Wartburg in Eisenach, Germany

The Wartburg (see figure 6) was selected as test site due to its high level of name recognition as well as to its prominent position among the European Cultural Heritages. The castle represents a long history going back to the 12th century. The Palas is the first of its kind in German and is well documented. Based on the results of intensive building research of the Wartburgstiftung (Foundation of Wartburg), detailed problems could be compiled in close contact with the responsible researches, architects and restorers.

In the Landgrafenzimmer, a room at the north site in the 1st floor of the Palas, the internal structure of the north wall to the staircase had to be investigated. Here, it was assumed that there had been a door which was walled up. The outer surface of the wall in the Landgrafenzimmer consists of plaster with ornaments and paintings. The other surface of the wall at the staircase, which was built in 1950, is covered with white painted plaster.

The aim of the investigations with radar, radar tomography, microseismic, geoelectric and impulse-thermography was to localise the former opening, to get information about the inner structure of the wall near the walled door and to analyse the moisture situation.

Here, as an example the results of pulse phase thermography (PPT) are presented. This relatively new approach of active thermography combines the method of data acquisition of impulse thermography (impulse heating of the surface and recording of the cooling down process) with the approach of frequency analysis (Weritz et al, 2003). The stored data received during

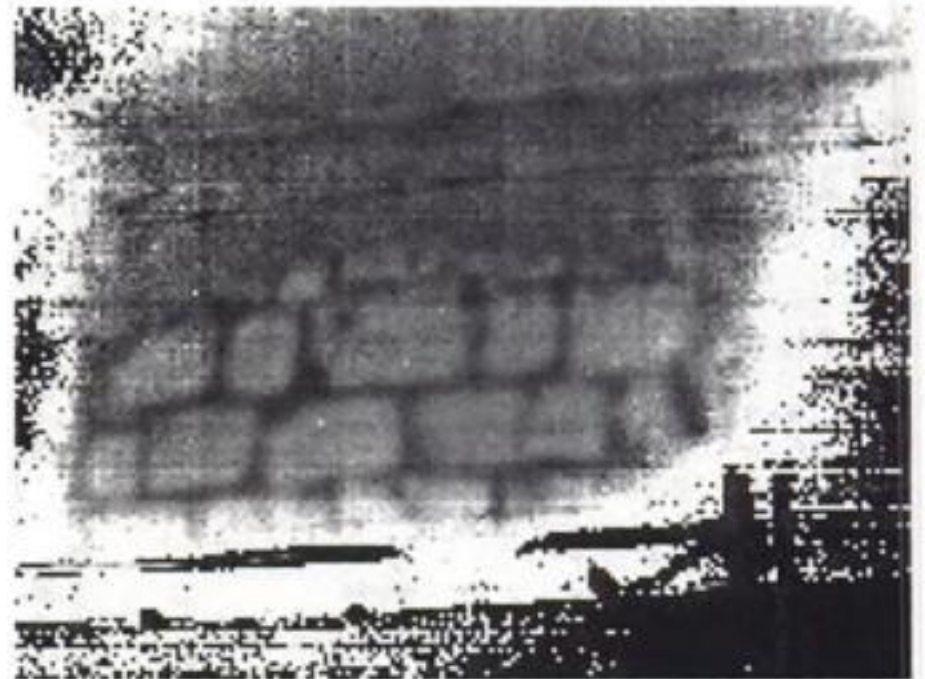


Figure 7. Phase image recorded with pulse-phase thermography showing the walled door behind the plaster at the Landgrafenzimmer of the Wartburg.



Figure 8. St Alessandro Church in Lucca, Italy.

the cooling down process is analysed in the frequency domain via Fast Fourier Transformation of the transient curve of each pixel in a series of thermal contrast images. This leads to changes in amplitude or phase of the corresponding images.

The wall was heated up for about 5 minutes and afterwards recorded for about 15 minutes using an infrared camera. The investigated area was about 3.5 m in horizontal and 1.2 m in vertical length and was located above a show-case. The phase image displayed in figure 7 clearly shows the masonry and mortar structure in the lower part of the wall with an arc-shaped borderline on its upper part. In the upper part of the wall no masonry-structures are visible.

4.4 St Alessandro Church in Lucca, Italy

St Alessandro Church (see figure 8) in Lucca is a rectangular plan building with a semicircular apse, divided into three naves. Upon the dating of the construction

of the Romanesque church, researchers have controversial hypotheses. Salmi individuates the presence of two different construction phases, belonging to the beginning and to the second half of the 12th century. In contrary to that, Ragghianti has considered the present building as a homogeneous construction realised during the bishopric of Anselmo da Baggio in the second half of the 11th century. Silva's most recent studies have recognised four medieval phases between the 9th and the 12th centuries. The archaeological survey results in two main construction periods (period I and period II), one period characterised by volume modifications (period III) and a last period (period IV) which involves restorations of the structure in its medieval configuration, divided into several phases.

Concerning the used constructive techniques, five main wall typologies with some modifications have been found.

The more ancient period is characterised by an external wall face in San Guiliano's marble perfectly squared disposed in the pseudoisodoma apparatus. Probably this technique is related to the ashlar where all six faces have been worked.

The type of masonry characterising the period II is similar to the one of period I on the external side, but the inner part of the ashlar has not been worked. There is still the tail for the scarf with the nucleus.

The stone masonries of the other periods refer to more usual types for the middle ages consisting of ashlar on horizontal and parallel courses (put down with various heights) and a probable nucleus with horizontal layers.

Investigations with radar, ultrasonics and impact-echo have been performed to analyse the internal structure of the walls at different positions. The main aim was to distinguish the four periods of construction that are documented from the historical-archaeological studies. Another objective was the investigation of cracks which are most probably related to soil subsiding.

In figure 9, results of measurements at an area inside the church with a size of $1 \times 1 \text{ m}^2$, investigated with ultrasonic in echo configuration, are presented. The image at the bottom left represents a C-scan (depth slice) at a depth of 93 mm showing strong reflections from the joints (black). At bottom right, the C-scan at a depth of 225 mm shows reflections from the backside of two stones (black). These results clearly show that the backsides of the different stones are at different depths, thus the backside of the leaf is not parallel to the surface.

The on-site investigations are planned to be performed partly with the involvement of an interested audience in the frame of workshops, seminars or demonstrations. It is one of the characteristics of the ONSITEFORMASONRY project to make project results accessible for the public and to involve

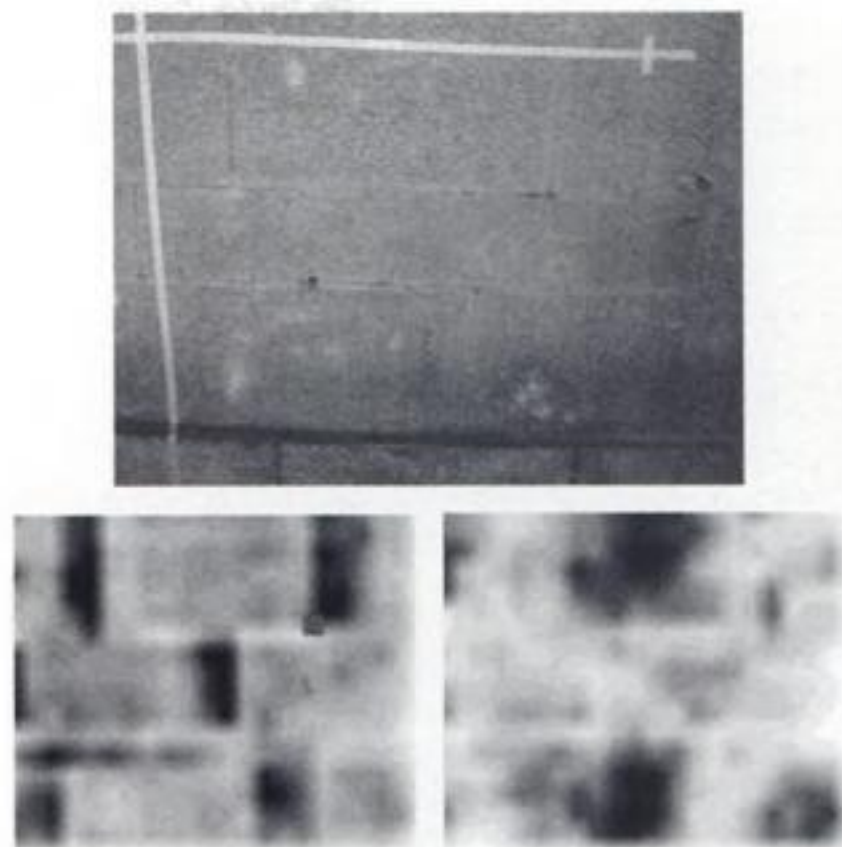


Figure 9. Top: Investigated area having a size of $1 \times 1 \text{ m}^2$. Bottom: C-scans (depth slices) recorded at a depth of 93 mm (left) and 225 mm (right) from ultrasonic data. The joints as well as the backside reflection from some stones are clearly visible.

especially the end-users into the project already at an early stage.

5 CONCLUSIONS AND OUTLOOK

One of the main results of ONSITEFORMASONRY until now is that although the structure of historic masonry is very inhomogeneous, it can be classified by a small number of structural elements. In most evaluations of historic buildings not the whole building complex but these elements are under consideration. The scientific and technical achievements give first guidelines to choose the most appropriate method to solve every problem related to different levels of assessment. To give a rigid procedure is not possible due to the large number of variations of single problems.

During the remaining period of the project, calibrations actions and various on-site investigations are running. For the development of guidelines and recommendations, close co-operation with all stakeholders is essential.

ACKNOWLEDGEMENTS

The project ONSITEFORMASONRY is funded by the European Commission in the 5th Framework Program. The presented results have been achieved by all Partners of the project, which are listed in chapter 1.

A public website has been established (www.onsite-formasonry.bam.de) to keep anyone interested in the project informed. Contributions and opinions from the reader are requested and can be forwarded to the Partners by e-mail.

REFERENCES

- Abbaneo, S., Berra, M., Binda, L. and Faticcioni, A., 1995, Non destructive evaluation of bricks-masonry structures: calibration of sonic wave propagation procedures, *Int. Symposium Non-Destructive Testing in Civil Engineering (NDT-CE)*, Berlin, Vol. 1, pp. 253–260.
- da Porto, F., Valluzzi, M. R. and Modena, C., 2003, Use of sonic tomography for the diagnosis and the control of intervention in historic masonry buildings. In: *Proceeding of the International Symposium on Non-destructive Testing in Civil Engineering*, DGZfP, Germany, 2003, CDROM and www.dgzfp.de.
- Krause, M., Maierhofer, Ch., Gardei, A., Kohl, Ch. and Wiggenhauser, H., 2003, Improvement and combination of echo methods for NDT of concrete elements. In: Naus, D.J. (ed.); *Proceedings PRO 29 of the 2nd International RILEM Workshop on Life Prediction and Management of Concrete Structures*, 5–6 May 2003, Paris, France, Bagnoux: RILEM Publications S.A.R.L. (2003) pp. 137–147.
- Lualdi, M., Zanzi, L. and Binda, L., 2003, Acquisition and processing requirements for high quality 3D reconstructions from GPR investigations. In: *Proceeding of the International Symposium on Non-destructive Testing in Civil Engineering*, DGZfP, Germany, 2003, CDROM and www.dgzfp.de.
- Maierhofer, Ch., Wöstmann, J. and Hennen, I. Ch., 2003, Non-destructive investigation of complex historic masonry structures with impulse radar. In: *Proceeding of the International Symposium on Non-destructive Testing in Civil Engineering*, DGZfP, Germany, 2003, CDROM and www.dgzfp.de.
- Marchisio, M., D'Onofrio, L., Forlani, E. and Cerri, S., 2000, The use of geophysical methods to study the masonry structures of monuments: an application for the restoration of the Cathedral of Nicosia (Sicily), *Proceedings of the 6th Meeting EEGS – ES*, Bochum, Sept. 3–7.
- Sansalone, M.J. and Streett, W.B., 1997, *Impact-echo, Non-destructive evaluation of concrete and masonry*, Bullbrier Press, Ithaca, N.Y., pp. 340.
- Weritz, F., Wedler, G., Brink, A., Röllig, M., Maierhofer, Ch. and Wiggenhauser, H., 2003, Investigation of concrete structures with Pulse Phase Thermography. In: *Proceeding of the International Symposium on Non-destructive Testing in Civil Engineering*, DGZfP, Germany, 2003, CDROM and www.dgzfp.de.

Combined in-situ tests for the assessment of historic masonry structures in seismic regions

V. Bosiljkov & M. Tomažević

Slovenian National Building and Civil Engineering Institute, Ljubljana, Slovenia

L. Binda, C. Tedeschi, A. Saisi & L. Zanzi

Department of Structural Engineering, Politecnico di Milano, Milano, Italy

F. da Porto, C. Modena & M.R. Valluzzi

Department of Structural and Transportation Engineering, University of Padua, Italy

ABSTRACT: The knowledge of the structural behaviour of existing masonry requires a multilevel approach, with proper application of diagnosis and assessment methodologies. The paper presents the results of some recent in-situ tests carried out in collaboration by the Slovenian National Building and Civil Engineering Institute, the Polytechnic of Milan and the University of Padova, on the walls of the Pišce Castle, located in the Eastern part of Slovenia. In order to calibrate different test methodologies a combination of DT (direct shear tests on a double-panel), MDT (single and double flat jacks) and NDT (georadar, direct sonic transmission and tomography) were performed. The aim of the study was to define the morphological, compositional and structural characteristic by direct inspection and MDT, to qualify the mechanical properties of the masonry by MDT and DT, to compare results obtained by the different level of obtrusiveness procedures, and, finally on the basis of these results, to evaluate load bearing capacity of the Castle as well as its seismic resistance by means of push-over analysis.

1 INTRODUCTION

The case study presented herein, represent an example of NDT, MDT and DT based approach in numerical modeling of historic masonry structures. Following the extensive in-situ testing program carried out at Pišce castle (Slovenia) from 10th till 20th of July 2003, within the framework of the 5th European Framework project ONSITEFORMASONRY, the seismic analysis of the Western part of Pišce castle by means of push-over method has been evaluated.

Investigation of the Western part of Pišce castle was conducted to determine as-built and current conditions as well as mechanical properties of historic masonry. It was done through application of different techniques: in-situ shear test, radar, impact-echo, flat-jack, sonic test, videoboroscopy, microseismic waves, coring and sampling as well as the laboratory tests on mortar and stone samples. Partners involved in the testing campaign of the Western part of Pišce castle were: Bundesanstalt für Materialforschung und – prüfung (Germany), Politecnico di Milano (Italy), Slovenian National Building and Civil Engineering Institute (Slovenia), University of Padua and University of Pisa

(Italy). In this paper some of the results of importance for the structural analysis of the building are presented and commented.

Following the results of DT and MDT tests, an attempt to calibrate some of the NDT tests have been also made. The results of numerical analysis provided valuable information of load-bearing capacity of the structure, possible causes for the observed crack pattern and validation of some of the results gained through on-site investigations.

2 DIAGNOSIS STRATEGIES

A correct intervention on a historic structure should start from an accurate diagnosis of the building in order to minimize the interferences of the intervention with the historicity of the architectural document. Furthermore, the study of the building rules and structural details, such as the wall sections, has a great importance in the mechanic behaviour of the structure.

The structural performance of a masonry can be understood provided the following factors are known: its geometry; the characteristics of its masonry texture,

single or multiple leaf walls, connection between the leaves, joints empty or filled with mortar, physical, chemical and mechanical characteristics of the components (stones, mortar); the characteristics of masonry as a composite material. In order to fulfill these needs an experimental on site investigation is required and recommended also by Codes of Standards in several countries.

NDT can be helpful in finding hidden characteristics, such as internal voids and flaws and characteristics of the wall section (Schuller et al. 1994, Valle et al. 1998, da Porto et al. 2003), which cannot be known otherwise than through destructive tests. Up to now most of the ND procedure can give only qualitative results. The application to masonry of NDT, although advanced, can be frustrating due to several factors, like the different masonry typologies and materials, the high inhomogeneity of the materials, the interpretation of the results of each single technique but also the harmonization of the results. Furthermore, most of the NDT's come from other research field and need a specific calibration.

The solution of very difficult problems cannot be reached with a single investigation technique, but with the complementary use of different techniques (Binda et al. 2003a,b). Therefore the designer is asked to interpret the results and use them at least as comparative values between different parts of the same masonry structure or by using different ND techniques. To this purpose it is important the production of guidelines for the correct application of investigation techniques to diagnosis problems of different classes of masonries (Binda et al. 2000).

Often MDT or slightly destructive techniques should be applied in strategic points of the structure in order to solve the more difficult problems of hidden situations.

However, an ultimate approach represents DT procedure for the evaluation of compressive or shear (tensile) strength, as well as stiffness parameters and ductility of as-built historic masonry. This approach is not completely destructive, however the tested walls should be repaired after applied DT tests. This approach is inevitable for precise and accurate assessment of the structural behaviour of the building.

The diagnosis process should be based on an accurate survey, which should document the current state of the building. A preliminary in-situ survey is useful in order to provide details on the geometry of the structure and in order to identify the points where more accurate observations have to be concentrated. Following this survey a more refined investigation has to be carried out, identifying irregularities (vertical deviations, rotations, etc.). In the meantime the historical evolution of the structure has to be known in order to explain the signs of damage detected on the building. The crack pattern should be classified and accurately

documented by pictures and on the geometrical survey. The definition of the structural model can be carried out only on the base of the geometrical survey but also of the crack pattern.

3 NUMERICAL STRATEGIES

In general, the seismic analysis of masonry structures can be done by using lumped parameter models (LPM), structural element model (SEM) or finite element models (FEM). Since for ordinary masonry buildings, the first vibration mode shape is the predominant one, there is usually no need for sophisticated non-linear dynamic and the LPM models are quite rare.

SEM approximates the actual structural geometry more accurately by describing individual structural elements such as piers and walls. In the case of single or multistory buildings due to their regularity and simplicity an equivalent static analysis in two orthogonal directions by using SEM can provide reliable information regarding the seismic safety under expected seismic loads. Nevertheless, since seismic loading can exercise the structural system to and beyond its maximum resistance capacity, the SEM models usually have to be used with static non-linear analysis. In that case a step-by-step procedure is followed, using decreased stiffness values under increasing lateral loads. Nonlinear element behaviour is prescribed in the form of nonlinear lateral deformation-resistance relationships, depending on the boundary conditions and failure mode of masonry elements. Usually the bi-linear or tri-linear behaviour of SE is considered. The storey resistance envelope is calculated by step-wise drifting of the storey for small values. The SE's are deformed equally (due to the rigidity of floor structure) and internal forces are induced according to the assumed shape of resistance envelope of each SE. In the case of torsional effects (due to relatively displacement of the mass centre to the centre of stiffness of the storey) the displacements of individual SE are modified.

Masonry is a composite, heterogeneous, non-linear structural material. As with other composite materials, also with masonry the mechanical properties are conditioned with the properties of composite elements, their volume ratio and the properties of bond between the units and the layers of mortar. Moreover, the properties and behaviour of masonry is strongly affected by the orientation of the main principle stresses towards the bed joints. Following the aforementioned, the main strategies for application of FEM can be adopted for the masonry as follows:

- simplified micro-modelling - usable for small elements and shear wall with openings, where

expanded units are represented by continuum elements whereas the behaviour of the mortar joints and unit-mortar interface is represented by discontinuous elements.

- homogenization – is aimed to solve the problem of modelling of large masonry structures, by treating masonry as a homogeneous material. Mechanical properties of masonry are predicted from the properties of its constituents, i.e. units and mortars.
- macro-modelling – for modelling whole structures where masonry is regarded as an anisotropic composite material (constitutive models).

Each of those FEM strategies has advantages and disadvantages. However, when analyzing old historical building, where a limited parameters from different NDT/MDT techniques can be obtained, the effective FEM analysis by applying sophisticated constitutive material laws could be questionable.

For the Western part of Pišece Castle, SEM model with applied push-over analysis were adopted for the verification of the seismic resistance. Main input parameters were determined from the results of in-situ shear tests as well as the results from single and double flat-jack tests.

4 CASE STUDY – WESTERN PART OF PIŠECE CASTLE

The castle of Pišece was built at the first half of the 13th century as defence fortification against the Hungarian attacks by archbishop of Salzburg. First records about the castle dated from 13th century (1268 AD). Till 14th century it belonged to knights of Pišece. By the end of 16th century (1595 AD) castle was sold to Inocent Moscon. Since that time till the end of Second World War (1945), it belonged to Moscon family. After the Second World War, the castle became property of state and was used as social apartments. From the year 1998 the castle stands empty.

The oldest part of the castle is Romanic tower build in first half of 13th century with two and half meter thick walls, peripheral castle walls and Romanic chapel. The important renovations were made in year 1568 and the round tower was added on NW (North-West) side of the castle. In the baroque time some architectural details such as small tower over the chapel were added. In XVIII century considerable changes were made on the tower of Pišece Castle and its height has been reduced by removing the top floor of the tower. The last renovations were made in 1867 with neoromantic and neogothic decorations with partial reconstructions of existing walls and by closing some of the openings in the castle.



Figure 1. Western part of Pišece Castle.

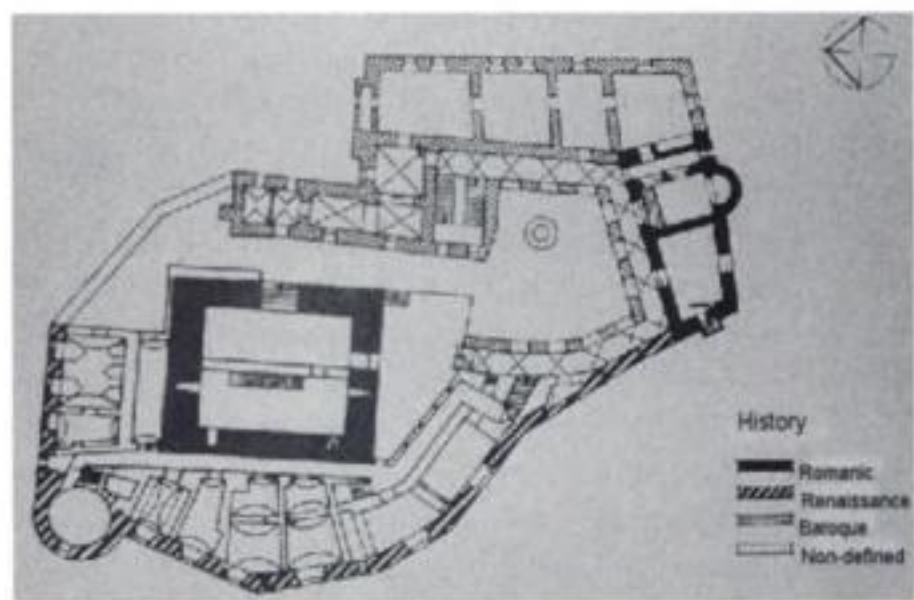


Figure 2. History of building of Pišece Castle.

5 LAYOUT OF THE WESTERN PART AND MORPHOLOGY OF THE WALLS

From the structural point of view the Castle represent classical example of masonry structures for Slovenian region. It consists of main defence tower, attached buildings around it, a chapel and defence wall. Structural elements that determine the load-bearing capacity of the castle are mainly solid walls.

The Western part of the castle (Fig. 3), was built later in renaissance period and it is partly attached to the main tower. It is to be expected that its seismic behaviour would be strongly affected by the presence of stiff and strong tower in its vicinity and thus two directions of seismic analysis were determined as it is presented in Figure 3.

6 ON SITE TESTS

The walls of the Western part of Pišece castle appeared very inhomogeneous with signs of past interventions. On-site tests were carried at Positions 4a & b (Fig. 3) in order to control peculiar problems and situations.

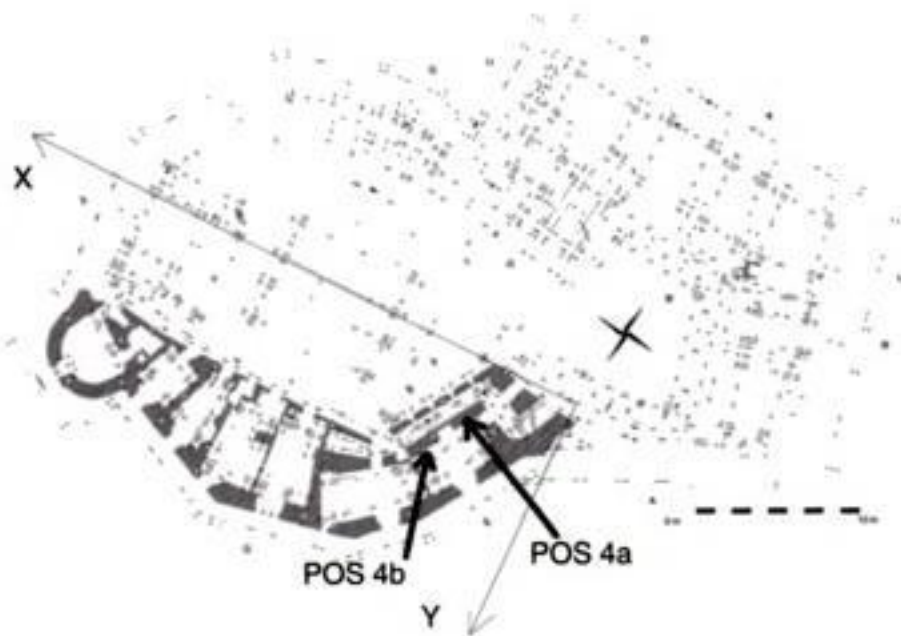


Figure 3. Two directions of seismic analysis of the Western Part of Pišec Castle and layout of tested positions.

The first inspection was made by radar profiles at Position 4b that clearly showed a position where the signal could not pass through the wall section although the thickness was not particularly large (~90 cm). The same results were obtained with sonic test. Later on the flat-jack tests were carried out at same wall to measure the value of the local vertical compressive stress and the stress-strain behaviour of the material. Finally coring of the wall at that position and laboratory tests on sampled material have been evaluated.

Positions 4a & b had almost the same state of compressive loading and morphology of the walls. Thus in the vicinity of Position 4b, an in-situ shear test were carried out at the wall at Position 4a. In-situ shear test was accompanied by sonic tests that were carried out before and after the shear test in order to quantify test results of sonic tests on intact and severely cracked masonry material.

6.1 NDT tests

6.1.1 Radar investigation

The first inspection was made by radar profiles (Figs 4 and 5) that clearly showed a position where the signal could not pass through the wall section although the thickness is not particularly large (about 90 cm). Profile and time acquisitions were carried out with 1 GHz and 500 MHz antennas. The time acquisitions were performed in positions 5 to 10 placing a metal shield on the backside of the wall during the second half of the experiment. Moving from left to right positions, the shield reflection is absent (positions 5, 6, 7), then it appears as a weak signal (position 8) and finally as a good signal (positions 9 and 10). To show this transition, the radar data collected at positions 8, 9 and 10 are plotted in Figure 4b. Where the radar signal could penetrate, an average velocity of 11 cm/ns was measured which is a rather common value for a stone masonry.

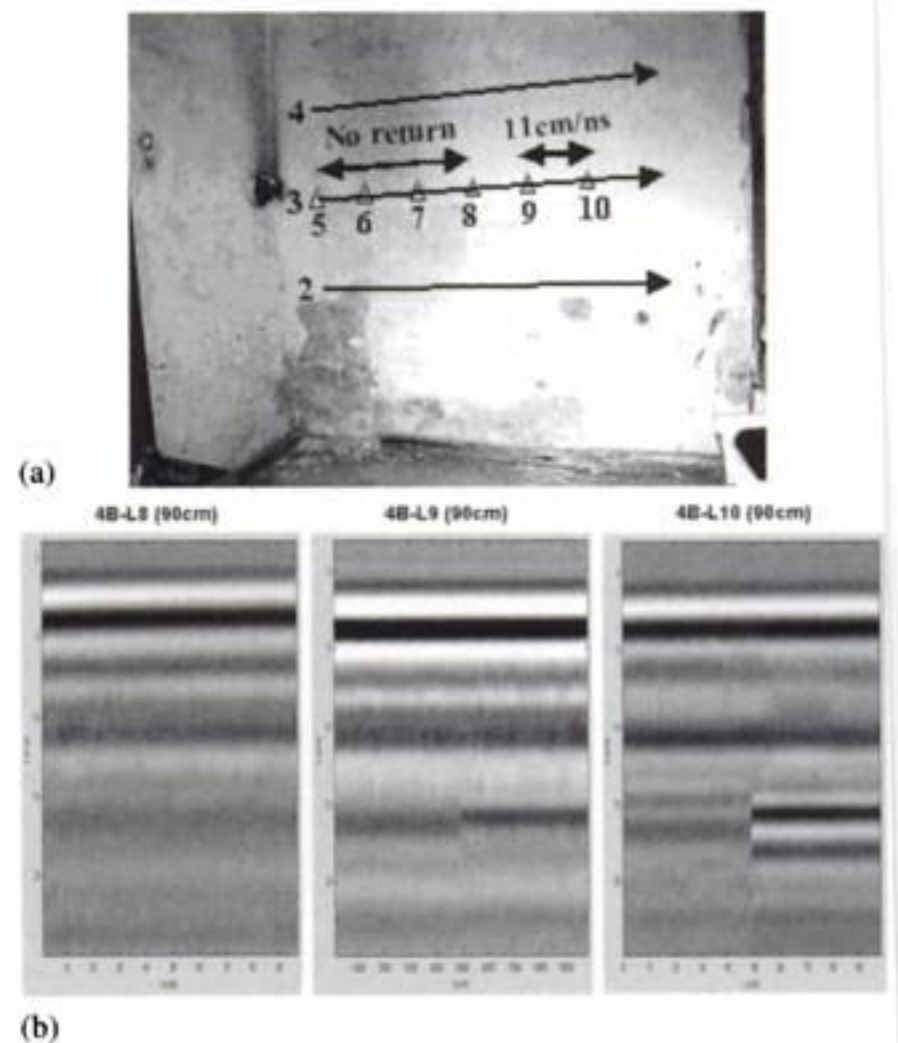


Figure 4. Geometry of the radar survey (a) and time radar data (b) acquired at positions 8, 9 and 10.

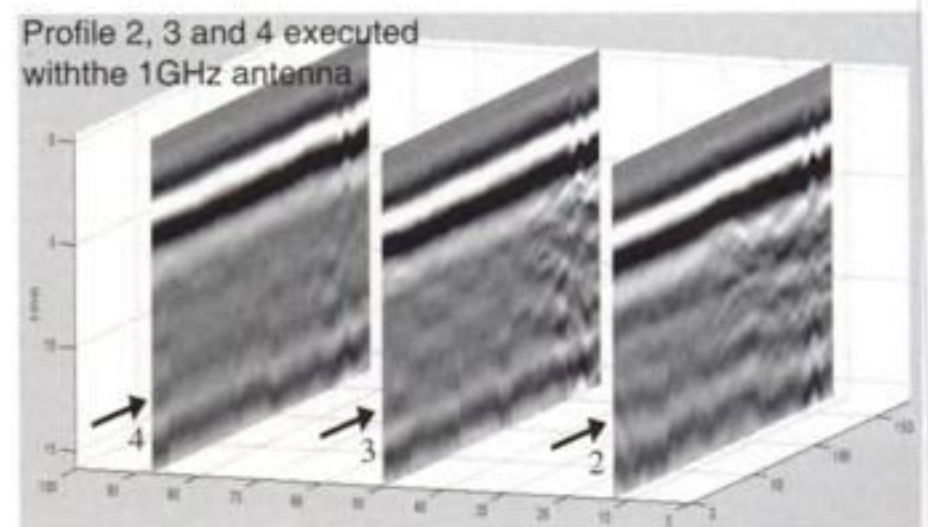


Figure 5. Results of the radar test along the profile 2, 3 and 4.

The profiles acquired by high frequency radar (Fig. 5) confirm a low penetration on the left side where no reflections and/or diffractions appear after the background signal.

The no return positions were avoided for the flat jack tests that were instead located in the area shown in Figure 10a.

6.1.2 Sonic tests and tomographies

Direct sonic tests were carried out in Position 4b, in correspondence of other non-destructive and slightly destructive tests. Figure 6a shows the sonic velocity map compared to the no return area revealed by the radar test in Position 4b. The area where the radar was unable to reach the backside of the wall is associated with low sonic velocities. This indicates the presence

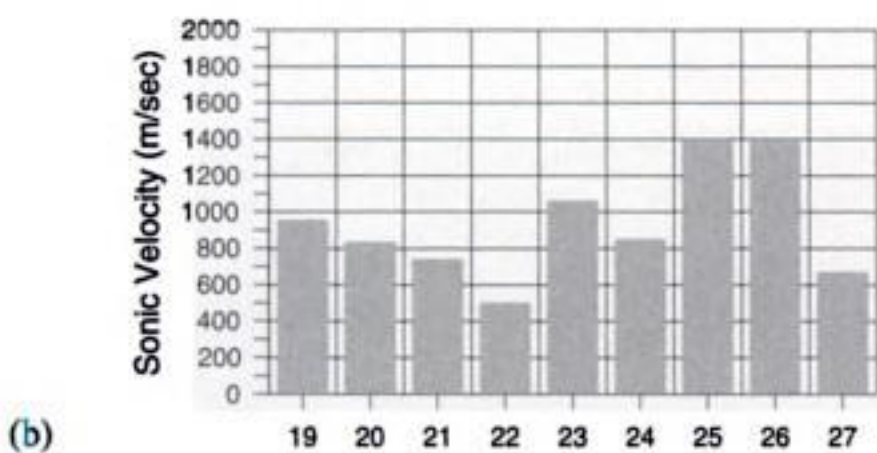
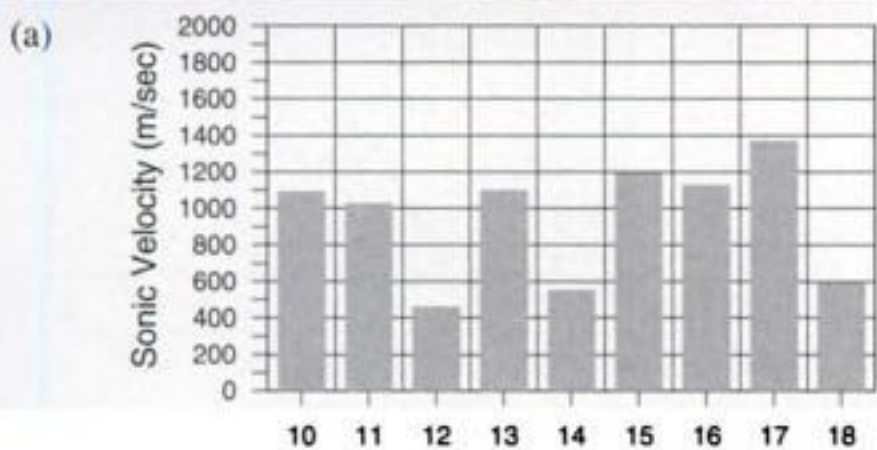
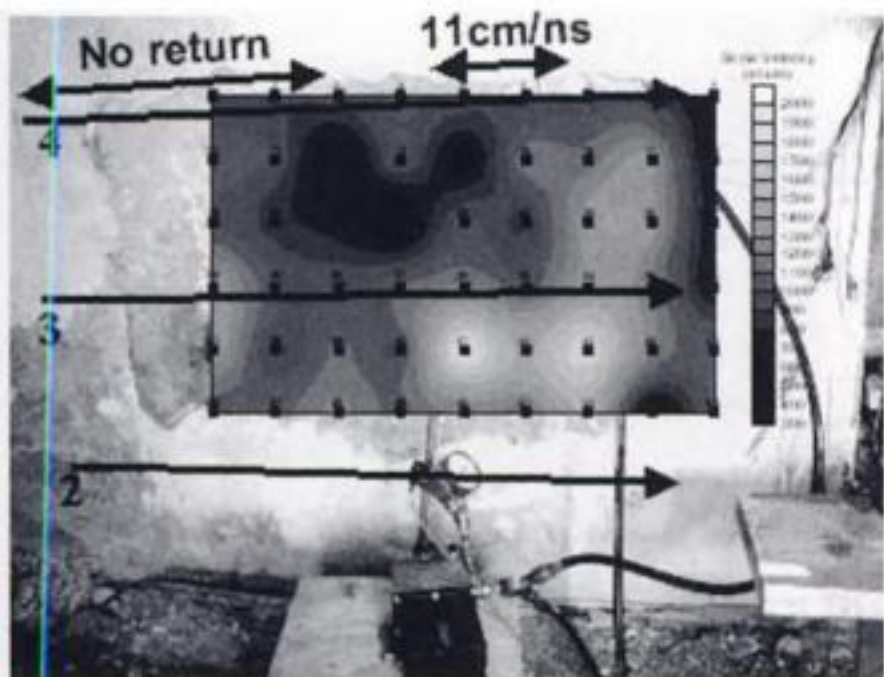


Figure 6. Results of the sonic tests in the position POS 4b.

of a void or a deteriorated masonry that results in a poor elastic response for the sonic test and in a high absorption effect for the radar test. Besides these low values, the sonic velocities found by means of direct sonic tests were ranging from about 1000 to about 1400 m/s. Higher values were found locally, as shown in Figure 6.

Direct sonic tests and tomographies were carried out also in Position 4a, before and after the execution of the shear test. The main aim of the tests was to characterize the wall morphology and to calibrate the values of sonic velocities on the undamaged and damaged masonry wall. Two horizontal tomographies and one vertical tomography were carried out. Figure 7 shows a scheme of the tests performed.

The mean values of sonic velocity found in the upper and lower horizontal tomographies and in the vertical tomography were respectively equal to 1260 m/s, 1500 m/s and 1080 m/s. From the tomographic rendering, it was possible to notice the presence of a non-homogeneous section, but it was not possible to detect

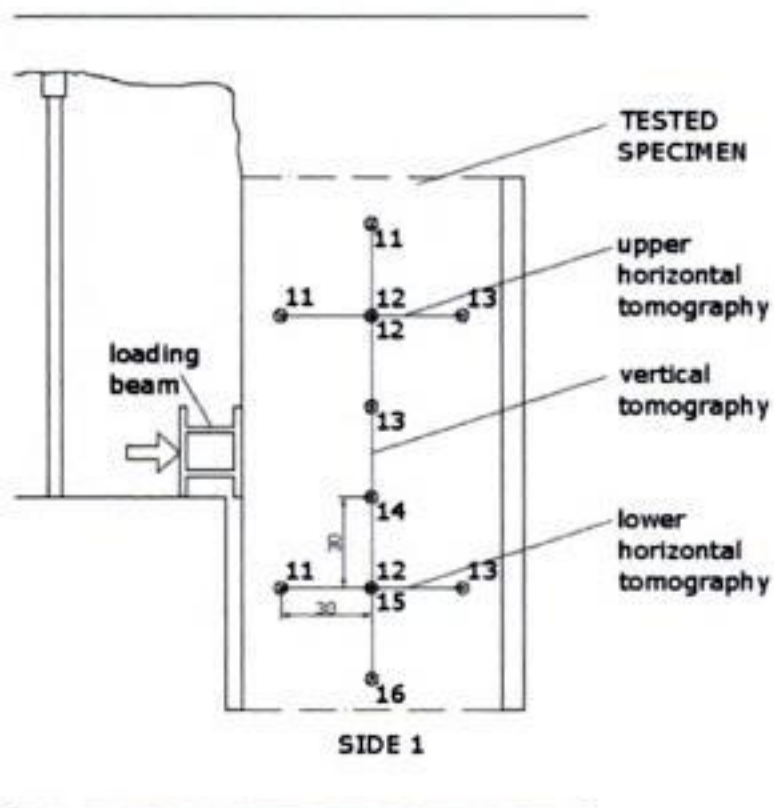


Figure 7. Scheme of the vertical and horizontal sonic tomographies.

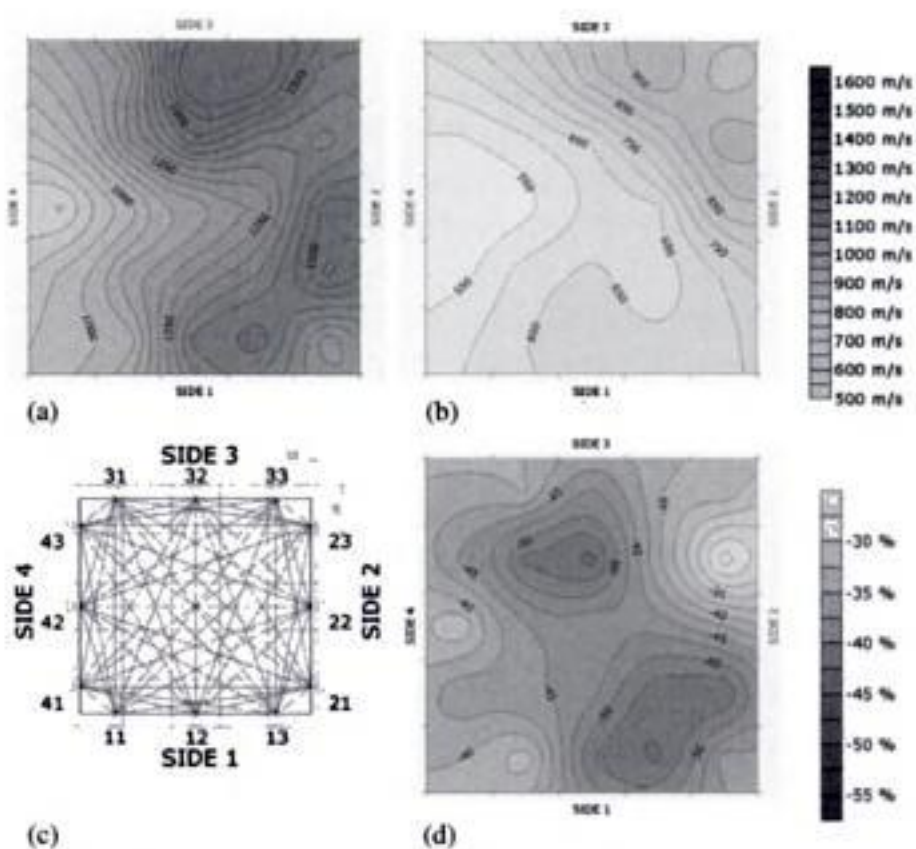


Figure 8. Results of the upper horizontal tomography before (a) and after (b) the shear test; scheme of acquisition points and mesh for data processing (c); percentage decrease of sonic velocity before and after the shear test (d).

the presence of distinct masonry leaves. Figure 8 shows the results found on the upper horizontal section.

The mean decrease of sonic velocity found in the upper and lower horizontal tomographies, after carrying out the shear tests, were equal to 45% and 32%. The corresponding decrease of shear modulus, calculated for the upper and lower part of the tested specimen from the elastic effective stiffness and the secant stiffness in the inelastic range, was respectively equal to 48% and 26%. A comparison was made also between the decrease of velocity found by means of direct sonic

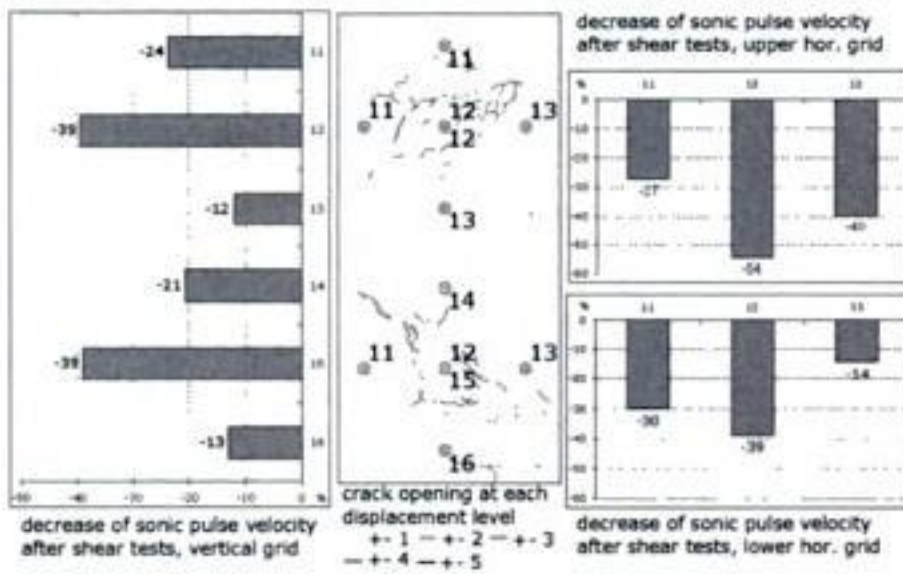


Figure 9. Comparison between the decrease of sonic pulse velocity in direct tests and the crack pattern due to the shear test.

tests on the three grids of test positions for the tomography, and the crack pattern survey carried out during the shear test. The results of this comparison can be seen in Figure 9.

6.2 MDT tests

In order to evaluate the mechanic characteristic of the masonry and to calibrate the results of the NDT, slightly destructive tests were carried out.

6.2.1 Flat-Jack tests

The flat jack results show a good behaviour of the masonry (Fig. 10b) with an elastic modulus around 1490 N/mm^2 and with the level of local compressive stresses of $\sigma_0 = 0.143 \text{ N/mm}^2$ (analytically calculated σ_0 was 0.154 N/mm^2).

6.2.2 Coring

Coring at the same position (Position 4b) where the flat-jack, radar and sonic tests were executed revealed non-homogenous structure of testing masonry. It consisted of rubble stone masonry with large gaps between stones filled with gravels lied in poor lime mortar (Fig. 11).

Additional laboratory tests on samples from mortar specimens revealed the low value of soluble Silica which imply the lime as a binder. The structure of the stone material revealed from the cored sample showed that it consists of two types of stone. Petrographic tests on stone samples, revealed Lithothamnium limestones with following characteristics: density 20 kN/m^3 , compressive strength 125 MPa and modulus of elasticity 50.9 GPa and Calcernit stones (dark colour) with compressive strength up to 250 MPa .

6.2.3 Videoboroscopy

Videoboroscopy shows a non homogeneous but rather solid masonry (Fig. 12), which confirmed the good quality of the masonry.

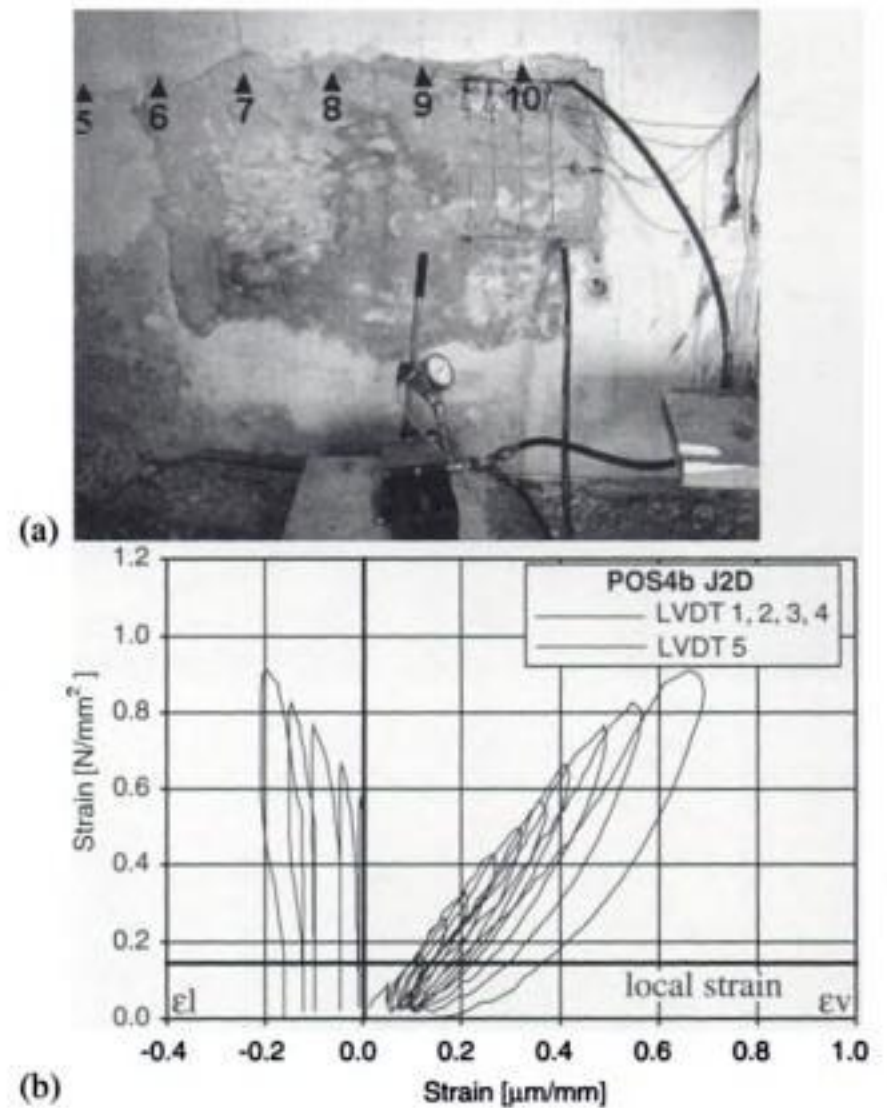


Figure 10. Localisation and result of the double flat jack test Position 4b.

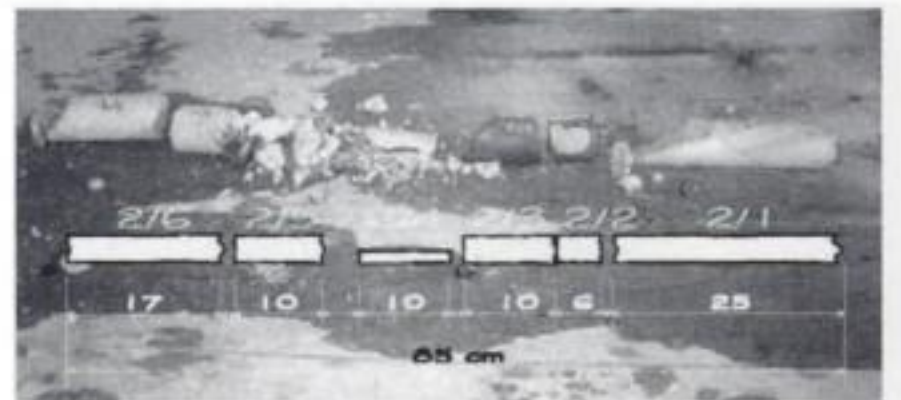


Figure 11. Cored specimen from Position 4b.



Figure 12. Videoboroscopy in the Position 4b.

6.3 DT tests

6.3.1 In-situ shear test

In-situ shear test was carried on the wall (Position 4a) previously agreed with representatives of Institute for

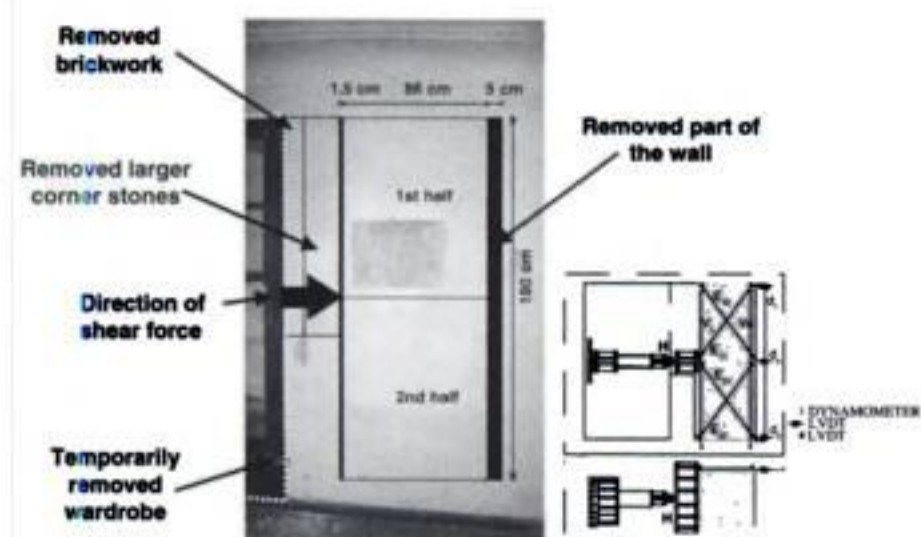


Figure 13. Preparing the specimen for the In-situ shear test.



(a)



(b)

Figure 14. In-situ shear test: (a) before and (b) after the test.

the Protection of Cultural Heritage of Slovenia. Execution of in-situ test was essential for the obtainment of mechanical properties needed for the assessment of the seismic resistance of the Western Part of the Castle. Removal and partial destruction of the tested wall is presented in Figures 13 and 14.

Lateral load was imposed in cyclic manner (one cycle per pre-defined displacement), with increasing

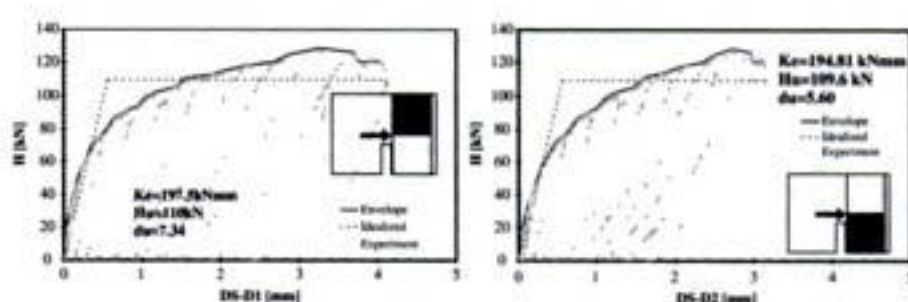


Figure 15. Results of testing of upper and lower part.

Table 1. Results of In-situ shear test.

	Upper part	Lower part
H_u (kN)	110	110
K_e (kN/mm)	198	195
d_u	7.3	5.6
f_t (MPa)	0.14	0.14
G (MPa)	432	424

the amplitude of the displacement up to the limit state of the specimen. The failure of the specimen was pre-defined as the attainment of the 80% of the maximum lateral resistance in softening region. The results of lateral tests are presented in Figure 15 and Table 1, where: H_u – analytically calculated idealized lateral resistance of the element; K_e – effective stiffness of masonry element; d_u – ductility of the masonry element; f_t – tensile (shear) strength of the masonry and G – shear modulus of the masonry calculated from the elastic effective stiffness.

7 SEISMIC ANALYSIS OF THE WESTERN PART

For the seismic analysis of the Western part following assumptions were made: rigid horizontal floor diaphragm action, predominant first vibration mode shape, contribution of an individual wall depends on the lateral displacement attributed to that wall and the shape of its resistance envelope and the walls of composite section were considered as separate along the vertical joint (or cracks observed with crack pattern survey) between their parts. Calculations were performed in two orthogonal directions (Fig. 3).

Main steps in non-linear analysis were: the calculation of the weight of building and stiffness of individual walls, determination of base shear and its distribution among the walls according to their stiffness. Seismic resistance was calculated on the basis of assumed ultimate resistance mechanism, which includes the redistribution of action effects to individual walls according to the attributed ductility capacity (storey resistance envelope). And finally following the energy and ductility based bi-linear idealization of the relationship between the resistance and relative storey

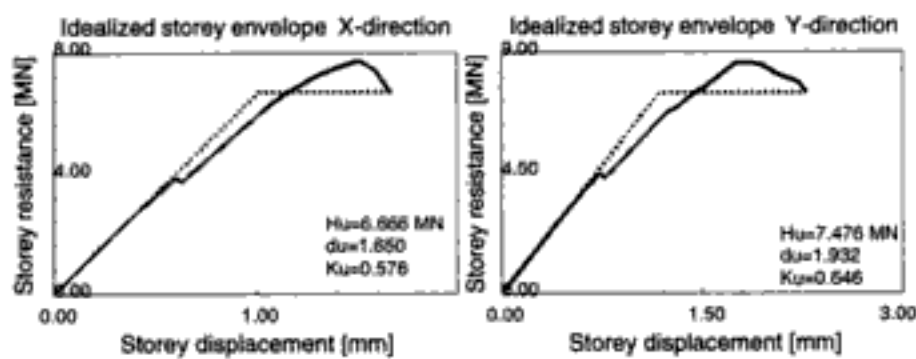


Figure 16. Relationship between the resistance and relative storey drift of the storey for X and Y direction respectively.

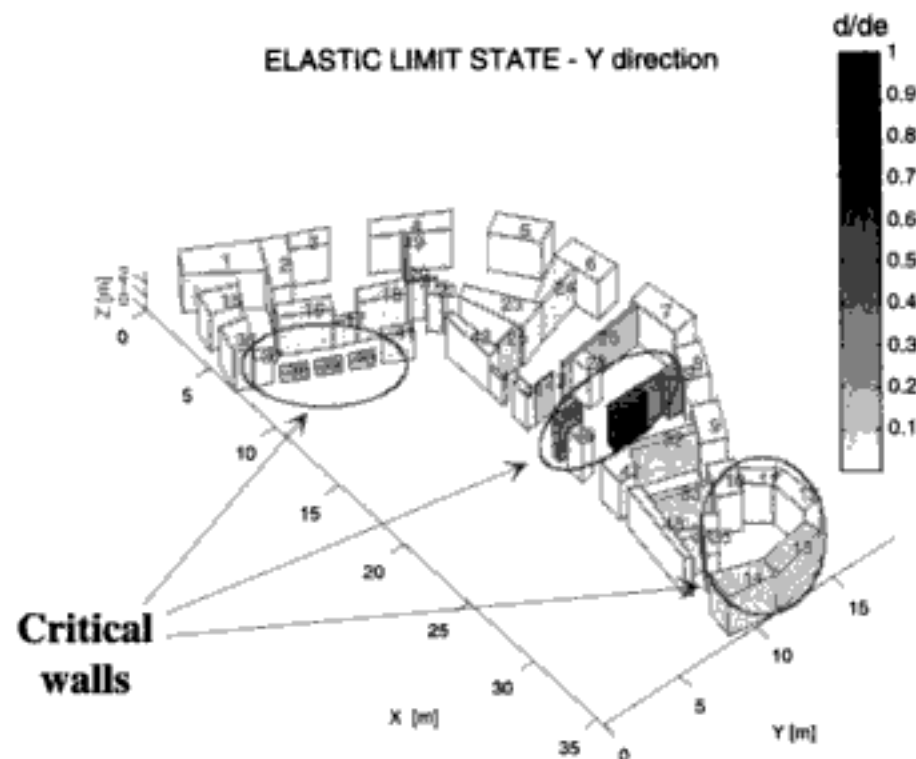


Figure 17. Elastic limit state – Y-direction.

drift of the storey under consideration, the comparison with design shear provisions were made.

Parameters for seismic analysis that were considered in this numerical investigation were: geometry of walls (derived through geometric and crack pattern survey), modulus of elasticity of masonry and compressive strength of masonry (double flat-jack test), shear modulus of the masonry and ductility (in-situ shear test) and vertical stresses in the elements (analytically and single flat-jack test).

Following the results of analysis presented in Figure 16, the ultimate design seismic resistance coefficient for X ($SRC_{du} = 0.576$) and Y ($SRC_{du} = 0.646$) directions respectively, have been compared with the design base shear coefficient BSC_d . In the case of Pišce Castle, for the design ground acceleration of 0.2 g and importance factor of 1.4, the BSC_d was calculated as 0.47.

Although the seismic analysis of Western Part of Pišce Castle has revealed that its seismic resistance is satisfying (which should not be surprising, considering that the ratio of areas of all walls towards the overall area of critical section was over 20%), the numerical analysis have shown also some weaknesses of the structure (Fig. 17), like are the short walls along the corridor, walls with chimney flues and already cracked round walls at the north part.

The numerical investigation was carried out under several assumptions. One of these was the rigid floor action, which for the Western Part of Pišce Castle still has to be achieved, since the floors in that part are wooden one and only a few anchors for tying the walls in the floor level were noticed during the investigations.

8 CONCLUSIONS

A great deal of research is still necessary for the interpretation of the NDT results and for their correlation with the masonry characteristics. However, from this case study it can be concluded that both radar and sonic tests have revealed a hidden chimney flues at Position 4b. Results of flat-jack tests at same position have been analytically verified with the differences between measured and calculated values of normal stresses less than 10%. Results of sonic tests carried out at Position 4a, before and after in-situ shear tests were significantly different.

Results from flat-jack tests and in-situ shear tests were than incorporated in non-linear seismic analysis of the Western part of Pišce Castle. Following results of geometry and crack pattern survey, main structural elements of the building have been defined. The results of seismic analysis revealed some weak points of the structure as well as possible origin of the large vertical cracks at the round tower of the north part of the building.

The on site investigation procedures should be calibrated and controlled in order to verify their effectiveness and particularly the possible application to each peculiar masonry problem. Since no test is usually self-sufficient to give the requested information, the complementarity of the different tests (in-situ shear, sonic and radar tests, flat-jack, etc.) has also to be studied for the definition of the necessary physical and mechanical parameters of masonries.

ACKNOWLEDGEMENT

The research activity was performed within the framework of the ONSITEFORMASONRY research project, coordinated by C. Maierhofer of BAM, at present still in progress and funded by the European Commission (research project N. EVK4-2002-00546).

REFERENCES

- Binda, L., Saisi, A., Tiraboschi, C. 2000. Investigation procedures for the diagnosis of historic masonries, *Construction and Building Materials*, vol.14, n.4, 199–233.
- Binda, L., Saisi, A., Zanzi, L. 2003a. Sonic tomography and flat jack tests as complementary investigation procedures

for the stone pillars of the temple of S.Nicolo' l'Arena, *Non Destructive Testing and Evaluation Int.*, vol.36, n.4, 215–227.

Binda, L., Lualdi, M., Saisi, A., Zanzi, L. 2003b. The complementary use of on site non destructive tests for the investigation of historic masonry structures, 9th North American Masonry Conference 9NAMC, Clemens, South Carolina, 978–989.

da Porto, F., Valluzzi, M.R., Modena, C. 2003. Use of sonic tomography for the diagnosis and the control of intervention in historic masonry buildings, *International symposium Non-Destructive Testing in civil engineering,*

NDT-CE 2003, Berlin, Germany September 16–19, (CD-ROM).

Schuller, M., Berra, M., Faticcioni, A., Atkinson, R., Binda, L. 1994. Use of tomography for diagnosis and control of masonry repairs. *Proc. 10th International Brick/Block Masonry Conference*, Calgary, Canada, July 1994, pp. 438–447.

Valle, S., Zanzi, L., Binda, L., Saisi, A., Lenzi, G. 1998. Tomography for NDT applied to masonry structures: Sonic and/or EM methods. *Arch bridges*. A. Sinopoli Editor, Balkema, Rotterdam, pp. 243–252.

Structural evaluation of historic walls and columns in the Altes Museum in Berlin using non-destructive testing methods

C. Maierhofer^a, M. Hamann^b, C. Hennen^c, B. Knupfer^d, M. Marchisio^e, F. da Porto^f,
L. Binda^g & L. Zanzi^g

^a *Federal Institute for Materials Research and Testing (BAM), Berlin, Germany*

^b *Institute for Applied Science in Civil Engineering (IaFB), Berlin, Germany*

^c *Stiftung Luthergedenkstätten in Sachsen-Anhalt, Lutherstadt Wittenberg, Germany*

^d *GEOCISA, Research and Development, Madrid, Spain*

^e *University of Pisa, Dept. of Civil Engineering, Pisa, Italy*

^f *University of Padova, Dept. of Construction and Transport, Padova, Italy*

^g *Politecnico di Milano, Dept. of Structural Engineering, Milano, Italy*

ABSTRACT: The methodologies developed in ONSITEFORMASONRY were applied to assess the structure and material properties of selected structural elements in the Altes Museum in Berlin-Mitte. Since at all time the Altes Museum was of great concern in the archival studies, a lot of information exist about former destruction and restoration which support the interpretation of data recorded with the different testing methods.

1 INTRODUCTION

Analysing the damages and other problems affecting historical constructions for their structural evaluation, methodologies based on the application of non-destructive (NDT) and minor destructive (MDT) testing methods have been designed during the ONSITEFORMASONRY-project according to the type of damage or problem, the construction typology, the level of assessment and the environmental conditions. These methodologies are being applied on real cases like the Altes Museum in Berlin for their validation.

The Altes Museum (old museum) in the city centre of Berlin was designed by Karl Friedrich Schinkel and was built between 1823 und 1830 on the Lustgarten. Figure 1 shows a view from the Lustgarten. The building was designed with an atrium containing pillars and a central cupola related to the Roman Pantheon and having antique temples as an archetype. It represents the eldest exhibition hall in Berlin. During the Second World War parts of the Altes Museum burned down, and it was rebuilt in 1966.

In 1999, the planning stage started for a broad reconstruction in the frame of a master plan concerning the whole Museumsinsel (museum island) taking into account contemporary requirements for a museum building. Extensive investigations have to be performed to assure structural integrity and to provide a basis for a sustainable and considerable conversion of the building.



Figure 1. Altes Museum in Berlin-Mitte, view from the Lustgarten.

At all time the Altes Museum was of great concern. Thus archival studies of the Technical University of Berlin provided a lot of information about the structure. These studies are of fundamental interest for ongoing NDT and MDT in the frame of the European Research Project ONSITEFORMASONRY.

With radar, geoelectric, microseismic, sonics, impulse-thermography and flat-jack, different testing problems have been solved which are described in more detail below.

2 OBJECTIVES

The Altes Museum has been chosen as pilot site because several questions are also typical for other historic structures in general. In the frame of reconstruction, testing problems mainly occur related to

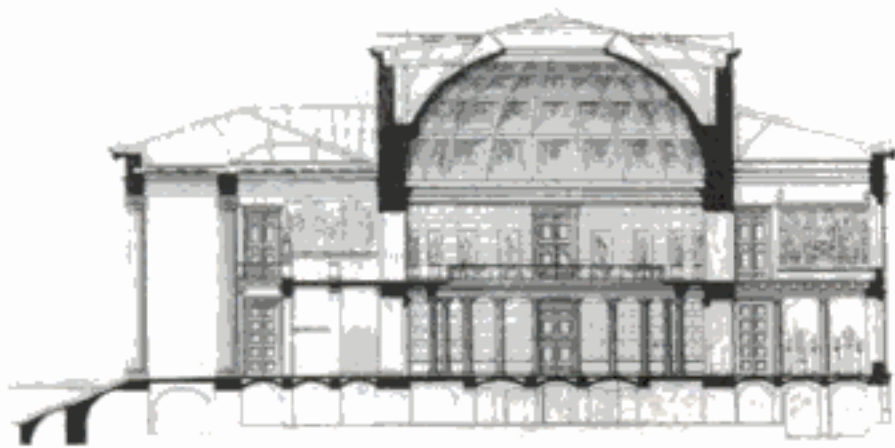


Figure 2. Cross-section of the Altes Museum showing the different construction elements in the entrance hall, in the rotunda and in the cellar.

the inner structure of different structural elements like columns, floors, ceilings and walls. In this paper, the following objectives have been analysed (see also Figure 2):

- Investigation of the inner structure of the outside columns in the entrance hall of the museum. Here, the outer column located at the west part of the entrance hall was selected for solving the following questions: How are the single drums connected to each other? Is it possible to locate the different materials used for restoration at the cylindrical shell? A scaffold was raised for performing measurements along the whole length. Radar and ultrasonic investigations in reflection as well as in tomographic mode had been planned.
- Localisation of plaster delaminations at the columns in the rotunda. These columns belong to the original asset from 1830. The columns consist of massive sand stone which is covered with lime plaster having a thickness of 2 to 3 cm. This plaster is the carrying layer for the visible stucco marble layer of 3 to 6 mm. The sand stone core is massive and it is expected that it consists of single drums. The whole surface of the columns is covered with a net of small cracks. The cracks are very thin, but few of these have a width of up to 2 mm. By knocking on the surface, different types of delaminations can be accessed: Delaminations of the stucco marble layer, delaminations of the plaster and a combination of both. One column (no 14) had been selected for investigations with impulse-thermography to locate and quantify these delaminations.
- Investigation of the structure and moisture content of an inner carrying wall in the cellar. The foundation of the Altes Museum is based on wooden piles, which have been positioned in a dense grid. The top of these piles is covered with wooden frame constructions. These are the basis for the foundation consisting of natural lime stone. The walls constructed on this basement are made of bricks. Only parts of the building have a cellar. The level of the ground water is at 31 mNN (normal level), while the floor of the cellar is at approx. 31.71 mNN.

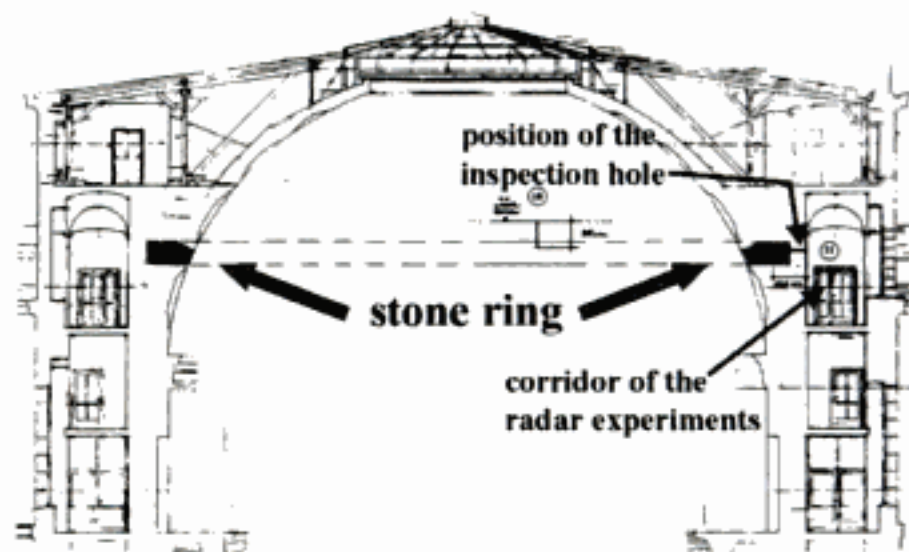


Figure 3. Structure of the supposed reinforcement stone ring and position of the investigations.

Therefore, at least the basement consisting of natural stone is exposed to moisture. The inner carrying wall which was selected for the investigations is accessible from both sides, one side is covered with mortar. From the floor up to a height of 70 cm, the wall consists of a pedestal made of lime stone. Above the pedestal, there is still stonework made of lime stone up to a total height of 2.0 m. The connection to the ceiling was closed by two to three layers of brickwork. At both sides of the wall, there are wall porches which are connected to the wall. At the side without mortar, the wall shows a crack with widths from 0.5 to 3 cm at the area close to the outer wall. The crack follows the steps of the joints from the lower edge of the ceiling down to the floor. For the investigation of the inner structure, for the determination of the moisture distribution and for analysing the load measurements, investigations had been performed at this wall with radar, geoelectric, microseismic, sonic tests and flat-jack.

- Structural investigation of the sand stone ring. Figure 3 shows the assumption of the architects regarding the existence of a stone ring embedded inside the brick masonry structure supporting the dome. The objective of the investigations was to validate this assumption and to derive as many information as possible regarding the morphology of the ring. Thus, radar measurements had been carried out in reflection mode.

3 METHODOLOGIES

3.1 Radar

Radar is based on the transmission of short electromagnetic impulses by an antenna at frequencies between 300 MHz and 2.5 GHz (Daniels, 1996). These impulses are reflected at interfaces with changing dielectric properties of the materials. Also the propagation velocity depends on the dielectric properties. Since moisture is influencing this parameter, radar can also be applied to detect an enhanced moisture content

and to determine the moisture distribution. With radar, reflection measurements from one surface as well as tomographic measurements from both sides are usually performed to obtain information about the internal structure of the structural element under investigation (Maierhofer et al, 2000; Colla et al, 2000; Maierhofer et al, 1998).

3.2 Sonics

Sonic tests consist in transmitting stress waves within the frequency range of acoustic waves (20 Hz to 20 kHz), generated by an instrumented hammer, and in measuring their travel time by means of accelerometers. For given masonry typologies it is possible to find a relationship between the sonic velocity and the elastic properties of masonry (Riva et al, 1997). In general, sonic tests can be applied to get qualitative information on the morphology, consistency and state of conservation of masonry (Berra et al, 1992; Abbaneo et al, 1996). Besides direct and indirect tests, carried out through the thickness or on the same side of the wall, also sonic tomographies can be performed. In that case, the measures of sonic pulse velocity are combined along different ray-paths on a cross section of masonry, and are subsequently processed in order to define mean values of velocity on each portion of the wall section itself (Valle et al, 1998; da Porto et al, 2003).

3.3 Geoelectric

The geoelectrical tomography is the reconstruction of the distribution of the electrical resistivities in the body of a structure obtained by current injections across many different couples of electrodes.

Two different methods can be used: *transparency tomographies* or *inverted pseudo-sections* when only one side of the structure is accessible.

The *transparency tomographies* use an experimental disposition of the electrodes corresponding to the *cross-hole tomography* in the subsoil: in this case 2 series of electrodes are fixed along 2 profiles on the opposite faces of a masonry structure. The electrodes are connected in different combinations, performing a high number of measurements (typically several hundreds). The cross-section covered by the ray paths is ideally divided into a number of cells (pixels). Their resistivity is computed by means of complex iterative routines. The numerical output (resistivity of each cell) must be converted into an *image* of the distribution of the velocities in the cross-section to render it usable.

Another technique, the *inverted pseudo-section*, uses only one profile with many electrodes on one face of the structure. Measurements are made with the technique of the so-called *resistivity pseudo-sections* by connecting 4 electrodes at a time with one of the typical arrays used in geoelectrics. A high number of

measurements (several hundreds) is performed. The measured data, namely the apparent resistivities, can be directly plotted versus some kind of pseudo-depths to build the so called pseudo-sections. These are purely qualitative images.

By means of a complex inversion process, the distribution of true resistivities versus true depth can be obtained, that is, another kind of geoelectrical tomography. This is sometimes referred as the impedance tomography.

In both cases multi-electrode (24, 48 or more) automatic switching geo-resistivity-meters are necessary. Very high quality instruments are required. A particular care must be taken to ensure a good electric contact of the electrodes with the surface of the wall (Marchisio et al, 2000; Cosentino et al, 1998; Marchisio et al, 2002).

3.4 Impulse-thermography

Impulse-thermography (IT) is an active approach for a quantitative thermal scanning of the surface of various structures and elements. A thermal pulse is applied to a surface causing a non stationary heat flow. During the cooling-down process the emitted thermal radiation is observed with an infrared camera. The propagation of the heat into the body depends on material properties like thermal conductivity, heat capacity and density of the inspected object. If there are inhomogeneities in the near surface region of the structural element this will result in measurable temperature differences in the local area of the surface (Maierhofer et al, 2002).

A relatively new approach of IT is the pulse phase thermography (PPT) (Vavilov et al, 1998; Maldague et al, 1996; Maldague, 2001). The stored data received during the IT is analysed in the frequency domain via Fast Fourier Transformation of the transient curve of each pixel in a series of thermal contrast images. This leads to changes in amplitude or phase of the corresponding images. The main advantage of PPT lies in the phase images, which are reported to be less influenced by surface infrared and optical characteristics. That also means less sensitivity to non-uniform heating compared with the thermal contrast images of IT (Maldague, 2001).

3.5 Single and double flat-jack

The objective of the flat-jack test is to obtain the local state of stress in compression of a masonry element that works under vertical stress. The method is based on stress release.

The general procedure of this test consists on restoring the vertical displacement caused by a horizontal slot made in a loaded masonry. The distance between three or four points fixed across the slot is measured by gages before and after cutting. The device used to restore the displacement is a flat-jack; oil is pumped

in the jack until the distance between the gage points is restored to the initial situation.

In order to obtain the local state of stress, the restoring pressure has to be corrected taking into account two coefficients that depend on the mechanical characteristic of the flat-jack, calibrated in laboratory, and on the relation between the geometry of the slot and the shape of the flat-jack.

A double flat-jack test is carried out by two flat-jacks inserted in two parallel slots at a convenient distance and pumping oil into both so that a compression test is performed. In fact, the two jacks delimit a masonry sample of appreciable size to which a uni-axial compression stress can be applied. Measurement bases for removable strain-gauge or LVDTs on the sample face provide information on vertical and lateral displacements. Several unloading and re-loading cycles can be performed at increasing stress levels in order to determine the deformability modulus, an important parameter in the masonry classification (Binda et al, 2004). It is interesting to compare these last results to the stress level measure in order to verify the actual state of the masonry in relation with its potentialities (Binda et al, 1999).

4 RESULTS

4.1 Structure of columns in the entrance hall

4.1.1 Radar

For getting an overview four evenly distributed traces in direction of the longitudinal axis (vertical) of the selected column were recorded with the 900 MHz antenna along the whole height (10.2 m). A measuring wheel mounted to the antenna performed measurement triggering and recording of the path. Figure 4 shows one of these radargrams. Clear signals related to the surface and to the backside reflection can be detected. The travel time of the backside echo increases when going from top to bottom corresponding to an increase of the diameter of the column. Close to the surface reflection, hyperbolas occur representing the reflection of the joints between the different drums. Due to the high intensity of these reflections, it is assumed that these joints contain plumb layers that were used as a non-seizing compound for the alignment of the column drums.

For detailed investigations on the joints between the drums, horizontal traces at different areas close and far from the joints were recorded. The measurements were performed radial along the surface of the column with the 1.5 GHz antenna. One of these radargrams below a joint is shown in the bottom of Figure 5. Due to the cannelures the backside reflections appears in a wave-like shape. Noticeable reflections can be detected at a depth between 70 and 75 cm. The position and intensity of this reflection is changing with the angular position

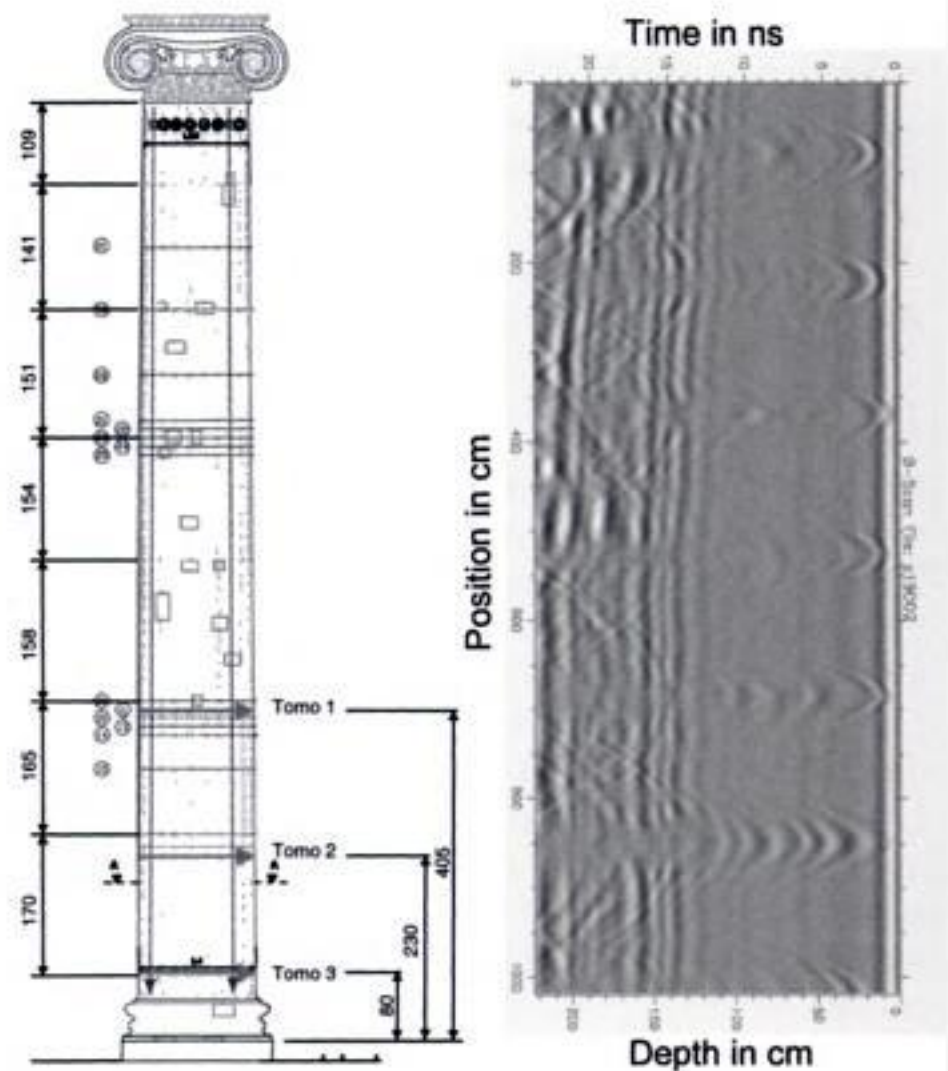


Figure 4. Investigated column (left) and radargram of a vertical trace (right) recorded along the total height of the column with the 900 MHz antenna. The hyperbolas are related to the joints between the drums.

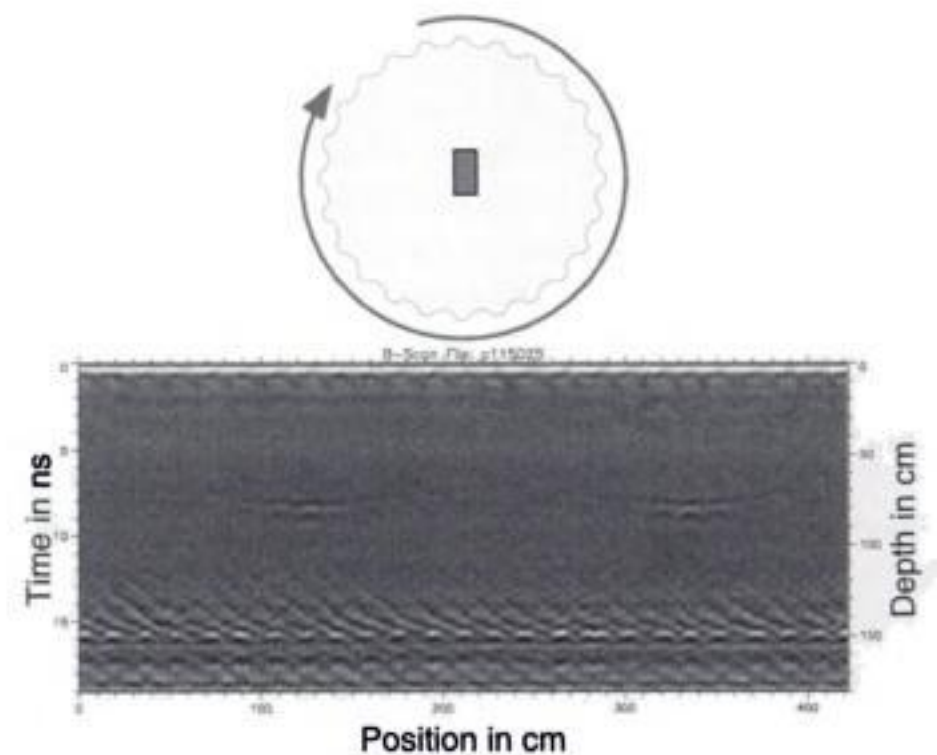


Figure 5. Top: Rectangular void in the upper part of each drum used for transportation and alignment. Bottom: Radargram of a horizontal trace recorded with the 1.5 GHz antenna in the upper part of one of the drums.

of the antenna around the column (trace of antenna: 360°). The reflections at opposite antenna positions (180°) are similar. From this reflection profile it can be concluded, that in the middle of the drum below the joint, a rectangular hole exists (with a length of ca. 7 to 10 cm and a width of 2 to 3 cm) which was used for

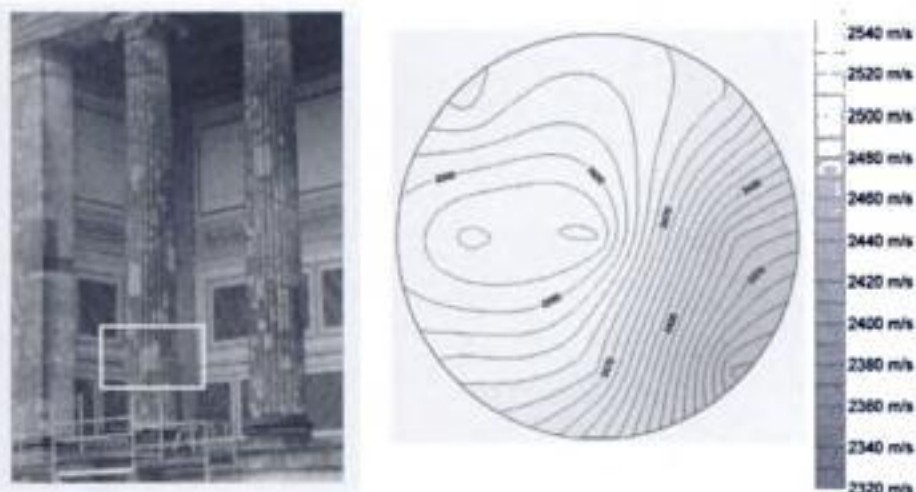


Figure 6. Investigated column (left), tomographic reconstruction of the section (right).

mounting, see figure 5, top. This hole was only located at the top of each drum and was presumably used for mounting and alignment of the drums. There were no hints to metal compounds as pins between the drums, only this lead dies.

It was also possible to locate the restored areas, but the thickness of the replaced structures could not be resolved.

4.1.2 Sonics

On the same column, also a sonic tomography was carried out in order to check the distribution of different materials. A horizontal section, 1.10 m high from the level of the entrance floor and 0.10 m above the lower ashlar, was chosen for the sonic tomography (Figure 6, left and tomo 3 in Figure 4, left). A very simple acquisition grid with six points located on the outer perimeter of the column was chosen to carry out the tests. Three measurements per point have been recorded and they were subsequently processed with software purposely developed in Visual Basic 6 and based on the theoretical non rectilinear propagation of elastic waves. The investigated section was divided into nine large square pixels.

The tomographic reconstruction gave uniform values of velocity in the section, with velocities included between 2330 and 2540 m/s (about 8% scatter, Figure 6, right). The lowest values of velocities were actually located around an area restored with a pigmented mortar after the bombing that damaged the columns.

No other differences were found in the column composition, such as the presence of large inner core, etc. It has to be noted that a higher number of transmitting/receiving points, in order to have the cross section more densely investigated, would have improved the accuracy of the obtained results. The sonic tomography allowed detecting areas built with different materials (macroscopic phenomena consistent with the tested cross section dimension) but its resolution is too low, also in terms of wavelength, to detect the position of small iron fasteners or minor irregularities.

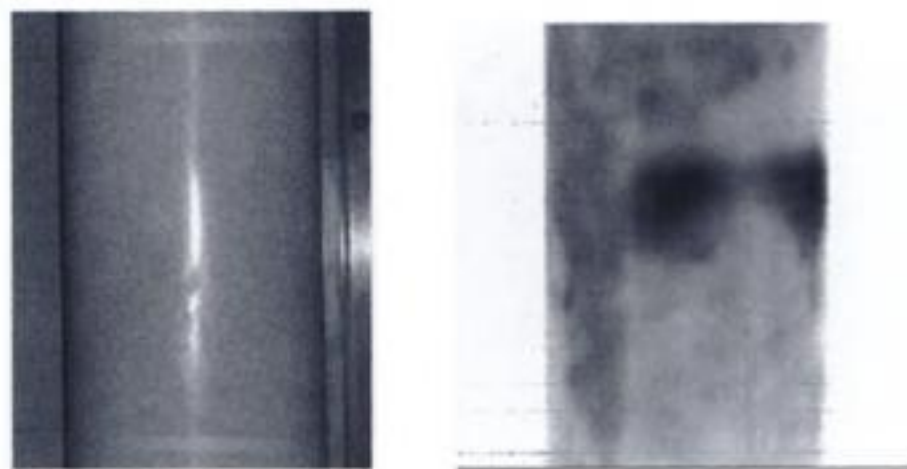


Figure 7. Photo (left) and phase image (right) of the same area of the column after a heating of 5 min. The delaminations appear in the phase image as dark areas.

4.2 Plaster detachments at columns in the rotunda

4.2.1 Impulse-thermography

The experimental set-up consists of a thermal heating unit, an infrared camera and a computer system, which enables digital data recording in real time. For the heating of the surface of the columns a conventional electric fan heater has been used with a heating power of 2000 W avoiding temperatures at the surface higher than 50°C. The infrared camera is an Inframetrics SC1000 with a PtSi-focal plane array detector with a resolution of 256 vs. 256 pixels. It detects the emitted radiation in a wavelength range from 3 to 5 μm . For accessing all parts of the column, a lift was used. Large areas with delaminations appear in the lower parts of the column as demonstrated in the dark parts of the phase image in Figure 7 right after 5 min of heating. From comparisons with results obtained at test specimens with different mortar thickness in the laboratory, it is assumed that these delaminations belong to the stone/mortar interface. But this assumption was not proved with destructive tests.

4.3 Properties of a carrying wall in the cellar

For the investigation of the structural and material parameters of the inner carrying wall in the cellar (plan view in Figure 8, part of the wall with a large crack is shown in Figure 9), several tomographic and indirect and direct transmission investigations had been performed with sonics, microseismics, geoelectric and radar. Flat-jacks had been applied at four positions as shown in Figure 8.

4.3.1 Sonics

Direct sonic tests were carried out on two positions of the load bearing wall in the cellar (P1 and P2 in figure 8). In correspondence to the flat-jack tests, the tests were carried out on a 6 \times 8 grid (six rows and eight columns, 15 cm \times 15 cm) of transmitting/receiving points, for a total of 48 points. The thickness of the wall was 1.71 m. A single measurement per point has been

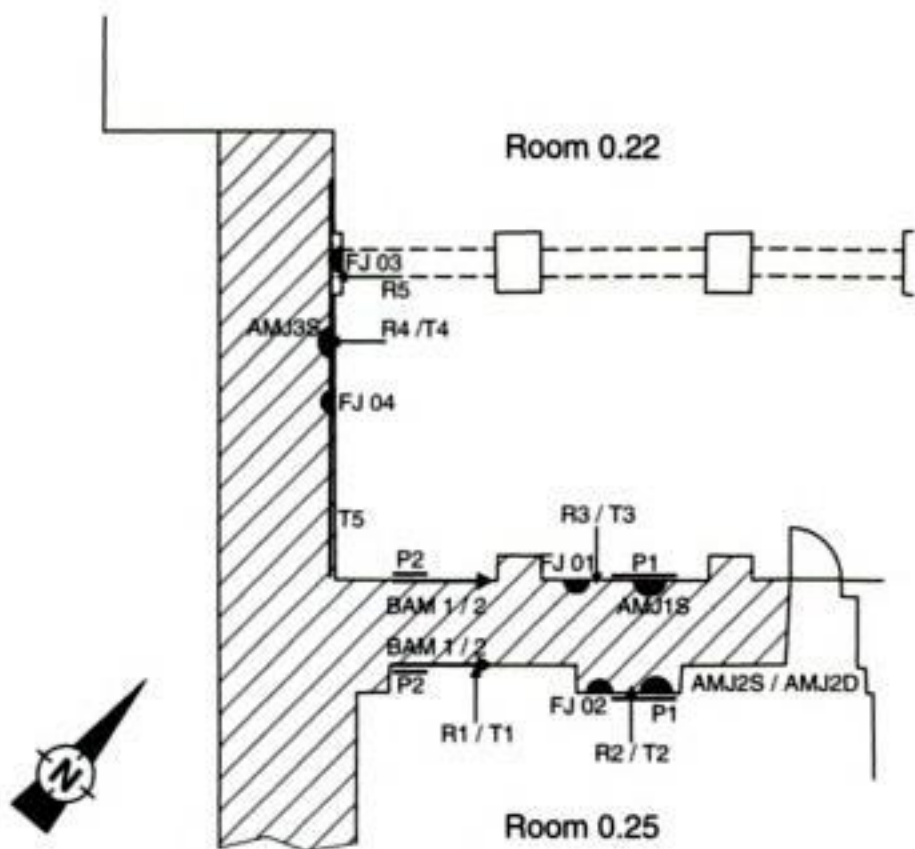


Figure 8. Part from the plan view of the cellar showing the cross-section of the investigated inner wall and the different measurement positions. P1, P2: Direct sonic tests. R1 to R5: Microseismic profiles. T1 to T5: Geoelectric profiles. BAM1, BAM2: Radar tomography profiles. AMJ1S to AMJ3S: Single flat-jack by Polimi. AMJ2D: Double flat-jack by Polimi. FJ01 to FJ04: Single flat-jack by Geocisa.

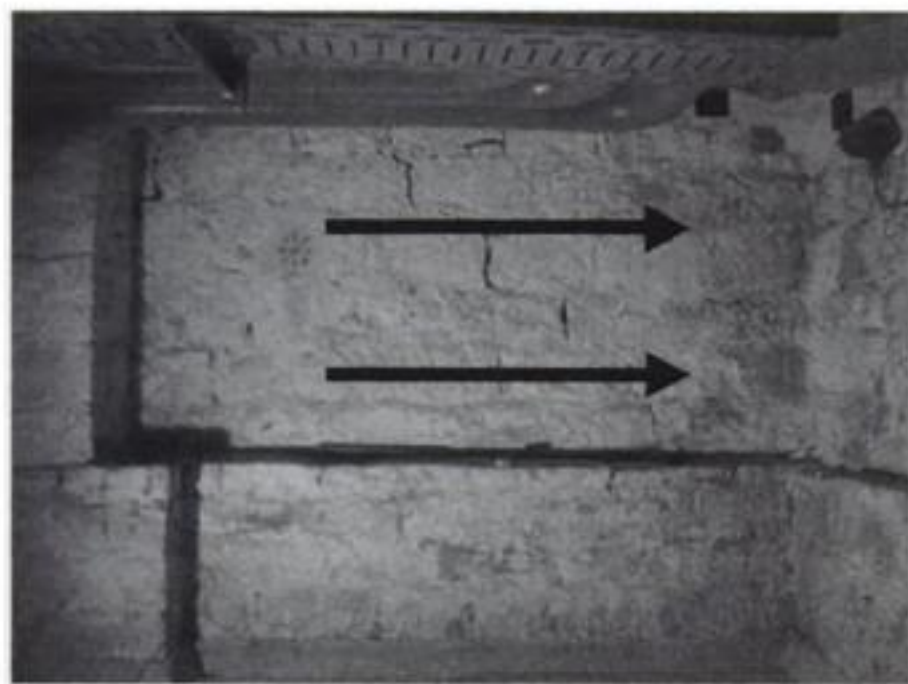


Figure 9. Part of the investigated inner carrying wall in the cellar showing a large crack. The arrows mark the position of the radar traces for tomography.

recorded. The velocities ranged between 1600 and 2600 m/s, with a high scatter (38%), about 1000 m/s. The results of position P1 are presented in Figure 10.

The mean value is 2150 m/s. The upper part of the tested area presented lower velocities and the lower part of the tested area was characterised by higher values. This might be related to higher moisture content in the bottom of the wall, considering that the presence of moisture results in apparent increases of sonic velocity (Riva et al, 1998). This trend was observed

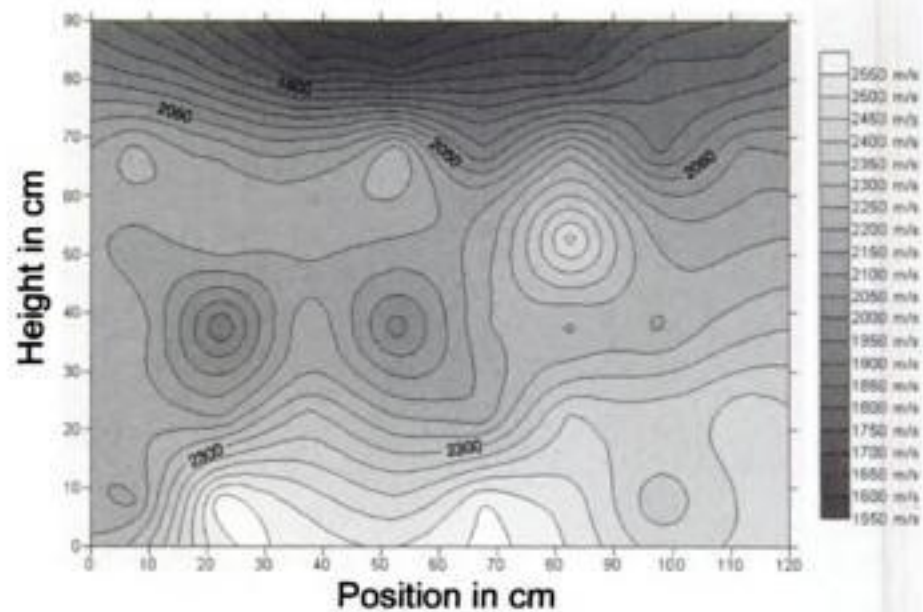


Figure 10. Sonic velocity distribution as obtained from direct tests at position P1.

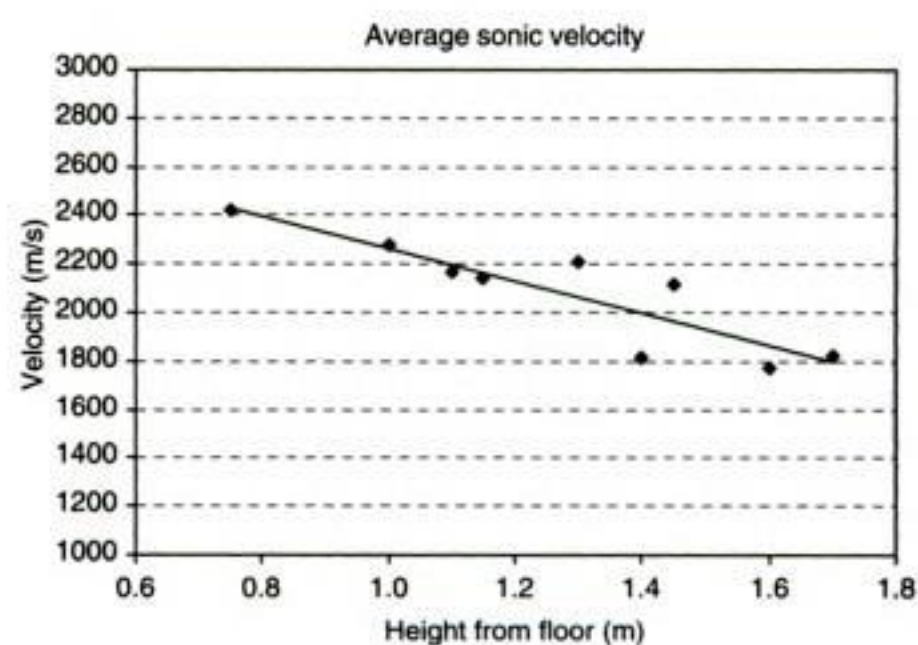


Figure 11. Sonic velocity measured in direct tests on test area P1 and P2 versus height from floor.

also in other tested area in the cellar. The mean values of direct sonic measurements taken at different heights on the cellar wall are shown by Figure 11.

The values of sonic velocities are typical of masonry in fair good/good condition (Berra et al, 1992; Forde et al, 1985). With similar thickness, multi-leaf stone masonry walls with internal filling with poor mechanical properties, internal voids and detachment of the external layers, in bad conservation condition, usually give lower values of velocity (Riva et al, 1997).

4.3.2 Microseismics

Seismic velocity profiles were performed on the basement wall of the cellar in five positions (R1 to R5 in Figure 8).

Some examples of seismic velocity profiles are shown in Figure 12.

The figures show the so-called *dromochrones*, that is the arrival times for a single shot plotted versus the distances from the shot point. The slope of the straight parts of the dromochrones are the reciprocal of the propagation velocity of the micro-seismic waves.

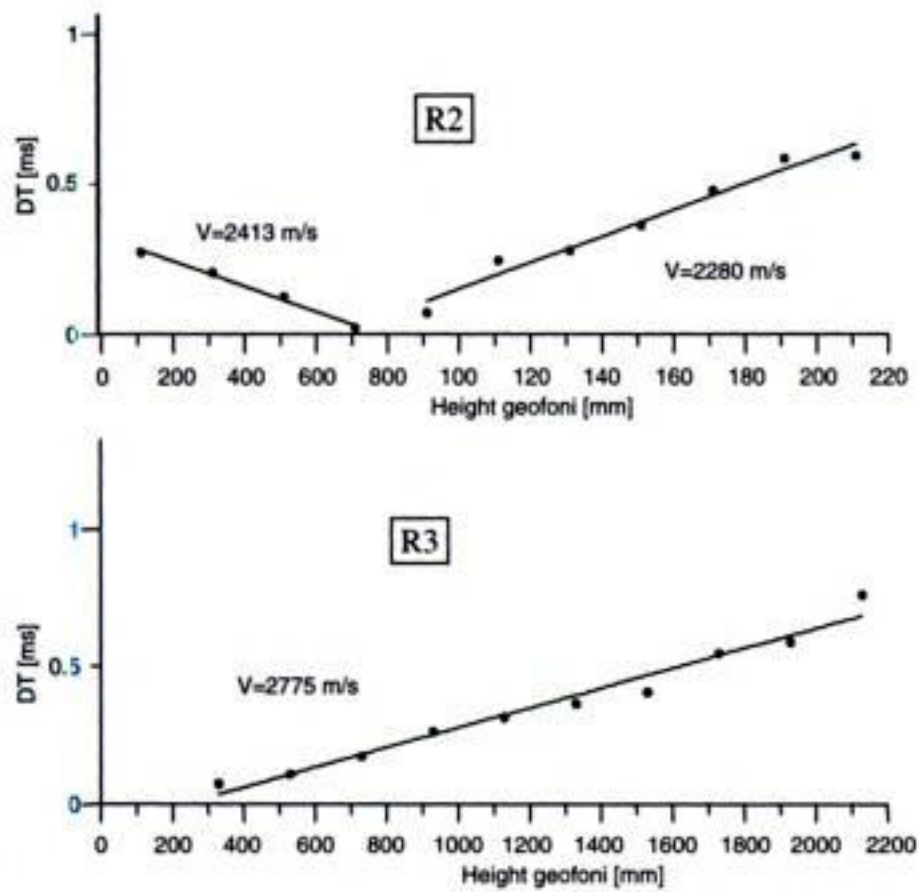


Figure 12. Velocity profiles recorded with microseismics.

The velocities of the elastic (or seismic) waves in a homogeneous body depend on the elastic properties of the body and on its density.

The propagation velocity of the pressure (longitudinal) waves, V_p , is given by:

$$V_p = \sqrt{\frac{\lambda + 2\mu}{\delta}} = \sqrt{\frac{E}{\delta} \cdot \frac{1 - \nu}{(1 + \nu)(1 - 2\nu)}}$$

while the propagation velocity of the shear (transversal) waves, V_s , is given by:

$$V_s = \sqrt{\frac{\mu}{\delta}} = \sqrt{\frac{E}{\delta} \cdot \frac{1}{2(1 + \nu)}}$$

where λ and μ are the constants of Lamè; E is the Young modulus; ν is the modulus of Poisson; δ is the density.

The elastic moduli can be derived from the velocities and density. These elastic moduli are referred as *dynamic elastic moduli* as they refer to very small stress and deformations, while the static values are measured with much higher values.

If both V_p and V_s are known, the Poisson ratio can be computed:

$$\frac{V_p}{V_s} = \sqrt{\frac{2(1 - \nu)}{1 - 2\nu}}$$

All the velocity profiles are well consistent. Velocity values are high (from 2400 to 2800 m/s). These values correspond to dynamic elastic moduli values of 80000–110000 DaN/cm² (Gucci et al, 1997; Marchisio et al, 2002).

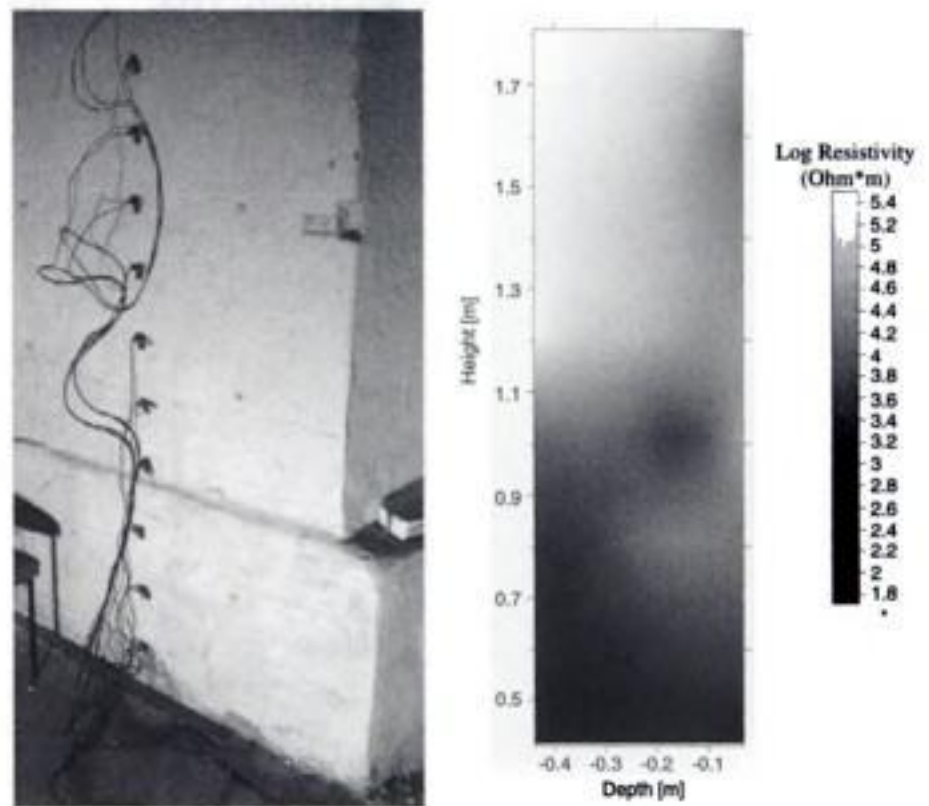


Figure 13. Left: Electrode array for geoelectrical measurements. Right: Reconstructed electrical resistivity distribution in the wall calculated from geoelectrical measurements (T2).

4.3.3 Geoelectric

Electrical tomographies were performed on the basement wall of the cellar at five positions. There are 4 vertical electrical tomographies (from T1 to T4) and 1 horizontal electrical tomography (T5) (Figure 8).

In Figure 13, the geoelectric measurements at T2 are shown together with the reconstructed tomogram. In the lower part, the material is relatively more conductive. Probably this is due both to change of material and presence of moisture.

4.3.4 Radar

Radar measurements in transmission mode were performed along the two traces marked in Figure 9 using two 900 MHz antennas (BAM1 and BAM2 in Figure 8). The transmitting antenna was placed at the wall in a fixed position, while the receiving antenna was moved along the measuring trace on the opposite side of the wall from left to right with constant velocity. The next measurement was carried out with the sending antenna shifted of about 10 cm. The measurement was then completed in a similar way (shifting of transmitter after each trace) with a total of 15 sending positions.

The data were reconstructed by TOMOPOLI (Valle et al, 1998). The respective velocity distributions are shown in Figure 14. The velocities in the lower tomogram are lower than in the top tomogram which might be related to a higher moisture content in the bottom of the wall. In both tomograms, two areas with higher velocity can be recognised being perpendicular to the x-axis and parallel to the z-axis. The position of these areas can be correlated to the position of the crack as shown in Figure 9. In the area of the crack, there might be several voids which have a higher penetration velocity for electromagnetic waves.

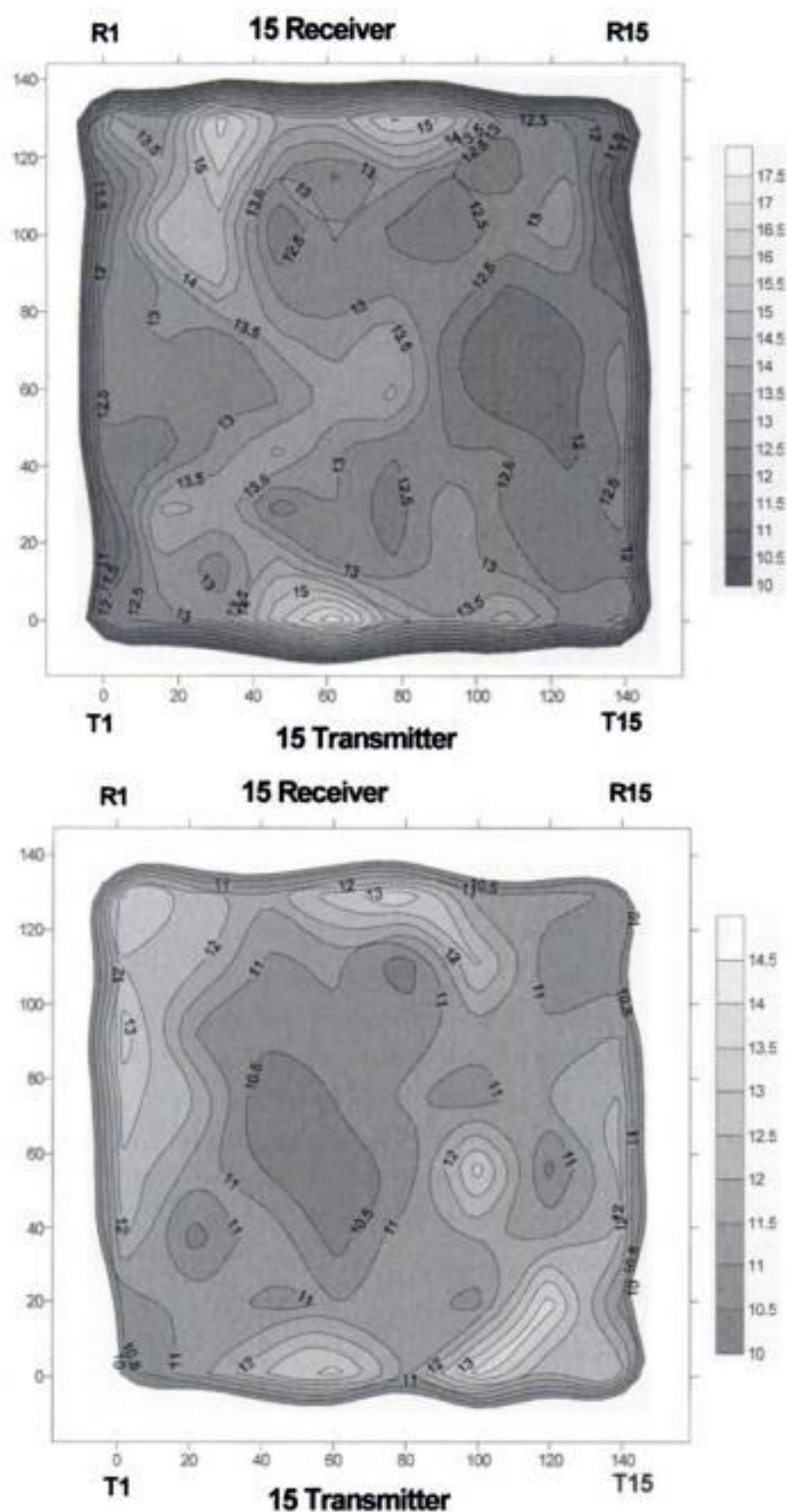


Figure 14. Reconstructed horizontal velocity distribution along the cross section of the basement wall. Top: Profile along the top trace (BAM1). Bottom: Profile along the bottom trace (BAM2). The values are in 10^{-1} m/ns.

4.3.5 Flat-jack

Polimi and *Geocisa* carried out several single flat-jack tests localised at 4 positions at the inner carrying wall and at the outside wall as shown in Figure 8.

The test procedure used by *Polimi* was performed according ASTM test (ASTM, 1999) (AMJ1S, AMJ2S, AMJ2D, AMJ3S) taking into account 4 measurement points and cutting in the mortar joint.

Geocisas single flat-jack tests (FJ01 to FJ04) follows an own developed procedure also based on ASTM, but modifying some testing conditions for a faster and friendly use equipment: at each position, three gage points are placed centred in the future slot as the flat-jack has smaller dimensions and the cut is



Figure 15. Flat-jack inside the slot.

performed in the stone assuring good contact conditions between the flat-jack and the masonry (stone). To guarantee a correct measure the surface of the wall is arranged and points are fixed with a rigid adhesive. The initial distance between gage points is the reference measure to achieve the test. The control of the gage displacement was done with a mechanical extensometer with an accuracy of 0.001 mm. The slot was made with a diamond circular saw (radius 115 mm), the cutting was guided to ensure a horizontal plane using a platform fixed to the wall (see Figure 15).

The flat-jacks used in both procedures have circular shapes. In the first case, the size was $350 \text{ mm} \times 250 \text{ mm} \times 4 \text{ mm}$, with a calibration factor of 0.88 and a geometrical factor of 0.93. In the second procedure, the length of this flat-jack is 211 mm, the depth is 70 mm and it is 3 mm thick. The calibration constant was determined at laboratory and the value obtained is 0.5. The geometrical factor is 1.0 because the prepared slot has the same shape as the flat-jack.

After cutting the slot the distance between gage points was measured, obtaining a closing movement. The flat-jack was introduced into the slot as shown in Figure 15, increasing gradually the internal pressure while the distance between gage points is controlled until the distance is restored to the reference measure.

The use of a flat-jack of smaller dimensions allows the testing of elements of smaller dimensions as columns.

Figure 16 shows the results of the single flat-jack test carried out by *Polimi*. The recovery of the slot displacements was reached in all the measuring points, almost at the same stress.

A double flat-jack test (AMJ2D) was carried out by *Polimi* at the inner carrying wall as shown on figure 8 according to ASTM (ASTM).

The results are summarised in Table 1.

The stress-strain diagram of the double flat-jack test AMJ2D (not shown here) demonstrates the good

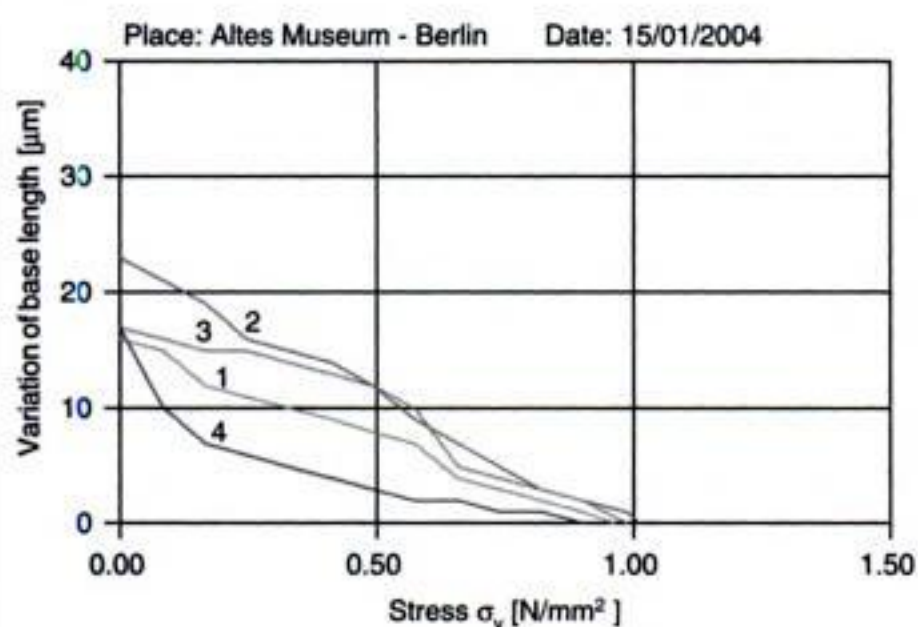


Figure 16. Results of the flat-jack tests carried out according ASTM (AMJ2S).

Table 1. Results of single and double flat-jack tests presenting the local state of stress and the Young modulus at the different positions.

Position	Single flat-jack AMJxS Local state of stress (N/mm ²)	Single flat-jack FJx Local state of stress (N/mm ²)	Double flat-jack AMJ2D Young modulus (N/mm ²)
1	1.13	1.50	–
2	0.96	1.00	33900
3	0.79	0.9	–
4	–	0.7	–

characteristics of the masonry in terms of compressive strength and elastic properties.

4.4 Stone ring reinforcement in the dome

The radar experiment was planned in a position of a corridor where the supposed stone ring should be quite close to the internal wall (Figure 3).

4.4.1 3D radar

For a more reliable interpretation of the radar images, the experiment was executed in 3D mode by collecting a number of dense parallel profiles on an area of about 80 cm × 80 cm. The data were processed with a 3D software obtaining a 3D data volume that confirms the existence of the stone ring (Figure 17). The two reflections observed at about 45 and 80 cm were respectively interpreted as the reflection from the stone ring and from the interface separating the first and the second stone layer of the structure. A hole was also drilled in the position where the stone ring should be closer to the corridor wall and a sandstone block was actually found behind a 50 cm brick wall.

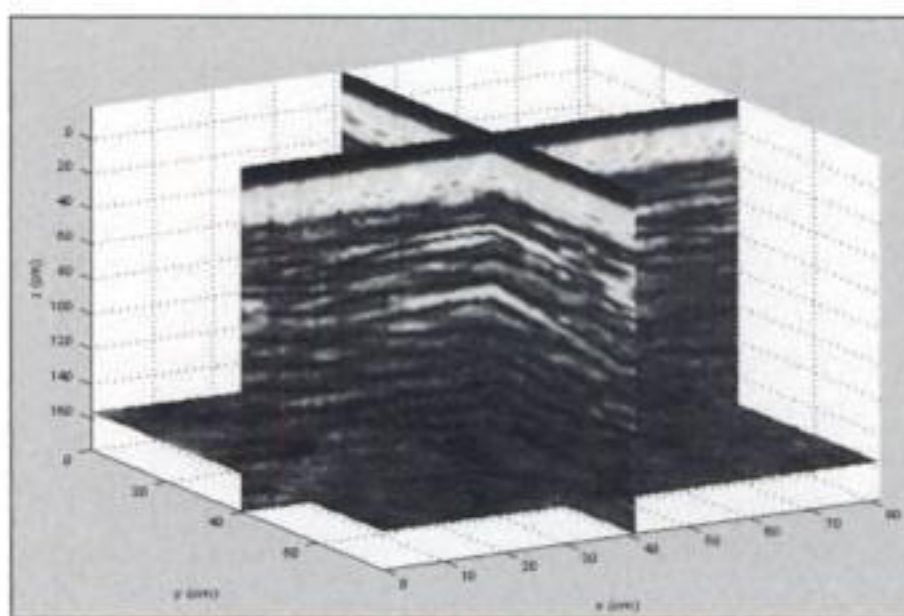


Figure 17. Cross-sections of the 3D radar data showing two main reflections at about 45 and 80 cm.

5 CONCLUSIONS AND OUTLOOK

5.1 Structure of columns in the entrance hall

With radar, the joints between the drums could be located very easily. The high intensity of these reflection could be related to possible plumb layers between the joints as non-seizing compound. Related to the connections between the single drums, metal compounds like pins could be most probably excluded. At the top of each column, a rectangular hole is expected which was used for mounting and alignment of the drums.

With radar reflection as well as with sonic tomography, the repaired areas could be located. But it was not possible to determine the depth of these structures. The uniform values of sonic velocities vary between 2330 and 2540 m/s. The lowest areas of velocity were located around a repaired area.

5.2 Plaster detachments at columns in the rotunda

With impulse-thermography, it was possible to detect delaminations which are most probably related to the stone/mortar interface. But this assumption was not proved with destructive tests. Also, it is planned to compare the experimental results with numerical simulations.

5.3 Properties of a carrying wall in the cellar

The main objectives of the multifaceted investigations of the carrying wall in the cellar were the analysis of the inner structure and the moisture content. As NDT and MDT methods radar, sonics, microseismics, geoelectric and single and double flat-jack have been combined.

Related to the internal structure, the sonic investigations resulted in acoustic velocities between 1600 and 2600 m/s with a mean value of 2150 m/s. With microseismics, velocities between 2400 and 2800 m/s were

obtained. These values are typical for fair good/good condition of masonry. But it should be regarded that these are mean values over the whole cross section, thus only an averaged parameter is given. At the bottom of the wall, the sonic as well as the microseismic investigations give higher velocities in comparison to the results at the top. This might be explained by a higher load and/or by a higher moisture content.

The radar tomograms appear homogeneous, some readings could be related to the crack at this area. The radargrams recorded in reflection configuration and not presented here showed a more or less inhomogeneous structure related to stones having different size and inhomogeneous joints.

The single flat-jack tests show mainly the same stress at all positions. The stress strain diagram of the double flat-jack investigation demonstrate good characteristics of masonry related to compressive strength and elastic properties. A load set of the museum by a simple engineering method gave significant differences to the stress results of the single flat-jack tests. The local determination of the elastic modulus by double flat-jack gave comparatively high values (33000 N/mm^2). An additional investigation by endoscopy has shown differences in the masonry conditions over the depth. Due to the high measured values of the elastic modulus in the outside part of the wall and the results of endoscopy it is to assume a concentrated load distribution over the wall section.

A simplified 3D linear elastic FE model of the west wing of the museum is under development. On the bases of the NDT tests carried out, it is possible to make some assumptions for a more reliable modeling of the structure. The model can be calibrated on the bases of the flat-jack tests results. It will be thus possible to simulate the behavior of the structure and simulate the presence of possible interventions.

Information about the moisture situation could be gained from geoelectric and radar measurements. The results of the geoelectric measurements give a higher conductivity at the bottom of the wall. This is consistent with the horizontal radar tomograms, which showed lower velocities in the lower part. Both readings can be correlated to a higher moisture content at the bottom of the wall. At the height of the lower radar tomogram, small cores (12 mm in diameter) were extracted and the moisture content was determined by weighting. At depth between 0 and 30 cm, a moisture content from 0 to 2 Vol% (moisture content relatively to the total volume) was determined. This increases up to 10 Vol% at depth deeper than 30 cm.

5.4 Structural investigation of the sandstone ring

With 3D radar, the sandstone ring was investigated in horizontal direction from the outside of the dome on an area of about $80 \text{ cm} \times 80 \text{ cm}$. It was possible to observe reflections at depth between 45 and 80 cm, which could

be related to the reflection from the stone ring and from an interface separating the first and second stone layer. Videoscopic investigations of a borehole in this area should the beginning of the sandstone at a depth of about 50 cm (behind a 50 cm thick brick wall).

ACKNOWLEDGEMENTS

This work was funded by the European Commission under the 5th Framework Program.

For the assistance in preparation of the measurement campaigns we thank Mrs. Röver (Technical University, Berlin) and Mrs. Rüger (German Federal Office for Architecture, Berlin).

REFERENCES

- Abbateo, S., Berra, M., Binda, L. (1996): Pulse velocity test to qualify existing masonry walls: usefulness of waveform analyses. Proc. 3rd Conference on non-destructive evaluation of civil structures and materials; Boulder, Colorado, September 1996; pp. 81–95.
- ASTM (1999): Standard test method for in situ compressive stress within solid unit masonry estimated using the flat-jack method. ASTM C 1196-95, Philadelphia, ASTM.
- ASTM, Standard test method for in situ measurement of masonry deformability properties using the flat-jack method. ASTM C 1197-92, Philadelphia.
- Berra, M., Binda, L., Anti, L., Faticcioni, A. (1992): Non destructive evaluation of the efficacy of masonry strengthening by grouting techniques. Proc. International workshop on effectiveness of injection techniques for retrofitting of stone and brick masonry walls in seismic areas; Polytechnic of Milan, March 1992; pp. 63–70.
- Binda, L., Tiraboschi, C. (1999): Flat-Jack Test as a Slightly Destructive Technique for the Diagnosis of Brick and Stone Masonry Structures. Int. Journal for Restoration of Buildings and Monuments, Int. Zeitschrift für Bauinstandsetzen und Baudenkmalpflege, Zurich, pp. 449–472.
- Binda, L., Cantini, L., Tiraboschi, C. (2004): Caratterizzazione e classificazione di murature storiche in zona sismica mediante prova con martinetti piatti. XI Cong. Naz. "L'Ingegneria Sismica in Italia", ANIDIS, Genova, 25–29 Gennaio 2004, CD-ROM, E4-07, ISBN 88-86281-89-7.
- Colla, C., Maierhofer, Ch. (2000): Investigation of historic masonry via radar reflection and tomography. Proc. on 8th Intern. Conf. on Ground Penetrating Radar, Gold Coast, Australia, CDROM.
- Cosentino, P., Luzio, D., Martorana, R., D'Onofrio, L., Marchisio, M., Ranieri, G. (1998): Tomographic Pseudo-Inversion of Pole-Pole and Pole-Dipole Resistivity Profiles. Atti SAGEEP, Chicago, 22–26 Marzo 1998.
- da Porto, F., Valluzzi, M.R., Modena, C. (2003): Use of sonic tomography for the diagnosis and the control of intervention in historic masonry buildings. International Symposium Non-Destructive Testing in Civil Engineering, NDT-CE 2003, Berlin, Germany, CDROM.
- Daniels, D. (1996): Surface-Penetrating Radar, The Institution of Electrical Engineers, London.

- Forde, M.C., Birjandi, K.F., Batchelor, A.J. (1985): Fault detection in stone masonry bridges by non-destructive testing. Proc. 2nd International Conference Structural Faults & Repair, Engineering Technics Press, Edinburgh, pp. 373–379.
- Gucci, N., Marchisio, M., D’Onofrio, L., Mazzeo, D. Sassu, M. (1997): Prove microsismiche in controllo di carico su pannelli di muratura. Atti VIII° Convegno ANIDIS, Taormina, 21–24 Settembre 1997.
- Maierhofer, Ch., Brink, A., Röllig, M., Wigggenhauser, H. (2002): Impulse thermography for locating voids and honeycombing in concrete structures supported by numerical simulations. In: Häupl, P. and J. Roloff (eds.); Proceedings of 11. Symposium of Building Physics, 26.-30. September 2002, Dresden, S. 242–252.
- Maierhofer, Ch., Leipold, S., Schraurich, D., Binda, L., Saisi, A. (1998): Determination of the moisture distribution in the outside walls of S. Maria Rossa using radar. Proc.: 7th Int. Conference on Ground Penetration Radar (GPR), Lawrence, USA, 27.-30. May 1998, Kansas, USA: Radar Systems and Remote Sensing Laboratory, Vol. 2, pp. 509–514.
- Maierhofer, Ch., Wöstmann, J. Schaurich, D., Krause, M. (2000): Radar investigations of historical structures. In: Proc. Non-Destructive Testing in Civil Engineering, Uomoto, T. (ed.), Elsevier, Tokyo, pp. 529–537.
- Maldague, X. (2001): Theory and practice of Infrared Technology for non-destructive testing, John Wiley and Sons, Inc.
- Maldague, X., Marinetti, S. (1996): Pulse Phase Thermography. J. Appl. Phys. Vol. 79, No. 5, pp. 2694–2698.
- Marchisio, M., D’Onofrio, L., De Falco, A., Baroncini, V., Morandi, D. (2002): Non-destructive testing on masonry structures: a series of different methodologies applied on the cathedral of Lucca. Proceedings of the 8th Meeting EEGS – ES, Aveiro, Sept. 9–12, 2002.
- Marchisio, M., D’Onofrio, L., Forlani, E., Cerri, S. (2000): The use of geophysical methods to study the masonry structures of monuments: an application for the restoration of the Cathedral of Nicosia (Sicily). Proceedings of the 6th Meeting EEGS – ES, Bochum, Sept. 3–7, 2000.
- Riva, G., Bettio, C., Modena, C. (1998): Valutazioni quantitative di caratteristiche meccaniche di muratura in pietra esistenti mediante prove non distruttive. Materiali e Struture, “L’ERMA” di Bretschneider Ed., n° 1.
- Riva, G., Bettio, C., Modena, C. (1997): The use of sonic wave technique for estimating the efficiency of masonry consolidation by injection. Proc. 11th International Brick/Block Masonry Conference, Shangai, China, October 1997, pp. 28–39.
- Valle, S., Zanzi, L., Binda, L., Saisi, A., Lenzi, G. (1998): Tomography for NDT applied to masonry structures: Sonic and/or EM methods. In “Arch bridges”, A. Sinopoli Editor, Balkema, Rotterdam, pp. 243–252.
- Vavilov, V., Marinetti, S., Grinzato, E. and Bison, P. G. (1998): Thermal tomography, characterization and pulse phase thermography of impact damage in CFRP, SPIE Vol. 3361, pp. 275–281.

Geo-electrical techniques as a non-destructive appliance for restoration purposes

R. Keersmaekers, F. Van Rickstal & D. Van Gemert

Department of Civil Engineering, Katholieke Universiteit Leuven, Belgium

ABSTRACT: The use of geo-electrical survey techniques for restoration purposes proved useful as a non-destructive tool for the diagnosis of a deteriorated masonry structure. A short overview of the development of the technique is given, starting with apparent resistivity maps and continuing with the relative difference maps. In the recent past new developments in geophysics were adapted and implemented for the conditions of masonry structures. The measurements are carried out to construct a pseudo-section, which is the graphical representation of the apparent resistivity values for a 2D-section of the wall. Inverse modelling enables to reproduce the resistivity distribution in the masonry structure that matches with the obtained data of apparent resistivity. Two on site measuring campaigns are presented in this paper. Finally, to parallel actual research areas are elucidated. The aim is to combine an automated measuring system with AC-current power supply creating realistic expectations for the on-line validation of mortar injections in the near future.

1 INTRODUCTION

1.1 Importance

Destructive research of materials has important disadvantages in the field of restoration. First of all, the authenticity of the material is not respected. Secondly, from a scientific point of view, the information obtained is very locally and therefore not representative for the overall situation of the construction.

Geo-electrical survey of masonry is a suitable non-destructive tool for the diagnosis of a deteriorated structure, for judging the need of restoration, for controlling the efficacy of injections. The limited dimensions of masonry structures, contrary to the situation at soil investigation and the high degree of heterogeneity complicate the interpretation of the measurements.

This paper first briefly formulates the research done in the past in a way that the incorporation of new ideas and the results from implemented experiments based in these ideas becomes clear and useful for restoration specialists.

1.2 Measurement principle: Ohm's law

Two current electrodes (C1 and C2 in Figs. 1 & 2) create an electrical field inside the assessed material. Two other probes (P1 and P2) measure the resulting potential. Ohm's law allows calculating the apparent resistivity value ρ_a .

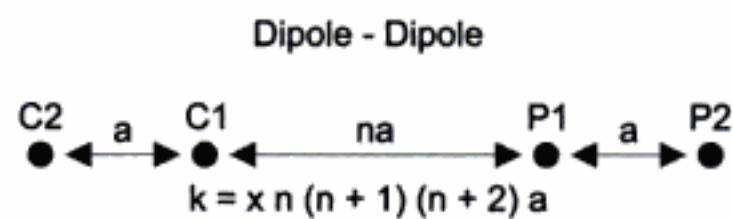


Figure 1. Dipole-dipole electrode configuration with k the geometrical factor.

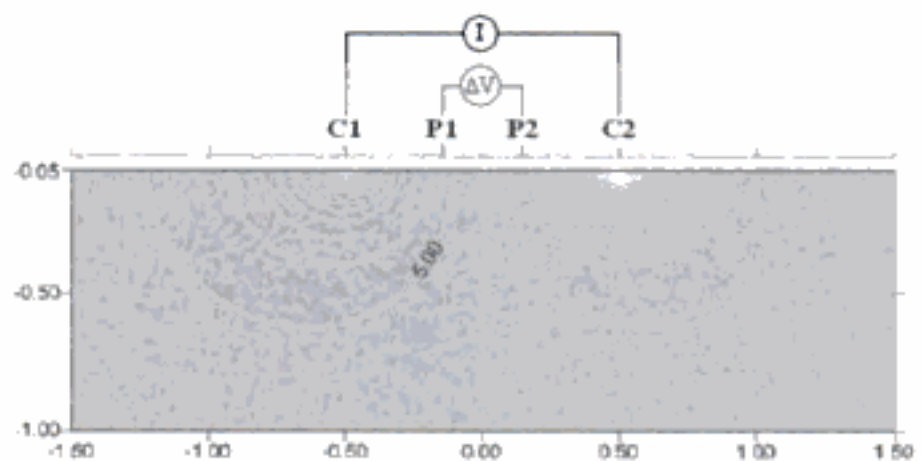


Figure 2. Resulting potential lines in a half infinite medium as the result of the injected current. Wenner-alpha electrode configuration.

The word “apparent resistivity” is used because this value is the resistivity value that would be measured in case of a perfectly homogeneous material. In reality this is not the case. The underground and the wall both have a heterogeneous resistivity distribution.

Various combinations of current and potential electrodes are applied. For each electrode configuration

a different value of the geometrical factor k gives the relation between the resistivity, the injected current and the measured potential difference between P1 and P2. Figure 1 shows the dipole-dipole configuration and its geometrical factor.

2 CURRENT STATE OF TECHNOLOGY

2.1 Relative difference map: filtering of unwanted influences

The history of the development of a specific geo-electrical technique for restoration purposes started with apparent resistivity maps, on which the diagnosis of a deteriorated masonry structure was made.

The problem hereby is that unwanted boundary conditions such as changing moisture content, the presence of soluble salts and geometric boundaries have a big influence on the measurements and are able to completely scatter the interesting information about the present anomalies. The interpretation of the internal state of the structure becomes ambiguous.

In the past two doctoral theses were finished at the Reyntjens laboratory dealing with the filtering of the measurements so that only the relevant anomalies in the masonry wall remain (Janssens 1993, Venderickx 2000). Figure 3 shows an example of a relative difference map which prevails the location of the anomalies in the wall.

The most disturbing factors are the geometric boundaries, changing moisture content and the presence of soluble salts in the masonry. To exclude the influence of the geometry, the resistivity values are numerically calculated in the presumption that all material is perfectly homogeneous. The relative difference map is then the visual representation of the difference between measured and calculated theoretical resistivity values, relative to the theoretical values.

Only the present anomalies are visualized now. The influence of the changing moisture content is filtered out in a similar way.

2.2 Pseudo-section

In the recent past new developments in geophysics within the field of geo-electrical survey of soils, were adapted and implemented for the conditions of masonry structures (Van Rickstal 2003, Keersmaekers 2003). The measurements are carried out to construct a pseudo-section, which is the graphical representation of the apparent resistivity values for a 2D-section of the masonry wall.

This technique was developed in geo-physics to get an image of the different layers of the underground. A number of electrodes are placed into the ground. Every electrode can be either a current or a potential electrode.

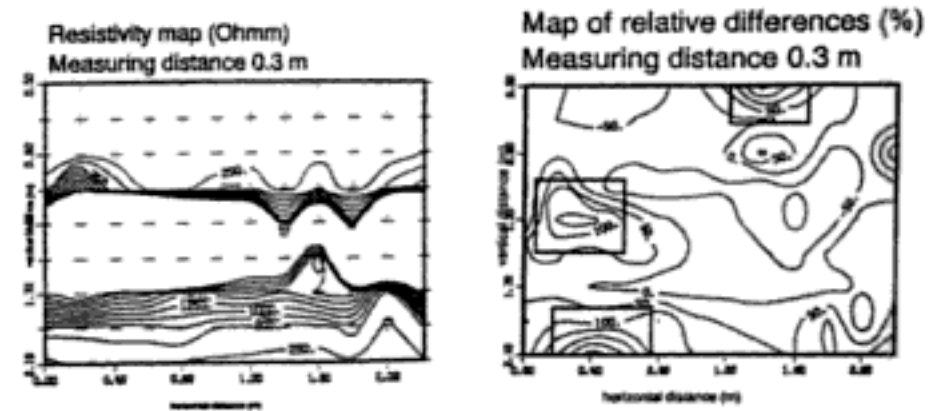


Figure 3. The present anomalies in the masonry of the wall around the park Arenberg (Leuven) are completely lost by the influence of the interface between two different kinds of masonry (left). The relevant anomalies clearly show up using the relative difference map (right) (Janssens 1993).

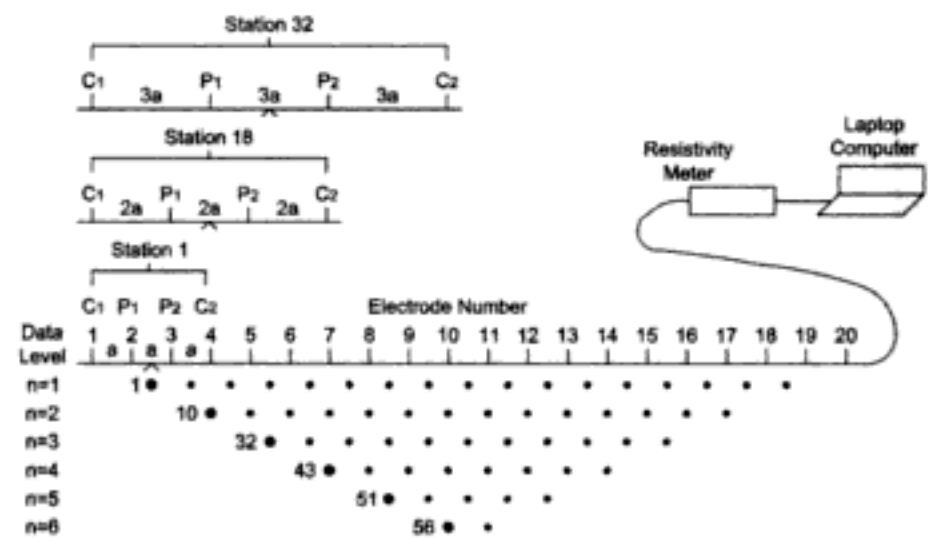


Figure 4. 2D electrical survey; electrode configuration (array) Wenner-alfa; necessary measurements to build up a pseudo-section of the underground.

The line of electrodes is called the survey line. The further apart the electrodes are positioned, the deeper the measured zone of the wall. The measured resistivity value is assigned to a fixed point that depends on the electrode configuration and the electrode spacing. First a series of measurements is made scanning the survey line using a small electrode spacing ($n = 1$ on Figure 4). Then the electrode spacing is doubled every time the survey line is scanned ($n = 2, 3, 4, \dots$), thus producing a pseudo-section (Fig. 4).

The general problem of this method is the direct interpretation of the 2D pseudo-section because this section is the result of apparent resistivity values. Therefore, it is not possible to draw conclusions about the real resistivity distribution of the underground (internal structure of the masonry) based on the measured pseudo-section.

The following example illustrates this. With the Res2Dmod programme (Geotomo software 2002) a model of a typical historic masonry wall is created (Fig. 5b).

The air behind the wall and the cavity in the wall are modeled as high resistivity material. The software is able to calculate the pseudo-section for any electrode configuration. In this example the dipole-dipole array is used (Fig. 1) with 30 electrodes,

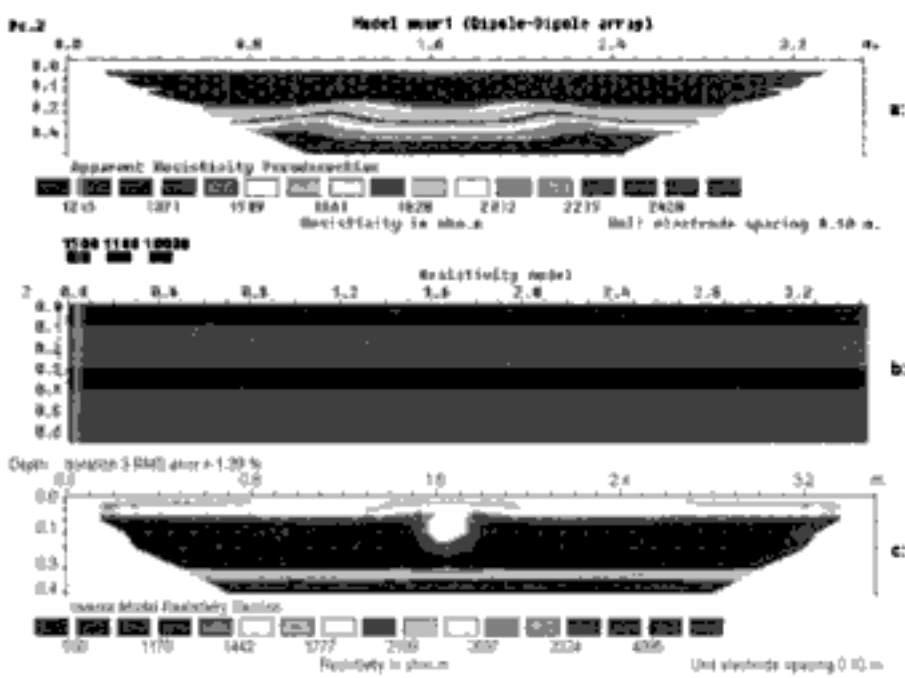


Figure 5. Model (a), inversion result, (b) calculated pseudo-section using dipole-dipole array, (c) of a 40 cm thick historic masonry wall build up using an inner and outer layer of natural stone filled with a rubble core.

10 cm electrode spacing. The calculation itself is called forward modeling and is based on a numerical scheme.

Figure 5a gives the calculated pseudo-section. The cavity in the wall is not visible. An interpretation based on Figure 5a concerning the internal structure of the wall fails to find the cavity in the model. To obtain a representation of the real resistivity distribution it is necessary to “invert” the pseudo-section, as shown hereafter.

2.3 Inverse modelling

Inverse modelling enables to reproduce the resistivity distribution in the masonry structures that originates in the obtained pseudo-section. The programme Res2Dinv is actually the most commonly used and most user friendly inversion software, based on finite techniques, for geophysical surveys (Geotomo software 2002).

The philosophy is to construct a model representing a certain distribution of the underground (wall) resistivity of which the calculated pseudo-section is the same as the measured pseudo-section. The underground is therefore divided in blocks or elements and each block is given a certain resistivity value.

A least-square fitting between the calculated and the measured pseudo-section determines how the model parameters (the resistivity values of the different blocks) have to change in the next iteration in order to improve the least-square fitting of the calculated and the measured pseudo-section (Loke 2002, Keersmaekers 2003).

Figure 5c gives the result of the inversion of the pseudo-section for the dipole-dipole array as calculated in Figure 5a. The cavity in the wall is clearly visible on the inversion. Also the boundary of the leaf at the side of the electrodes can be seen in the inversion

result. To improve the inversion result, the thickness of the wall was fixed at 40 cm. In the first iteration the elements that represent the air behind the wall was given a fixed resistivity value of 10 kΩm. This means that the software can not change the model parameters for these elements during iteration. Note that the layer of natural stone at the rear side of the wall is not clearly visible. This gives a first indication about the reduced resolution with increasing depth of investigation which indeed was verified during two on site measuring campaigns.

Theoretical analysis, using the simulation technique as described above, was carried out to examine different electrode configurations for their suitability to be implemented for the conditions of masonry structures (Keersmaekers 2003). The pole-pole, Wenner-Schlumberger, Wenner-alfa and dipole-dipole arrays were studied. Analogously to figure 5b different models of historic masonry were constructed using the Res2Dmod forward modelling software. The pseudo-section was then calculated for the different arrays. The number of electrodes and electrode spacing remained constant. The calculated pseudo-section was then imported in the Res2Dinv software to invert. This result was compared with the initial Res2Dmod model.

Figure 5c already showed that the dipole-dipole array was able to find the cavity in the wall. The Wenner-Schlumberger array gave also an inversion result pointing out the presence of the cavity, but less clear than the dipole-dipole. Inversion based on the pseudo-section produced with the Wenner-alfa array resulted in a rather poor increase of resistivity where the cavity was expected. The pole-pole array did not perform at all: the resolution of this array seemed very poor.

This theoretical analysis pointed out that the dipole-dipole array will probably deliver the best results when measurements are done in practice. The Wenner-Schlumberger array should also be considered. The Wenner-alfa and pole-pole arrays are most probably not suited for use on masonry structures. These conclusions were verified in two on site measuring campaigns.

Another important conclusion is that the obtained resolution depends on the electrode spacing. The closer the electrodes are placed, the higher the resolution of the survey. The number of electrodes (and the number of measurements) quickly rises when the electrode spacing is reduced. In practice a survey must compromise between number of measurements and wanted resolution.

2.4 Case studies

2.4.1 Diagnose of the internal structure of a wall

An old deteriorated limestone wall, part of the surrounding houses of the castle in Melsbroek (Belgium),

was the subject of a first series of surveys. The aim was the determination of the internal structure of the 40 cm thick wall. Three different arrays were examined: the Wenner-alfa, the Wenner-Schlumberger and the dipole-dipole array. All arrays used the same survey line consisting of 30 electrodes (steel nails in the joints) with 0,1 m spacing. The total length of the survey line is 2,9 m.

The model, constructed for simulation purposes in Figure 5b, is an abstract representation of this limestone wall. The same model was used to compare the surveys and to determine the most convenient measurement configuration.

During the survey, some interesting observations were made:

First, there is the problem of the "self-potential" of the wall. This means that when no current is injected in the wall, there is a small potential difference measured over the potential electrodes. Subtracting this potential from the potential measured with current injected eliminates its influence. The self-potential can also be excluded by changing the polarity of the injected current. The latter gave better inversion results.

The origin of this phenomenon can be electrostatic charging due to the wind. Also differences in salt and moisture content can cause small differences in electronegative values resulting in small galvanic cell leading to potential differences measured when no current is injected.

The best known origin for this "self-potential" is de polarisation of the electrodes (see Dahlin 2000 for a good overall description). This happens when an electrode recently used to inject current, is used to measure potential differences. The interface between the electrode and the wall is charged up when DC-current is injected. The discharge of the electrode can take a few minutes. The effect of this discharge can be taken into account by alternating the polarity of the current injected (Fig. 6).

What is measured are the potential differences $\Delta V_1, \Delta V_2, \Delta V_3 \dots$. What is necessary to calculate a proper value of the apparent resistivity are $\Delta V_1 - \text{s.p.}, \Delta V_2 - \text{s.p.}, \Delta V_3 - \text{s.p.}$. Mathematical reduction delivers a simple equation for the wanted

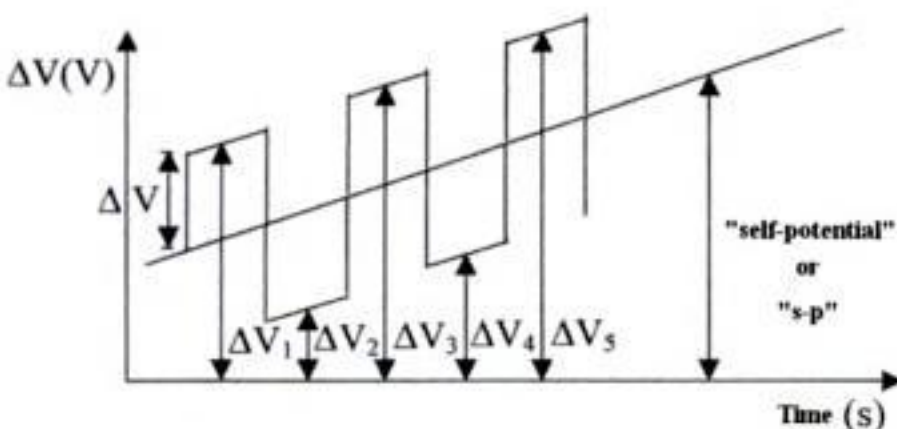


Figure 6. Superposition of potential difference and self-potential.

potential difference ΔV . The influence of the self-potential is filtered out (Venderickx 2000).

$$\Delta V = \frac{\Delta V_1 - 2 \cdot \Delta V_2 + \Delta V_3}{4} \quad (1)$$

Note that the above equation is only valid when the charge or discharge of the self-potential is linear.

Another problem is the limited current that can be injected. The reason is probably the capacitive action of the wall but this phenomenon has to be investigated more detailed. If the voltage over the current electrodes is increased, suddenly the wall reacts as a huge resistivity and the injected current drops to zero. This leads to unnaturally high apparent resistivity values that have a negative effect on the inversion result. Therefore, the current must be evaluated closely when increasing the voltage.

Figure 8a shows the measured pseudo-section. It is not possible to draw conclusions about the internal state of the structure based on this pseudo-section. Again, the importance of inversion is obvious. Figure 8b shows the inversion result when no fixed



Figure 7. Left: PC and electrical source, right: dipole-dipole parallel measurement with electrode spacing $a = 0,2 \text{ m}$ and $n = 1, 2, 3, 4$ and 5 .

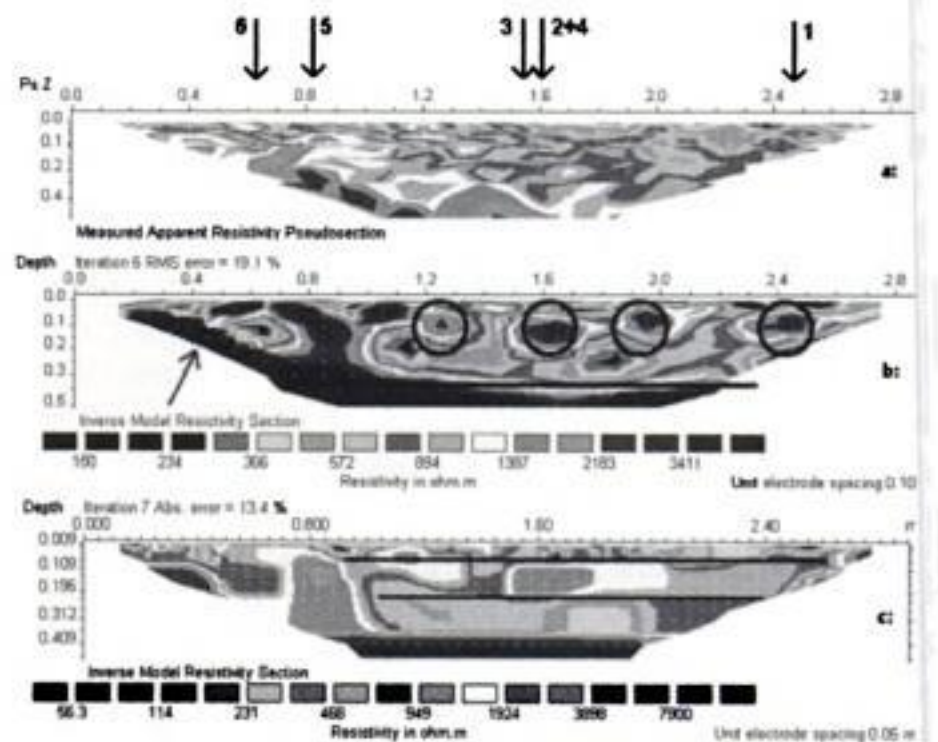


Figure 8. a: Measured pseudo-section and drilling hole positions for endoscopic investigation, b: inversion result dipole-dipole without fixed resistivity of air behind the wall, c: inversion result dipole-dipole with fixed resistivity of air behind the wall.

resistivity region is implemented before inversion. The black line shows that the dipole-dipole array is able to give a satisfactory idea of the thickness of the wall. In reality the wall is indeed 40 cm thick.

The black arrow on Figure 8b indicates that the found thickness of the wall decreases in the left zone of the measured region. In reality, the wall has a constant thickness of 40 cm.

The reason for this is shown in Figure 9. At the rear side of the wall a big hole beneath the survey line leads to an increased resistivity in the inversion result. Due to the fact that the current distribution in the structure is 3D, this geometrical boundary influences the result.

The high resistivity values of Figure 8b at x-positions 2,0 m and 2,4 m were not verified by endoscopic examination. At x-position 1,2 m and 1,6 m drill holes in the wall showed indeed the presence of cavities that explain the higher resistivity values in the inversion result (Fig. 9 left).

A better result of the inversion was obtained by fixing the resistivity of the area behind the wall (Figure 8c). The influence of the hole remains present in the inversion. Nevertheless, endoscopic examination confirmed the inversion result for drillings 1 to 4. Drilling hole 1 showed a good consolidated masonry.

Drillings 2 to 4 learned that this area is heavily deteriorated resulting in a series of cavities present in the centre of the wall (for example Figure 9 left).

The result of the Wenner-alfa and the Wenner-Schlumberger arrays were rather poor and will not be discussed here. This confirms the theoretical analysis (Keersmaekers 2003).

2.4.2 Handbogenhof Leuven: finding the buttresses at the rear side of a historical rampart

Another measuring campaign was made on the 12th century city wall "Handbogenhof" in Leuven. Figure 10 shows the front side and the rear side of this wall. Also the survey lines are indicated as the red and black lines on the pictures. The aim of the experiment was not to determine the inner state of the structure, but to find the buttresses at the rear side of the historical rampart.

Two survey lines were measured. The red measurement line is designed to find the two buttresses in the inversion result. This line has a length of 11,6 m

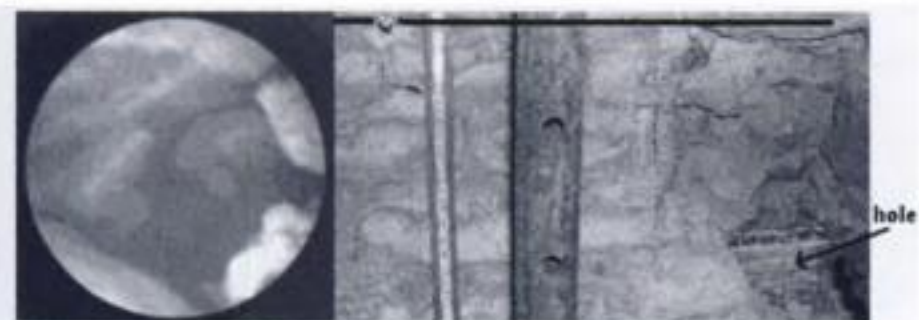


Figure 9. Left: endoscopy of drilling hole 4, right: the hole under the survey line influences the measurements.

using 30 electrodes with 40 cm spacing. The second survey line concentrates on one buttress in the middle of the line. This line has a length of 9,6 m using 25 electrodes with 40-cm spacing. In the latter case the number of measurements is reduced. Simulations as in chapter 3 indicated that the dipole-dipole array would give the best results. Based on the positive practical experience, this array was selected to carry out this experiment. Simulations indicated that an electrode spacing of 40 cm should be sufficient to detect the contours of the wall with a limited number of measurements (Keersmaekers 2003).

The influence of the self-potential is excluded by changing the polarity of the injected current. This gave better inversion results compared to subtraction of the zero potential. Again, the current was closely monitored to prevent current drop out (capacitive action of the wall) so that normal apparent resistivity values could be measured.

The pseudo-section (Fig. 11a) fails to show the buttresses at the rear side of the wall. Inversion is required. Comparing Figures 11b and 11c learns that the method proved capable to indicate the presence of both buttresses (yellow areas of lower resistivity), but their contours do not match perfectly with the real horizontal section of the wall (Fig. 11c).

Two drilling holes were endoscopically examined. As expected, the electrodes were too far apart (40 cm) to get relevant information about the inner state of the masonry. For aiming to find the contours of the wall,



Figure 10. Front side (left) and rear side (right) of the city rampart Handbogenhof.

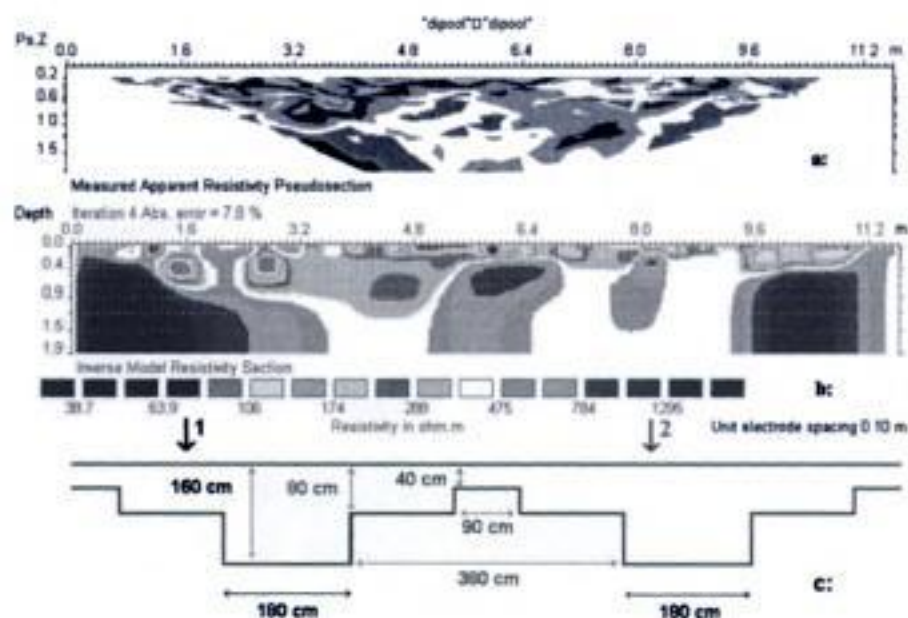


Figure 11. a: Measured pseudo-section, b: inversion result; both buttresses are found, c: on scale section of the real wall.

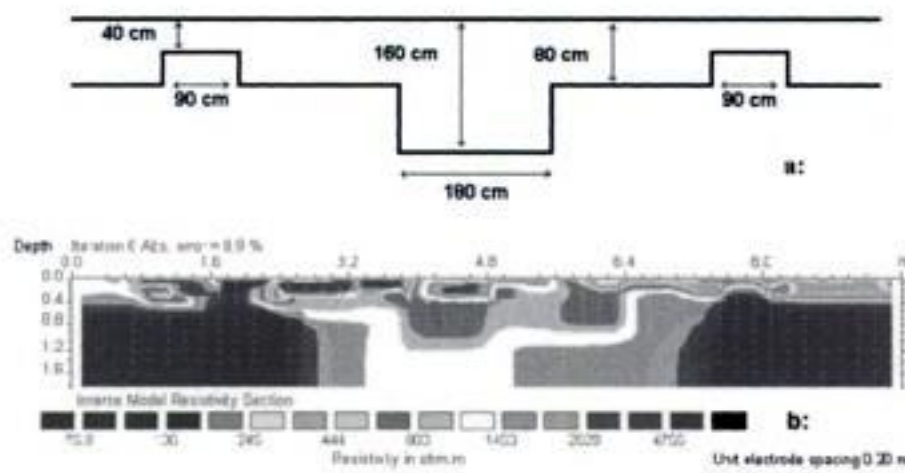


Figure 12. a: On scale section of the real wall, b: inversion result; the buttress and two shooting niches.

the survey proved sufficient, but the poor resolution failed to provide information on the deterioration of the wall. The niche (Fig 11c in the centre) is not recognised for the same reason. These niches are old shooting holes.

A second series of data points were located with one buttress in the middle of the survey line. The inversion result clearly proves the presence of the buttress as the yellow area in Figure 12b. Both niches on both sides of the buttress can now be recognised. The thickness of the wall however, is underestimated (50 to 60 cm instead of the expected 80 cm). The problem of the self-potential was well resolved by alternating the current, but this method has the drawback that it nearly doubles the measuring time.

2.5 Evaluation

The new developments in geophysics were successfully implemented in geo-electrical survey of masonry. A new step forward is taken towards the refinement of the geo-electrical method. The benefit of inverse modelling is illustrated.

The inversion enables to reproduce the resistivity distribution in the masonry structures that originates in the obtained pseudo-section. Inverse modelling apparently allows visualising the inner condition of the structure more accurately than previously possible.

The analysis of the data, obtained during two on site measuring campaigns, clearly shows that the interpretation of the inverse model is much easier than the interpretation of the apparent resistivity maps (the measured pseudo-section). The results of these experiments were verified by endoscopic examination of the measured structure.

Theoretical and practical experience is gained with the inversion technique. The dipole-dipole array leads to the best theoretical and practical results. The method also proved to be capable of finding the buttresses at the rear side of a historical rampart.

Great potential is expected for the method, but further research is necessary to improve the performance. The average survey time can be reduced using an

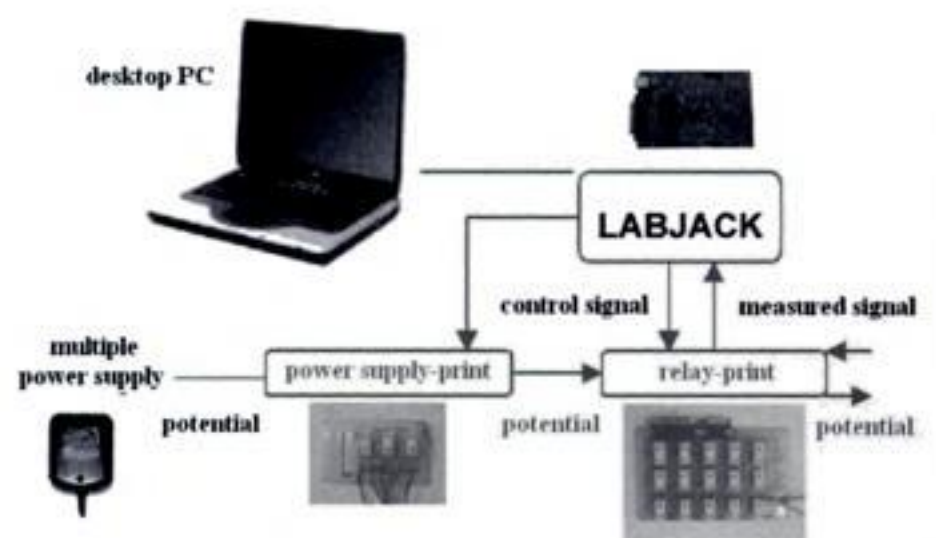


Figure 13. Schematic representation of the different parts of the automated measurement system.

automatic source that sequentially powers the electrodes and measures the potentials. Also the measurement itself should stabilize more quickly to allow faster survey times.

3 ACTUAL RESEARCH

3.1 Automated measurement system

The biggest limitation of this new measuring technique is that the number of measurements quickly rises when great resolution is needed. Currently, an automated measuring device is being developed and tested. With this measuring equipment, surveys can be carried out more quickly and with limited manual intervention.

Figure 13 shows the schematic representation of the different parts of the automated measurement system (Neuhard & Waes 2004).

Automated measuring systems are already commercially available for use in geological applications. The disadvantages of purchasing a commercial system are the high cost, but more importantly, the insufficient flexibility for research purposes. It is, for example, without mayor adaptations, not possible to use AC-current source signals. All the systems available on the market work stand alone, using DC-batteries. The reason is that geophysicists perform surveys everywhere, regardless the presents of a plug-socket.

Research is being done on the use of AC-current source signals, as will be elucidated further, and it is profitable to build an automated system which can work both with DC-and AC-current. For this reasons the initiative was taken to build a customized automatic measuring system.

The modularity of the system permits to extend it to control as much electrodes as needed. Software is developed that generates the control program automatically, using only the number of electrodes needed and the type of electrode configuration. The system is now in a test phase, the basic modules are tested on a limited number of electrodes. It will soon be possible to perform some case studies with the equipment.

with the obtained data of apparent resistivity (pseudo-section). Inverse modelling apparently allows visualising the inner condition of the structure more accurately than previously possible. The analysis of the data, obtained during two on site measuring campaigns, clearly shows that the interpretation of the inverse model is many times easier than the interpretation of the apparent resistivity maps (the measured pseudo-section). The results of these experiments were verified by endoscopic survey of the measured structure.

The biggest limitation of this new measuring technique is that the number of measurements quickly rises when great resolution is needed. Currently, an automated measuring device is being developed and tested. With this measuring equipment surveys can be carried out more quickly and with limited manual intervention.

Another problem using the conventional DC-current as power supply is the polarisation effect of the electrodes and the capacitive effect of the masonry structure itself, both contributing to the inaccuracy of the measurement. To obtain good data it is necessary to wait until both effects stabilize. This can take a few minutes and extends the survey time considerably. Fundamental research examining AC-current as power supply shows that a measurement immediately stabilizes in stead of drifting for a few minutes. The polarisation effect of the electrodes and the capacitive effect of the masonry structure can be diminished using AC-current signals.

Combining the automated measuring system with AC-current power supply creates realistic expectations for the on-line validation of mortar injections in the near future.

REFERENCES

- Cole, K.S. & Cole, R.H. 1941. Dispersion and absorption in dielectrics. I. alternating current field. *Journal of Chemical Physics* 1, p 341–351, 1941.
- Dahlin, T. 2000. Short note on electrode charge-up effects in DC resistivity data acquisition using multi-electrode arrays. *Geophysical Prospecting*, 48, p 181±187.
- Geotomo software, 2002. Guide of the software Res2Dmod and Res2Dinv version 3.5. Download from <http://www.geoelectrical.com/>
- Janssens, H. 1993. Geo-elektrische controle van consolidatie-injecties bij metselwerk, Ph.D. Thesis, KULeuven, Department of Civil Engineering.
- Keersmaekers, R. 2003. De geo-elektrische methode toegepast op metselwerk-structuren: implementatie van recente ontwikkelingen. Masterthesis, KULeuven, Department of Civil Engineering.
- Loke, M.H. 2002 Tutorial: 2D and 3D electrical imaging surveys. Download from <http://www.geoelectrical.com/>
- Neuhard, J. & Waes, T. 2004. Geo-Electrical Measuring Module. Masterthesis, ACE-GROEPT Polytechnic academy, Department of automatisisation.
- Oldenburg, D.W. & Li, Y. 1994. Inversion of induced polarization data. *Geophysics*, 59, 1994, p 1327–1341.
- Oldenburg, D.W. & Yuval. 1997. Computation of Cole-Cole parameters from IP data. *Geophysics*, 62, 1997, p 436–448.
- Pelton, W.H. et al. 1978. Mineral discrimination and removal of inductive coupling from multifrequency IP. *Geophysics* Vol 43, 1978, p 588–609.
- Van Rickstal, F.; Keersmaekers, R. & Van Gemert, D. 2003. Geo-electrical investigation of masonry walls: developments and case studies. Department of Civil Engineering, KULeuven, Belgium. Paper presented at the 6th meeting of the Materials Science and Restoration Society – Sept. 2003, Karlsruhe, Germany.
- Van Rickstal, F. & Vanhellefont, Y. 2002. Niet-destructief opzoeken van scheuren in metselwerk en pleisters. Technieken en case studies. WTA, NL/VL, Seminar, Sint-Truiden, ed. D. Van Gemert, KULeuven.
- Venderickx, K. 2000. Evaluatie van geo-elektrische metingen op metselwerkstructuren. Ph.D. Thesis, KULeuven, Department of Civil Engineering.
- Verboomen, J. 2004. gedetailleerde studie van de Tesla-transformator: Optimalisatie en Toepassingen. Masterthesis, KULeuven, Department of Electrical Engineering.
- Welter, A.; Seichter, M. & Kampe, A. 1996. Induced-Polarization modelling using complex electrical conductivities. *Geophysical Journal International*, 127, p 387–398.

The use of radar techniques and endoscopy in investigating old masonry: the case of Dafni Monastery

E. Vintzileou

Laboratory of Reinforced Concrete, National Technical University of Athens

A. Miltiadou-Fézans

Directorate of Technical Research for Restoration, Hellenic Ministry of Culture

V. Palieraki

Laboratory of Reinforced Concrete, National Technical University of Athens

N. Delinikolas

1st Ephoreia of Byzantine Antiquities, Hellenic Ministry of Culture

ABSTRACT: This paper summarizes the results obtained from the application of two investigation techniques, namely radar and endoscopy, in the masonry of the Katholikon of Dafni Monastery (Attica). The two techniques were applied with the aim to investigate the type of construction of the perimeter masonry of the monument. The application of the two techniques proved to be very efficient, since their results offered reliable information regarding the thickness of stones, hence, the thickness of the internal filling material in the three-leaf stone masonry of the monument.

1 INTRODUCTION

Dafni Monastery, situated at approximately 10 km from Athens on the way to Eleusis, is one of the major Byzantine monuments in Greece (Millet, 1899, Bouras, 1998, Delinikolas et al., 2003). The Katholikon of the Monastery (Figure 1) has suffered serious damages during the September 1999 earthquake that affected the region of Attica.

Within the framework of a strategic plan¹ undertaken by the Ministry of Culture for the conservation of the monument (its mosaics included), a series of research programs were carried out with the aim to acquire information that is necessary for the assessment of the monument and, subsequently, for the stage of interventions. A part of the research programs was dealing with the evaluation of the mechanical characteristics of masonry.

The investigation of the construction type of masonry constitutes an important step towards the



Figure 1. The Katholikon of the Dafni Monastery.

evaluation of the mechanical properties of masonry. Given the architectural value of the monument, and the resulting constraints regarding the techniques that can be applied, and taking into account the limitations of each investigation technique, the decision was made to apply a combination of two techniques, namely radar and endoscopy, in order to reach enhanced reliability of the data. In fact, radar technique (a non destructive one) was the main one to apply to the

¹ A Scientific Committee was set by the Ministry of Culture, to follow the progress of the investigations, studies and works. Members of this Committee are Professors Ch. Bouras, T.P.Tassios, H.Mariolakos and N.Zias.

monument. Endoscopy was applied in places where the information obtained by the radar technique was considered of low reliability. It should be noted, however, that endoscopy, thanks to the direct visual contact of the observer with the interior of masonry, offered additional valuable information regarding the type of construction materials, and the presence of internal discontinuities in masonry.

For both techniques, the equipment available at the Laboratory of Reinforced Concrete/National Technical University of Athens was used.

2 A SHORT DESCRIPTION OF THE APPLIED TECHNIQUES

2.1 Radar technique

Using a radar system, consisting of a central unit and various antennas, electromagnetic signals are emitted through the material under investigation. The antenna is moved along a straight line on the surface of the considered material or element. When the signal meets an interface (be it a void or a discontinuity within the material or a different material), part of the emitted radiation is reflected and recorded by the central unit and part of it travels deeper into the material. Thus, by appropriately processing the recorded reflected pulse, one may have a picture, more or less clear of the in-depth geometry of the investigated element.

Radar technique was first applied in the field of geophysical investigation. Its application especially in masonry structures is still rather limited, although this non-destructive technique seems to be adequate for structures of high architectural values. It has to be admitted that the numerous interfaces that the electromagnetic pulse can meet when traveling through masonry are of unknown nature, they may cause multiple reflections of the pulse, thus giving a rather unclear picture of the internal state of masonry.

2.2 Endoscopy

This technique, borrowed from medical applications is a slightly destructive method. Holes (approximately 25 mm in diameter) are drilled in masonry. After meticulous cleaning of the hole from dust and loose material, the endoscope is introduced into the hole. The core of the endoscope, consisting of optical fibres, allows for direct observation of the walls of the hole. In addition, pictures can be taken at any depth of the hole.

It should be mentioned that, since the diameter of the drilled holes is rather small, the application of this technique is acceptable even in case of structures of high architectural value.

3 APPLICATION OF TECHNIQUES – PROBLEMS ENCOUNTERED

(a) It is well known (Daniels, 1996) that, when using the radar technique, the accuracy of the picture depends on the frequency of the emitted signal: Low frequency signals allow for more in-depth investigation giving, however, less clear results; on the contrary, higher frequency signals result to rather limited penetrability. Nevertheless, in this case, the obtained picture is clear for the limited depth that is investigated. Given the scope of this application, a rather high frequency antenna was selected (1500 MHz). In fact, available historical data regarding previous interventions on the monument (Delinikolas et al., 2003), as well as cores taken in selected locations prove that the (approximately 0,80 m thick) masonry of the Katholikon is a three-leaf masonry. Thus, the scope of the investigation was (i) to obtain data regarding the thickness of stones in both the internal and the external leaves and (ii) to check whether there are stones connecting the two leaves of masonry. On the other hand, the radar technique was not expected to give reliable information regarding the intermediate leaf, given its nature (it consists of rubble material-pieces of stones and bricks loosely cast in mortar) and the numerous interfaces between various materials. It has to be mentioned that the applicability of the radar technique in Dafni Monastery was investigated, during a preliminary stage, by the specialized staff of LCPC-France (Côte et al., 2002). This investigation gave very promising results.

(b) Although the aim of the research was to investigate the type of masonry construction along all perimeter walls of the monument, the investigation was finally limited to parts of the south and west walls. For example, the application of the technique in the eastern wall of the church was not feasible, due to the complex geometry of the wall (Figure 2, the section is polygonal from outside and curved from inside),

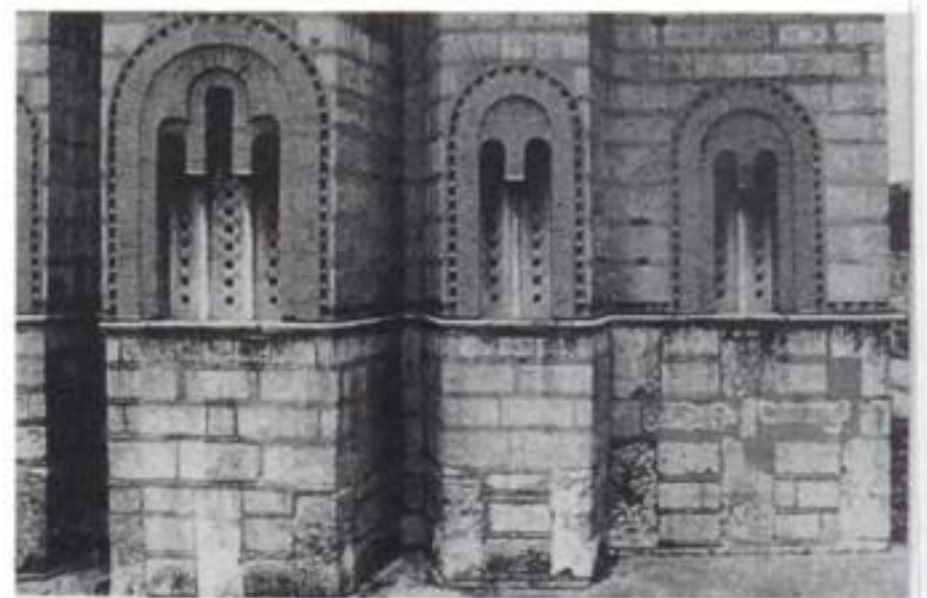


Figure 2. The eastern wall of Katholikon.

dotted lines in the upper part of the picture (one of them is marked with a circle on Figure 4) show the location of mortar joints among consecutive stones. The location of joints is manually introduced to the respective file by the observer during scanning of the path and they allow for easier interpretation of the results. This is the reason why it is preferable to apply the technique on uncovered masonry (without plaster). The continuous dark gray line (indicated on Figure 4 by the white arrow) constitutes the reflection of the surface of masonry. Raw data, as presented in Figure 4, are not liable to interpretation. Thus, using the possibilities offered by the software accompanying the equipment, the file containing the raw data is subject to various modifications (such as overall gain, migration, etc.). In this way, a new file is created (Figure 5a). The vertical axis is now in meters (in depth of masonry). One can distinguish on the graph, at a depth of approximately equal to 0,25 m, a zone of disturbance. This zone corresponds to the end face of the series of stones scanned along path G. The findings are then presented in a drawing (Figure 5b) showing (in scale) the length and the thickness of the stones.

It should be reminded here that a relatively high frequency antenna was used with the aim to obtain as accurate as possible results regarding the thickness of stones. In fact, as shown in Figure 5, the data corresponding to the part of masonry deeper than the first leaf of stones cannot be evaluated.

On the same Figure 5, a white ellipse shows a hyperbola, which was assumed to indicate the location of a metallic material in the internal leaf of the wall. In order to check whether this assumption was correct, that region was investigated also by endoscopy, as described in the following section.

5 RESULTS OBTAINED BY ENDOSCOPY

As mentioned in the Introduction, endoscopy was applied mainly in order to check the validity of radar measurements in some locations, in which the obtained picture was not clear enough. The results of observation using the endoscope are presented as shown in Figures 3, 6–8: The location of the drilled hole is first indicated on the respective drawing (e.g. E21 on Figure 3). A detail of the region in which the hole (25 mm in diameter) is drilled is shown in Figure 6a, together with a sketch based on the visual inspection by the observer (Figure 6b). The presentation is completed with the pictures taken by the observer (Figure 7).

As shown in Figures 6b and 7, endoscopy has confirmed the findings of radar measurements in the same location (compare with Figure 5). In fact, the thickness of stones was measured and it was found practically equal to that determined by the radar measurements.

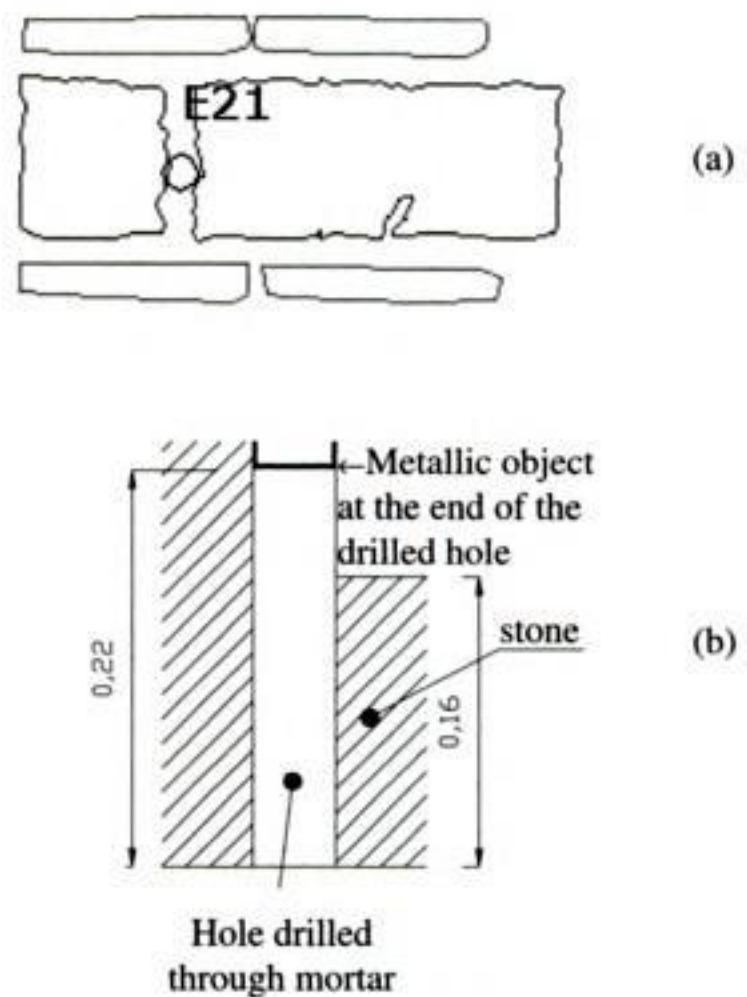


Figure 6. (a) Detail of the region of E21, (b) Sketch of the results of observation.

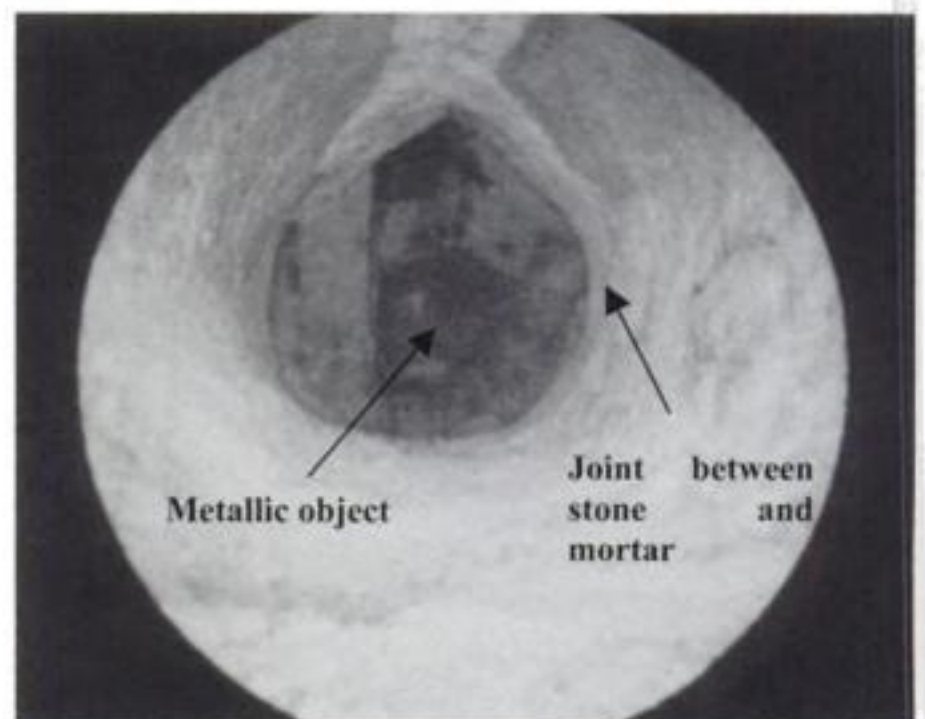


Figure 7. Picture taken inside the hole of E21. The limit of the right stone is shown (compare with Figure 6b), as well as the metallic object in the far front of the hole.

In addition, a metallic object² (detected also by the radar) was found, as shown in Figure 7.

It should be noted that the observation through endoscope offers, thanks to the direct visual contact of the observer with the inside of masonry, the possibility of detecting discontinuities and holes (Figures 8

² During the extensive interventions carried out in 1895, the original materials were used for reconstruction. Cracked stones were also used. In such cases, iron [-shaped connectors (like the one detected by endoscope) were used to bridge the crack.

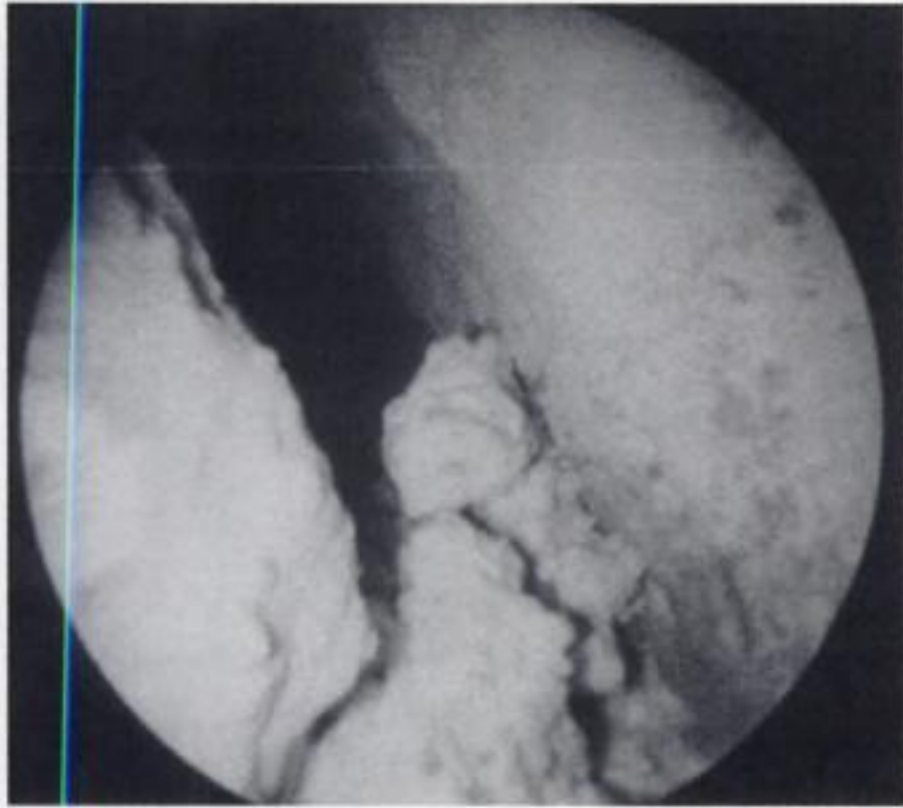


Figure 8. Picture from E6: One may observe two stones, as well as the mortar between them. It is obvious that the joint between the two stones is only partially filled.

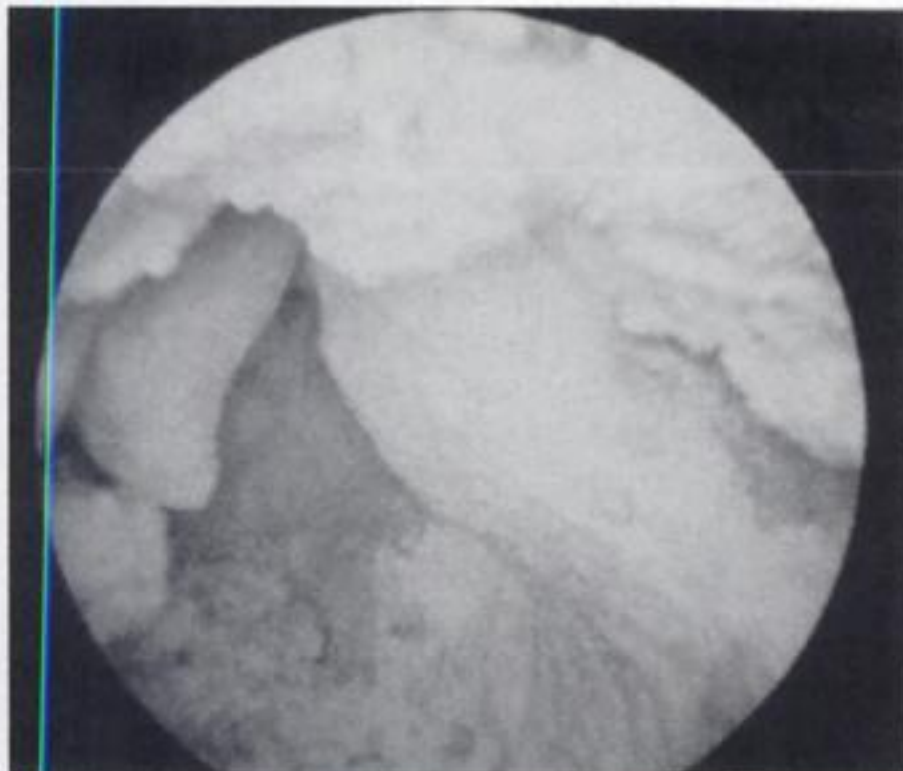


Figure 9. Picture from E6. The nature of the material filling the space between the two leaves of masonry can be seen: It consists of mortar and pieces of stone. Holes in the filling material are apparent.

and 9), as well as to obtain qualitative information about the state of materials (Figure 10).

This kind of information is valuable during the decision making stage for interventions. In fact, it may allow for a rough estimation of the percentage of voids within masonry, which in turn affects the proportioning of grouts to be injected, as well as the anticipated strength enhancement of masonry. It may also affect the procedure of injecting grouts. In fact, special measures have to be taken to avoid damages to mosaics when large internal holes are present at their vicinity.

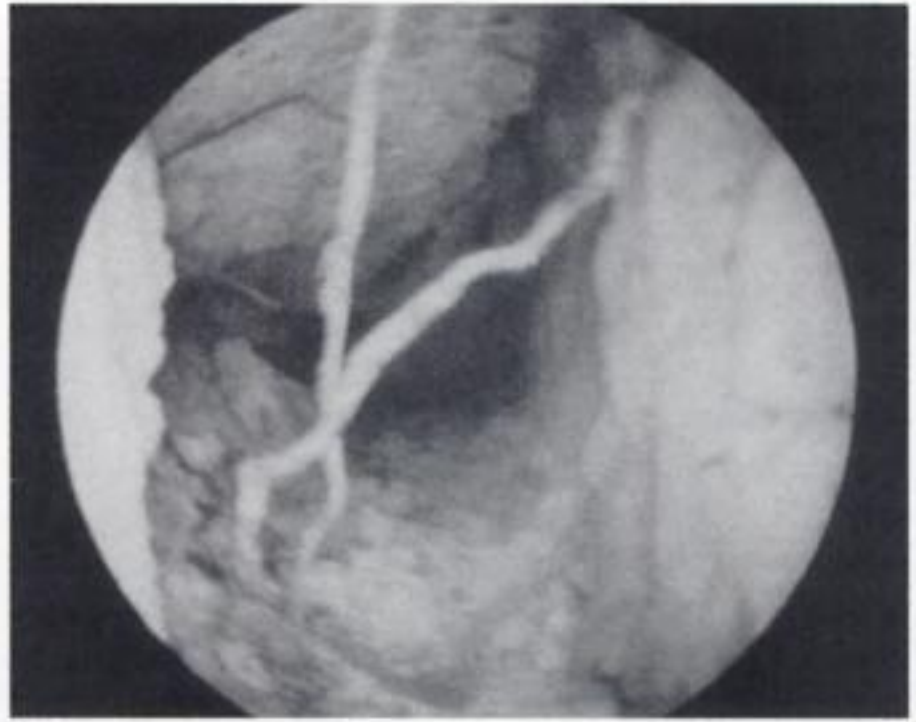


Figure 10. Picture from E19. The mortar between stones is disintegrated. Roots of a plant can also be seen.

It has to be mentioned, however, that this last aspect has not yet been thoroughly investigated.

6 COMPARISON OF RESULTS OBTAINED BY RADAR AND ENDOSCOPY

Figure 11 shows some plots of horizontal sections of masonry, as obtained by radar. In each plot, the part of the path for which results by endoscopy as well are available, is magnified and presented on top of the complete path. It may be observed that in several cases, the measurements of the two methods correlate remarkably well (as in the two first paths). In other cases, however, it seems that the thickness of stones was not accurately determined on the basis of radar measurements.

In general, the results of endoscopy are considered to be more accurate, since they are based on visual inspection. Thus, the pictures taken by radar measurements are where needed corrected accordingly. Nevertheless, in some cases, inspection through endoscope was proved to be inconclusive: Holes for inspection through endoscope were drilled mostly through mortar joints, to allow for the thickness of adjacent stones to be determined. However, the fact that either the mortar joint is excessively thick or the back face of the stones is not perfectly cut (Figure 12), does not always allow for the end face of stones to be clearly detected.

In such cases, the results of both techniques were re-evaluated and the most reliable ones were selected as final. It should be noted, however, that even in cases of disagreement between the two methods, the basic geometry of masonry in its depth is not substantially affected (see Figure 11). In fact, the purpose of this investigation is served by the applied techniques in a satisfactory way.

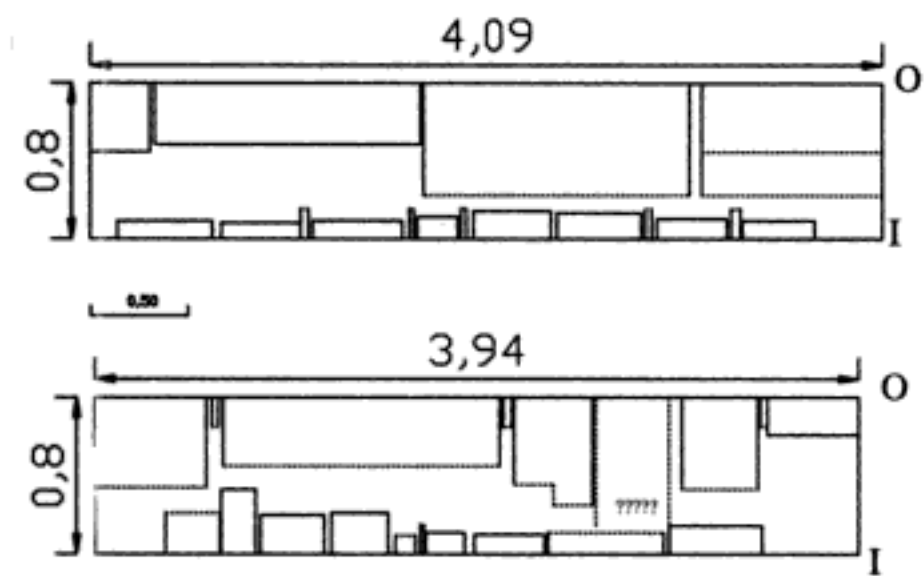


Figure 14. Horizontal section of masonry in the lower zone.

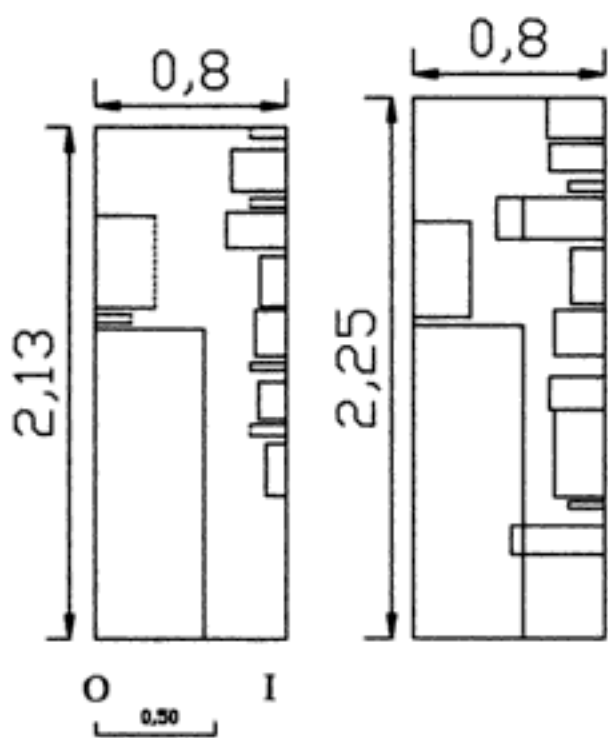


Figure 15. Vertical sections of masonry in the lower zone.

considered to be continuous, since there are no transverse stones connecting the external leaves between them.

This picture was confirmed by measurements in the vertical direction (Figure 15). On the basis of the available measurements, one may conclude that the lower zone consists in an outer strong leaf, of average thickness equal to 0,39 m, an inner weak leaf, approximately 0,17 m thick and an intermediate leaf of filling material 0,24 m thick approximately.

Figure 16 shows three horizontal sections representing the type of construction of the part of walls from the lower row of windows up to the arches and domes (Figure 13). In Figure 17, vertical sections of masonry in the same zone are presented. One may observe that (a) there is still a difference of thickness between the outer and the inner leaf of masonry. Nevertheless, this difference is less pronounced than for the lower zone of masonry. In fact, the average thickness of the outer leaf is approximately equal to 0,28 m, whereas the average thickness of the inner one is of 0,20 m approx.), (b) due to the smaller thickness of stones of the external leaf,

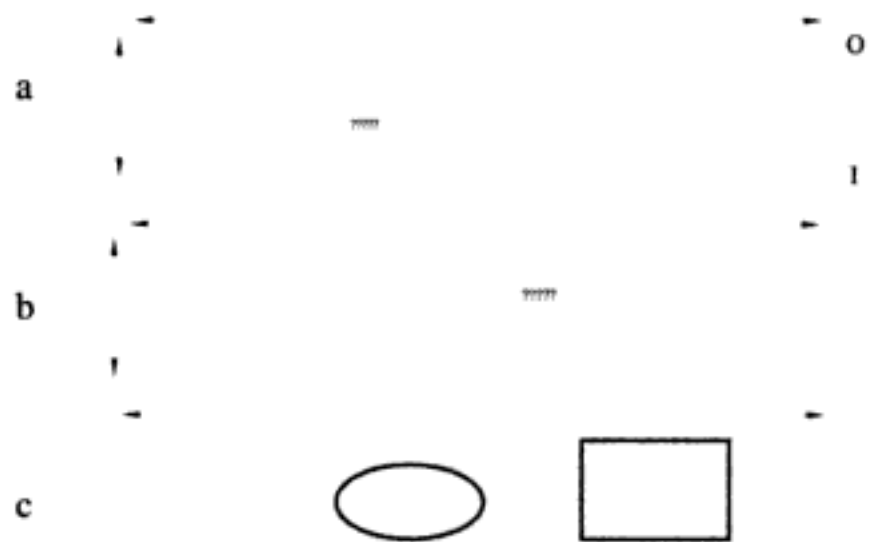


Figure 16. Horizontal sections of masonry in the upper zone.

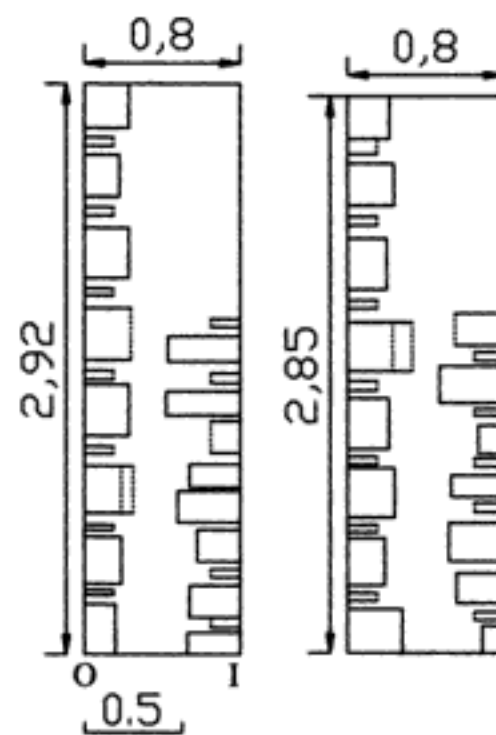


Figure 17. Vertical sections of masonry in the upper zone.

the average thickness of the filling material is larger than in the lower part of masonry (approximately equal to 0,32 m), (c) in some cases (see Figure 16c), in the inner leaf, there are stones placed with their length along the thickness of the wall, thus reducing locally the thickness of the filling material.

A general remark valid for either zone of masonry is that the construction type is much more complex than that of a masonry consisting of three leaves of practically constant thickness both horizontally and vertically. In fact, in masonry of the Dafni Monastery, the use of stones varying in thickness, both in-length and in-height of masonry leads to increased interface between external leaves and filling material. Thus, a positive effect of the geometry on the mechanical properties of masonry could be expected.

The information gathered thanks to the investigation presented in this paper will serve the purpose of determining the mechanical characteristics of masonry. As mentioned in the Introduction, part of the strategic plan of preservation of the monument is

devoted to the estimation of the mechanical properties of masonry. At a first stage, an attempt was made to estimate some basic mechanical properties, such as the compressive strength of masonry. To this purpose, samples of stones were tested in Laboratory and their compressive strength, tensile strength, Young's modulus of elasticity and Poisson's ratio were determined. In addition, the fragments test (Tassios et al., 1989) was applied to pieces of mortar taken out of various zones of masonry. Thus, the tensile strength of mortar was determined. On the basis of the available literature, this tensile strength was translated into compressive strength of mortar. Subsequently, in order to estimate the compressive strength of masonry, several empirical formulae were applied. Those formulae, which express the compressive strength of masonry as a function of the compressive strength of constitutive materials, resulted to unacceptably scattered values for the compressive strength of masonry. It is obvious that the adoption of the lower value, that might constitute a sensibly conservative assumption in case of a building of rather low architectural value, is definitely unacceptable in case of a monument like the Katholikon of the Dafni Monastery. In fact, such a conservative assumption would lead to extensive interventions that might not be needed and that would inevitably alter the architectural value of the monument. Thus, the decision was taken to construct wallettes following the construction type determined on the basis of radar and endoscopy investigations and to test them in compression or in shear, in order to reach reliable data regarding the characteristics of masonry. In addition, since the Central Archaeological Council has already approved the proposal for injecting grouts to the monument, the wallettes-after testing-will be injected and then retested, in order to measure their improved mechanical properties. This part of the research is in the stage of construction of wallettes.

A last comment regarding the accuracy of the results obtained by the two techniques should be added here. In Figures 14 to 17, where the profiles obtained from both sides of masonry are plotted together, one may see also the regions of uncertain data (marked on the profiles by dotted lines). The following can be observed: (a) The presentation of both single-side profiles allows for further correction of the data obtained by radar and endoscopy. In fact, as shown-for example-in the last profile of Figure 16, in the region marked with an ellipse, the thickness of the stone belonging to the outer leaf of the wall was not reliably determined. However, the fact that the thickness of the respective stone of the inner leaf was accurately measured, suggests that the smaller of the two possible thicknesses should be adopted for the stone in the outer leaf, (b) There are cases, however, in which the uncertainty regarding the thickness of some stones remains (see, for example, the part of the same profile marked with a rectangle).

Nevertheless, one could accept this inaccuracy, since the overall geometry of masonry does not seem to be affected by the uncertainties related to the dimensions of a limited number of stones.

8 CONCLUSIONS

On the basis of the material presented in this paper, one may conclude that

(a) The application of radar techniques to masonry can yield reliable results regarding the geometry of masonry in-depth. To this purpose, however, rather high frequency antennas should be used; thus, the depth for which the results are accurate enough is limited to part of masonry thickness.

(b) The combination of this non-destructive technique with the slightly destructive technique of endoscopy may enhance the accuracy of the results. In addition, endoscopy may provide information regarding the nature and the state of materials inside masonry.

(c) For the purpose of the investigation that serves the needs of preservation of the Dafni Monastery, the two techniques provided sufficient information that allowed for the construction type of masonry to be determined in various parts of the monument.

ACKNOWLEDGMENTS

The work presented in this paper would not have been possible without the cooperation with Dr Ph. Côte and Dr X. Dérobert (LCPC, France) who trained us in using the equipment and processing the data. Their competence and their kind assistance are gratefully acknowledged.


Thanks are due to the Members of the Scientific Committee for Dafni Monastery, Professors Ch. Bouras, T.P. Tassios, H. Mariolakos and N. Zias.

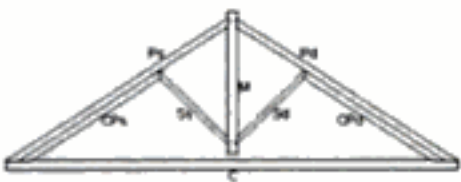
The constant support of V.Chandakas, General Director for Restoration, Museums and Technical Works, M. Fountoukou, Director for the Restoration of Byzantine and Post Byzantine monuments, E. Tsofopoulou, Director of the 1st Ephoreia of Byzantine Antiquities, N. Charkiolakis, Head of the Section for the studies on Byzantine monuments and A. Christofidou Head of the Section for the Execution of works of the Directorate for Restoration of Byzantine and Post-byzantine Monuments is gratefully acknowledged.

The project was carried out by the Directorate for the Restoration of Byzantine and Post-Byzantine Monuments of the Hellenic Ministry of Culture in cooperation with the Laboratory of Reinforced Concrete, National Technical University of Athens; the project was funded by the European Union and the Hellenic Ministry of Culture.

DIAGNOSI DEL LEGNO STRUTTURALE IN OPERA: INDAGINE VISIVA
SCHEDA DI RILEVAMENTO n. 1.

Sito: Abbazia di S. Lorenzo ad Septimum - Aversa - Corpo lato sud chiostro
 Tipologia dell'elemento strutturale: Capriata Palladiana semplice

Ubicazione planimetrica: C I est
 Datazione storica:
 Schema dell'elemento strutturale 



Collegamenti nodali:
catene: elemento in legno chiodato su lato sud, manca su lato nord
Aggiunta di collegamento metallici tra catena e CP destro

Specie legnosa: Castagno
 Contenuto di umidità: (vedi indagine strumentale eseguita con igrometro elettrico)
 Condizioni ambientali: Completamente esposto ad agenti atmosferici sul lato nord, coperto da soli coppi sul lato destro e da tavole + assotto + coppi sul lato sinistro
 Classe di rischio biologico:

Numero di elementi: 8 Sottoschede allegate: 8

Indagini strumentali da eseguire: Resistograph [x] - Ultrasuoni [x] - Prove di laboratorio [x]

Data: 11.02.2004 Rilevatore: Felice Russo

Allegato n.1/8 SCHEDA n.1

Elemento: Catena
 Specie legnosa: (se diversa) Castagno
 Dimensioni: l = 9,80 sez. circolare ϕ = 20 cm

Diffetti:	1*	2*	3*
Stessi	max 1/5 <input type="checkbox"/>	max 1/5 <input type="checkbox"/>	max 1/5 <input checked="" type="checkbox"/>
Lesioni varie	assenti <input type="checkbox"/>	assenti <input type="checkbox"/>	limitate <input checked="" type="checkbox"/>
Crevi da gelo	assenti <input checked="" type="checkbox"/>	assenti <input type="checkbox"/>	limitati <input type="checkbox"/>
Coperture	assenti <input checked="" type="checkbox"/>	assenti <input type="checkbox"/>	limitate <input type="checkbox"/>
Nodi singoli	max 1/5 <input checked="" type="checkbox"/> max 30 mm	max 1/5 <input type="checkbox"/> max 70 mm	max 1/2 <input type="checkbox"/>
Gruppi di nodi	max 1/5 <input checked="" type="checkbox"/>	max 2/5 <input type="checkbox"/>	max 3/4 <input type="checkbox"/>
Infezioni fittonce			
In sezione radiale	max 7% <input checked="" type="checkbox"/>	max 12% <input type="checkbox"/>	max 20% <input type="checkbox"/>
In sezione tangenziale	max 7% <input checked="" type="checkbox"/>	max 12% <input type="checkbox"/>	max 30% <input type="checkbox"/>
Festucazioni radiali di rive	non passanti <input checked="" type="checkbox"/>	non passanti <input type="checkbox"/>	non passanti <input type="checkbox"/>
Spessore anelli	min 8 mm <input type="checkbox"/>	min 3,3 mm <input type="checkbox"/>	min 3,3 mm <input checked="" type="checkbox"/>

Alterazioni degradative: Attacco da parte di insetti xilofagi, presenza di rovine e fori di uscita, presenza di muffe

Zone critiche: Nodo catena - puntone : presenza di nodi di grandi dimensioni

Note:

Figure 1. Visual inspection form. Up: survey form used to investigate each truss. Down: standard enclosure to categorize each element of the truss.

damages and deteriorations by xylophagous insect, fungi or mould. The analysis of all these features is useful to operate a kind of classification of the quality

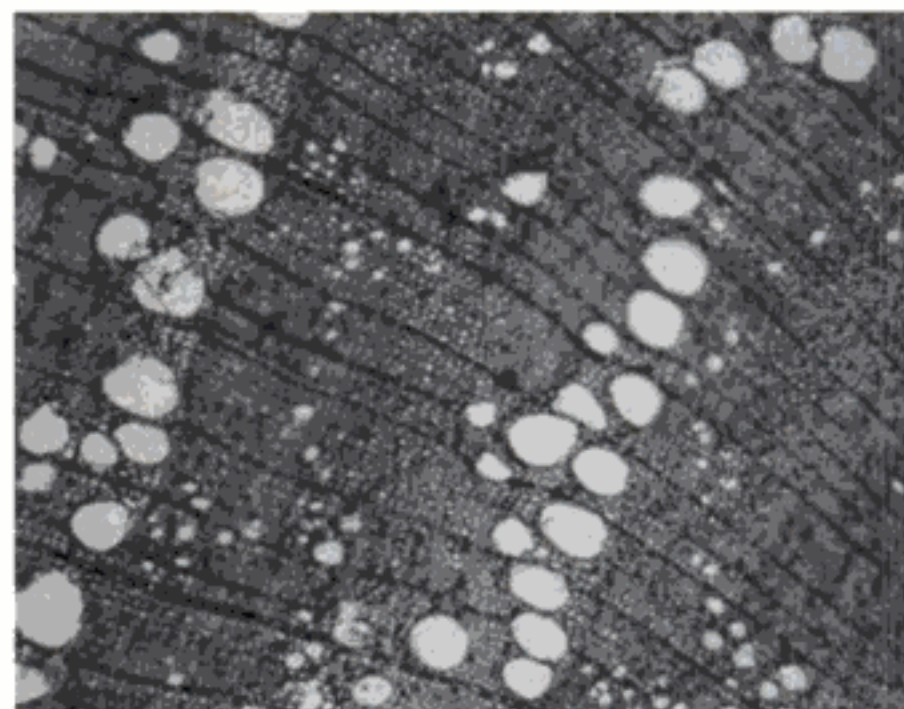


Figure 2. Image of a sample of chestnut wood from an investigated truss 50 times magnified by optical microscope. Courtesy Dr. E. Allevato, botanist.

of each element similar to that one used to categorize new structural timber up to standard.

In this first phase the collaboration between different professional competences turns out essential to carry on a reliable research work: in the specific case the research group availed of the consultancy of a botanist and an entomologist.

An appropriate form was arranged and then filled up in situ during the inspection of each truss. The first page of the form includes information about the whole truss, and then the features of each structural element are reported as enclosures.

The position of each truss has been schematically transferred on a map and marked with reference to the filled pages. Every connection and each notable detail has been photographed noting down the position on the corresponding form, and then little specimens of the material have been removed from damaged zone to identify the botanic species of wood by optical microscope.

The visual inspection is also essential to settle on the kind of instrumental checks to carry out afterwards. The choice has to be done on the basis of the physical properties to find, of the accessibility of the site, of the possibility to operate on protected elements belonging to the cultural heritage. During this stage a selection of the specimens to test in situ by NDTs and then in laboratory has to be done, defining the sample of the survey.

2.2 Instrumental inspection

This phase, also defined as "second level surveying" and performed in situ too, consists of the evaluation of the conservation conditions, defects and alterations of the structures in internal or not visible parts and of the identification of physical and mechanical characteristics by the use of appropriate portable devices.

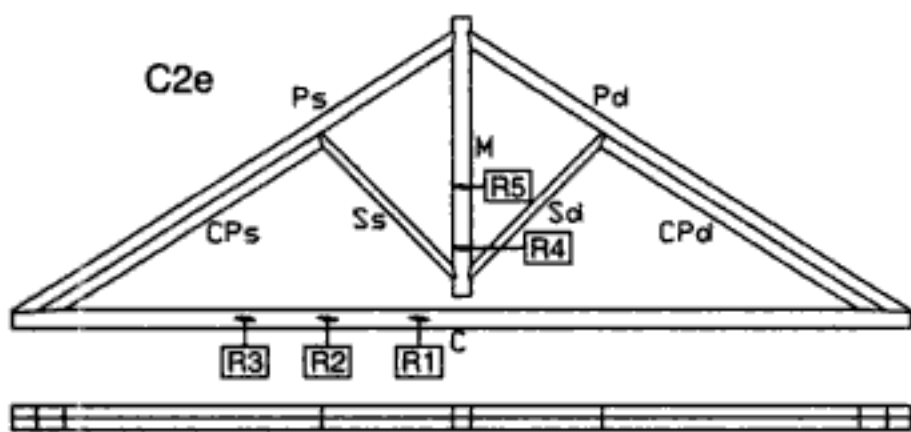


Figure 10. Location of NDT on the truss.

- Identification of the botanic species of wood
- Examination of the principal macroscopic defects and the superficial deterioration degree
- Evaluation of environmental factors linked damage
- Assessment of the organic damage
- Graphical restitution of the results
- Instrumental in situ inspection:
 - Choice of the specimens to test according to the preceding inspection
 - Choice of each cross section to test
 - Dendrochronological surveying
 - Measurement of the moisture content of wood by electrical hygrometer
 - Carrying out of the drilling test by *Resi F400*
 - Analysis of the lay-out diagrams and choice of the cross section to test by ultrasonic wave
 - Carrying out of the ultrasonic test
 - First qualitative evaluation of the results

In this part of the research work the professional competences employed are: structural engineers, botanists, entomologists, instrument operators.

3.3 Tests execution

The visual inspection has been carried out on all the trusses of the described roof structure. Each element has been analyzed to check the conservation state, the geometrical characteristics and to locate the critical zones. Besides, the presence of damages and defects and the stress condition have been evaluated, to select the sections to investigate by NDTs.

Then 113 drilling tests by *Resi F400* have been carried out on 8 tie-beams, 10 king-posts, 4 struts and 2 principal rafters.

After the drilling ones, 105 ultrasonic tests were carried out, 100 of them as local test through cross sections along the radial direction, next to the locations of the drilling ones, and 5 as global test along the longitudinal direction, considering a 2 m range of the log.

The ultrasonic test is greatly influenced by the thermo-hygrometric conditions of the tested material,

Table 1. Moisture content measurements for each kind of truss element.

Truss element	Average MC (%)	Max MC (%)	Min MC (%)
Tie-beam	16.6	24.0	12.5
King-post	15.2	17.0	13.4
Strut	15.1	18.4	13.3

so together with it, temperature and moisture content of each element was accurately measured by an electric hygrometer (Table 1).

The output of the ultrasonic test is time taken by the wave to cross the section, so the wave speed can be obtained knowing the path length.

4 ANALYSIS OF THE NDTs RESULTS

4.1 Drilling test

The *Resi* test lay-out diagrams have been analyzed discovering the defect owning zones and selecting the results to consider in the statistical processing. Then a reference factor of the investigated sections quality has been calculated.

This parameter called “conventional absorbed power” (CAP) represents the ratio between the subtended area of the diagram and the corresponding x-coordinate length (Piazza & del Senno 2002). This quantity can be correlated to the average density of the material in every corresponding zone.

A statistical analysis of all the measurements has been processed to evaluate the data scattering in each cross section and for each group of truss components: tie-beam, king-post, struts. Analyzing the drilling tests lay-out, a data selection was carried out to check cross sections without defects and anomalies and to reject the results obtained in damaged sections.

The aim of this selection is to operate first an identification of the mechanical characteristics of a quite homogeneous material (that can be considered as good quality) and then estimate the variation of all the considered parameters because of the presence of defects and deterioration.

The diagrams in Figures 11–13 show the values of CAP in the selected sections and the tendency line allows grasping the values scattering.

The data analysis of the ultrasonic tests has been processed according to the just exposed criterion, too.

The diagrams below (Figs 14–16) show the values of the ultrasonic speed in the selected sections and the tendency line.

The statistical analysis of the results allows assessing the data scattering for each kind of element of the truss (tie-beam, king-post, struts). The average

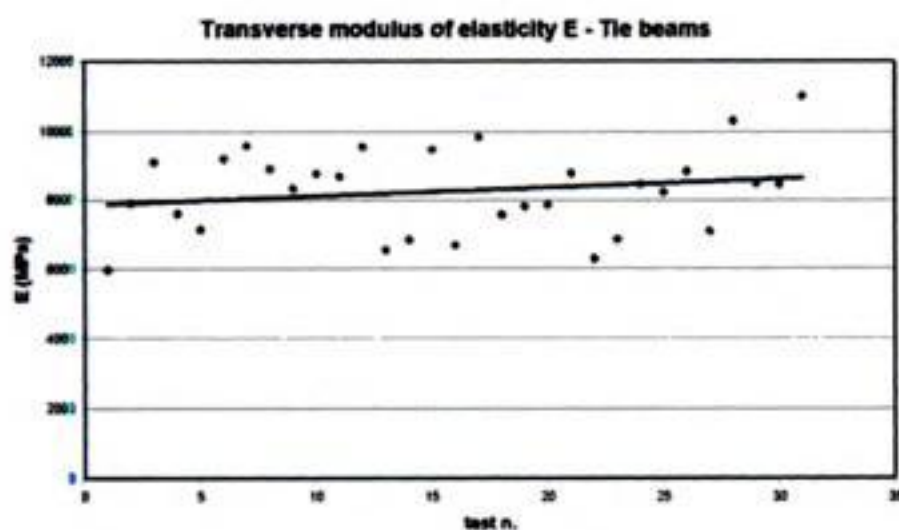


Figure 17. Tendency of transverse modulus of elasticity for tie beams.

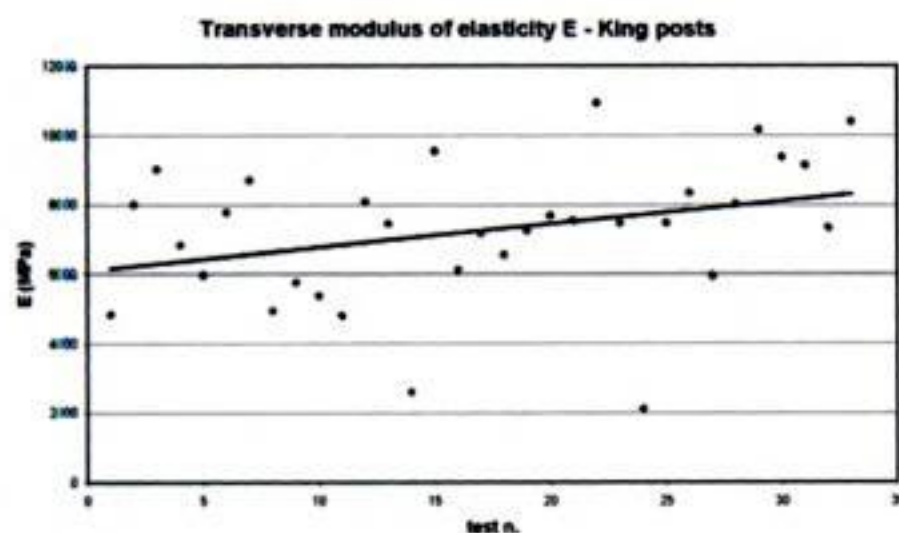


Figure 18. Tendency of transverse modulus of elasticity for king posts.

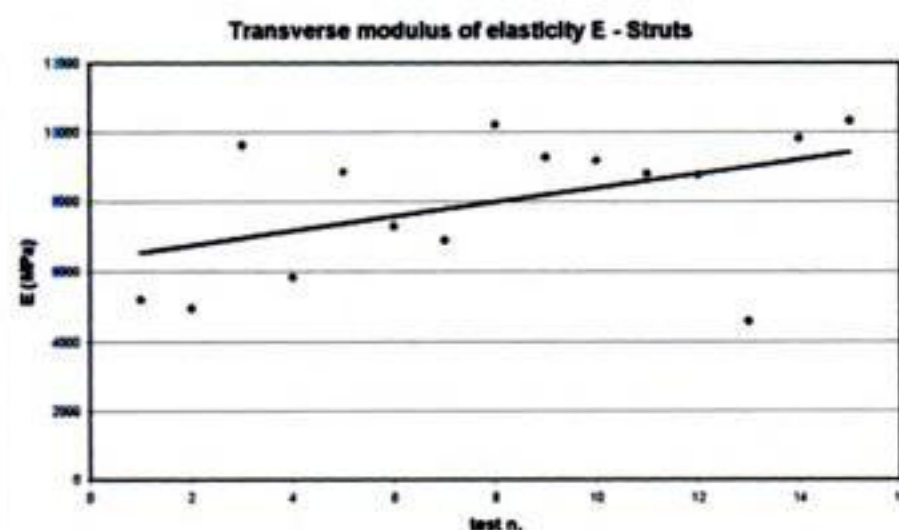


Figure 19. Tendency of transverse modulus of elasticity for struts.

a value of the material density lower than the average one taken from literature and quite reliable.

In this phase of the research work the density of the material has been not measured directly, so a characteristic value of chestnut wood density (5th percentile) was taken into account and verified on two specimens.

The diagrams below (Figs 17–19) show the values of the transverse modulus of elasticity in the selected sections and the tendency line.

The average value of the transverse modulus of elasticity estimated for each selected section is reported in the table below (Table 4). As first approximation

Table 4. Average value of the modulus of elasticity for each kind of truss element.

Truss element	E transverse (MPa)	E longitudinal (MPa)
Tie-beam	826	12705
King-post	723	11131
Strut	855	13161

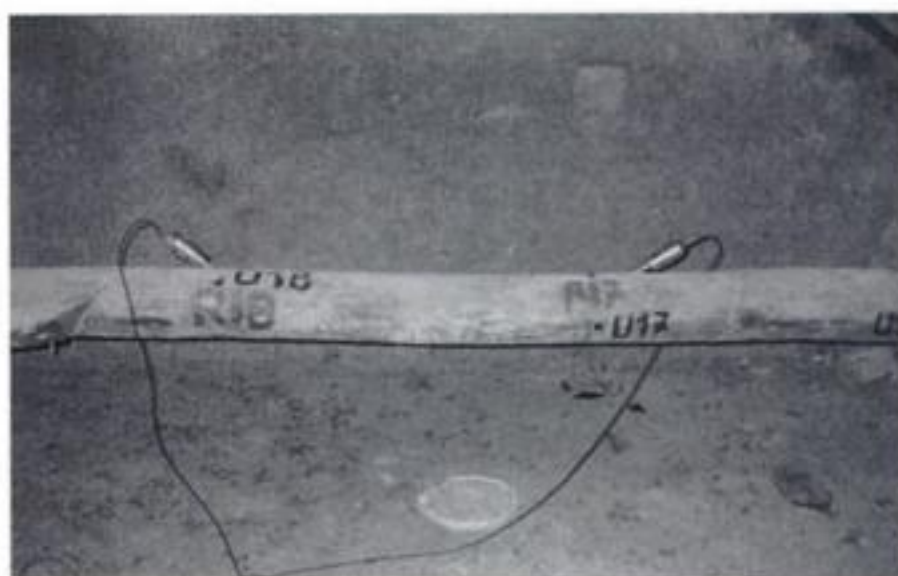


Figure 20. Longitudinal ultrasonic measurements.

and to estimate reference assessments to compare with the results of the laboratory tests, the values of the longitudinal modulus have been derived from the transverse ones according to a proportionality factor resulting from the hardwood resistance classification by EN 338.

We can notice that the indirectly estimated values are near to the average values deducible from literature.

The US tests carried out on some tie beam and king post, along the longitudinal direction, confirm the results of $E_{\text{longitudinal}}$ estimated by the exposed criterion.

5 CONCLUSIONS

The combined use of both drilling and US tests allows to check the homogeneity of each investigated cross sections and to select the results to formulate an estimation of the modulus of elasticity for a material lack in defects and anomalies, as first step.

The procedure let to reach a more reliable evaluation of the results that will be verified running laboratory tests.

The proposed methodology will consent to evaluate more precisely the mechanical characteristics of existing structures by the means of not much expensive and easy to run NDTs.

The possibility to set the procedure, carrying out vast survey campaigns on different species specimens, can let a simpler and reliable interpretation of NDTs not yet standardized.

ACKNOWLEDGEMENTS

The authors wish to thank TECNO IN S.r.l. for the carrying out of instrumental investigation, in particular Eng. A. Sorrentino for his technical assistance. Thanks to Dr. G. Di Pasquale and Dr. E. Allevato of the Laboratory of Applied Ecology, *Arbopave*, Agricultural Science Faculty of University of Naples "Federico II" for the identification of the botanic species.

REFERENCES

- Calvi, G. & Croce, U. 1989. Indagini sperimentali per l'applicazione di metodi non distruttivi alle strutture di legno. In G. Tampone (ed), *Il Restauro del legno*. Milano: Hoepli.
- Chen, C.-J., Tsai, P.-H., Hsu, M.-F. & Chang W.-S. 2003. In-situ evaluation of timber roof structures of historic buildings. *STREMAH VIII*. Halkidiki:WIT Press.
- del Senno, M. & Piazza, M. 2003. Behaviour and rehabilitation of queen post timber trusses: a case study. *STREMAH VIII*. Halkidiki:WIT Press.
- Galimard, P. 2002. Estimation of the mechanical properties of ancient timber beams. In C. Bertolini Cestari, J.A. Faria & A. Soikkeli (eds), *European Timber Building as an Expression of Technological and Technical Cultures*. Paris: Elsevier.
- Giordano, G. 1986. *Tecnologia del legno*. Torino: UTET.
- Giordano, G. 2001. *Tecnica delle costruzioni in legno*. Milano: Hoepli.
- Kappel, R. & Mattheck, C. 2003. Inspection of timber construction by measuring drilling resistance using Resistograph F300-S. *STREMAH VIII*. Halkidiki:WIT Press.
- Migliore, M.R. & Ramundo, F. 2003. La Diagnostica Non Distruttiva nel Legno Strutturale. In *Atti della Giornata di studi sul tema: Diagnostica per la tutela dei materiali e del costruito*. Sito Reale di S. Leucio-Caserta.
- Piazza, M., Baldassino, N. & Zanon, P. 1996. In situ evaluation of the mechanical properties of timber structural elements. In *Proceedings of the X Symposium on NDT of Wood*. Lausanne.
- Piazza, M. & del Senno, M. 2001. Proposals and criteria for the preliminary evaluation, the design and the execution of works on ancient load bearing timber structures. In C. Bertolini Cestari (ed), *Wooden Handwork/Wooden Carpentry:European Restoration Sites*. Paris: Elsevier.
- Piazza, M. & del Senno, M. 2002. Applicabilità di indagini strumentali. *L'edilizia n.4*.
- Rinn, F. 1994. Resistographic inspection of construction timber, poles and trees. In *Proceedings of Pacific Timber Eng. Conference*. Australia.

Compressive behavior and NDT correlations for chestnut wood (*Castanea sativa* Mill.)

A.O. Feio & P.B. Lourenço

University of Minho, Department of Civil Engineering, Portugal

J.S. Machado

LNEC, National Laboratory for Civil Engineering, Timber Structures Division, Portugal

ABSTRACT: The goal of the present work consists in the characterization of the mechanical behavior of chestnut wood under compression perpendicular to the grain. After a review of the problems usually involved in characterizing timber under this type of loading, a mechanical test was set-up. The timber specimens used in the testing program were divided in two groups: (a) new chestnut wood (NCW), which has never been used structurally even so it comes from logs that could be used as such; and (b) old chestnut wood (OCW), which were already used in structural elements from ancient constructions (date and precise origin unknown). The mechanical behavior of the specimens is discussed taking into account the orientation of the annual growth rings along the direction of the load. Correlations between mechanical properties and NDT (ultrasonic pulse velocity and drilling resistance) are also provided, taking into account the density of the wood.

1 INTRODUCTION

Timber is one of the most used materials in the roofs and floors of monumental constructions in Portugal. In particular, chestnut (*Castanea sativa* Mill.) is usually present in noble constructions, given not only its mechanical and durability properties, but also its aesthetic characteristics.

Carefully conservation or rehabilitation of existing constructions implies extensive knowledge about the constituent material from which the structure was made, both from the mechanical point of view and from the physical point of view. This knowledge constitutes the support to evaluate the short-term structural behavior and to foresee the continuous adaptation and capacity of response of the material under adverse factors (long-term structural behavior).

The last decades witnessed developments in the testing techniques and equipments that allow, diminishing the subjectivity and increasing the level of the structural analysis, diagnosis and inspection of historical constructions. NDT have an own special interest due to the fact that their application does not affect the present structural integrity and safety of the structure.

These methods can be classified in two distinct groups: Global Test Methods (GTM) and Local Test Methods (LTM) (Bertolini et al. 1998). The first ones

include the application of the ultrasonic and vibration methods. The LTM, with the utilization of the Resistograph (Rinn, 1994) and the Pilodyn (Gorlacher, 1987) as the most common NDT devices, play usually a role support in the visual grading of the wooden elements and structures. The application concerns the evaluation of the incidence and severity of defects in the material state of conservation (Machado & Cruz, 1997), with the aim of comparing the residual section with the variations of density, usually associated with the loss of mass. These methods present several advantages such as their practical utilization, transport and efficiency.

Presently these methods are used alone or at the same time with others NDT methods or techniques. The effectiveness (in terms of results) could be increased if some laboratorial tests were used to study the variability of the mechanical characteristics of the wooden elements (Uzielli, 1992).

The main scope of the present work consists in the characterization of the mechanical behavior of chestnut wood (*Castanea sativa* Mill.) under compression perpendicular to the grain. The mechanical characterization aims at obtaining the elastic properties (namely the modulus of elasticity and the Poisson coefficient) and the compressive strength perpendicular to the grain, in laboratory with a predefined set-up for mechanical testing. Correlation of these properties with NDT techniques will be analyzed also.

The mechanical behavior of the tests specimens is discussed taking into account the orientation of the annual growth rings with respect to the direction of the applied load.

2 DESCRIPTION OF THE EXPERIMENTAL TESTS

2.1 Specimens size and orientation

The average size of the tests specimens was originally $5 \times 5 \times 30$ cm. Ultrasonic tests were carried out in these specimens and, afterwards, all of them were cut in three samples of $5 \times 5 \times 10$ cm: two of specimens were tested in laboratory up to failure and the other specimen was used for the NDT tests (Resistograph and Pilodyn 6J).

In total, 164 specimens of chestnut wood were tested. The specimens were divided in two groups: new chestnut wood (NCW), which has never been used structurally even so it comes from logs that could be used as such, and old chestnut wood (OCW), which were already used in structural elements from ancient constructions (date and precise origin unknown). All wood comes from the Northern region of Portugal.

The specimens were also divided in different groups taking into account the orientation of the annual growth rings with respect to the direction of the applied force. Therefore, four groups were considered: (a) diffuse, (b) diagonal, (c) tangential and (d) radial, as shown in Figure 1.

All the specimens were previously conditioned in a climatic room capable of keeping a temperature of $20 \pm 2^\circ\text{C}$ and a humidity of $65 \pm 5\%$. The tests specimens were considered conditioned when the density variation is smaller than 0.5% in a period of two hours, as recommended by the NP-614 standard. The densities were measured through an electronic weighing machine with a precision of 0.01 g.

2.2 Destructive tests

The experimental research was carried out at the Structural Testing Laboratory of the National Laboratory for Civil Engineering, using a universal testing machine Baldwin, with a load cell of 300 kN. A power supply Schenk equipment was used, together with a HBM system (Spider 8) for the acquisition and amplification of the data, see Figure 2a.

The tests were carried using NBr7190/97 standard being the test velocity 6×10^{-3} mm/s, in the cyclical phase, and 6×10^{-2} mm/s in the last step (during the failure phase). This normative change was necessary, because the tests were performed under displacement control and not under force control, as prescribed by the standard.

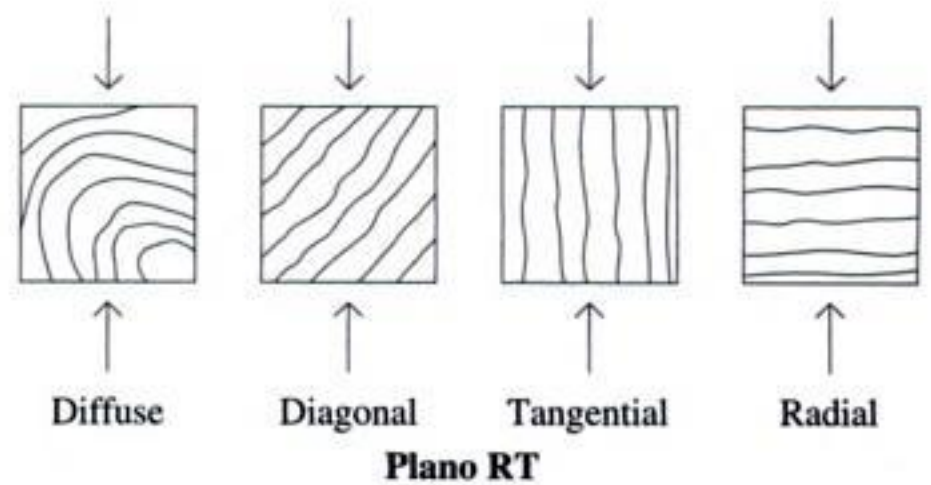


Figure 1. Orientation of the annual growth rings with respect to the direction of the applied load.

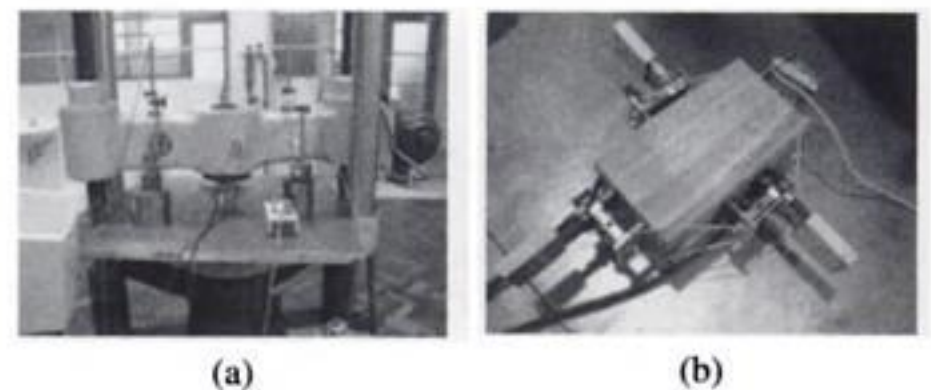


Figure 2. Laboratorial tests: (a) general view and (b) instrumented specimen.

Previously, a series of calibration tests of the apparatus was carried out, for the purpose of verifying the agreement between the vertical displacements in the faces of the tests specimens, measured using mechanical strain gauges, and the vertical displacements in the arms of the test machine, measured by means of LVDT's. Four mechanical strain gauges (one in each one of the faces) were used to measure the horizontal displacements and two additional LVDT's were placed in the arms of the test machine measuring the vertical displacements. As shown in Figure 2b, three mechanical strain gauges from HBM (DD1 type) and one mechanical strain gauge from Schenck were used. This last transducer was not always effective in measuring the displacements due to insufficient adhesion.

The normal compressive strength ($f_{c,90}$) is the conventional value determined by the residual specific deformation of 2%, following the NBr7190/97 standard. The stiffness of wood, in the direction perpendicular to the grain, is determined by its modulus of elasticity. This is equal to the slope of the linear part on the stress-strain relationship (Fig. 3), defined by the points $(\sigma_{10\%}; \varepsilon_{10\%})$ and $(\sigma_{50\%}; \varepsilon_{50\%})$ corresponding respectively to 10% and 50% of the conventional stress, in compression perpendicular to the grain, and it is represented by:

$$E_{c,90} = \frac{\sigma_{50\%} - \sigma_{10\%}}{\varepsilon_{50\%} - \varepsilon_{10\%}} \quad (1)$$

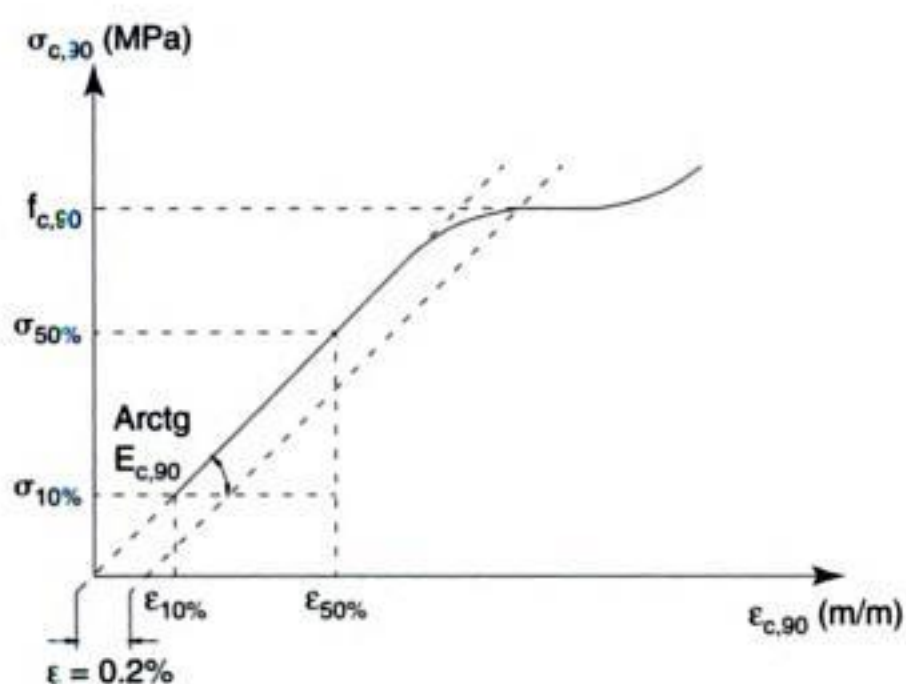


Figure 3. Stress-strain relationship.

where $\sigma_{10\%}$ and $\sigma_{50\%}$ are the normal stresses corresponding to 10% and 50% of the conventional stress, and $\epsilon_{10\%}$ and $\epsilon_{50\%}$ are the specific strains corresponding to the values of $\sigma_{10\%}$ and $\sigma_{50\%}$.

The relative moisture and the temperature during the tests were registered by an electronic device. During the tests, the average values of temperature and relative moisture were $24 \pm 2^\circ\text{C}$ and $52 \pm 12\%$, respectively.

2.3 Non-destructive tests

2.3.1 Ultrasonic tests

During the tests the ultrasonic equipment Pundit/Plus was used, with cylinder-shaped transducers of 150 kHz. The tests were divided in three distinct types of signal transmission: (1) Indirect Method; (2) Direct Method, parallel to the grain, and (3) Direct Method, perpendicular to the grain. The elastic properties of wood were estimated by the measurement of stress wave propagation time in these directions, assuming a continuous and homogeneous material. The transmission technique of elastic waves based on the Indirect Method was used in all the faces, for the case of diagonal and diffuse tests specimens (Fig. 1). For the case of radial and tangential tests specimens, the transducers were used in two opposite faces, depending on the orientation of annual growth rings, see Figure 4a. Average values were considered.

In the Direct Method, perpendicular to the grain, contiguous sections of the same specimen were used (the distance between each section was 6 cm), see Figure 4c, and once again average values were considered. In all tests, coupling between the transducers and specimens was assured by a conventional hair gel and a constant pressure was applied by means of a rubber spring, allowing adequate transmission of the elastic wave between the transducers and the specimen under testing.

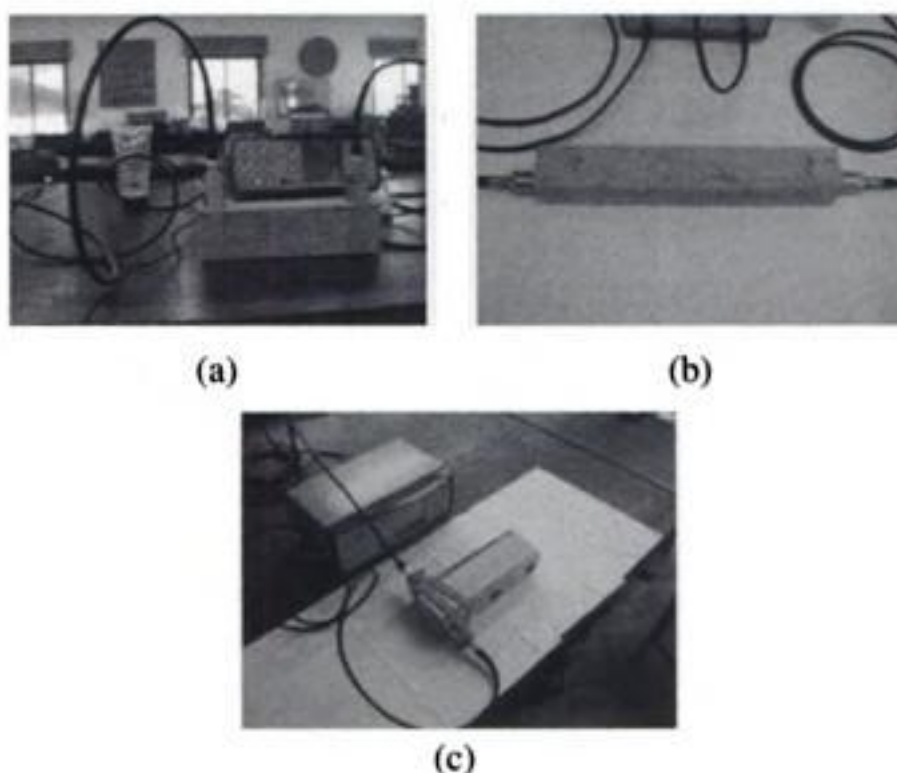


Figure 4. Test set-up: (a) Indirect Method, (b) Direct Method, parallel to the grain and (c) Direct Method, perpendicular to the grain.



Figure 5. NDT devices: (a) Resistograph and (b) Pilodyn 6J.

2.3.2 Resistograph tests

The use of the Resistograph allowed to obtain the density profile of the used tests specimens, see Figure 5a. Drilling was made parallel to plan RT (plain TL and LR), which, in real cases, represents the accessible face of the timber elements.

For all the specimens, as a function of the obtained graphs with the Resistograph, a resistographic measure (RM) was determined. The selected resistographic measure represents the ratio between the integral of the area of the diagram and the height of the tests specimens (see Eq. 2). Using this quantity, the Resistograph results can be easily compared with the values of density and the strength values.

$$RM = \frac{\int_0^h Area}{h} \quad (2)$$

2.3.3 Pilodyn 6J tests

The Pilodyn 6J is a device that allows, through the release of a spring that transforms the elastic potential energy into impact energy, to measure the penetration of a metallic needle with 2.5 mm of diameter.

This impact is responsible for the penetration of the needle in the surface of the specimens, allowing to register the depth penetrated by the needle in plan TR or in plan RT of the specimens, see Figure 5b. The Pilodyn 6J was used with the aim of correlating the density of each specimen with the depth reached with the needle of the device (surface hardness or resistance to superficial penetration).

2.3.4 Density determination

Density was measured according to NP-616 standard. Given the conditioning conditions of the specimens, the average density is determined for a moisture content of 12%, given by:

$$\rho_{12\%} = \frac{m_{12\%}}{V_{12\%}} \quad (3)$$

Table 1. Radial specimens: NCW.

	E (MPa)	Poisson			$\sigma_{0,2\%}$ (kPa)
		ν_{LR}	ν_{TR}	ν_{LT}	
Average	800,6	0,04	0,32	0,13	7806,9
Max.	985,6	0,06	0,39	0,18	10896,8
Min.	621,0	0,03	0,21	0,10	5344,8
No.			19		
CV	13	18	12	16	19

Table 2. Radial specimens: OCW.

	E (MPa)	Poisson			$\sigma_{0,2\%}$ (kPa)
		ν_{LR}	ν_{TR}	ν_{LT}	
Average	846,3	0,05	0,32	0,16	8011,6
Max.	1058,9	0,08	0,45	0,20	12045,5
Min.	562,7	0,04	0,23	0,11	5365,0
No.			12		
CV	17	22	21	15	26

Table 3. Diagonal specimens: NCW.

	E (MPa)	Poisson			$\sigma_{0,2\%}$ (kPa)
		ν_{LR}	ν_{TR}	ν_{LT}	
Average	551,5	0,04	0,26	0,16	6233,0
Max.	673,1	0,05	0,32	0,19	7400,0
Min.	453,8	0,02	0,13	0,12	5224,4
No.			20		
CV	10	22	16	13	10

3 DESTRUCTIVE TESTS

The results of the destructive tests, following the grouping detailed above, are presented taking into account the orientation of the annual growth rings along the direction of the force. The tables presented next (Table 1 to Table 8), provide the values obtained for all groups.

Table 4. Diagonal specimens: OCW.

	E (MPa)	Poisson			$\sigma_{0,2\%}$ (kPa)
		ν_{LR}	ν_{TR}	ν_{LT}	
Average	620,8	0,04	0,26	0,16	6623,1
Max.	929,2	0,06	0,32	0,23	9124,8
Min.	421,6	0,02	0,21	0,11	4376,3
No.			26		
CV	21	21	12	19	21

Table 5. Tangential specimens: NCW.

	E (MPa)	Poisson			$\sigma_{0,2\%}$ (kPa)
		ν_{LR}	ν_{TR}	ν_{LT}	
Average	527,6	0,05	0,28	0,18	6667,4
Max.	660,2	0,07	0,39	0,23	8792,5
Min.	331,0	0,04	0,23	0,16	5170,9
No.			18		
CV	15	17	13	12	14

Table 6. Tangential specimens: OCW.

	E (MPa)	Poisson			$\sigma_{0,2\%}$ (kPa)
		ν_{LR}	ν_{TR}	ν_{LT}	
Average	572,4	0,06	0,32	0,18	7484,2
Max.	687,6	0,08	0,38	0,23	9199,2
Min.	467,6	0,05	0,29	0,14	6310,0
No.			12		
CV	12	13	8	13	10

Table 7. Diffuse specimens: NCW.

	E (MPa)	Poisson			$\sigma_{0,2\%}$ (kPa)
		ν_{LR}	ν_{TR}	ν_{LT}	
Average	592,7	0,06	0,36	0,17	6523,3
Max.	751,8	0,08	0,44	0,22	9307,2
Min.	516,0	0,03	0,30	0,07	4684,8
No.			22		
CV	12	19	9	18	16

4 CORRELATIONS BETWEEN NON-DESTRUCTIVE AND DESTRUCTIVE TESTS

4.1 Ultrasonic tests

It is well known that stress waves velocity can be directly related to the elastic properties of timber.

The propagation velocity of the longitudinal stress waves in an elastic media depends essentially on the stiffness and the density of the media itself. On the other hand, it is normally possible to measure the propagation time of a set of elastic waves in the axial direction of the wooden elements or in the perpendicular directions to this (it is stressed again that the

propagation time is an average time obtained from the measurement of the faster elastic waves).

For prismatic, homogeneous and isotropic elements and for those with section width smaller than the stress wavelength, the relation:

$$E_{din} = v^2 \times \rho \quad (4)$$

holds, where E_{din} represents the dynamic modulus of elasticity (N/mm^2); v is the propagation velocity of the longitudinal stress waves (m/s) and ρ is the density of the specimens (kg/m^3).

For practical purposes, the relation between the dynamic modulus of elasticity and the static value $E_{med,static}$ is particularly relevant ($E_{din} > E_{med}$). Generally (Wood Handbook, 1974), a linear relation is adequate:

$$E_{med} = a \times E_{din} - b \quad (5)$$

Table 8. Diffuse specimens: OCW.

	E (MPa)	Poisson			$\sigma_{0,2\%}$ (kPa)
		ν_{LR}	ν_{TR}	ν_{LT}	
Average	618,3	0,06	0,35	0,18	6559,6
Max.	705,9	0,08	0,43	0,24	7968,0
Min.	479,2	0,04	0,29	0,10	4730,4
No.			29		
CV	8	18	9	16	14

Table 9. Dynamic modulus of elasticity (MPa) (Direct Method, perpendicular to the grain).

	Tangential		Diagonal		Diffuse		Radial	
	New	Old	New	Old	New	Old	New	Old
Av.	1456	1662	2256	2109	1664	1867	2997	3083
No.	19	12	11	16	10	13	18	13
CV	16	9	19	18	13	25	19	14

Table 9 to Table 11 provides the values measured for all specimens. The obtained values with the ultrasound test emphasize the good relation between the dynamic and static moduli of elasticity.

Figure 6 illustrates different correlations obtained between the dynamic modulus of elasticity, taking into account the orientation of the annual growth rings along the direction of the force, considering the Direct Method, perpendicular to the grain, for the NCW group.

4.2 Resistograph tests

Figure 7 and Figure 8 show the correlations between the resistographic measure and the density of each

Table 10. Dynamic modulus of elasticity (MPa) (Indirect Method).

	Tangential		Diagonal		Diffuse		Radial	
	New	Old	New	Old	New	Old	New	Old
Av.	12932	12008	12189	13237	13306	12391	13084	12897
No.	19	12	11	16	10	13	19	12
CV	16	26	14	21	12	16	16	22

Table 11. Dynamic modulus of elasticity (MPa) (Direct Method, parallel to the grain).

	Tangential		Diagonal		Diffuse		Radial	
	New	Old	New	Old	New	Old	New	Old
Av.	14445	14540	13368	15091	16057	14601	14445	14525
No.	19	12	11	16	10	13	18	13
CV	19	22	15	13	13	21	19	22

density. In future communications, the issue of correlations between non-destructive parameters and strength values will be addressed.

Taking into account the subjectivity of the results associated with the Resistograph, the concept of resistographic measure needs revising, to reduce reading errors and increase graphical interpretation.

ACKNOWLEDGMENT

The first author gratefully acknowledges Foundation for Science and Technology (FCT), for PhD grant SFRH/BD/6411/2001. The authors acknowledge also the support of Augusto de Oliveira Ferreira e Companhia Lda. (offer of specimens), and personnel of the Timber Structures Division and the Structural Testing Laboratory of LNEC.

REFERENCES

- Bertolini, C., Brunetti, M., Cavallaro, P. & Macchioni N. 1998. A non destructive diagnostic method on ancient timber structures: some practical application examples. *Proceedings of 5th World Conference on Timber Engineering, Montreux*. Presses Polytechniques et Universitaires Romandes, Vol. I, p. 456–465.
- Bodig, J. 1965. The effect of anatomy on the initial stress-strain relationship in transverse compression. *Forest Products Journal*. 14, p. 197–202. May, 1965.
- Gorlacher, R. 1987. Non destructive testing of wood: an in-situ method for determination of density. *Holz as Roh- und Werkstoff*. Vol. 45, p. 273–278.
- Machado, J.S. & Cruz H. 1997. Avaliação do estado de conservação de estruturas de madeira. Determinação do perfil densidade por métodos não destrutivos. *Revista Portuguesa de Engenharia de Estruturas*. 42, p. 15–18.
- Norma Brasileira. 1997. *NBr7190/97 – Projeto de Estruturas de Madeira*.
- Norma Portuguesa. 1973. *NP-614 Madeiras – Determinação do teor em água*.
- Norma Portuguesa. 1973. *NP-616 Madeiras – Determinação da massa volúmica*.
- Rinn, F. 1994. Resistographic inspection of construction timber, poles and trees. *Proceedings of Pacific Timber Engineering Conference*. Gold Coast, Australia. July, 1994.
- Tabarsa, T. & Chui, Y.H. 2001. Characterizing microscopic behaviour of wood under transverse compression. Part II. Effect of species and loading direction. *Wood and Fiber Science*. Vol. 33 (2), p. 223–232. April, 2001.
- Uzielli, L. 1992. Evaluation of timber elements bearing capacity. *L'Edilizia*. 12, p. 753–762.
- Wood Handbook. 1974. *Forest Service Agricultural Handbook*. No 72, U.S.D.A.

Inspection & NDT to verify structural reliability of historic wooden roofs in the ex-Meroni spinning-mill

F. Augelli, C. Colla & R. Mastropirro
Polytechnic University of Milan, Milan, Italy

ABSTRACT: The Meroni spinning-mill, an industrial archaeological complex of historic and cultural importance, is the only surviving testimonial – integral, although in decay – of former economic activity in the province. In view of its preservation, inspections and NDT have been carried out on the wooden roof structures to verify and quantify the material consistency, to determine the degree of decay and risk of collapse. The inspection phases involved: identification of wood species; determination of natural durability and class of biological risk; location and evaluation of defects, alterations, critical zones; pathologies; environmental and wood moisture condition; evaluation of residual bearing resistance, photographic survey. The data plotting and reporting has been organized in thematic maps, catalogue of all structural elements, considerations of reliability, assessment of residual resistant sections and initial intervention indications. Local decay has been identified and explained in terms of a prolonged lack of maintenance, responsible for partial loss of material.

1 INTRODUCTION

The Meroni spinning-mill complex is located in the historic centre of the small town of Soncino, near Cremona, Italy. It has recently been the object of a national architecture competition wanted by the Town Council, which owns it (Comune di Soncino 2002). The proposals ought to foresee the salvage of the architecture from the abandon, its restore and re-use with a social function. The historic and cultural importance of this industrial archaeological pole is enhanced by its position in the ancient urban mesh, since it lies adjacent to the Sforza fortress inside the still existing town wall. The silk mill, a large construction for the dimensions of Soncino, represents the last testimony still integral, although in decay, of such economic activity in the province.

In the 19th century, the mill construction, though it has a very ancient core, assumes the shape of the street block delimiting inside a large quadrangular yard with the decantation basins. Each of the buildings, constructed in different historical periods, has its own peculiar characteristics. Noteworthy in this respect are the two long buildings, one to the North and the other to the South. The former was originally destined to dry the cocoons. Its roof system presents a series of 10 traditional trusses with 4 struts. The latter is a 19th century neoclassical building with a high chimney. Herein were the spinning mills and the roof presents 12 trusses with metal beam and 2 struts. Despite metal carpentry

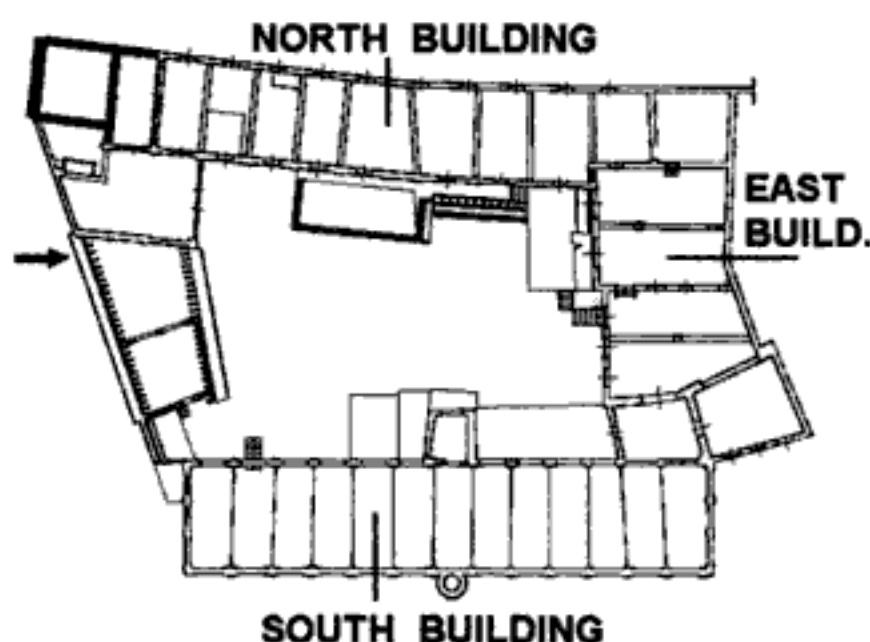


Figure 1. Plan view of the spinning mill's first floor, with indication of the truss positions in the North and South buildings.

at the joints between the wooden elements, of retention caps and stirrups, many are the elements in precarious equilibrium in both buildings. The eastern side of the block, in terms of height and characteristics, is made up of 3 distinct buildings, once used as warehouse (Fig. 1).

2 INSPECTION AIMS & PROCEDURE

In view of the project requirements, inspections and micro-destructive investigations have been carried out on appointment by the City technical office and in

of environmental and wood moisture conditions via non destructive testing (NDT) measurements; evaluating the residual bearing resistance of the individual items by means of penetration resistance tests in the areas of decay, whether real or suspected (zones not directly accessible, such as at the bearing points and joints) together with photographic surveys. The data plotting and reporting is articulated on the basis of thematic maps (in scale 1:100 and 1:50) as follows: the classification of each wooden item in a catalogue, considerations concerning their structural reliability, assessment of residual resistant sections and the initial intervention indications (Tampone 1996). The number of elements inspected amounted to more than 185. Due to space constraints only the investigations and sample results from the South building (Figs 2–3) will be presented.

3 ROOF CONSTRUCTION

In the South building, 12 trusses are included in the main roof structure. Each extremity of the trusses leans on the brick masonry walls of the North and South facades. The trusses are made up of a metal tie beam, principal rafters, a king post and 2 struts (Fig. 4). Bridle joints were used for the struts and dovetail joints

were used on the king post with addition of metal carpentry (sagittal hob-nailing at the extrados). Cast iron retention caps holding the rafters' low end are fixed to the metal beam, which crosses the rafters and the back of the caps to which it is bolt screwed. Cleats are nailed to the principal rafters in order to prevent purlins and struts from sliding on the inclined members. The king post's side skidding is limited by metal stirrups which tie its low end to the tie beam. The trusses, equally spaced, are positioned about 6 m above the floor level. The East side of the roof ends in a pavilion so the primary frame elements are hip-rafters.

Purlin and ridge beams are positioned above the trusses and, above them, in orthogonal direction, are to be found the secondary rafters. The roofing is laid on a floor with boards nailed onto the rafters. In a small portion, the boards have been replaced with corrugated fibre cement sheeting. The covering is made of a double layer of bent terracotta tiles; the tiles are missing in the area with the corrugated roofing.

To face extremely precarious decay situations, the structural roofing was partially replaced in the past and more recently (3 trusses were replaced and this involved re-using the metal carpentry).

All of the material made of wood (most of which has regular square-edged section), with the exception of the recently substituted secondary rafters, has



Figure 4. View of the South building's trusses from the East end of roof.

undergone a preservation treatment, probably using creosote. This oil, which is obtained from the batch distillation of pit-coal, has given a black colour to the wood surface and this coating treatment has made it extremely difficult to inspect the timber (to identify species, defects and pathology).

4 MACROSCOPIC IDENTIFICATION OF THE WOOD

The identification of the wood species was carried out by means of a macroscopic inspection method (UNI 4390 1959, UNI EN 844-7 1999), by recognition procedures using the naked eye or with the aid of a magnifying glass (10x or 30x), to determine the presence or absence of anatomic elements. Sometimes these macro elements are so obvious that identification of the species – or, at least, of the *order, genus and family* – is very likely. Such markers include: wood porosity and colour differences between annular rings; differences between sapwood and heartwood; visibility, shape and dimensions of the rays; the presence of resin and/or pitch pockets; distinctive smells; wood colour and pattern; etc.

Owing to the accumulation of dirt on the surface and deposits, sample inspection areas (dimensions 30 × 30 mm and 1 mm depth) had to be carved out to observe uncontaminated wood. Careful examination demonstrated that Ulmaceae and elm wood (*Ulmus campestris*) were used for the principal rafters of the trusses. The most recent wood used tends to be softwood from the pine family (larch-wood).

5 WOOD QUALITY AND WORKMANSHIP

The UNI and UNI EN standards grade the timber quality (UNI EN 518 1997, UNI EN 975-1 1999, UNI 11035-1 2003, UNI 11035-2 2003, UNI ISO 1029 1984) on the basis of a number of parameters including the abundance of “defects”. These are mainly:

- quality of workmanship;
- lack of homogeneity and defects such as knots, angle grain, deformations, checks.

5.1 Wood workmanship

Regarding the timber elements which make up the roof main frame, the quality of the workmanship is mixed (UNI EN 844-3 1998): purlins and ridge beams are of rough-hewn timber with wane edges or round logs; in the trusses, the king-post and principal rafters are sawn and frequently planed. Even on the worked pieces, edges are frequently not straight. In such cases there are irregular, semicircular or prismatic sections

or rough-edged sections with taper greater than one tenth of the section. The most recent elements are square-sawn and square-edged with wane allowance.

5.2 Wood knottiness

Large knots are common (larger than 50 mm diameter) and also knot nests (diameter smaller than the section height). Unsound knots and knotholes have also been observed. In these situations, a reduction coefficient of 0.75 was suggested in the calculations of the residual bearing resistance.

5.3 Grain direction and shrinkage shake

Equally frequent are members with angle grain (between 10°–15°), wavy grain or, in the case of round logs, spiral grain. At times, shrinkage shakes have been observed, of the large and deep kind, but normally there are no through shakes. Occasionally, damage due to angle grain was detected, near knots in traction areas. Cup shakes were detected frequently. For those members with angle grain, reduction coefficients of bearing resistance were recommended.

5.4 Physiologic alterations and growth defect

With respect to wood quality and workmanship, no significant wood warping, due to growth defects, was observed (UNI EN 844-9 2000).

6 NATURAL RESISTANCE

According to current standards (UNI EN 335-1 1993, UNI EN 335-2 1993), the natural durability of the in-situ members is as follows:

- Elm, little resistance to fungi attack; not resistant to wood borers (*anobium punctatum*);
- Larch, medium resistance to fungi attacks; not resistant to wood borers (*anobium punctatum* and *hylotrupes bajulus*).

7 CLASS OF BIOLOGICAL RISK

Biological risk is the hygiene-health state of wood preservation in-situ. It is necessary to determine the adverse situations in which wood may risk bio-attack, due to moisture. Regarding biological risk, it is standard to rate wood from 1 to 5 (1 being protected wood, 5 being material in salt water).

In the buildings which are being inspected, ventilation is furnished by the absence of windowpanes in the windows and glass panels in the entrance doors.

The following situations have been observed during inspection:

- In general, the biological risk rating is type 1 (protected wood and low risk of direct wetting, wood moisture normally below 20%), and the only kind of rot is that associated with wood borers;
- locally, where water leaks inside because of roofing rot (ridge beam areas), the class of biological risk rises to 3 (the wood is not completely protected and the moisture content is frequently greater than 20%); the primary rot risk is associated with fungi, the secondary risk with insects. The bearings of the trusses in the masonry walls are also to be included in class 3, although at present they are not moist.

The building is subject to condensation phenomena which increment both the environmental and the wood moisture content.

8 PATHOLOGIES

Wood pathologies are included in the visual grading of the elements considered. The visual inspection of active and non-active pathologies revealed the presence, extent and nature of aggressors, together with the characteristics of the damage found (UNI EN 844-10 2000, UNI EN 844-11 2000, UNI EN 1311 1999): saprophyte and parasitic insect attack (shape, dimension and colour of flight holes and bore dust) co-exist with the typical aggressors of the species present on the site. Likewise, when possible, stains were examined to ascertain the presence of pathologies (infections) or harmless alterations. Possible rot infections were evaluated with the aid of an acoustical method. This reliable standard technique consists in listening to mallet's blows. This technique was used on all the bearing points, close to the masonry (the areas with the highest infection risk) and, where possible, extended to all the areas which the macroscopic inspection had categorized as suspected active or idle infected areas (Ceccotti et al. 1998, Macchioni & Mannucci 2000, Bonamini et al. 2001).

In addition, a gimlet was used to test wood solidity and a chisel to evaluate locally the depth of attacks, hence enabling decay quantification. On account of first level examination (visual inspection), the preservation state of the material at some bearing points in the masonry was assessed using invasive investigation techniques. More detailed explanations are provided below.

Leaving detailed evaluation to the catalogue of the single items, the following general observations can be made:

- Elm members are being attacked by saprophyte anobium coleopters (*Anobium punctatum* and/or

Oligomerus ptilinoides) up to 10–15 mm depth, limited to edge areas (remains of sap wood).

- Infections are local and mostly non-active. More serious attacks are to be found close to the truss bearings, where stagnation and lack of ventilation have favoured spore taking root and hyphae proliferation. Extended areas of brown rot have been observed even on members with higher resistance to fungi attacks (Fig. 5).

9 INSPECTIONS USING ELECTRONIC EQUIPMENT

In addition to the above-mentioned visual inspections, other investigations were undertaken with the aid of an electronic thermo-hygrometer for wood and of an instrumented dynamometric drill (Mannucci & Togni 2000).

9.1 Environmental conditions

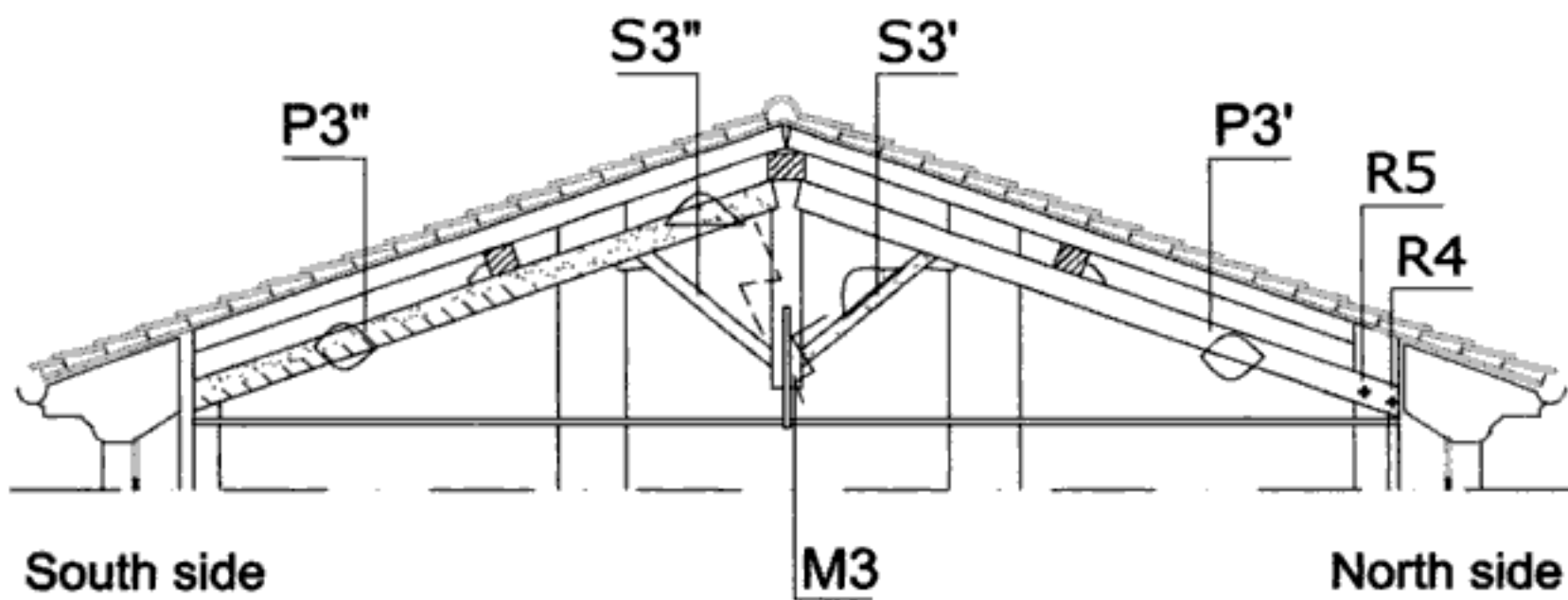
Before carrying out investigations on wood using electronic equipment, the environmental conditions – temperature and moisture – were ascertained. Temperature and moisture have an appreciable effect on the moisture values of building materials, particularly on wood. An electronic probe with an active electrode was employed.

9.2 Wood moisture condition

Non-insulated nail electrodes were employed to monitor wood moisture (UNI EN 844-4 1999, EN 13183-2 2003). The electrodes were driven deep into the wood (about 60 mm) by means of a hammer mass used percussively. The penetration depth is a function of the wood section to be tested (Giordano, 1993). In the case to hand the elements were rather large (300 × 300 mm on average). Consequently the nails had to be driven completely into the wood. The equipment measures the electric conductivity as a function of moisture: the greater the wood moisture, the greater the conductivity (Kupfer 1997, Weiß & Ungerers 1995).

9.3 Wood penetration resistance

The scope of the penetration resistance test (or instrumented dynamometric drill) is to verify the presence of inner wood holes and shakes, and fungi attack (Rinn 1989, Rinn et al. 1990, Colombo 2000, Tampone et al. 2002). The 3-mm diameter tip, 385-mm length needle, proceeds by a combined forward and rotation movement at constant speed. As the drill bores into the tested material, a chart or profile is created on chemical paper. The penetration depth (in mm) is reported on the x-axis, whilst the drill resistance is to be found



P Principal rafters
 M King post
 S Braces
 R4₊ Test location

DEFECTS

/ Angle grain

••• Knettiness

^ Natural tapering

DISARRANGEMENT

~ Crack

~ Spiral grain

- - - Shrinkage shake

◊ Ring shake

↻ Rotation on axis

DECAY

••••• Infestation

/ / / / / Infestation Infection

/ / / / / Infection

| | | | | Infiltration

Figure 6. Truss No. 3: graphical report of collected data and test positions.

10 ENVIRONMENTAL TEMPERATURE AND MOISTURE

Before testing on wood, moisture and temperature conditions in the attic were monitored. The figures obtained (Table 1) were used to correlate environmental moisture with wood moisture, hence to ascertain anomalous values when compared with figures in standard tables. To obtain measurements inside the building, the probe was raised 2 m from the working level. Furthermore, values were monitored at 2 m height from ground level, both inside and outside.

11 AVERAGE WOOD MOISTURE

After cleaning the wood in the test areas (dust/dirt and altered layers were removed, where possible), the equipment was calibrated according to the temperature at the time of testing and to the species of wood. The test positions were selected in areas where there

Table 1. Environmental and wood moisture conditions.

Name	Member	Species	Timber moist. (%)	Air moist. (%)	Temp. (°C)
U1	P1''	Elm	19.7	56.2	26.9
U2	P1''	Elm	18.4	56.2	26.9
U3	P1'	Elm	20.5	56.2	26.9
U4	P2'	Elm	19.7	53.5	30.4
U5	P2'	Elm	17.5	53.5	30.4
U6	P3''	Elm	19.6	53.5	30.4
U7	P3'	Elm	17	53.5	30.4
U8	P4''	Elm	17	50.8	32.4
U9	P4'	Elm	17.5	50.8	32.4
U10	P5''	Elm	18.4	50.8	32.4
U11	P5'	Elm	17.2	50.8	32.4
U12	P6'	Elm	22.8	72	23.8
U13	P7'	Elm	17.5	72	23.8
U14	P9''	Elm	19.3	64	26.7
U15	P10'	Larch	12.9	51.3	30.8
U16	FPN	Larch	17.9	55	29.5

lower than ideal values. In the right conditions, they will begin to spread if they have not been previously treated.

Wood moisture values are high, as measured on both the North and the South bearings of the trusses, probably because of dew phenomena, although the whole building is well ventilated due to the absence of windowpanes.

12 PENETRATION RESISTANCE TESTS

Before beginning the tests, the equipment's sensitivity was calibrated on the species to be tested. The testing positions were chosen on the basis of the previously collected thermo-hygrometer data. Calibration tests were then carried out on sound wood.

Penetration resistance tests were mainly carried out close to the bearing points of the trusses, with the aim of evaluating the condition of the wood inside the masonry section. For this reason, the tests were carried out at 45°, with the aid of a specific tool mounted on a drill. The test ended when the drill reached the maximum extension of the needle or when the needle had completely penetrated the wood section. In figure 7 one of the penetration resistance profiles, obtained from truss number 3, is shown. The interpretation of the test is reported in Table 2.

13 CONCLUSIONS

The Meroni spinning mill wooden roof structures were inspected and tested in relation to the preservation project. As the result of a prolonged lack of maintenance, the elements have been subjected to widespread local water leakage for many years. This has given rise to irreversible decay in the material in limited areas, and particularly in high-risk areas such as at the bearings.

In the South building's trusses, four of the main rafter's ends need to be replaced. Four further rafters are to be wholly replaced because of abundance of defects and pathologic conditions. Any attempts to preserve these elements would be uneconomical and technically difficult. The wood salvaged from the rejected members could be re-used for prostheses, providing that the wood be of the same type and from the areas which are free from defects and decay. It is suggested that traditional wood-wood joints be used aided by metal carpentry. Where there is total member replacement it is advisable to employ high-grade (durable and strong) timber which is pre-treated in autoclave.

No particular intervention was reputed necessary with respect to the other truss members, apart from considerations regarding safety margins, to be

analytically verified, and a good cleaning involving appropriate preservation treatment.

REFERENCES

- Bonamini, G., Noveri, M., Togni, M. & Uzielli, L. 2001. Ispezione e diagnosi in opera. In L. Uzielli (ed.), *Il manuale del legno strutturale 1*. Rome: Mancosu.
- Ceccotti, A., Ruffino, M., Bonamini, G. & Uzielli, L. 1998. *Restauro conservativo di capriate lignee. La pieve di S. Marino, progettazione, prove di lavoro, fasi esecutive*. Turin: CLUT.
- Colombo, P. 2000. I metodi della scienza per la conoscenza della fabbrica. *Recupero e Conservazione* 34: 56–57.
- Comune di Soncino 2002. *Concorso nazionale di Progettazione per il Recupero e Ristrutturazione del complesso Ex-Filanda Meroni*. Soncino: Comune di Soncino. CD-Rom.
- EN 13183-2. 2003. Moisture content of a piece of sawn timber – Part 2: Estimation by electrical resistance method.
- Giordano, G. 1993. *Tecnica delle costruzioni in legno*. 4th ed. with A. Ceccotti & L. Uzielli. Milan: Hoepli.
- Kupfer, K. 1997. Moderne Verfahren und Geräte zur Materialfeuchtemessung. In *Feuchttag 1997; Proc. nat. symp., Weimar, 1997*. Weimar: MFPA an der Bauhaus Universität.
- Lavisci, P. & Mannucci, M. 1999. Strutture di legno. Analisi e diagnosi. *Recupero e Conservazione* 26: 26–27.
- Macchioni, N. & Mannucci, M. 2000. Strutture di legno. Tecniche di indagine per la valutazione del degrado biologico. *Recupero e Conservazione* 33: 38–42.
- Mannucci, M. & Togni, M. 2000. Tecniche di indagine strumentale per la valutazione di caratteristiche meccaniche. *Recupero e Conservazione* 31: 54–60.
- Rinn, F. 1989. Eine neue Bohrmethode zur Holzuntersuchung. *Holz-Zentralblatt* 34: 67–81.
- Rinn, F., Becker, B. & Kromer B. 1990. Ein neues Verfahren zur direkten Messung der Holzdicke bei Laub- und Nadelhölzern. *Dendrochronologia* 7: 31–47.
- Tampone, G. 1996. *Il restauro delle strutture di legno*. Milan: Hoepli.
- Tampone, G., Mannucci, M. & Macchioni, N. 2002. *Strutture di legno*. Milan: DeLettera.
- UNI EN 335-1:1993, "Durability of wood & wood based products. Definition of hazard classes of biological attack. General".
- UNI EN 335-2:1993, "Durability of wood & wood based products. Definition of hazard classes of biological attack. Application to solid wood".
- UNI EN 518:1997, "Structural timber. Grading. Requirements for visual strength grading standards".
- UNI EN 844-3:1998, "Round and sawn timber – Terminology – General terms relating to sawn timber".
- UNI EN 844-4:1999, "Round and sawn timber – Terminology – General terms relating to moisture content".
- UNI EN 844-7:1999, "Round and sawn timber – Terminology – General terms relating to anatomical structure of timber".
- UNI EN 844-9:2000, "Round and sawn timber – Terminology – General terms relating to features of sawn timber".
- UNI EN 844-10:2000, "Round and sawn timber – Terminology – General terms relating to stain and fungal attack".

The historic side-walls of the Navigli canals in Milano: in situ and laboratory tests for the structural conservative project

A. Migliacci, P. Ronca, P. Crespi & G. Franchi

Depart. of Structural Engineering, Politecnico di Milano, Milan, Italy

F. Bianchi

Mapei S.p.A., Milan, Italy

S. Di Martino

Municipality of Milano, Milan, Italy

ABSTRACT: The paper gives significance at first to an historic overview of the origin and development of the network of the Navigli canals, strictly related to the history and growth of Milano itself. Focusing the architectonic and historical meaning of the today remaining canals, the significance of the salvage of the related structural components is underlined. The calibration procedure of some different in situ and complementary laboratory tests on the side walls in a “pilot site work”, and, subsequently in different positions, where the first rehabilitation site work has been open, are described. The aim is of suggesting a guide line for the conservative rehabilitation project of the ancient masonry walls, under those specific physical conditions and requests of the Antiquities National Authority, that are similar to those which may be found in citadels walls or even in the different structural components of the masonry arch bridges.

1 HISTORIC OVERVIEW

The Milano's city history is strictly bound to the geographical history of rivers and water routes, characterizing, since at least the Roman time, geological configuration of the northern Italy's land. Figure 1 testifies of the hydro-network (canals and rivers) surrounding Milano during the last centuries of the Roman empire. The three concentric lines define the city border, starting from the center part, of Roman, medieval (about XIII century) and Spanish period (XVII century), all characterized by water defense ditches, that became navigable canals.

Through rivers and canals, Milano became, since the XIV century, one of the most important commercial venue with Switzerland. The commercial harbor downtown Milano had his major development during XVI and XVII centuries, with a network of Naviglis crossing the town and reaching even the boundary of the Venetian Republic. Milano developed its peculiar attitude of commercial city, thanks mostly to this hydraulic network.

The problem of different levels among lakes, rivers and the Milano's harbor (even 56 meters) was solved with a system of locks, some of them designed by



Figure 1. Hydro-network surrounding Milano at the end of Roman empire.

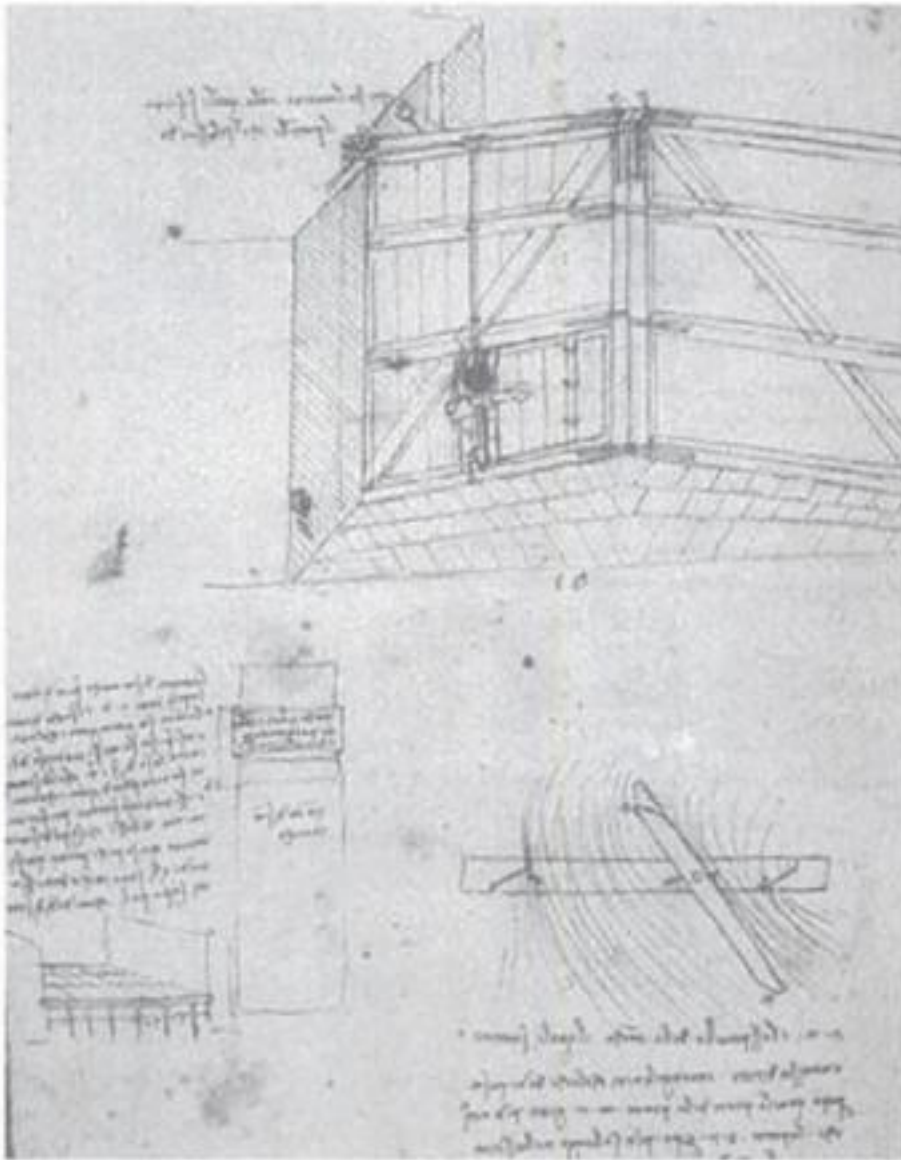


Figure 2. Codice Atlantico by Leonardo da Vinci.



Figure 3. Lock called "Conca dell'Incoronata".

Leonardo da Vinci (Fig. 2). The lock called "Conca dell'incoronata", built according to the engineeristic suggestions of Leonardo, was visible in its overall complex hydraulic system until some decades ago, see Figure 3.

The Navigli network reached its largest extension, more than 250 km, during the nineteenth century; many nobile villas and powerful monasteries were built near the sites of the Navigli and they are still standing today. During the last decades of the XIX



Figure 4. The today "via Laghetto" very close to the cathedral.



Figure 5. The today "via della chiusa" downtown Milano.

century, mainly because of the railway development, the commercial appeal of the Navigli declined.

The landscape in the surrounding and downtown Milano were indubitably characterized by the crossing Navigli water route network, whose memory are the actual numerous toponomastic names; the pictures in Figures 4 and 5 recall the views of the today streets, still called "via Laghetto" (small lake street) and "via della chiusa" (lock street). The first decades of XX century are testimony of a city crossed by numerous arch bridges, even with important decorations (see Figure 6 "ponte delle sirene"). Starting from the forties, the works of covering the water canals downtown Milano began, destroying even hydraulic plants, as shown in Figure 7.



Figure 6. "Sirene" bridges, today no more visible.



Figure 7. Navigli covering site-works.

2 ACTUAL REMAINING HYDRAULIC STRUCTURES

During the first half of the XX century, due to the increasing need of car routes, the Naviglis downtown Milano were covered destroying many hydraulic plants, as was the main part of the harbor. What remain inside Milano of these canals now is under the Conservation Architectural Authority. In the last 20 years the both sides of the Naviglis still crossing the city became the artistic quarter and a live commercial and tourist attraction, like happened in many European cities, see for example the restored locks and canal of Figure 8, in central London.

But, since many decades, the maintenance of the structural components, like foot-arch-bridges, locks and most of all side walls was abandoned, living the structures in very unsafe conditions. Moreover, intensive building constructions, increasing in the cars and



Figure 8. Example of recent restoration downtown London.



Figure 9. Example of today's sidewall.

busses traffic, progressive excavations for civic services worked together against the safe of stability of the side walls, in particular those of the canal called Naviglio Grande, being its structures the most ancient.

Scarce are the documents describing the building techniques of the side walls. It is possible to suppose that only at the end of XVIII century the compacted soil banks confined by wooden piles, have been in some parts renewed using stones or even brick masonry. Only from the beginning of XIX century (Napoleon period) the maintenance of the side walls started with the use of cementitious mortar to bound the bricks (Celona & Beltrame 1982, Maffei 1984, Bruschetti 1972). Actually the static interventions were sporadic and limited, giving the results at present visible: the walls are a patchwork of different materials and construction techniques, as it is shown, just an example, in Figure 9.

The ancient walls are mostly hidden; moreover there is no written documentation of the material, geometry and type of foundation used. From the archives, it is possible to guess that the brick or block section of the

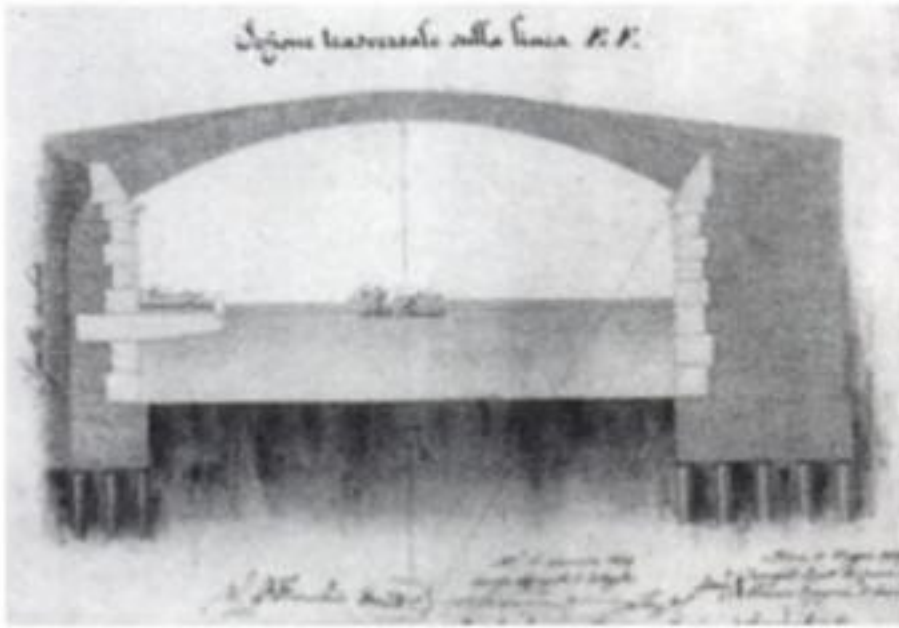


Figure 10. Example of project with wooden pile foundations.



Figure 11. Rests of wooden piles.

wall were built on wooden pile foundations, as shown in examples of Figures 10 and 11.

The problem of knowing the actual geometry was first analyzed by computing the minimum dimensions required to guarantee the equilibrium of the wall as it is summarized on Table 1. This Table takes into account different geometries for a simple rectangular cross section gravity wall, in terms of height H and width b , and for the soil properties (specific weight $\gamma_s = 20 \text{ kN/m}^3$ and friction angle $\phi_s = 30^\circ$). A specific weight of the

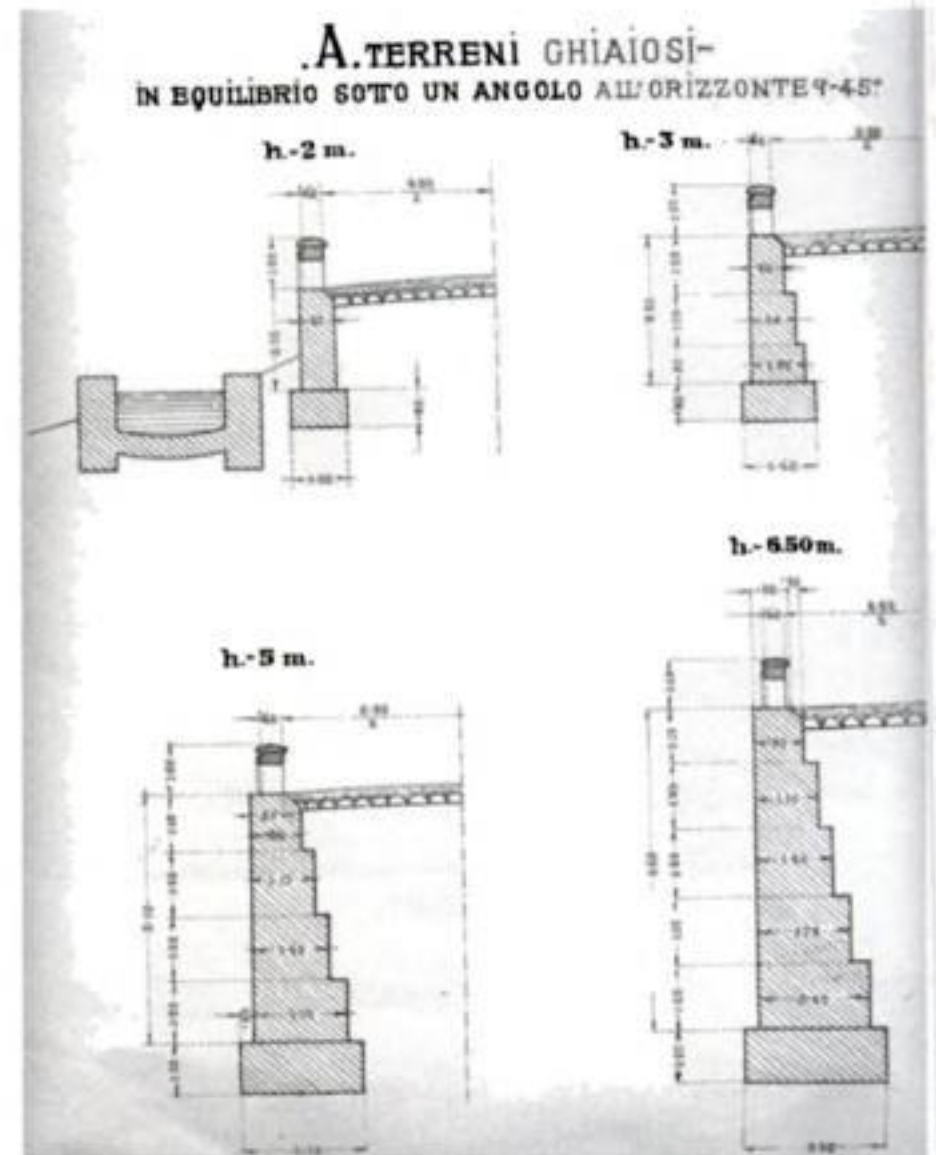


Figure 12. Suggestion from masonry hydraulic wall manual.

Table 1. The allowable minimum geometric requirements for the "gravity wall".

b [m]	H [m]	W [kN/m]	S_s [kN/m]	S_q [kN/m]	M_R [kNm/m]	M_S [kNm/m]
0,50	3,00	27	30	10	7	45
0,75	3,00	41	30	10	15	45
1,00	3,00	54	30	10	27	45
1,25	3,00	68	30	10	42	45
1,50	3,00	81	30	10	61	45
0,50	2,50	23	21	8	6	28
0,75	2,50	34	21	8	13	28
1,00	2,50	45	21	8	23	28
1,25	2,50	56	21	8	35	28
1,50	2,50	68	21	8	51	28

masonry $\gamma_m = 18 \text{ kN/m}^3$ has been assumed, and a live load $q = 10 \text{ kN/m}^2$ has been applied. According to different cases, the capacity of the wall versus the external actions in terms of the resisting M_R and applied M_S moments are shown in the last two columns. These simplified calculations clearly show the minimum level below which equilibrium conditions can not be satisfied, moreover hypothesizing compact material inside the wall.

Because it is impossible to use large and deep excavations all along the wall, unless traffic is restrained in a large section of the town, and also because of

the presence of a network of active underground civic services, it was decided to perform a program of in situ and laboratory tests with the double aim of either achieving better characterization of the actual local geometry and physic and mechanical properties, either optimizing the calibration procedures of non destructive tests, in particular those based on radar and sonic principles.

3 IN SITU AND LABORATORY TESTS

A program of in situ and laboratory tests has been performed with the double aim of better characterization of the actual geometry and the mechanical properties of the wall under consideration. The following tests were performed and mutually related (Bonizzi 2003) during the spring period without water in the channel: localized excavations in the inner part of the side-wall, geotechnical boreholes, core-drills, endoscopic inspections and laboratory test for the material characterization. It was immediately clear that the results of radar technique were unreliable because of the persistence presence of water in the walls and in the surrounding soil, as it was confirmed also by the laboratory tests on mortar and bricks.

Here just some significant results are reported and correlated, for their correct implementation and useful indications for the best structural conservative rehabilitation project.

The most significant discovery obtained from the campaign of the in situ tests can be summarized as follows:

- not only the material, but also the width of the wall is mostly variable;
- generally foundations are absent, or, at least, the wall is provided by a limited enlargement.

The tests on material samples, based on X ray techniques, termogravimetry, PH measurement and more chemical and mechanical analysis are reported on Mapei (2003). Here we just underline the material physical properties found, strictly correlated with the mechanical properties:

- the mortar presents no more cementitious component;
- high porosity either for the mortar as for the bricks (Figs 13, 14);
- high water absorption;
- average mechanical good conditions for the bricks;
- low presence of soluble salts, as the consequence of a wash out process.

A campaign of sonic tests was performed and calibrated by using small nearby excavations that gave direct information on actual geometry and consistency of the wall. The knowledge of these parameters

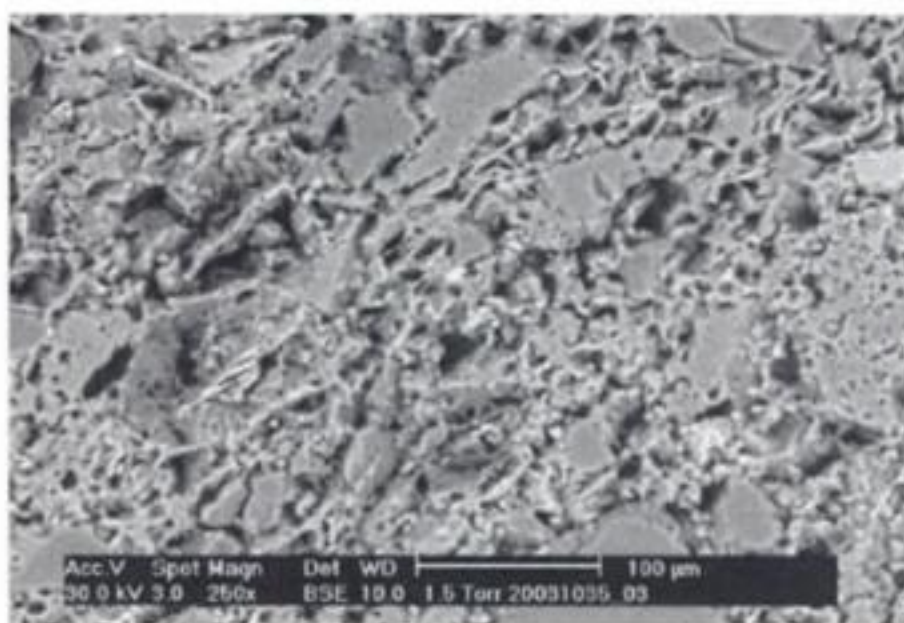


Figure 13. Brick electronic microscopy.



Figure 14. Mortar enlargement showing the absence of cementitious component.

allowed the selection of the best suitable sonic frequency and wave length to use for computing a consistent velocity, which is the basic parameter for defining the possible thickness and the average materic consistency of the wall. As a matter of fact, wave attenuation is useful to obtain information on how to relate the sonic wave to the physical degradation of the wall. As it is known, sonic techniques to characterize a medium properties are successfully used in the case of metallic material or for detecting underground discontinuities. In the case of brick masonry, the method has been tested and calibrated in the field and in laboratory prototypes, mostly in the last decades. As it was shown (Ronca 1993, Ronca 1995) by testing samples constructed with pre-established percentages of voids in the mortar layers, the methods using ultrasonic frequencies are not best suited to detect small voids, frequently present in the walls of historic buildings, which are responsible of consistent reductions of mechanical properties of masonry structures.

city. Non destructive tests can be used with the aim to determine the realistic value of parameters, such as shape, homogeneity and actual thickness of walls that have been built or reconstructed during the centuries. For these purposes a coordinated in situ and laboratory tests have been implemented, with a focus on calibration procedures of sonic wave propagation technique.

ACKNOWLEDGEMENT

The authors acknowledge the regional and municipality administrations for their continuous assistance, the technicians of the MAPEI S.p.A. laboratory, Prof. J. Cascante of Waterloo University, Canada and Mr A. Bonizzi, graduate student at that time, who helped everybody of us in achieving the best results.

REFERENCES

- Bonizzi, A. 2003. *Indagini e taratura di prove non distruttive in situ per il consolidamento conservativo dei muri spondali dei Navigli: nuovi sviluppi delle prove soniche*. Civil and Environmental engineering degree thesis, Politecnico di Milano, Milano, Italy.
- Bruschetti, G. 1972. *Istoria dei progetti e delle opere per la navigazione interna del Milanese*. Cisalpino Goliardica.
- Celona, T. & Beltrame, G. 1982. *I navigli milanesi, storia e prospettive*. Provincia di Milano.
- Maffei, L. 1984. *Navigli '80*. Gammalibri.
- Mapei 2003. *Rapporto sull'analisi de campioni di muratura dei muri spondali dei Navigli*.
- Ronca, P. 1993. Experimental investigations on masonry specimens with ultrasonic method; reliability and actual limits. *ARCO 1st Nat. Congr.*, Rome, Italy.
- Ronca, P. 1995. Critical review of two non-destructive tests for old buildings. *Fourth International Masonry Conference*, London, UK.
- Ronca, P., Cascante, G., Crespi, P. & Franchi, G. 2004. Leonardo da Vinci's Channel System of Milano: preliminary tests on the side walls for the restoration design project. *SAGEEP 2004*, Colorado Springs, USA.
- Zerwer, A., Cascante, G. & Hutchinson, J. 2001. Verification and finite element simulation of surface waves. *Journal of Geotechnical and Geoenvironmental Engineering*, ASCE, Vol. 128, No. 3, pp. 250-261.

Application of ultrasonic Rayleigh wave to testing of masonry materials

M. Skłodowski

Institute of Fundamental Technological Research Polish Academy of Sciences, Warszawa, Poland

ABSTRACT: The paper describes the use of ultrasonic edge transducers for testing the properties of masonry materials, both fresh-made and weathered, and after the treatment with colloidal silica. The method proposed is completely non-destructive because no additional coupling material is used, and this is particularly important in the case of testing historical structures where no damage or pore filling should be introduced. The paper presents principles of surface Rayleigh wave measurement by means of edge transducers, as well as basic theoretical considerations and the experimental setup. Finally, the results are given of laboratory testing of marbles and bricks as well as of in situ testing of brick masonry originating from a gothic church in Poland.

1 INTRODUCTION

Rayleigh wave was primarily used in stone testing for measurement of elastic constants of stones (Pinińska 1986). This comes from the fact that elastic constants can be expressed by means of longitudinal, compressive and transversal, shear wave velocities.

Let us denote the measured velocities of shear and longitudinal waves as V_s and V_l respectively. Then the material constants called “dynamic material constants” can be expressed by the equations

$$\nu_d = \frac{0.5 - (V_s/V_l)^2}{1 - (V_s/V_l)^2}$$

$$E_d = \rho V_l^2 \frac{(1 + \nu_d)(1 - 2\nu_d)}{(1 - \nu_d)}$$

where ν_d is the Poisson's ratio, E_d is the Young's modulus and ρ is the material density.

The shear wave velocity can be evaluated via Rayleigh surface wave V_R velocity measurements which can give a good approximation of the former according to formula $V_s = V_R/0.9$, valid for typical values of the Poisson's ratio.

Generally, surface wave velocity measurements are made using industrial transducers in the frequency range of a few MHz. The measurements are taken mostly on metals, and they use the influence of the second critical longitudinal wave incidence angle on the border between the polymethyl-metacrylate (PMMA) wedge and the tested material. Introducing the wave

with the PMMA wedge needs also some coupling media.

An interesting study of the Rayleigh wave propagation in Dionysos Marble in the Athens Acropolis Parthenon (Stavropoulou et al. 2003) was done with transducers made of a mixture of tungsten particles embedded in epoxy resin. The authors report that transducers were not strong enough so unfortunately several pairs of them were had to be used for completing the research.

Rayleigh waves can also be generated in various materials by means of solid state lasers built on Neodimium doped Yttrium Aluminium Garnet crystals (Nd:YAG laser) using an ablation generation mechanism. This kind of technique can give a valuable insight into the material heterogeneity (Owino et al. 1999) but equipment cost is very high and the portability is much lower than that of edge probes.

The edge probes (Peński 1984) can introduce the surface wave in various kinds of materials without any coupling. This is very important in the case of porous materials where coupling media can get inside and thus significantly modify wave propagation conditions.

The described probes generate the Rayleigh wave which penetrates an outer skin layer of the tested material to the depth of a few millimeters only. Thus measured wave velocities and/or attenuations are not influenced by bulk material properties which makes the method suitable for a detection of changes of elastic properties of the surface of materials. This property seems to be very suitable for evaluation of stone strengthening procedures based on impregnation of a material with colloidal silica.

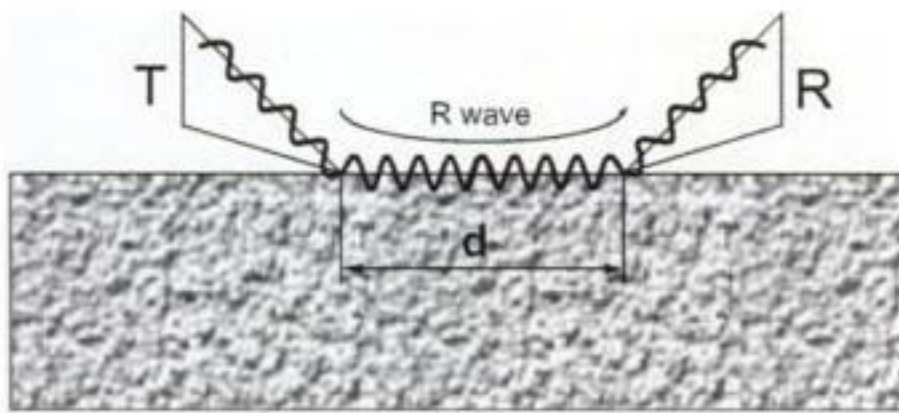


Figure 1. Schematic diagram of surface wave generation with edge probes.

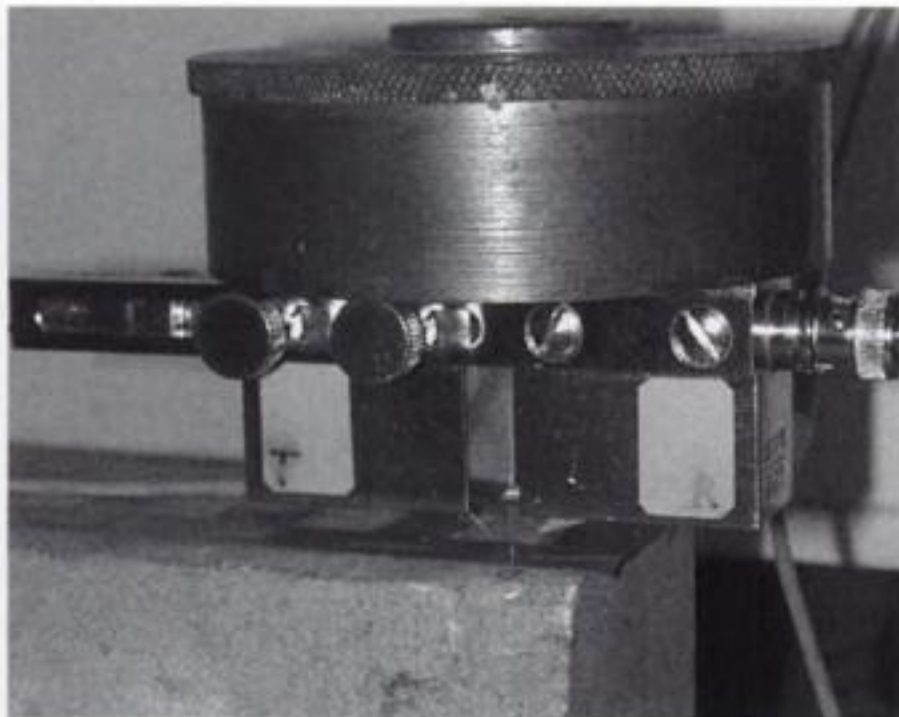


Figure 2. Edge probes pressed against the surface of a stone specimen prepared for impregnation.

2 MEASUREMENT METHOD

2.1 Wave generation

Piezo-transducers are glued to the surface of steel edges which guide the ultrasonic wave to the edge nibs (Pęski & Ranachowski 1988) which are pressed against the specimen surface as shown in Figure 1. Measurements are made using one transmitting and one or two receiving transducers spaced at known distances along a straight line on the surface of the specimen.

Up to present the edge probes for frequencies from 1 MHz to 4 MHz were constructed and used. The amount of energy delivered to the surface of materials depends strongly on the surface conditions but pressing the probes with a force of approx. 10 N, as shown in Figure 2, usually solves the problem.

2.2 Wave velocity measurement

There is a high attenuation of ultrasonic waves in most building industry materials like stones, rocks, concrete etc. for the frequency range used in the described experiments. As a result a short distance of a few

centimeters between transmitting and receiving transducers must be maintained, and hence a short measurement base should be used for ultrasonic wave velocity measurements (Skłodowski et al. 2002). Fortunately enough, the short measurement base is an advantage in the case of detecting local anomalies in tested material. For greater distances, averaging the measurements along a full path can give the desired value together with variation of the measured velocity.

The developed experimental equipment consists of a portable computer, a defectoscope card and an oscilloscope card, put together with batteries into a metal case, with the edge probe being connected to the defectoscope card (Skłodowski et al. 2003). Rated frequency of the probe is 1.25 MHz.

All elements of the equipment can be seen in Figure 4 which shows measurement of the surface wave propagation in brick masonry in a gothic church.

The equipment was calibrated prior to the experiments by measuring propagation time of the surface wave along two different distances between edge nibs. Calibration measurements were taken using a steel caliper, PMMA, glass and aluminum specimens to make sure that the calculated time delays of the probe and electronic devices are correct.

The propagation time of the surface wave was calculated using correlation procedure in the spectral domain of the recorded signals and a time shift between the wave recorded in calibration experiments and the wave measured was found.

3 EXPERIMENTS

3.1 In laboratory

Brick and marble materials were chosen for experimental studies of surface wave propagation in both unimpregnated and impregnated specimens.

A brick was excavated during reconstruction works in a XIV century church but is actually not that old.

Marble materials were of two types. One marble specimen was from Sweden and was exposed to natural weathering conditions during the period of one year (within TEAM Project of EU 5th FP). Two other specimens were of Goia Marble: one specimen was of fresh intact rock and the other specimen was exposed to one cycle of heating in 70°C. All four samples were tested under air-dry conditions, both before and after the impregnation.

An example of specimen preparation is shown in Figure 3.

Parallel lines marking a contact position of the edge nibs of the probe were drawn with a pencil on the specimen surface. Then a plastic adhesive tape was used to define individual measurement cells of area of 2 cm² each as well as to separate one cell from another. Then

Table 1. Colloidal silica impregnants.

Impregnant	Type	Active ingredient	Application range
No. 1	Strengthenener	Silicic acid ethyl ester	Fine to coarse pored sandstones, volcanic rocks (e.g. tuff), weathered bricks
No. 2	Hydrofobizing impregnation agent	Alkylalkoxy silane	Porous, cementitious building materials as sand-lime brick, natural stone, fairfaced brick masonry work,
No. 3	Surface repellent	Aqueous silicone compound	Building materials on floor and wall areas, interior and exterior



Figure 4. Measurement of surface wave propagation in brick masonry of a gothic church.

positions on both walls. At each point the surface wave velocity was measured in horizontal and vertical directions of the wave propagation so altogether 16 measurements were carried out on each of the walls.

Figure 4 shows the measurement in point 3 on the south wall, taken in the vertical direction. Wave profiles in time and spectral domains were also recorded.

4 RESULTS

4.1 Measurements in situ

In situ measurements showed that in highly deteriorated bricks there exists a multi-layered structure of the surface. These material layers have thickness smaller than the length of the applied ultrasonic wave. As a result no surface wave can propagate but a multi-wave signal is detected instead.

Qualitative results confirm greater deterioration of the south wall where only ten recordings out of 16

measurements were successful while in contrast on the north wall of the tower the wave transmission through the bricks was recorded in all 16 cases.

Rayleigh wave velocities were successfully measured on the north wall at three measurement points (1800 m/s, 1310 m/s and 1890 m/s).

At the same time there was no successful Rayleigh wave measurements on the south wall, and recorded wave profiles of the measurements carried out on this wall show more clearly multi-wave nature of the received signals.

The developed portable equipment allowed us to perform the in situ measurements and wave profiles recording for nearly two hours before computer batteries run down.

4.2 Laboratory results

Laboratory experiments with the brick showed no reliable signals before impregnation and also in the case of low silica concentration (0.25, 0.5 and 1.0 l/m² of impregnant No. 1). However, for higher concentrations (1.5 and 2.0 l/m² of impregnant No. 1) Rayleigh waves were recorded, and their respective velocities were 1230 m/s and 1340 m/s.

Figure 5 shows receiver response in time domain before impregnation and Figure 6 its response at the same point on the brick after impregnation with surface density of impregnant No. 1 equal to 2.0 l/m². One should notice also the difference in vertical scales in the both figures.

Naturally weathered marble treated with two impregnants also showed partial recovering of its elastic properties because after impregnation Rayleigh wave was observed in two out of three points for which the measurement was impossible before impregnation.

All laboratory results are summarized in Figure 7.

Good quantitative results were obtained for Goia Marble. Elastic properties were improved by

wave velocities for impregnated fresh and thermally weathered specimens were practically the same.

ACKNOWLEDGEMENTS

The research described in this paper was conducted with financial support of the EU 6 Framework Program (MCDUR, Contract G6RD-CT2000-00266, & ACOUTHERM, Contract GRD3-2001-60001) as well as of the Polish State Committee for Scientific Research (63/E-89/SPB/5.PR UE/DZ 150/2003-2004).

Samples of colloidal silica for impregnation treatment were kindly supported by Remmers-Poland.

REFERENCES

- Pęski, Z. 1984. Nowa metoda generowania fali powierzchniowej. In: *13 Krajowa Konferencja Badań Nieniszczących, Kozubnik*. (in Polish).
- Pęski, Z. & Ranachowski, J. 1988. *Patent Pending 142739*, Poland.
- Pinińska, J. 1986. Surface wave velocity as a laboratory non-destructive control of the rock properties. In *Proc. 5th Intern. IAEG Congress, 20–25 October 1986, Buenos Aires*. Rotterdam, Boston: Balkema.
- Owino, J.O. & Jacobs, L.J. 1999. Attenuation measurements in cement-based materials using laser ultrasonics. *Journal of Engineering Mechanics* 125(6): 637–647.
- Skłodowski, M., Pinińska, J., Łukaszewski, P., Bobrowska, A. & Gutkiewicz, P. 2002. Report on Ultrasonic surface wave velocity measurements. *MCDUR-ACUTHERM 6FP Project (unpubl)*.
- Skłodowski, M., Pinińska, J., Łukaszewski, P., Bobrowska, A. & Gutkiewicz, P. 2003. Report on Ultrasonic surface wave velocity measurements. *MCDUR-ACUTHERM 6FP Project (unpubl)*.
- Stavropoulou M., Exadaktylos G., Papamichos E., Larsen I. & Ringstad C. 2003. Rayleigh wave propagation in intact and damaged geomaterials. *Int. J. Rock Mech and Min. Sci.* 40(3): 377–387.
- Remmers (UK) Ltd. 2004. <http://www.remmers.co.uk/>

Mosaic-grouting monitoring by ground-penetrating radar

P. Côte & X. Dérobert

Laboratoire Central des Ponts et Chaussées, Bouguenais, France

A. Miltiadou-Fézans

Directorate of Technical Research for Restoration, Hellenic Ministry of Culture, Athens, Greece

N. Delinikolas

1st Ephoria of Byzantine Antiquities, Hellenic Ministry of Culture, Athens, Greece

N. Minos

Directorate for the Conservation of Ancient Monuments, Hellenic Ministry of Culture, Athens, Greece

ABSTRACT: Due to the 1999 Athens earthquake, both the masonry structure and the mosaics of the Katholikon of Dafni's Monastery have suffered severe damages. In order to design the appropriate intervention scheme for mosaic conservation, first for the detection and mapping of delaminated mosaic's areas, and second for the monitoring the movement of the grout during injection, using a non-destructive testing such as ground-penetrating radar, presents a great interest. Two experimental studies have been realized on the mosaics. The first one concerns GPR mapping on some mosaics in-situ, in order to find out the exact location of doubtful zones including delamination, changes of structures (i.e. recent repairs) or buried heterogeneities. The second one is focused on the GPR monitoring of mosaic grouting. Thus, a physical model has been built, including known voids in order to develop a survey methodology. Results show that one can follow the grouting spreading inside the physical model.

1 INTRODUCTION

The Katholikon (church) of Dafni's Monastery is one of the most important monuments of the middle-byzantine period (Millet 1899, Bouras 1998, Delinikolas et al. 2003), already inscribed in the World Heritage List of UNESCO and well known for its excellent mosaics from 11th century. Due to the 1999 Athens earthquake both the masonry structure and the mosaics have suffered severe damages (Miltiadou-Fezans et al. 2003). In order to design the appropriate intervention scheme, the detection and mapping of mosaic's areas, which have been detached from the masonry, using non destructive testing, presents a great interest. On the other hand, as the application of injection techniques by means of suitable hydraulic grouts is often used in the case of detached mural mosaics, the possibility of using non destructive procedures to monitor the movement of the grout during injection could be very useful in order to assure that the voids are filled without endangering the mosaics' substrata.

Non-Destructive Testing (NDT) methods have begun to be commonly used, for historical buildings'

investigations, for only few years. Old masonry structures from civil engineering, such as bridges, present similar pathologies than masonry historical buildings. That is why NDT can participate actively to the evaluation of such structures (Colla et al. 1997, McCann & Forde 2001, Binda et al. 2003).

The Ground-Penetrating Radar (GPR) is a very useful technique, lying in a high-speed acquisition rate. GPR is mainly dedicated to the detection and location of hidden heterogeneities in the structures at depths from 5–6 cm (at very high frequencies, over 1 GHz) to up to a meter (at lower frequencies, about 500 MHz) (Maierhofer & Leipold 2001).

For particular cylindrical structures, like pillars, NDT tomography technique have been developed in order to obtain qualitative information, while mapping a 2D-transversal section, on the detected heterogeneities (Valle et al. 1999, Flint et al. 1999).

In the present application, two experimental studies have been realized on Byzantine mosaics. The first one concerns GPR mapping on some mosaics in-situ, related with their very near bearing-structure, in order to locate doubtful zones including delamination,

changes of structures (i.e. recent repairs) or buried heterogeneities. The second one is focused on the GPR monitoring of mosaic grouting.

2 MOSAIC MAPPING

2.1 Presentation of the problem

Many of mosaics have been damaged due to earthquakes that occurred throughout the history of the monument. In the masonry drums of the dome and the arches, that support squinches, there are many cracks visible on the surface.

The load bearing elements of the church are three-layered masonry walls, consisting of two stone masonry layers and a zone in-between with loose filling material. The mosaics are attached to the walls by mortar, the quality of which has a great importance for an adequate sustainability.

For a reliable preservation of these mosaics, it is necessary to evaluate correctly the very-near structure bearing them, and localize any voids behind the surface. Visual inspections and manual-sonic investigations represent the classical procedure for conservators in order to evaluate the substrata of the mosaics (Fig. 2a), and proceed to a specific repair.

In Fig. 2, an example of mapping is shown, realized in-situ by the conservators on the mosaic presented in Fig. 1 (Chrisopoulos et al. 2002). It has to be noticed that the surface of the mosaic is concave. The main limitation of such an evaluation is related to the manual-sonic mapping itself, which is a subjective method, able to obtain only a limited information coming from human-expert senses. Moreover, it is very difficult to have any information about the depth where the voids or heterogeneities are located.



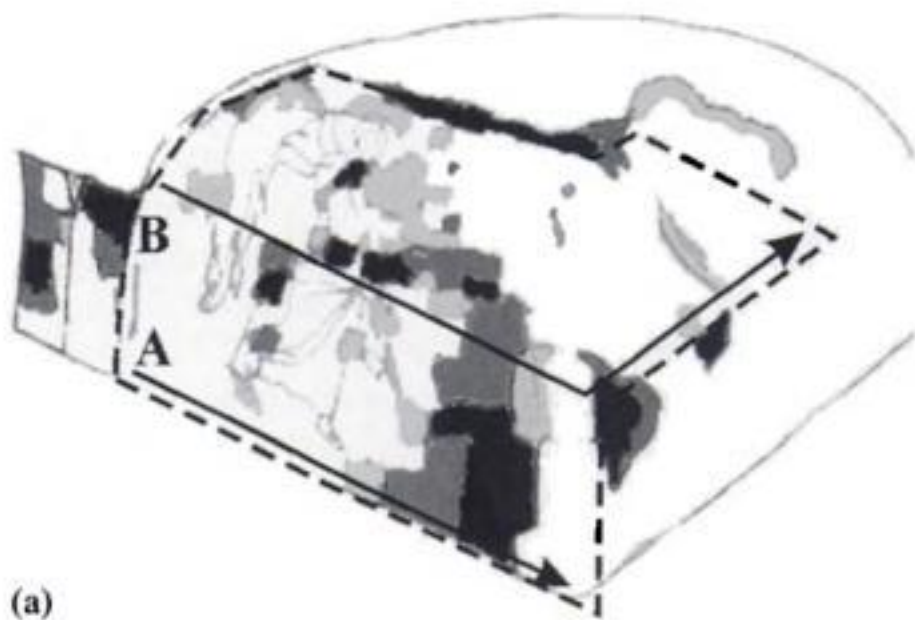
Figure 1. The mosaic “Evangelismos – Annonciation” under GPR testing. Gummed paper positions the GPR profile while protecting the mosaic.

Thus, the maps prepared by the conservators are indicating four zones, where the white color corresponds to sound areas, the light-gray color to slightly detached areas, the dark-gray color to detached areas and finally the black to very detached areas.

Therefore, NDT techniques could be very useful for a complementary and more detailed evaluation of mosaic substrata and masonry state.

2.2 GPR mapping

The principle of GPR consists of an electromagnetic pulse transmitted to the structure, at very high frequencies, with a 1.5-GHz central frequency antenna. The receiving antenna then records GPR impulse signals that contain echoes from the reflections generated by the inner layered structures. The juxtaposition of time



(a)



(b)

Figure 2. Presentation of the current maps prepared by the mosaic’s conservators. (a) Manual-sonic map. white color corresponds to sound areas, light-gray color to slightly detached areas, dark-gray color to detached areas and black to very detached areas. (b) Visual inspection map indicating the damages after the 1999 earthquake. Black areas represent dislocated parts of the supporting masonry, while grey areas correspond to surface cracks.

signals enables to construct a time-section – or GPR profile – (the time unit is the nanosecond), presented with a false gray-color scale, related to the amplitude of the signals, and which gives information of the geometry of the investigated structure (an example of GPR profile is given further in Fig. 4).

Thanks to specific processing from parallel GPR profiles (shown in the dotted area, from Fig. 2a, where arrows positioning the GPR profiles), maps can be constructed from chosen trenches of the investigated medium. Although, a high central-frequency GPR-antenna has been used (1.5 GHz), the expected information, delamination or recent repair just behind the mosaic, is located in the GPR surface echo.

Thus, the energy of the first peak of parallel profiles has been summarized in a map after a subtraction of a calibration signal recorded in a supposed sound area (Fig. 3).

NDT mapping enables to locate areas, which can be considered as more or less different from the chosen calibration zone. Processing is automatic and focuses the human factor on his competence: the interpretation and evaluation of the masonry structure.

Thus, one can roughly discriminate two main areas, a lighter one in the upper part of the map (above the

profile B, in Figs 2a and 3) which properties are close to the ones of the calibration area, and a darker one in the bottom part which could correspond to a different type of structure. Moreover, some details can be seen through the variations of gray-level. These two kind of structures can also be identified on the vertical GPR profile (Fig. 4); the upper part, over 1-m high, shows large deep-echoes which indicate a quite different structure behavior than the lower part of the profile.

Concerning the lower structure, between profiles A and B, one can notice some dark area around of the calibration zone, which shape (dotted line in Fig. 3) could correspond to the one of the detached areas, detected by manual-sonic sounding (in Fig. 2a).

Moreover, in the middle upper part of the GPR map, an area reinforced by a mesh of bars, corresponding to a recent repair, has been localized in a considered sound area (in Fig. 2a). From the horizontal GPR profiles, which were used for the map Fig. 3, five vertical bars have been detected, 10-cm spaced and about 80-cm long. Similarly, vertical GPR profiles have shown ten horizontal bars, 10-cm spaced and about 40-cm long (Fig. 4). It has to be noticed that although the date and the area of the repair was known, the existence of steel reinforcements was not reported in the relevant reports.

Thus, the gray-level scale GPR mapping should offer a complementary instrument in the hands of the mosaic's conservators in order to discriminate various levels of zoning. The evaluation of such approach is still in progress.

A second example, realized on the Virgin Birth mosaic, is illustrated in Fig. 5. The manual-sonic map is compared to the GPR reflectivity map. In this case, the contrasts observed with both methods are smaller than in the previous case (Annonciation mosaic). One of the advantages of the GPR technique comes from the fact that it is possible to compare several mosaics using the same procedure. Then, one could classify the whole set of mosaics of the church with the typology based on the observed degradation. Indeed, the relative subjectivity of the manual-sonic classification do not authorize such comparison between several mosaics.

3 GROUTING CONTROL

3.1 Physical model

The second approach of GPR investigation has focused on monitoring weak-structured mosaic grouting. Thus, a physical model has been built with pieces of thick lime plaster put together with lime mortar, including known void areas in order to develop the survey methodology and define the performances and limits that one can expect.

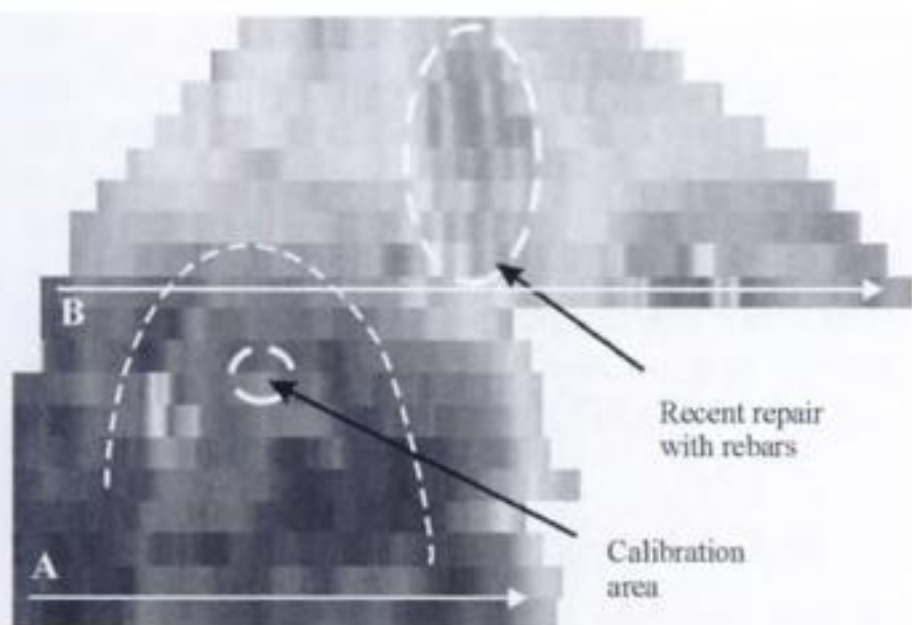


Figure 3. Horizontal GPR mapping of the mosaic presented in Fig. 1. Dark areas correspond to highest differences from the calibration zone.

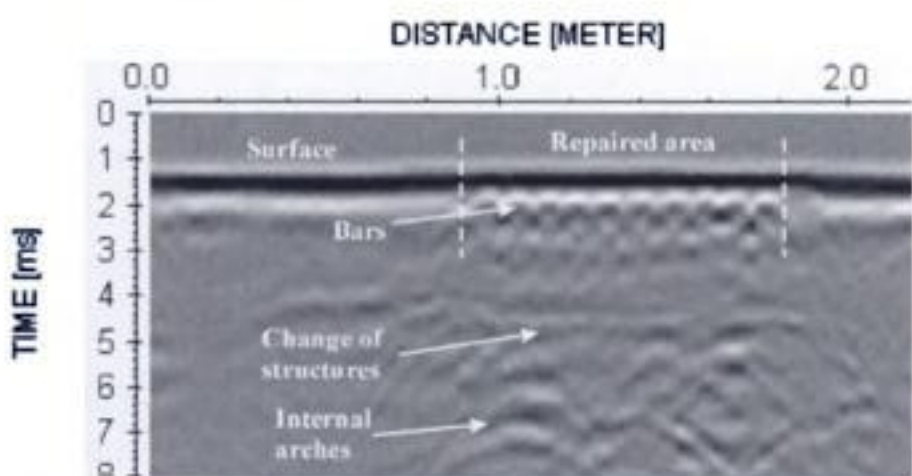
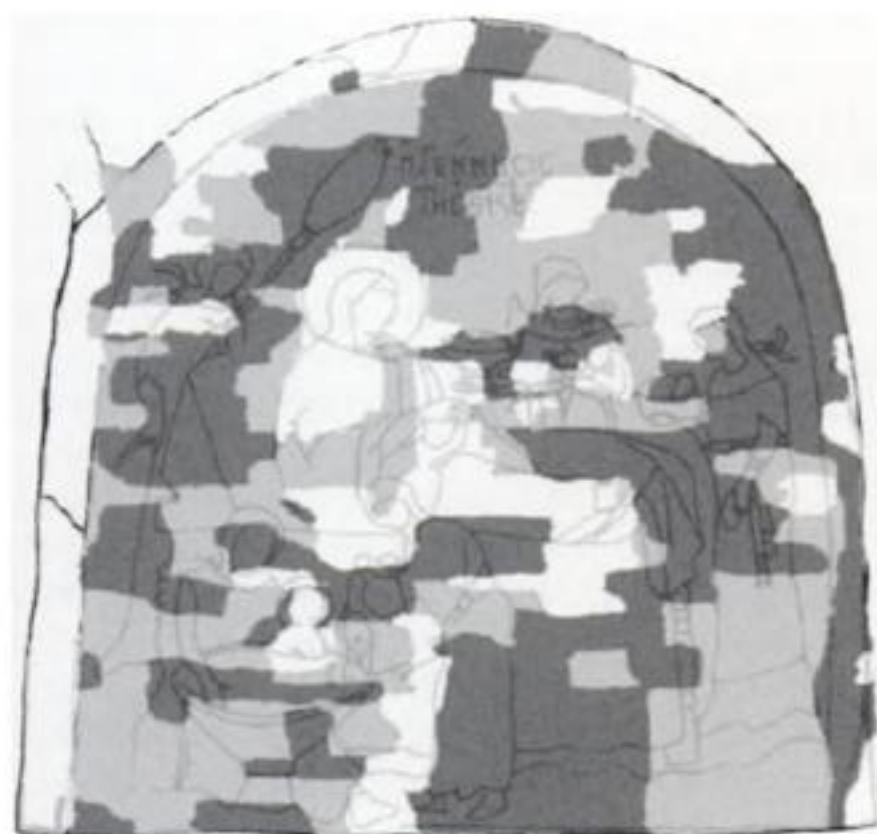
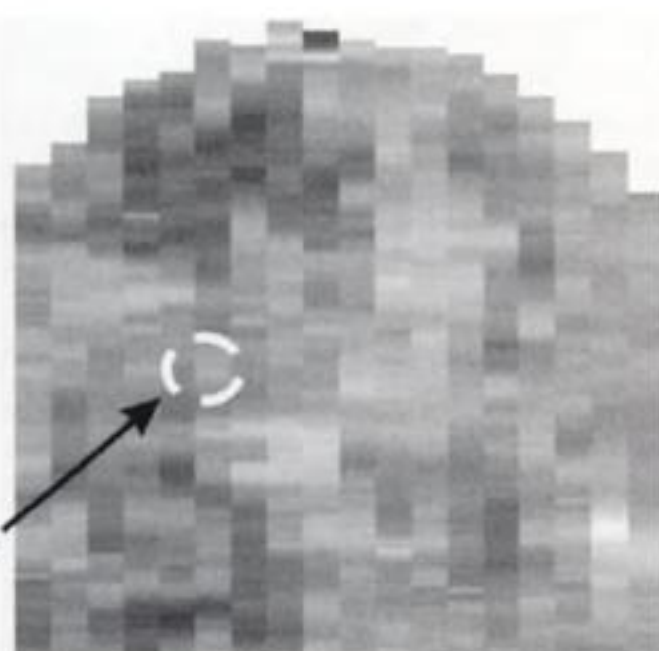


Figure 4. Vertical GPR profile done on the repaired area (down to top).



(a)



Calibration
area

(b)

Figure 5. Mosaic of the Virgin Birth. (a) Manual-sonic map prepared by the mosaic's conservators. (the false-gray level scale corresponds to the one Fig. 2). (b) Vertical GPR map. Dark areas correspond to highest differences from the calibration zone.

The model has been constructed in the Laboratory of the Directorate for the Conservation of Ancient Monuments, in order to be used for the observation of the efficiency of grouting. It consists of two parallel lime mortar plates (42×53 cm, 3,5–4,5 cm thick), which are not completely connected (adjacent).

Before the connection of the edges of the two plates of the specimen, the upper one was cut into smaller pieces, in order to create a non-uniform surface, trying to imitate the existence of cracks in the masonry. The smaller pieces were connected with mortar on the surface. The connection of the plates as well as the filling of cracks was made by lime mortar. The inner surfaces of the plates were not smooth, while the inner voids were about 3 mm to 2 cm wide. Then, the model was



Figure 6. Grouting of the model by a syringe (on the right), and evacuation of the grout through the plastic tubes. Arrows indicate the GPR profiles.

borded by a gypsum plaster panel in order to present a smooth plane to GPR profiles and to avoid important border effects.

For this experiment there were installed three plastic tubes of 5 mm diameter, named A, B and C. The model was positioned with a slope in order to enable the filling of the voids by gravity while grouting (Fig. 6).

The experiment started by injecting the grout that consisted by a special material for conservation works (Ledan TB1) and de-ionised water in proportion 1:2 in volume, while a water-soluble blue colour mineral additive was added.

The grout was injected by position A and the grout came out by positions B and C. The total quantity of grout was 1650 ml (33 syringes of 50 ml).

3.2 Methodology

The GPR principle lays on the measurement of the upper and lower interfaces of the model, assuming that any grouting will induce some GPR delay for the echo from the back interface. Two measurement lines have been chosen, a vertical and a diagonal one, with a 1.5 GHz central-frequency antenna. After every elementary grouting, with a 50-ml syringe, GPR acquisition is realized and averaged on two profiles. Thirty-three elementary injections have been done in more than two hours.

3.3 Results

Double-travel times, picked after every grouting in the model, are summarized in Figs 7 and 8. While grouting, empty areas are filled inducing changes in the EM-characterization of the structure. As result, the averaged velocity is decreasing thus the double-travel

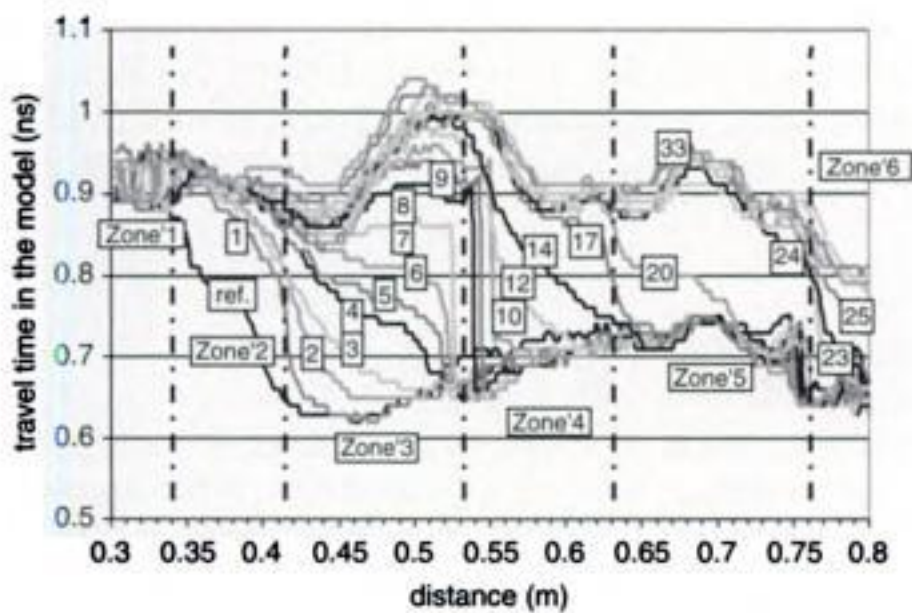


Figure 7. Time variation of the model during grouting on the diagonal profile (estimated $V = 0.1$ m/ns).

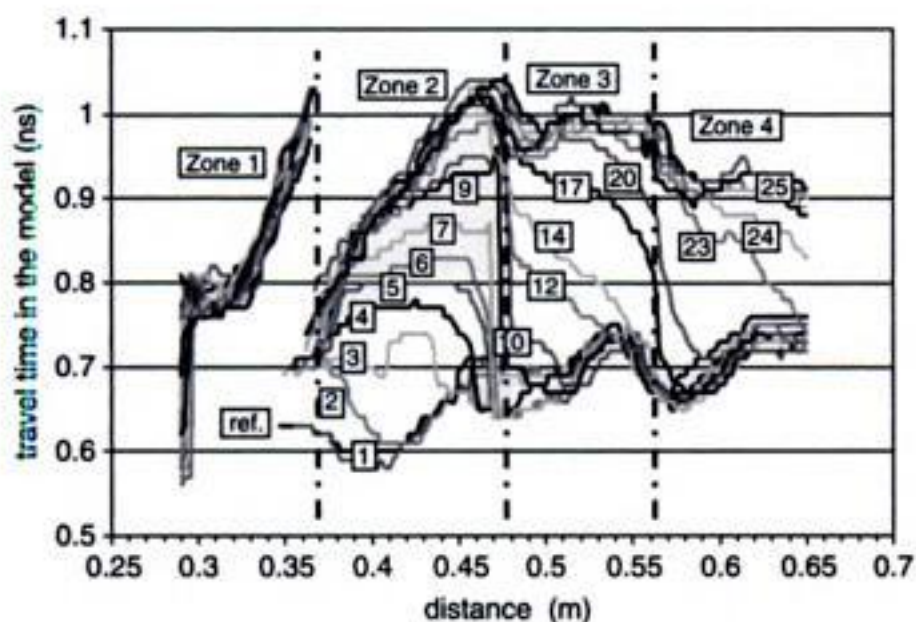


Figure 8. Time variation of the model during grouting on the vertical profile (estimated $V = 0.1$ m/ns).

time increasing. Visible drift from the bottom of the model (left part of the curves Figs 7 and 8) to the top (right part of the curves) is noticed after every elementary grouting, giving a spatial information on the filling location.

Different zones can be distinguished from the diagonal and vertical GPR curves. They are separated by vertical dashed lines in Figs 7 and 8. As the model has been disposed with a slope, while grouting, successive empty cavities have been filled from the bottom to the top, due to the gravity.

The Fig. 9 presents the GPR interpretation in term of grouting location during the grouting process, while combining the information from Figs 7 and 8. Thus, the interpretation proposes the localization of five main grouted zones.

Moreover, one can estimate the elementary volumes of grout for every area, thus giving an average of thickness. Indeed, one can obtain a rough quantitative information considering that a time resolution under 0.05 ns corresponds to about 1 to 2 mm voids filled with grout.

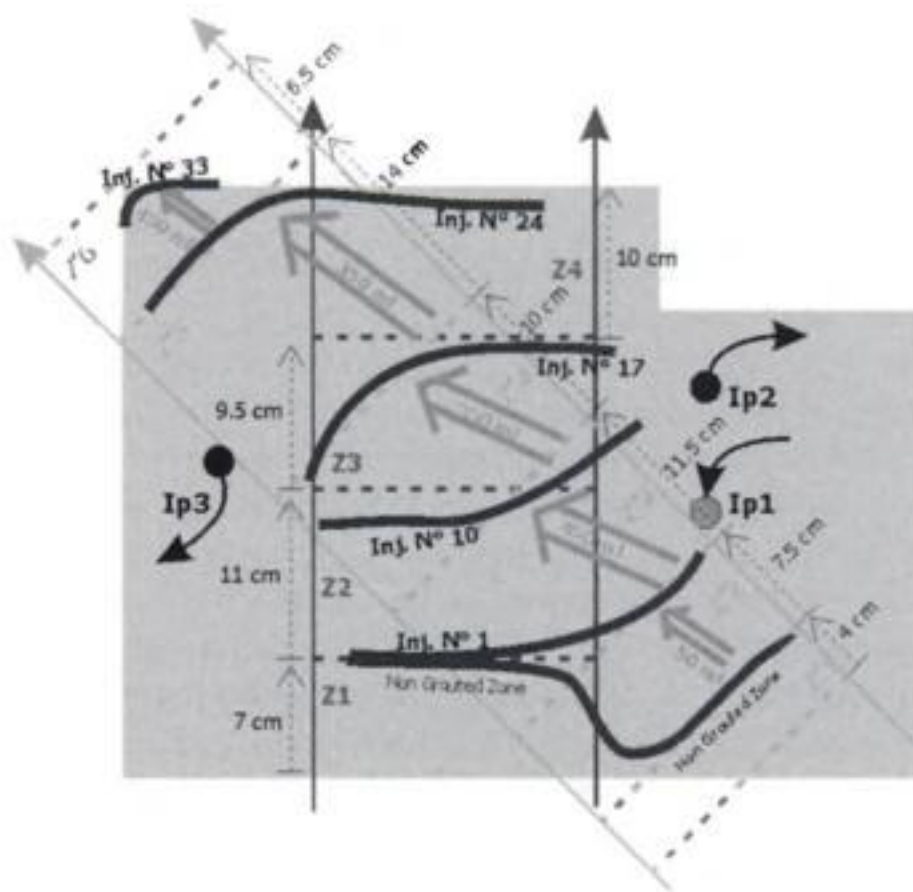


Figure 9. Zonation of the grout front during the grouting process.



Figure 10. Physical model after grouting, cut in the diagonal direction. Values written on the edge correspond to the distance presented Fig. 7.

Although the ratio between the wavelength and the thickness of the voids is too high theoretically for a detection of them, it has been possible due to the moistening of the internal masonry around the grout. Therefore, an important part of the masonry, including the grout, is wet enough to delay the GPR signals and characterize a shift in the double-travel times picking.

Figure 10 presents the result of grouting after sawing the masonry model. One can find on the edge the x-axis of the six zones detected by GPR and shown in Fig. 7. Although, one must be careful while comparing linear (cutting) and planar (3D-reduced-to-2D GPR signals) information, coherent similarity can be found.

4 CONCLUSION

Two GPR approaches related to the investigation of mosaics and their restoration have been presented in this article. The first one is dedicated to the mapping of the energy of the surface echo, which is related to the very near bearing structure. This kind of NDT should be very helpful for conservators in order to obtain a more reliable diagnosis.

The second technique concerns the control of grouting during the process, which enable to locate and quantify the grout inside the first centimeters of the masonry. The experimental feasibility has been demonstrated on a physical model. This point enables us to forecast a methodology of grouting evaluation, in terms of quality, extension and quantity, for ancient mosaics in-situ.

ACKNOWLEDGMENT

The authors want to thank D. Chrissopoulos, E. Anamaterou and F. Georganis, Conservators of Art Works, as well as their team, for their collaboration for the comparison of the NDT with their mapping, the design of the test model and its disposal for this current study.

The fulfillment of the whole project had the constant support of V. Chandakas, General Director for Restoration, Museums and Technical Works, M. Fountoukou, Director for the Restoration of Byzantine and Post-Byzantine Monuments, E. Tsofopoulou, Director of the 1st Ephoreia of Byzantine Antiquities, N. Charkiolakis, Head of the Section for the Studies on Byzantine Monuments and A. Christofidou, Head of the Section for the Execution of Works of the Directorate for the Restoration of Byzantine and Post-Byzantine Monuments.

It has to be acknowledged as well that the application of NDT techniques has constantly the support of the Scientific Committee for Dafni's Monastery Studies and Works, composed by Prof. Ch. Bouras, Prof. T.P. Tassios, Prof. H. Mariolakis and Prof. N. Zias.

The project has been realized by the Directorate for the Restoration of Byzantine and Post-Byzantine

Monuments of the Hellenic Ministry of Culture in collaboration with the "Laboratoire Central des Ponts et Chaussées, Bouguenais, France" and it was funded by the European Union together with the Hellenic Ministry of Culture.

REFERENCES

- Binda, L., Zanzi, L., Lualdi, M. & Condoleo, P. 2003. Complementary of non destructive techniques in the diagnosis of damaged historical structures. *Struct. Faults & Repairs Conf. Proc.*, London, July 2003, p. 9.
- Bouras, Ch. 1998. The Daphni monastic complex reconsidered. AETOS studies in Honor of C. Mango, B.G., Teubner Stuttgart & Leipzig [with an extensive bibliography].
- Colla, C., Das, P.C., McCann, D. & Forde, M.C. 1997. Sonic, electromagnetic and impulse radar investigation of stone masonry bridges. *NDT&E Int.*, 30(4): 249–254.
- Chrisopoulos, D., Anamaterou, D. & Georganis. 2002. Documentation study for the mosaics of the Katholikon of Dafni's Monastery after the 1999 earthquake. *Directorate for the Conservation of Ancient Monuments*, Hellenic Ministry of Culture.
- Delinikolas, N., Miltiadou-Fezans, A., Chorafa, E., Zaroyianni, E., 2003. Study on restoration of the Katholikon of Dafni Monastery, Phase A-Architectural and Historical Survey, Hellenic Ministry of Culture.
- Flint, R.C., Jackson, P.D. & McCann, D.M. 1999. Geophysical imaging inside masonry structures. *NDT&E Int.*, 32: 469–479.
- Maierhofer, C. & Leipold, S. 2001. Radar investigation of masonry structures. *NDT&E Int.*, 34: 139–147.
- McCann, D. & Forde, M.C. 2001. Review of NDT methods in the assessment of concrete and masonry structures. *NDT&E Int.*, 34: 71–84.
- Millet, G. 1899. Le monastère de Daphni, Histoire, Architecture, Mosaïques. *Monuments de l'Art Byzantin*, I, Paris.
- Miltiadou-Fezans, A., Tassios, T.P., Delinikolas, N., Chorafa, E., Zaroyianni, E. & Chandrinou, I. 2003. Earthquake structural problems and urgent measures undertaken to support the Katholikon of Daphni's Monastery in Athens-Greece. *Proc. 8th Int. Conf. STREMAH*, Halkidiki, Greece, may 2003.
- Valle, S., Zanzi, L. & Rocca, F. 1999. Radar tomography for NDT: comparison of techniques. *Journ. Appl. Geophys.*, 41: 259–269.

Ultrasonic testing of properties of mortars

P. Cikrle, J. Adánek & M. Stehlik

Brno University of Technology, Faculty of Civil Engineering, Brno, Czech Republic

ABSTRACT: This paper describes the comparison tests of physical-mechanical properties of mortar on bodies made in forms and on bodies sampled directly from the joints of brick masonry. The goal of the tests was to verify the possibilities of the testing of mortar with low compression strength approximately from 0,4 to 2,5 MPa, which appears commonly in historical masonry constructions. For non-destructive testing of mortar, the ultrasonic pulse method was used and by common standardized procedures the following properties of mortar were determined: volume mass, compression strength, tensile strength in bending and static modulus of elasticity.

On the basis of the test results of various mortar samples with the strength of approx. 0,4 to 2,5 MPa, a statistically important dependence of the velocity of the ultrasonic waves pulse spread on the physical-mechanical properties of mortar – compression strength, tensile strength in bending, static elasticity modulus – was determined.

1 INTRODUCTION

The objective of this part of work was to verify the possibility of applying non-destructive mortar testing on specimens made in moulds and on specimens sampled directly from brick masonry joints. Ultrasonic pulse method was used in the non-destructive mortar testing. Common standard procedures then determined the following mortar properties: volumetric mass, compression strength, flexural strength and the static elasticity modulus. To determine the correlation between the propagation velocity of ultrasonic wave pulses and the abovementioned physical-mechanical properties, four mortar mixes were prepared based on the same lime-cement binder and differing only by their ratios of binder and filler (sand) volumes. Much attention was paid to the effect of water extraction and also to the influence of moisture on the physical-mechanical properties of mortars. Considering the current changes in the effective mortar-testing regulations, two sets of trial specimens were made from each mix. Set-I was made in steel, 40 × 40 × 160 mm moulds with open tops; the excess water was not extracted. Set-II was made using steel frames of the same moulds where the bottom part was replaced with a glass plate. The excess water was extracted from the set-II mortar during its mixing and moulding by means of several layers of gauze and filter paper [ČSN EN 1015-11]. Apart from these trial specimens of regular shapes, mortar was also laid between two bricks so that it could mature in a natural way as it does in masonry. By cutting the produced mortar joints, we obtained

set-III trial specimens. The sets I and II were split into two parts – the first group of specimens was tested in a water saturated state (denoted 'sat') and the second group was tested in a state of natural moisture content (denoted 'moi'). As it was not possible to obtain enough set-III specimens from the joints, they were only tested in the state of natural moisture content.

2 PREPARATION OF MORTAR SAMPLES AND PRODUCTION OF TRIAL SPECIMENS

2.1 Material used

The basic type of the mortar used was a masonry mortar 2.5 N/mm² – manual work, bagged. Its properties were declared to be as follows:

- Grain size: 0–4 mm;
- Volumetric mass of dry mix: 1600 kg/m³;
- Water consumption per one 40-kg bag: approx. 6.5 l;
- Guaranteed flexural strength after 28 days: min. 0.8 N/mm²;
- Guaranteed compression strength after 28 days: min. 2.5 N/mm²;
- Workability time: 3 hours.

The aim of the tests was to verify the possibility of testing mortars with low compressive strength of around 0.4 to 2.5 N/mm², which can commonly be found in historic masonry structures. To achieve the different mortar strengths, the basic bagged mortar mix was mixed with sieved sand with grain sizes from 0 to 4 mm in 4 different proportions. The sand was from

Černovice and its moisture content was lower than 1%. The ratio of the basic mix to the sand for mixes A to D was as follows:

- Mix A: basic mix 33%, sand 67%;
- Mix B: basic mix 50%, sand 50%;
- Mix C: basic mix 67%, sand 33%;
- Mix D: basic mix 100%, sand 0%.

2.2 Trial specimens

The mortar was mixed by a drill with a mixing bit. Fresh-mortar workability tests were carried out for all trial mixes. The plasticity of mortar on shaking table ranged between 170 and 180 mm. The following trial specimens were made from each of the four mixes A to D:

- **Set I:** Six $40 \times 40 \times 160$ -mm prisms in steel moulds according to ČSN 72 2440; the excess water was not extracted.
- **Set II:** Six $40 \times 40 \times 160$ -mm prisms in steel frames on glass plates according to the new standard EN 1015-11; the excess water was extracted by means of two layers of gauze and six layers of filter paper.
- **Set III:** Five bedding mortar joints between two bricks, approx. 10 mm thick. To ensure the same mortar height in the joint, steel prisms of cross section 10×10 mm ran the length of the brick. Specimens were cut from the brick joints to be tested for mortar compressive and flexural strengths. These were prisms of approximate dimensions $20 \times 20 \times 10$ mm for compression strength and prisms of approximate dimensions $20 \times 10 \times 80$ mm for flexural strength.

All trial specimens were processed and stored until the time of testing in the same manner according to EN 1015-11 in order not to introduce other factors to the test results. Half of the prisms from sets I and II were water-soaked for three days before the tests.

3 METHODOLOGY OF MECHANICAL TESTS ON MORTARS

3.1 Flexural strength

The test was carried out in a mechanical testing machine using prisms from sets I and II and the $20 \times 20 \times 100$ mm prisms (set III); see Figure 1.

The trial specimens were placed in a three-point loading system of cylinders perpendicularly to the tamping direction. The flexural strength f_f in N/mm^2 is calculated from the following formula:

$$f_f = 1.5 \frac{F l}{b d^2}, \quad (1)$$

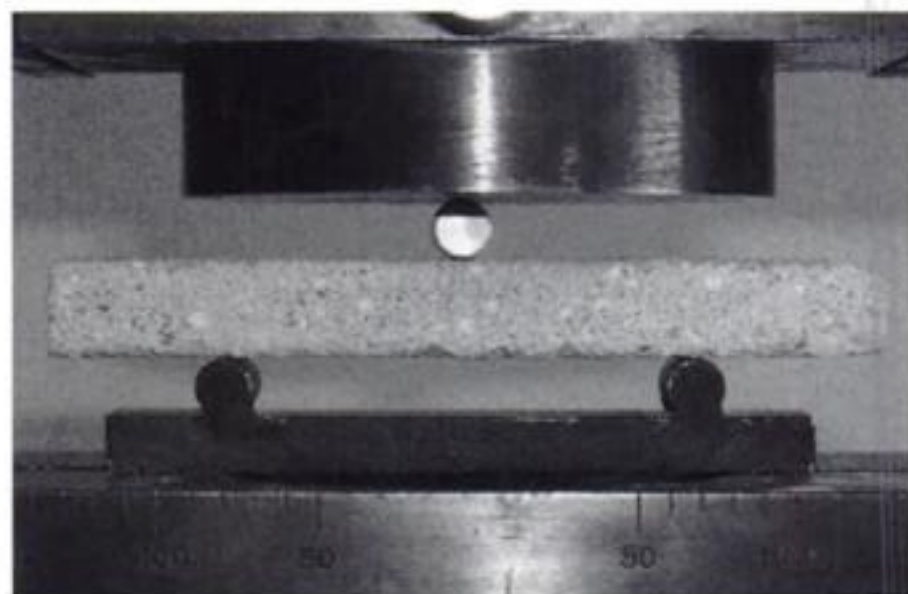


Figure 1. The flexural test on specimens from batch “D”, set III.

where F = maximum load, l = the axis distance between the supports, b = the trial specimen width, and d = the trial specimen height.

3.2 Compressive strength

Prism fragments from the flexural test were used in the compression strength test. A testing device with two steel pressure plates of dimensions 40×40 mm was used. Steel plates of dimensions 20×20 mm were used for specimens sampled from the joints. The compression strength f_c in N/mm^2 is calculated from the following formula:

$$f_c = \frac{F}{A}, \quad (2)$$

where F = the maximum load, and A = the compressed area.

3.3 Volumetric mass

This test was carried out according to the standard procedures. Dimensions of the set-I and set-II trial specimens were measured using a calliper rule; the specimens were weighed and their volumetric mass was calculated. The volumetric mass of specimens sampled from the joints was measured by means of hydrostatic weighing.

3.4 The dynamic elasticity modulus

This test was based on measuring the propagation time of ultrasonic wave pulses through the given material. Measurements were carried out using the TICO ultrasonic instrument with external 150-kHz probes (the frequency was chosen in view of the dimensions of the specimens). The value of the dynamic elasticity modulus E_u in compression and tension in N/mm^2 can be calculated from the formula

$$E_u = \rho v_l^2 \frac{1}{k^2} 10^{-6} \quad (3)$$

Table 1. Results of the mortar tests for different casting procedures and moisture conditions.

Property	Set	Water saturation	Batch			
			A	B	C	D
Compression strength f_c [N/mm ²]	I	moi	0.22	0.67	0.91	2.74
		sat	0.16	0.62	0.49	1.55
	II	moi	0.35	1.05	1.50	3.85
		sat	0.28	1.05	0.75	2.18
	III	moi	0.46	1.69	2.86	5.19
Flexural strength f_f [N/mm ²]	I	moi	0.042	0.085	0.210	0.637
		sat	0.000	0.096	0.151	0.421
	II	moi	0.068	0.189	0.461	0.905
		sat	0.028	0.112	0.214	0.649
	III	moi	–	–	1.030	2.440
Volumetric mass ρ [kg·m ⁻³]	I	moi	1798	1838	1835	1794
		sat	2008	2091	2072	2026
	II	moi	1834	1849	1849	1823
		sat	2069	2074	2062	2031
	III	moi	1913	2020	1946	1953
Propagation velocity of US waves v_L [ms ⁻¹]	I	moi	562	1128	1190	1900
		sat	620	865	1025	1800
	II	moi	732	1393	1482	2195
		sat	885	1350	1485	2170
	III	moi	1483	2427	2410	2979
Dynamic elasticity modulus E_d [N/mm ²]	I	moi	511	2107	2341	5827
		sat	695	1408	1959	5908
	II	moi	894	3232	3694	7904
		sat	1458	3402	4093	8605
	III	moi	3811	10741	10782	15605
Static elasticity modulus E_c [N/mm ²]	I	moi	0	1786	2381	4710
		sat	–	–	–	–
	II	moi	0	2907	3750	6357
		sat	–	–	–	–

where ρ = the volumetric mass of material, v_L = the ultrasonic propagation velocity, and k = a dimensionless coefficient characterizing the size of the specimens (ČSN 73 1371).

3.5 Static modulus of elasticity

The static elasticity modulus was calculated based on the measured values, which were obtained from strain gauges during the repeated loading and unloading of specimens. The test methodology was based upon the ČSN ISO 6784 standard of concrete testing. The loading intensity (for concrete) is chosen so that the basic (lower) stress is 0.5 N/mm² and the upper stress is one third of the maximum compressive strength of concrete $f_c/3$. Due to the low mortar compressive strength, the basic stress was lowered. The static compression elasticity modulus E_c (N/mm²) is calculated from the following formula

$$E_c = \frac{\Delta\sigma}{\Delta\varepsilon} = \frac{\sigma_a - \sigma_b}{\Delta\varepsilon} \quad (4)$$

where σ_a = the upper stress, σ_b = the basic stress in N/mm², and $\Delta\varepsilon$ = the dimensionless average change of the relative deformation.

4 RESULTS OF THE PHYSICAL MECHANICAL MORTAR TESTS

The volumetric mass, compressive strength, flexural strength, propagation velocity of ultrasonic wave pulses, dynamic and static elasticity moduli were determined for the trial specimens made of the four mortar types described in paragraph 2.2. Table 1 presents the average results of all mortar tests. The individual mortar types with different binder to filler ratios are denoted A, B, C, D (in ascending order of the binder content). Set I was cast in steel moulds and the excess water was not extracted; set II was cast in steel moulds and the excess water was extracted by means of gauze and filter paper; set III was made from specimens sampled from the brick joints.

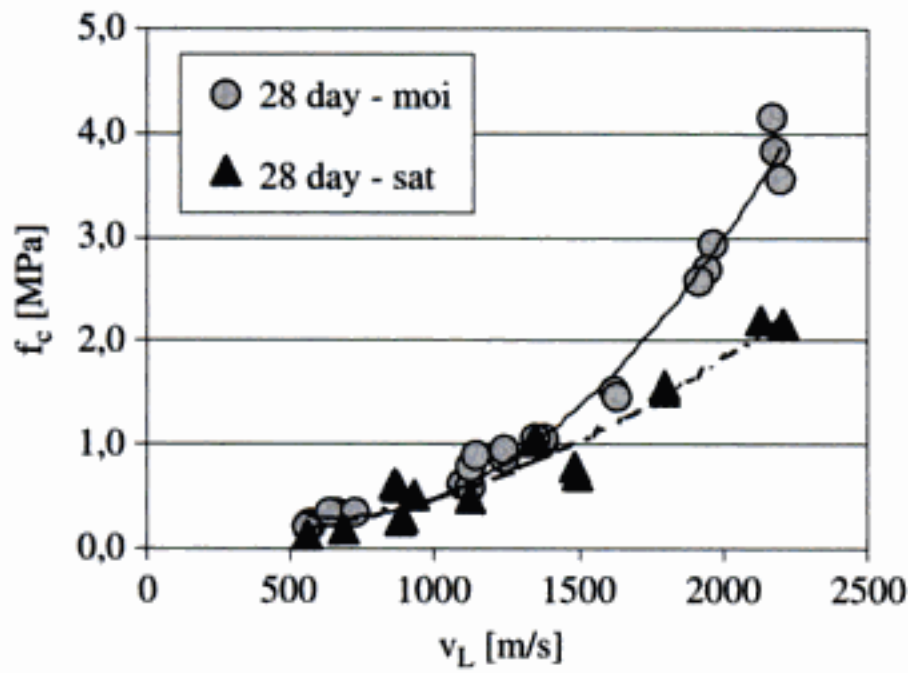


Figure 5. Dependence between compression strength and propagation velocity of ultrasonic waves.

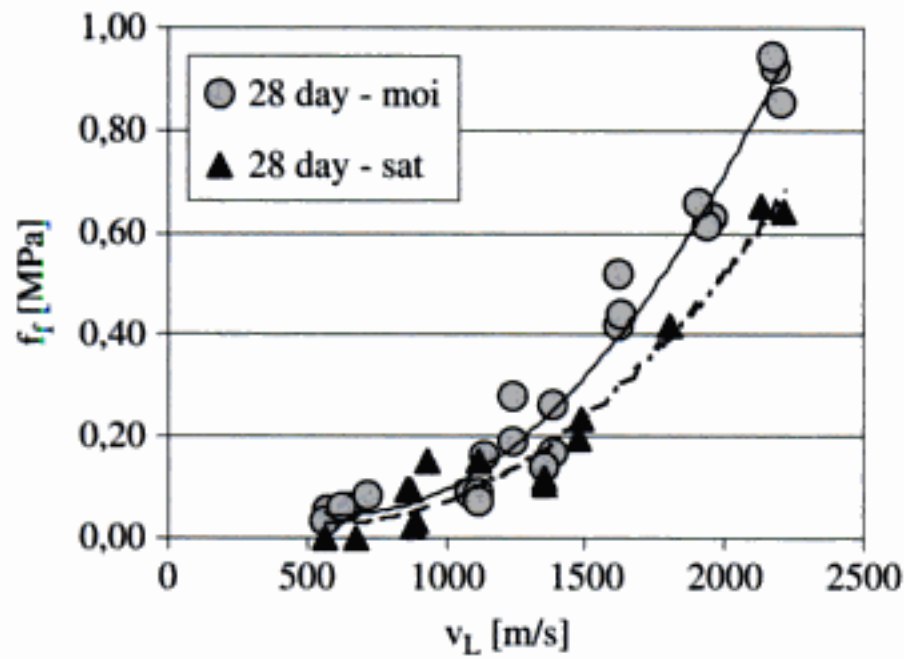


Figure 6. Dependence between tensile strength and propagation velocity of ultrasonic waves.

tested mortar types with compressive strengths from 0.4 N/mm^2 to 2.5 N/mm^2 responds sensitively to the changing mortar compression strength and the effect of mortar density is also noticeable. This was observed, for example, for mix B that had lower compressive and flexural strengths but, at the same time, it had a higher volumetric mass than mix C – the propagation velocity of ultrasonic waves was similar for both mixes. It follows then that, based on the propagation velocity of ultrasonic waves, it is possible to roughly determine the compression and tensile strengths for the given mortar type – see Figures 5 and 6. However, to obtain more accurate results, it is necessary to determine another parameter – the mortar volumetric mass or, even better, its water-absorption capacity.

The propagation velocity of US waves increased from 700 m/s to 1000 m/s for specimens cut from the joints. The ultrasonic measurement thus verified the results of the compressive and flexural tests. The influence of water saturation on the velocity of US waves was not very significant for the tested mortars.

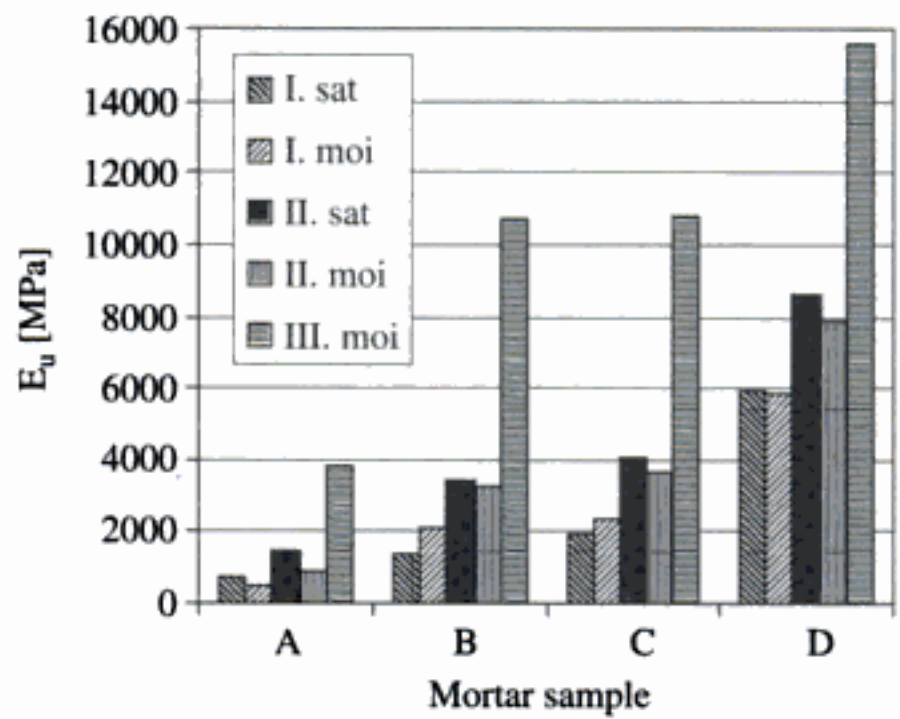


Figure 7. Dynamic modulus of elasticity of mortars in dependence on moisture state and ageing.

4.4 Dynamic elasticity modulus of mortars

The dynamic elasticity modulus was calculated using the measured propagation velocity of ultrasonic waves and the volumetric mass of the material. Mutual comparison of the individual mixes and specimen types is therefore comparable with the propagation velocity of US waves. Values of the dynamic moduli ranged from 500 N/mm^2 (mix A) to 5800 N/mm^2 (mix C) for set-I specimens without water extraction; from 900 N/mm^2 to 7900 N/mm^2 for set-II specimens with water extraction; and from 3800 N/mm^2 to 15600 N/mm^2 for set-III specimens from the joints; see Figure 7.

These results seem to be very important for the experimental verification of masonry pier properties since the elasticity modulus values measured using the trial specimens are probably up to two times lower than the elasticity modulus values for joint mortar.

4.5 Relation between static and dynamic elasticity moduli of mortar

The static elasticity modulus was determined using $40 \times 40 \times 160 \text{ mm}$ prisms according to the concrete-testing methodology only for set-I and II specimens with natural moisture content. It was not possible to test mix-A specimens due to their low compression strength and problems involved in attaching the measuring instruments. The trend observed in the previous tests was confirmed again – mortar mixes with higher compression and flexural strengths and excess-water extraction show higher values of the static elasticity modulus.

The dynamic elasticity modulus values were only slightly higher than the static elasticity modulus values. This result was rather surprising as – according to our experience from mortar testing – the ratio of the static to the dynamic mortar elasticity modulus

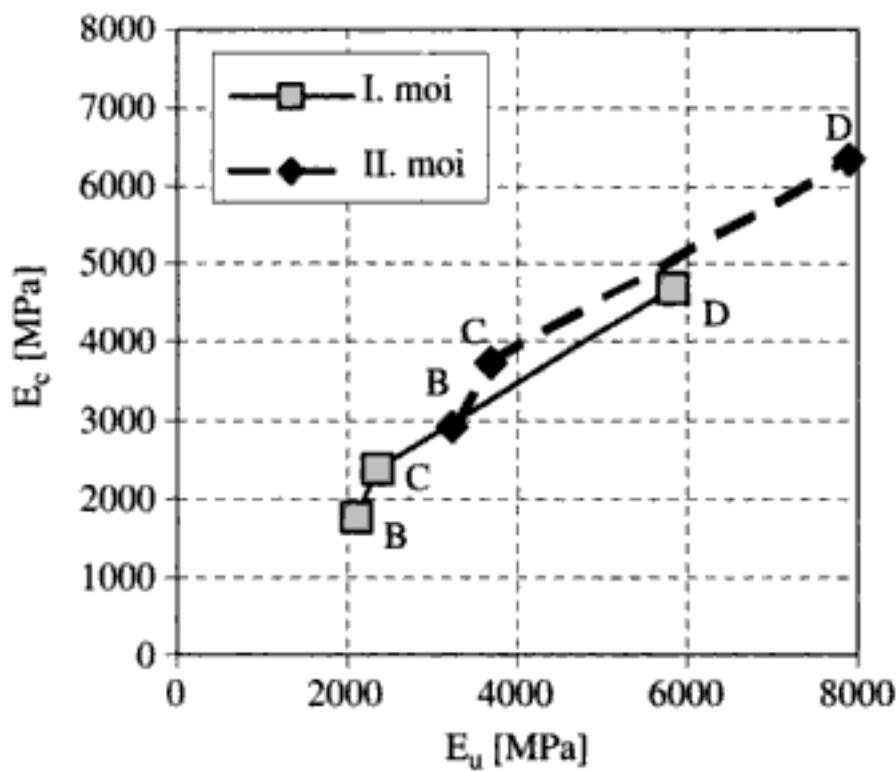


Figure 8. Dependence between static and dynamic modulus of elasticity of mortar.

is between 0.5 and 0.9 and for mortars of lower strength, the dynamic modulus is usually twice the static modulus.

A very good correlation between the static and dynamic moduli was identified during our experiment as can be seen in Figure 8. This means that based upon the ultrasonic measurements, not only the strength but also the static modulus values could be roughly determined for mortar within the masonry joints.

5 CONCLUSIONS BASED ON MATERIAL TESTS

Based on the test results for various mortar specimens of compression strength ranging approximately from 0.4 N/mm^2 to 2.5 N/mm^2 , it can be stated there is a relation between the propagation velocity of ultrasonic wave pulses and the mechanical properties of the mortar – the compression and flexural strengths and

the static elasticity modulus. Also the volumetric mass and moisture content of mortar had an appreciable effect on the results of the ultrasonic measurements. It is precisely within the range of 0.4 to 2.5 N/mm^2 where the differences in the propagation velocity of US waves are relatively high which means that the ultrasonic method is highly sensitive in this range and it will be probably possible to use it successfully in practical on-site measurements of buildings.

Another result of the experiment consisted in verifying the influence of excess-water extraction from the mortar – this was most pronounced for mortars from the masonry joints. Ultrasonic measurements showed a large increase of strength as well as elasticity moduli for mortars from the masonry joints as compared with the specimens cast into moulds even if water was extracted by gauze and filter paper. This finding is particularly important for experimental work and models of masonry structures behaviour.

ACKNOWLEDGEMENT

In this article there are presented results of a research Intention EESD Programme “ONSITEMASONRY”, EVKA-2002-00546, and Project MSM 261100007.

REFERENCES

- Drdacky, M., Valek, M. & Prochazka, P. 1999. Spalling of Historic Mortars. In Proc. preprint of the “International Workshop *HISTORIC MORTARS – Characteristic and Tests*: pp. 1/10 10/10. Paisley, Scotland, May 1999.
- Drdacky, M., Lesak, J., Michoinova, D., Svoboda, J. & Urushadze, Sh. *Contact Less Method for Identification of Cohesion Loss in Lime Mortar Renders*. Proc. *Experimental Stress Analysis*. 41-46. CTU Prague, 2001.
- Drdacky, M. & Michoinova, D. Lime Mortars with Natural Fibres. In *Brittle Matrix Composites 7*. 7th International Symposium (A.M.Brandt, V.C.Li,I.H.Marshall,eds.). 523–532. Cambridge and Warsaw, ISBN 1-85573-796-8.

Dynamic behaviour and structural monitoring

The influence of bells' movement on the adjacent masonry vibrations

O. Fischer & S. Urushadze

Institute of Theoretical and Applied Mechanics, Academy of Sciences of the Czech Republic, Prague

ABSTRACT: The gable wall standing over the entrance into a neo-gothic church and fixed on both sides of its base into towers, swayed with well-visible amplitudes out of its plane in the rhythm of the swinging of the bells. The gable is of triangular shape with the height of 8.60 m and base-width 9.0 m, not being supported horizontally by the roof or by any other stiffening structure. The measurements revealed that the bells excite the vibrations of towers and of the basement of the gable with moderate amplitudes, while the cantilever of the gable wall amplifies the motion by the resonance-effect. The impression of the gable motion was made worse due to the beat-effect of superposition of more bells (up to 6, with the masses between 150 and 1000 kg) with slightly different swaying frequencies (0.44 thru 0.52 Hz). The way of reinforcing the wall is now being sought with respect to the cultural heritage conserving aspects.

1 INTRODUCTION

The triangular gable wall in the western front of the cca 100 years old neo-gothic cathedral in Prague-Vysehrad was observed to vibrate out of its plane during ringing. Our Institute was asked to measure these vibrations and to assess their influence on the stability (safety) of the wall. In what follows, the measurements of wall-motion have been described and the results analyzed. Simple shaking-table experiments, modelling the behaviour of the damaged wall, have been added.

2 DESCRIPTION OF THE STRUCTURE AND OF ITS BEHAVIOUR

The cathedral in question was built at the boundary between the 19th–20th centuries from traditional materials (stone, bricks, covered with slate on wooden truss), having about 30 × 56 m in plane; its two towers are about 60 m high (see Figure 1). The church interior was recently refurbished and also its structure seems to be in good order and condition. Its triangular gable wall over the main entrance starts at the height of 19.60 m above the church floor, its width between both church towers is 9.0 m and the height of its rectangular part fixed into the towers is 2.60 m. The height of the free-standing triangular part is 8.70 m and the cross on its top reaches the height 30 m. The gable wall does not lean against the wooden construction of the roof covering the main nave of the church. The masonry of the gable is 0.57 m thick, but the niches containing

statues, of total width (from 5 to 1) × 1.20 m, reduce it up to 0.27 m. (the photo annexed).

The towers are of square cross-section 7 × 7 m, the bells are hung in classical wooden stools placed at the level about 29 m. There are two old bells in the southern tower (J1, J2), four recently mounted ones in the northern tower (S1–S4). All bells exert swaying motion driven separately by electric motors. Besides, there is a set of 12 stable bells with clappers controlled by computer in northern tower, used for playing several songs. The characteristics of the bells are given in Tab. 1. The amplitude of all bells' swaying is about ±45 deg. Both old stools in the southern tower are evidently damaged and need to be repaired.

Standing in the entrance and looking up along the gable, the swaying of its top could be sometimes observed during ringing, similarly also when looking from the window of the tower the movement of the gable edge versus the roof slates. The movement in general was not stationary, its amplitude swayed,

Table 1. Parameters of the bells.

Bell no.	Tone	m [kg]	θ [m]	f [Hz]
J1	e ₁	cca 1000	1.23	0.44
J2	f sharp ₁	cca 600	?	0.44
S1	a ₁	650	0.93	0.50
S2	c sharp ₂	300	0.78	0.54
S3	d ₂	180	0.63	0.58
S4	d sharp ₂	150	0.56	0.60

Note: The frequencies of bells' swaying were averaged from the measured response.

especially when several bells were ringing together. In order to define better the phenomenon, to assess its influence and to decide about adequate measures, the measurements of vibrations of the gable and expert examination was ordered.



Figure 1. The western front of the Church of the Royal Chapter House of St. Peter & Paul in Prague – Vysehrad.

3 MEASUREMENT OF THE VIBRATIONS

There were 12 measuring points chosen on the front wall of the church, as shown on Figure 1, viz:

- 5 positions along the height of the southern tower, incl. its top and bell-floor level
- 4 positions on the gable wall, incl. its base and top
- 3 positions on the northern tower.

Our facility was able to pick up and register 6 signals simultaneously. Different combinations were chosen for different excitations, viz

- each of the bells separately
- all bells together.

The pickups used were of the production of Wilcoxon Research CMSS 916VD: the signals were stored in a standard notebook and analyzed with the ONO SOKKI CF-350Z analyzer. Every registration lasted 1 minute or more, from which the RMS of the displacements and the frequency peaks were evaluated. As the registrations were more or less of the sinusoidal shape, the informative maximum amplitudes were checked as $\sqrt{2} \times \text{RMS}$ value. Some results (amplitudes and frequencies, the most important underlined) are given in Tab. 2, some frequency analyses are shown on Figures 2, 3.

The results of the measurements can be summarized as follows:

(a) The biggest response was excited by two old bells in the southern tower due to their biggest mass and to the bad order of their stools. The frequencies of all measured motions correspond with the swaying of the bells, its double and triple; similar results were obtained in (Bennati et al. 2002).

(b) The amplitudes of the tower and the front wall (incl. the base of the gable) are smaller than 0.5 mm and can not in the least endanger the structure. Mostly the 3rd harmonic (1.32–1.50 Hz) prevails in the response of the towers.

Table 2. Response of the gable to the ringing of old bells (southern tower, bells J1, J2) observed frequencies [Hz] and displacements (RMS) [mm].

Point no	Position	Bell J1 frequencies	Bell J1 RMS	Bell J2 frequencies	Bell J2 RMS
12	Southern tower, top	0.44;0.88 <u>1.32</u>	0.154	<u>1.32</u>	0.325
20	Southern tower above bells	0.44;0.88; <u>1.32</u> ;1.77	0.108	0.44;0.88 <u>1.32</u>	0.218
2	Southern tower, bells	0.44;0.88 <u>1.32</u> ;1.77	0.080	0.44;0.88 <u>1.32</u>	0.218
21	Southern tower, gable base level	0.44; <u>0.88</u> 1.32;1.77	0.051	0.44;0.88 <u>1.32</u>	0.058
22	Southern tower bottom	0.44; <u>0.88</u> 1.32;1.77	0.054	0.48; <u>0.88</u> 1.34;1.78	0.048
6	Gable top	<u>0.88</u> ;1.76 2.64	7.163	<u>0.88</u> ;1.33 1.77;2.66	4.944
7	Gable low	0.44; <u>0.88</u> ; <u>1.32</u> ;1.77	0.063	<u>1.32</u>	0.233
4	Gable base	0.44; <u>0.88</u> 1.32;1.77	0.053	0.88; <u>1.32</u>	0.078
11	Northern tower, gable base level	0.44; <u>0.88</u> 1.76	0.050	0.50; <u>0.88</u> 1.78	0.040

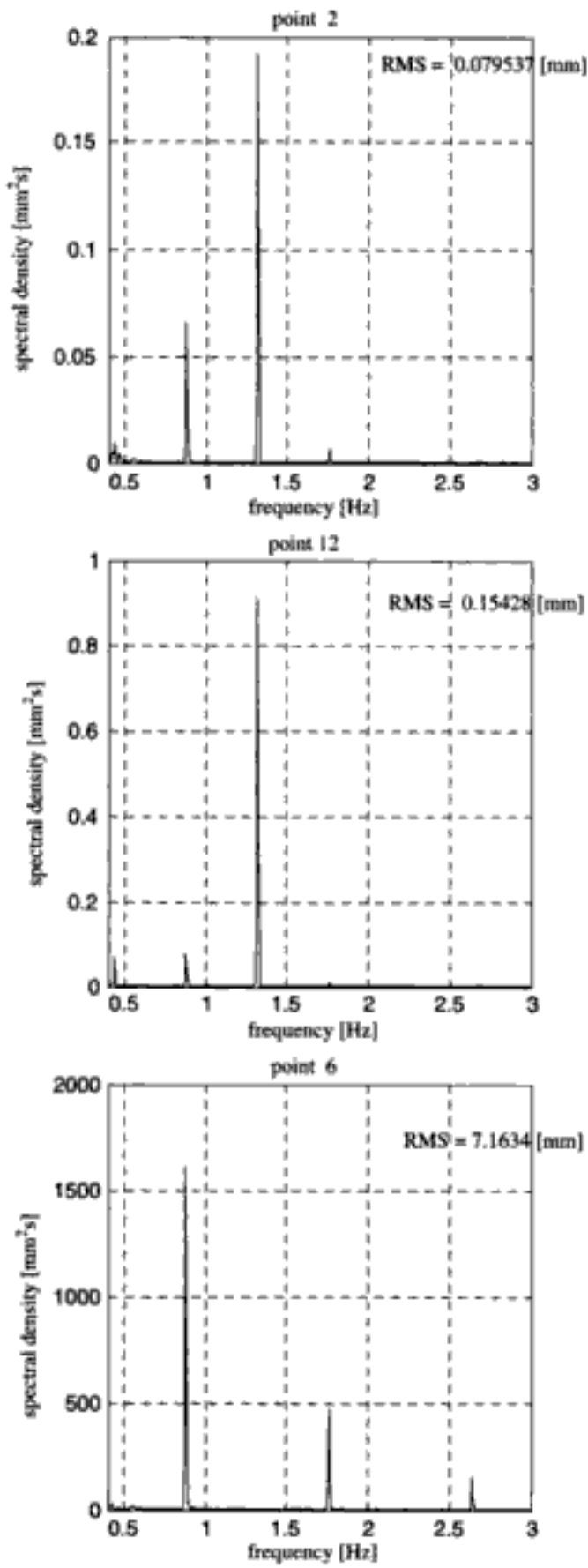


Figure 2. Frequency response of some points to the ringing of the biggest bell J1.

(c) The top of the free standing triangular gable vibrated with visible amplitudes, up to 18 mm, with prevailing frequency corresponding to the 2nd harmonic of the fundamental frequency of southern bells' swaying (0.88–1.18 Hz).

4 EFFECT OF BELL'S SWAYING ON THE CONSTRUCTION

Neglecting the mass of the clapper, the bell can be considered as a physical pendulum, which is described by its mass m , eccentricity of suspension r (distance between the centre of gravity and the axis of rotation) and distribution of its mass around the centre

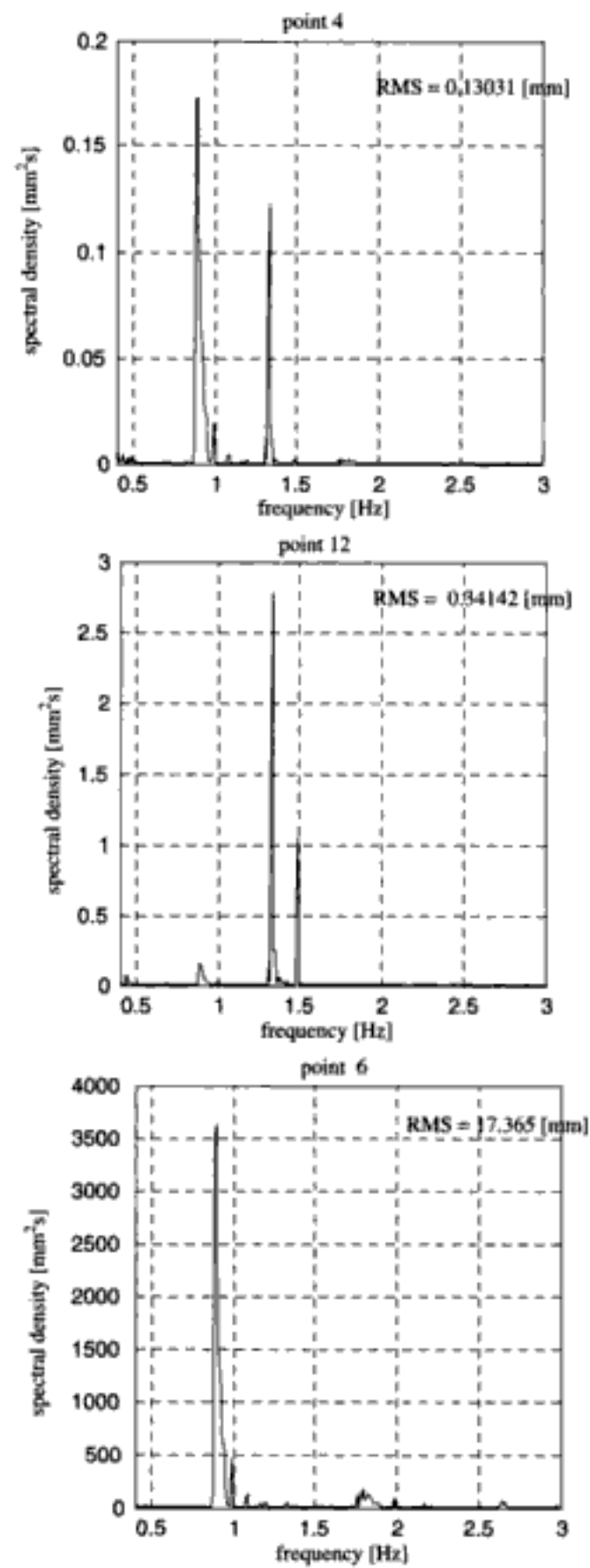


Figure 3. Frequency response of some points to simultaneous ringing with all bells.

of gravity, given e.g. by the radius of inertia with respect to the centroidal axis parallel to the axis of bell's rotation, i_s , or by the ratio

$$\kappa = \frac{i_s}{r} \quad (1)$$

This coefficient κ can also be determined from the period of small free vibration (total period, both ways movement), for which it holds (g – acceleration of gravity).

$$T_0 = 2\pi \sqrt{\frac{I_{red}}{g}}$$

in which the reduced pendulum length is,

$$l_{red} = r + \frac{i_s^2}{r} = r(1 + \kappa^2). \quad \text{Then}$$

$$T_0 = 2\pi \sqrt{\frac{r}{g} \sqrt{1 + \kappa^2}}, \quad \text{or } \kappa = \sqrt{\frac{T_0^2}{4\pi^2} \cdot \frac{g}{r} - 1}. \quad (2)$$

A physical pendulum, swaying with the angle-amplitude $\pm\varphi_0$, acts in its general angle-elongation φ on the supporting point by a force with horizontal and vertical components (Dašek V. 1955).

$$H = \frac{mg}{1 + \kappa^2} (2 \cos \varphi_0 - 3 \cos \varphi) \sin \varphi$$

$$V = \frac{m \cdot g}{1 + \kappa^2} (3 \cos^2 \varphi - 2 \cos \varphi_0 \cdot \cos \varphi + \kappa^2) \quad (3)$$

Supposing the bell's motion as harmonic, viz

$$\varphi(t) = \varphi_0 \sin\left(\frac{2\pi}{T_0} t\right) \quad (4)$$

the horizontal reaction can be expressed as

$$H(t) = \frac{mg}{1 + \kappa^2} \gamma(t), \quad (5)$$

in which the dimensionless time-function $\gamma(t)$ is defined by both previous expressions (3) and (4). Its time-course, for the values corresponding to the bells J1, J2, i.e. for

$$T_0 = \frac{1}{0.44} = 2.273 \text{ s};$$

$$\varphi_0 = 45^\circ = 0.785 \text{ rad}$$

is given on the Figure 4. Maximum of the vertical reaction is evidently in the moment when the bell passes

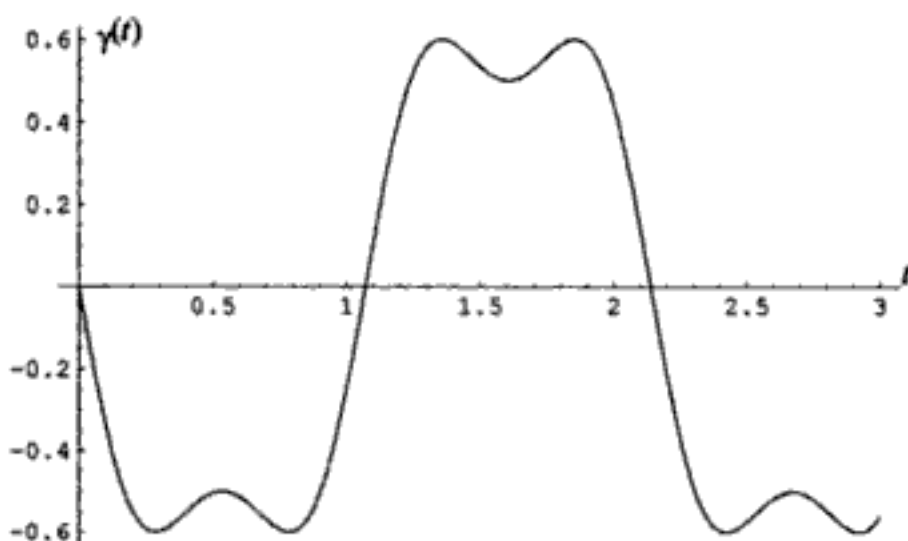


Figure 4. Time function $\gamma(t)$ describing the time-course of the horizontal reaction of the bell.

through its equilibrium position $\varphi = 0$, maximum horizontal force corresponds to the angle φ_m given by zero value of the derivative of (3), namely

$$\frac{d\gamma(t)}{d\varphi} = 3 \sin^2 \varphi + 2 \cos \varphi_0 \cdot \cos \varphi - 3 \cos^2 \varphi = 0 \Rightarrow$$

$$\varphi_m = \arccos\left[\frac{1}{6} \left(\cos \varphi_0 + \sqrt{\cos^2 \varphi_0 + 18}\right)\right] \quad (6)$$

Here $\varphi_m = 33.41^\circ$. In our case, during one cycle ($t = 0$ thru 2.273 s), this maximum (absolute value) occurs four times, namely, according to (4), for

$$t = \frac{T_0}{2\pi} \arcsin \frac{\varphi}{\varphi_0} \Rightarrow \frac{2.273}{2\pi} \arcsin \frac{33.41}{45} =$$

$$= 0.303 \text{ s}, \quad \text{and then } 0.834, 1.439, 1.970 \text{ s}$$

The function $\gamma(t)$ can be developed into a Fourier series

$$\gamma(t) = (2 \cos \varphi_0 - 3 \cos \varphi) \cdot \sin \varphi \doteq$$

$$\doteq b_1 \cdot \sin\left(2\pi \frac{t}{T_0}\right) + b_3 \cdot \sin\left(6\pi \frac{t}{T_0}\right) \quad (7)$$

in which (in our case)

$$b_1 = \frac{2}{T_0} 4 \int_0^{T_0/4} \gamma(t) \cdot \sin\left(\frac{2\pi t}{T_0}\right) dt = 0.673;$$

$$b_3 = \frac{2}{T_0} 4 \int_0^{T_0/4} \gamma(t) \cdot \sin\left(\frac{6\pi t}{T_0}\right) dt = 0.179$$

As it can be seen, the excitation effect of a swaying bell has two harmonic components, the first and third. The higher ones are unimportant (e.g. $b_5 = 0.0065 < 4\% b_3$). Both these frequencies, the fundamental one and its triple, can be identified on the measured responses, but this analysis does not say anything about the double, which is also very important in the response. It probably comes from the fact that in this case the bells do not sway as a pure pendulum, the driving force of which depends on the elongation, but they are also driven by electric motors, which exert the force depending on velocity. The exact analysis of this phenomenon has not been done till now, but it seems evident that the phase of such an excitation is shifted by $\pi/2$ and evidently adds cosine-members into the excitation (7). The double frequency was also observed in (Bennati et al. 2002), where the bells were driven by motors, while in (Fischer O. & Pirner M. 2002), where the bell was moved by human force, only the first and 3rd frequencies were found.

5 EVALUATION OF THE RESULTS OBTAINED

The only important vibrations found on the construction are those of the free standing triangular gable over the church entrance. This evidently behaves as a cantilever and – due to the resonance effect – amplifies the negligible excitation of the base into about centuple response of the top. Nevertheless, such a trivial explanation has some shortcomings, viz.

- according to even an approximate calculus, the natural frequency of the triangular gable wall about 1 Hz is unrealistically low
- the resonant amplification by centuple would require unrealistically low damping of 0.5%
- the observed resonance frequency band 0.88–1.18 Hz ($f_o \pm 15\%$) does not match with this low damping.

All these discrepancies seem to reveal that the gable wall does not behave like a linear elastic structural element, i.e. that its masonry has been damaged in some way, most probably by the ageing process and weathering of the mortar in the joints between stones. In order to elucidate the influence of this phenomenon, a simple experiment on the shaking table was arranged.

6 SHAKING TABLE EXPERIMENT OF A BRICK-COLUMN

A column of 590/140 mm comprising 22 layers from 2 (or 1 + 2 halves) pieces of perforated bricks (290/140/65 mm, 3.57 kg) was “built” on shaking table 1.25 × 1.55 m exerting unidirectional horizontal

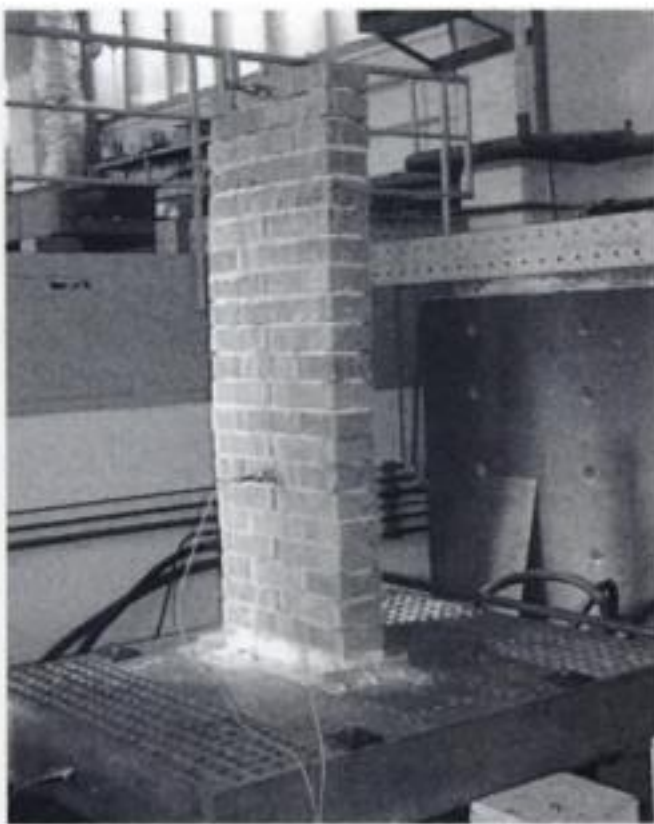


Figure 5. Brick column with plastic sheets in horizontal layers on shaking table.

excitation, controlled by electro-hydraulic dynamic system MTS 204.51. In the first case, the bricks were left bare (total height 1.43 m), in the second the joints were filled by mortar, but the horizontal ones were separated by thin plastic sheets (height 1.56 m) – see Figure 5. Two transducers were fixed horizontally in the heights of 475 and 1384 mm (525 and 1554 mm). The columns were tested for free vibrations after a release from static deflection and for harmonic excitation with step-wise increasing and decreasing frequencies starting with small amplitudes and repeated with larger ones. The response is of course strongly non-linear: (i) the “resonance curves” are different for increasing and decreasing frequencies, (ii) the natural frequencies increase with smaller amplitudes, and (iii) the damping is smaller for small amplitudes. One set of measured values is given in Tab. 3 as example, some resonance curves are shown on Figures 6 and 7.

Table 3. Natural frequencies $f_{(1)}$ [Hz] and logarithmic decrement δ of free vibrations of the column made without mortar and with separated horizontal layers.

	Bare bricks	Separated layers
f_o	1.96–2.53	2.53–3.57
δ	0.138–0.078	0.322–0.431

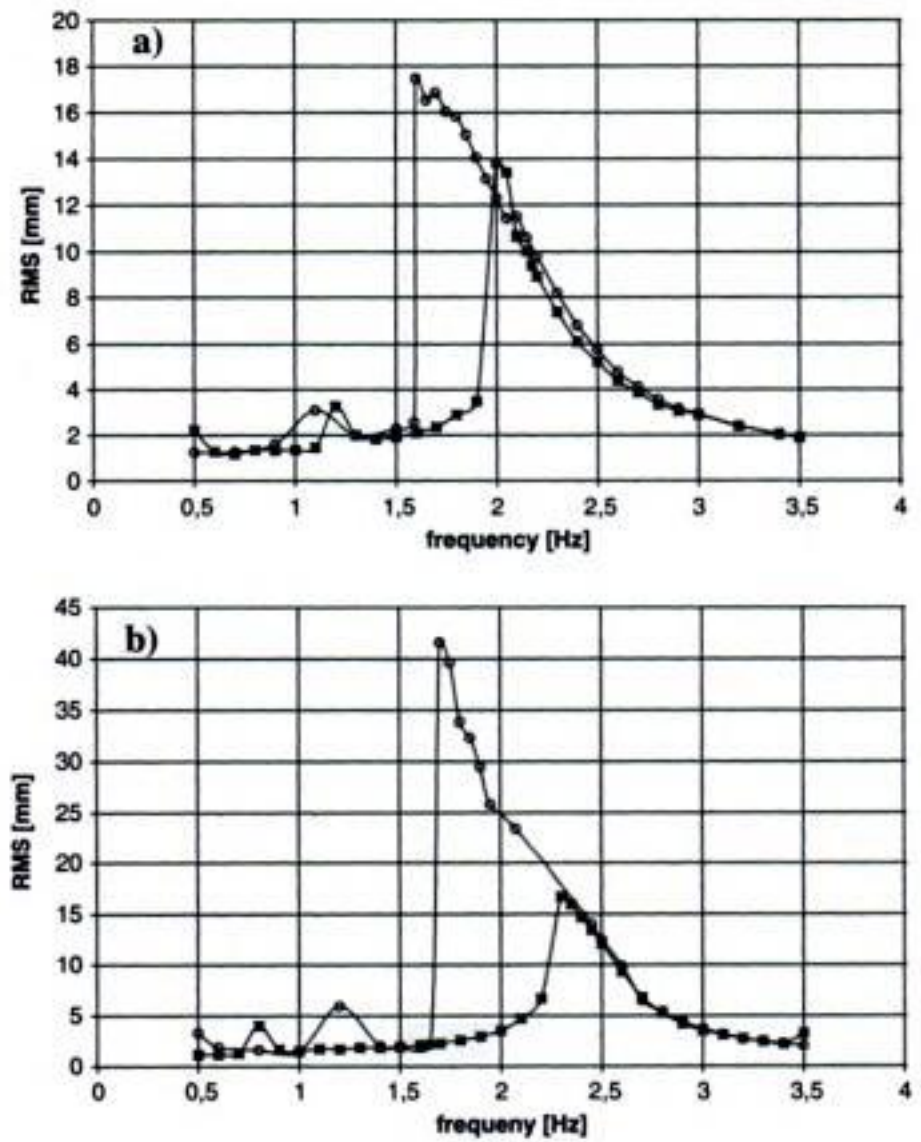


Figure 6. Stationary response of the bare brick column (ratio of the RMS of the motion of the top and of the table) to harmonic excitation with increasing (■) and decreasing (○) frequencies. a – excitation 0.2 mm, b – 0.30 mm.

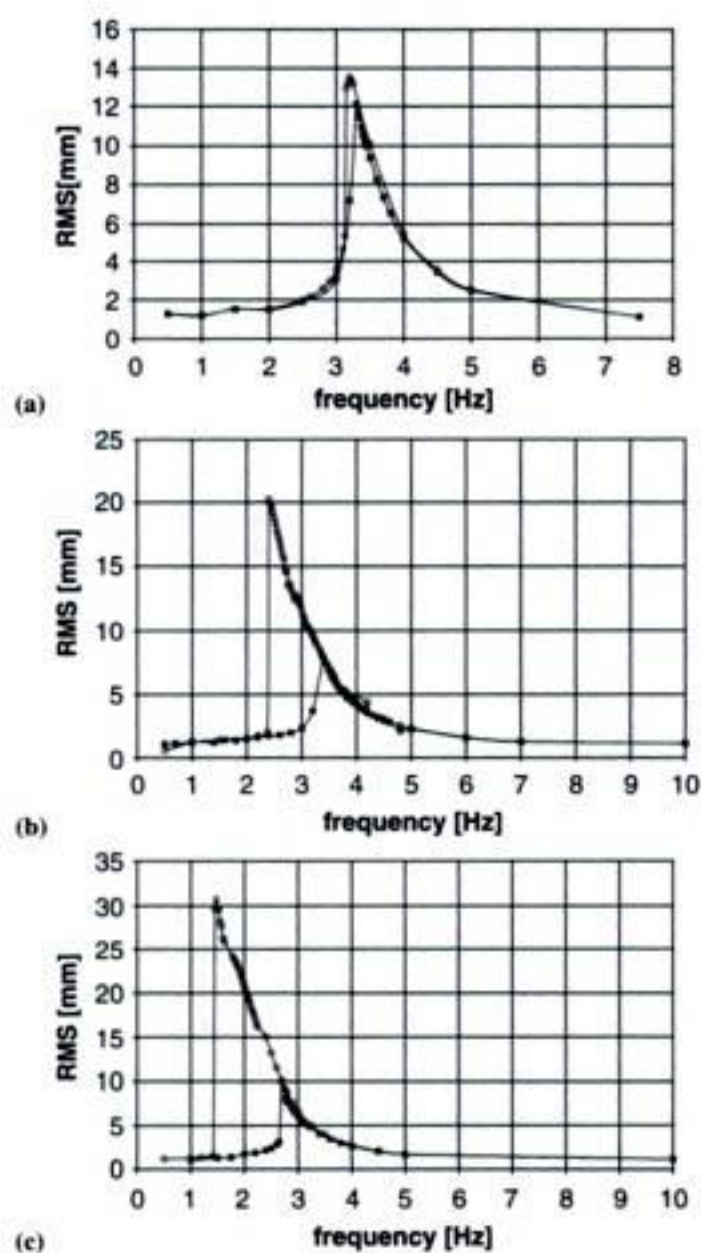


Figure 7. Stationary response of the brick column (ratio of the RMS of the motion of the top and of the table) to harmonic excitation with increasing (■) and decreasing (○) frequencies. a – excitation 0.046 mm, b – 0.12 mm, c – 0.24 mm.



Figure 8. The wobbling gable.

The experiment has confirmed that the above given discrepancies can be explained by nonlinear behaviour of masonry, the joints of which are opening to a certain extent, thus the wall vacillates, together with bending.

7 CONCLUSIONS

The presented analyses and measurements have revealed that

- the swaying bells excite the structure by considerable horizontal forces with frequencies of one, two and three multiple of the bells' motion. This excitation can be amplified by resonance effect of an arbitrary structural element, which is tuned to one of these frequencies.
- the gable wall of the church under consideration is most probably damaged due to the ageing process of its masonry, and has to be retrofitted either by restoration the mortar joints or by reinforcing the gable, e.g. by an additional supporting system inside the church garret.

ACKNOWLEDGEMENT

The measurement on the church building were ordered and paid by the Royal Chapter House; some concurring analyses and research were financed by the Grant Agency of the Academy of Sciences within the project No B2071303. Also the support of EVK-2001-00091 - ONSITEFORMASONRY and ITAM AV OZ 2071913 research plane are gratefully acknowledged.

REFERENCES

- Bennati S., Salvatore W., Nardini L. & Della Maggiora M. 2002. Bell's dynamic action on a historical masonry tower. In Grundmann & Schuëller (eds). *Proc. 7th European conference EURODYN 02, Munich, 7–11 September 2002*. ISBN 90 5809 510 X, pp. 1495–1504. Rotterdam: Balkema.
- Dašek V. 1955. *Dynamics* (in Czech). Praha. Academia.
- Fischer O. & Pirner M. 2002. An attempt of reducing vibrations of a slender steel belfry (in Czech). In Academy of Sci. eds. *Proc. conf. Engineering Mechanics 2002. Inst. of thermomechanics*. 13-16.5.2002, Svratka, pp 47–49. Fulltext on CD, 9 pgs.

Validated structural analysis of Gothic vaulted systems

E. Erdogmus & T.E. Boothby

The Pennsylvania State University, University Park, USA

ABSTRACT: A validated analytical procedure for vaulted unreinforced masonry structures is proposed in this study. The structural analyses necessary in this research are carried out by the finite element analysis method (FEM). The ribs of a gothic rib vault are modeled using linearly elastic solid elements, while the vault webs are modeled using linearly elastic shell elements. The analytical models are then validated using *in situ* nondestructive vibration experiments, by the comparison of analytical and experimental mode shapes and natural frequencies of the vaulting system. Appropriate boundary conditions are determined by the verification of mode shapes, and material properties are verified by comparison of natural frequencies. National Cathedral in Washington, DC, U.S.A. is studied as a controlled case as it has known material properties and construction history. These analysis and validation methods studied on NC will be then applied to European medieval structures in the continuation of this research.

1 INTRODUCTION

Gothic architecture initiated in France in the 12th century and spread through Europe for four centuries. Within the last few hundred years, other structures around the world such as the National Cathedral (NC) in Washington, DC were also constructed in Gothic style. The main component in these unreinforced masonry structures is the complex assembly of vaulted roof systems, for which, there are not well-established and dependable analysis techniques. The available methods are rigid-plastic analyses, elastic analyses, two-dimensional graphical analyses and a current trend of computer analyses mostly based on the finite element method. However, none of these methods has been validated by experiments conducted on the real structures (Boothby, 2001).

A validated analytical procedure for vaulted systems is evident is proposed in this study. The structural analyses necessary in this research are carried out using three-dimensional finite element analysis method (FEM). The analytical models are then validated using *in situ* nondestructive experiments.

For the case of a Gothic vaulted roof structure, besides the complexity of the structural behavior, material properties and support conditions are unknown. Static load testing or sample extraction, which would reveal information about these parameters are not possible on these historically important structures. Therefore, nondestructive testing is called upon for the validation of FEM. In this study, *in situ* vibration experiments and experimental modal

analyses are used for the updating and validation of the model.

The proposed methods are first studied on a structure with better-known properties and history, the National Cathedral (NC). Therefore, the ribbed vaults in the choir of NC are modeled, the analytical models are experimentally validated, and the results of this study are presented in this paper. The findings, results and improvement suggestions from this study will be applied to similar studies on medieval European structures in the future.

1.1 Washington National Cathedral

The construction of the NC, the sixth largest cathedral in the world, continued for more than 83 years (September 29, 1907 to September 29, 1990). Frederick Bodley, England's leading Anglican Church architect, was the first head architect with Henry Vaughan as the supervising architect. After Bodley and Vaughan had passed away following World War I, American architect Philip Hubert Frohman became the principal architect. The cathedral was built in the Decorated Gothic style, a style in English architecture that lasted from 1270 to 1380. The cathedral was engineered and constructed like the medieval churches, using only quarried stone with no steel reinforcement in any part of the building and no mass-produced elements. Even though the exact dates are unknown, the choir vaults, which will be analyzed in this study, were finished around the 1930's, when the transepts were opened for public use. The even-level-crown,

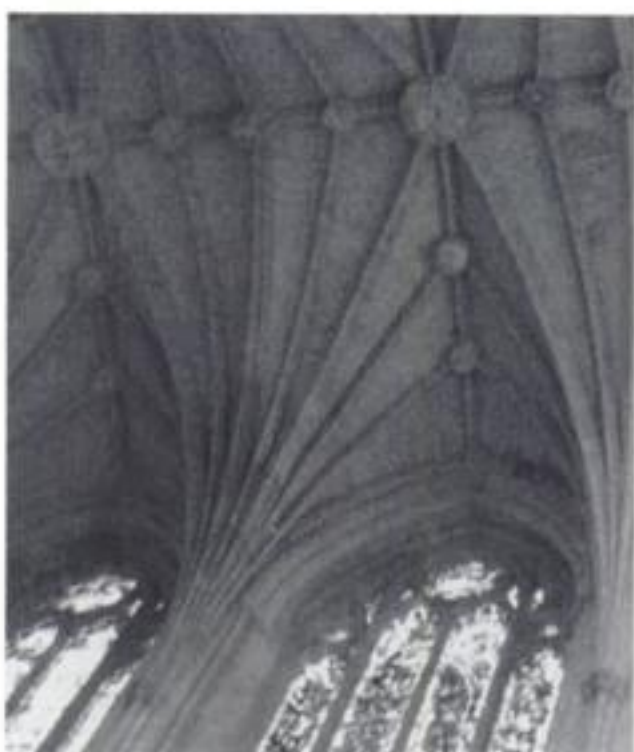


Figure 1. Tierceron vaults in the choir of National Cathedral.

Tierceron rib vaults, which cover the rectangular plan bays of the church, are constructed using Indiana limestone (Fig. 1) (www.cathedral.org; Ed. Fallen, 1995).

2 FINITE ELEMENT MODEL CREATION

The finite element model creation starts with the geometric modeling. The models of NC are created using the scaled drawings from the NC archives (National Cathedral Archives) and on-site observation.

After the geometric model is created, numerous unknown parameters are added to the model for a structural analysis, such as the material properties and the boundary conditions. These parameters affect the structural behavior of the model greatly and it is impossible to have confidence in these parameters without verification from some experimental data. For that reason, some experiments on the vaults of NC are conducted, which reveal information about the structural behavior. Once these parameters are updated in the analytical models based on experimental findings, the analyses to be performed on these models will be more reliable. The final boundary conditions and the material properties for this model, as updated by the experimental results are presented in the subsequent sections.

2.1 Finite element model material properties

The models are created with the assumptions of linear behavior and homogenous material. The initial assumption for linear behavior is proved to be appropriate after the review of dynamic experiment results, because the impacts from different magnitudes of impact (heel drops vs. hammer impact) generate similar behavior on the structure, as will be presented later



Figure 2. The National Cathedral three-vault finite element model (software: ANSYS) and the experimental setup schematic shown on the finite element model.

Table 1. Masonry assembly stiffness values.

Mortar (E in GPa)	Joint thickness		Masonry (E in GPa)	E_{eff} (GPa)	
	(mm)	(in)			
Max	1.4	6.4	(1/4)	31	21
	1.4	9.5	(3/8)	31	18
Average	0.85	6.4	(1/4)	31	18
	0.85	9.5	(3/8)	31	15
Min	0.31	6.4	(1/4)	31	10
	0.31	9.5	(3/8)	31	8

in this paper. The homogeneous material assumption, which considers effective material properties for the masonry unit and mortar assembly rather than separate entities for units and masonry joints, is adopted for simplification of the finite element analysis procedure.

The material properties are gathered from various sources such as literature (www.langstone.com), laboratory experiments on an Indiana lime stone sample, and calculations to account for the mortar unit assembly assumption. Depending on the stiffness of the mortar and the thickness of the mortar joint, the effective stiffness of the assembly varies. Table 1 summarizes the possible Modulus of Elasticity (E-value) ranges for masonry assembly with type O mortar and Indiana lime stone. The mortar E-values are from McNary & Abrams (1985) and E value for the Indiana lime stone is from laboratory testing. The mortar joint thicknesses vary between 9.5 mm and 6.4 mm (3/8"–1/4").

According to the information given in Table 1, the modulus of elasticity for the masonry-mortar assembly for the finite element model ranges between 8 GPa to 21 GPa, depending on the condition and thickness of the mortar joints. When the model is updated by the experimental results, the optimum value for the masonry assembly stiffness is found to be 12 GPa. This is partially due to the fact that the masonry in the vaults

Table 2. Final material properties for NC finite element model.

Material	Modulus of elasticity (GPa)	Density (kg/m ³)	Poisson's ratio
Masonry assembly	12	2100	0.2
Concrete surcharge	24	2100	0.15

buttresses and connection of the roof trusses to the exterior wall.

3 EXPERIMENTAL PROCEDURES AND RESULTS

In this research, the experimental modal analysis techniques are used to validate the finite element models of the complex vaulted systems. This is an application of dynamic experiments that the design of experiments constitutes an important part of the procedure. Therefore, experience from similar experiments performed on other types of structures is called upon. Hanagan et al. (2003) investigate the variables that affect experimental modal analysis of floor systems, some of which are discussed in the following sections and are used in this study to determine the experimental procedures.

3.1 Experimental equipment and setup

In this study, three different excitation methods are used: heel drops, shaker excitation and hammer impacts. The heel drop is a man-made impact created by raising up on one's toes and dropping the heels onto the floor. The heel drop impact force is measured using a force plate constructed by attaching four shear beam load cells to the corners of a thick aluminum plate (Hanagan, et al., 2003). The force plate used for heel drops in this study, has a calibration coefficient of 3916 N/volt. The instrumented hammer is another convenient tool to excite a floor system because of its portability. The instrumented hammer used is PCB Piezotronics ICP[®] Impulse Hammer Model 086C20. The hammer has options for creating the impact, including a selection of tips with varying hardness. Since the hammer is instrumented, the force plate is not required and the hammer can be connected directly to the data acquisition system. However, in this set of experiments another custom designed force plate, with a calibration coefficient of 801 N/volt is used to measure the force created by the hammer.

The force plate, which is used for the heel drops, is also used for the shaker. Due to the heavy weight and low coherence caused by some technical problems with the available shaker at hand, the shaker is not used in these experiments extensively. However, as better data is available from shaker excitation for one of the setups (Row4), the data from that experiment is used for determining the mode shape and is presented in this paper as evidence for the consistency of the results regardless of the excitation type and thus the linearity of the structural behavior.

Seven PCB Piezotronics model 393A03 seismic accelerometers, with a sensitivity of 1 V/g are used as vibration transducers and were placed in various arrays. The experiments on the NC vaults cover

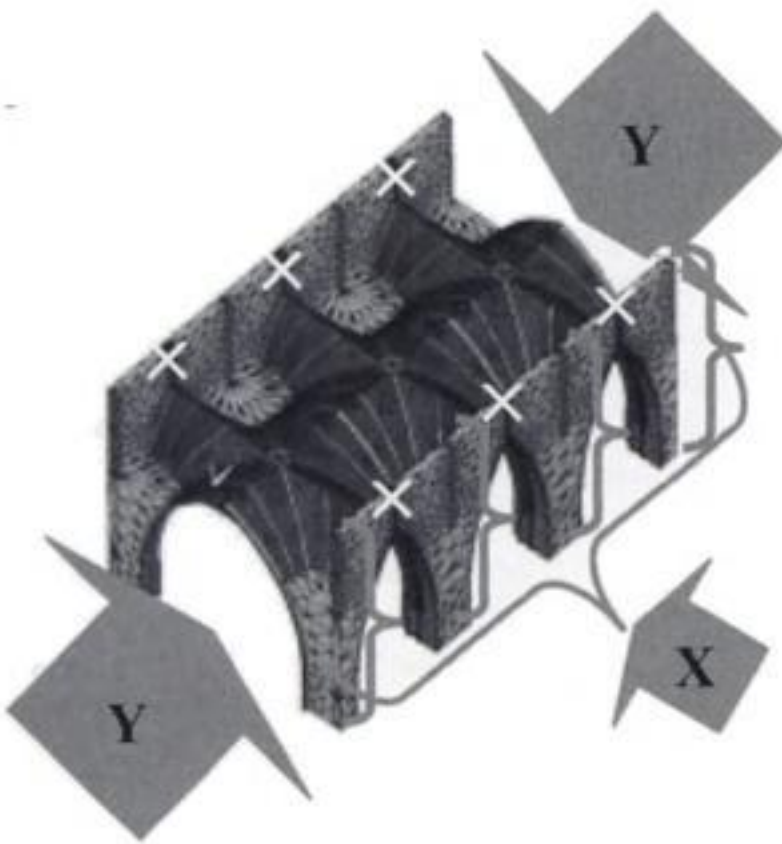


Figure 3. Final boundary conditions as updated by the experimental findings.

has lost some of its initial stiffness due to loss of mortar and cracks at some joints, which results in an E-value at the lower end of the range.

The other material properties required are the density and the Poisson's ratio of the masonry assembly, and the material properties for the surcharge, which is concrete in the case of NC. Table 2 presents the experimentally validated final values for these parameters.

2.2 Finite element model boundary conditions

The boundary conditions are applied based on observations and are then updated by experimental results to match the experimentally observed mode shape. The final boundary conditions, as illustrated in Figure 3, are as follows: The sides of the arches are restrained in the Y direction to account for the adjacent vaults. The top portion of the side arches is restrained in the vertical direction to account for the vertical-movement-limiting effects of the adjacent arches. Parts of the exterior wall are restrained in the X direction to account for the wall buttresses, flying

mode of the system. Figures 5 and 6 present these plots for the heel drop tests in the NC, for the sensor located immediately adjacent to the driving point for the setup shown in Figure 4. As can be seen from both plots, there is an apparent mode with a natural frequency of 36 Hz.

Since the force input is normalized and plotted for every frequency, FRF allows for averaging and comparing data from several excitations even though the applied force intensity varies. The coherence function measures how well the output is linearly related to the input for every frequency, and is rated on a 0 to 1 scale. Coherence measurements approaching unity indicate a linear trend between output and input, and in most cases represent high confidence in the measured data (Hanagan et al., 2003; Raebel, 2000). The coherence for the heel drop measurements for the sensor next to the driving point is presented in Figure 5 and it suggests good quality data except the 0–5 Hz low frequency range, where the ambient noise interferes with the generated vibrations.

Figure 7 shows the FRF from a hammer impact at the same driving point. As can be seen, the low coherence for hammer impact covers a larger range of lower frequencies (0–25 Hz). This is mainly because the hammer impact is a low amplitude excitation, that can generate lower frequency vibrations and therefore the data is more susceptible to the ambient noise. On the other hand, the FRF plots for these two different excitation levels are very similar, which supports the assumption of linear behavior for this structural system.

The deflected shape of the structure from the experimentally observed mode shape is gathered from the imaginary plots, as this representation of the FRF also includes the sense of the acceleration for each sensor (Figs 8 & 9). By noting the positive and negative motion of each sensor, the deformed shape for the testing scheme illustrated in Figures 1 and 4 is plotted in Figure 10.

By comparing this experimentally observed deformed shape with the analytically established mode

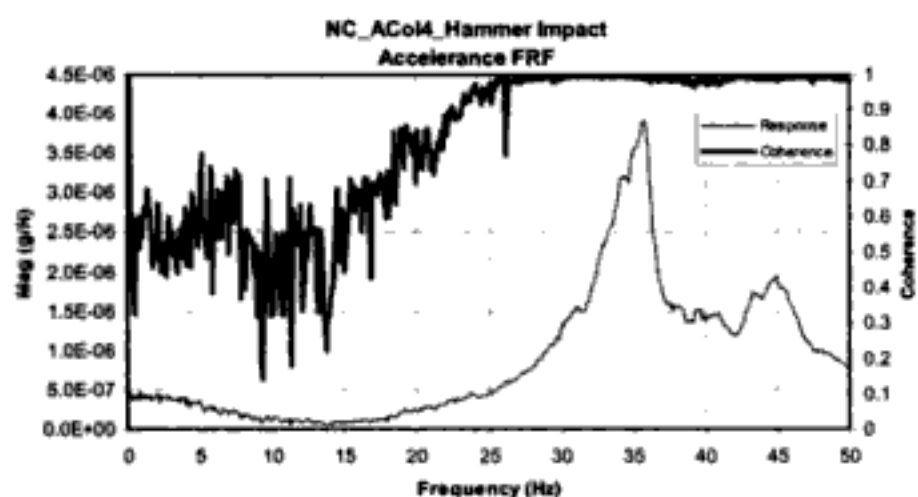


Figure 7. FRF magnitude and coherence plot for hammer impact for the NC experiment setup col4.

shapes, it is possible to validate the boundary condition assumptions, because the mode shape is determined mainly by boundary conditions. Other parameters such as the material properties (Masonry and surcharge stiffness, density and Poisson's ratio) have no effect on the mode shape, although they affect the natural frequency of this mode shape.

An additional experimental result of interest is the FRF plotted in displacement units, because the displacement at zero frequency gives the inverse of the system stiffness, i.e. the system flexibility. Since the sensors measure acceleration, the data collected must be converted to displacement units

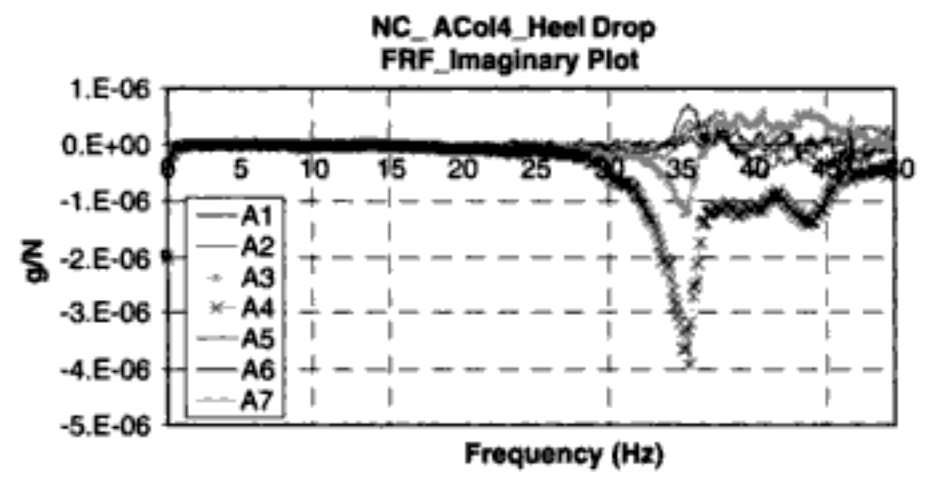


Figure 8. Imaginary plot for heel drop excitation for all sensors in the NC experiment setup col4.

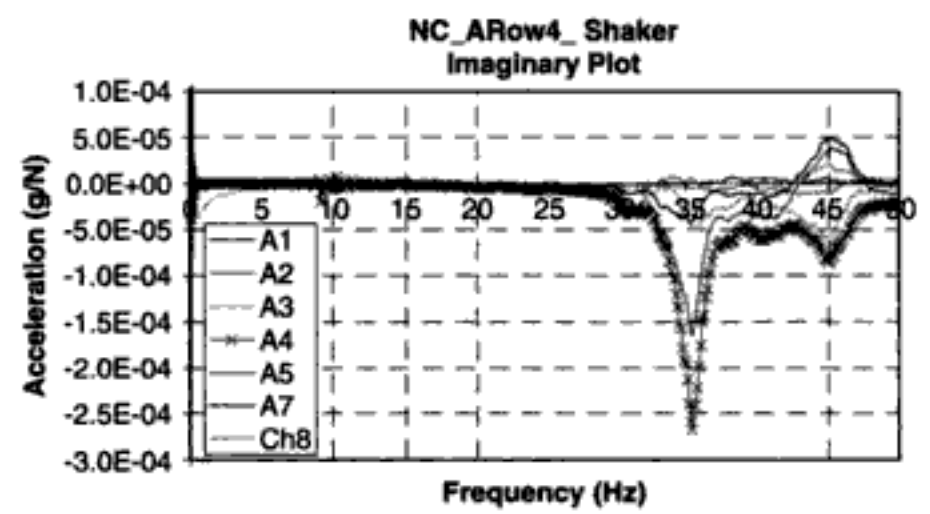


Figure 9. Imaginary plot for shaker excitation for all sensors in the NC experiment setup row4.

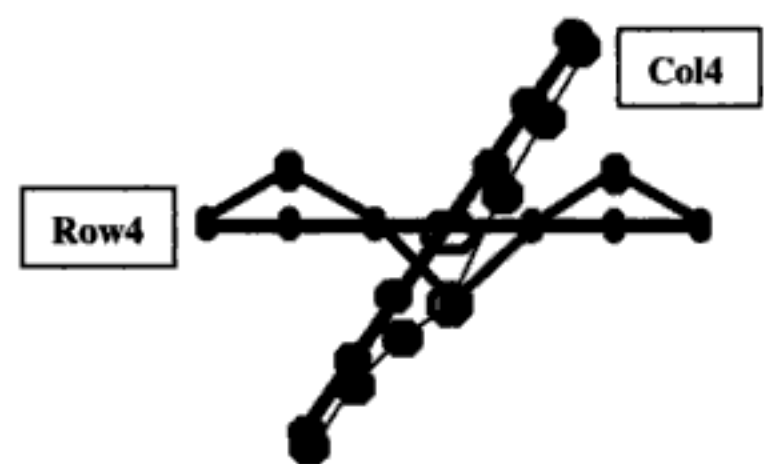


Figure 10. Deformed shape of the top beams detected by the grid of accelerometers at 36 Hz.

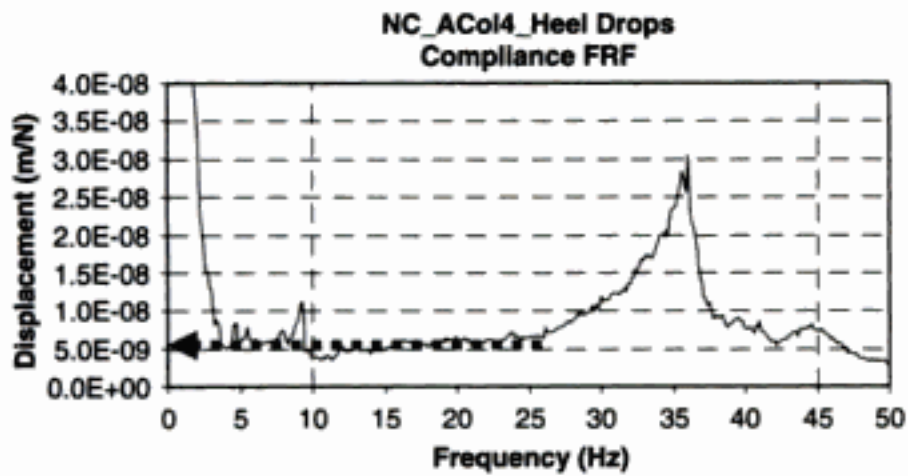


Figure 11. Displacement FRF for the NC experiment setup col4.

using the relationship between the acceleration and displacement as shown by Equation 1.

$$\ddot{X} = -\omega^2 X \quad \text{or} \quad X = \frac{\ddot{X}}{-\omega^2} \quad (1)$$

Where, \ddot{X} is the acceleration
 X is the displacement
 ω is the circular natural frequency

The data collected by the accelerometer next to the driving point during heel drops is converted to displacement units by Equation 1, and plotted as shown in Figure 11.

If the acceleration at zero frequency were actually zero, then the equation would result in a singularity and would be solved for by an indefinite integral solution. Thus, the conversion between the acceleration and displacement units in theory is not trivial but it is possible. However, in practice, this conversion generates some problems. The ambient noise results in very small vibration amplitudes at the lower frequencies, which is also apparent from the low coherence between 0–5 Hz, as shown in Figure 5. Therefore, the displacement plot is not reliable at these lower frequencies. But if a displacement FRF for a simple system is inspected, it is observed that there is a plateau starting at about the root of the resonant peak of a natural frequency and ending at 0 Hz. Therefore, the value at 25 Hz can be extrapolated in the plot in Figure 10 to 0 Hz and hence result in an approximate value for the system stiffness of 5E-9. Although approximate, this system stiffness value can then be compared to analytically established values to see if they are in the same order of magnitude.

4 MODEL VALIDATION

The finite element model is analyzed by linear elastic, undamped modal analysis for a comparison with the experimental results. The modal analysis equation

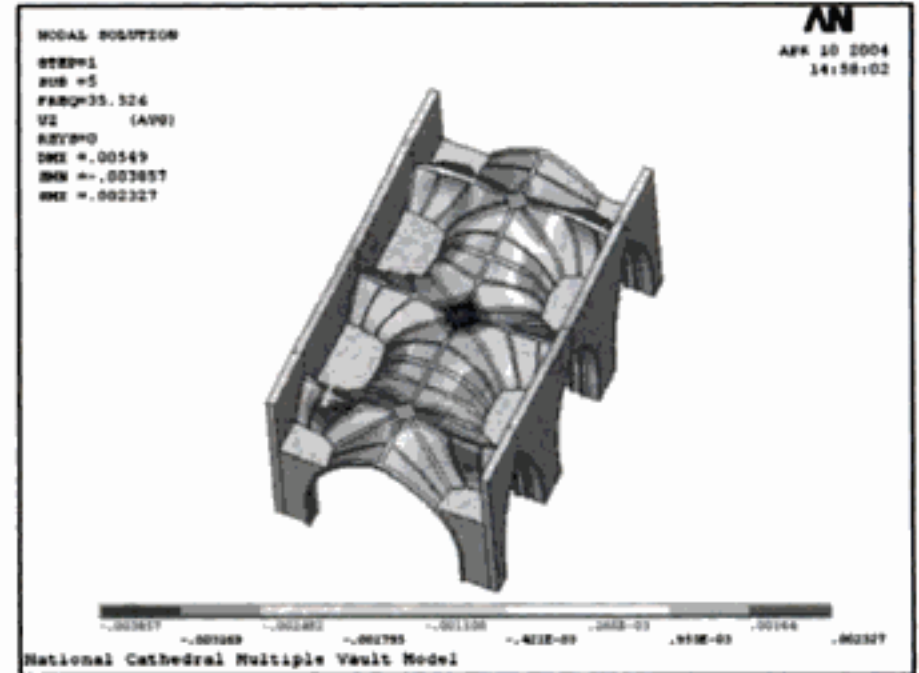


Figure 12. The deformed shape and vertical displacements plot on the full three-vault model.

used by the finite element analysis software ANSYS is given by Equation 2 (ANSYS, 2003).

$$[K]\{\varphi_i\} = \omega_i^2 [M]\{\varphi_i\} \quad (2)$$

Where, $[K]$ is the stiffness matrix
 $\{\varphi_i\}$ is the mode shape vector (eigenvalue) of mode i
 ω_i is the natural circular frequency of mode i
 ω_i^2 is the eigenvalue
 $[M]$ is the mass matrix

When such an analysis is performed on the three-vault model of NC, the 5th mode of vibration, which is the lowest mode with a substantial vertical movement at the sensor points, presents a similar deformed shape as the experimentally observed one, at 35.5 Hz. These results are for the previously described final material properties and boundary conditions, and present a very good agreement with the experimental results. Hence the model is validated with the *in situ* experiments. The results for this mode shape are shown in Figure 12 on the full model and Figure 13 shows the deformed shape for the top ribs only.

If Figure 13 is compared to Figure 10, it is seen that the analytically determined mode shape for the top ribs are in very good agreement with the experimentally observed deformed shape.

In order to determine the system stiffness analytically, a static unit load is applied to the point, which is the driving point during the experiments and the displacement at this point is sought. Figure 14 presents the graphical results for this static analysis.

The system flexibility (inverse of system stiffness) determined by this analytical model is 4E-09 m/N while the experimentally gathered approximate value is 5E-09 m/N. The two are in the same order of magnitude. The error is due to the low coherence of

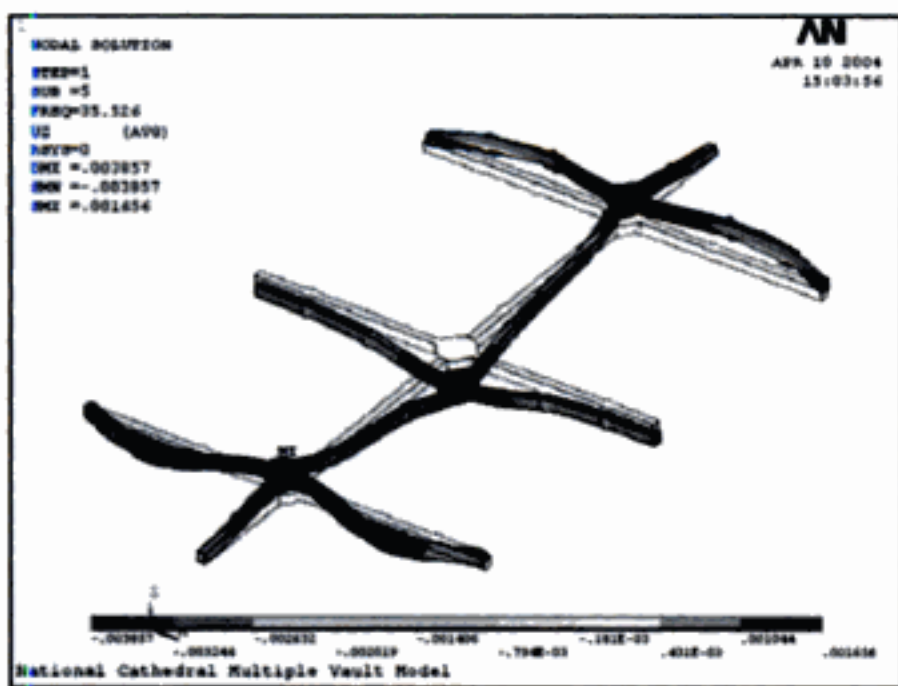


Figure 13. The deformed shape and vertical displacements illustrated only on the top beams of the three-vault model.

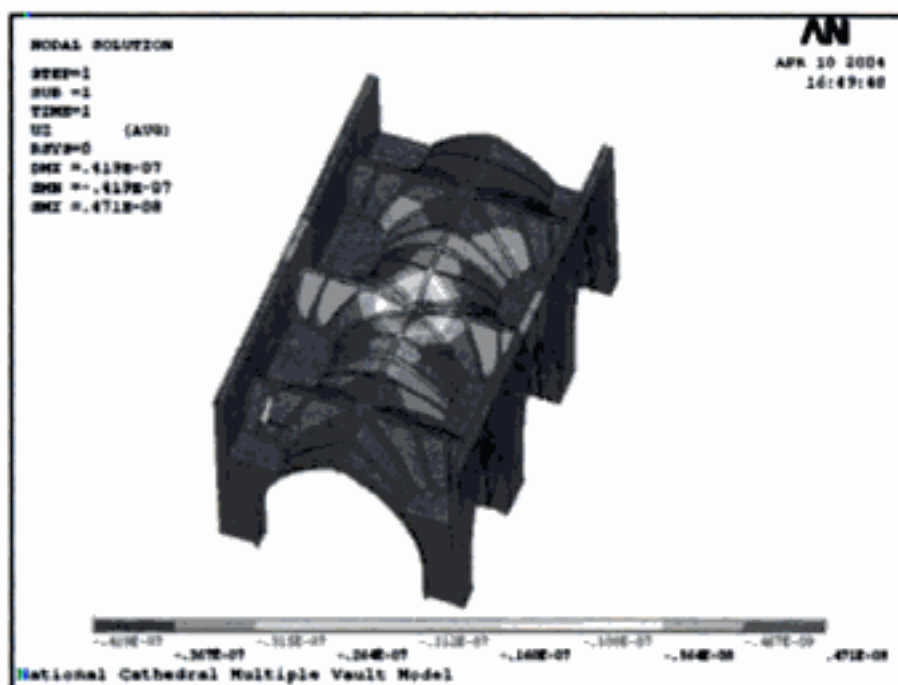


Figure 14. The static analysis with unit load for system stiffness.

the experimental data at the lower frequencies and the errors emerging from the manual post-processing conducted to gather the displacement data from the acceleration data.

5 SUMMARY AND DISCUSSIONS

In this study, the experimentally observed mode shape of the tested structure and the natural frequency of this mode are compared to the analytical model results for the validation of analytical models. As the applied boundary conditions result in a mode shape that is in very good agreement with the experimentally observed mode, the next step is to determine the most accurate material properties within the appropriate range, which is gathered through a combination of lab experiments and literature. Effective stiffness values are calculated to account for the combined properties of the Indiana lime stone and type O mortar.

With these material properties, the analytical natural frequency is in very close agreement with the experimentally recorded natural frequency. The analytical system stiffness is also compared to an approximate experimental value, which are in the same order of magnitude. Although there is 25% error in this comparison, this error is mostly due to the approximately calculated value of the displacement at zero frequency. As a result of all three types of comparisons and updating, the analytical model is successfully validated by the nondestructive vibration experiments.

Besides proposing a validation method for the complex three-dimensional finite element models of the stone vaulted systems, this study reveals several useful facts about the dynamic testing of such structures. For instance, it is observed that the heel drops give more coherent results than the impulse hammer impacts. However, as heel drops are not possible on most vaulted systems, an instrumented hammer, which presents the advantages of convenience and portability, is recommended, since it gives comparable results for the mode shape and natural frequency.

Another finding through various experimental trials in this study is that, the structure behaves linearly under dynamic loading and thus linear analysis on the structure is appropriate.

The work presented in this study is an excerpt from an ongoing research project, but it reveals some very useful conclusions for the future work of the study, which explores the extrapolation of the proposed methods to European medieval structures. For these cases where the material properties are also unknown, the vibration experiments on the structure itself and the knowledge from similar structures with calibrated models, such as established here for NC, can be used for model validation.

ACKNOWLEDGEMENTS

The authors would like to thank to Professor Linda Hanagan, the National Cathedral administration, Joe Alonso and Professor Robert Mark for their support and patience. The assistance of Guoliang Jiang and Carlos Gomez are also greatly appreciated.

REFERENCES

- ANSYS Incorporation, (2003). *ANSYS Elements Reference*.
- Boothby, T.E. (2001). "Analysis of Masonry Arches and Vaults," *Prog. Struct. Engng Mater.* Vol 3, 246–256.
- Hanagan, L.M., Raebel, C.H., and Trethewey, M.W. (2003). "Dynamic Measurements of In-Place Steel Floors to Assess Vibration Performance." *Journal of Performance of Constructed Facilities, ASCE*, 17(3), 126–135.
- <http://www.cathedral.org>
- <http://www.langstone.com/indiana.htm>

McNary, W.S., and Abrams, D.P. (1985), "Mechanics of Masonry in Compression," *Journal of Structural Engineering, ASCE*, Vol. 111, No. 4, 857–870.

Raebel, C.H. (2000). "Development of an experimental protocol for floor vibration assessment," *Masters Thesis*, Pennsylvania University.

Washington National Cathedral Guidebook, (1995) Ed. Anne-Catherine Fallen, Research & Design, Ltd., Washington National Cathedral, Washington.

Washington National Cathedral Archive, Washington National Cathedral, Washington, DC.

A first approach to study an 18th century belltower

S. Ivorra

Departamento de Mecánica de los Medios Continuos y Teoría de Estructuras, Universidad Politécnica de Valencia, Spain

M.J. Palomo & G. Verdú

Departamento de Ingeniería Química y Nuclear, Universidad Politécnica de Valencia, Spain

F. Pallarés

Departamento de Física Aplicada, Universidad Politécnica de Valencia, Spain

ABSTRACT: This paper describes the analysis performed for the characterization of the dynamic structural behavior of the belltower of Nuestra Sra. de la Misericordia Church in Campanar (Valencia, Spain). Subsequently to the geometrical analysis of the belltower structure, different numerical models were calibrated based on dynamic tests to determine the bending and torsion frequencies of the tower. This work was complemented with the analysis of the inertia forces caused by bell swinging and the possible dynamic amplification factor as a consequence of the close values between the excitation and belltower frequencies. This study was performed prior to the restoration of the bells and to the installation of new automatic bell systems.

1 INTRODUCTION

The belltower of Nuestra Sra. de la Misericordia Church in Campanar (Valencia) was built by the Valencian architect José Mínguez, and it was finished in 1740. From its construction, the church has been restored in several occasions. The last works were developed in 1987, conducted by the architect Francisco Esquembre; some metallic elements were incorporated for bracing the bells' housing body. By the end of 2003 the three old bells were restored and were again installed in the tower together with a new bell. All of them possess the traditional Valencian yoke and computer-based automatic systems that simulate the typical Spanish bell swinging system.

2 GEOMETRICAL DESCRIPTION

The belltower presents a square plant with 5.6 m per side; it possesses the three typical bodies characteristic of the belltowers built in this period: basement, belltower and crown. The building technique consists of solid brick and mortar, except for the central pane of the first body, which uses masonry. The thickness of the walls is 1.20 m at the wall base. Two well-differentiated building sections can be noticed with respect to the type and thickness of the mortar and

to the working technique. The first section comprises the first 12.50 m whereas the second section comprises from this height to the crown of the tower. This, together with the data available in the documents of the Church Archive indicates the existence of an earlier tower on which the present tower was erected.

The height of the tower crown is 42 m. Despite its apparent symmetry, it is conditioned by the fact that one of the tower walls lies on one of the buttresses of the central nave of the Church.

3 FORMAL COMPOSITION

The belltower consists of the three main bodies mentioned in the previous section (Base, bell house and crown) – figure 2, separated by two big cornices. The base is square-shaped, with 5.60 m. per side. The first body is a square-base prism with a height of 23 m, which houses the baptistery. This opening originally reached approximately a third of the height of this body, topped with an ogival arch that can be seen in one of the rooms inside the tower. The arch is partially walled towards the inner room of the tower with a wall supported by a wooden beam, and totally walled towards the church by walls supported by two arches: a half-point arch and a carpanel arch; this arch covers a false vault that covers the baptistery.

square-shaped. It presents two symmetry axes, only broken inside by the staircase that gives access to this floor and that communicates with the upper floor, placed on the SE corner, and slightly integrated in the wall. This body presents four brick arches, one arch per side, which house the bells. The arches are flanked by four pillars, with a top pyramid at the corners.

The transition to the last body is through an arched buttress, placed at the four diagonals of the transition level to a smaller square-shaped central body that forms the crown of the tower, ended with a Valencian blue glazed tile dome. This body houses the clock bells.

4 CONSTRUCTION TECHNIQUE

The construction technique consists of solid brick and mortar, except for some sections in the first body, made of masonry. There are two building techniques clearly differentiated with respect to the materials, type and thickness of the mortar used and the building method. The first section goes up to the walled ogival window on the N façade (16 m), whereas the second section goes from here to the crown. The Baroque top of the clock bell house, architecturally well solved with respect to the perfect connection between the base body and the top dome, is however constructively defective with respect to its structural conception. The bell house body ends with a vault that forms a platform where the upperbody is supported. Since this presents a smaller section, load transfer does not occur on the perimetral walls but in the middle of the platform. The arches located in the lateral sides at 45° do not perform any structural function, since they do not alter substantially the load transfer system. This causes important inclined stresses on the base of the vault that tend to be corrected by stone pillars and pinnacles. This increases the vertical component but causing a horizontal force that with time, and the vibration generated by the bells, the effects of the old mechanic swinging system, and other external factors have caused small cracks in the arches of the bells body and vault base. Except for some stone pieces, all the ornamental elements are made of ceramic pieces, brick and concave and convex rounded pieces. All the structure is painted and covered mainly with sand-lime mortar, though some repairs and patches used sand and cement mortar. At present, the tower has been painted on it outside.

5 EXPERIMENTAL ANALYSIS

Different dynamic tests were performed on the tower in order to determine its dynamic characteristics, that is, its vibration modes in bending and torsion as well as the overall damping of the system.

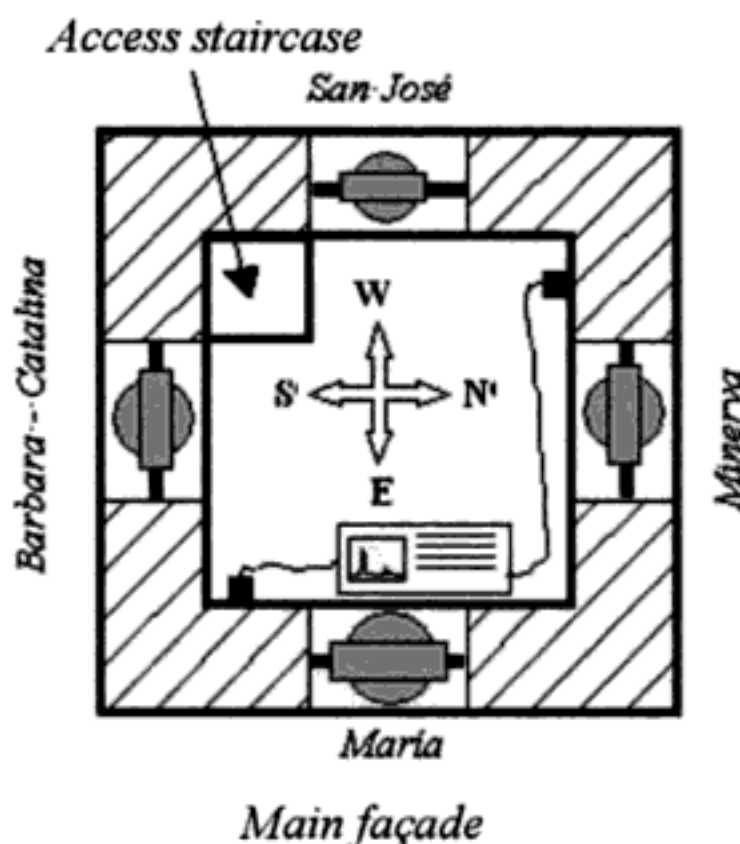


Figure 3. Location of the bells in the tower. Location of the accelerometers for dynamic testing.

The works of Bachmann (1997) and Casolo (1998) fix the main frequencies in torsion and bending between 0.9 and 2 Hz for slender towers.

From the equation (1) proposed by the NCSE 2002 we can obtain the values of the estimated frequencies of the tower:

$$\omega_1 = \frac{\sqrt{L}}{0.06 \cdot H \cdot \sqrt{2 \cdot L + H}}$$

$$\omega_2 = 3 \cdot \omega_1$$

$$\omega_3 = 5 \cdot \omega_1 \quad (1)$$

where:

L : plant dimension of the building in the direction of the oscillation.

H : building height.

This particular building structure is supposed to have a natural frequency of 1.2 Hz or higher, since the stiffness of the structure will be greater as a result of having a contact zone with the church nave. According to the classification of buildings specified in the standards mentioned, this structure possesses a first period comprised between $0.75 \text{ s} < T < 1.25 \text{ s}$ so that it can be considered a slender construction

For dynamic testing, two piezoelectric accelerometers were placed at the height of the bell house, as shown in Figures 3 and 4. The working range of the accelerometers is between 0.5 and 2000 Hz, with a conversion factor of 1 V/g. With this arrangement the E-W and N-S vibrations of the tower can be measured. The dynamic data generated on the tower by environmental vibrations were recorded at the same time by the two channels of a YOKOWAWA instrument with a sampling frequency of 200 Hz.

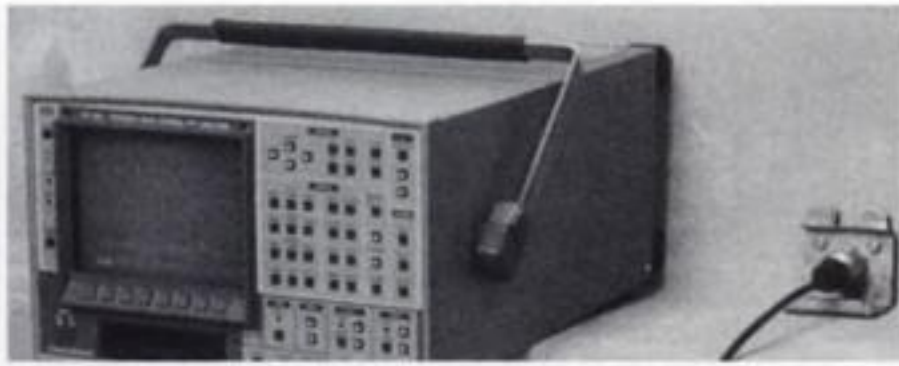


Figure 4. Accelerometer anchorage.

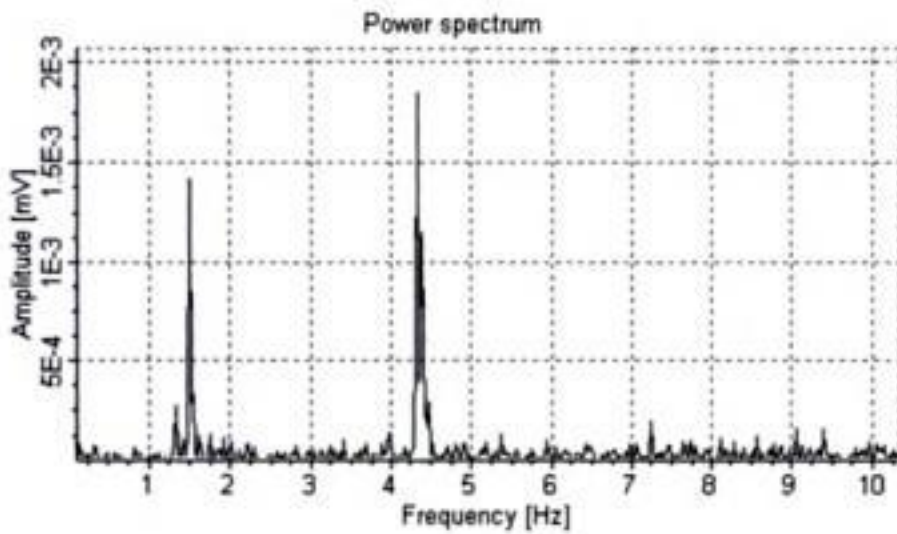


Figure 5. Power Spectrum of the tower for the E-W direction.

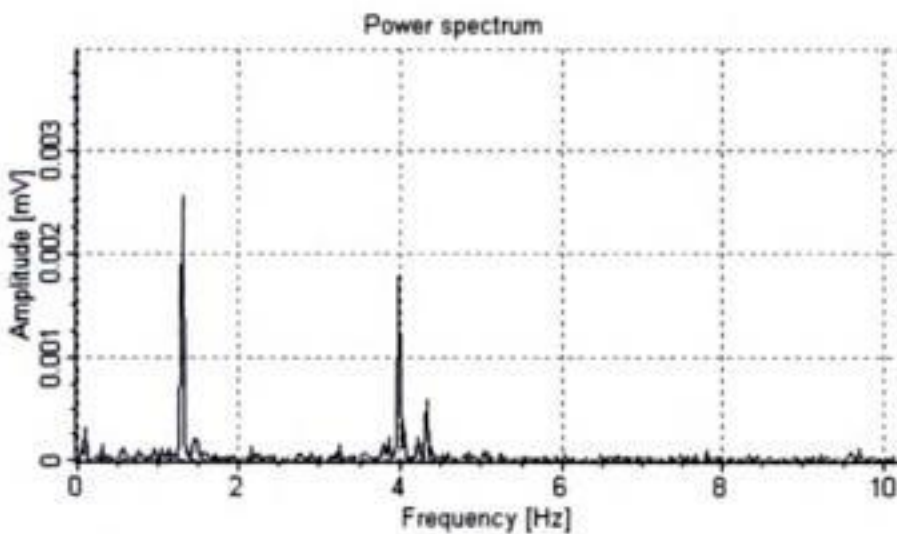


Figure 6. Power Spectrum of the tower for the N-S direction.

From the recordings of the environmental vibrations the Power spectral Response of the structure was obtained for the E-W and N-S directions, shown in Figures 5 and 6 and described in Table 1.

These graphs were used to identify the mode parameters described in Table 1.

Once a natural frequency has been detected, it is very easy to produce large structural deformations with small energy input. Using the oscillation of San José bell at 1.294 Hz and stopping the device and allowing the tower's free vibration slowly, the logarithmic viscous damping decrement can be easily derived from the measured time history. (Meskouris, 2000). For this tower we obtain an approximate damping ratio of 0.0159.

Table 1. Frequencies of the tower.

Direction	Frequency (Hz)	Mode classification
E-W	1.489	Bending
	4.321	Torsion
	4.370	Bending
N-S	1.294	Bending
	3.979	Bending
	4.321	Torsion



Figure 7. Minerva bell rotating around its axis.

6 CHARACTERISTICS OF THE BELLS

The bells of this tower swing by the Spanish system – Ivorra, 2001, 2004 where a big counterweight provides a high level of balance and the bells, directly anchored on the tower windows, rotate continuously in the same direction – Figure 7. To determine the characteristics of these bells we have carried out laboratory tests on the bells of this tower. To that purpose, one of the authors developed a work protocol (Ivorra (2002)) based on the works of Heyman & Therefall (1976) and Wilson (1992). Tables 2 and 3 show the results obtained for all the bells of this tower.

Considering the bell as a compound pendulum, we calculated the horizontal and vertical forces induced in the tower by the bell's swinging. Figure 8 shows the temporal variation of the horizontal force for María bell. From the dynamic test, we calculated all possible dynamic amplification factors (D.A.F.) generated by

Table 2. Characteristics of the bells of the tower.

Bell name	Total weight (N)	Bronze weight (N)	Total W/bronze W	Unbalance (m)
Bárbara Catalina	3000	1510	1.99	0.074
San José	7250	4160	1.74	0.090
Minerva	10100	5740	1.76	0.088
María	16000	9160	1.75	0.090

Table 3. Dynamic characteristics of the bells of the tower.

Bell name	Swing velocity rad/s (Hz)	Inertia (kg · mm ²)	Admin. horizontal force	Admin. vertical force
Bárbara Catalina	5.2 (0.8)	5.9	0.277	1.237
San José	4.2 (0.7)	28.19	0.211	1.182
Minerva	3.8 (0.7)	56.28	0.161	1.143
María	2.6 (0.4)	84.04	0.161	1.144

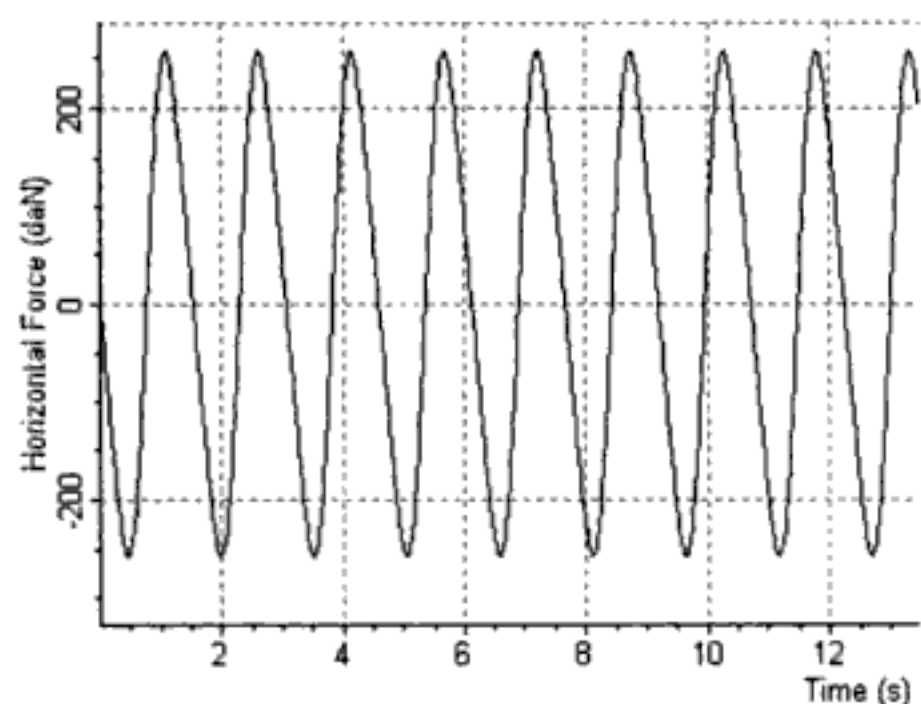


Figure 8. María Bell. Horizontal force temporal variation.

the interaction of the tower frequencies and the bells excitation.

A frequency analysis of the variable forces induced by the swinging of housed bell or bells is needed to assess the reliability of the supporting structure. Due to their geometry, the materials used in their construction and the traditional disposition of the bells, most towers show significantly higher stiffness to axial loading than to torsion or bending, making therefore more critical the horizontal component of the induced forces (Müller, 1963). Figure 9 shows the RMS spectrum for the horizontal force induced by María Bell swinging by the Spanish System. The results obtained from the frequency analysis of the four bells are shown in Table 4.

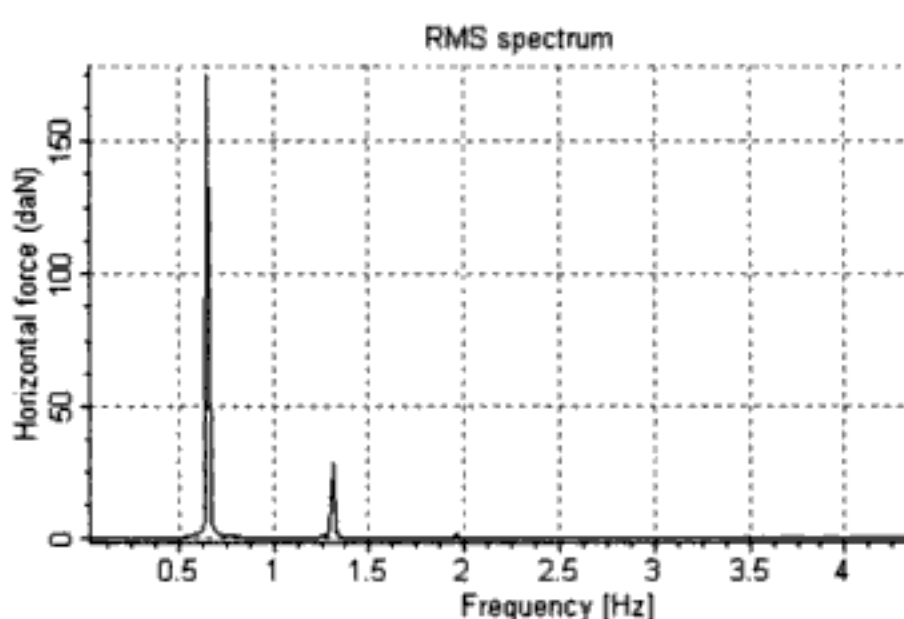


Figure 9. María Bell. RMS spectrum of horizontal force.

Table 4. Analytical harmonics of horizontal force.

Bell name	First (Hz)	Second (Hz)	Third (Hz)
Bárbara Catalina	0.935	1.871	2.086
San José	0.741	1.483	2.224
Minerva	0.659	1.317	1.976
María	0.654	1.308	1.963

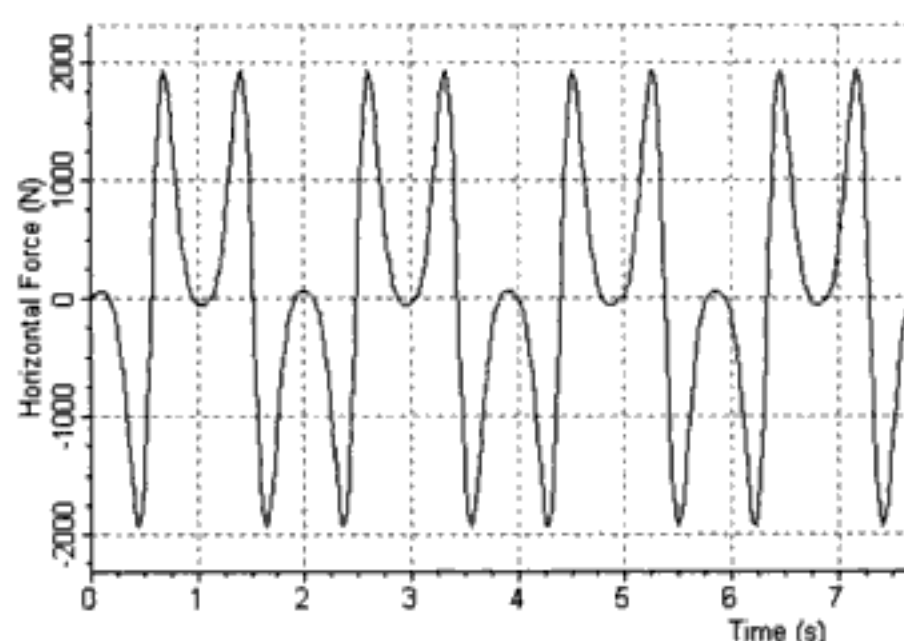


Figure 10. Characteristic temporal variation of the horizontal bell force swinging by the Central European System.

Note that for this bell swinging system the dominant harmonic corresponds to the first one, as can be seen in Figure 9. Applying the DIN4178 standard, we also calculated the horizontal forces induced by the bells under the Central European swinging system – Figure 10. A frequency analysis was performed – Figure 11 and we concluded that for this bell swinging system the dominant harmonic corresponds to the third one, as described in the standards. This is a significant difference between both bell swinging systems.

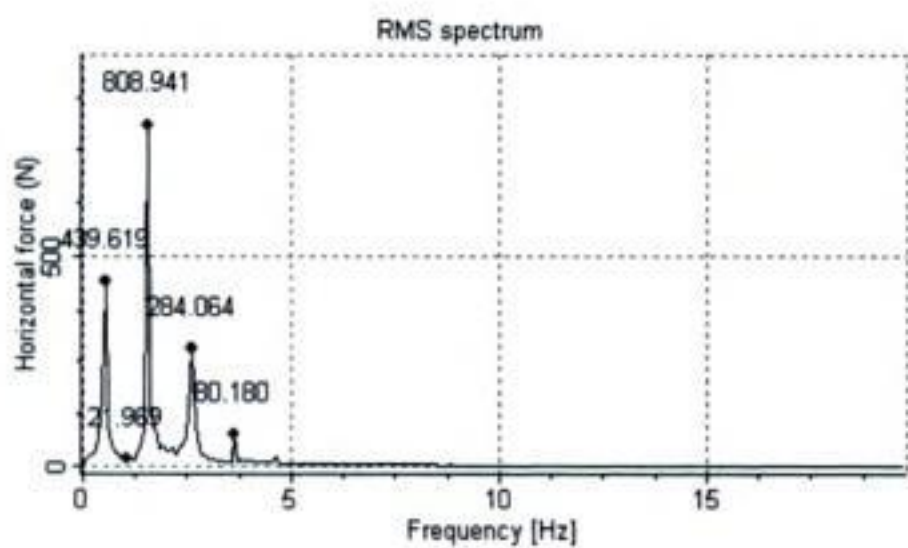


Figure 11. RMS spectrum of the horizontal bell force swinging by the Central European System.

7 NUMERICAL ANALYSIS

Subsequently to the accurate analysis of the geometry of the tower, different numerical models were developed to assess the structural response of the tower to the excitations caused by bell swinging. All the numerical models were calibrated through the dynamic tests performed. Considering the initial behavior of the tower as a cantilever beam with box square cross section with one degree of freedom, the relationship between the material's elastic modulus and the tower's first natural frequency value is:

$$E = \frac{4 \cdot M \cdot L^3}{b^4 - (b - e)^4} \cdot \omega^2 \text{ (N/m}^2\text{)} \quad (2)$$

where:

M = mass of the tower

L = crown height

b = width of the square tubular section

e = wall thickness

ω = s.d.o.f natural frequency.

From Equation (2) we can deduce directly that an increase in the elastic modulus involves an increase in the system's frequency; an increase in the specific weight of the material (mass) involves a decrease in the system's frequency; and an increase in stiffness involves an increase in the system's natural frequency. These considerations for 1 d.g.f. systems can be extrapolated to m.d.o.f. systems.

For the development of these simple models, the following hypotheses have been considered:

- The specific weight of the material is supposed to be constant for the whole tower, 18 kN/m³, following the NBE AE standards – 88 for solid brick structures. In beam models weight is considered to be uniformly distributed.
- The Poisson's ratio of the masonry was held constant and equal to 0.15.

Table 5. Elastic modulus in W-E and N-S direction for simplified models.

Direction	Degrees of freedom	First natural frequency (Hz)		Elastic Modulus (N/mm ²)
		Measured	Model	
E-W	26	1.489	1.489	4746
N-S	26	1.294	1.295	3.579
E-W	52	1.489	1.489	4746
N-S	52	1.294	1.295	3.579
E-W	104	1.489	1.487	4746
N-S	104	1.294	1.297	3.579



Figure 12. West façade.

- The mechanical behavior of the material was considered to be linear elastic, since we applied the method of modal superposition.
- All degrees of freedom are restrained in the base of the tower.
- The belltower possesses a limited N-S horizontal displacement as a consequence of the N wall of the central nave of the church. The height of this section reaches 11.5 m. This constraint will be considered through the mean elastic modulus of the tower calculated by the iterative procedure in which the bending first natural frequency value obtained in the dynamic test is made to coincide with that of the numerical method.
- The model is based on the flexural vibration of the Timoshenko beam where shear deformations are considered and the rotary inertia of deep cross-sections may be significant.

From these hypotheses different simplified models were evaluated; the results are summarized in Table 5.

These results show that the stiffness of the tower in the E-W direction is greater than in the N-S direction. The effects of the E-W displacement is conditioned by the great stiffness of the wall of the central nave of the church, which supports part of the N side of the tower (Figure 12).

- Meskouris, K., 2000, Structural Dynamics, Models, Methods, examples. Ernst & Sohn (Eds.). Berlin, 143–156.
- Müller, F.P., 1963. Statische und dynamische probleme beim bau on glockentürmen, Deutsche Bauzeitung, no 12, 1–4
- NBE AE-88, 1988. Acciones en la edificación. Ministerio de Fomento, España
- NCSE 2002. Norma de Construcción Sismorresistente. Ministerio de Fomento, España
- Niederwanger, G., 1997. Structural Repair of Damaged Old Bell Towers Based on Dynamic Measurements. Structural studies, Repairs and Maintenance of Historical Buildings Ed. Sanchez. Computational Mechanical Publications. Southampton, 321–330
- Schutz, K. G., 1994, Dynamische Beanspruchung von Glockentürmen. Bauingenieur 69, Springer-Verlag , 211–217
- Wilson, J.M., Selby A., 1993. Engineering a Cathedral, London, Thomas Telford Ltd., London, 77–100

Dynamic-based F.E. model updating to evaluate damage in masonry towers

C. Gentile & A. Saisi

Department of Structural Engineering, Politecnico of Milan, Milan, Italy

ABSTRACT: The paper presents the experimental and analytical modal analysis of a masonry bell-tower, dating back to the XVII century. The tower, about 74 m high, is characterised by the presence of major cracks on the Western and Eastern load-bearing walls. The field test was carried out by ambient vibration testing; both the classical *Peak Picking* spectral technique and the more advanced *Frequency Domain Decomposition* procedure were used to extract the modal parameters (natural frequencies and mode shapes) from ambient vibration data. In the theoretical study, vibration modes were determined by using a 3D finite element model. The experimental data were first used to verify the main assumptions used in the models through rough comparison of measured and predicted modal parameters; furthermore, some structural parameters of the model were updated in order to enhance the match between theoretical and experimental modal parameters.

1 INTRODUCTION

Investigations on the structural safety of ancient masonry towers have recently become of increasing concern, probably as a consequence of some dramatic events which occurred like the sudden collapse of the Civic Tower in Pavia in 1989 (Binda et al. 1992, Binda et al. 1995). Generally, such investigations include:

- accurate survey of the crack pattern and geometric assessment;
- non-destructive and slightly destructive tests, like flat-jack tests or sonic pulse velocity tests;
- various other laboratory tests on cored samples;
- finite element modelling and theoretical analysis.

In the paper, the results of the dynamic-based assessment of an historic masonry bell-tower, adjacent to the Cathedral of Monza (a town about 20 km far from Milan, Italy), are presented and discussed. Dynamic-based assessment of a structure generally involves the comparison between the experimental modal parameters identified during full-scale tests and the predictions of finite elements analysis, as it is schematically shown in the flow-chart of Fig. 1. The figure clearly outlines the main steps of a dynamic-based assessment procedure:

1. Full-scale dynamic testing;
2. Experimental modal analysis (*EMA*), i.e. the extraction of modal parameters (natural frequencies and mode shapes) from experimental data;

3. Finite element analysis (*FEA*) and correlation with the experimental results;
4. Model updating (Mottershead & Friswell 1993).

Full-scale dynamic tests were carried out to complement an extensive experimental program planned to assess the structural condition of the tower since the West and East sides of the building exhibited wide, passing-through and potentially dangerous vertical cracks.

The *EMA* was carried out in the frequency domain by using the classical *Peak Picking* spectral techniques (Bendat & Piersol 1993) and the *Frequency Domain Decomposition* procedure (Brincker et al. 2001). The fundamental mode, with a natural frequency of about 0.59 Hz, involves dominant bending in the E-W direction with significant bending participation in the opposite N-S direction as well. Notwithstanding the nearly symmetric shape, the identified modes of the system generally show coupled motion in the two main E-W and N-S directions; thus, the *EMA* suggests either a significant interaction between the bell-tower and the Cathedral or a non-symmetric stiffness distribution (as the one expected basing on the crack distribution).

In the theoretical study, vibration modes were determined by using a 3D finite element model. Experimental modal data were then used to verify the main assumptions adopted in formulating the model and to adjust some uncertain structural parameters. The updated model, characterised by relatively low

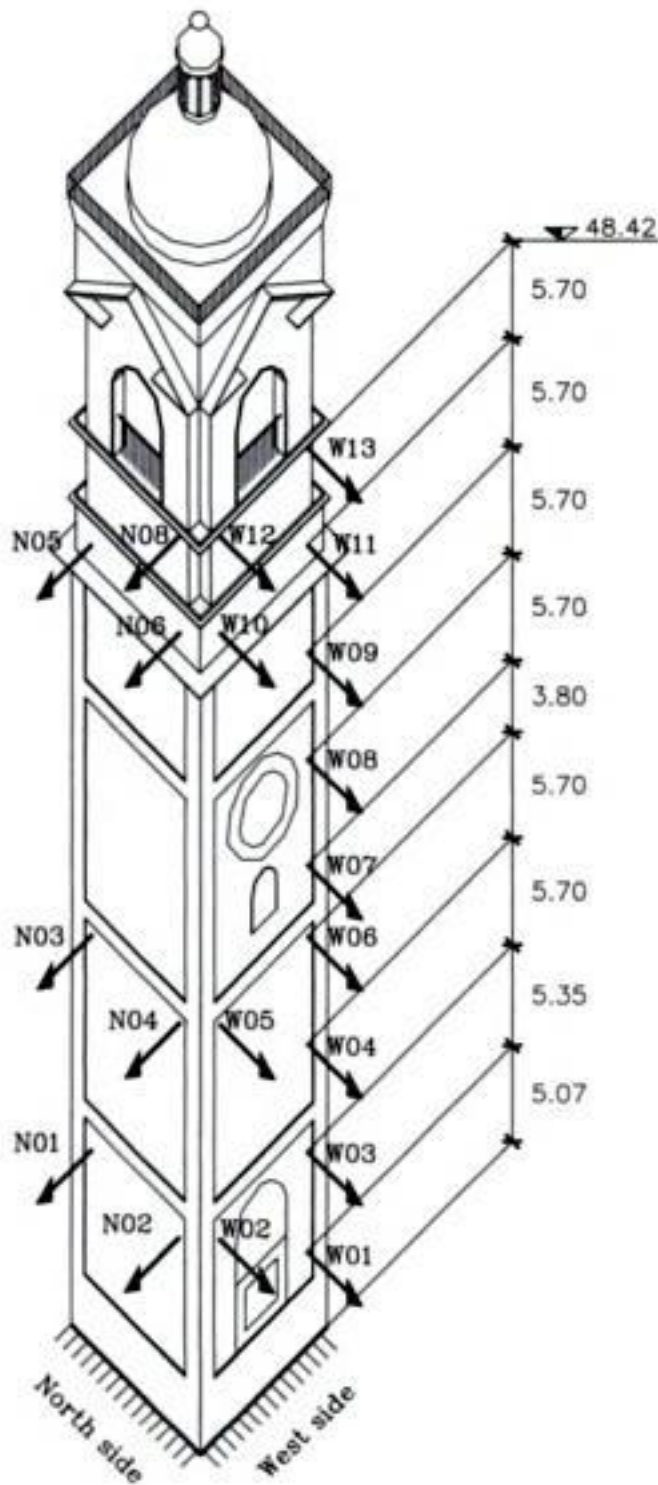


Figure 4. Sensor locations.

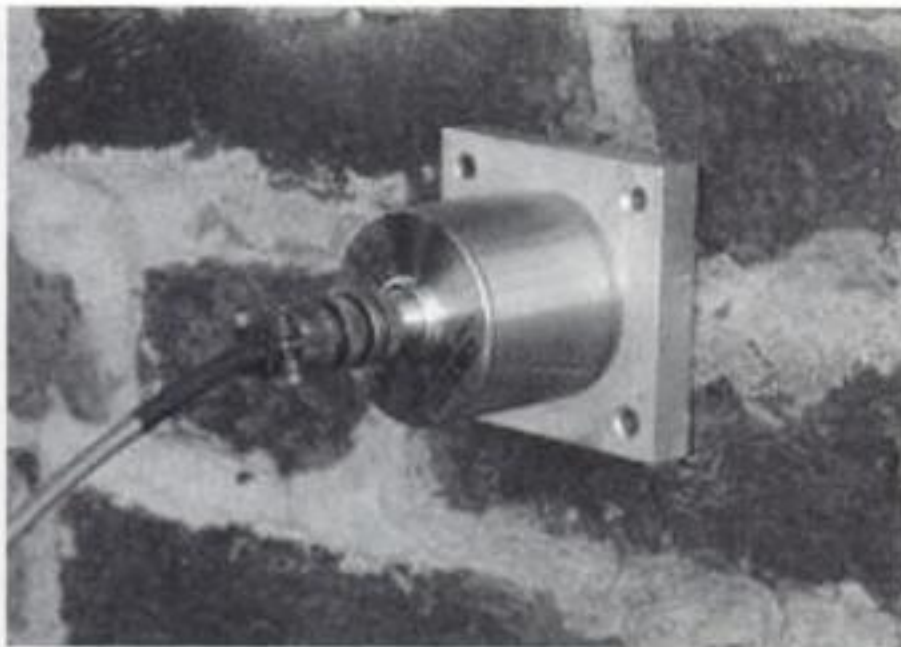


Figure 5. WR-71 accelerometer.

or velocity responses to be recorded. Two-conductor cables connected the accelerometers to a computer workstation with a data acquisition board for A/D and D/A conversion of the transducer signals and storage of digital data.

Ambient vibration response (in terms of both acceleration and velocity) was acquired in about 38 minute records per channel at a sample rate of 200 Hz to provide good waveform definition.

Due to the low level of ambient excitation that existed during the tests, the maximum recorded velocity ranges up to about 0.15 mm/s.

4 MODAL IDENTIFICATION PROCEDURES

The extraction of modal parameters from ambient vibration data was carried out by using two different output-only procedures: *Peak Picking* method (PP, Bendat & Piersol 1993) and *Frequency Domain Decomposition* (FDD, Brincker et al. 2001). Both methods are based on the evaluation of the spectral matrix (i.e. the matrix of cross-spectral densities) in the frequency domain:

$$G(f) = E[A(f)A^H(f)] \quad (1)$$

where the vector $A(f)$ collects the acceleration responses in the frequency domain, superscript H denotes complex conjugate transpose matrix and E denotes expected value. The diagonal terms of the matrix $G(f)$ are the (real valued) auto-spectral densities (ASD) while the other terms are the (complex) cross-spectral densities (CSD):

$$G_{pp}(f) = E[A_p(f)A_p^*(f)] \quad (2a)$$

$$G_{pq}(f) = E[A_p(f)A_q^*(f)] \quad (2b)$$

where the superscript $*$ denotes complex conjugate.

Both ASDs and CSDs were estimated from recorded data samples by using the modified periodogram method (Welch 1967); according to this approach an average is made over each recorded signal, divided into M frames of $2n$ samples, where windowing and overlapping is applied. In the present application, smoothing is performed by 8192-points Hanning-windowed periodograms that are transformed and averaged with 50% overlapping; since $\Delta t = 0.005$ s, the resulting frequency resolution is $1/(8192 \times 0.005) \approx 0.0244$ Hz.

4.1 Peak picking

The more traditional approach to estimate the modal parameters of a structure (Bendat & Piersol 1993) is often called *Peak Picking* method. The method leads to reliable results provided that the basic assumptions of low damping and well-separated modes are satisfied. In fact, for a lightly damped structure subjected to a white-noise random excitation, both ASDs and CSDs reach a local maximum at the frequencies

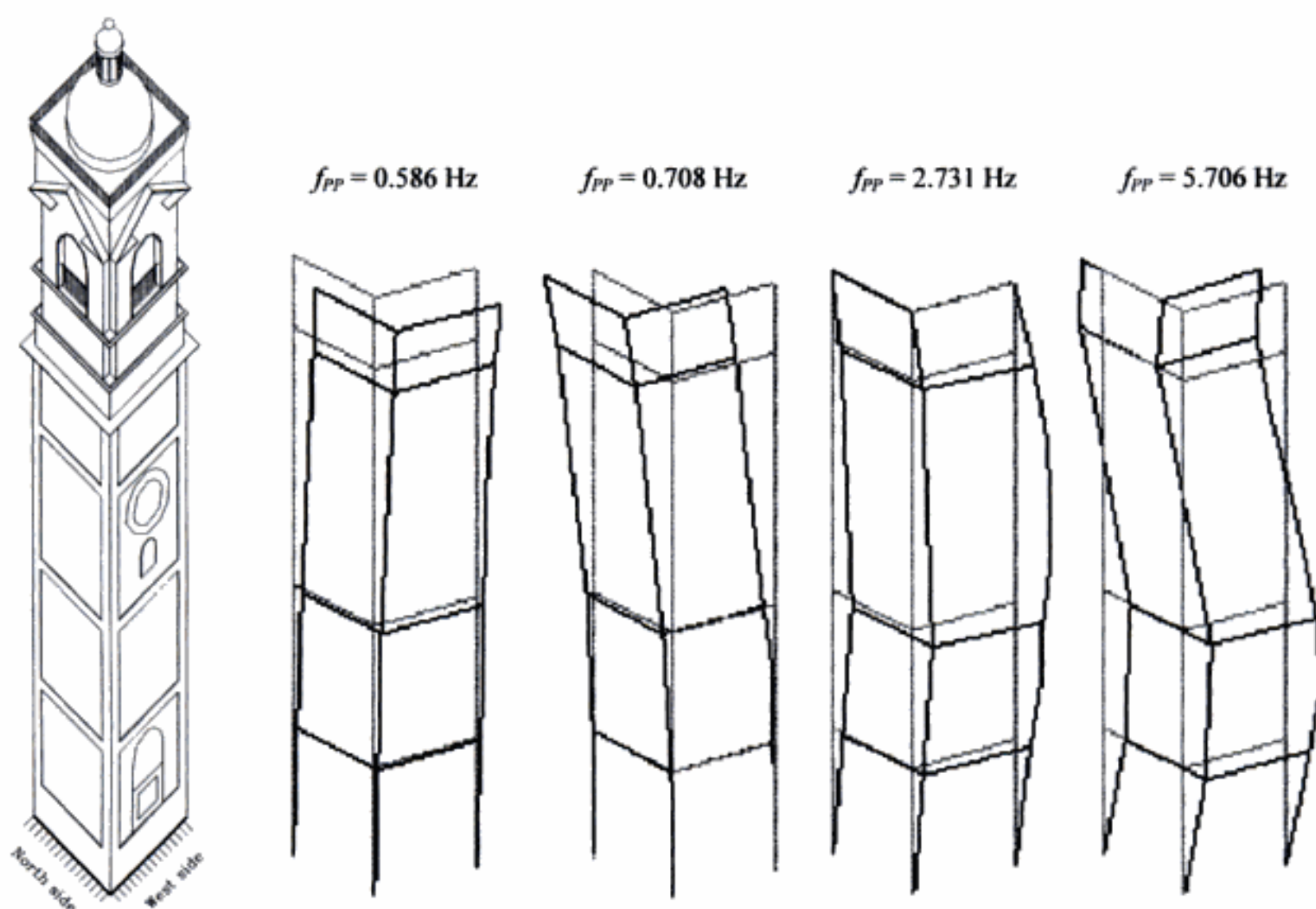


Figure 7. Vibration modes identified during ambient vibration tests (*PP*).

This hypothesis was further investigated by using a 3D finite element model.

Furthermore, Table 1 compares the corresponding mode shapes obtained from the two different identification procedures through the frequency discrepancy $D_F = |(f_{PP} - f_{FDD})/f_{PP}|$, the *MAC* and the *NMD*. Inspection of the correlation values listed in Table 1 clearly highlights a very good agreement between the two methods in terms of both natural frequencies (with the maximum differences not exceeding 2.05%) and modal deflections (with minimum *MAC* value of about 0.96).

Finally, the experimentally determined bending modes of the tower are shown in Fig. 7.

6 STRUCTURAL MODELING AND UPDATING

6.1 Finite element model

A finite element model of the bell-tower was created basing on the geometric survey. The tower was modeled by using 8-node brick elements while the dome was represented by 4-node shell elements. A relatively large number of finite elements have been used in the model, so that a regular distribution of masses could be obtained and all the main openings in the

load-bearing walls could be reasonably represented. The model consisted of 4944 nodes, 3387 solid elements and 80 shell elements with 14286 active degrees of freedom. A three-dimensional view of the model is shown in Fig. 8.

In formulating the model, the following hypotheses were adopted:

- the Tower footing was fixed;
- a weight per unit volume of 18.0 kN/m^3 was assumed for the masonry;
- the Poisson's ratio of the masonry was held constant and equal to 0.15;
- the connection between the Southern wall of the bell-tower and the facade of the Cathedral was accounted for by introducing rigid constraints normally to the wall; in the orthogonal direction the interaction between the tower and the Cathedral was simulated by an uniform distribution of linear elastic springs of constant k (Fig. 8). The range of variation of k was estimated in order to ensure a broad correspondence between theoretical and experimental mode shapes.

A non-homogeneous distribution of the Young's modulus was considered in order to adequately represent the damaged areas of the tower; specifically, six different values of the elastic modulus were considered in the model. Since the major cracks were placed

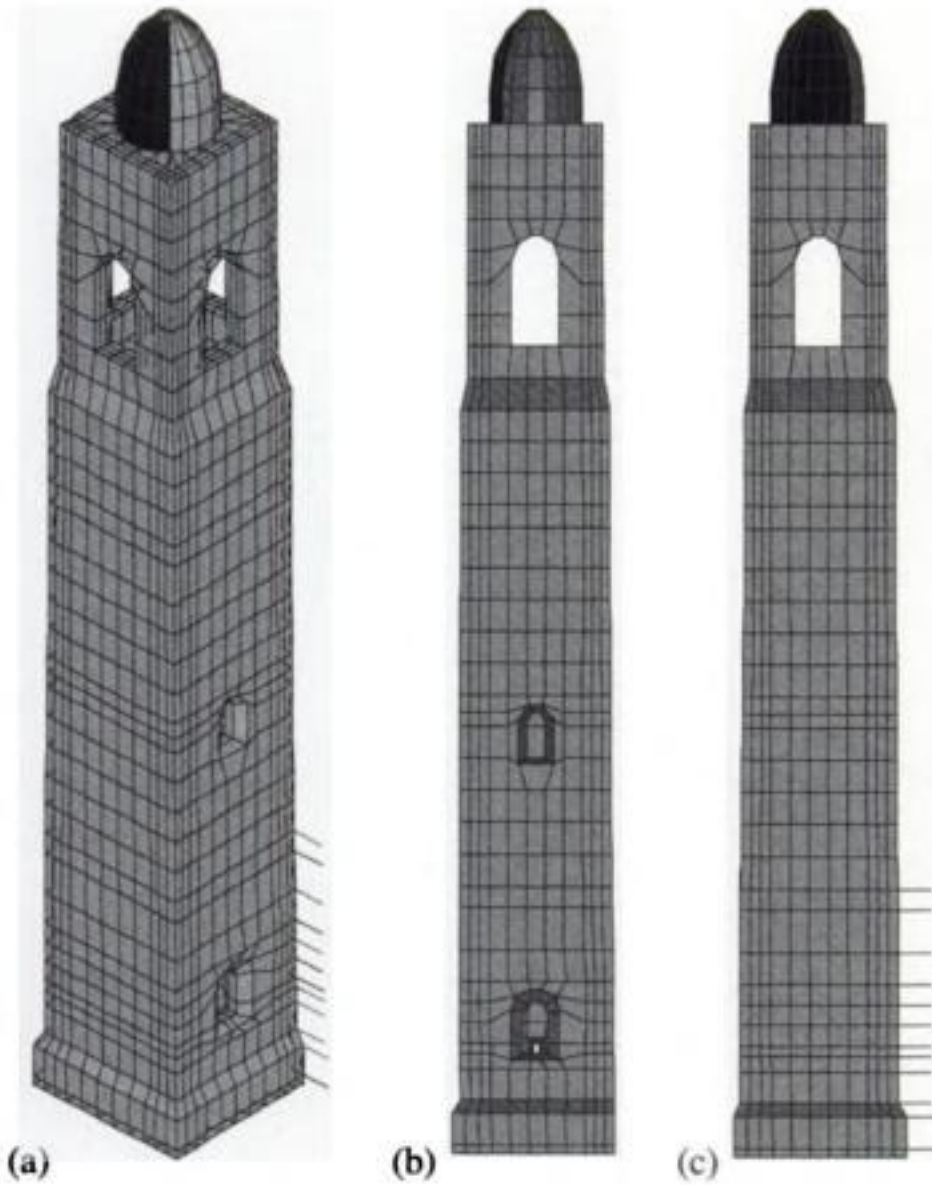


Figure 8. Finite element model of the bell-tower: (a) 3D view; (b) West side; (c) North-side.

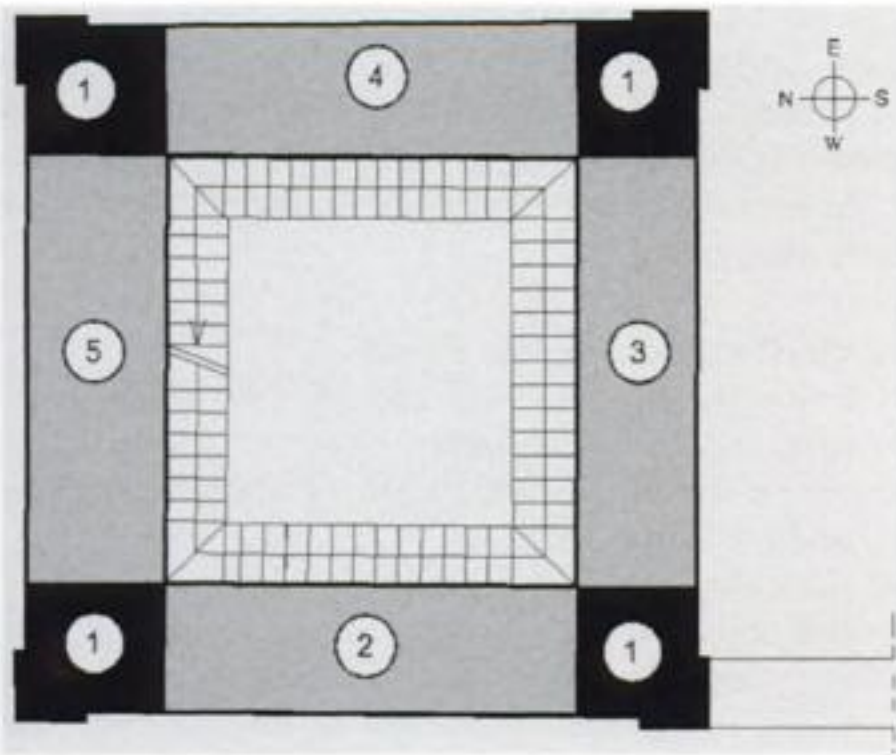


Figure 9. Distribution of the elastic properties up to 23.0 m.

along the East- and West- sides of the building up to about 20.0–23.0 m, the lower part of the tower (up to 23.0 m) was divided into five sub-regions by distinguishing the four sides and the corner properties, as it is shown in Fig. 9; a further elastic modulus was introduced to represent the average behavior of the masonry in the upper part of the tower.

Thus, the finite element model updating was carried out with respect to the set of seven structural parameters summarised in Table 2:

1. the Young's moduli E_i ($i = 1, 2, \dots, 5$) in the lower part of the tower;
2. the Young's modulus E_6 in the upper part of the tower;
3. the elastic constants k of the springs placed along the contact area between the Cathedral and the bell-tower in the direction of the Southern wall.

6.2 Finite element model updating

The uncertain structural parameters were estimated by minimizing the difference between theoretical and experimental natural frequencies. Specifically, two different well-known identification algorithms were used: the Douglas-Reid (*DR*) procedure (Douglas & Reid 1982) and the inverse sensitivity (*IS*) method (Collins et al. 1974).

According to the *DR* approach (Gentile et al. 2002), the dependence of the natural frequencies (or in general of a response parameter) of the model on the unknown structural parameters X_k ($k = 1, 2, \dots, N$) is approximated around the current values of X_k , by the following:

$$f_i^*(X_1, X_2, \dots, X_N) = \sum_{k=1}^N [A_{ik} X_k + B_{ik} X_k^2] + C_i \quad (7)$$

where f_i^* represents the approximation of the i -th frequency of the finite element model and the $(2N + 1)$ coefficients A_{ik} , B_{ik} and C_i must be determined before the evaluation of the unknown structural parameters by a least-square minimisation of the difference between each f_i^* and its experimental counterpart f_i^e :

$$J = \sum_{i=1}^M w_i \varepsilon_i^2 \quad (8)$$

$$\varepsilon_i = f_i^e - f_i^*(X_1, X_2, \dots, X_N) \quad (9)$$

where w_i is a weight constant.

However, eq. (7) represents a reasonable approximation in a range, around a "base" value of the structural parameters X_k^B , limited by lower X_k^L and upper values X_k^U ($k = 1, 2, \dots, N$); thus, the coefficients A_{ik} , B_{ik} , C_i are dependent on both the base value of the structural parameters and the range in which such parameters can vary.

In the *IS* procedure, the natural frequencies f of the updated model are written in a Taylor series expansion as:

$$f = f^B + S(X - X^B) \quad (10)$$

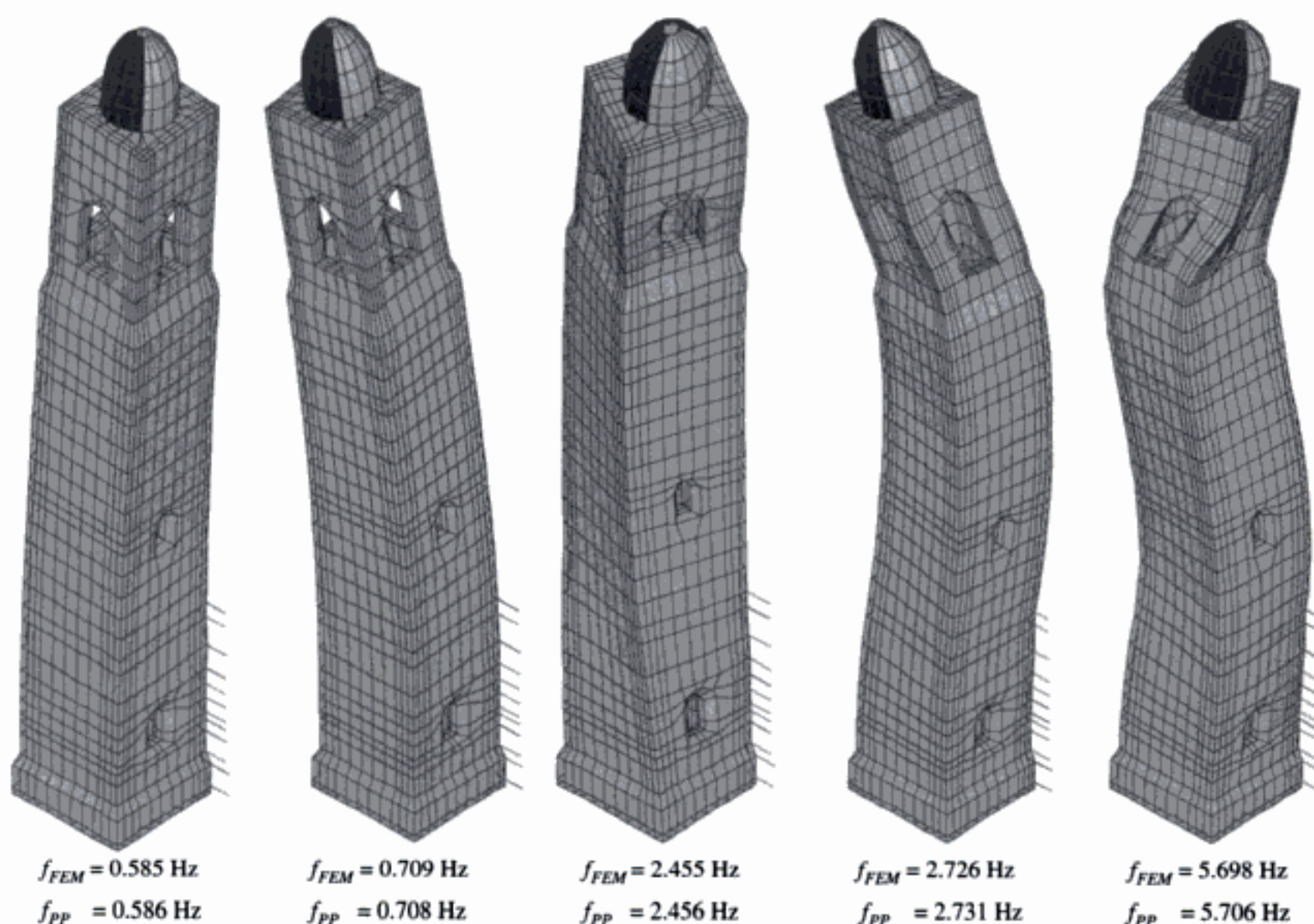


Figure 11. Vibration modes of the updated model (Douglas-Reid method).

Table 3. Comparison between theoretical (updated model, Douglas-Reid method) and experimental modal parameters.

Mode No.	f_{PP} (Hz)	f_{FEM} (Hz)	MAC	NMD (%)
1	0.586	0.585	0.9874	11.30
2	0.708	0.709	0.9745	16.19
3	2.456	2.455	0.8614	40.11
4	2.731	2.726	0.8602	40.32
5	5.706	5.698	0.8721	38.30

of mode shapes is fairly good since the MAC is always greater than 0.86 but significant average differences are highlighted by the NMD . Such differences are probably to be related either to the simplified distribution of the model elastic properties (which were held constant for large zones of the structure) or to a relative lack of accuracy in the experimental evaluation of the higher mode shapes.

7 CONCLUSIONS

Theoretical and experimental dynamic investigation of a historic masonry bell-tower is described in the

paper. The following conclusions can be drawn from the study:

1. Within the frequency range 0–10 Hz, 5 vibration modes were clearly identified;
2. The measurement of structural response to the ambient levels of vibration mainly induced by the bells ringing has proved to be an effective means for the identification of the dynamic properties of masonry towers, although in the some measurement points the signal-to-noise ratio turned out to be quite low;
3. A very good agreement was found between the modal estimates obtained from classical *Peak Picking* (Bendat & Piersol 1993) and *Frequency Domain Decomposition* (Brincker et al. 2001) methods;
4. No experimental evidence was found that would suggest the existence of non-linear behavior of the tower during the tests;
5. The fundamental mode of the bell-tower, with a natural frequency of about 0.59 Hz, involves dominant bending in the E-W direction with significant bending participation in the opposite N-S direction as well; the coupled motion in the two main E-W and N-S directions characterizes all the tower mode shapes;

6. The comparison between measured and predicted modal parameters was used to verify the assumptions adopted in formulating the model. Specifically, a good match between theoretical and experimental modal parameters was reached for relatively low values of the model Young modulus in the most damaged regions of the tower. Furthermore, the dynamic-based model updating, carried out by using two different methods, led to consistent structural parameters (distribution of Young's modulus in the masonry) which are in close agreement with the results of double flat-jack tests;
7. The dynamic-based assessment of masonry towers seems a promising approach to evaluate damage in such structures provided that an accurate geometric survey is available and in the hypothesis that the damage scenario mainly involves the lower regions of the building, where high eigen-sensitivity has to be expected.

ACKNOWLEDGEMENTS

The research was supported by the Italian Ministry of University and Research (M.I.U.R.), under grant Cofin03.

The authors are indebted with Prof. L. Binda; without her involvement and advice, this research would not have been possible.

Dr. N. Gallino is gratefully acknowledged for the help in developing the application of *IS* identification procedure.

Furthermore, the authors would like to thank M. Antico, L. Cantini, and M. Cucchi for the assistance in conducting the field tests.

REFERENCES

- Abdel-Ghaffar, A.M. & Housner, G.W. 1978. Ambient vibration tests of suspension bridge, *J. Eng. Mech. Div. ASCE* **104**: 983–999.
- Allemang, R.J. & Brown, D.L. 1983. Correlation coefficient for modal vector analysis, *Proc. 1st Int. Modal Analysis Conference*.
- Bendat, J.S. & Piersol, A.G. 1993. *Engineering applications of correlation and spectral analysis*, 2nd Ed., Wiley Interscience.
- Binda, L. et al. 1992. The collapse of the Civic Tower of Pavia: a survey of the materials and structure, *Masonry International*, **20**(6): 11–20.
- Binda, L. et al. 1995. The failure of ancient Towers problems for their safety assessment, *Proc. 4th STREMAH*.
- Binda, L. & Poggi, C. 1997. *Assessment of the mechanical behaviour of materials and structures of the bell-tower adjacent to the Cathedral of Monza by on-site tests and numerical simulation* (in Italian), Dept. of Struct. Engng., Politecnico di Milano, Milan, Italy.
- Binda, L. et al. 2000. On site and laboratory investigation on materials and structure of a bell-tower in Monza, *Int. Zeitschrift für Bauinstandsetzen und bauDenkmalpflege*, **6**(1): 41–62.
- Brincker, R. et al. 2001. Modal identification from output-only systems using frequency domain decomposition, *Smart Materials & Structures*, **10**: 441–445.
- Douglas, B.M. & Reid, W.H. 1982. Dynamic tests and system identification of bridges, *Journal Struct. Div. ASCE*, **108**, 2295–2312.
- Gentile, C. et al. 2002. Dynamic investigation of a historic masonry bell tower, *Proc. 6th International Masonry Conference*.
- Golub, G.H. & Van Loan, C.F. 1996. *Matrix Computations*, 3rd Ed., J. Hopkins University Press.
- Maya, N.M.M. & Silva, J.M.M. (Eds.) 1997. *Theoretical and experimental modal analysis*, Research Studies Press Ltd, Hertfordshire.
- Mottershead, J.E. & Friswell, M.I. 1993. Model updating in structural dynamics: a survey, *J. Sound and Vibration*, **167**: 347–375.
- Waters, T.P. 1995. *Finite element model updating using measured frequency response functions*, Ph.D. Thesis, Department of Aerospace Engng., University of Bristol.
- Welch, P.D. 1967. The use of Fast Fourier Transform for the estimation of Power Spectra: a method based on time averaging over short modified periodograms, *IEEE Transactions*, **AU-15**: 70–73.

Seismic resistance of masonry towers

D. Abruzzese & A. Vari

University of Rome "Tor Vergata", Italy

ABSTRACT: The paper deals with structural identification of masonry structures. Dynamic analysis and dynamic tests are the main tools adopted in this study, focused on "tall masonry structures", to evaluate the static and dynamic behaviour of a masonry structure. The masonry material is assumed with limited but not negligible tensile stress. Some analytical model has been developed, tuned with the results of the dynamic tests and adopted to evaluate the dynamic vulnerability of the structure. The subsoil and the foundation are considered involved in the dynamic behaviour of the tower. The analysis allows to assess the seismic risk of tall masonry towers. As case study a middle-age tower in Rome has been investigated. The results permit to evaluate the seismic intensity which could lead the Tower to the collapse.

1 INTRODUCTION

1.1 Seismic vibration of masonry tower structures

In the last decades the research in the monumental and historical structures developed widely, considering and improving methodology and techniques for diagnosis and restoration. Some interesting studies in this field are related with seismic behaviour of the masonry towers structure, mainly since several collapses registered in Italy (Pavia, Florence, Bologna), in Europe and eastern Asia (China). The knowledge of the behaviour of these monuments seems very difficult to be achieved, because the uncertainties about the masonry material elastic characteristics and resistance and the soil and foundation condition, mostly under dynamic condition.

1.2 Recent studies and methodology

Many authors investigated the problems related with such kind of masonry structures. Some important results have been achieved dealing with the behaviour of the soil and foundation of leaning Tower (C. Viggiani, L. Binda), or on the dynamic characterization by mean of measurement of vibration performed on the towers in Pavia (G.M. Calvi, G. Macchi, A. Pavese). Main goal of these studies is to collect more information about the towers in order to restore or to reinforce the structures for a better protection against the earthquakes, the most heavy load condition for such a kind of monument.

As for other structures, the knowledge of mechanical characteristics of the masonry material, the geotechnical properties of the foundation soil and

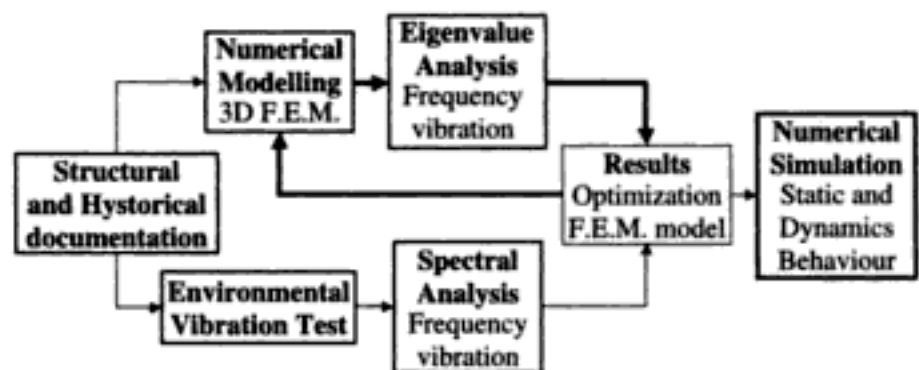


Figure 1. Methodology adopted in the paper.

the soil-structure dynamic interaction are fundamental to understand the whole behavior of the tower. The dynamic soil-structure interaction can be considered not yet fully investigated, and in the paper will be focused the importance of the matter in order to investigate the seismic vulnerability the structure.

The use of measurement of vibration technique is highly efficient to evaluate the mechanical characteristics of the material when correlated with the results obtained with advanced models solved with finite element analysis.

The results obtained with such a process can be utilized to evaluate the efficiency of possible reinforcement. In Fig. 1 the diagram shows the methodology adopted to characterize the dynamic and static parameter of the Tower studied in this paper.

2 EXPERIMENTAL INVESTIGATIONS

2.1 Structural characterization

The paper describes the research performed on the Capocci's Tower in Rome. After a collection of

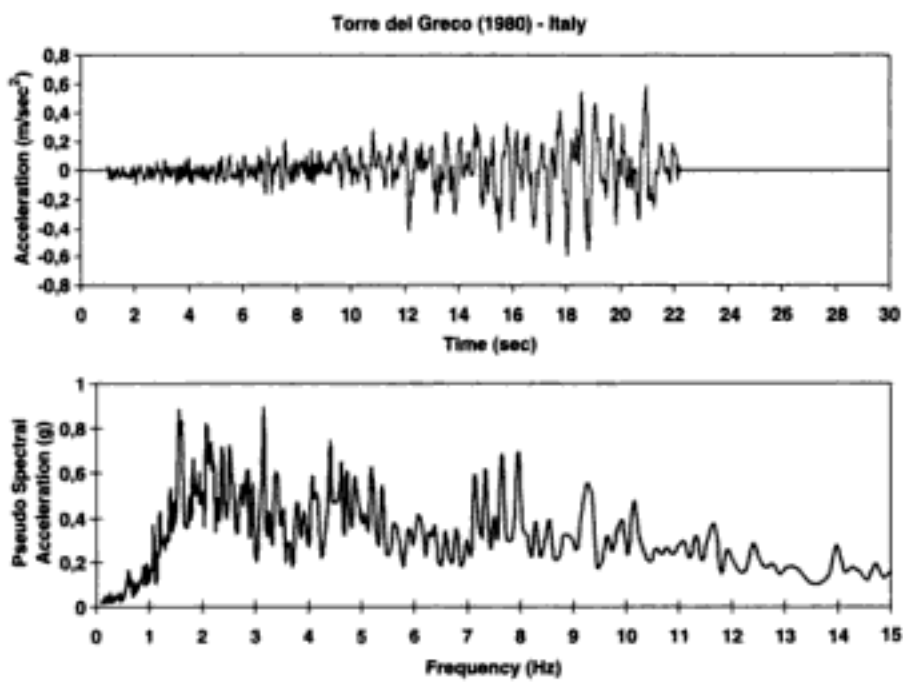


Figure 10. Accelerogram used as seismic load at the base of the tower and response spectrum.

of the response spectra we can notice large number of peaks in the frequencies between 0.5 and 3.5 Hz, with other peaks around 4.5 Hz, 8 Hz, 9 Hz.

Considering the natural frequencies of the tower, the frequency contents of this earthquake can activate the main natural vibrations of the structure, resulting even amplified.

3.3 Results

The analysis of the vulnerability of the structures consists mainly of searching the potential collapse mechanism, related to the load applied.

The model 3 has been made in order to evaluate in a more economic and concise way the global behaviour of the three-components system soil-foundation-structure. Then an interface element between the soil and the foundation with visco-elastic-plastic behaviour has been used to take into account the interaction of the structure and the foundation without disregard the non linear characteristics of the soil (internal friction, plasticity effects, hardening).

As for the previous cases, the preparation and optimization of the model has been made on the base of results obtained with the other models already studied (1 and 2) and on the base of the on site measurement.

The tuning process provided the results shown in the Table 3.

Tall masonry structures, as towers, chimney, bell towers, have in seismic action the most heavy load condition. We wanted to evaluate the collapse mechanism and the limit value of the seismic load compatible with the structure by using in a step-by-step analysis the recorded signal of the earthquake mentioned scaled with different amplification factor A_i .

In the analysis we use a time step of 0.0325 sec, the total length of the record is 30 sec, where only in the first 20 sec. We apply the earthquake. This way we can also analyse the behaviour of the tower after the

Table 3. Comparison between the natural frequencies of the three models and the frequencies measured on site.

Natural frequency	Experimental (Hz)	Model 1 (Hz)	Model 2 (Hz)	Model 3 (Hz)
1° flex X	2.00	1.958	2.00	1.942
1° flex Y	2.17	2.201	2.344	2.325
1° tors	6.70	6.696	6.752	6.552
2° flex X	8.52	8.683	8.545	8.533
2° flex Y	9.01	9.238	9.277	9.327

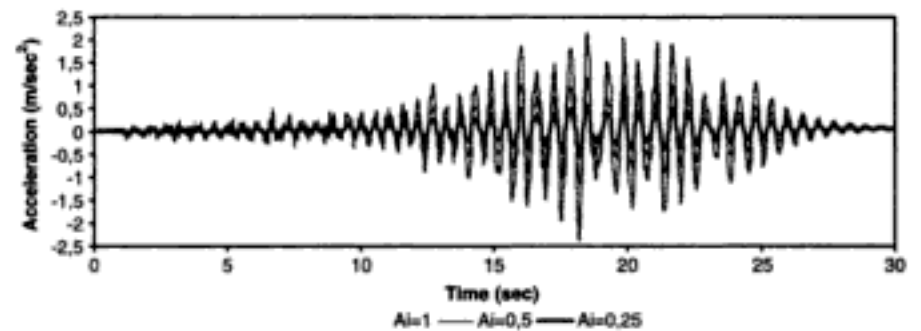


Figure 11. Seismic acceleration applied at the foundation of the tower with different amplification factor A_i .

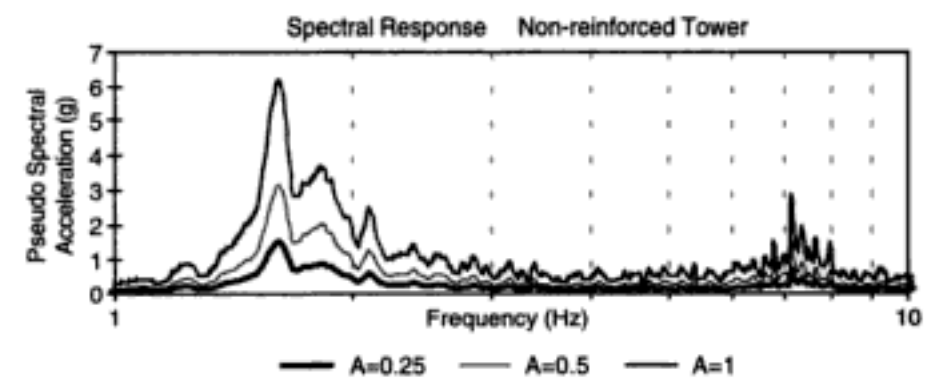


Figure 12. Response spectra on the top of the tower for the three different amplifications A_i .

end of the earthquake. The results of this analysis are summarize in the Figs. 11–13. As the amplification A_i of the seismic action raises some cracks appear on the top of the basement, due mostly to the shear stress of not much likely effect of some blocks “exploded” for the peak of the stresses.

As well as the A_i parameter arises, and until the structure reaches the collapse (Fig. 12c), highest stresses appear always at the foundation, due to the tensile stress attained between the foundation structure and the soil.

From the analysis it is evident the importance of the connection between foundation and upper structure, because the highest stress appear in the transition zone. It can be useful to mention that the interface elements we used in the analysis are helpful also to analyse in detail collapse mechanisms also for the soil, but in this case they did not occur.

From the analysis of the response spectra we can remark that the most relevant frequencies noticed do not change as the seismic amplification change. Along

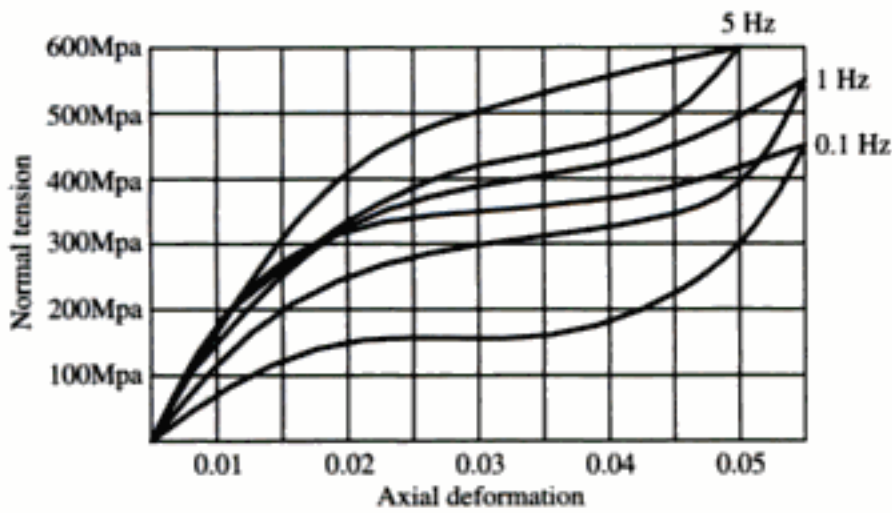


Figure 15. Hysteresis cycle vs. the load frequency. (ISTECH Project, 1999).

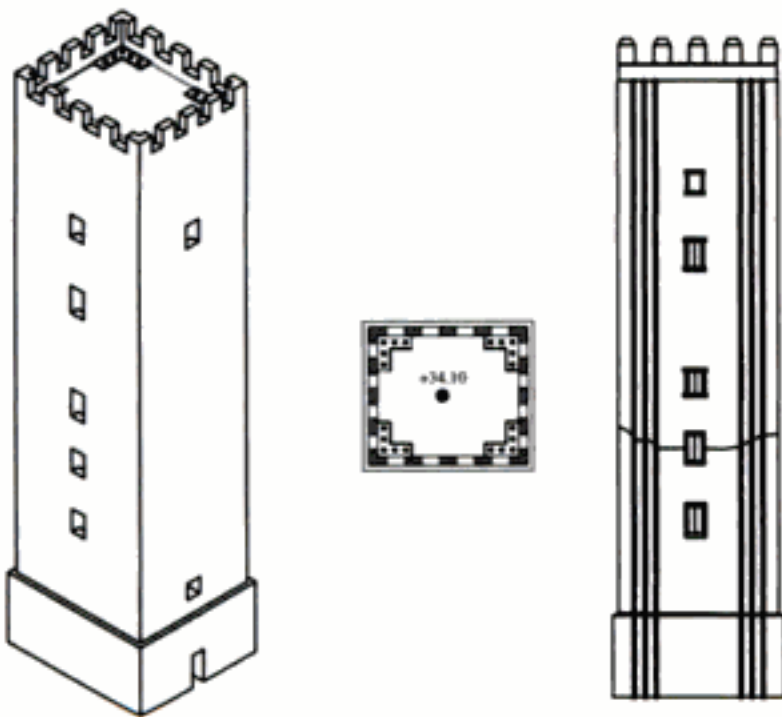


Figure 16. Sketch of the hypothesis of reinforcement with steel bar equipped with SMAD.

seismic forces. The results of the ISTECH project shown, through numerical analysis and experimental tests, that memory shape alloy devices are more efficient than traditional steel chain bars. SMA devices have been used in several monumental structures such as S. Francesco basilica, in Assisi, and in the bell-tower of S.Giorgio's church in Trignano.

4.1.2 Application of SMA devices to the Capocci's Tower

The Capocci's Tower at the moment do not show cracks neither soil/foundation deformations, and this condition can guarantee a quite good mechanical behaviour. The reinforcement hypothesis then should be a seismic improvement, by using modern technologies such as memory shape alloy.

The structural reinforcement should improve the anchorage between the structure and the foundation, and give to the tower a larger reserve if stressed by tensile stress. This hypothesis originates and has been suggested from the collapse mechanism that has already been studied and described before.

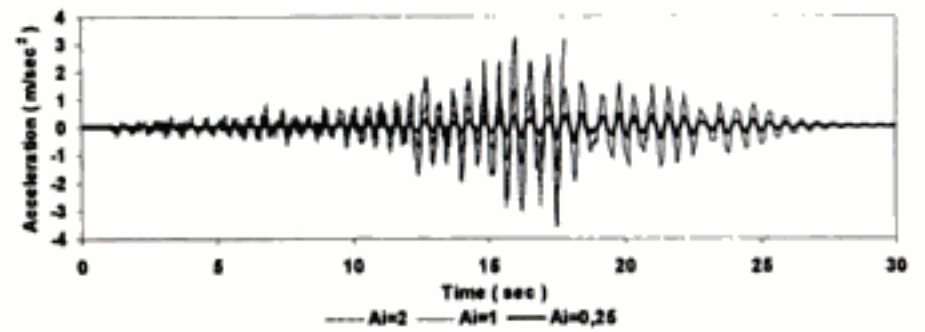


Figure 17. Accelerations evaluated at the top of the tower for different amplification of the earthquake.

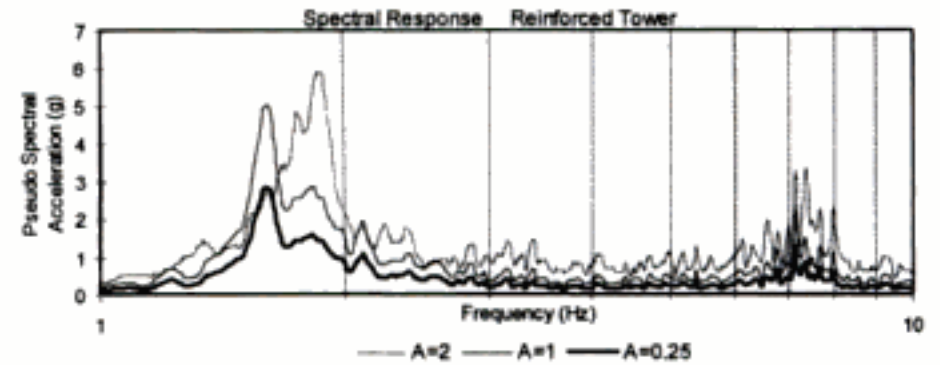


Figure 18. Response spectra of the accelerations for different amplification of the earthquake.

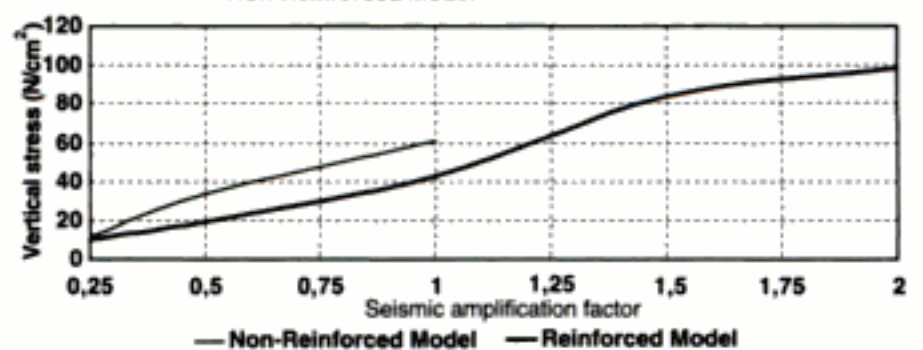
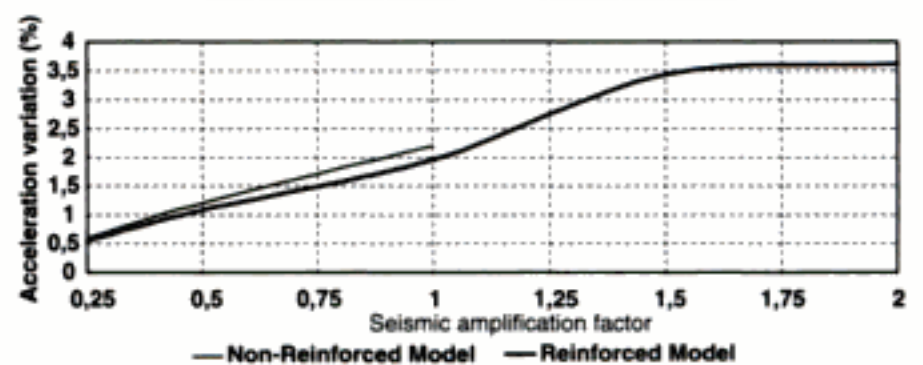
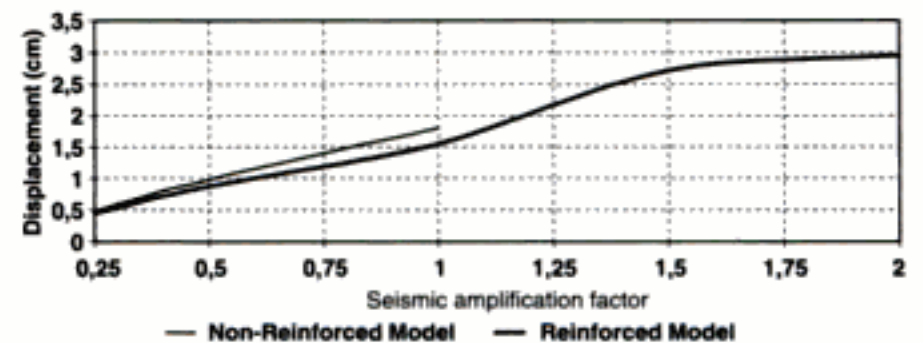


Figure 19. Improvement of the behaviour of the tower: displacements, acceleration, maximum stress.

This effect could be obtained by giving a pre-compression to the external vertical walls, by steel chain bars at corners; the chain bar should be dimensioned according to the required pre-compression. The suggested design of the reinforcement foresees 5 chain bars in each corner, all of them equipped with a SMA device, which gives to the masonry a compressive

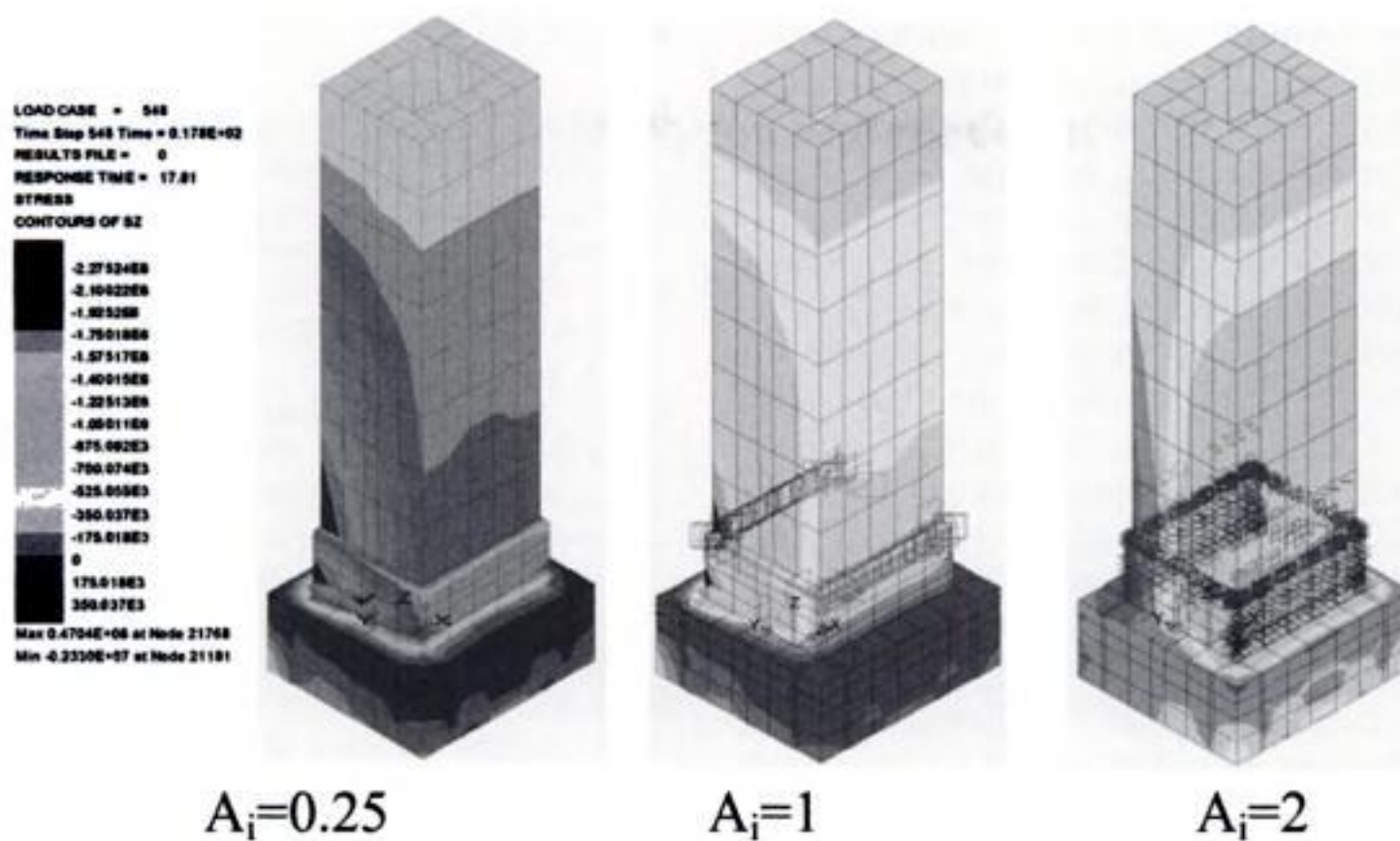


Figure 20. Distribution of the vertical stresses. At the collapse, with amplification $A_i = 2$, the cracks appear all over the foundation.

pre-stress of about 0.1 MPa average (Fig. 16). The chain bars connected with the SMADs could be steel bars anchored with the basement in a suitable way, or modern, stainless, carbon bars.

The 3D model should be modified introducing the effect of the pre-compression, performed by the chain, and through the analysis of the *model* could be evaluated the improvement after the intervention. The value of pre-compressive stress would be almost invariable during the different loading steps, thanks to the SMA devices, besides they allow the structure to dissipate a large amount of energy during the hysteresis cycles, in case of seismic loads.

4.1.3 Seismic analysis of reinforced tower

The seismic vulnerability of the “simulated” reinforced tower will be evaluated loading it again with the chosen earthquake, in the same way than before, i.e. with increasing value of the amplitude until the structure will collapse.

In Figs. 17–18 the accelerations and the response spectra are shown, as result of the calculation at the top of the tower; in Fig. 20 the distribution of stresses is shown, at peak of the seismic action. We can notice that the growth of accelerations at the top of the tower is not linear with the amplification (A_i) at the base. In the reinforced structure the building could resist to higher values of stress, and, as final result, we can state that the collapse is reached with an amplification value that is twice as non-reinforced case ($A_i = 2$), as we could expect.

Besides, in the reinforced tower the stresses decrease drastically by 35%, at the same amplification value (A_i). (Fig. 19)

The global structural stiffness of the Tower do not change significantly, due to the particular typology of the reinforcement. In the reinforced tower model there are frequencies slower than the natural frequency of the original tower, when the collapse occur, while in the original tower model it does not happen. The SMAD reinforcement let the tower have a plastic behaviour and dissipate a larger part of seismic energy (dissipation due to the SMADs’ hysteresis cycle).

The typology of collapse is the same as the previous case, but this time the whole foundation is involved in the collapse mechanism. At the last step, before collapse, we can observe in the same time, masonry’s plastic behaviour, in compression, but also cracks due to high tensile stresses (Fig. 20).

5 CONCLUSIONS

The problem of protection of ancient masonry monuments against seismic actions is very complex. The technicians working on the monument should pay attention to the importance of the building, considering carefully the structural problem without neglect historical and artistic aspects connected with the monument. Studies on monuments should consider that restoration’s aim is mainly to preserve them from decay, as well as to protect them from damages due to seismic and dynamic actions.

Besides, if we talk about tall masonry buildings, such as towers, we can’t forget to analyse the condition of foundation soil, which is strictly connected to the seismic behaviour of the whole structure. Here we can recall one of the most famous examples of

the interaction between soil and the structure is the leaning Pisa Tower, studied and solved successfully.

The influence of foundation soil is very important in the dynamic analysis, because it represents the restraint condition of the structure; so it could strongly influence the structure behaviour, mostly when subsidence are affecting the foundation.

In the paper it has been tentatively analysed the dynamic behaviour of high masonry buildings, such as middle age towers, trying to obtain a more satisfactory results with the help of environmental vibration measurement. These data were necessary to determine mechanical characteristics of masonry and foundation soil in the case study, the Capocci Tower.

The finite element model of the tower simulated the building's behaviour under seismic forces and its collapse mechanism, considering the interaction with the foundation soil. Moreover the model was improved with the introduction of a modern structural reinforcement system, with the use of shape memory alloys (SMA), that increased seismic resistance by 100%.

It is important to notice that after this kind of consolidation, if the metallic devices at the end of the bars are connected with masonry in the correct way, the structure keeps the same mass and stiffness. This is very important in order to obtain a invariable dynamic behaviour when the seismic forces change frequency.

ACKNOWLEDGEMENT

The authors wish to acknowledge the Italian M.A.E. (Min.of For.Aff.) to support the research in the framework of the international cooperation with Chinese University of Yangzhou.

REFERENCES

- Bonzi, A., Pizzigalli, E., Eusebio, M., Ravasio, F., 1997. Dynamics test and monitoring of the Leaning Tower of Pisa. Aims, methodology and results. In *ISMES, Italian group of IABSE, Colloquium, Seriate 1997*.
- Calvi, G.M., M.J.N. Priestly, "Investigations of the Collapse of a Medieval Masonry Tower", *The TMS Journal*, 9.1, 1990.
- Fanelli, M.A., 1997. Plectron V° : Dynamic identification for towers 1997. In *ISMES, Italian group of IABSE, Colloquium, Seriate 1997*.
- Giuseppetti, G., Galimberti, C., Mazzà, G., 1997. The experience of ENEL spa Ricerca/CRIS in the field of architectural heritage preservation. In *ISMES, Italian group of IABSE, Colloquium, Seriate 1997*.
- Hoer, C., Moan, T., Remseth, S. "System identification of structures exposed to environmental loads", *Proc. of EURO DYN '93*, vol.2, 1993.
- Macchi, G. Inspection Methods and Technologies – Keynote Lecture. In *ISMES, Italian group of IABSE, Colloquium, Seriate 1997*.
- Pavese, A., 1997. Structural role of the colonnade in the Leaning Tower of Pisa. In *ISMES, Italian group of IABSE, Colloquium, Seriate 1997*.
- Pavese, A., "Diagnosi di Torri Medioevali mediante Identificazione Dinamica", *Monitoraggio delle strutture dell'ingegneria civile*, a cura di P.G.Malerba, CISM, Udine, 1995.
- Pizzigalli, E., Ravasio, F., Mazza, D., Terzi, E., Di Lullo, S., 1997. Static and dynamic characterization of Gombito Tower in Bergamo. In *ISMES, Italian group of IABSE, Colloquium, Seriate 1997*.
- Yuan Jianli, Li Shencai. "On the method to model ancient brick and stone pagodas by dynamic parameters", *Earthquake Resistant Engineering*, n.1, 1998.

Techniques of structural identification for the monitoring of historical buildings: first experimental results for a masonry tower

P. Carusi, V. Sepe & A. Viskovic

Università di Chieti-Pescara "G.D'Annunzio", Dept. PRICOS, Pescara (Italy)

ABSTRACT: The techniques of structural identification, and in particular those of modal parameters of linear or linearised models, represent an important tool for analysing existing structures. Like all civil structures, monumental buildings are constantly subject to environmental actions (wind, traffic, microtremors of the ground), that can allow identification avoiding the costs related to artificial excitations, but that are usually unmeasured. In the framework of a research on the application to this kind of structures of the identification techniques with unknown input, already implemented for other kind of buildings, this paper report the preliminary results of an experimental investigation on a masonry tower located in the East-Central part of Italy.

1 INTRODUCTION

The increasing interest in the seismic safeguarding of buildings with strategic or historical interest and the recent seismic new classification of the Italian territory ask to the public administrations to define synthetic criteria to assign priorities for retrofitting or restoration interventions.

The techniques of structural identification, and in particular those of modal parameters of linear or linearised models, represent an important tool for analysing existing structures. In fact, synthetic information on damage occurred to buildings can be obtained comparing the value of such modal parameters (first of all natural frequencies and damping coefficients) before and after the seismic event.

Like all civil structures, monumental buildings are constantly subject to environmental actions (wind, traffic, microtremors of the ground); the objective difficulty of characterizing and measuring the significant parameters of such types of actions, has motivated the study of techniques of identification under unknown input, which are based on the measurement of the structural response alone in some points; such techniques also have the advantages of a limited number of operations to carry out on the building, the small number of sensors for the measurement of structural response and the non-interruption of the normal functionality of the building; moreover, they do not require the additional costs related to devices for acting artificial excitations (Brownjohn et al., 1989–1992; Farrar & James, 1997; Katafygiotis et al., 1998; Luz & Wallaschek, 1992; Quek et al., 1999; Torkamani &

Ahmadi, 1988; Wang & Haldar, 1994–1997, Wilson & Liu, 1991). Moreover, the high precision of the measurement instruments allows to record accurately vibrations due to very low actions, for which a linear structural model could be sufficient even in presence of previous damage.

As regards structural systems with linear behaviour, one of the writers and co-authors (Capecchi et al., 2002–2004; De Angelis et al., 2003) have recently introduced a procedure in the frequency domain for the identification of the modal parameters (components of the modal shapes, natural frequencies and modal damping) in the case of unknown and possibly non stationary seismic excitation. The procedure, which can be transferred to the time domain (De Angelis et al., 2004), is based on the observation that the ratios of the Fourier transforms of the responses in different points of the building, turn out to be independent of the forcing itself, and therefore can give experimental information for the identification of modal parameters.

This procedure, that has successfully been applied to framed plane and three-dimensional structures, can be extended, from a theoretical point of view, to more complex structures, as monumental ones.

However, this task has not yet been dealt with in the present paper, that is part of a research in progress on the techniques of structural identification for historical and monumental building, a theme that is receiving an increasing attention above all in Italy (Bartoli & Blasi, 1995; Binda et al., 1992–1995; Croci, 2001; Pavese, 1992).

As a first step of the quoted research, this paper refer on the preliminary results of an in-situ investigation

1.40 m, and the overall height of the tower is about 29 metres.

3 FINITE ELEMENT MODEL OF THE TOWER

A model of the tower was implemented using the commercial finite elements (FEM) code Algor®.

Considering the objective of the study, which was to identify the average values of some mechanical parameters, through a comparison between the modal characteristics of the model and those which were obtained during on-site tests, the FEM model was very accurate from the geometrical point of view, while the material was assumed homogeneous and isotropic; quite obviously this dramatic simplification, certainly appropriate for the said objective, excludes the possibility of getting reliable information on the very local stress state.

In the first phase of the research, reported in this paper, attention was devoted to the identification of the mass density and the elastic modulus of the brickwork through comparison of the natural frequencies of the tower and of its FEM model; in this model, the mass density and the elastic modulus have been varied in a relatively large interval, corresponding to typical values of the characteristics of the masonry typology at issue (cf. Beolchini, 2000), while a constant value of 0.18 has been considered for the Poisson coefficient. Some results on the FEM analysis are reported in Table 1, where F1, T1, F2 and V1 denote the first flexural mode (Figure 3), the first torsional mode (Figure 4), the second flexural mode (Figure 5) and the first vertical mode, respectively.

Quite obviously, as a consequence of the double symmetry of the tower cross sections (square or circular), each one of the flexural modes is a multiple mode, corresponding to possible oscillations in any one of the vertical central planes of the structure.

Table 1. Modal frequencies of the FEM model for different values of density and elastic modulus.

Density (kg/m ³)	Elastic modulus (kN/mm ²)	Natural frequency (Hz)			
		Mode F1	Mode T1	Mode F2	Mode V1
1800	3	2,54	7,36	9,84	12,05
1800	5	3,28	9,50	12,71	15,53
2000	2	1,97	5,70	7,62	9,34
2000	2,5	2,20	6,38	8,52	10,44
2000	3	2,41	6,98	9,34	11,44
2000	3,5	2,60	7,54	10,08	12,35
2000	4	2,78	8,07	10,78	13,20



Figure 3. First modal shape (1st flexural) of the FEM model: plan (top), lateral view (middle) and axonometric view (bottom).

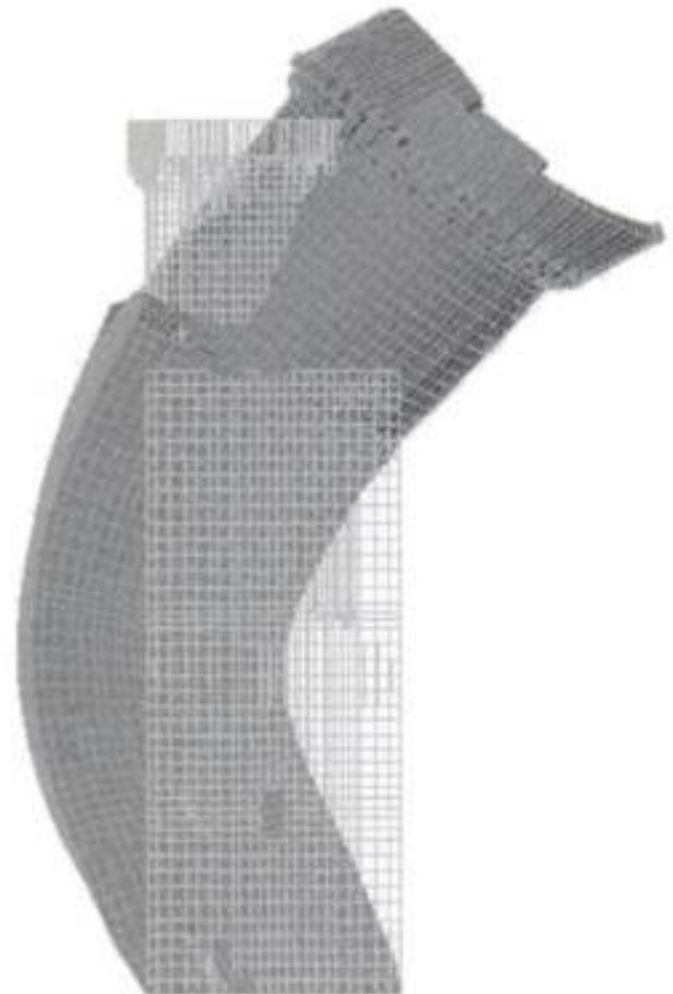
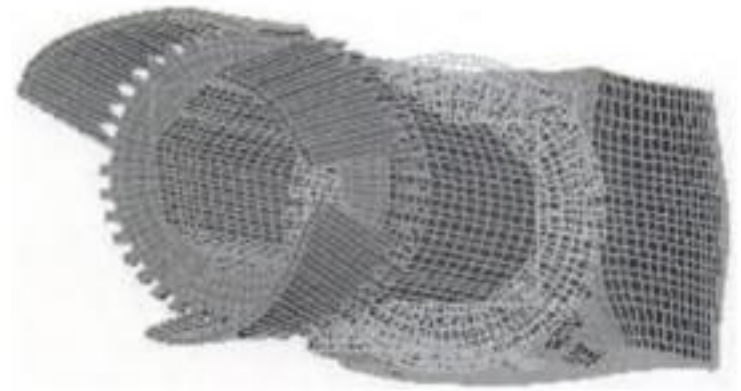
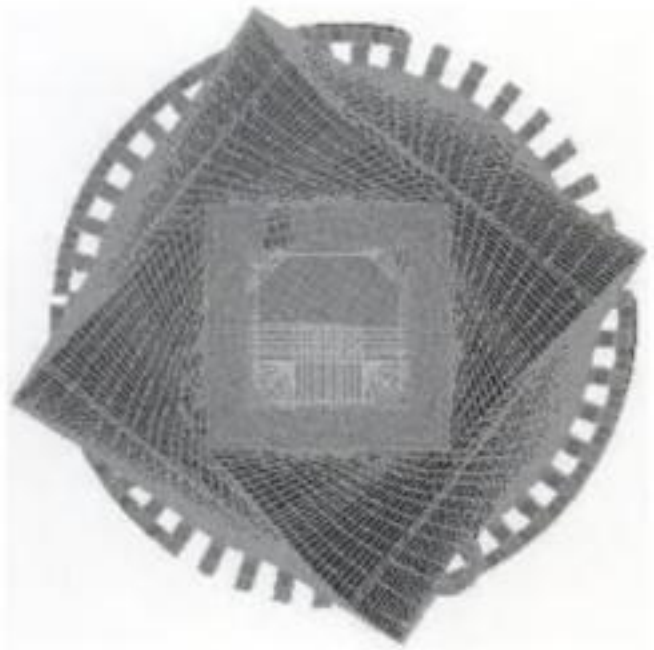


Figure 4. Second modal shape (1st torsional) of the FEM model: plan (top), lateral view (middle) and axonometric view (bottom).

Figure 5. Third modal shape (2nd flexural) of the FEM model: plan (top), lateral view (middle) and axonometric view (bottom).

4 IN-SITU DYNAMIC MEASUREMENTS

Due to the importance and peculiarity of the monument, it was considered useful to perform in-situ test to get further information on some mechanical characteristics of the tower.

Preliminary dynamic in-situ measurements have been so far performed by the Department of Structures (Dip. PRICOS) of the University of Chieti- Pescara. In these tests, that should continue in the next months, precision accelerometers are used to record the very low intensity vibrations due to external "noise" and ambient loads, namely due to the vibration induced by an aerial platform (Figure 1) and by other building-yard equipments operating near the tower during the investigation and restoration works planned by the local authorities.

For the first series of tests three accelerometers of the type PCB 393 AO3 were used; they were placed on the structure by way of an articulated aerial platform (Figure 1). Namely, the three sensors, arranged with a horizontal axis of measurement, were all placed (Figure 6) on the concrete floor which separates the cylindrical part of the tower from the prismatic part underneath; in fact, the FE model of the structure (see Section 3) shows how the first modes of vibration are characterized by oscillations of a global type, both flexural or torsional.

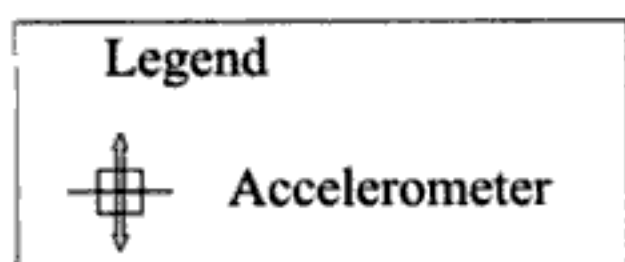
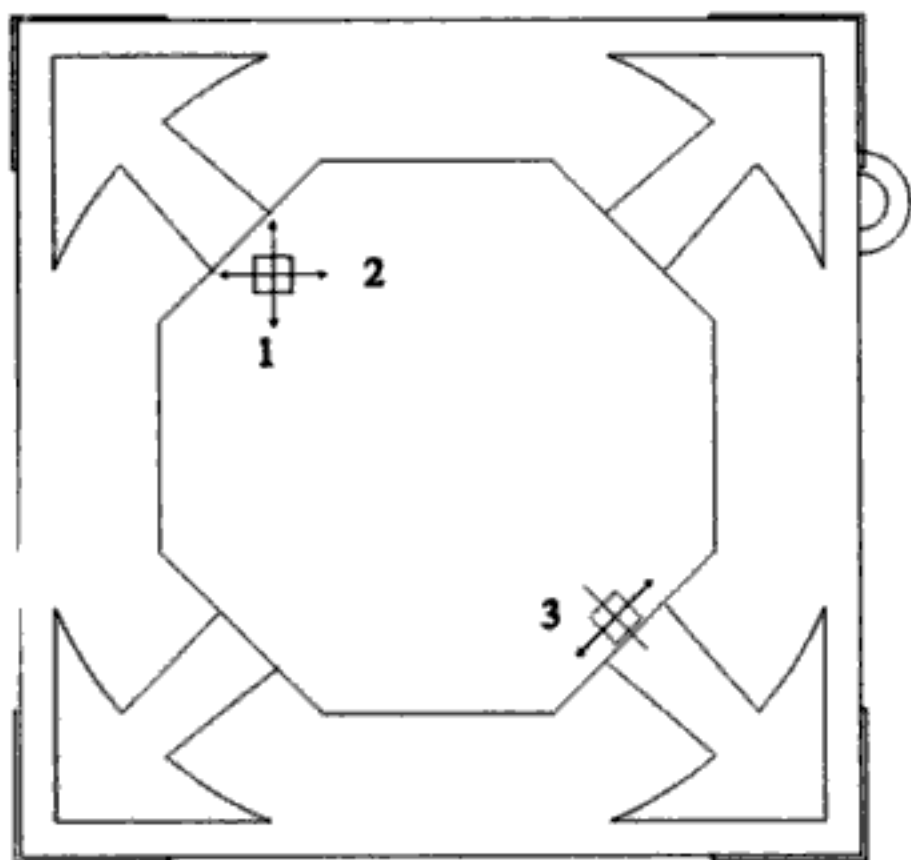


Figure 6. Position of the accelerometers on the r.c. floor between the square and the circular parts of the tower.

Local oscillations of single parts or the structure, corresponding to modes with higher frequencies, will be the objective of future investigation, that require a larger number of sensors.

In this phase of the analysis accelerometers records have been performed of the low intensity structural vibrations due to the vibration induced by an aerial platform (Figure 1) and by other building-yard equipments operating near the tower; such tests are denoted in the following with the letter A followed by the number of the sensor and the number of the sequence of the test (e.g. A_s2_05). Other tests, denoted respectively with the letters B and C, were carried out with a local type of excitations, consisting of a person jumping rhythmically on the concrete floor (mass of about 90 kg, jumps with period of about one second) in a vertical direction (tests denoted with B) or in a lateral direction (tests denoted with C).

The recorded accelerations, some examples of which are shown in Figure 7, have then been filtered and transformed in the frequency domain, through the classical technique of Fast Fourier Transform (FFT).

The FFT of the records in Figure 7 are shown in Figure 8. In spite of some uncertainty, probably due to the low intensity of the vibrations, and in spite of some anomalies that are currently being investigated, most of the tests have shown peaks of frequencies of 2.4 Hz, 7.8 Hz and 13 Hz, approximately.

Considering the location and orientation of the sensors, the first two frequencies can be associated with the first flexural mode and the first torsional mode, respectively (Section 3).

The comparison between the experimental values of frequency with those given by the FE model for different mechanical characteristics (Table 1), allows to get identified values of the mass density and of the elastic modulus of about 2000 kg/m^3 and 3.5 kN/mm^2 , respectively.

It must be said, however, that such values represent only an average estimate for low-intensity vibrations, and therefore the possibility of values locally higher or lower cannot be excluded in this phase of the study; in particular, parts of masonry with mechanical characteristics lower than the average, due to the presence of hollows or local cracks must be investigated experimentally.

What is more difficult in this phase is the interpretation of the third peak of the FFT, that, with this very low level of vibrations, can be also sometimes difficult to distinguish from peaks due to background noise.

The comparison with the results given by the FE model allows to consider, for this third peak, the hypotheses both of a contribution of the second flexural mode, which should however be only slightly relevant at the concrete floor level where the sensors are located (Figure 5), or of the first vertical mode,

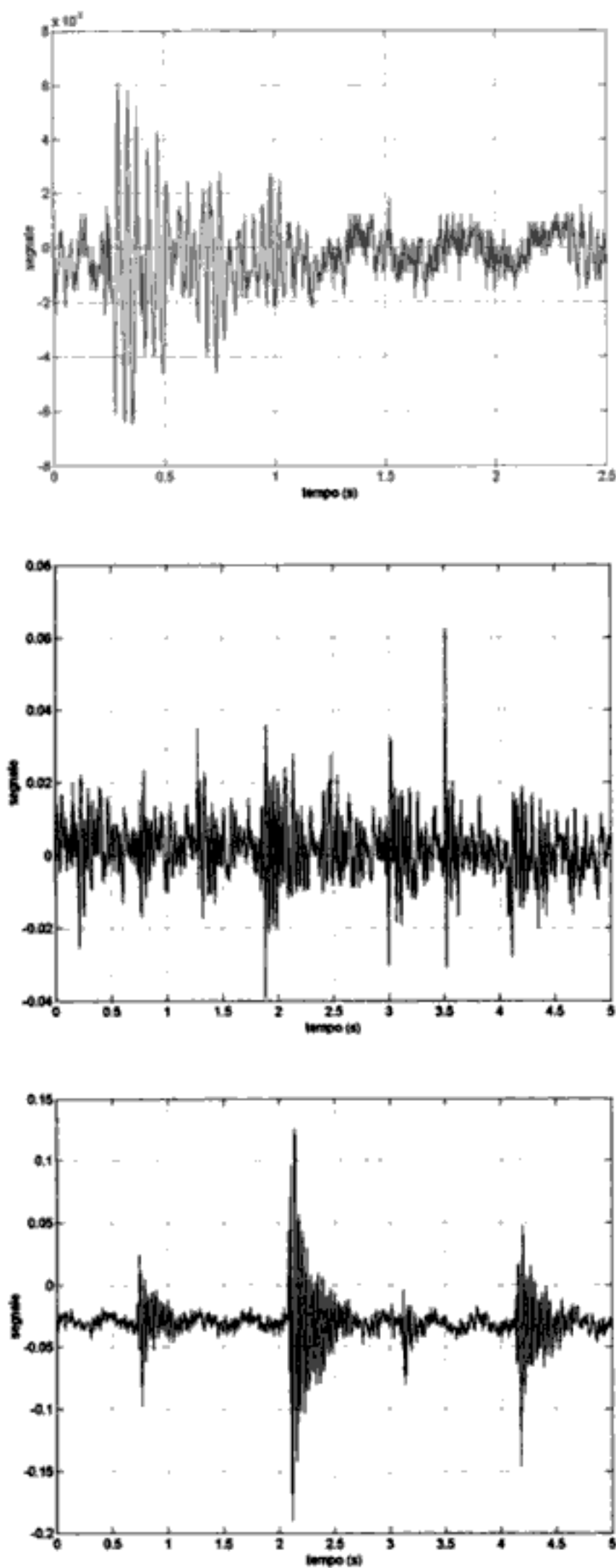


Figure 7. Example of recorded acceleration time-histories. top: sensor #2, type A excitation, 2.5 seconds
middle: sensor #3, type B excitation, 5 s
bottom: sensor #2, type C excitation, 5 s.

which is certainly activated by the last two modalities of excitation considered (B and C), but whose presence in the FFT should denote an error (imperfect horizontality) in the location of the sensors.

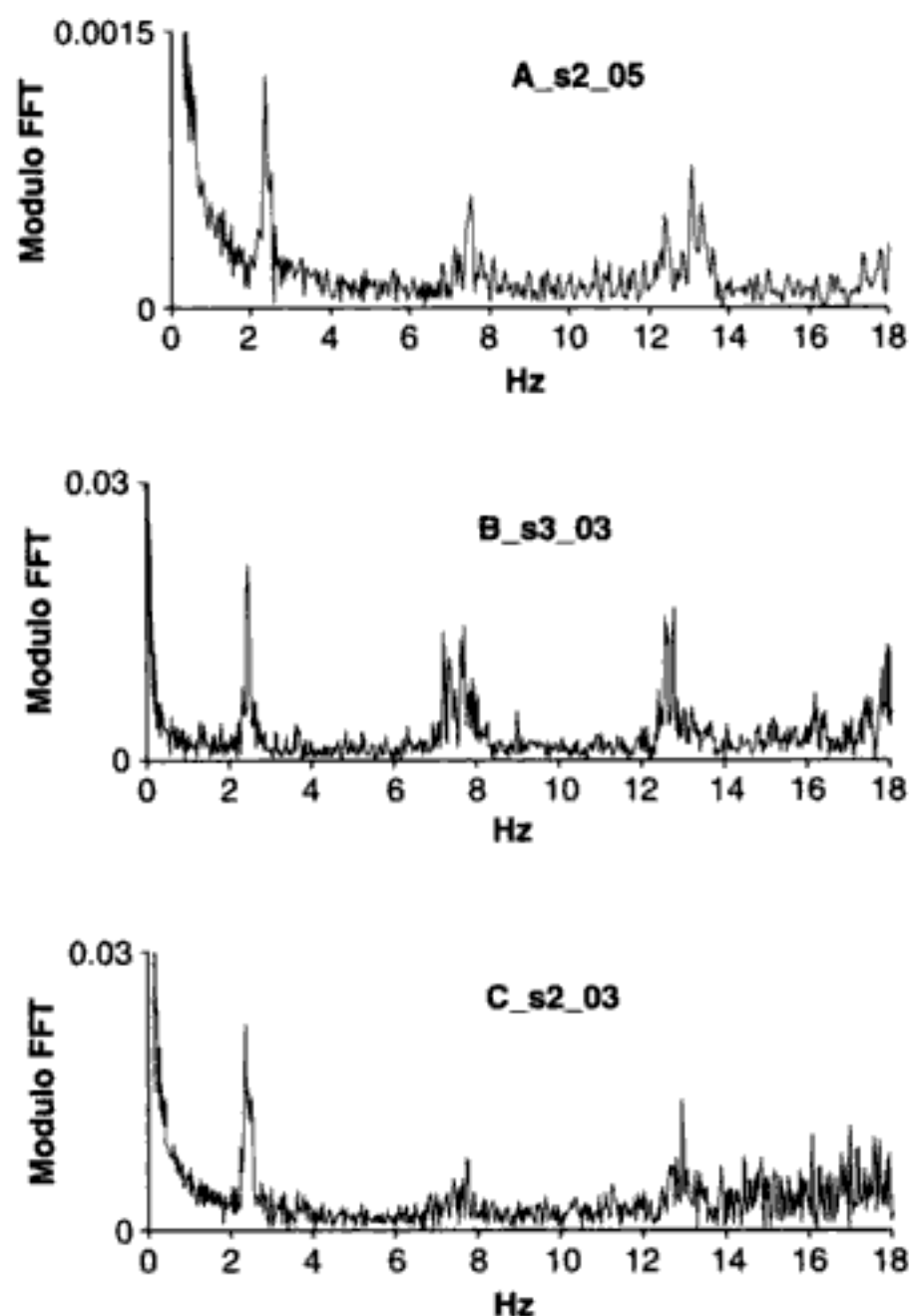


Figure 8. Modulus of the Fourier Transforms of the acceleration time-histories in Figure 7.

Further numerical investigations, still in progress, are trying to clarify these aspects.

5 CONCLUDING REMARKS

This paper refer on the very preliminary results of an in-situ investigation recently performed on a masonry tower. In the experimental campaign, that should continue in next months provided the availability of financial support, only low intensity ambient excitation have been used (namely, due to the vibration induced by an aerial platform (Figure 1) and by other building-yard equipments operating near the tower).

At the moment, the comparison between the experimental values of frequencies with those given by the FE model for different values of the density and elastic modulus, have only allowed to get identified average values for the mass density and for the elastic modulus of the masonry.

Further investigations, still in progress, are trying to apply to this structure the techniques already implemented by one of the writers (see Capecchi et al., 2002–2004; De Angelis et al., 2003–2004) for other kinds of buildings, and to perform a more accurate

updating of the FE model of the tower, taking into account both global and local vibration shapes.

However, the results reported in this paper confirm that a satisfactory investigation of this kind of structures can be performed under ambient (low intensity and no-cost) excitations, without the need of using artificial excitations (e.g. due to vibrodyne), that are often incompatible with the safeguard of the historical heritage.

ACKNOWLEDGEMENTS

The mayor and the administration of Trasacco are gratefully acknowledged for making available technical support for the experimental tests reported in this paper.

V. Sepe acknowledges also the financial support of the University of Chieti-Pescara (ex MIUR 60%, 2002 and 2003, Faculty of Architecture).

REFERENCES

- Bartoli G., Blasi C., Il sistema di monitoraggio della cupola di Santa Maria del Fiore: problematiche relative al funzionamento degli strumenti ed alla gestione dei dati, in *Monitoraggio delle strutture dell'Ingegneria Civile* (Editor P.G. Malerba), International Centre for Mechanical Sciences CISM, 1995, ISBN 88-85137-09-1, 183–202 (in Italian).
- Beolchini G. Parametri meccanici e legami costitutivi delle murature di pietrame, in *Patrimonio storico architettonico e terremoto; diagnosi e interventi di recupero* (V. De Vecchis editor), 2000, 143–154 (in Italian).
- Binda L., Gatti G., Mangano G., Poggi C., Sacchi Landriani G. The collapse of the Civic Tower of Pavia: a survey of the materials and structure, *Masonry International*, 1992, vol.6, n.1, 11–20.
- Binda L., Mirabelli Roberti G., Abbaneo S. The diagnosis research project, in *Monitoraggio delle strutture dell'Ingegneria Civile* (Editor P.G. Malerba), International Centre for Mechanical Sciences CISM, 1995, ISBN 88-85137-09-1, 49–72.
- Brownjohn J.M., Dumanoglu A.A., Severn R.T., Blakeborough A. Ambient vibration survey of the Bosphorus suspension bridge. *Earthquake Engineering and Structural Dynamics* 1989; **18**, 263–283.
- Brownjohn J.M., Dumanoglu A.A., Severn R.T. Ambient vibration survey of the Fatih Sultan Mehmet (second Bosphorus) suspension bridge. *Earthquake Engineering and Structural Dynamics* 1992; **21**: 907–924.
- Capecchi D., De Angelis M., Sepe V. Identification of structures subject to unknown seismic excitation. 3rd *Joint Conference GIMC and AACME*. Giulianova (Italy), June 2002.
- Capecchi D., De Angelis M., Sepe V. Modal model identification with unknown nonstationary base motion. *Meccanica* 2004; **39**: 31–45.
- Croci G. Conservazione e restauro dei Beni Architettonici, UTET, 2001 (in Italian)
- De Angelis M., Sepe V., Capecchi D. Identification of Modal Parameters with Unknown Input, *Problems in Structural Identification and Diagnostics: general aspects and applications* (Ed. Davini and Viola), *CISM Courses and Lectures n.471*, 2003, ISBN 3-211-20492-X.
- De Angelis M., Sepe V., Sibilio E. 2004. Tecniche nel dominio delle frequenze e nel dominio del tempo per l'identificazione di strutture sotto forzanti non misurate, *Proceed. 11-th Italian Conference on Earthquake Engineering*, Genova, 25–29 January 2004 (in Italian).
- Ewins D.J. Modal testing: theory and practice. *Research Study Press—J. Wiley & Sons*, 1986.
- Farrar C.R., James G.H. III System identification from ambient vibration measurements on a bridge. *Journal of Sound and Vibration* 1997; **205**(1): 1–18.
- Katafygiotis L.S., Mickelborough N.C., Yuen K.V. Statistical identification of structural modal parameters using ambient response data. *Proceedings 3rd International Conference on Computational Stochastic Mechanics*, Island of Santorini, Greece, 1998, 93–102.
- Luz E., Wallaschek J. Experimental modal analysis using ambient vibration. *The International Journal of Analytical and Experimental Modal Analysis* 1992; **7**(1): 29–39.
- Pavese A. Studi sul comportamento dinamico di torri in muratura e loro modellazione, PhD Thesis, Dipartimento di Meccanica Strutturale, Università di Pavia, 1992 (in Italian).
- Quek S.T., Wang W., Koh C.G. System identification of linear mdof structures under ambient excitation. *Earthquake Engineering and Structural Dynamics* 1999; **28**: 61–77.
- Torkamani M.A.M., Ahmadi A.K. Stiffness identification of a tall building during construction period using ambient test. *Earthquake Engineering and Structural Dynamics* 1988; **16**: 1177–1188.
- Wang D., Haldar A. Element-level system identification with unknown input. *Journal Engineering Mechanics (ASCE)* 1994; **120**(1): 159–176.
- Wang D., Haldar A. System identification with limited observations and without input. *Journal Engineering Mechanics (ASCE)* 1997; **123**(5): 504–511.
- Wilson J.C., Liu T. Ambient vibration measurements on a cable-stayed bridge. *Earthquake Engineering and Structural Dynamics* 1991; **20**: 723–747.

The dynamic behaviour of the façade of the Basilica S.Maria di Collemaggio

E. Antonacci & G.C. Beolchini
DISAT, Università di L'Aquila, Italy

ABSTRACT: Experimental dynamic tests were performed to frame the dynamic behaviour of the façade of the Basilica S.Maria di Collemaggio. Selected points of the façade were hit using an instrumented hammer to excite as many modes as possible. Recorded accelerograms were used to evaluate the transfer functions of instrumented points. The experimental transfer functions allowed to identify the dynamic properties of the structure: natural frequencies, modal displacements and damping factors. The experimental results were used to calibrate the parameters of a numerical model. In this paper numerical and experimental analyses are presented and discussed.

1 INTRODUCTION

The Basilica S.Maria di Collemaggio is one of the most attractive churches in Central Italy (Figure 1). Dating back to the XV century, the Basilica has a nave and two side aisles. The nave is 61 m in length and 11.3 m in width; reaching a height of 18.25 m. The two side aisles are 7.8 and 8 m in width, delimited by two external walls, both 12.5 m high.

Following a recent earthquake the Basilica underwent some light repair work, thus moderately strengthened to improve its transversal behaviour. A light steel truss structural system was mounted at roof level to improve the link between the walls; furthermore, the walls were injected with cement mortar to enhance the mechanical properties of the masonry. A numerical and experimental study allowed to define the dynamic behaviour of the Basilica (Antonacci et al. 2001a, b). A parametric analysis was performed by FE models to predict and frame the transversal response of the church before and after the retrofitting. Experimental tests allowed the determining of the dynamic behaviour, in particular of the modal parameters and the efficiency of structural elements. Dynamic test results were used to validate and update finite element models of the structure. They also gave information on overall behaviour which cannot be evaluated by the numerical models. In fact, in such structures this depends not only on the mechanical properties of materials but also, if not mainly, on the connections between structural components.

The façade, approximately rectangular in shape, has a thickness varying from 0.70 m, at the top, up to 1.20 m near its foundation. It is not as regular as it



Figure 1. The Basilica S. Maria di Collemaggio.

may seem at first glance. In the front there are three fields separated by vertical parastas. The right field, adjacent to the octagonal squat tower, is wider than the other two: this gave ancient pilgrims a better perspective as they arrived from the left path which was then the main access to the Basilica.

Its arrangement is not well defined. Basically, at least three leaves of different materials constitutes the wall. The actual façade is the result of at least two major structural interventions. The first performed after the earthquake in Fucino in 1915, which strongly damaged the upper left corner, consisted in a reinforced concrete grid and a leaf of brick masonry at the rear of the façade to improve its resistance out of plane. Furthermore, this reinforcement was stiffened by means of four vertical brick corbels laying on longitudinal

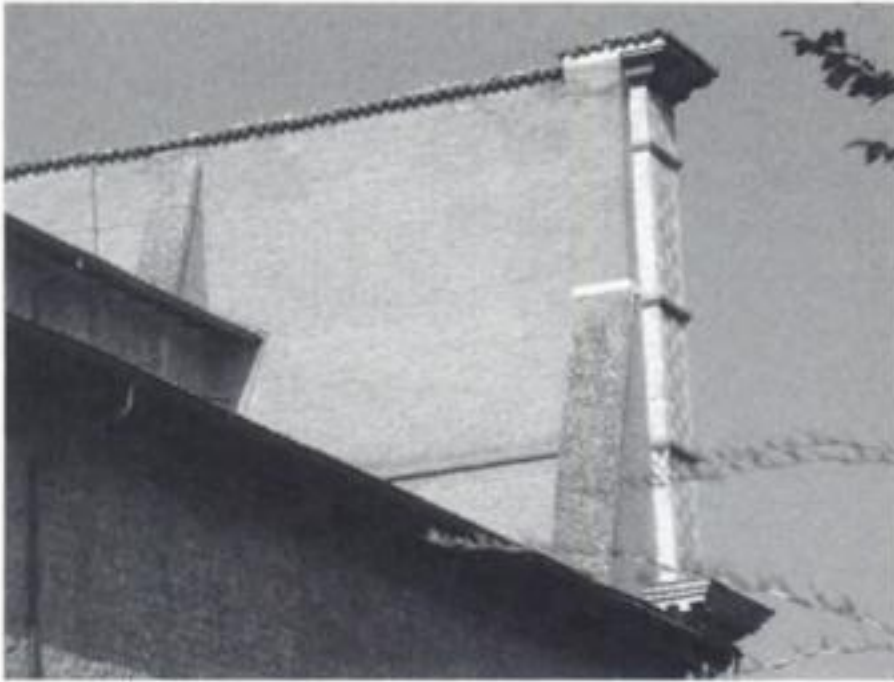


Figure 2. The vertical brick corbels behind the façade.

walls (Figure 2). Corbels are approximately triangular; those on lateral walls have a rectangular extension up to the top of the façade. The second intervention, around 1970, consisted in adding three meters of stone masonry at the top of longitudinal walls which were lowered after the 1703 earthquake.

Thus, the actual arrangement of the façade is not very clear. Although the layers seem well ordered, there is some uncertainty as to their mutual connections. Furthermore, the artistic value of the façade does not allow for the use of traditional techniques, even those of minor destructiveness, to determine the mechanical parameters of materials necessary to calibrate a reliable numerical model: in any case, they can only give restricted information, sometimes contradictory, and thus not automatically valid for other parts of the structure.

Research was carried out to define the global structural layout of the façade: thermographic (Paoletti et al. 2001) and georadar analyses (Tallini et al. 2002) permitted to locate the position of some inclusions and discontinuities; in addition the thicknesses of the wall, varying from 0.70 m in the upright corner to 1.20 m at the base, were established. Dynamic tests were carried out to describe the behaviour of the façade, as already done for the longitudinal wall.

2 DYNAMIC TESTS

The dynamic tests were carried out by exciting the façade at low intensities through an instrumented hammer (frequency interval: $0 \div 500$ Hz; force interval: $0 \div 22000$ N; average sensitivity: 0.22 mV/N; resonance frequency: 2.7 kHz; mass: 5.4 kg). A total of 23 accelerometers (sensitivity: 5 V/g; full scale: 2g; bandwidth: $0.5 \div 25$ Hz; resolution: 0.002% of full scale) registered responses in each test. Several tests were carried out, with different positions of the instruments and impact locations, in order to excite and measure as

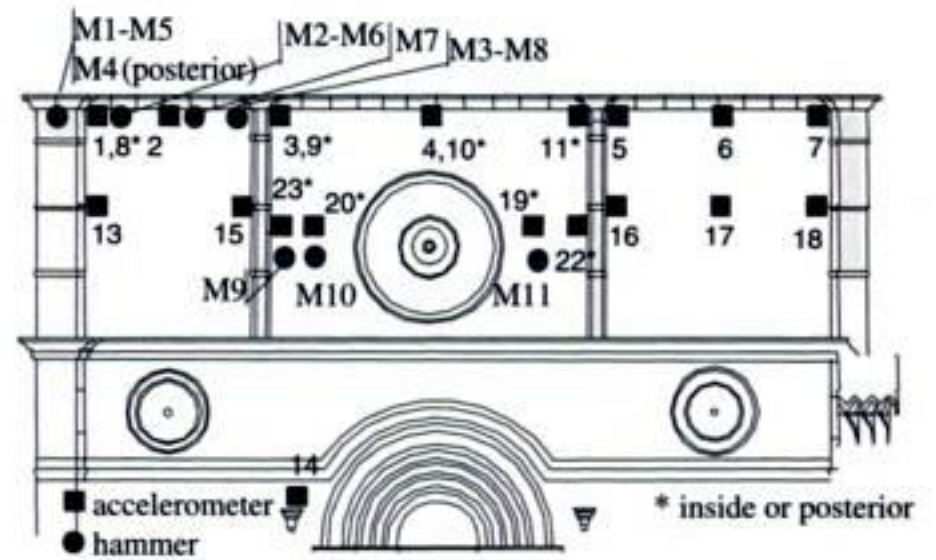


Figure 3. Accelerometers and hammer impact points.

many modes as possible. Hammer blows hit the walls at the level of accelerometers to give a horizontal pulse nominally perpendicular to the wall; in each test several blows were used in each point. The position of accelerometers and hammer impact points are given in Figure 3.

The tests were carried out in two distinct periods. In the first cycle only the accelerometers at the top of the façade (from 1 to 11) and inside the Basilica (from 19 to 23) were used; the corresponding impact points were from M1 to M4. Eight of the accelerometers at the top were arranged in pairs, one on the front side of the façade, the other one behind it: this allowed to control the connection between the layers of the wall. In the second cycle, accelerometers 2, 6, 8, 9 and 11 were removed and mounted in positions from 13 to 18. An accelerometer, mounted in 14, controlled the movements of lower part of the façade which resulted insignificant. M5 up to M11 denote hammer impact points of the second cycle of tests.

3 EXPERIMENTAL RESULTS

Recorded accelerograms were used to evaluate the transfer functions of instrumented points; experimental responses were filtered by exponential window to amplify the first part of records. Transfer functions were obtained by averaging the transforms of significant accelerograms, from 2 to 8 in each test, divided by the transform of the corresponding excitation (Ewins, 1984). Only accelerograms with coherence greater than 0.8 were considered, so a ratio signal/noise of 12 dB is ensured.

The amplitude of some typical transfer functions is shown in Figure 4. In Figure 4a, b the responses of coupled instruments A1–A8 and A3–A9 are compared. Even if the simultaneous examination of the phases, or the complex representation, can give a comprehensive description of the responses, the diagrams permit the recognition of at least five major resonant peaks in the $3.9 \div 10$ Hz range.

Table 1. Identified frequencies (Hz): hammer impact point M1.

Accelerometer	Mode				
	1	2	3	4	5
A1	3.83	4.46	5.02	8.54	9.51
A2	3.95	4.47	5.02	–	9.51
A3	3.95	4.47	5.02	–	9.51
A4	3.95	4.48	5.02	7.27	9.52
A5	3.96	4.48	5.02	7.26	9.52
A6	3.96	4.46	5.01	7.25	–
A7	3.96	4.46	5.02	–	–
A8	3.82	4.46	5.02	–	–
A9	3.95	4.47	5.02	–	9.49
A10	3.95	4.30	5.02	–	9.48
A11	3.95	4.47	5.02	7.26	9.49
Mean	3.95	4.47	5.02	7.26	9.47

Table 2. Mean values of identified frequencies (Hz): hammer impact points M2 to M8.

Test	Mode				
	1	2	3	4	5
M2	3.93	4.45	5.00	–	9.47
M3	3.97	4.46	5.00	7.22	9.41
M4	3.95	4.46	5.02	7.24	9.48
M5	4.00	4.53	5.27	7.22	9.63
M6	4.01	4.55	5.28	7.24	9.76
M7	4.03	4.53	5.30	7.19	9.74
M8	4.04	4.53	5.29	7.21	9.72

Table 3. Identified modal damping factors (%): hammer impact point M1.

Accelerometer mode	Mode				
	1	2	3	4	5
A1	1.5	0.7	1.0	–	–
A2	0.5	1.0	1.3	–	1.2
A3	0.6	1.1	1.5	–	1.2
A4	0.7	1.2	1.1	1.1	1.3
A5	0.8	1.6	1.0	1.2	1.3
A6	1.1	0.9	0.5	1.5	–
A7	1.2	0.9	0.7	–	–
A8	1.7	0.7	1.0	–	–
A9	0.6	1.1	1.6	–	1.4
A10	1.6	0.5	0.5	–	0.6
Mean	0.96	1.12	1.06	1.22	1.85

ignored, first of all because it appears to depend on a local mode; furthermore, the related experimental transfer functions are rather low around it, and the signal is comparable to noise.

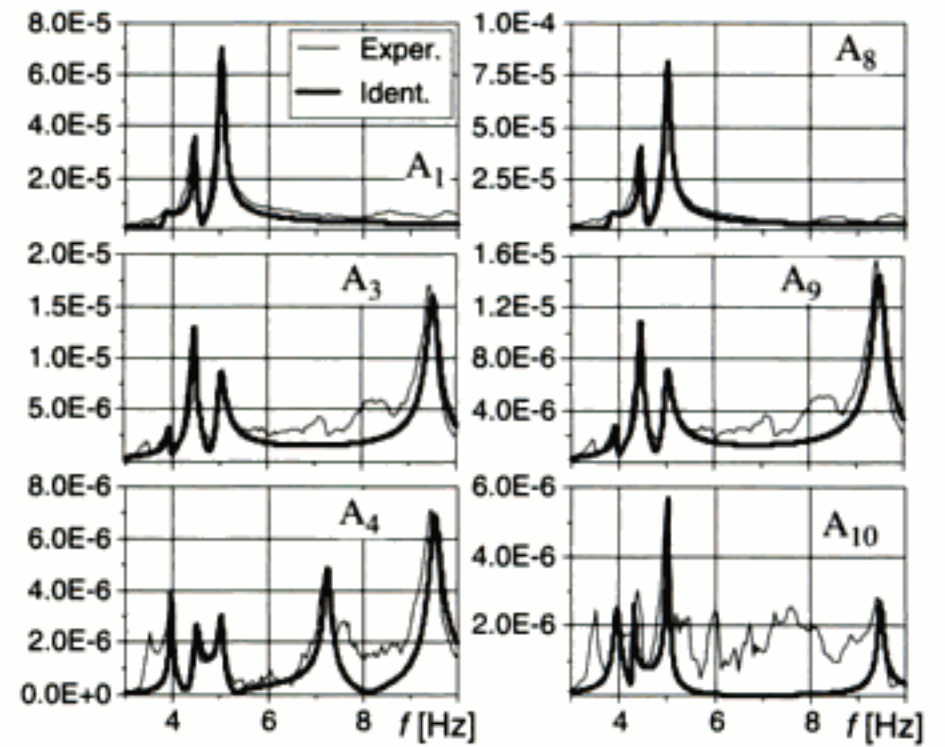


Figure 5. Experimental and identified transfer functions.

An example of identified modal frequencies is given in Table 1 where test M1 is considered. The frequencies are very close to mean values, with the exception of the frequencies of modes 1 and 4 evaluated by experimental transfer function of accelerometers A1 and A8. The differences certainly depend on their very low responses at corresponding frequencies, as shown in Figure 4a, where the peaks are actually not very evident.

The mean values of identified frequencies by other tests are shown in Table 2. The frequencies of tests M2 to M4, carried out in the first cycle, as test M1, confirm the data in Table 1: the scattering around the mean values is in the range of sampling frequency (0.05 Hz) used during the tests. The frequencies identified by second cycle data (M5 to M8) are very close to those of the first one. They are some fractional percent higher; the slight difference is probably due to the modified atmospheric conditions during second group of tests.

Notwithstanding the low excitations, the identified modal damping factors are not negligible, as shown in Table 3, where only the results of M1 test are indicated. Damping factors identified by the other tests are in the same ranges of those of Table 1.

Some examples of identified frequency response functions are plotted in Figure 5.

If only A1 and A8 are considered (Figure 5), there is an excellent match between the identified and experimental frequency response curves. Only the first three peaks of identified response functions are clearly visible in the plots, due to the low values of modal constant χ identified for modes 4 and 5.

The agreement between identified and experimental plots is still satisfying if only the main peaks of A3 and A9 are considered. In the interval 5 to 9 Hz was not possible to identify the modal parameters of fourth mode. Furthermore the resonance around

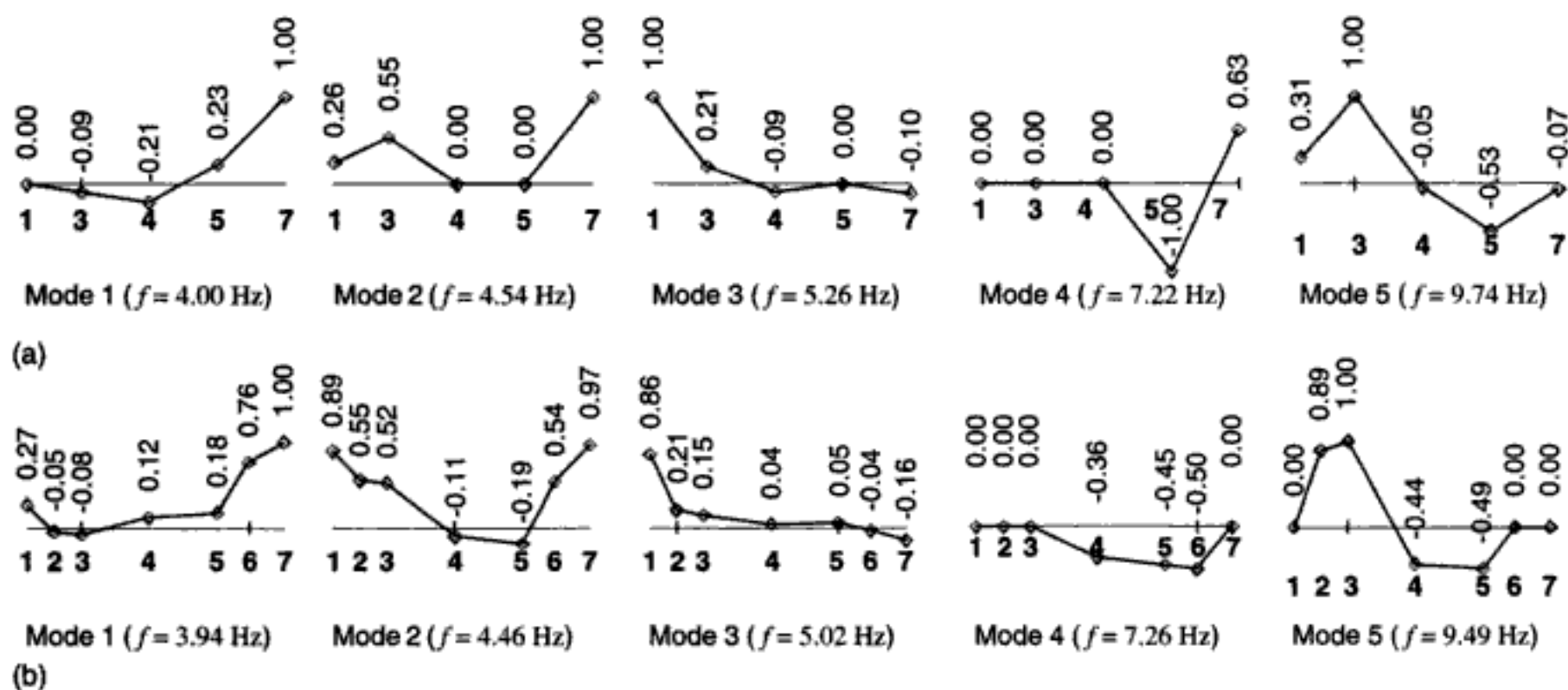


Figure 6. Identified modal shapes at top of façade: a. M5 test, b. M1 test.

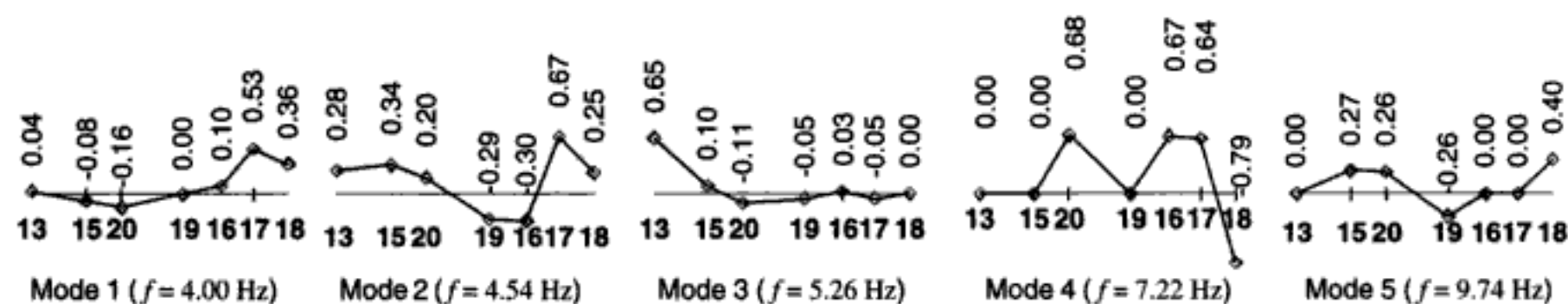


Figure 7. Identified modal shapes at rose window level (MS test).

8.5 Hz seems to be produced by local vibration, as well as that at 3.5 Hz.

If the responses of A4 and A10 are compared the discrepancies in the interval 5 to 9 Hz are apparent. In addition, the presence of the peak around 3.5 Hz in the experimental transfer functions is very noticeable, notwithstanding every effort to identify its modal parameters failed because its association to local vibrations.

Modal shapes complete the description of modal model of the façade. They help to understand its dynamic behaviour and give essential information to characterize numerical models presented later.

An example of identified modal shapes is given in Figure 6, where the modal deformations at the top of the façade identified by M5 and M1 test are compared. The first modal shape corresponding to M5 shows that the left side of the façade seems fixed (point 1, Figure 6a), due to the higher stiffness of restraints; this behaviour is confirmed by other tests with the exceptions of M1 (point 1, Figure 6b) and M4, where the hammer's hit excites local vibrations. The second mode is approximately symmetric, with horizontal tangent in the middle of façade: it is similar to the first mode of a free beam. Third mode is basically anti-symmetric with respect to the first one. Fourth mode seems to bend only the right side of façade and, only

in test M1, its central segment. In first analyses it was considered associated to a local vibration, due to its absence in other responses: it could be considered a true fourth mode, as confirmed by numerical evaluations given later. Fifth mode is semi-symmetric: it seems a second mode of a free beam. Modal shapes of Figure 7, with the exception of mode 4 that appear very disturbed, enrich the description of Figure 6, confirming previous suggestions: the façade behaves as a plate supported by restraints with variable deformability.

5 NUMERICAL MODELS

Even if the façade does not have any symmetry, it can be considered as a rectangular plate where three vertical fields are visible: fields are separated by parastas (Figure 1). The plate is connected with longitudinal walls, behind parastas, that can probably be considered as fixed restraints. The vertical brick corbels laying at the top of walls should be considered as flexible supports, even if many uncertainties condition their modelling: different height, connection with reinforced concrete grid made after the 1915's earthquake and with three meters of new stone masonry added over all longitudinal walls in 1970's interventions.

Some linear finite element models were developed to reproduce modal shapes and frequencies by varying the set of mechanical parameters describing the façade. Only a single layer was adopted to describe the façade; in fact, the attempt of taking into account the three layers that constitute the actual structure has to be considered not very useful, due to many uncertainties depending on their thicknesses, connections and mechanical properties. Therefore, each element in a section has to be considered representative of a complex arrangement of at least two or three layers with different thicknesses and moduli of elasticity.

The mesh of the models has been adapted in order to respect all possible geometric characteristics of the façade, such as the openings, imperfections and restraint. Standard plate-shell elements (1001 in number) were used to reproduce, as accurately as possible, the real geometry of façade. In the optimised mesh an element average size of 1.0 m was considered; plate-shell elements have a thickness varying from 0.70, around the central rose window, up to 1.2 m, when they represent the parastas. In each band the material is assumed to have linear elastic behaviour, and homogeneous and isotropic characteristics.

Soil-structure interaction has been neglected, therefore the façade was considered fixed to the soil. Cylindrical hinges were used to model the links among façade and longitudinal walls, which are supposed to be rigid. The presence of brick corbels behind the façade has been taken in account by adopting an increased thickness of plate-shell elements.

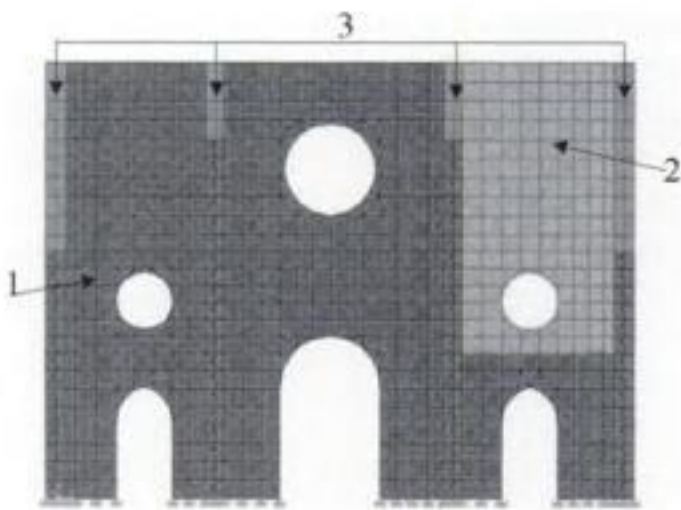


Figure 8. Model A (numbers denote section types).

Table 4. Mechanical parameters of model A.

Parameter	Section		
	1	2	3
Thickness (m)	1.0	0.8	1.0
Modulus of elasticity (MPa)	2940	3430	7850
Weight per unit volume (kN/m ³)	15.7	15.7	19.6

Many models were defined to frame the dynamic responses; only three of them are described in the paper.

The first rough model (A) was preliminarily used to locate the frequencies of façade before tests. Its geometry is described in Figure 8. Only three sections were used, with parameters guessed or chosen on the basis of historical documents. Its mechanical parameters, tuned after first experiments, are summarized in Table 4. Almost all the façade is described by section 1; section 2 is used to represent the upper right part of façade, whereas section 3 characterizes the parastas.

The more refined model B takes into account the thicknesses and irregularities pointed out by thermographic analyses (Paoletti et al. 2002) and georadar (Tallini et al. 2003). Elements representing parastas (Section 3) are unchanged, whereas thicknesses of other elements is denoted by section number (in centimeter), as shown in Figure 9; modulus of elasticity and weight per unit volume is that of Section 2 in Table 4.

The last model (C) is one of the attempts to improve the agreement between numerical and experimental results: in this attempt thicknesses of parastas (Figure 10) and the restraints between façade and corbels have been modified.

Frequencies evaluated by numerical models above are summarized in Table 5. Frequencies of first rough model A are already similar to those identified by

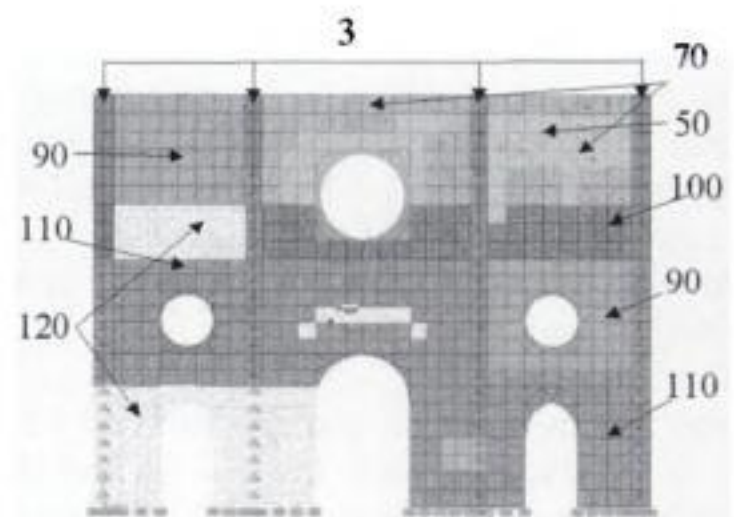


Figure 9. Model B.

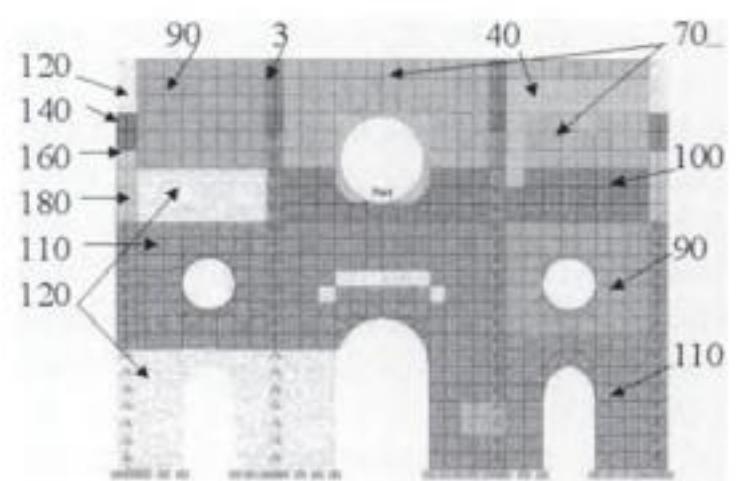


Figure 10. Model C.

experimental transfer functions: the first two frequencies are less than those experimental, whereas other three are rather higher. Frequencies of model B show that a more refined description of thicknesses draw numerical results to experimental estimates; in any case, they show that it is not sufficient, even if rather satisfying, to vary only thicknesses, without taking into account other essential parameters such as mechanical properties or connections among elements. Model C is, at the moment, that gives the better estimate of identified frequencies.

Besides comparing frequencies it is necessary to consider modal shapes. Their aerial view are plotted in Figures 11, 12 and 13.

In Figure 11 the modal shape of first mode is similar to the corresponding of Figure 6, that was obtained only by M1 test; other tests gave results similar to the plot of first mode in Figure 6a, which agrees with that of Figure 12. All other modal shapes of Figure 11

differ from those identified, plotted in Figure 6: second numerical mode is semi-symmetrical, whereas the identified one is not; third and fourth numerical modes are both symmetrical and different from identified modes. In the fifth mode deformations in first field are slighter with respect to that measured.

Modal shapes of model B (Figure 12) give a more satisfying approximation of experimental behaviour if only first, second and, partially, fifth modes are considered. Their frequencies are in any case still different from those identified. Furthermore, third and fourth modes still exhibit an approximately symmetric behaviour which does not occur in the façade.

Model C, on the whole, is able describe with sufficient accuracy the experimental behaviour: frequencies as well as modal shapes agree with identified parameters. It is still a simple model, where only one layer of masonry is considered and only two values of moduli of elasticity are used: notwithstanding, it seems able to give a reliable outline of the behaviour of façade out of its plane.

Table 5. Frequencies of numerical models and mean values of identified frequencies (Hz).

Mode	Model			Identified
	A	B	C	
1	3.68	3.79	3.76	4.00
2	4.15	4.73	4.93	4.50
3	6.20	5.81	5.44	5.20
4	7.81	7.77	7.80	7.22
5	11.20	10.20	9.16	9.60

6 CONCLUSIONS

The dynamic behaviour of the Basilica S. Maria di Collemaggio was analysed using both numerical and experimental methods.

Dynamic test allowed framing general aspects of the behaviour of the façade out of its plane. Furthermore, notwithstanding the low intensity of excitations, they pointed out some localised deficiencies in



Figure 11. Modal shapes by Model A.



Figure 12. Modal shapes by Model B.

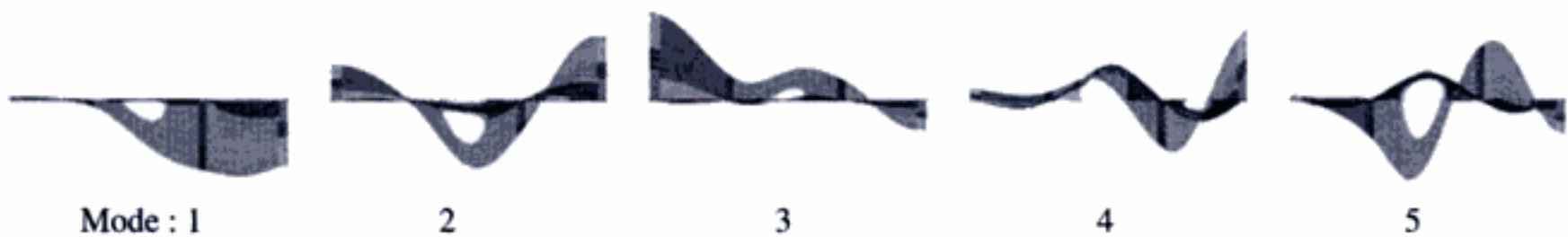


Figure 13. Modal shapes by Model C.

connections among structural components, thus confirming the results of thermographic and georadar analyses. The research can give useful suggestions to decide the strategy of future interventions to reinforce the façade.

The contemporary use of FE and experimental modal analysis allowed a satisfying numerical prediction to be made, even if nonlinearity are present in the façade, still at low excitations, and the links, constraints and elements can not be always correctly modelled.

The appreciable quality of hammer tests demonstrated the possibility of using a relatively inexpensive and uncomplicated tool to integrate and calibrate numerical prevision.

The repetition of dynamic tests in the future will permit the monitoring of the façade of the Basilica and, more generally, will allow to control variations due to degradation of structure or material.

REFERENCES

- Antonacci, E., Beolchini, G.C., Di Fabio, F. & Gattulli, V. 2001a. Retrofitting effects on the dynamic behaviour of S.Maria di Collemaggio, *Computational Methods and Experimental Measurements, CMEM2001, Proc. intern. congress, Alicante, 6–8 June 2001*, Southampton: WIT Press.
- Antonacci, E., Beolchini, G.C., Di Fabio, F. & Gattulli, V. 2001b. The dynamic behaviour of the Basilica S.Maria di Collemaggio, *Studies in Ancient Structures, SAS2001; Proc. intern. congress, Istanbul, 9–3 July 2001*.
- Ewins, D.J. 1984. *Modal testing: Theory and Practice*, Research Study Press Ltd., Letchworth, Hertfordshire: John Wiley & Sons Inc.
- Goyder, H.G.D. 1980. Methods and applications of structural modelling from measured structural frequency response data, *Journal Sound Vibration*, 68: 209–230.
- Paoletti, D. & Schirripa, G. 2002. Thermographic analyses of façade of the Basilica S.Maria di Collemaggio (in Italian). *Internal Report of Laser Lab., DENE, University of L'Aquila*.
- Ranalli, D., Scozzafava, M. & Tallini, M. 2004. Ground penetrating radar investigations for restoration of historical building: the case study of Collemaggio Basilica (L'Aquila, Italy), *Journal of Cultural Heritage*. 5: 91–99.

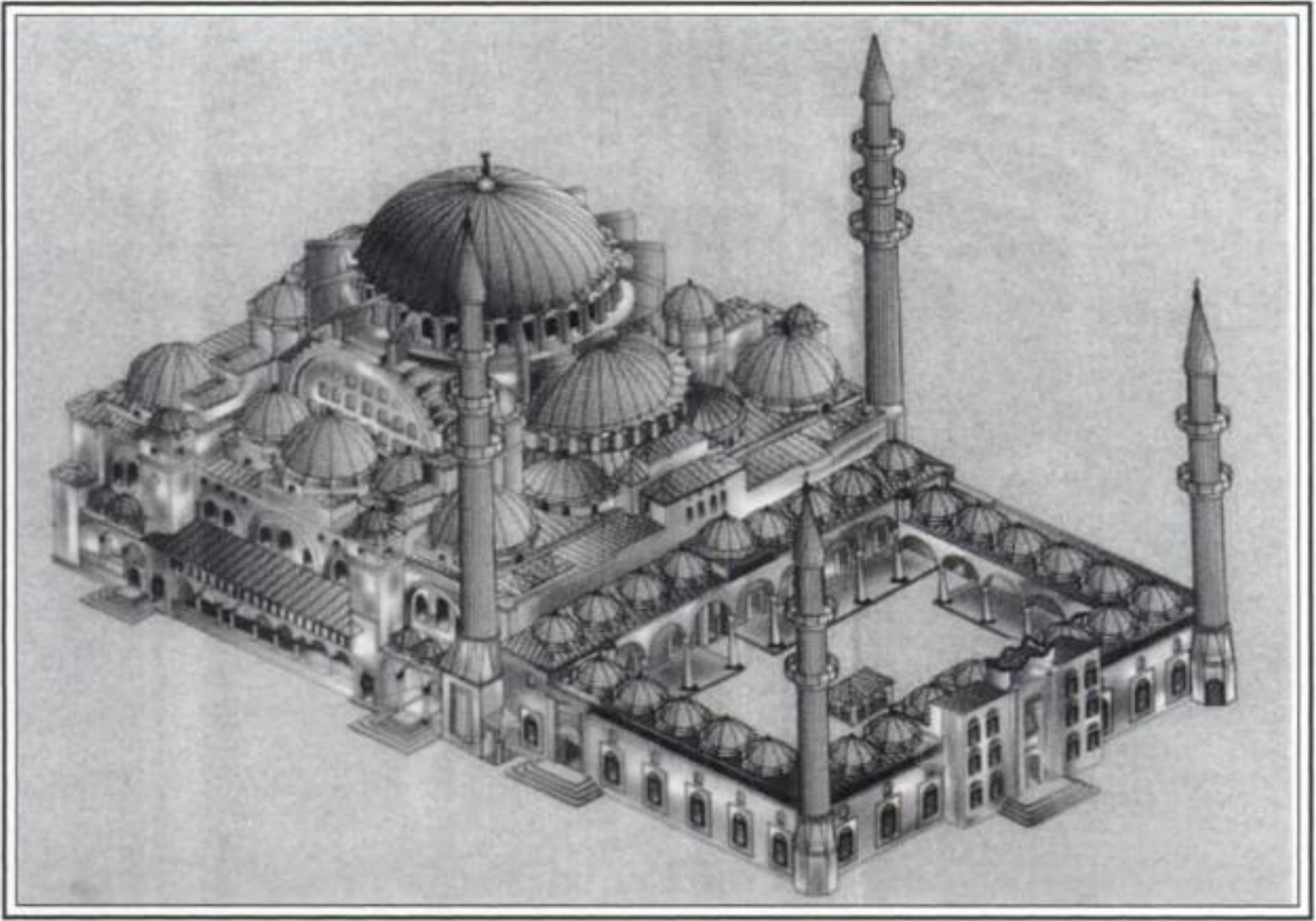


Figure 1. 3-Dimensional view of Suleymaniye Mosque.

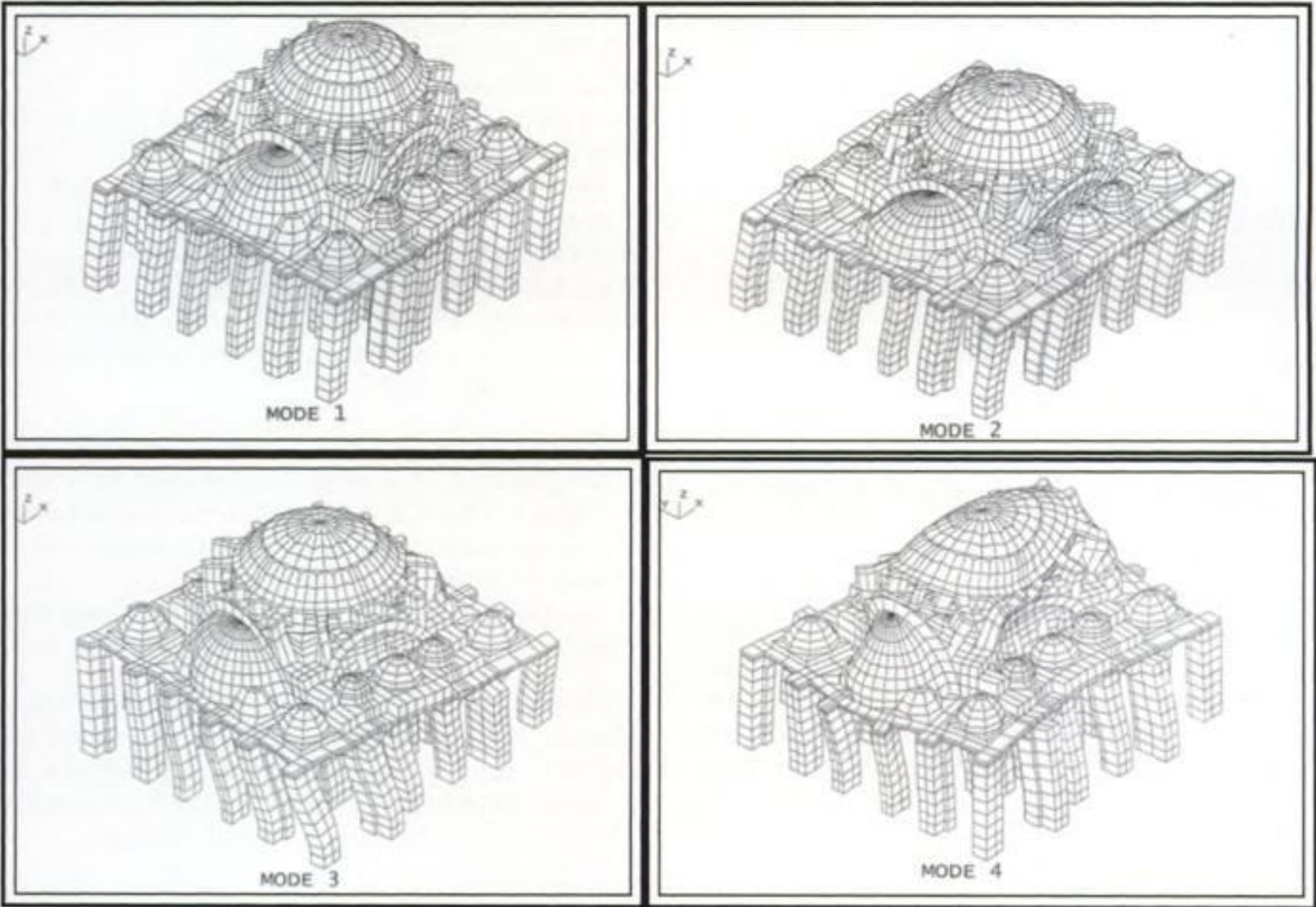


Figure 2. Modal analysis mode 1-2-3-4.

improved by utilising the following modifications:

- A detailed study was carried out to determine an optimum number of structural elements. For this purpose the total number of elements were raised to 3989 and the corresponding total number of nodes to 6980.
- Small domes were added to the model which were previously excluded.

- Foundation level was lowered 2.5 m below the ground level.
- Four different boundary conditions were analysed for different combinations of material properties.

The frequencies corresponding to the first five modes are given in table 5, (Fig. 2)

4.2 Analysis

The results of the various dynamic runs under different combinations of material properties and boundary conditions are summarized in Table 6.

Four different boundary conditions were analysed for four different combinations of material properties. Several dynamic runs were carried out and finally a model with nearest frequency values to those of ambient vibration tests was selected as the improved model which was used for the spectral response analysis under a scenario earthquake for İstanbul. Table 7 gives the material properties used in the analysis.

Table 8 below can be used to compare the results obtained from ambient vibration tests, earthquake

Table 5. Results of modal analysis.

Modes	Frequency (Hz)
Mode 1 (Lateral mode in the north-south direction)	3,244
Mode 2 (Lateral mode in the east-west direction)	3,420
Mode 3 (Torsional mode)	4,305
Mode 4 (Diagonal Torsional mode)	4,734
Mode 5 (Lateral squeezing in east-west and north-south direction)	4,745

Table 6. Table of dynamic runs.

Model name	Description	Natural frequencies					Input no
		F1	F2	F3	F4	F5	
Sup1 A1	Fix in XYZ at - 5.3 m	3,07	3,23	3,76	4,81	4,93	1
		2,84	2,99	3,65	4,17	4,18	2
		2,89	3,03	3,03	4,28	4,30	3
Sup2 A2	Fix in XY at - 2.8 m	3,24	3,41	4,02	5,01	5,12	1
		2,96	3,12	3,89	4,32	4,33	2
		3,02	3,17	3,91	4,44	4,44	3
B2	Spring in XY at - 2.8 m A1	3,08	3,29	3,82	4,85	4,91	1
		2,85	3,03	3,70	4,20	4,22	2
		2,90	3,08	3,72	4,31	4,34	3
Sup3 A3	Fix in XYZ at - 2.8 m A1	3,52	3,75	4,45	5,35	5,44	1
		3,15	3,34	4,26	4,56	4,60	2
		3,24	3,41	4,30	4,71	4,73	3
Ambient tests		3,38	3,44	4,26	4,71	5,85	
Sup4 A4	Fix in XY at - 2.8 m A1	3,14	3,33	3,89	4,90	5,03	1
		2,89	3,06	3,78	4,25	4,26	2
		2,94	3,11	3,80	4,36	4,38	3
B4	Spring in XY at - 2.8 m A1	3,14	3,33	3,89	4,90	5,03	1
		2,89	3,06	3,78	4,25	4,26	2
		2,94	3,11	3,80	4,36	4,38	3
A5	Fix in XYZ at - 2.8 m A1	3,72	3,74	4,47	5,36	5,45	1
		3,16	3,35	4,28	4,56	4,6	2
		3,37	3,56	4,59	4,88	4,38	3
B5	Fix in XYZ at - 28 m A1	3,53	3,74	4,47	5,36	5,45	1
		3,16	3,35	4,28	4,56	4,61	2
		3,24	3,56	4,59	4,88	4,93	3
A6	Fix in XYZ at - 28 m	4,04	4,31	5,34	6,04	6,08	1
		3,46	3,68	4,94	4,94	5,06	2
		3,58	3,79	5,02	5,14	5,23	3

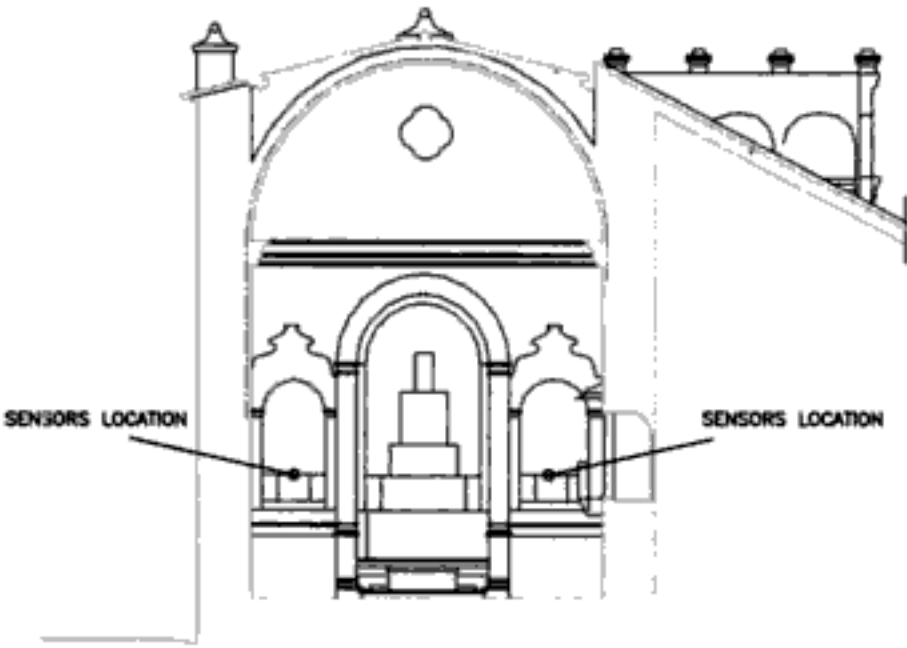


Figure 6. Location of sensors in this preliminary test.

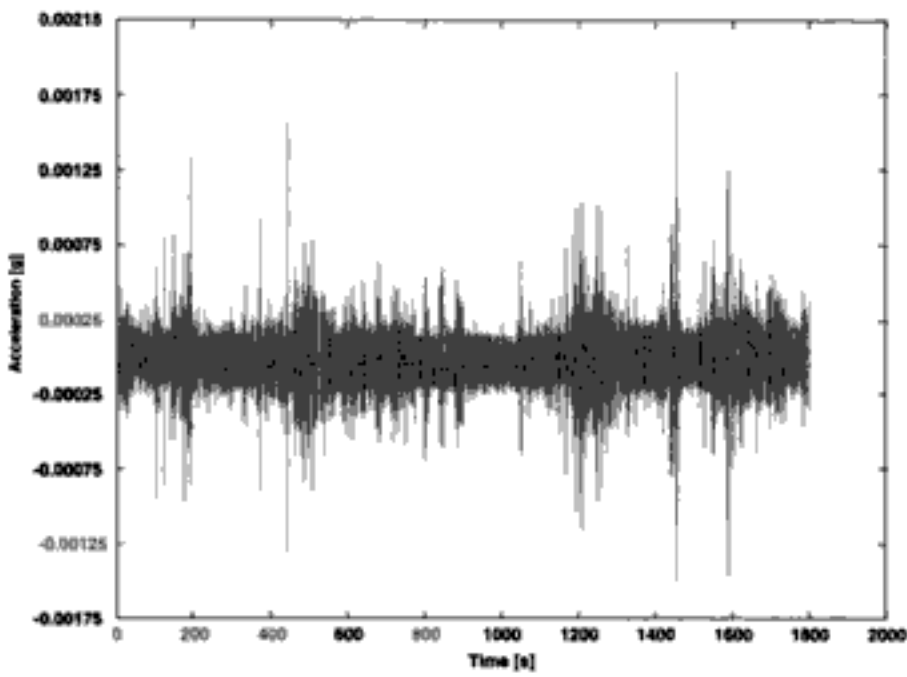


Figure 7. Accelerogram recorded on March 2003, inside the church.

data acquisition system (DAS) with dynamic range of 114 dB, and output data format with 24 bits.

To obtain the fundamental frequency of the church, a preliminary test was made: acceleration data was recorded for 30 minutes and a sampling frequency of 250 Hz was used.

Figure 7 presents an acceleration record where we can see the amplitude of vibrations inside the church in ambient vibration conditions.

Data processing was performed using Artemis Extractor version 3.4, SVBs (2002). The power spectral densities matrices are obtained using the Frequency Domain Decomposition. This technique decomposes approximately the spectral density matrix of the system response into a set of SDOF systems using Singular Value Decomposition; the singular values are estimates of the spectral density of the SDOF systems, and the singular vectors are estimates of the mode shapes Ventura (2001).

Analysis of the Figure 8 enables the clear identification of the first frequency (fundamental) of 3.3 Hz.

4 THE FINITE ELEMENT MODEL

In order to obtain a finite element model of the structure it is necessary to use idealisations of material behaviour and geometry. Geometry of ancient historical structures may be rather complex as often there is no clear distinction between decorative and structural elements (Lourenço, 2001).

The FEM has been developed using the computer program SAP 2000 version 7.10 (Computers & Structures, 1998). This program can be used for linear and

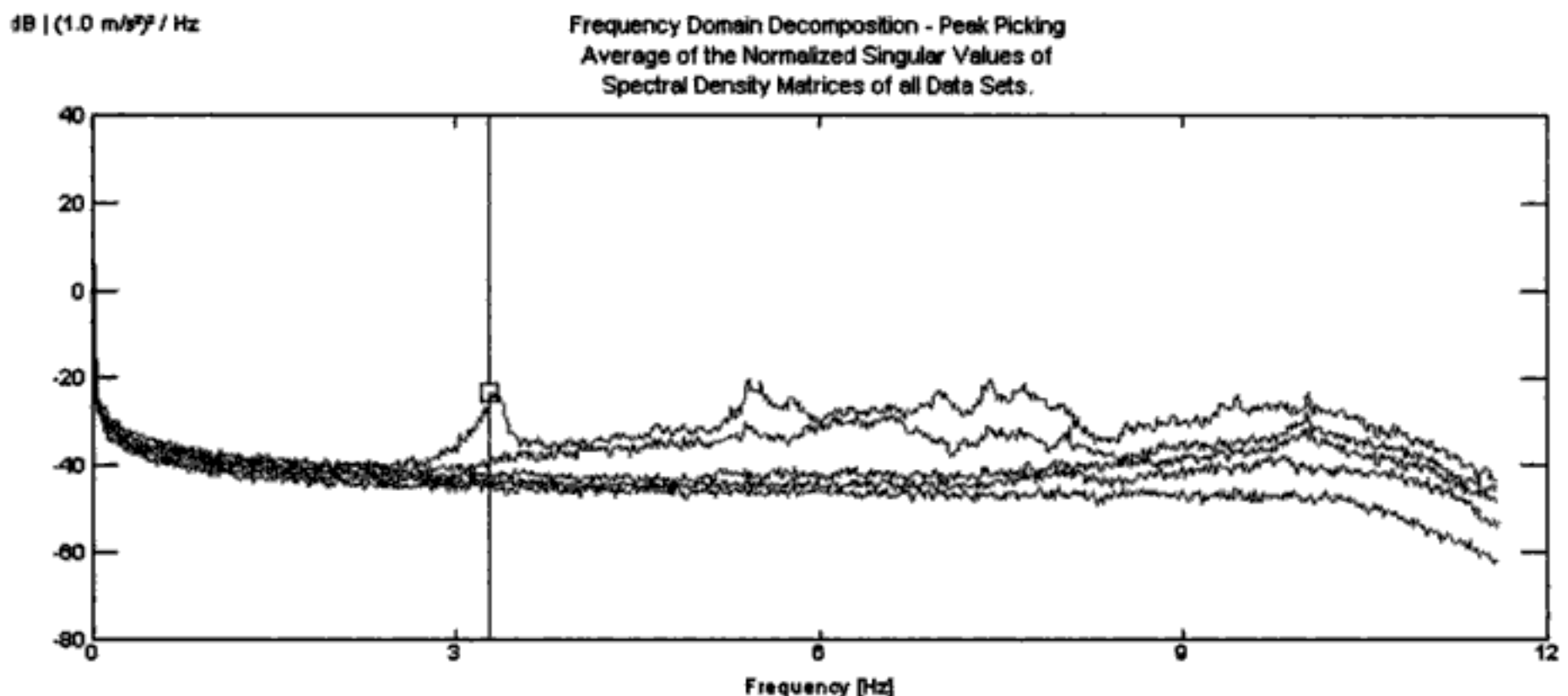


Figure 8. Singular values of spectral densities matrices using FDD.

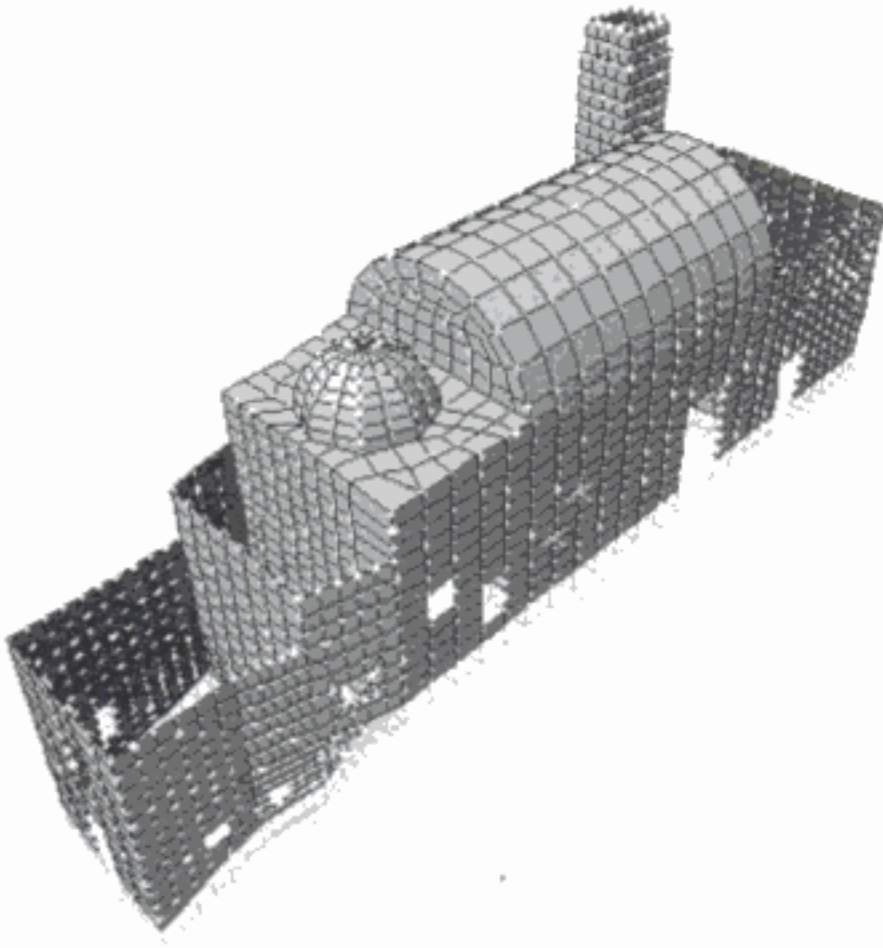


Figure 9. Numerical model.

non-linear, static and dynamic analyses of a three-dimensional model of the structure. In our study the program has been used to determine the fundamental frequencies and the corresponding mode shapes of structure, based on its physical and mechanical properties.

In the preliminary phase, it is assumed that all the materials of the structure have the following characteristics: (i) they are homogeneous and isotropic; (ii) modulus of Elasticity, $E = 0.7 \text{ GPa}$ (based on a preliminary ambient vibration test); (iii) Poisson's ratio 0.2; iv) linear elastic behaviour is assumed. The geometry of the structure is idealised considering the structure to be made of shell elements.

Figure 10 shows the 1st mode shape, obtained by the finite element modelling; it corresponds to a translation in the transversal direction, with a frequency of 3.3 Hz. The modulus of elasticity has been tuned in order to identify the model from the experimental result.

The second mode shape, obtained from the FEM, involves mainly the bell tower (see Figure 11).

5 FINAL CONSIDERATIONS

In order to obtain an accurate estimate of natural frequencies and mode shapes the sensors should be placed at the base of the vault see Figure 12. Those tests are scheduled for July 2004 as they require the availability of an auxiliary structure that will be used during rehabilitation works.

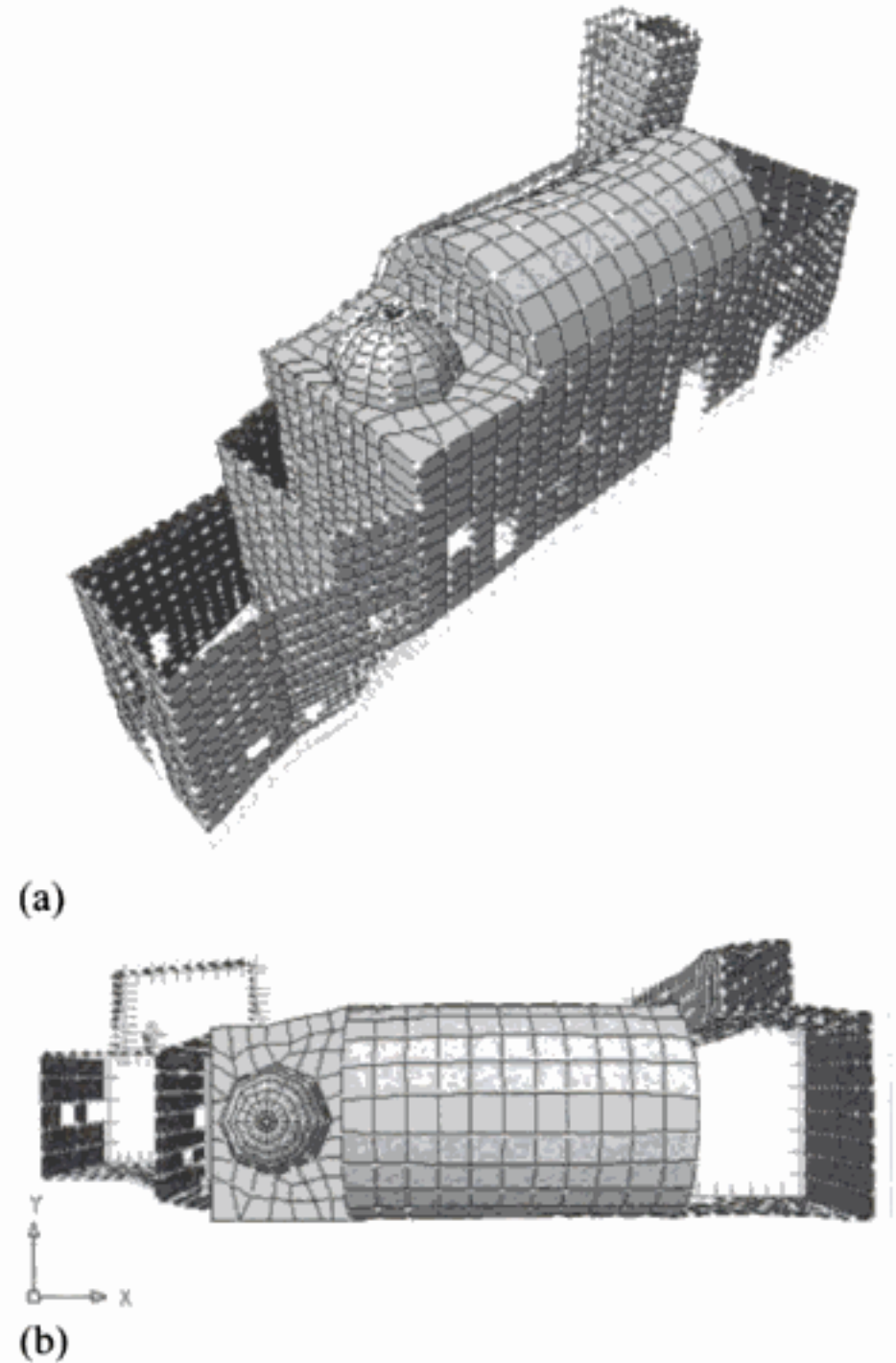


Figure 10. 1st mode shape, with a frequency of 3.3 Hz; (a) 3D view; (b) plan view.

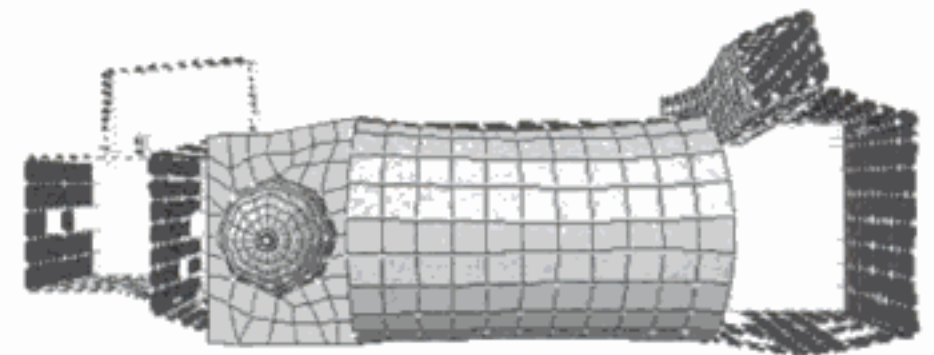


Figure 11. 2nd mode shape, with a frequency of 3.99 Hz.

From the structural point of view, the main concern of the rehabilitation process is the presence of longitudinal cracking along the vault. In order to study this effect, one possibility is the simulation of the crack, by considering a reduction of the modulus of Elasticity in the vertical direction. This hypothesis will be verified experimentally with a new sensors location (see Figure 12).

Procedures to evaluate dynamic behavior, of historical structures, under seismic load are not yet quite well established so any quantitative information on

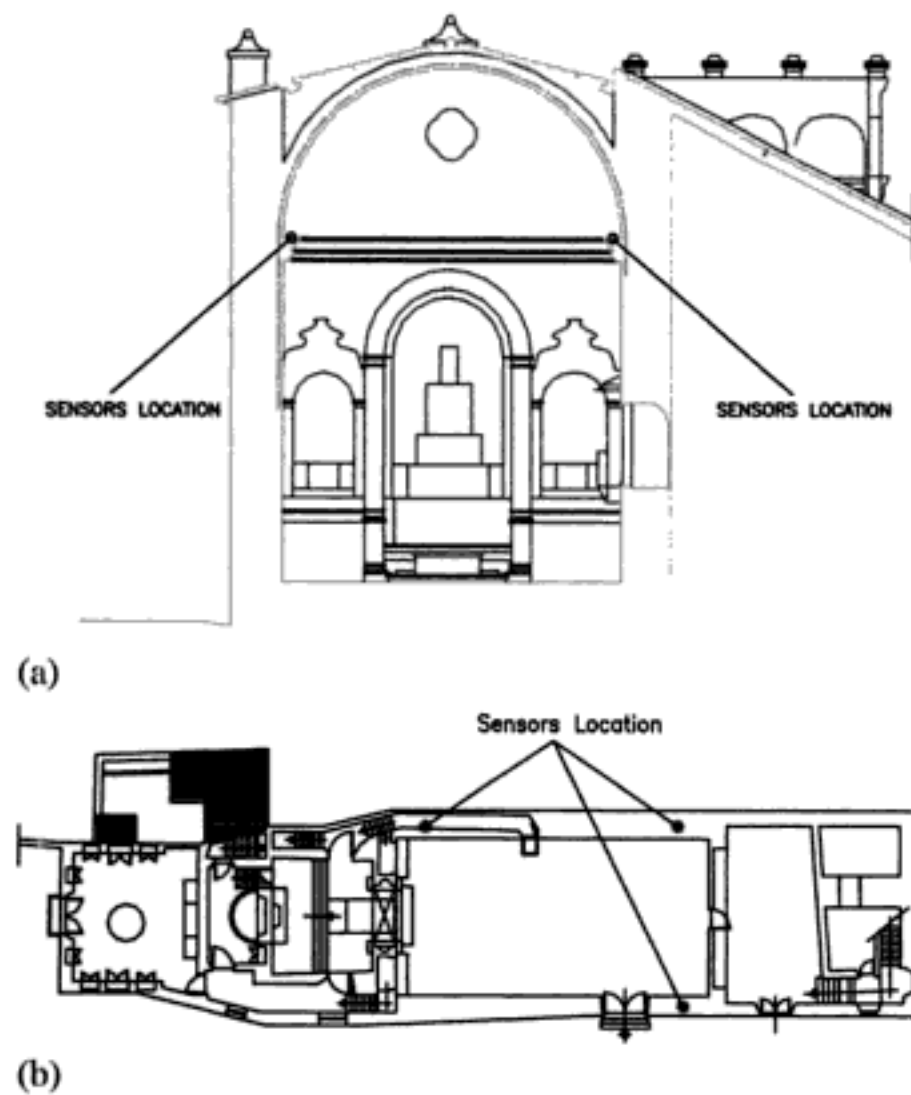


Figure 12. Future sensors location, in order to obtain mode shapes: (a) transversal section; (b) plan section.

their dynamic properties is important to understand and to infer their seismic performance.

6 THE SEISMIC BEHAVIOUR

The damage observation to historical monuments after strong earthquakes has shown that churches are one of the most vulnerable typologies among ancient structures (Lagomarsino and Podestà, 2003a). This is due to the presence of slender walls, wide halls (the nave), vaults of large span, etc.

Learning from the past earthquakes, a methodology has been established for the seismic vulnerability analysis, which is able to forecast the possible collapse mechanisms in churches (Lagomarsino and Podestà, 2003b). However, the method may be used for a risk analysis at territorial level, conducted on all the churches in a Region, in order to obtain a list of vulnerability and decide on the priorities for mitigation strategies.

In the case of a single church, a statistical approach is not suitable and a structural analysis should be performed. To this aim, some simplified approaches can be adopted, which consider the theorems of limit analysis for masonry structures (Lagomarsino et al. 2004).

However, in this case the availability of ambient vibration tests and the possibility of building up a detailed finite element model (thanks to a detailed geometric survey), suggest us to perform a detailed non linear finite element analysis.

In order to evaluate the seismic performance of a masonry structure, identified by ambient vibrations, a proper non linear constitutive model is necessary for the masonry material. The one developed by Lagomarsino and Calderini (2004) will be adopted; it considers the masonry as a composite material, made by blocks and mortar joints, in which various micromechanical failure mechanisms (openings, sliding with friction, crushing, etc.) are homogenized in a continuum damage model, suitable for the finite element procedure.

Pushover static non linear incremental analyses will be performed, in order to evaluate the capacity of the church in terms of total base shear and displacements. The seismic analysis uses the capacity spectrum method (Fajfar, 2000).

ACKNOWLEDGMENTS

The authors wish to thank Instituto Politécnico de Lisboa for financial support of project Caravela (50-2003) and Architect Frederico Paula for his collaboration.

REFERENCES

- Baptista, M.A., Mendes, P., Campos Costa, A., Sousa Oliveira, C., Afilhado, A., Silva, P. 2004. Use of Ambient Vibration Test for Modal Evaluation of a 16 Floor Reinforced Concrete Building In Lisbon, Portugal. *Proc. of 13th World Conference on Earthquake Engineering*, Paper 1985, Vancouver, B.C., Canada, August 1-6.
- Brincker, R., Ventura, C.E., Andersen, P. 2002. Why Output-Only Modal Testing is a Desirable Tool for a Wide Range of Practical Applications. online.
- Computers & Structures Inc. 1998. *SAP 2000 Integrated Finite Element Analysis and Design of Structures*, Berkeley, California, USA.
- Fajfar, P. 2000. A Nonlinear Analysis Method for Performance-Based Seismic Design. *Earthquake Spectra*, 16 (3), pp. 573-592.
- Ferreira, P., Proença, JMFM 2001. Identificação Modal do Corpo 4 do Hospital de Santa Maria, em Lisboa. Inferência da Vulnerabilidade Sísmica., *SÍSMICA 2001 - 5º Encontro Nacional de Sismologia e Engenharia Sísmica*, Açores, 2001, pp. 381-393.
- Lagomarsino, S., Calderini, C. 2004. A Micromechanical Damage Model for Complex Masonry Structures. *Proc. 13th International Brick and Block Masonry Conference*, Amsterdam, July 4-7, pp. 1195-1204.
- Lagomarsino, S., Podestà, S. 2004(a). Seismic vulnerability of ancient churches: I. Damage assessment and emergency planning. *Earthquake Spectra*, 20 (2), pp. 377-394.
- Lagomarsino, S., Podestà, S. 2004(b). Seismic vulnerability of ancient churches: II. Statistical analysis of surveyed data and methods for risk analysis. *Earthquake Spectra*, 20 (2), pp. 395-412.

- Lagomarsino, S., Podestà, S., Resemini, S. 2004. Observational and mechanical models for the vulnerability assessment of monumental buildings. *Proc. of the 13th World Conference on Earthquake Engineering*, Paper 942, Vancouver, B.C., Canada, August 1–6.
- Lourenço, P.B. 2001. Analysis of historical constructions: From thrust-lines to advanced simulations. *Historical Constructions, possibilities of numerical and experimental techniques*, Guimarães, pp. 91–116.
- Shelley, E.O., Ordaz, M., Singh, S.K., Lemo, J. 2000. Estimation of Seismic Hazard to Rehabilitate the Temple of La Compañia in Puebla, Mexico. *Proc. Int. Millennium Congress – Archi 2000, Unesco*.
- SVBs, 2002. *Structural Vibration Solutions ApS: ARTeMIS Extractor, Release 3.2, User's Manual*. Denmark.
- Ventura, C.E., Schuster, N.D. 1996. Structural dynamic properties of a reinforced concrete high-rise building during construction. *Canadian Journal of Civil Engineering*, 950–972.
- Ventura, C.E., Brincker, R., Dascotte, E., Andersen, P. 2001. FEM Updating of the Heritage Court Building Structure. *Proc. 19th Int. Modal Analysis Conference (IMAC), Florida, USA*, pp. 324–330.

notable structural and metallurgical non-homogeneity. Inner oxidization, inclusions, cavities and a substantial fragile behavior were put in evidence whereas, the average composition looked like that of a C30 steel.

Moreover, average Young modulus was evaluated so as to enable the vibration tests to yield accurate estimates of the tensile forces acting in the remaining tie beams. In fact, vibration tests (using impact hammer) on the old three tie beams were able to exclude any possible overloading due to the sudden fracture and to give a reference value of the tensile force the new tie beam was to be given. In fact, the three tie beams, n. 2, 3, 4 in Figure 2, showed tensile forces of 86, 90, 81 kN respectively. Finally, resort was made to the magnetostriction technique (based on Magnetic Barkhausen Effect) to verify if this relatively new method can be profitably applied to the evaluation of stress states in historical metals.

As a matter of fact, the method needs to be calibrated by working on an unstressed similar material and, this was the case for the old (broken) tie beam.

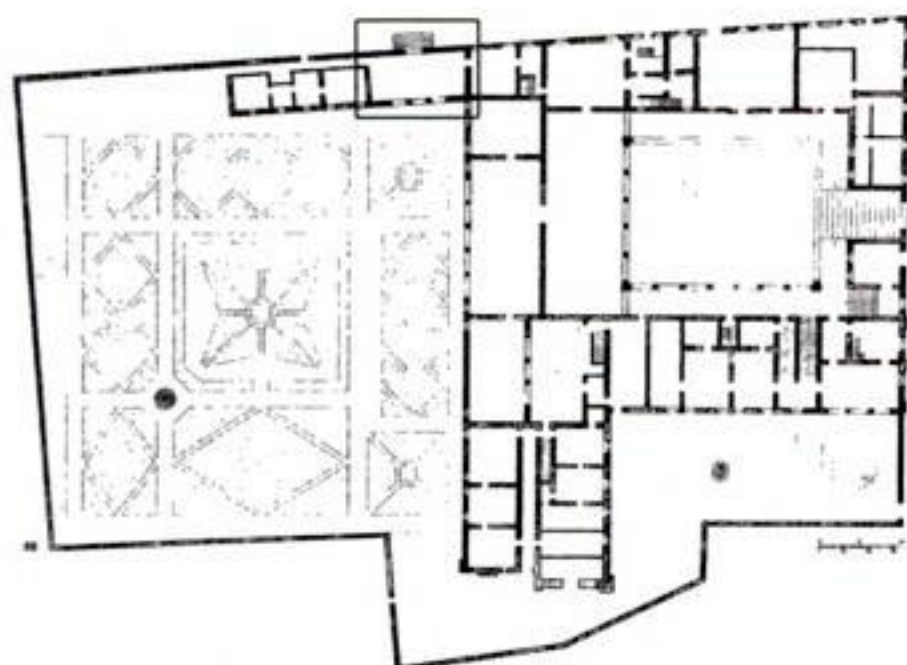


Figure 1. Plan of Museum of Spina showing the pavilion vault arcade under investigation.

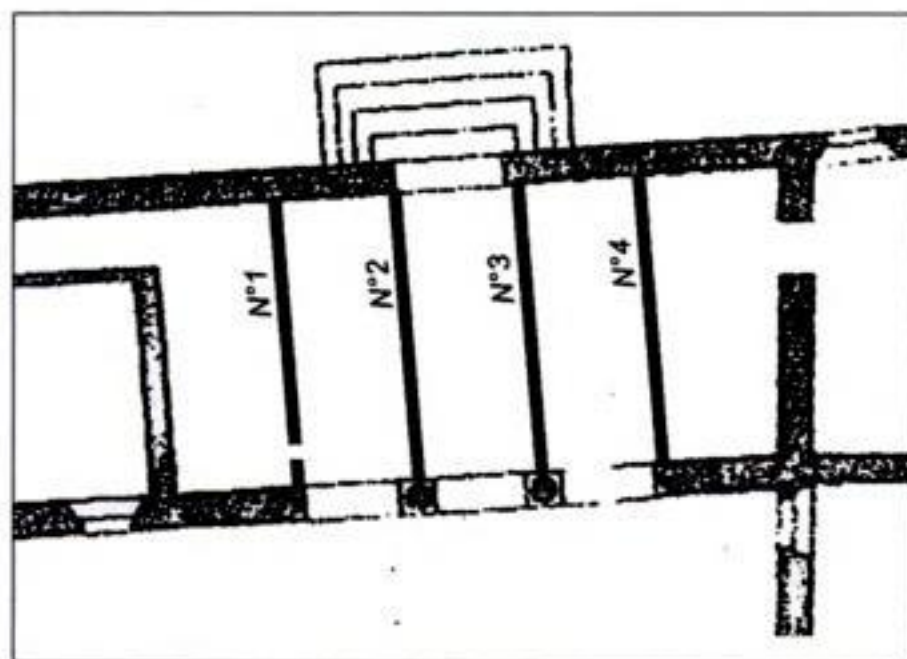


Figure 2. Plan of the pavilion vault arcade showing the four tie beams.

Finally, at the end of the year 2003, it was decided to insert, in the place of the old tie-beam, a drawn steel rod with threaded ends, to be anchored by means of ribbed plates. In turn, the plates were built into the masonry (subjected to a proper consolidation) and, working at the two extremities, a tensile force of 90 kN was imposed by means of a dynamometric wrench.

The vibration tests, as well as the magnetostriction technique confirmed the value of the force imposed to the new tie beam; yet, the analogous vibration test, repeated thirty days later at a similar temperature level, revealed a reduction of the tensile force more than 50% whereas the adjacent tie beam showed a reduction of 5 kN. Apparently, the masonry had recovered part of the suffered distortions causing a notable reduction of the anchoring force in the new tie beam. Hence, supplementary vibration tests were planned to monitor the future behavior.



Figure 3. Image of the pavilion vault arcade under investigation.



Figure 4. Image of the tie beams n. 2, 3, 4.

2 METALLURGICAL TESTS

The old tie beam was subdivided into 5 main segments from which specimens were obtained (Figure 5) to perform metallurgical and mechanical tests.

For tensile tests, two distinct zones were chosen, i.e.: segment 4 (with fewer internal defects) and segment 2, which presented the highest number of defects and was close to the fracture point. Moreover, segment 2A was used for chemical and metallographic analyses, segment 3A was used for hardness tests and segment 5A was used for hardness and metallographic tests. Finally, segments 1 and 5 were used for the evaluation of Young elastic modulus.

2.1 X-rays and microscopic tests

X-rays showed the main defects due to forging process, i.e.: extensive longitudinal cracks with more or less accentuated transversal ramifications with openings growing from the core to the surface (Figure 6).

The heads of the fracture (Figure 7) showed that there had been no significant reduction of area, and no development of plastic deformation.

Observation through electronic microscope showed that the surfaces were diffusely corroded. There was a significant external area showing the morphology of a cleavage fracture, a type of low energy fracture quite different from discontinuous yielding that shows evident plastic deformation spreading along well defined crystallographic planes. The cleavage fracture had the particular form of the "river" pattern, (Figure 8) slightly 'polluted' by the products of corrosion. The

fracture had a crystalline appearance with a characteristic shine that covers areas over one half of the circular sector.

2.2 Chemical analysis

First of all, sample 2A was analysed by optical emission spectrometer. In Table 1, the resulting chemical composition is shown. As is known, the method may find it difficult to yield reliable results in terms of carbon and sulphur; hence, the same sample was subjected to chemical analysis for combustion using a



Figure 7. Details of heads of fracture: sample 3A on the left, and sample 2A on the right.

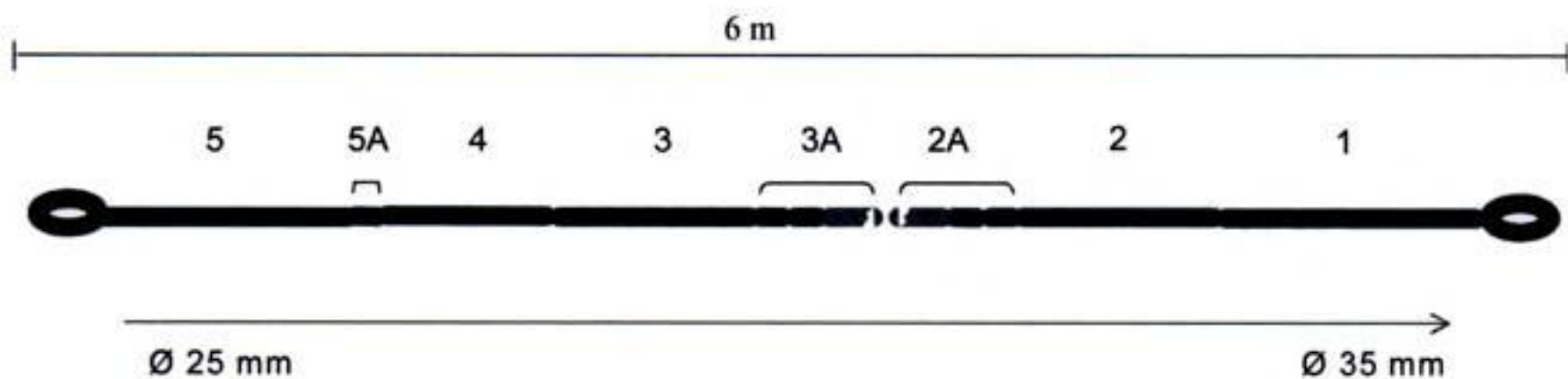


Figure 5. Segmentation of the old tie beam for the experimental analyses.



Figure 6. Detail of positive x-ray with transversal cracks on segment 5.

high frequency induction oven and IR sensors (Table 2). The chemical composition suggested to assimilate the material under investigation to a C30 type steel.

2.3 Metallographic tests

Optical microscope analysis was also necessary to observe inclusions and microstructure subject to chemical attacks: useful information for an explanation of the “thermal history” of the sample. A lot of inclusions was found in the centre of the samples, with gray stripes of two different tones, which, in morphological terms, suggest aluminates or silicates (confirmation was obtained using electronic microprobe (EDS)). Following metallographic attack with Nital 2%, several different microstructures were found confirming a high heterogeneity level: a ferritic type structure with limited perlitic areas in the joints of the ferritic granules; a very compact perlitic structure, a ferritic, bainitic and perlitic structures occurring without any evident explanation and some intergranular cracks, corresponding to austenitic grains. These cracks have rendered the material response even more fragile.

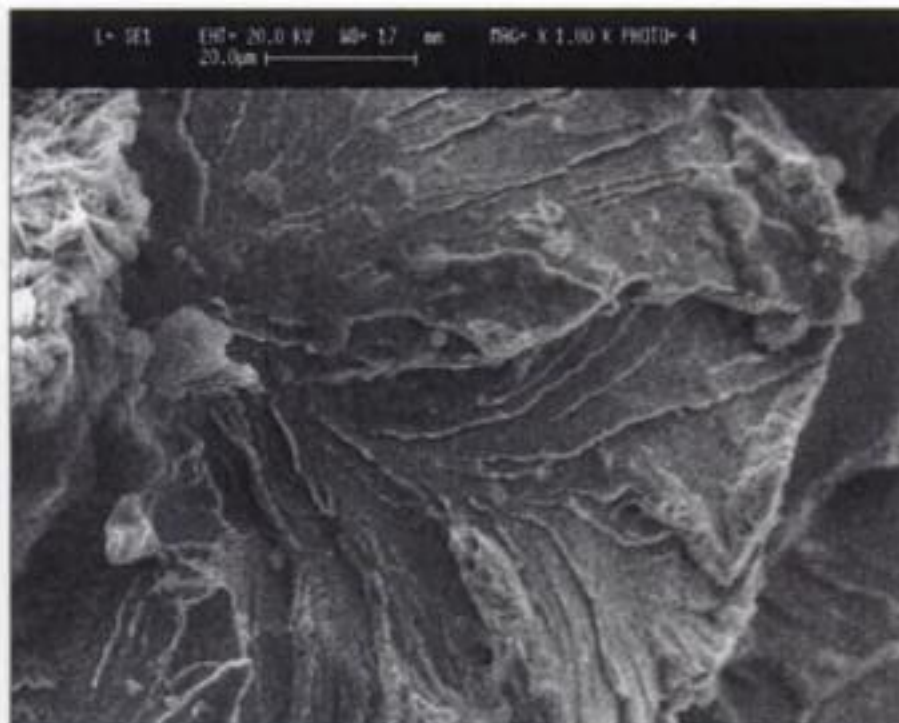


Figure 8. “River Pattern” of a cleavage fracture present in the fracture head 2A.

Table 1. Chemical composition of sample “2A” obtained using spectrometer with optical emission.

Test	C	Si	Mn	P	S	Cu	Cr	Ni	Al	Mo	V	Ti	W	Pb	Zn
1	15.56	8.03	0.815	0.001	O.R.*	0.568	0.289	0.167	1.546	0.807	0.316	0.313	1.498	2.235	2.456
2	0.692	0.278	0.148	0.001	O.R.	0.017	0.005	0.006	0.043	0.142	0.005	0.007	0.029	0.048	0.048
3	8.950	1.995	0.458	0.002	O.R.	0.275	0.150	0.085	0.606	0.395	0.159	0.146	0.760	1.202	1.260
4	25.41	6.677	1.211	0.001	O.R.	0.656	0.324	0.178	1.399	0.970	0.367	0.380	1.574	2.495	2.542
5	10.86	13.84	1.988	0.003	O.R.	0.122	0.069	0.034	0.521	0.179	0.088	0.078	0.289	0.859	0.641
6	0.177	0.507	0.144	0.001	O.R.	0.146	0.079	0.007	0.082	0.008	0.008	0.010	0.038	0.100	0.081

* O.R.: out of range.

3 MECHANICAL TESTS

3.1 Hardness tests

Hardness tests showed surface values approximately twice as those evaluated in the central area. In section 3A (next to the fracture, Figure 9) values were found higher than in 5A. The average Vickers hardness values for two test point lines were almost identical (135 and 137 HV10). A peak of hardness of 213 HV10 in section 3A could indicate a greater fragility induced by the forging process. It should be emphasized that the average diameter in section 5 is smaller than those of sections 2 and 3.

3.2 Tensile tests

Two cylindrical specimens, obtained from segment 4 (far from the head of the fracture, with few inner defects) and from segment 2 (close to the fracture, with high defect density), were subjected to a tensile test. The results confirmed the fragile behavior suggested by metallurgical tests. Figure 10 shows the stress-strain curve for the specimen obtained from segment 4.

3.3 Young modulus test

The Young modulus test was carried out on two different specimens obtained by segments marked 1 and 5. It was performed using two different systems for strain acquisition: one mechanical strain gauge (M in Figure 11a) and three electrical strain gauges (E1, E2, E3 in Figure 11a). The electrical gauge gives a localized value of the strain whereas the mechanical gauge refers the extension to a fifty millimeters base. Actually, two

Table 2. Carbon/Sulphur analysis using combustion method (LECO instruments).

Elements	Analysis 1	Analysis 2	Analysis 3	Average value
C	0.284	0.324	0.307	0.305
S	0.0066	0.0062	0.0063	0.0064

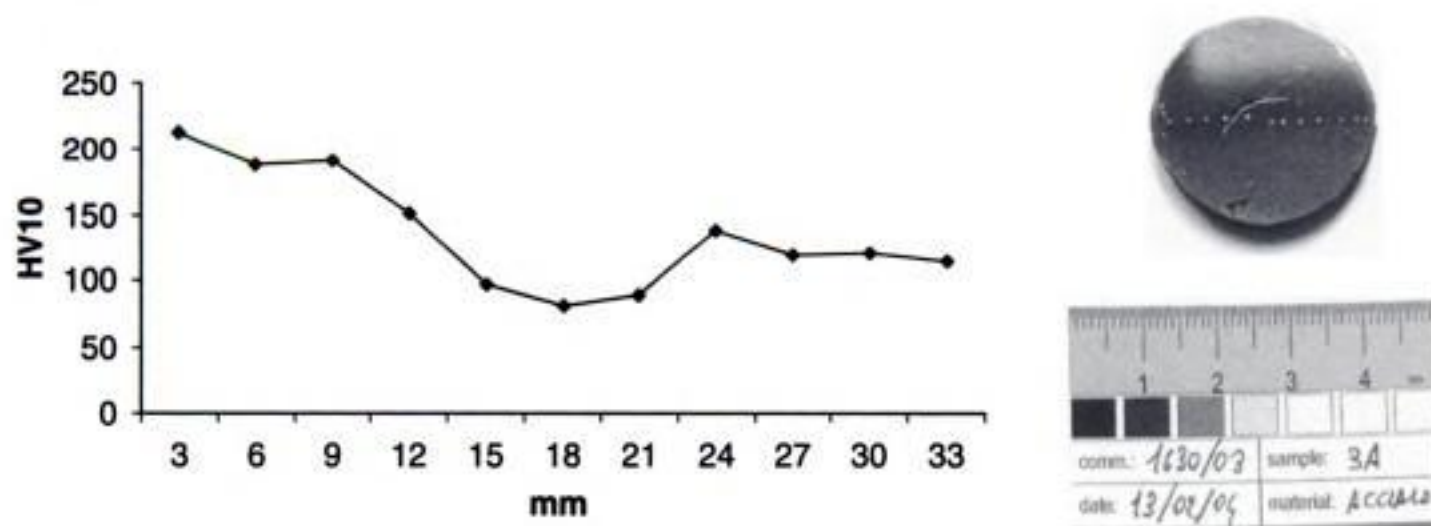


Figure 9. HV10 hardness test point lines along the diameter of sample 3A (near the fracture head).

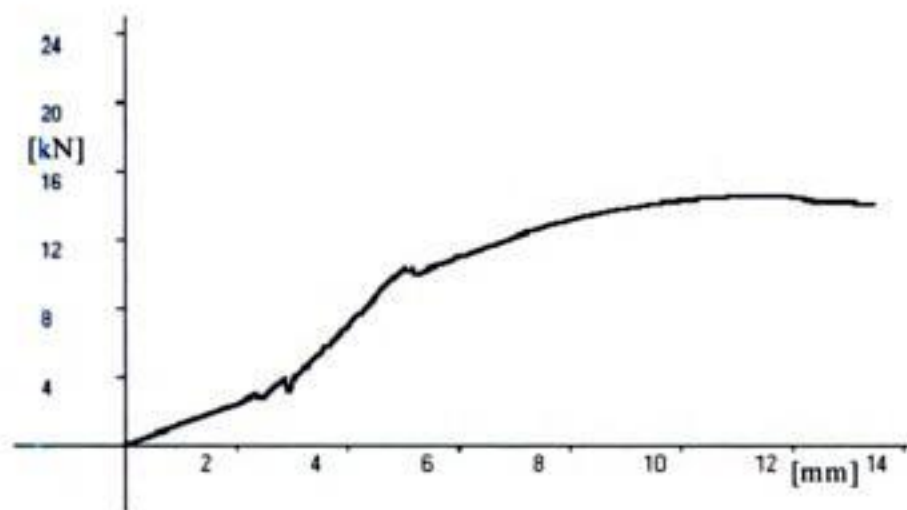


Figure 10. Stress-strain curve (Diameter = 6.35 mm, Area = 31.67 mm²; Maximum load = 14.49 kN; Yield stress = 322.39 N/mm², Tensile strength R_m = 457 N/mm²).

displacement transducers, working on a 340 mm base, were also adopted to verify that local and average values were not in conflict. The stress-strain diagrams were plotted up to 150 kN of the axial force value. The four records for specimen 1 are reported in figure 11b whereas Table 3 summarizes the main results for both the specimens.

4 VIBRATION ANALYSIS

Static and dynamical methods have been proposed aimed at determining tensile forces acting in tie-beams of masonry arches or vaults and, in general, dynamic methods require lesser experimental effort. In fact they need the response of few accelerometers rigidly connected to the beam under investigation when it vibrates due to a given perturbation. Some formulations (Livingston et al. 1995, Calderini & Lagomarsino 2003) work on vibration frequencies only and the evaluation of the tensile force has resort to a proper error function, whereas other formulations make use of both static deflections and vibration frequencies (Blasi & Sorace 1994).

4.1 Theoretical background

In the present case, for the vibration analysis, a method recently proposed (Tullini & Laudiero 2003, Tullini & Laudiero 2004) was adopted which gives both the tensile force acting in the tie-beam and the rotational stiffness of the constraints offered by the side walls. To this purpose, three accelerometers are required to know a vibration frequency ω and three amplitudes v_1, v_2, v_3 of the corresponding modal shape. As is known, the equation governing the vibrations of Euler-Bernoulli beam of length L and uniform cross section, subjected to end rotational constraints of stiffness k_0 e k_1 , and to an axial force N can be written as (Graff 1975):

$$v''''(x) - n v''(x) - \lambda^4 v(x) = 0 \quad 0 < x < 1, \quad (1)$$

subjected to the boundary conditions, where

$$n = \frac{NL^2}{EJ}, \quad \lambda^4 = \omega^2 \frac{\mu L^4}{EJ}, \quad \beta_0 = \frac{k_0 L}{EJ}, \quad \beta_1 = \frac{k_1 L}{EJ},$$

$$x = \frac{X}{L}, \quad (2)$$

E, μ and J represent Young modulus, linear density and cross section inertia moment respectively and, finally, the positive sign of N corresponds to traction. The solution to equation (1) is:

$$v(x) = C_1 \cos q_1 x + C_2 \sin q_1 x + C_3 \cosh q_2 x + C_4 \sinh q_2 x \quad (3)$$

with:

$$q_1^2 = \frac{1}{2} (\sqrt{n^2 + 4\lambda^4} - n), \quad q_2^2 = q_1^2 + n \quad (4)$$

where q_1 is determined by the frequency characteristic equation and the boundary conditions yield constants C_1-C_4 . When the accelerometers are placed at $L/4$,

composition, high heterogeneity and relatively fragile behaviour of ancient forged tie beams were quite surprising and seem to require a very cautious approach. Laboratory metallurgical tests highlighted these unusual properties and gave basic information necessary to develop strengthening design. Vibration tests had previously been developed in laboratory conditions but (laboratory) mechanical tests gave reference values that enabled the authors to rely on in situ tests as well. Metallurgical tests made possible magnetostriction analysis that requires specific calibration curves for a given material. In spite of more or less refined analyses, masonry has extraordinary resources; in fact, it can undergo a drift of 28 mm between the vault abutments without giving rise to appreciable overloading of adjacent tie beams and without showing significant sufferings. At the same time, it can recover part of the suffered distortions and change the value tensile forces acting in tie beams, perhaps cyclically, according to season conditions.

ACKNOWLEDGEMENTS

The authors would like to acknowledge the respective contributions. G. Mezzadri was in charge for the strengthening design. Elletipi (Laboratory) S.r.l. in Ferrara developed chemical, metallurgical and mechanical tests. Department of Ingegneria of University of Ferrara was responsible for the vibration analyses. Studio V.M. in Ferrara developed magnetostriction tests.

REFERENCES

Blasi, C. & Sorace, S. 1994. Determining the axial force in metallic rods. *Structural Engineering International*, Vol. 4(4), 241–246.

- Calderoni, C. & Lagomarsino, S. 2003. Una metodologia diagnostica per l'identificazione dinamica del tiro nelle catene metalliche antiche. Atti del XVI Congresso AIMETA di Meccanica Teorica e Applicata. Ferrara, 9–12 September 2003, CD-ROM.
- Di Francesco, C., Fabbri, R. & Bevilacqua, F. *Atlante degli elementi costruttivi tradizionali nell'architettura ferrarese*, (Motta Editore), Milano, in printing.
- Ewins, D.J. 1984. *Modal Testing: Theory and Practice*. John Wiley & Son, New York.
- Graff, K.F. 1975. *Wave motion in elastic solids*. Clarendon Press, Oxford.
- Grandis, D., Mezzadri, G. & Strozzi, S. 2001. Analisi dei livelli di rischio strutturale nell'edilizia storica. Atti del Convegno *Crolli e Affidabilità delle Strutture Civili*. Venezia, 6–7 December 2001.
- Jiles, D. 1991. *Introduction to magnetism and magnetic materials*. Chapman & Hall, New York.
- Lagomarsino, S. 2001. *Sicurezza e conservazione delle chiese in zona sismica in Modelli Chiese*. DISEG, HTML Document: <http://adic.diseg.unige.it/Marche/Marche.htm>.
- Livingston, T., Béliveau, J.G. & Huston, D.R. 1995. Estimation of axial load in prismatic members using flexural vibrations. *Journal of Sound and Vibration*, Vol. 179 (5), 899–908.
- Tullini, N. & Laudiero, F. 2003. Valutazione dello sforzo normale in travi prismatiche tramite parametri modali flessionali. Atti del XVI Congresso AIMETA di Meccanica Teorica e Applicata. Ferrara, 9–12 September 2003, CD-ROM.
- Tullini, N. & Laudiero, F. 2004. Valutazione sperimentale del tiro nelle catene mediante prove dinamiche. Atti del XI Congresso Nazionale "L'Ingegneria Sismica in Italia". Genova 25–29 January 2004, CD-ROM.

Dynamic identification and model updating of historical buildings. State-of-the-art review

J.C. Araiza Garaygordóbil

Civil engineering school, University of Colima, Mexico

ABSTRACT: Nowadays, structural design and analysis are commonly performed with the finite element (FE) method. A FE model simulates the physical behavior of the structure and can be used to predict the responses under a different combination of loads and assess the structural integrity. However, even with the great advances in the field of structural modeling, an initial FE model is often a poor representation of the actual structure – particularly in the field of ancient structures, because of a high number of simplifying assumptions that depend on engineering judgment. This participation pretends to give the reader an overview of the state-of-the-art on dynamic identification of historical buildings. The document includes a resume of: previous literature reviews, the excitation techniques, the measurement equipments and finally several references of the application of dynamic testing on ancient structures developed during the last few years.

1 INTRODUCTION

The interest in the ability to monitor a structure and detect damage at the earliest possible stage exists not only on ancient-structures engineering but also throughout the civil, mechanical and aerospace engineering communities. Vibration-based damage detection relies upon the fact that a local stiffness change affects the global dynamic characteristics of the structure. In the static variant, displacements (instead of accelerations) are measured while a static load is applied to the structure. The main advantage of this method is that measurements at one location are sufficient to assess the condition of the whole structure. The measurement location may differ from the location of the damage. This participation contains a review of the technical literature concerning the detection, location, and characterization of structural damage in bridges via techniques that examine changes in measured structural vibration response.

Ideally, a robust damage detection scheme will be able to identify that damage has occurred at a very early stage, locate the damage within the sensor resolution being used, provide some estimate of the severity of the damage, and predict the remaining useful life of the structure. The method should also be well-suited to automation. To the greatest extent possible, the method should not rely on the engineering judgment of the user or on an analytical model of the structure. A less ambitious, but more attainable, goal would be to develop a method that has the features listed above, but that

uses an initial measurement of an undamaged structure as the baseline for future comparisons of measured response.

2 PREVIOUS STATE-OF-THE-ART AND LITERATURE REVIEWS

The promising perspective of vibration-based health monitoring inspired many researchers all over the world. A detailed survey of the technical literature and interviews of selected experts to determine the state of the art of the damage-detection field (using modal analysis procedures) was presented by Richardson (1980). The survey focused on structural integrity monitoring for nuclear power plants, large structures, rotating machinery, and offshore platforms, with by far the largest amount of literature associated with rotating machinery. Doebling, et al. surveyed and classified the literature in a rigorous report published by Los Alamos National Laboratory (1996). Several doctoral dissertations that address damage detection and related issues have recently been published. Each dissertation contains a literature survey and a development of the theory relevant to its scope. These dissertations include Casas (1988), Rytter (1993), Hemez (1993), Kaouk (1993), Doebling (1995), Peeters (2000) and Araiza (2003). Mottershead and Friswell (1993) present a survey of the literature related to dynamic finite element model (FEM) updating, which has been used extensively for structural damage detection. Their review

contains a list of references on the topic of model updating. This participation summarizes and compares the work presented by the previously mentioned authors and adds the references generated recently.

3 EXCITATION TECHNIQUES

On the field of ancient structures, the process of dynamic identification has not been widely studied, however, different authors have compared and classified the sources of excitation for dynamic testing on bridges. Bridge engineering is perhaps the area in which dynamic testing has suffered the stronger development. Salawu and Williams (1995) provide a review of full-scale dynamic testing of bridges where methods of excitation are examined. Farrar, et al. (1999) summarized the various methods that have been used to excite bridge structures during dynamic testing. Peeters et al. (2000) evaluated the various sources of excitation that have been applied on bridge Z24, in Switzerland. These authors evaluated both forced artificial sources such as shakers and drop weight and ambient, natural sources such as wind and traffic. The exhaustive use of testing in evaluation of bridges has resulted in the American Society of Civil Engineers (ASCE) Committee on Bridge Safety publishing a guide for field testing of bridges in 1980 (ASCE 1980). RILEM committee 20-TSB also proposed a standard for in-situ testing of bridges (1983). Both of the previous documents include details on excitation procedures.

The methods of exciting a bridge for dynamic testing fall into two general categories: (1) Measured-input tests; and (2) Ambient test. In general, tests with measured inputs are conducted on smaller bridges. For larger truss, suspension and cable stayed bridges; ambient tests become the only practical means of exciting the structure (Farrar, et al., 1999).

Methods for determining the modal characteristics (resonant frequencies, mode shapes and modal damping ratios) of structures subjected to measured inputs are well established, particularly when the input forcing function is well characterized. In the measured-input excitation testing of bridges, a wide variety of forcing techniques are used including various types of shakers, step relaxation, and various methods of measured impact. The methods of measured input excitation are summarized on detail in Farrar, et al. (1999).

Ambient excitation is defined as the excitation experienced by the structure under its normal operating conditions. All bridges are subjected to ambient excitation from sources as traffic, wind or seismic actions. This type of excitation has been largely used for both small and large bridge structures. Normally, ambient excitation cannot be measured during the test. For larger bridge structures, this is the only practical

means of exciting the structure. Ambient excitation is also used with smaller bridges when other constraints prevent the bridge from being taken out of service during the test (Farrar, et al., 1999). Casas (1995) reported the results of ambient vibration test on several bridges. Ambient vibration was measured under traffic conditions.

4 MEASUREMENT EQUIPMENT

The data acquisition portion of the structural health monitoring process involves selecting the types of sensors to be used, selecting the location where the sensors should be placed, determining the number of sensors to be used, and defining the data acquisition and storage hardware. Economic considerations play a major role in these decisions. Another consideration is how often the data should be collected. In some cases it is adequate to collect data immediately before and at periodic intervals after a severe event.

Data acquisition issues for bridge applications include the sensor type and the number of sensors, sensor location, sensor mounting, environmental effects on the sensors, signals recording, and record duration. Averaging, windowing and similar data processing parameters must also be determined. Another issue is determining the steps that could be taken to make the data acquisition as repeatable as possible.

The primary sensors used for bridge health monitoring are piezoelectric accelerometers. Force-balance accelerometers, electric resistance and vibrating-wire strain gages are also widely used. More recently, fiber-optic sensors utilizing Bragg grating (Todd, et al., 1999) have been studied as a means of increasing channel counts for bridge monitoring in a cost-effective manner. In addition to the motion measuring devices, anemometers and temperature sensors such as thermocouples are used to characterize the environmental variability. Data transmission and recording are done in manners similar to most mechanical vibration applications as summarized in (McConnell, 1995). Recent developments in wireless data acquisition systems have shown promise for large civil engineering structures (Straser, 1998). When ambient excitation sources are used, all channels of data are typically recorded simultaneously. The damage to be monitored and the number of available sensors typically dictate sensor placement.

5 APPLICATIONS OF DYNAMIC TESTING ON STRUCTURES

Although vibration-based structural health monitoring is applicable to a large range of structures, bridges are considered as the first and most important applications. In Europe, most of the bridges are reaching

their critical age and it is expected that the demands for maintenance will peak in 2010. Vibration-based monitoring is certainly a helpful tool in assessing the condition of these bridges and in making maintenance schedules. More recent long-span cable-stayed and suspension bridges are equipped with an embedded monitoring system consisting of sensors such as: accelerometers, potentiometers, displacement transducers, inclinometers, strain gauges, or temperature sensors. Examples of instrumented bridges exist all over the world. As reported in Farrar (1999), one of the best-equipped bridges is probably the Tsing Ma Bridge in Hong Kong. The bridge was built in 1997, has a main span of 1377 m and is monitored by nearly 600 sensors. Available literature give examples of bridge monitoring not only for damage detection, but also for different applications such as: quality control during the construction; model updating; warning system for traffic closure when the bridge is subjected to excessive wind loading; or condition assessment about its serviceability and ultimate limit state.

At present, bridges are generally rated and monitored during biennial inspections, largely with the use of visual inspection techniques. There is the possibility that damage could go undetected at inspection or that cracks in load-carrying members could grow to critical levels between inspection intervals (Gorlov, 1984). Since 1979, numerous studies involving the development and application of damage detection techniques for bridge structures have been reported. Kato and Shimada (1986) perform vibration measurements on an existing prestressed concrete bridge during a failure test. Salane, et al. (1981) used changes in the dynamic properties of a three-span highway bridge during a fatigue test as a possible means of detecting structural deterioration resulting from fatigue cracks in the bridge girders. Turner and Pretlove (1988) perform a numerical vibration analysis on a simple beam representation of a bridge subjected to random traffic loading. Biswas, et al. (1990) discuss the state of degradation of bridges in the US. Spyarakos, et al. (1990) performed a series of experiments on a set of beams designed to have dynamic responses similar to actual bridges. Mazurek and DeWolf (1990) present strong arguments in favor of a continuous automated vibration monitoring system for highway bridges, citing several unexpected collapses and near collapses of bridges. Tang and Leu (1991) performed experiments on a defective prestressed concrete girder bridge. They found that mode shape changes might be a more effective indicator of damage in bridges than frequency shifts. Law, et al. (1992) performed vibration tests on a one-fifth-scale model of a reinforced concrete beam-slab bridge deck. The model had five pre-cast main beams connected transversely by five diaphragms. The model was statically loaded incrementally to failure.

Raghavendrachar and Aktan (1992) performed impact tests on a three-span reinforced concrete bridge with a goal of detecting local or obscure damage, as opposed to severe, global damage. The authors concluded that modal parameters may not be reliable as damage indicators if only the first few modes are measured. An extensive survey and analysis of structural damage detection has been completed by Kim and Stubbs (1993). The authors assessed the relative impact of model uncertainty on the accuracy of nondestructive damage detection in structures. Aktan, et al. (1994) assess the reliability of modal flexibility as an indicator of bridge condition by comparing the measured flexibility to the flexibility obtained using a static-load truck test. In Biswas, et al. (1994) the authors study crack detection in a scale model of a bridge structure.

Farrar, et al. (1994) presented the results of a damage-detection experiment performed on the I40 bridge over the Rio Grande river in Albuquerque, NM. This bridge was designed so that the two main plate girders carry all the loads of the bridge. Samman and Biswas (1994) tested a scale model bridge consisting of a concrete slab bonded to three steel girders. Toksoy and Aktan (1994) use the measured flexibility matrix to assign a condition index to a bridge. By comparing cross-sectional deflection profiles from the flexibility matrices, they are able to detect structural damage and anomalies. Alampalli, et al. (1995) repeatedly tested a single span, steel girder bridge with an integral concrete deck in an undamaged condition to examine the variability in resonant frequencies, modal damping, and mode shape data caused by random test variations and environmental effects. Farrar and Cone (1995) present further analysis of the I40 bridge damage detection data set described by Farrar, et al. (1994). They identify the modal properties from the ambient test, when the bridge was undamaged, and from the forced-excitation tests for each of the damage cases. James, et al. (1995) presented the results of two damage-location techniques applied to the body of data from the I40 bridge damage detection test described by Farrar, et al. (1994). Liang, et al. (1995) apply their ETR damage-identification method to data obtained on the steel Peace Bridge over the Niagara River near Buffalo, NY.

Kou and De Wolf (1997) studied the influencing variables for the behavior of a continuous span highway bridge. Chin-Hsiung, et al. (1997) assessed a five-span continuous bridge using ground motion. Huang, et al. (1999) conducted free vibration tests on highway bridges, exciting the structures with a loaded truck. Paultre, et al. (2000) developed a series of dynamic tests to evaluate the dynamic properties and the dynamic amplification factor in a rehabilitated bridge.

On the field of ancient structures, the literature is not so wide. However, significant developments

have been identified. Ellis (1998) developed some non-destructive test, which was used to evaluate the integrity of 534 stone pinnacles of the Palace of Westminster in London. The objective of the test was to measure the fundamental natural frequency of the individual pinnacles so that the frequency of each pinnacle could be compared with the frequencies of similar pinnacles, thereby identifying any pinnacle, which was significantly different from the norm. Two types of test were established: an impact test for the smaller pinnacles, which involved attaching a transducer to a pinnacle; and a laser test for the larger pinnacles, which involved monitoring their ambient (wind) response.

Genovese and Vestroni (1998) developed experimental investigations of an old masonry building taking in account its non-linear behavior. Frequency response functions from small amplitude forced oscillations were used as experimental data to identify modal parameters. They found that the response is sensitive to the characteristics of the excitation and that the evolution of the dynamic behavior of the structure subjected to increasing levels of force is characterized by the decrease of the modal stiffness.

Koh, et al. (1995) apply a condensation method for local damage detection of multistory frame buildings to a numerical simulation of a 12-story plane-frame structure and a 6-story steel frame structure. Damage, ranging from 10% to 45.6% reductions in the story stiffness, was successfully identified without false indications in the undamaged floors. The method was found to be insensitive to reasonable assumed damping values for the structures.

Dynamic evaluation technique was used to assess the mechanical behavior with the objective of redesign and rehabilitate panel buildings in Prague (Gattermayerova and Bayer, 1998). Stress and strains were also determined by means of dynamic test in the base of a eight-storey panel building.

Forced vibration test carried out on an old masonry house using a vibrodyne and on a 1:5 scale model in laboratory were presented in 1996 (Vestroni, et al.). On this research project, professor Vestroni and his co-workers induced in a first step small amplitude oscillation to determine the dynamic characteristics of the structure. The evolution after large amplitude oscillations furnishes a correlation between modal quantities and structural damage. The found forced vibration test as a very effective tool for an understanding of the dynamic behavior of masonry buildings. The role of identification techniques in processing experimental data is shown to be fundamental to a correct interpretation of test results and to extend their meaning beyond the studied cases.

Some examples of dynamic testing of historical masonry constructions are presented by Sigmund and Herman (1998). Different sources of excitation are compared in this paper. Dynamic data is used to setup

numerical models and to simulate extreme loading conditions. The authors conclude that dynamic testing can be a valuable tool on model updating of ancient structures.

Ambient vibration tests have a number of features, which make them particularly attractive over other methods. A study of the use of ambient vibration for evaluation of masonry buildings was presented by Slastan and Foissner (1995). The authors developed different experiment in high and low-rise masonry buildings. The use of dynamic testing under ambient vibration was found helpful in the model updating process.

Bensalem, et al. (1995) developed experiments on a laboratory brickwork bridge under dynamic excitation and measurements. The proposed method was used to characterize dynamic behavior of masonry bridges. A linear dynamic finite element model was also developed to predict the arch's behavior at each load step. Not only hammer excitation but also mass shakers were used on the test. The hammer was found superior to the steady state or shaker methods.

Roca and Molins (1997) applied dynamic testing on the inspection of three different masonry bridges in Spain. The analysis of experimental data and its comparison with numerical simulations were used to adjust the proposed numerical model. The models were used afterwards to estimate the ultimate capacity of the structure. The authors conclude that dynamic testing can be successfully used as an inspection tool on the masonry bridges presented.

6 CONCLUSIONS

There are three necessary components for the success of a dynamic test in an ancient structure: Pre-define of the objectives of the test; all test's details must carefully organized; and finally, the results must be presented in a manful fashion. From the authors' own experience, it can be extracted that redundancy in instrumentation is always helpful and that best instrumentation give the best ratio between accuracy and cost.

To summarize, it appears that over the past 15 years there has been repeated application of modal properties of ancient structures to the fields of damage detection and structural monitoring. The work has been motivated basically by several catastrophic failures in one hand, and by dramatic reduction of equipment's costs, in the other. Earlier work utilized primarily modal frequency changes to detect damage, but more recent work has shown that frequency changes are insufficient. Changes in mode shapes are more sensitive indicators and might be more useful for detection of the defect location. Damping changes have not generally been found to be useful for damage detection in bridges or historical buildings. Finally, is worth

considering some other methods of computing damage from modal properties that are being developed, such as dynamic flexibility measuring; strain mode shapes changes or neural network-based methods.

REFERENCES

- Aktan, A.E., K.L. Lee, C. Chuntavan, and T. Aksel, 1994. Modal Testing for Structural Identification and Condition Assessment of Constructed Facilities. Proc. of 12th International Modal Analysis Conference, 462–468.
- Alampalli, S., G. Fu, and E.W. Dillon, 1995. On the Use of Measured Vibration for Detecting Bridge Damage. Proc. Fourth International Bridge Engineering Conference, 125–137.
- American Society of Civil Engineers Committee on Bridge Safety, 1980. A Guide For Field Testing of Bridges, New York.
- Araiza, J.C. 2003. Dynamic assessment of structural building components; Ph.D. Thesis, Department of Construction Engineering, Technical University of Catalonia (UPC), ISBN: 84-688-1937-9. DL: B-24073-2003. Spain. February 2003.
- Bensalem, A., C., Fairfield, and A. Sibbald, 1995. Non-destructive testing for arch bridge assessment, Proceedings of the First International Conference on Arch Bridges, Bolton, UK. 3–6 September.
- Biswas, M., A. Pandey, and S. Bluni, 1994. Modified Chain-Code Computer Vision Techniques for Interrogation of Vibration Signatures for Structural Fault Detection. Journal of Sound and Vibration, 175(1), 89–104.
- Casas, J.R. 1995. Dynamic Modeling of Bridges: Observations from Field Testing. Transportation Research Record, 1476.
- Casas, J.R. 1988. El estudio de la respuesta dinámica como método de inspección y control de tableros de puentes de hormigón armado y pretensado. Ph.D. dissertation. Technical University of Catalunya, Spain.
- Chin-Hsiung Loh, and Zheng-Kuan Lee 1997. Seismic monitoring of a bridge: assessing dynamic characteristics from both weak and strong ground excitations. Earthquake Engineering & Structural Dynamics 26, 269–288.
- Doebling S.W., C.R. Farrar, M.B. Prime, and D.W. Shevitz 1996. Damage Identification and Health Monitoring of Structural and Mechanical Systems From Changes in Their Vibration Characteristics: a Literature Review. Research report LA-13070-MS, ESA-EA Los Alamos National Laboratory, Los Alamos, NM, USA.
- Doebling, S.W., 1995. Measurement of Structural Flexibility Matrices for Experiments with Incomplete Reciprocity, Ph. D. Dissertation, University of Colorado, Boulder, CO, Department of Aerospace Engineering Sciences, CU-CAS-95-10.
- Ellis, B.R. 1998. Non Destructive dynamic testing of stone pinnacles of the palace of Westminster. Proceedings of the institution of Civil Engineers, Structures and Buildings UK.
- Farrar, C., A. Duffey, P. Cornwell, and S. Doebling, 1999. Excitation methods for bridge structures, Proceedings of International Modal Analysis Conference, Kissimmee, FL, Feb.
- Farrar, C.R., W.E. Baker, T.M. Bell, K.M. Cone, T.W. Darling, T.A. Duffey, A. Eklund, and A. Migliori, 1994. Dynamic Characterization and Damage Detection in the I-40 Bridge Over the Rio Grande, Los Alamos National Laboratory report LA-12767-MS.
- Gorlov, A.M., 1984. Disaster of the I-95 Mianus River Bridge – Where Could Lateral Vibration Come From. ASME Journal of Applied Mechanics, 51, 694–696.
- Hemez, F.M., 1993, Theoretical and Experimental Correlation Between Finite Element Models and Modal Tests in the Context of Large Flexible Space Structures, Ph. D. Dissertation, Dept. of Aerospace Engineering Sciences, University of Colorado, Boulder, CO.
- Kaouk, M., 1993, Finite Element Model Adjustment and Damage Detection Using Measured Test Data, Ph. D. Dissertation, Dept. of Aerospace Engineering Mechanics and Engineering Science, Univ. of Florida, Gainesville, FL.
- James, G., R. Mayes, T. Carne, T. Simmermacher, and J. Gooding, 1995. Health Monitoring of Operational Structures – Initial Results. Proc. of 36th AIAA/ASME/ASCE/AHS/ASC Structures, Structural Dynamics and Materials Conference, 2226–2236.
- Kaouk, M., 1993. Finite Element Model Adjustment and Damage Detection Using Measured Test Data, Ph. D. Dissertation, Dept. of Aerospace Engineering Mechanics and Engineering Science, Univ. of Florida, Gainesville, FL.
- Kato, M., and S. Shimada, 1986. Vibration of PC Bridge During Failure Process. ASCE Journal of Structural Engineering, 112, 1692–1703.
- Law, S.S., P. Waldron, and C. Taylor, 1992. Damage Detection of a Reinforced Concrete Bridge Deck Using the Frequency Response Function. Proc. of the 10th International Modal Analysis Conference, 772–778.
- Liang, Z., M. Tong, and G.C. Lee, 1995. Modal Energy Measurement of a Long Steel Bridge. Proc. 13th International Modal Analysis Conference, 226–232.
- Lifshitz, J.M. and A. Rotem, 1969, “Determination of Reinforcement Unbonding of Composites by a Vibration Technique,” Journal of Composite Materials, 3, 412–423.
- Mazurek, D.F. and J.T. DeWolf, 1990. Experimental Study of Bridge Monitoring Technique. ASCE Journal of Structural Engineering, 116, 2532–2549.
- McConnell, K.G. 1995. Vibration Testing Theory and Practice, John Wiley and Sons, Inc., NY.
- Mottershead, J.E. and M.I. Friswell, 1993, Model Updating in Structural Dynamics: A Survey. Journal of Sound and Vibration, 167(2), 347–375.
- Paultre, P., J. Proulx, and T. Bégin, 2000. Dynamic investigation of a hybrid suspension and cable-stayed bridge. Earthquake Engineering & Structural Dynamics, 29, 731.
- Peeters, B. 2000. System identification and damage detection in civil engineering, Ph.D. dissertation, Civil Engineering Department, Catholic University of Leuven, Belgium.
- Raghavendrachar, M. and A.E. Aktan, 1992. Flexibility by Multireference Impact Testing for Bridge Diagnostics. ASCE Journal of Structural Engineering, 118, 2186–2203.
- Richardson, M.H. 1980, Detection of Damage in Structures from Changes in their Dynamic (Modal) Properties-A survey, NUREG/CR-1431, U.S. Nuclear Regulatory Commission, Washington, D.C.
- RILEM Committee 20-TBS TBS-3 1983. Testing Bridges in situ. Mater. Struct. 96, 421–431.

- Roca, P., and C. Molins, 1997. Dynamic load test on masonry structures as inspection technique. *Inspection and Monitoring of the Architectural Heritage*, pp. 133–140. IABSE, Ferrari Editrice, Bergamo, Italia.
- Rytter, A., 1993, *Vibration Based Inspection of Civil Engineering Structures*, Ph. D. Dissertation, Department of Building Technology and Structural Engineering, Aalborg University, Denmark.
- Salane, H.J., J.W. Baldwin, and R.C. Duffield, 1981. Dynamics Approach for Monitoring Bridge Deterioration. *Transportation Research Record*, 832, 21–28.
- Salawu, O.S., and C. Williams, 1995, Bridge Assessment Using Forced-Vibration Testing. *Journal of Structural Engineering*, 121(2), 161–173.
- Samman, M.M., and M. Biswas, 1994. Vibration Testing for Nondestructive Evaluation of Bridges. *Journal of Structural Engineering*, 120(1), 290–306.
- Slastan, J.a., and P. Foissner, 1995. Masonry building dynamic characteristics evaluation by means of ambient vibration. *Proceedings of 10th European Conference on Earthquake Engineering Rotterdam*.
- Spyrakos, C., H.L. Chen, J. Stephens, and V. Govindaraj, 1990. Evaluating Structural Deterioration Using Dynamic Response Characterization. *Proc. Intelligent Structures*, Elsevier Applied Science, 137–154.
- Straser, E.G. 1998. *A Modular, Wireless Damage Monitoring System For Structures*. Ph D. Dissertation, Dept. of Civil Eng., Stanford Univ., Palo Alto, CA.
- Tang, J.P., and K.-M. Leu, 1991. Vibration Tests and Damage Detection of P/C Bridges. *Journal of the Chinese Institute of Engineers*, 14, 531–536.
- Todd, M.D., C.C. Chang, G.A. Johnson, S.T. Vohra, J.W. Pate and R.L. Idriss 1999. Bridge Monitoring Using a 64-Channel Fiber Bragg Grating System. *Proceedings of the 17th International Modal Analysis Conference*, Kissimmee, FL, pp. 1719–1725.
- Toksoy, T., and A.E. Aktan, 1994. Bridge-condition Assessment by Modal Flexibility. *Experimental Mechanics*, 34, 271–278.

Structural monitoring in the Villa Reale of Monza (MI), Italy

A. Del Grosso

Department of Structural and Geotechnical Engineering, University of Genoa, Genoa, Italy

A. Torre & G. Corte

D'Appolonia S.p.A., Genoa, Italy

G. Brunetti

Tecniter s.r.l., Cassina De' Pecchi (Mi), Italy

D. Inaudi

Smartec s.a., Manno, Switzerland

ABSTRACT: This paper presents the case study of a long-term monitoring of a historical building, performed through an integrated system of SOFO fiber optic sensors and conventional sensors, designed to control the structure's movements and the efficiency of the planned strengthening works.

The paper will discuss the features of the monitoring system, data reduction and interpretation techniques, and the usefulness of monitoring techniques in gathering knowledge on the real behaviour of historical structures.

1 INTRODUCTION

Nowadays, structural health monitoring (SHM) is becoming an increasingly diffused tool for the management and in-service safety evaluation of different categories of structures. As concerning civil engineering applications, this is mainly true in the field of transportation infrastructure and lifeline critical facilities. These developments are also pushing an intensive research activity and the number of papers on the subject published worldwide in specialized journals and conference proceedings has dramatically increased in the last few years.

This paper is aimed at discussing a special topic within the framework of civil engineering applications, related to the role that SHM techniques can play in the preservation and rehabilitation of architectural heritage. The problem can be considered of a significant cultural and economical importance in several countries in Europe and worldwide, where old civilization has left a significant number of monumental buildings and structures that must be protected against deterioration or submitted to a rehabilitation process in order to allow their reuse for public and private functions. Nonetheless, this topic has received very little attention in modern research on SHM techniques.

Internationally agreed standards for restoration (Chart of Venice – 1964, Chart of Krakow – 2000) require the rehabilitation process to be performed in full respect of the historical characteristics of a monument. This has led to establish the principle of reversibility, i.e. to require that any intervention should be conceived in such a way that the original conditions could be recovered theoretically at any time after the intervention has been performed. However, when the rehabilitation process concerns the structural characteristics of a monumental building, safety requirements imposed by modern codes lead to strengthening techniques very often conflicting with such principle. Consequently, we are forced to accept irreversible modifications of the original structure but, in this case, it is required that strengthening is performed at the minimal possible extent.

The mechanics of ancient structures is sometimes very difficult to analyze. Strength of aged materials is often unknown as well; distress phenomena may reveal unclear and structural geometry itself may be hidden by modifications of the building occurred after its construction. This has the consequence that conventional approaches to structural rehabilitation, based on structural surveys and diagnostic campaigns followed by design and construction, in an open-loop-like

4 CHARACTERISTICS OF THE MONITORING SYSTEM

At the moment three separate monitoring systems have been installed in the building at different times and with different purposes.

The systems have however been designed in view of their integration in an unique system. The base component of the monitoring systems, allowing for system integration, is represented by the SOFO™ fibre optics system.

Indeed, the SOFO system is able to incorporate through its reading unit SOFO deformation sensors, as well as conventional sensors.

The SOFO measuring system (Glisic & Inaudi 2002) is based on the principle of low-coherence interferometry (Fig. 3). The infrared emission of a light emitting diode (LED) is launched into a standard single mode fibre and directed, through a coupler, to the deformation sensors mounted on or embedded in the structure to be monitored, consisting in long-base temperature compensated fibre optic gages, containing two fibres. The measurement fibre is in mechanical contact with the structure itself and will therefore follow its deformations in both elongation and shortening. The second fibre, called reference fibre, is installed free in the same pipe. Mirrors, placed at the end of both fibres, reflect the light back to the coupler which recombines the two beams and directs them towards the analyzer. This is also made of two fibre lines and can introduce a well known path difference between them by means of a mobile mirror.

On moving this mirror, a modulated signal is obtained on the photodiode only when the length difference between the fibres in the analyzer compensates the length difference between the fibres in the structure to better than the coherence length of the source (in our case some hundreds of mm).

The fibre optic gages can be manufactured in length varying from 10 cm to 10 m and fixed on different supports. The sensors can measure the variation in length between an active and a reference fibre up to a precision of 2 microns. Each optical sensor must be connected to the reading unit through optical switches. One position of the switch can be attached to an ADAM

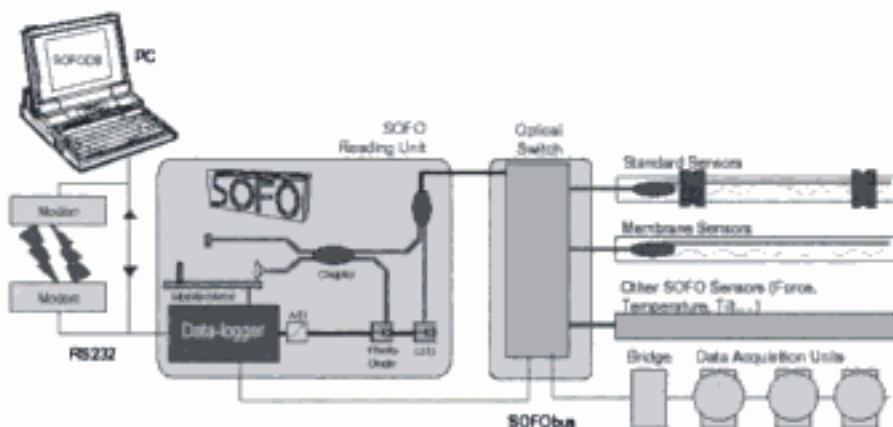


Figure 3. SOFO™ system architecture.

bridge, able to address a chain of data acquisition modules (ADAM) suitable for driving nets of conventional electric sensors.

The reading unit possesses local capabilities for data acquisition and storage (Glisic & Inaudi, 2002). For data processing and interpretation, the unit can be accessed locally or remotely by a computer system.

In the Villa, the reading unit is actually connected in a provisional location only to the subsystem in the South wing and it is being expanded to include the other two subsystems. Final positioning will be in the M&E control room of the South wing.

4.1 The South wing monitoring system

The South wing of the royal Villa of Monza has been equipped with 30 SOFO deformation sensors and 6 thermocouples: the deformation sensors are located in the orthogonal direction of the two mezzanine corridors, in such a way to measure the relative movements of the four masonry blocks in ten sections of the wing. Each sensor has nearly the same width of the corridor and has been provisionally fixed at the wall in correspondence of the springer of the vaults, but in their final configuration the sensors will be embedded in the reinforced concrete strengthening of the vaults. The position of the sensors at each level is shown in Figure 4.

Reading of the instruments is automatic and performed every four hours since February 2002, in order to record the daily variations of the temperature and the related displacements.

Due to the structural complexity, the uncertainty of the mechanical characteristics of the masonry and soil, the forecasting of the structural behavior will be carried out through a statistical data processing. A special purpose computer program (Sechi, 2002) has been conceived in order to correlate the relative displacements to their geometrical position in space and to external and internal temperatures. This program is composed from a sequence of modules:

- Three-dimensional geometric model of the South wing.
- Research of the maximum and minimum values.
- Definition of the trends.
- Attenuation of the irregular variations.

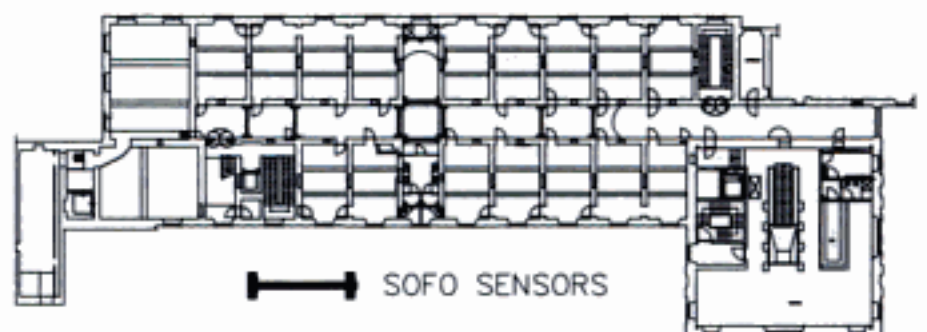


Figure 4. Location of the SOFO sensors in a mezzanine plan.

- Definition of the correlation between displacements and temperatures.
- Forecast of the future structural behavior.

The three-dimensional geometric model reproduces, schematically, the four masonry blocks, defined by the sensor position in the undeformed configuration: the relative displacements of the four blocks are obtained by calculating the new sensor coordinates for each session of measurement, supposing that the sensors keep transversally the same position (Fig. 5).

The research of the maximum and minimum values is performed in order to obtain the range in which the displacements occur.

The data sets show an irregular behavior due to short and long term variations. In order to obtain a first indication of the displacement evolution independently from the cyclic and seasonal variations, trends have been defined through least-square regressions on the entire data sets recorded on the monitoring period under consideration.

The attenuation of the irregular variations can be performed, in order to reduce the undesired variations, making a Fourier transformation of the data sets in a period of 1 year.

In Figure 6 the Fourier spectrum of the sensor 4 is represented, where the yearly and monthly variations of the displacements are characterized by the first 10

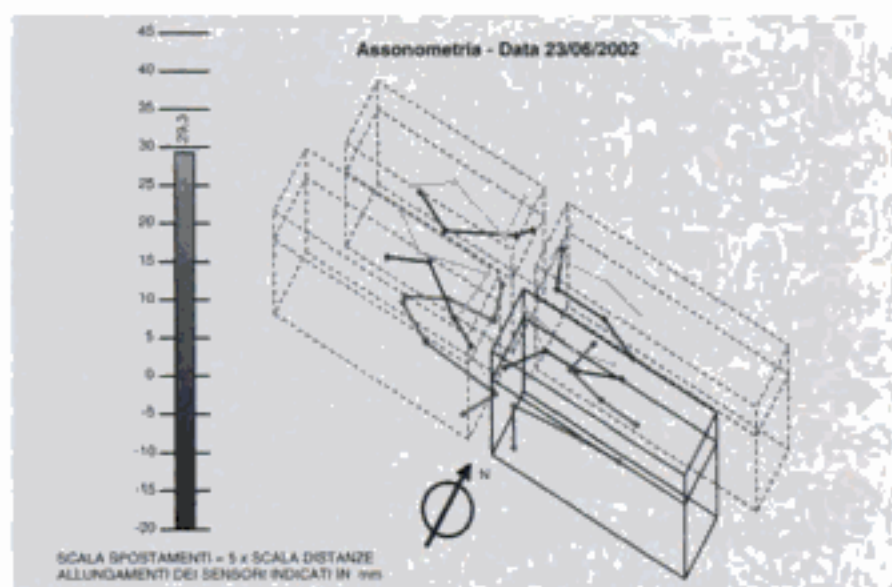


Figure 5. South Wing three-dimensional geometric model.

frequencies, and the daily variations by a peak at higher frequency.

After individuating the main frequencies, a filter function has been created in order to cut the higher frequencies. These frequencies represent the residual displacements (Fig. 7) due to the daily and random displacements and are used in order to obtain the range in which the 85% of the measures are statistically contained. In Figure 8 the displacement attenuation and the related confidence range are represented.

The same operations are performed on the temperature data of and the two trends are compared. Figure 9 shows that the two trends are similar until July 2003, but from that date on the displacements show a divergence from the temperatures.

After the first analyses on the displacements, a correlation between the displacements and the temperatures can be carried out, in order to determine, qualitatively, how the displacements are due to temperature variations.

High correlation coefficients mean that temperature is the main cause of the movement and low correlation coefficients mean that other effects may have caused these displacements.

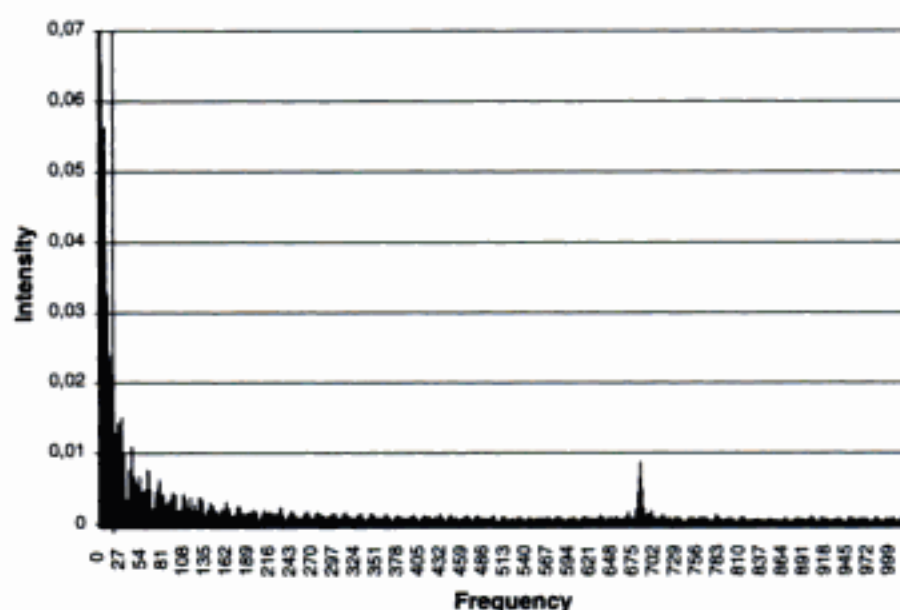


Figure 6. Fourier spectrum of displacements at sensor 4.

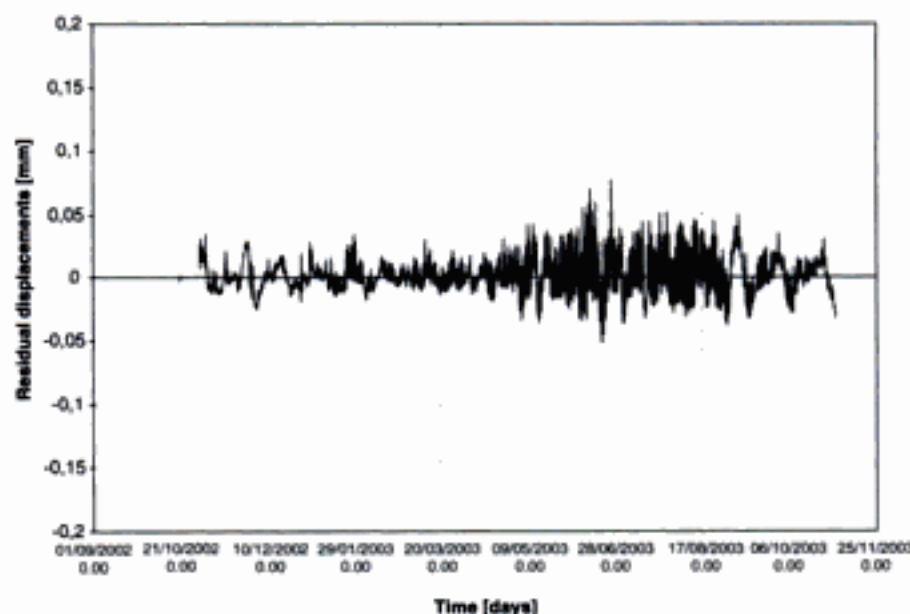


Figure 7. Residual displacements due to random and daily variations.

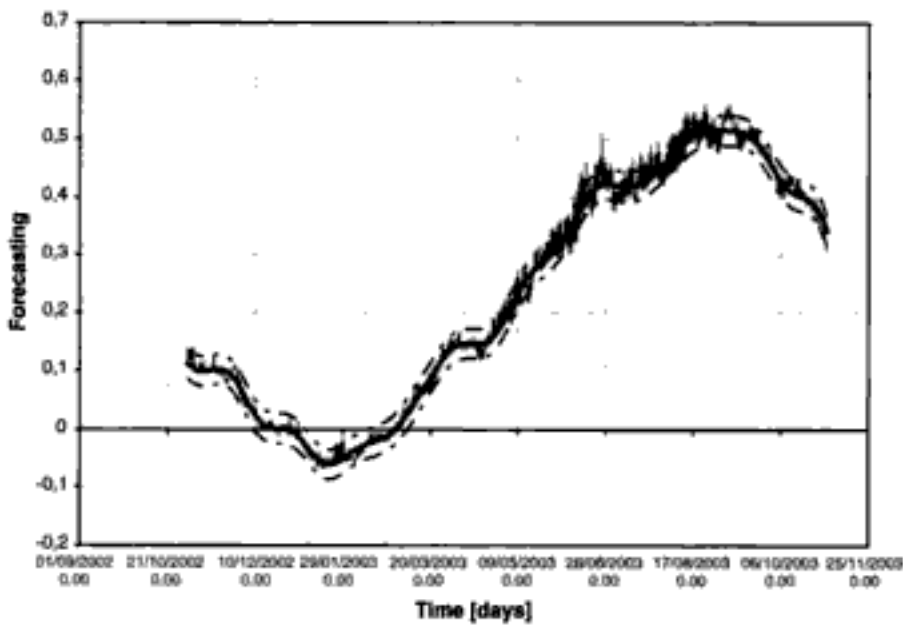


Figure 8. Displacement attenuation and confidence range.

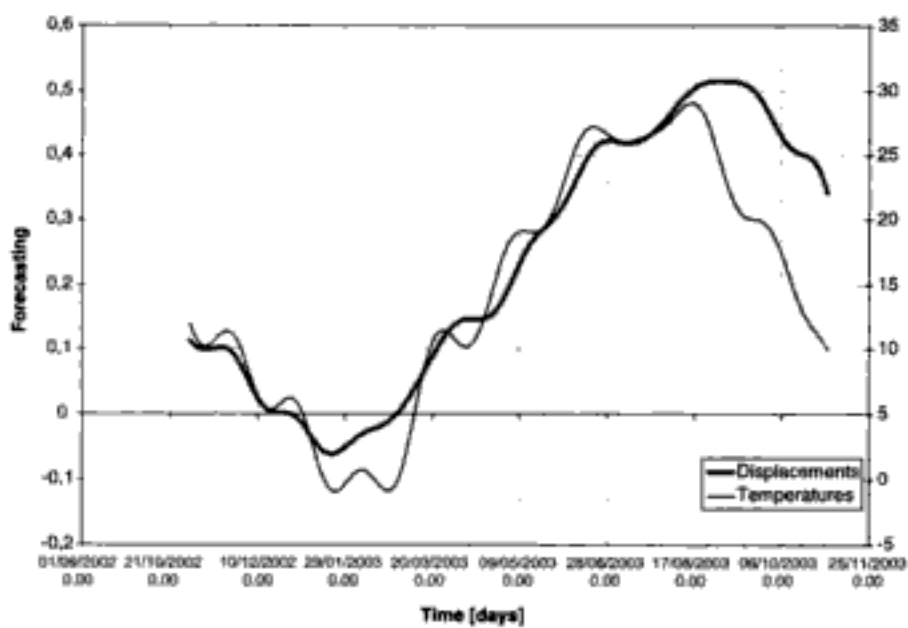


Figure 9. Comparison between temperature and displacement attenuations.

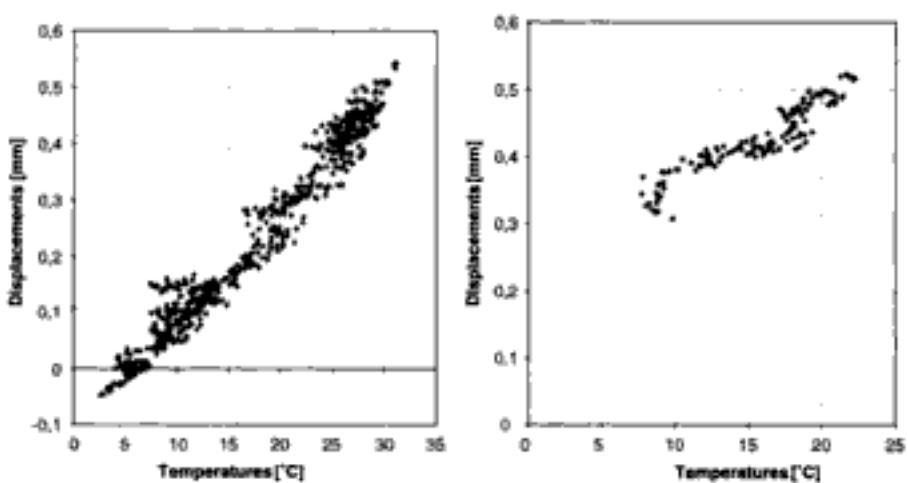


Figure 10. Correlation chart between displacements and temperatures.

It is possible that the structural response of a building occur with a delay mainly due to this thermal inertia, particularly significant in a masonry building. The definition of this delay can be carried out through the research of the maximum correlation coefficient, obtained by imposing several delays between the two data sets.

Figure 10 shows the correlation between displacements and temperatures for sensor 4, before and after

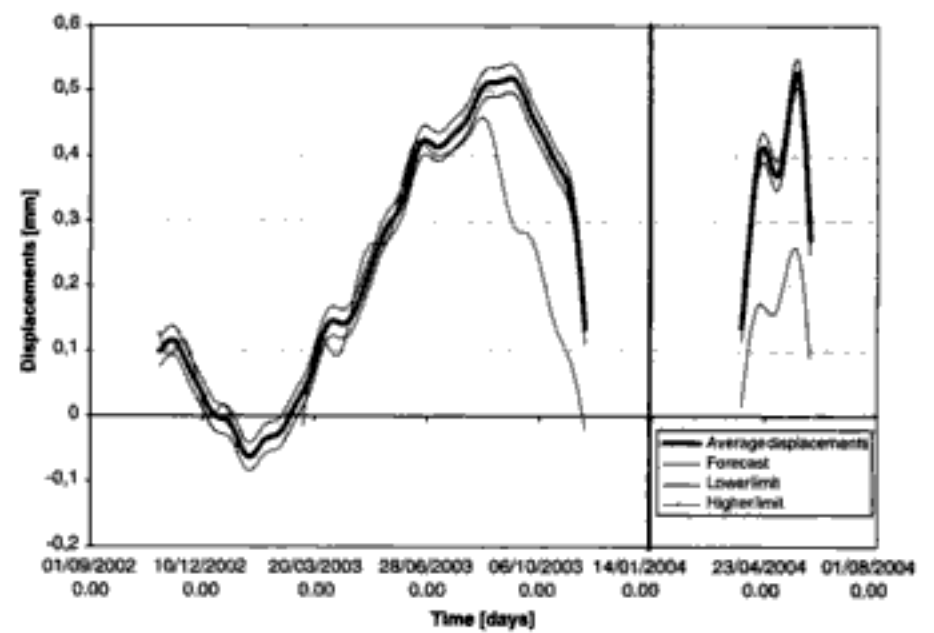


Figure 11. Displacement forecast before and after beginning of the rehabilitation works.

31 July 2003: in this case the delay in the structural response is practically null and the two charts show a high correlation in both cases: this fact indicates that the observed divergence is due to some non-linear effect.

Finally it is possible to performing a forecast of the structural behavior by a regression between displacements and temperatures. The forecast can be made on the data collected before starting the rehabilitation works, in order to compare the measurements that will be obtained during these works with the forecasted values.

Figure 11 shows a first forecast of the structural behavior since the beginning of the rehabilitation works. The time series present a lack of data between November 2003 and April 2004, due to a temporary break of the reading unit. The vertical line on 7 January 2004 represent the start of the rehabilitation works, then the monitoring of the first phase hasn't been performed. The forecast performed to May and June 2004 confirm the displacement hypothesis: in fact, the trends of the measured and forecasted displacements are similar. This is confirmed by the still significant correlation coefficient (0, 84) between the displacements and the temperatures.

4.2 The North wing monitoring system

The North wing of the royal Villa of Monza has been equipped with 12 SOFO deformation sensors installed in the two corridors of the two mezzanines in order to measure, as well as in the South wing, the global displacements of the four masonry blocks before the rehabilitation project. To this aim, the evolution of the main cracks has been measured through 18 standard deformation sensors. Finally, the system has been equipped with 6 thermocouples in order to measure the internal temperature variations.

As well as in the South wing, the SOFO sensors are provisionally installed, but the reading has been

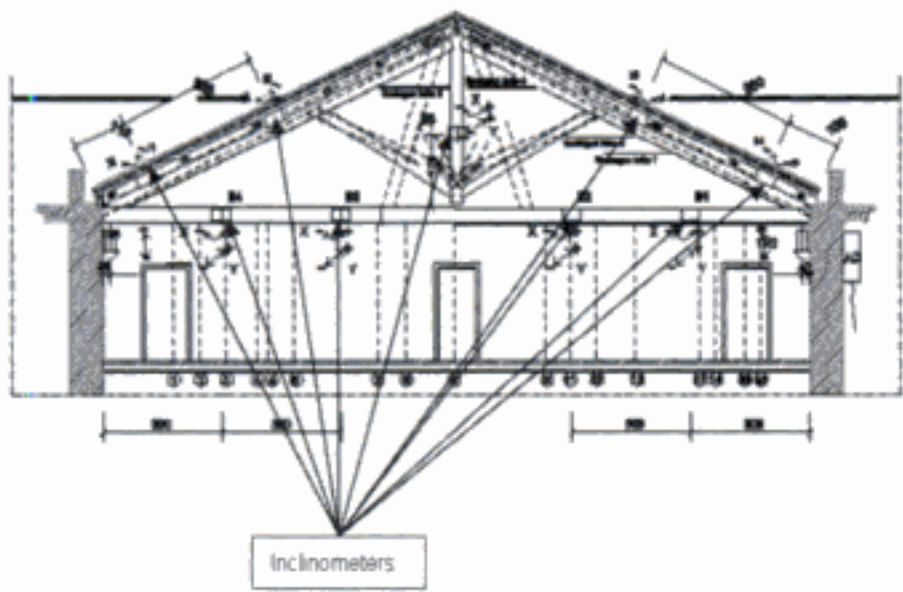


Figure 12. Location of the inclinometers on the truss.

performed manually nearly every month. In this case, the low number of data do not allow to carry out a statistical analysis as well as in the South wing. The system is actually being integrated into the reading unit of the South wing for automatic operation and data processing.

4.3 The Belvedere monitoring system

The Belvedere main truss was interested by torsional deformations of the chain and out-of-plane rotation of the king post, induced by three-dimensional effects of the timber structure. In order to control the deformations of the truss during the rehabilitation works and in-service phase, a monitoring system was installed on the main elements since July 2003.

This system, shown in Figure 12, is composed of 4 biaxial standard inclinometers on the chain, 4 mono-axial inclinometers on the struts, 1 biaxial inclinometer on the king post and temperature/humidity sensors, to control the environmental conditions. The system is equipped with a self-standing automatic data acquisition hardware that is being connected to the SOFO reading unit in the South wing through an ADAM device.

Monitoring has been performed in two phases, corresponding to the removal of the temporary supports used during the structural rehabilitation works, and to the first in-service period. The plots of the measured rotations are shown in Figures 13–15: from 23 September to 14 October 2003, the acquisition was accidentally interrupted.

The plots show that in the first phase of loading, a significant torsional deformation of the chain was detected. Due to this deformation it was decided to add a steel tendon by each side of the chain, in order to reduce the stresses in the old timber structure and provide a presidium.

After this intervention, the system has been kept on service with data acquisition every 4 hours, in order to record the displacements due to the thermal

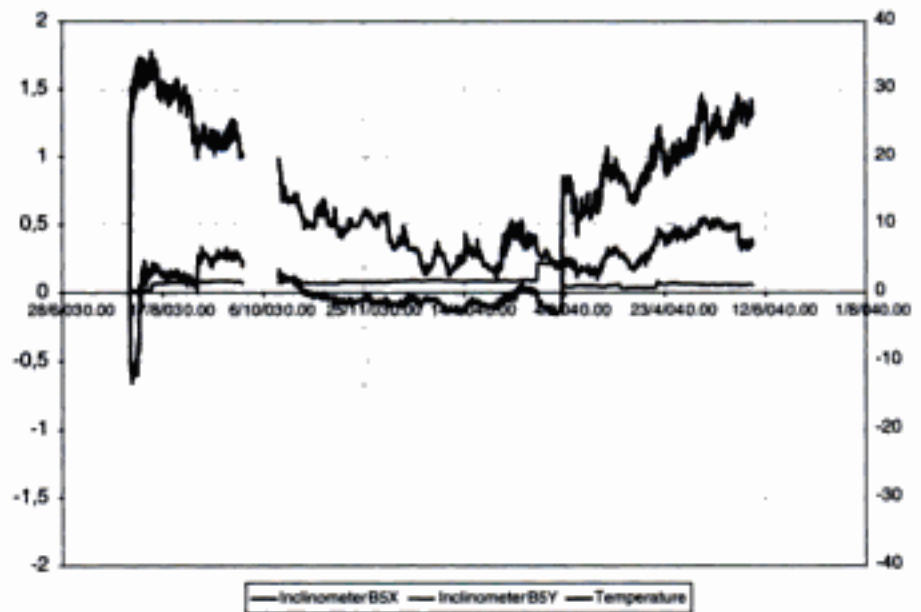


Figure 13. Rotations of the biaxial inclinometer on the king post.

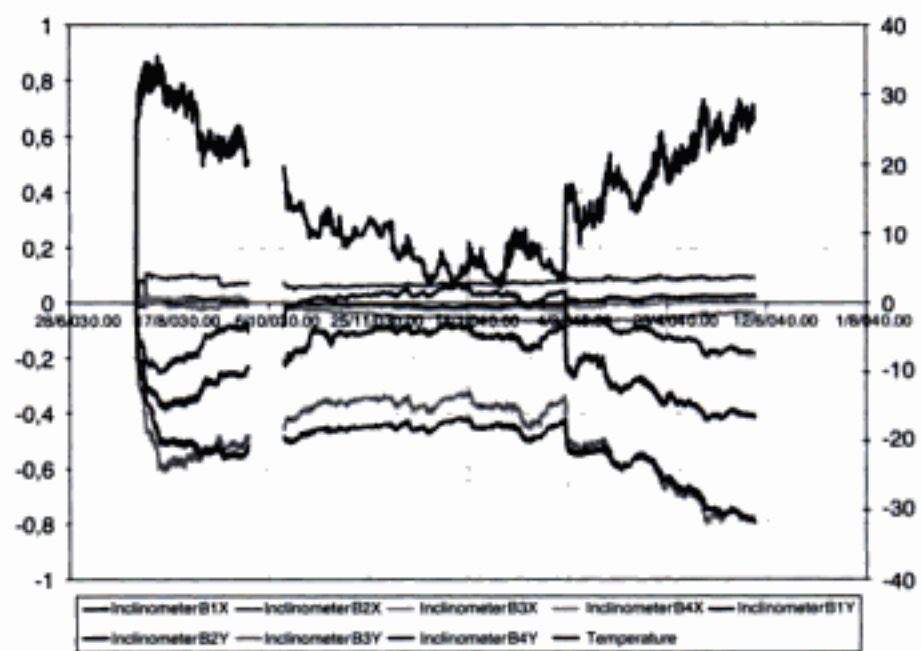


Figure 14. Rotations of the biaxial inclinometers on the chain.

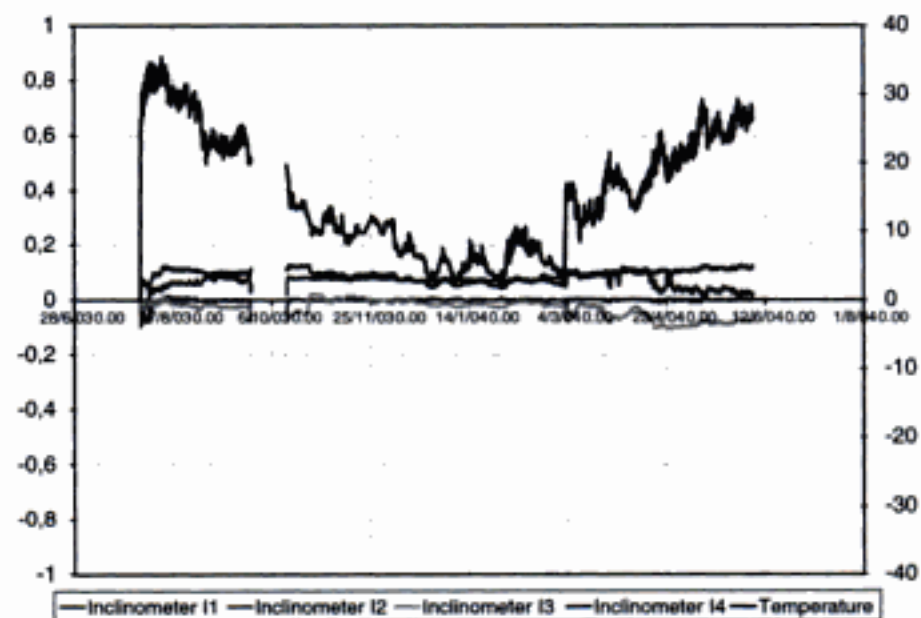


Figure 15. Rotations of the biaxial inclinometers on the struts.

variations: in this period, the torsional deformations of the chain follow mainly these variations.

The mono-axial inclinometers on the struts have shown small rotations ($<0.2^\circ$) during the works on

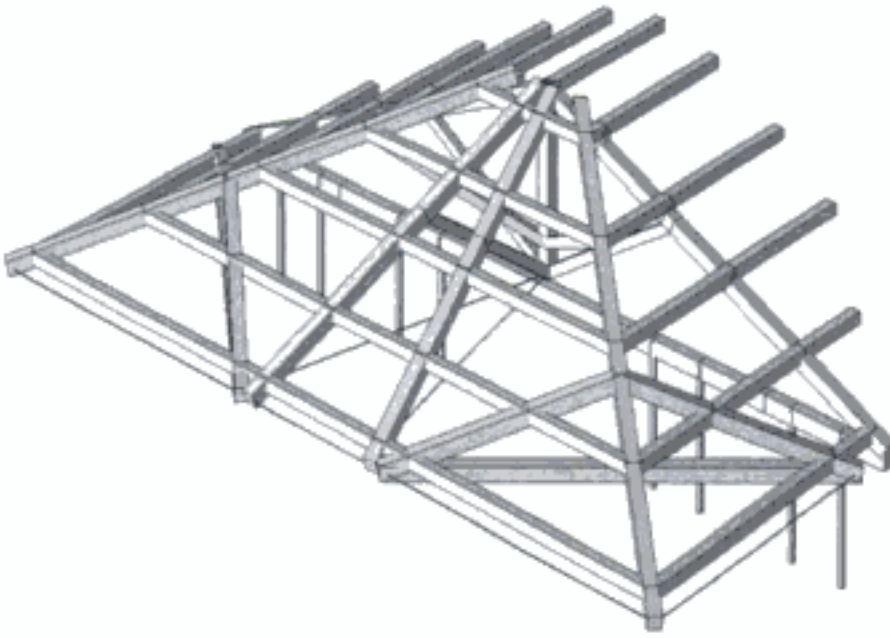


Figure 16. Finite element model of the roof.

the timber in July and August 2003, and practically no rotations at all during the first in-service phase.

The biaxial inclinometer on the king post has shown an out-of-plane rotation practically null after the removal of the temporary supports, due to the presence of the steel tendons between the king post and the pitch struts. These rotations increased unexpectedly on 19 February 2004 due to a release of a tendon's clamp. During the fixing of the problem, the monitoring system was used to restore the previous conditions. The in-plane rotation has followed substantially the trend of the temperature.

In order to provide an interpretation of the observed data, a finite element model of the structure has been developed. As indicated in Figure 16, the model comprises the three-dimensional arrangement of the original timber structure and the steel tendons introduced along the perimeter walls and between the king post and the two pitch struts to absorb the horizontal thrust. Eccentric wooden supports are modeled along the chain, in order to simulate its torsional behavior.

The parameters of the model have been optimized by fitting the response observed in the first phase with the computed rotations. The testing results have substantially confirmed these parameters.

The model will then be used to evaluate the conditions of the structure during the subsequent in-service phase.

5 CONCLUSIONS

The monitoring systems installed in the royal Villa of Monza have allowed to control the structural behavior of some parts after and before the rehabilitation works. In the case of the South wing monitoring system the interpretation of the displacements has been statistically carried out, due to the complexity of the structure. The Belvedere main truss displacements are interpreted by means of a numerical model optimized by fitting the response observed in the first phase with the computed rotations.

In the future, the presence of the permanent monitoring system, that include all system described in this paper, will guarantee the possibility of verifying the effectiveness of the interventions that are being carried out in the present phase and of eventually defining local interventions to improve soil conditions. For this reason the case described can represent an example of a monitoring-based structural rehabilitation process.

REFERENCES

- Glisic, B. & Inaudi, D. 2002. Long-Gage Fiber Optic Sensors for Global Structural Monitoring. *First International Workshop on Structural Health Monitoring of Innovative Civil Engineering Structures, ISIS Canada, September 19–20, 2002*
- Inaudi, D. Glisic, B. & Vurpillot, S. 2002. Database Structures for the Management of Monitoring Data. *First International Workshop on Structural Health Monitoring of Innovative Civil Engineering Structures, ISIS Canada, September 19–20, 2002*
- Sechi, M. 2002. Elaborazione dei dati dal monitoraggio strutturale della Villa Reale di Monza. *Laurea Thesis, Department of Structural and Geotechnical Engineering, University of Genoa*

Dynamic monitoring of an ancient masonry bridge on Carrara marble way

G. Chellini, P. Orsini & W. Salvatore

Department of Structural Engineering, University of Pisa, Pisa, Italy

ABSTRACT: The so-called *Vara bridges*, erected at the end on the Nineteenth Century, are of relevant historical importance. They were part of the Private Marble Railway of *Carrara* (Italy), built between the 1876 and the 1890. The bridges are placed in the first section of the line from *Carrara* to the quarries, transformed nowadays into a road street. So they are currently crossed by the trucks transporting marble from quarries to the highway and the port. Because of these reasons and the high loads interesting daily the structures, an accurate check of the bridge structural safety has been foreseen. In the present paper, besides some historical information, the first results of the experimental analyses performed on the Viaduct of *Canal Piccinino*, one of the *Vara bridges*, are illustrated and discussed.

1 INTRODUCTION

1.1 *The Private Railway of Carrara (Italy)*

The Society of Private Marble Railway of *Carrara* (Italy) was born the 29th of May 1874, and authorized with a King's Decree the 5th of November of the same year. The final aim was the connection of the quarries in the *Apuane Alps*, where the precious white marble is extracted, with the port of *Marina di Carrara* and the National Railway station at *Avenza*. The first railway run, between "Carrara-Miseglia-LaPiastra", started working the 19th of August 1876. Subsequently the railway was enlarged in order to improve the connection with the National Railway and to reach the quarries till "Ravaccione", "Canalgrande" e "Gioia", see Figure 1. Two different proposals were developed for this project, but too costly, so Eng. Leoni, technical responsible of the railway, instructed Eng. Sartorio to arrange the new design. After several discussions and disputes, the new runs were opened on the 15th of May 1890. (Canali, 1995)

Nevertheless the new railway became a threat for people that, since then, had successfully transported marble blocks by wagons pulled by oxen. Viaduct of *Vara*, showed in the Figure 2, was so mined and seriously injured, see Figure 3.

At the beginning of the XX century new works for the realization of other branches were executed, together with the restoration of the Viaduct of *Vara*, that was definitively executed in the 1932 as showed in the Figure 4. The society reached the maximum expansion in the 1926, when the transport of marble blocks reached the 5×10^6 kN.

The maximum length reached by the Railway of Marble in this period was equal to 21945 m, climbing till 455 m of altitude over the sea level, with an average value of the slope equal to 45‰.

The maximum slope was equal to 70‰, near to "Miseglia Superiore" e "Tarnone". The complete development of the railway is represented in the Figure 5.

The structures and infrastructural works were numerous and of uncommon importance: 15 galleries for a total length of 4537 m and 16 bridges and viaducts with free spans of arches between 10 and 30 m. The 25% of the total length of the railway was curved. (Betti Carboncini, 1984)

After the II World War the Society met new difficulties connected with the recovering of the railway. Moreover a flood seriously damaged almost the complete extension of the railway, adding new problems to the difficult management of the Society.

The traffic progressively decreased, till, in the 1962, a plan for the progressive substitution of the railway with a new road was promoted and quickly executed. The railway exercise stopped definitively on the 28th of February, 1969.

1.2 *Aims of the monitoring*

After the transformation from railway to road street, the traffic of trucks transporting marble increased more and more.

The old railway line is today the most important way to reach, starting from the quarries, the businesses near the city of *Carrara*, the highway and the port.

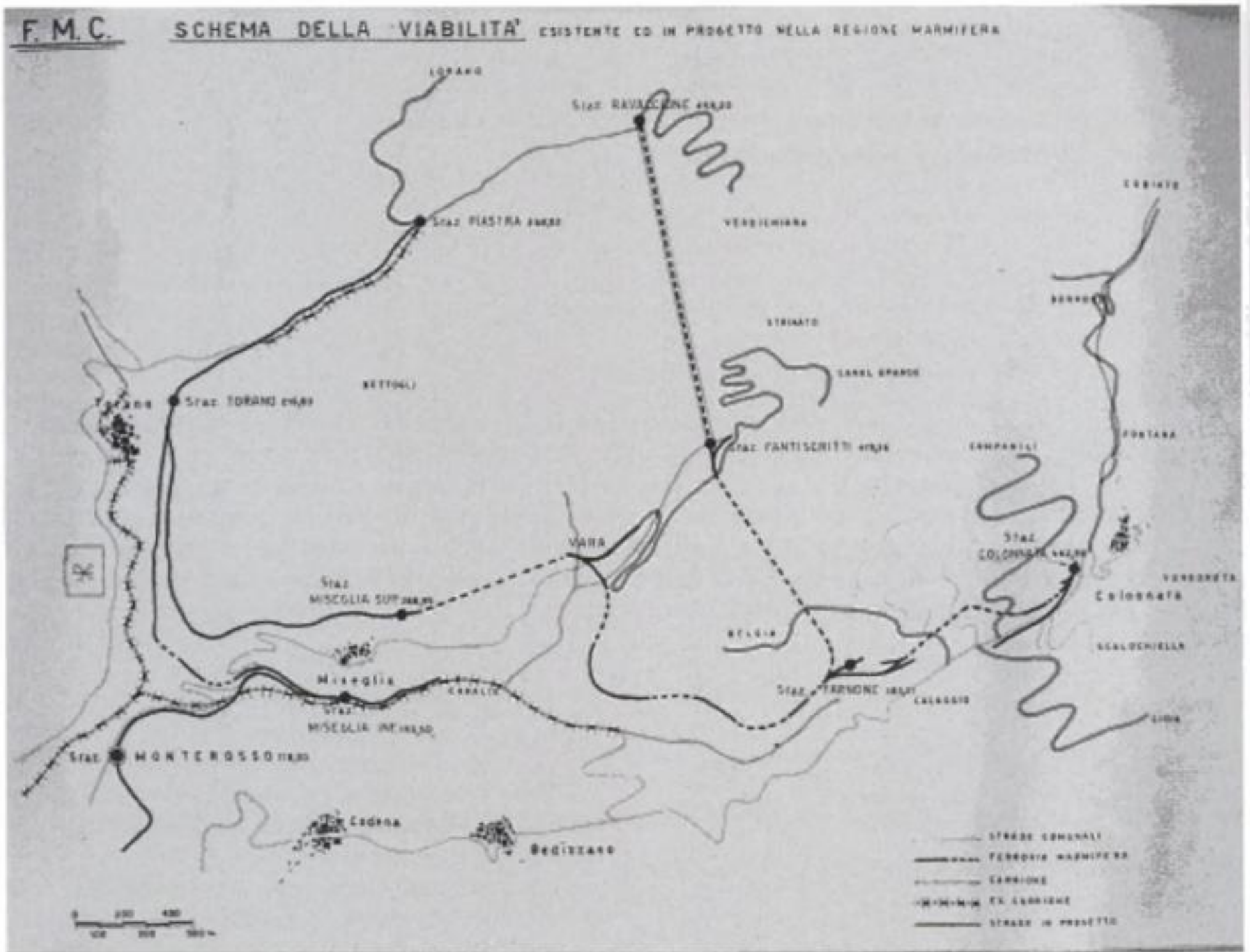


Figure 1. Existing and design railways; drawing of the XIX century (Archives of the Private Marble Railway of Carrara).



Figure 2. Viaduct of *Vara*, 1908. (Archives of the Private Marble Railway of Carrara).



Figure 3. Viaduct of *Vara* after mining, 1913. (Archives of the Private Marble Railway of Carrara).

It is so evident the crucial importance of continuous bridges exercise: any service interruption can compromise seriously the functioning of all the marble industry.

On the other hand, old bridges of the railway line, designed more than a century ago for different service

conditions and loads, are daily subjected to the high dynamic actions due to the transit of more than 600 heavy loaded trucks. Moreover they have been and are currently exposed to the possible debris slides due to the large amounts of marble stones accumulated on the sides of the mountains.

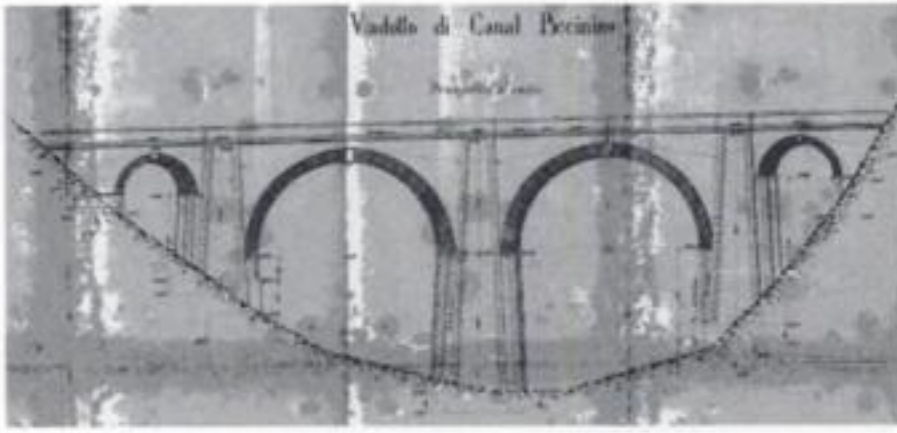


Figure 8. Front view of the Viaduct of *Canal Piccinino* as designed by Eng. Leoni, 1885 (Archives of the Private Marble Railway of *Carrara*).

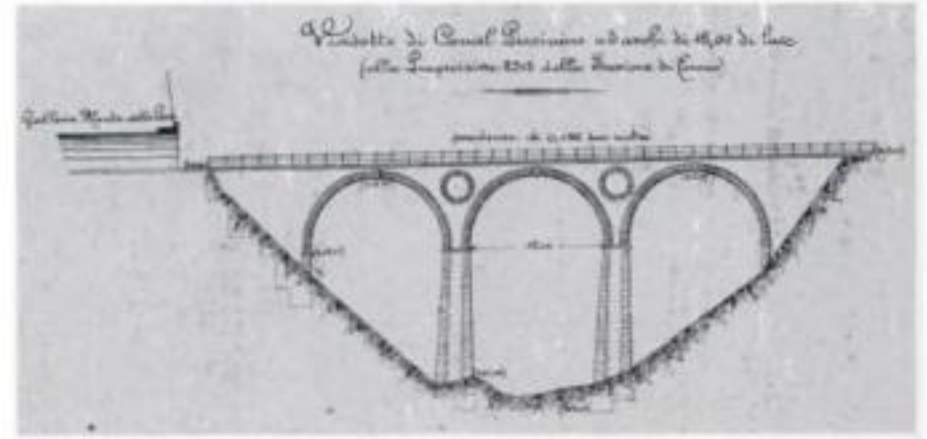


Figure 11. Front view of the Viaduct of *Canal Piccinino* as realized, picture of the XX century (Archives of the Private Marble Railway of *Carrara*).



Figure 9. Plan view of the Viaduct of *Canal Piccinino* as designed by Eng. Leoni, 1885 (Archives of the Private Marble Railway of *Carrara*).

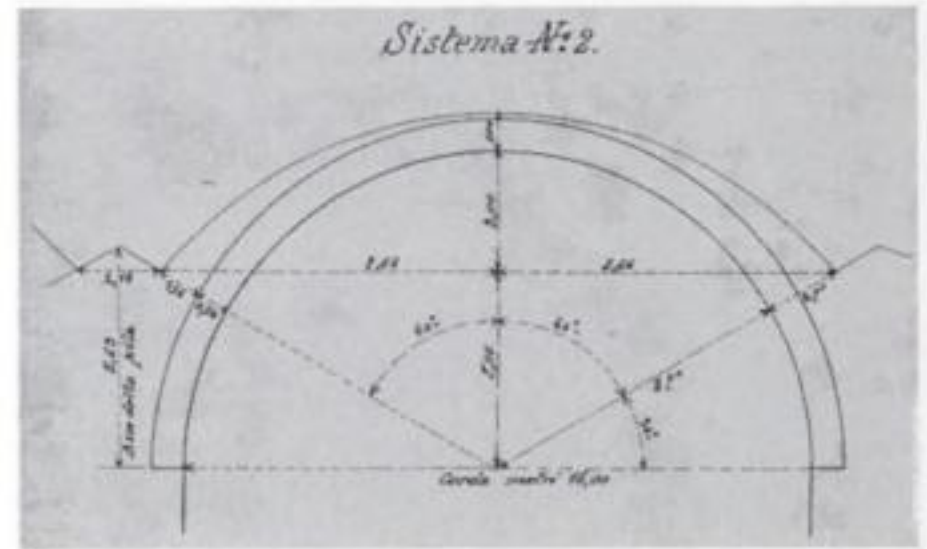


Figure 12. II solution for the reinforcement of the vaults; Viaduct of *Canal Piccinino*, May 7, 1889. (Archives of the Private Marble Railway of *Carrara*).

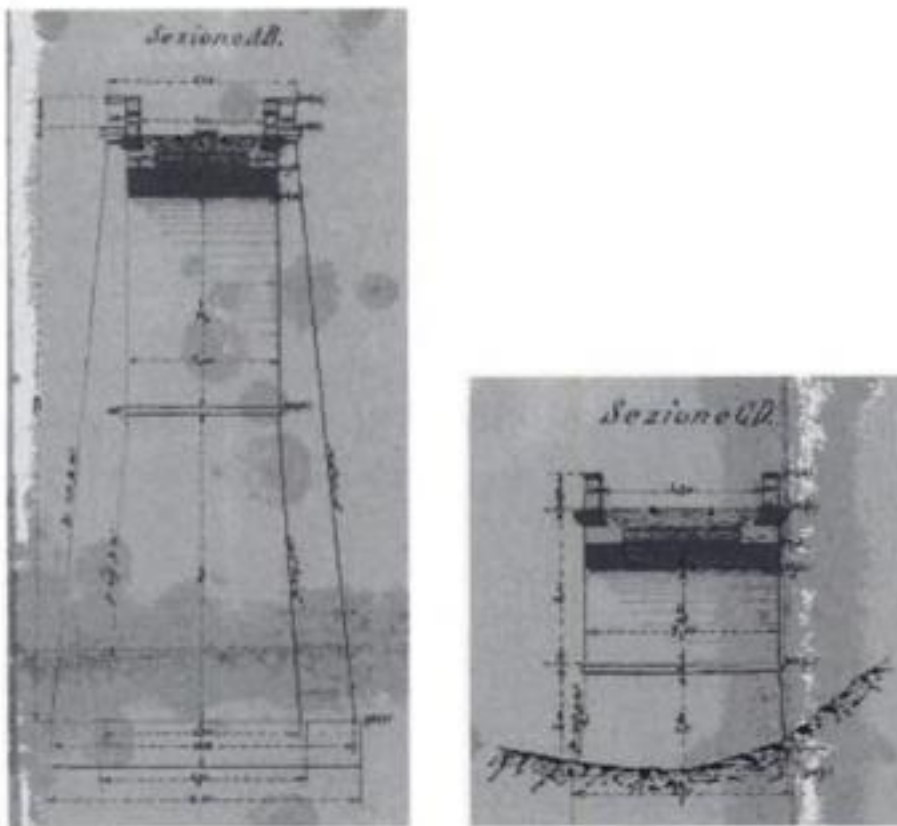


Figure 10. Cross sections of the Viaduct of *Canal Piccinino* as designed by Eng. Leoni, 1885 (Archives of the Private Marble Railway of *Carrara*).

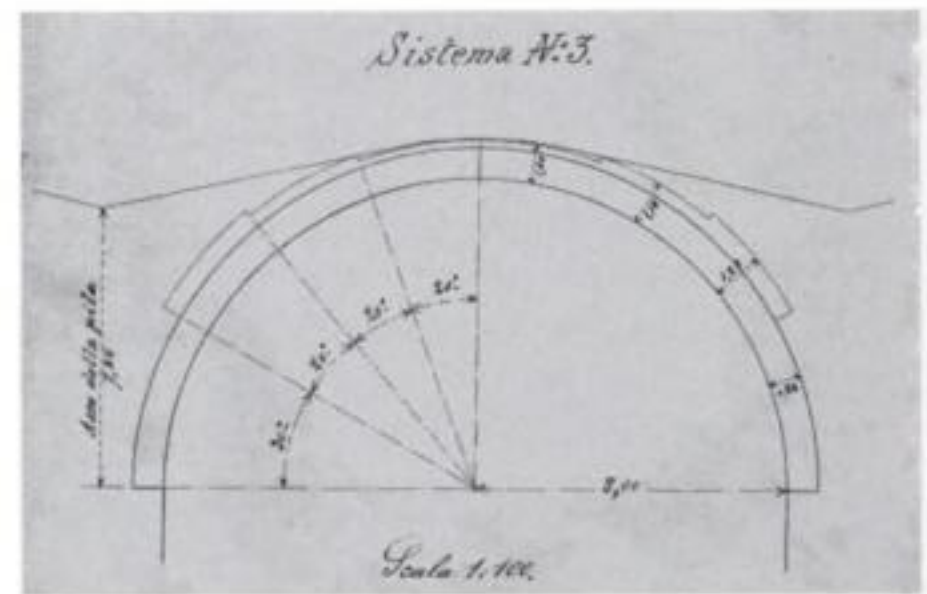


Figure 13. III solution for the reinforcement of the vaults; Viaduct of *Canal Piccinino*, May 7, 1889. (Archives of the Private Marble Railway of *Carrara*).

The Viaduct of *Canal Piccinino* was part of the first section, from “Torano” to “Gioia”. Its first design, proposed by Eng. Augusto Leoni on the 20th January 1885, foresaw four arches of different spans, as shown in the Figures 8, 9 and 10. Afterwards a new solution, characterized by three equal masonry arches with 16 m long spans, was built. A picture of the XX century, showed in the Figure 11, represents the realized design of the bridge.

The design of the viaduct was very accurate as confirmed by the studies executed during works, on the shapes of vault cross sections, represented in the Figures 12 and 13 and the related cost estimates, showed in the Figure 14. Other particular studies were needed to solve the problems arising in correspondence of the last arch for the presence of the crossroads between “Tarnone-Fantiscritti” and “Para”. Dedicated studies

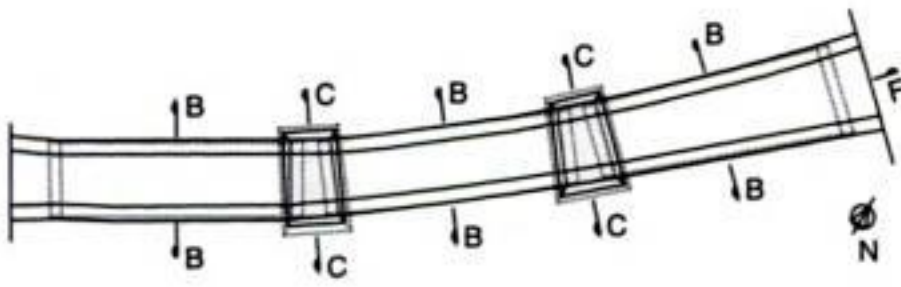


Figure 18. Plan view of the Viaduct of *Canal Piccinino*.

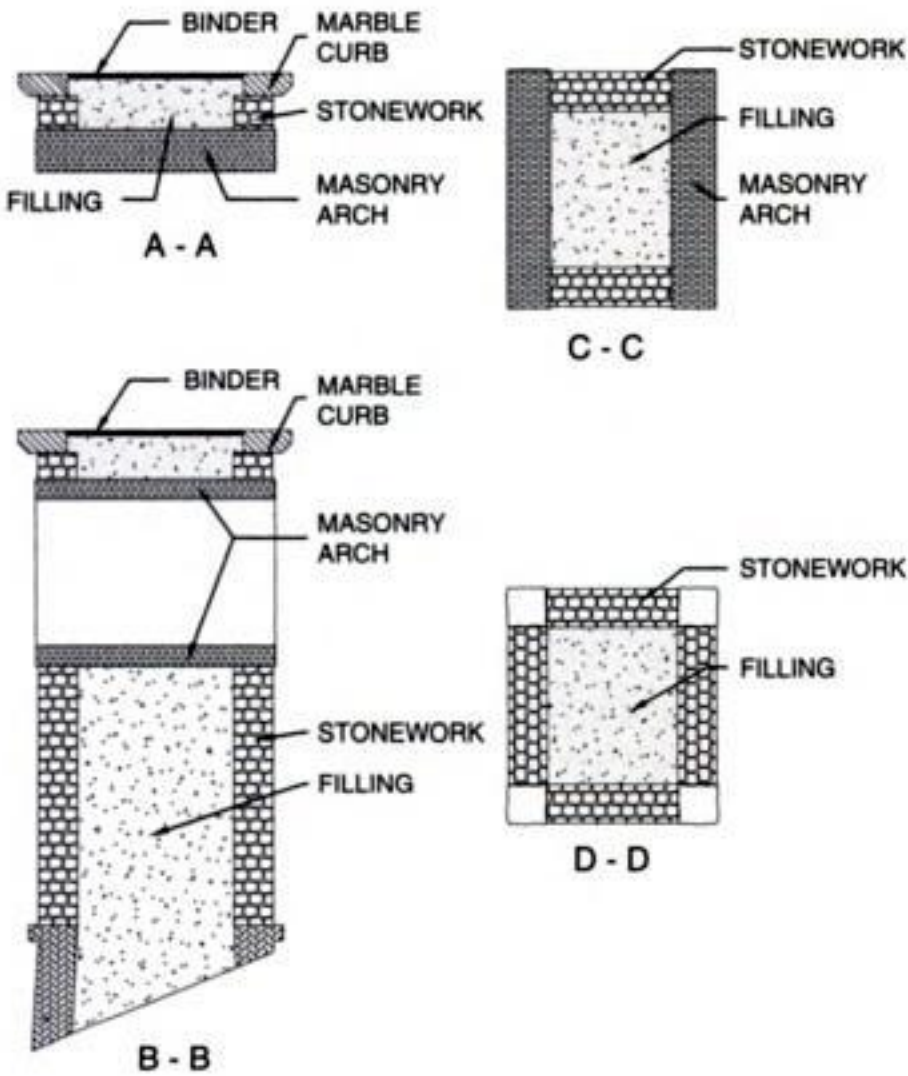


Figure 19. Typical cross-sections; Viaduct of *Canal Piccinino*.

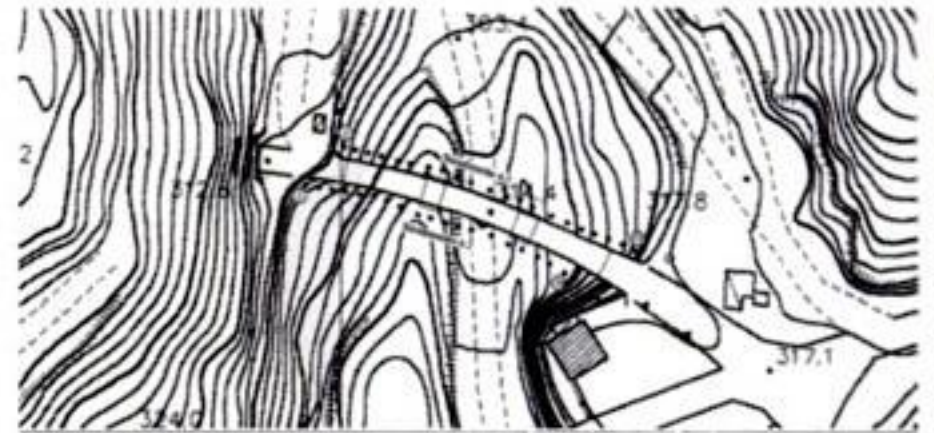
2.3 Geotechnical investigations

Being foundations not profound, for a better understanding of soil nature, accurate investigations have been executed studying dynamic wave refraction. Geophones arrangement is showed in the Figure 20, while the results obtained for the two sides of the viaduct, are illustrated in the Figures 21 and 22. It is evident that a profound layer of marble debris is present in the bed of the *Canal Piccinino*.

3 THE DYNAMICAL EXPERIMENTAL ANALYSES

3.1 Test design

In order to reproduce the actual working conditions, the response to impact actions transmitted by an heavy loaded truck – total weight 223 kN – passing across the viaduct has been measured, see Figure 23. On the road surface, in order to emphasize the dynamic action,



Località: PONTI DI VARA Tavola n.1
 LEGENDA
 Pila del ponte
 Viadotto di accesso all'opera
 Geofoni
 Sezione trasversale PONTI DI VARA 1-1
 Sezione trasversale PONTI DI VARA 1-2

Figure 20. Arrangement of geophones for soil investigations.

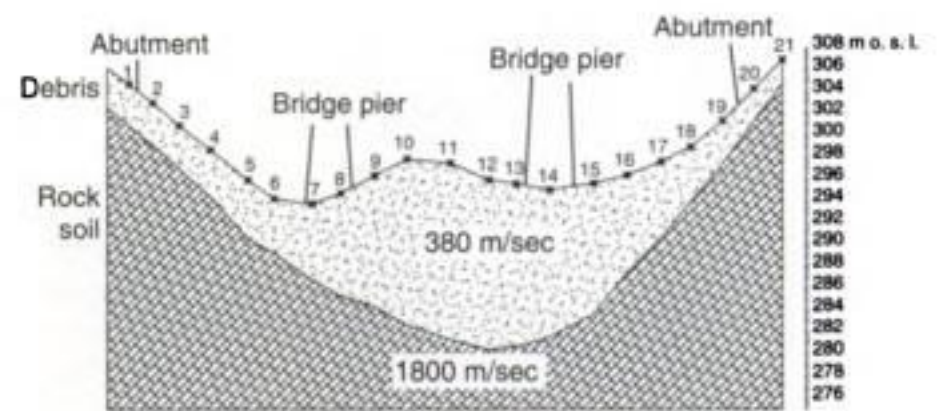


Figure 21. The first soil section.

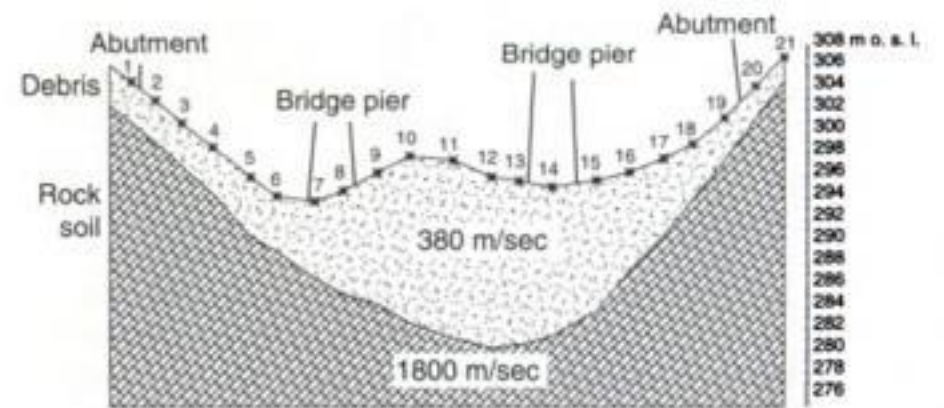


Figure 22. The second soil section.



Figure 23. The truck crosses the viaduct during the tests.

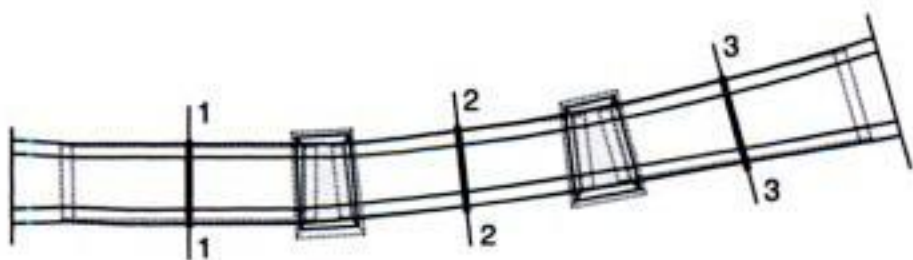


Figure 24. Positioning of the three artificial surface imperfections.



Figure 25. The truck crosses the viaduct and stops just after the first imperfection during the first test series.

three artificial imperfections of the asphalt have been built, one for each keystone of the three arches, as illustrated in the Figure 24.

The dynamic response of the bridge was recorded in different working conditions in order to excite all possible movements. In particular the truck was stopped after passing with the first axle load (weight equal to 74 kN) each imperfection, starting alternatively just before the same imperfection or from the abutment. In this way single jump or repeated jumps were realized. In the Figures 25 and 26 the truck stopping respectively just after the first and the second imperfections is showed.

At the end of the test series, a final measure was realized crossing with the truck the whole viaduct.

The accelerations were measured by a maximum of 17 piezoelectric accelerometers PCB 393 C (sensitivity $9.8 \times 10^{-4} \text{ m/s}^2$).

The signals were processed and acquired with a PCB 584 amplifier and National Instruments PCI-6031E multiplexing acquisition device. A sampling frequency of 800 Hz was chosen for data recording.

The accelerometer arrangement was designed in such a way to measure displacements and rotations of the bridge cross-sections in correspondence of the keystones of arches, of abutments and of piers.

The horizontal and vertical movements of piers cross-sections were also recorded.

In order to perform accurately all foreseen measures, three different configurations were adopted, analyzing separately the response of each arch to



Figure 26. The truck crosses the viaduct and stops just after the second imperfection during the second test series.

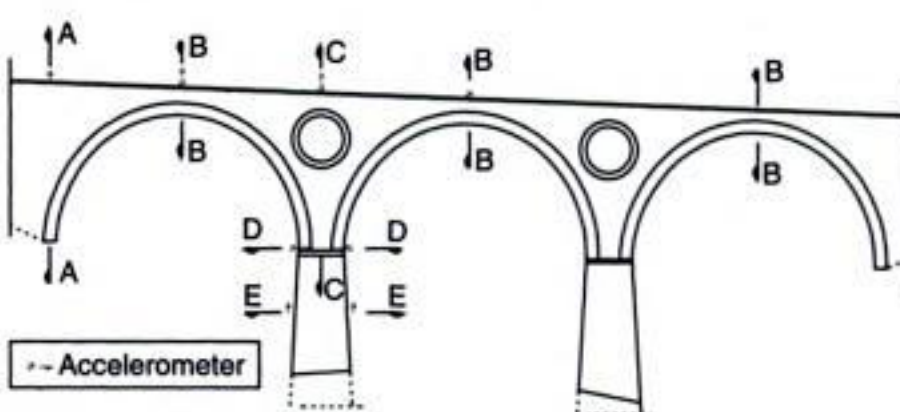


Figure 27. Front view of the accelerometers arrangement; I configuration.

the complete series of above described loading histories. The first configuration, corresponding to the first arch, and the second configuration, corresponding to the arch in the middle, are represented in the Figures 27–32. In particular Figures 27, 28 and 29 show front and plan views and cross-sections indicating accelerometer positioning in the first configuration, while the Figures 30, 31 and 32 represents the same drawings for the second. The third configuration, corresponding to the remaining lateral arch, is similar to the first one.

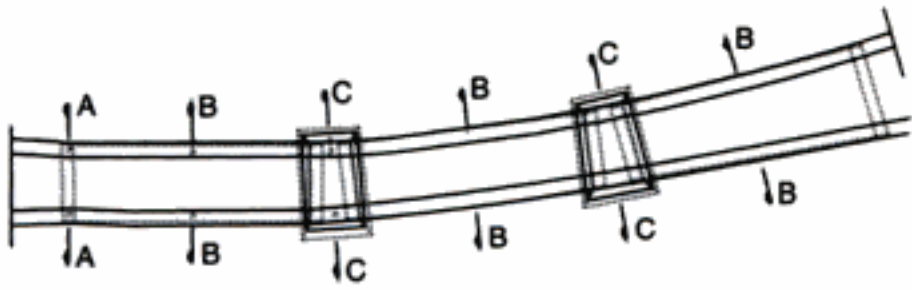


Figure 28. Plan view of the accelerometers arrangement; I configuration.

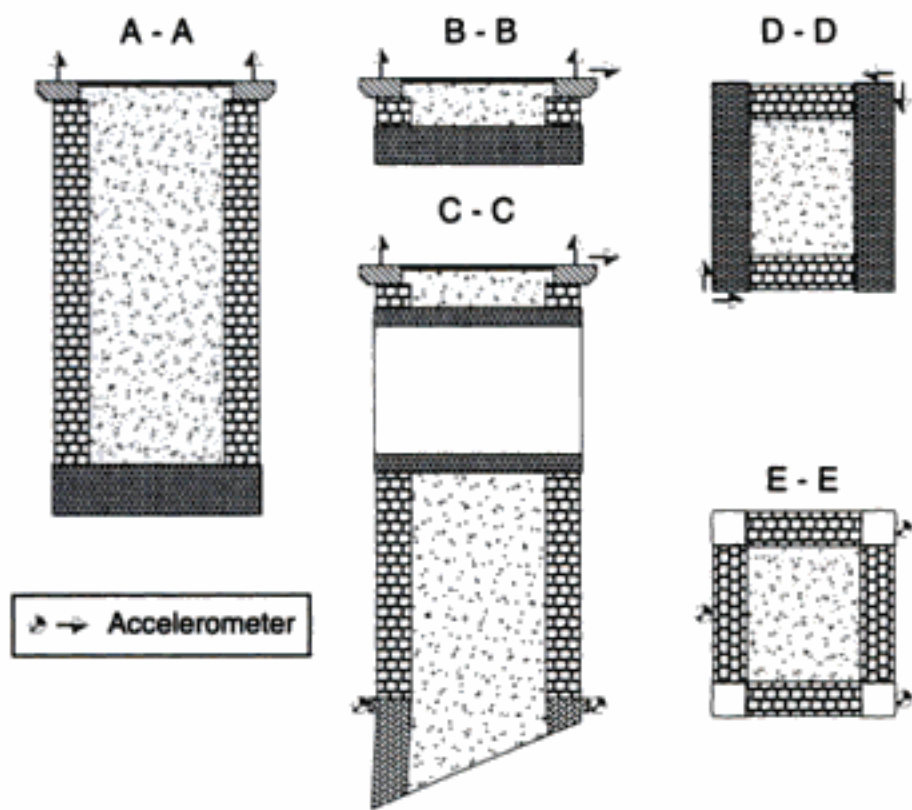


Figure 29. Accelerometers arrangement: cross sections; I configuration.

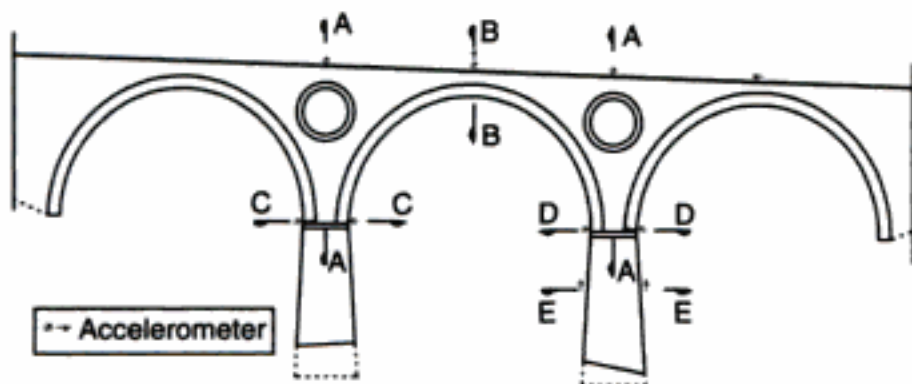


Figure 30. Front view of the accelerometers arrangement; II configuration.

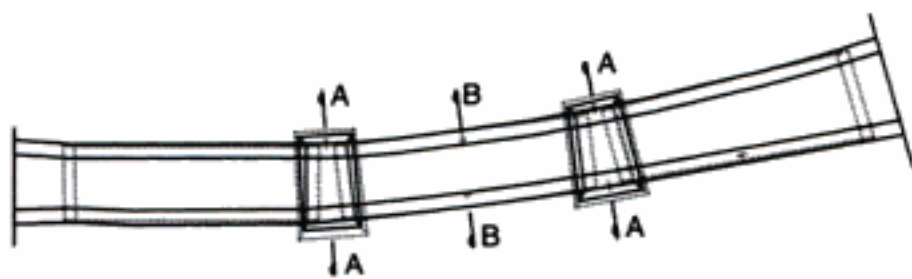


Figure 31. Plan view of the accelerometers arrangement; II configuration.

The recorded time response of the bridge in terms of horizontal acceleration measured in correspondence of the keystone of the middle arch, in the transverse direction, is represented in the Figure 33, referring to

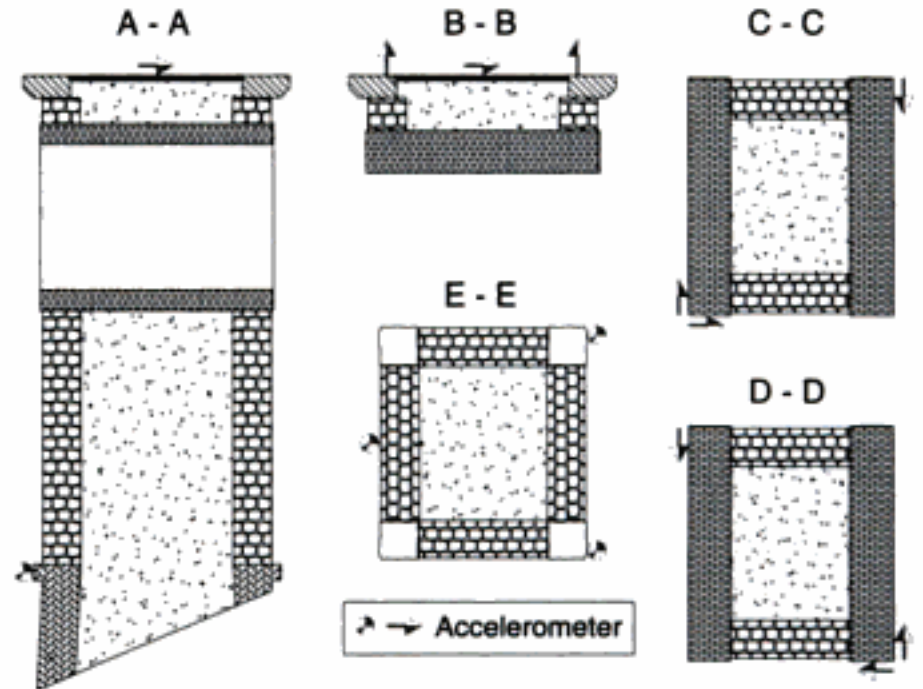


Figure 32. Accelerometers arrangement: cross sections; II configuration.

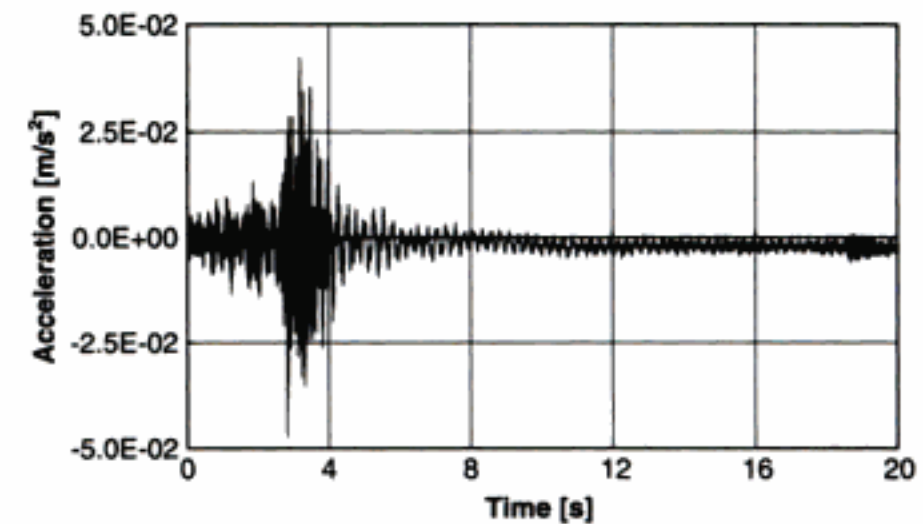


Figure 33. Time-variation measured law of the horizontal transverse acceleration in correspondence of the keystone of the middle arch; truck stopping just after the second imperfection.

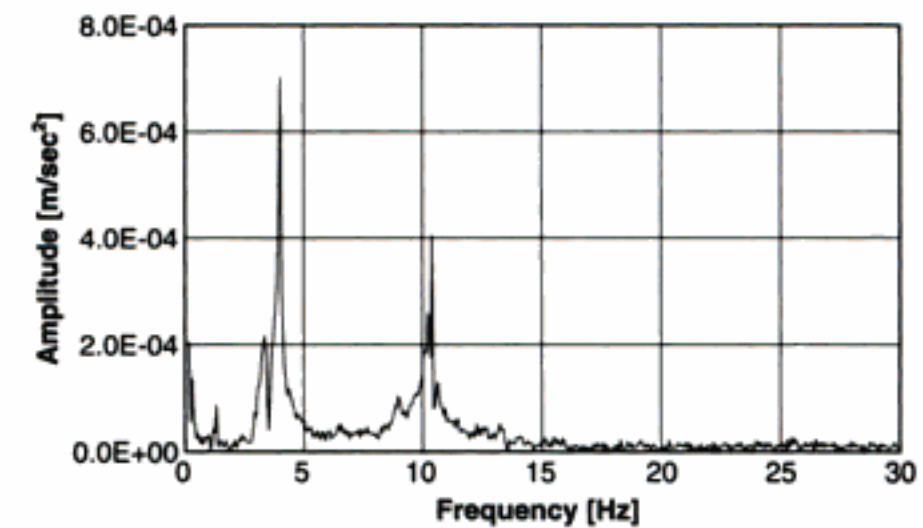


Figure 34. Fourier spectrum amplitude of the horizontal transverse acceleration in correspondence of the keystone of the middle arch; truck stopping just after the second imperfection.

the case of truck stopping just after the second surface imperfection.

In order to analyze the frequency content of the viaduct response, the Fourier transform of the same signal is represented in the Figure 34.

the second mode shape, and to the well definitions of all mode shapes, very close each other in some cases.

ACKNOWLEDGEMENTS

Authors are very grateful to the Municipality of Carrara for their help in performing tests.

REFERENCES

- Canali, D. 1995. *La ferrovia marmifera*. Cassa di Risparmio di Carrara, Carrara. (In Italian).
- Betti Carboncini, A. 1984. *I treni del marmo*. ETR Editrice Trasporti su Rotaie, Salò, Italy. (In Italian).
- Maia, N. M. M., Silva, J. M. M. 1997. *Theoretical and Experimental Modal Analysis*. Research Studies Press LTD, Baldock, Hertfordshire, England.

Structural integrity assessment of medieval towers

A. Carpinteri & G. Lacidogna

Department of Structural Engineering & Geotechnics, Politecnico di Torino, Italy

ABSTRACT: This investigation concerns the structural stability of two medieval buildings, “Torre Sineo” and “Torre Astesiano”, rising in the centre of Alba, a characteristic town in Piedmont (Italy). The geometrical and structural aspects of these masonry towers were analysed and tests were performed to assess the evolution of damage phenomena. The slant of the towers was determined with the customary topographic survey methods. NDT methods were used, instead, to determine the extent of damage and cracking and to assess the evolution of these phenomena over time. The damage processes underway in some portions of the masonry were monitored using the Acoustic Emission (AE) technique. The latter method makes it possible to estimate the amount of energy released during the fracture process and to obtain information on the criticality of ongoing processes. Finally, an *ad hoc* theory based on fractal concepts for assessing the stability of masonry structures from the data obtained with the AE technique is proposed.

1 INTRODUCTION

Non-destructive and instrumental investigation methods are currently employed to measure and check the evolution of adverse structural phenomena, such as damage and cracking, and to predict their subsequent developments. The choice of a technique for controlling and monitoring reinforced concrete and masonry structures is strictly correlated to the kind of structure to be analysed and the data to be extracted (Carpinteri & Bocca 1991; Binda et al. 2000). For historical buildings non-destructive evaluation (NDE) techniques are used for several purposes: (i) detecting hidden structural elements, such as floor structures, arches, piers, etc.; (ii) determining masonry characteristics, mapping the nonhomogeneity of the materials used in the walls (e.g., use of different bricks during the life of a building); (iii) evaluating the extent of the mechanical damage in cracked structures; (iv) detecting voids and flaws; (v) determining moisture content and rising by capillary action; (vi) detecting surface decay phenomena; and (vii) evaluating the mechanical and physical properties of mortar and brick, or stone.

This study addresses some of the afore-mentioned problems deemed of special significance. Towers geometry was defined through the customary survey methods. Damage, cracking and the evolution of these phenomena over time were assessed through a number of non-destructive techniques: thermographic exams were performed on the main sets of the towers subjected to cracking phenomena; tests with flat-jacks

were conducted in order to evaluate the range of stresses affecting the structures; at the same time, the cracking processes taking place in some portions of the masonry structures were monitored using the Acoustic Emission (AE) technique.

The AE technique has proved particularly effective (Carpinteri & Lacidogna 2001, 2002a, b, 2003), in that it makes it possible to estimate the amount of energy released during the fracture process and to obtain information on the criticality of the process underway. Strictly connected to the energy detected by AE is the energy dissipated by the structure being monitored. The energy dissipated during crack formation in structures made of quasi-brittle materials plays a fundamental role in the behaviour throughout their life. Strong size effects are clearly observed in the energy density dissipated during fragmentation. Recently, a multiscale energy dissipation process has been shown to take place in fragmentation, from a theoretical and fractal viewpoint (Carpinteri & Pugno 2002a, b, 2003). Based on Griffith's assumption of local energy dissipation being proportional to the newly created crack surface area, fractal theory shows that the energy will be globally dissipated in a fractal domain comprised between a surface and a volume in the Euclidean space. According to fractal concepts, an *ad hoc* theory is employed to monitor masonry structures by means of the AE technique. The fractal theory takes into account the multiscale character of energy dissipation and the strong size effects associated with it. With this energetic approach it becomes possible

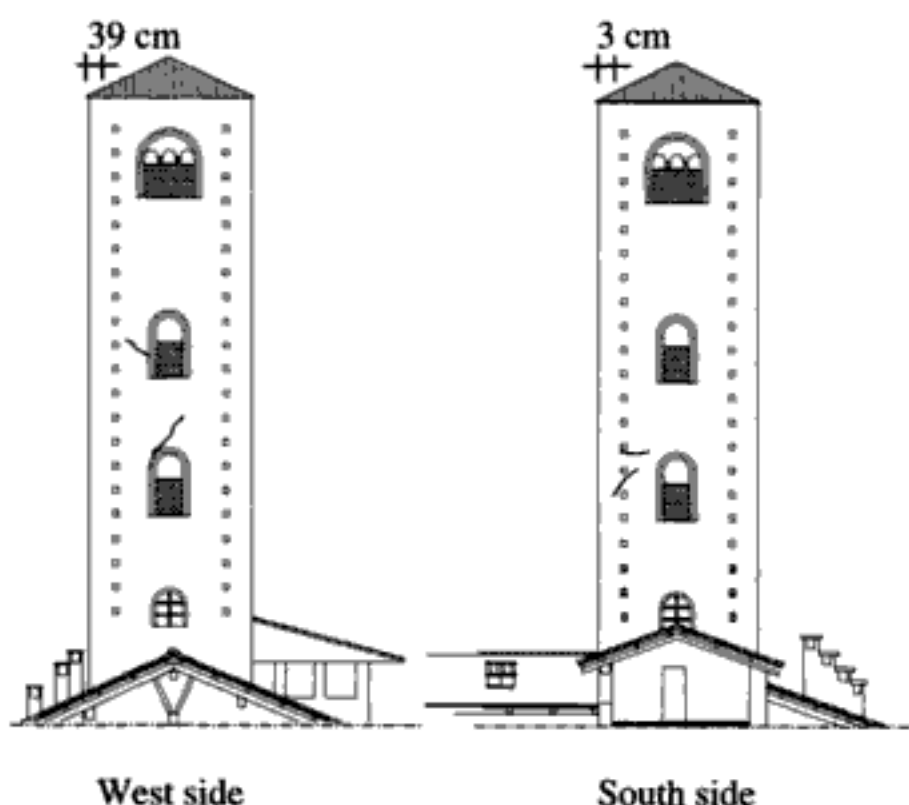


Figure 3. Torre Sineo. Elevations of two sides of the tower. Notice the presence of cracks near the openings and the deviation from verticality of the tower.

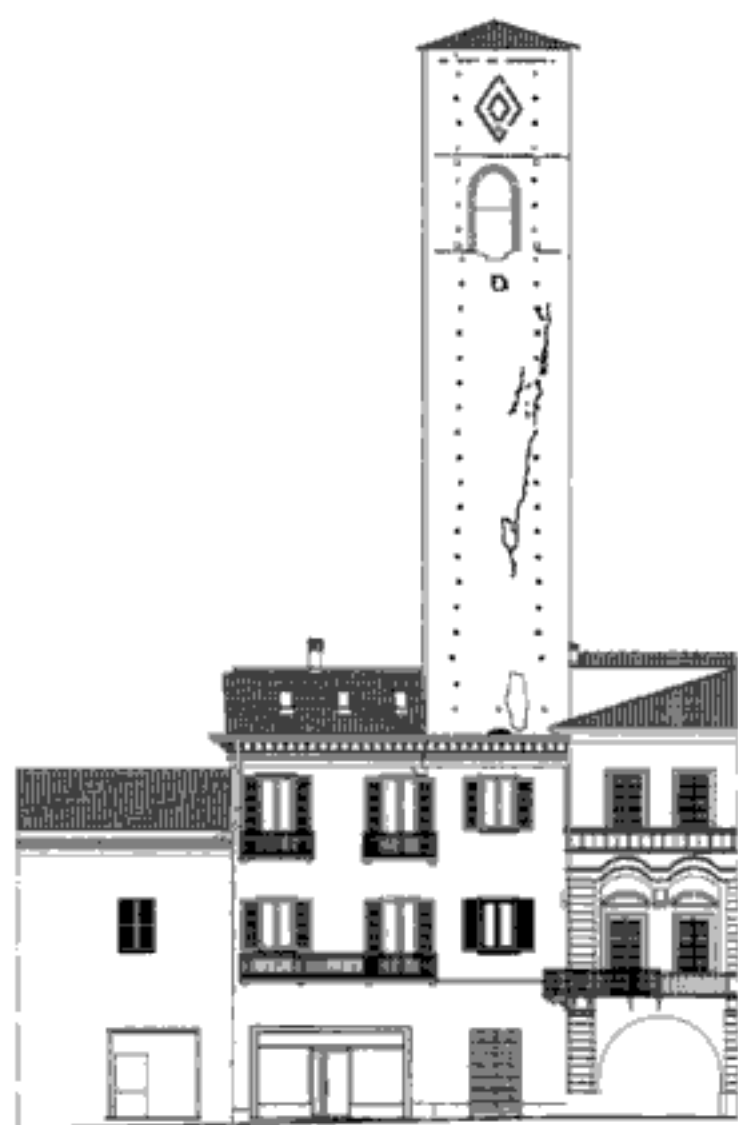


Figure 4. Torre Astesiano. Elevation view of the tower. Notice the presence of the main crack in the upper part of the tower.

designed to estimate stress values in the masonry at different levels and to assess the elastic modulus and failure strength in situ.

Compressive stresses in existing masonry structures are measured on site by inserting a thin, single flat-jack in a slot sawn into a mortar joint (ASTM, 1991a). This method is relatively non-destructive.

When a slot has been formed in the masonry, the compressive stresses present at that point cause the masonry above and below the slot to get closer. Accordingly, the compressive state of stress in the masonry can be measured by introducing a flat-jack into the slot and increasing the pressure applied until the original distance between the points above and below the slot has been restored: it corresponds approximately to the pressure applied by the flat-jack multiplied by factors accounting for the ratio, K_a , between the bearing area of the jack in contact with the masonry and the bearing area of the slot, and for the physical characteristic of the jack, K_m . The average compressive stress in the masonry, f_m , can be calculated as:

$$f_m = K_m K_a p, \quad (1)$$

where, p is the pressure required to restore the gauge points to their original distance. The double flat-jack test provides a relatively non-destructive method for determining the deformation properties of existing non-reinforced solid-unit masonry (ASTM, 1991b). The test is carried out by inserting two flat-jacks into parallel slots, one above the other, in a solid unit masonry wall. By gradually increasing the flat-jack pressure, a compressive stress is induced in the masonry comprised in between. The stress – strain relation can thus be obtained by measuring the deformation of the masonry. If the test is continued to local failure, it is also possible to determine the compressive strength, but this may damage the masonry area adjacent to the flat-jacks. The tangent stiffness modulus for any stress interval can be obtained as follows:

$$E_t = \frac{d\sigma_m}{d\varepsilon_m}, \quad (2)$$

where, $d\sigma_m$ is the increment of stress, and $d\varepsilon_m$ is the increment of strain. On the other hand, the secant modulus is given by:

$$E_s = \frac{\sigma_m}{\varepsilon_m}, \quad (3)$$

where, σ_m and ε_m are the stress and the strain in the masonry.

For Torre Sineo, vertical stress and the elastic modulus were determined on site at two different height levels, according to the scheme shown in Figure 5. The results are summarized in Figure 6 and Table 1.

Vertical stress and elastic modulus were also measured for the Torre Astesiano at different levels, according to the scheme shown in Figure 7. The results are summarized in Table 2.

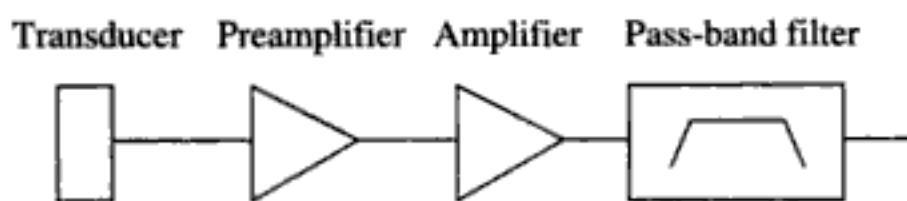


Figure 10. Acoustic Emission measurement system.

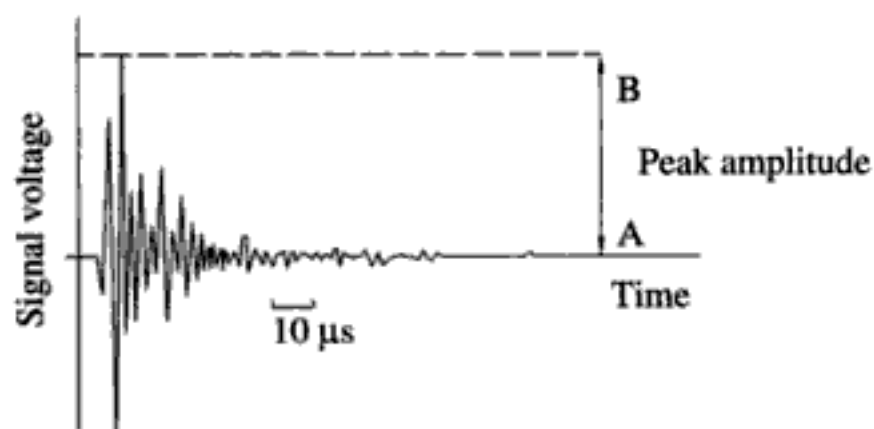


Figure 11. AE signal identified by the transducer.

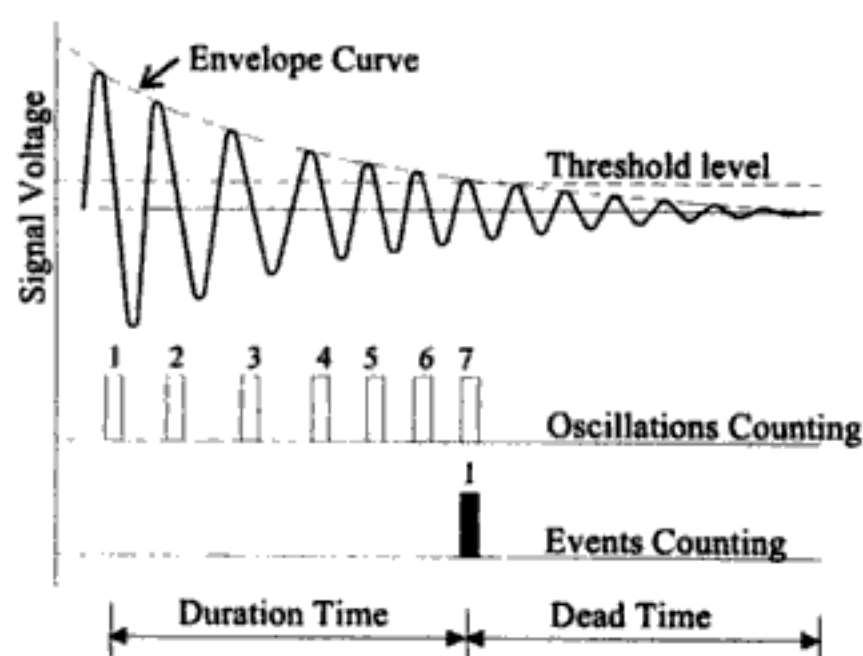


Figure 12. Counting methods in AE technique.

it is then filtered to eliminate unwanted frequencies, such as the vibrations caused by the mechanical instrumentation, which are generally lower than 100 kHz. Up to this point the signal can be represented as a damped oscillation. The signal is then analysed by a threshold measuring unit which counts the oscillations exceeding a certain voltage value.

This method of analysis is called Ring-Down Counting and is broadly used for the identification of defects with the AE technique. As a first approximation, the counting number, N , can be correlated to the quantity of energy released during the loading process and it can be assumed that the corresponding increments grow proportionally to the crack length. This technique also considers other procedures. For instance, by keeping track of the characteristics of the transducer and, in particular, of its damping, it is possible to consider all the oscillations produced by a single AE signal as unique events and to replace Ring-Down Counting with the Counting of Events (Fig. 12).

3.6 AE data acquisition system

The AE monitoring equipment adopted by the authors consists of PZT transducers fitted with a preamplifier and calibrated on inclusive frequencies between 100 and 400 kHz. The transducers are connected to switchboards equipped with a amplifier and a pass-band filter, a threshold level measuring unit, a recorder and an oscillation counter. The threshold level of the signal recorded by the system, fixed at 100 μ V, is amplified up to 100 mV.

The amplification gain, i.e. the output voltage (E_u) to input voltage ratio (E_i), according to the relationship $\text{dB} = 20 \log_{10} (E_u/E_i)$, turns out to be 60 dB. This is the signal amplification value usually adopted for the survey of AE events in concrete and in masonry structures. The oscillation counting capacity is limited to 255 every 120 seconds of signal recording. In this way a single *event* is the result of 2 recorded minutes.

Since, as specified in the literature, the maximum amplitude of direct non-amplified signals is about 100 μ V, neglecting the attenuation phenomena due to the distance from the point of generation of the signal, it can be assumed that the measuring system can detect only the most significant AE events reflecting the cracking of the material. With this system, the intensity of a single event is by definition proportional to the number N recorded in the time interval (Event Counting). Clearly, this hypothesis is fully justified at the occurrence of slow-crack growth (Holroyd, 2000).

4 AE DAMAGE DETECTION OF THE TOWERS

For the Sineo Tower, through AE monitoring, two cracks were detected in the inner masonry layer at the seventh floor level (Fig. 3): one next to a window and another nearby. The monitoring process revealed an on-going damaging process, characterized by slow crack propagation inside the brick walls. In the most damaged zone, crack spreading had come to a halt, the cracks having achieved a new condition of stability, leading towards compressed zones of the masonry.

In this particular case it can be seen that, in the zone monitored, each appreciable crack advance is often correlated to a seismic event. In the diagram shown in Figure 13, the cumulative AE function relating to the area monitored is overlaid with the seismic events recorded in the Alba region during the same time period; the relative intensity of the events is also shown. Seismic event data were provided by the National Institute for Geophysics and Volcanology in Rome. It can be seen that the behaviour of the tower is stable when the structure is subjected to vertical loads alone, whereas the structure is unable to respond elastically to shaking or horizontal actions.

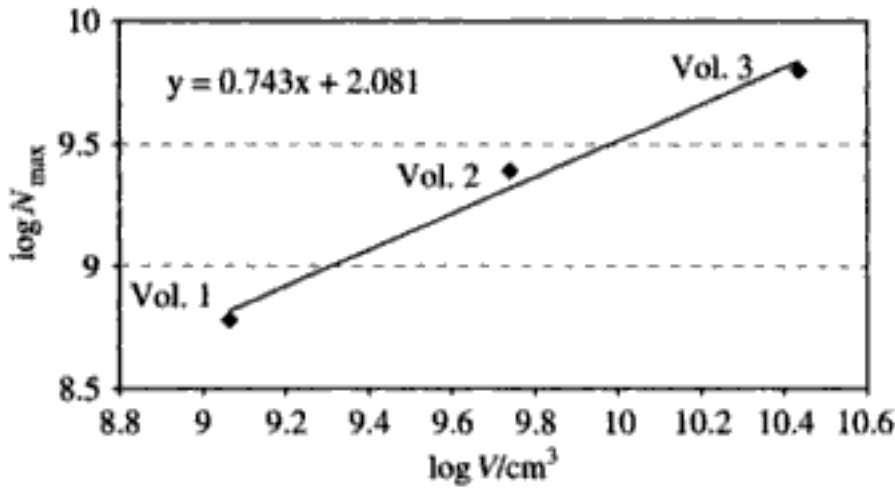


Figure 18. Volume effect on N_{max} .

experimental data, parameters D and Γ_{AE} (eq. (6)) can be quantified. Parameter D represents the slope, in the bilogarithmic diagram, of the curve correlating N_{max} to specimen volume. By best-fitting, we obtain $D/3 \cong 0.743$ (Fig. 18), so that the fractal exponent, as predicted by fragmentation theories, turns out to be of between 2 and 3 ($D \cong 2.23$). Moreover, the critical value of fractal AE density turns out to be: $\Gamma_{AE} \cong 8.00 \text{ cm}^{-2.23}$.

4.4 Damage level of the monitored volumes

During the observation period, which lasted 60 days for the Sineo Tower and 146 days for the Astesiano Tower, the number of AE events recorded for the former was $N \cong 2250$ (Fig. 13), and for the latter it was $N \cong 9000$ (Fig. 14). Through earlier tests performed on rubble filled masonry, 80 cm thick, and hence characterised by appreciable discontinuities, it was ascertained that the transducers were able to pick up the AE signals from a distance of up to 10 m from their points of application (Carpinteri & Lacidogna 2002b) and to a depth of 12 cm, i.e., over a length corresponding to the thickness of the outer layer of bricks.

Since the average width of the sides of the towers is about 500 cm, the total volume monitored by the transducers will be: $V \cong 500 \times 2000 \times 12 = 1.2 \times 10^7 \text{ cm}^3$. From eq. (6), using fractal exponent $D \cong 2.23$ and the critical value of fractal acoustic emission density, $\Gamma_{AE} \cong 8.00 \text{ cm}^{-2.23}$, we obtain a critical AE number of $N_{max} \cong 1.46 \times 10^6$. Introducing the values of N and N_{max} into eq. (8), we get $\eta \cong 0.154\%$ for Torre Sineo and $\eta \cong 0.616\%$ for Torre Astesiano. These values represent, in percentage terms, the amount of energy released with respect to the energy that would cause the ultimate damage of the monitored volumes.

Finally, in order to obtain indications on the rate of growth of the damage process in the towers, as given in eq. (9), the data obtained with the AE technique were subjected to best-fitting in the bilogarithmic plane. For the Sineo Tower, this yielded a slant $\beta_t \cong 0.648$, for the Astesiano Tower $\beta_t \cong 1.041$.

These results confirm how the damage process stabilised in the Sineo Tower during the monitoring

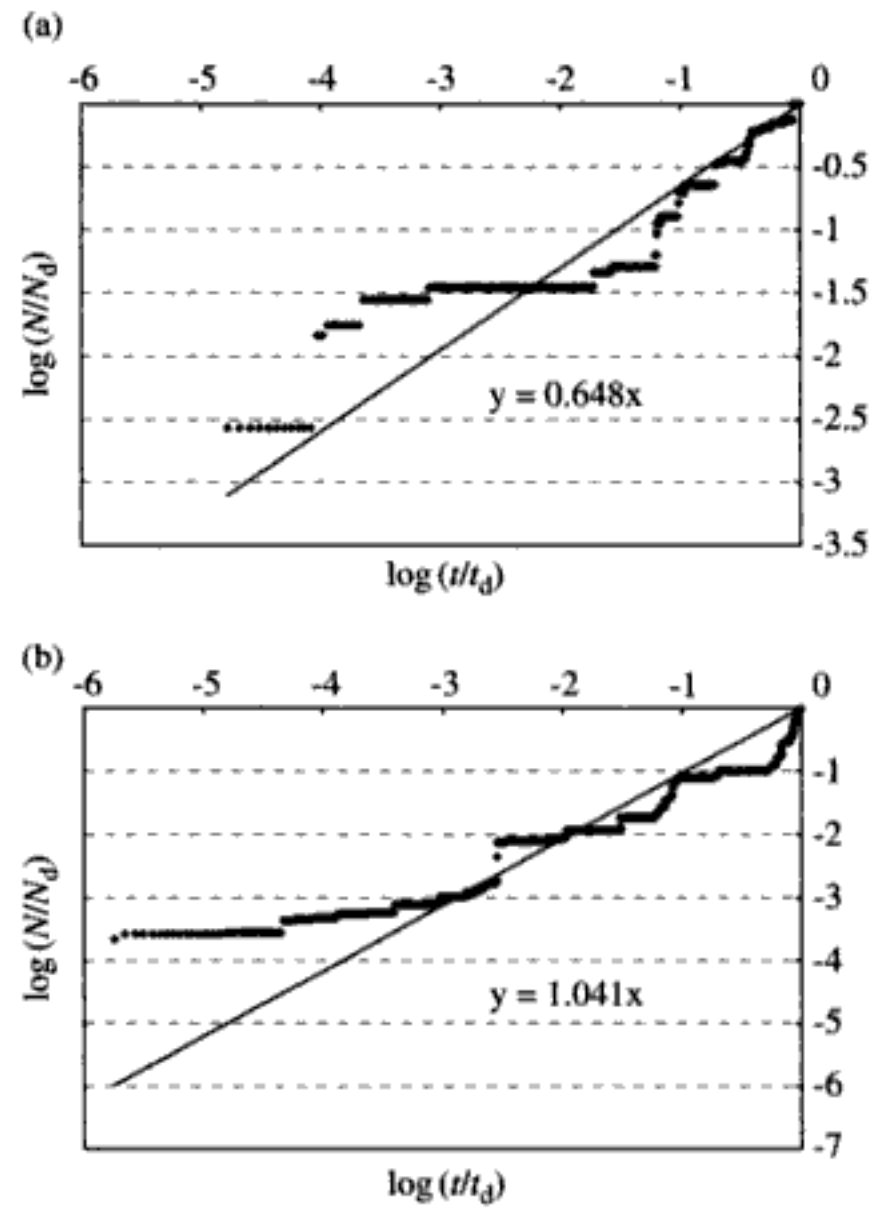


Figure 19. Evolution of damage: Torre Sineo (a), Torre Astesiano (b).

period, whereas for the Astesiano Tower it evolved towards a condition of instability according to a quasi-linear progression over time. In fact, if we introduce the values of N and N_{max} obtained for Torre Astesiano into eq. (9), with $\beta_t = 1.041$, we get $t/t_{max} \cong 7.532 \times 10^{-3}$. The lifetime of this structure is therefore defined, in terms of time before the maximum number of AE events is reached in the analysed zone, at about 53 years.

5 CONCLUSIONS

In view of the appreciable number of old structures still in use today, more attention should be paid to preservation and rehabilitation issues. A sound safety assessment cannot be based solely on the visual observation of cracks and signs of damage in structural elements. The evolution and interaction of different damage phenomena should be considered instead. This is why structural monitoring is taking on ever greater importance in the whole process of reliability assessment: in this connection, the AE technique can be highly effective.

This technique makes it possible to introduce a useful energy-based damage parameter for structural assessment which establishes a correlation between AE activity in a structure and the corresponding

Experimental and numerical analysis of the structural behaviour of St Stefano's bell-tower in Venice

A. Lionello & I. Cavaggioni

Landscape and Architectural Heritage Office, Venice

C. Modena & F. Casarin

Department of Constructions and Transportations Engineering, University of Padova

P.P. Rossi & C. Rossi

R.teknos s.r.l., Bergamo

ABSTRACT: The paper illustrates the results of two series of in situ tests for the analysis of the mechanical behaviour of the masonry structures: flat-jack tests, coring and video camera survey as well as a detailed crack-pattern survey. All the tests were carried out with the aid of climbers, without any kind of scaffolding. An automatic monitoring system was installed, including direct pendulum, crack-gauges, long-base extensometers, clinometers and thermal gauges for measuring air and masonry temperature. The diagrams of the measures recorded during a period of about two years are presented. A FE model was implemented in order to better interpret the results of both the experimental investigations and the monitoring.

1 FOREWORD

The construction of St. Stefano's bell-tower, facing the Malatin canal on the south-west side, started in 1450; the first stage of the construction was interrupted when the bell-tower was 27 m high due to an initial tilting movement of the tower, than in 1550 the second section was built following a different inclination: nevertheless it is not recognizable any discontinuity between the two masonry structures either relating to the structural characteristics or to the architectural language.

The St. Stefano's bell-tower is a single pipe structure with a squared plan (side 7.25 m); the thickness of the masonry at the level of the basement is 1.83 m and it reduces, by following offsets, to 0.95 m measured at the top of the tower. The construction is 61.90 m high and it measures 44 m up to the level of the bell's cell.

The first evidence of a leaning of 0.80 m towards the east-west side, dates 1774; in 1900 it was observed a sensible increasing of the leaning (about 7 mm per year) which leads the deviation from verticality to 1.70 m, measured at the level of the bell's cell.

After the fall of St. Marco's bell-tower the 14th of July 1902, the governmental commission, entrusted to verify the stability of St. Stefano's bell-tower, being seriously worried about the leaning, decided

to proceed with the demolition of the second section of the tower and ordered to build up the scaffolding necessary for the works.

Following sharp discussions about St. Stefano's bell-tower, the municipality decided to consult a second technical commission including the engineers Caselli and Antonelli from Turin; considering that the leaning was increasing homogeneously since long time without any recent impulse, the commission decided that it was possible to proceed with the conservation and the consolidation of the bell-tower in spite of the decay of the structure in some parts and partial failures in the foundation structures. Many proposals for the consolidation of the tower were submitted to the Municipality which finally charged, for the design and the direction of the works, the engineers Caselli and Antonelli who proposed both the consolidation and the strengthening of the bell-tower in order to guarantee its stability.

2 THE RESTORATION AND STRENGTHENING INTERVENTION OF 1904

The consolidation works carried out in 1904 are fully illustrated through the drawings and the technical reports produced by the designers, and by the daily

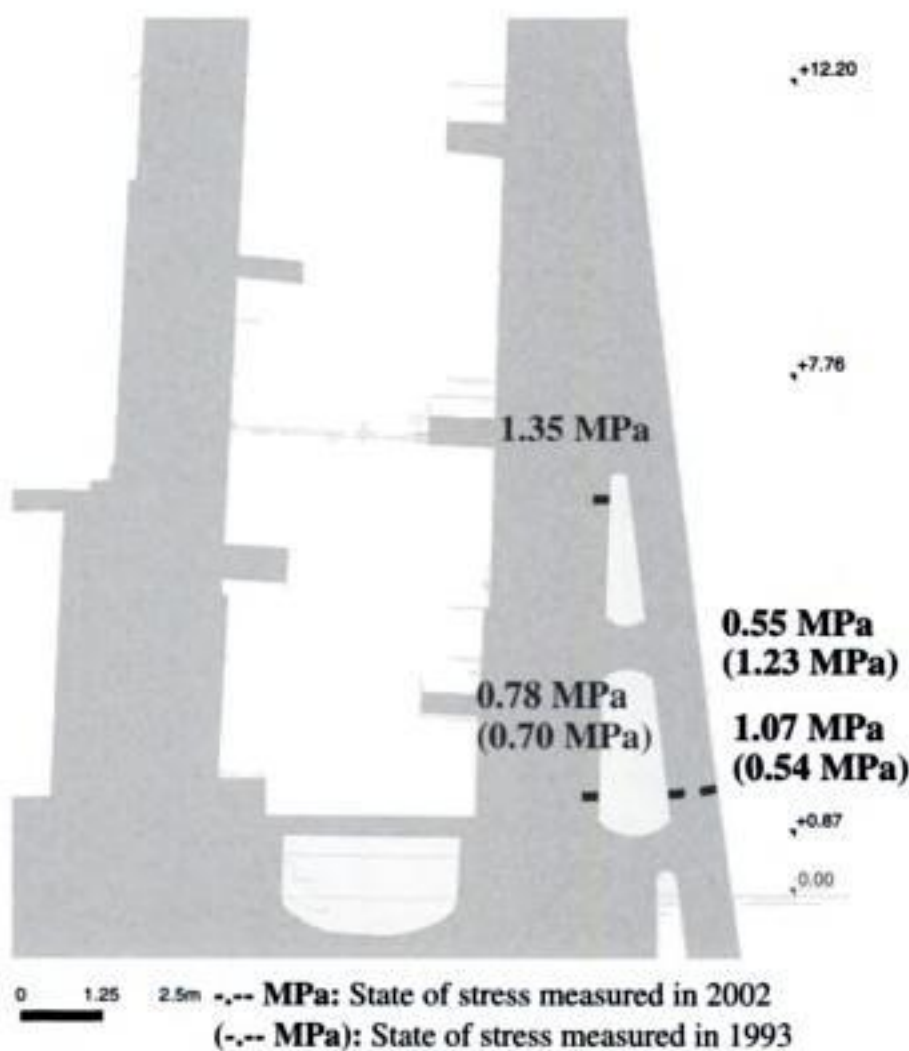


Figure 3. Measure of the state of stress in the east side of the bell-tower by flat-jack technique: comparison between the stress values measured in 2002 and 1993.

0.55 MPa. At the base of the east side of the tower the stress is nearly the same. The redistribution of the stresses in the buttresses could be partially related to the movements of the bell-tower in the period (9 years) between the two testing phases.

4 NUMERICAL MODEL

4.1 Description of the model

A 3-D FE model was chosen to evaluate the structural behaviour of St Stefano bell-tower. In particular the modelling aimed at detect the changing, in terms of principal compressive stresses, noticed in the masonry buttresses.

The model includes 17,650 brick and 540 shell plate elements, these last used for the belfry. The average dimension of the solid elements is 0.4 m in the buttresses, 0.5 m in the lower masonry walls of the tower, 1.0 m in the central/upper part.

The mechanical properties chosen to describe the materials follow the results of previous tests performed on the masonry structures. According to the experimental investigations, three sets of material properties were used. In particular, a Young modulus of 4000 MPa was chosen for the lower part of the bell-tower (from the foundations up to a height of 27 m), while for the upper elements an elasticity modulus of 2800 MPa was considered. A slightly higher elasticity modulus (5000 MPa) was assigned to the buttresses, dating back

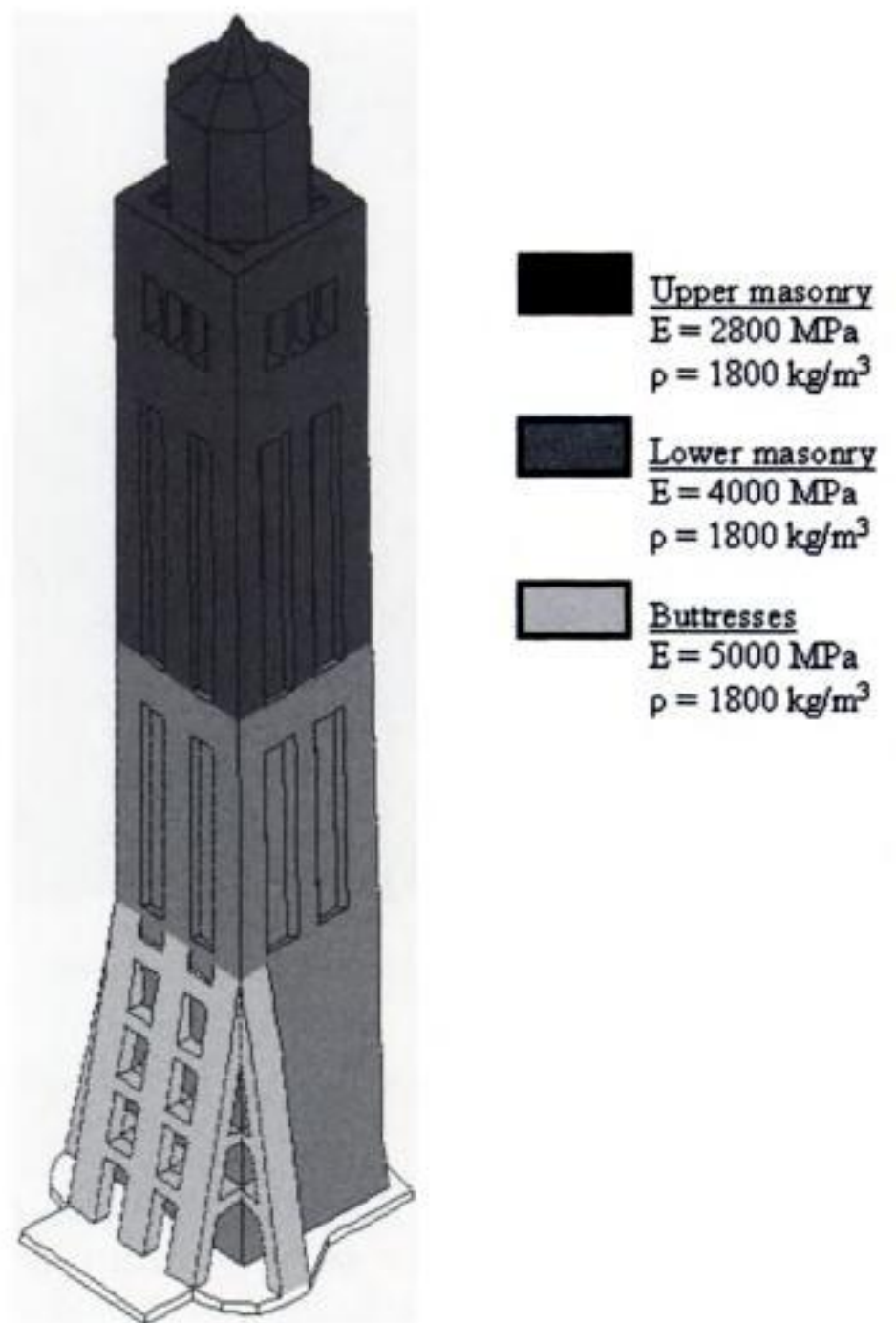


Figure 4. The 3-D model, materials and parameters.

to 1904. The density of all the sets of material (brick masonry) was kept constant and equal to 1800 kg/m^3 (Fig. 4).

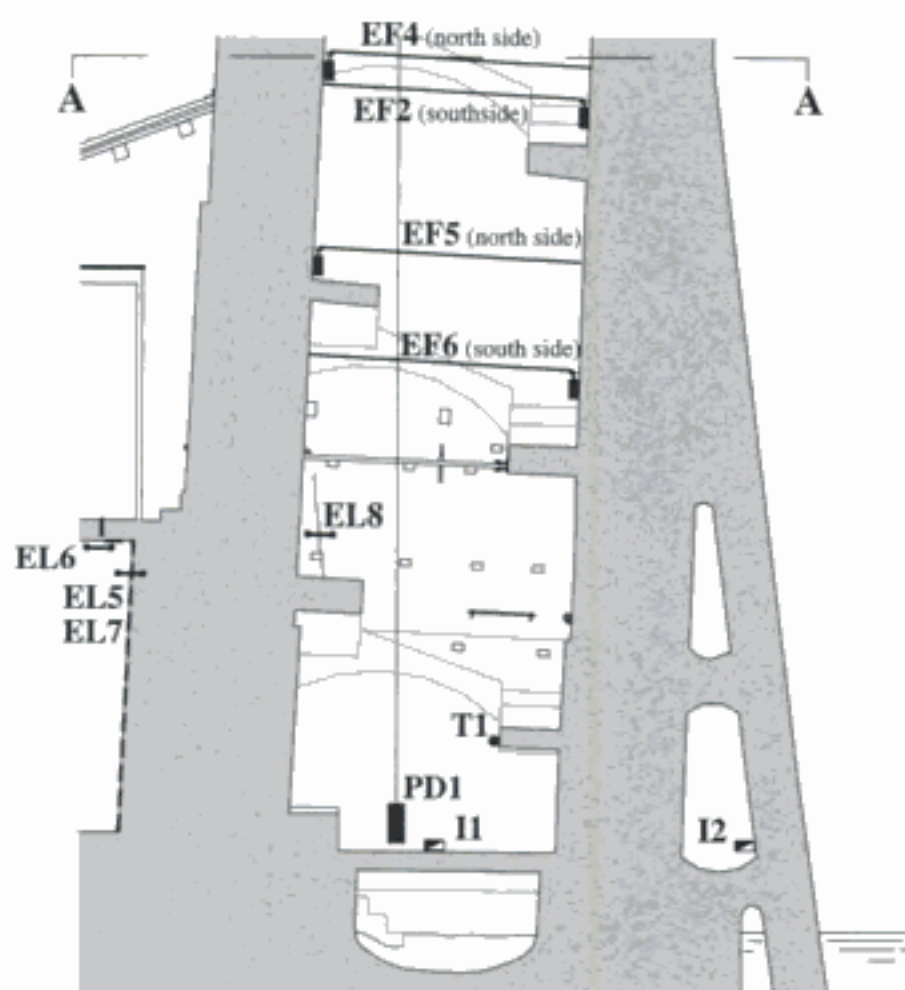
Firstly, the model was used to assess the mechanical behaviour of the tower in the year 1994, when the first measuring campaign was carried out. According to the survey results, the starting model presents an out of plumb, at the height of 44 m, of 1.98 m in the East direction, and of 0.12 m towards South.

Subsequently, different restraint conditions were imposed at the base of the model to fit the geometry of the bell-tower in 2002, according to the displacement tendency recorded by the direct pendulum. At the height of 44 m, an increase in terms of out of plumb of 10 and 2 mm towards East and South were considered, respectively.

4.2 Results of the modelling – 1994/2002

The analyses carried out, for both the models simulating the structural behaviour of the bell-tower in 1994 and 2002, are linear elastic.

The limits of a linear elastic analysis in identifying a masonry structure are well known, see Lourenço



SECTION A-A

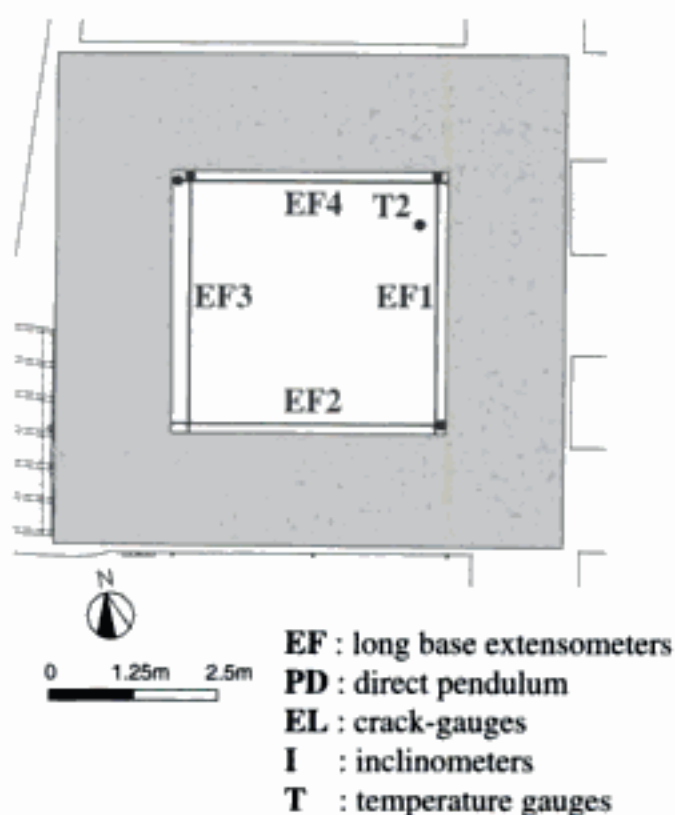


Figure 7. Scheme of installation of the instruments of the structural monitoring system.

5 MONITORING SYSTEM

As mentioned in paragraph 1, the movements of the bell-tower started just after the construction and were measured in 1770 and 1900. In 1904 a direct pendulum was installed and allowed an easier and more frequent control of the movement of the tower.

In 2001 the total deviation from the verticality of the bell-tower was 1.99 m.

The progressive movement which is involving the bell-tower advised the installation of a structural

automatic monitoring system able to check in real time the deformation behaviour of the tower.

The monitoring system, installed in 2001, includes the following instruments (Fig. 7):

- direct pendulum equipped with automatic teleco-ordinometer, for the measure of the absolute horizontal movements of the top of the tower at the level of the bell's cell (44 m);
- 6 long base extensometers which invar wire kept in tension by a weight, installed in two horizontal sections of the tower in order to measure the relative displacements between the opposite walls;
- 8 crack-gauges installed on the main vertical cracks of the tower and on the joint between the tower and the adjoining buildings on west side;
- 2 inclinometers for the measure of tilting at the base of the tower and at the base of the concrete plate which supports the buttresses;
- several thermal-gauges to measure the temperature of the air (internal and external) and inside the masonry at different depths from the outer wall.

All the instruments are connected to an automatic data acquisition and recording system which is equipped with a modem to transfer the data to a remote controller.

The scheme of installation of the main instruments is shown in Figure 7.

It must be pointed out that, in the designing phase of the monitoring system, the principle of "redundancy" was respected in order to have several instruments able to give information on the main movements of the tower.

6 ANALYSIS AND INTERPRETATION OF THE MONITORING SYSTEM DATA

The methodological approach for the analysis of the structural monitoring system data aimed at highlighting the deformation behaviour of the bell-tower by evaluating the trend of deformations.

Direct analysis of the time-history diagrams of each instrument allows an evaluation of the main characteristics of the phenomena involved, such as the main periodicities, the amplitude variations of the signal recorded, correlation with temperature measurements, possible significant strain trends, signal irregularities and interruptions. For example, Figure 8 shows the diagrams of the temperature of the air inside the tower and of the two components of the absolute horizontal movements of the top of the tower measured by the direct pendulum. In the diagrams the average daily values are plotted. This direct analysis is also important for planning numerical elaborations.

The methodological approach proposed for signal analysis of the static monitoring system data, illustrated in Figure 9, includes signal analysis, evaluation

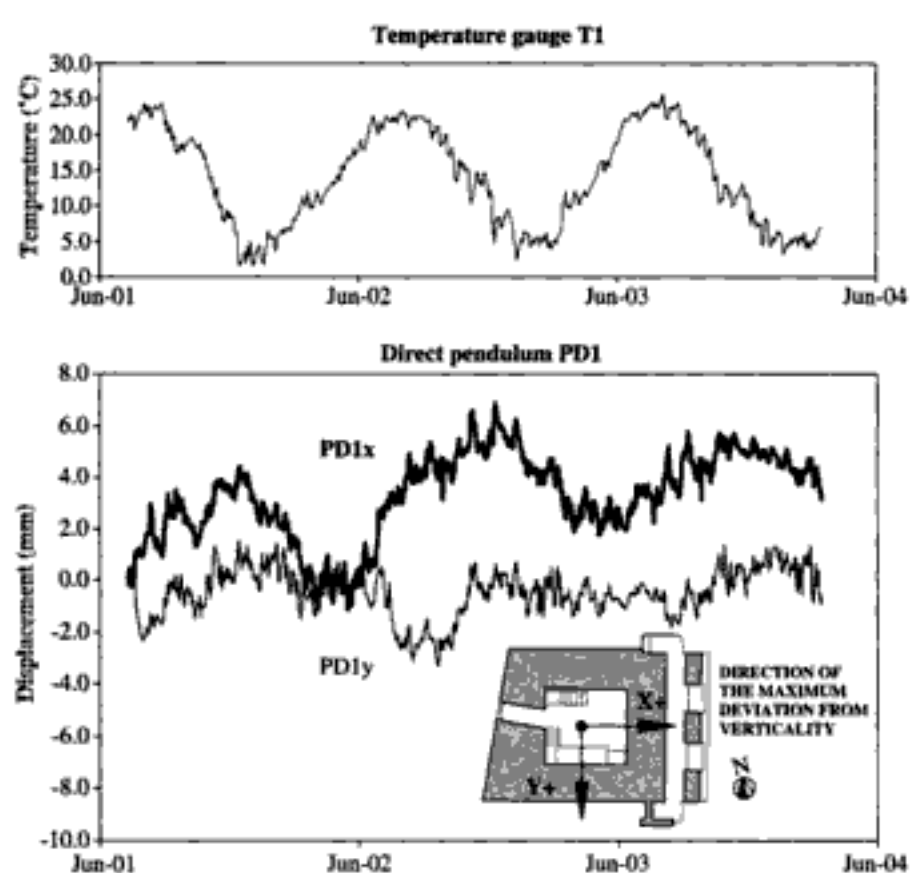


Figure 8. Diagrams of the data of the temperature gauge T1 and of the two components of the absolute horizontal movements of the top of the tower measured by the direct pendulum. The average daily values are reported.

of signal's harmonic component and evaluation of the signal trend.

Data processing can be described according to the following steps:

- 1) Signal irregularities and interruption: the elimination of signal interruption is an indispensable operation for any kind of data processing for frequency domain analysis. The irregularities are removed by cleaning the signal of anomalies due to accidental impacts against the instruments. These anomalies can cause an interpretation that does not correspond to the real phenomenon.
- 2) Treatment of signal for non stationarity: the signal analysis proposed is based on the assumption of stationarity of the stochastic process that represent the phenomenon. Thus, the signal must be made stationary.
- 3) Signal frequency analysis: this operation, consisting in the identification of the main periodicities of the phenomenon, is carried out analyzing the frequency characteristics of the signal by a transformation from time domain to that of frequency.
- 4) Main periodicities removal: this step involves filtering the signal in the frequency domain. This operation is analogous to treating the signal in time-domain by subtracting a sinusoid, containing the main period of the signal after having treated it for non stationarity.
- 5) Deformation trend estimation from filtered signal: the removal of main periodicities of the signal permits the use of a "least squares" linear regression to evaluate the annual deformation trend of the signal.

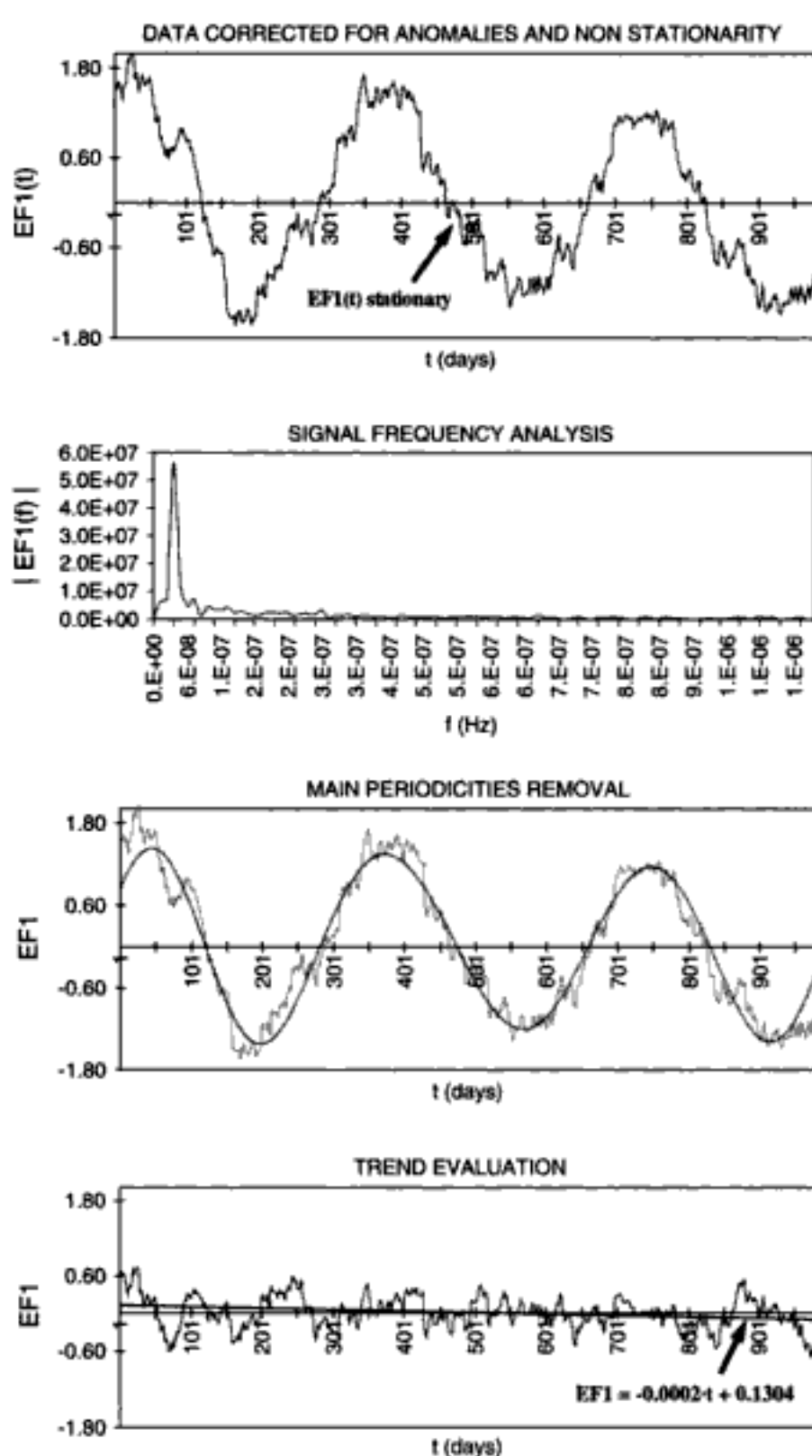


Figure 9. Methodological approach for signal analysis described for the data coming from the long base extensometer EF1. The analysis is implemented by the following steps: elimination of irregularities and non stationarity of the signal; signal frequency analysis; main periodicity removal by filtering the signal (in this case the main periodicity is about 341 days corresponding to a frequency of $3.39E-8$ Hz); trend evaluation by "least squares" linear regression. This trend obtained is pertinent to the stationary process: the real trend can be obtained by considering the method used to render signal stationary.

This trend is pertinent to the stationary process: the real trend can be obtained by considering the method used to render signal stationary.

In Figure 10, the results obtained for the direct pendulum (component in direction of maximum deviation from verticality) are shown.

The values of the annual trend estimated for the static monitoring system signals are presented in Table 1. The same analysis implemented for the temperature gauge T1 and T2, measuring the air

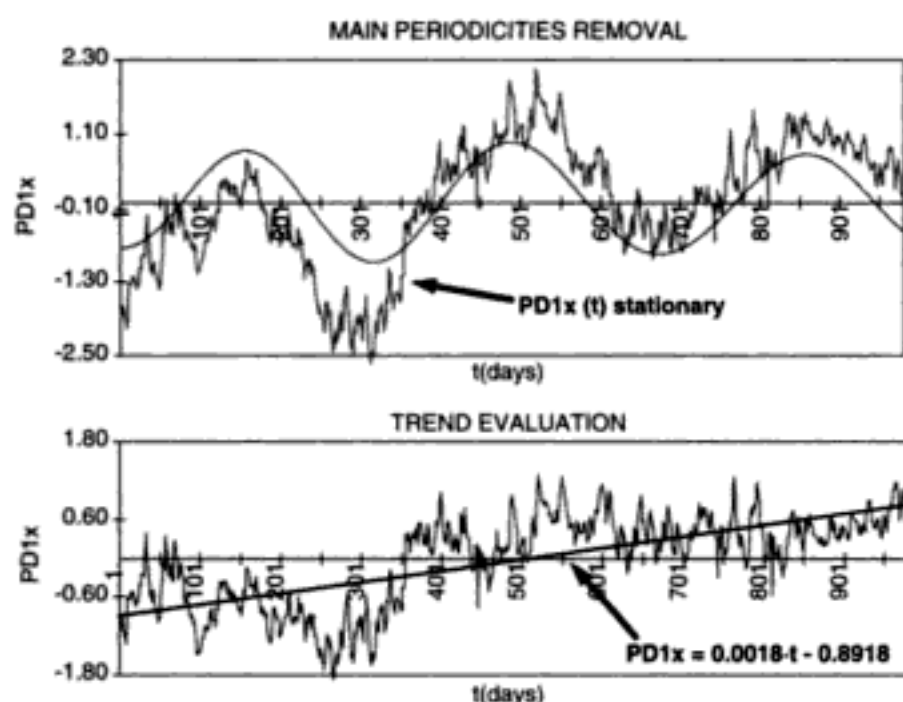


Figure 10. Signal analysis implemented for the direct pendulum (component in direction of maximum deviation from verticality). The trend of 0.0018 1/day obtained is pertinent to the stationary process: the real trend can be obtained by considering the method used to render signal stationary; for the X-component of the pendulum the real trend is 1.076 mm/year.

Table 1. Annual deformation trends.

Measurement device	Number	mm/year
Direct pendulum	PD1x	1.076**
	PD1y	0.218**
Long base extensometer	EF1	-0.022
	EF2	-0.044
	EF3	-0.014
	EF4	-0.022
	EF5	-0.021
	EF6	-0.021
Crack-gauges	EL1	0.013
	EL2	0.022
	EL3	0.008
	EL4	0.010
	EL5	0.063**
	EL6	0.235**
	EL7	0.139**
	EL8	0.005
Inclinometers	I1	-0.011*,**
	I2	-0.010*,**

* mrad/year.

** trends which are meaningful, according to the transducers' accuracy.

For the long base extensometer a positive (+) trend means a increase of the distance between the vertical walls; for the crack gauges a positive (+) trend means an opening of the crack; for the inclinometers a positive (+) trend means a tilting toward the maximum deviation from verticality; for the pendulum a positive (+) trend means a increase of horizontal movement of the top of the bell-tower in the directions of the maximum deviation from verticality, in according to the scheme of Figure 3.

temperature inside the bell-tower, gave as a result a trend of the temperature close to zero.

This means that a correction of the deformations trend of the tower, due to the influence of the temperature trend, was not needed.

In Table 1 are evidenced the annual trends which are meaningful according to the accuracy of the transducers of the instruments.

The analysis of the calculated trends clearly shows that the bell-tower is moving as a rigid body tilting at the base in the direction where the deviation of verticality is maximum:

- the absolute horizontal movements of the top of the bell-tower, measured by direct pendulum, shows a significant trend which is about 1.08 mm/year in the direction of maximum deviation from verticality (X-component) and 0.22 mm/year in the Y-component.
- all the long-base extensometers EF1÷EF6 and the crack-gauge EL1÷EL4 and EL8, installed on the bell-tower leafs, do not show significant deformation trends;
- the crack-gauges EL5, EL6 installed on the joint between the tower and the vertical walls of adjacent building, show a positive trend of opening of the joint with an average value of 0.10 mm/year;
- the inclinometers show a trend of the rotation of about 0.011 mrad/year toward the direction of maximum deviation from verticality.

7 CONCLUSIONS

The analysis of the data obtained by the monitoring system during the first three years of observation clearly shows that the bell-tower is moving like a rigid body which is tilting at the base. The moving of the cracks as well as the relative movements of the opposite faces of the tower is only influenced by temperature changes and no significant trend due to other causes is observed.

The absence of significant trends of the transversal deformation of the tower means that the steel chains which tie the tower are able to guarantee a sufficient confining effect.

It must be pointed out that after the installation of the monitoring system new chains made of high-resistance cables were installed by climbers in order to guarantee a reliable confining effect able to eliminate the transversal deformation of the tower.

On the contrary, the absolute horizontal movements of the tower, measured by direct pendulum, show a significant trend which is about 1.08 mm/year in the direction of maximum deviation from verticality. This value is a little bit higher than the value (1.0 mm/year) measured by the old pendulum which was installed

Analytical and numerical approaches

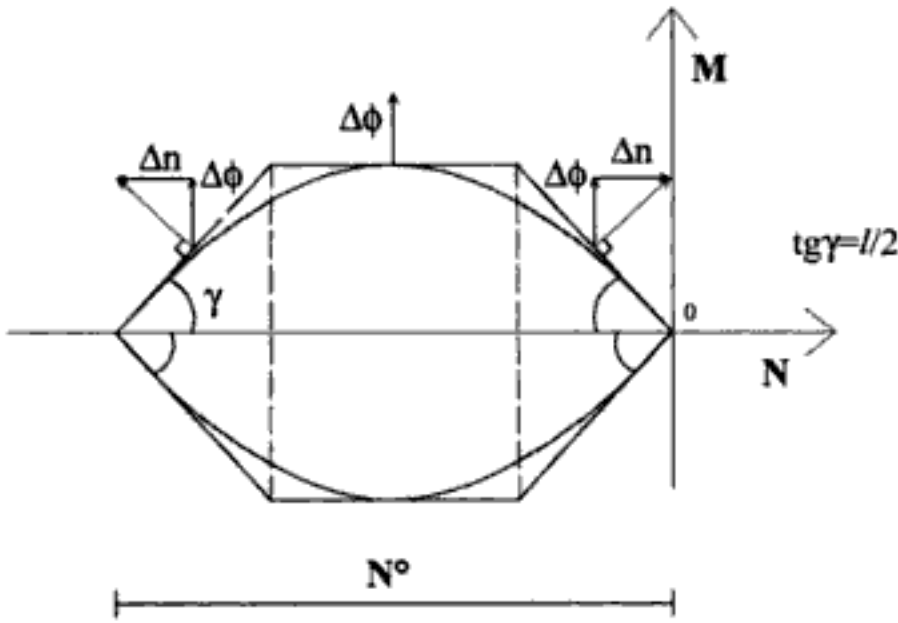


Figure 5. Limit surface for rocking (circumscribed polygon).

Instead, when a limited compressive strength is supposed, we have two formulations according to the kind of linearized domain:

$$\begin{bmatrix} \operatorname{tg}\varphi_0 & 1 & 0 \\ \operatorname{tg}\varphi_0 & -1 & 0 \\ 1/2 & 0 & 1 \\ 1/2 & 0 & -1 \\ 0 & 0 & 1 \\ 0 & 0 & -1 \\ -1/2 & 0 & 1 \\ -1/2 & 0 & -1 \end{bmatrix} \cdot \begin{bmatrix} N \\ T \\ M \end{bmatrix} - \begin{bmatrix} 0 \\ 0 \\ 0 \\ 0 \\ \sigma_0 l^2 s / 8 \\ \sigma_0 l^2 s / 8 \\ \sigma_0 l^2 s / 2 \\ \sigma_0 l^2 s / 2 \end{bmatrix} \leq \begin{bmatrix} 0 \\ 0 \\ 0 \\ 0 \\ 0 \\ 0 \\ 0 \\ 0 \end{bmatrix} \quad (4)$$

$$\mathbf{D}_i \mathbf{X}_i - \mathbf{TN}_i \leq \mathbf{0} \quad (5)$$

or:

$$\begin{bmatrix} \operatorname{tg}\varphi_0 & 1 & 0 \\ \operatorname{tg}\varphi_0 & -1 & 0 \\ 3l/8 & 0 & 1 \\ 3l/8 & 0 & -1 \\ 1/8 & 0 & 1 \\ 1/8 & 0 & -1 \\ -1/8 & 0 & 1 \\ -1/8 & 0 & -1 \\ -3l/8 & 0 & 1 \\ -3l/8 & 0 & -1 \end{bmatrix} \cdot \begin{bmatrix} N \\ T \\ M \end{bmatrix} - \begin{bmatrix} 0 \\ 0 \\ 0 \\ 0 \\ \sigma_0 l^2 s / 16 \\ \sigma_0 l^2 s / 16 \\ 3\sigma_0 l^2 s / 16 \\ 3\sigma_0 l^2 s / 16 \\ 3\sigma_0 l^2 s / 8 \\ 3\sigma_0 l^2 s / 8 \end{bmatrix} \leq \begin{bmatrix} 0 \\ 0 \\ 0 \\ 0 \\ 0 \\ 0 \\ 0 \\ 0 \\ 0 \\ 0 \end{bmatrix} \quad (6)$$

$$\mathbf{D}_i \mathbf{X}_i - \mathbf{TN}_i \leq \mathbf{0} \quad (7)$$

where s is the block's thickness and \mathbf{TN}_i is the vector of the known terms.

Obviously, the domain (4) – circumscribed polygon – gives the same results of the domain (2) for $N \leq N_0/4$, being $N_0 = \sigma_0 l s$. The more restrictive domain (6), instead, gives advantage over safety.

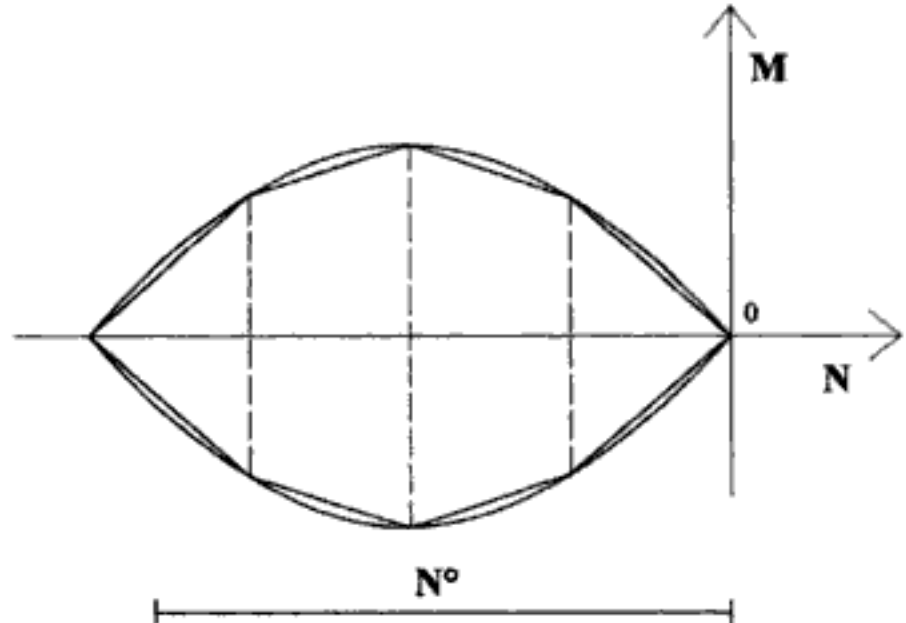


Figure 6. Limit surface for rocking (inscribed polygon).

2.3 Governing conditions

If n and m are respectively the number of the blocks and of interfaces, the equilibrium conditions are:

$$\mathbf{A} \mathbf{X} + \mathbf{F}_0 + \alpha \mathbf{F}_1 = \mathbf{0} \quad (8)$$

and the yield domain's conditions are:

$$\mathbf{Y} = \mathbf{D} \mathbf{X} - \mathbf{TN} \leq \mathbf{0} \quad (9)$$

where \mathbf{A} is a $(3n \times 3m)$ matrix, \mathbf{X} is a $3m$ -vector, \mathbf{F}_0 and \mathbf{F}_1 are $3n$ -vectors, α is the unknown collapse multiplier, \mathbf{D} is a $(km \times 3m)$ matrix – where k is 4, 8 or 10 according to yield domain selected (2), (4) or (6) – and finally \mathbf{TN} is a (km) vector of known terms.

In operating terms it is better to split \mathbf{X} in two sub-vectors $\mathbf{X}_1, \mathbf{X}_2$, where the second $3(m-n)$ sub-vector collects the “iperstatic” unknowns.

Consequently, the problem is formulated in the following manner:

maximize α
subject to

$$\mathbf{A}_1 \mathbf{X}_1 + \mathbf{A}_2 \mathbf{X}_2 + \mathbf{F}_0 + \alpha \mathbf{F}_1 = \mathbf{0} \quad (10)$$

$$\mathbf{Y} = \mathbf{D}_1 \mathbf{X}_1 + \mathbf{D}_2 \mathbf{X}_2 - \mathbf{TN} \leq \mathbf{0} \quad (11)$$

$$\alpha \geq 0 \quad (12)$$

being \mathbf{A}_1 a $(3n \times 3n)$ invertible matrix, or better, reformulated only in the unknown \mathbf{X}_2 and α , as:

maximize α
subject to

$$\mathbf{Y} = \mathbf{D} \mathbf{X}_2 + \mathbf{D}_0 \alpha - \mathbf{TN}_0 \leq \mathbf{0} \quad (13)$$

$$\alpha \geq 0 \quad (14)$$

being: $\mathbf{D} = \mathbf{D}_2 - \mathbf{D}_1 \mathbf{A}_1^{-1} \mathbf{A}_2$, $\mathbf{D}_0 = -\mathbf{D}_1 \mathbf{A}_1^{-1} \mathbf{F}_1$,
 $\mathbf{TN}_0 = \mathbf{D}_1 \mathbf{A}_1^{-1} \mathbf{F}_0 + \mathbf{TN}$.

eighteen rigid voussoirs, each one subjected to own load P_i (Fig. 10). The yield domain utilized is that defined in (2).

The lowest value of the thickness h has been defined in function of different values of $\text{tg}\phi_0$.

When is $\text{tg}\phi_0 \geq 0,396$ we have $h_{\min} = 1,059$ m and the correspondent collapse configuration is showed in Figure 11. Instead, when is $0,396 < \text{tg}\phi_0 \leq 0,310$ we have $1,062 \text{ m} < h_{\min} \leq 1,996$ m; in Figure 12 the collapse configuration for $\text{tg}\phi_0 = 0,35$ and correspondent to $h_{\min} = 1,525$ m is showed.

The results obtained are practically the same of those presented by Sinopoli (1996).

4.3 Axi-symmetric dome

We have studied an axi-symmetric dome having the middle radius $R = 10$ m, thickness $s = 1$ m and

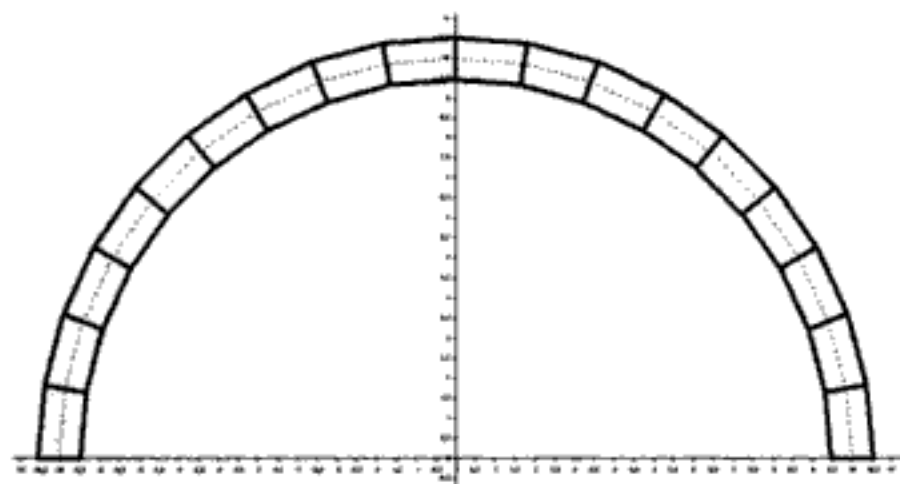


Figure 10.

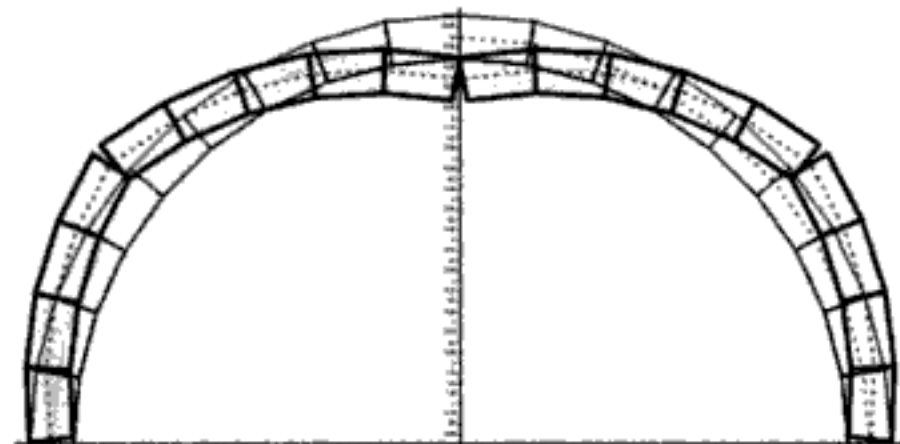


Figure 11.

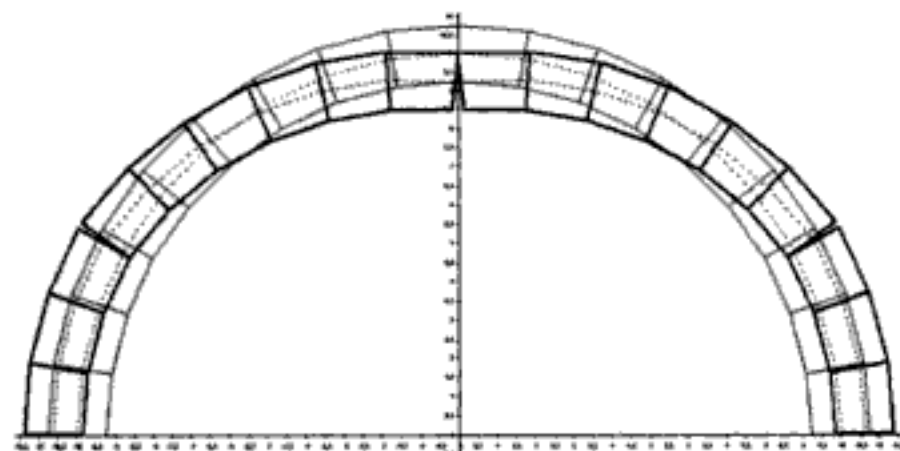


Figure 12.

$\text{tg}\phi_0 = 0,75$, subjected to only dead load. Because of simmetry, we analyse one slice alone discretized by nine rigid blocks. The yield domain utilized is that defined in (4). In Figure 13 the middle plane of this slice is showed. We have obtained the collapse load's multiplier $\alpha = 17,8584$. The correspondent collapse configuration is showed in Figure 14.

For the same dome with $R = 10$ m we have defined the lowest admissible thickness s (Fig. 15). The value 0,42 obtained for s/R is practically the same of that presented by Heyman (1966).

5 CONCLUSIONS

In this paper we have presented a very simple numerical method suitable for determining the load collapse

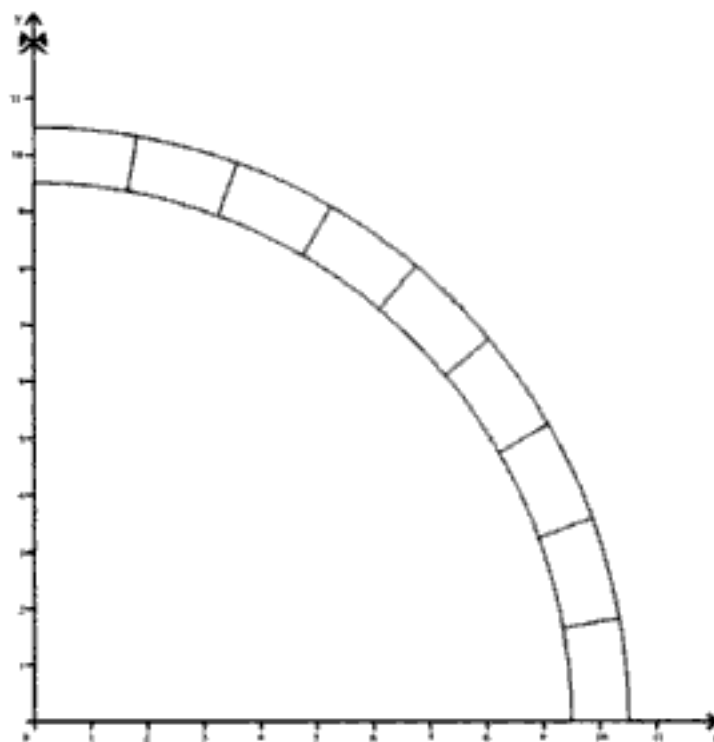


Figure 13.

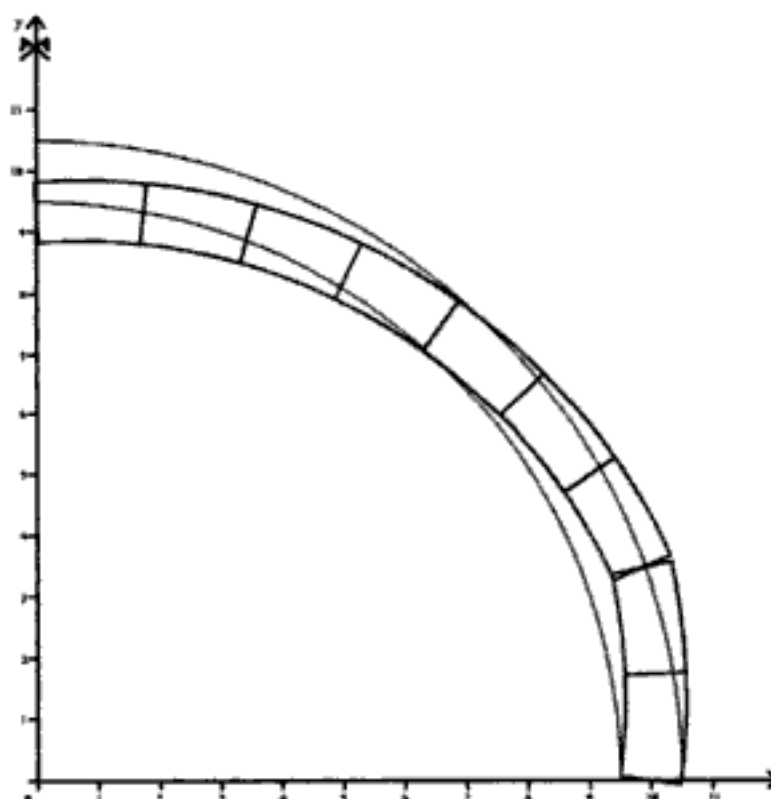


Figure 14. Collapse configuration.

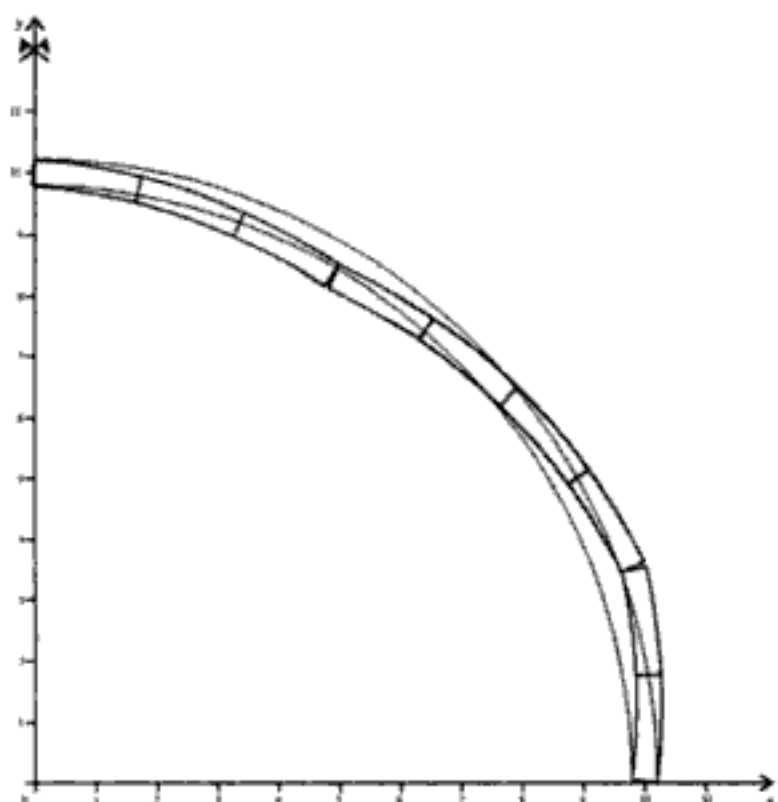


Figure 15. Collapse configuration for the dome having lowest thickness.

multiplier for masonry structures by a linear formulation founded on the static theorem of limit analysis. By the applications carried out we have verified that:

- the utilization of the static theorem permits to work only with the iperstatic unknowns and to obtain the solution by the very simple *Excel's solver*;
- the introduction of a limit for the compressive strength permits to solve problems otherwise insoluble;
- the increasing of the block's number doesn't give sensibility better results.

REFERENCES

- Baggio, C. & Trovalusci, P. 1998. Limit Analysis for No-Tension and Frictional Three-Dimensional Discrete Systems. *Mechanics of Structures and Machines*. 26 (3): 287–304.
- Como, M. & Grimaldi, A. 1983. Analisi limite di pareti murarie sotto spinta. In Atti del *Convegno Gruppo di Ricerca C.N.R. "Ingegneria Strutturale"*, Udine 30 Giugno 1983.
- Del Piero, G. 1995. Materiali non resistenti a trazione e analisi limite. In Atti del *Convegno "Giornata di Studio AIDIS"*, Capri, Maggio 1995.
- Ferris, M.C. & Tin-Loi, F. 1999. Limit Analysis of Frictional Block assemblies as a Mathematical Program with Complementary Constraints. *International Journal of Mechanical Sciences* (43): 209–224.
- Franciosi, V. 1984. L'attrito nel calcolo a rottura delle mura-ture. *Giornale del Genio Civile*: 215–234.
- Gilbert, M. & Melbourne, C. 1994. Rigid-block Analysis of Masonry Structures. *The Structural Engineer* 21 (72): 356–361.
- Heyman, J. 1966. The Stone Skeleton. *International Journal Solids Structures* (2): 249–279.
- Heyman, J. 1968. The Safety of Masonry Arches. *International Journal Mechanical Sciences* (11): 363–385.
- Kooharian, A. 1953. Limit Analysis of Voussoir (segmental) and Concret Arches. In *Proceedings American Concrete Institute* (89): 397.
- Lucchesi, M., Padovani, C., Pasquinelli, G. & Zani, N. 1996. L'analisi limite per gli archi in muratura. In Atti del *Convegno "La Meccanica delle Murature tra Teoria e Progetto"*, Messina 18–20 Settembre 1996. Bologna: Pitagora.
- Sinopoli, A., Corradi, M. & Focè, F. 1996. Sviluppi recenti sulla Statica dell'arco murario in relazione alle teorie storiche pre-elastiche. In Atti del *Convegno "La Meccanica delle Murature tra Teoria e Progetto"*, Messina 18–20 Settembre 1996. Bologna: Pitagora .

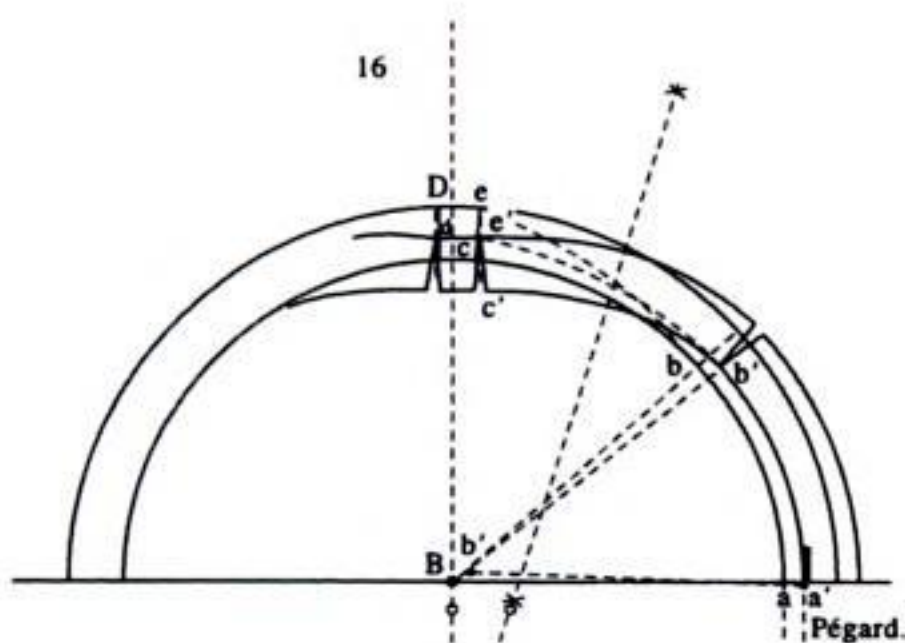


Figure 2. Deformed arch in the church at Vézelay, France due to spreading supports (Viollet-le-Duc 1854).

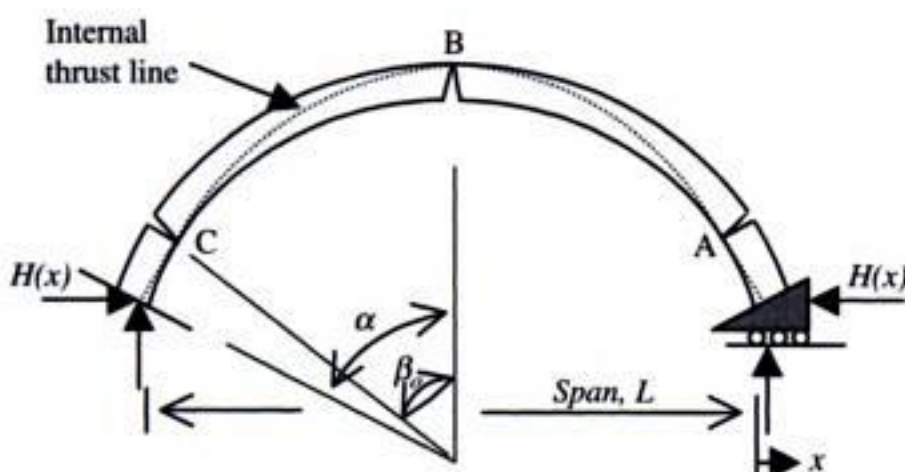


Figure 3. Circular arch segment with spreading abutments at state of minimum thrust.

horizontal thrust, H , changes as a result. It is well-known that a perfectly constructed arch supported on rigid supports can resist a range of thrust values between the maximum thrust and minimum thrust (Heyman 1995). However, most arches exist in a deformed state due to movements of the supports. The arch thrust may cause the abutments to spread apart, increasing the span of the arch. As soon as the abutments spread apart, the arch exists in a state of minimum thrust. The smallest outward movement of the abutments will cause the arch to form three hinges (A, B, and C in Figure 3). At this point the arch is statically determinate and the abutment thrust can then be determined uniquely from the geometry and the location of the hinges. In this case there are intrados hinges at A and C, and an extrados hinge at B. (For small angles of embrace, α , the intrados hinges will form at the abutments.) If the span continues to increase, the arch will deform according to rigid-body kinematics. Eventually the arch will collapse due to the excess displacement or in some cases, the thrust of the deformed arch may exceed the capacity of the buttresses supporting the arch.

Solving for the collapse state of a masonry arch on spreading supports is not a trivial problem. Ochsendorf (2002) showed that the location of the intrados hinge

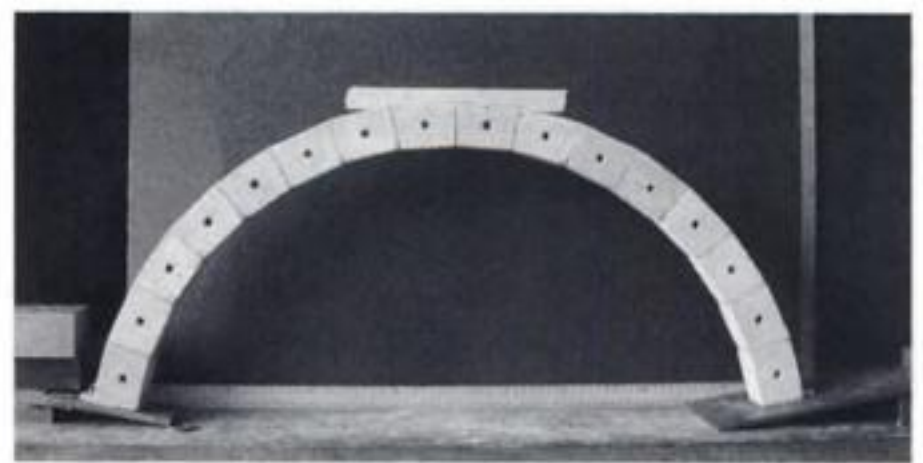


Figure 4. Undeformed masonry arch of 10° voussoirs.

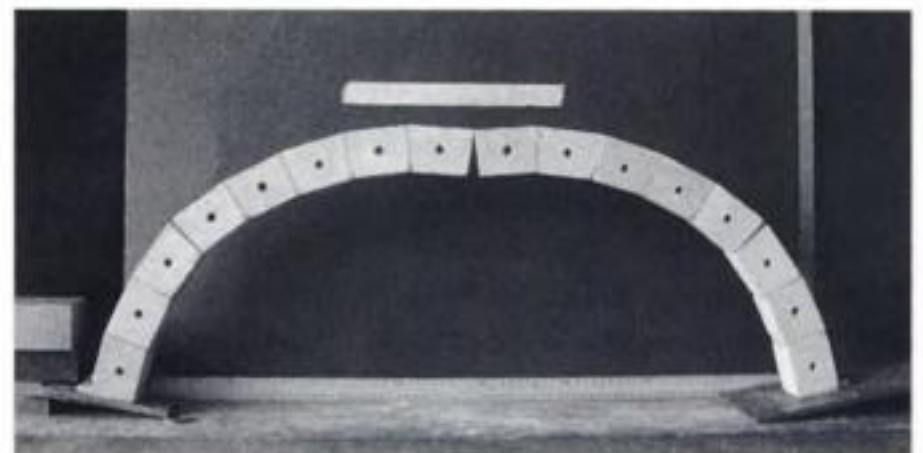


Figure 5. Deformed arch on spreading supports just before collapse.

at an angle of β_0 from the vertical can change as the arch geometry changes. A detailed discussion of this problem is beyond the scope of this paper, which aims to illustrate the need for such displacement-based analysis of masonry structures. While hundreds of papers have addressed the load capacity of masonry arches, surprisingly few have considered the displacement capacity of arches and the influence of displacements on the horizontal thrust of masonry arches.

To investigate this problem, the author conducted experiments on model arches on spreading supports (Ochsendorf 2002). Figures 4 and 5 illustrate the undeformed arch and the collapse state for a circular arch of 10-degree voussoirs subtending a total angle of embrace of 160 degrees. The thickness of the model arch is 13% of the centerline radius. In this case, the intrados hinge forms initially at $\beta_0 = 50^\circ$ from the crown of the arch, though the hinge shifts to $\beta_0 = 60^\circ$ at the collapse state. The collapse mechanism is a symmetrical five-hinge mechanism in theory, though only four hinges are required for collapse. The arch collapses when the span is increased by approximately 8% at which point the minimum horizontal thrust has increased by more than 50%. At the collapse state, the crown of the arch has descended by an amount almost equal to the thickness of the arch. Thus, small changes in the support conditions can lead to gross deformations and eventual collapse, with drastic changes in the internal forces in the structure. Such gross deformations are visible in many Romanesque and Gothic vaults throughout Europe.

In the case of historic masonry buildings, the stability of the arch or vault will often depend on the resistance of the arch to support movements and this is an area which requires further research. Such an approach has more physical meaning than applying heavy loads on building vaults. The author is currently investigating the collapse conditions for arches of various geometries, including pointed arches. Such two-dimensional results can then be extended into three dimensions to consider the collapse of domes and vaults.

3 LEANING BUTTRESSES

The deformation of arches is often due to the movement of walls or buttresses which lean over time. Outward leaning is the greatest threat to the stability of a wall or buttress. Most masonry buttresses exist in a state of leaning, which increases throughout the life of the structure. In general, the lean of a buttress may be due to any or all of the following:

- Deformation and subsidence in the foundations during construction;
- Construction defects or small movements between stones;
- Elastic deformation of the masonry and mortar (usually small);
- Additional subsidence due to changes in the soil conditions (caused by consolidation of the soil, enhanced by changes in the water table, adjacent excavations, long term creep of the foundations, etc.);
- Ratcheting movements of the stones due to vibrations of the structure (from earthquakes, bell-ringing, wind loading, etc.); and
- Seasonal effects of temperature and moisture over long periods of time.

As the buttress leans, the eccentric loading on the foundations can cause additional leaning, which will continue to increase during the life of the structure. The lean of the buttress causes an increase in the span of the vault or arch, which will increase the thrust of the arch. In some cases, the increased thrust of the arch may exceed the decreased horizontal thrust capacity of the leaning buttress, leading to collapse as a result of deformations.

A leaning buttress overturns at a lower load than the same buttress in a vertical position, due to the horizontal shift of the centroid of the buttress. Even small amounts of leaning will significantly alter the equilibrium conditions. For buttressed vaults, a small amount of leaning in the buttress, such as 1° from vertical, will alter the line of thrust and increase the applied thrust of the vault (Huerta and López 1997). For example, consider an arch spanning five meters, which is supported at a height of 10 meters. If each buttress leans

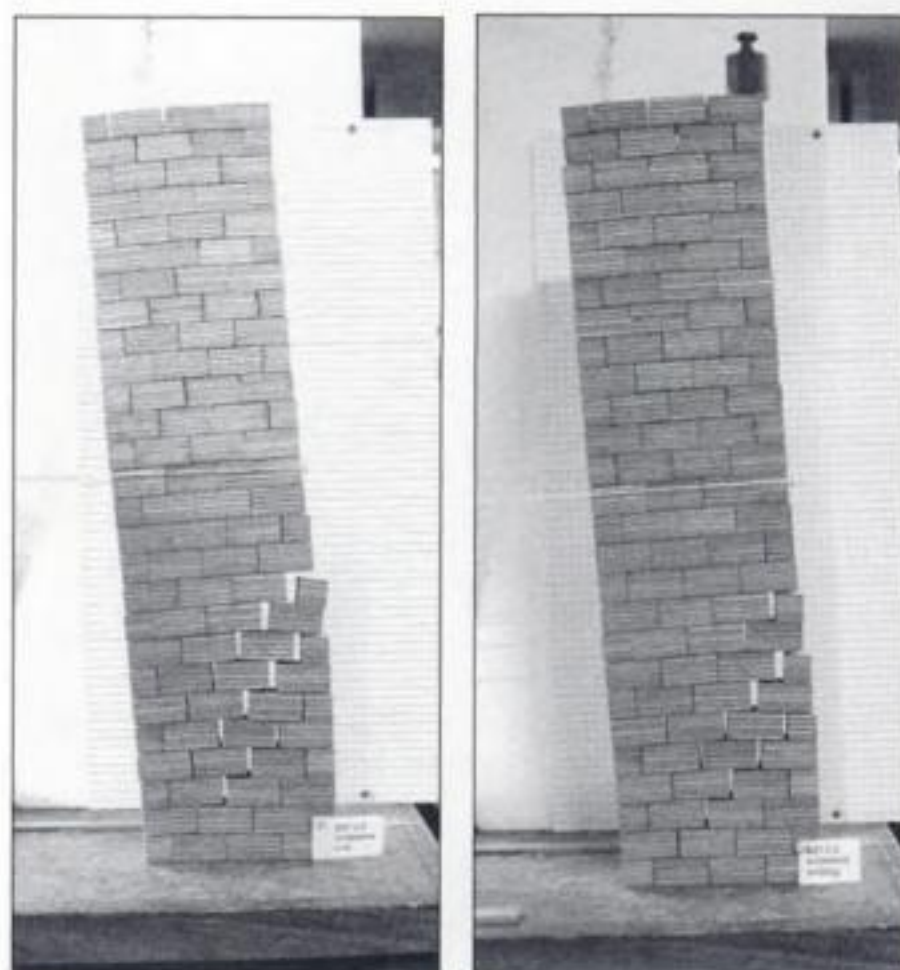


Figure 6. Tests on model rectangular buttresses showing the collapse state of a buttress due to horizontal thrust at mid-height.

outward by one degree, then the horizontal movement at the height of the arch will be approximately 0.17 meters on each side. Over the arch span of 5 meters, this constitutes an increase in span of approximately 7%, which is sufficient to cause the collapse of many typical masonry arches.

In addition, recent work by Ochsendorf et al. (2003, 2004) has illustrated the potential for a fracture to form in a masonry buttress at the collapse state, reducing the capacity for horizontal thrust by up to 30%. Experiments on model buttresses have illustrated the existence of this fracture for buttresses under horizontal loads (Ochsendorf 2002). Figure 6 illustrates two model buttress configurations at the collapse state. The buttress on the right is loaded with a vertical surcharge in addition to the horizontal load, while the buttress on the left is subjected only to its own weight and the horizontal force. The fracture is slightly different in each case as a result.

As the buttress leans outward, the centroid of the buttress shifts. Typical values of lean for historic buildings may be on the order of one or two degrees, though in extraordinary cases, such as the tower of Pisa, the lean from vertical can approach five degrees or more. Regardless, for values of lean less than five degrees it is appropriate to approximate the movement of the centroid using the small angle assumption that it is a linear decrease in buttress capacity for small angles. As the centroid of the buttress shifts horizontally, the load capacity of the buttress is reduced linearly. The exact reduction in capacity depends on the geometry of the buttress.

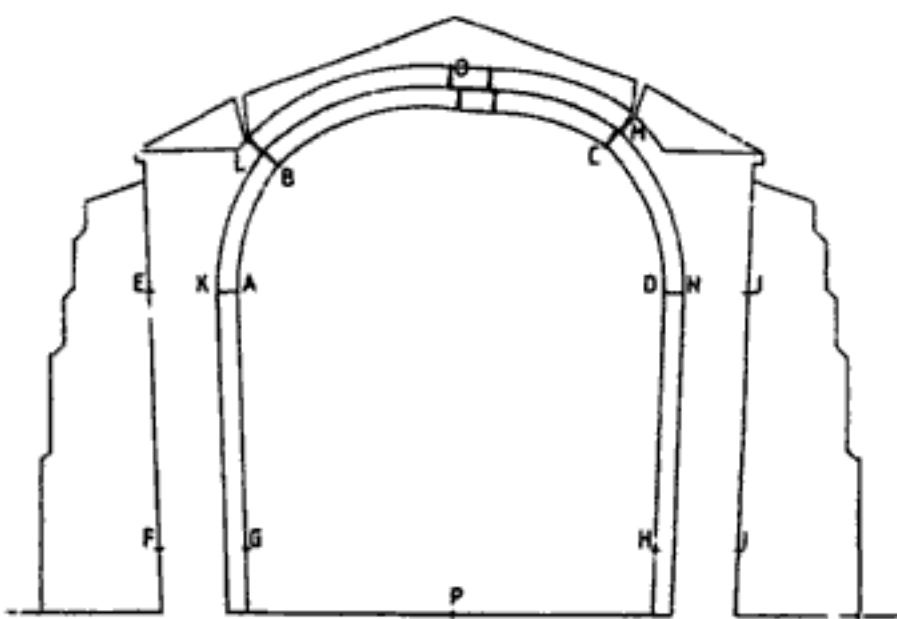
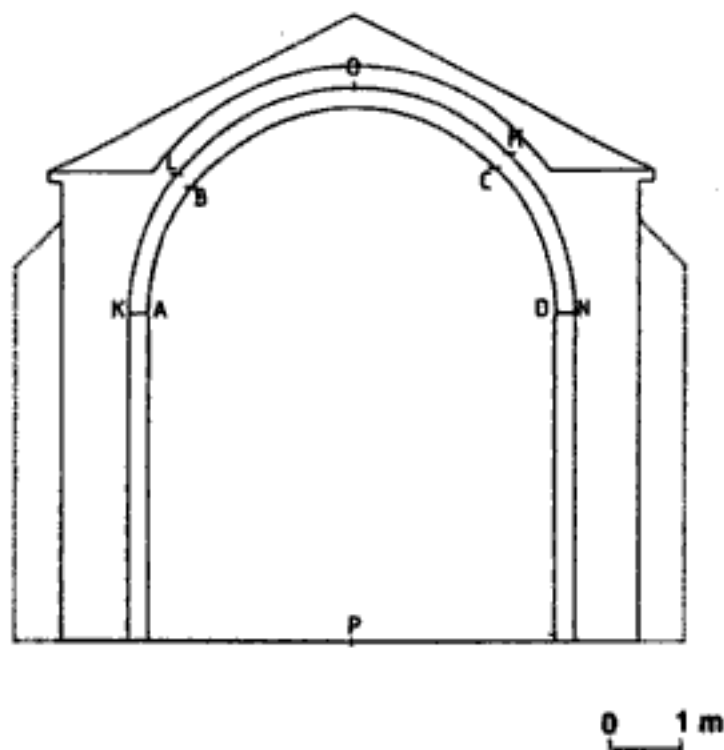


Figure 7. Severe deformations in a barrel vault (Huerta and López 1997).

4 ARCH ON LEANING BUTTRESSES

The results for an arch on spreading supports can be combined with the analysis of the leaning buttress to gain a greater appreciation for the stability of an arch on leaning buttresses. This problem has been encountered by several researchers in recent years, such as Huerta & Lopez (1997) and Deshpande (2001), and is illustrated in Figure 7. For such a deformed structure, it is crucial to understand the source of the displacements and to determine the capacity of the structure for increased displacement.

The author's PhD dissertation examined this problem in detail and concluded that there are two dominant modes of collapse due to the outward leaning of the buttress (Ochsendorf 2002). In some cases, the arch may collapse before the buttress capacity is reached, in a mode defined as "strong-buttress" failure. For strong-buttress failure, the support displacements are too large for the arch to stand and the arch collapses, even though the thrust of the arch has not exceeded the capacity of the leaning buttress. Alternatively, failure may occur by a "weak-buttress" mode,

in which the horizontal thrust capacity of the buttress is exceeded. In this case, one buttress gives way due to the increased thrust of the arch. As the buttress leans outward, the arch collapses. Though the buttress capacity is exceeded, the arch will collapse and the buttress will remain standing. Once the arch collapses, it will no longer exert a horizontal overturning force and the center of mass of the buttress will remain within the thickness of the buttress. Thus, even in the case of "weak-buttress" failure, the buttress will not collapse. For all cases, the displacement-based approach provides insight into the possible collapse modes for a vaulted masonry structure.

5 DISCUSSION

The use of a displacement-based approach for the assessment of vaulted masonry structures provides many advantages. The arguments in favor of this approach can be summarized as follows:

- 1) Small movements in the geometry of masonry structures can greatly alter the equilibrium configuration and can lead to collapse.
- 2) In order to assess the safety of historic monuments, engineers should be most concerned with the collapse state, rather than the current state or previous state. By determining the magnitude of displacements required to cause collapse, engineers can assess the relative stability of a structure.
- 3) In the case of historic buildings, collapse is more likely to occur from excessive support displacements than from excessive loading.
- 4) This method can provide a measure of comparison which is useful for assessing a large group of structures. For example, 30 masonry churches in a particular region can be evaluated quickly to see which require more detailed analysis.
- 5) A displacement-based approach has physical meaning since the foundations of historic monuments are often insufficient, causing walls and buttresses to lean outwards.
- 6) Such an approach can be implemented using various structural analysis methods. It can be carried out as an extension of conventional limit analysis by considering the blocks as rigid, or it can be applied to elastic models by introducing support displacements to a non-linear finite element model.
- 7) There is scope for much additional work in this area, in particular for the consideration of three-dimensional collapse mechanisms in masonry towers and vaults as a result of support displacements.

6 CONCLUSIONS

This paper has proposed a general analytical approach for masonry structures based on the application of

only very small traction forces can be transferred at joints level;

2. infinite compression strength. In most cases, collapse of masonry structures is not governed by compression failure, but is due to cracks opening and mechanism formation. This assumption is slightly non-conservative;
3. sliding of a stone, or of part of the structure, upon another cannot occur.

With these assumption, the only possible collapse mode is the rotation of adjacent blocks about a common point, so that masonry behaves as an assemblage of rigid bodies held up by compressive contact forces. The collapse is characterized by the formation of hinges among the single parts.

Uniqueness and safe theorems can be then respectively expressed as follows:

“If a thrust line representing an equilibrium condition for the structure under certain loads lies fully within the masonry, and allows the formation of sufficient hinges to drive the structure into a mechanism, then the structure is about to collapse. Further, in case of proportional loads, the load proportionality factor at collapse is unique.”

“If a thrust line, in equilibrium with the external loads and lying wholly within the structure, can be found, then the structure is safe.”

With these statements and under the outlined hypotheses, collapse analysis of masonry structures basically consists in seeking a thrust line, which is actually the graphical representation of equilibrium conditions, passing through a number of hinges sufficient to transform the structure into a mechanism.

Though the approach is conceptually simple and well posed from a theoretical point of view, a few points on its applicability and reliability can be arisen. First of all, infinite compression strength is assumed, while experience has shown how structures made of materials with poor mechanical properties often do not develop mechanism-like collapse, rather large portions of masonry crush. Possibly, finite values of compression strength can be accounted for by moving the position of the hinges from the external boundary towards the inside of the masonry.

Secondly, it must be said that though limit analysis actually reveals the weakest points of the structure and provides a bound of the admissible horizontal action, it neglects, due to material assumptions, a few structural inelastic capacity issues, so that the safety assessment turns out to be fairly pessimistic.

3 A FULLY GEOMETRICAL FORMULATION

Masonry portals, made of two vertical elements and a rectilinear horizontal element, is very often found in any masonry structures (fig. 1).

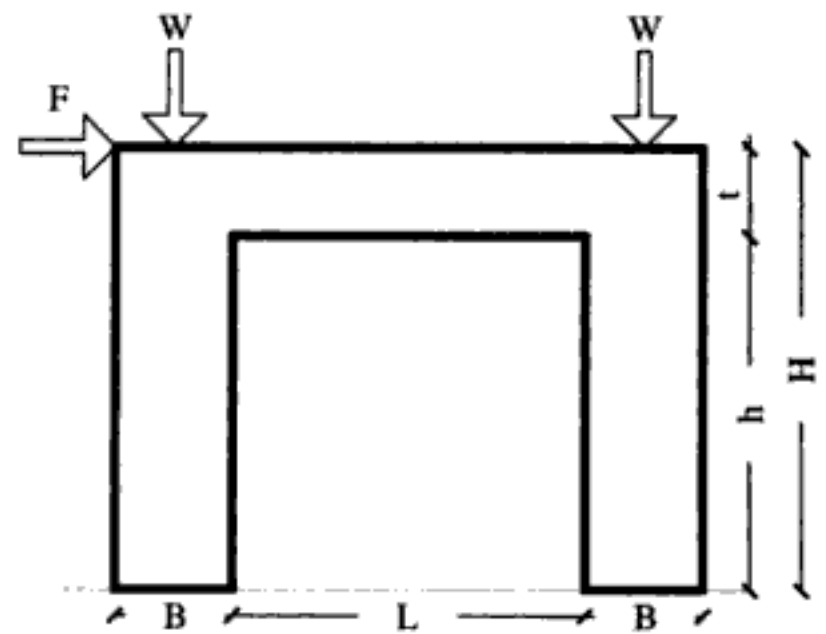


Figure 1. Geometry and loads of a masonry portal.

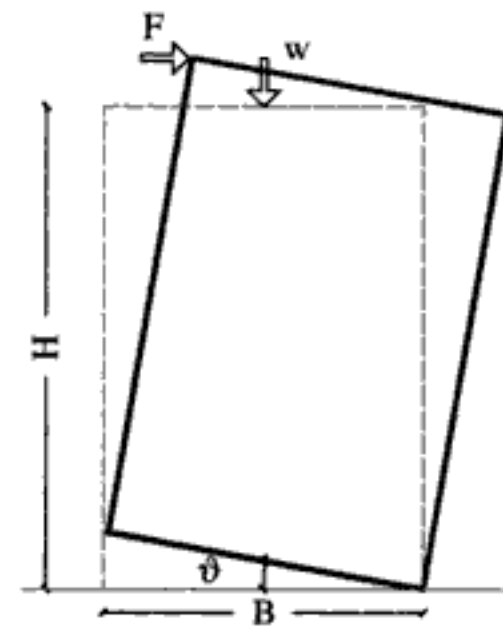


Figure 2. Rocking of the panel.

In this paper, a fully geometrical formulation for the evaluation of horizontal collapse load is proposed. It is opinion of the authors, that direct geometrical approach can be easy to use and the procedure fast to implement.

Within this framework collapse multiplier of the distribution given in figure 2 for a single rocking panel is derived through trivial equilibrium equation:

$$\frac{F}{W} = \frac{B}{2 \cdot H}$$

where F is the applied force, W the total weight, B the width and H the height of the masonry panel.

For portal frames an analogy can be observed with the single panel rocking behavior if the possible mechanisms are sketched. Four mechanism classes are chosen, in the following regarded as I mechanism (*frame mech.*), II and III mechanism (*mixed mech.*) and IV mechanism (*storey mech.*) as represented in figure 3.

Each mechanism features 4 hinges that give the structure a single lagrangian degree of freedom. Once the kinematic chain has been drawn, the principle

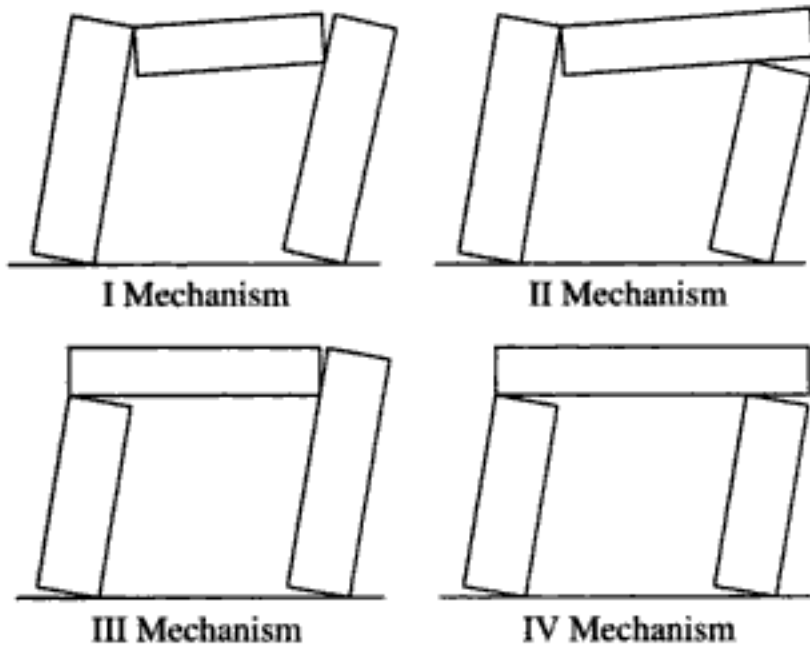


Figure 3. Masonry portal – collapse mechanisms.

of virtual works can be applied to each mechanism, stating an equilibrium equation which gives the load multiplier F/W_{tot} . The minimum of the four multipliers is assumed to be the collapse multiplier for the portal $F/W_{tot,real}$.

3.1 Kinematic multipliers

3.1.1 I mechanism (frame mechanism)

Figure 4a shows geometrical configuration and loads of the portal, while in figure 4b the kinematic chain of the mechanism is represented.

Operating on the kinematic chain, simple geometrical considerations give:

$$\varphi_3 \cdot B = \varphi_2 \cdot L \quad (1)$$

$$\varphi_1 \cdot d_1 = \varphi_3 \cdot d_3 \quad (2)$$

$$\vartheta \cdot d_1 = H \Rightarrow d_1 = \frac{H}{\vartheta} \Rightarrow d_1 = \frac{H \cdot L}{t}$$

$$d_3 = d_1 - B - L \Rightarrow d_3 = \frac{H \cdot L}{t} - B - L \Rightarrow$$

$$d_3 = \frac{H \cdot L - B \cdot t - L \cdot t}{t}$$

substituting the expressions of d_1 and d_3 in (2):

$$\varphi_1 \cdot \frac{H \cdot L}{t} = \varphi_3 \cdot \frac{H \cdot L - B \cdot t - L \cdot t}{t}$$

let

$$\psi = \frac{H \cdot L}{H \cdot L - B \cdot t - L \cdot t}$$

then:

$$\varphi_3 = \psi \cdot \varphi_1$$

$$\varphi_2 = \psi \cdot \frac{B}{L} \cdot \varphi_1$$

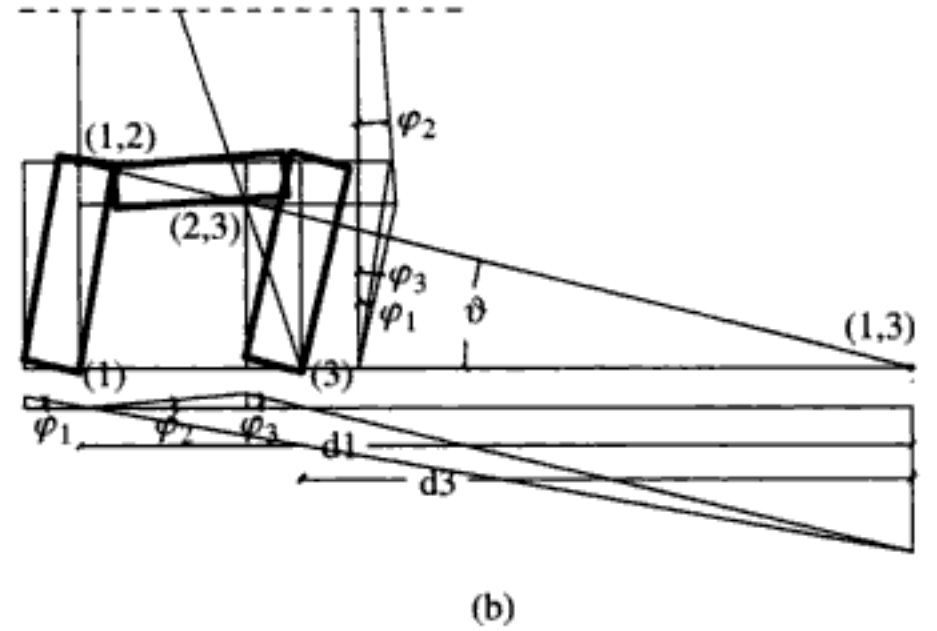
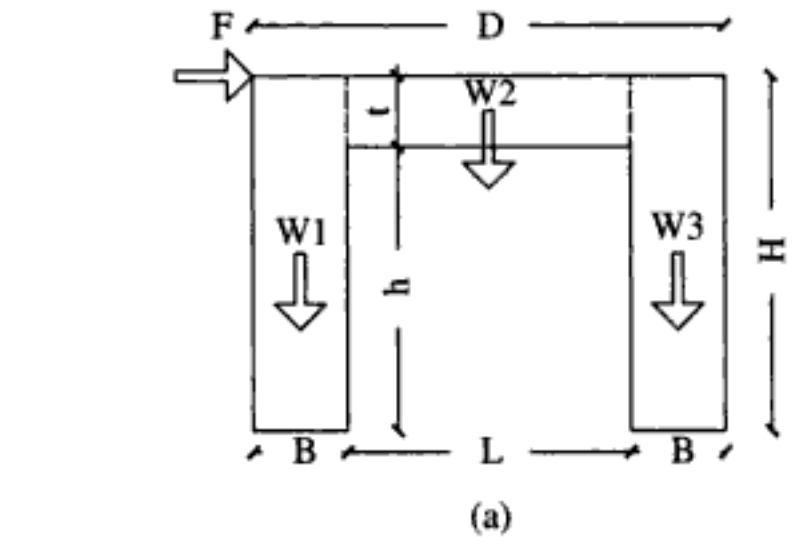


Figure 4. I mechanism – (a) geometry and loads; (b) kinematic chain.

The principle of virtual work then gives:

$$F \cdot \varphi_1 \cdot H = W_1 \cdot \varphi_1 \cdot \frac{B}{2} + W_2 \cdot \varphi_2 \cdot \frac{L}{2} + W_3 \cdot \varphi_3 \cdot \frac{B}{2}$$

From which the collapse multiplier for type I mechanism can be derived:

$$\frac{F}{W_{tot}} = \frac{B}{2 \cdot H} \cdot \frac{W_1 + W_2 \cdot \psi + W_3 \cdot \psi}{W_{tot}}$$

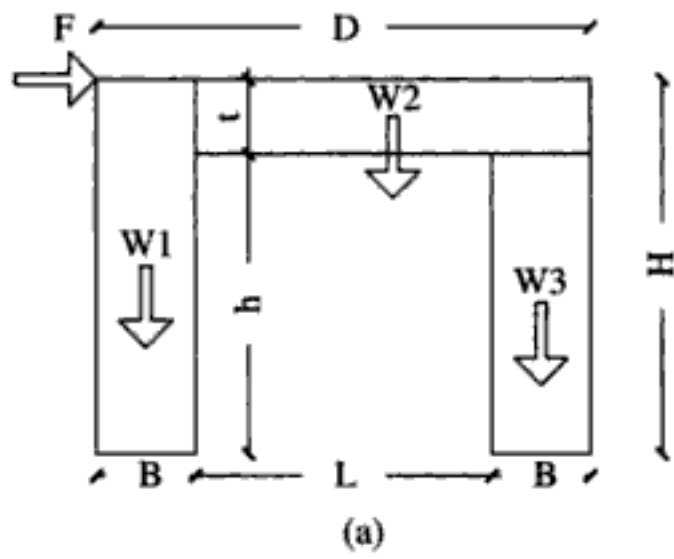
3.1.2 II mechanism (mixed mechanism)

Following the same procedure as outlined above, the collapse multiplier for the other mechanisms is here derived.

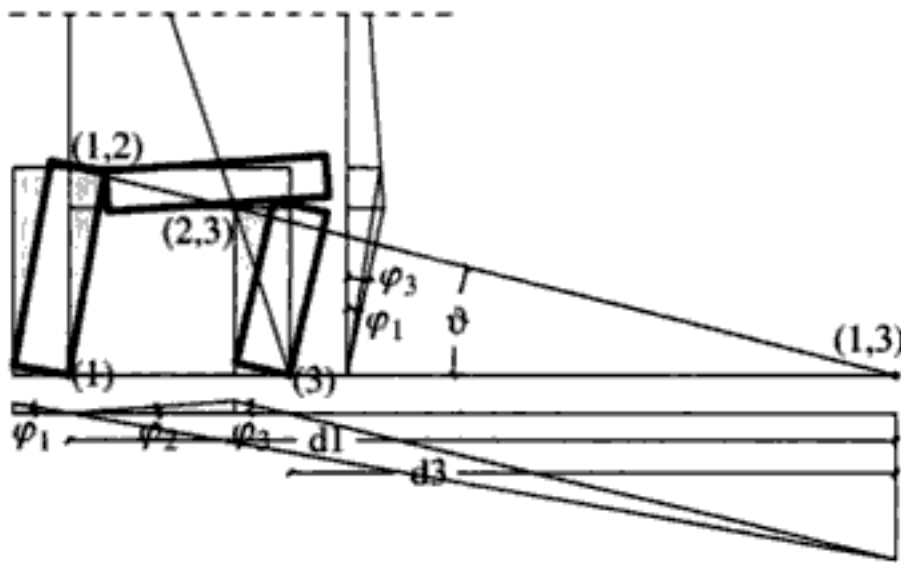
As in the previous case, figure 5a shows geometrical configuration and loads of the portal, while in figure 5b the kinematic chain of the mechanism is shown.

Geometrical relations are the same as for type I mechanism, and the equilibrium condition, written the principle of virtual works, is:

$$F \cdot \varphi_1 \cdot H = W_1 \cdot \varphi_1 \cdot \frac{B}{2} + W_2 \cdot \varphi_2 \cdot \frac{B+L}{2} + W_3 \cdot \varphi_3 \cdot \frac{B}{2}$$



(a)



(b)

Figure 5. II mechanism – (a) geometry and loads; (b) kinematic chain.

The collapse multiplier for II mechanism is then:

$$\frac{F}{W_{tot}} = \frac{B}{2 \cdot H} \cdot \frac{W_1 + W_2 \cdot \psi \cdot \frac{B+L}{L} + W_3 \cdot \psi}{W_{tot}}$$

3.1.3 III mechanism (mixed mechanism)

Figures 6a and 6b respectively show the geometrical configuration/loads of the portal and the kinematic chain for the mechanism.

The following geometrical relations can be written:

$$\varphi_1 = \varphi_3$$

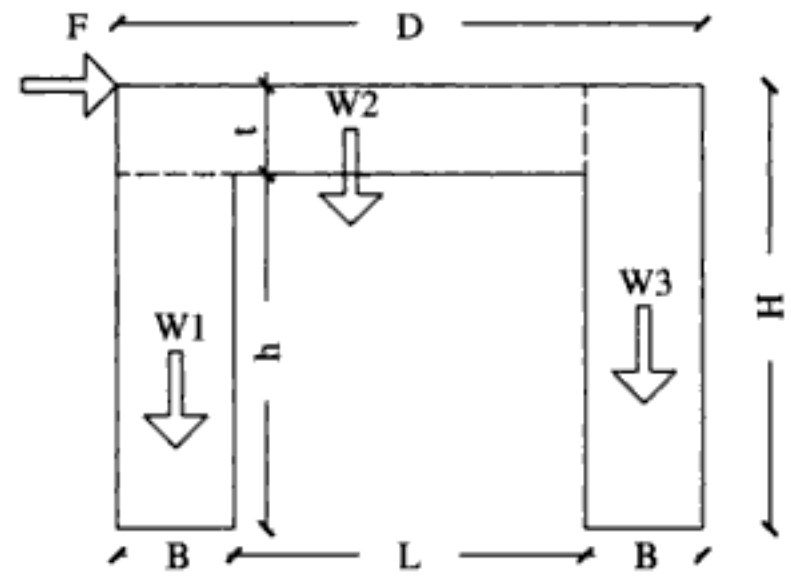
$$\varphi_2 = 0$$

equilibrium condition is:

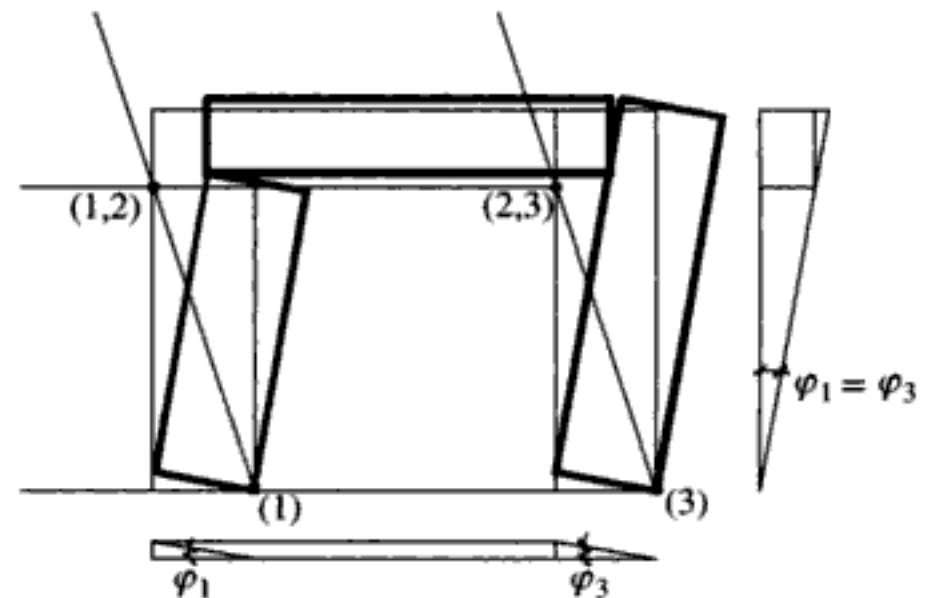
$$F \cdot \varphi_1 \cdot (H - t) = W_1 \cdot \varphi_1 \cdot \frac{B}{2} + W_2 \cdot \varphi_1 \cdot B + W_3 \cdot \varphi_3 \cdot \frac{B}{2}$$

and then the collapse multiplier is:

$$\frac{F}{W_{tot}} = \frac{B}{2 \cdot h} \cdot \frac{W_1 + 2 \cdot W_2 + W_3}{W_{tot}}$$



(a)



(b)

Figure 6. III mechanism – (a) geometry and loads; (b) kinematic chain.

3.1.4 IV mechanism (storey mechanism)

For this mechanism, geometrical configuration and loads of the portal and the kinematic chain of the mechanism are represented in figures 7a and 7b.

Geometrical relations are the same as for III mechanism. The principle of virtual works gives:

$$F \cdot \varphi_1 \cdot (H - t) = W_1 \cdot \varphi_1 \cdot \frac{B}{2} + W_2 \cdot \varphi_1 \cdot B + W_3 \cdot \varphi_3 \cdot \frac{B}{2}$$

from which the collapse multiplier can be derived:

$$\frac{F}{W_{tot}} = \frac{B}{2 \cdot h} \cdot \left(\frac{W_1 + 2W_2 + W_3}{W_{tot}} \right)$$

or:

$$\frac{F}{W_{tot}} = \frac{B}{2 \cdot h} \cdot \left(1 + \frac{W_{beam}}{W_{tot}} \right)$$

where: $W_{beam} = W_2$.

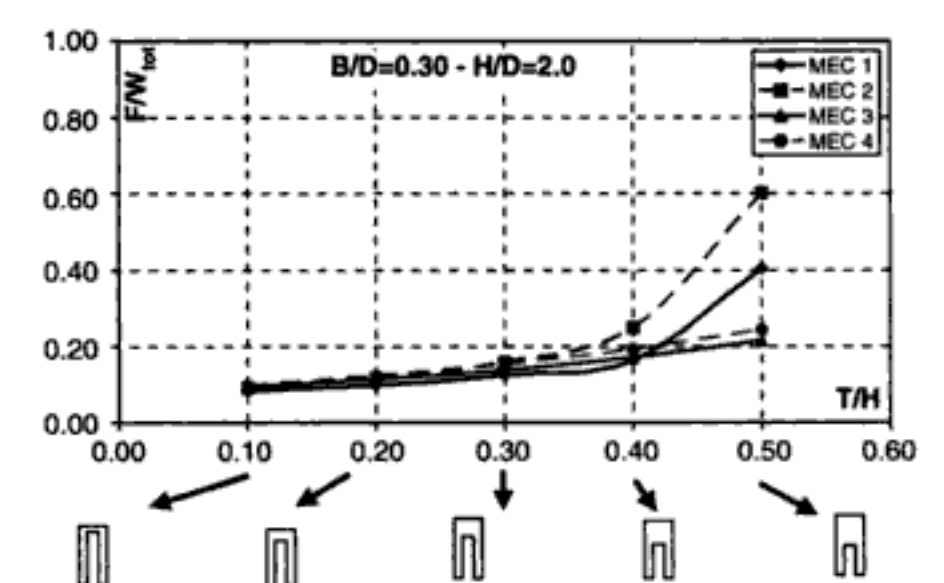
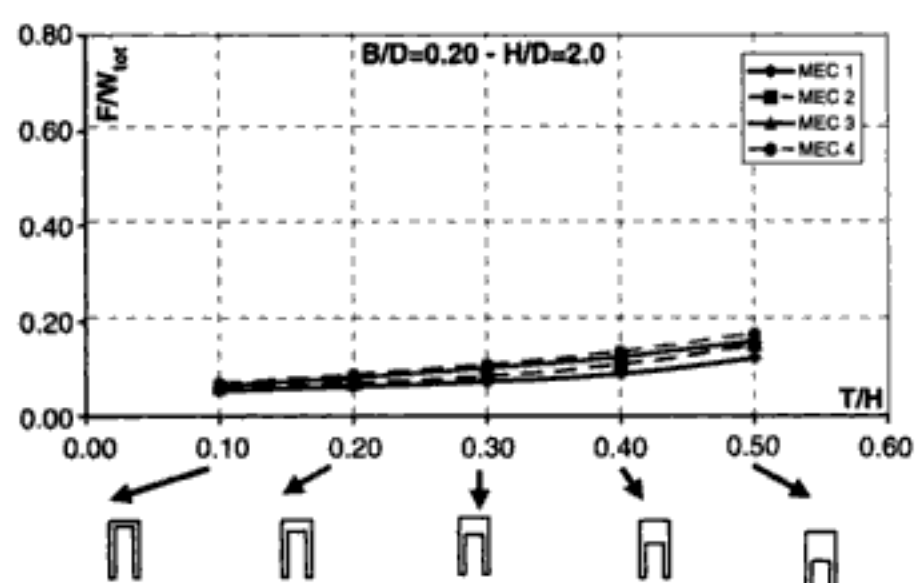
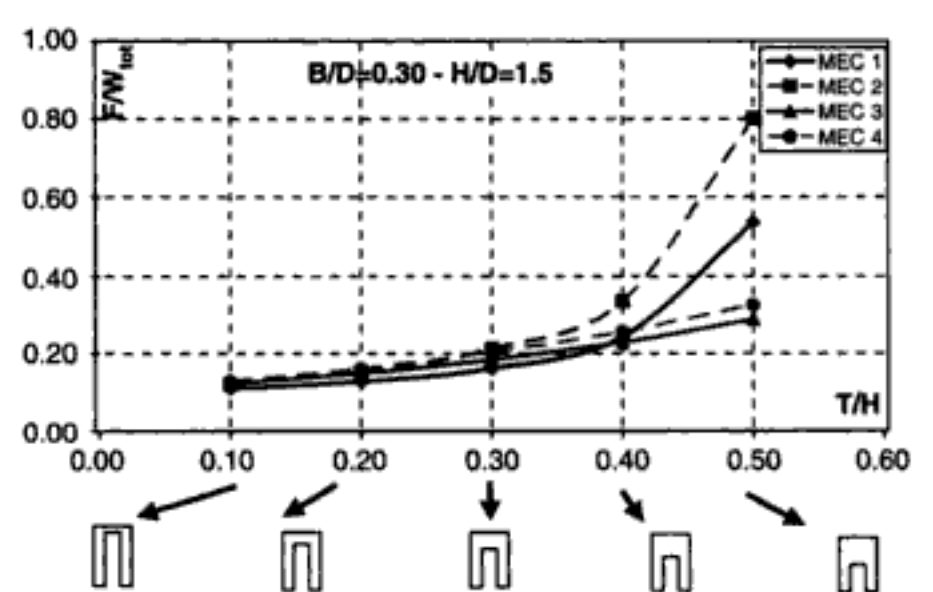
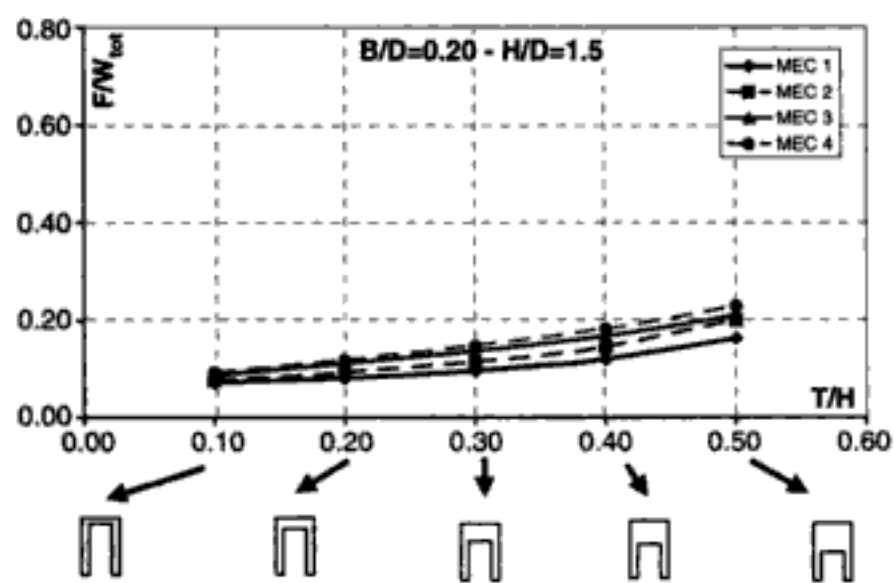
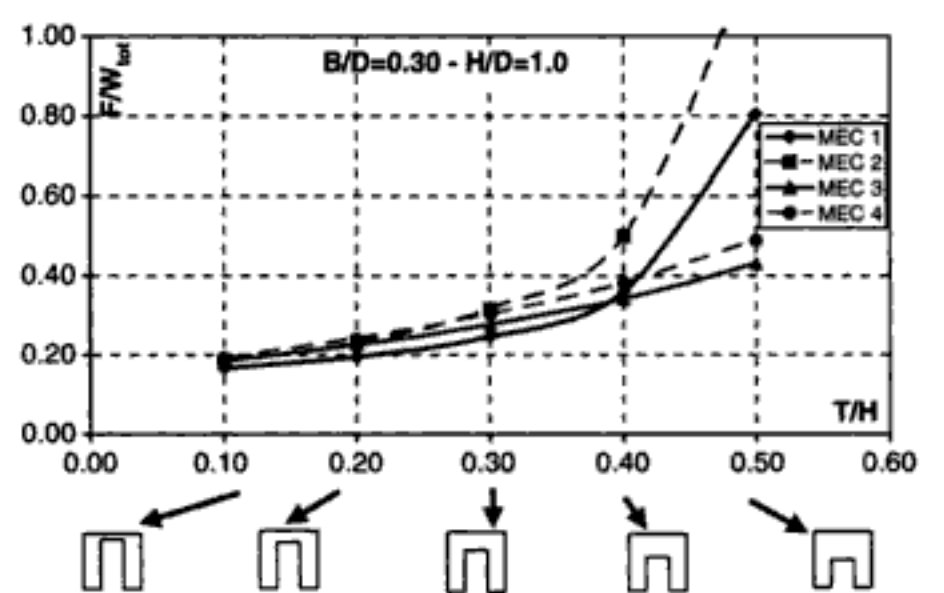
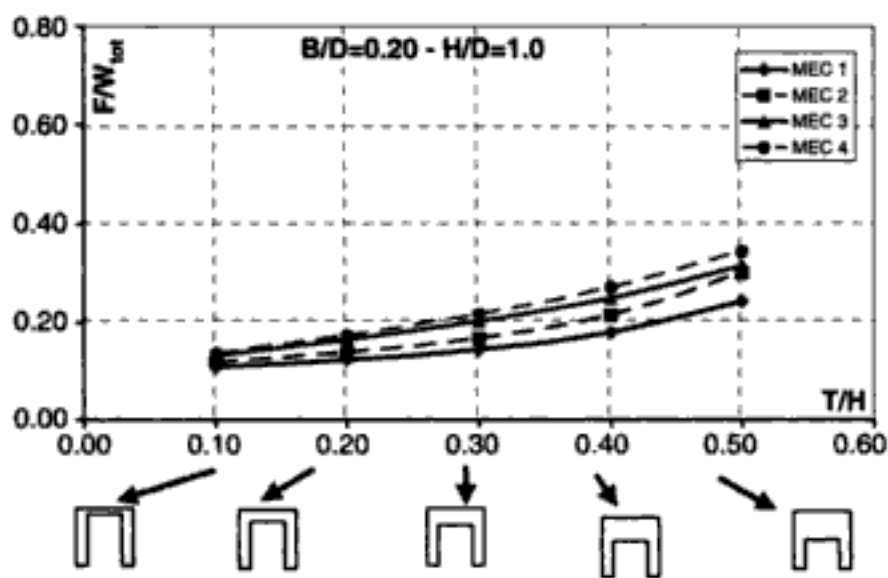
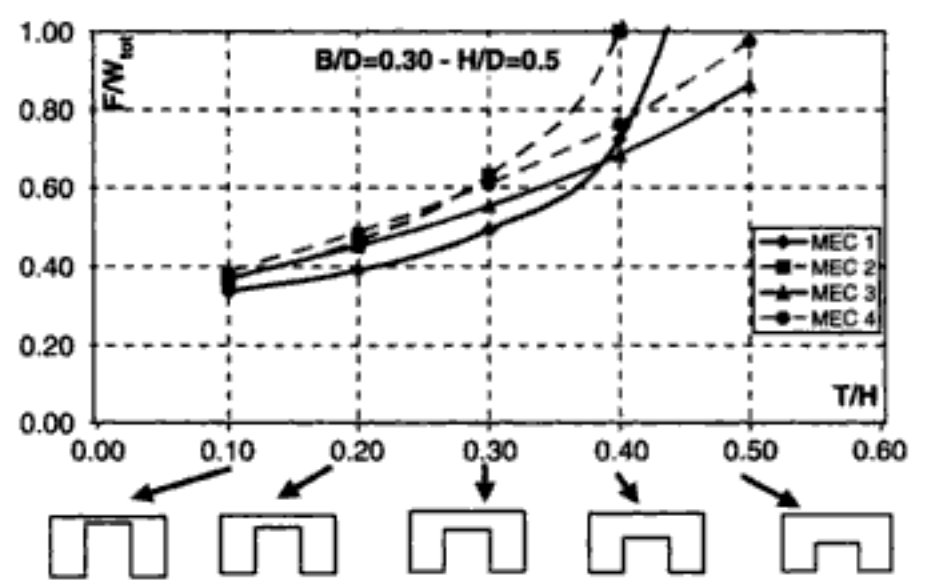
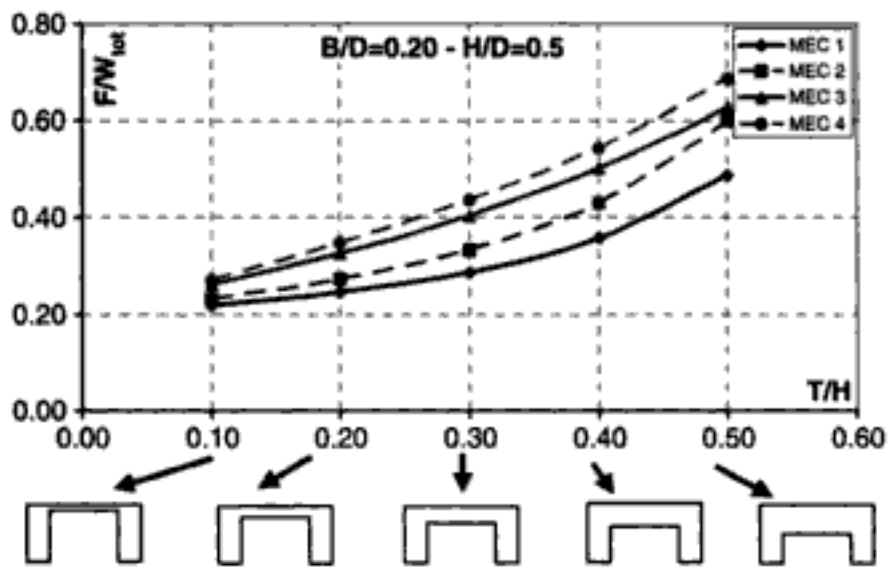


Figure 11. Collapse multipliers for $B/D = 0.2$.

Figure 12. Collapse multipliers for $B/D = 0.3$.

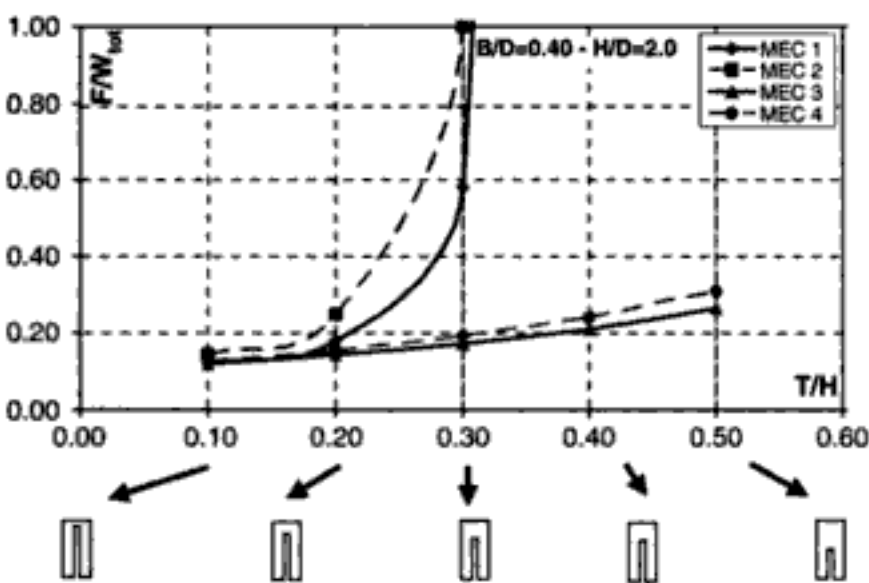
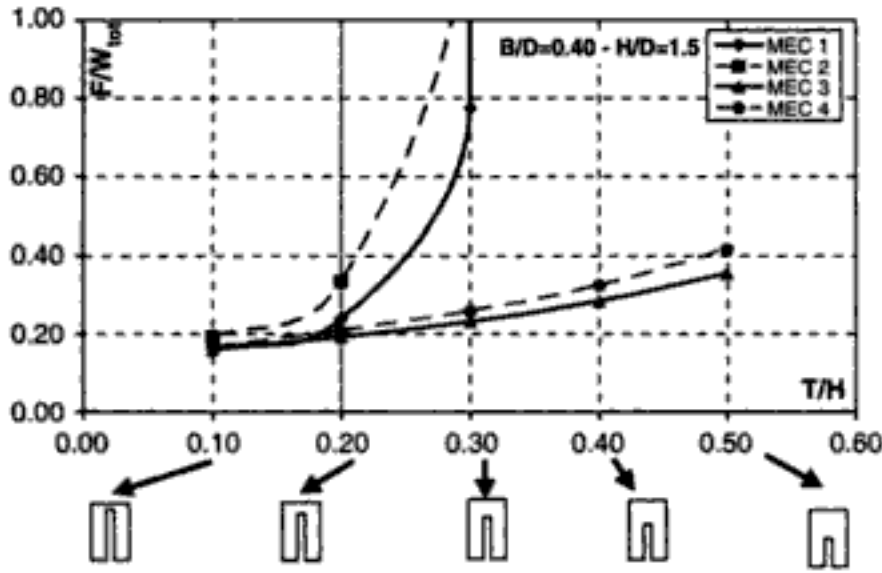
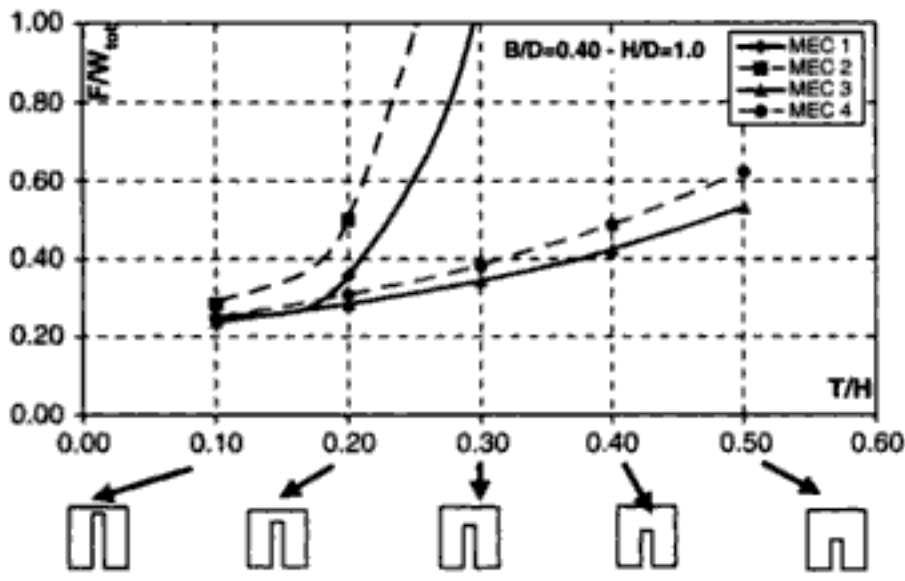
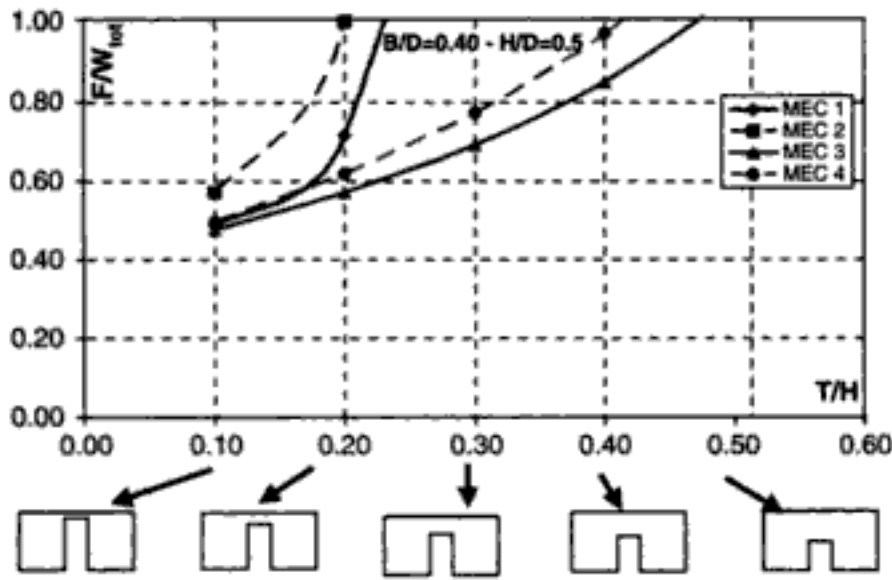


Figure 13. Collapse multipliers for $B/D = 0.4$.

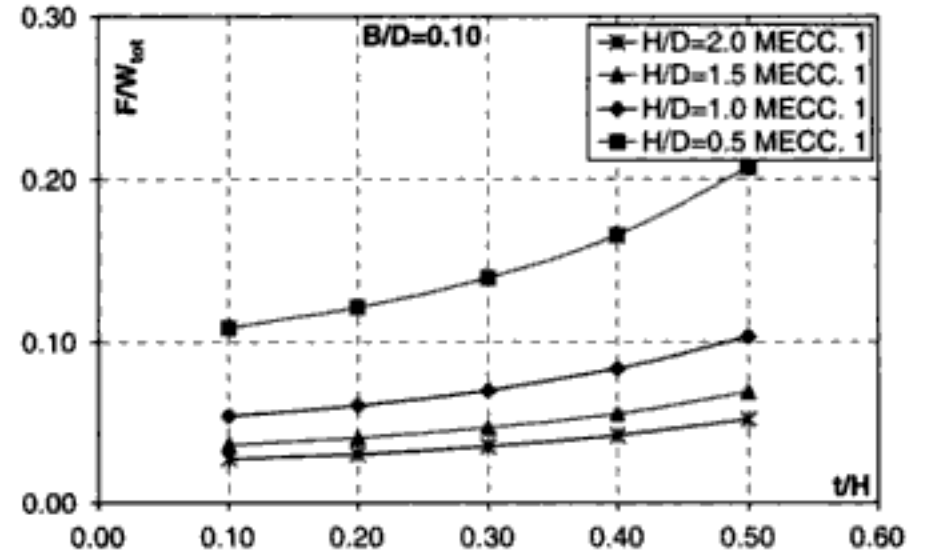


Figure 14. Synthetic diagrams.

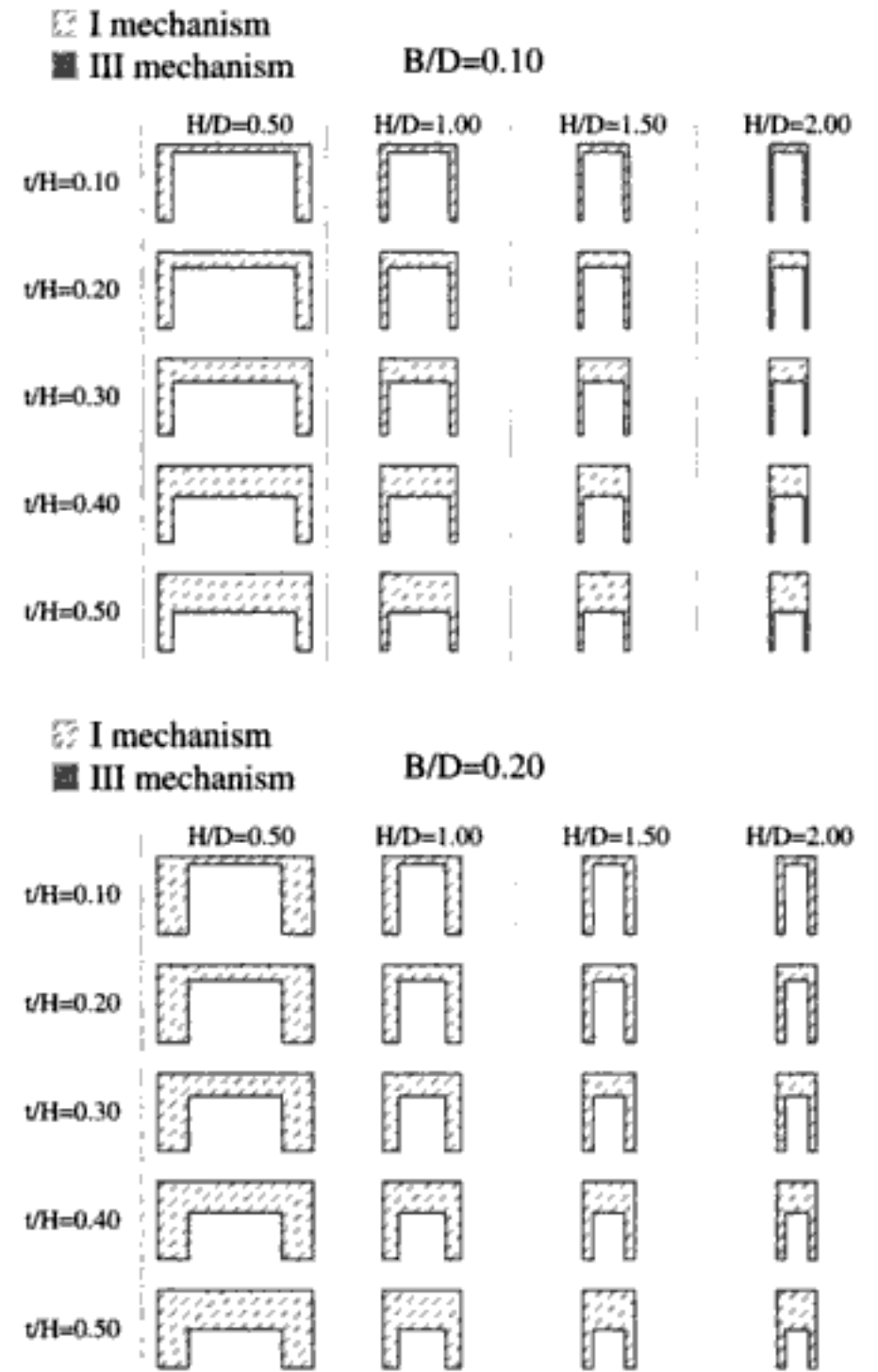


Figure 15. Geometrical configurations for different geometrical ratios values; prevalence of I or III mechanism: $B/D = 0.1$; $B/D = 0.2$.

In figure 14, for I mechanism the collapse multiplier is expressed as a function of t/H with fixed B/D value and for different H/D ratios.

Further, it is possible to define ranges of the fundamental ratios in which a mechanism prevails upon the others (fig. 15).

in which the maximum error is anyway less than 8.5%.

8 CONCLUSIONS

In this paper an exhaustive analysis of masonry portals through limit approach has been presented. In this aim, by adopting the hypotheses made in (Heyman, 1966), the analysis is extended to the portal frame which is a very recurrent element in historical buildings and is analyzed under the loading case of horizontal actions.

The formulation proposed in this paper removes the hypotheses made in previous studies (Como et al., 1983) on similar structures. In this manner, the formulation allows the possibility of deriving in a closed form solution the horizontal capacity of portal masonry frames in absence of reinforcing ties.

The closed form solution have been then used for performing an extensive parametric analysis on 80 structural schemes characterized by considerably varying geometrical proportions.

Abacuses are given for an immediate use for design purposes.

Finally, an approximate solution is proposed for evaluating the horizontal capacities of such schemes. The approximate formula has a very sound mechanical basis since it splits the multiplier in three factors each of them being very simple and immediate in its mechanical significance.

The formula has been tested for all the 80 cases providing excellent results with errors always less than 6%.

We believe that the results provided in this paper both in terms of closed form and approximated solutions might be very valuable for the designer in evaluating the capacity of portal masonry frames of historical buildings to horizontal action which are related to their seismic strength.

ACKNOWLEDGEMENT

This research has been partially supported by CNR "Progetto Finalizzato Beni Culturali" and has been developed in the context of the activities of "Centro di Competenza CRdC BENECON".

REFERENCES

- Abruzzese D., Como M. & Lanni G. 1990. *On the Horizontal Strength of the Masonry Cathedrals*. 9ECEE Conference Committee in Moscow. Elsevier Science.
- Abruzzese D., Como M. & Lanni G. Some results on the strength evaluation of vaulted masonry structures. *Structural Studies of Historical Buildings IV*. 1. Computational Mechanics Publications.
- Como M. & Grimaldi A. 1983. *Analisi limite di pareti murarie sotto spinta*. Quaderni di teoria e tecnica delle strutture. 546. Università di Napoli: Istituto di Tecnica delle Costruzioni.
- Coulomb C.A. 1773. Essai sur une application des regles de maximis et minimis à quelques problemèmes de statique relatifs à l'architecture. *Mem. de Math. Et Phys.*: 343. Paris: Acad. Roy. des Sciences.
- De Luca A., Giordano A. & Mele E. 2003 submitted. A procedure for the assessment of the seismic capacity of triumphal arches. *Engineering Structures*. Elsevier Science.
- Giordano A., Mele E. & De Luca A. 2002. Numerical modelling of masonry structures through different approaches. *Engineering Structures*. 24: 1057–1069. Elsevier Science.
- Heyman J. 1966. The Stone Skeleton. *International Journal of Solids and Structures*. 2: 249–279. Pergamon Press.
- Heyman J. 1969. The safety of masonry arches. *International Journal of Solids and Structures* 11: 363–385. Great Britain: Pergamon Press.
- Koorian A. 1953. Limit Analysis of voussoir (segmental) and concrete arches. *Journal of American Concrete Institute*. 89: 317–328.
- Massonet C.H. & Save M. 1980. *Calcolo plastico a rottura delle costruzioni*. Milano: CLUP.

Staircases as cantilevers or arches? – a question for limit analysis

E.A.W. Maunder

Department of Engineering, University of Exeter, UK

ABSTRACT: The questions of determining the load capacity and possible modes of load transfer are considered for “cantilever” staircases, i.e. where the treads appear to cantilever from a side wall, but where such a description is inadequate or inappropriate on closer inspection. Alternative modes of action are proposed in terms of arch actions in a flight of treads with discontinuous thrust lines. The discontinuities are balanced by torsional moments from the side wall. The questions are then addressed via limit analysis as an optimization problem with an implicit appeal to the lower bound theorem of plasticity. The problem is posed as a non-linear one and solutions, as exemplified for granite staircases in Castle Drogo, are presented based on a generalized reduced gradient algorithm using a spreadsheet format.

1 INTRODUCTION

Staircases are a vital component of multi-storey structures. They may be purely functional or form spectacular aesthetic features, and they can involve many different structural systems from simply supported inclined spans to dog-leg frames and curved spirals. This paper is concerned with a particular structural form which relies on interactions between treads as voussoirs combined with torsional reactions to individual treads from a stairwell.

It may be speculated that such a form originated in the 16th century in the works of the Italian renaissance architect Andrea Palladio with his development of systematic geometric design principles in three dimensions. In the modern translation by Tavernor & Schofield (1997) it is clear that Palladio recognized and advocated staircases supported by an outer wall without support in the middle. Similar structural concepts appear to have been extended to spectacular staircases with large oval stairwells in the 18th century, e.g. in the Greenwich Naval Hospital as recently discussed by Eatherley & Brady (2004), and Sharpham House in Devon as discussed by Cherry & Pevsner (1989).

Price (1996) has provided good explanations of the structural principles and the important roles of torsional moments provided to the treads by the supporting wall of the stairwell, and the interactions between treads even if these are only provided by small horizontal overlaps as observed in Palladio’s design for the monastery of the Carita in Venice. Price (1996) also explains the structural significance of rebates between treads, in that they allow inclined thrusts to be transmitted in a similar way as occurs between

voussoirs of an arch. Indeed arching action alone in the manner of a flying buttress has been noted by Sutherland (1994).

However there is a danger that the underlying structural concepts could be misunderstood by present day architects and others involved with maintenance and refurbishment. The term “cantilever” is a commonly used adjective, e.g. Cherry & Pevsner (1989), and whilst this term may be used as a generic one for the type of staircase under consideration there is an obvious risk that the term may be taken too literally as indicated by the recent collapses reported by Parker (2004).

The question in the title of this paper is a somewhat oversimplified one, since the torsional moments allow cantilever and arch modes of action to share the load with considerably more capacity than can be justified by either of the separate modes. Such questions are reminiscent of those raised in the debate on dam design in the early 20th century, Smith (1972), when arch and/or gravity (cantilever) modes of action were being considered. It appears that, without recourse to elastic theories, European designers at least decided themselves how a dam should work by placing reliance, perhaps unwittingly, on the lower bound theorem of plasticity.

These questions can be answered using non-linear numerical optimization techniques in the context of a limit analysis. This paper considers the optimization problem as one of maximizing a load factor applied to live loads with all other variables being static ones, i.e. stress resultants which are sufficient to determine all stresses of interest, subject to constraints which are generally non-linear. To the author’s knowledge the

staircase problem has not been considered before in this way although the underlying philosophy is similar to that discussed by Maunder & Harvey (2001).

The opportunity has also been taken to demonstrate optimization using a spreadsheet and a generalized reduced gradient algorithm as available in Excel. For relatively small scale problems such tools appear to be very suitable and they have the advantage of providing a transparent approach to computational aspects with both the intermediate workings and the final results displayed along with appropriate graphical output – all at the control of the engineer, Gottfried (1998).

The paper continues in Section 2 to describe an equilibrium model for limit analysis. An example of a typical granite staircase in Castle Drogo, the most recent castle to have been built in the UK, is considered in Section 3 where optimized solutions for load transfer are illustrated with thrust line diagrams as for an arch. This example is also considered in the context of a parametric study, as advocated by Eatherley & Brady (2004), when there are uncertainties in the data, e.g. the depths of embedment and the safe bearing stresses. Conclusions and proposals for further work are contained in Section 4.

2 AN EQUILIBRIUM MODEL

2.1 A tread as a cantilever

Each tread is embedded into a supporting wall which provides as reactions a bending moment M , a vertical shear force V and a torsional moment T . The moment M and shear V are assumed to be transmitted via contact with the horizontal surfaces of a rectangular section. The torsion T is assumed to be transmitted via both horizontal and vertical surfaces. All transmission is assumed via uniform normal bearing stresses σ_v or σ_h

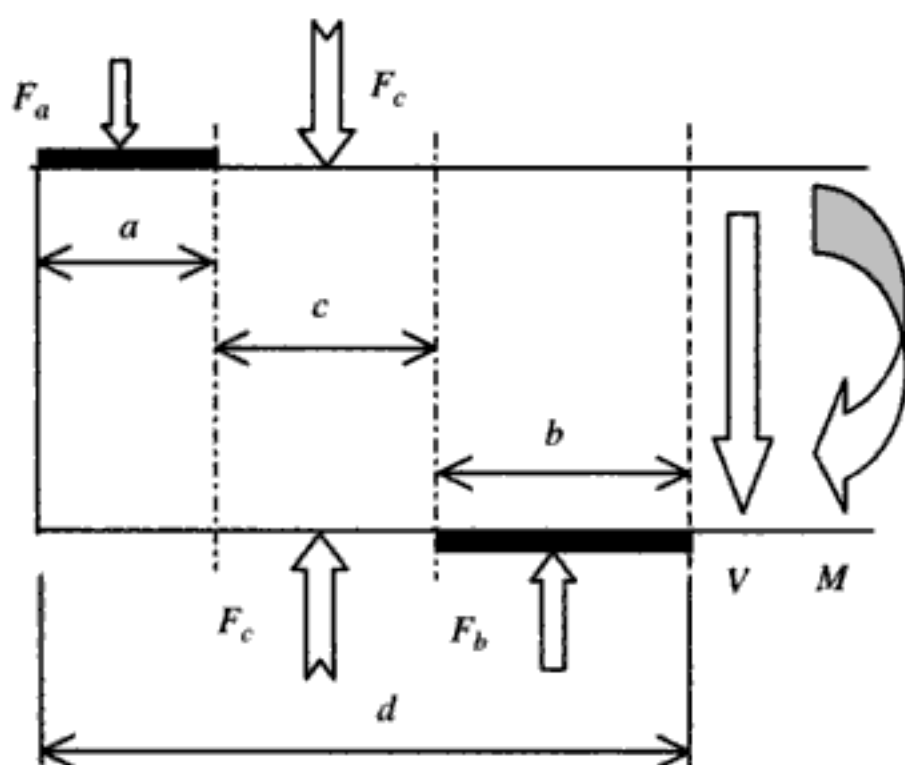


Figure 1. Vertical contact forces on a tread.

on allocated contact areas. These areas are somewhat arbitrary, but are selected and optimized to maximize the stress resultants.

The horizontal areas for σ_v are indicated in Figure 1 where d denotes the embedment length. The stress resultants must satisfy the equilibrium Equations (1).

$$-F_a + F_b = V$$

$$F_a(d - 0.5a) - F_b \cdot 0.5b = M \quad (1)$$

$$F_c z = T_v$$

where z is the lever arm of the torsional couple T_v formed by the pair of forces F_c . These equations can be put into non-dimensional forms as in Equation (2).

$$-\xi + \eta = r_1$$

$$\xi - 0.5\xi^2 - 0.5\eta^2 = r_2 \quad (2)$$

$$1 - \xi - \eta = r_3$$

where

$$\xi = \frac{a}{d}, \quad \eta = \frac{b}{d}$$

and

$$r_1 = \frac{V}{\sigma_v w d}; \quad r_2 = r_1 \frac{M}{V d} = r_1 r; \quad r_3 = \frac{4T_v}{\sigma_v w^2 d}$$

where w denotes the width of a tread. The torsion component T_v is maximized in the above equation with the relevant contact areas extending over half the width of the tread and $z = 0.5w$.

For a fixed ratio r combined shear and torsion becomes limited by Equation (3).

$$r_1^2 + 2r_1 + 4r \cdot r_1 + r_3^2 = 1 \quad (3)$$

Equation (3) represents an arc of a circle in r_1, r_3 space illustrated in Figure 2, with the maximum magnitude

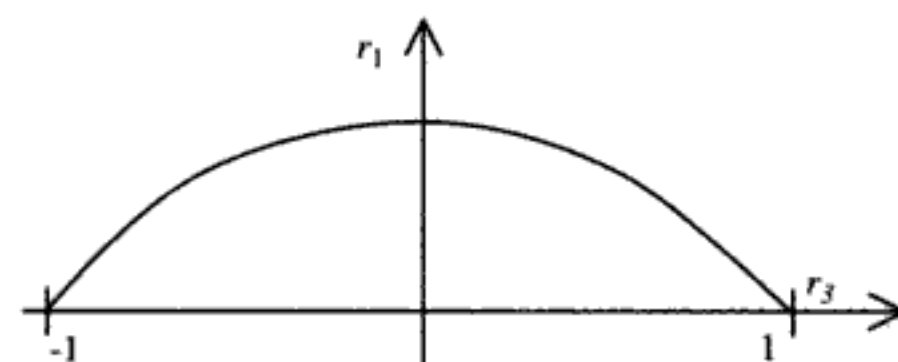


Figure 2. Shear/torsion interaction diagram.

of r_3 being 1 when $r_1 = 0$, and the maximum value of r_1 being given by Equation (4) when $c = r_3 = 0$.

$$r_1 = (2 + 4r + 4r^2)^{0.5} - 2r - 1 \quad (4)$$

A torsion component T_h is provided by bearing stresses σ_h on the vertical faces as indicated in Figure 3 and defined in Equation (5).

$$F_e(h - e) = T_h \quad (5)$$

T_h is maximized with the vertical contact areas extending over height $e = 0.5h$, and then T_h is given by Equation (6).

$$T_h = \sigma_h \frac{h^2 d}{4} \quad (6)$$

2.2 A flight of treads as an arch

Treads butt together at waist sections like voussoirs of an arch or flying buttress with adjacent landings acting as abutments. This mode of action is shown in Figure 4 with a typical thrust line to support the weight of the treads.

However for the thrust line to be admissible it needs to lie within the waist sections without overstressing the contact areas between adjacent treads. With reference to Figure 5, and again assuming uniform compressive stress on the contact area with a maximum value of σ_u , the axial stress resultant is equivalent to an axial force N and a bending moment M about the central axis.

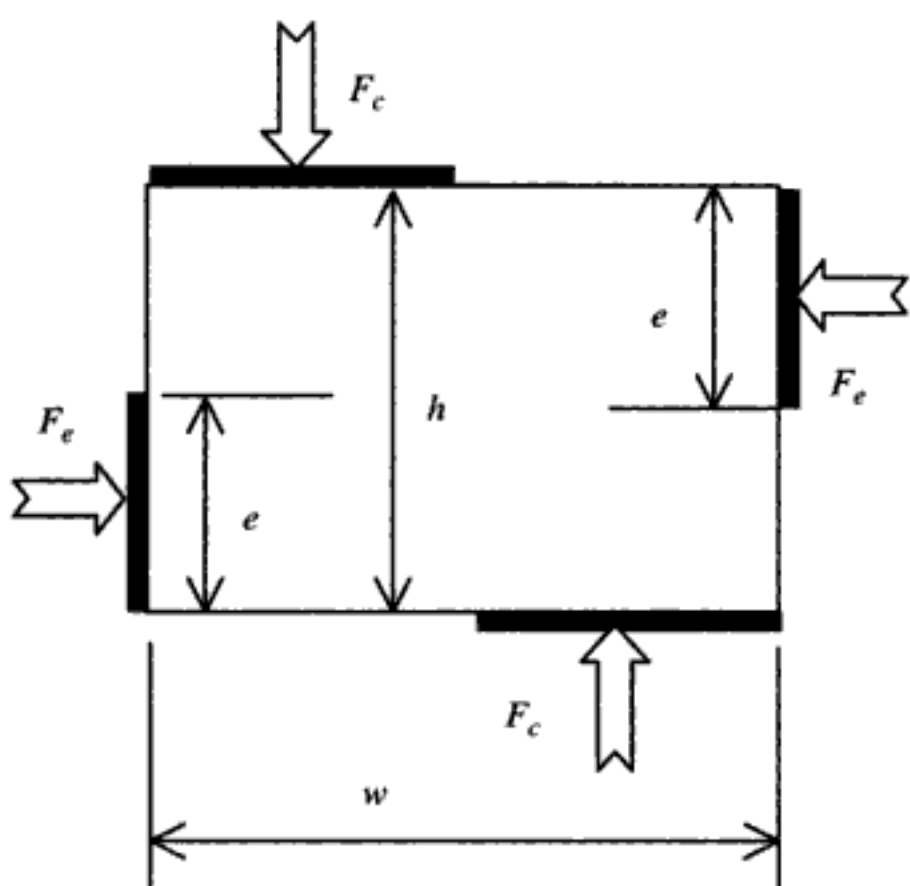


Figure 3. Torsional contact forces on a tread.

When the maximum stress σ_u applies, the stress resultants are related by Equation (7).

$$r_4 = \frac{M}{tN_u} = \frac{1}{2} \frac{N}{N_u} \left(1 - \frac{N}{N_u} \right) = \frac{r_3}{2} (1 - r_3) \quad (7)$$

where r_3 and r_4 are the non-dimensional terms representing N and M respectively, and $N_u = \sigma_u t l$ where l denotes the length of the outstand of a tread from the wall. Equation (7) defines limiting curves in r_3, r_4 space as illustrated in Figure 6.

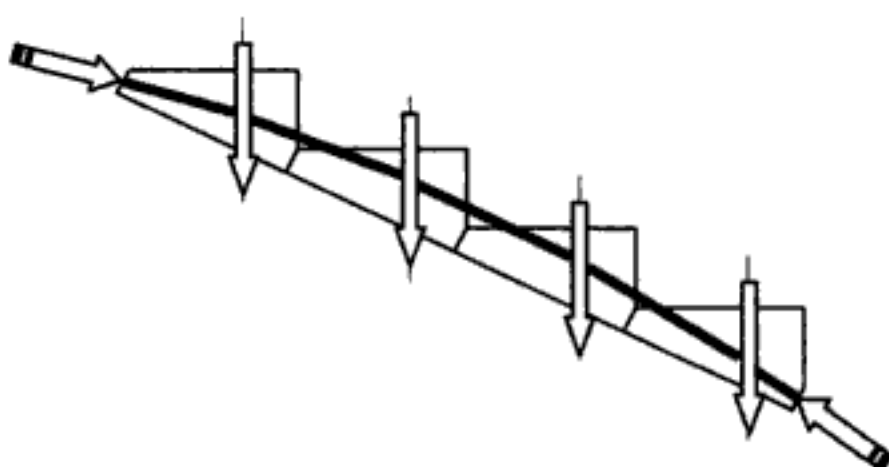


Figure 4. Continuous thrust line for arch action.

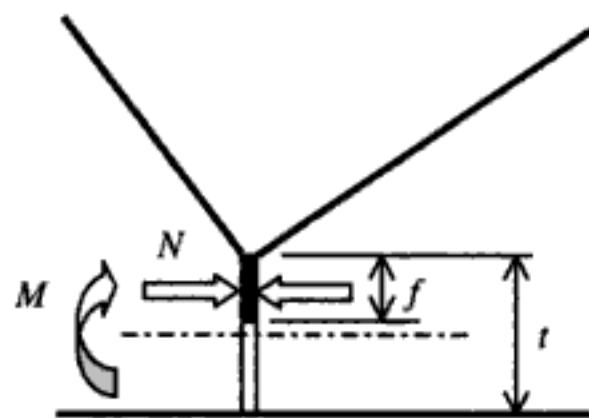


Figure 5. Detail of tread interaction.

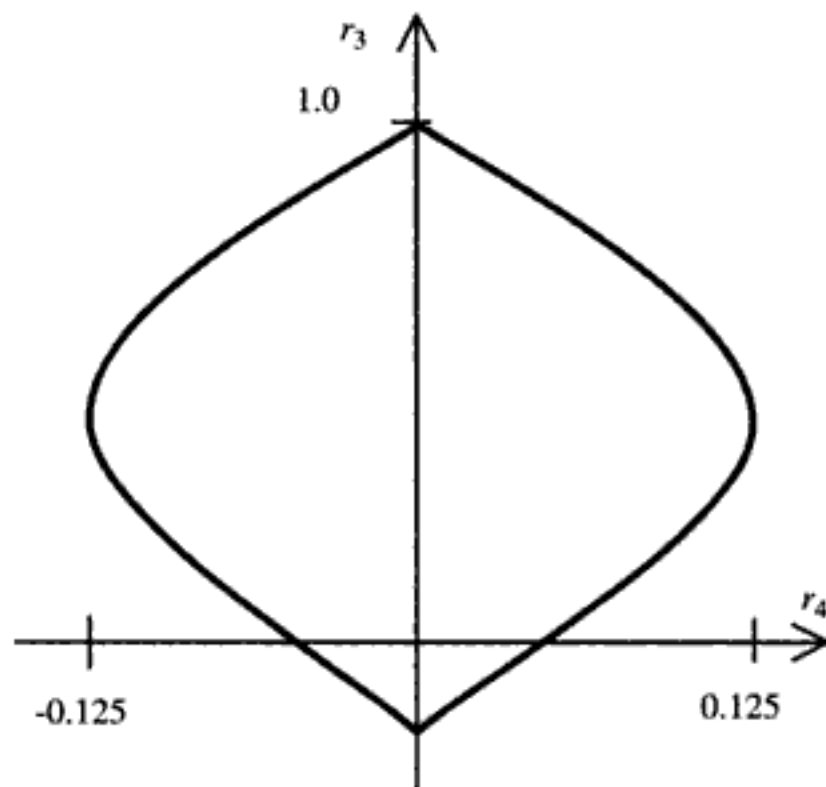


Figure 6. Thrust/moment interaction diagram.

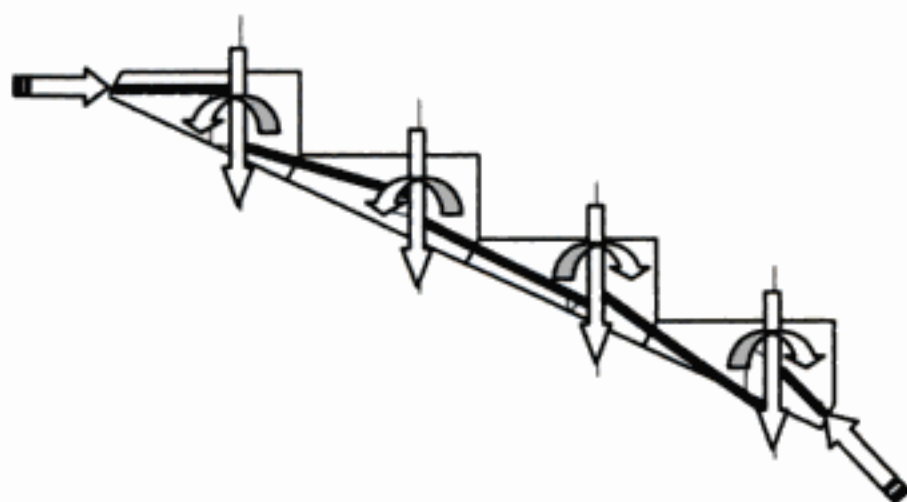


Figure 7. A discontinuous thrust line solution.

In general thrust line solutions can only be made admissible by allowing for discontinuities within the treads which are balanced by torsional moments introduced from the wall as indicated in Figure 7.

2.3 Non-linear optimization

The optimization problem is now posed which seeks to combine the modes of action described above in Sections 2.1 and 2.2 so as to maximize the live load capacity within the stress limits σ_v , σ_h , and σ_u .

The total vertical loads on the stairs are represented by the combination of dead and live loads in Equation (8), where λ denotes the live load factor.

$$W_{Total} = W_{Dead} + \lambda \cdot W_{Live} \quad (8)$$

The objective is to maximize λ . The variables other than λ are static quantities comprising: the shear forces V supported by cantilever action; the torsional moments T_v and T_h provided by the wall; plus three biactions X selected to render the arch statically determinate when $X = 0$.

The linear constraints correspond to the limits imposed on T_h by Equation (6) and to limits imposed by friction between the treads and/or the treads and the supporting landings.

Non-linear constraints in quadratic form correspond to the limits imposed on combinations of V and T_v by Equation (3), and to the limits imposed on combinations of N and M by Equation (7).

3 NUMERICAL EXAMPLES BASED ON STAIRCASES IN CASTLE DROGO

Castle Drogo, near Drewsteignton in Devon, is generally considered to be the last castle built in England in the early part of the 20th century according to Cherry & Pevsner (1989). Its structure is largely one of granite although it also contains early examples of reinforced concrete. The staircase that has been studied

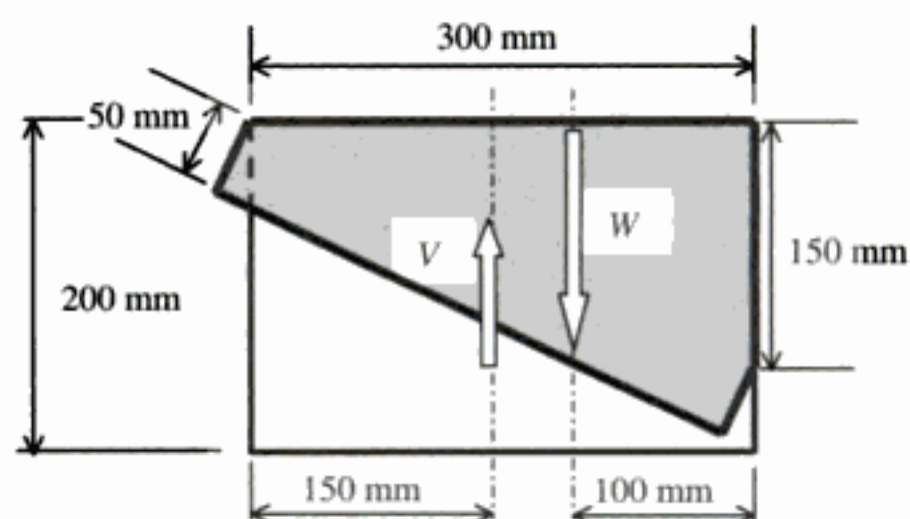


Figure 8. Cross-sections of a tread.

is contained within the North Tower which was originally used as a service wing with a separate staircase. Hence it was ensured that the paths of the servants and family remained separate! The staircase is an impressive granite structure rising up through five storeys, constructed with large granite landing slabs and flights of four treads formed from large blocks of solid granite which are referred to by Cherry & Pevsner (1989) as "cantilevered stone steps". The treads and landings receive support from an enclosing masonry wall. Through the centre of the staircase is an oak balustrade that stands independently from the stairs themselves.

Each tread has a cross-section which approximates to a right-angled triangle, however where a tread is embedded in a wall the section changes to one which approximates to a rectangle. The key dimensions are given in Figure 8 after minor simplification.

Following the work of Parker (2002) the length of embedment into a wall is estimated at $d = 230$ mm, and the self weight of a tread is estimated at 1.042 kN with its line of action inset 100 mm from the leading edge. For simplicity live loads are assumed to have the same line of action.

A typical flight of 4 treads is shown in Figure 4. It should be observed that the treads are not rebated, but the interfaces at the waist are formed on planes normal to the plane of the soffit and so, with the aid of friction, allow for inclined thrusts. For subsequent reference the treads are numbered 1 to 4 from the top of a flight downwards, and the waist sections are numbered 1 to 5 from the top downwards.

The arch, as a 2D structure, is three times statically indeterminate. The release system adopted for the definition of biactions consists of: the axial force N_3 at section 3, and the moments M_1 and M_5 at sections 1 and 5. The basic number of static variables is thus $3 + 4 \times 3 = 15$, however the optimization algorithm requires the use of non-negative variables. Consequently the number of moment variables is doubled to include moments of both senses leading to a total number of non-negative static variables = $5 + 4 \times 5 = 25$.

The total number of constraints applied is $22 = 5 + 3 \times 4 + 5$ made up from 5 for the arch sections, 12

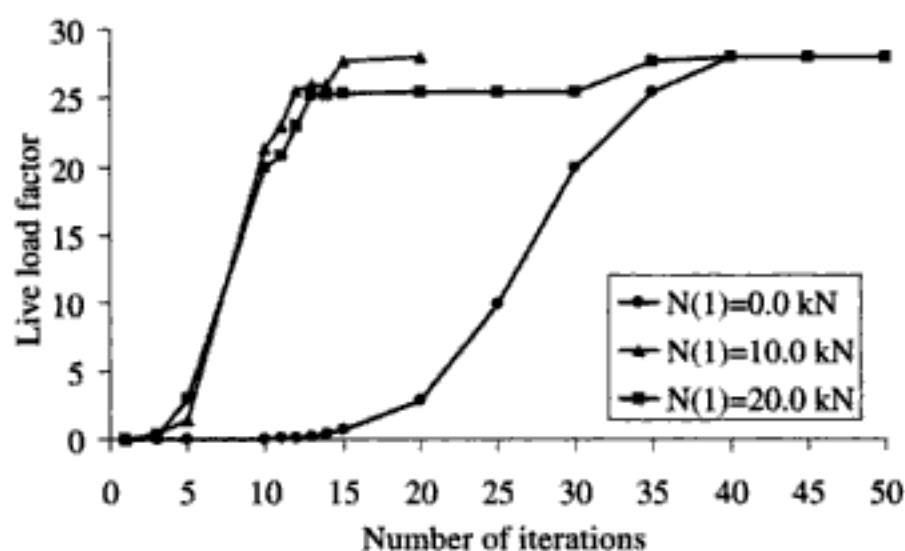


Figure 9. Convergence of live load factor λ .

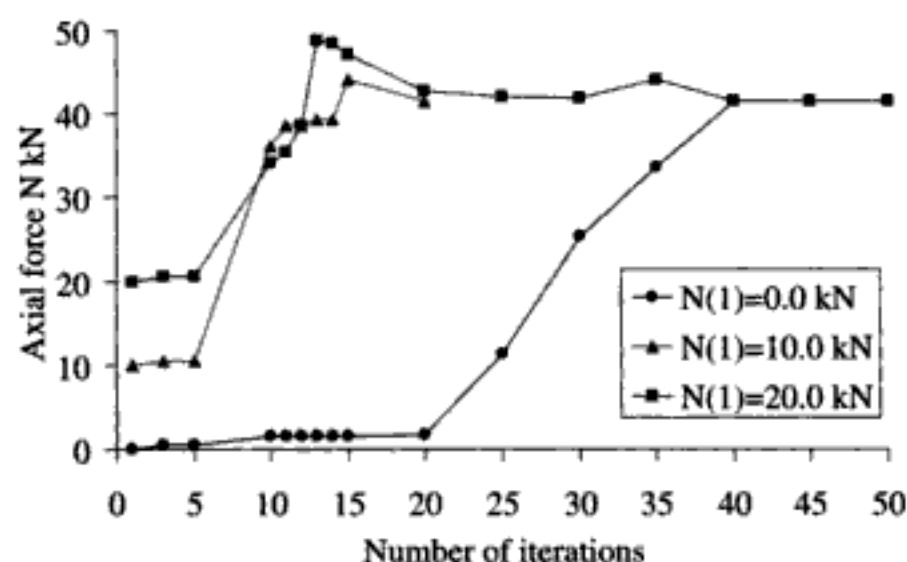


Figure 10. Convergence of axial force N_3 .

for the treads, and 5 to account for friction at sections 1 to 5. The constraints are functions of three normal stress components which are initially considered at the following values:

$$\sigma_u = 1.0 \text{ N/mm}^2, \sigma_v = \sigma_h = 0.5 \text{ N/mm}^2 \quad (9)$$

These values have been set at much lower values than would correspond to the strength of the granite in order to account for the lower strengths normally expected at mortared joints, e.g. see Genna & Ronca (2001).

Due to the non-linear nature of some of the constraints there is a choice for solution method between using linearised constraints in a linear programme, as in Maunder (1993), or to use a non-linear programme. The Excel spreadsheet has the facility to invoke a non-linear generalized reduced gradient (GRG) algorithm which appears to be well suited to the staircase problem – the non-linear constraints being well defined in convex quadratic forms.

3.1 Convergence studies

Figures 9 and 10 illustrate typical convergence behaviour when the stress limits are as given in

Equation (9), the friction coefficient $\mu = 0.5$, and the live load is restricted to tread 2.

All variables are initially set to zero except for the axial force N_3 in section 3. This force serves as a measure of the arching action. The initial value has the physical significance of an axial prestressing force which is then allowed to vary. The initial values are shown as $N(1)$ in Figures 9 and 10.

The operational parameters of GRG were set to an absolute value for the constraint tolerance of 10^{-6} , and a relative value of 1 in 10^6 for the convergence criterion, i.e. the iterations stop when the relative changes in the objective function λ are less than 10^{-6} over 5 iterations. These parameters lead to the same solutions within 45 iterations with monotonic convergence, although as can be seen in Figure 9 the solution initiated with $N(1) = 20 \text{ kN}$ converged to a lower value when the convergence criterion was raised to 10^{-5} . Clearly the value of initial prestress has a significant effect on the number of iterations required. However as soon as $\lambda > 0$, the self weight becomes supportable and all subsequent solutions are feasible even if not optimal. This reflects one of the benefits of an optimization method based on equilibrium.

Figure 10 shows non-monotonic convergence of the axial force from various initial values. When $N(1) = 0$, almost half the number of iterations is needed to mobilize significant arching action. A check on convergence is provided by the evidence in the spreadsheet that arching and cantilever actions are fully mobilized and only the frictional constraints may not be attained. The final solution shows $\lambda = 28.0$ and only 23.3% of the total load is supported by the treads as cantilevers, the remaining 76.7% being supported by the arch.

3.2 Sensitivity studies

A number of parameters, e.g. the depth d of embedment of the treads, the limiting bearing and contact stresses, and the friction coefficient between the treads are likely to have uncertain values. In which case it is prudent to consider ranges of values in sensitivity analyses, and such analyses are now demonstrated for the example of Castle Drogo.

With live load on tread 2 only, Figures 11 to 14 illustrate the effects on live load factors λ and the percentage of the total limit load supported by cantilever action as parameters are varied from a standard set of values with:

$$d = 225 \text{ mm}; \sigma_v = \sigma_h = 0.5 \text{ N/mm}^2, \text{ and}$$

$$\sigma_u = 1.0 \text{ N/mm}^2; \mu = 0.5.$$

The following observations can be made:

- Both the load factor and the proportion of cantilever action are approximately linearly dependent on d .

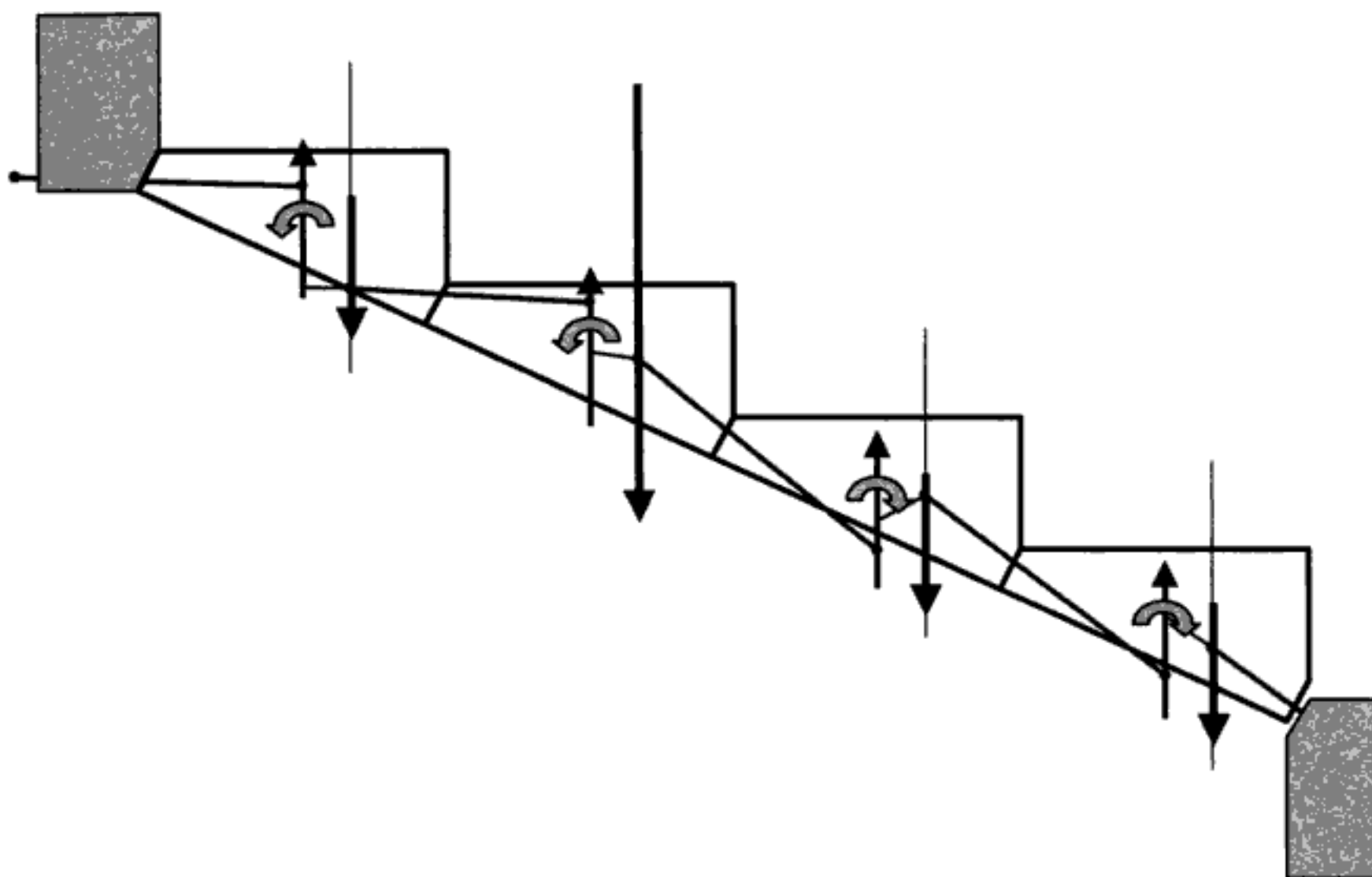


Figure 16. Complete optimized solution for live load on tread 2 only.

- Up to a bearing stress of about 0.8 N/mm^2 the load factor increases approximately linearly with stress and the proportion of cantilever/arch action tends towards a constant value. Higher values of bearing stress permit greater torsional restraints and potentially greater arching action, but this type of action then becomes constrained by friction in both sections for the top tread. Consequently further load requires a greater use of the cantilever actions.
- Up to a contact stress of about 0.6 N/mm^2 the load factor increases and the cantilever action decreases. These changes are mainly influenced by frictional constraints for the top tread. Friction tends not to be fully mobilized as the contact stress increases further, but the arch action then becomes limited by the torsional restraints from the wall, and little further load can be taken for contact stress higher than about 1.0 N/mm^2 .
- For low values of the friction coefficient μ up to about 0.15 the limit loads are constrained by friction on both sections of the top tread. Higher values of μ allow a relative increase in arch action and a greater load with friction still mobilized on section 1. For $\mu > 0.5$ no frictional constraints are mobilized, and the load and mode of action do not change.

3.3 Optimized solutions

Figures 15 and 16 and Table 1 detail optimized solutions for equal loads on all treads, and with live load on

Table 1. Stress-resultants for complete optimized solutions.

Stress-resultant	Equal loads on each tread	Live load only on tread 2
W_1 kN	11.14	1.04
W_2 kN	11.14	28.35
W_3 kN	11.14	1.04
W_4 kN	11.14	1.04
V_1 kN	0.44	0.00
V_2 kN	2.60	2.43
V_3 kN	2.61	2.61
V_4 kN	0.00	2.14
T_1 kNm	-3.433	-3.656
T_2 kNm	-1.320	-1.787
T_3 kNm	-0.004	1.127
T_4 kNm	3.656	2.194
P_1 kN	34.87	32.21
P_2 kN	36.48	32.26
P_3 kN	39.83	42.66
P_4 kN	44.58	41.64
P_5 kN	52.25	40.95

tread 2 only, based on the standard set of parameters. For the equal load case it is observed that self-weight could be supported by (a) cantilever action alone with a load factor of about 2.50, or (b) arch action alone with a load factor of about 1.0, or (c) the optimized solution as illustrated in Figure 15 with a load factor of about 10.0.

Systems of arches and columns strengthened with FRP at the extrados

U. Ianniruberto

Department of Civil Engineering, University of Rome "Tor Vergata", Rome, Italy

Z. Rinaldi

Department of Mechanics, Structures and Environment, University of Cassino, Cassino, Italy

ABSTRACT: The topical problem of the maintenance and upgrading of the masonry building heritage has led, in these last years, to an increasing interest in new and suitable material and technologies. As a consequence the application of composite material, also on masonry structures, is nowadays considered an assessed and quite usual practice. Nevertheless the adoption of new techniques requires a deep knowledge of the behavior of the reinforced structure and a definition of adequate models able to simulate it. Aim of this paper is the evaluation of the structural behavior of a system of arch and columns, strengthened with FRP at the extrados and loaded by a vertical force at the crown and by two horizontal forces at the abutments of the arch. The scope is pursued by means of a proposed methodology, which, with some simplifying assumptions, allows defining the failure interaction locus of the strengthened structure. The effectiveness of the strengthening intervention is evaluated on the basis of these strength domains defined in the plane of loads.

1 INTRODUCTION

The preservation of the existing masonry structures, particularly in seismic areas is nowadays considered a topic of great interest. In this framework, in the last years, the use of innovative systems to retrofit and/or reinforce structures has been widely developed in the field of civil engineering. Specifically the use of composite sheets (FRP) applied at masonry structures surfaces represents a very attractive solution in the field of research as well as to practical and professional applications. The advantages provided by this material are well known (light material, ease of installation, no corrosion problems, a high specific strength) and the reversibility of the intervention is also a very positive aspect.

Anyway even if applications on real structures are spreading, many uncertainties still remain on the effective global response of the reinforced structure, and particularly on the models to be adopted for the design of the reinforcement, and then for the behavior simulation.

In this work a reference masonry structure made by two piers and an arch, subjected to vertical and horizontal forces, is analyzed. The choice of this peculiar scheme is motivated by its frequent presence in many masonry structures that characterize European historical constructions.

In the following the case of the complete reinforcement of the surface at the extrados of the masonry frame will be considered. This arrangement of the reinforcement prevents the opening of "classical" hinges at the un-reinforced side of the structure, similarly to the case of the reinforcement of the intrados (Ianniruberto & Rinaldi, 2004) and in the case of arches loaded by vertical forces (Como et al., 2001). Then, no kinematically admissible mechanisms can occur in the structure and the classical limit analysis theorems (Kooharian, A. 1953, Heyman, 1966 and 1982), cannot be applied for the evaluation of the collapse behavior of the reinforced construction. The ultimate strength of the structure is governed by local failures due to masonry crushing, masonry slip at a mortar bed or FRP debonding.

In a previous paper the authors analyzed the collapse response of a system of arch and column reinforced at the intrados only. It was highlighted the enhancement of the structural capacity due to the application of FRP sheets, particularly for horizontal actions, and the influence of the debonding phenomenon of the composite material.

Aim of this paper is to show an analytical model for the evaluation of the bearing capacity of the reference masonry frame reinforced at the extrados taking into account failure criteria at both local and global level. Moreover the ultimate domains of the reinforced

structure subjected to combined vertical and horizontal loading conditions, are defined and discussed.

2 COLLAPSE ANALYSIS OF THE UNSTRENGTHENED MASONRY FRAME

The influence of the FRP reinforcement applied at the extrados of a system of piers and arch will be evaluated with reference to the masonry frame, shown in Figure 1, loaded by combined vertical and horizontal concentrated forces. The frame has a square cross section whose side is equal to 0.42 m.

In order to judge the effectiveness of the intervention, the collapse multiplier of the masonry frame without any reinforcement is evaluated within a limit analysis approach based on the classical constitutive hypothesis of rigid-in-compression no-tension material (Heyman, 1982). In this framework for each assigned kinematically admissible collapse mechanism it is possible to define the relationship between the horizontal and vertical loads corresponding to the onset of that failure mode. Then the collapse domain

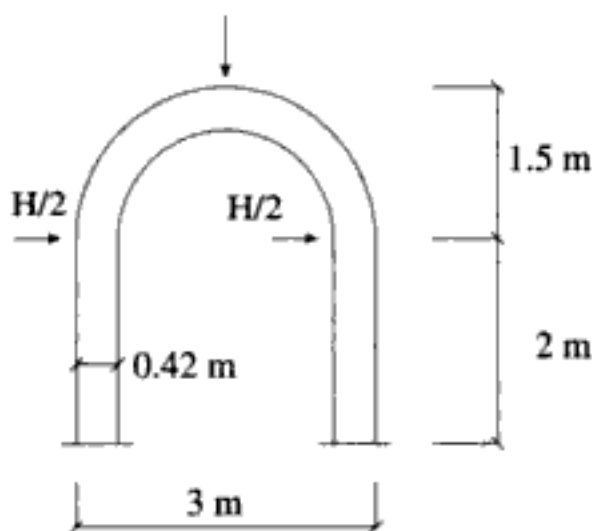


Figure 1. The reference masonry frame.

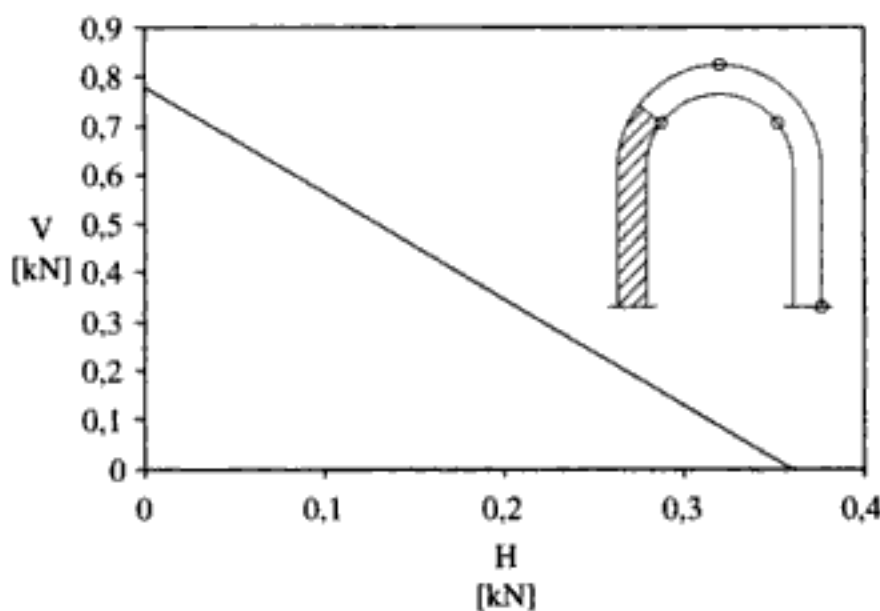


Figure 2. The collapse locus and the collapse mechanism of the un-reinforced masonry frame.

of the structure is obtained by the inmost envelop of the curves related to each possible mechanism.

In this particular case the interaction loci is characterized by a linear pattern and it is related to the asymmetric mechanism reported in Figure 2.

3 BEHAVIOR OF THE MASONRY FRAME STRENGTHENED WITH FRP AT THE EXTRADOS

The strengthening intervention on the reference scheme of Figure 1 is carried out by reinforcing with a composite sheet the entire surface at the extrados of the frame.

It is assumed that the fibers are not bonded below both base sections of the piers. This arrangement of the strengthening sheet is the most frequent because the foundation wall below the column is usually thicker than the pier, which lies on it.

The lack of anchorage length at the bottom implies that the thrust line must lie in the thickness of the pier at the base section.

When the FRP sheets are applied to the entire extrados of the structure, the classical mechanism of the un-reinforced structure can never form and therefore the failure criteria used in the un-strengthened case, which refers to a global collapse, is no more appropriate to evaluate the failure load of the structure. Indeed, as shown in many experimental results, completely reinforced structures exhibit brittle failures due to the crushing of the masonry (Briccoli Bati & Rovero, 1999), the shear failure at the brick-mortar interface (Valluzzi et al., 2001), the debonding of the sheets.

Furthermore in the examined case also the possibility of a global overturning of the entire structure must be taken into account because of the assumption of sheets not bonded below the springing sections.

In order to apply the mentioned failure criteria the evaluation of the internal stresses is required. This paper shows a model that, in the framework of some simplifying assumptions, provides a method to calculate the internal forces in each cross section of the structure, given the horizontal and vertical loads. Then the application of a failure criterion provides the failure locus related to the selected collapse mode. The inmost envelope of the obtained curves gives the failure locus of the reinforced structure.

The behavior of the FRP reinforced scheme is analyzed simulating a load process where the vertical load is kept constant and the horizontal forces increases.

If the structure is loaded only by a concentrated vertical force V at the crown, as soon as V is greater than the collapse load of the un-reinforced frame, the thrust line moves outwards at the haunches and the collapse occurs when three symmetrical hinges are

The comparison with the un-reinforced structure highlights a great increase of the bearing capacity of the reinforced structure even when the ultimate strain is set equal to $0.2 \varepsilon_{f,u}$.

In this last case the limit strain is so low that, under pure horizontal loads, the debonding occurs before the overturning of the entire structure

5 CONCLUSIONS

The paper shows an analytical model to evaluate the strength of a masonry frame made by two piers and an arch under a vertical force at the crown and two horizontal concentrated loads at the abutments of the arch. The model can be easily used to design the strengthening intervention, but it requires the knowledge of both the material properties of the masonry and the limit strain of the fibers, accounting for the FRP debonding.

The parametric analysis performed to evaluate the influence of this phenomenon shows the great sensitivity of the failure loads at the reduction of the maximum strain available in the sheets before the occurrence of the debonding.

The comparison with the un-reinforced case proves the effectiveness of the FRP reinforcement of the extrados that allows the development of a great increase of strength even when the limit strain in the composite material is very low.

REFERENCES

- Briccoli Bati, S. & Rovero, L. 1999. Consolidamento di archi in muratura con composito in fibra di carbonio. In Atti del II Convegno Materiali e Tecniche per il Restauro, Cassino, Ottobre.
- Como, M., Ianniruberto, U. & Imbimbo, M. 2001. On the structural capacity of masonry arches strengthened by FRP. In Proceedings Third International Conference on Arch Bridges, Paris, September 2001.
- Eurocode 6 – Design of masonry structures, ENV 1996.
- FIB Bulletin. 2001. Externally bonded FRP reinforcement for RC structures. Bulletin d'Information N. 14, Lausanne.
- Focacci, F. 2003. Rinforzo di archi in muratura con cavi scorrevoli. Proc. of the 16th AIMETA Congress of Theoretical and Applied Mechanics.
- Heyman, J. 1966. The Stone Skeleton. In Inter. Journ. Of Solids and Structures, 2.
- Heyman, J. 1982. The Masonry Arch. Ellis Horwood Limited Publ., Chichester.
- Kooharian, A. 1953. Limit Analysis of voussoir and concrete slabs. Int. Journ. American Concrete Institute, 24.
- Ianniruberto, U. & Rinaldi, Z. 2004. Resistenza laterale di portali in muratura rinforzati con FRP all'intradosso. Proc. Of the XI National Conference ANIDIS 04, Genova, Italy.
- Valluzzi, M. R., Valdemarca, M. & Modena, C., 2001. Behaviour of brick masonry vaults strengthened by FRP laminates. ASCE Journal of Composite for Constructions. Vol. V. No 3, August.

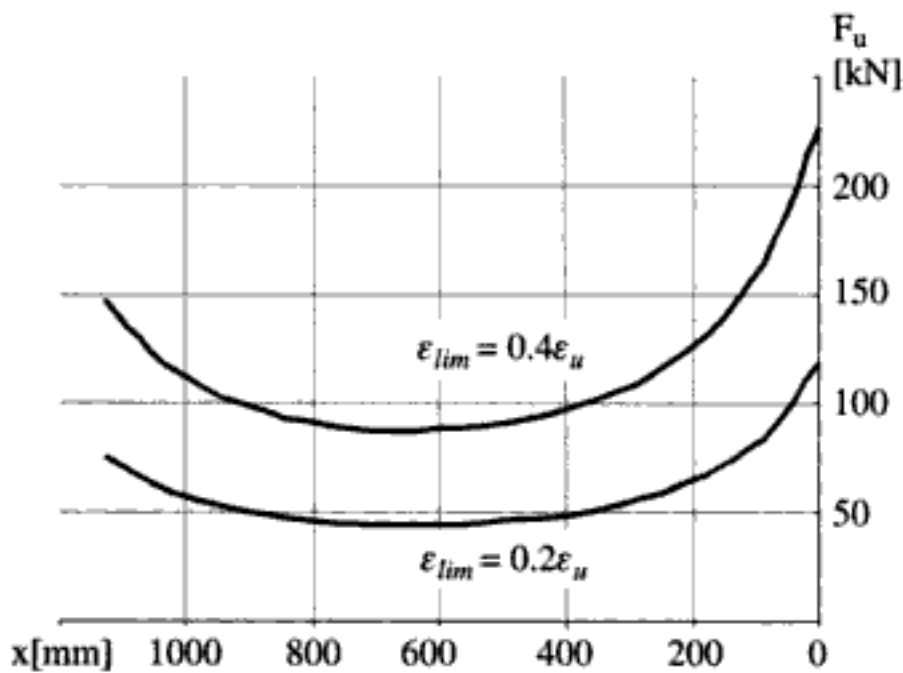


Figure 3. FRP reinforcement at the intrados: Ultimate load versus load application point.

As a consequence of the hinge pattern, the reinforced arch, close to the collapse, behaves as a statically determined structure. This allows the evaluation of the internal loads and then, by imposing the flexural failure criterion in the critical section, the definition of the ultimate load.

The debonding of the sheets is taken into account by reducing the ultimate strain in the fiber ε_{uFRP} , according to the approach suggested in the FIB Bulletin n.14, (2001) for FRP reinforced concrete structure.

Due to the lack of experimental and theoretical results two values of the limit strain in the FRP are considered: $\varepsilon_{lim} = 0.4\varepsilon_{uFRP}$ and $\varepsilon_{lim} = 0.2\varepsilon_{uFRP}$. For both these conditions the ultimate load is plotted versus its application points in Figure 3.

As expected the failure is always governed by the FRP debonding and then the reduction of the limit strain from 0.4 to $0.2\varepsilon_{uFRP}$ leads to a shifting of the curve towards lower values of the ultimate capacity.

The critical section, where the failure occurs, is located at the load application point, for every load position. The maximum bearing capacity is reached when the vertical load is at the crown (about 225 kN and 120 kN for $\varepsilon_{lim} = 0.4\varepsilon_{uFRP}$ and $\varepsilon_{lim} = 0.2\varepsilon_{uFRP}$, respectively), while the minimum ultimate load is attained when the force is located at the haunch (about 90 kN and 50 kN for $\varepsilon_{lim} = 0.4\varepsilon_{uFRP}$ and $\varepsilon_{lim} = 0.2\varepsilon_{uFRP}$, respectively).

3 NUMERICAL MODEL

The collapse behaviour of the reference arch is evaluated also by means of a F.E.M. program – Fiber-implemented by (Petrangeli, 1999).

The structural cross-sections are modelled with fibre elements, in the classical hypothesis of plane sections. Due to this assumption the FRP debonding needs to be simulated, once again, by fictitiously

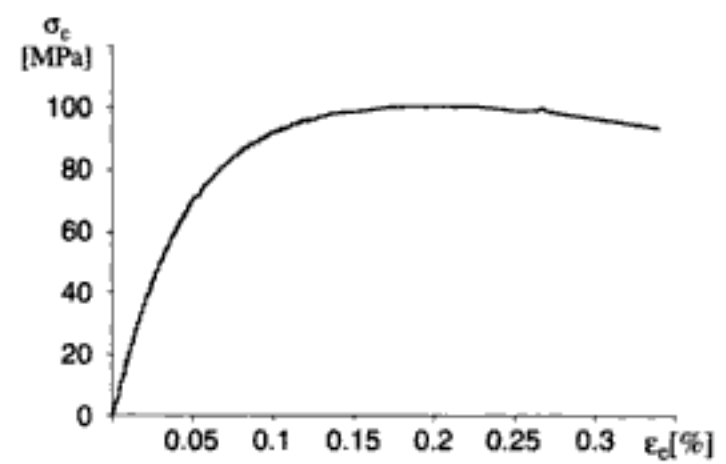


Figure 4. Numerical analysis: masonry constitutive law.

reducing the ultimate strain of the composite material. Improvement of the model through the introduction of an interface element, able to simulate the phenomenon and also to validate the adopted simplified procedure is now in progress. The main purpose of this study will be the assessment of the reduction factor to be applied at the ultimate FRP strain, in order to account for the debonding, particularly in the case of masonry-curved surfaces.

The fiber number in which each section is divided, equal to 30, and the number of elements constituting the arch, equal to 26, are defined on the basis of preliminary sensitivity analyses.

The masonry is simulated as a no-tension material, with the non-linear compression behaviour reported in Figure 4, limited to an ultimate strain equal to 0.35%, in agreement with the constitutive law assumed in the analytical model. The FRP sheets are considered unable to sustain any compressive stress and are characterised by an elastic behaviour. The material properties agree with the ones adopted for the analytical model (Tab. 1).

The analyses have been performed both in displacement and force control, by increasing the external action up to the structure failure.

A preliminary study is carried out with reference to the un-reinforced scheme, in order to evaluate the effectiveness of the program in simulating the arch behaviour and in particular its collapse mode, governed by a mechanism formation.

The comparison between analytical and numerical results is reported in Figure 5, where the collapse load (F_u) is plotted versus the distance of the point load from the keystone. The numerical results, as can be noted, are quite perfectly coincident with the ones obtained through the application of the classical limit analysis approach.

Furthermore the numerical thrust lines at collapse are plotted for three positions of load and are in perfect agreement with the ones required by the static and kinematics theorems, as can be observed in Figure 5 where the points in which the thrust line touches the surface of the arch are indicated with the classical symbol of hinge.

the strain pattern and in particular of the thrust line can be followed for each load step.

The comparison among the collapse behaviour of the reinforced arches, evaluated with the two models, gives very satisfactory results, both in terms of failure mode and collapse load values.

The position of the hinges assumed in the proposed analytical model is well confirmed by the numerical results together with the adopted hypothesis of a collapse behaviour evaluated on a statically determined structure.

Finally the paper shows the reliability of the analytical model that proves to be a very simple and powerful tool for the evaluation of the collapse behaviour of masonry arches entirely reinforced at the extrados and loaded by vertical point loads.

REFERENCES

- Briccoli Bati, S., & Rovero, L. 1999. Consolidamento di archi in muratura con composito in fibra di carbonio. In Atti del II Convegno Materiali e Tecniche per il Restauro, Cassino, Ottobre.
- Como, M., Ianniruberto, U., & Imbimbo, M. 2000. La resistenza di archi murari rinforzati con fogli in FRP. In Atti del Convegno Nazionale "La meccanica delle murature rinforzate con FRP-materials: modellazione, sperimentazione, progetto, controllo", Venezia, Dicembre 2000.
- Como, M., Ianniruberto, U., & Imbimbo, M. 2001. On the structural capacity of masonry arches strengthened by FRP. In Proceedings Third International Conference on Arch Bridges, Paris, September 2001.
- Como, M. 1992. Equilibrium and collapse Analysis of Masonry Structures. In *Meccanica*, Vol. 27, No. 3, Kluwer, Acad. Publ.
- Eurocode 6 – Design of masonry structures, ENV 1996.
- Faccio, P., Foraboschi, P., & Siviero, E. 1999. Volte in muratura con rinforzi in FRP. In *L'Edilizia*, De Lettera Ed., Milano, n.7/8 pp. 44–50.
- FIB Bulletin N° 14, 2001. Externally bonded FRP reinforcement for RC structures.
- Foraboschi, P. 2000. FRP reinforcement used to upgrade masonry arch bridges to current live loads. In *Proc. Of Advanced FRP Materials for Civil Structures*, Bologna, Italy, 19/10, pp. 109–119.
- Heyman, J. 1966. The Stone Skeleton. In *Inter. Journ. Of Solids and Structures*, 2.
- Heyman, J. 1982. *The Masonry Arch*. Ellis Horwood Limited Publ., Chichester.
- Kooharian, A. 1953. Limit Analysis of voussoir and concrete slabs. *Int. Journ. American Concrete Institute*, 24.
- Ianniruberto, U., Fabiani, & F.M., Rinaldi, Z. 2004. Collapse behaviour of FRP reinforced masonry arches: a parametric enquire. IMTCR04, Liguori Ed., Lecce, June.
- Petrangeli, M., Pinto, P., Ciampi, V. 1999. Fiber element for cyclic bending and shear of RC structures, I: Theory. *Journal of Engineering Mechanics*, 125, 9, Sept. 1999, pp. 994–1001.
- Valluzzi, M.R., Valdemarca, M., & Modena, C., 2001. Behaviour of brick masonry vaults strengthened by FRP laminates. *Journal of Composite for Constructions*. Vol. V. No , August.

Table 4. Probability to exceed $\bar{\epsilon}_v$ for different σ_v .

Ex. pr. of $\bar{\epsilon}_v = 1.25e - 005$	σ_v (N/mm ²)
10%	2.35
63%	4.30
90%	5.40

Table 5. Probability to exceed $\bar{\epsilon}_h$ for different σ_v .

Ex. pr. of $\bar{\epsilon}_h = 1.25e - 005$	σ_v (N/mm ²)
10%	3.00
63%	4.23
90%	4.75

stress level in the case of vertical strain. On the contrary, at 63% and 90% of the cases the exceedance of the chosen threshold strain-rate is performed at a lower stress level in the case of horizontal strain, exactly like in the creep test. In fact, at low stress values the material response is still visco-elastic, therefore the higher strain is shown in the loading direction. This was not evident in the case of creep tests because the load history of the different prisms was not the same and less regular data were available, therefore on a statistical basis the phenomenon was not evident. At higher stress level, approaching failure, the tendency is inverted: the material response turns into visco-plasticity with visible crack appearance corresponding to dilatant behavior, as shown by Figure 3, where at stress levels higher than about 2.5 MPa the horizontal strain appears to be higher and developing at a higher rate than the vertical ones. Again, this is confirmed also by the crack patterns (Figures 4 and 5).

5 APPLICATION TO THE BELL TOWER OF MONZA

The proposed probabilistic approach has been applied for the first time to a real case trying to evaluate the results of the monitoring of a massive historic building subjected to persistent load. The Bell Tower of Monza, a XVI century structure built in solid brickwork masonry, had suffered major and diffused cracks due to high compression (Fig. 12).

After the constitution of a Technical Committee in 1976 the building, together with the Cathedral, was subjected to a systematic control, setting up 31 fixed basis, 7 of which on the Tower corresponding to the major cracks. The basis had a length of about 400 mm, and the measurements were taken, starting in January 1978, every month during the first three years and every three months subsequently. The instrument used was a millesimal deformometer. After the recorded

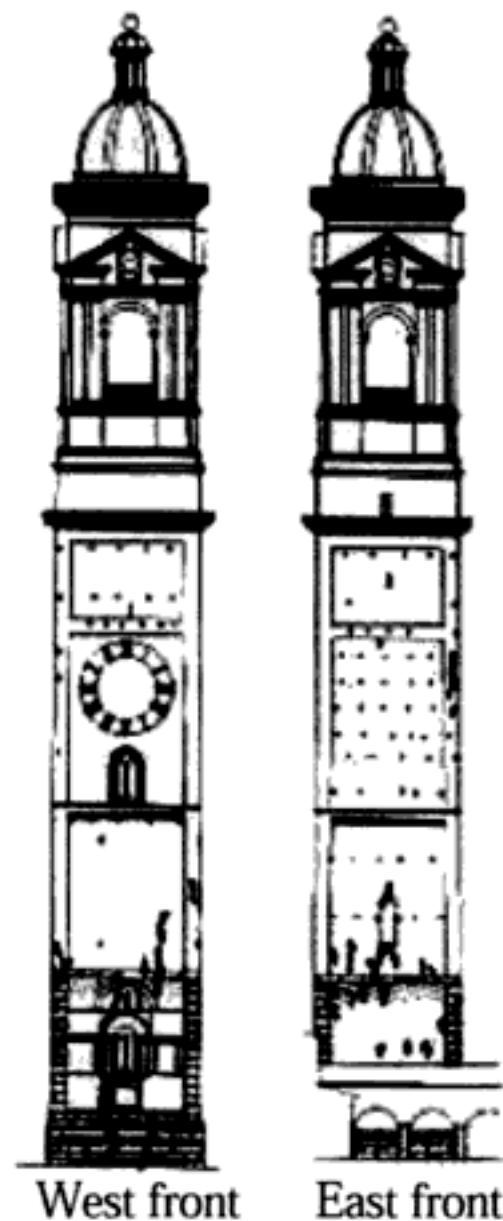


Figure 12. Crack pattern of the Bell Tower of Monza.

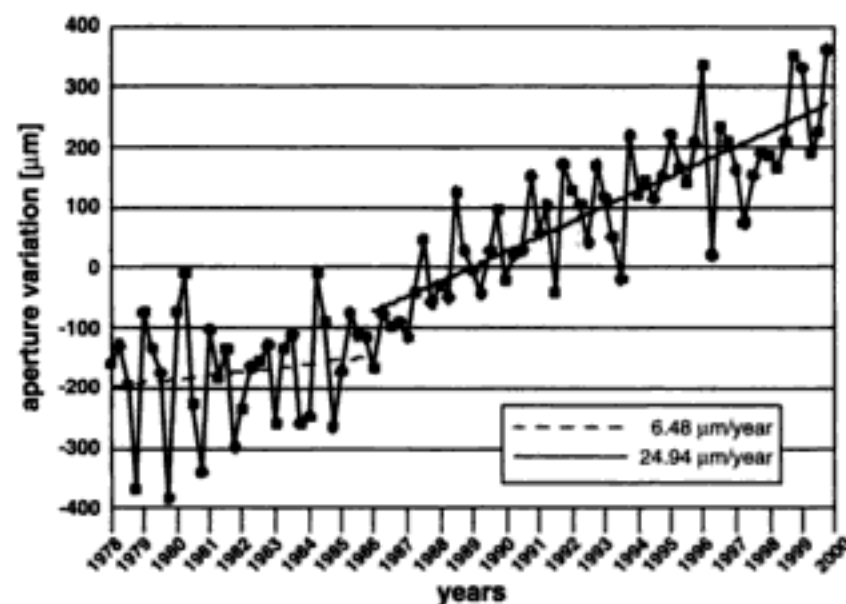


Figure 13. Monitoring of the Bell Tower of Monza: opening variation of a crack vs. time.

increase of the cracks aperture on the Tower and an anomalous geometry recorded on the Cathedral, in 1992 a new Committee was constituted by Politecnico di Milano, who installed a static control system, that included the continuation of the geometric evaluation of the cracks. Each of the previous basis was substituted by a couple of new basis placed above and below the other ones, having a length of 200 mm, the readings being taken at the same periodicity. Considering the data collected until 1999 (Figure 13), the influence of thermal variation on the crack opening can clearly be observed.

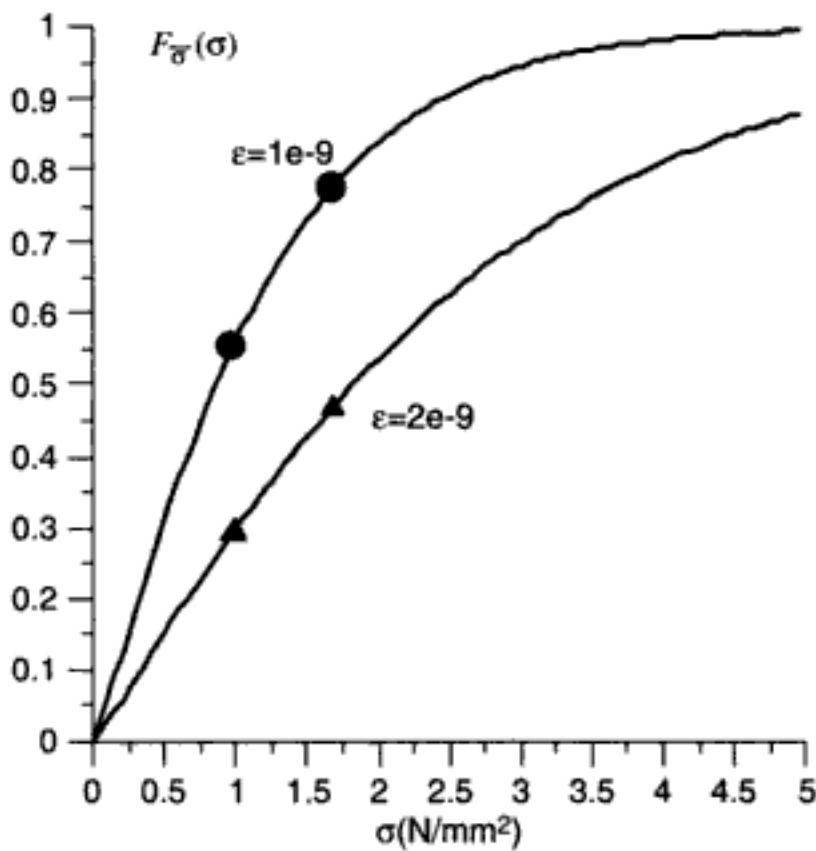


Figure 14. Experimental (● – ▲) and theoretical (—) fragility curves.

Nevertheless, tracing a regression line between the data, a neat increase of the aperture in time is visible; in the case of the base shown in Figure 13 a rate of aperture of 6.48 micron/year can be measured until 1986 and a higher rate of 24.94 micron/year can be measured subsequently, clearly indicating a worsening of the Tower static conditions. After the static survey, a consolidation intervention on the Tower was required, which is still in progress.

In order to compare the rate of crack opening of the Tower with the strain rate measured in the laboratory, the monitoring readings were divided by the base length and the rate in $\mu\text{m}/\text{mm}$ over seconds was calculated. Relating this calculated rate with the values of the vertical stress, locally measured by flat jack tested at the same height of the crack monitoring, the fragility curves shown in Fig. 14 were built for the Tower cracks for two different thresholds $\bar{\epsilon}$. In this case the strain-rate recorded is lower than the strain-rate obtained by creep and pseudo-creep laboratory tests.

Here the modeling appears an hazardous, but on the basis of the results obtained by laboratory tests it is possible to suppose the same distribution (Weibull distribution) for modeling the probability of exceedance of the $\bar{\epsilon}$ thresholds chosen. Although two data are not sufficient to investigate the Weibull shape, however the results obtained look like an interesting example of possible application of the procedure at a real cases, whether more suitable data were available.

6 CONCLUSIONS

A probabilistic model has been applied to the study of the long term behaviour of masonry specimens subjected in laboratory to creep and pseudo-creep.

The chosen model seems to appropriately interpret the experimental results also capturing the passage between visco-elastic and visco-plastic behaviour. An attempt of applying the procedure to the results of long term monitoring of displacements, particularly of crack opening, was carried out. The research will continue with the aim of providing a tool for preventing the masonry failure under particular states of stress.

ACKNOWLEDGEMENTS

The research was carried out with the support of MIUR Cofin 2000. Dr. G. Cardani is gratefully acknowledged for the data elaboration.

REFERENCES

- Binda, L., Gatti, G., Mangano G., Poggi, C. & Sacchi Landriani, G. 1990. La Torre Civica di Pavia: indagini sui materiali sulla struttura, *L'Edilizia e L'Industrializzazione*, n.11, pp. 713–735.
- Binda, L., Anzani, A. & Mirabella Roberti, G. 1997. The failure of ancient towers: problems for their safety assessment, *Conf. on Composite Construct. – Conventional and Innovative*, IABSE, Innsbruck, pp. 699–704.
- Anzani, A., Binda, L. & Mirabella Roberti, G. 2000. The effect of heavy persistent actions into the behaviour of ancient masonry, *Materials and Structures*, 33, pp. 251–261.
- Garavaglia, E., Lubelli, B. & Binda, L. 2000. Service life modelling of stone and bricks masonry walls subject to salt decay, *Proc. of Integrated Life-Cycle Design of Materials and Structures*, A. Sarja Ed., RILEM/CIB/ISO, Pro 14, Technical Research Center of Finland (VTT), Helsinki, 1, pp. 367–371.
- Binda, L., Garavaglia, E. & Molina, C. 1999. Physical and mathematical modelling of masonry deterioration due to salt crystallisation, *Proc. of 8th Int. Conf. on Durability of Building Materials and Components*, M.A. Lacasse, D.J. Vanier Editors, NRC-CNRC, Ottawa, 1, pp. 527–537.
- Taliencio, A.L.F. & Gobbi, E. 1996. Experimental investigation on the triaxial fatigue behaviour of plain concrete, *Magazine of Concrete Research*, 48(176), pp. 157–172.
- Garavaglia, E., Lubelli, B. & Binda, L. 2002. Two different stochastic approaches modeling the deterioration process of masonry wall over time, *Materials and Structures*, 35, pp. 246–256.
- Evans, D.H. 1992. *Probability and its Applications for Engineers*, Marcel Dekker, Inc., New York, NJ, USA.
- Melchers, R.E. 1987, *Structural reliability – analysis and prediction*, Ellis Horwood LTD, Chichester, West Sussex, England, pp. 400.
- Bekker, P.C.F. 1999. Durability testing of masonry: statistical models and methods, *Masonry International*, 13(1), pp. 32–38.
- Anzani, A., Binda, L. & Garavaglia, E. 2003. “The vulnerability of ancient buildings under permanent loading: a probabilistic approach” *Proc. of 2nd Int. Symp. ILCDES 2003, Integrated Life-Cycle Design of Materials and Structures*, Kuopio, Finland, December 1–3, 2003, RIL/VTT Ed., Helsinki, Finland, UE., Vol. I, pp. 263–268.

Out-of-plane behaviour of multiple-leaf stone masonry

G. Mirabella Roberti & L. Donati

DSA, Department of History of Architecture, Iuav University of Venice, Italy

A. Fontana

DIS, Department of Structural Engineering, "Politecnico" University of Milan, Italy

ABSTRACT: In ancient stone-masonry buildings, thick walls are very often made by different leaves, connected through the thickness in a more or less efficient way, so that the real mechanical behaviour for out-of-plane actions is not completely predictable. That behaviour affects not only the response to lateral loading (such as seismic actions) but also the response to ordinary, eccentrically applied vertical loading (such as floor loadings). Some recent experimental and numerical works dealing with different arrangements of three-leaves masonry walls, suggested a deeper study of the problem, focusing on the capacity of the interior leaf of transferring shear forces between the two external leaves. By means of a 2D finite element model with simple non-linear capabilities, some typical vertical cross-sections of three leaves wall in stone masonry with different block arrangements have been examined, in different load conditions, referring both to vertical and horizontal loads (due to wind or seismic actions).

1 INTRODUCTION

1.1 Stone masonry construction

Stone masonry construction is widely diffused in historic buildings, not only in Italy, and give rise a very large and articulated typological classification. They are often highly dishomogeneous and irregular, depending on the material employed (often found near the site), on the skill of the builders and on the technical knowledge of the time. Moreover, very often also apparently regular masonry is made by multiple leaves, with stone ashlar in the two external leaves and a core of weaker material, frequently without any cohesion, that may also constitute the greater part of the thickness. In these walls the transversal connection is also lacking, relying only in the block interlocking or seldom in some passing-through stone.

The weak load carrying capacity of this kind of masonry, often completely exploited against vertical loads, become dramatically insufficient against seismic actions, as many recent earthquakes demonstrated also in Italy: see for example some buildings in the Umbria-Marche regions.

It must be noticed that the recent Italian code (published in 2003) for seismic protection, extending the definition of seismic areas, state that in the next five years every building defined "of strategic interest" has to be verified according to the code, and eventually



Figure 1. Failure of a multi-leaf stone wall, from Nocera Umbra (Italy).

reinforced or consolidated: many public buildings, like hospitals, schools, libraries, etc. that belong to this category, are made by multiple-leaf stone-masonry walls.

1.2 Previous researches

In recent years very few researches has been developed in this subject, both from experimental and numerical approach. Starting in the '90, many works are developed in the research group of the *Politecnico di Milano* (see Binda & Fontana 1991, Binda et al. 1993, 1994) particularly on the shear transfer mechanism with different arrangements; a research on multi-leaf brick masonry was developed in Karlsruhe (Egermann et al. 1993). Recently, some numerical interpretation have been developed (Drei & Fontana 2000, 2001), and the results of a new experimental campaign have just been published (Binda et al. 2003a, b, Anzani et al. 2004), that constitute a starting point for the present work.

2 THE NUMERICAL SIMULATION

2.1 Objectives

A problem that still needs a deeper understanding is the mechanism of load transfer among the leaves, relying only on the geometrical configuration of the interfaces and on the bond and the friction between the stone and the inner fill.

For this reason a quite simplified geometrical model was adopted, based on the specimen tested in Milan. Different loading conditions were applied, which can reproduce two limiting cases related to the seismic action, increasing the horizontal load transmitted by the floor to the wall, in the hypothesis of (i) a stiff connection (no rotation allowed on top) or (ii) a weak connection (rigid rotation on the top). The presence of an upper level was simulated by constant vertical load, and only static actions were taken into account.

2.2 Geometrical model and material properties

The model was developed by means of a commercial program Strand7, using plate elements with 9 nodes to build a FE mesh in plane stress conditions. The non linearity of the behavior was concentrated in the interfaces between stone and mortar and stone and filling, adopting special "point contact" elements, able to simulate transversal friction and detachment in tension (see for ex. Rots & Lourenço 1993).

Two basic arrangements of the blocks were selected, simulating the presence of a continuous (smooth) vertical joint (Figs 2, 3, left) or the presence of some indentation allowing interlocking between external leaves and the inner fill (Figs 2, 3, right). Moreover, two different height/thickness ratio (h/t 1.5, Fig 2 and

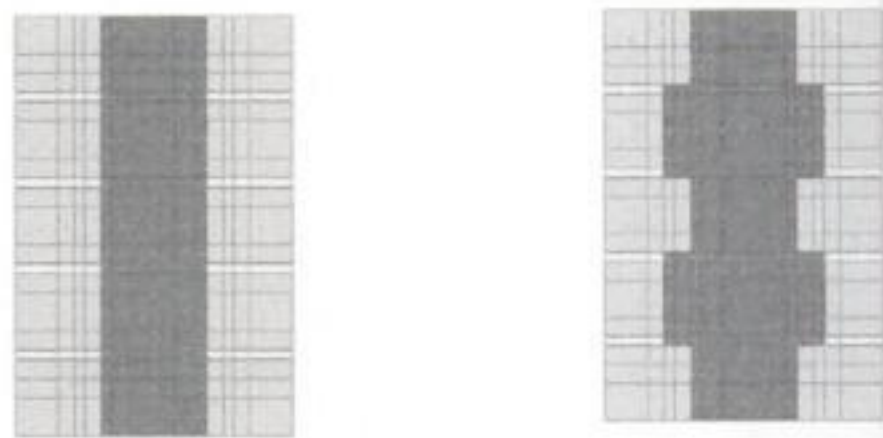


Figure 2. Specimens with height/thickness ratio of 1.5: without offsets (left) and with offsets (right).

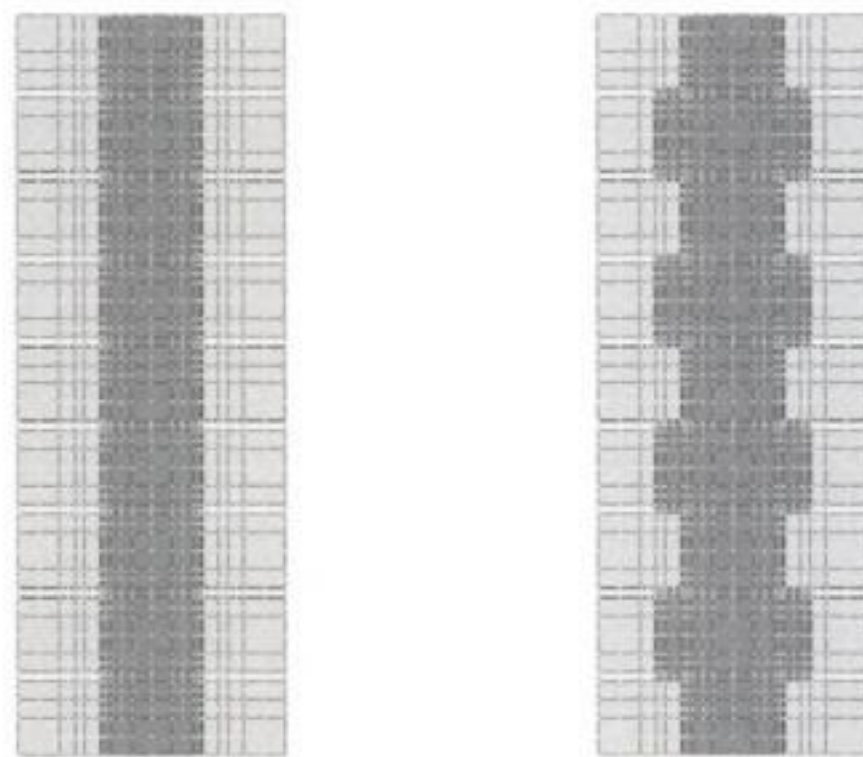


Figure 3. Specimens with height/thickness ratio of 2.75: without offsets (left) and with offsets (right).

h/t 2.75, Fig. 3) were chosen, in order to analyze the effect of the wall slenderness.

The materials adopted in this study reproduce those used by Binda et al., 2003a; a sandstone (called *Serena* stone) and a limestone (the *Noto* stone) respectively for the external blocks, and pieces of the same material mixed with mortar for the filling; an hydraulic lime mortar was employed in bed joints (the elastic properties are reported in Table 1). In order to evaluate the influence of the infill, a nonlinear material model was used, following the Drucker-Prager yield criterion:

$$\sigma_{DP} = \alpha J_1 + \sqrt{J_2'} \leq K',$$

where J_1 is the hydrostatic stress and J_2' is the second invariant of the deviatoric stress; the parameters α and K' are defined, using the cohesion c and the internal friction angle ϕ (see Table 1), as:

$$\alpha = \frac{2 \sin \phi}{\sqrt{3(3 - \sin \phi)}}, K' = \frac{6c \cdot \cos \phi}{\sqrt{3(3 - \sin \phi)}}$$

Three different combinations of the materials were chosen, simulating a variation in stiffness ratio

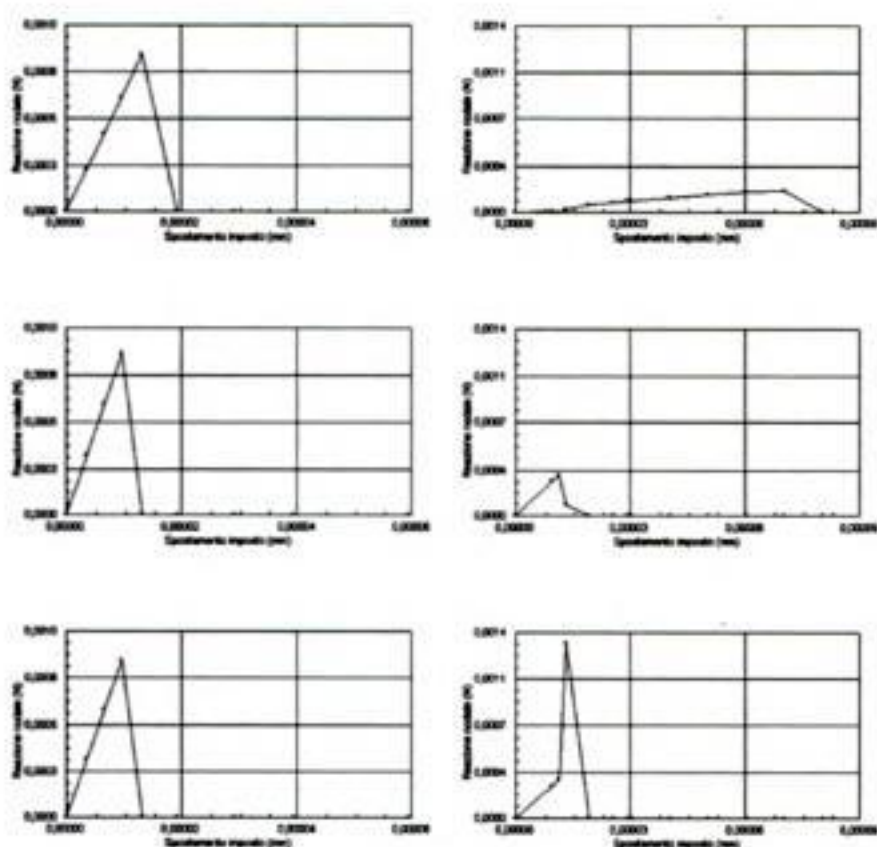


Figure 7. Specimens without offset, rigid rotation. Horizontal load-displacement plot for E_f/E_a 1/5 (top), 1/10 (middle), 1/15 (bottom); h/t 1.5 (left), h/t 2.75 (right).

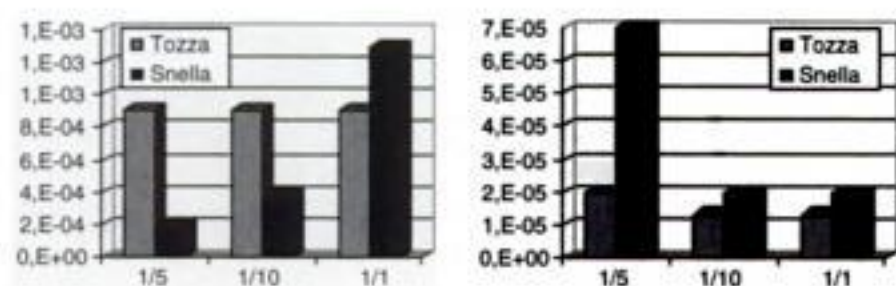


Figure 8. Comparison of ultimate load (left) and maximum displacement (right) for models without offset, rigid rotation. h/t 1.5 (light), h/t 2.75 (dark).

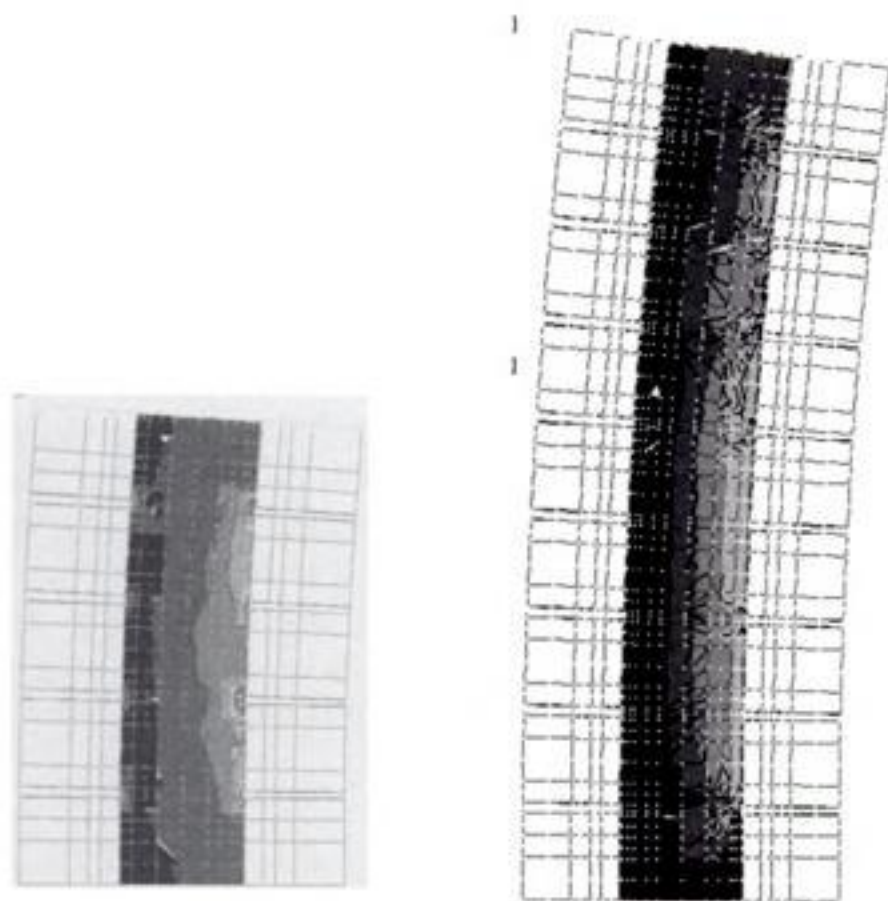


Figure 9. Contour plot of the DP stress – models without offset, rigid rotation.

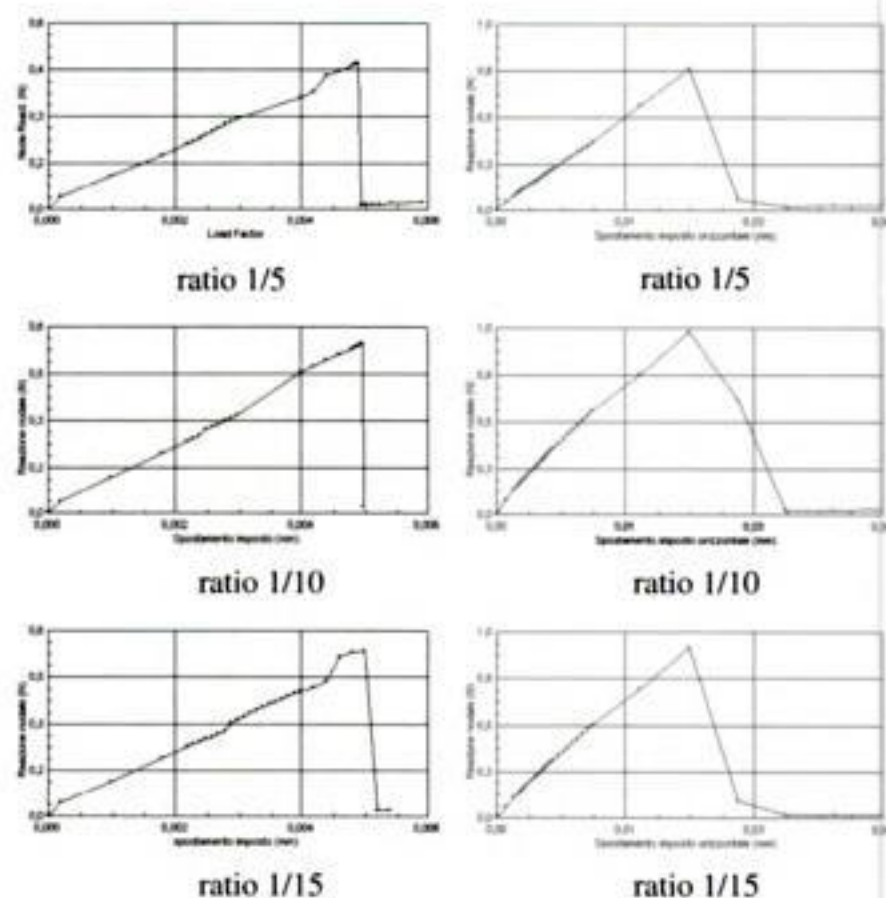


Figure 10. Horizontal load-displacement plot for models with offset, rigid translation; h/t 1.5 (left), h/t 2.75 (right).

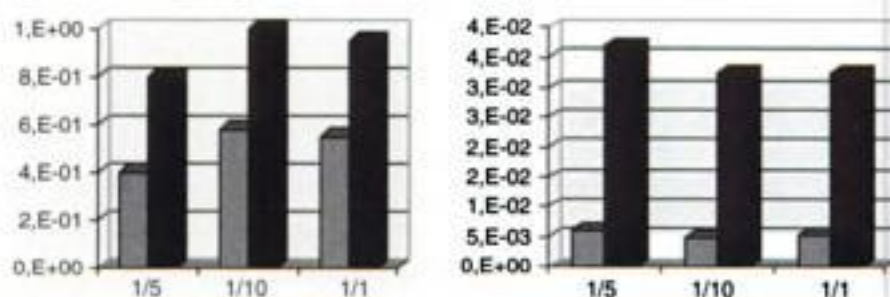


Figure 11. Comparison of ultimate load (left) and maximum displacement (right) for models with offset, rigid translation. h/t 1.5 (light), h/t 2.75 (dark).

exhibit a more brittle behaviour: the reduced number of bed joints limits the allowable overall deformation compared to slender specimens, as can be seen in Figures 10 and 11.

On the other hand, the DP stress contour plots (Fig. 12) show clearly the formation of a diagonal shear band, particularly in the case of smaller specimens.

2.3.4 Rigid translation, without offset

In this case, although the maximum load is very much lower than in the case with offset, nevertheless there is a sensitive increase compared to the bending-like boundary condition. Also in this case, the slender specimen behaves better (see the comparison in Fig. 13), showing a higher value of peak load and more ductility (Fig. 14, on the right).

The contour plots of the DP stress (Fig. 15) show the formation of a triple shear band, depending on the double bending configuration of the deformed shape, very clear in the less slender specimen.

- masonry. *Proc. 13th IB²MaC, Int. Brick/Block Masonry Conference, Amsterdam, 2004.*
- Binda L., Fontana A., Mirabella Roberti G., 1993. Modelling of the mechanical behaviour of multiple-leaf stone walls, *Proc. 2nd Int. Symp. STRUMAS Computer Methods in Structural Masonry, Swansea U.K. 1993*, pp. 229–241.
- Binda L., Fontana A., Mirabella Roberti G., 1994. Mechanical behaviour and stress distribution in multiple-leaf stone walls, *Proc. 10th IB²MaC, Int. Brick/Block Masonry Conference, Calgary 1994*, pp 51–59.
- Binda L., Anzani. A., Fontana A., 2003a. Mechanical behaviour of multiple-leaf stone masonry: experimental research. *Proc. Int. Conf. Structural Faults & Repair, London 2003.*
- Binda L., Fontana A., Anzani. A., 2003b. Multi-leaf masonry: shear transfer at interfaces. *Proc. 6th Int. Symp. STRUMAS, 'Computer Methods in Structural Masonry', Rome 22–24/9/2003*, pp. 1–6.
- Drei A., Fontana A., 2000. Response of multiple-leaf walls to horizontal forces. *Proc. 12th IB² MaC, Int. Brick/Block Masonry Conference, Madrid, 2000.*
- Drei A., Fontana A., 2001. Influence of geometrical and material properties on multiple-leaf walls behaviour, *Proc. 7th STREMAH, Struct. Studies Repairs and Maintenance of Architecture Heritage, Bologna, 2001.*
- Egermann R., Frick B., Neuwald C., 1993. Analytical and experimental approach to the load bearing behavior of multiple-leaf masonry. *Proc. 3rd STREMAH, Struct. Studies Repairs and Maintenance of Architecture Heritage, Bath*, pp. 383–390.
- Rots J.G. & Lourenco P.B., 1993. Fracture simulation of masonry using non-linear interface elements, *Proc. 6th NAMC, North American Masonry Conference, Philadelphia, Pennsylvania, 6–9/6/1993*, pp. 983–993.

Numerical modelling of a small mortar dome towards the restoration of a *cruzeiro* in Portugal

P.B. Cachim & A.L. Velosa

Department of Civil Engineering, University of Aveiro, Portugal

ABSTRACT: 'Cruzeiros' are a part of portuguese cultural heritage and should therefore be preserved. Although usually only minor maintenance procedures are necessary, in the specific case described, the 'cruzeiro' had been subject to severe damage and the basis for its reconstruction had to be thoroughly studied. All original materials in good conditions (stone) were maintained but it was necessary to build a new dome; for this several mortars were tested taking into account the specific characteristics they must meet. A hydraulic lime mortar was then chosen, guaranteeing compatibility with the existing structure and the dome shape was reformulated in order to reproduce the original dome. A finite element analysis of the whole structure was carried out in order to ensure that the tensile stresses developed during the construction and predicted lifetime of the dome were acceptable.

1 INTRODUCTION

Intervention in monuments is guided by the principles of the Venice Charter (ICOMOS, 1964), respecting authenticity. In this particular case, a portuguese 'cruzeiro', typical religious construction disseminated throughout the country with an extremely varied architecture, had been seriously damaged by a car accident. Due to its peculiar configuration, consisting of a small dome built over a cross, it is considered a construction with historic interest and is included in the list of National Monuments.

The damage caused by the accident (Figure 1) revealed a dome made from a mixture of cement and coarse sand, possibly an intervention of the 1950s and certainly not the original one, as was later confirmed by ancient photographs. In terms of the remaining structure, most columns remained in a good state, but part of the cross was missing.

In this scenario, and taking into account that the actual dome brought about no additional architectural value and was severely damaged, a decision was made to rebuild the dome in a fashion similar to the original one and to maintain all original pieces of the monument. Therefore, the architrave and columns were maintained with minor repair resumed to broken zones and the mortar used in all joints was formulated from the chemical and mineralogical analysis of existing joint mortar.

For the dome itself, an attempt was made to use aesthetically compatible materials, eliminating Portland cement as a possibility for the binder. Apart



Figure 1. State of the monument prior to the intervention.

from the lack of visual compatibility, this material may introduce soluble salts into the remaining monument, favouring stone decay. The execution of this kind of structure, with a relatively wide span and thickness, in a non-cementitious mortar required a detailed structural analysis and special building procedures.

1.1 Brief historical insight

Cruzeiros are a part of Portuguese religious architecture, usually fulfilling the purpose of creating paths devoted to prayer. The examples found are usually composed by a cross, supported by a pedestal; only in a few cases, this cross has a covering that may be in the form of a dome. Cruzeiro de Sangalhos is included in that category. This type of covering structure seems to

will also provoke some displacements at the base of the dome.

Case A, Figure 5 exhibits a *slab-type* behavior which is very demanding for the dome with the tensile stresses located at the bottom face in its centre.

A much more interesting behavior from the structural point of view is observed in case B, where an *arch-type* behavior is achieved (Figure 6). The tensile stresses are also located at the bottom face of the dome but also on the outer face in the zone of convexity.

Since the compressive stresses were not essential for the analysis a comparison between the tensile stresses in the two cases was made. The maximum tensile stress in case A is almost five times bigger than in case B (characteristic value of 156 kPa in case B).

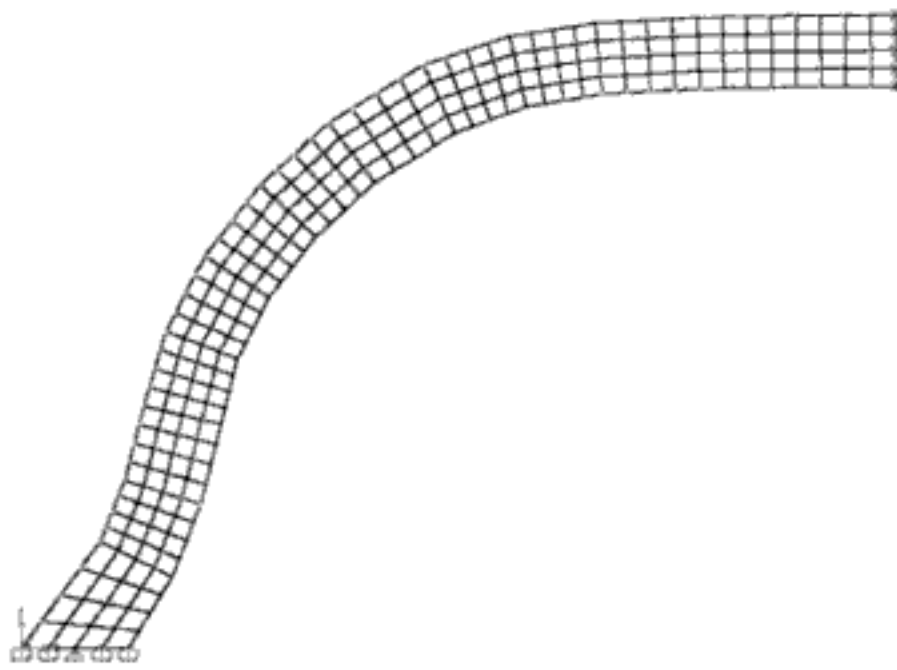


Figure 4. Finite element mesh.

The tensile stresses in case A are much higher than the allowable tensile strength, so the arch-type behavior must be imposed to the structure.

The vertical displacement of the centre of the dome for case B is 0,1 mm which is a perfectly acceptable value.

Therefore, it is necessary to restrain the horizontal displacement of the dome at its interface with the architrave. This could be achieved by providing a rough surface at the architrave before the placement of mortar.

3.2.2 3-D results

A detailed 3-D modelling of the structure was carried out afterwards. In the final model, it was assumed that perfect bond exists between the architrave and the dome. However, the architrave is not prevented from moving in the horizontal direction so an intermediate behavior for the dome can be observed. The finite element mesh is reproduced in Figure 7.

The stresses obtained are plotted in Figures 8 and 9. The design tensile stress is 240 kPa (characteristic value equals 160 kPa) and is, therefore, below the design tensile strength (300 kPa).

The maximum displacements observed were measured in the middle of the architrave and at the top of the dome. The displacement reads 0,14 mm which is clearly a very small value. The deformed shape is shown in Figure 10.

In the architrave biaxial bending was observed. The moments in each direction are 0,22 and 0,18 kNm (characteristic values). These moments lead to a design

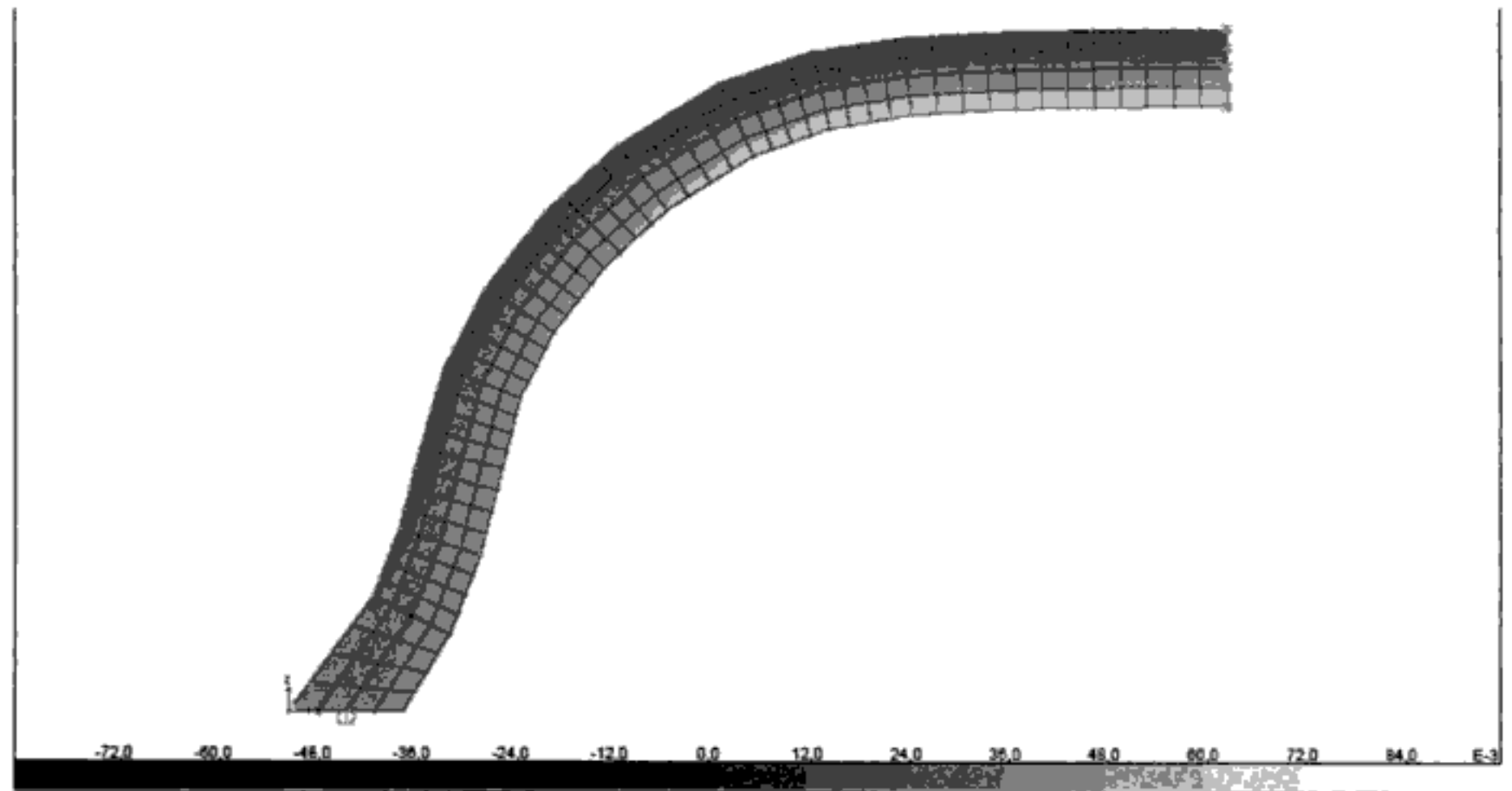


Figure 5. Results with free displacements.

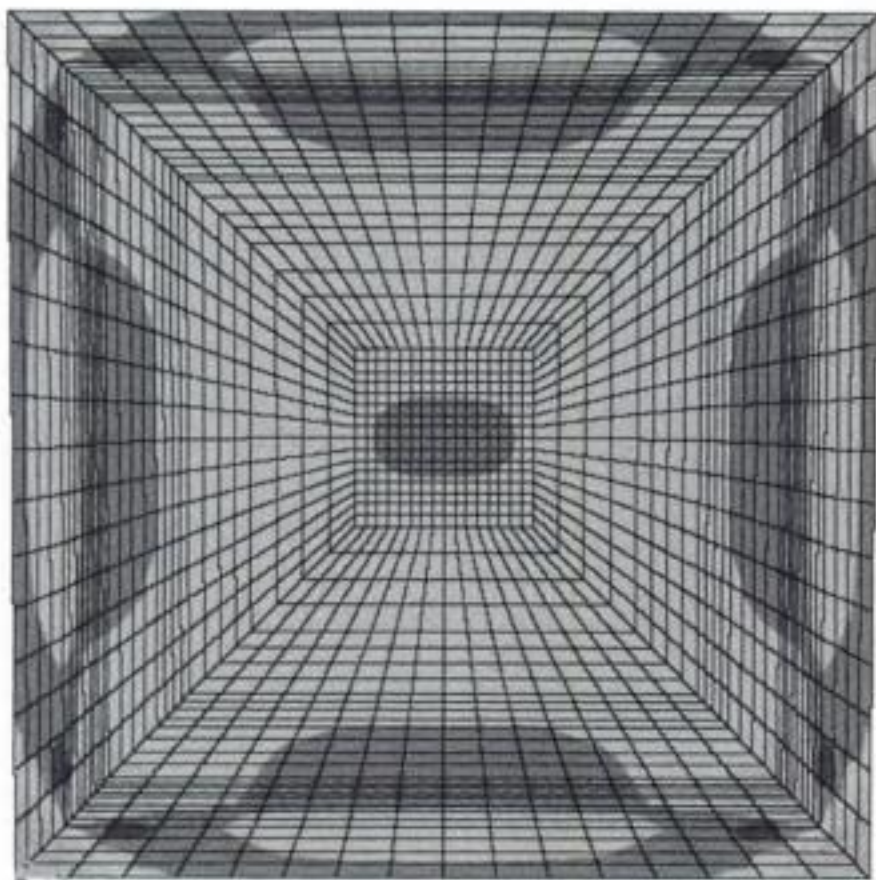


Figure 9. Vertical stresses (bottom face).



Figure 10. Deformed structure.

This means that at the base of the columns, the tensile stress at the joint mortar between the foundation and the columns was 0,19 MPa. This value is well below the tensile strength of this mortar. The wind load was found to be less severe than the seismic load.

With respect to car crushing, it was decided that local authorities will provide adequate protection for



Figure 11. Joint mortars.

the cruzeiro, since it will be impossible for the structure itself to sustain the impact of a car.

4 INTERVENTION

The dome mortar needed to be applied on a rather big extension and with a significant width. Therefore, several specifications were applied in order to improve its performance: a fiber mesh was applied on both sides of the dome, 0,5 cm from the surface and water was sprinkled on the outer surface twice a day. However, the dome execution was particularly delicate due to excessive temperature that occurred in that day (37°C); in order to minimize cracking it was specified that water sprinkling should take place more often, specially in the hottest times of day and a light colored covering was placed over it in order to avoid excess heat. To improve the performance of the dome a galvanized steel mesh was placed as indicated in Figure 12. This mesh was not considered in the structural analysis.

Concerning the joint mortars, these were formulated based on the analysis of existent mortars. Prior to their application, it was specified that the adjacent stone must be brushed and cleaned in order to provide a rough and particle free surface that would favor a good adhesion (Figure 11).

To improve the structural performance of the dome, a galvanized steel mesh with 4,5 mm bars spaced 10 cm was added at both faces 2 cm below surface. This mesh was not considered in the structural analysis and was placed as an additional security device. Its main function is to increase the stiffness of the dome reducing the horizontal displacements of the base thus attaining an arch-type behavior.

A schematic drawing of the dome was elaborated as shown in Figure 12.

Despite all the adverse atmospheric conditions during the intervention and the large width of the dome no severe cracks were observed.

The mechanical behaviour of mortars in triaxial compression

R. Hayen

Arte Constructo, Schelle, Belgium

K. Van Balen & D. Van Gemert

Department of Civil Engineering, K.U. Leuven, Leuven, Belgium

ABSTRACT: Most commonly the mechanical behaviour of the masonry composite is derived from the complex interaction in between the masonry units, stone and/or brick, and the mortar joint. While generally mortars are described by means of their mechanical properties in uni-axial compression, equilibrium within the masonry composite most often results in the presence of a horizontal confinement within the mortar joint. A series of tests on mortar samples in a state of triaxial compression evidences a clear change in mechanical behaviour and failure mechanism compared to the mechanical behaviour of the mortar in uni-axial compression. In order to describe the mechanical behaviour of the masonry composite from the individual materials, an adequate modelling of the mechanical behaviour in triaxial compression of the mortar becomes necessary. This paper describes the mechanical behaviour of mortar in triaxial compression and the first step towards the modelling of the mechanical behaviour.

1 INTRODUCTION

The main objective for the presented study is to understand the differences in material behaviour of the composite masonry constructed with different mortar types; e.g. putty lime, hydraulic lime, cement or lime-cement mortars. While lime mortars generally obtain a lower compressive strength than nowadays cement-based mortars, its influence on the overall strength of the masonry structure is minimal and the possibility of the former to adapt to settlements is extraordinary (Figure 1) and still not understood, as mentioned amongst others by Sahlin (1971) and Van Balen (1991).

Masonry is a composite material, built up of brick or natural stone units and a mortar as binder matrix. Both composing materials are different in nature. Both brick and natural stone can be considered as an elastic brittle material with a certain compressive strength and some tensile strength, which is often considered only one tenth of its compressive strength. Mortar is generally also considered an elastic brittle material, however, with a much higher deformability with regard to the brick or natural stone units. Due the composite nature of masonry and the important difference in deformability of the composing materials, the stresses and strains will be divided in a complex manner between the brick units and the mortar matrix. The commonly accepted linear elastic approach on the redistribution



Figure 1. Settlement of a historical masonry structure without actual structural failure of the structure.

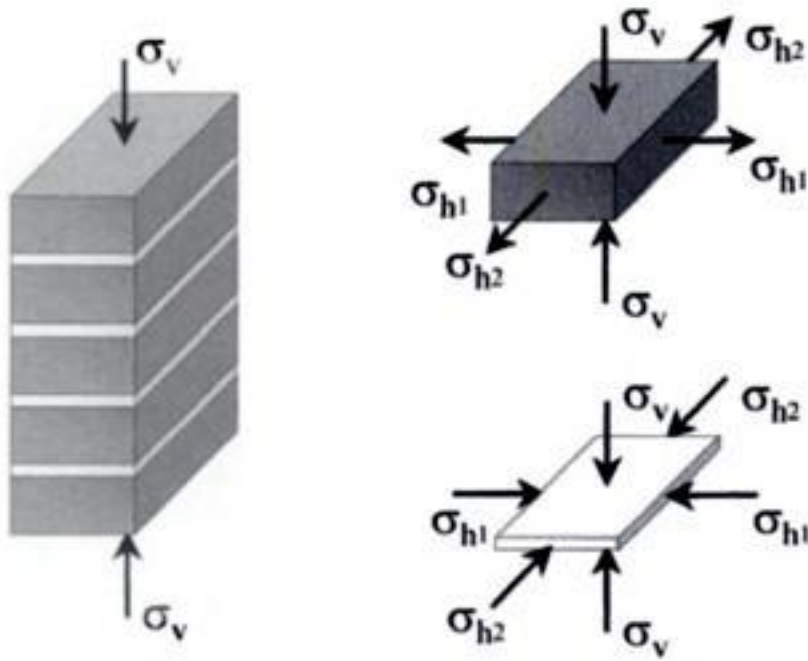


Figure 2. Redistribution of the stresses in a masonry composite structure.

of the strains and stresses within a masonry composite structure was originally introduced by Francis et al. (Hendry 1998). They put forward that the vertical loads, coming from the dead load on a load-bearing structure, result in a horizontal confinement on the mortar within the horizontal joint, as it tries to move out horizontally from between both bricks due to its elevated deformability. On the other hand, equilibrium within the composite masonry structure results in the built-up of horizontal tensile stresses at the brick's contact surface with the mortar (Figure 2).

A linear elastic approach incorporates, inevitably, a constant value for the Young's modulus E_y and the coefficient of Poisson ν for both the brick or natural stone unit and the mortar. Furthermore, an equal distribution of the confining stresses on the masonry units and the mortar over the total height of each element is considered. As such, a linear elastic approach implies the presence of a constant relationship in between the vertical load on the structure and the resulting confining stresses within the mortar joint. This relationship σ_h/σ_v , which shall be denoted as κ for the following paragraphs, can be calculated analytically and is determined by means of equation (1) by Tassios (1988):

$$\kappa = \frac{\sigma_h}{\sigma_v} = \frac{\frac{t_m}{t_b} \left(\nu_m - \frac{E_m}{E_b} \nu_b \right)}{\frac{t_m}{t_b} \frac{E_m}{E_b} (1 - \nu_b) + (1 - \nu_m)} \quad (1)$$

where E_b , E_m = Young's moduli of the brick and mortar, respectively; ν_b , ν_m = the coefficients of Poisson of the brick and mortar, respectively; and t_b , t_m = the heights of the brick unit and the mortar joint, respectively.

From the linear elastic approach it is clear that the determination of the elastic properties, the Young's

moduli and the coefficients of Poisson, are utterly important in order to evaluate the occurrence and the importance of the confining stresses within the mortar joint in the first place, without even considering any effect of a non linear deformation of the individual materials. While in general the Young's moduli are determined experimentally, the coefficient of Poisson is most often approached from literature data assuming a mean coefficient of Poisson, in the case of the mortar, of about 0.20.

2 ANALYSIS OF THE MATERIAL BEHAVIOUR IN COMPLEX LOADING CONDITIONS

2.1 Introduction

The following paragraphs outline the change in material behaviour and failure mechanism of a mortar upon triaxial loading. It is important to note that, apart from the actual values of compressive strength and the associated deformations, no important differences are found for different mortar types upon their overall mechanical behaviour in triaxial compression, as has been described in Schueremans (1999), Hayen (2001) and Hayen (2003). The analysis of the influence of the triaxial loading condition on the material behaviour is therefore valid for mortar in general, independent of the type and composition of the mortar (e.g. putty lime, hydraulic lime, cement or lime-cement mortar).

2.2 From brittle to elasto-plastic deformation

Upon triaxial loading an evident change in material behaviour can be discerned, as is demonstrated in Figure 3, where the deformations of a putty lime mortar are represented in both uni-axial and triaxial loading conditions. From the analysis of the development of the stress-strain relationship with an increasing κ -value the following observations can be deduced:

- a change in material behaviour is observed from brittle in a uni-axial loading condition to a combined elastic and plastic behaviour in triaxial loading conditions, from rather low confining pressures up to hydrostatic compression. From κ as low as 0.15 the influence of the rather limited confining pressure is important, resulting initially in some post-peak plastic behaviour and gradually, as κ increases, altering the mechanical behaviour to an elasto-plastic material. A similar change in material behaviour has been recorded for several other materials as e.g. porous chalk, porous sandstone and concrete by Homand (2000), Wong (1997) and van Mier (1986), respectively.
- while in general in a linear elastic approach a certain value for the coefficient of Poisson is assumed, the results of the mechanical behaviour in uni-axial

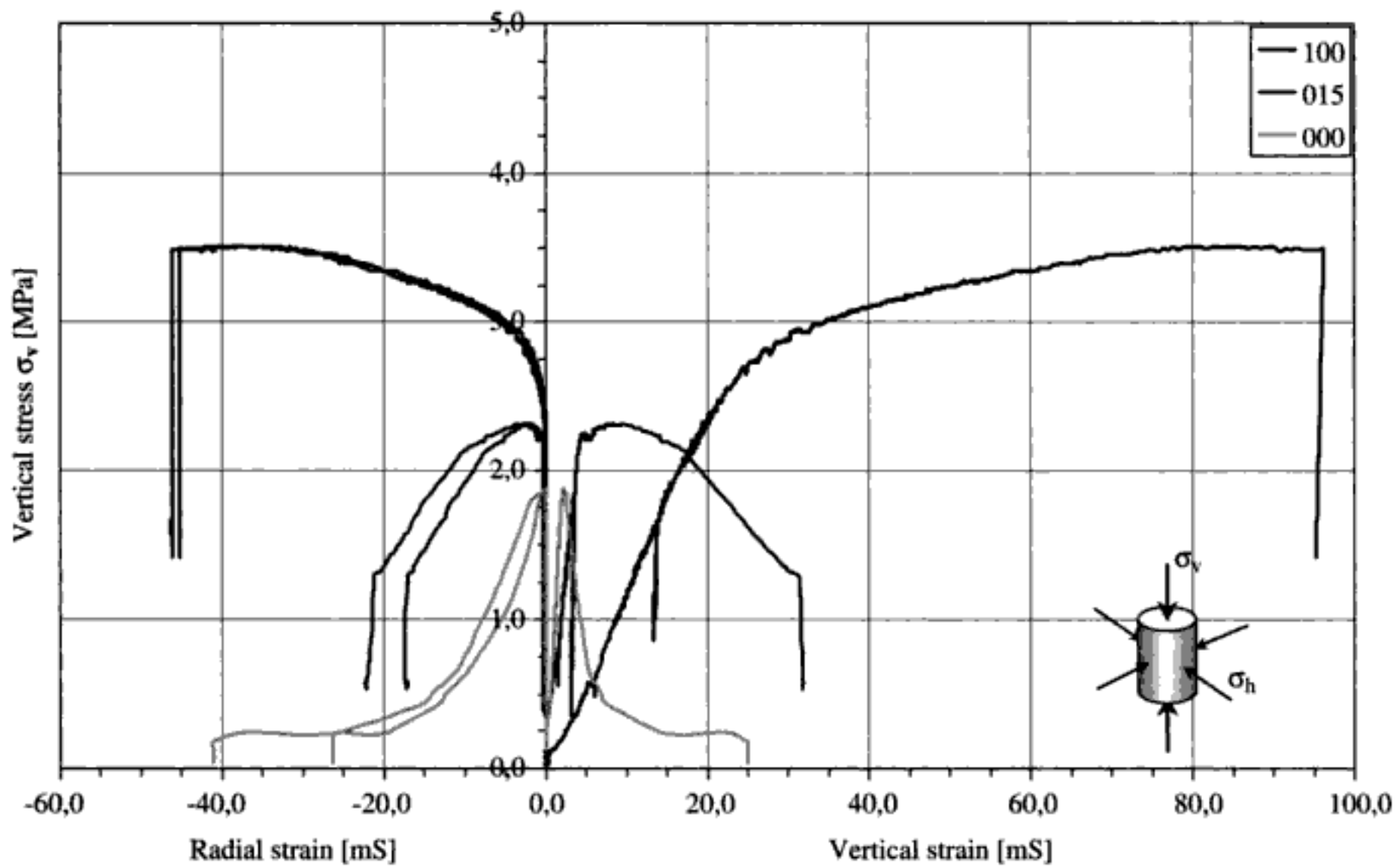


Figure 3. Vertical and horizontal deformations in uni-axial and triaxial loading conditions. The legend represents κ in hundredths of a unit.

as well as in triaxial loading conditions yield no evidence for such an approach. On the contrary, the initial lack in horizontal deformation does evidence the absence of an actual coefficient of Poisson.

The instantaneous relationship in between the vertical and horizontal displacements, being represented in Figure 4 in the case of the uni-axial compression test on a putty lime mortar sample, clearly evidences the initial absence of any horizontal deformation in the mortar. Only as the vertical compression on the mortar sample approaches the compressive strength of the material the horizontal deformations do occur quite suddenly in uni-axial compression. In a state of triaxial compression the horizontal deformations become more and more plastic in nature as the influence of the horizontal confining pressure on the overall mechanical behaviour of the mortar increases.

- a tendency towards an increase in deformability in the elastic region at higher κ -values. The collected data is however rather limited and too scattered in order to formulate a relationship between the change in modulus of elasticity E_y and κ .
- an important increase in strength is observed with only a slight increase in the contribution of the horizontal confining pressure on the overall loading condition. This is fairly evident in the graphical representation of the corresponding horizontal and vertical loading conditions at failure, the

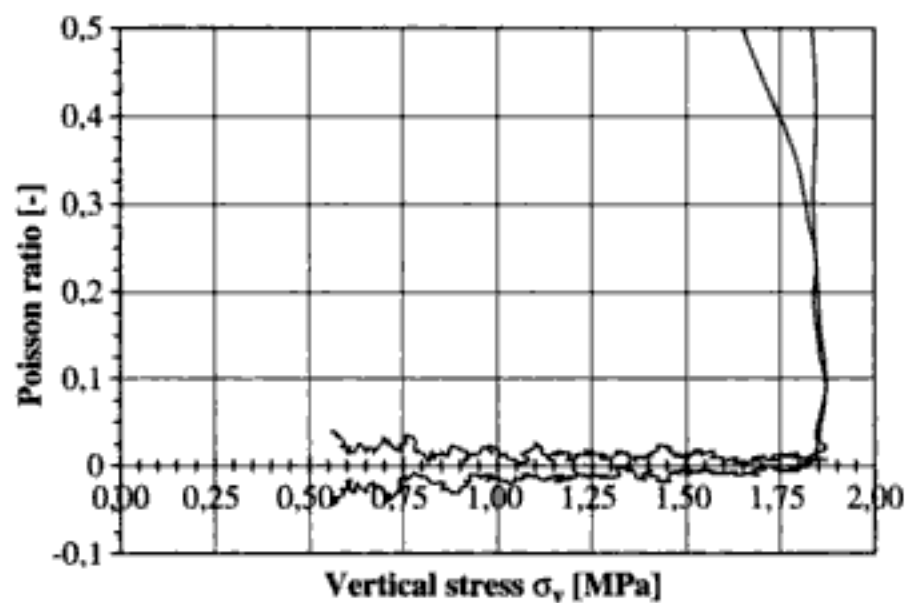


Figure 4. Evolution of the Poisson ratio in function of the applied uni-axial load in the case of a putty lime mortar.

triaxial yield criterion in the $\sigma_{II} = \sigma_{III} = \sigma_h$ plane, in Figure 5.

2.3 From shear failure to pore collapse

Analysis of the volumetric deformation upon triaxial loading, represented in Figure 6 for a moderately hydraulic lime mortar, evidences a change in failure mechanism at values of κ above 0.25 (at κ equal to 0.25 both failure mechanisms have been observed for the different mortar types).

Under uni-axial loading or triaxial loading conditions with a relative limited horizontal component ($\kappa < 0.25$), the recorded volumetric deformations, as well as the evolution of the Poisson's ratio throughout the test, evidence the existence of a shear failure mechanism. After an initial decrease in volume, probably due to the closing of existing cracks and anomalies within the mortar structure, an increase in volume is rather soon observed as a network of very fine vertical cracks starts to grow and shear bands develop. The mortar sample finally collapses along diagonal shear bands accompanied by a substantial increase in volume over the middle section of the cylindrical mortar sample.

For triaxial loading conditions with an important horizontal confining pressure ($\kappa > 0.25$), failure of the mortar no longer coincides with an increase in volume. Hence, no shear failure mechanism is observed. Instead a rather constant decrease in volume is observed right to the end of the triaxial test, setting forward the possibility of a pore collapse mechanism. The existence of such a pore collapse mechanism has been demonstrated by Vlado (1996) and Bésuelle (2000) in the case of porous rocks. In most cases the triaxial tests were however broken off before the actual failure of the mortar was observed, due to the limited measurement range of the triaxial test apparatus (these points are referred to as non broken in Figure 3), at least if failure is defined as a decrease in bearing capacity of the mortar sample. Careful study of the mortar samples after the triaxial tests proved that, although the bearing capacity of the mortar was unaffected, the internal structure of the mortar was almost completely destroyed and the mortar internally was turned to powder. Failure itself, therefore, was not observed as a decrease in bearing capacity, but rather by the collapse of the internal structure of the mortar. If and how the bearing capacity of the mortar finally will fade away, could not be derived from the current study.

2.4 Evidence for a pore collapse mechanism

The study of the internal pore structure of very weak lime mortars, let alone the study of a deteriorated lime mortar after triaxial compression, is a problem on its own which faces a lot of problems regarding the validity of the test results. The most important issue is the influence of the test conditions on the pore structure of the weak sample. In order to at least put forward some evidence of a pore collapse mechanism several tests were explored and combined; the determination of the total pore volume through vacuum submersion and the analysis of the pore structure by means of mercury intrusion and scanning electron microscopy.

The results obtained are represented in Figure 7a, for the total porosity by vacuum submersion in the case of an hydraulic lime mortar, and Figure 7b, for the pore

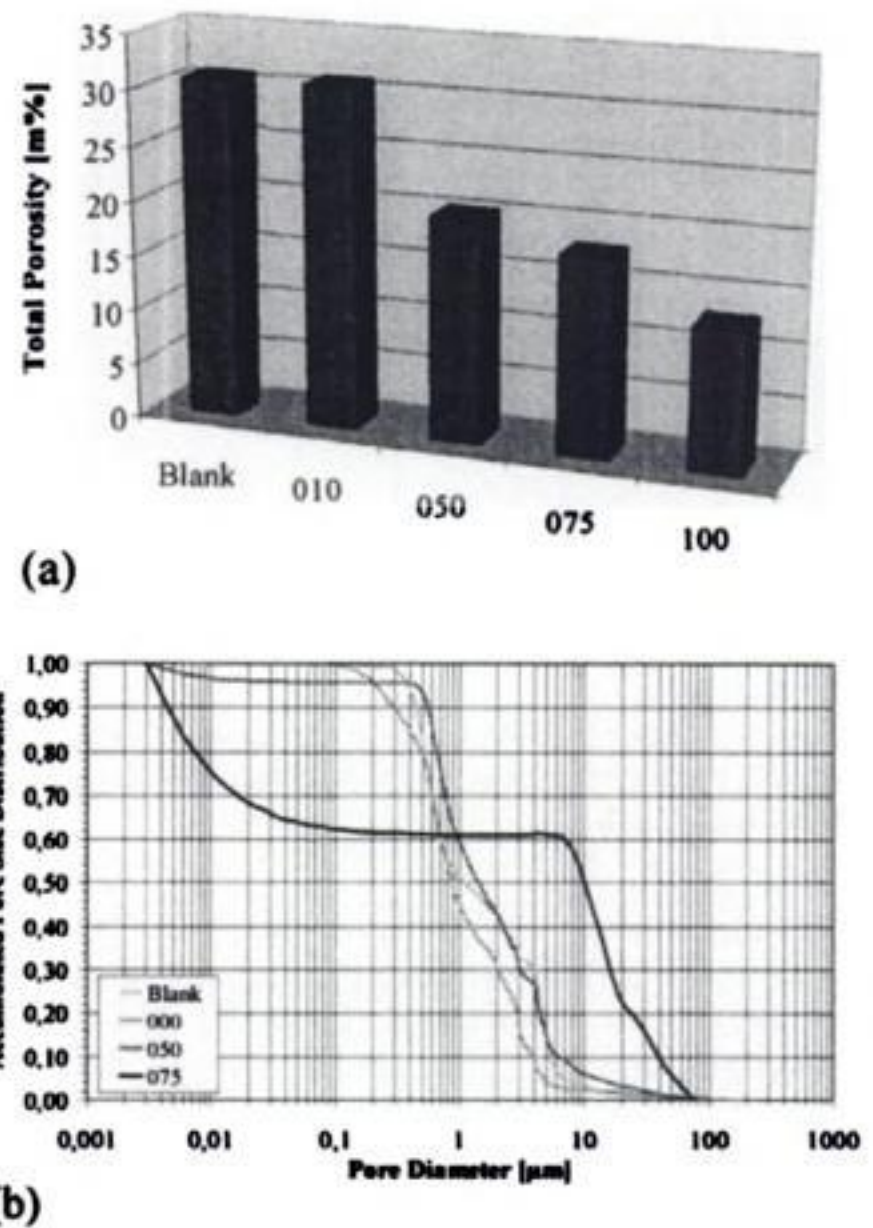


Figure 7. (a) Total pore volume by vacuum submersion. (b) Pore size distribution by mercury intrusion. The legend represents k in hundredths of a unit.

size distribution by mercury intrusion in the case of a putty lime mortar. Both studies show some evidence for the alteration of the internal pore structure of the mortar upon triaxial loading conditions for κ above 0.50. For the hydraulic lime mortar the decrease in total porosity, even considering a normal variation in material properties of the material, is substantial. The study of the pore structure by mercury intrusion on the other hand shows that the internal structure of the putty lime mortar undergoes an important transformation. The triaxial loading condition, again in the case of the presence of an important horizontal component, is responsible for the formation of both a network of fine to large cracks and the closing of the medium sized pores. This was also recorded by means of the SEM-images, where indeed the formation of a network of fine cracks from grain to grain was confirmed.

3 THEORETICAL BACKGROUND FOR THE CHANGE IN FAILURE MECHANISM

The occurrence of intersecting diagonal shear bands in uniaxial vertical compression is generally attributed to the formation of a network of interacting vertical cracks (Van de Steen 2001), which are induced by the

The effect of the masonry pattern on the global behaviour of vaults

C. Calderini & S. Lagomarsino

Department of Structural and Geotechnical Engineering, University of Genoa

ABSTRACT: A micromechanical damage model for the finite element modelling of complex masonry structures is presented. The model considers masonry material as a continuum medium constituted by an iterative and ordered assembly of bricks (or stones) and mortar. The constitutive equations are based on the homogenization theory and consider the non linear stress–strain relationship in term of mean stress and mean strain. Specific aim of the study is the analysis of the influence of the block assembly on the global behaviour of masonry vaults. An incremental structural analysis of a simple domed vault subjected to a concentrated asymmetric load is presented in order to demonstrate the effectiveness of the model.

1 INTRODUCTION

Masonry constructions are made of a continuum where the resistant structure is not univocally defined. The structure depends on geometry, stiffness and mass distribution, chronological succession of the building works, subsequent alterations. Moreover, it depends on the acting forces and on the damage state of the constituent material. For these reasons, full-scale models are required for the analysis of masonry structures.

The identification the residual life of the structure is one of the main problem in the study of historical constructions. In fact, differently than for new construction, the analyst does not know in which stage the structure is at present. It depends, besides its complex events, on the history of damage. From an experimental point of view, monitoring is the main tool to identify damage evolution; although, it is well recognized the exigency of numerical tools for evolutive analysis (Page 1978, Pietruszczak & Niu 1991, Gambarotta & Lagomarsino 1997, Lourenço et al. 1997, Luciano & Sacco 1997, Papa & Nappi 1997, Berto et al. 2002).

Objective of the present study is to develop a constitutive model for complex masonry structures, able to predict their behaviour from the linear elastic range, through cracking and degradation until complete loss of strength. The finite element method is adopted as a framework for the numerical implementation.

Masonry is constituted by an assembly of blocks connected by joints. Under this definition, a number of different materials and structures can be included. The constitutive model presented in this paper has been

developed for a specific and widely diffused class of masonry structures, whose main characteristics are:

- prevalence of bidimensional structural elements (vaults, domes, walls of limited thickness);
- blocks size much lower than structural elements size;
- presence of mortar joints.

On the basis of this assumptions, the model has been formulated with a micromechanical approach, considering the hypothesis of plane stress. In the micromechanical theory, the behaviour of a composite material is described in terms of macro (or average) stress and strain. This approach provides the continuum constitutive properties in terms of properties and structures of the microconstituents.

The analysis of the influence of the block assembly on the global behaviour of masonry structures is one of the main objective of this study.

The constitutive model is based on the models presented in Alpa & Monetto (1994) and in Gambarotta & Lagomarsino (1997).

2 THE CONSTITUTIVE MODEL

Masonry is considered as a composite material, made of a periodically arranged set of blocks connected by mortar joints. The model distinguishes two different types of mortar joints: bed joints, continuous on their plane and usually set perpendicularly to the compressive principal stresses, and discontinuous head joints. A *running* pattern is assumed (Fig. 1).

$$\bar{\sigma} = (\sigma_x, \sigma_y, \tau)^T \quad (5)$$

The definition of the average elastic tensor has not been an aim of this study. Different elastic homogenization techniques has been presented recently in literature (Anthoine 1995, Lourenço & Zucchini 2000, Cecchi & Rizzi 2001).

The definition of the inelastic contributions is based on different damage mechanisms.

Mechanism *M1* represents damage phenomena in mortar bed joint generated by a tensile stress normal to their plane ($\sigma_y > 0$). The related strain contribution is the following:

$$\bar{\epsilon}_y^{M1} = \eta_{mb} \alpha_{mb} c_{mn} H(+\sigma_y) \sigma_y, \quad (6)$$

where $\alpha_{mb} > 0$ is the bed mortar joint damage variable, c_{mn} is the extensional inelastic compliance parameter characterizing the mortar joint, and H is the Heaviside function taking in account the unilateral response of the interface.

Mechanism *B1* is activated by the analogous tensile force ($\sigma_y > 0$), but involves blocks. Although mortar joints are usually weaker than blocks, in some particular cases (for example for pozzolanic mortars typical of Southern Italy) blocks could be weaker and, consequentially, subjected to the damage phenomena taken in account from this mechanism. The associated inelastic strain is:

$$\bar{\epsilon}_y^{B1} = (1 - \eta_{mb}) \alpha_b c_{bnt} H(+\sigma_y) \sigma_y, \quad (7)$$

where $\alpha_b > 0$ is the blocks damage variable and c_{bnt} is the extensional inelastic compliance parameter characterizing the blocks when they are subjected to a tensile stress.

Mechanism *M2* describes the damage in mortar bed joint due to a tangential stress acting on their plane (τ). Slidings associated to this tangential stress are limited or locked, through friction phenomena, by a compressive stress ($\sigma_y < 0$). The mechanism produces a sliding dependent on the applied stress τ and on the friction acting on mortar-block interface f :

$$\bar{\gamma}^{M2} = \eta_{mb} \alpha_{mb} c_{mt} (\tau - f), \quad (8)$$

where c_{mt} is the tangential inelastic compliance parameter characterizing the mortar joint.

Mechanism *B2* describes the damage of blocks when they are subjected to an analogous tangential stress. It generates the following inelastic strain contribution:

$$\bar{\gamma}^{B2} = (1 - \eta_{mb}) \alpha_b c_{bt} \tau, \quad (9)$$

where c_{bt} is the inelastic tangential compliance parameter of blocks.

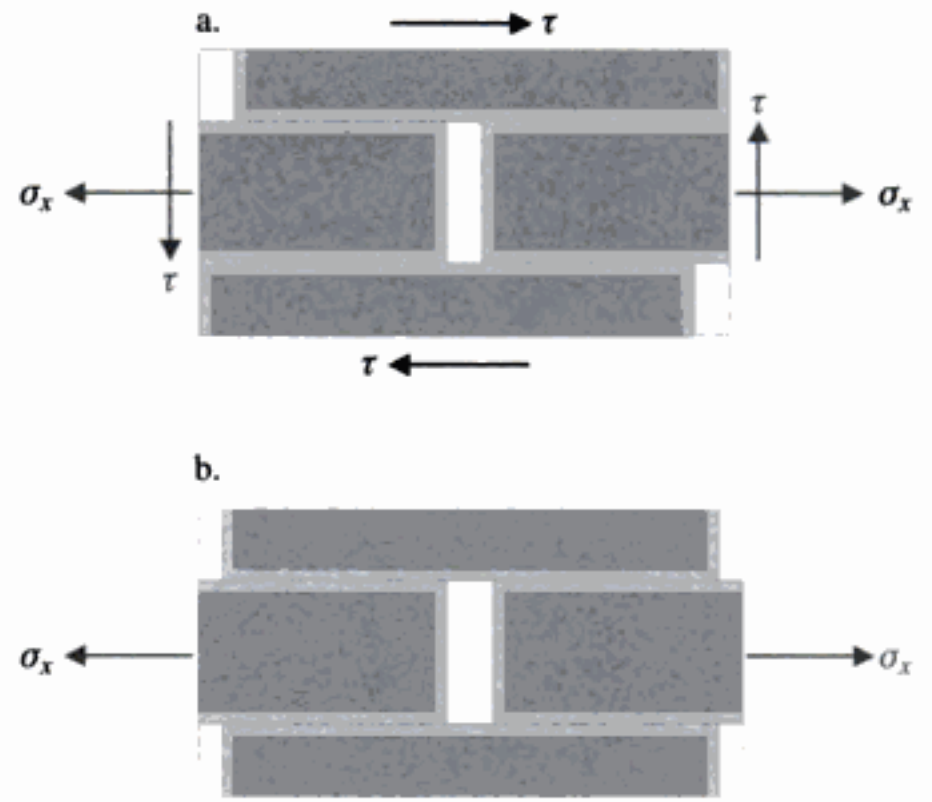


Figure 5. Different damage pattern for mechanism *M3*.

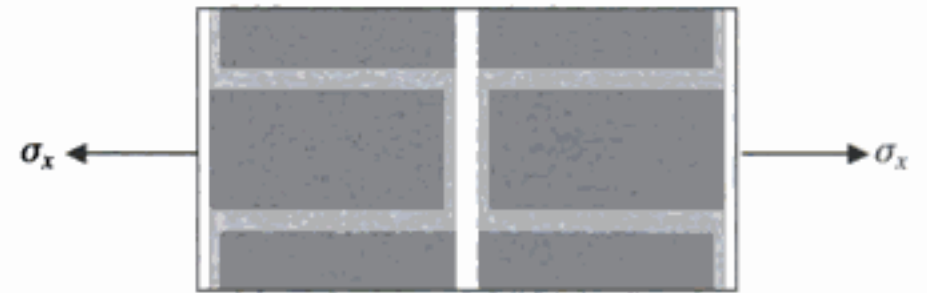


Figure 6. The damage mechanism *MB*.

Mechanism *M3* involves simultaneously mortar bed and head joints and represents the typical phenomena of loss of interlocking in the masonry. It is activated by a tensile stress acting on the plane of mortar head joints ($\sigma_x > 0$) and/or a tangential stress acting on the plane of mortar bed joints (τ). It produces normal extensions of the mortar head joints associated with slidings on mortar bed joints. Analogously to the mechanism *M2*, it is assumed that slidings are limited or locked by a friction force associated to a compressive stress $\sigma_y < 0$. When both normal and tangential stresses are acting on the reference volume, the damage pattern has a typical stair-shape (Fig. 5a). When only a normal stress acts on the reference volume, the damage pattern has the shape illustrated in Figure 5b.

Mechanism *MB* is a mixed mechanism that involves both mortar head joints and blocks. It is activated by a tensile stress acting on the plane of the mortar head joints ($\sigma_x > 0$) and produces a normal extension of the volume along x (Fig. 6).

Mechanisms *M3* and *MB* interact. In fact, when a tensile stress acts locally on the mortar head joints, the damage can involve either mortar bed and head joints or mortar head joints and blocks. The occurrence of the two mechanism depends on various parameters: the strength ratio between mortar and blocks; the compressive force acting on mortar bed joints; the aspect

joints associated with slidings on mortar head joints, produced by a shear stress acting on the volume. In the present model, such mechanism has been disregarded since its effects on the failure domain is negligible, at least for standard masonry patterns.

Finally, the inelastic strain tensors have the following form:

$$\bar{\epsilon}_{mb} = \begin{Bmatrix} 0 \\ \bar{\epsilon}_y^{M1} \\ \bar{\gamma}^{M2} + \bar{\gamma}^{M3} \end{Bmatrix}, \quad (20)$$

$$\bar{\epsilon}_{mh} = \begin{Bmatrix} \bar{\epsilon}_x^{M3,MB} \\ 0 \\ 0 \end{Bmatrix}, \quad (21)$$

$$\bar{\epsilon}_b = \begin{Bmatrix} \bar{\epsilon}_x^{MB} + \bar{\epsilon}_x^{B3} \\ \bar{\epsilon}_y^{B1} + \bar{\epsilon}_y^{B4} \\ \bar{\gamma}^{B2} \end{Bmatrix}. \quad (22)$$

2.2 Damage evolution laws

The expressions of the inelastic strain contributions imply that the internal variables α_{mb} , α_{mh} and α_b (besides the friction stresses f and f_h) must be known at any step of the loading history through evolution equations. The proposed model assumes two different kinds of evolution laws, accordingly to different damage mechanisms.

The first criterion concerns the damage associated to normal stresses and is based on fracture mechanics theory. The hypothesis is advanced that damage (assumed as a crack growth) may be activated ($\alpha_b > 0$) if the density of damage energy release rate Y equals the damage toughness of the material R . If $Y < R$ there is no damage evolution. It follows that admissible states must satisfy the following condition:

$$\phi = Y - R \leq 0. \quad (23)$$

Accordingly to this criterion, the following three damage evolution conditions have been introduced in the model:

$$\phi_{mb} = Y_{mb} - R_m \leq 0, \quad (24)$$

$$\phi_{mh} = Y_{mh} - R_m \leq 0, \quad (25)$$

$$\phi_b = Y_b - R_b \leq 0, \quad (26)$$

where Y_{mb} , Y_{mh} and Y_b are the dissipations in the infinitesimal step associated to the damage in mortar bed joints, mortar head joints and blocks, respectively; R_m is the toughness function of the mortar; R_b is the

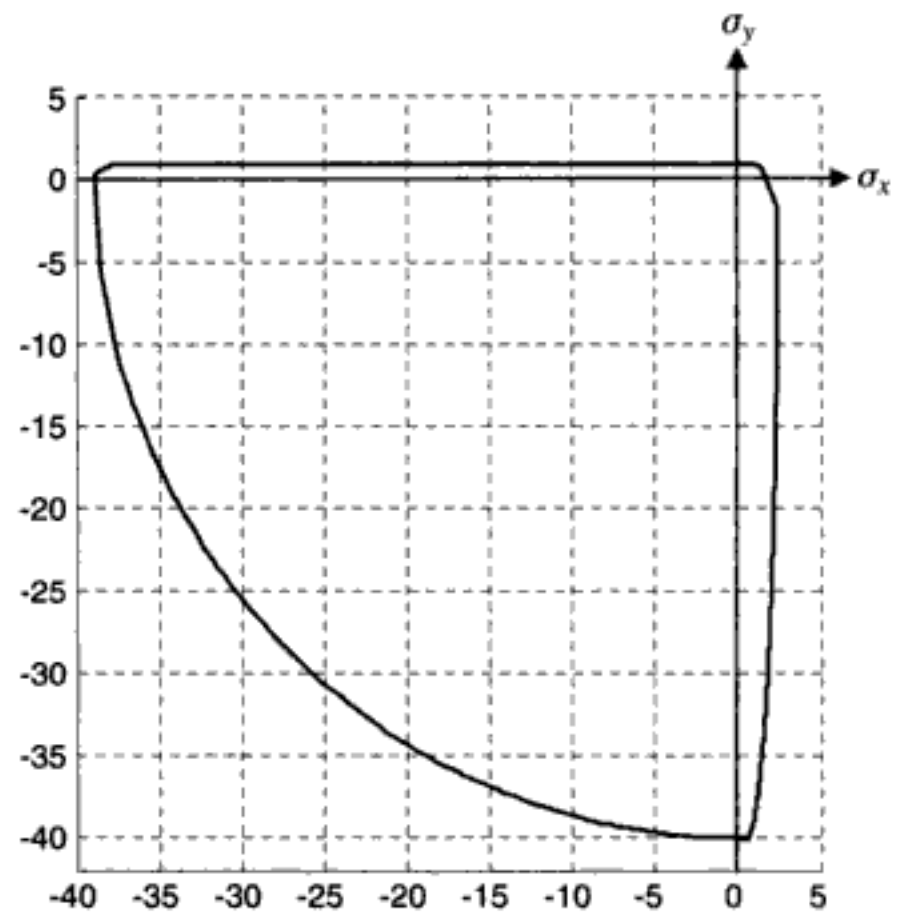


Figure 9. Equivalent stress domain in the plane σ_x/σ_y ($\tau = 0$).

toughness function of the blocks. It is worth noting that each damage condition is associated to a specific damage variable α_{mb} , α_{mh} and α_b .

The second criterion regards the friction phenomena on the mortar-block interface. The hypothesis that the friction stresses f and f_h must satisfy the Coulomb condition, conduces to the following additional damage conditions (a *non-associated* flow rule is assumed):

$$|f| + \mu \sigma_y \leq 0, \quad (27)$$

$$|f_h| + \mu \left(\sigma_y + 2 \frac{\eta_{mh}}{\eta_{mb}} |\tau| \right) \leq 0. \quad (28)$$

The terms in round bracket in equation (28) represents a effective normal stress acting on mortar bed joints in mechanisms $M3$. It can be observed that the tangential stress, appearing in absolute value, reduces the effect of the compressive normal stress in limiting slidings.

2.3 Limit strength domain

Eqs. (24)–(28) defines a set of ellipsoids and planes in the equivalent stress space (i.e. σ_x , σ_y , τ) whose intersection defines the current admissible field of the material. It is worth noting that the obtained surface is closed and, for standard parameters, convex. The multi-surface limit domain is represented in Figures 9–13. Figure 9 and 10 shows two section of the domain in the planes σ_x/σ_y and σ_y/τ , respectively. It can be noted that the domain in plane σ_y/τ is analogous to the one obtained in Gambarotta & Lagomarsino (1997).

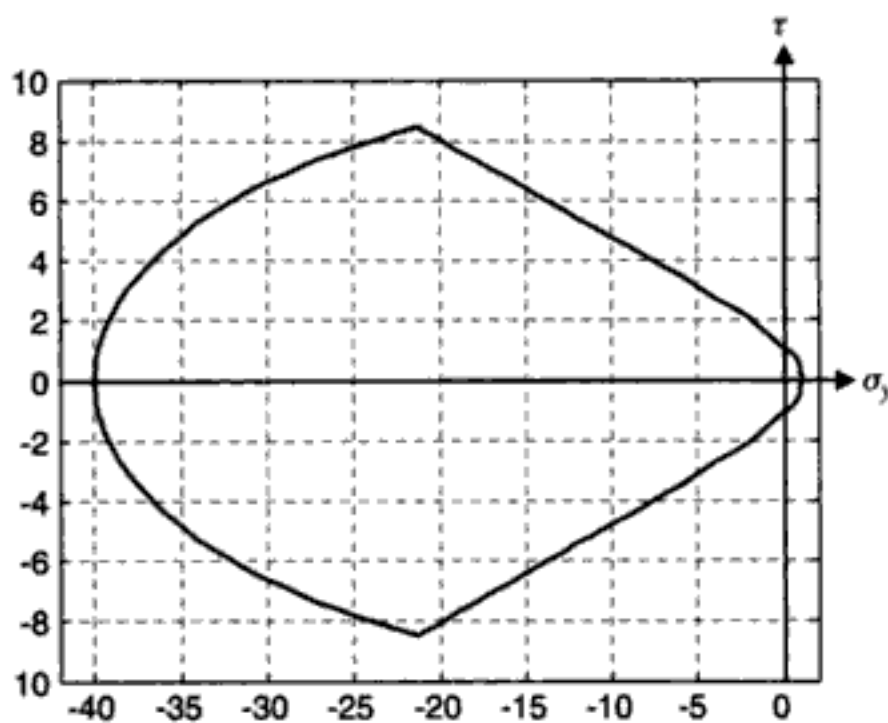


Figure 10. Equivalent stress domain in the plane σ_y/τ ($\sigma_x = 0$).

Figure 11 illustrates the domain in the plane σ_x/τ ($\sigma_y = 0$) for two types of masonry patterns. It can be observed that:

- the resistance along x associated to mechanism $M3$ increases as a function of the block aspect ratio b/h (see Alpa & Monetto 1994);
- the resistance along x associated to mechanism MB decrease as a function of the block aspect ratio b/h ;
- the resistance along x of a masonry with a good interlocking ($b/h = 4$) is globally higher;
- with reference to mechanism $M3$, the shear strength of masonry decreases as a function of the tensile stress applied normally to the mortar head joints.

Figure 12 shows the effect on the limit domain of the compressive stress normal to the mortar bed joints (σ_y). It can be observed that for low stress states, the compression increases the shear resistance of the masonry, limiting the sliding associated to mechanisms $M2$ and $M3$; for higher stress states, the failure of the blocks tends to prevail (mechanisms $B2$, $B3$ and $B4$).

The complete three-dimensional limit domain of the constitutive model in the stress-space is represented in Figure 13.

3 APPLICATION

The model has been implemented in a *general purpose* finite element program (ANSYS). The solution of the incremental problem for the definition of the internal state variables has been carried out by linearizing the problem through the Newton-Raphson method.

In order to study the influence of different patterns on the global behaviour of masonry structures, an ideal domed vault, subjected to a concentrated asymmetric

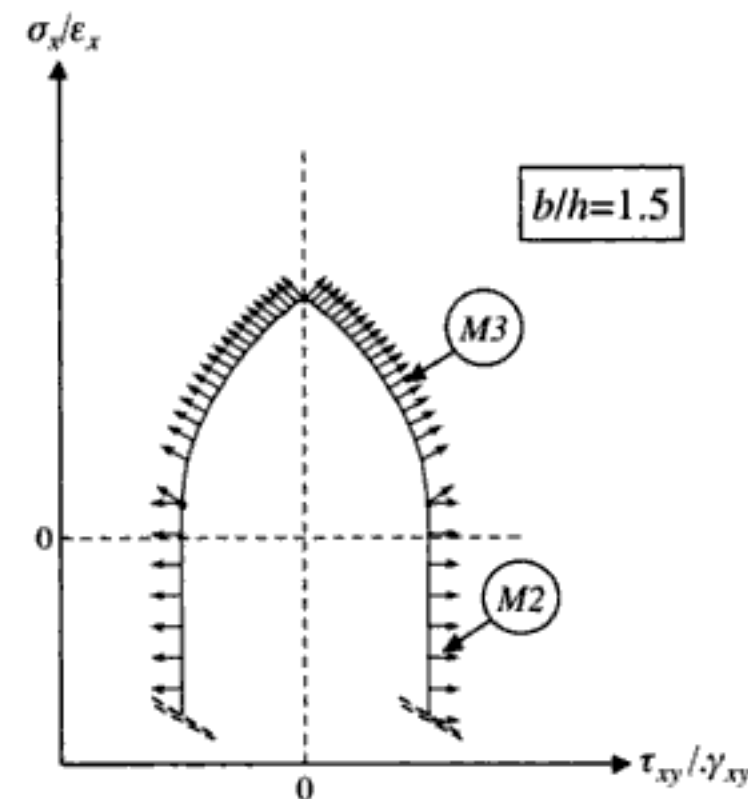
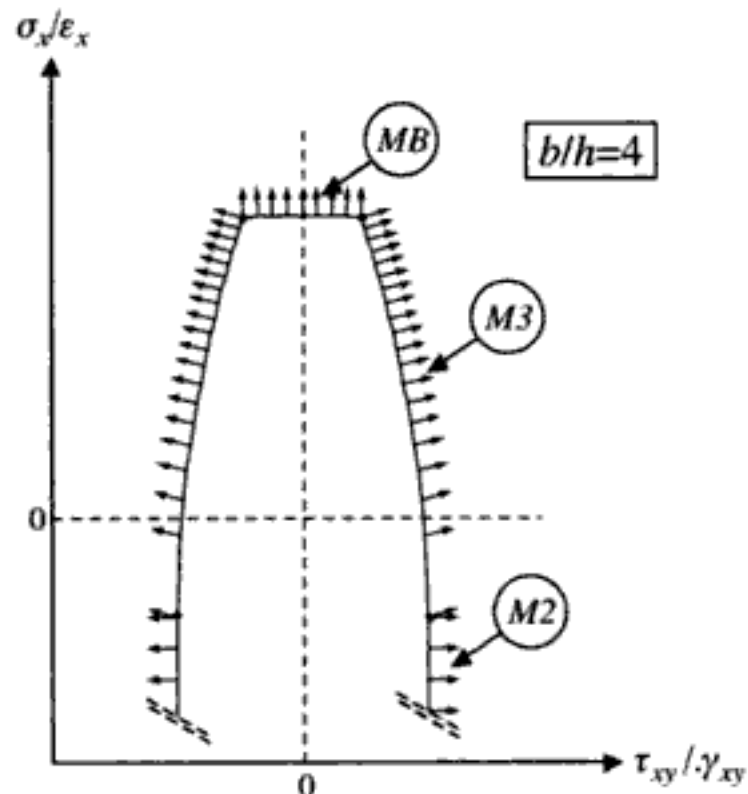


Figure 11. Equivalent stress domain in the plane σ_x/τ ($\sigma_y = 0$) for two masonry with different block aspect ratios b/h .

load, has been analysed. It is well known that this kind of vaults can be built with different block arrangements. Figure 14 illustrates two typical arrangements: in case a , above, the blocks are set along the circumferences of the vault; in case b , below, the blocks are set along four diagonal segments.

The model of the vault is illustrated in Figure 15, where P is the applied load. Multi-layered shell elements have been used. The vault has a squared plane of 4×4 meters and is 10 cm thick. The concentrated load represents, for example, a roof wood beam acting on the vault. It has been possible to represent the two different block arrangements by rotating the local coordinate system of each elements.

The analysis has been carried out in two steps: in the first one, the only own weight has been applied;

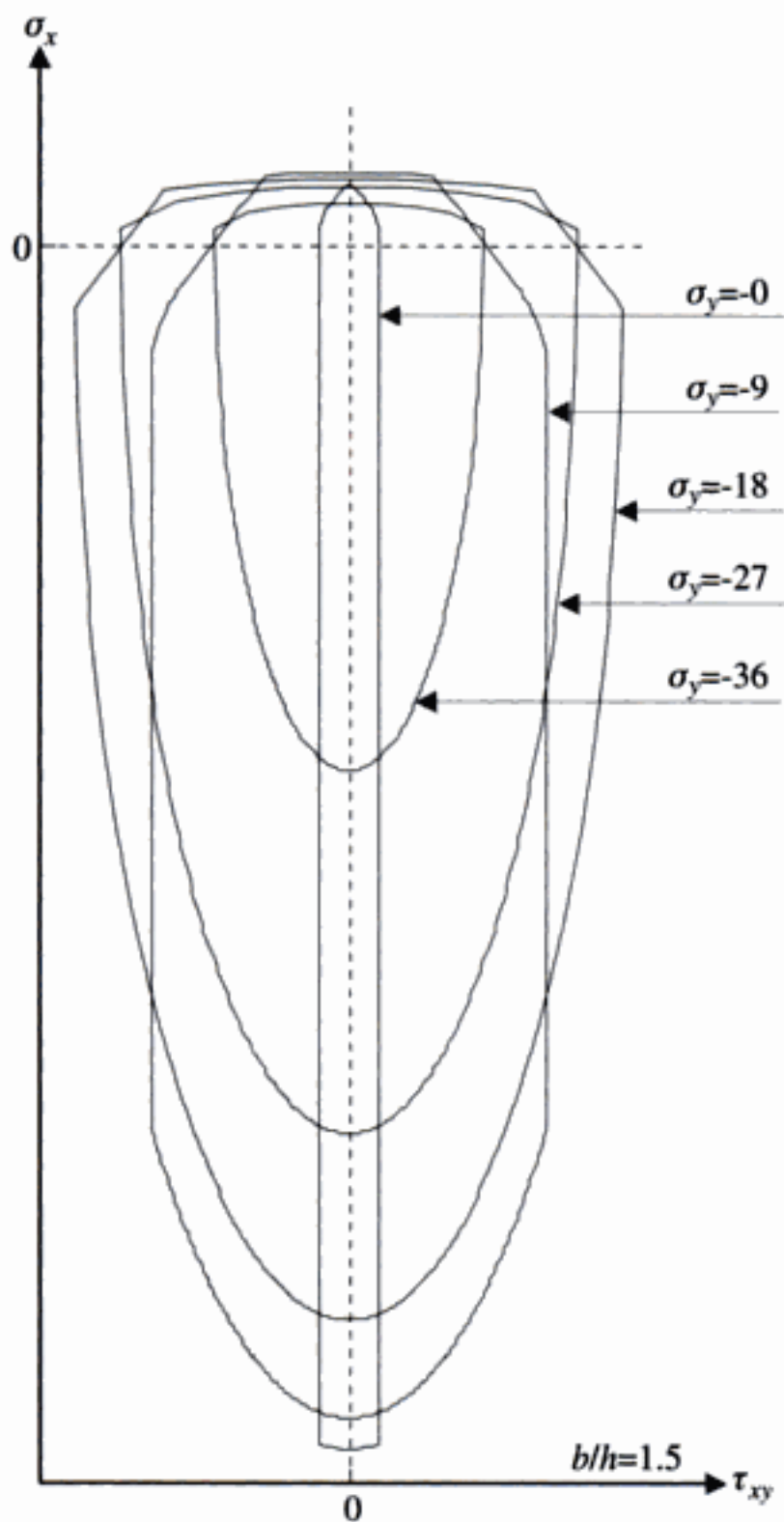


Figure 12. Effect of the compressive stress σ_y on the limit strength domain (Kg/cm^2).

in the second one, the concentrated load P has been superimposed.

Tables 1 and 2 shows the results obtained in the first step; they are expressed in term of circumferential and tangential stresses at the extrados and intrados of the vault. It can be observed that the behaviour of the structure is different in the two cases. In particular, the stress diffusion in the vault globally differs and, in the case b , the tangential stresses are locally higher.

The incremental collapse analysis of the structure under the concentrated load P demonstrated how the collapse load P_c of the vault with masonry pattern a is higher than the one of the vault with masonry pattern b : $P_{c(a)} = 6200 \text{ Kg}$ and $P_{c(b)} = 5800 \text{ Kg}$. Tables 3–5 illustrate the stress states in the two cases at collapse. The main differences can be observed in the tangential stresses at the intrados. In fact, in case a , the tangential stresses are concentrated around the load

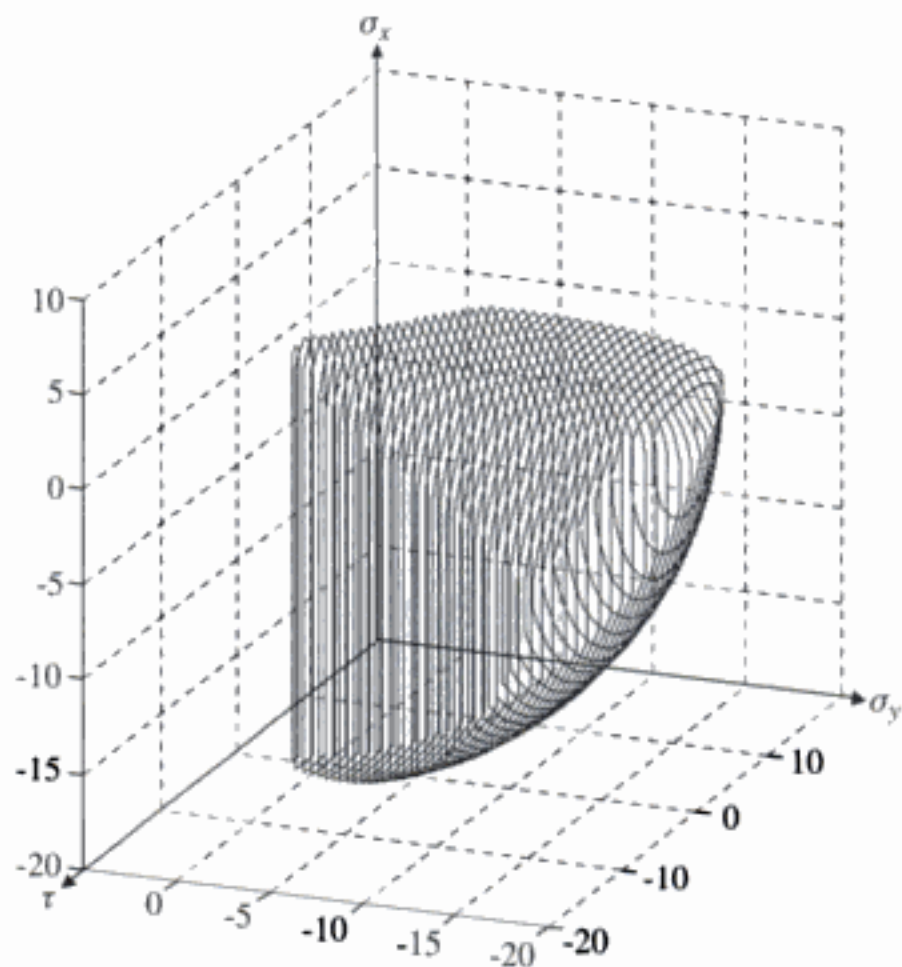


Figure 13. Three dimensional limit domain of the constitutive model.

Case a



Case b

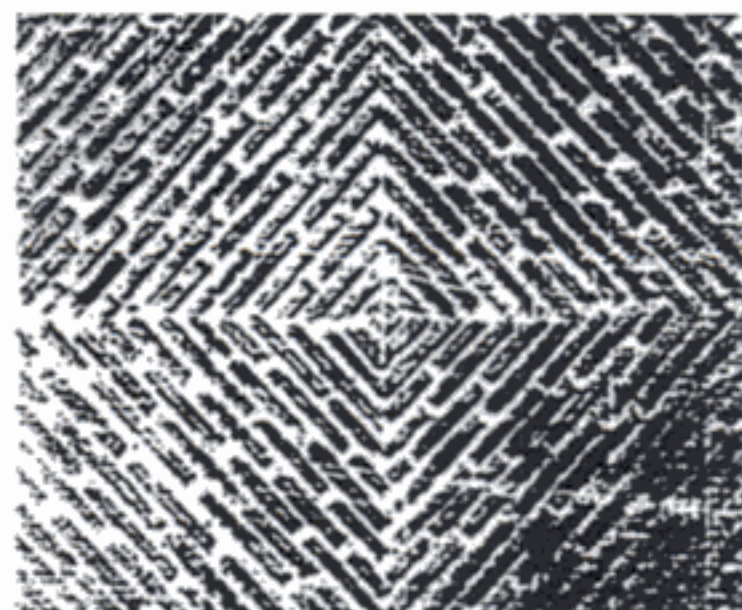


Figure 14. Different masonry pattern of domes vaults: the circular pattern a and the segmental pattern b .

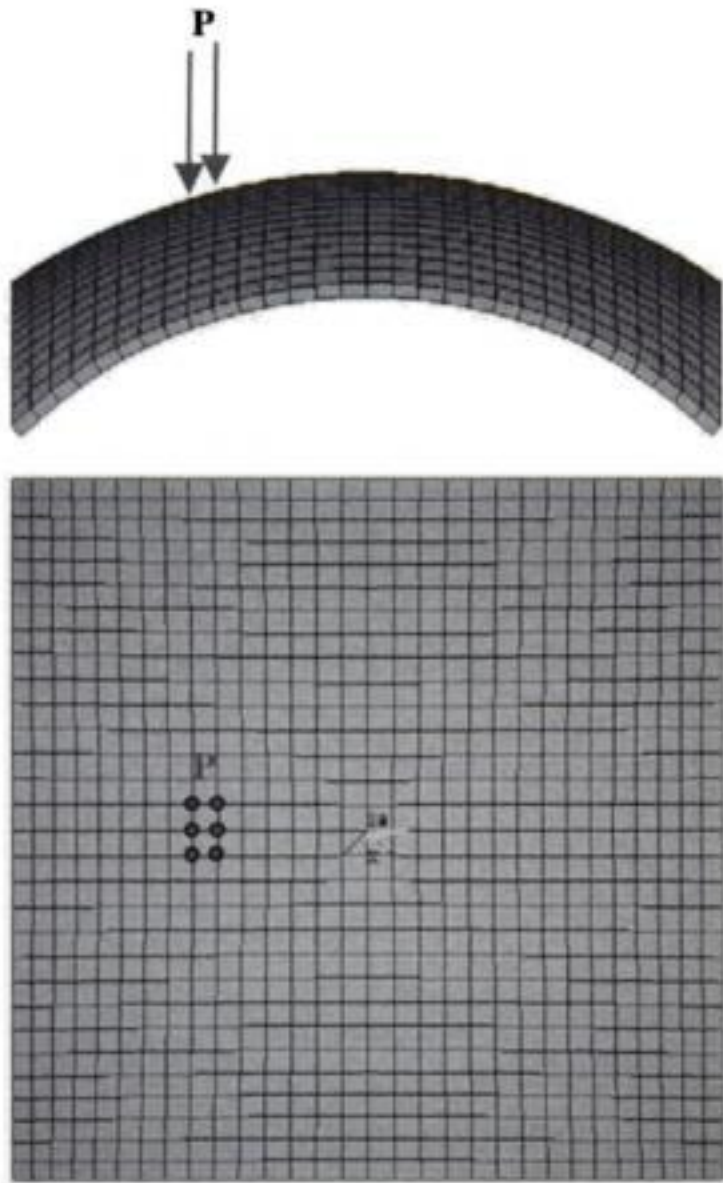
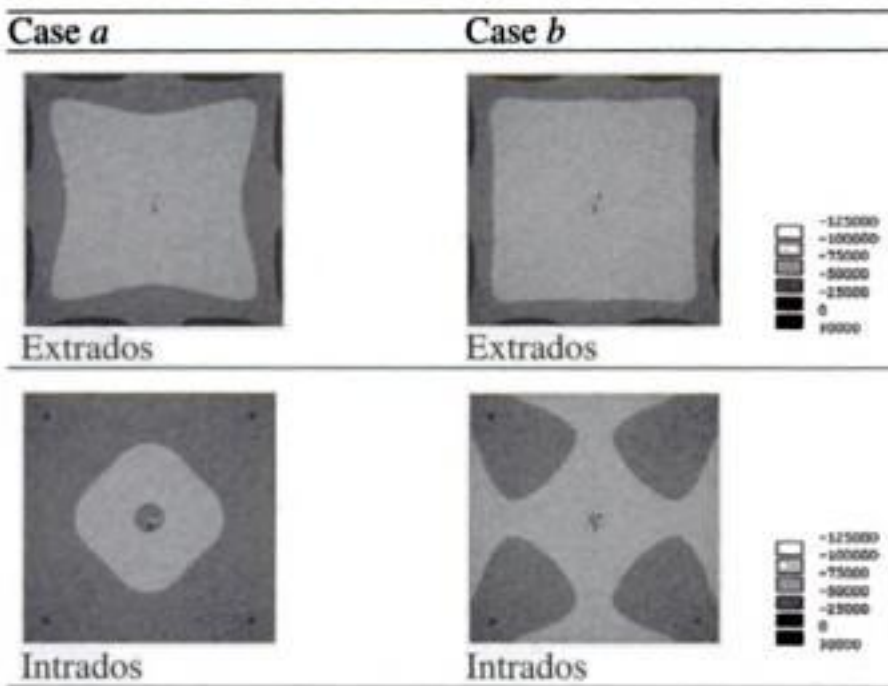


Figure 15. The FEM model of the vault.

Table 1. Circumferential stresses in the vault, loaded with its own weight (Kg/cm^2).



application point and have a circumferential distribution; in case *b* they are concentrated along two diagonals in correspondence of the load application point. This phenomenon is also evident in the damage patterns illustrated in Tables 6–7. In particular, Table 6 represents the mortar bed joints damage variable α_m for the two cases. It is worth noting that in case *a* the damage of the mortar bed joints at the intrados is concentrated in the zone of the load *P*, while in case *b*

Table 2. Tangential stresses in the vault loaded with its own weight (Kg/cm^2).

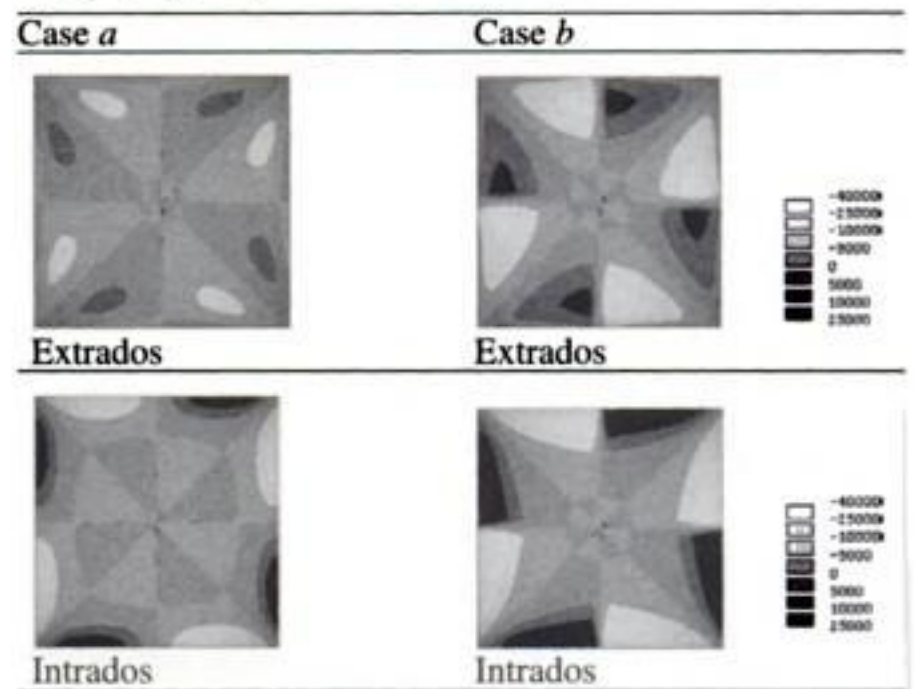


Table 3. Circumferential stresses in the vault, at the collapse state under the concentrated load *P* (kg/cm^2).

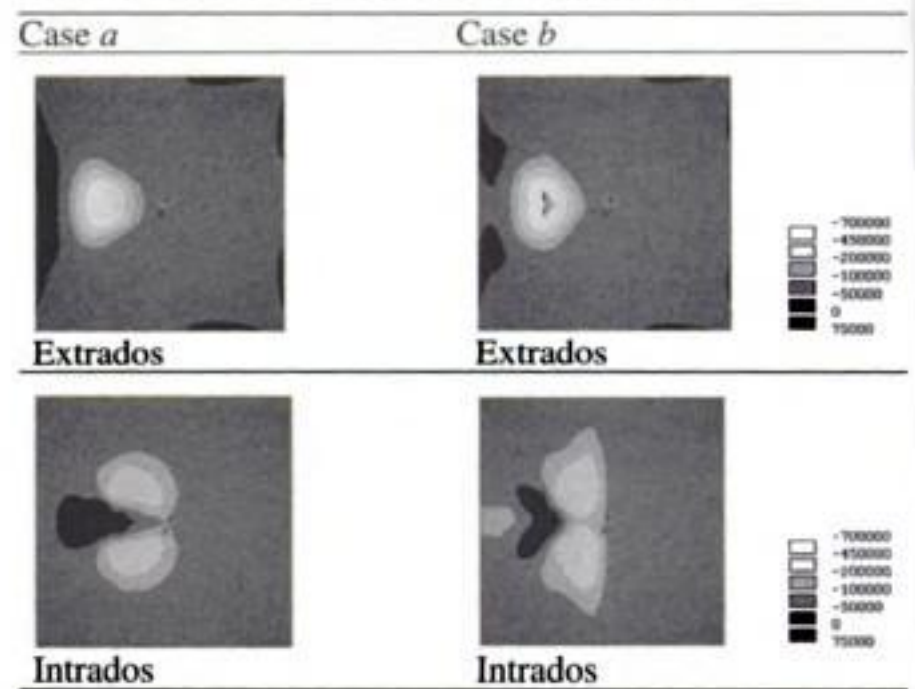
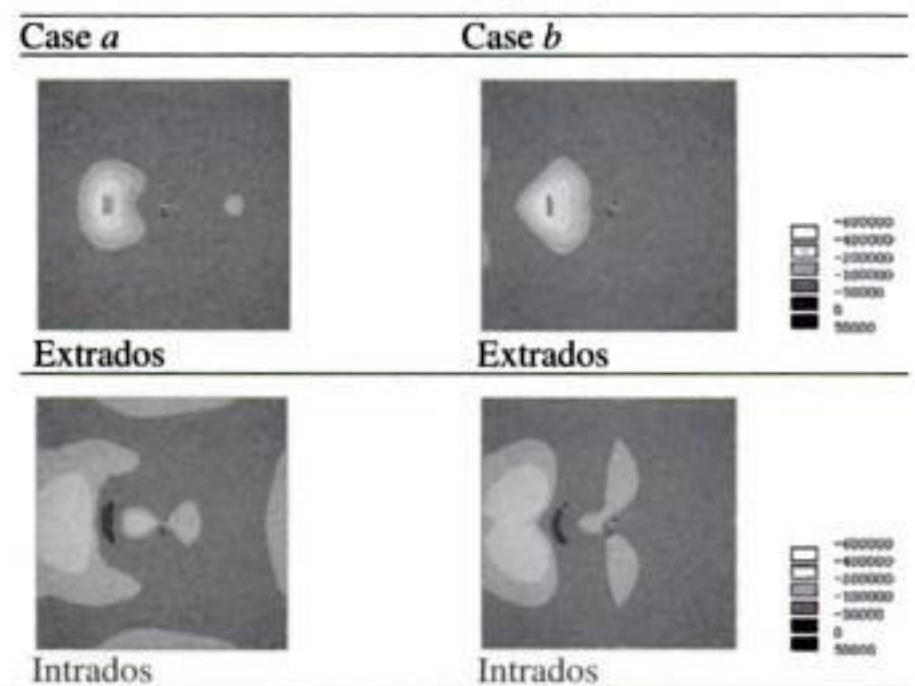


Table 4. Meridian stresses in the vault, at the collapse state under the concentrated load *P* (kg/cm^2).



- Luciano, R. & Sacco, E. 1997. Homogenization technique and damage model for old masonry material. *Int. J. Solids Struct.* 34(24): 3191–3208.
- Page, A.W. 1978. Finite element model for masonry. *Journal of Structural Division, ASCE* 104(ST8): 1267–1285.
- Papa, E. & Nappi, A. 1997. Numerical modelling of masonry: a material model accounting for damage effects and plastic strains. *Appl. Math. Modelling* 21: 319–335.
- Pietruszczak, S. & Niu, X. 1991. A mathematical description of macroscopic behaviour of brick masonry. *Int. J. Solids Struct.* 29(5): 531–546.
- Zucchini, A. & Lourenço, P.B. 2002. A micro-mechanical model for the homogenization of masonry. *Int. J. Solids Struct.* 39: 3233–3255.

Non linear step by step analysis for masonry structures using changing shape finite elements – new developments and implementations

P. D'Asdia, A. Viskovic & C. Brusaporci

Department PRICOS, University "G. D'Annunzio" of Chieti – Pescara, Italy

ABSTRACT: The procedure, named PEFV, is based on a mathematical model schematizing the masonry by macro-finite elements. The particularity and the favourable features of this procedure, compared with the general purpose ones, is the way of dealing with the non linear behaviour of masonry materials. This method, in fact, doesn't simulate non linearity modifying the properties and the mechanical characteristics of the finite elements "material". On the contrary it is seen as a geometrical problem: at each load step the shape of the mathematical model is updated to reproduce the configuration variations of the resistant (and working) portions of the walls, excluding the volumes of masonry under tensile stresses, or cracked, or generally no more co-operating. In such a way the accuracy of this procedure is not "mesh dependent" but only "load step dependent". The last developments allow also to take into account well connected different walls, on the whole height of their junction, with "L" or "T" horizontal configurations.

1 INTRODUCTION

The method, named PEFV and developed by D'Asdia & Viskovic (1993), based on variable shape finite elements, is aimed to the non-linear analysis of multi-storeyed masonry buildings, not reinforced or reinforced with bars or chains (prestressed or not prestressed), under horizontal actions.

The method is aimed both to the analysis of multi-storeyed masonry single walls, under in plane actions, and to the analysis of spatial masonry boxed building structures, more generally loaded.

In the previous implementations for three dimensional boxed buildings, the method was taking into account the case of a reduced continuity in the corners, with good connections only at the floors levels.

In the present paper it is presented the sub-procedure to take into account well connected corners on the whole masonry height.

The program for PC implementations is written in C++ language, to take advantage, writing a F.E. procedure, of the object oriented programming philosophy.

2 THE SINGLE SIMPLE MASONRY PANEL MACRO ELEMENT

The F.E. mesh employs a reduced number of elements for each masonry panel (Fig. 1).

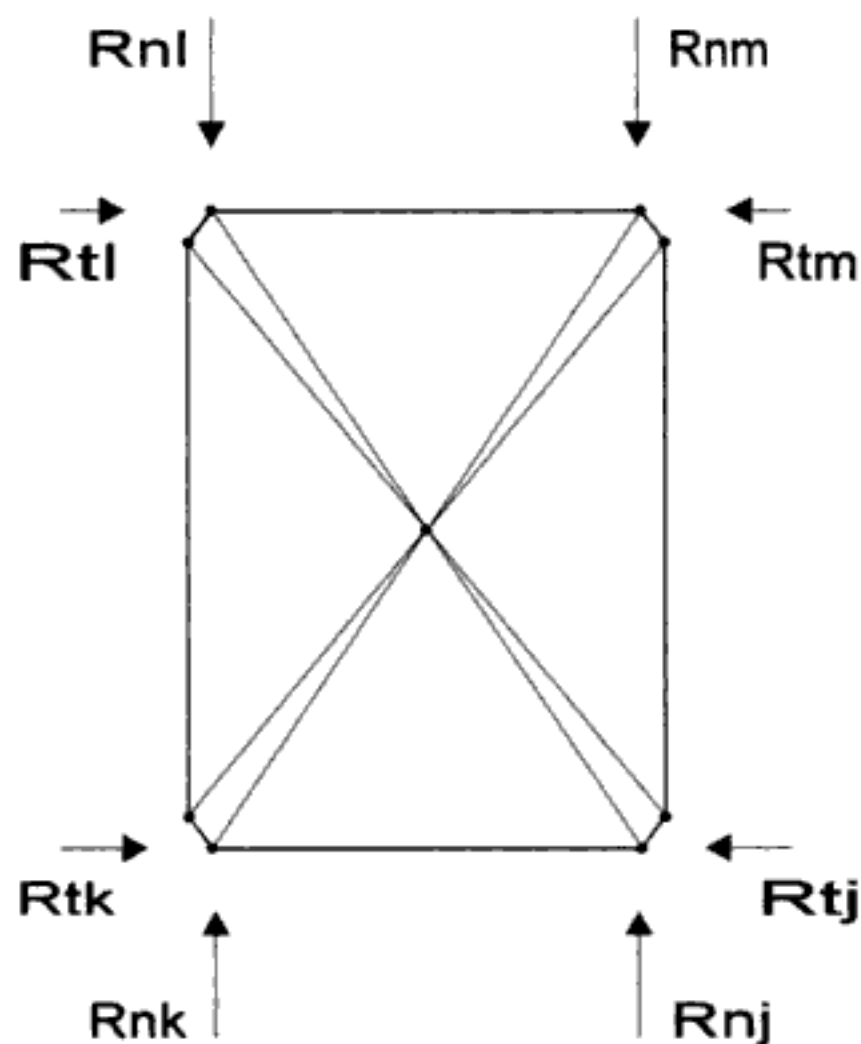
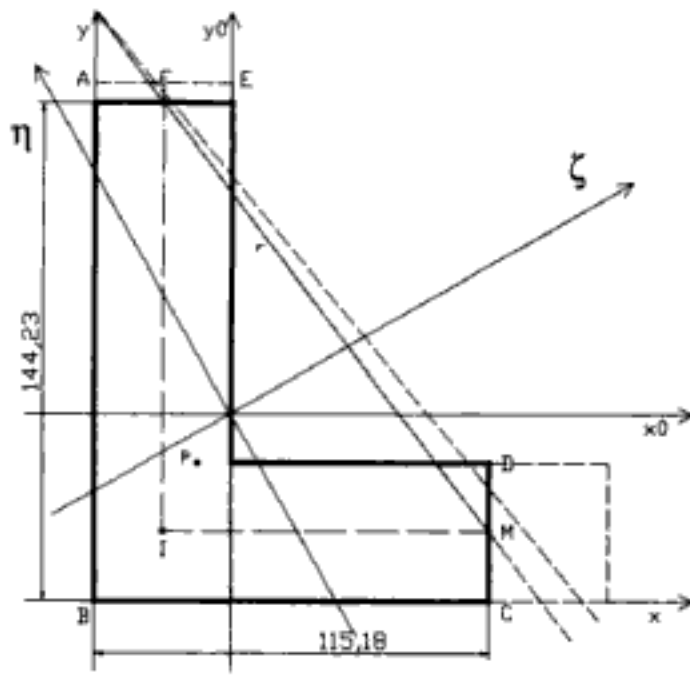
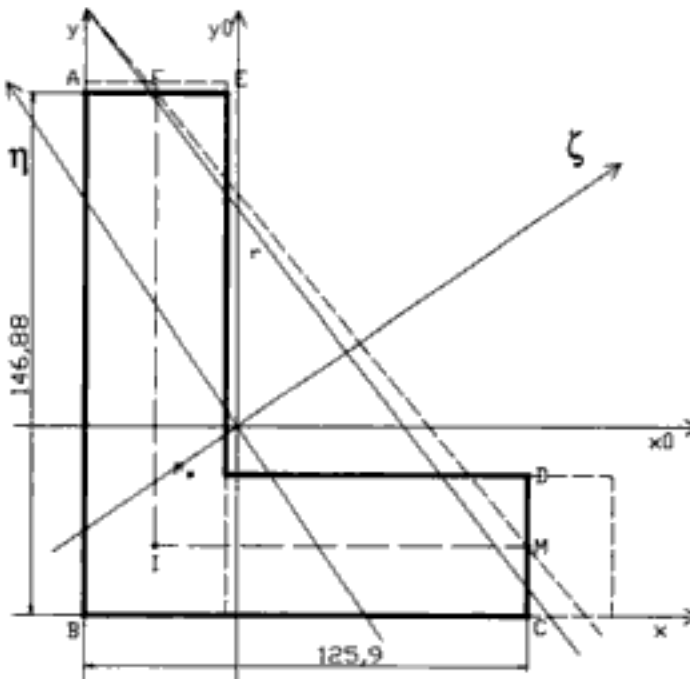


Figure 1. Generic panel mesh.

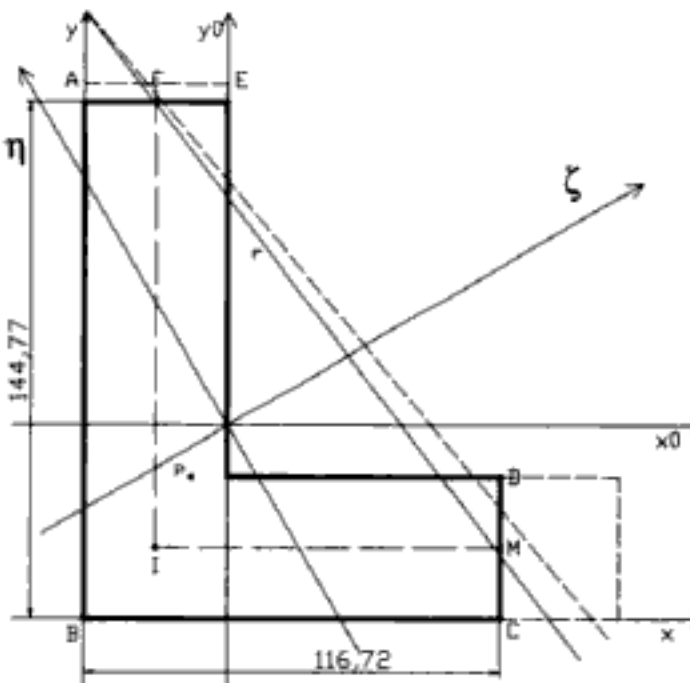
The procedure follows step by step the evolution of the resisting parts of the wall: when horizontal loads increase, the shape of the elements changes eliminating the zones where the masonry is no more working,



Iteration 1



Iteration 2



Iteration 3

Figure 7. Three iterations to find out the neutral axis position, given the resultant force position "P", in a well connected corner.

procedure is so efficient that generally are necessary no more than three or four iterations. Moreover, in the PEFV program, the load steps are so relatively little that the iterations, for the neutral axis positioning at each load step, are constantly less than four.

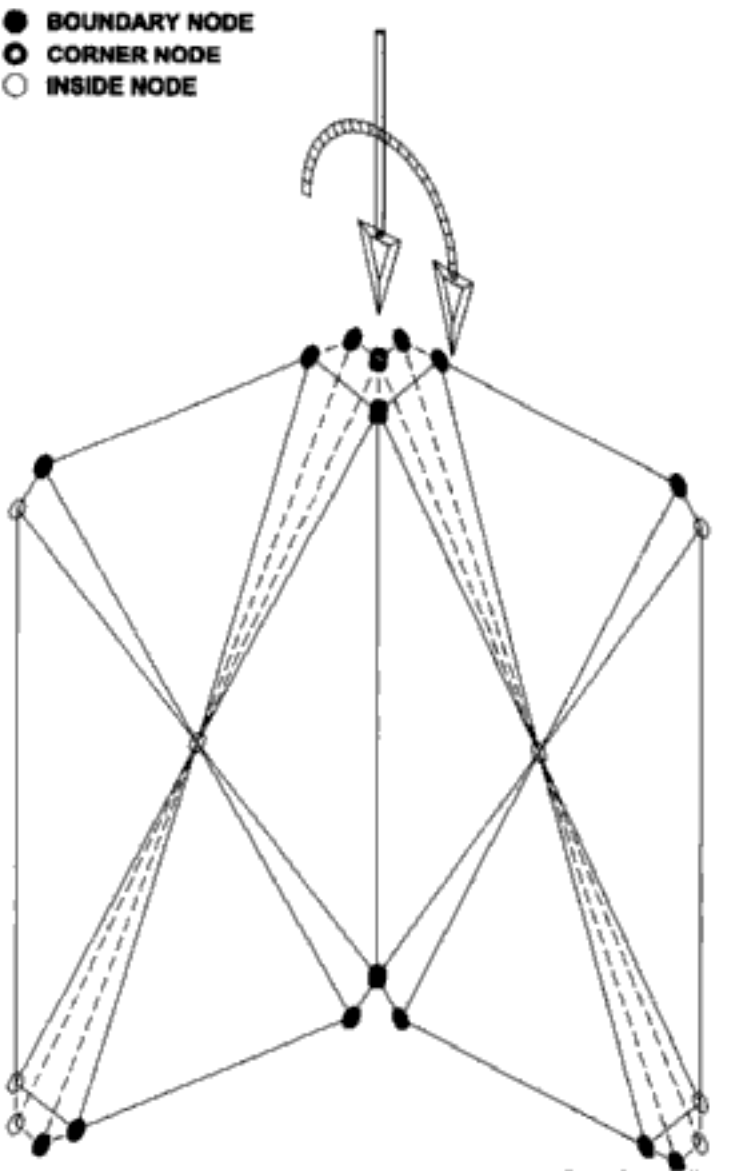
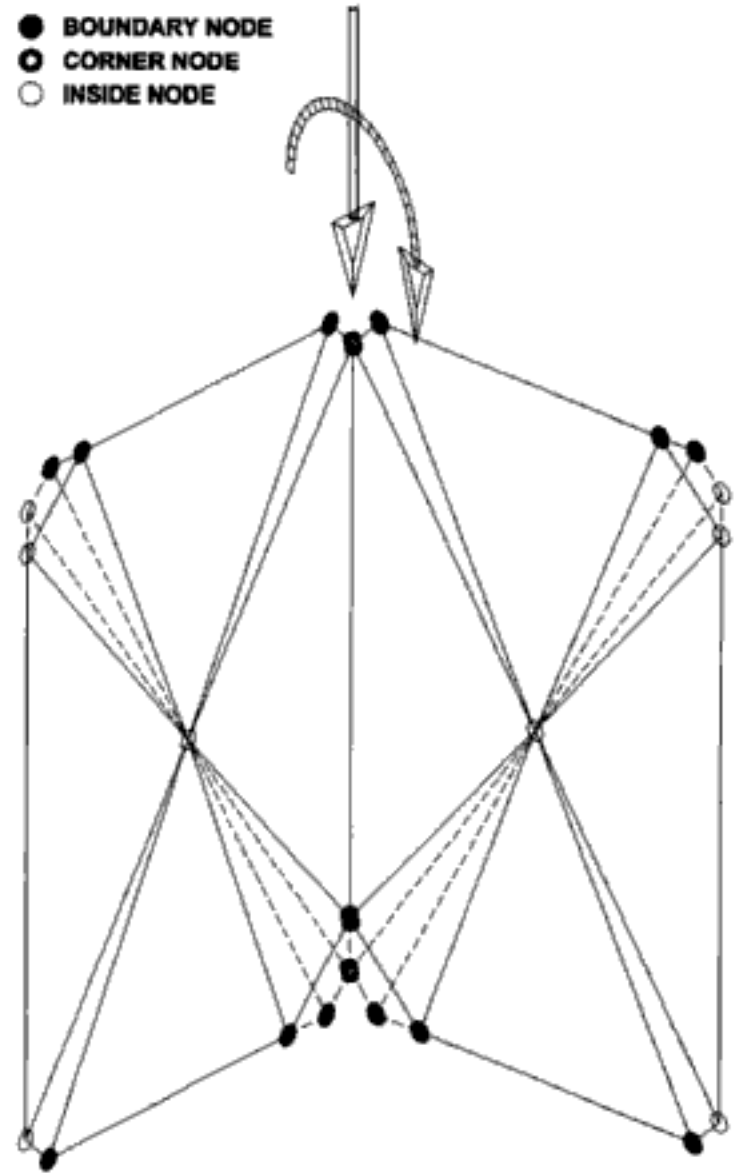


Figure 8. Two of the possible way in the decrement of a generic corner substructure working sections.

Construction sequence in the finite element analysis of Romanesque churches

L.A. Van Gulick

Lafayette College, Easton, PA, USA

ABSTRACT: French Romanesque churches typically incorporate thick masonry vaults over nave side aisles, over galleries, when present, and often over central nave spaces. Construction sequence can play an important role in determining undeformed configurations for these vaults due to deformations of supporting members occurring prior to vault erection. Finite element analyses that do not include this effect can significantly overestimate building deformations and stresses. The feasibility of using element “birth/death” capability to include the effects of construction sequence in three-dimensional finite element analysis of French Romanesque churches is demonstrated. Also demonstrated is the potential importance of these effects.

1 INTRODUCTION

Structural analyses of medieval buildings using contemporary engineering analytical techniques can contribute to a better understanding of their structural function and the historical development of their characteristic structural forms. The analyses can also help to understand the history of structural modifications that the buildings may have experienced due to problems encountered (Mark 1982).

Linear finite element analyses can identify local areas of significant tension, cracking, and possible resultant structural distress under normal service loading conditions, including wind load. Localized tension and cracking on exterior surfaces was almost certainly of particular concern to medieval builders due to the possibility of progressive damage from cycles of freezing and melting of water from rain or snow penetrating into the cracks. This concern can be assumed to have played a significant role in the development of medieval structural forms.

Nonlinear finite element analyses can include the effects of mortar cracking and other nonlinear material behavior on deformations and stresses in un-reinforced masonry structures, including French Romanesque churches (Navedo et al. 1998), (Boothby & Rosson 1999), (Fanning & Boothby 2001). They are necessary whenever nonlinear phenomena, particularly cracking, cause a significant redistribution of stresses. They are certainly necessary for predicting structural collapse or describing the large plastic displacements frequently found in medieval buildings.

Major French Romanesque churches typically incorporate thick masonry groin, axial half-barrel, or transverse barrel vaults over nave side aisles and, when present, galleries. Central nave spaces, when vaulted, are usually covered by thick axial barrel vaults, but transverse barrel or groin vaults are occasionally encountered.

Construction of the churches often extended over several decades, or more. Vertical structural components, including exterior and interior walls, supporting piers, columns, and arcades were usually built first, and the enclosed space created covered by a timber-framed roof. Masonry vaults over side aisles, and galleries, were sometimes constructed simultaneously with the vertical structural components; sometimes afterwards. Vaulting of the central spaces was almost invariably the last stage in the construction process. Vaults under construction were supported by wooden centering until they were complete and ready to become self-supporting.

Deformations of vertical components due to self-weight and roof weight occurred before central vault erection, and on occasion side aisle and gallery vault erection, began. Support locations for vaults and their resultant undeformed shapes reflected this deformation. Supporting centering also affected vault undeformed shape.

Three-dimensional finite element analyses are well-suited for studying the structural function of French Romanesque vaulted churches and helping to develop a better understanding of the development of their structural forms.

by the present thin *colonettes*, probably in the seventeenth century (Mark 1992), (Morganstern 1996).

Now open to the elements, the central nave was never vaulted, but was originally covered by a timber-framed roof, as were the galleries.

Archeological evidence in the building fabric and documentary information from contemporaneous Norman churches have led scholars to believe that the nave of Notre-Dame may have originally been spanned by either one or three diaphragm arches rising from the Romanesque *dosserets* (Morganstern 1996). These arches would have been intended to help support the tall clerestory walls against deformations and stresses resulting from the inward thrust of the gallery vaults below them and wind loading on both the walls themselves and on the roof above them. Seventeenth century changes to the upper part of the building to accommodate false vaults and lack of definitive documentary evidence leave room for scholarly differences of opinion on the question of the original existence of the arches.

Several years ago, the author joined a team of scholars led by James Morganstern involved in a continuing investigation of Notre-Dame at Jumièges (Morganstern 2002). Finite element analyses of the building have addressed the possible structural functions of the arches and hence the possibility that Romanesque builders may have included them in the original construction.

Notre-Dame at Jumièges furnished a logical starting point in the consideration of construction sequence in finite element analysis of French Romanesque churches. Although its central nave space was not vaulted, diaphragm arches would have been among the last elements added to the building and would have played a structural role similar to that of central vaults. A study of the effects of construction sequence would, however, be easier to implement and interpret for the arches than for the central vaults of other churches. Experience obtained in applying birth/death capability for this purpose and demonstrated success in doing so will facilitate similar studies of centrally vaulted buildings.

No other nonlinear effects were considered in this analysis of Notre-Dame. They do not appear necessary for its intended objective and would have unnecessarily complicated it. Archaeological evidence indicates that the construction sequence followed for the side aisle and gallery groin vaults makes its inclusion in the analysis similarly unnecessary.

3 ANALYSIS

Basic geometric information was obtained from drawings furnished by Morganstern that were produced by the Atelier Photogrammétrique of the Inventaire



Figure 3. Finite element model.

Général, E.L.P. It was supplemented by on-site visits and slides taken by the author.

The analysis was carried out using general-purpose finite element code ANSYS, Release 7.1 (ANSYS 2003). Ten-node SOLID92 tetrahedral elements with quadratic displacement shape functions were used because they are particularly well-suited for describing the complex three-dimensional geometry typical of French Romanesque churches.

Based on axial and transverse symmetry considerations under dead weight, i.e. gravity, loading, a solid model of one quarter of a typical bay of the building was constructed. A “bottom-up” approach proceeding from key points to lines to surfaces to volumes was followed. Boolean operations were frequently employed to find surface and line intersections. The diaphragm arch was constructed as a separate volume to facilitate selecting the associated elements for birth and death operations.

The solid model was meshed to obtain the finite element model. Mesh density was varied in critical regions during preliminary stages of the analysis to best describe localized tensile stresses. The final version of the one quarter bay finite element model contains 43,729 nodes and 27,807 elements (Fig. 3). Nodes at ground level were fixed in all degrees of freedom and appropriate symmetry displacement boundary conditions applied.

Displacements and stresses under gravity loading were first computed without considering the effects of construction sequence. Results are shown in Figures 4–6.

Figure 4 shows the deformed shape of the building with deformations “scaled up” to make them clearly visible. Vertical displacements are seen to be generally greater near the central nave space than at the outer walls of the gallery and side aisle. This tends to produce a downward slope toward the interior of horizontal surfaces and an inward slope of vertical surfaces. Vertical displacements are greater in the vicinity of the simple



Figure 4. Deformed shape without construction sequence effects – gravity.

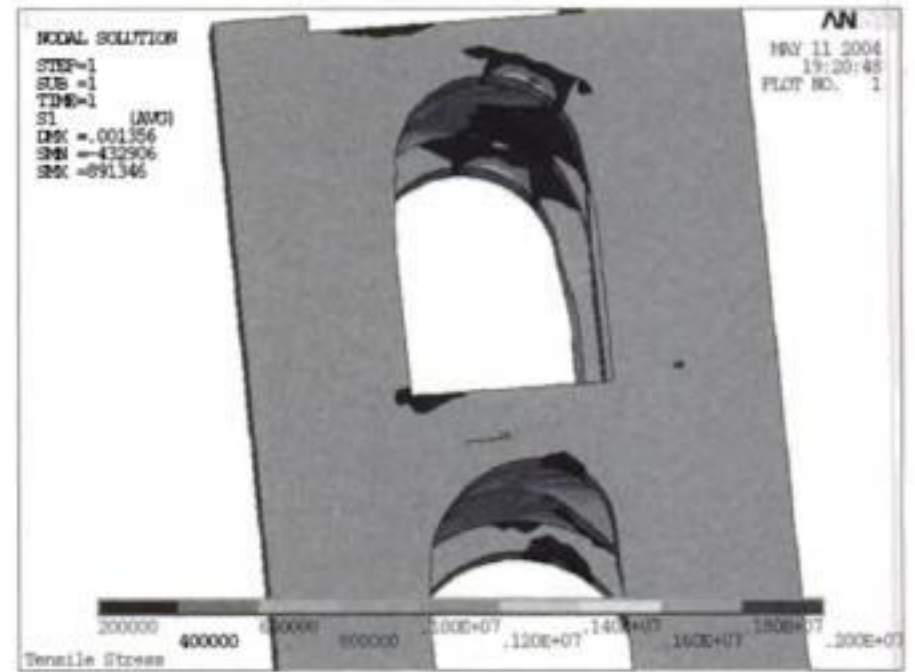


Figure 6. Tensile stresses in gallery and side aisle transverse arches and vault intrados without construction sequence effects – gravity.

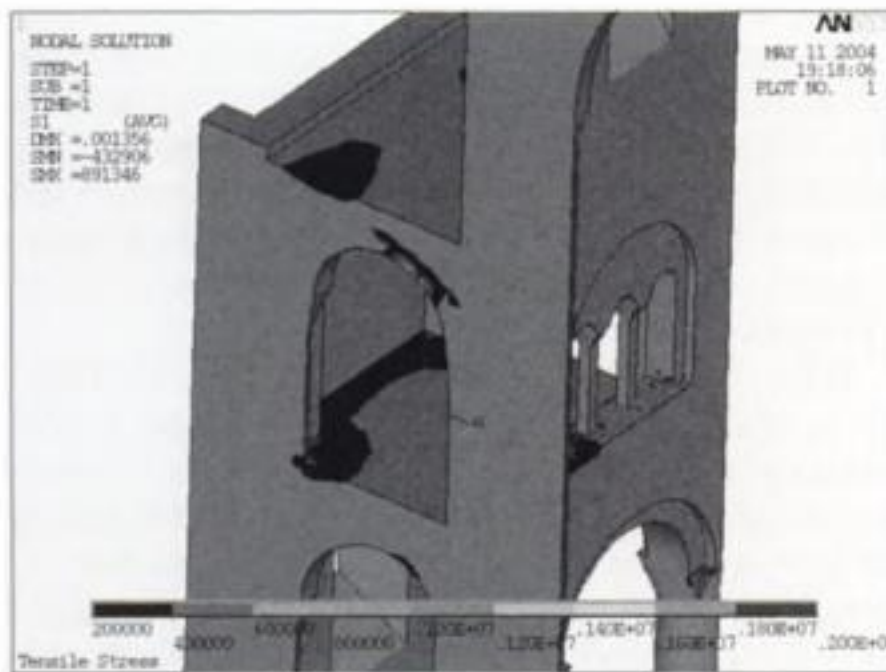


Figure 5. Tensile stresses in gallery balustrade, floor, and vault extrados without construction sequence effects – gravity.

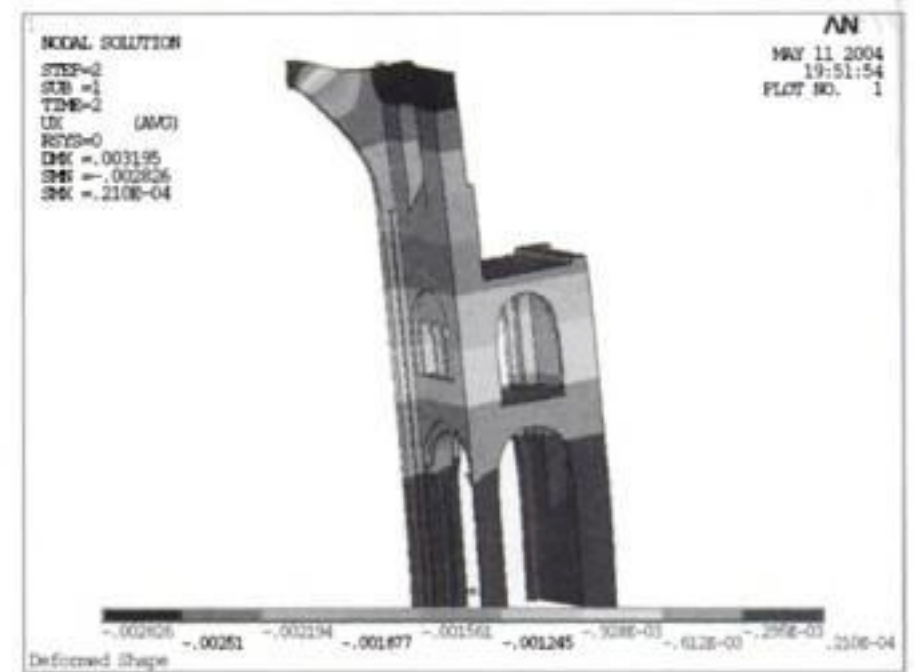


Figure 7. Deformed shape with construction sequence effects – gravity.

column than near the compound pier, producing axial bending in the gallery floor and balustrade.

Inward horizontal displacements due to side aisle and gallery vault thrusts and differential vertical displacements are especially noticeable near the top of the gallery level at both the inner and outer wall. Above the gallery level, the outward thrust of the diaphragm arch reduces these displacements and the clerestory wall shows a noticeable outward slope. The result is a compound “S-shaped” bending pattern.

Figures 5–6 show the regions of the model in which tensile stresses exceed an assumed nominal 200 kPa cracking level for medieval mortar (Mark 1982). Observed stress patterns are consistent with the deformations.

Tensile stresses seen in the gallery transverse arches (200–900 kPa), gallery and nave vault intrados and side aisle transverse arches (200–400 kPa), are due to the compound bending noted above. This bending also

produces tensile stresses (200–400 kPa) in the rear of the gallery floor and limited areas of the gallery vault extrados. Tensile stresses (200–400 kPa) in a limited area of the balustrade below the gallery opening result from axial bending

Gravity loading computations that described a two-step construction sequence were next carried out. Arches were “killed” before the first step of the computations and then “born” stress-free in the resulting deformed configuration. The second step of the computations included the effects of the newly-born arches.

Figure 7 shows the deformed shape of the building with the newly-born arches. It is quite different from the previous result (Fig. 4). Inward horizontal displacements in the upper portion of the building are no longer reduced by outward arch thrusts and reach their peak level at the top of the clerestory wall. The compound bending previously seen is not present.

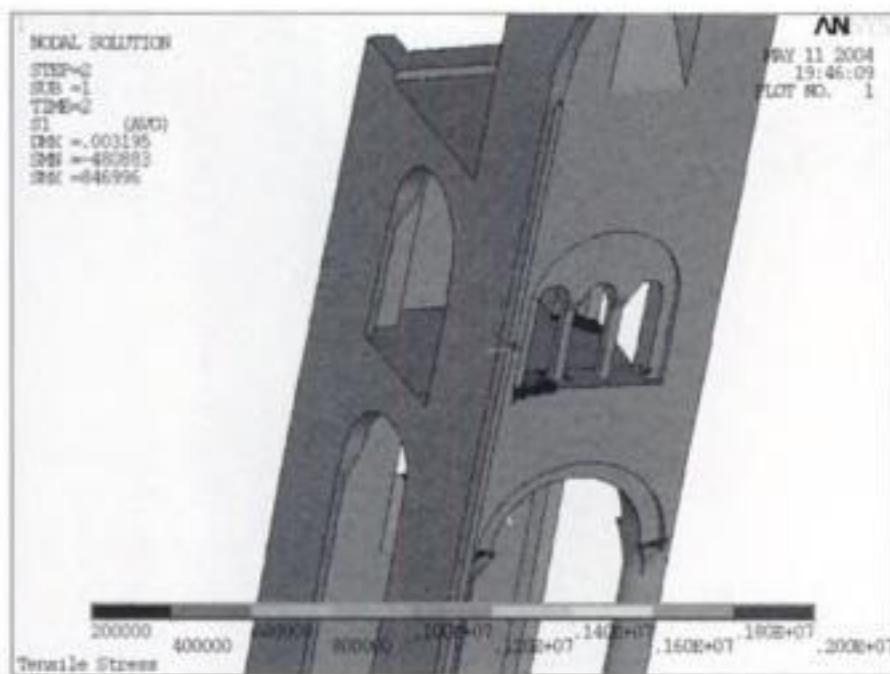


Figure 8. Tensile stresses in gallery balustrade and floor with construction sequence effects – gravity.

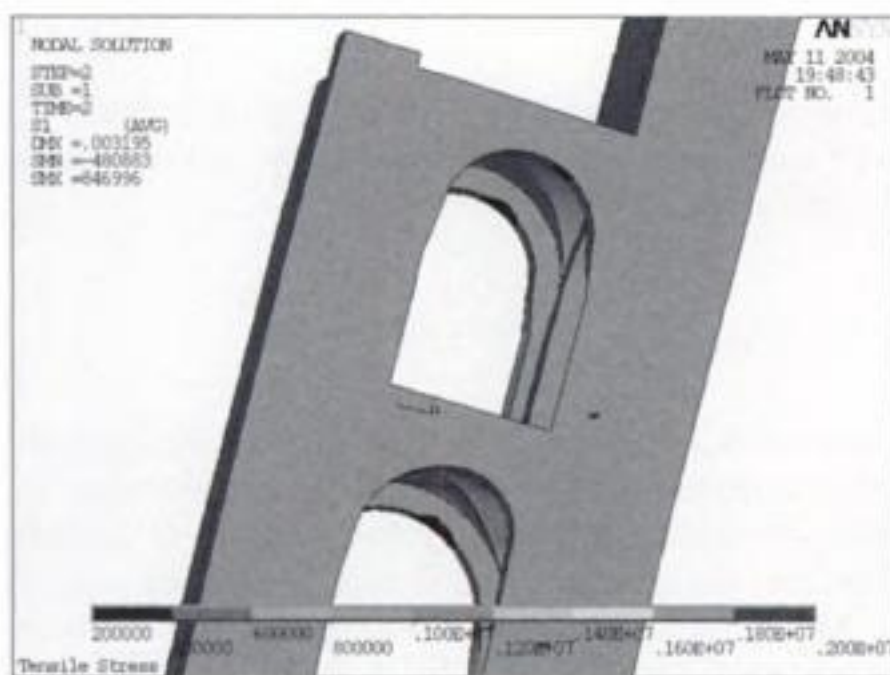


Figure 9. Tensile stresses in gallery and side aisle transverse arches with construction sequence effects – gravity.

As a result of the absence of compound bending, the tensile stresses previously noted in gallery and side aisle vaults and transverse arches, and the gallery floor are essentially eliminated. Only low level (200–400 kPa) tensile stresses in extremely limited regions of these components remain (Figs 8–9). The tensile stress due to axial bending in the balustrade below the gallery opening remains, but is unchanged from its already relatively low level.

Stresses and displacements have been markedly changed by the consideration of construction sequence in the analysis. The basic character of the displacement pattern is different. Tensile stresses have been much reduced, both in magnitude and in the extent of regions in which they occur.

Including the effects of wind load in computations meant that transverse symmetry could no longer be invoked. A half-bay model (Fig. 10) was accordingly obtained by reflection of the quarter-bay model about the center plane of the nave. It includes 121,044



Figure 10. Reflected finite element model.

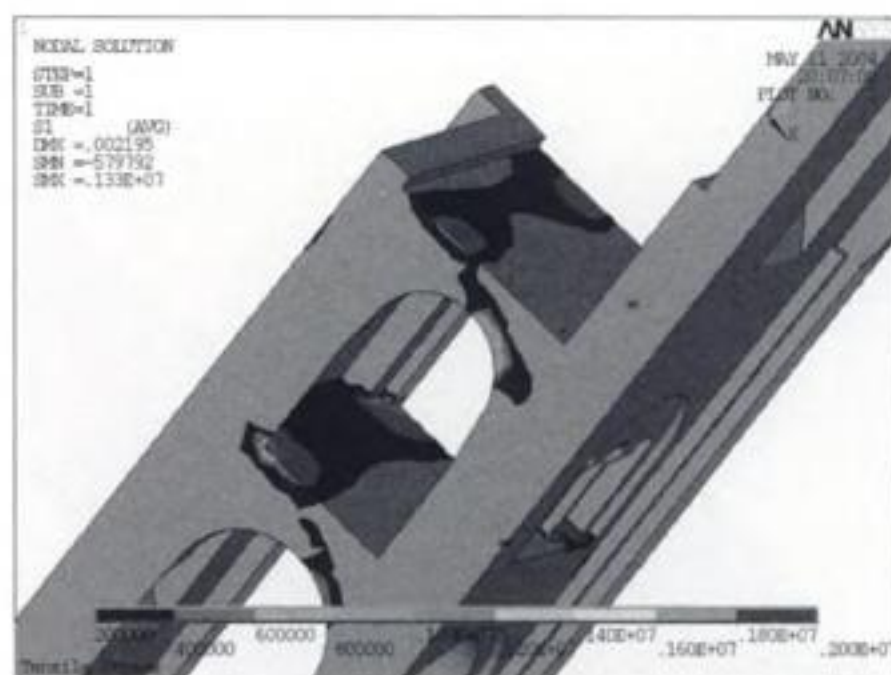


Figure 11. Tensile stresses in Leeward gallery vault extrados and floor without construction sequence effects – combined loading.

nodes and 78,762 elements. Computations of stresses and displacements due to combined gravity loading and “worst-case” wind loading on exterior walls, as well as roof wind load, were carried out with the model.

Tensile stresses in the leeward half of the model that do not include the effects of construction sequence are shown in Figures 11–12. They are substantially greater than those in the windward half, which are little changed by the action of the wind.

Tensile stresses (200–600 kPa) in the rear portion of the gallery vault extrados are seen in Figure 11, as are stresses (200–800 kPa) in the rear half of the gallery floor. Figure 12 shows large regions of tensile stress in the gallery transverse arches (200 kPa–1.3 MPa), gallery vault intrados, (200–800 kPa), side aisle transverse arches (200–600 kPa), and side aisle vault intrados (200–400 kPa) Also shown are small regions of tensile stress (200–400 kPa) on the exterior surfaces of the lower pier buttress and rear gallery wall.

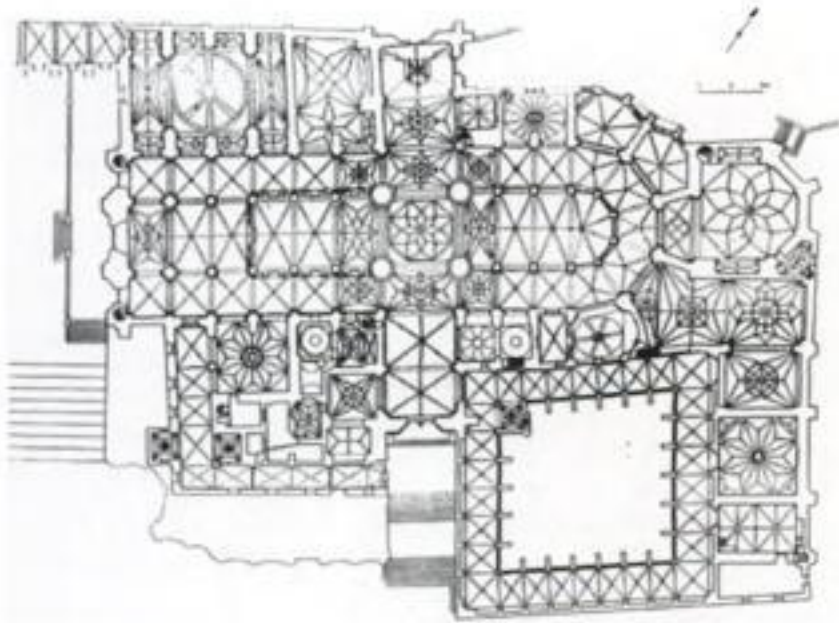


Figure 1. Plan of the Cathedral (Karge 1989).



Figure 2. External aspect of the Cathedral (Andres 1993).

perform a similar retaining function for the transepts as well. A freestanding octagonal tower marks the crossing and is supported on four heavy piers.

The zone of the apse is where most of the construction phases can be identified. A first ring of radial chapels was added after the Renaissance and traces of other lesser chapels can still be seen at the external perimeter of the apse. The entire Cathedral is flanked by chapels, most of which have been accommodated in various configurations and styles between the outer pier buttresses and therefore affect only locally the structural scheme of the Cathedral.

The transept constitutes actually the limit between the two main construction phases of the apse and the nave, as stylistic differences can testify (Karge 1989).



Figure 3. The interior of the Cathedral.

Additionally, a study of the plan (Fig. 1) shows a misalignment between the axes of these two parts, most probably due to the need to re-use the foundations of the pre-existing Romanesque Cathedral.

The crossing tower (Fig. 3) is a focal point of the scheme not only because of its position, volume and decoration but also due to the major reconstruction of the entire crossing area its collapse caused in 1539. The heavy pilasters that were then incorporated provide further stiffness to the ends of the choir and the nave and to some extent compartmentalise structurally the building.

The elevation of the nave follows the typical division into nave arcade, triforium and clerestory (Fig. 4) and the differences with that of the choir are mainly stylistic. The compound piers are formed by a cluster of 8 shafts that join the ribs of the vaults above, providing an aesthetic unity that will be discussed later. The nave arcade is a pointed arch with a not very deep section, which means the *tas-de-charge* ending of the wall above has a large offset (Fig. 4). As a consequence, the blind triforium passage formed behind a single arch span is quite shallow. The top windows occupy the most part of the clerestory but apparently they do not compromise the lateral stability of the wall as will be seen below.

The dimensions of the elevation however depend significantly on the vaulting system. Quadripartite ribbed cross vaults of good quality ashlar masonry were used, following the French type bond of laying the units in courses parallel to the edges. The vaults in the nave (Fig. 5a) span over a 5.3×10.4 m compartment.

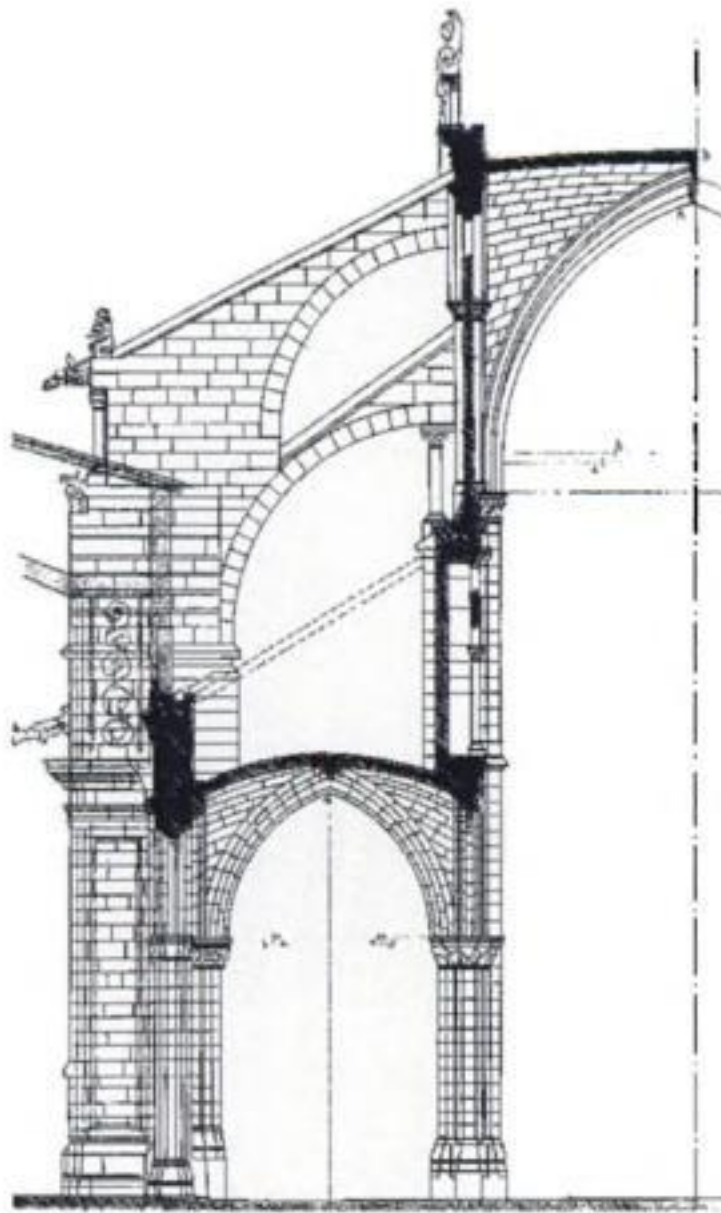


Figure 4. Cross section of the nave – third bay from the façade.



(a) Nave vault



(b) Aisle vault

Figure 5. The main vaulting types of the Cathedral.

The longitudinal vertex is emphasised by a rib that runs along the main axis of the nave, while the vaults next to the transept and the façade are formed by a more complex net of tierceron ribs (Fig. 3). An interesting feature of the transverse vault is that it is stilted, so the corresponding thrusts are applied with an offset from the springing.

The vaults at the aisles span over a 6.3×5.3 m compartment (Fig. 5b). As the transverse vertices however are longer a smooth curve was applied to reduce the deflections.

The transverse thrusts of the vaults are contained using the classic system of double flying buttresses upon large pier buttresses, which are capped by a sculpture functioning as the necessary pinnacle (Bork 1997). At the interior, the springings of the nave vaults meet over a wider area and thrust is spread more efficiently around the head of the rampant arch with the help of rubble filling the conoid pockets behind the spandrel walls.

All the stone units of the Cathedral are made of accurately dressed limestone (caliza de Hontoria) and the joints are very thin and uniform. The load-bearing capacity of the stone masonry appears to be in a very good condition in general. No major faults have been reported in the cathedral itself (Alonso et al 1994) except at the steeples due to an inappropriate use of cast iron reinforcement in 1900 and subsidence at the cloister.

The study of the structural behaviour of the Cathedral can be simplified to that of a typical bay of the nave as there are sufficient transverse structures that function as diaphragms (plates with high in-plane stiffness), isolating parts of the building into areas with an almost uniform stress regime. The third bay from the façade appeared to be quite representative in terms of structural layout and support or even decoration (Fig. 1). The section and plan in Figure 4 were produced from an in-situ survey, critical analysis of existing measured surveys (Karge 1989, MEC 1983, Velazquez Bosco 1885) and the establishment of a system of proportions that could have been used in the original design (Merino 1993, Karge 1989).

The configuration of the bay as originally designed, while ignoring time-dependent deformations, had to be determined in order to understand the inherent stability of the original project. The analysis of the initial state can therefore indicate areas of weakness or high stress concentration and allow certain present signs of distress to be interpreted.

2.2 Construction history

The most important phase in the development of the Cathedral is the foundation and construction of the original design that succeeded a previous Romanesque Cathedral. On 20 July 1221 the foundation stone was laid and with some interruptions and minor changes

- Andrés Ordax, S. 1993. *La Catedral de Burgos, Patrimonio de la Humanidad*. Edileasa, León.
- Azkarate Garai-Olaun, A. 2001. *Catedral de Santa María, Vitoria-Gasteiz: plan director de restauración*. Fundación Catedral Santa María, Vitoria.
- Bilson, J. 1906. Amiens Cathedral and Mr. Goodyear's "refinements" – a criticism. *J. Royal Inst. British Architects*, 3rd series, vol. XIII, No. 15.
- Bork, R., Mark, R., Murray, S. 1997. The openwork flying buttresses of Amiens Cathedral. *J. Soc. Archit. Hist.*, 56(4).
- Croci, G., Viskovic, A., Sabbadini, F. 1995. Some aspects of the structural behaviour of gothic cathedrals. *Spatial structures: heritage, present and future, Proc. IASS Int. Conf.*, Milan.
- Fitchen, J. 1961. *The construction of Gothic Cathedrals*. Clarendon Press, Oxford, UK.
- Hendry, A. W., Sinha, B. P., Davies, S. R. 1997. *Design of masonry structures*. E&FN Spon, London.
- Jagfeld, M. 2000. *Tragverhalten und statische Berechnung gemauerter Gewölbe: Untersuchungen mit der Finite-Elemente-Methode*. Shaker, Aachen.
- Karge, H. 1995. *La catedral de Burgos y la arquitectura del siglo XIII en Francia y España*. Consejería de Cultura y Turismo, Valladolid.
- Martinez y Sanz, M. 1866. *Historia del Templo de la Catedral de Burgos*. Imp. de Anselmo Revilla, Burgos.
- Martinez, J. L., Martín-Caro, J. A., Torrico, J., León, J. 2000. The "Silla de la Reina" tower in the Cathedral of León. *Proc. 12th Int. Brick/Block Masonry Conf.*, Madrid.
- MEC (Ministerio de Educación y Cultura) 1983. Measured survey of the Cathedral of Burgos. Façade elevation, longitudinal section and plan in 1:100.
- Merino de Cáceres, J. M. 1993. Metrología y simetría en las Catedrales de Castilla y León. *Conf. Proc. Medievalismo y neomedievalismo en la arquitectura Española, Las Catedrales de Castilla y León.*, Ávila.
- PINACAL 2004. Database of building stones in the Castille and Leon region. http://www.pinacal.es/datos_tecnicos/iframe/iframe_var2.asp?variedad=Piedra de Hontoria
- Rico Santamaria, M. 1985. *La Catedral de Burgos*. Heraclio Fournier, Vitoria.
- Stalley, R. 1999. *Early medieval architecture*. Oxford History of Art, Oxford University Press, Oxford.
- Theodossopoulos, D., Sinha, B. P., Usmani, A. S. 2003. Case Study of the Failure of a Cross Vault: Church of Holyrood Abbey. *J. Architectural Engrg. Am. Soc. Civil Engineers (ASCE)*, vol. 9(3), pgs. 109–117.
- Torres Balbas, L. 1952. Arquitectura gótica. *Ars hispaniae: Historia universal del arte hispánico*; v.7.
- Velázquez Bosco, R. 1885. Cross section of the zone of the nave. In *Ricardo Velázquez Bosco*, exhibition catalogue, MEC (Ministerio de Educación y Cultura), Madrid 1991.

Comparison of the masonry structures analysis using the co-rotational formulation and a simplified proposal

Antonio Agüero

Universidad Politécnica de Valencia, Departamento de mecánica de los medios continuos y teoría de estructuras, Valencia (España)

Francisco J. Pallarés

Universidad Politécnica de Valencia, Departamento de física, Valencia (España)

ABSTRACT: The purpose of the present article is to compare the analysis of masonry structures using the co-rotational formulation and a simplified proposal to calculate the second order effects. In the simplified proposal the non-linear displacement are obtained as: $\{d_{NL}\} = \{d\} + \{a_1/[P_1/(P-1)]\}\{\phi_1\}$. where $\{d\}$ are the linear displacement, $[K_L]\{d\} = \{F_{ext}\}$, $\{\phi_1\}$ is the buckling mode associated with the smaller buckling load $\{P_1\}$ ($[K_L] + P_1/P \cdot [K_G]\}\{\phi_1\} = \{0\}$). The coefficients $\{a_j\}$ are given by $\{a_j\} = (\{\phi_j\}^T \{F_{ext}\}) / (\{\phi_j\}^T [K_L] \{\phi_j\})$ these can be easily obtained using the orthogonality properties of the buckling modes respect to the linear stiffness matrix $[K_L]$ and the geometric matrix $[K_G]$.

From the various examples presented it can be concluded that the simplified proposal provides very accurate results. Furthermore the time required to solve the analysis as well as the number of parameters used is smaller, this means that it will be easier to control the physical meaning of the results.

1 INTRODUCTION

The objective of the present article is to compare the analysis of masonry structures using the co-rotational formulation and a proposal that calculates the second order effects in a simplified form.

The advantages of this simplified proposal are:

1. Provides very accurate results so this method can be used to perform a nonlinear geometric analysis of the structure.
2. Furthermore the time required to solve the analysis is smaller.
3. As well as the number of parameters used is smaller, so it will be easier to control the physical meaning of the results.

Many practical applications can be performed, for example 4.1.2 could be used to analyse the second order and imperfections effects on a masonry chimney.

Three are the kinematics descriptions currently used to describe the kinematics equations and the equilibrium equations these are: The "Total Lagrangian" (TL), the "Update Lagrangian"(UL) and the "Co-rotational" (CR).

In first place a brief resume of the co-rotational formulation is presented. In second place the proposed

method is described. In third place some examples are used to validate the simplified proposal.

The Co-rotational formulation has its roots in the old idea of splitting the total movement into a rigid solid movement and a purely deformational. Two reference configurations are used: The unloaded and the Co-rotational, this is obtained through a rigid solid movement from the unloaded configuration. The deformation of the element is measured from the Co-rotational configuration and is admitted that the movements referred to such configuration are very small, so it is allowed to apply the linear kinematics. When this hypothesis is not fulfilled, in some element, these must be divided into more. This formulation presents the advantage that uncouples the material nonlinearities from the geometric nonlinearities. The material nonlinearities are taken into account by considering the behaviour with respect to the co-rotational configuration and the geometric nonlinearities are incorporated into the analysis by considering the rigid solid movement of the element axes.

2 CO-ROTATIONAL FORMULATION

The Co-rotational approach has roots on a very old idea: the separation of rigid body and purely

deformational motions in solid and continuum mechanics. It originally arose in theories of small deformations coupled with large rigid motions.

Given the *global displacements*: $(U_1, V_1, W_1, \varphi_{x1}, \varphi_{y1}, \varphi_{z1}, \Phi_1)$ and $(U_2, V_2, W_2, \varphi_{x2}, \varphi_{y2}, \varphi_{z2}, \Phi_2)$; (U, V, W) are movements about axis x, y and z ; $(\varphi_x, \varphi_y, \varphi_z)$ are the total rotations about x, y and z, Φ is the warping where the rotation matrix is given by Rodrigues (1840):

$$[R_T] = e^{[W]} = [I] + \frac{\sin(\varphi)}{\varphi} [W] + \frac{1}{2} \left(\frac{\sin(\varphi/2)}{\varphi/2} \right)^2 \cdot [W]^2$$

$$[I] = \begin{bmatrix} 1 & 0 & 0 \\ 0 & 1 & 0 \\ 0 & 0 & 1 \end{bmatrix}$$

$$[W] = \begin{bmatrix} 0 & -\varphi_z & \varphi_y \\ \varphi_z & 0 & -\varphi_x \\ -\varphi_y & \varphi_x & 0 \end{bmatrix}$$

The rigid solid rotation $[R_{SR}]$ rotates the unloaded local axes $[T_A]$ of the element into the new configuration $[T_B]$:

$$[T_B] = [R_{SR}] \cdot [T_A]$$

The *deformational displacements* $\{\theta_{y1}, \theta_{z1}, \Phi_1, u_2, \theta_{xD}, \theta_{y2}, \theta_{z2}, \Phi_2\}$ can be obtained extracting the rigid solid from the total:

$$[R_D] = [R_T] \cdot [R_{SR}]^{-1} = [R_T] \cdot [R_{SR}]^T$$

As the deformational rotations are small these can be expressed as:

$$[R_D] = [I] + [W] = \begin{bmatrix} 1 & -\theta_z & \theta_y \\ \theta_z & 1 & -\theta_x \\ -\theta_y & \theta_x & 1 \end{bmatrix}$$

$u_2 = L_f - L_0$; where L_f is the final length and L_0 is the initial length.

$(\theta_x, \theta_y, \theta_z)$ are the deformational rotations about x, y and z .

3 DESCRIPTION OF THE PROPOSED METHOD

The method presented in this paper is based on:

1. A linear analysis of the structure used to obtain the primary internal forces and moments.
2. An initial stability analysis used to obtain the secondary internal forces and moments.
3. The orthogonality properties of the buckling modes to simplify the analysis.

3.1 Nonlinear analysis of the structure with geometric imperfections

The first variation of the potential in a double symmetric section is given by:

$$\delta V^* = \int \left[EA u_p' u_p' + Ely w_p'' w_p'' + Elz v_p'' v_p'' + GI_T \theta_p' \theta_p' + Ela \theta_p'' \theta_p'' \right] dx - f_{x1} u_{p1} - f_{y1} v_{p1} - f_{z1} w_{p1} - f_{x2} u_{p2} - f_{y2} v_{p2} - f_{z2} w_{p2} - M_{x1} \theta_{p1} - M_{y1} \theta_{p1} - M_{z1} \theta_{p1} - M_{x2} \theta_{p2} - M_{y2} \theta_{p2} - M_{z2} \theta_{p2} - Bi_1 \phi_{p1} - Bi_2 \phi_{p2} - \int \left[p_x u_p + p_y v_p + p_z w_p + m_x \theta_p \right] dx - \int My \cdot \left[(v' + v') \theta_p' + (\theta_x' + \theta_x') v_p' \right] dx - \int P \cdot \left[(v' + v') v_p' + (w' + w') w_p' + r_o^2 (\theta_x' + \theta_x') \theta_p' \right] dx$$

where the subindex "p" stands for perturbation movements.

Equilibrium equations of the structure:

$$([K_L] + [K_G]) \{d_{NL}\} = \{F_{ext}\} - [K_G] \{d_{imp}\}$$

where $[K_L]$ is the linear stiffness matrix, $[K_G]$ is the geometric stiffness matrix,

Governing equilibrium equations of the beam column:

$$EA \frac{d^2 u}{dx^2} = -P_x$$

$$Ely \frac{d^4 w}{dx^4} + P \frac{d^2 w}{dx^2} = -P \frac{d^2 w_i}{dx^2} + p_z$$

$$Elz \frac{d^4 v}{dx^4} + My \frac{d^2 \theta_x}{dx^2} + P \frac{d^2 v}{dx^2} = -My \frac{d^2 \theta_{xi}}{dx^2} - P \frac{d^2 v_i}{dx^2} + p_y$$

$$(-GI_T + Pr_o^2) \frac{d^2 \theta_x}{dx^2} + My \frac{d^2 v}{dx^2} + Ela \frac{d^4 \theta_x}{dx^4} = -Pr_o^2 \frac{d^2 \theta_{xi}}{dx^2} - My \frac{d^2 v_i}{dx^2} + m_x$$

where P and My are the primary axial and bending moments, A, Iz, Iy, It and Ia are the cross sectional properties area inertia about z, y torsional modulus and warping modulus. (v_i, w_i, θ_{xi}) are the geometric imperfections.

The displacements are given by:

$$u(x) = a_1 + a_2 \cdot x - \frac{P_x}{2 \cdot E \cdot A} x^2$$

$$v(x) = a_3 \cdot \sinh(\mu \cdot x) + a_4 \cdot \cosh(\mu \cdot x) + a_5 \cdot \sinh(\beta \cdot x) + a_6 \cdot \cosh(\beta \cdot x) + a_7 + a_8 \cdot x + \frac{My \cdot m_x + p_y \cdot (G \cdot It - P \cdot r_o^2)}{2 \cdot (P \cdot (G \cdot It - P \cdot r_o^2) + My^2)} x^2 + v_{wi}(x)$$

$$w(x) = a_9 + a_{10} \cdot x + a_{11} \cdot \cos(k \cdot x) + a_{12} \cdot \sin(k \cdot x) + \frac{P_z}{2 \cdot P} x^2 + w_{wi}(x)$$

$$k = \sqrt{\frac{P}{E \cdot Iy}}$$

$$\theta_x(x) = \eta \cdot (a_3 \cdot \sinh(\mu \cdot x) + a_4 \cdot \cosh(\mu \cdot x)) + \psi \cdot (a_5 \cdot \sinh(\beta \cdot x) + a_6 \cdot \cosh(\beta \cdot x)) + a_{13} + a_{14} \cdot x + \frac{My \cdot p_y - m_x \cdot P}{2 \cdot (P \cdot (G \cdot It - P \cdot r_o^2) + My^2)} x^2 + \theta_{wi}(x)$$

$$\mu = \frac{\sqrt{P \cdot (Iz \cdot r_o^2 + Ia)} + \sqrt{4 \cdot Iz \cdot Ia \cdot My^2 + P^2 + 2 \cdot P \cdot \rho \cdot (Ia - Iz \cdot r_o^2) + P^2 \cdot (Iz \cdot r_o^2 \cdot (Iz \cdot r_o^2 - 2 \cdot Ia) + Ia^2)}}{\sqrt{2 \cdot E \cdot Iz \cdot Ia}}$$

$$\beta = \frac{\sqrt{P \cdot (Iz \cdot r_o^2 + Ia)} - \sqrt{4 \cdot Iz \cdot Ia \cdot My^2 + P^2 + 2 \cdot P \cdot \rho \cdot (Ia - Iz \cdot r_o^2) + P^2 \cdot (Iz \cdot r_o^2 \cdot (Iz \cdot r_o^2 - 2 \cdot Ia) + Ia^2)}}{\sqrt{2 \cdot E \cdot Iz \cdot Ia}}$$

$$\eta = -\frac{E \cdot Iz \cdot \mu^2 + P}{My}; \psi = -\frac{E \cdot Iz \cdot \beta^2 + P}{My}$$

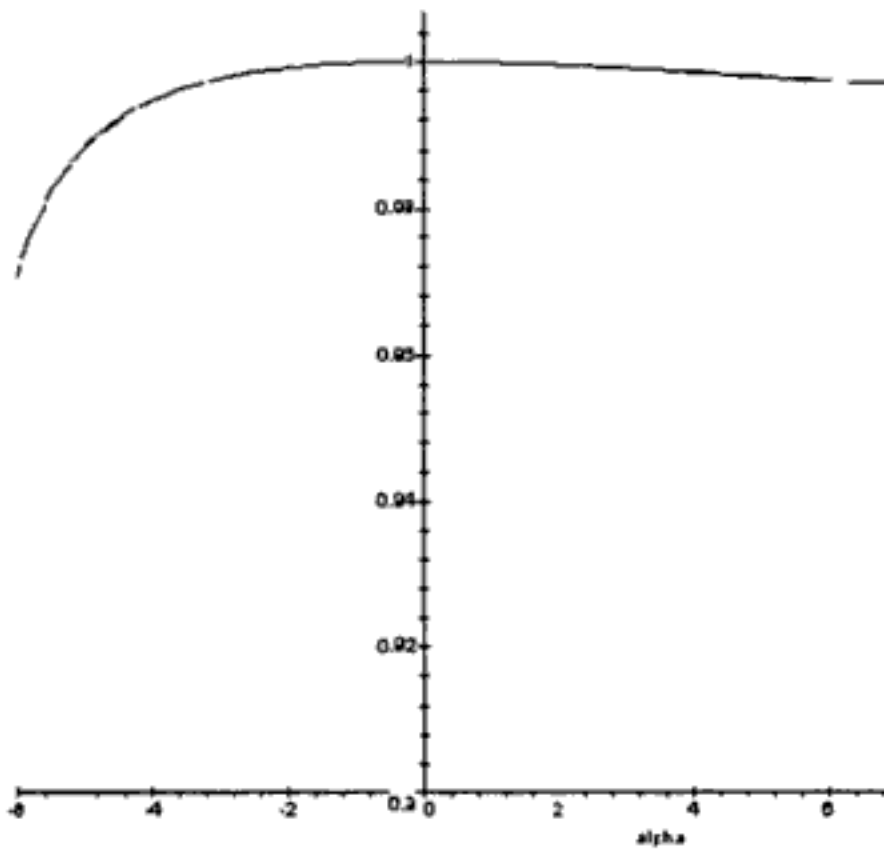


Figure 8. $\frac{\Delta_{aproximado}}{\Delta_{exacta}}$ and $\frac{\Delta_{aproximada_MEF}}{\Delta_{exacta}}$ vs $\alpha = \frac{P \cdot L^2}{E \cdot Iz}$.

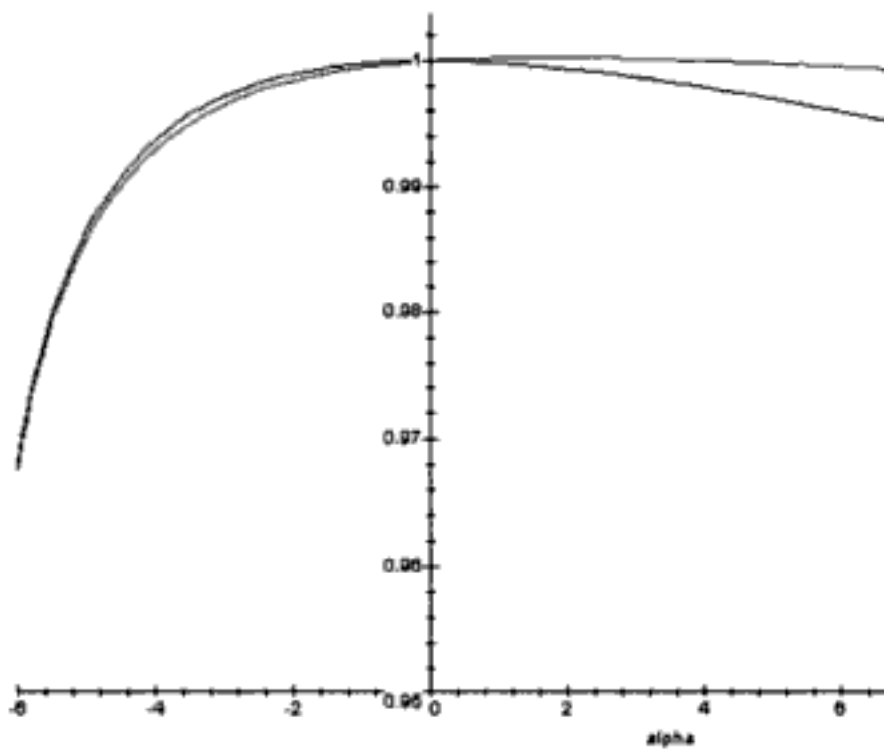


Figure 9. $\frac{\theta_{1aproximado_propuesta}}{\theta_{1exacta}}$ (red) and $\frac{\theta_{1aproximada_MEF}}{\theta_{1exacta}}$ (blue) vs $\alpha = \frac{P \cdot L^2}{E \cdot Iz}$.

The nonlinear “analytical” displacements are:

$$\{\Delta \theta_1 \theta_2\} = \frac{-H \cdot L^2}{2(P \cdot L^2(6+s) - E \cdot Iz(s^2(1-c^2) + 12s(1+c)))} \{(s+6)L - s(1+c) - s(1+c)\}$$

5 CONCLUSIONS

From the examples presented can be concluded that the simplified proposal provides very accurate results so this method can be used to perform a nonlinear geometric analysis of the structure. Furthermore the time required to solve the analysis as well as the number of parameters used is smaller, this means that it will be easier to control the physical meaning of the results.

REFERENCES

- Chen, W.F. & Atsuta. “Theory of beam columns Vol. 2; Space behaviour and design”. Mc Graw Hill, U.S.A. 1976.
- Crisfield, M.A., “Non-linear finite element analysis of solids and structures”, volume 2, John Wiley and Sons. 1997.
- Culver, C.G. “Initial imperfections in Biaxial Bending Equations”. Journal of the structural Division. ASCE. Vol. 92, No ST2 Proc. Paper 4772, April, pp. 63–83. (1966a).
- Mendola, L.L. (1997) “Influence of nonlinear constitutive law on masonry pier stability”. Journal of structural engineering, ASCE, pp. 1303–1311.
- Mendola et al. (1995) “Stability of masonry walls subjected to seismic transverse forces”. Journal of structural engineering, 121 (11), pp. 1581–1587.
- Trahair, N.S. “Flexural-torsional buckling of structures”. E&FN SPON. (1993).

Analysis of masonry structures by discrete finite element method

Iraj H.P. Mamaghani

Department of Civil Engineering, University of North Dakota, Grand Forks, North Dakota, USA

ABSTRACT: Masonry structures are comprised of a finite number of distinct interacting blocks that have a length scale relatively comparable with the structure of interest. Therefore, they are ideal candidates for modeling as discrete systems instead of modeling them as continuum systems. The discrete finite element method (DFEM) developed by the author to model discontinuum media consisting of blocks of arbitrary shapes is adopted in the static and dynamic analysis of masonry structures. The developed DFEM is based on the principles of the finite element method incorporating contact elements. DFEM considers blocks as sub-domains and represents them by solid elements. Contact elements, which are far superior to joint or interface elements, are used to model the block interactions such as sliding or separation. In this study, first the DFEM is briefly reviewed. Then, through some typical illustrative examples, the applicability of the DFEM to analysis of masonry structures, such as arches, towers, and walls, are examined and discussed.

1 INSTRUCTION

Blocky structures are the primary engineering structures that human beings have designed. Most of the historical structures, which are found all over the world, are this type of structure. They were built for different purposes such as flood prevention, road bridges, gravity dams, defense, castles, slope stabilization, and so on. Examples of such structures are shown in Figure 1.

Because of modern civilization and land problems there is a need for demolishing some of them and replacing them by modern structures. On the other hand, it will be quite necessary to preserve some of these structures, which are historically valuable. Thus, analysis of these structures and, if required, repairing and reinforcing them against failure, has paramount importance. Therefore, a well-defined numerical analysis method for these kinds of structures is needed.

Analysis of masonry structures has been receiving a particular interest among civil engineers and rock mechanics. In recent years, several techniques have been developed to analyze rock masses consisting of distinct blocks in the field of rock mechanics. A comprehensive review of these techniques was presented by Kawamoto and Aydan (1999). The limiting equilibrium analysis by Hoek and Bray (1977) and Aydan et al. (1989) and some numerical analysis methods such as the finite element method (FEM) with joint or interface element by, among others, Goodman et al. (1968),

distinct element method (DEM) by Cundall (1971), and discontinuities deformation analysis (DDA) by Shi (1988) can be accounted for. In spite of all these techniques, it is difficult to say that a unique technique that guarantees satisfactory results is developed. Although DEM and DDA can be used for static and dynamic analyses of discontinuum media, the treatment of rate-dependent behavior of materials in these methods is nothing to do with the actual ones. For example, DEM introduces a forced damping to suppress oscillations. DDA adopts very large time steps so that artificial damping occurs as a result of numerical integration.

Mamaghani and Aydan proposed the discrete finite element method (DFEM), which is based on the principles of the finite element method for analysis of blocky systems under static and dynamic loading (Mamaghani 1993, Mamaghani et al. 1994, 1999). It consists of a mechanical model to represent the deformable blocks and contact models that specify the interaction among them. In the DFEM, a visco-elastic constitutive law for linear behavior and a visco-elasto-plastic constitutive law for nonlinear behavior of blocks and contacts are used together with the updated Lagrangian scheme. The DFEM can handle large block motions within the framework of the finite element method. In this paper, first the modeling of masonry structures discontinuities and DFEM formulation are briefly presented. Then, the applicability of the DFEM to static and dynamic analysis of masonry structures are checked out and discussed.

3 DISCRETE FINITE ELEMENT METHOD (DFEM)

The developed DFEM, in analyzing and assessing the stability of rock block systems such as masonry structures, is based on the finite element method. It consists of a mechanical model to represent the deformable blocks and contact models that specify the interaction among them. The deformation of blocks is assumed to be small unless they are allowed to rupture. Small displacement theory is applied to the deformable blocks while blocks can take finite displacement. The large deformation of blocky systems is associated with the separation, translation, and rotation of blocks. Blocks are polygons with an arbitrary number of sides, which are in contact with the neighboring blocks and are idealized as a single or multiple finite elements. Block contacts are represented by a contact element.

3.1 Equations of motion

The equations of motion employing the principle of virtual work and conventional finite element discretization procedures are obtained for a typical finite element, in a condensed form, as follows (Mamaghani 1993, Mamaghani et al. 1994):

$$M\ddot{U} + C\dot{U} + KU = F \quad (5)$$

where,

$$M = \int_{\Omega_e} \rho N^T N d\Omega \quad (6)$$

$$C = \int_{\Omega_e} B^T D_v B d\Omega \quad (7)$$

$$K = \int_{\Omega_e} B^T D_e B d\Omega \quad (8)$$

$$F = \int_{\Omega_e} N^T b d\Omega + \int_{\Gamma_e} \bar{N}^T t d\Gamma \quad (9)$$

3.2 Modeling of contacts

The contact element is used to model contacts of blocks in masonry structure discontinuities. Let us consider a two-noded element lm in two-dimensional space and take two coordinate systems oxy and $o'x'y'$ as shown in Figure 3. Assuming that, the strain component $\varepsilon_{y'y'}$ is negligible; the remaining strain components take the following form:

$$\varepsilon_{x'x'} = \frac{\partial u'}{\partial x'}, \quad \gamma_{x'y'} = \frac{\partial v'}{\partial x'} \quad (10)$$

Let us assume that the shape functions are linear such that:

$$N_l = 0.5(1 - \xi), \quad N_m = 0.5(1 + \xi) \quad (11)$$

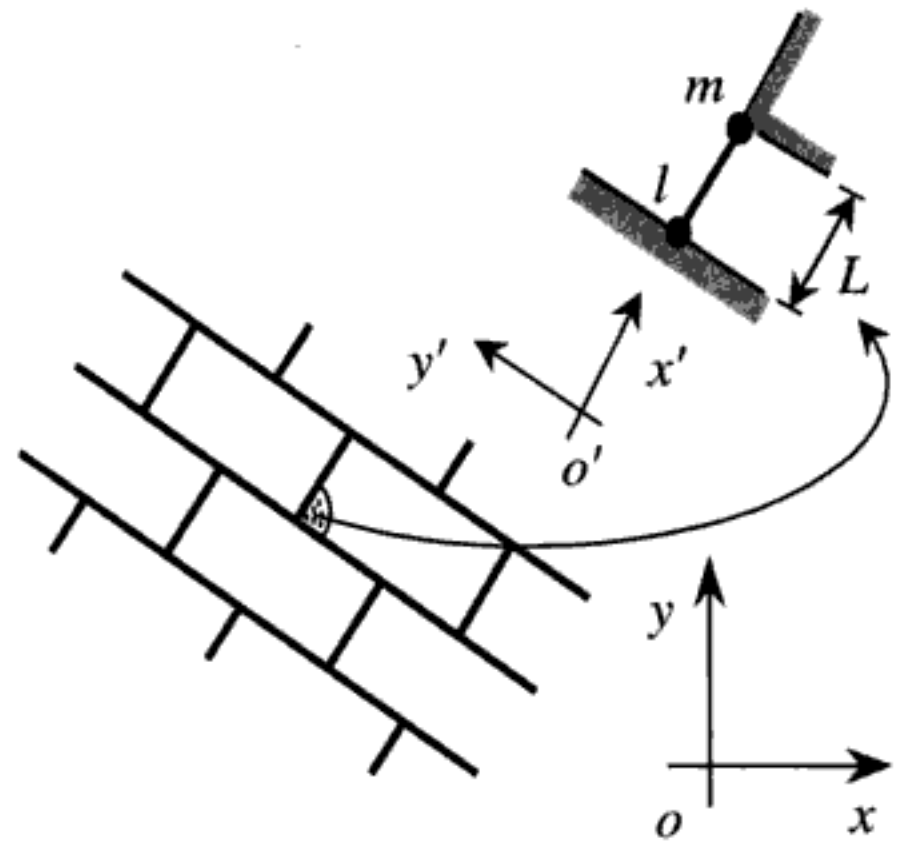


Figure 3. Modeling blocks contact.

where $\xi = (-2x' + x'_l + x'_m)/L$, and $L = x'_m - x'_l$. Then, the relation between the strains and nodal displacements becomes:

$$\begin{Bmatrix} \varepsilon_{x'x'} \\ \gamma_{x'y'} \end{Bmatrix} = \frac{1}{L} \begin{bmatrix} -1 & 0 & 1 & 0 \\ 0 & -1 & 0 & 1 \end{bmatrix} \begin{Bmatrix} U'_l \\ V'_l \\ U'_m \\ V'_m \end{Bmatrix} \quad (12)$$

Thus, the stiffness matrix of contact element in the local coordinate system is explicitly obtained as:

$$K' = \begin{bmatrix} k'_n & 0 & -k'_n & 0 \\ 0 & k'_s & 0 & -k'_s \\ -k'_n & 0 & k'_n & 0 \\ 0 & -k'_s & 0 & k'_s \end{bmatrix} \quad (13)$$

in which,

$$k'_n = E_n \cdot \frac{A_c}{x'_m - x'_l} \quad (14)$$

$$k'_s = G_s \cdot \frac{A_c}{x'_m - x'_l} \quad (15)$$

Here, A_c is the contact area; E_n and G_s are normal and shear elastic moduli of discontinuity, respectively. The stiffness matrix in the local coordinate system is then transformed to the stiffness matrix in the global coordinate system by the following relationship:

$$K = T^T K' T \quad (16)$$

by 50 times to make more visible the mode of failure (deformed configuration) from the initial configuration. Figure 7c shows that the arch is slid at the base at the time step 23 under Acc. No. 1 and the crown blocks of the arch starts to fall apart while the side columns are still stable. Figure 7c shows that, under Acc. No. 1 at the time step 50, the arching action disappears and the crown blocks fall apart. The columns slide relative to the base and they tend to topple in two opposite directions. The blocks tend to separate within the side columns, see Figure 7c for the time step 50.

Figure 7d shows that, under Acc. No. 2 at the time step 23, there is no slide at the base of the arch while the crown blocks are separated and tend to fall apart. At the time step 23, the side columns of the arch exhibit relatively stable behavior under Acc. No. 2 as compared with the Acc. No. 1, Figures 7c and d. However, under Acc. No. 2 at the time step 50 (10 seconds), the side columns of the arch slide at the base and the arching action disappears while the blocks start to fall apart.

As expected, the toppling (failure) modes of the side columns of the arch differ depending on the nature of the imposed form of acceleration waves, as shown in Figures 7c and 7d for the time step 50.

Figure 7b shows the displacement responses with time of a nodal point at the top most-right corner of the arch corresponding to the Acc. No. 1 and Acc. No. 2. The results in Figure 7b indicates that, as expected, the displacement of the side column of the arch with time is much severe under the Acc. No. 1 as compared with the Acc. No. 2, especially in the early stage of loading. Figures 7c and 7d show that, under both of the imposed acceleration waves, the reaction of the toppled columns forces the crown block to move upward. This is because of the geometrically symmetric configuration of the structure and outward inclination of the crown block contact interfaces at the center of symmetry; Figure 7a. As can be realized by examining the displacement response curves in Figure 7b, the real value of the upward displacement is very small as compared with the dimension of the crown block. It should

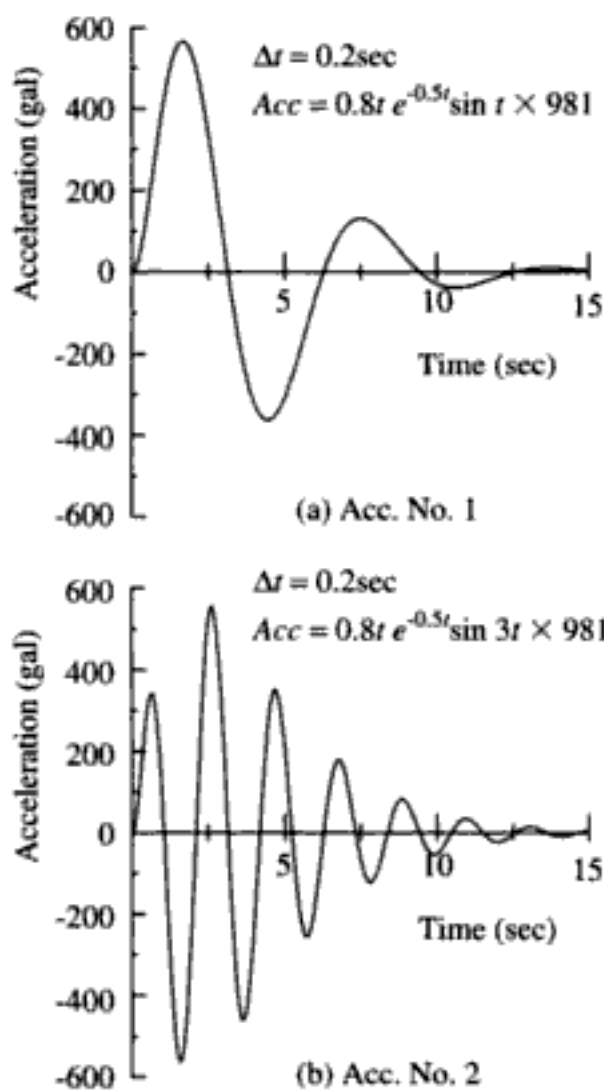


Figure 6. Lateral acceleration waves acting on foundation.

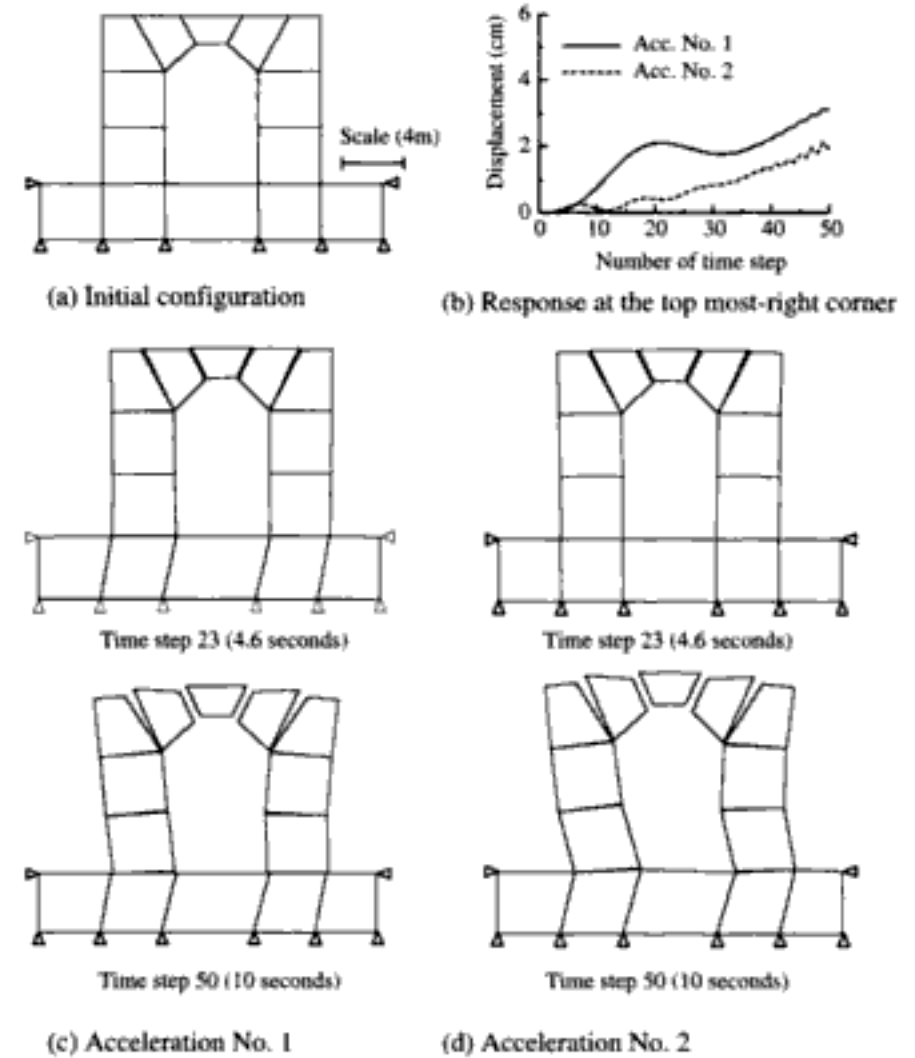


Figure 7. Initial and deformed configurations and displacement response with time of the arch.

Table 2. Material properties of rock blocks and contacts.

Properties of blocks					Properties of contacts					
λ (MPa)	μ (MPa)	λ^* (MPa · s)	μ^* (MPa · s)	ρ (kN/m^3)	E_n (MPa)	G_s (MPa)	E_n^* (MPa · s)	G_s^* (MPa · s)	h (mm)	φ (°)
30	30	30	30	25	5.0	2.5	5.0	2.5	5	35

be noticed that in Figures 7c and d, the displacement is amplified using the illustration scale factor (50 times the actual scale) to make the failure mode of the whole structure more visible.

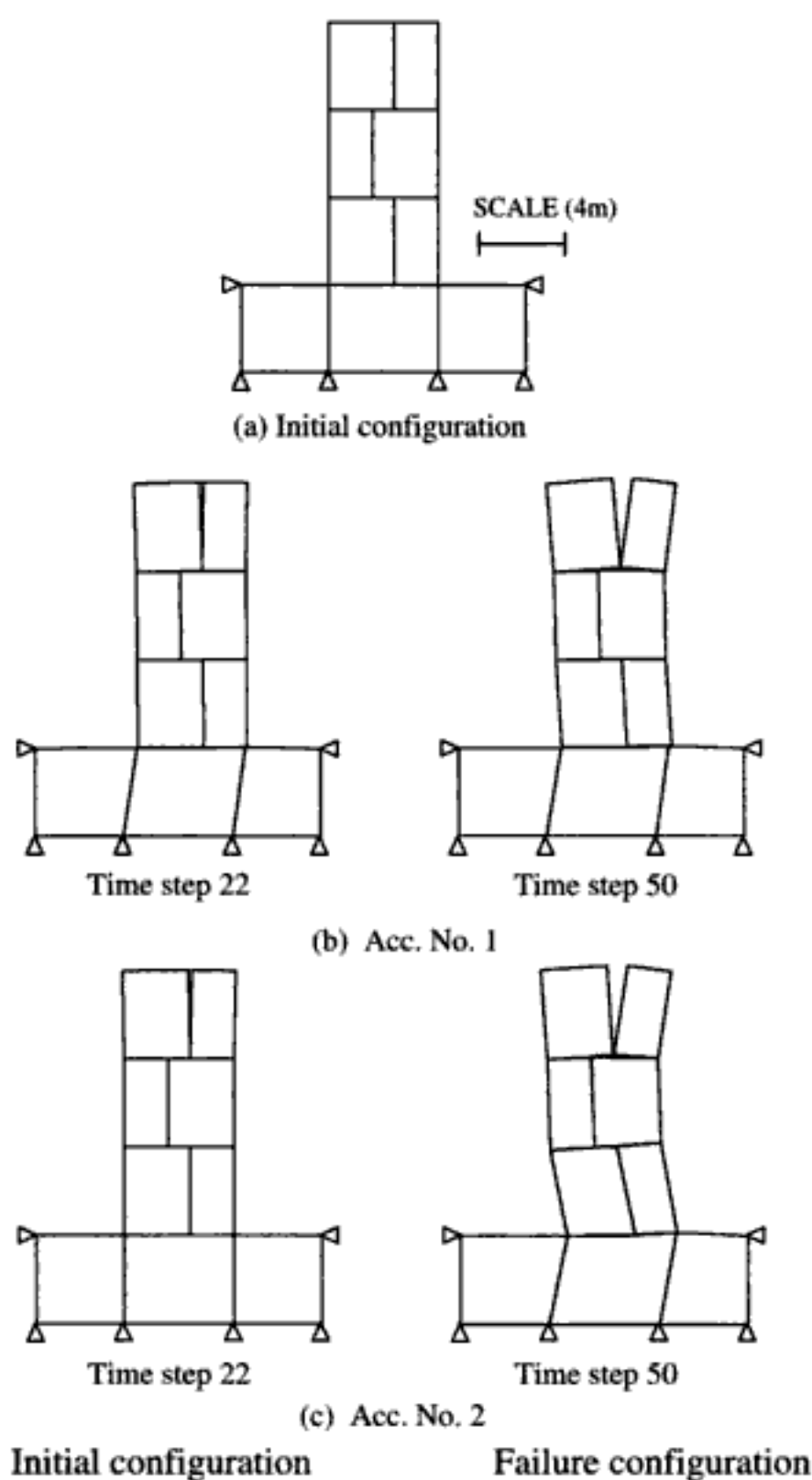


Figure 8. Initial and deformed configuration of the masonry tower.

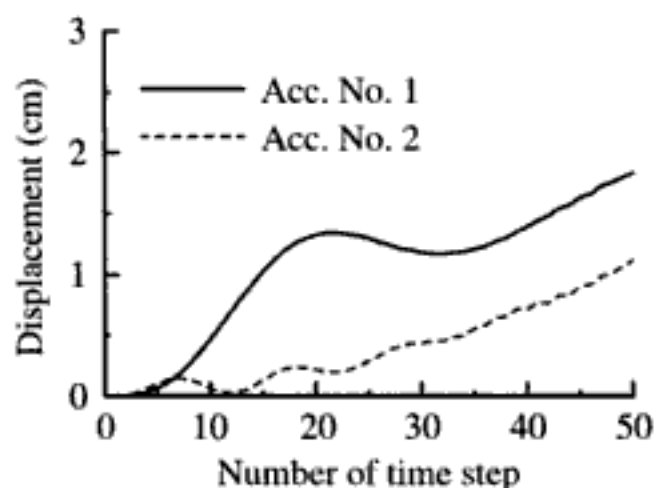


Figure 9. Displacement response with time at the top most-right corner of the tower.

4.4 Dynamic analysis of masonry towers

Figures 8a, 8b, and 8c show the initial and deformed configurations of a masonry tower at the time steps of 22 (4.4 seconds) and 50 (10 seconds) corresponding to the Acc. No. 1 and Acc. No. 2, respectively. Figure 8b shows that when the tower is subjected to Acc. No. 1, there is a sliding at the base of the tower at time step 22 and the most upper blocks start to detach at the top of the tower. At time step 50, relative sliding and separation occurs along block contacts and the two most upper blocks tend to topple in two opposite directions. Figure 8c shows that, under Acc. No. 2, there is no sliding of the tower at the base while the most upper blocks of the tower are separated and tend to topple at time step 22. At time step 50, there is a relative slide at the base of the tower and blocks are slid and detached along block contacts. Figure 9 shows the displacement response versus the number of time step for a nodal point at the top most right corner of the tower (monitoring node) corresponding with both of the imposed acceleration waves. As shown in Figure 9, the toppling of the top most-right block of the tower is more severe under Acc. No. 1 as compared with the Acc. No. 2.

Comparison of the responses in Figures 8 and 9 also show that the failure mode of the tower depends on the nature of the imposed acceleration wave. The tower shows relatively stable behavior under Acc. No. 2 with a small period as compared with that of the Acc. No. 1 with a large period at the time step 22. However, the tower does not return to its original position and ceases to be stable at the end of shaking under both of the imposed forms of the acceleration waves, see Figure 8 for time step 50. It is worth noting that, as shown in Figure 8, the response of the tower is quite similar to those may be expected in actual earthquakes.

Although the examples discussed above are very simple structures, they illustrate the fundamental features of the developed DFEM. It is also possible to consider and analyze more complicated masonry structures by the DFEM. Nevertheless, more experimental information is required on the constitutive parameters of blocks and contacts before conducting the analysis of such structures.

5 CONCLUSIONS

This paper was concerned with static and dynamic analysis of masonry structures which are comprised of a finite number of distinct, interacting blocks that have the length scale relatively comparable with the structure of interest, using the discrete finite element method (DFEM) recently developed by the author. The DFEM is based on the principles of the finite element method incorporating contact elements. It considers blocks as sub-domains and represents them by solid elements. Contact elements are used to model the

block interactions such as sliding or separation. The DFEM calculates displacements at the joints as well as deformation within the blocks, which can be used to follow the processes of the failure mechanism of slopes under static as well as dynamic loading. Through some typical illustrative examples, the applicability of the DFEM to static and dynamic analysis of masonry structures were investigated and discussed. It has been shown that the DFEM is capable of simulating large displacement of blocky systems. It was found that the DFEM is a promising method for studying behavior of masonry structures under static and dynamic loading. However, the hyperbolic scheme of the DFEM is still in its formative phase for which both experiments on viscous characteristics of blocks and contacts, as well as a numerically stable time-discretisation scheme, are felt to be necessary.

REFERENCES

- Aydan, Ö., Mamaghani, I.H.P. & Kawamoto, T. 1996. Applications of discrete finite element method (DFEM) to rock engineering structures. *NARMS'96, 2nd North American Rock Mechanics Symposium Tools and Techniques in Rock Mechanics*, Canada, pp. 2039–2046.
- Aydan, Ö., Shimizu, Y. & Ichikawa, Y. 1989. The effective failure modes and stability of slopes in rock mass with two discontinuity sets. *Rock Mechanics and Rock Engineering*, Vol. 22(3), pp. 163–188.
- Cundall, P.A. 1971. A computer model for simulating progressive large-scale movements in blocky rock systems. *Proc. Int. Symp. on Rock Fracture*, II-8, Nancy, France.
- Goodman, R.E., Taylor, R. & Brekke, T.L. 1968. A model for the mechanics of jointed rock. *J. of Soil Mech. and Found. Eng. Div.*, ASCE, SM3, Vol. 94(3), pp. 637–659.
- Hoek, E. & Bray, J.W. 1977. Rock slope engineering. *The Institution of Mining and Metallurgy*, Revised Second Edition, London.
- Kawamoto, T. & Aydan, Ö. 1999. A review of numerical analysis of tunnels in discontinuous rock masses. *Int. J. Numer. Anal. Meth. Geomech.*, 23, pp. 1377–1391.
- Mamaghani, I.H.P. 1993. Numerical analysis for stability of a system of rock blocks. *Master Thesis*. Department of Civil Engineering, Nagoya University, Nagoya, Japan.
- Mamaghani, I.H.P. & Aydan, Ö. 2000. Stability analysis of slopes by discrete finite element method. *GeoEng 2000*, November 19–24, Melbourne, Australia.
- Mamaghani, I.H.P., Aydan, Ö. & Kajikawa, Y. 1999. Analysis of masonry structures under static and dynamic loading by discrete finite element method. *Journal of Structural Mechanics and Earthquake Engineering*. Japan Society of Civil Engineers, JSCE, No. 626/I-48, pp. 1–12.
- Mamaghani, I.H.P., Baba, S., Aydan, Ö. & Shimizu, Y. 1994. Discrete finite element method for blocky systems. *Proc. of the Eighth Int. Conf. on Computer Methods and Advances in Geomechanics (IACMAG)*, Morgantown, USA, Vol. 1, pp. 843–850.
- Shi, G.H. 1988. Discontinuous deformation analysis: a new numerical model for the statics and dynamics of block system. *PhD Thesis*. Dept. of Civil Engineering, University of California, Berkeley.
- Tokashiki, N., Aydan, Ö., Shimizu, Y.T., & Mamaghani, I.H.P. 2001. A stability analysis of masonry walls by discrete finite element method (DFEM). *Proc. of the 10th Int. Conf. on Computer Methods and Advances in Geomechanics (IACMAG'01)*, 7-12 January 2001, Tucson, Arizona, USA.

Why does the Endless Column seem everlasting?

C.A. Safta

University Politehnica of Bucharest, Romania

ABSTRACT: The paper firstly presents the geometrical data used for shaping the Endless Column, located in Targu-Jiu, Romania, as well as the physical data about site and environment. Recent investigations in the subsonic wind tunnel have shown the influence of Column shape on wind flow around it. The influence of Geometry on Kármán's alternate vortices and wind gusts was further analytically searched. Finally, the virtual analysis was devoted to wind flow around horizontal and vertical cross-sections. The answer to title question is affirmative, indeed.

1 INTRODUCTION

The dynamic parameters of the Endless Column were measured in situ at Targu Jiu only in 1984 after 47 years since its erection, with the participation of Column builder Stefan Georgescu-Gorjan. It was found that the period of natural oscillations in fundamental mode is near 2 seconds (Georgescu 2004). This large value is typical for very flexible structures. The History of Science is mentioning many damages caused to similar constructions like submarine periscopes, industrial smoke stacks and gas pipelines. The failure of Tacoma suspension bridge near Seattle in 1940 is also due to its high flexibility (Yamada 2004). However, the Endless Column by its motionless standing, has never drawn attention on any danger coming from wind or earthquakes. Only after the maintenance works carried out between 1996 and 2000 some questions about its stability to wind were raised. On the basis of some laboratory tests performed in Italy it was established that the Column has a reliable behaviour under wind actions (Lungu 2002). On the other hand by a comparative study and theoretical analysis it was found that the Column is aeroelastically stable (Safta 2002a, b). Subsequent studies have shown that the Column is not only stable but even aeroelastically indifferent (Safta 2003). Finally, after some investigations on a model in wind tunnel, new data have been brought for supporting the aeroelastic stability of the Column (Safta 2004).

There are many column-like monuments but the Column in Targu Jiu is the only endless in the world. Its infinity is not an adjective resulting from a mystic rich imagination, a legend or a fairy tale. The endlessness of the Column is a reality based on the laws of automorphism as it was topologically demonstrated

(Sofronie 2001, 2003). Brancusi succeeded this performance with the aid of Geometry. By combining the geometrical properties of his modules he bridged according to his own statement the earth with the sky. Particularly, with his masterpiece it seems Brancusi either defined the wind or on the contrary succeeded to tame and control its force. The paper tries to disclose the influence of Column shape on wind power.

2 GEOMETRY AND SHAPE

The Endless Column in Targu Jiu is composed by cast iron modules threaded along a central steel pillar. Each module is shaped as a decahedron with eight identical isosceles trapeziums as equally inclined faces and two identical squares as bases (Fig. 1).

The decahedron has five symmetry plans, four vertical and one horizontal. Since the eight faces are slightly swelled out the inclined sides of the hexagons in the four vertical plans of symmetry are a little curved. Due to the existing horizontal plan of symmetry at the middle of module height, the decahedron shaped as above can be regarded as composed by two congruent hexahedra with common squared bases. Both types of polyhedral shapes satisfy the topological relationship

$$F + V = E + C \quad (1)$$

where F = number of faces; V = number of vertices; E = number of edges; and $C = 2$ is Euler's characteristic.

As metrical relations, the sides of the two base squares have 45 cm, the sides of middle square have 90 cm while the height of each hexahedron is 90 cm that means the total height of decahedral module is

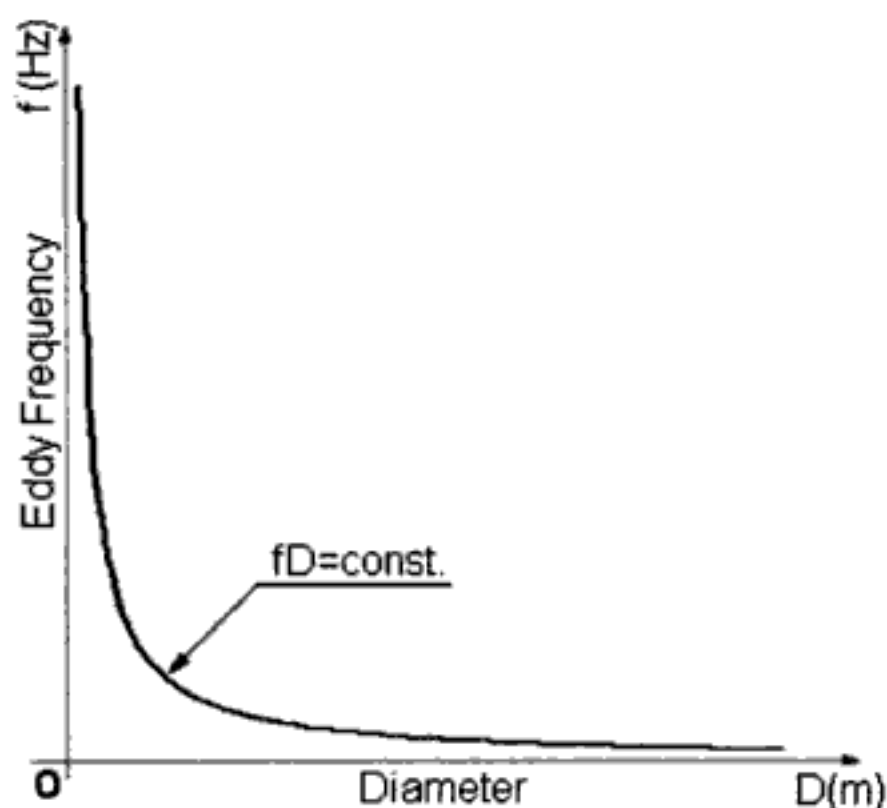


Figure 7. Strouhal's hyperbola.



Figure 8. Elastic structure.

6 GEOMETRY AND GUST ACTION

The gust action is a transient phenomenon of short duration. Assume a gust force $Q(t)$ applied on the top of Column producing a horizontal displacement $u(t)$, (Fig. 8).

By using again the dynamic equilibrium of the disturbing force $Q(t)$ with the inertia force F_i and the elastic force F_e , one obtains

$$F_i + F_e = Q(t). \quad (12)$$

Explicitly the equation of motion becomes

$$m \frac{d^2 u}{dt^2} + ku = Q(t) \quad (13)$$

or

$$\frac{d^2 u}{dt^2} + \omega^2 u = q(t) \quad (14)$$

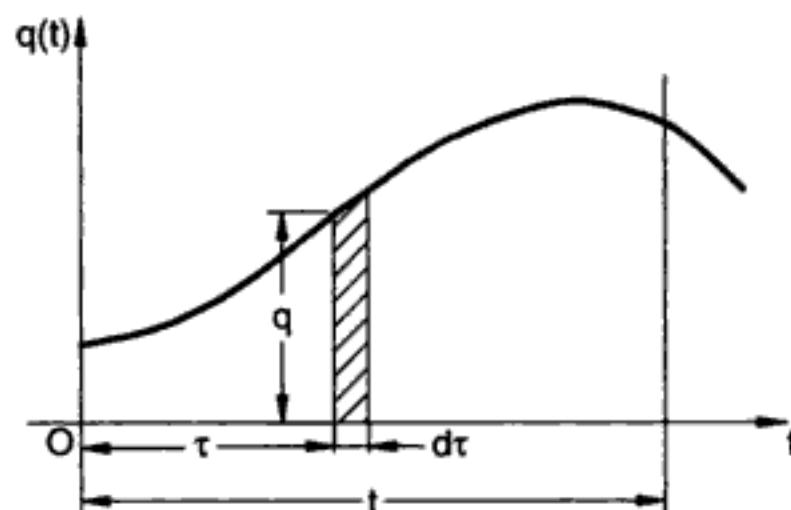


Figure 9. Gust impulse.

where $m = W/g$ mass of oscillating structure; W = weight of structure; g = gravity acceleration; $k = 3EI/l^3$ spring constant; $\omega^2 = k/m$ natural circular frequency; and $q = Q/m$ gust force per unit of mass.

Since at the initial moment, $t=0$, the structure is at rest, i.e. $u=0$, but with an initial velocity v_0 , equation (14) assumes the solution

$$u = \frac{v_0}{\omega} \sin \omega t. \quad (15)$$

To calculate this displacement, the continuous action of the force q is represented by a series of elementary impulses (Fig. 9).

As a result of the unit impulse $dv_0 = q d\tau$ occurring at the instant τ , the structure experiences an increment of velocity

$$du = \frac{dv_0}{\omega} \sin \omega(t - \tau)$$

or replacing dv_0 with its value $q d\tau$ one finds

$$du = \frac{q}{\omega} \sin \omega(t - \tau) d\tau \quad (16)$$

Applying the superposition principle over the whole interval of time t , one obtains the dynamic response of structure to gust action

$$u = \frac{1}{\omega} \int_0^t q \sin \omega(t - \tau) d\tau. \quad (17)$$

This is Duhamel's convolution integral, firstly solved in 1934 by M.A. Biot (Kármán & Biot 1940). It contains both free and forced oscillations produced by the disturbing force $Q(t)$. A realistic representation of gust force is given by the function

$$Q(t) = Cte^{-at} \quad (18)$$

where C and a are constants that can be chosen so as to give the desired strength Q_{\max} of the structure at

- Safta, C.A. 2002a. Device for preventing the oscillations induced by wind in metallic stacks and gas pipelines. Bucharest: Romanian Patent Office OSIM No. A 00928.
- Safta, C.A. 2002b. The Aeroelastic Stability of the Column. *Bulletin of the Technical University of Civil Engineering Bucharest*, 51(1): 51–55.
- Safta, C.A. 2003. Aeroelastic Indifference of the Endless Column. *Proc. of the 28th Congress of the American-Romanian Academy*. Targu Jiu, Romania, 2–8 June 2003, Paper EGAM #10.
- Safta, C.A. 2004. Stability to wind of the Endless Column. *Proc. of the Romanian-Japanese Workshop “Wind Engineering and Cultural Heritage”*, UNESCO Bucharest, Romania, 8 March, 2004. Paper #4.
- Sofronie, R.A. 2001. Brancusi and the obsession of gravity. *Proc. of the International Congress of ICOMOS and UNESCO. Special Session BRANCUSI*. Paris, France, 12 September 2001. Paper #1.
- Sofronie, R.A. 2003. Ideomorphic concept of the Endless Column. *Proc. of the 28th Congress of the American-Romanian Academy*. Targu Jiu, Romania, 2–8 June 2003, Paper HAFA #4.
- Timoshenko, S.P. & Young, D.H. 1965. *Theory of Structures*. New York: McGraw-Hill Book Company Inc.
- Yamada, H. 2004. Wind and Long-Span Bridges. *Proc. of the Romanian-Japanese Workshop “Wind Engineering and Cultural Heritage”*, UNESCO Bucharest, Romania, 8 March 2004. Paper #1.

Structural analysis of Küçük Ayasofya Mosque in İstanbul

M. Massanas, P. Roca & M. Cervera
Universitat Politècnica de Catalunya, Barcelona, Spain

G. Arun
Yıldız Teknik Üniversitesi, İstanbul, Turkey

ABSTRACT: The paper describes a preliminary structural analysis of Küçük Ayasofya Mosque in İstanbul carried out by means of a continuum damage formulation specifically developed for the study of large buildings made of brittle material such as masonry. A discussion of the results obtained in the simulation of different actions such as gravity loads, differential settlements and earthquake, is presented.

1 INTRODUCTION

The Küçük Ayasofya Mosque, the former Church of Sts. Sergius and Bacchus, is a Byzantine construction built during 527–536 A.D. in İstanbul. It consists of an octagonal nave enlarged by four semi-circular niches surrounded by a two-storey ambulatory. The octagonal nave is covered by a large ribbed dome consisting of 16 shell sectors combining alternately concave and flat surfaces.

The building is showing significant structural disorders such as large deformations at the piers and at the dome and important cracks across the vertical walls and dome surfaces. Due to its historical interest—together with the concern generated by its current damaged condition – Küçük Ayasofya has deserved attention from different researchers and some studies are now available (Özsen and Bairam, 1995, on the structure, Aköz and Yüzer, 1995, on material properties, Arun, 2001, on survey, Yüzügüllü and Durukal, 1997, on the effects of train traffic, or Alkiş et al., 2003 on the deformations of the building). However, a more detailed and general assessment is still needed in order to accurately evaluate its structural condition, characterize active processes causing deterioration and define possible repair or strengthening actions. Surveillance carried out during the last years has shown that, although most of the lesions exhibited by the building are very ancient, the opening of some of the cracks is still progressing.

The present paper describes a preliminary structural analysis of Küçük Ayasofya Mosque carried out by means of a formulation based on the mechanics of continuum damage. This formulation was specifically

developed for the study of large buildings made of brittle materials such as masonry and has already been used for the analysis of historical constructions (Roca, 2001).

The study consists of the simulation of different actions (gravity, soil settlements and earthquake) and is aimed at the characterization of their possible effects on the building. The analysis focuses on the possible contribution of such actions to the generation of the main observable lesions. This paper presents preliminary results obtained for a partial model elaborated from the information available on geometry and materials of the building.

2 DESCRIPTION OF THE BUILDING

The construction of the Church of the Sts. Sergius and Bacchus started at the beginning of the Justinian mandate, about the year 527 and was finished before the year 536. It was built as the basilique of the Palace of Hormisdas, the residence of Justinian in Constantinople as the heir to the throne. The building was placed in an irregular space between the palace and the church of the Sts. Peter and Paul, with which it shared the nartex, atrium and propileum (Krautheimer, 1965). From 1504 on, after the Ottoman conquer of Constantinople, the building has been used as a mosque with the new name of Küçük Ayasofya Camii; except for the West main entrance, of Ottoman style, the rest of the building, the main architectural components of the inner structure (the dome, piers and niches) are original and have only been subject to minor decorative alterations.



Figure 1. Deformation of piers.

The building has experienced a number of accidents across its life, among them the fire of 1758 and numerous important earthquakes. Several parts of the building have been reconstructed due to the destruction caused by the latter, or other possible actions; this is the case of most of the external walls and ambulatories with the exception of some sectors of the North wall.

During 1870–1871 a main railway line was built only a few meters apart from the South-West wall of the building. Later, from 1950 to 1960, the platform of the railway line was elevated to 2.5 m above the ground level of the building; this modification meant the formation of a new embankment in part retained by the South wall itself.

During most of the 20th century (if not during most of the entire life of the building), lack of maintenance has contributed very much to the deterioration of the dome. Water filtration was affecting the dome until a lead cover was provided to the roof in 1970. The roof is currently being restored.

The structural damage shown by the structure of Küçük Ayasofya Mosque (Figs. 1–3) is possibly

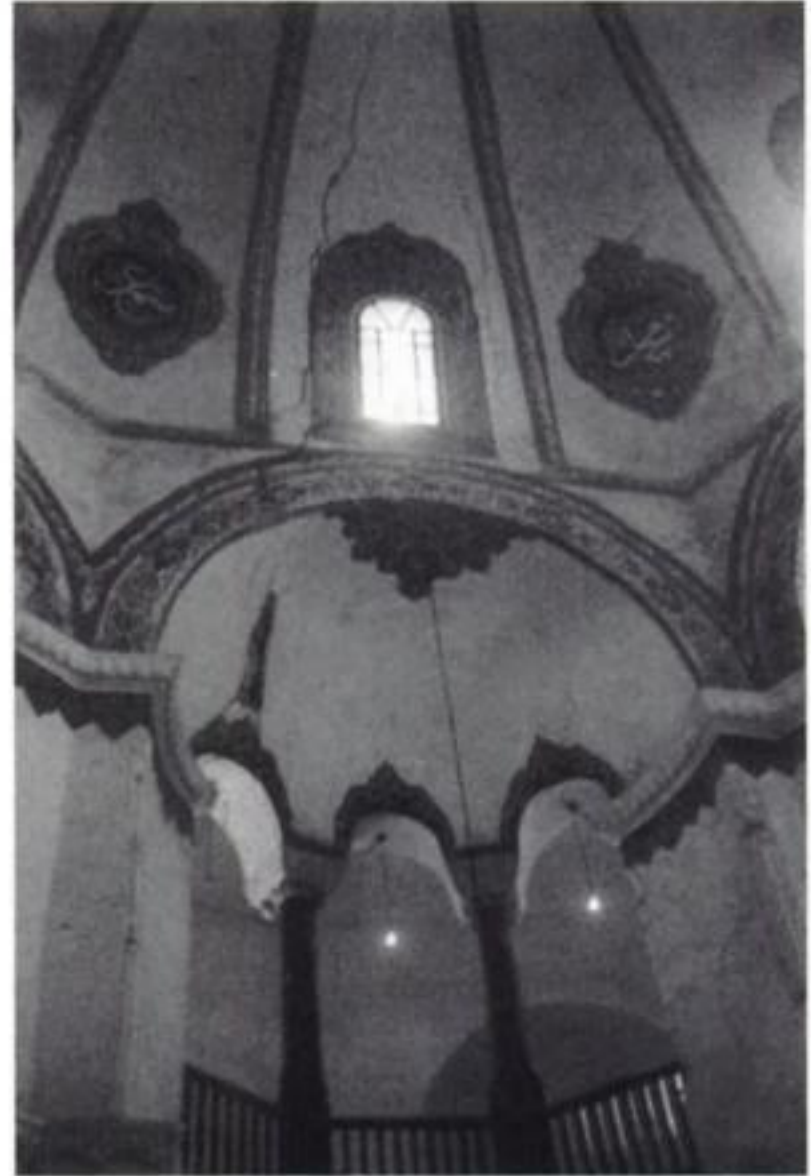


Figure 2. Cracking of the dome and semi-circular spandrels.



Figure 3. View of the interior.

connected to some of the above mentioned facts. Among other existing lesions, important cracks affecting the nave, the semi-circular niches and the ambulatory are observed. Figure 4 describes the main cracks experienced by the dome and the semi-circular spandrels of the South-East quadrant. Five different crack systems (numbered 1 to 5 in Figure 4) can be seen close to the crown of the arch of the apse (1), along the shell sector over the pier (2), in the semi-circular spandrel of the niche and then across the upper shell sector (3),

Finally, the damage indices d^+ and d^- are explicitly defined in terms of the corresponding current values of the damage thresholds, so that they are monotonically increasing functions such that $0 \leq d^\pm (r^\pm) \leq 1$. These damage functions can be expressed according to the behaviour that is desired to simulate. For example, linear hardening/softening behaviour would have the following expression:

$$d^\pm (r^\pm) = (1 - H_d^\pm) \left(1 - \frac{r_0^\pm}{r^\pm} \right) \quad (5)$$

where H_d^\pm is a constant, defined as a material property, different for tension and compression. In case of softening ($H_d^\pm < 0$), this parameter must be related to the fracture energy G_f of the material, and to the characteristic length of the finite element mesh, to ensure mesh-size objective results. More details on the formulation can be found in Cervera (2003).

4 STRUCTURAL MODEL

It must be noted that the structure does not show perfect lateral symmetry due to the overall irregularity of its plan. Due to this, an accurate analysis would require a complete modelling of the entire building. As a first step, the preliminary study here presented has been carried out on a simpler model consisting of a quadrant of the building (Fig. 5). The South-East quadrant has been selected for this purpose. The model includes 230,000 tetrahedral solid elements with maximum dimension of 0.5 m in walls and dome, 0.4 m in piers and 0.1 m in columns (Fig. 5). All structural elements include at least 4 tetrahedral elements across their minimum dimension.

Based on the information available on the materials, only four different sets of material properties have been defined for, respectively, the stone of the monolithic columns in niches sand ambulatory walls, the stone masonry of the main piers, the brick masonry of vaults and dome and the masonry of walls. The latter consists of brick masonry stiffened with stone blocks of different nature (limestone, argillaceous limestone and travertine) embedded in 4–5 cm thick mortar beds.

A compressive strength (f_c) of 30 N/mm² and a density (γ) of 25 kN/m³ has been defined for the stone columns. The corresponding values considered for the both the brick or brick and stone masonries are $f_c = 4.5$ N/mm² and $\gamma = 18$ kN/m³. A Young modulus of $1000 \cdot f_c$ and a Poisson coefficient of 0.2 have been defined for all materials. The tensile strength has been estimated as $0.07 \cdot f_c$ in the case of stone and masonry stone and $0.05 \cdot f_c$ for brick masonry.

Future studies should consider a more detailed distinction among the different materials and masonries,

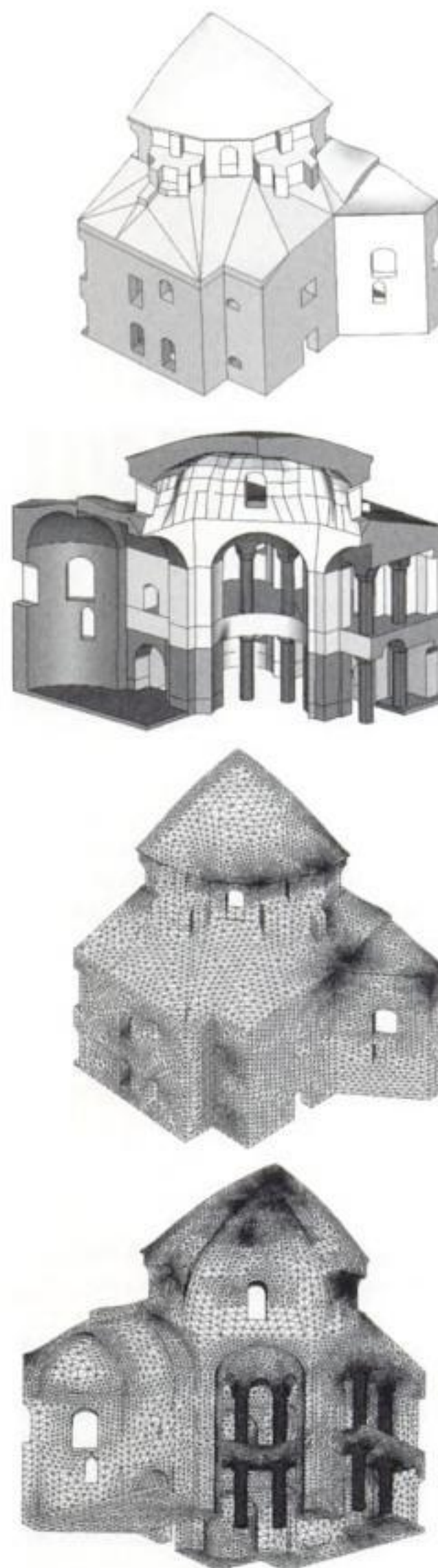


Figure 5. Geometry of structural model and FE mesh.

together with a more accurate estimation of the different material properties; this, in turn, requires further research on the existing materials and their mechanical properties.

5 SIMULATION OF DIFFERENT ACTIONS

5.1 Dead loading

The model has been first used to analyze the resulting distribution of stresses and damage caused by the only effect of the dead load. A conventional instantaneous analysis, with all dead loading simultaneously applied, has been performed for that purpose. Figures 6a and 6b respectively show the distribution of the tensile ratio and the maximum compression stresses obtained for the analyzed quadrant.

Dead loads produce mostly compression stresses across the structure. However, cracking develops at mid-span of the apse arch, where the tension ratio reaches a value above 1 (with maximum of 1.6). Moderate tensile stresses appear at the spandrels of the semi-circular niches, with tensile ratio up to 0.6 (maximum tension stress of 0.14 N/mm^2).

In the rest of the structure, the distribution of compression is far from being uniform. Although most of the walls and shell sectors reach average compression values within 0.2 to 0.4 N/mm^2 , several regions exist showing maximum compression stresses below 0.015 N/mm^2 . These regions include all the spandrels existing below the windows of the tambour. As expectable, these windows prevent the arches from receiving a significant part of the load of the dome by forcing the deviation of the vertical compression forces towards the piers. This effect can be described as the generation of a set of relieving arches within the dome, which spring from the piers and rise to the region above the windows. The region below the relieving arches is subjected to very low confinement and is thus likely to experience cracking, in the long term, due to the contribution of other possible actions.

According to the analysis (and for the material properties considered), the piers experience only very little horizontal displacements between 0.2 and 0.3 mm . As something expectable (but to a remarkable extend), the instantaneous analysis can not predict large deformations such as those actually shown by the building. However, a very significant, long-term amplification of these deformations is conceivable across a long historical period. In fact, large deformations affecting piers, buttresses and other structural components are commonly observed in ancient constructions. In many cases, such large deformations are one or more orders of magnitude superior to those that can be predicted by instantaneous or short-term numerical analysis, even if non-linear material or geometrical effects, or even a conventional treatment of primary creep at short or mid-term, are considered. Different actions and phenomena occurring during the construction process and also during the long-term, historical life of the building, such as repeated low-intensity earthquakes, thermal or hygrometric cycles, or long-term

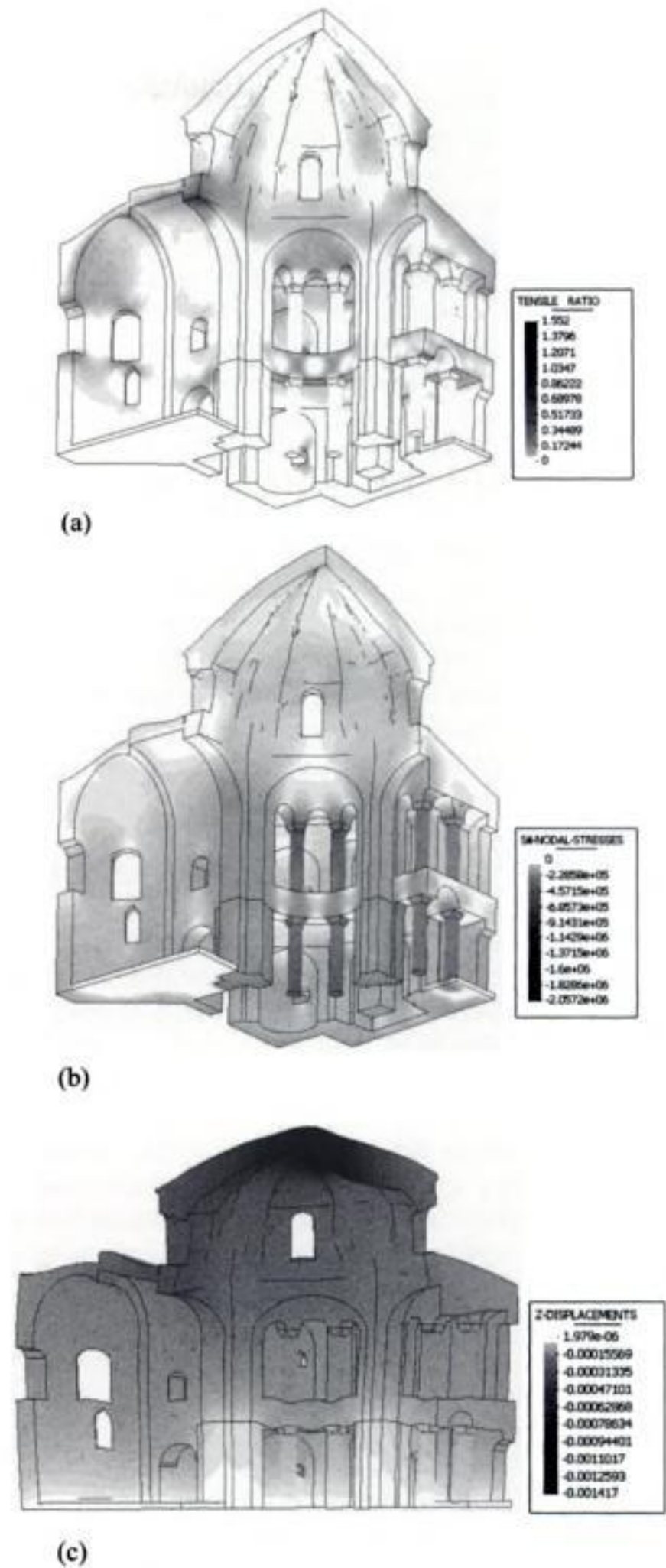


Figure 6. Distribution of (a) the tensile ratio, (b) maximum compression stresses in N/m^2 and (c) deformations, for gravity loading.

damage related to creep, may have contributed very significantly to increase the overall deformation of the structure. Since the more persistent action is gravity, it is not strange that the increase of deformation manifests as a monotonic, non-asymptotic amplification of the initial deformed shape due to dead load.

Figures 9a and 9b show the obtained distribution of tensile ratio. For forces acting in $-x$ direction, the calculation predicts the appearance of significant tensile damage (tensile ratio above 1) in the crown of the apse arch, the semicircular spandrels and upper region of the dome in the case of forces acting in the $-x$ direction. Tensile damage is predicted in the semicircular and lateral spandrels over columns and sector shells located over the piers for forces acting in the $-y$ direction. Additional, intense but localized damage appears in the lintels over the columns and window arches. Most of the damage appears in regions which the analysis for dead load showed to be particularly sensitive (as those related to cracks 1–4 in Figure 4). In particular, a moderately damaged region, appearing for forces applied both in the $-x$ and $-y$ directions,

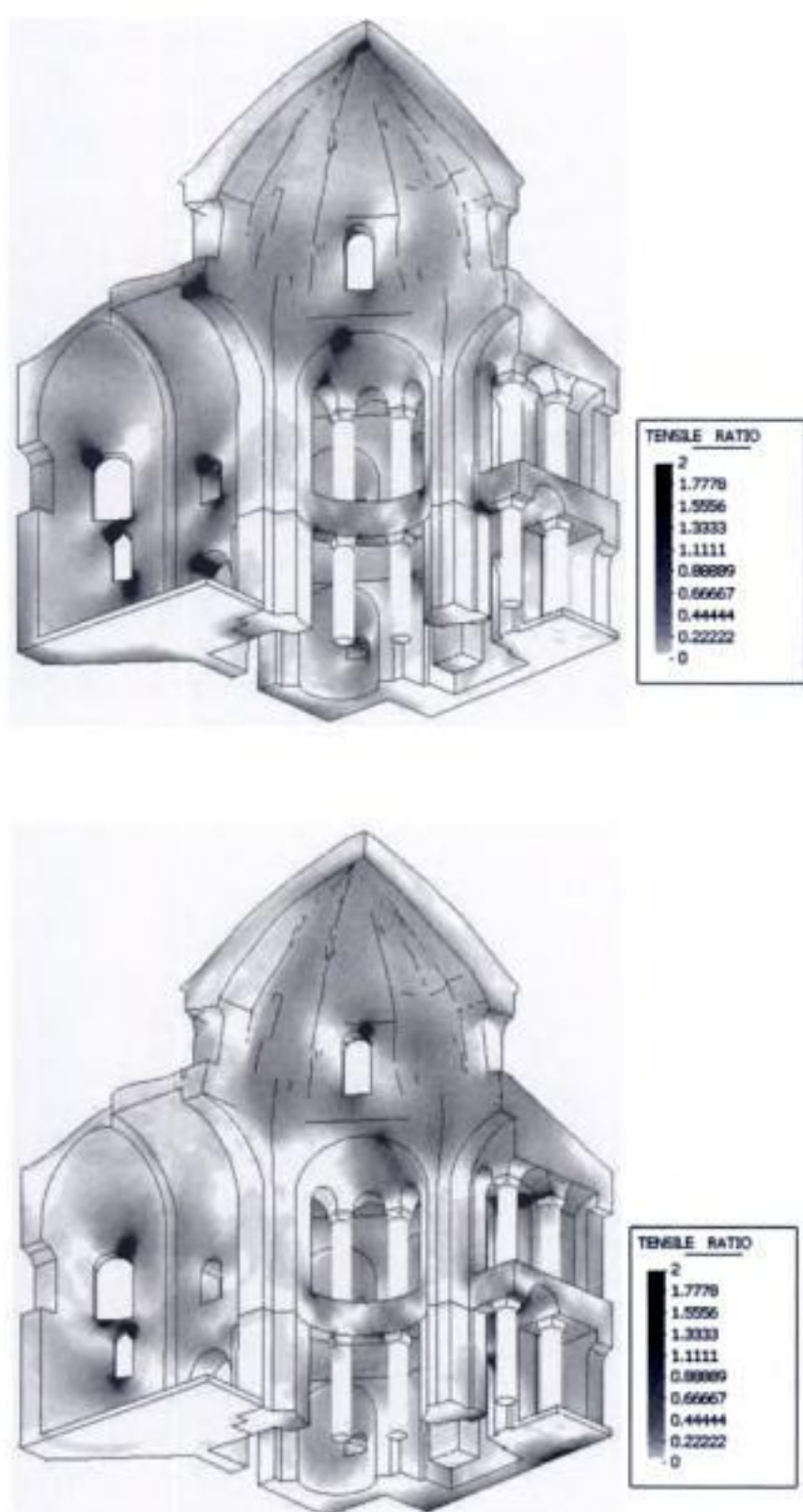


Figure 9. Distribution of tensile damage for seismic forces applied in the $-x$ (above) and $-y$ (below) directions (zones damaged in tension correspond to tensile ratio ≥ 1).

can be related with the vertical crack existing along the intersection of the flat surfaces of the shell sector over the pier (crack 2 in Figure 4). Severe damage (with high tensile ratio) is experienced in regions located below the windows of the tambour, as the semicircular spandrels and lateral arches which close the apse and ambulatory.

A maximum compression ratio of 0.56 is obtained in the analyses, meaning that no damage related to compression stresses is produced.

6 CONCLUSIONS

A preliminary analysis of Küçük Ayasofya Mosque in İstanbul has been undertaken based on a tension-compression damage FE formulation. The analysis, carried out on a structural model comprehending a quadrant of the structure, has allowed a certain insight on the effect of different actions (dead loads, local pier-column differential settlements and earthquake) and their possible contribution to cause the main lesions shown by the building.

The authors intend to continue the study after the extension of the formulation to new capabilities now in development (such as dynamic analysis in the time-domain).

A more complete structural model, comprehending the entire construction, is also needed to account for the influence of the remarkable construction irregularities and to allow an accurate seismic analysis. A more detailed model would require, in turn, more information available on the geometry, materials and historical actions having affected the construction. Significant actions for the building, such as traffic on the close railway line or the overall soil settlements, are still to be analyzed.

REFERENCES

- Aköz, F., Yüzer, N, 1995, Investigation of material properties of Küçük Ayasofya Mosque – The Church of Sts. Sergios and Bacchus in İstanbul. *Architectural Studies of Historical Buildings IV*, Southampton: Computational Mechanics Publications.
- Alkiş, A., Demirel, H., Doğan, U., Düpe, R., Gerstenecker, C., Krockner, R., Arun, G., Snitil, B., 2001, Deformation Observations at the church of Sergios and Bacchus by Photogrammetric Tools. *Studies in Ancient Structures*, İstanbul: Yıldız Technical University.
- Arun, G., 2001, Investigations on Küçük Ayasofya Mosque–The Church of Sts. Sergios and Bacchus in İstanbul. *On-site Control and Evaluation of Masonry Structures*, Bagnaux: Rilem publications s.a.r.l.
- Cervera, M., 2003, *Viscoelasticity and Rate-dependent Continuum Damage Models*. Pub. M79, Barcelona: Center for Numerical Methods in Engineering.

- Krautheimer, R., 1984, *Early Christian and Byzantine Architecture*. Pelican History of Art Series. 4th ed.: Yale Univ.
- Özsen, G.A., Bairam, E., 1995, Structural evaluation of the dome of Küçük Ayasofya – Sts. Sergius and Bacchus. *Architectural Studies of Historical Buildings IV*, Southampton: Computational Mechanics Publications.
- Roca, P., 2001, Studies on the structure of Gothic cathedrals. *Structural Analysis of Historical Constructions III*. Guimaraes: Universidade do Minho.
- Yüzügüllü, Ö, Durukal, E. 1997, The effects of Train Traffic on the Küçük Ayasofya Mosque in İstanbul. *Studies in Ancient Structures*, İstanbul: Yıldız Technical University.

Prevision of settlement-induced cracking in historical building masonry façades

J.G. Rots

Delft University of Technology, Delft, The Netherlands

S. Invernizzi

Politecnico di Torino, Torino, Italy; visiting research fellow Delft University of Technology

ABSTRACT: In the present paper the case study of an historical masonry building is presented in order to assess the settlement-induced cracking due to recent underground tunneling. A comprehensive numerical analysis is carried out in the framework of classical nonlinear smeared crack models. The building structure is analyzed by modeling the most important 2D sections, respectively parallel and orthogonal to the tunnel trace. The results obtained from the numerical simulation allow assessing the critical angular distortion after which some mitigation countermeasures are necessary to avoid the façade cracking. This value can be compared with the expected one, as well as with results provided by real-time monitoring during the tunnel excavation. A future development of the study could be directed to assess the effectiveness of possible structural strengthening.

1 INTRODUCTION

The “Industrieele” (Industrial) Club was founded in April 1913 as a centre owing to serve the growing needs of Dutch industry and trade in the Netherlands. It was a national society with headquarters in the capital, Amsterdam. It was quickly apparent that important business was best conducted in the proper and refined surroundings and so during the three years that followed, the impressive building “Industria” on Dam Square (No 27) gradually took shape by the architect Foeke Kuipers design.

Initially, there were problems with the foundations. The excavations stumbled on the remains of a disused sluice, which had originally been built in the 13th century, after the dam across the Amstel river had been constructed. All the complicated construction in the centuries previous to the foundation of Industria meant the builders had a difficult task ahead of them. The floor of sluice was no longer supported by poles, these having sunk under their own weight. Despite all these setbacks, as well as a builder’s strike lasting 6 months, and the start of the First World War, the building was finished on the 8th of January 1916.

Nowadays, the building is going to be interested by the new underground line tunneling that will be traced nearby. Therefore, a reliable assessment of the settlement-induced damage due to the Tunnel Boring



Figure 1. View of the Industria building from the Dam square in Amsterdam.

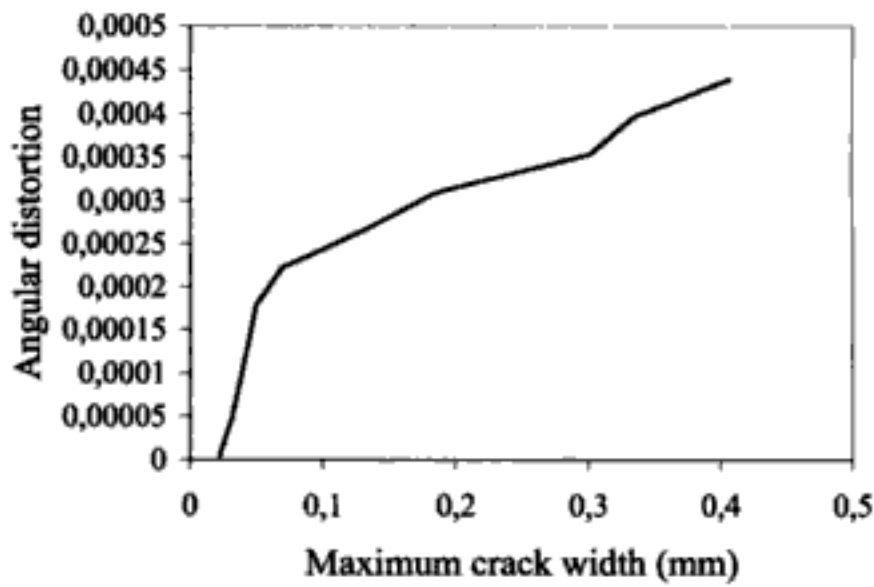


Figure 9. BACK façade cracking response to settlements.

4.3 SECTION model

The SECTION scheme is obtained from a section of the building placed parallel and right beneath the BACK façade. Therefore, the model is composed of an outer masonry wall and an inner RC frame. In the central part, the foundation wall is absent, and the RC frame is placed directly upon the foundation reverse beam.

Being larger than the BACK façade, the SECTION scheme is relatively closer to the tunnel centerline. This results in a more curved settlement profile. On the other hand, the SECTION scheme is more flexible than the previous one, and this is an advantage since imposed settlements cause less severe stress in the structure.

The crack pattern in the SECTION scheme is shown in Figure 10. The first cracks that nucleate are those in the upper region of the outer masonry wall.

When the angular distortion increases, also the lower zones of the outer masonry wall crack. Figure 10 shows a prevalent shear type crack pattern, with cracks that follow a curved path rather than run straight through the façade.

The diagram in Figure 11 quantifies the angular distortion vs. maximum crack width for the SECTION scheme. The behavior does not differ significantly from the previous ones, and is characterized by a basically bilinear response.

4.4 ROKIN façade

The ROKIN façade face the Rokin road, beneath which the tunnels will be drilled.

This is the largest façade of the building, i.e. the one with the lower height over width ratio.

Also the kind of settlement profile profoundly differs from the previous cases. Due to the fact that the tunnels run parallel to the façade, the settlement profile does not increase monotonously. In other words, there are two regime configurations, respectively before the tunnel front travel under the building, and well after, for which the differential settlements are zero.

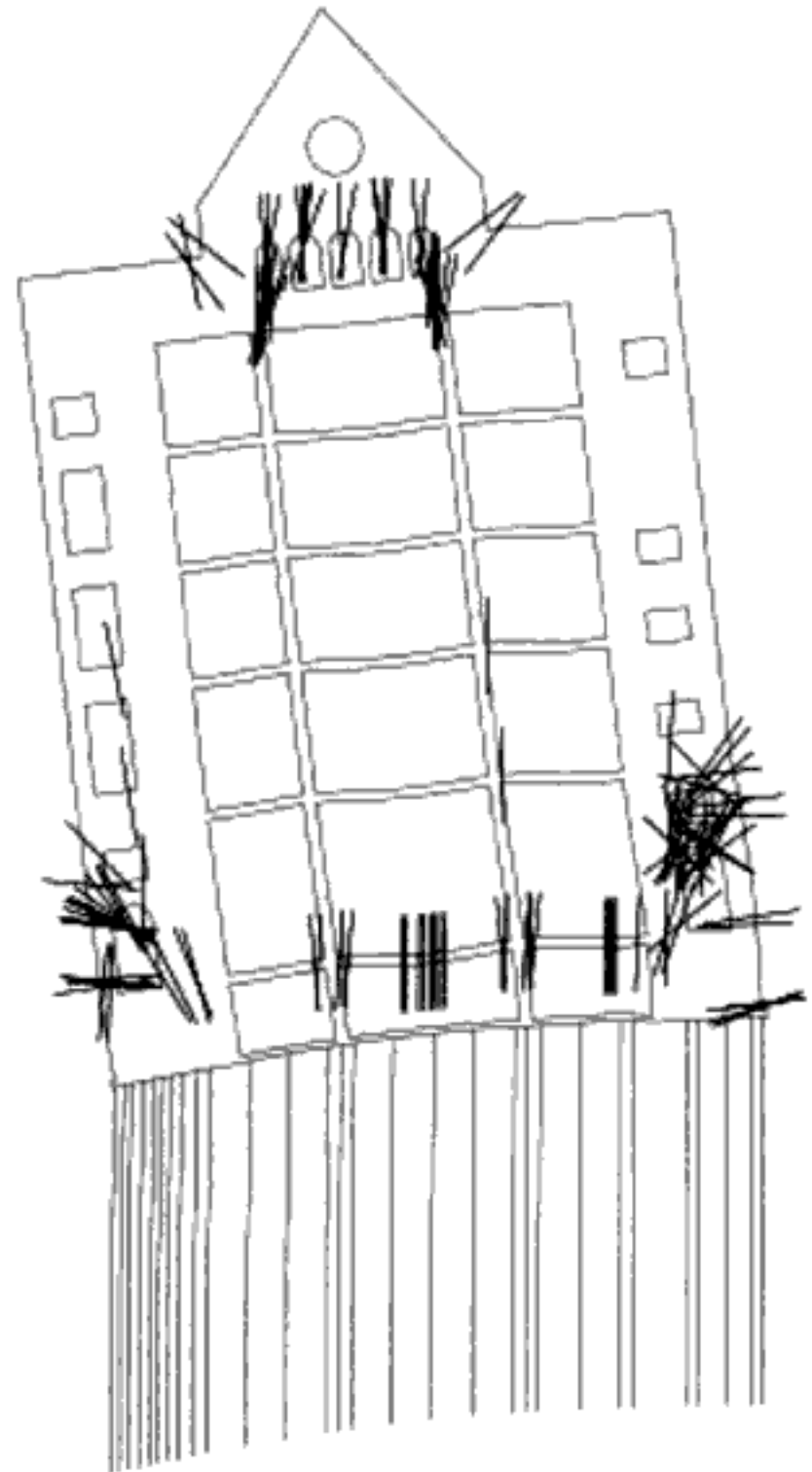


Figure 10. SECTION crack pattern (tunnels are on the left side).

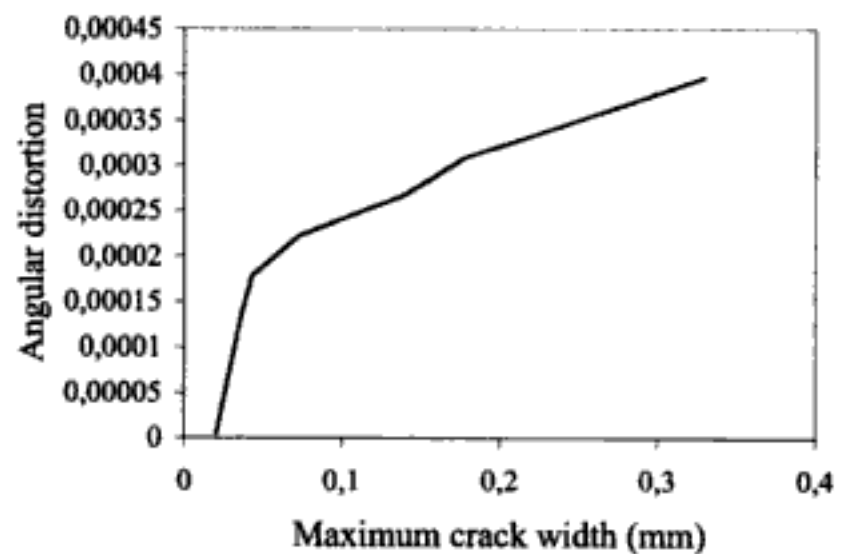


Figure 11. SECTION model cracking response to settlements.

The dangerous differential settlements are experienced by the façade only in the transitory phase. An example is shown in Figure 12, where the tunnel front is coming from the left side of the façade (i.e. coming

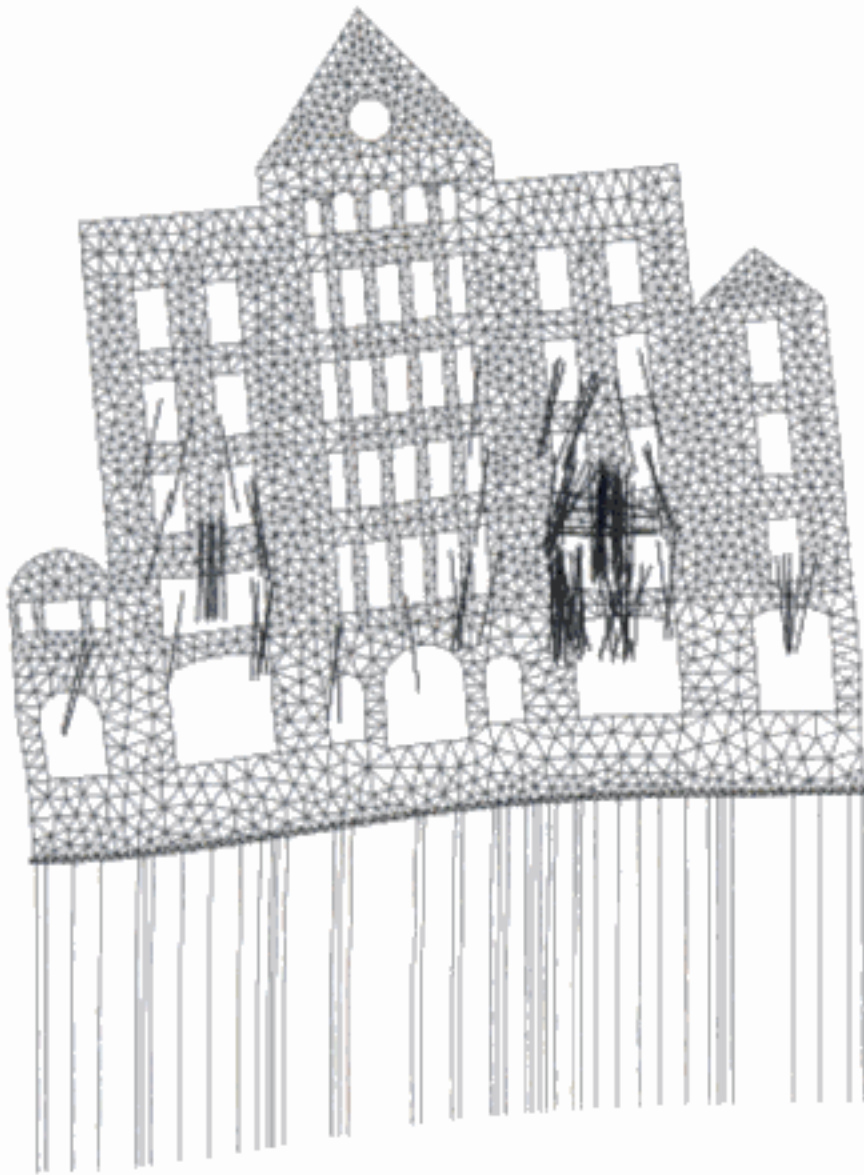


Figure 12. ROKIN façade mesh and crack pattern.

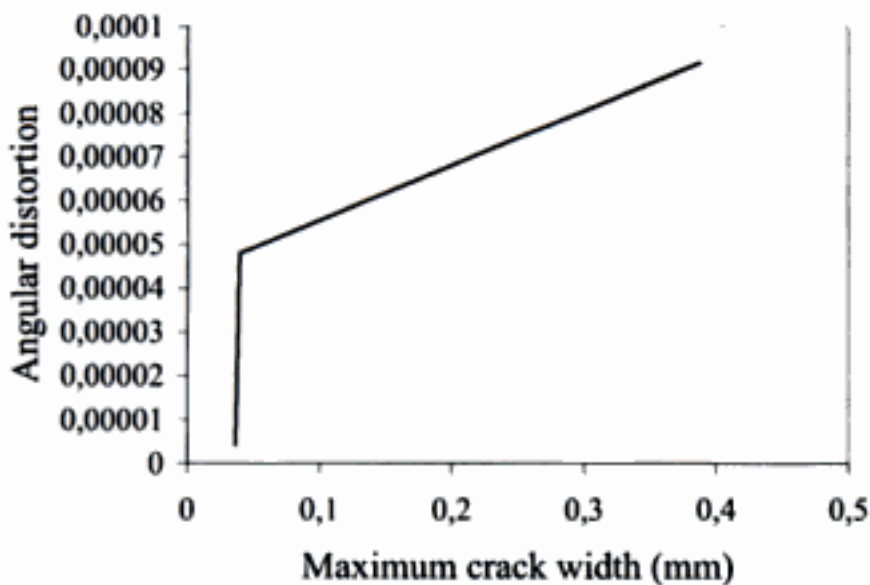


Figure 13. ROKIN façade cracking response to settlements.

from the Amsterdam Central Station). Of course, the most critical front position is the one that causes the larger distortions in the façade.

In Figure 12, it is also possible to see the unstructured triangular mesh used to discretize the plane stress problem (the element side is about 250 mm). Moreover, Figure 12 shows the ROKIN façade crack pattern. It is worth noting that the right half of the façade presents a more pronounced fracture pattern. This is due to the fact that it is in the hogging part of the trough profile. On the other hand the left half is in the sagging zone, and shows a less severe crack pattern.

This confirms some comments made in the previous sections.

Finally, the behavior of the angular distortion vs. maximum crack width for the ROKIN façade is shown in Figure 13. Once again, the typical bilinear curve suggest the definition of a critical angular distortion, after which the crack opening increases rapidly, and therefore some mitigation countermeasures, like compensation grouting or structural strengthening, are useful to avoid an excessive façade cracking.

5 CONCLUSIONS

In the present paper the case study of an historical masonry building has been presented. Nowadays, the building is going to be interested by the new underground line tunneling that will be traced nearby. Therefore, a reliable assessment of the settlement-induced damage due to the Tunnel Boring Machine (TBM) is necessary in order to design properly the possible countermeasures (e.g. compensation soil grouting or structural strengthening).

A comprehensive numerical analysis has been carried out in the framework of classical nonlinear smeared crack models. The building structure is analyzed by modeling the most important 2D sections, respectively parallel and orthogonal to the tunnel trace. The model includes a representation of the pile foundation, while settlements of the deep soil layer are assigned based on geotechnical evidences.

Some conclusions can be outlined from the analysis of the most relevant 2D schemes, which follows. The relative position of the façade with respect to the tunnel centerline plays a central role, where the so-called hogging zone is definitely more critical than the sagging one. This can appreciate clearly from the ROKIN façade, interested by the longitudinal settlement trough, where the resulting crack pattern is not symmetric and concentrated in the hogging zone.

In addition, the height over width ratio influences the structural response. Ratios close to one preferably lead to rigid body motion of the façade, while low values of ratio are rather characterized by the deformation of the façade.

In the present case study the presence of a deep concrete foundation wall also influence the upper masonry wall behavior. The concrete wall basically bends under the effect of settlements. On the other hand, some of the façades (e.g. DAM) are crossed by straight cracks, while others (e.g. BACK and SECTION) are mainly characterized by shear type curved crack patterns.

Finally, in the scheme named SECTION the outer masonry wall interact with an inner RC frame, and the foundation concrete wall is not continuous. This results in a more flexible scheme, which does not suffer from settlements more than the other façades. This should

at least in part justify the habit, in common practice, to limit the analysis to the front façades.

The results obtained from the numerical simulation allow assessing the critical angular distortion after which some mitigation countermeasures are required to avoid the façade cracking. This value can be compared with the expected one, as well as with results provided by real-time monitoring during the tunnel excavation.

A future development of the study could be directed to assess the effectiveness of possible structural strengthening.

ACKNOWLEDGEMENTS

Financial support from Delft Cluster, COB and the Netherlands Technology Foundation STW is acknowledged.

REFERENCES

- Boonpichetvong, M., & Rots, J.G. 2003. Settlement damage modeling of historical buildings. In N. Bicanic, R. de Borst, H. Mang & G. Meschke (eds.), *Computational modeling of concrete structures; Proceedings of Euro-C 2003*: 655–665. Lisse: Balkema.
- Burland, J.B., Standing, J.R. & Jardine, F.M. (eds.) 2001. *Building response to tunneling. Case studies from the Jubilee Line Extension*. London: Thomas Telford.
- Feenstra, P.H. 1993. *Computational aspects of biaxial stress in plain and reinforced concrete*, Ph.D. Dissertation, Delft University of Technology, Delft, the Netherlands.
- Feenstra, P.H., Rots, J.G., Arnesen, A., Teigen, J.G. & Høiseth, K.V. 1998. A 3D constitutive model for concrete based on a co-rotational concept, In R. de Borst et al. (eds), *Proc. Int. Conf. Computational Modeling of Concrete Structures*: 13–22. Rotterdam: Balkema.
- Mair, R.J. & Taylor R.N. 1997. Bored tunneling in the urban environment. In *Proc. 14th Int. Conf. Soli Mech. And Foundation Engineering 2*: 2353–2385. Amsterdam: Balkema.
- Mair, R.J., Taylor R.N. & Burland J.B. 1996. Prediction of ground movements and assessment of risk of building damage due to bored tunnelling. In R.J. Mair and R.N. Taylor (eds), *Geotechnical aspects of underground construction in soft ground*: 713–718. Rotterdam: Balkema.
- Rots, J.G. 1988. *Computational modeling of concrete fracture*, Ph.D. Dissertation, Delft University of Technology, Delft, the Netherlands.

Cracking simulation in a plain structure using the finite element method

L. Pani, B. De Nicolo & Z. Odoni

Department of Structural Engineering, University of Cagliari, Italy

ABSTRACT: This paper outlines the procedure developed to simulate the cracking mechanism in the stone masonry façade of Santa Chiara Church (Cagliari). The static damage growth is demonstrated, from the first crack to the fully developed crack pattern. The procedure is implemented in specifically developed program, based on an iterative process and storage of intermediate results, utilising FEM. The program was first tested on simple structural models whose solution is known from the theory of Structural Mechanics, and then on a real structure. The results show a very good reliability and the manageability of the program. Furthermore, the program easily allows the designer to adjust specific variables in order to achieve the expected results.

1 INTRODUCTION

Throughout the world, many designers, engineers and researches are studying in order to exploit historic masonry structures to their potential. This interest derives from the consciousness that historic masonry structures are part of the cultural heritage and as such are to be preserved and reused. For many centuries, stone structures have been built in accordance with empirical design criteria, which guaranteed high safety factors. For the careful restoration of this cultural patrimony there is a need for computational modelling, which can show the real mechanical behaviour of stone masonry (Bull 2001).

In order to model the structural behaviour of stone masonry, several hypothesis are necessary on the material constitutive law (elastic, elastic-plastic model, heterogeneous or homogeneous material, mortar/stone interaction, etc.) due to the uniqueness of each building.

Today's commercial FEM programs do not always allow following, step by step, the dynamic process of crack formation. In fact it is necessary to have easy means which can perform damage simulation of both materials and structures, and allow introducing probable modifications of the governing parameters. In the present study, a FEM-based program has been developed, which allows investigating the behaviour of stone masonry subject to static damage and/or material degradation. The reliability of the program was tested with a number of applications on simple beams, in order to compare the results with those obtained according to the theory of Structural Mechanics.

Afterwards, the program has been applied to a real plane structure whose geometry and cracking state is known.

2 CASE STUDY: THE FAÇADE OF SANTA CHIARA CHURCH

The Santa Chiara Church, situated in the historical quarter of Stampace in Cagliari, Italy, was built in the second half of 13th century.

The building is the remaining part of a monastery, neglected to the ravages of time and ultimately destroyed by the bombing during the Second World War. The church has a rectangular layout, with a barrel vault ceiling spanning 7.50 m (Fig. 1). Several restoration

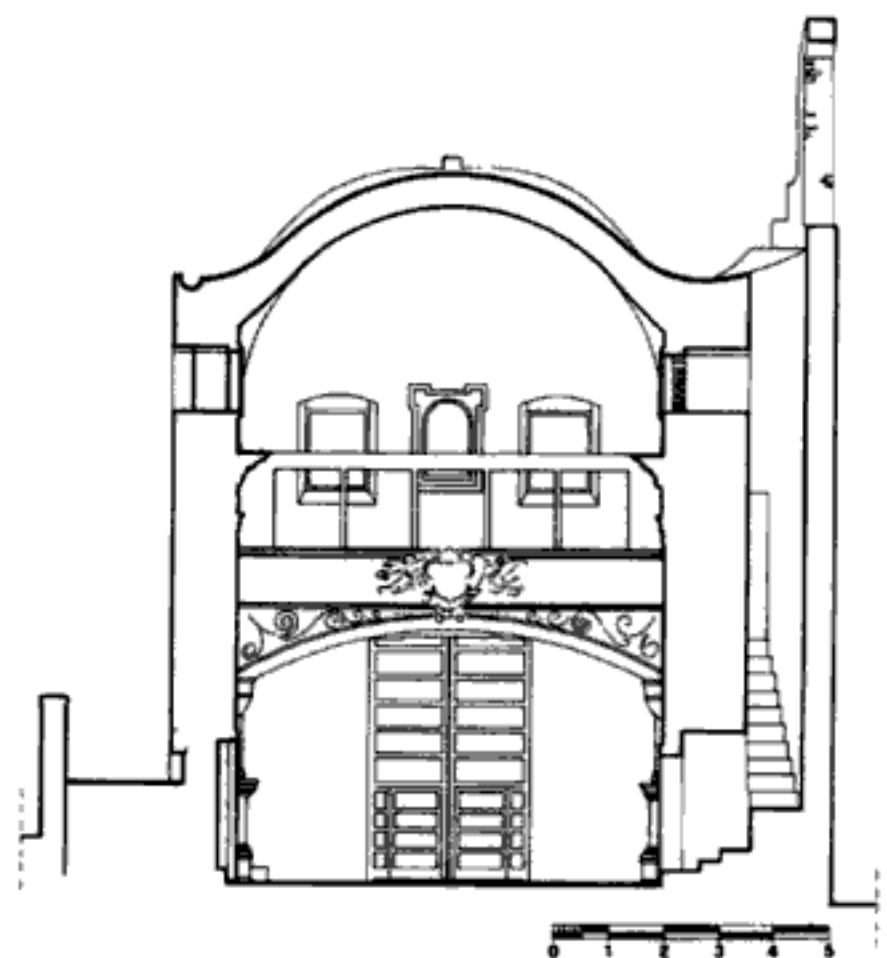


Figure 1. Section of the church.



Figure 2. A detail of façade at the cornice.

works had been carried out both on the load-bearing walls and on the vault (Ingegno 1993).

The façade, whose average thickness is 1,35 m, is independent from the remaining building and is exclusively an vertical wall (Fig. 2).

The façade has structural problems, which led to extensive cracking and is in need for restoration. The cracks start from the architrave of the main door and from the windows, and then almost vertically towards the stone cornice. The cracks are evident both on the inner and outer side. Hence, it was necessary to determine the reason for this cracking, before a new restoration work.

2.1 The stone masonry

The façade was built with limestone blocks, with variable size and shape and little worked. The stones were laid with lime and soil mortar, and the interstices among the stones were filled with stone chips.

Limestone is typical of Cagliari and its hinterland. Its chemical and mechanical properties are quite variable. Table 1 shows the average values of the material properties, obtained from an extensive in-situ experimental investigation of a variety calcareous stones from Cagliari (Barroccu et al. 1981, Concu et al. 2003).

The architrave of the main door is made of juniper wood, and appears rather damaged.

Table 1. Chemical, physical and mechanical properties of masonry.

γ_s	KN/m ³	dry specific weight	18
γ_{sw}	KN/m ³	saturated specific weight	24
n	%	porosity	5.6
σ_c	MPa	dry compressive strength	24.5
σ_{cw}	MPa	sat. compressive strength	9.8
σ_t	MPa	dry tensile strength	0.95
σ_{tw}	MPa	saturated tensile strength	0.32
E	MPa	modulus of elasticity	2070
CaCO ₃	%	content	85

The following parameters have been assumed for modelling the damaged juniper wood: $E_{j||} = 2000$ MPa, $\sigma_{t||} = 0,9$ MPa, whereas the values $E_{j||} = 11000$ MPa, $\sigma_{t||} = 30$ MPa have been used for the undamaged condition.

3 THE BASIC FORMULATION

3.1 Model for masonry

In order to schematize the material behaviour, a linear elastic model is assumed. The tensile and compressive strength are assumed at the saturated state, considering the great hygroscopicity of limestone. The E-modulus of masonry is assumed about 25% lower than that of limestone ($E = 1500$ MPa), in order to account for the presence of mortar joints. Masonry is assumed to be an homogeneous and isotropic material.

However, to introduce some non-homogeneity, the E-modulus is assumed to randomly vary of $\pm 10\%$ around the chosen value. In fact, the program allows assigning different properties to every single element.

3.2 Procedure

The procedure can be schematized as follows:

1. First step
 - preliminary computation of stress and strain at the structure nodes,
 - search for nodes at which the strain exceeds the cracking limit,
 - mesh refinement in the surrounding nodes area.
2. Iteration
 - computation of stress in the refined structure,
 - search for more strained nodes where cracking is possible,
 - if the last requirement is positive, triangle separation at that node.

The loading condition was the self weight (dead load). The tensile strain limit of cracking for masonry is defined based on the De S. Venant-Grashof criterion.

Furthermore, since in the hypothesis of homogeneous and isotropic masonry a crack occurs in a plane orthogonal to the direction of the maximum tensile stress, to determine these critical points reference was made to the principal stresses based on Mohr theory (Mastrodicasa 1993).

4 THE PROGRAM

The various components described above have been implemented on PC, in a finite element program, written ad hoc in TURBO PASCAL, using pointer-type variables.

When the data amount exceeds the RAM of the computer, data are stored in external files, and in mixed storage (RAM and files) when data amount is relatively moderate.

The program code is modular and is divided into logical subsets, each composed of one or more procedures. The main subsets are explained below.

The logical procedure can also be applied to 3D structures.

The program can generate readable files for commercial graphical software packages: Autocad-LT reads the input data file and print the structural model, Surfer 5.0 reads the result files and plots the colour contour of stress and displacement components.

4.1 Choice of the element

The façade is represented in the model by meshes of six-nodes triangular plane stress elements (Krishnamoorthy 1994, Zienkiewicz & Taylor 2000).

This element is chosen for its geometric versatility and excellent performance in stress analysis of structures with high stress concentrations. The triangular shape allows all side orientation compatible with geometric shape of cracks.

Furthermore, the mid-side nodes allow separating the triangles also at the intermediate points, once the limit of crack condition has been obtained.

4.2 Input data

The diagram in Figure 3 shows the procedure of data input.

In "Geometric data of Structure", nodes and elements are automatically generated, while their orientation for each zone is fixed by the user, in order to detail the cracking as much as possible.

The physical and mechanical properties for each element are stored in "Material characteristic".

In order to simulate the non-homogeneity of material, it is possible to replace the values of material properties with others, obtained from percentage variation with random law around fixed value.

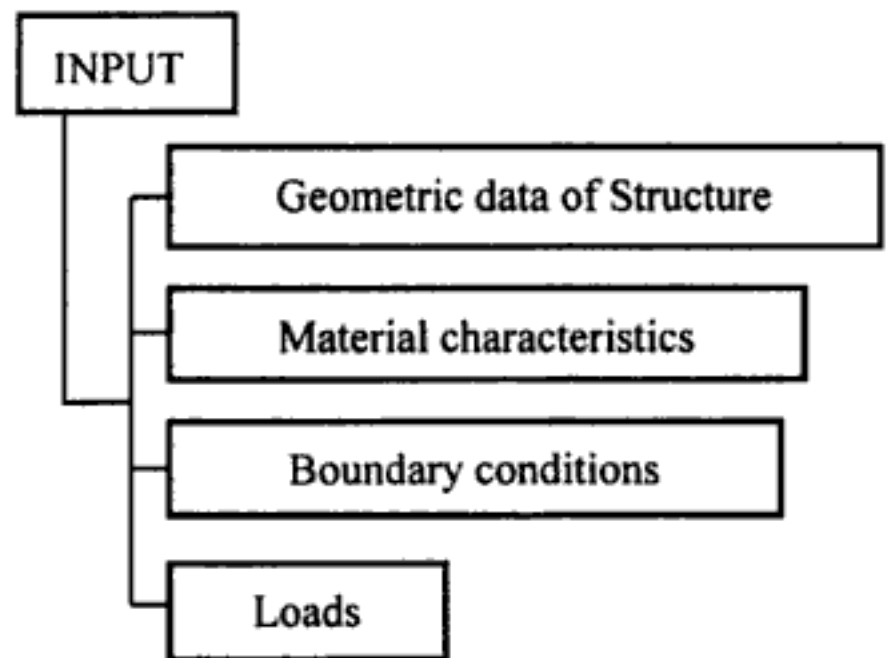


Figure 3. Data input procedure.

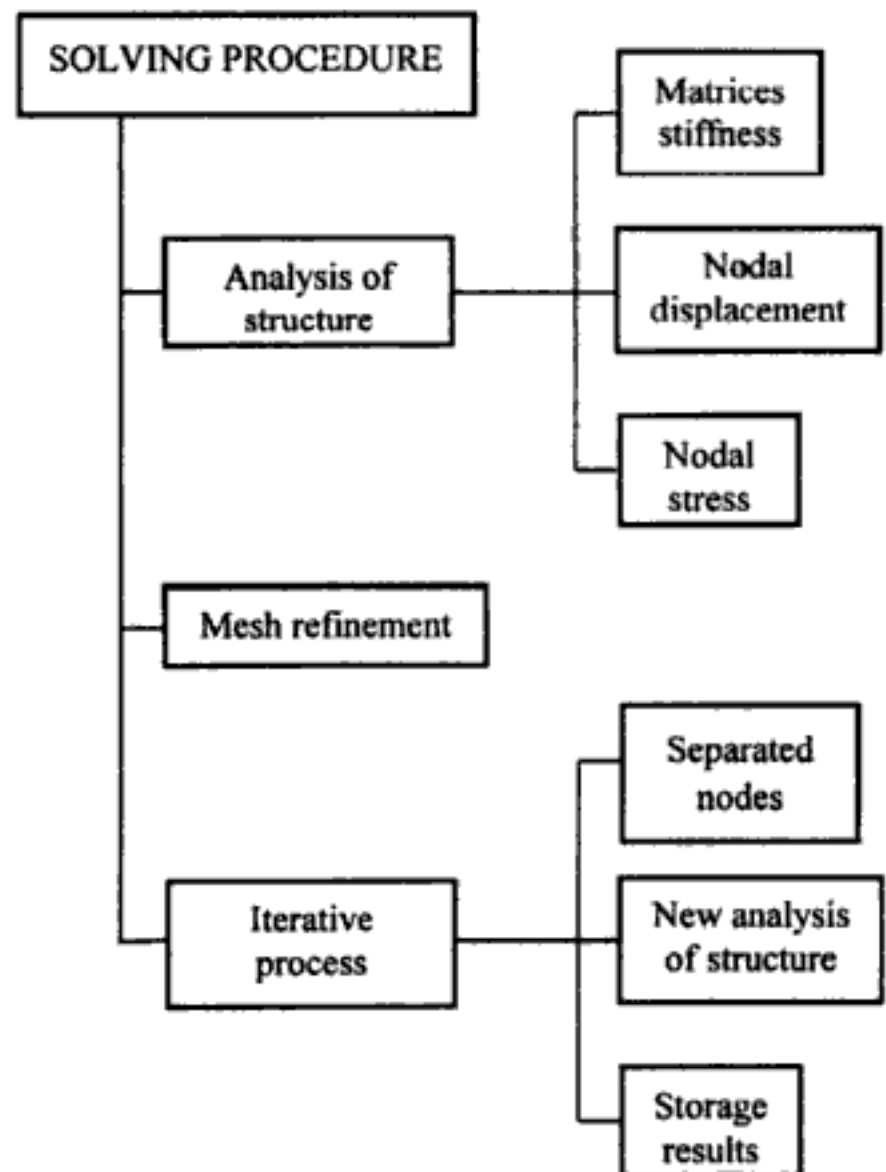


Figure 4. Solving procedure.

The procedure can review the material characteristics for each element. The constraints are specified in "Boundary conditions", while "Loads" describe how the structure is loaded.

4.3 Solving procedure

The calculation consists of three part (Fig. 4).

In "Analysis of structure", the element stiffness matrices and the nodal loads are calculated and

Table 2. Limits Standards SN 640 312, Structural Category IV, Building that are particularly vulnerable or worth preserving.

<i>Continuous or steady state vibration</i>	
Frequency (Hz)	Max velocity (in/s)
10–30	0,12
30–60	0,12-0,2
<i>Transient or impact vibration source sources</i>	
Frequency (Hz)	Max velocity (in/s)
10–60	0,3
60–90	0,3–0,5

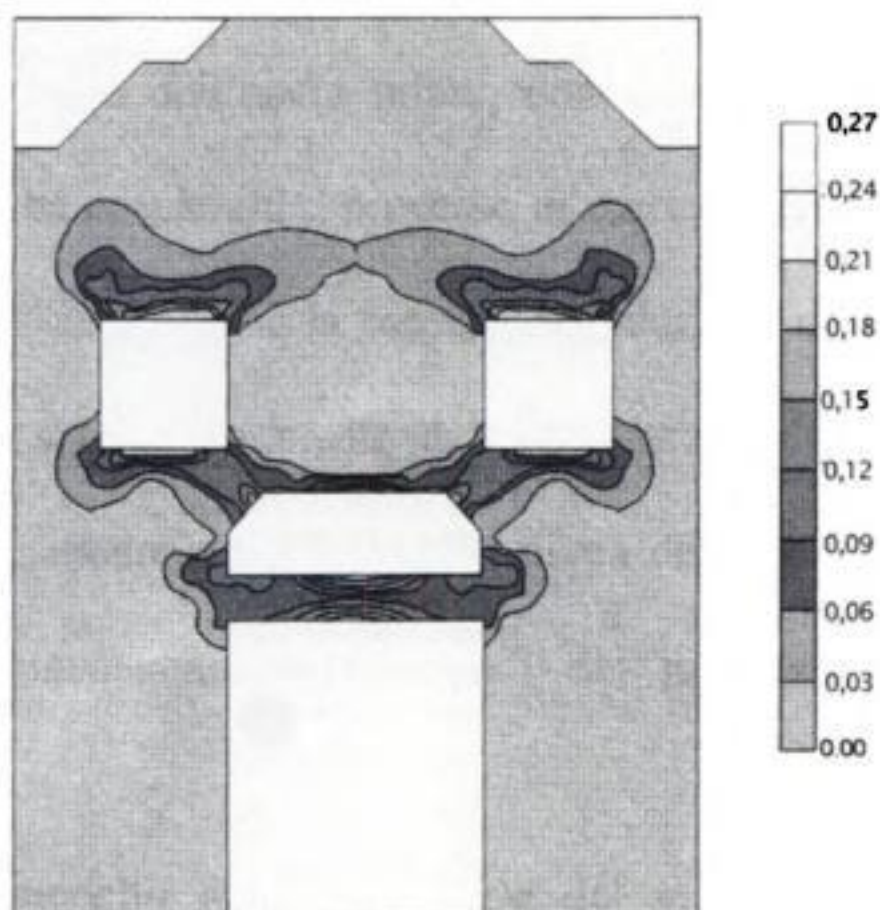


Figure 7. Main tensile stress (MPa) with architrave undamaged.

The reference limits have been assumed in accordance with Standard DIN 4150-3 and Standards SN 640 312 (Table 2). The values of the natural frequencies of the façade are very different than the limit proposed for both hypotheses. However the vibration produced by organ and bomb may have also contributed to establish the actual state of cracking.

The performed analysis showed that the hypothesis of the “settlement of the main door juniper wood architrave” provides a cracking map equal to the actual one. This hypothesis is confirmed by Figure 7, which shows the principal tensile stresses in the façade, calculated assuming the juniper wood architrave to be undamaged.

Figure 8 shows the result of a new calculation with the hypothesis of damaged juniper wood architrave. Stress concentrations are observed in the areas around the openings and near the arch above the main door.

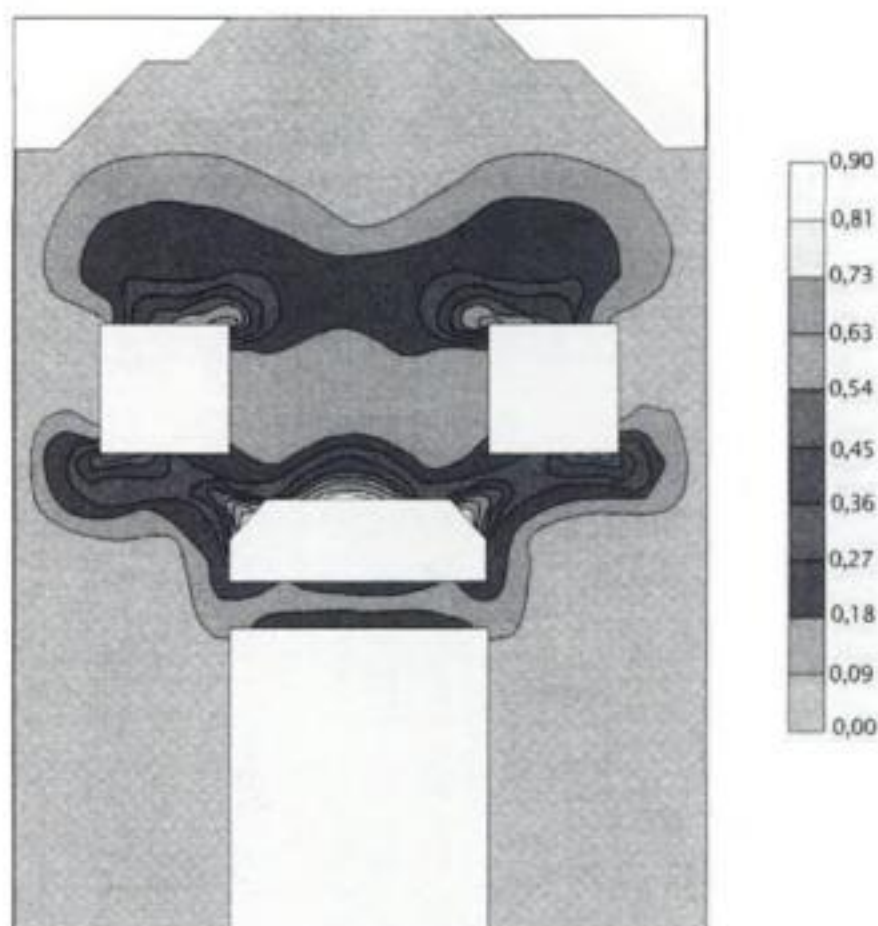


Figure 8. Main tensile stress (MPa) with architrave damaged.

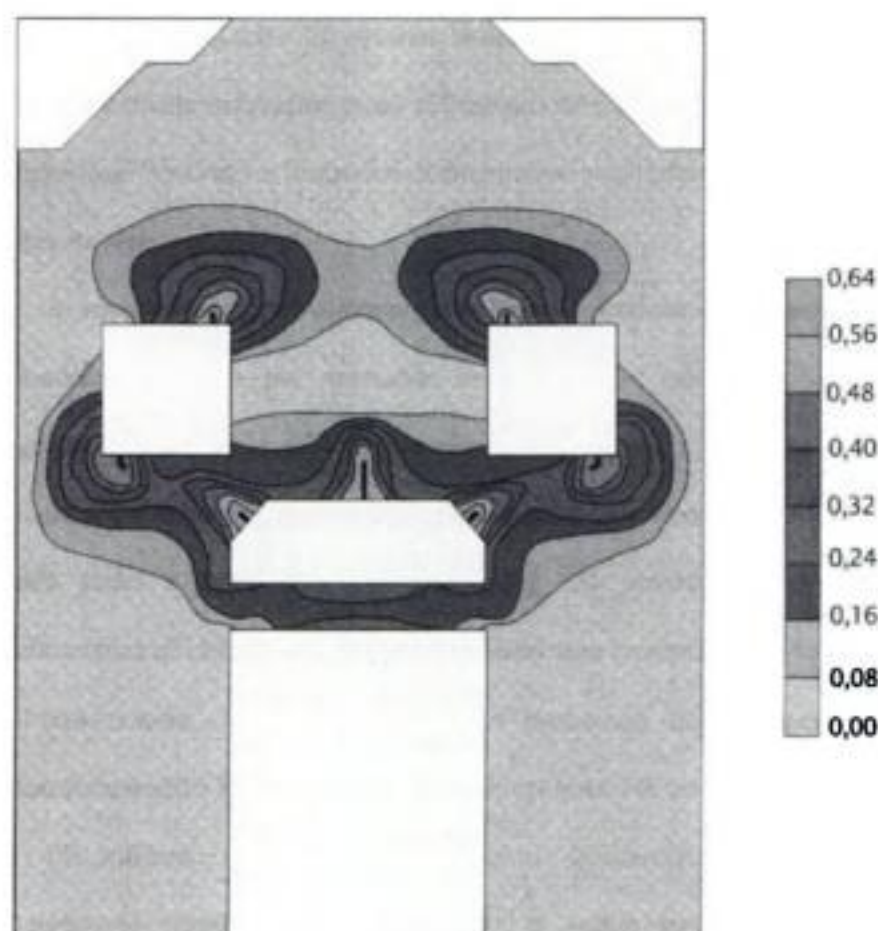


Figure 9. Main tensile stress (MPa) and cracks in their final state.

The principal tensile stresses were obtained after the iterations of the previously described procedure until the stabilisation of cracking, in accordance with De S. Venant-Grashof criterion.

The principal tensile stresses are represented in Figure 9, and the cracks in their final state are pointed out.

- Gottardi, G. 1323
 Greco, R. 1175
 Gubana, A. 745
- Hahmann, L. 977
 Hamann, M. [331](#)
 Hayen, R. [611](#)
 Hennen, C. [331](#)
 Higgins, S.R. 1273
 Hirs, J. 1367
- Ianniruberto, U. [577](#), 583
 Ignoul, S. 719, 1349
 Inaudi, D. [505](#)
 Indirli, M. 1235
 Infanti, S. 1229
 Invernizzi, S. 687
 Ivorra, S. [429](#), 1149
- Jaeger, W. 753, 1267
 Jaquin, P.A. 1315
 Jespersen, T. 763, 1341
- Kala, J. 1367
 Kansal, A. 1069
 Kaya, S.M. 477
 Keersmaekers, R. [343](#)
 Kelley, S.J. 1257
 Kırca, Ö. [87](#), [223](#)
 Knupfer, B. [331](#)
 Köpp, C. 313
 Ksandr, K. 1367
 Kwiecień, A. 1357
- La Mendola, L. [281](#), [867](#)
 Lacidogna, G. [523](#)
 Laefer, D.F. [191](#), [255](#)
 Lagomarsino, S. 483, 619, 1091, 1157
 Landolfo, R. 1039
 Lanza, F. 1001
 Lanza, L. 489
 Laudiero, F. 489
 Lionello, A. [533](#), [781](#), 1323
 Lo Gatto, G. [183](#)
 Locke, R. 1215
 Lockrem, A. 1215
 Lodigiani, A. 771
 Lokošek, E. 1305
 Lourenço, P.B. 51, 299, 369
- Macchi, G. 771, 1375
 Machado, J.S. [369](#)
 Magenes, G. 1079
 Maierhofer, C. 313, 331
 Malangone, P. 1019
 Malyszko, L. [291](#)
- Mamaghani, [LHP 659](#)
 Mancini, L.C. 177
 Mandara, A. 803, 1207, 1247
 Manganiello, M. 1039
 Marano, G.C. 1175
 Marchetti, L. 1061
 Marchi, A. 1421
 Marchi, G. 1323
 Marchisio, M. [331](#)
 Martín, M. 1149
 Marzo, A. 945
 Masia, M.J. 829
 Maskey, P.N. 1103
 Massanas, M. [679](#)
 Mastropirro, R. 377
 Mattarucco, A. 1001
 Matteo, J.A. 1335
 Maunder, E.A.W. [569](#)
 Mazzalai, P. 813
 Mazzolani, F.M. 903, 923, 945, 1247
 Mechling, J.M. [265](#)
 Mele, E. 557
 Meli, R. 1121
 Melo, Â. 51
 Mendes, P. 483
 Menichelli, C. 967
 Mezzadri, G. 489
 Migliacci, A. [387](#)
 Migliore, M.R. 361
 Miklós, M. 1403
 Mileto, C. 159
 Miltiadou-Fézans, A. [351](#), [401](#), 1285
 Minch, M.Y. [137](#), [795](#)
 Minos, N. [401](#)
 Mirabella Roberti, G. [597](#)
 Mirandola, D. 167
 Modena, C. [75](#), [321](#), [533](#), [837](#), 911, 967, 1061, 1323
 Mucciarella, M. 1235
- Nardoni, G. 489
 Nencioni, S. 1395
 Niglio, O. [203](#)
 Nisizaki, L. 1395
- Ochsendorf, J.A. 551
 Odoni, Z. [695](#)
 Olsson, K.G. 935
 Ombres, L. 847
 Orsini, P. [513](#)
- Palacio, A.G. 1409
 Palieraki, V. [351](#)
 Pallarés, F. [429](#)
 Pallarés, F.J. [653](#), 1149
- Palomo, M.J. [429](#)
 Palumbo, G. 803
 Pani, L. [695](#)
 Papia, M. [281](#)
 Parodi, S. 1091
 Pecora, C. 1395
 Pedroni, S. 1295
 Peña, F. 1121, 1165
 Penazzi, D. 1051
 Penna, A. 1157
 Petrescu-Comnene, M. 1273
 Piazza, M.P. 957
 Pina-Henriques, J. 299
 Pistola, F. 1235
 Pistone, G. [121](#)
 Podestà, S. 1091
 Podnar, H. 1305
 Popa, L. 1403
 Portioli, F. 1039
- Quagliarini, E. 883
- Raffagli, A. 787
 Ragazzini, A. 1323
 Ramundo, F. 361, 1207
 Rauci, M. 1019
 Ray, A.S. [239](#)
 Re, L. [121](#)
 Reda Taha, M.M. 829
 Resemini, S. 1091
 Restrepo-Vélez, L.F. 1079
 Riggio, M.R. 957
 Rinaldi, Z. [577](#), [583](#)
 Riva, G. [131](#)
 Roca, P. [63](#), [679](#)
 Romano, A. 557
 Ronca, P. [273](#), [387](#)
 Rossi, C. [533](#), [781](#), [1323](#)
 Rossi, P.P. [533](#), [781](#), 1323
 Rots, J.G. 687
 Rush, A.S. [255](#)
 Russo Ermolli, E. 991
 Russo, V. [153](#)
- Safta, C.A. [667](#)
 Saisi, A. 321, 439, 837, 1061
 Salvatore, W. [513](#)
 Sassu, M. 1029
 Schueremans, L. 1349
 Schuller, M. 1215
 Sciolti, M.S. 875
 Sendova, V. 1187, 1257
 Sepe, V. [461](#)
 Shrive, N.G. 829
 Silvestri, L. 813
 Skłodowski, M. [395](#)
 Sofronie, R.A. 735

Spadoni, B. 1235
 Speranza, E. 1235
 Spina, G. 1207
 Sponchioni, A. 167
 Springhetti, L. 813
 Stazi, A. 883
 Stehlik, M. [407](#)
 Stevens, P. 1349
 Stoll, V. 753
 Stuart, [B.H. 239](#)
 Szołomicki, J. [137, 795](#)

Tassios, T.P. 707
 Tedeschi, C. 321
 Thelin, C. 935
 Theodossopoulos, D. 643, 1383
 Thomas, P.S. [239](#)
 Tokay, [Z.H. 213](#)
 Tolles, E.L. 1197
 Tomaževič, M. [15, 321](#)

Torre, A. [505](#)
 Torresani, S. 813
 Toumbakari, E.E. 707
 Tralli, S. 489
 Tullini, N. 489
 Tuztaşı, U. 231

Olivieri, D. [203](#)
 Urushadze, S. [415](#)

Valletta, G. 1395
 Valluzzi, M.R. 321, 837, 911, 967, 1061
 Van Balen, K. [611, 1349](#)
 Van Gemert, D. [343, 611, 707, 719, 1349](#)
 Van Gulick, L.A. [635](#)
 Van Rickstal, F. [343, 719](#)
 Vari, A. [451](#)
 Vegas López-Manzanares, F. 159

Velosa, A.L. 603
 Verdú, G. [429](#)
 Vermeltfoort, A.T. 1413
 Victor, L.M. 483
 Villaschi, J.N.S. 177
 Vintzileou, E. [351, 707, 1285](#)
 Viskovic, A. 461, 629
 Voiello, G. 145

Wasserman, [L. 245](#)
 Wendland, D. [111](#)
 Wendrich, A. 313

Yeomans, D. 1111
 Yuzugullu, O. 477

Zambrano, A. 1019
 Zanzi, L. 321, 331
 Zaroyianni, E. 1285
 Zerbo, V. 891

Structural Analysis of Historical Constructions contains about 160 papers that were presented at the IV International Seminar on Structural Analysis of Historical Constructions that was held from 10 to 13 November, 2004 in Padova Italy. Following publications of previous seminars that were organized in Barcelona, Spain (1995 and 1998) and Guimarães, Portugal (2001), state-of-the-art information is presented in these two volumes on the preservation, protection and restoration of historical constructions, both comprising monumental structures and complete city centres.

These two proceedings volumes are focused on the possibilities of numerical and experimental techniques in the maintenance of historical structures. In this respect, the papers, originating from about 30 countries, are subdivided in the following areas:

- Historical aspects and general methodology.
- Materials and laboratory testing.
- Non-destructive testing and inspection techniques.
- Dynamic behaviour and structural monitoring.
- Analytical and numerical approaches.
- Consolidation and strengthening techniques.
- Historical timber and metal structures.
- Seismic analysis and vulnerability assessment.
- Seismic strengthening and innovative systems.
- Case studies.

Structural Analysis of Historical Constructions is a valuable source of information for scientists and practitioners working on structure-related issues of historical constructions.

